

Northumbria Research Link

Citation: Jennings, Claire (2011) Chromatographic Analysis of Recombinant Lysostaphin Expressed in Escherichia coli. Doctoral thesis, Northumbria University.

This version was downloaded from Northumbria Research Link:
<https://nrl.northumbria.ac.uk/id/eprint/14689/>

Northumbria University has developed Northumbria Research Link (NRL) to enable users to access the University's research output. Copyright © and moral rights for items on NRL are retained by the individual author(s) and/or other copyright owners. Single copies of full items can be reproduced, displayed or performed, and given to third parties in any format or medium for personal research or study, educational, or not-for-profit purposes without prior permission or charge, provided the authors, title and full bibliographic details are given, as well as a hyperlink and/or URL to the original metadata page. The content must not be changed in any way. Full items must not be sold commercially in any format or medium without formal permission of the copyright holder. The full policy is available online: <http://nrl.northumbria.ac.uk/policies.html>



**Chromatographic Analysis of
Recombinant Lysostaphin
Expressed in *Escherichia coli***

Claire Elizabeth Jennings

A thesis submitted in partial fulfilment
of the requirements of the University of
Northumbria for the degree of Doctor
of Philosophy

Research undertaken in the School of
Life Sciences

2011

Abstract

Lysostaphin (EC.3.4.24.75) is an extracellular glycyglycine endopeptidase produced exclusively by *Staphylococcus simulans* biovar *staphylolyticus* (ATCC 1362, NRRL B-2628). The zinc-containing endopeptidase demonstrates specific and potent staphylolytic activity therefore shows great promise for the treatment of blood-borne and biofilm-associated staphylococcal infections. The gene encoding mature lysostaphin has therefore been cloned and expressed using *Escherichia coli*, the most widely used expression host for recombinant protein production.

This research demonstrated that when recombinant lysostaphin is expressed in *E. coli* BL21(DE3), the resulting catalytically-active product exhibits considerable micro- and macro-heterogeneity. Using a variety of chromatographic modes, including IEX, GF, IMAC, HIC and RP, several variants of recombinant lysostaphin were resolved indicating differences in charge, mass and hydrophobicity. The degree of charge heterogeneity observed was influenced by a number of factors, including expression temperature, amino acid sequence, optical density at point of induction and duration of culture. Rapid analysis of *N*-terminally His-tagged recombinant lysostaphin demonstrated that charge variant formation occurred in a time-dependent manner, whereby basic protein variants became steadily converted to more acidic variants.

LC-MS analysis of *N*-terminally His-tagged recombinant lysostaphin indicated that the protein was likely to have become truncated during expression. Comparison of WCX and LC-MS analysis suggested that amino acids were lost from the *N*-terminus to produce basic variants, whilst loss of *C*-terminal lysine₁₆ may have explained the detection of more acidic variants. As intact mass measurements acquired during LC-MS analysis of *N*-terminally His-tagged recombinant lysostaphin did not match exactly with theoretical intact protein masses, it was thought that the protein variants were also subject to enzymatic or chemical PTMs. These conclusions were made using supporting evidence that was acquired during GF, SDS-PAGE and CXC analysis.

Overall these findings are of concern for the production of recombinant protein production using *E. coli*. However this research suggested that chromatography can be used to sensitively detect and monitor product heterogeneity, so that a more homogeneous product could be produced by careful adjustment of expression, harvest and formulation conditions.

List of Contents

1	INTRODUCTION.....	1
1.1	<i>Escherichia coli</i>	1
1.1.1	Recombinant protein expression in <i>E. coli</i>	1
1.1.2	Quality control during recombinant protein production.....	3
1.2	Post-translational modifications (PTMs).....	4
1.2.1	Types of PTM.....	4
1.2.1.1	<i>N</i> -terminal modifications of recombinant proteins expressed in <i>E. coli</i>	5
1.2.1.2	Enzyme-mediated side chain modifications of recombinant proteins expressed in <i>E. coli</i>	7
1.2.1.3	Chemical side chain modifications of recombinant proteins expressed in <i>E. coli</i>	8
1.3	Heterogeneity of recombinant proteins expressed in <i>E. coli</i>	9
1.3.1	Sequence variation	9
1.3.2	Protein instability	13
1.4	Recombinant lysostaphin	13
1.4.1	Applications of lysostaphin	14
1.4.2	Chromatographic analysis of recombinant lysostaphin expressed in <i>E. coli</i>	19
2	CLONING, EXPRESSION AND PURIFICATION OF RECOMBINANT LYSOSTAPHIN.....	21
2.1	Introduction.....	21
2.2	Methods.....	22
2.2.1	Bacterial strains	22
2.2.2	Chemicals	22
2.2.3	Equipment.....	22
2.2.4	Buffers and solutions.....	22
2.2.5	Agarose gel electrophoresis of DNA and protein preparations	22
2.2.6	Polyacrylamide gel electrophoresis (PAGE)	22
2.2.7	Quantitation and detection of DNA and protein	23

2.3	Cloning of the gene encoding lysostaphin	24
2.3.1	Introduction	24
2.3.1.1	Cloning of the lysostaphin gene	25
2.3.1.2	Cloning of the gene encoding lysostaphin in <i>E. coli</i>	26
2.3.2	Methods	28
2.3.2.1	Media	28
2.3.2.2	Enzyme and buffer composition.....	28
2.3.2.3	Bacterial strains	28
2.3.2.4	Vectors	28
2.3.2.5	Kits	29
2.3.2.6	PCR amplification of the lysostaphin gene.....	29
2.3.2.7	Primer design and plasmid DNA constructs.....	29
2.3.2.8	Cloning using the Zero Blunt [®] cloning system.....	31
2.3.2.9	Cloning into pET-vector system	31
2.3.3	Results.....	32
2.3.3.1	Purification of genomic DNA from <i>S. staphylolyticus</i>	32
2.3.3.2	PCR amplification of mature lysostaphin domain encoding sequence from <i>S. staphylolyticus</i> genomic DNA	32
2.3.3.3	Cloning of the mature lysostaphin domain encoding sequence using the Zero Blunt [®] cloning system	33
2.3.3.4	Cloning of the lysostaphin gene using pET vector cloning system	34
2.3.3.5	Sequencing of plasmid DNA	36
2.3.3.6	ClustalW alignment of the known mature lysostaphin domain encoding sequence (with <i>N</i> -terminal His- tag encoding sequence added) and the acquired DNA sequence from pET construct 1	36
2.3.3.7	Identification of mis-matched nucleotides within the mature lysostaphin domain encoding sequence	39
2.3.4	Discussion.....	41
2.4	Expression of recombinant lysostaphin in <i>E. coli</i>	44
2.4.1	Introduction	44
2.4.1.1	Expression of recombinant lysostaphin in <i>E. coli</i>	45
2.4.2	Methods	47
2.4.2.1	Media	47
2.4.2.2	Chemicals.....	47
2.4.2.3	Buffers.....	47
2.4.2.4	Bacterial strains	47

2.4.2.5	Media supplementation.....	47
2.4.2.6	Bioinformatic prediction of expected molecular weight.....	48
2.4.2.7	Expression from recombinant lysostaphin gene constructs.....	48
2.4.3	Results.....	49
2.4.3.1	Expression of recombinant lysostaphin gene constructs in <i>E. coli</i>	49
2.4.3.2	Cytoplasmic expression of <i>N</i> -terminally His-tagged recombinant lysostaphin (construct 1).....	50
2.4.3.3	Expression of recombinant lysostaphin (constructs 2, 3, 4 and 5).....	51
2.4.3.4	Expression of recombinant lysostaphin using different expression media ..	52
2.4.3.5	Expression of recombinant lysostaphin using different expression media volumes ..	52
2.4.4	Discussion.....	54
2.5	Purification of recombinant lysostaphin.....	56
2.5.1	Introduction	56
2.5.1.1	Purification of recombinant lysostaphin.....	57
2.5.2	Methods	60
2.5.2.1	Buffers.....	60
2.5.2.2	Chemicals.....	60
2.5.2.3	Equipment	60
2.5.2.4	Purification of recombinant lysostaphin.....	60
2.5.3	Results.....	61
2.5.3.1	Ammonium sulphate fractionation.....	61
2.5.3.2	HIC using Phenyl Sepharose™ high performance media and an ÄKTA™ purification system	62
2.5.3.3	GF using HiLoad™ 16/60 Superdex 200 media and a FPLC system.....	65
2.5.3.4	AXC using Source™ 30Q media and an ÄKTA™ purification system....	67
2.5.3.5	CXC using Source™ 30S media and an ÄKTA™ purification system....	68
2.5.3.6	IMAC using Chelating Sepharose™ Fast Flow media and an ÄKTA™ purification system	70
2.5.3.7	Large-scale purification of recombinant lysostaphin by IMAC using Chelating Sepharose™ Fast Flow media and an ÄKTA™ purification system	73
2.5.3.8	Large-scale purification of recombinant lysostaphin by IMAC using Chelating Sepharose™ Fast Flow media and a peristaltic pump	75

2.5.3.9 Purification of recombinant lysostaphin from <i>E. coli</i> cell lysate using and Ultimate™ 3000 system and a ProPac® IMAC-10 column	76
2.5.3.10 IMAC using ProPac® IMAC columns (2 x 250 mm)	78
2.5.3.11 IMAC using ProPac® IMAC columns (4 x 250 mm)	79
2.5.4 Discussion.....	82
2.6 Discussion	86
3 SEPARATION OF RECOMBINANT LYSOSTAPHIN ISOFORMS	88
3.1 Introduction.....	88
3.2 Methods.....	90
3.2.1 Buffers	90
3.2.2 Equipment.....	90
3.2.3 Sample preparation.....	90
3.3 Column selection.....	91
3.3.1 Introduction	91
3.3.1 Methods	93
3.3.1.1 Column selection	93
3.3.2 Results.....	94
3.3.2.1 Protein separation using ProPac® SAX-10 column and DX500 chromatography system.....	94
3.3.2.2 Protein separation using ProPac® SCX-10 column and DX500 chromatography system.....	95
3.3.2.3 Protein separation using ProPac® WCX-10 column and DX500 chromatography system.....	95
3.3.2.4 Protein separation using ProPac® WCX-10 column and Ultimate™ 3000 chromatography system.....	98
3.3.2.5 Validation of ProPac® WCX-10 column.....	100
3.3.2.6 Protein separation using ProSwift® SCX-1S column and an Ultimate™ 3000 system	101
3.3.2.7 Protein separation using ProSwift® WCX-1S column and an Ultimate™ 3000 system	102
3.3.2.8 Validation of ProPac® MAb SCX beta test column	103
3.3.2.9 Protein separation using ProPac® MAb SCX beta test column and an Ultimate™ 3000 system.....	104

3.3.3 Discussion.....	105
3.4 Optimisation of protein isoform separation.....	107
3.4.1 Introduction	107
3.4.2 Methods	110
3.4.2.1 Optimisation of protein isoform separation.....	110
3.4.2.2 Separation of protein isoforms using optimised conditions.....	110
3.4.2.3 Optimisation of protein separation using ProPac® MAb SCX columns .	110
3.4.3 Results.....	111
3.4.3.1 Optimisation of protein isoform separation using the ProPac® WCX column.....	111
3.4.3.2 Optimisation of sample loading conditions	111
3.4.3.3 Optimisation of sample preparation	113
3.4.3.4 Optimisation of gradient conditions	115
3.4.3.5 Optimisation of mobile phase conditions.....	117
3.4.3.6 Optimisation of column length.....	118
3.4.3.7 Optimisation of column diameter	118
3.4.3.8 Optimisation of fraction collection	123
3.4.3.9 Timed fraction collection	123
3.4.3.10 Peak recognition.....	124
3.4.3.11 Analysis of recombinant lysostaphin using optimised conditions.....	127
3.4.3.12 Influence of culture temperature upon charge heterogeneity of recombinant lysostaphin	128
3.4.3.13 Separation of alternative recombinant protein preparations	134
3.4.3.14 Optimisation of protein isoform separation using the beta-test ProPac® MAb column.....	139
3.4.3.15 Optimisation of sample loading conditions.....	139
3.4.3.16 Optimisation of chromatographic gradient conditions.....	140
3.4.3.17 Optimisation of mobile phase conditions.....	141
3.4.3.18 Optimisation of column length.....	141
3.4.4 Discussion.....	144
3.5 Rapid analysis of recombinant lysostaphin isoforms.....	148
3.5.1 Introduction	148
3.5.1.1 Rapid analysis of recombinant lysostaphin	150
3.5.1.2 Optimisation of sample preparation during rapid analysis	152
3.5.1.3 Maximising sample through-put during rapid analysis.....	153

3.5.1.4	Optimisation of chromatographic conditions	154
3.5.2	Methods	156
3.5.2.1	Optimisation of rapid analysis	156
3.5.3	Results	157
3.5.3.1	Rapid analysis of recombinant lysostaphin using a ProPac [®] SCX (2 x 250 mm) column	157
3.5.3.2	Influence of optical density at point of induction upon charge heterogeneity	161
3.5.3.3	Comparative analysis of cell lysate using ProPac [®] SCX (2 x 250 mm) and ProPac [®] WCX (4 x 500 mm) columns	166
3.5.3.4	Rapid analysis of recombinant lysostaphin using a ProPac [®] WCX (2 x 250 mm) column	168
3.5.3.5	Optimisation of cell lysate preparation during rapid analysis using a ProPac [®] WCX (2 x 250 mm) column	169
3.5.3.6	Rapid analysis of recombinant lysostaphin using a ProPac [®] WCX (2 x 500 mm) column	172
3.5.3.7	Maximising sample through-put during rapid analysis using a ProPac [®] WCX (2 x 500 mm) column	174
3.5.3.8	Culture analysis using a ProPac WCX [®] (2 x 500 mm) column	178
3.5.3.9	Investigation of the influence of optical density at the point of induction upon the charge heterogeneity of recombinant lysostaphin	178
3.5.3.10	Optimisation of chromatographic conditions	186
3.5.3.11	Investigation of the influence of time upon the charge heterogeneity of recombinant lysostaphin	189
3.5.3.12	Extended investigation of the influence of time upon the charge heterogeneity of recombinant lysostaphin	199
3.5.3.13	Rapid analysis of recombinant lysostaphin using a ProPac [®] MAb SCX (4 x 250 mm) column	203
3.5.4	Discussion	207
3.6	Discussion	211
4	CHARACTERISATION OF RECOMBINANT LYSTOSTAPHIN	223
4.1	Activity of recombinant lysostaphin	224
4.1.1	Introduction	224
4.1.1.1	Staphylolytic activity of lysostaphin	226

4.1.1.2	Elastolytic activity of lysostaphin	228
4.1.1.3	Lysostaphin as a zinc metalloprotein	229
4.1.1.4	Activity of recombinant lysostaphin	231
4.1.2	Methods	233
4.1.2.1	Media	233
4.1.2.2	Buffers	233
4.1.2.3	Bacterial strains	233
4.1.2.4	Sample preparation	233
4.1.2.5	Equipment	233
4.1.2.6	Homology-based identification of consensus zinc binding residues in the amino acid sequence of recombinant lysostaphin	233
4.1.2.7	Lysostaphin assay	233
4.1.2.8	Assay of recombinant lysostaphin	234
4.1.3	Results	235
4.1.3.1	Homology-based identification of consensus zinc binding residues in the amino acid sequence of recombinant lysostaphin	235
4.1.3.2	Growth of <i>S. aureus</i> for turbidometric assay	236
4.1.3.3	Assay of staphylolytic activity of recombinant lysostaphin	237
4.1.3.4	Assay of <i>N</i> -terminally His-tagged recombinant lysostaphin (construct 1)	238
4.1.3.5	Influence of expression media upon the activity of recombinant lysostaphin	238
4.1.3.6	Influence of expression location upon the activity of recombinant lysostaphin	239
4.1.3.7	Influence of purification upon the activity of recombinant lysostaphin ..	240
4.1.3.8	Influence of lyophilisation upon the activity of recombinant lysostaphin	241
4.1.3.9	Assay of charge variants following WCX separation	242
4.1.3.10	Assay of charge variants following WCX separation during culture analysis	246
4.1.4	Discussion	248
4.2	IMAC analysis of recombinant lysostaphin	252
4.2.1	Introduction	252
4.2.1.1	Recombinant lysostaphin and <i>N</i> -terminal His-tag heterogeneity	257
4.2.2	Methods	263
4.2.2.1	Buffers	263
4.2.2.2	Equipment	263

4.2.2.3	Sample preparation	263
4.2.2.4	WCX analysis of His-tag heterogeneity.....	263
4.2.2.5	WCX analysis of IMAC purified protein	263
4.2.3	Results.....	264
4.2.3.1	WCX analysis of His-tag heterogeneity.....	264
4.2.3.2	IMAC Purification of <i>N</i> -terminally His-tagged recombinant lysostaphin	266
4.2.3.3	PAGE analysis of IMAC samples and fractions.....	270
4.2.3.4	WCX analysis of IMAC purified protein	274
4.2.3.5	IMAC purification of <i>C</i> -terminally His-tagged recombinant lysostaphin	276
4.2.3.6	PAGE analysis of IMAC samples and fractions.....	278
4.2.3.7	WCX analysis of IMAC purified protein	280
4.2.3.8	IMAC purification of recombinant lysostaphin	282
4.2.3.9	PAGE analysis of IMAC samples and fractions.....	285
4.2.4	Discussion.....	288
4.3	GF analysis of recombinant lysostaphin	298
4.3.1	Introduction	298
4.3.1.1	Aggregation during recombinant protein expression	298
4.3.1.2	Aggregation during protein purification	299
4.3.1.3	Aggregation during storage and formulation	300
4.3.1.4	Protein structure and aggregation.....	301
4.3.1.5	Aggregation of recombinant lysostaphin	301
4.3.2	Methods	305
4.3.2.1	Buffers.....	305
4.3.2.2	Equipment	305
4.3.2.3	Sample preparation	305
4.3.2.4	PAGE analysis of protein stability after prolonged storage.....	305
4.3.2.5	GF Analysis	305
4.3.3	Results.....	306
4.3.3.1	PAGE analysis of protein stability after prolonged storage.....	306
4.3.3.2	Influence of lyophilisation on the solubility of recombinant lysostaphin	307
4.3.3.3	GF of fractions eluted following IMAC purification.....	308
4.3.3.4	GF of fractions eluted following IMAC purification under denaturing conditions	310
4.3.3.5	GF of fractions eluted following WCX separation of recombinant lysostaphin isoforms	312

4.3.4 Discussion.....	324
4.4 LC-MS analysis of recombinant lysostaphin	328
4.4.1 Introduction	328
4.4.2 Methods	329
4.4.2.1 Buffers.....	329
4.4.2.2 Equipment	329
4.4.2.3 Sample preparation	329
4.4.2.4 Intact LC-MS analysis.....	329
4.4.3 Results.....	331
4.4.3.1 Intact MS analysis of recombinant lysostaphin.....	331
4.4.4 Discussion.....	343
4.5 Discussion	346
5 DISCUSSION.....	353
5.1 Cloning, expression and purification of recombinant lysostaphin	353
5.2 Separation of recombinant lysostaphin.....	354
5.3 Activity of recombinant lysostaphin	357
5.4 IMAC analysis of recombinant lysostaphin	357
5.5 GF analysis of recombinant lysostaphin	359
5.6 LC-MS analysis of recombinant lysostaphin	359
5.7 Heterogeneity of recombinant lysostaphin.....	361
5.8 Truncation of recombinant lysostaphin.....	365
5.9 PTM of recombinant lysostaphin.....	367
5.10 Consequences of product heterogeneity.....	370
5.11 Detection and remediation of product heterogeneity	372
5.12 Recombinant lysostaphin as a zinc glycyl-glycine endopeptidase	374
5.13 Conclusions	375

5.14	Further work.....	376
6	REFERENCES.....	378
7	APPENDIX.....	394
7.1	Cloning, Expression and Purification of Recombinant Lysostaphin	394
7.1.1	Cloning of the gene encoding lysostaphin	409
7.1.2	Expression of recombinant lysostaphin	442
7.1.3	Purification of recombinant lysostaphin	475
7.2	Separation of Recombinant Lysostaphin Isoforms.....	496
7.2.1	Column selection.....	518
7.2.2	Optimisation of protein isoform separation	520
7.2.3	Rapid analysis of recombinant lysostaphin isoforms	548
7.3	Characterisation of Recombinant Lysostaphin	593
7.3.1	Activity of recombinant lysostaphin	593
7.3.2	IMAC analysis of recombinant lysostaphin	618
7.3.3	GF Analysis of recombinant lysostaphin.....	624
7.3.4	LC-MS Analysis of recombinant lysostaphin.....	630

Acknowledgements

Firstly I would like to thank Professor Gary Black for recognizing my abilities and providing opportunities to perform research under his supervision and guidance. I really appreciated that he was always available with help and advice when it really mattered. Many thanks also to Dr Ken Cook for sharing his love of chromatography and for investing much time and interest in my research.

Thank you to all my colleagues and friends in Lab A307 who supported and entertained me throughout the long days, nights, highs and lows of research. Particular thanks to Dr Lakshmy Manickan and Dr Caroline Orr, who gave me so many special memories and moments that I will never forget.

I would also like to acknowledge Northumbria University, the Centre for Excellence in Life Sciences (CELS) who funded this research and Avecia Biologics Ltd for providing the inspiration for this project.

Special thanks must also go to:

- Dr Justin Perry for his contributions to this project.
- Dr Meng Zhang, for the cloning of recombinant oxidoreductase and recombinant Ayr1p
- Mr Andrew Porter for assistance with LC-MS/MS analysis.
- Dr Achim Treumann and Mr David Blinco at NEPAF for advice and assistance with intact LC-MS analysis.
- Dr Julia Smith and Bruker Daltonics for LC-MS advice
- Mr Geoff Sparrow for solving an array of unfortunate IT disasters.
- Mr Ed Ludkin for technical advice during chromatography.
- Dr Paul Bassarab and Dr Katherine Stapleton for chemistry and IT advice.

Finally I would like to thank my family for all their support during this PhD. I am extremely fortunate to have such dedicated parents, Diane and Brian, who have done everything they could to help and encourage me. Thanks also to my grandmother, Mrs Doris Euston for her continued interest, my brother David, and my aunts, uncles and cousins who have supported me throughout. During the past four years, my patience, persistence, strength and determination have been tested to levels beyond that which I ever expected to encounter. This kind of achievement was therefore not possible without the support of my family and friends.

Declaration

I declare that this work contained in this thesis has not been submitted for any other award and that it is my own work. I also confirm that this work fully acknowledges opinions, ideas and contributions from the work of others.

Name: Claire Elizabeth Jennings

Signature:

Date:

Abbreviations

aa	Amino acid
ACN	Acetonitrile
APS	Ammonium persulphate
AIM	Autoinduction media
ASF	Ammonium sulphate fractionation
ATCC	American Tissue Culture Collection
AXC	Anion exchange chromatography
BPB	Bromophenol blue
BSA	Bovine serum albumin
C-terminal	Carboxy-terminal
CE	Capillary electrophoresis
CHO	Chinese hamster ovary
CXC	Cation exchange chromatography
CFE	Cell-free extract
°C	Degrees Celsius
Da	Dalton
DNA	Deoxyribonucleic acid
DSM	Deutsche Sammlung von Mikroorganismen
DTT	Dithiothreitol
EMA	European Medicines Agency
ESI	Electrospray ionisation
FA	Formic acid
GMP	Good manufacturing practice
GF	Gel filtration
H	Hour(s)
HIC	Hydrophobic interaction chromatography
HPLC	High performance liquid chromatography
IEX	Ion exchange chromatography
IMAC	Immobilised Metal Affinity Chromatography
Kbp	Kilobase pair(s)
L	Litre (L)
LB	Luria-Bertani media
LC	Liquid Chromatography
M	Molar

mA	Milliamps
MALDI	Matrix assisted liquid desorption ionisation
Min	Minute(s)
MM	Minimal media
mm	millimetre(s)
mAb	Monoclonal antibody
MHRA	Medicines and Healthcare products Regulatory Agency
MRSA	Methicillin resistant <i>S. aureus</i>
MS	Mass spectrometry
MS/MS	Tandem mass spectrometry
m/z	Mass-to-charge ratio
NCBI	National Center for Biotechnology Information
NRRL	Northern Regional Research Laboratory
N-terminal	Amino-terminal
NTA	Nitriloacetic acid
ORF	Open reading frame
ORSA	Oxacillin-resistant <i>S. aureus</i>
PAGE	Polyacrylamide gel electrophoresis
PCR	Polymerase chain reaction
PEEK	Polyether ether ketone
pI	Isoelectric point
PI	Post-induction
POI	Point of induction
PS-DVB	Polystyrene divinyl benzene
PTM	Post-translational modification
RNA	Ribonucleic acid
RP	Reversed phase
S	Second(s)
SAX	Strong anion exchange
SCX	Strong cation exchange
SDS	Sodium dodecyl sulphate
SEC	Size exclusion chromatography
TB	Terrific broth
TEMED	<i>N,N,N',N'</i> -Tetramethylethylenediamine
TFA	Trifluoroacetic acid
TOF	Time of flight
Tris	Tris(hydroxymethyl)aminomethane,

UV	Ultraviolet
VISA	Vancomycin-intermediate susceptible <i>S. aureus</i>
V	Volts
v/v	volume per volume
w/v	weight per volume
WCX	Weak cation exchange
x g	Times gravity
α	Alpha
β	Beta
λ	Lambda
μ	Micro
2D-LC	Two-dimensional liquid chromatography
18.2 M Ω /cm H ₂ O	18.2 mega ohm per centimetre water

1 Introduction

1.1 Escherichia coli

Escherichia coli is a rod-shaped, Gram-negative bacterium, which was first described as *Bacterium coli* in 1885 by Theodor Escherich. The bacterium became officially recognised as *Escherichia coli* in 1958, to acknowledge its discoverer (Kuhnert *et al.*, 2000). *E. coli* is a widespread bacterial species, which includes a wide range of strains which can be highly pathogenic, leading to considerable morbidity through localised and systemic infections (Kuhnert *et al.*, 2000). Alternatively *E. coli* strains can be avirulent strains, contributing to the normal flora of the intestine. Many avirulent strains have been characterised and are used as safe laboratory strains for genetic, molecular biological and biotechnological purposes. Due to the widespread nature and versatility of *E. coli*, the structure of this bacterium has been studied extensively

As a Gram-negative bacterium, *E. coli* possess a three-layer envelope which adjoins the cytoplasmic space. This envelope consists of an outer membrane and an inner plasma membrane which surround the periplasmic space. *E. coli* was one of the first microorganisms to be genome sequenced, which provided enhanced knowledge of gene expression in this organism. The 4.6 Mbp genome of *E. coli* K12 was published in 1997 and was found to encode 4288 proteins (Blattner *et al.*, 1997). Although the exact function of around 30% of the open reading frames (ORFs) which encode the *E. coli* genome are unknown, knowledge of *E. coli* genetics has provided an insight into how the organism grows, replicates and responds within environmental conditions (Richmond *et al.*, 1999). Prior advances in knowledge of *E. coli* genetics also lead to the development of recombinant DNA technology, which has revolutionised the large-scale production of specific, biologically important proteins.

1.1.1 Recombinant protein expression in *E. coli*

In 1982, recombinant insulin, the very first therapeutic protein derived from *E. coli* was approved for therapeutic use in the treatment of insulin-dependent diabetes (Johnson, 1983). Using recombinant DNA technology, the mature gene sequence encoding insulin could be efficiently expressed within *E. coli*, providing large amounts of recombinant insulin. Due to high yields and efficiency, *E. coli* rapidly became popular for the production of a variety of recombinant proteins used for industrial purposes, such as amylases, cellulases and proteases, or therapeutic purposes,

such as hormones, monoclonal antibodies (mAbs), cytokines and interferons (Schellekens, 2005, Swartz, 2001, Eiteman and Altman, 2006, Bylund *et al.*, 2000). Long-term use of *E. coli* has led to improvements in genetic handling and therefore the organism has well-characterised genetics, which can be exploited to full potential during recombinant protein expression (Ghosh Moulick *et al.*, 2007).

E. coli provides economical protein production due to being able to grow rapidly in inexpensive media (Zhang and Greasham, 1999). Host expression strains have been genetically engineered to enhance recombinant protein production, through improvements in DNA transcription, RNA translation, protein expression and stability (Eiteman and Altman, 2006). The versatility of heterologous expression is increased further by advances in gene cloning which has permitted periplasmic expression and expression of recombinant fusion proteins, to facilitate protein purification or enhance solubility. Provided that expression conditions are selected appropriately, *E. coli* replicates rapidly leading to an increased cell density and high yields of recombinant product within a short period of time. The success and extent of protein expression is however dependent on a number of factors, such as expression media conditions, the mode and scale of culture, expression host strains and bacterial growth kinetics. Stringent monitoring is essential to ensure reproducibility of recombinant protein manufacture, especially as the complexity of the prokaryotic cellular milieu and small alterations in culture conditions can alter the yield, stability and structure of a recombinant protein (Jenzsch *et al.*, 2006).

E. coli remains the most commonly used expression host for the production of recombinant proteins derived from eukaryotic or prokaryotic origins for industrial, therapeutic, diagnostic and research purposes (Eiteman and Altman, 2006, Xu *et al.*, 2008). Although other prokaryotic expression hosts, such as *Lactococcus lactis*, *Bacillus subtilis* or *Campylobacter jejuni* are available for recombinant protein production, *E. coli* remains the most dominant prokaryotic expression host (Georgiou, 1988, Chou, 2007, Mierau *et al.*, 2005a, Westers *et al.*, 2004, Wacker *et al.*, 2002, Linton *et al.*, 2005). Eukaryotic expression hosts also exist from yeast species such as *Pichia pastoris* or *Saccharomyces cerevisiae* or using insect or mammalian cells, such as Chinese hamster ovary (CHO) (Kang *et al.*, 2000, Choi *et al.*, 2006, Leonard *et al.*, 1990). Despite the availability of a variety of expression hosts, nine out of a total of 31 therapeutic proteins approved between 2003 and 2006 were derived from *E. coli*, demonstrating the popularity and importance of the organism as a prokaryotic expression host (Chou, 2007, Ioannou, 2006).

1.1.2 Quality control during recombinant protein production

Following expression, the recombinant protein is purified from cellular contaminants as part of good manufacturing practice (GMP) as such impurities may impinge on the safety of therapeutic proteins (Rathore *et al.*, 2003). Protein purification typically requires the application of a number of preparative techniques to achieve an acceptable level of purity and therefore increases the duration and cost of recombinant protein production. Once purified, the protein may undergo formulation, through the addition of buffering agents and excipients which enhance the stability of the recombinant protein. In addition, the yield and quality of the recombinant product must be assessed so that culture conditions and expression systems can be optimised if required (DePhillips *et al.*, 1994).

The quality of recombinant protein products is paramount, especially in the case of protein therapeutics which are strictly regulated by drug quality standards. Regulatory authorities, such as the Medicines and Healthcare products Regulatory Agency (MHRA) or European Medicines Agency (EMA) publish guidelines which specify the levels of purity, stability, safety and efficacy that a recombinant product must satisfy. As recombinant proteins are derived from living organisms, quality control is a much more complex affair due to variable influence of cell physiology and growth conditions upon the integrity of the expressed protein. It is therefore essential that the structure and formulation of a recombinant protein is thoroughly characterised to ensure that drug immunogenicity is not encountered during clinical trials or following therapeutic administration (Pavlovic *et al.*, 2008).

When producing recombinant proteins, it is therefore desirable to produce homogeneous proteins which ideally display identical activity and conformational structure to that of the native protein. Many eukaryotic proteins typically undergo post-translational modification (PTM) to achieve their native state. As prokaryotic systems are regarded as being much simpler than eukaryotic systems, it has been reported that *E. coli* is not able to produce more complex, modified or processed forms of recombinant proteins (Sugase *et al.*, 2008, Demain and Vaishnav, 2009). Therefore *E. coli* is regarded as the preferred host for the expression of therapeutic proteins that do not require PTM to achieve biological function (Jenzsch *et al.*, 2006, Choi and Lee, 2004).

Despite past reports, growing evidence has demonstrated that recombinant proteins expressed in *E. coli* can display considerable product heterogeneity, which occurs as

a result of post-translational processing events which follow expression. Recombinant proteins can also undergo chemical modifications or aggregation during purification, storage or formulation. Such structural alterations can result in micro- and macro-heterogeneity, which could interfere with the function or stability of the protein. It is also concerning that greater product complexity could lead to unexpected immunogenicity during therapeutic use.

1.2 Post-translational modifications (PTMs)

PTMs are covalent modifications, which occur following the transcription of DNA into RNA and the translation of RNA into proteins. The polypeptide chains that compose a protein structure are constructed of unique sequences of amino acid residues. The translated protein structure can exhibit further variability due to sequence alterations, such as amino acid substitutions or splicing variations that can occur during translation. The nascent or folded polypeptide can then be subjected to co- or post-translational modifications following chemical or enzyme-catalysed reactions (Walsh *et al.*, 2005). PTMs increase the complexity of the protein structure further and greatly expand the proteome of an organism. In addition to increasing biological diversity, PTMs alter the biophysical and biochemical properties of a protein and therefore have important implications for cellular processes that the protein governs. The structural changes imposed by PTMs can control or lead to induction of enzymatic activity, direction of intra- or extra-cellular translocations and can influence protein stability and degradation (Arfin and Bradshaw, 1988). Such PTMs are reversible, allowing greater control of cellular processes, whilst other modifications are permanent and can only be removed through replacement of the modified molecule.

1.2.1 Types of PTM

PTMs can occur following the covalent addition of a chemical group to a side chain residue of a protein or through covalent cleavage of the peptide backbone. Electron rich, nucleophilic side chains of amino acids possess the propensity to undergo covalent addition of electrophilic fragments of cosubstrates (Figure 1.1) (Walsh *et al.*, 2005). Amino acids containing nitrogen, oxygen or sulphur atoms can, depending on their ionization state, function as nucleophiles during covalent modification. The nucleophilic group chemically mediates the transfer of the electrophile, during derivatization of the protein side chains. The terminal regions of a protein also

possess nucleophilic groups which have the potential to undergo covalent modification, with the amino group at the *N*-terminus and the carboxyl group at the *C*-terminus (Walsh and Jefferis, 2006).

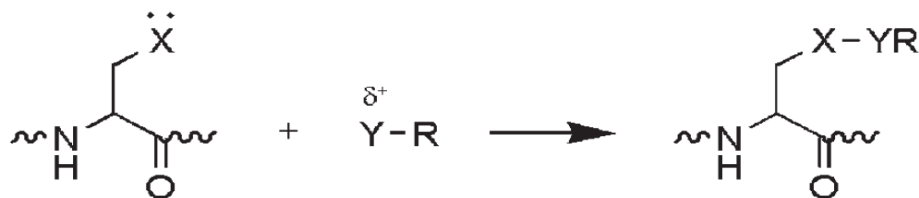


Figure 1.1: Chemical mechanism of covalent modification. Nucleophilic amino acid side chains become covalently modified by an electrophilic fragment of a cosubstrate (Walsh *et al.*, 2005)

Nucleophilic groups promote terminal and side chain modifications; however the incidence of such covalent interactions is facilitated by the existence of enzymes that efficiently catalyse the formation or removal of specific PTMs. Through the action of a variety of modification-specific enzymes, a diverse range of electrophilic fragments can be transferred by nucleophilic attack, leading to an array of PTMs. Common PTMs include phosphorylation, glycosylation, methylation and oxidation, however more than 200 kinds of PTM can occur following covalent addition of electrophilic groups (Polevoda and Sherman, 2007, Walsh, 2006). At present it is unknown exactly how many of these modifications can occur within *E. coli*, however it is already evident that a significant number can readily occur, influencing the structure of native and recombinant proteins. Consequently sequence variants and PTMs have been found to occur at nucleophilic groups at the *N*-terminus or side chain of recombinant proteins, through chemical or enzyme-catalysed reactions (Xie *et al.*, 2009).

1.2.1.1 *N*-terminal modifications of recombinant proteins expressed in *E. coli*

N-terminal heterogeneity is not uncommon following expression of a recombinant protein within *E. coli* (Table 1.1). The heterogeneity appears to arise as a consequence of prokaryotic protein synthesis and associated *N*-terminal processing mechanisms. Recombinant protein expression can exacerbate the heterogeneity of *N*-terminal sequences, due to the heightened synthetic demands that heterologous expression imposes on the expression host.

Table 1.1: N-terminal modifications of recombinant proteins expressed in *E. coli*

Modification	Recombinant Protein	Reference
Retention of N-terminal methionine	Interleukin-1 beta	Wingfield <i>et al.</i> , 1987a
	Growth hormone (hGH)	Nakagawa <i>et al.</i> , 1987
	Interleukin 2 (IL-2)	Nakagawa <i>et al.</i> , 1987
	Proapolipoprotein A-I	Moguilevsky <i>et al.</i> , 1993
	Growth hormone	Nishimura <i>et al.</i> , 1998
Retention of N-formylmethionine	Growth hormone II (EGH)	Sugimoto <i>et al.</i> , 1990
	Granulocyte colony-stimulating factor	Clogston <i>et al.</i> , 1992
	Interleukin-5	Rose <i>et al.</i> , 1992
	Histone A (hmfA)	Sandman <i>et al.</i> , 1995
	Cytochrome P450 (5 mutants)	Dong <i>et al.</i> , 1996
	Fatty acid-binding protein (H-FABP)	Specht <i>et al.</i> , 1994
N ^ε -Acetylation	Eglin C	Grutter <i>et al.</i> , 1985
	Leukocyte interferon A	Takao <i>et al.</i> , 1987
	Interferon-γ	Honda <i>et al.</i> , 1989
	Interleukin-1β (mrIL-1 β)	Lischwe <i>et al.</i> , 1993
	Stathmin-like domains RB3 and RB3' (RB3SLD and RB3SLD')	Charbaut <i>et al.</i> , 2002
	Tissue inhibitor of metalloproteinases-4 (TIMP-4)	Troeberg <i>et al.</i> , 2002
	Prothymosin α	Wu <i>et al.</i> , 2006
	F1-V	Bariola <i>et al.</i> , 2007
	N-terminal domain of TIMP (N-TIMP-1)	Van Doren <i>et al.</i> , 2008
	Thymosin α 1-L12 (Tα1-L12)	Fang <i>et al.</i> , 2010
N ^ε -Methylation	Ag1624	Lahnstein <i>et al.</i> , 1993
	Haemoglobin (rHb1.1)	Apostol <i>et al.</i> , 1995
	Histidine-rich protein II	Schneider <i>et al.</i> , 2005

1.2.1.2 Enzyme-mediated side chain modifications of recombinant proteins expressed in *E. coli*

Recombinant protein expressed in *E. coli* can also be susceptible to a number of enzyme-mediated side chain modifications. Acetylation, phosphorylation and methylation are the most frequently reported of these modifications (Table 1.2).

Table 1.2: Enzymatic modifications of recombinant proteins expressed in *E. coli*

Modification	Recombinant Protein	Reference
Acetylation	Somatotropin (Bovine)	Violand <i>et al.</i> , 1994
	Somatotropin (Porcine)	Violand <i>et al.</i> , 1994
	Placental lactogen	Violand <i>et al.</i> , 1994
	Tissue factor pathway inhibitor (TFPI)	Violand <i>et al.</i> , 1994
	Basic fibroblast growth factor (hbFGF) mutein CS23 (CS23)	Suenaga <i>et al.</i> , 1999
	RANTES S24F	d'Alayer <i>et al.</i> , 2007
Phosphorylation	Aurora A catalytic domain	Du <i>et al.</i> , 2005a
	PAK1 catalytic domain	Du <i>et al.</i> , 2005a
	PAK7 catalytic domain	Du <i>et al.</i> , 2005a
	PKA catalytic subunit	Du <i>et al.</i> , 2005a
	Aurora 2 catalytic domain	Du <i>et al.</i> , 2005a
	StkSA1	Lomas-Lopez <i>et al.</i> , 2008
	NE2398 CBS domain	She <i>et al.</i> , 2010
	RPA3416 CBS domain	She <i>et al.</i> , 2010
	PH0267 CBS domain	She <i>et al.</i> , 2010
	Atu1752 CBS domain	She <i>et al.</i> , 2010
	AF0847 CBS domain	She <i>et al.</i> , 2010
	TV1335 CBS domain	She <i>et al.</i> , 2010
	MJ0653 CBS domain	She <i>et al.</i> , 2010
Atu1337 ABM domain	She <i>et al.</i> , 2010	
Methylation	Growth hormone (Genotropin®)	Hepner <i>et al.</i> , 2005

1.2.1.3 Chemical side chain modifications of recombinant proteins expressed in *E. coli*

In the absence of enzyme-mediated catalysis, side chain modification of nucleophilic groups of amino acids can occur readily through nucleophilic attack. Deamidation, glycation and oxidation of recombinant proteins has been most frequently reported to occur (Table 1.3).

Table 1.3: Non-enzymatic modifications of recombinant proteins expressed in *E. coli*

Modification	Recombinant Protein	Reference
Deamidation	Interleukin-1 α (IL-1 α)	Wingfield <i>et al.</i> , 1987b
	Growth hormone II (EGH)	Sugimoto <i>et al.</i> , 1990
	Neu differentiation factor	Hara <i>et al.</i> , 1996
	Stem cell factor (rhSCF)	Hsu <i>et al.</i> , 1998
	Serine hydroxymethyltransferase	Solstad and Flatmark, 2000
	Lymphotoxin (rhLT)	Xie <i>et al.</i> , 2003
	Growth hormone (Genotropin [®])	Hepner <i>et al.</i> , 2005
	Growth hormone (Nutropin AQ [®])	Jiang <i>et al.</i> , 2009
	Immunoglobulin G Fc fusion protein	Ren <i>et al.</i> , 2009
Glycosylation	GRK-2	Geoghegan <i>et al.</i> , 1999
	ZAP-70	Geoghegan <i>et al.</i> , 1999
	Phosphatidylinositol-3 kinase (c-P85)	Geoghegan <i>et al.</i> , 1999
	Spo0F	Yan <i>et al.</i> , 1999b
	FKBP	Yan <i>et al.</i> , 1999a
	Src tyrosine kinase (SH3 domain)	Kim <i>et al.</i> , 2001
	Interferon γ (rhIFN- γ)	Mironova <i>et al.</i> , 2001, Mironova <i>et al.</i> , 2003
	Interferon alfacon-1	Mironova <i>et al.</i> , 2008
Oxidation	Insulin-like growth factor I (IGF-I)	Forsberg <i>et al.</i> , 1990
	Growth hormone II (EGH)	Sugimoto <i>et al.</i> , 1990
	Interleukin-5	Rose <i>et al.</i> , 1992
	Neu differentiation factor	Hara <i>et al.</i> , 1996
	Growth hormone (Genotropin [®])	Hepner <i>et al.</i> , 2005
	Growth hormone (Norditropin [®])	Hepner <i>et al.</i> , 2006
	<i>N</i> -terminal domain of TIMP (<i>N</i> -TIMP-1)	Van Doren <i>et al.</i> , 2008
	Growth hormone (Nutropin AQ [®])	Jiang <i>et al.</i> , 2009
	Immunoglobulin G Fc fusion protein	Ren <i>et al.</i> , 2009

1.3 Heterogeneity of recombinant proteins expressed in *E. coli*

It is evident that recombinant proteins expressed in *E. coli* are susceptible to a wide range of PTMs, which can occur as a consequence of post-translational processing, the nucleophilicity of amino acid groups and enzyme-mediated modification mechanisms. In the majority of studies, particular modifications were specifically detected or reported in isolation, however more recent studies suggest that recombinant proteins expressed in *E. coli* can be susceptible to a combination of multiple modifications (Hepner *et al.*, 2005, Hepner *et al.*, 2006). Furthermore it is unclear how many different kinds of modification can occur in *E. coli* and as a result recent studies have reported the detection of less common or novel modifications, such as succinylation or S-thiolation (Zhang *et al.*, 2011, Liu *et al.*, 2009) .

1.3.1 Sequence variation

In addition to PTM, proteins may exhibit sequence variation through loss or substitution of amino acids. Such sequence variation can occur under normal growth conditions, however it seems probable that hyper-expression of a recombinant protein could increase the likelihood of translational errors by overwhelming the translational apparatus and proof-reading mechanisms of *E. coli* (Schneider *et al.*, 2005, Scorer *et al.*, 1991). The physiological stress associated with recombinant protein expression may therefore adversely affect translational fidelity (McNulty *et al.*, 2003). Mis-translational events can also arise due to genetic mutation or codon bias, which can lead to processing errors such as protein truncation, protein elongation or amino acid substitutions.

Due to nature of recombinant DNA technology, errors in sequence information can occur at any stage of gene expression (Scorer *et al.*, 1991). For instance, point mutations, insertions or deletions within a recombinant gene sequence could alter the subsequent amino acid sequence of the translated recombinant protein. Nucleotide insertions, deletions or point mutations can lead to frame-shifting or amino acid substitution depending on where the mutation occurs. Frame-shift mutations and deletions are thought to occur more frequently than amino acid exchanges however (Hepner *et al.*, 2005). The implications of a mutation are less severe if the mutation happens at the third base encoding a particular codon, due to the “Wobble hypothesis” for codon-anti-codon pairing. If a mutation occurs within one of the first two bases of a codon then the amino acid is likely to become substituted.

Sequence variation can also arise due to codon bias, which can occur when expressing a foreign recombinant gene that originates from a host whose codon utilization preferences differ markedly from that of *E. coli*. During normal protein expression, different organisms have a bias towards a specific subset of codons, which have evolved according to cellular gene expression levels (Bonekamp and Jensen, 1988). During recombinant protein expression, translation of the target protein may be complicated by an absence of rare codons which are required to translate the protein in its desired form. Codon bias can therefore lead to misincorporation errors, as the lack of rarer tRNA molecules leads to ribosomal stalling, frame-shifting and misincorporation of more abundant tRNA molecules (McNulty *et al.*, 2003, Kane *et al.*, 1992). The degree of mis-translation is also dependent on the amino acid sequence of the recombinant protein being expressed. Furthermore expression culture conditions can influence the synthesis and subsequent availability of essential codons (Kane *et al.*, 1992) .

The incidence of amino acid substitution has been reported several times during recombinant protein expression (Table 1.4). Amino acid substitutions alter the primary structure of a protein, which can have implications for secondary and tertiary protein structure, in addition to potentially influencing the biological activity of a protein (McNulty *et al.*, 2003). The exchange of amino acids may therefore affect the quality of a recombinant biopharmaceutical as substituted residues may lead to product heterogeneity (Hepner *et al.*, 2005) .

Table 1.4: Recombinant proteins with amino acid substitutions when expressed in *E. coli*

Recombinant Protein	Origin	<i>E. coli</i> Strain	Detection Methods	Reference
Interleukin-2	Human	K12	Edman degradation FAB-MS Amino acid analysis	Tsai <i>et al.</i> , 1988
Somatotropin	Bovine	W3110G	IEF RP-HPLC Amino acid analysis	Bogosian <i>et al.</i> , 1989
Growth hormone	Human	Not specified	HIC Edman degradation	Gellerfors <i>et al.</i> , 1990
Haemoglobin	Human	Not specified	Amino acid analysis ESI-MS Edman degradation	Apostol <i>et al.</i> , 1997
Foot protein type 5 (Mgfp-5)	<i>Mytilus galloprovincialis</i>	BL21(DE3)	MALDI-TOF	Hwang <i>et al.</i> , 2004
Growth hormone (Genotropin®)	Human	K12	ESI-LC-MS/MS	Hepner <i>et al.</i> , 2005
Growth hormone (Norditropin®)	Human	MC1061	ESI-LC-MS/MS	Hepner <i>et al.</i> , 2006
Histidine-rich protein II	<i>Plasmodium falciparum</i>	BL21(DE3)	MS	Schneider <i>et al.</i> , 2005

As shown in Table 1.5, a variety of amino acid residues can be substituted within the amino acid sequence of a recombinant protein. Methionine, glutamine and arginine appear to have been most frequently reported as having undergone substitution. Translation of arginine residues in *E. coli* is known to be problematic as the arginine codons are considered rare, occurring at a frequency of less than 1% (McNulty *et al.*, 2003). In addition, rarer arginine codons, such as AGG are translated much slower than more abundant arginine codons, such as CGU (Bonekamp and Jensen, 1988).

Table 1.5: Amino acid substitutions observed in recombinant proteins expressed in *E. coli*

Recombinant Protein	Expected Amino Acid	Observed Amino Acid	Reference
Interleukin-2	Methionine	Norleucine	Tsai <i>et al.</i> , 1988
Somatotropin	Methionine	Norleucine	Bogosian <i>et al.</i> , 1989
Growth hormone	Glutamine	Valine	Gellerfors <i>et al.</i> , 1990
	Glutamine	Lysine	
Haemoglobin	Leucine	Norvaline	Apostol <i>et al.</i> , 1997
Foot protein type 5 (Mgfp-5)	Alanine	Threonine	Hwang <i>et al.</i> , 2004
Growth hormone (Genotropin [®])	Arginine	Lysine or Glutamine	Hepner <i>et al.</i> , 2005
	Arginine	Glycine	
	Methionine	Isoleucine	
Growth hormone (Norditropin [®])	Methionine	Valine	Hepner <i>et al.</i> , 2006
Histidine-rich protein II	Histidine	Glutamine	Schneider <i>et al.</i> , 2005

Amino acid substitutions typically involve misincorporation of regular amino acids, however non-usual amino acids, such as norleucine, norvaline and isoleucine have also been incorporated into recombinant proteins (Kane *et al.*, 1992). Norleucine, an analogue of methionine is known to substitute for internal and *N*-terminal methionine residues (Tsai *et al.*, 1988). At high intracellular norleucinyl tRNA levels, the analogue competes with methionyl tRNA for formylation and incorporation during protein translation (Bogosian *et al.*, 1989). Similarly norvaline is an analogue of leucine and can be misincorporated into recombinant proteins following intracellular accumulation. Both norvaline and norleucine arise as a consequence of branched-chain amino acid biosynthetic pathways in *E. coli* (Soini *et al.*, 2008).

Codon bias may also result in premature termination of protein synthesis, whereby a truncated nascent polypeptide dissociates from the ribosome (McNulty *et al.*, 2003). Protein truncation can also occur as a result of proteolytic processing. *E. coli* possesses several proteases, which are located within different intracellular compartments and are responsible for maintaining the cellular proteome. Proteases degrade abnormal or foreign recombinant proteins to ensure that the location and activities of native cellular proteins remain regulated (Narayanan and Chou, 2009,

Walsh *et al.*, 2005). Recombinant proteins often become truncated or degraded through the action of cellular proteases (Table 1.6), however such sequence variants are only typically investigated when the biological activity of therapeutic proteins become compromised.

Table 1.6: Truncated recombinant proteins expressed in *E. coli*

Recombinant Protein	Origin	<i>E. coli</i> Strain	Detection Methods	Reference
Interleukin-6 (IL-6)	Human	JM83	Circular dichroism Edman degradation	Proudfoot <i>et al.</i> , 1993
Phenylalanine hydroxylase (hPAH)	Human	HMS174(DE3) BL21(DE3)	IEF Edman degradation	Martinez <i>et al.</i> , 1995
β 2-microglobulin	Human	BL21(DE3)	ESI-MS	Esposito <i>et al.</i> , 2000
Growth hormone (Nutropin AQ [®])	Human	Not specified	LC-MS/MS FT-ICR MS	Jiang <i>et al.</i> , 2009

1.3.2 Protein instability

Further product heterogeneity can also result from physical or chemical instabilities. Chemical instabilities occur as a consequence of making or breaking covalent bonds in the intra- and inter-molecular protein structure, whilst physical instabilities do not change the chemical composition of the protein but rather result in denaturation and aggregation (Manning *et al.*, 2010). Protein instability is covered in further detail in Section 4.3.

1.4 Recombinant lysostaphin

Post-translational modification or processing of recombinant proteins can only become apparent through analytical characterisation of protein structure and function. As only a limited selection of recombinant proteins have been characterised in such a manner, it is currently unclear whether all recombinant proteins are likely to display heterogeneity upon expression in *E. coli* or whether this phenomenon is only related to a small subset of proteins.

Recombinant lysostaphin is one such protein which had been found to demonstrate product heterogeneity upon expression in *E. coli* (Kara *et al.*, 2006). The protein is

produced by heterologous expression after cloning the gene sequence encoding mature lysostaphin, which is derived from the genome of *Staphylococcus simulans* biovar *staphylolyticus* (ATCC 1362, NRRL B-2628). The gene sequence of lysostaphin (EC.3.4.24.75) is encoded as a preproenzyme, which is processed by *S. staphylolyticus* to produce a mature, monomeric glycyglycine endopeptidase. Lysostaphin is exclusively produced by *S. staphylolyticus* and mediates specific hydrolysis of the pentaglycine cross-bridges present within peptidoglycan cell walls (Heath Farris *et al.*, 2003, Surovtsev *et al.*, 2007). As lysostaphin selectively targets the pentaglycine cross-links of peptidoglycan, only staphylococcal strains are susceptible to lysis, whilst other genera are resistant (Turner *et al.*, 2007, Huber and Huber, 1989, Boyle-Vavra *et al.*, 2001). The mechanisms of catalysis are described further in Section 4.1.1.

1.4.1 Applications of lysostaphin

Lysostaphin has been shown to lyse over fifty strains of *S. aureus*, regardless of phage type, antibiotic resistance, cell wall condition or degree of bacterial capsulation (Trayer and Buckley, 1979). In addition to *S. aureus*, the endopeptidase can also target the cell walls of other staphylococcal species that have cell walls featuring pentaglycine residues, such as *S. simulans*, *S. epidermidis* and *S. carnosus* (Bardelang *et al.*, 2009, Mierau *et al.*, 2005a, Wu *et al.*, 2003). As lysostaphin demonstrates selective lysis of staphylococcal strains, the enzyme is used for a number of clinical and therapeutic applications. As a prototypical peptidase, lysostaphin is also commonly employed as a research tool in biotechnology (Firczuk *et al.*, 2005). Staphylococcal cells are resistant to conventional lysis methods, therefore the action of lysostaphin can be used to liberate cellular constituents, such as intracellular enzymes, nucleic acids and cell membrane components (Park *et al.*, 1995). Cell wall lysis is also useful when differentiating staphylococcal strains or during genetic studies in which DNA is isolated from staphylococcal strains (Thumm and Götz, 1997).

Due to its potent anti-staphylococcal activity, lysostaphin has been considered as an antibacterial agent for over 40 years. The prevalence of other antibiotics and difficulties in achieving protein purity restricted widespread use and development of lysostaphin as an antibacterial agent. However developments in recombinant DNA technology and the emergence of multi-drug resistant bacteria lead to renewed

interest in lysostaphin for clinical and therapeutic purposes. Due to the enzyme's ability to lyse *S. aureus* regardless of resistance to other antibiotics, recombinant lysostaphin has been shown to kill multi-drug resistant strains, such as methicillin resistant *S. aureus* (MRSA), oxacillin-resistant *S. aureus* (ORSA) and vancomycin-intermediate susceptible *S. aureus* (VISA) (Yang *et al.*, 2007, Climo *et al.*, 2001, Walsh *et al.*, 2004).

The growing emergence of antibiotic-resistant staphylococcal infections poses a major problem in clinical settings, particularly amongst immunosuppressed and immunocompromised individuals affected by cutaneous and blood-borne infections. Many studies have therefore been performed on animal, but also human models to assess the efficacy of recombinant lysostaphin in the therapy of localised and systemic infections (Table 1.7). Such investigations have indicated that lysostaphin can effectively kill Staphylococcal cells at low minimal inhibitory concentration (MIC) values of between 0.0039 and 15.4 µg/ml, depending on staphylococcal strain (Dajcs *et al.*, 2000, Climo *et al.*, 1998, Wu *et al.*, 2003, Harrison and Zygmunt, 1967, Patron *et al.*, 1999, McCormick *et al.*, 2006, Oluola *et al.*, 2007). These values indicate that lysostaphin can inhibit the visible growth of staphylococcal cells at extremely low concentrations, suggesting that the enzyme offers extremely sensitive and potent cell lysis.

Table 1.7: Studies in which lysostaphin has been administered topically or parenterally to human or animal models with successful suppression or eradication of localised or systemic staphylococcal infections.

Reference	Animal Model	Target infection	Mode of Administration	MIC value [†] (µg/ml)
Schuhardt and Schindler, 1964	Mouse	Systemic	Intraperitoneal or subcutaneous	Not specified
Harris <i>et al</i> , 1967	Human	Nasal colonisation	Topical	Not specified
Harrison <i>et al</i> , 1967	Mouse	Renal	Intravenous	0.095
Dixon <i>et al</i> , 1968	Mouse	Renal	Intravenous	Not specified
Quickel <i>et al</i> , 1971	Human	Nasal colonisation	Topical	Not specified
Stark <i>et al</i> , 1974	Human	Systemic	Intravenous	Not specified
Oldham and Daley, 1992	Cow	Mastitis	Sub-cutaneous	Not specified
Climo <i>et al</i> , 1998	Rabbit	Aortic valve endocarditis	Intravenous	0.015-0.030
Patron <i>et al</i> , 1999	Rabbit	Aortic valve endocarditis	Intravenous	0.0039
Dajcs <i>et al</i> , 2000	Rabbit	Keratitis	Topical	0.031-0.063
Dajcs <i>et al</i> , 2001	Rabbit	Endophthalmitis	Topical	Not specified
Dajcs <i>et al</i> , 2002	Rabbit	Keratitis	Topical	Not specified
Kokai-Kun <i>et al</i> , 2003	Rat	Nasal colonisation	Topical	Not specified
Walsh <i>et al</i> , 2004	Mouse	Nasal colonisation	Topical	Not specified
McCormick <i>et al</i> , 2006	Rabbit	Endophthalmitis	Topical	0.74-15.4
Kokai-Kun <i>et al</i> , 2007	Mouse	Systemic	Intravenous	Not specified
Oluola <i>et al</i> , 2007	Rat	Systemic	Intraperitoneal	0.125

[†] MIC values were determined against single or multiple lysostaphin-susceptible bacterial strains. In some cases where the MIC values were not specified, the applied lysostaphin concentrations were deliberately augmented to enhance therapeutic efficacy.

Table 1.7 details a number of studies in which lysostaphin has demonstrated efficacious suppression or eradication of localised and systemic staphylococcal infections. Lysostaphin preparations can be administered topically or via intraperitoneal, subcutaneous or intravenous injection. Topical application of lysostaphin to nasal or ocular infections has demonstrated considerable success in a number of studies indicating that effective formulations exist to tackle and prevent cutaneous infections, not only in research but also clinical trials (Yang *et al.*, 2007, Cisani *et al.*, 1982, Dajcs *et al.*, 2000, Dajcs *et al.*, 2002). Intravenous administration of lysostaphin has also been shown to eradicate localised and systemic staphylococcal infections in a number of animal models. However Walsh *et al.* (2004) found that greater than 95% of the enzyme is cleared from serum circulation within an hour of administration (Walsh *et al.*, 2004). In order to maintain serum protein concentrations and minimise the requirement for frequent dosing, the protein formulation may require optimisation to extend serum half-life.

Lysostaphin has also been applied to treat staphylococcal infections of the mammary glands (mastitis) in animals. Mastitis has major economic implications for dairy farming, by adversely influencing animal welfare and reducing overall dairy yields. Lysostaphin has been used to successfully treat bovine mastitis, without encountering resistance. The endopeptidase treatment has traditionally been administered through sub-cutaneous injection of lysostaphin purified following expression in either bacterial or mammalian cells (Williamson *et al.*, 1994). However in recent years, lysostaphin has been expressed transgenically in the mammary glands of animals (Fan *et al.*, 2004, Klein *et al.*, 2006, Donovan *et al.*, 1996, Kerr *et al.*, 2001, Mitra *et al.*, 2003, Fan *et al.*, 2002). This approach was found to effectively protect livestock against intra-mammary staphylococcal infections as the lysostaphin gene remains functional in mammalian cells, despite its prokaryotic origins (Williamson *et al.*, 1994).

In addition to the treatment of staphylococcal infections, recombinant lysostaphin has also been used to suppress biofilm formation, particularly on medical devices, such as catheters (Turner *et al.*, 2007). Like many other bacterial strains, staphylococcal cells have a tendency to form a multi-layered population of cells known as biofilms. Biofilms are 1000-1500 times more resistant to antibiotics than their more dispersed counterparts, therefore are much more difficult to eradicate and often necessitate removal of indwelling medical devices (Wu *et al.*, 2003). However lysostaphin has been found to be active against *S. aureus* within biofilms, but is also known to rapidly

disrupt the extracellular matrix of biofilms colonizing plastic and glass surfaces (Wu *et al.*, 2003). Shah *et al.* (2004) found that lysostaphin-coated catheters were less readily colonized by several strains of *S. aureus* and therefore could be used prophylactically to prevent the incidence of catheter-related staphylococcal infections (Shah *et al.*, 2004).

Although lysostaphin shows great promise as an anti-staphylococcal agent, the activity of the enzyme may ultimately become compromised by the development of endopeptidase resistance. *S. staphylolyticus* renders itself resistant to the action of lysostaphin through modification of the polyglycine cross-bridges within peptidoglycan. Some staphylococcal species also demonstrate complete resistance to lysostaphin, whilst others exhibit decreased susceptibility, such as *S. epidermidis* and *S. haemolyticus*. Lysostaphin-resistant staphylococcal strains exhibit similar modifications of the poly-glycine cross-links as *S. staphylolyticus*, in that glycine residues become substituted with serine or alanine residues. This resistance can arise following mutations of the femA gene, which typically mediates the addition of the glycine residues within the cross-bridge. Essentially mutation of this gene results in production of a monoglycine cross-linker, which however renders the cells susceptible to the action of β -lactam antibiotics (Kiri *et al.*, 2002, DeHart *et al.*, 1995, Climo *et al.*, 2001).

The incidence of reduced susceptibility to lysostaphin highlights the importance of using lysostaphin, in combination with other antibacterial agents to achieve maximal cell lysis during therapeutic interventions. For instance, using lysostaphin in combination with lysozyme, an endo- β -muramidase, can potentiate the anti-staphylococcal efficacy of lysostaphin (Cisani *et al.*, 1982). Lysostaphin has been used in combination with other antibiotic agents, such as vancomycin to provide enhanced elimination of staphylococcal infections or biofilms (Climo *et al.*, 1998, Walencka *et al.*, 2005, Walencka *et al.*, 2006). Furthermore recombinant lysostaphin has been used in combination with antimicrobial peptides, such as ranalexin or monoclonal antibodies raised against staphylococcal cell wall components with increased efficiency of infection eradication (Walsh *et al.*, 2004).

The efficacy of lysostaphin applied alone and in combination with other anti-staphylococcal agents has exemplified the biopharmaceutical importance of recombinant lysostaphin production. However the purity and potential immunogenicity of all recombinant biopharmaceuticals must be considered prior to

clinical use in the interests of drug safety. The studies in Table 1.7 indicated that lysostaphin retains biological activity *in vivo* without eliciting immune responses following administration. In addition, the enzyme was thought to be digested by intestinal proteinases, without demonstrating oral toxicity (Williamson *et al.*, 1994). Also Dajcs *et al.*, (2002) did not observe immunogenicity, even following immunization of rabbits with anti-lysostaphin antibodies (Dajcs *et al.*, 2002).

In the majority of studies, immunogenicity has not been notably observed following topical or parenteral administration of lysostaphin to human subjects (Quickel *et al.*, 1971, Climo *et al.*, 1998). A few isolated cases have reported immunogenicity following administration, however due to the emergence of more stringent clinical trial regulations, lysostaphin has not been readily administered to human models, which limits the availability of data concerning the potential immunogenicity of the protein (Daley and Oldham, 1992, Stark *et al.*, 1974). Sensitisation experiments performed in animals indicated that lysostaphin did not elicit an immune response until 18-21 administrations had been performed (Daley and Oldham, 1992). It is therefore possible that individuals who have been previously exposed to lysostaphin may have only become sensitized if an excessive dosing regime was prescribed.

Recombinant lysostaphin may elicit greater immunogenicity due to product impurity or heterogeneity following purification after expression in prokaryotic or eukaryotic hosts. Immunogenicity would be a major concern due to the production of antibodies which could neutralize enzyme activity or increase drug clearance (Walsh *et al.*, 2004).

1.4.2 Chromatographic analysis of recombinant lysostaphin expressed in *E. coli*

Recombinant lysostaphin shows great promise as an anti-staphylococcal agent and therefore high level production of such a therapeutically important protein is essential. The protein has been shown to be expressed at high levels in *E. coli*, however this has been associated with product heterogeneity (Kara *et al.*, 2006). As the quality and homogeneity of recombinant protein preparations must be closely controlled and regulated, it was imperative that the extent and origins of this heterogeneity was investigated.

This research therefore aimed to provide an insight into the heterogeneity of recombinant lysostaphin following cloning and expression in *E. coli* (Kara *et al.*,

2006). Through purification and separation of protein isoforms using LC it was possible to assess the heterogeneity of recombinant lysostaphin, before characterising the activity, stability and structure of protein variants using LC separation and LC-MS analysis. Due to the implications of sequence variation, post-translational processing and modifications upon protein structure function and heterogeneity, it was imperative that structure of recombinant lysostaphin was appropriately characterised. This research therefore had a number of aims.

Aims:

- To clone the gene encoding recombinant lysostaphin using *E. coli* cloning vectors.
- To express recombinant lysostaphin in *E. coli* expression hosts.
- To purify recombinant lysostaphin from *E. coli* using single or multiple chromatographic modes.
- To separate recombinant lysostaphin isoforms using chromatography.
- To evaluate the extent of product heterogeneity following expression in *E. coli* using single or multi-dimensional chromatographic separation.
- To assess the influence of culture conditions upon the heterogeneity of recombinant lysostaphin preparations.
- To characterise the functional and structural properties of recombinant lysostaphin, through activity assays, chromatographic and mass spectrometric analysis.
- To identify post-translational processing events or modifications that may have contributed to the heterogeneity of recombinant lysostaphin.

2 Cloning, Expression and Purification of Recombinant Lysostaphin

2.1 Introduction

In order to investigate the heterogeneity of recombinant lysostaphin, the protein had to be produced and purified prior to chromatographic analysis. The gene encoding lysostaphin was therefore cloned in *E. coli* following identification and amplification of the appropriate gene sequence from within the genomic DNA of *Staphylococcus staphylolyticus*. The amplified gene sequence was firstly cloned into pCR-Blunt, before sub-cloning the insert DNA into pET-vector cloning systems. Appropriate pET-vectors were selected to permit subsequent expression of recombinant lysostaphin with or without additional *N*- or *C*-terminal hexahistidine tags, which facilitate subsequent purification. In addition PelB leader sequences were incorporated into some of the gene constructs to permit translocation of recombinant lysostaphin to periplasm of *E. coli*.

Following cloning, the recombinant lysostaphin gene constructs were expressed in *E. coli* BL21(DE3) to allow subsequent purification and characterisation of the resulting recombinant protein. Although the expression host strain was kept constant, expression conditions such as induction conditions, cultures volumes, media composition, temperature and expression location were varied during the course of research to establish which factors could influence the expression of recombinant lysostaphin. Once expressed, a variety of chromatographic techniques were tested to achieve efficient purification of recombinant lysostaphin so that protein heterogeneity could be investigated. Rapid recovery of target protein was essential to minimise potential proteolysis or modification caused by enzymes or reactive intermediates present within the cell lysate.

Aims:

- To clone the gene encoding recombinant lysostaphin using pCR-Blunt and pET-vector cloning systems.
- To express recombinant lysostaphin in *E. coli* BL21(DE3).
- To efficiently purify recombinant lysostaphin from *E. coli* using single or multiple chromatographic modes.

2.2 Methods

2.2.1 Bacterial strains

Bacterial strain information, storage and culture is described in Appendix 7.1-Appendix 7.7.

2.2.2 Chemicals

All chemicals used in this research and their preparation are outlined in Appendix 7.8 and Appendix 7.9.

2.2.3 Equipment

All key pieces of laboratory equipment and chromatographic columns required at each stage of the research are outlined in Appendix 7.10 and Appendix 7.11.

2.2.4 Buffers and solutions

All buffer and solution compositions are outlined in Appendix 7.12.

2.2.5 Agarose gel electrophoresis

DNA preparations were analysed using analytical agarose gel electrophoresis to assess molecular weight or purity (Appendix 7.13), whilst preparative agarose gel electrophoresis was used to separate and extract DNA (Appendix 7.14).

2.2.6 Polyacrylamide gel electrophoresis (PAGE)

SDS-PAGE was performed under denaturing conditions to assess the purity and molecular weight of proteins following recombinant expression, purification, separation or digestion (Appendix 7.15).

2.2.7 Quantitation and detection of DNA and protein

DNA and protein concentrations were established using UV spectrometry (Appendix 7.23). The presence of protein was determined using Bradford's reagent (Appendix 7.24).

2.3 Cloning of the gene encoding lysostaphin

2.3.1 Introduction

Lysostaphin (EC.3.4.24.75) is an extracellular glycyglycine endopeptidase, produced exclusively by *Staphylococcus simulans* biovar *staphylolyticus* (ATCC 1362, NRRL B-2628). The zinc-containing endopeptidase can lyse staphylococcal cells by specifically cleaving the pentaglycine cross-links in their peptidoglycan cell walls (Firczuk *et al.*, 2005, Fedorov *et al.*, 2003). Lysostaphin was originally isolated from cell-free filtrates of *Staphylococcus staphylolyticus* by Schindler and Schuhardt (1960) and the gene encoding lysostaphin was subsequently identified and sequenced by Recsei *et al.* (1987) (Schindler and Schuhardt, 1964, Trayer and Buckley, 1979, Recsei *et al.*, 1987).

The lysostaphin gene is carried on pACK1, a β -lactamase expressing plasmid which is the largest of the five plasmids of *S. staphylolyticus* (Sharma *et al.*, 2006). The pACK1 plasmid also carries an endopeptidase resistance gene (*epr*), which renders *S. staphylolyticus* resistant to the lytic action of lysostaphin (Chan, 1996). Resistance is acquired by modification of pentaglycine cross-links of peptidoglycan, through the substitution of glycine residues with serine residues. The expression of *epr* is regulated, therefore cell cultures are known to be susceptible during the early exponential phase but resistant during the post-exponential phase. However as *S. staphylolyticus* synthesises lysostaphin as a preproenzyme, there is time during the processing of preprolysostaphin to acquire resistance (DeHart *et al.*, 1995).

The entire coding region of the lysostaphin gene is comprised of 1482 bp that encode preprolysostaphin, which is 493 amino acids (aa) in length. The sequence encodes three distinct domains: a secretory signal peptide (36 aa) at the *N*-terminus; a hydrophilic propeptide (211 aa) from which there are 15 conserved repetitive sequences (13 aa each) and the hydrophobic mature lysostaphin (246 aa) (Thumm and Götze, 1997, Recsei *et al.*, 1987) (Figure 2.1).



Figure 2.1: A schematic representation of the three domains of the uncleaved lysostaphin preproenzyme (adapted from Klein *et al.*, 2006)

At the *N*-terminus of the sequence, the signal peptide region consists of a hydrophilic region (6 aa) and a hydrophobic region (21 aa), which forms a β -pleated sheet (Heinrich *et al.*, 1987). The exact site of signal peptide cleavage is not yet known, however the entire sequence of the gene has been elucidated (Appendix 7.35). Unlike the signal peptide sequence, the repetitive sequences within the hydrophilic propeptide region have a strong tendency to undergo α -helix formation. The repetitive sequences are 13 aa long and whilst the first 14 identical repeats encode for A-E-V-E-T-S-K-A-P-V-E-N-T, the 15th repeat encodes A-E-V-E-T-S-K-A-L-V-Q-N-R (Heinrich *et al.*, 1987). The amino acid sequence and structure of mature lysostaphin is discussed further in Chapter 4 .

During expression in *S. staphylolyticus*, the 42 kDa preprolysostaphin is exported from the bacterial cytoplasm by signal peptide-mediated translocation. During cell wall secretion, the *N*-terminal 36 aa signal peptide is cleaved by a signal peptidase to produce catalytically active prolysostaphin (Fedorov *et al.*, 2003). However mature lysostaphin is around 4.5 fold more active than prolysostaphin, therefore the mature peptide is produced by extracellular cleavage of the propeptide following translocation (Thumm and Götz, 1997). In *S. staphylolyticus*, the conversion of prolysostaphin to lysostaphin is catalysed by a cysteine protease that is entrapped within the cell wall matrix or non-covalently associated with cell wall polymers (Grundling *et al.*, 2006, Bunn *et al.*, 1998). Extracellular cleavage of prolysostaphin yields the mature and catalytically-active 27 kDa protein, lysostaphin (Szweda *et al.*, 2001).

2.3.1.1 Cloning of the lysostaphin gene

Due to the importance of lysostaphin as a therapeutic agent, the lysostaphin gene has been cloned and expressed using a variety of expression hosts. Recombinant lysostaphin preparations are commercially available and have been used extensively for research purposes (Kokai-Kun *et al.*, 2003, Kokai-Kun *et al.*, 2007). The gene encoding lysostaphin has been cloned and the encoded product expressed using both eukaryotic and prokaryotic cloning and expression systems (Klein *et al.*, 2006, Mierau *et al.*, 2005b, Recsei *et al.*, 1987). The gene has primarily been cloned in *E. coli* vectors, as described in

Table 2.1, but has also been cloned using the NICE cloning system in *Lactococcus lactis* (Mierau *et al.*, 2005a, Mierau *et al.*, 2005b).

Table 2.1: Cloning of recombinant lysostaphin in *E. coli*

<i>E. coli</i> Strain	Cloning Vector	Restriction sites	Reference
JM83	pUC19	Not specified	Heinrich <i>et al.</i> , 1987
JM105	pUC8	<i>Mbol</i> <i>Bam</i> HI	Recsei <i>et al.</i> , 1987
HB101	pBR322	<i>Mbol</i> <i>Bam</i> HI	Williamson <i>et al.</i> , 1994
JM83	pET-29b(+)	<i>Nde</i> I <i>Bam</i> HI	Chan, 1996
TOP10F	pTYB12	<i>Bam</i> HI	Szweda <i>et al.</i> , 2001

2.3.1.2 Cloning of the gene encoding lysostaphin in *E. coli*

In order to investigate the homogeneity of recombinant lysostaphin expressed in *E. coli*, the lysostaphin gene was cloned in *E. coli* TOP10 and XL1-Blue, in preparation for expression in *E. coli* BL21(DE3). Prior to cloning, the lysostaphin gene sequence was amplified from the genomic DNA of *S. staphylolyticus* using PCR. PCR primers were synthesised in order to facilitate directional cloning of the insert DNA into pET-vector cloning systems. However, following PCR, the amplified gene sequence was first cloned into the cloning vector, pCR-Blunt.

Following cloning in pCR-Blunt, the cloned lysostaphin gene was then subcloned into pET-22b or pET-28a depending on the requirement for fusion tag sequences. The *N*-terminally His-tagged regions of recombinant proteins can exhibit phosphorylation, gluconoylation and phosphogluconoylation when in expressed in *E. coli* (Du *et al.*, 2005a, Du *et al.*, 2005b, She *et al.*, 2010). Therefore recombinant lysostaphin was cloned in pET-22b and pET-28a allowing expression of the protein without a His-tag sequence, but also expression with an *N*-terminal or a *C*-terminal His-tag sequence. This cloning strategy was designed to allow investigation of the effects of terminal His-tag sequences on recombinant protein heterogeneity, with a view to identification of possible terminal modifications.

Lysostaphin gene constructs were also created to allow expression of the recombinant protein in different cellular locations within *E. coli*. The lysostaphin gene was therefore subcloned into pET-22b and pET-28a allowing cytoplasmic expression

of recombinant lysostaphin or expression within the periplasm, following PelB mediated transfer of the expressed protein to the periplasm. This cloning strategy was developed to ultimately allow assessment of the influence of expression location upon the heterogeneity of recombinant lysostaphin.

Aims:

- To amplify the gene sequence encoding mature lysostaphin using PCR.
- To clone the gene sequence into pCR-Blunt.
- To clone the gene sequence into the appropriate pET vector.

2.3.2 Methods

2.3.2.1 Media

All media compositions are outlined in Appendix 7.25.

2.3.2.2 Enzyme and buffer composition

Enzyme and buffer compositions are outlined in Appendix 7.26.

2.3.2.3 Bacterial strains

E. coli TOP10 and *E. coli* XL1 Blue were cultured for the preparation of chemically and electrocompetent cells for transformation with recombinant plasmids containing the lysostaphin gene. *Staphylococcus staphylolyticus*, biovar of *Staphylococcus simulans* (DSM 20723, NRRL B-2628) was grown for the extraction of genomic DNA for cloning of the lysostaphin gene.

2.3.2.4 Vectors

Cloning of the lysostaphin gene was achieved using the cloning systems described in Table 2.2. Vector maps for all of the plasmids are shown in Appendix 7.29, Appendix 7.30 and Appendix 7.31.

Table 2.2: Cloning systems used during gene cloning

Vector System	Application	Supplier
Zero Blunt Cloning System	Cloning of lysostaphin gene using pCR-Blunt	Invitrogen Ltd, UK
pET Vector Cloning System	Cloning of lysostaphin gene using pET-28a and pET-22b	Merck4Biosciences, UK

2.3.2.5 Kits

Gene cloning procedures were performed using a number of molecular biology kits, as described in Table 2.3. The composition of buffers used in each kit is provided in Appendix 7.32.

Table 2.3: Molecular biology kits used during gene cloning

Kit	Application	Supplier
DNeasy Mini Spin Kit	Extraction of genomic DNA from <i>S. staphylolyticus</i>	Qiagen Ltd, UK
QIAprep Spin MiniPrep Kit	Plasmid DNA extraction	Qiagen Ltd, UK
QIAquick Gel Extraction Kit	Gel extraction of DNA	Qiagen Ltd, UK
Plasmid Maxi Kit	Plasmid DNA extraction	Qiagen Ltd, UK

2.3.2.6 PCR amplification of the lysostaphin gene

In order to clone the lysostaphin gene, *S. staphylolyticus* was cultured (Appendix 7.33) and the genomic DNA of the organism extracted using a DNeasy mini spin kit (Appendix 7.34) to allow PCR amplification of the lysostaphin gene.

2.3.2.7 Primer design and plasmid DNA constructs

Primers were synthesised (MWG Biotech AG, Germany) to allow amplification of the section of the gene that encodes the mature lysostaphin ORF (Gen Bank Accession No. X06121) (Appendix 7.35). Primers were designed to contain restriction sites at their 5' ends. In addition, the primers were designed to enable cloning of the lysostaphin gene with or without fusion tags (*N*-terminal His-tags, *C*-terminal His-tags and PelB leader sequences) (Table 2.4). PCR was performed as described in Appendix 7.36 and Appendix 7.37. The resulting PCR products were firstly cloned in pCR-Blunt vector using the Zero Blunt[®] Cloning system and then subcloned in the pET vector cloning system using pET-22b or pET-28a vectors

Table 2.4: Primer sequences, pET-vectors, fusion tags and expression locations of lysostaphin constructs

Construct	Primer Sequences	Vector	Restriction Sites	Fusion Tags	Expression Location
1	<i>LSNdelFP</i> : 5'-CAT ATG GCT GCA ACA CAT GAA CAT TCA-3' <i>LSXholSRP</i> : 5'-CTC GAG TCA CTT TAT AGT TCC CCA AAG-3'	pET-28a	<i>NdeI</i> <i>XhoI</i>	N-terminal His-tag	Cytoplasmic
2	<i>LSNdelFP</i> : 5'-CAT ATG GCT GCA ACA CAT GAA CAT TCA-3' <i>LSXholSRP</i> : 5'-CTC GAG TCA CTT TAT AGT TCC CCA AAG-3'	pET-22b	<i>NdeI</i> <i>XhoI</i>	None	Cytoplasmic
3	<i>LSNdelFP</i> : 5'-CAT ATG GCT GCA ACA CAT GAA CAT TCA-3' <i>LSXholNSRP</i> : 5'-CTC GAG CTT TAT AGT TCC CCA AAG AAC-3'	pET-22b	<i>NdeI</i> <i>XhoI</i>	C-terminal His-tag	Cytoplasmic
4	<i>LSNcolFP</i> : 5'-CCA TGG CTG CAA CAC ATG AAC ATT CA-3' <i>LSXholNSRP</i> : 5'-CTC GAG CTT TAT AGT TCC CCA AAG AAC-3'	pET-22b	<i>NcoI</i> <i>XhoI</i>	C-terminal His-tag PelB leader sequence	Periplasmic
5	<i>LSNcolFP</i> : 5'-CCA TGG CTG CAA CAC ATG AAC ATT CA-3' <i>LSXholSRP</i> : 5'-CTC GAG TCA CTT TAT AGT TCC CCA AAG-3'	pET-22b	<i>NcoI</i> <i>XhoI</i>	PelB leader sequence	Periplasmic

2.3.2.8 Cloning using the Zero Blunt[®] cloning system

Following PCR, the lysostaphin ORF was cloned into pCR-Blunt through ligation of the PCR product (744bp) with pCR-Blunt vector (3.5 Kb) (Appendix 7.38). *E. coli* TOP10/ XL1-BLUE were grown (Appendix 7.39) for the preparation of electrocompetent cells (Appendix 7.40). The electrocompetent cells were then transformed with the ligated vector DNA by electroporation (Appendix 7.41). Following transformation and overnight incubation, plasmid DNA was extracted from pCR-Blunt clones (Appendix 7.42) and was subjected to restriction digestion to establish whether the extracted DNA contained the appropriate insert DNA fragment (Appendix 7.43).

2.3.2.9 Cloning into pET-vector system

In order to clone the mature lysostaphin domain encoding sequence into pET-28a or pET-22b, plasmid DNA isolated from the pCR-Blunt clones was restriction digested (Appendix 7.43), subjected to preparative gel electrophoresis (Appendix 7.14) and the DNA insert fragment gel extracted using a QIAquick[®] gel extraction kit (Appendix 7.44). *E. coli* transformed with pET-vector DNA were cultured (Appendix 7.45), so that pET vector DNA could be prepared (Appendix 7.46) and restriction digested (Appendix 7.43) prior to ligation with the insert DNA fragment. Recombinant pET vector DNA was then used to transform *E. coli* BL21 (DE3) cells for protein expression as described in Appendix 7.73. Plasmid DNA was extracted from transformed cells and sequenced to ensure that the mature lysostaphin domain encoding sequence was encoded correctly (Appendix 7.42 and Appendix 7.48).

2.3.3 Results

2.3.3.1 Purification of genomic DNA from *S. staphylolyticus*

Genomic DNA was extracted from *S. staphylolyticus* and agarose gel electrophoresis was used to confirm that the genomic DNA had been extracted successfully (Figure 2.2).

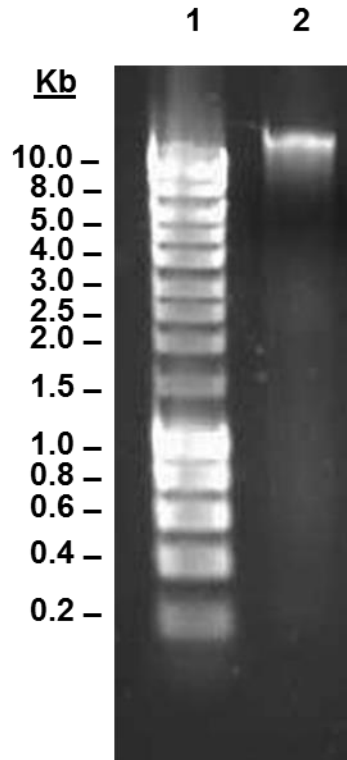


Figure 2.2: 1% (w/v) agarose gel electrophoresis of purified genomic DNA from *S. staphylolyticus*. Lane 1: Bioline 10 Kb Hyperladder size standard; Lane 2: Purified genomic DNA

2.3.3.2 PCR amplification of mature lysostaphin domain encoding sequence from *S. staphylolyticus* genomic DNA

The mature lysostaphin gene sequence was amplified from *S. staphylolyticus* genomic DNA using PCR. Primers were designed to allow amplification of the mature lysostaphin domain encoding sequence to permit cloning of the sequence and expression of mature lysostaphin without or with fusion tags. Following PCR, the PCR products were analysed by agarose gel electrophoresis to ensure that the amplified products were the correct size. As shown in Figure 2.3A, PCR products for constructs 1, 2, 4 and 5 amplified successfully on the first attempt, however amplification of the PCR product for construct 3 was unsuccessful initially. Repetition of PCR using the same conditions was successful and the PCR product for construct was amplified correctly (Figure 2.3B).

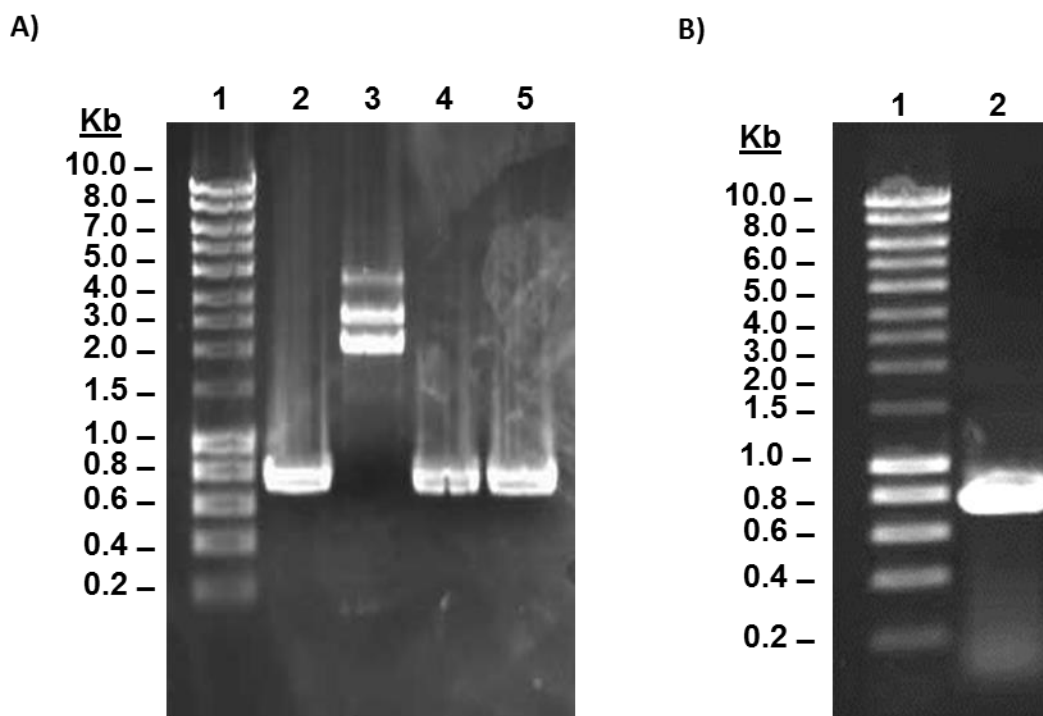


Figure 2.3: PCR amplification of the section of lysostaphin gene encoding mature lysostaphin from *S. staphylolyticus* genomic DNA. A) Lane 1: Bioline 10 Kb Hyperladder size standard; Lane 2: PCR product for construct 1 and 2, Lane 3: Unsuccessful amplification of PCR product for construct 3; Lane 4: PCR product for construct 4; Lane 5: PCR product for construct 5. B) Lane 1: Bioline 10 Kb Hyperladder size standard; Lane 2: PCR product for construct 3

2.3.3.3 Cloning of the mature lysostaphin domain encoding sequence using the Zero Blunt® cloning system

Following PCR, the amplified mature lysostaphin domain encoding sequences were ligated into the 3.5 Kb pCR-Blunt vector and transformed into *E. coli* TOP10. Plasmid DNA was extracted from overnight cultures of *E. coli* TOP10 inoculated using transformed colonies. The extracted plasmid DNA was restriction digested with *Nde*I and *Xho*I or *Nco*I and *Xho*I depending on which PCR product had been ligated into the pCR-Blunt vector (Figure 2.4).

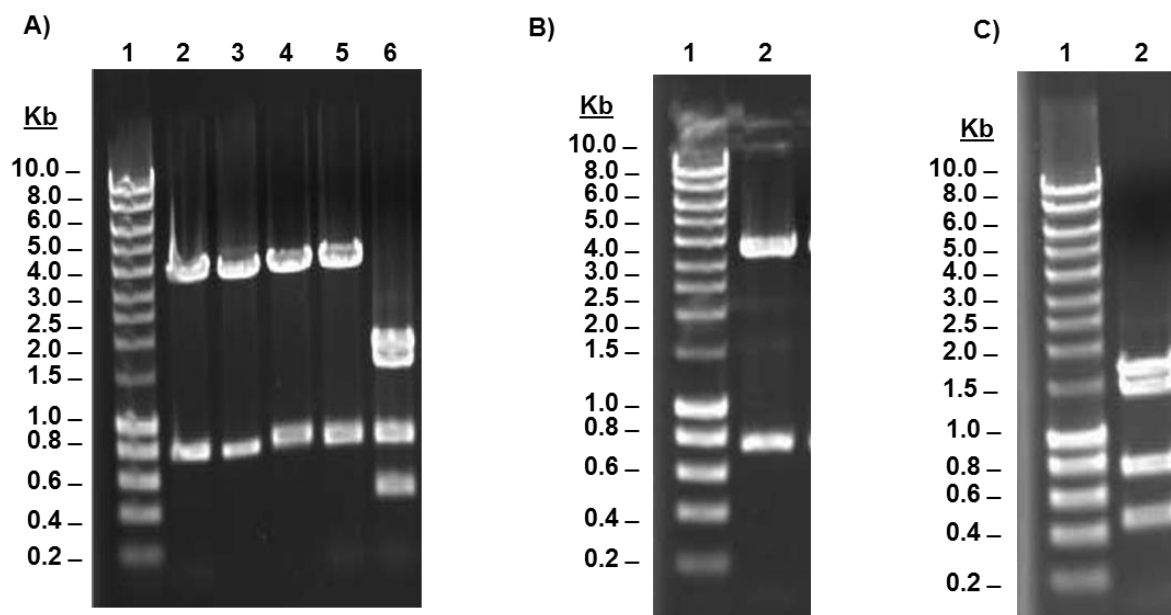


Figure 2.4: Restriction digestion of pCR-Blunt recombinants. A) Lane 1: Bioline 10 Kb Hyperladder size standard; Lanes 2-5: pCR-Blunt construct 1 and 2 (*NdeI* and *XhoI* digest); Lane 6: pCR-Blunt construct 4 (*NcoI* and *XhoI* digest). B) Lane 1: Bioline 10 Kb Hyperladder size standard; Lane 2: pCR-Blunt construct 3 (*NdeI* and *XhoI* digest). C) Lane 1: Bioline 10 Kb Hyperladder size standard; Lane 2: pCR-Blunt construct 5 (*NcoI* and *XhoI* digest).

As shown in Figure 2.4, each PCR product was cloned successfully in pCR-Blunt vector. Restriction digestion using *NdeI* and *XhoI* released the insert DNA from the 3.5 Kb pCR-Blunt vector. Due to internal *NcoI* restriction sites in the pCR-Blunt vector, digestion with *NcoI* and *XhoI* yielded the insert DNA fragment and two pCR-Blunt vector fragments of 500 bp and 1500 bp. Following restriction digestion and gel extraction, the insert DNA fragment from each pCR-Blunt construct was ligated into appropriately restriction digested pET vector DNA.

2.3.3.4 Cloning of the lysostaphin gene using pET vector cloning system

Following ligation, the recombinant pET vector DNA was transformed into *E. coli* TOP10 or *E. coli* XL-1 Blue. Plasmid DNA was extracted from overnight cultures, which had been inoculated with transformed *E. coli* colonies. The plasmid DNA was restriction digested with *NdeI* and *XhoI* or *NcoI* and *XhoI* depending on which insert DNA fragment had been subcloned into the pET vector (Figure 2.5).

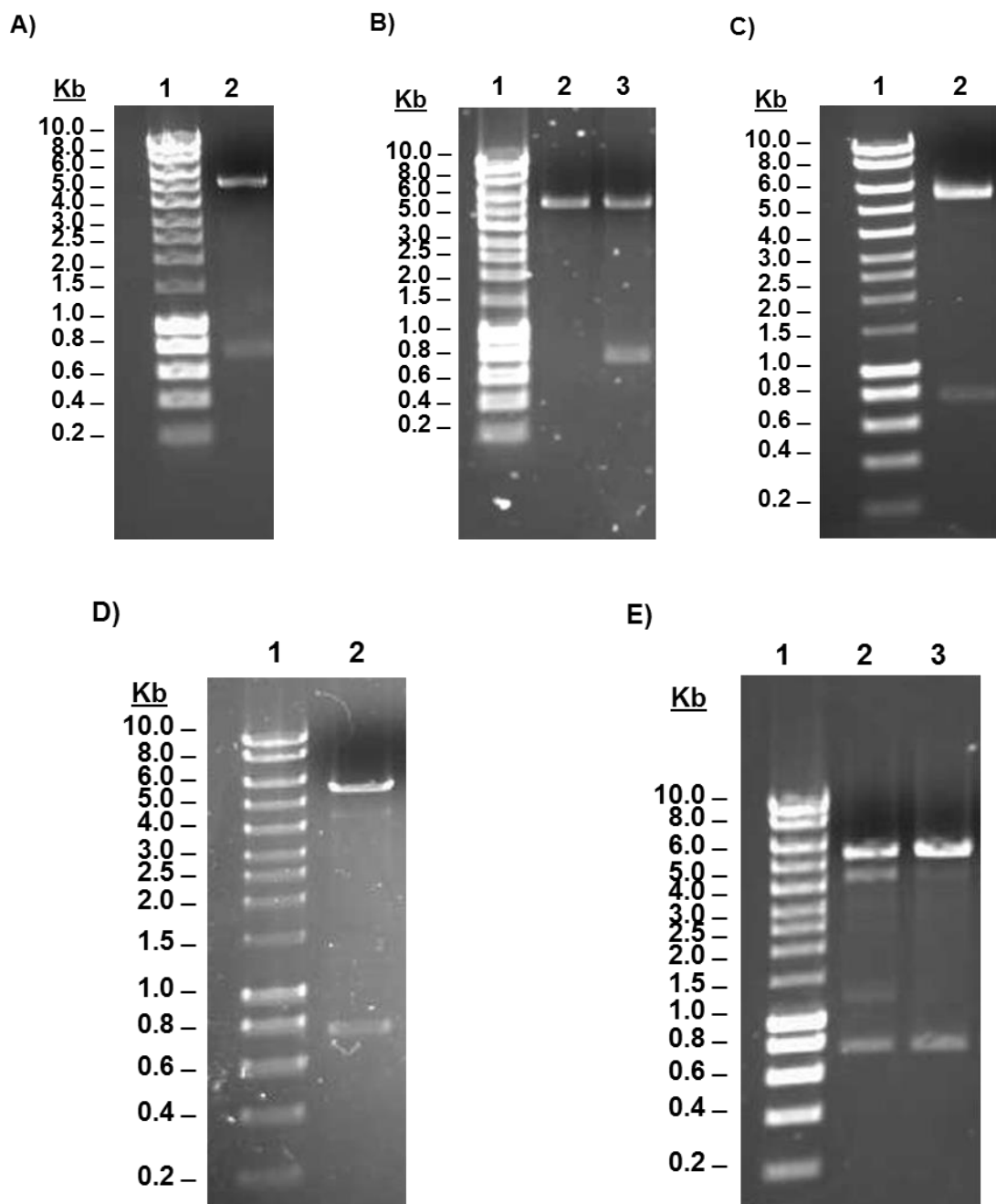


Figure 2.5: Restriction digestion of pET vector recombinants. A) Lane 1: Bioline 10 Kb Hyperladder size standard; Lane 2: pET construct 1 in pET-28a (*NdeI* and *XhoI* digest). B) Lane 1: Bioline 10 Kb Hyperladder size standard; Lane 2: pET-22b without insert DNA (*NdeI* and *XhoI* digest), Lane 3: pET construct 2 in pET-22b (*NdeI* and *XhoI* digest). C) Lane 1: Bioline 10 Kb Hyperladder size standard; Lane 2: pET construct 3 in pET-22b (*NdeI* and *XhoI* digest). D) Lane 1: Bioline 10 Kb Hyperladder size standard; Lane 2: pET construct 4 in pET-22b (*NcoI* and *XhoI* digest). E) Lane 1: Bioline 10 Kb Hyperladder I size standard; Lane 2: pET construct 5 in pET-22b (*NcoI* and *XhoI* digest); Lane 3: pET construct 5 in pET-22b (*NcoI* and *XhoI* digest).

As shown in Figure 2.5 (A-E), each insert DNA fragment was successfully subcloned in pET-22b or pET-28a. Restriction digestion using *NdeI* and *XhoI* or *NcoI* and *XhoI* released the insert DNA fragment from the pET-22b vector (5493 bp) or the pET-28a vector (5369 bp),

providing confirmation of gene cloning. pET constructs 1-3 were then sequenced to establish the accuracy of the cloned lysostaphin gene sequence.

2.3.3.5 Sequencing of plasmid DNA

pET constructs 1-3 were sequenced to ensure that the mature lysostaphin gene was accurately encoded. The quality of the sequenced data was generally very high and chromatographic representation of the sequence data demonstrated largely non-overlapping and evenly-spaced peaks (Appendix 7.49, Appendix 7.50 and Appendix 7.51). To establish if the acquired sequence data matched with the expected nucleotide sequences (Appendix 7.52, Appendix 7.53, Appendix 7.54, Appendix 7.55, Appendix 7.56 and Appendix 7.57) ClustalW alignments were performed to identify any nucleotide mis-matches.

2.3.3.6 ClustalW alignment of the known mature lysostaphin domain encoding sequence (with an *N*-terminal His-tag encoding sequence added) and the acquired DNA sequence from pET construct 1

The known mature lysostaphin domain encoding sequence (with *N*-terminal His-tag encoding sequence added) is presented in Appendix 7.52. The sequence acquired from construct 1 is presented in Appendix 7.53. The known and acquired sequences were then compared by ClustalW analysis and the results are presented in Figure 2.6.

```

Expected      ATGGGCAGCAGCCATCATCATCATCACAGCAGCGGCCTGGTGCCGCGCGGCAGCCAT 60
N-terminally ATGGGCAGCAGCCACCCCTCT--AAAAGCACAGCAGCGGCCTGGTGCCGCGCGGCAGCCAT 58
***** * _ ** : * : _ * *****

Expected      ATGGCTGCAACACATGAACATTCAGCACAAATGGTTGAATAATTACAAAAAGGATATGGT 120
N-terminally ATGGCTGCAACACATGAACATTCAGCACAAATGGTTGAATAATTACAAAAAGGATATGGT 118
*****

Expected      TACGGTCCTTATCCATTAGGTATAAATGGCGGTATCCACTACGGAGTTGATTTTTTTATG 180
N-terminally TACGGTCCTTATCCATTAGGTATAAATGGCGGTATGCACTACGGAGTTGATTTTTTTATG 178
*****

Expected      AATATTGGAACACCAGTAAAAGCTATTTCAAGCGGAAAAATAGTTGAAGCTGGTTGGAGT 240
N-terminally AATATTGGAACACCAGTAAAAGCTATTTCAAGCGGAAAAATAGTTGAAGCTGGTTGGAGT 238
*****

Expected      AATTACGGAGGAGGTAATCAAATAGGTCCTTATTGAAAATGATGGAGTGCATAGACAATGG 300
N-terminally AATTACGGAGGAGGTAATCAAATAGGTCCTTATTGAAAATGATGGAGTGCATAGACAATGG 298
*****

Expected      TATATGCATCTAAGTAAATATAATGTTAAAAGTAGGAGATTATGTCAAAGCTGGTCAAATA 360
N-terminally TATATGCATCTAAGTAAATATAATGTTAAAAGTAGGAGATTATGTCAAAGCTGGTCAAATA 358
*****

Expected      ATCGGTTGGTCTGGAAGCACTGGTTATTCTACAGCACCCACATTTACACTTCCAAGAATG 420
N-terminally ATCGGTTGGTCTGGAAGCACTGGTTATTCTACAGCACCCACATTTACACTTCCAAGAATG 418
*****

Expected      GTTAATTCATTTTCAAATTCAACTGCCCAAGATCCAATGCCTTTCTTAAAGAGCGCAGGA 480
N-terminally GTTAATTCATTTTCAAATTCAACTGCCCAAGATCCAATGCCTTTCTTAAAGAGCGCAGGA 478
*****

Expected      TATGGAAAAGCAGGTGGTACAGTAACTCCAACGCCAATACAGGTTGAAAACAACAAA 540
N-terminally TATGGAAAAGCAGGTGGTACAGTAACTCCAACGCCAATACAGGTTGAAAACAACAAA 538
*****

Expected      TATGGCACACTATATAAATCAGAGTCAGCTAGCTTACACCTAATACAGATATAATAACA 600
N-terminally TATGGCACACTATATAAATCAGAGTCAGCTAGCTTACACCTAATACAGATATAATAACA 598
*****

Expected      AGAACGACTGGTCCATTTAGAAGCATGCCGCAGTCAGGAGTCTTAAAAGCAGGTCAAACA 660
N-terminally AGAACGACTGGTCCATTTAGAAGCATGCCGCAGTCAGGAGTCTTAAAAGCAGGTCAAACA 658
*****

Expected      ATTCATTATGATGAAGTGATGAAACAAGACGGTCATGTTTGGGTAGGTTATACAGGTAAC 720
N-terminally ATTCATTATGATGAAGTGATGAAACAAGACGGTCATGTTTGGGTAGGTTATACAGGTAAC 718
*****

Expected      AGTGGCCAACGTATTTACTTGCCGTGAAGAACATGGAATAAATCTACTAATACTTTAGGT 780
N-terminally AGTGGCCAACGTATTTACTTGCCGTGAAGAACATGGAATAAATCTACTAATACTTTAGGT 778
*****

Expected      GTTCTTTGGGGAACATAAAAGTGA 804
N-terminally GTTCTTTGGGGAACATAAAAGTGA 802
*****

```

Figure 2.6: ClustalW alignment of the known mature lysostaphin domain encoding sequence (with N-terminal His-tag encoding sequence added) and the acquired DNA sequence from pET construct 1

As shown in Figure 2.6, a number of mis-matched nucleotides were found within the initial part of the sequence data. However further examination of the sequence chromatographic data, as shown in Figure 2.7 indicates that the mis-matched bases occurred within a region of the sequence where the chromatographic trace was particularly noisy. The correct

nucleotide bases could be identified within the noisy region, suggesting that the mis-matches bases were falsely identified during sequencing.

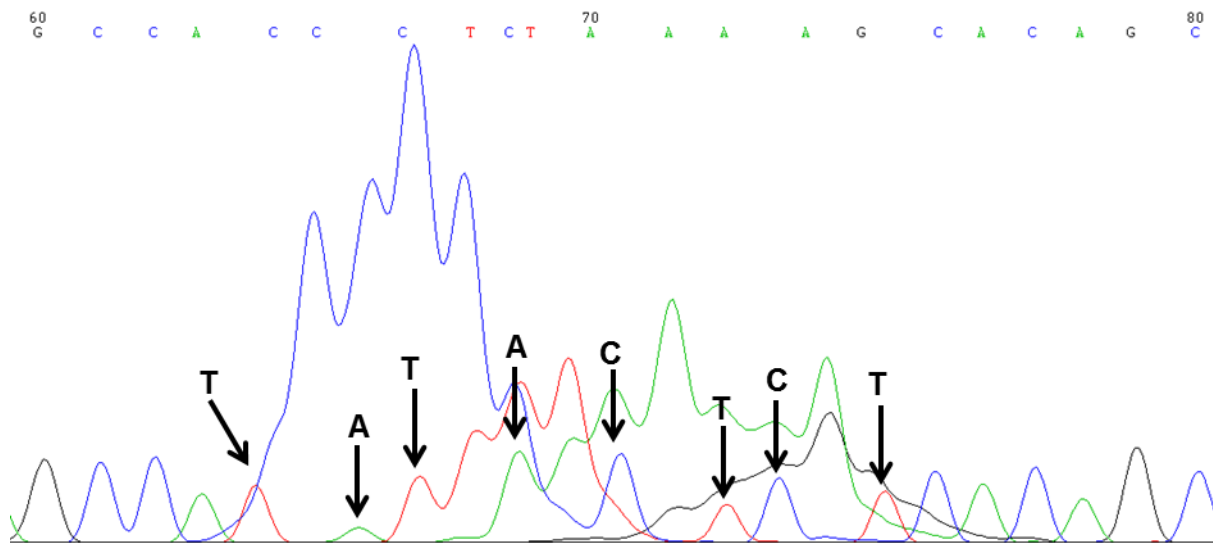


Figure 2.7: Mis-indentification of bases during sequencing of pET construct 1. Mis-identified bases are indicated.

Apart from mis-matches in the initial region of sequence data, ClustalW alignment also identified two other mis-matched nucleotides at positions 203 and 563. Inspection of the chromatographic sequence data revealed the genuine presence of guanine rather than cytosine at both mis-matched positions (Figure 2.8).

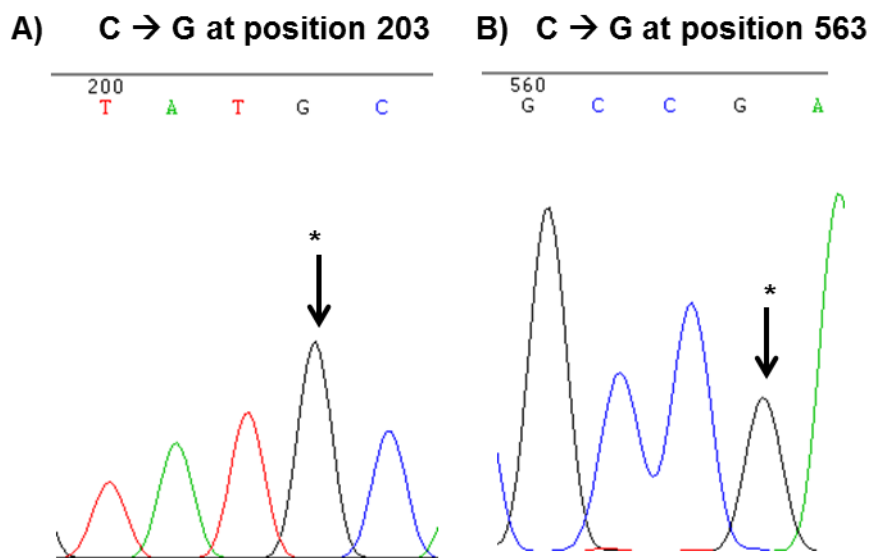


Figure 2.8: Sequence data supporting base differences supported by ClustalW. The positions of substituted bases are marked by an asterisk.

ClustalW analysis of sequence data obtained following sequencing of pET constructs 2 and 3 (Appendix 7.58 and Appendix 7.61 respectively) also revealed a number of mis-matched bases within the initial part of the sequence data. Further examination of the chromatographic data acquired during sequencing of pET constructs 2 and 3 also indicated that the mis-matched bases occurred within a region of the sequence where the chromatographic trace was particularly noisy (Appendix 7.59 and Appendix 7.62). The correct nucleotide bases could therefore be identified within the noisy region suggesting that the mis-matched bases were falsely identified during sequencing. In addition to mis-matches in the initial region of sequence data, ClustalW alignment also identified two other mis-matched nucleotides at positions 147 and 507 for pET construct 2 (Appendix 7.60 A and B) and positions 148 and 508 for pET construct 3 (Appendix 7.63 A and B). In both cases, examination of the chromatographic sequence data revealed the genuine presence of guanine rather than cytosine at each of the mis-matched positions.

2.3.3.7 Identification of mis-matched nucleotides within the mature lysostaphin domain encoding sequence

Sequencing of plasmid DNA encoding the mature lysostaphin domain (pET constructs 1-3) revealed the presence of two apparent nucleotide mis-matches. Both changes involved the genuine identification of guanine rather than expected cytosine nucleotides. These mis-matched bases could be identified as occurring at cytosines at position 96 and 456 within the sequence of the mature lysostaphin domain encoding sequence (Figure 2.9). The corrected sequence of the mature lysostaphin domain encoding sequence is presented in Appendix 7.65.

ATGGCTGCAACACATGAACATTCAGCACAAATGGTTGAATAATTACAAAAAGGATATGGTTACGGTCC
 TTATCCATTAGGTATAAATGGCGGTATCCACTACGGAGTTGATTTTTTATGAATATTGGAACACCAGTA
 AAAGCTATTTCAAGCGGAAAAATAGTTGAAGCTGGTTGGAGTAATTACGGAGGAGGTAATCAAATAG
 GTCTTATTGAAAATGATGGAGTGCATAGACAATGGTATATGCATCTAAGTAAATATAATGTTAAAGTAG
 GAGATTATGTCAAAGCTGGTCAAATAATCGTTGGTCTGGAAGCACTGGTTATTCTACAGCACCAT
 TTACTTCCAAAGAATGGTTAATTCATTTTCAAATCAACTGCCCAAGATCCAATGCCTTTCTTAAAG
 AGCGCAGGATATGAAAAGCAGGTGGTACAGTAACTCCAACGCCCAATACAGGTTGGAAAACAAAC
 AAATATGGCACACTATAAATCAGAGTCAGCTAGCTTACACCTAATACAGATATAATAACAAGAACG
 ACTGGTCCATTTAGAAGCATGCCGAGTCAGGAGTCTAAAAGCAGGTCAAACAATTCATTATGATG
 AAGTGATGAAACAAGACGGTCATGTTTGGGTAGTTATACAGGTAACAGTGGCCAACGTATTTACTT
 GCCTGTAAGAACATGGAATAAATCTACTAATACTTTAGGTGTTCTTTGGGGAAGTATAAAGTGA

Figure 2.9: DNA sequence encoding the mature lysostaphin domain. Cytosine bases which appear to have been substituted in plasmid DNA sequences are indicated (position 96 and 456).

To assess how these nucleotide mis-matches influenced the resulting amino acid sequence of the mature lysostaphin domain, the expected and sequenced DNA sequences were translated *in silico* to derive the anticipated amino acid sequences (Appendix 7.67) and compared using ClustalW analysis (Figure 2.10). Incorporation of guanine rather than cytosine at position 456 did not alter the translation of proline₁₅₂, whilst incorporation of guanine rather than cytosine at position 96 resulted in the translation of methionine₃₂ rather than isoleucine₃₂.



Figure 2.10: ClustalW alignment of the expected amino acid sequences of the mature lysostaphin domain obtained following incorporation of guanines rather than cytosines at position 96 and 456. Exchange of cytosine at position 456 did not alter the translation of proline₁₅₂, whilst exchange of cytosine at position 96 resulted in the translation of methionine₃₂ rather than isoleucine₃₂.

2.3.4 Discussion

Using a combination of PCR and gene cloning techniques, the mature lysostaphin domain encoding sequence was successfully amplified and cloned in *E. coli*. DNA sequencing was used to provide more accurate confirmation that the exact nucleotide sequence had been cloned. However a number of nucleotide mis-matches were observed following sequencing of pET constructs 1-3, which were attributable to some false and true nucleotide differences.

Processed sequencing data is typically represented by chromatographic traces consisting of evenly spaced, non-overlapping peaks that correspond to labelled fragments that terminate at a specific nucleotide in the sequence (Ewing *et al.*, 1998). However the chromatographic traces may deviate from this pattern in some regions of the sequence. For instance, the chromatographic trace commonly becomes noisy within the first 50-70 bases of a sequence, resulting in mis-identification of nucleotides. Noisy traces and unevenly spaced peaks tend to occur as a consequence of the detection of unreacted dye-primer or dye-terminator molecules and the anomalous migration of very short DNA fragments (Ewing *et al.*, 1998). Therefore following examination of sequencing chromatograms, it was possible to establish that nucleotide mis-matches occurring between the first 60 and 80 bases of the sequence could be attributable to chromatographic noise.

Sequencing data obtained from the subsequent 400-500 bases is typically of high quality, with an error rate of around 4% (Lipshutz *et al.*, 1994, Kelley *et al.*, 2010). The quality of sequencing data acquired after the first 80 nucleotides was high, with a chromatographic distribution of even, non-overlapping peaks. However the obtained sequence data also demonstrated two incidences of base mis-identification, whereby nucleotide positions 96 and 456 were composed of guanine rather than cytosine bases. The credibility of these mis-matches was augmented by their presence in all three sets of sequencing data. These nucleotide mis-matches could be explained by a number of factors including mis-amplification of the gene sequence during PCR or simply inaccurate gene sequence information.

PCR is known to occasionally introduce mutations into the amplified DNA sequence through mis-incorporation of nucleotides by the polymerase (Wendland, 2003). In this work, PCR amplifications were performed using KOD Hot Start Polymerase, which offers efficient and high-fidelity amplification of DNA, due to the possession of 3'-5' exonuclease-dependent proofreading activity. It was therefore less likely that the apparent base changes observed during sequencing arose due to errors during PCR amplification. Furthermore it is unlikely

that DNA extension errors could account for the observed errors which occurred at the exactly the same nucleotides, despite the DNA being generated in separate PCR reactions.

Primers were designed to allow amplification of the DNA sequence encoding the mature lysostaphin sequence within the preprolysostaphin gene. The preprolysostaphin gene sequence (X06121) (Appendix 7.35) was acquired from the nucleotide database maintained by the National Centre for Biotechnology Information (NCBI) and was submitted by Heinrich *et al* (1987) after initial identification of the lysostaphin gene sequence. The accuracy of the sequence is therefore dependent on database maintenance by NCBI and the accuracy of DNA sequencing performed by Heinrich *et al* (Heinrich *et al.*, 1987). Heinrich *et al* performed dideoxy-DNA sequence analysis as described by Sanger *et al*, 1977 which was reported to achieve reasonably accurate determination of sequences ranging between around 15 and 200 nucleotides (Sanger *et al.*, 1977, Gargis *et al.*, 2010). Given the “reasonable accuracy” of DNA sequence analysis used to determine the sequence of lysostaphin, it seemed probable that the determined nucleotide sequence may not have been entirely accurate.

This theory is supported by the work of Gargis *et al* (2010), who sequenced the pACK1 plasmid of *S. staphylolyticus*, but did not acknowledge nucleotide mis-matches within the lysostaphin gene sequence (Gargis *et al.*, 2010). As the pACK1 plasmid contains the gene for lysostaphin, the sequence of pACK1 was compared to the sequence of the mature lysostaphin by ClustalW analysis. ClustalW analysis revealed that the lysostaphin-encoding region of the pACK1 plasmid contained guanine rather than cytosine at nucleotide positions 96 and 456 (Appendix 7.64). Therefore the sequence data acquired in this work and the sequence of pACK1 clearly demonstrate that cytosine bases at 96 and 456 of lysostaphin were incorrectly determined during sequence analysis by Heinrich *et al* (1987). Changes in the expected nucleotide sequence consequently influenced the resulting amino acid sequence following expression of the recombinant protein. Whilst incorporation of guanine rather than cytosine at position 456 would not alter translation of proline₁₅₂, incorporation of guanine rather than cytosine at position 96 would result in the translation of methionine₃₂ rather than isoleucine₃₂. Methionine has a mass of 149 Da which is greater than the mass of isoleucine (131 Da), therefore this amino acid difference will have slightly increased the predicted mass of recombinant lysostaphin following expression.

Although this single amino acid difference was not likely to have interfered with the activity of recombinant lysostaphin, it would have interfered with characterisation of the primary structure of lysostaphin. With this knowledge, the pET constructs encoding the mature lysostaphin domain were expressed in *E. coli* so that the structure and function of

recombinant lysostaphin could be characterised to ensure that the cloned gene sequence encoded the desired product.

2.4 Expression of recombinant lysostaphin in *E. coli*

2.4.1 Introduction

As described in Section 2.3.1, the lysostaphin gene encodes a proenzyme, which is processed by *S. staphylolyticus* to produce a mature, monomeric glycyglycine endopeptidase. The native mature lysostaphin is composed of 246 amino acids and has a molecular weight of around 25 kDa (Recsei *et al.*, 1987). The endopeptidase achieves optimal staphylolytic activity at pH 7.5 and is a basic protein with an isoelectric point (pI) of 9.5 (Heinrich *et al.*, 1987). The mature lysostaphin domain expressed in *E. coli* will now be referred to as recombinant lysostaphin in this thesis. Recombinant lysostaphin exhibits the same activity as the native protein.

Recombinant lysostaphin has been produced using eukaryotic expression hosts, such as mammalian cells and transgenic animals (Klein *et al.*, 2006, Williamson *et al.*, 1994, Wall *et al.*, 2005, Kerr *et al.*, 2001). Recombinant lysostaphin is more frequently produced using prokaryotic expression hosts, including *E. coli*, *L. lactis*, *Bacillus subtilis* and *Lactobacillus casei* (Gaier *et al.*, 1992, Mierau *et al.*, 2005a, Mierau *et al.*, 2005b, Mitra *et al.*, 2003). Higher amounts of recombinant lysostaphin can be yielded from *E. coli*, therefore *E. coli* is frequently used to express recombinant lysostaphin for research and commercial purposes, as demonstrated in Table 2.5 (Kokai-Kun *et al.*, 2007, Oddone *et al.*, 2007).

Table 2.5: Expression conditions for the production of recombinant lysostaphin in *E. coli*

Expression Strain	Expression System	Vector	Inducer	Expression Media	Fusion Proteins	Reference
JM105	pUC	pUC8	None	L	Not specified	Recsei <i>et al.</i> , 1987
JM83	pET	pET-29b(+)	IPTG	LB	Not specified	Chan, 1996
ER2566	IMPACT-CN	pTYB12	IPTG	LB	Chitin-bound intein tag	Szweda <i>et al.</i> , 2001
BL21(DE3)	pET	pET-23b(+)	IPTG	LB	C-terminal His-tag	Szweda <i>et al.</i> , 2005
BL21(DE3)	pBAD	pBAD/Thio-TOPO	IPTG	LB	N-terminal His-tag Thioredoxin tag	Szweda <i>et al.</i> , 2005
BL21(DE3)	pET	pET-15b	IPTG	LB	N-terminal His-tag	Sharma <i>et al.</i> , 2006

As shown in Table 2.5, recombinant lysostaphin has been expressed in a number of expression strains and vectors, with incorporation of various fusion tags. In the majority of cases, *E. coli* was propagated in LB and protein expression was induced through the addition of IPTG. Recombinant lysostaphin was expressed and harvested from the cytoplasm of *E. coli*, although Chan, 1996 reported that lysostaphin activity could also be detected in the periplasmic and extracellular fractions of recombinant *E. coli* (Chan, 1996).

2.4.1.1 Expression of recombinant lysostaphin in *E. coli*

Following cloning, the recombinant lysostaphin gene constructs were expressed in *E. coli* to permit subsequent purification and characterisation of the resulting recombinant protein. The recombinant plasmid DNA was transformed into *E. coli* BL21(DE3) to see if recombinant lysostaphin could be successfully expressed. The recombinant lysostaphin gene constructs were engineered to permit expression in the cytoplasm or periplasm. As lysostaphin displays activity against staphylococcal strains only, expression of recombinant lysostaphin in *E. coli* was unlikely to result in cell toxicity or death of host cells. As expression of recombinant lysostaphin has previously been achieved in *E. coli* BL21(DE3) using pET vectors, it was expected that the lysostaphin gene constructs would express successfully in this work (Szweda *et al.*, 2005, Sharma *et al.*, 2006).

Once expression had been established, expression experiments were performed to establish which factors could influence expression of recombinant lysostaphin. Expression variables such as different expression media, induction conditions and culture volumes were assessed. Recombinant protein expression was performed using rich and minimal media in shake-flasks. Depending on the amount of recombinant lysostaphin required for protein analysis, culture volumes varied between 50 ml and 1 L. To achieve higher amounts of recombinant lysostaphin, cell lysates were pooled from multiple batch cultures and expression levels upon scale up were assessed. Sodium dodecyl sulphate polyacrylamide gel electrophoresis (SDS-PAGE) analysis was used to provide an initial assessment of the molecular weight and solubility of recombinant lysostaphin.

Aims:

The initial aim of this work was:

- To establish whether the recombinant lysostaphin gene constructs could be successfully expressed within the cytoplasm or periplasm of *E. coli* using SDS-PAGE analysis.

If recombinant lysostaphin was expressed correctly then further experiments could be performed:

- To assess the solubility of expressed recombinant lysostaphin using SDS-PAGE and solubilising buffer analysis.
- To evaluate expression in minimal and complex media.
- To assess expression levels upon scale-up of cell culture.

2.4.2 Methods

2.4.2.1 Media

All media compositions are outlined in Appendix 7.68.

2.4.2.2 Chemicals

All chemical compositions are outlined in Appendix 7.69.

2.4.2.3 Buffers

All buffer compositions are outlined in Appendix 7.70

2.4.2.4 Bacterial strains

Recombinant protein expression was performed following transformation of *E. coli* BL21(DE3).

2.4.2.5 Media supplementation

All cultures were supplemented with an antibiotic, according to the antibiotic selectivity of the pET vector used during recombinant protein expression. During IPTG-based induction of protein expression, the lactose analogue, IPTG was added to the culture to induce protein expression. Antibiotics and IPTG were added to cultures at the concentrations reported in Table 2.6. The media supplements were prepared by dissolving the required chemical in sterile 18.2 MΩ/cm H₂O, before storing at 4°C for up to one week.

Table 2.6: Antibiotic and chemical supplements used during the expression of recombinant lysostaphin

Chemical	Media	Working Concentration (µg/ml)	Stock Concentration (mg/ml)	Dilution
Kanamycin	LB	50	10	1/200
Kanamycin	AIM	100	10	1/100
Ampicillin	LB/AIM	100	10	1/100
IPTG	LB/AIM/TB/MM	240	24	1/100

2.4.2.6 Bioinformatic prediction of expected molecular weight

To establish the predicted amino acid sequence following translation from each recombinant lysostaphin gene construct, nucleotide sequences were submitted to the Translate tool (Expasy Proteomics Server, Swiss Institute of Bioinformatics), available at <http://expasy.org/tools/dna.html>. The submitted nucleotide sequences were based on the corrected lysostaphin gene sequence as determined by sequencing data, as described in Section 2.3.3.7. The predicted amino acid sequence was then submitted to the ProtParam tool (Expasy Proteomics Server, Swiss Institute of Bioinformatics), available at the <http://expasy.org/tools/protparam.html>. The theoretical molecular weight and other physiochemical properties of each recombinant lysostaphin construct were determined using the results of ProtParam analysis. Theoretical masses were calculated based on the assumption that the zinc binding domain was not occupied.

2.4.2.7 Expression from recombinant lysostaphin gene constructs

After cloning of the mature lysostaphin gene sequence, extracted recombinant pET vector DNA was transformed into chemically competent *E. coli* BL21(DE3) to permit protein expression. Chemically competent cells were prepared (Appendix 7.72) and transformed (Appendix 7.73). Transformed *E. coli* were then inoculated into media which was carefully prepared prior to recombinant protein expression in shake flask cultures (Appendix 7.74). Recombinant protein expression was achieved following autoinduction (Appendix 7.75) or IPTG induction (Appendix 7.76) and the expressed protein was extracted following cytoplasmic (Appendix 7.77) or periplasmic protein expression (Appendix 7.78).

2.4.3 Results

2.4.3.1 Expression of recombinant lysostaphin gene constructs in *E. coli*

Following cloning in Chapter 1, the recombinant plasmid DNA was transformed into *E. coli* BL21(DE3) and a number of expression experiments were performed to assess how efficiently the recombinant lysostaphin gene constructs were expressed during culture and under a variety of expression conditions. Initial experiments focused on whether induction of protein expression resulted in the successful and soluble expression of recombinant lysostaphin in the cytoplasm or following signal peptide-mediated translocation to the periplasmic space. Bioinformatics analysis was performed to establish the theoretical molecular weight of each of the recombinant lysostaphin gene constructs following expression (Table 2.7). The expected nucleotide and amino acid sequences and ProtParam analysis results are presented in Appendix 7.80-Appendix 7.94.

Unfortunately ProtParam could only provide the theoretical masses of the apoprotein form of recombinant lysostaphin, which does not have a bound zinc molecule. At this stage of analysis, it was unclear whether recombinant lysostaphin was expressed in an apoprotein or holoprotein form or how the addition of zinc would influence the mass of recombinant lysostaphin. Therefore theoretical apoprotein masses were used to assess the masses of expressed proteins during SDS-PAGE analysis, until further characterisation of recombinant lysostaphin could be performed and theoretical metalloprotein masses obtained (Chapter 4).

Table 2.7: Theoretical molecular weight and number of amino acids encoding recombinant lysostaphin gene constructs.

Construct	Fusion Tags	Number of Amino Acids	Apoprotein Mass (kDa)
1	N-terminal His-tag	267	29337.8
2	None	247	27075.4
3	C-terminal His-tag	255	28140.5
4	C-terminal His-tag PelB leader sequence	255	28140.5
5	PelB leader sequence	247	27075.4

2.4.3.2 Cytoplasmic expression of *N*-terminally His-tagged recombinant lysostaphin (construct 1)

Cytoplasmic expression of *N*-terminally His-tagged recombinant lysostaphin was induced in *E. coli* BL21(DE3) and the cell lysate containing the resulting recombinant protein was harvested and analysed by PAGE. The cell lysate was found to contain a hyper-expressed protein with a molecular weight of around 29 kDa that was indicative of the presence of *N*-terminally His-tagged recombinant lysostaphin, which has a theoretical molecular weight of 29337.8 kDa (Figure 2.11).

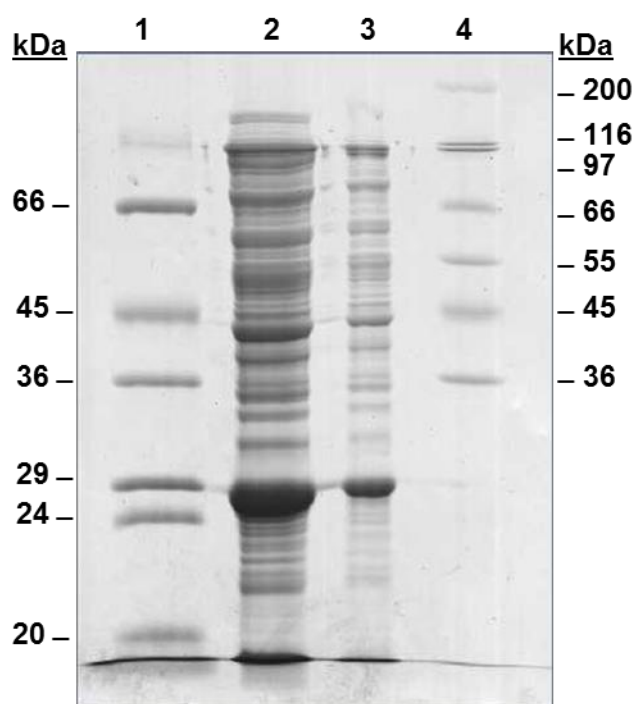


Figure 2.11: Cytoplasmic expression of *N*-terminally His-tagged recombinant lysostaphin (construct 1) in *E. coli* BL21(DE3) cultured in AIM. Cell-free extract (CFE) was analysed by 12% (v/v) SDS-PAGE. Lane 1: Sigma low molecular weight markers; Lane 2: CFE (1:10); Lane 3: CFE (1:100); Lane 4: Sigma high molecular weight markers.

PAGE analysis revealed that *N*-terminally His-tagged recombinant lysostaphin could be hyper-expressed within the cytoplasm of *E. coli* and therefore this form of recombinant lysostaphin was expressed many times to produce recombinant lysostaphin for subsequent analysis and characterisation. Following expression, the solubility of proteins within the harvested cell lysate was tested by adding solubilising buffer to cell lysate, before PAGE analysis. As shown in Figure 2.12, the solubilised cell lysate sample contained a stronger protein band at 29 kDa, than was detected in cell lysate that was not treated with solubilising

buffer. This indicated that a small proportion of *N*-terminally His-tagged recombinant lysostaphin may have become insoluble upon cytoplasmic expression.

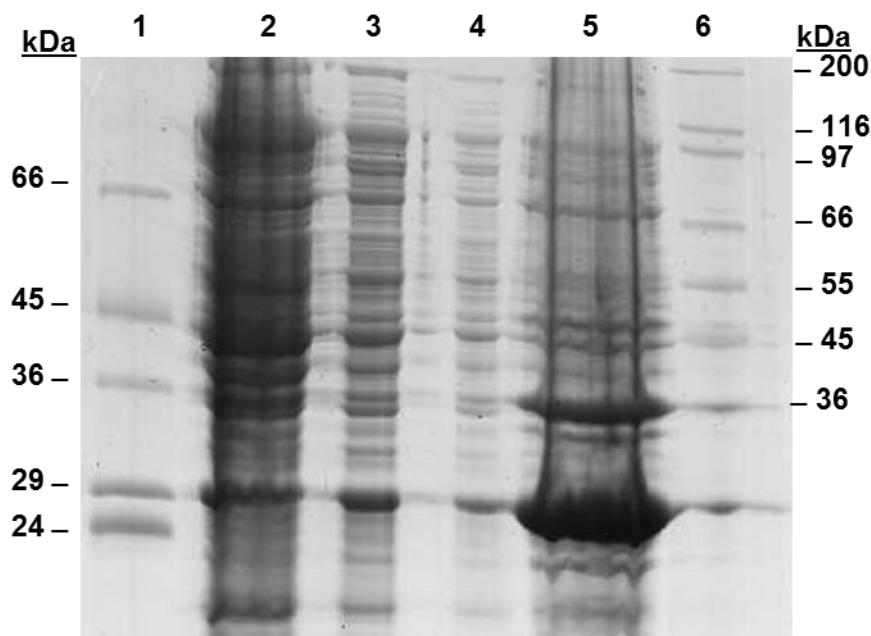


Figure 2.12: Cytoplasmic expression of *N*-terminally His-tagged recombinant lysostaphin in *E. coli* BL21 (DE3) cultured in AIM. CFE was analysed by 12% (w/v) SDS-PAGE. Lane 1: Sigma low molecular weight markers; Lane 2: CFE (neat); Lane 3: CFE (1:10); Lane 4: CFE (1:100); Lane 5: CFE in solubilising buffer; Lane 6: Sigma high molecular weight markers.

2.4.3.3 Expression of recombinant lysostaphin (constructs 2, 3, 4 and 5)

PAGE analysis of cell lysate following cytoplasmic expression of recombinant lysostaphin (constructs 2 and 3) demonstrated hyper-expression of protein with a molecular weight corresponding with the expected values, indicating the presence of recombinant lysostaphin (Appendix 7.95 and Appendix 7.96 respectively). Both forms of the protein appeared to remain soluble upon expression in *E. coli* BL21(DE3).

PAGE analysis of cell lysate following periplasmic expression of recombinant lysostaphin (constructs 4 and 5) demonstrated hyper-expression of protein with a molecular weight corresponding with the expected values, indicating that the PelB leader sequence effectively translocated recombinant lysostaphin across the inner membrane to the periplasmic space (Appendix 7.97 and Appendix 7.99 respectively). Repeated expression of both forms of the protein indicated that recombinant lysostaphin remained soluble upon expression in *E. coli* BL21(DE3) (Appendix 7.98 and Appendix 7.100). However PAGE analysis also revealed that the periplasmic lysate also featured over-expression of other proteins, with molecular

weights of around 36 and 45 kDa, which may have had a detrimental effect on the expression levels of recombinant lysostaphin through their activity or interference with translocation.

2.4.3.4 Expression of recombinant lysostaphin using different expression media

Initial expression experiments suggested that the recombinant lysostaphin gene constructs could be transcribed and translated in *E. coli* BL21(DE3), yielding a protein with a molecular weight that corresponded with the molecular weight of recombinant lysostaphin. Initially expression experiments were performed by culturing the *E. coli* in AIM, whereas in subsequent experiments *E. coli* was optionally fermented using either LB, minimal media (MM) or terrific broth (TB), whilst protein expression was induced through the addition of IPTG.

Expression of *N*-terminally His-tagged recombinant lysostaphin (construct 1) was demonstrated in AIM, LB, TB and MM (Appendix 7.101), though greater expression levels were observed in more complex media (LB and TB) or semi-defined media (AIM) and protein solubility appeared highest when the protein was expressed in LB (Appendix 7.102). Expression of recombinant lysostaphin (construct 2) and *C*-terminally His-tagged recombinant lysostaphin was found to occur to a greater extent in AIM than LB (Appendix 7.103 and Appendix 7.104 respectively). However due to the popularity and convenient formulation of LB media, LB became the preferred media type for preparation of recombinant lysostaphin during the optimisation of preparative and analytical chromatographic methods.

2.4.3.5 Expression of recombinant lysostaphin using different expression media volumes

The yield of recombinant lysostaphin (construct 1) could be increased by augmenting expression media volume from 50 ml to 1 L, without compromising expression levels. Protein yield could be increased further by harvesting cell lysate originating from 1, 5 and 15 L of culture (Figure 2.13). Although there were no major discernible differences between protein expression levels with increased expression media volumes, it was unclear whether pooling shake flask cultures increased protein heterogeneity if individual cultures suffered from batch-to-batch variability.

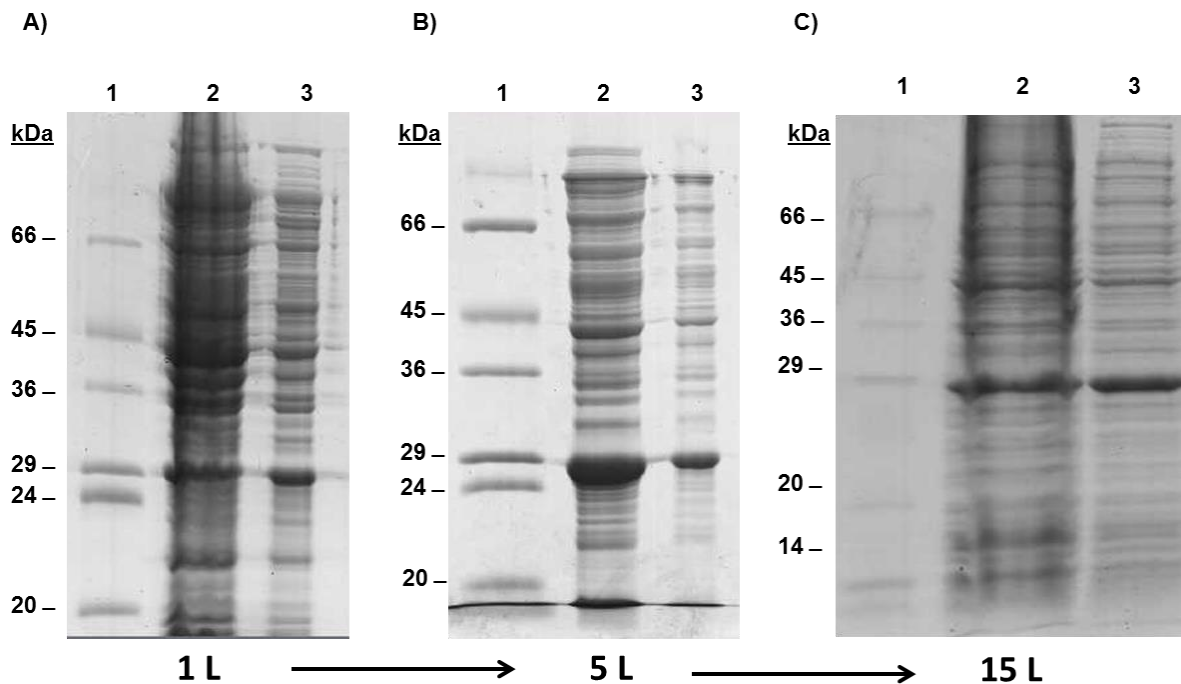


Figure 2.13: PAGE analysis of cytoplasmic cell lysates resulting from overall culture volumes during the expression of *N*-terminally His-tagged recombinant lysostaphin (construct 1) in *E. coli* BL21(DE3) cultured in AIM. Overexpression of a protein with a molecular weight of around 29 kDa was observed in cell lysates derived from 1 L batch culture or after pooling 5 or 15 x 1L batch cultures, indicating successful expression of *N*-terminally His-tagged recombinant lysostaphin. A) CFE resulting from 1L batch culture; Lane 1: Sigma low molecular weight markers; Lane 2: CFE (neat); Lane 3: CFE (1:10). B) CFE resulting from 5 x 1L batch cultures; Lane 1: Sigma low molecular weight markers; Lane 2: CFE (neat); Lane 3: CFE (1:10). C) CFE resulting from 15 x 1L batch cultures. Lane 1: Sigma low molecular weight markers; Lane 2: CFE (neat); Lane 3: CFE (1:10).

2.4.4 Discussion

Following protein expression in *E. coli*, it was evident that all five recombinant lysostaphin gene constructs could be successfully expressed in *E. coli* BL21(DE3). Each recombinant lysostaphin gene construct appeared to have been expressed efficiently within the cytoplasm. Successful expression was indicated by SDS-PAGE, through the observation of protein bands that corresponded with the expected molecular weights of proteins encoded by the recombinant lysostaphin gene constructs. Furthermore recombinant lysostaphin with pelB leader sequences (constructs 3 and 4) appeared to undergo effective translocation from cytoplasm to periplasm, which is not always guaranteed (Malik *et al.*, 2006, Chou, 2007). PelB leader sequences are cleaved by signal peptidases upon translocation through the inner membrane. PAGE analysis suggested that pelB leader sequence had been effectively removed, as the observed protein bands matched the expected molecular weight of *N*-terminally processed recombinant lysostaphin, in the presence and absence of a C-terminal His-tag.

Recombinant lysostaphin was expressed exclusively using *E. coli* BL21(DE3), however the cloned plasmids harbouring the lysostaphin gene could have been transformed into alternative *E. coli* strains. Alternative *E. coli* B or K-12 strains are often employed when expression is problematic, however in this work *E. coli* BL21(DE3) was shown to provide efficient expression of recombinant lysostaphin therefore the use of alternative expression strains was not deemed necessary. Furthermore, the influence of strain diversity upon the expression of recombinant lysostaphin was not investigated in this work, as the chemical and enzymatic modifications described in Section 1.2.1 were not found to be strain-specific, occurring in variety of popular *E. coli* expression strains.

All of the expression experiments indicated that the recombinant lysostaphin gene constructs could be used to express recombinant lysostaphin in a largely soluble form. A crude test of solubility was performed by treating cellular proteins with solubilising buffer prior to PAGE analysis. Solubilising buffer treatment solubilised any insoluble fractions of the recombinant protein preparation, however in the majority of instances, recombinant lysostaphin appeared to remain soluble following expression, which is desirable during recombinant protein production.

However on several occasions, PAGE analysis revealed that *N*-terminally His-tagged recombinant lysostaphin (construct 1) appeared to be produced in soluble and insoluble fractions. The insolubility of *N*-terminally His-tagged occurred intermittently and became apparent through frequent expression of this particular construct. It was likely that the

apparent insolubility probably arose as a consequence of hyper-expression of recombinant lysostaphin and therefore could probably be minimised through alteration of culture temperatures or the addition of lower concentrations of IPTG during induction. Protein insolubility can lead to undesirable protein aggregation, therefore *N*-terminally His-tagged recombinant lysostaphin was analysed by gel filtration, as described in Section 4.3, as a test of protein aggregation.

All of the recombinant lysostaphin gene constructs appeared to express well in different types of expression media. Expression experiments were primarily performed using AIM or LB, however due to convenience and popularity, LB became the preferred choice of expression media. Recombinant lysostaphin appeared to remain soluble when expressed in LB, whereas insoluble fractions were frequently observed upon expression in AIM. Furthermore, the use of LB and IPTG-based induction may have provided greater control over induction conditions, than auto-induction of protein expression. Auto-induction is dependent on cellular metabolism therefore induction occurs during growth saturation at a point which is determined by intrinsic cell physiology. IPTG-based induction therefore provides greater knowledge and control over the optical density at which protein expression is induced within a culture.

Most expression experiments were performed using 50-1000 ml of expression media, however when larger yield of recombinant lysostaphin were required, the cell lysates from up to 15 L of culture were combined. Pooling of cell lysates from multiple batch cultures proved to be a successful method of providing larger amounts of recombinant lysostaphin, in the absence of a continuous culture strategy. PAGE analysis of cell lysates resulting from the combination of multiple batch cultures suggested that batch-to-batch variability did not appear to dramatically increase the overall heterogeneity of the cell lysate. However this strategy may have increased the heterogeneity of recombinant lysostaphin through the combination of different protein isoforms, therefore this strategy was avoided where possible.

Due to the reactive nature of the cellular compartments of *E. coli*, recombinant lysostaphin would have been exposed to a cellular milieu which may have been detrimental to its structure, stability or function. It was therefore desirable to rapidly isolate the recombinant protein from the cell lysate by protein purification, as described in Section 2.5.

2.5 Purification of recombinant lysostaphin

2.5.1 Introduction

A protein purification strategy typically aims to purify a target protein in a rapid and efficient manner, whilst retaining biological activity and structural integrity. An optimised purification strategy can permit maximal recovery of pure and active protein from the complex starting material from which the protein was derived. Cell lysates, such as those obtained from *E. coli* contain a mixture of macromolecules, including several thousand proteins, from which the target protein must be purified (Marshak, 1996). As recombinant DNA technology, enables high level expression of a target protein, it has become simpler to isolate a target protein. Nevertheless it is imperative that the hyper-expressed target protein is separated from active cellular proteases that could detrimentally affect protein structure upon their release by cellular disruption.

Careful preparation of cell lysate is therefore important to ensure the target protein does not undergo proteolysis prior to purification. Cell lysate preparation should be optimised to ensure that protein stability and activity is appropriately influenced by pH, ionic strength, temperatures and reducing agents. Cell lysate is therefore typically prepared at low temperatures using buffers which are compatible with the target protein, but also with subsequent assay measurements or chromatographic analysis. Such downstream applications often determine the level of purification required, as proteins with therapeutic uses must be purified to a very high level, whilst protein used in industrial applications can be of lower purity.

As proteins are composed of different numbers and sequences of amino acids, they tend to differ in their physical and chemical characteristics. Furthermore, polypeptides are folded to create distinct tertiary structures, which influences the size, shape and reactivity of the protein (Marshak, 1996). Unique biochemical properties, such as mass, charge, stability, solubility, hydrophobicity or affinity are exploited during protein purification to isolate the target protein. A number of these techniques were employed during the separation or purification of recombinant lysostaphin, as presented in Table 2.8. Many of these separation techniques are dependent on molecular interactions, involving hydrogen bonds, hydrophobic and ionic interactions, which vary with temperature, pH and ionic strength. An understanding of the nature and strength of these molecular interactions can therefore facilitate protein purification, through optimisation of purification conditions.

Table 2.8: Modes and principles of separation techniques used in protein purification

Separation Process	Separation Mode	Principle of Separation
Precipitation	Ammonium sulphate	Solubility
	Acetate	Solubility
	Trichloroacetic acid	Solubility
Chromatography	Immobilised metal affinity chromatography	Specific ligand binding
	Hydrophobic Interaction	Hydrophobicity
	Reversed-Phase	Hydrophobicity, size
	Ion Exchange	Charge
	Gel Filtration (Size exclusion)	Size, shape
Filtration	Ultrafiltration	Size, shape
	Dialysis	Size, shape

2.5.1.1 Purification of recombinant lysostaphin

Following expression of recombinant lysostaphin, it was imperative that the target protein was recovered from the cell lysate as swiftly and efficiently as possible, to minimise proteolysis or modification of the recombinant product. To achieve this, a protein purification strategy for the isolation of recombinant lysostaphin was identified and optimised. Complete protein purification often requires the application of several separative techniques, however in this instance purification of recombinant lysostaphin in a single purification step was desirable.

By minimising the number of purification steps, the yield and activity of purified recombinant lysostaphin could also be maximised and maintained. To ensure that the activity of recombinant lysostaphin had been preserved during purification, the staphylolytic activity was assayed (Section 4.1). To confirm that protein yields and purity were maintained through the course of purification, protein concentration was monitored by UV spectrometry, whilst purity was determined by SDS-PAGE analysis. Maximal retention of expressed recombinant lysostaphin was essential to ensure that enough protein was available for subsequent analysis and characterisation, as described in Chapters 3 and 4. Whilst some analytical techniques such as mass spectrometry, theoretically only required femtomolar amounts for protein identification, biological assays and chromatographic separation of protein isoforms required larger, micromolar amounts of protein to accomplish analysis.

During the optimisation of a purification strategy, a number of purification techniques were employed, including ammonium sulphate fractionation (ASF), immobilised metal affinity chromatography (IMAC), ion exchange chromatography (IEX), hydrophobic interaction

chromatography (HIC), gel filtration (GF) and ultrafiltration. Some techniques were selected according to convenience, such as ASF, due to its ease and compatibility with HIC. ASF was also used on several occasions to concentrate protein sample prior to chromatographic purification. Ultrafiltration was used to effectively desalt and concentrate samples prior to and following a chromatographic separation. Recombinant lysostaphin expressed in *E. coli* has traditionally been purified using affinity chromatography, however in this work a variety of chromatographic separations were performed to assess whether recombinant lysostaphin could be successfully isolated by different chromatographic mechanisms (Chan, 1996, Szweda *et al.*, 2001, Sharma *et al.*, 2006).

The success of chromatographic separation was ultimately influenced by the physicochemical properties of each of the expressed recombinant lysostaphin constructs. Following bioinformatic analysis of the amino acid sequences of recombinant lysostaphin constructs, certain biochemical properties could be predicted, as described in Table 2.9. Evidently, recombinant lysostaphin constructs harbouring His-tag sequences could theoretically be purified efficiently and directly using IMAC. Recombinant lysostaphin constructs without affinity fusion tags had to be purified using alternative chromatographic approaches, such as IEX, HIC and GF. As PTMs have been known to occur at His-tag sequences of proteins, His-tagged recombinant lysostaphin constructs were also purified using these techniques, to establish whether modified protein isoforms were excluded from purified recombinant lysostaphin preparations during IMAC.

Table 2.9: Expected physicochemical properties of expressed recombinant lysostaphin gene constructs, as determined by ProtParam analysis.

Construct	Fusion Tags	Apoprotein Mass (kDa)	Theoretical isoelectric point (pI)
1	N-terminal His-tag	29337.8	9.72
2	None	27075.4	9.59
3	C-terminal His-tag	28140.5	9.52
4	C-terminal His-tag and PelB leader sequence	28140.5	9.52
5	PelB leader sequence	27075.4	9.59

The theoretical isoelectric points of the recombinant lysostaphin constructs indicate that recombinant lysostaphin is a fairly basic protein. This trait would essentially lead to the

protein bearing an overall negative charge at neutral pH, suggesting that the protein would be purified more successfully using CXC rather than AXC.

The aims of this work were:

- To successfully isolate recombinant lysostaphin from extracted cell lysates using a single or multiple chromatographic techniques.
- To purify maximal amounts of the expressed recombinant protein.
- To create an optimised purification strategy allowing rapid purification of recombinant lysostaphin.
- To retain the biological activity of recombinant lysostaphin.
- To produce His-tagged recombinant lysostaphin preparations, purified using affinity purification or non-affinity based chromatography, for comparison of product heterogeneity.

2.5.2 Methods

2.5.2.1 Buffers

All buffer compositions are outlined in Appendix 7.105.

2.5.2.2 Chemicals

All chemical compositions are outlined in Appendix 7.106.

2.5.2.3 Equipment

All equipment used during the purification of recombinant lysostaphin is outlined in Appendix 7.107.

2.5.2.4 Purification of recombinant lysostaphin

Recombinant lysostaphin was purified from cell-free extract (CFE) following protein extraction. ASF was tested as an initial differential purification technique and was occasionally used to concentrate protein samples during the course of protein purification (Appendix 7.109). Harvested cell lysate was applied to ion exchange columns during AXC (Appendix 7.112) and CXC (Appendix 7.113). Recombinant lysostaphin constructs expressed without His-tags were purified in one-step using CXC or two-steps, using HIC (Appendix 7.110) and GF (Appendix 7.111). Constructs expressed with His-tags were purified in one-step with IMAC, but were also purified by CXC to ensure that potential protein isoforms harbouring His-tag modifications were not eliminated from the final purified protein preparation.

IMAC was performed using Chelating Sepharose™ Fast Flow columns in conjunction with an ÄKTA™ prime plus purification system (Appendix 7.114) or Eylea microtube peristaltic pump during large-scale purification (Appendix 7.115). Dialysis (Appendix 7.118) and lyophilisation (Appendix 7.119) was used to concentrate purified protein following large-scale purification. Alternatively IMAC purification was performed using ProPac® IMAC-10 columns and an Ultimate™ 3000 Titanium system (Appendix 7.116 and Appendix 7.117). Following small-scale purifications, resulting fractions were analysed by PAGE and fractions containing the target protein were concentrated by ultrafiltration (Appendix 7.120).

2.5.3 Results

Following expression of the recombinant lysostaphin gene constructs in *E. coli* BL21(DE3), experiments were performed to purify the recombinant protein from other contaminating cellular proteins from *E. coli*.

2.5.3.1 Ammonium sulphate fractionation

ASF was tested as an initial crude differential purification technique to remove less hydrophilic contaminating proteins from the protein preparation. Following expression in *E. coli* BL21(DE3), harvested cell lysate was analysed by SDS-PAGE (Appendix 7.121) and precipitated using between 20 and 60% (w/v) ammonium sulphate. SDS-PAGE analysis of resuspended protein suggested that recombinant lysostaphin became insoluble at 20% (w/v) ammonium sulphate and therefore ASF could not provide differential purification on the grounds of solubility (Figure 2.14). Precipitation of recombinant lysostaphin with 50-60% (w/v) ammonium sulphate was subsequently used to provide sample concentration, however this was found to have detrimental effects on protein solubility during resuspension, as described in Sections 2.5.3.3 and 2.5.3.8.

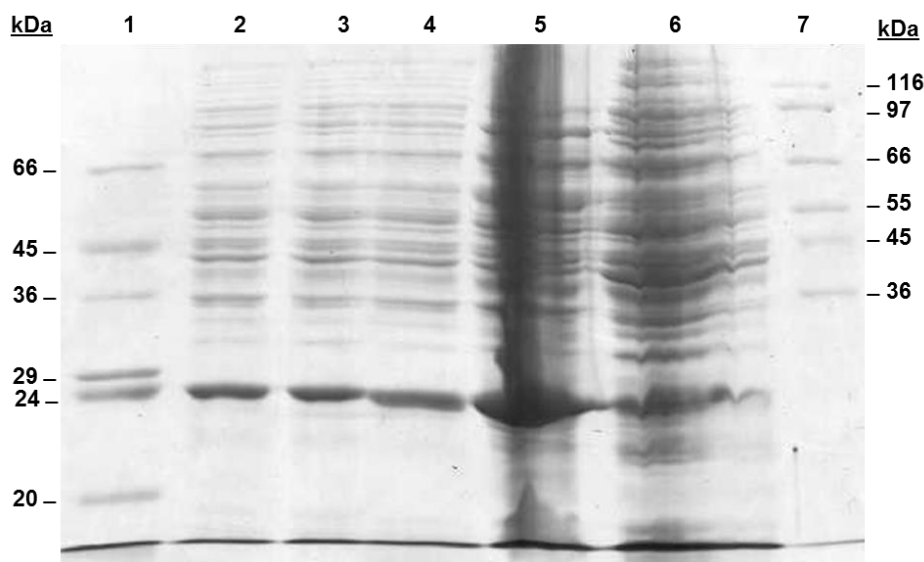


Figure 2.14: ASF of recombinant lysostaphin (construct 2). Lane 1: Sigma low molecular weight markers; Lane 2: 20% (w/v) ammonium sulphate (pellet); Lane 3: 30% (w/v) ammonium sulphate (pellet); Lane 4: 40% (w/v) ammonium sulphate (pellet); Lane 5: 60% (w/v) ammonium sulphate (pellet); Lane 6: 60% (w/v) ammonium sulphate (supernatant); Lane 7: Sigma high molecular weight markers.

2.5.3.2 HIC using Phenyl Sepharose™ high performance media and an ÄKTA™ purification system

Following ASF, the pelleted protein was subjected to HIC, which resulted in the elution of a series of poorly separated peaks (Figure 2.5). According to SDS-PAGE, these peaks reflected the retention of recombinant lysostaphin and other *E. coli* cellular proteins (Figure 2.15).

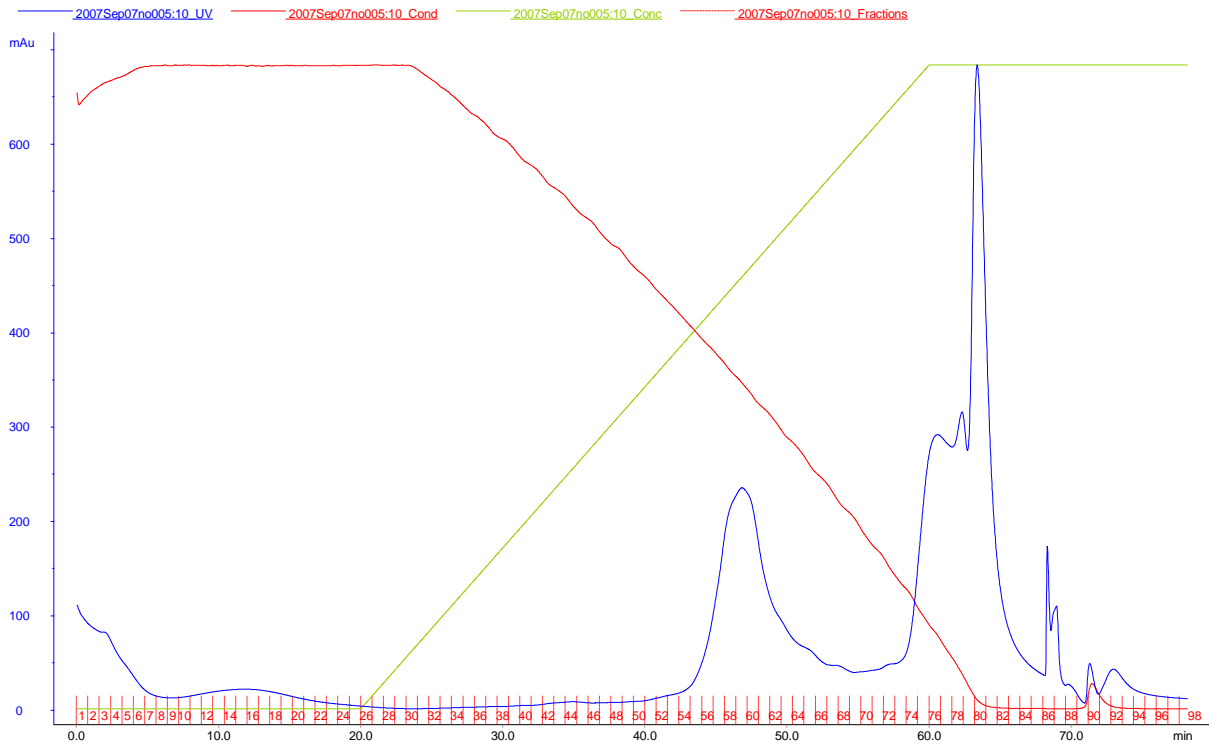


Figure 2.15: Purification of recombinant lysostaphin (construct 2) using HIC. Cell lysate extracted from recombinant *E. coli* BL21(DE3) cultured in AIM was applied to the Phenyl Sepharose™ high performance column. Bound protein was eluted by applying a decreasing ammonium sulphate concentration (1.5-0 M). Fractions 73-80 contained recombinant lysostaphin.

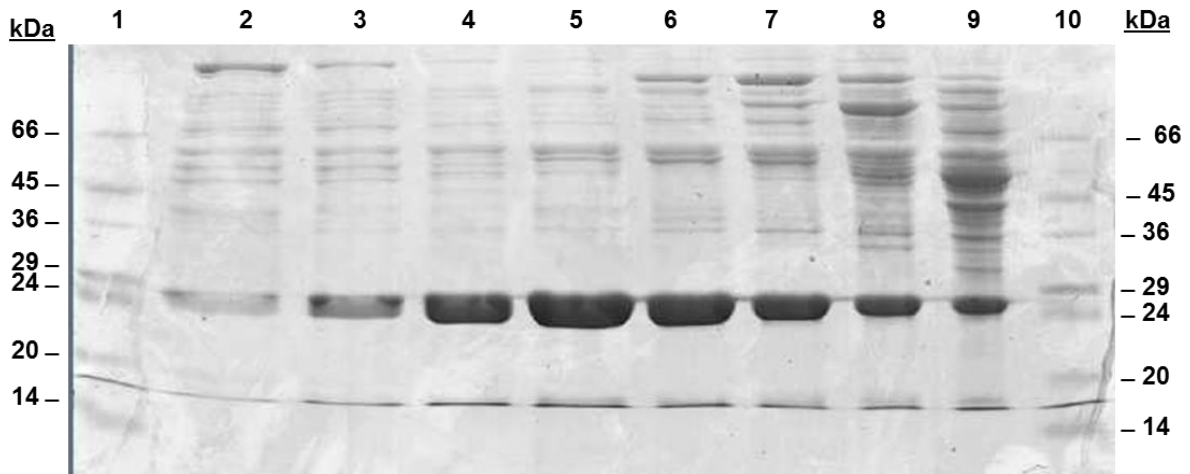


Figure 2.16: SDS-PAGE analysis of fractions eluted during HIC of cell-lysate containing recombinant lysostaphin (construct 2). Lane 1: Sigma low molecular weight markers; Lane 2: Fraction 73; Lane 3: Fraction 74; Lane 4: Fraction 75; Lane 5: Fraction 76; Lane 6: Fraction 77; Lane 7: Fraction 78; Lane 8: Fraction 79; Lane 9: Fraction 80; Lane 10: Sigma low molecular weight markers.

HIC was performed again following application of cell lysate containing C-terminally His-tagged recombinant lysostaphin (construct 3) (Appendix 7.126), which resulted in the resolution of a number of peaks that reflected the presence of recombinant lysostaphin and contaminating *E. coli* proteins (Figure 2.17 and Figure 2.18).

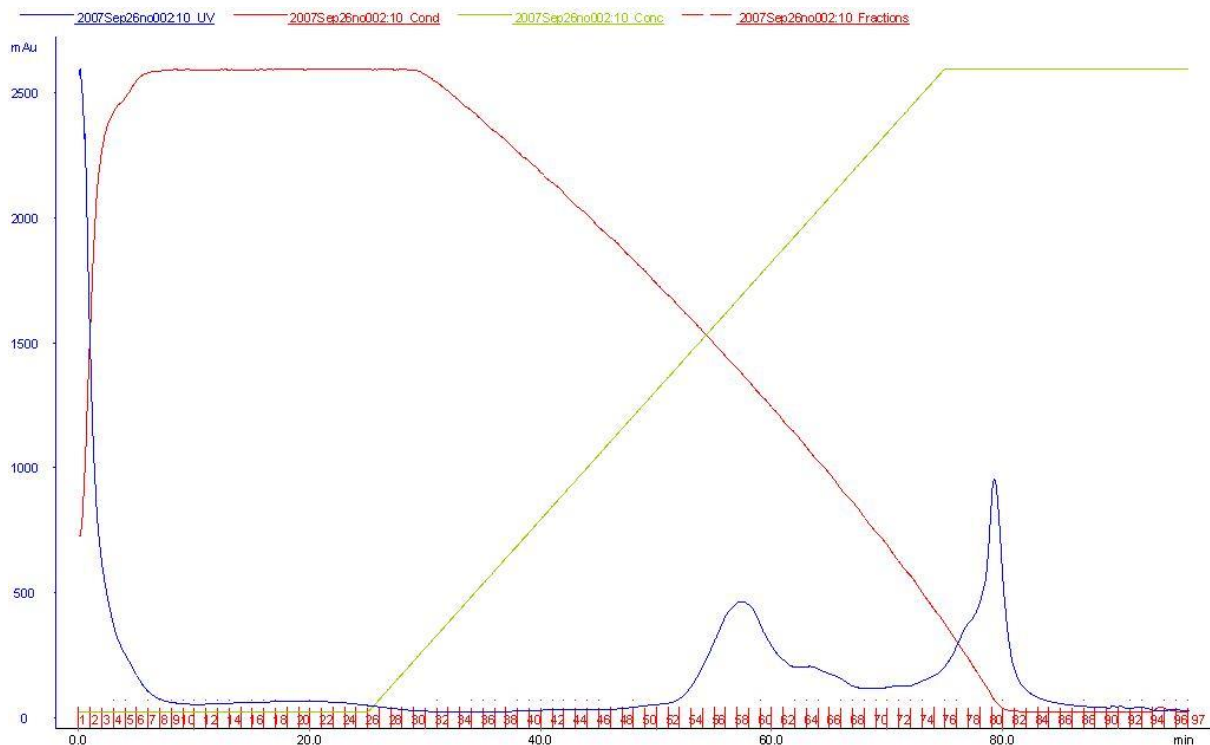


Figure 2.17: Purification of C-terminally His-tagged recombinant lysostaphin (construct 3) using HIC. Cell lysate extracted from recombinant *E. coli* BL21(DE3) cultured in AIM was applied to the Phenyl Sepharose™ high performance column. Bound protein was eluted by applying a decreasing ammonium sulphate concentration (1.5-0 M).

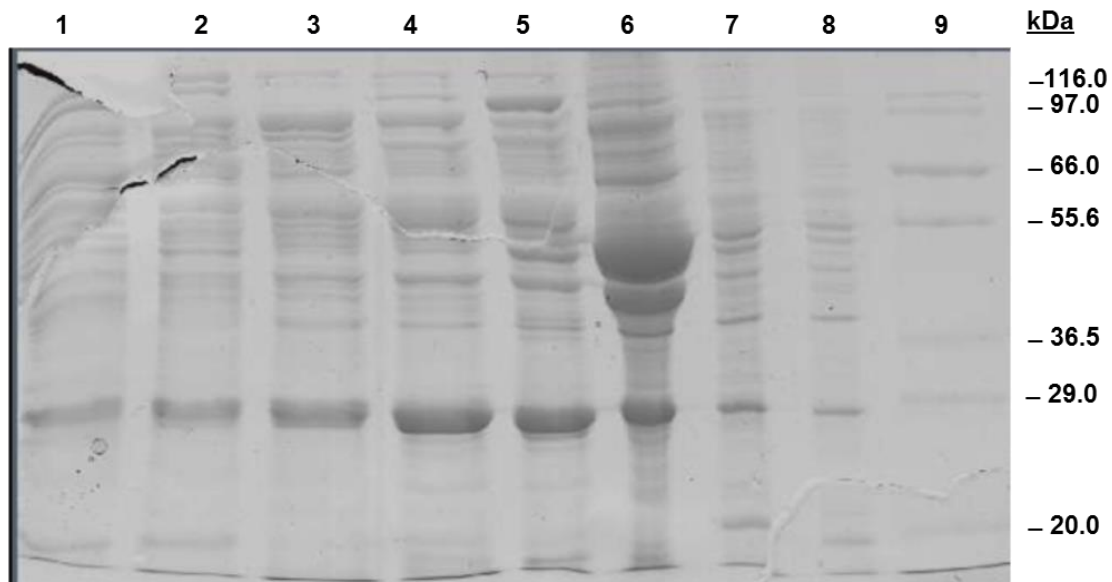


Figure 2.18: SDS-PAGE analysis of fractions eluted during HIC of cell-lysate containing C-terminally His-tagged recombinant lysostaphin (construct 3). Fractions 70-80 were pooled and precipitated by ammonium sulphate fractionation prior to concentration by ultrafiltration. Lane 1: Fraction 70; Lane 2: Fraction 72; Lane 3; Fraction 74; Lane 4: Fraction 76; Lane 5: Fraction 78; Lane 6: Fraction 80; Lane 7: Fraction 82; Lane 8: Fraction 84; Lane 9: Sigma high molecular weight markers.

2.5.3.3 GF using HiLoad™ 16/60 Superdex 200 media and a FPLC system

Following HIC, the fractions containing recombinant lysostaphin (construct 3) were pooled and subjected to ASF before resuspending the pellet and concentrating the protein by ultrafiltration. Sample concentration was hindered by protein solubility issues, however the sample was ultimately concentrated and injected onto a GF column (Figure 2.19). GF resulted in the elution of a number of peaks, one of which contained recombinant lysostaphin, as confirmed by SDS-PAGE (Figure 2.20).

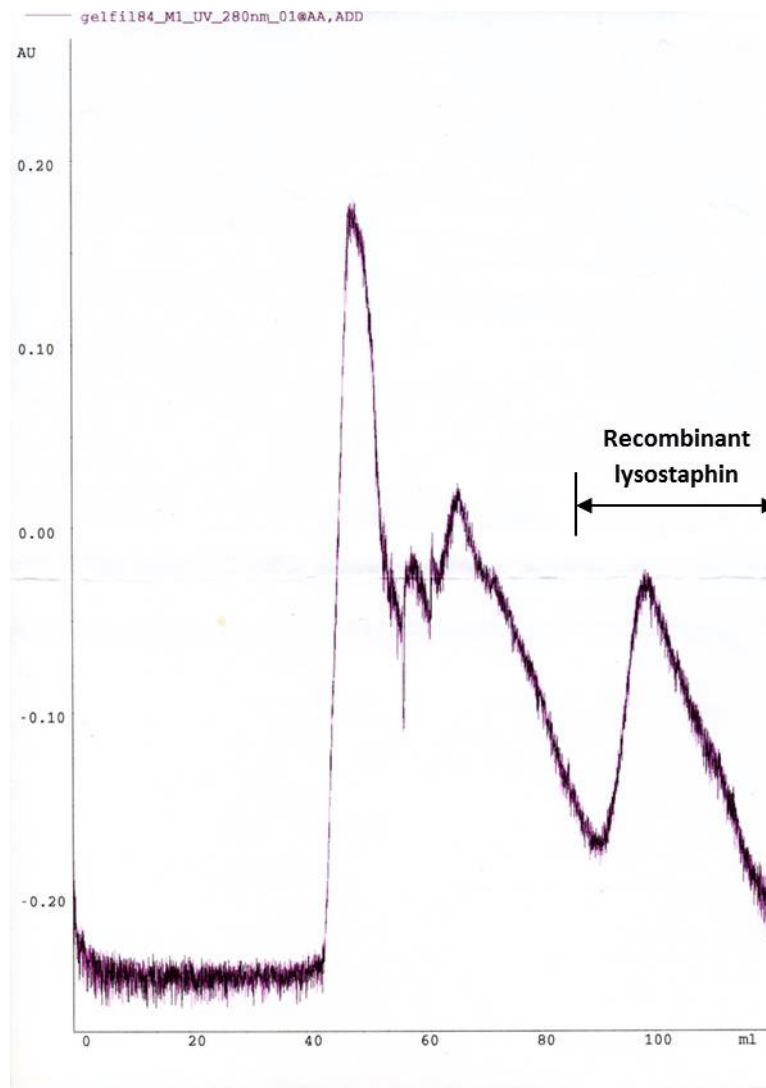


Figure 2.19: Purification of C-terminally His-tagged recombinant lysostaphin (construct 3) using GF. Concentrated protein purified using HIC was applied to HiLoad 16/60 Superdex 200 prep grade column. Bound protein was eluted by isocratic elution.

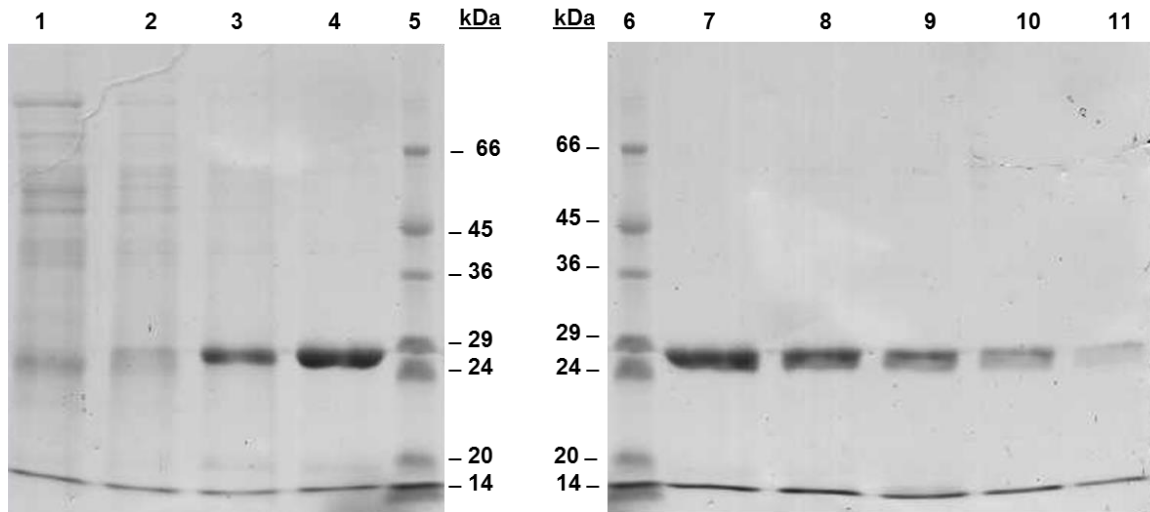


Figure 2.20: SDS-PAGE analysis of fractions eluted during GF of protein eluted during HIC. Fractions 19-26 were pooled and concentrated by ultrafiltration. Lane 1: Fraction 18; Lane 2: Fraction 19; Lane 3; Fraction 20; Lane 4: Fraction 21; Lane 5: Sigma low molecular weight markers; Lane 6: Sigma low molecular weight markers; Lane 7: Fraction 22; Lane 8: Fraction 23; Lane 9: Fraction 24; Lane 10: Fraction 25; Lane 11: Fraction 26.

The fractions containing recombinant lysostaphin were pooled and concentrated prior to SDS-PAGE (Figure 2.21). Whilst HIC and GF provided high-level purification of recombinant lysostaphin, the purified sample was of low concentration and may have degraded during the course of purification and storage.

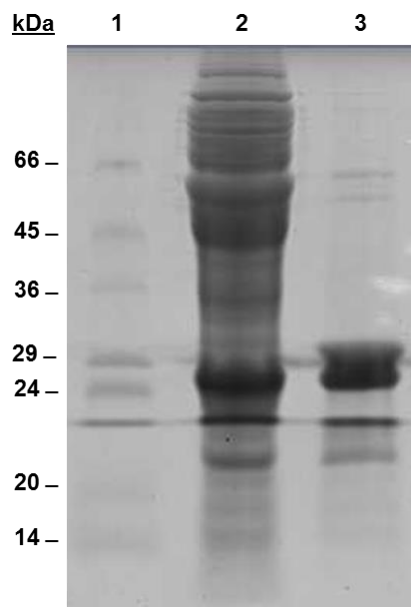


Figure 2.21: SDS-PAGE analysis of the recombinant protein preparation after HIC and following HIC and GF. Lane 1; Sigma low molecular weight markers; Lane 2; Protein sample following HIC; Lane 3: Protein sample following HIC and GF.

2.5.3.4 AXC using Source™ 30Q media and an ÄKTA™ purification system

As HIC could not provide complete purification of recombinant lysostaphin, IEX was performed with the intention of directly purifying the recombinant protein from the cell lysate. Cell lysate was subjected to AXC, which resulted in retention of multiple proteins (Figure 2.22); however SDS-PAGE analysis revealed that the detected peaks represented retention of *E. coli* cytoplasmic proteins instead of recombinant lysostaphin (Figure 2.23). AXC was repeated following application of cell lysate containing recombinant lysostaphin (constructs 4 and 5) (Appendix 7.122 and Appendix 7.124), however once again SDS-PAGE analysis revealed that the target protein was not retained (Appendix 7.123 and Appendix 7.125) and therefore AXC could not be used to purify recombinant lysostaphin.

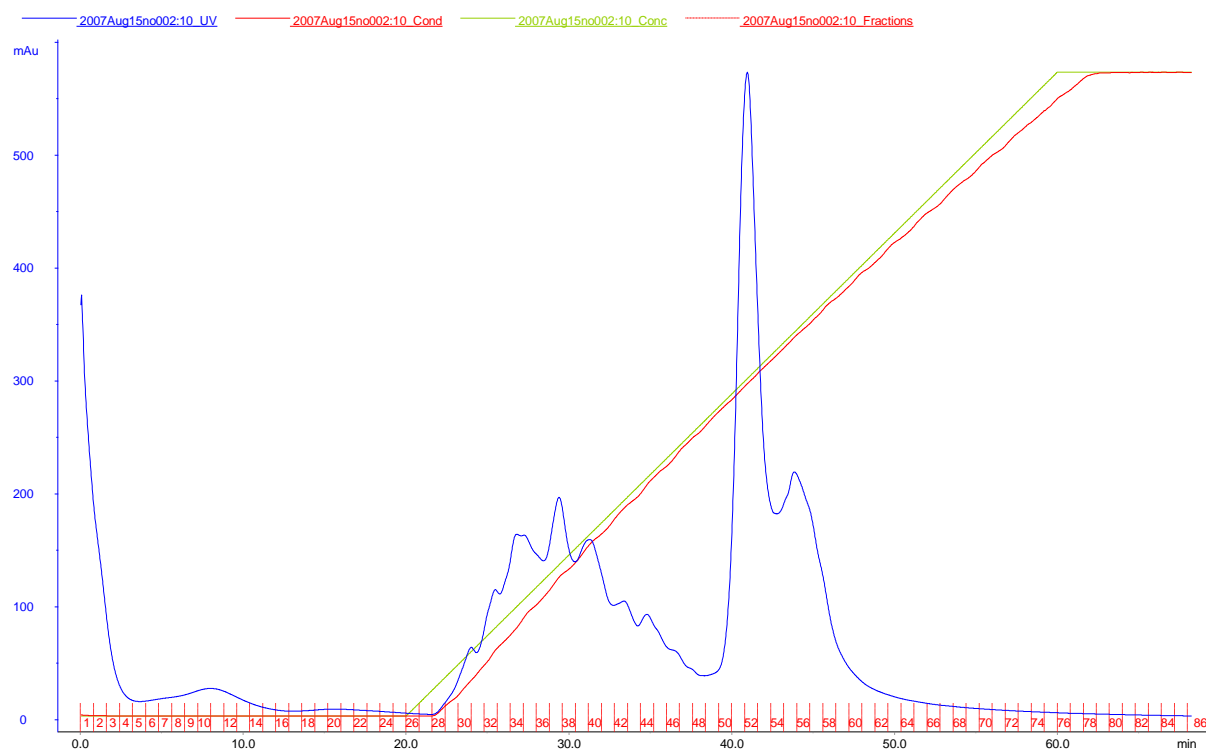


Figure 2.22: Purification of recombinant lysostaphin (construct 2) using AXC. Cell lysate extracted from recombinant *E. coli* BL21(DE3) cultured in AIM was applied to the Source™ 30Q column. Bound protein was eluted by applying an increasing NaCl concentration (0-1.0 M)

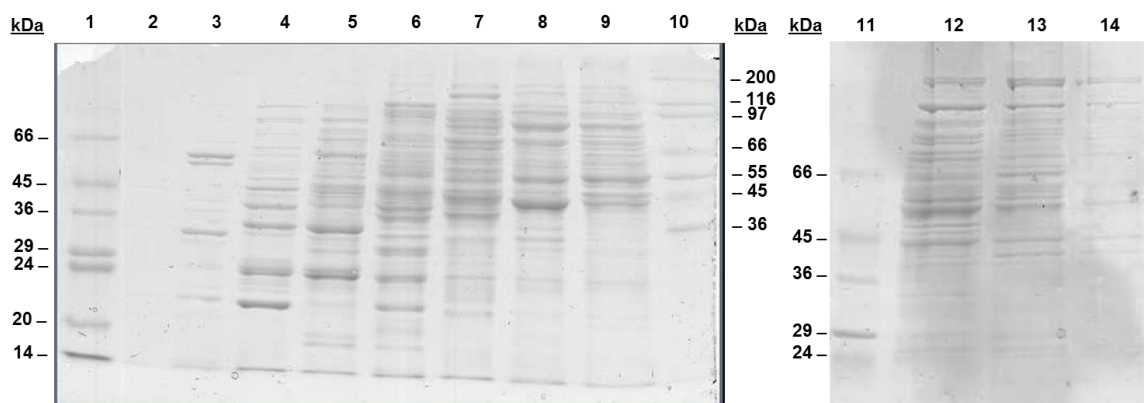


Figure 2.23: SDS-PAGE analysis of fractions eluted during AXC of cell-lysate containing recombinant lysostaphin (construct 2). Lane 1: Sigma low molecular weight markers; Lane 2: Fraction 28; Lane 3: Fraction 30; Lane 4: Fraction 32; Lane 5: Fraction 34; Lane 6: Fraction 36; Lane 7: Fraction 38; Lane 8: Fraction 40; Lane 9: Fraction 42; Lane 10: Sigma high molecular weight markers; Lane 11: Sigma low molecular weight markers; Lane 12: Fraction 44; Lane 13: Fraction 46; Lane 14: fraction 48.

2.5.3.5 CXC using Source™ 30s media and an ÄKTA™ purification system

Cell lysate was also subjected to CXC, which resulted in the resolution of a single major peak (Figure 2.24). SDS-PAGE analysis revealed that CXC efficiently separated recombinant lysostaphin (construct 2) from *E. coli* cytoplasmic proteins, providing a high degree of purification (Figure 2.25). CXC also provided efficient purification of *N*-terminally His-tagged recombinant lysostaphin (construct 1) on two separate occasions (Appendix 7.127 and Appendix 7.129). Once again SDS-PAGE of eluted fractions revealed that CXC could selectively purify the target protein from the cell lysate (Appendix 7.128 and Appendix 7.130).

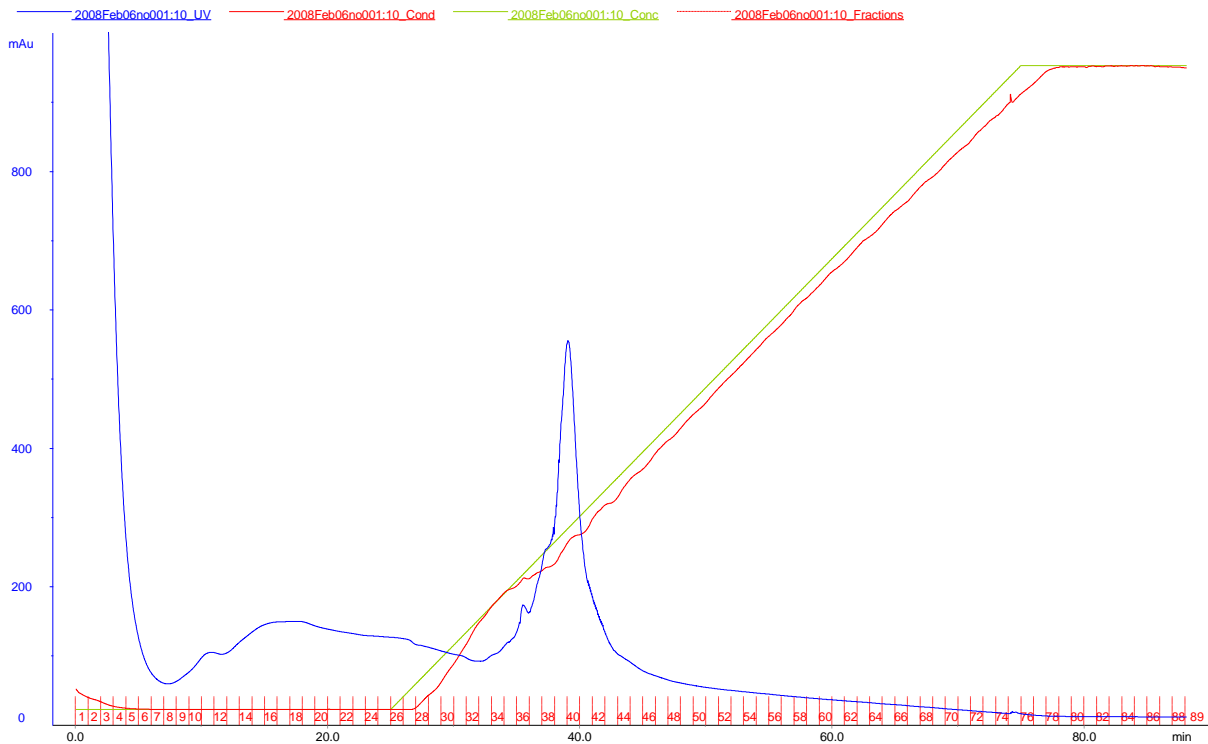


Figure 2.24: Purification of recombinant lysostaphin (construct 2) using CXC. Cell lysate extracted from recombinant *E. coli* BL21(DE3) cultured in AIM was applied to the Source™ 30s column. Bound protein was eluted by applying an increasing NaCl concentration (0-1.0 M).

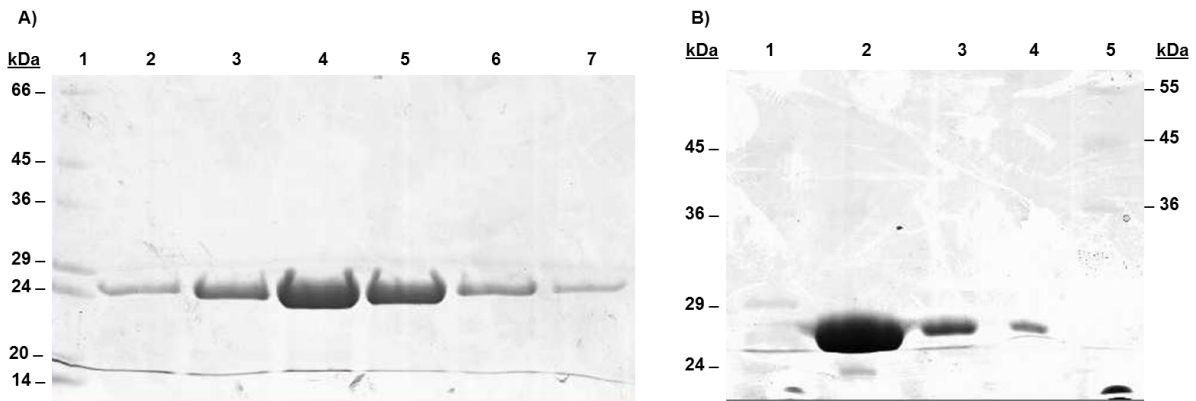


Figure 2.25: SDS-PAGE analysis of CXC fractions and purified recombinant lysostaphin (construct 2). A) Fractions eluted during CXC of cell-lysate containing recombinant lysostaphin (construct 2). Eluted CXC fractions 35-41 were pooled and concentrated by ultrafiltration. Lane 1: Sigma low molecular weight markers; Lane 2: Fraction 34; Lane 3: Fraction 36; Lane 4: Fraction 38; Lane 5: Fraction 40; Lane 6: Fraction 42; Lane 7: Fraction 43. B) Concentrated protein after pooling and ultrafiltration of fractions eluted during CXC of cell-lysate containing recombinant lysostaphin (construct 2). Lane 1: Sigma low molecular weight markers; Lane 2: concentrated protein (neat); Lane 3: concentrated protein (1:10); Lane 4: concentrated protein (1:100); Lane 5: Sigma high molecular weight markers.

2.5.3.6 IMAC using Chelating Sepharose™ Fast Flow media and an ÄKTA™ purification system

As three of the five expressed recombinant lysostaphin gene constructs featured His-tag sequences, recombinant lysostaphin (constructs 1, 3 and 4) could be purified using IMAC. Initial IMAC purifications were performed using an ÄKTA™ prime plus purification system, whilst later purifications were performed using an Ultimate™ 3000 Titanium system. IMAC purification of cell lysate containing recombinant lysostaphin (construct 3) resulted in elution of a narrow, well resolved peak, suggesting purification of the target protein (Figure 2.26). A high degree of protein purification was confirmed following PAGE analysis of the fractions eluted during IMAC (Figure 2.27).

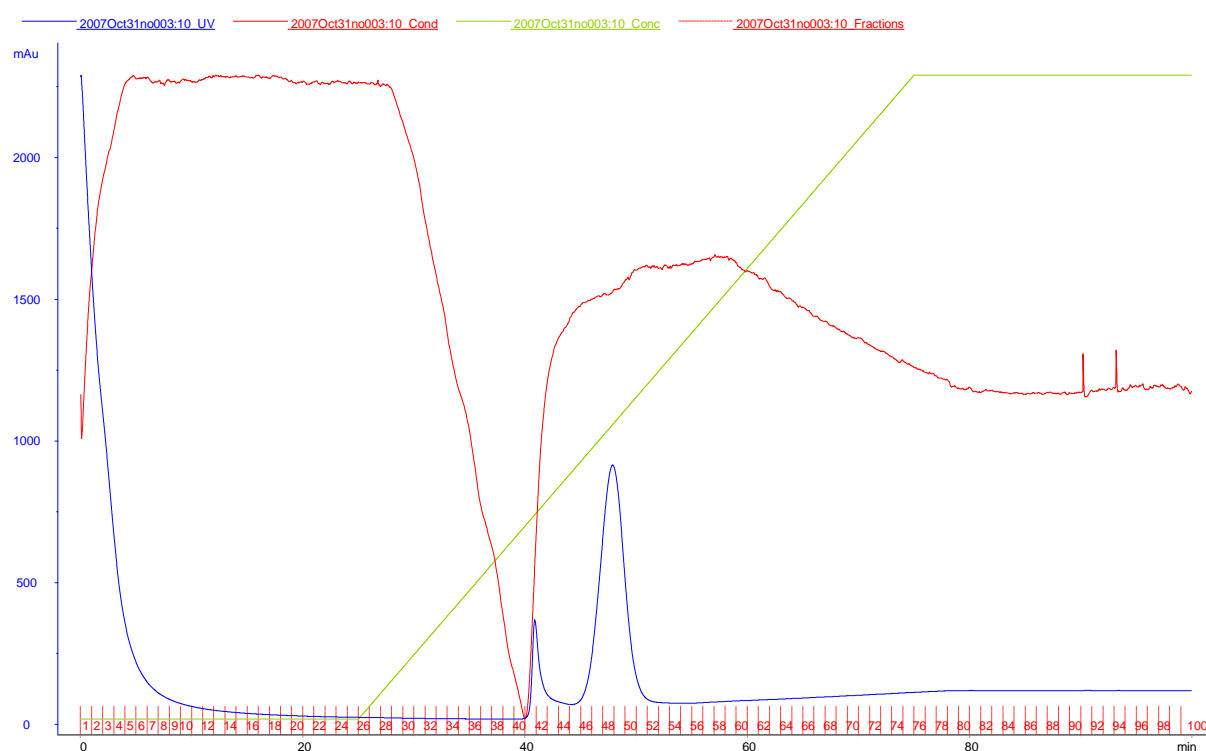


Figure 2.26: Purification of C-terminally His-tagged recombinant lysostaphin (construct 3) using IMAC. Cell lysate extracted from recombinant *E. coli* BL21(DE3) cultured in AIM was applied to the Chelating Sepharose™ Fast Flow media column. Bound protein was eluted by applying an increasing imidazole concentration (20-500 mM).

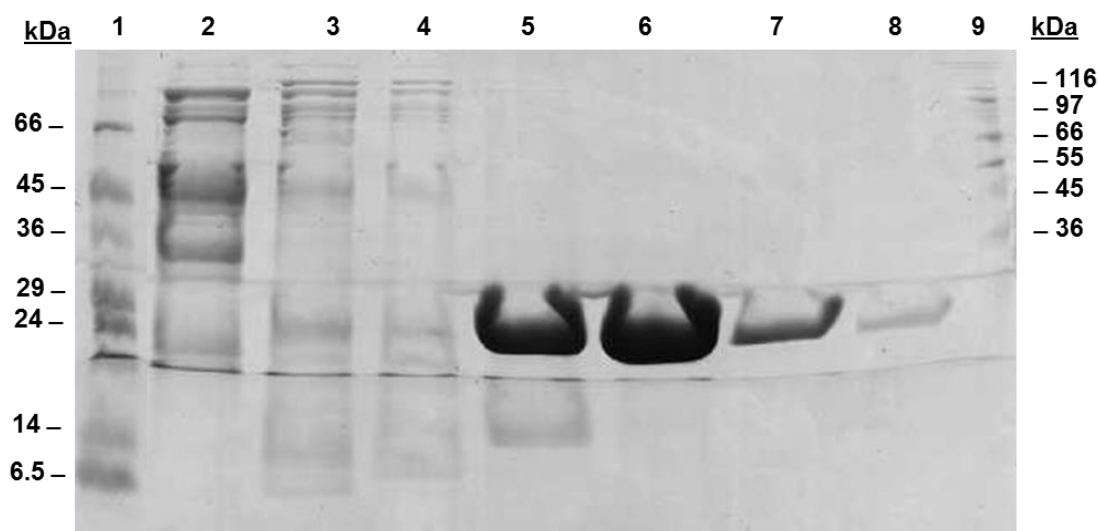


Figure 2.27: SDS-PAGE analysis of fractions following IMAC purification of C-terminally His-tagged recombinant lysostaphin (construct 3). Lane 1: Sigma low molecular weight markers; Lane 2: Fraction 41; Lane 3: Fraction 43; Lane 4: Fraction 45; Lane 5: Fraction 47; Lane 6: Fraction 49; Lane 7: Fraction 51; Lane 8: Fraction 53; Lane 9: Sigma high molecular weight markers.

To remove low molecular weight contaminants, fractions containing purified recombinant lysostaphin were concentrated and subjected to GF (Figure 2.28). SDS-PAGE of eluted fractions demonstrated that recombinant lysostaphin has been purified to a very high degree (Figure 2.29). Further IMAC purifications of recombinant lysostaphin (construct 1 and construct 4) were performed (Appendix 7.131 and Appendix 7.133) leading to a high-level of purification which was confirmed by SDS-PAGE (Appendix 7.132 and Appendix 7.134). As IMAC provided a high degree of purification within a single chromatographic step, secondary purification with GF was not considered efficient or necessary.

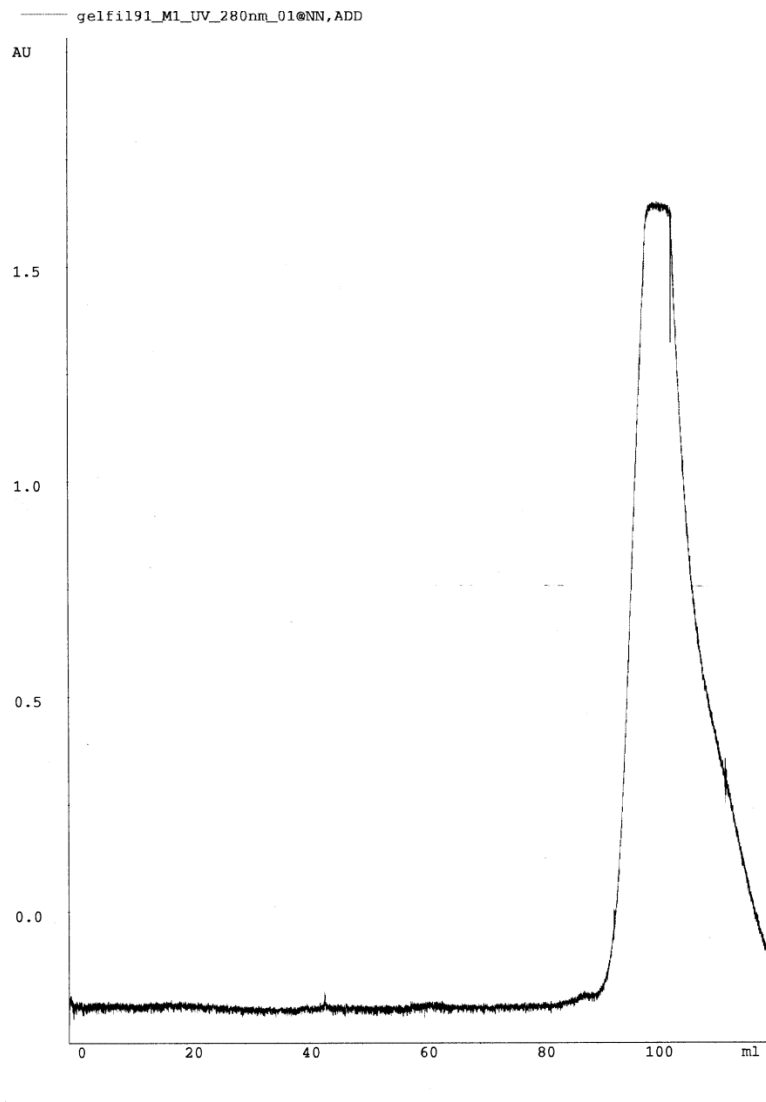


Figure 2.28: Purification of C-terminally His-tagged recombinant lysostaphin (construct 3) using GF. Concentrated protein purified using HIC was applied to HiLoad 16/60 Superdex 200 prep grade column. Bound protein was eluted by applying an isocratic gradient.

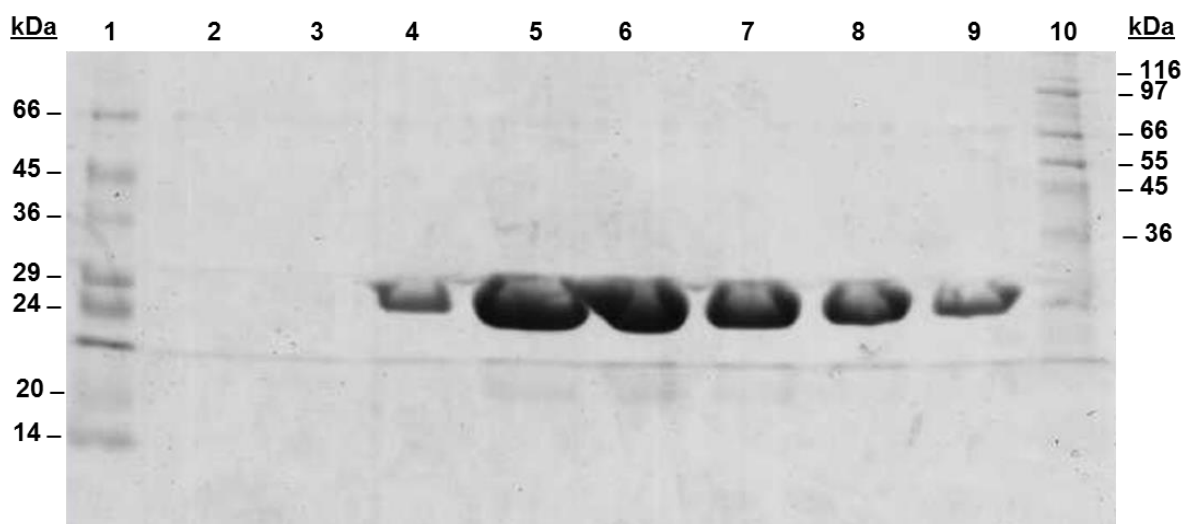
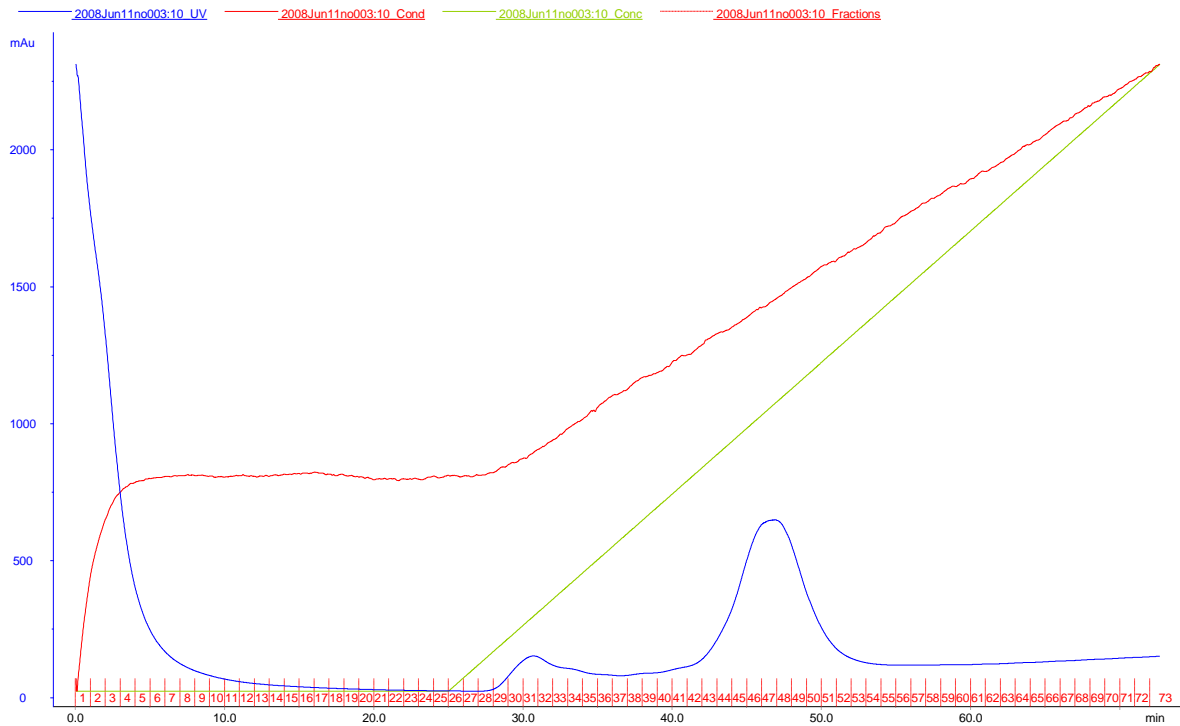


Figure 2.29: SDS-PAGE analysis of fractions following IMAC and GF purification of C-terminally His-tagged recombinant lysostaphin (construct 3) derived from *E.coli* BL21(DE3) cultured in AIM. Lane 1: Sigma low molecular weight markers; Lane 2: Fraction 17; Lane 3: Fraction 18; Lane 4: Fraction 19; Lane 5: Fraction 20; Lane 6: Fraction 21; Lane 7: Fraction 22; Lane 8: Fraction 23; Lane 9: Fraction 24; Lane 10: Sigma high molecular weight markers.

2.5.3.7 Large-scale purification of recombinant lysostaphin by IMAC using Chelating Sepharose™ Fast Flow media and an ÄKTA™ purification system

When cell lysate was harvested from multiple batch cultures, multiple IMAC purifications were performed consecutively to ensure that the increased concentration of recombinant protein did not overwhelm the binding capacity of the IMAC stationary phase. Due to shared usage, it was more practical to perform multiple IMAC purifications rather than re-pack the chelating sepharose column and re-program the ÄKTA™ chromatographic program to accommodate the larger bed volume of the stationary phase. Therefore cell lysate containing recombinant lysostaphin (construct 3) was applied to the IMAC column over two consecutive separations (Figure 2.30). PAGE analysis suggested that recombinant lysostaphin was purified effectively from cell lysate from 4 L of culture; however this approach was not practical when purifying the target protein from larger culture volumes (Figure 2.31).

A)



B)

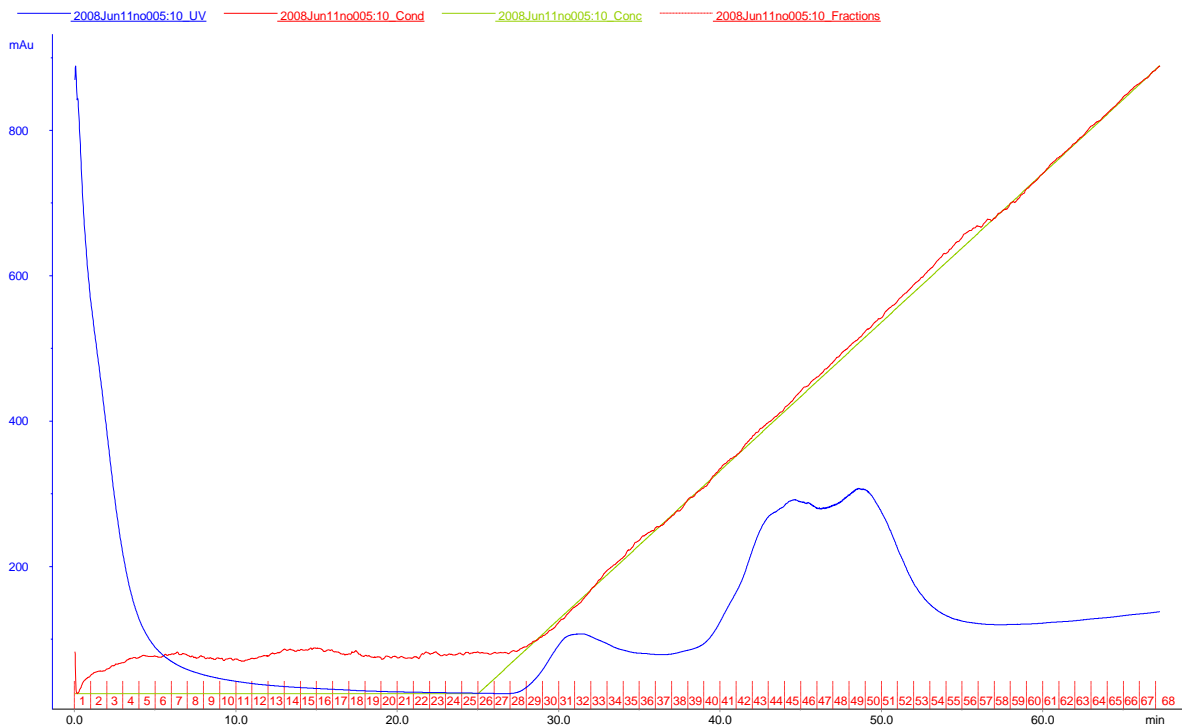


Figure 2.30: Purification of *N*-terminally His-tagged recombinant lysostaphin (construct 1) using IMAC. Cell lysate extracted from recombinant *E. coli* BL21(DE3) cultured in 4 x 1 L AIM was applied to the Chelating Sepharose™ Fast Flow media column. Bound protein was eluted by applying an increasing imidazole concentration (20-500 mM). A) First application of CFE, B) Second application of CFE.

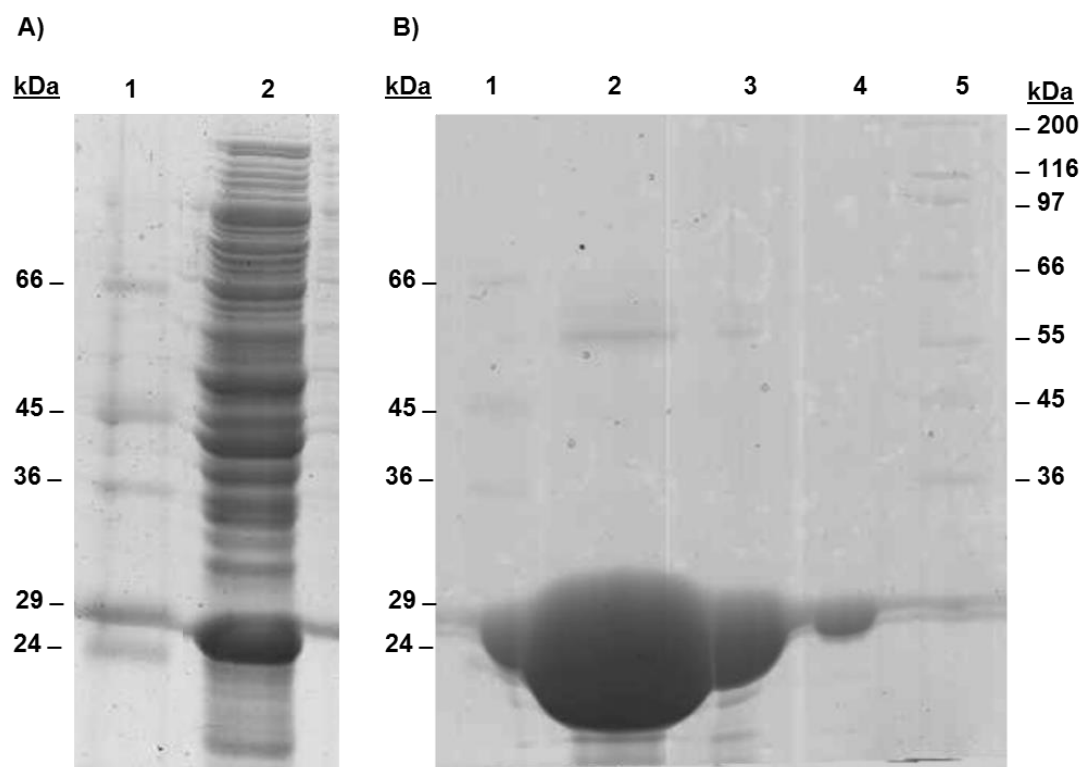


Figure 2.31: SDS-PAGE analysis of C-terminally His-tagged recombinant lysostaphin (construct 3). A) Expression of construct 3 in *E. coli* BL21(DE3) grown in AIM (4L culture volume). Lane 1: Sigma low molecular weight markers; Lane 2: CFE (neat). B) Concentrated purified recombinant lysostaphin following multiple IMAC purifications. Lane 1: Sigma low molecular weight markers; Lane 2: concentrated protein (neat); Lane 3: concentrated protein (1:10); Lane 4: concentrated protein (1:100); Lane 5: Sigma high molecular weight markers

2.5.3.8 Large-scale purification of recombinant lysostaphin by IMAC using Chelating Sepharose™ Fast Flow media and a peristaltic pump

To purify larger amounts of recombinant protein in an efficient manner, IMAC purification was performed using a peristaltic pump and a chelating sepharose column with greater binding capacity. Cell lysate containing recombinant lysostaphin (construct 1) (Appendix 7.101 B and Figure 2.13.C) was applied to a nickel column and purification was achieved by step elution using a peristaltic pump. SDS-PAGE analysis suggested that the highest concentration of protein was eluted following application of elution buffer containing 300 and 400 mM imidazole (Figure 2.32). The eluted protein was concentrated by lyophilisation, however following resuspension, recombinant lysostaphin protein did not regain full solubility, which interfered with the effectiveness of subsequent chromatographic analysis (Section 3.4.3.3).

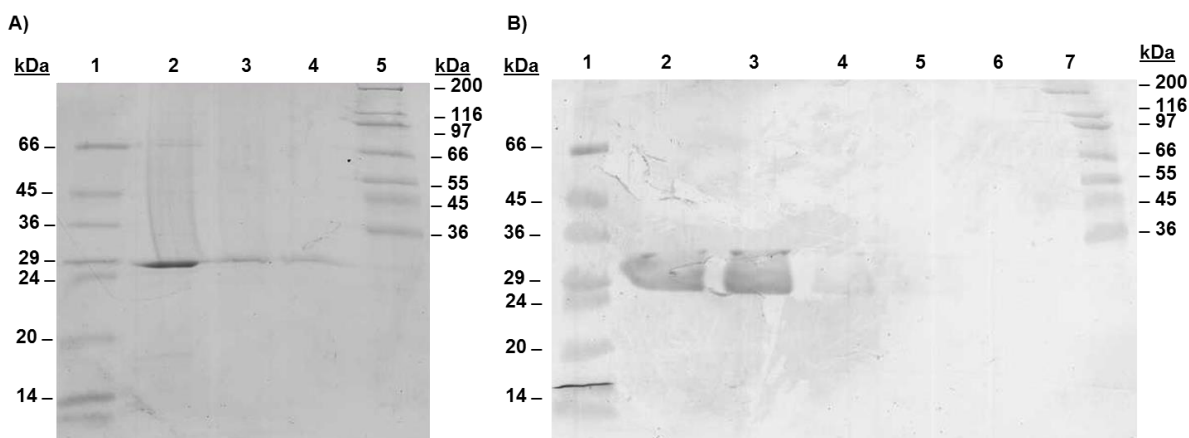


Figure 2.32: SDS-PAGE analysis of IMAC fractions following IMAC purification of *N*-terminally His-tagged recombinant lysostaphin (construct 1) produced in *E.coli* BL21(DE3). A) IMAC purification of recombinant lysostaphin derived from 15 x 1 L shake-flask cultures of AIM. Lane 1: Sigma low molecular weight markers; Lane 2: 200 mM imidazole elution; Lane 3: 300 mM imidazole elution; Lane 4: 400 mM imidazole elution; Lane 5: Sigma high molecular weight markers. B) IMAC purification of recombinant lysostaphin derived from 14 x 1 L shake-flask cultures of LB. Lane 1: Sigma low molecular weight markers; Lane 2: 200 mM imidazole elution (A); Lane 3: 200 mM imidazole elution (B); Lane 4: 300 mM imidazole elution; Lane 5: 400 mM imidazole elution; Lane 6: 500 mM imidazole elution; Lane 7: Sigma high molecular weight markers.

2.5.3.9 Purification of recombinant lysostaphin from *E. coli* cell lysate using an Ultimate™ 3000 system and a ProPac® IMAC-10 column

As IMAC purification using the ÄKTA™ system was fairly time consuming (Figure 2.33), IMAC purifications were also performed using an Ultimate™ 3000 system with a ProPac® IMAC-10 (4 x 250 mm) column (Figure 2.34). SDS-PAGE analysis of fractions eluted during comparative IMAC purifications demonstrated that the ProPac® IMAC column provided a higher degree of protein purification than the Chelating Sepharose™ Fast Flow column did (Figure 2.35). Due to operating at a lower flow rate (0.5 ml/min) than the Chelating Sepharose™ Fast Flow column (5 ml/min), total elution volumes were reduced, which beneficially reduced the duration of sample concentration. The ability to rapidly purify His-tagged proteins was explained in further depth in a Dionex customer application note, entitled “Rapid His-tag Purification of Recombinant Proteins using Dionex ProPac IMAC columns” (Appendix 7.135).

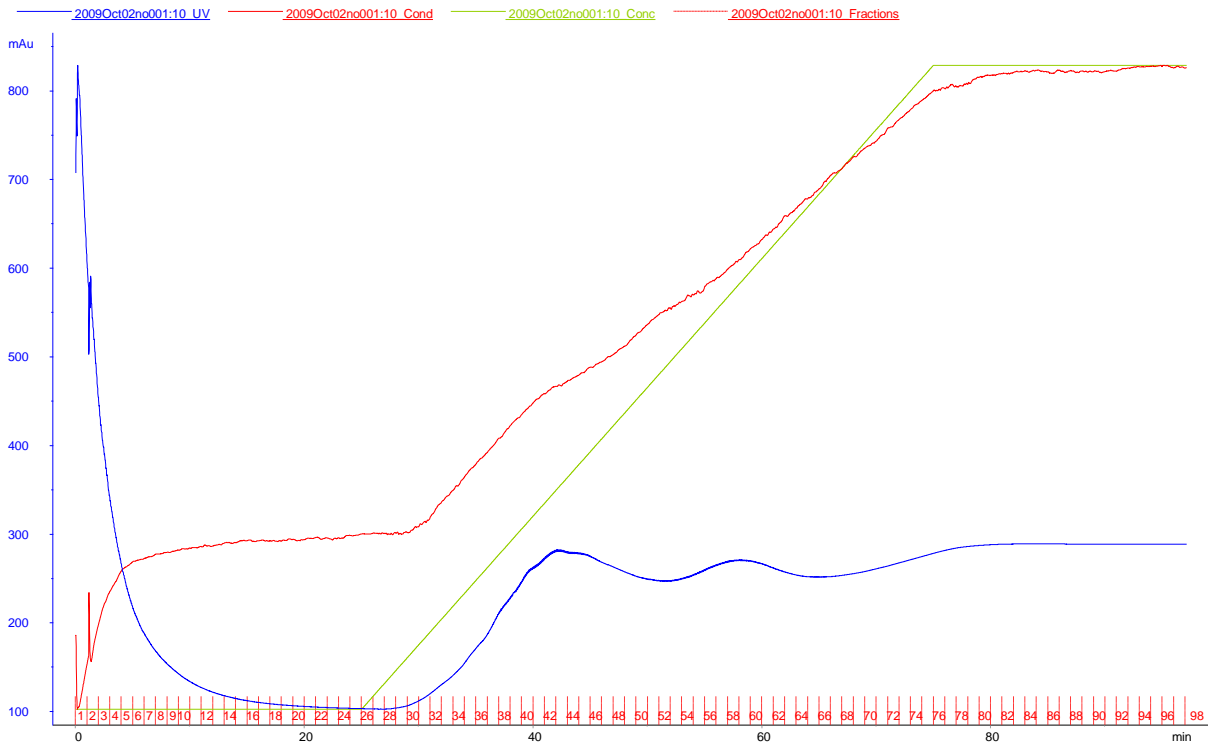


Figure 2.33: IMAC purification of recombinant lysostaphin (construct 1) using a Chelating Sepharose™ Fast Flow column and ÄKTA™ purification system.

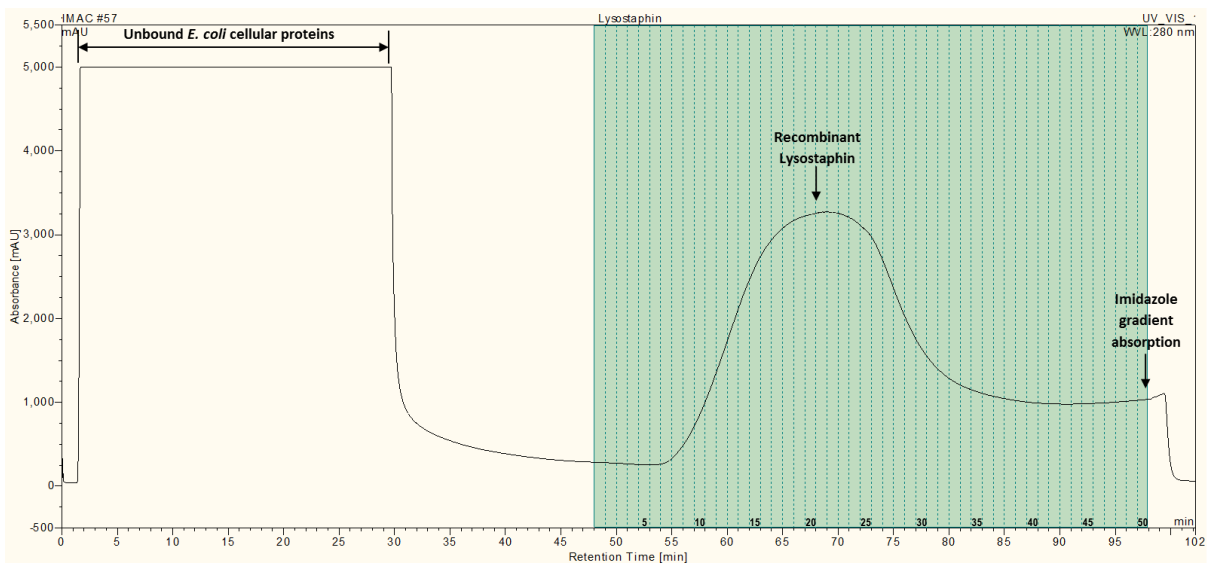


Figure 2.34: IMAC purification of recombinant lysostaphin (construct 1) using a ProPac® IMAC-10 column (4.0 x 250 mm) and Ultimate™ 3000 system. Fractions were collected by time between 48 and 98 min and fractions 7, 11, 15, 19, 23, 27, 31 and 35 were analysed by SDS-PAGE. The increasing imidazole concentration was detected at 280 nm, as indicated. This background absorbance was removed in subsequent chromatograms, through arithmetic combination against a blank UV trace.

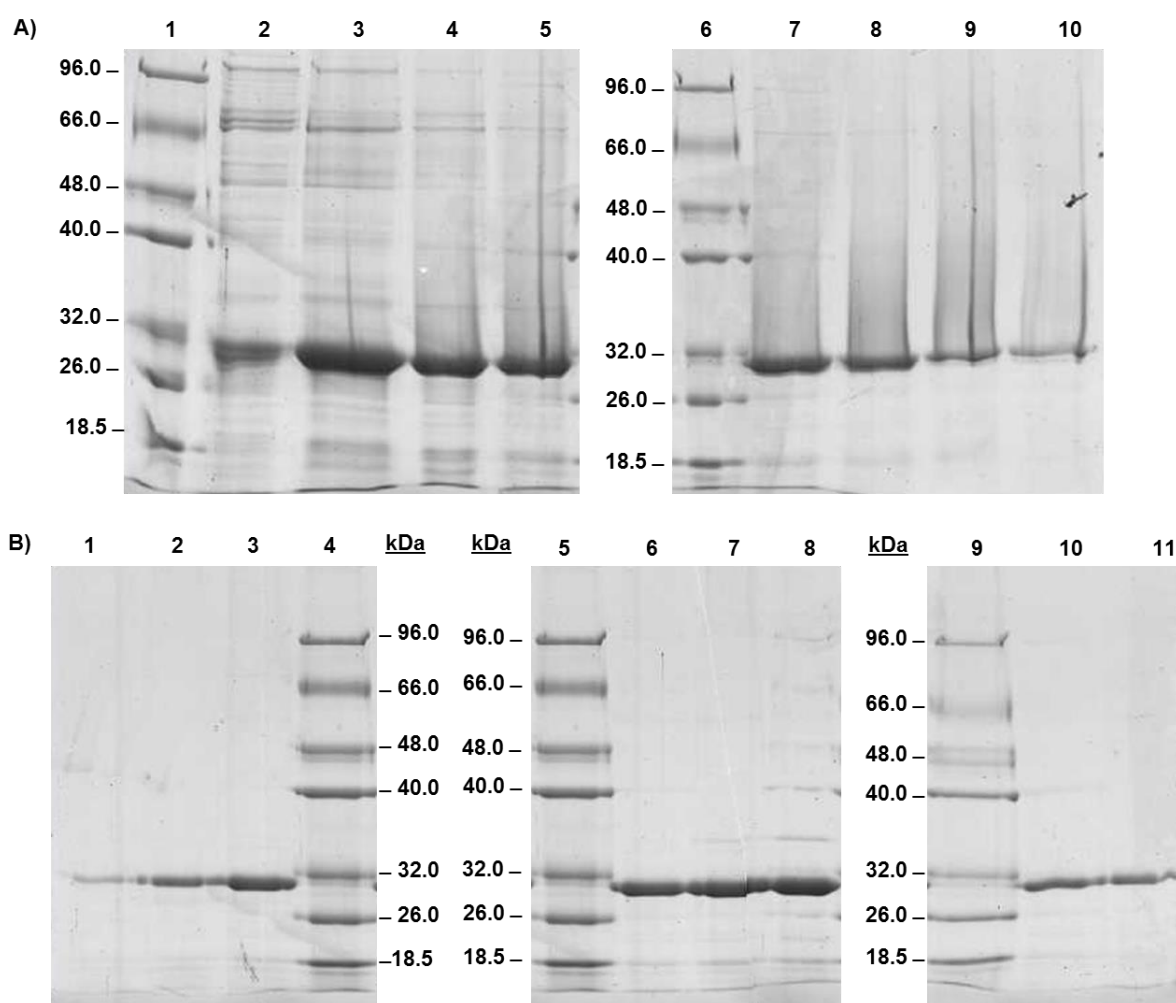


Figure 2.35: SDS-PAGE analysis of IMAC fractions following purification of *N*-terminally His-tagged recombinant lysostaphin (construct 1) derived from *E.coli* BL21(DE3) cultured in LB. A) IMAC purification performed using an ÄKTA™ purification system. Lane 1: NZY molecular size markers; Lane 2: Fraction 34 (neat); Lane 3: Fraction 38 (neat); Lane 4: Fraction 42 (neat); Lane 5: Fraction 46 (neat); Lane 6: NZY molecular size markers; Lane 7: Fraction 50 (neat); Lane 8: Fraction 54 (neat); Lane 9: Fraction 58 (neat); Lane 10: Fraction 62 (neat). B) IMAC purification performed using an Ultimate™ 3000 purification system. Lane 1: Fraction 7 (1:10); Lane 2: Fraction 11 (1:10); Lane 3: Fraction 15 (1:10); Lane 4: NZY molecular size markers; Lane 5: NZY molecular size markers; Lane 6: Fraction 19 (1:10); Lane 7: Fraction 23 (1:10); Lane 8: Fraction 27 (1:10); Lane 9: NZY molecular size markers; Lane 10: Fraction 31 (1:10); Lane 11: Fraction 35 (1:10).

2.5.3.10 IMAC using ProPac® IMAC columns (2 x 250 mm)

ProPac® IMAC-10 columns were also available in a 2 x 250 mm format which permitted faster IMAC purification due to a reduced column volume. The overall binding capacity of the column was initially unknown, however injection of varying amounts of purified recombinant lysostaphin, demonstrated that the column could comfortably bind 8 µg and 40

μg of protein with minimal flow-through of non-binding protein (Figure 2.36). However the application of 40 μg resulted in considerable band broadening due to longitudinal diffusion.

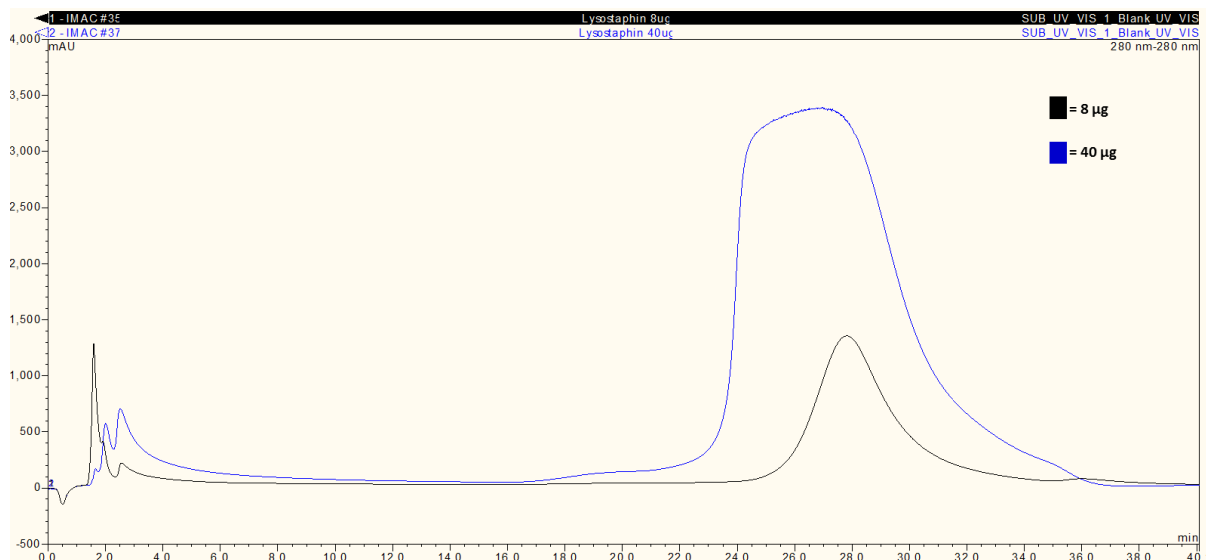


Figure 2.36: Comparison of peak height following application of 8 and 40 μg of purified *N*-terminally His-tagged recombinant lysostaphin.

2.5.3.11 IMAC using ProPac[®] IMAC columns (4 x 250 mm)

To achieve a greater binding capacity, IMAC purification was performed using a ProPac[®] IMAC-10 column with a 4 mm diameter. The chromatographic method was modified to allow CFE loading and the capacity of the 4 x 250 mm column was assessed by applying cell lysate harvested from 2 L of culture expressing recombinant lysostaphin (construct 3), with the intention that the capacity of the column would be exceeded. The first application of cell lysate resulted in a single peak with a high UV absorbance reading at 280 nm (Figure 2.37).

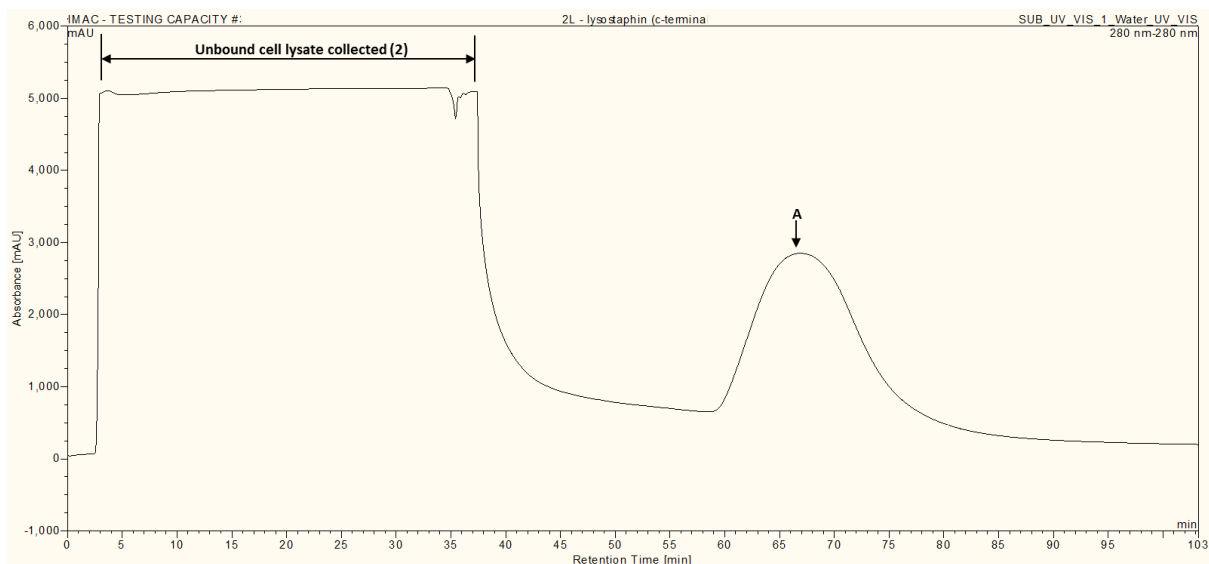


Figure 2.37: Purification of recombinant lysostaphin (construct 3) from *E. coli* cell lysate (1) using an Ultimate™ 3000 System and ProPac® IMAC-10 (4 x 250 mm). A single peak reflecting purified recombinant lysostaphin (construct 3) was observed (peak A). Unbound cell lysate (2) was collected manually as indicated and re-applied to the column.

The unbound cell lysate (2) was collected manually (outside of the fraction collection period) and re-applied to the ProPac® IMAC column to purify any recombinant lysostaphin which was still left in the unbound cell lysate. Figure 2.38 demonstrates that application of unbound cell lysate (2) to the column resulted in another single peak (Peak B). The peak height of Peak B was very similar to that of Peak A suggesting that the column capacity of the ProPac® IMAC column was reached at a peak height of 3000 mAU. The total amount of purified recombinant lysostaphin eluted within peak B was determined to be 9.72 mg. PAGE analysis confirmed that both peaks A and B contained a protein with the same molecular weight as recombinant lysostaphin (construct 3), regardless of differences in peak retention times (Figure 2.39).

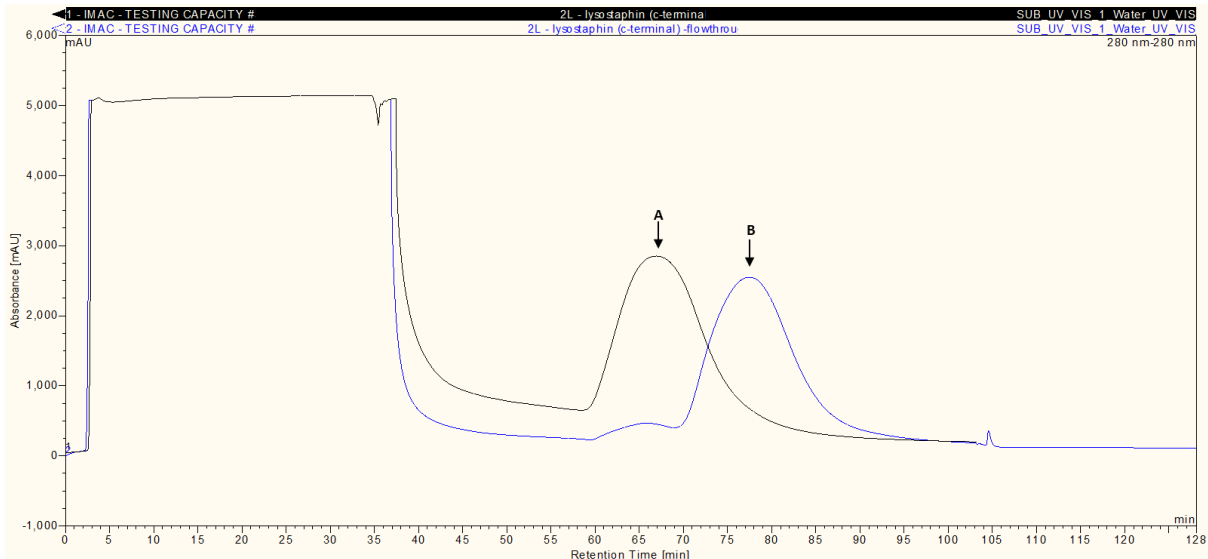


Figure 2.38: Comparison of elution peaks following the application of cell lysate (1) and re-application of unbound cell lysate (2) flow-through. The re-application of unbound cell lysate resulted in elution of a single peak (B) at a retention time which was longer than that of the elution of peak A after initial application of cell lysate.

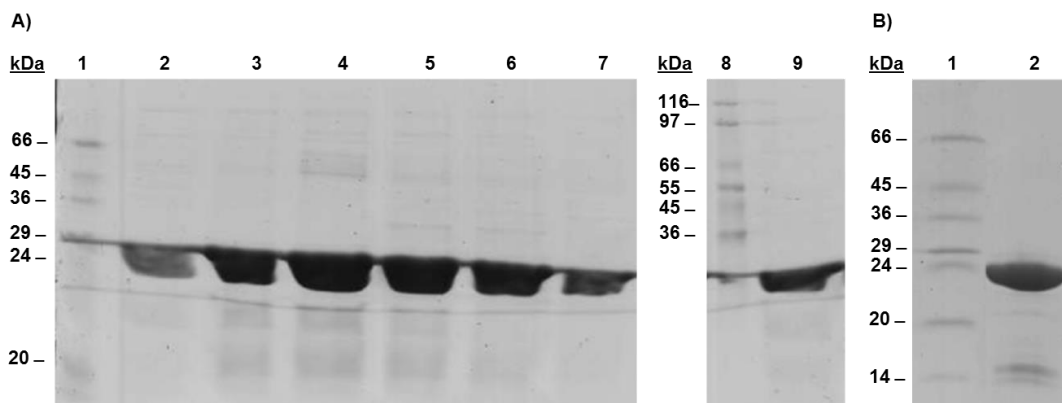


Figure 2.39: SDS-PAGE analysis of IMAC fractions and concentrated purified protein following IMAC purification of C-terminally His-tagged recombinant lysostaphin (construct 3) derived from *E.coli* BL21(DE3) cultured in LB. A) IMAC fraction collected during elution of peak A. Lane 1: Sigma low molecular weight markers; Lane 2: Fraction 5; Lane 3: Fraction 11; Lane 4: Fraction 14; Lane 5: Fraction 17; Lane 6: Fraction 20; Lane 7: Fraction 23; Lane 8: Sigma high molecular weight markers; Lane 9: Fraction 27. B) Concentrated protein pooled from IMAC fractions 31-34 collected during elution of peak B. Lane 1: Sigma low molecular weight markers; Lane 2: concentrated protein (neat).

2.5.4 Discussion

After testing a number of protein purification techniques, it was evident that recombinant lysostaphin could be efficiently and successfully separated from contaminating *E. coli* proteins following recombinant protein expression. By performing protein purification it became apparent that sufficient amounts of recombinant lysostaphin could be recovered following batch culture, permitting subsequent separation and characterisation of the recombinant product. In addition, it became clear that recombinant lysostaphin could be effectively purified using single chromatographic separations, which was extremely desirable given the increased potential for protein modifications or degradation to occur over extended periods of time.

Despite its ease and convenience, ASF did not offer differential purification of recombinant lysostaphin on the grounds of solubility. Though recombinant lysostaphin was predicted to be a relatively hydrophilic protein, this putative hydrophilicity did not prevent precipitation of recombinant lysostaphin at fairly low concentrations of ammonium sulphate. Although ASF was not effective for purification, ammonium sulphate precipitation was also employed as a mode of sample concentration during protein purification. Recombinant lysostaphin could be effectively precipitated, however it was found that the recombinant protein could not be successfully resuspended following precipitation in two instances, prior to GF and following large-scale IMAC purification.

These findings indicated that ammonium sulphate precipitation had a detrimental influence on the solubilisation of recombinant lysostaphin. In order to achieve solubilisation, the precipitated protein molecules must regain monomolecular dispersion, without participating in non-native intra- or inter-molecular interactions (Tsumoto *et al.*, 2003). Full solubilisation can often require the addition of inorganic salts, such as sodium chloride, which increases ionic strength and encourages protein solubility (Vuillard *et al.*, 1995). Whilst resuspension of precipitated protein in buffers containing inorganic salts may have resolubilised recombinant lysostaphin, this approach was not desirable given that the presence of fairly high salt concentrations can interfere with consequent biological assays, electrophoresis or IEX.

Although ASF cannot provide successful purification of recombinant lysostaphin, the technique is highly compatible with HIC. However HIC also did not offer efficient separation of recombinant lysostaphin from contaminating *E. coli* proteins. SDS-PAGE analysis revealed that a second chromatographic purification step was required to achieve protein purification. Subsequent GF provided a high degree of protein purification following HIC,

indicating that recombinant lysostaphin could be successfully purified using a combination of HIC and GF. However, GF offers low productivity and high resolution that is only once the protein sample has been concentrated to a volume which reflects less than 5% of the total column volume (Jungbauer, 2005). Prior sample concentration increases the length of time taken to recover recombinant lysostaphin from contaminating protein, which could have increased the incidence of protein degradation or modification during handling and storage.

As HIC could not offer purification in a single chromatographic step, IEX was performed using AXC to see if recombinant lysostaphin could be efficiently purified. As ProtParam analysis revealed that all of the recombinant lysostaphin constructs had a theoretical pI of between 9.52 and 9.72, it was expected that as a basic protein, recombinant lysostaphin would be unlikely to bind at neutral pH during AXC. This prediction was confirmed following AXC of cell lysates containing recombinant lysostaphin (constructs 2, 4 and 5), which did not appear to bind to the anion exchange resin. As the majority of cellular proteins are acidic, a very high number of proteins bound to the anion exchange resin, as revealed by SDS-PAGE. It therefore would have been extremely difficult to isolate recombinant lysostaphin from the *E. coli* cellular proteins had the protein been successfully retained during AXC.

Whilst recombinant lysostaphin could not be successfully purified during AXC, CXC was found to provide an excellent degree of protein purification. SDS-PAGE analysis revealed that fractions eluted during CXC contained very few contaminating proteins, suggesting that only a limited number of proteins present within the *E. coli* cell lysate could be retained on the cation exchange resin. CXC therefore provided fairly rapid, one-dimensional chromatographic purification of recombinant lysostaphin in the presence and absence of His-tag sequences, a trait which was exploited to further advantage in Chapter 3.

His-tagged recombinant lysostaphin was also purified using IMAC which was performed using an ÄKTA™ purification system or an Ultimate™ 3000 Titanium system. Both chromatographic systems offered preparative purification of recombinant lysostaphin, however the Ultimate™ 3000 system was primarily developed for analytical separations, as described in Chapter 3. Initial preparative purifications performed using the ÄKTA™ system and a chelating fast-flow sepharose column generally resulted in a high degree of purification, without the need for any additional purification steps prior to protein analysis. In one instance, IMAC was followed by GF to remove a few low molecular weight contaminants, however it was found that the extra purification provided by GF was not worthwhile given the additional time and cost of purification.

When producing larger amounts of recombinant lysostaphin, it was still possible to successfully purify recombinant lysostaphin using consecutive IMAC purifications. However this approach extended the duration of purification which was not desirable. Large-scale IMAC purification using a greater capacity chelating sepharose column and peristaltic pump was therefore performed and provided high quality purification. However due to the use of step elution, recombinant lysostaphin was recovered in fractions of a large volume, which meant that lengthy sample concentration was required using dialysis and lyophilisation. The analytical quality of the lyophilised recombinant lysostaphin was examined in Section 3.4.3.3 and 4.3.3.2.

To reduce the duration of purification, IMAC purification was also performed using ProPac[®] IMAC-10 columns and an Ultimate[™] 3000 system. After performing comparative IMAC purifications using the chelating sepharose and ProPac[®] IMAC-10 columns, SDS-PAGE analysis revealed that a greater degree of purity could be obtained using the ProPac[®] IMAC-10 columns, over a shorter purification period (Appendix 7.135). The duration of purification could be reduced further by using a 2.0 mm diameter ProPac[®] IMAC column, however greater binding capacity could be achieved using a ProPac[®] IMAC column with a 4.0 mm diameter. In testing column capacity, it became apparent that the chromatographic peaks were subject to retention time shifting. This phenomenon often arises due to variation in mobile phase pH or ionic strength, though in this instance may have been explained by *N*-terminal His-tag heterogeneity as discussed in Section 4.2.

This work demonstrated that recombinant lysostaphin could be purified to near homogeneity using CXC. His-tagged recombinant lysostaphin could also be purified to a high degree using IMAC via ÄKTA[™] or Ultimate[™] 3000 systems. The ability to purify recombinant lysostaphin was imperative to prevent PTM of the expressed protein by enzymes or reactive intermediates present in the cell lysate. Following purification, recombinant lysostaphin could be effectively desalted and concentrated by ultrafiltration, which is commonly used for pre-concentration prior to protein analysis (Eykamp, 1991). Although ultrafiltration devices have been developed to allow rapid desalting and concentration of proteins, current ultrafiltration membranes are fairly thick and therefore it often takes hours or days for unwanted molecules to pass through the membranes (Striemer *et al.*, 2007). During which time the recombinant protein may become aggregated or undergo non-enzymatic modifications, such as glycation or deamidation, which often propagate upon extended processing or storage (Mironova *et al.*, 2003, Ren *et al.*, 2009).

During protein purification, protein yield and activity are typically monitored during and following chromatographic steps. The overall amount of purified protein was dependent on

the recombinant lysostaphin construct, expression media composition and volume and the chosen purification strategy. Following purification, 1-60 mg of recombinant lysostaphin was recovered from litre batch cultures. Evidently increased protein amounts were obtained following purification of cell lysate derived from larger culture volumes. In addition, purifications performed using preparative resins tended to provide higher yields due to providing greater binding capacity. However analytical ProPac[®] IMAC-10 columns offered faster purification and a better degree of protein purification than preparative IMAC columns.

The activity of purified recombinant lysostaphin preparations was regularly monitored to ensure staphylolytic activity was retained following protein processing and purification, as described in Section 4.1. Purified recombinant lysostaphin was also subjected to chromatographic separation with the intention of separating and identifying distinct protein isoforms, as documented in Chapter 3.

2.6 Discussion

The gene sequence encoding the mature lysostaphin domain from *S. staphylolyticus* was amplified and cloned in *E. coli* using a combination of PCR and gene cloning techniques. Cloning of the mature lysostaphin domain was uneventful and led to the production of five pET vector constructs, which could be used to express recombinant lysostaphin with or without *N*- or *C*-terminal His-tags, within the cytoplasm or the periplasm of *E. coli* BL21(DE3). However sequencing of the pET vector constructs 1, 2 and 3 led to the elucidation of two nucleotide mis-matches within the lysostaphin gene sequence published by Heinrich *et al.*, (1987). These nucleotide mis-matches were confirmed by the work of Gargis *et al.* (2010), who sequenced the pACK1 plasmid of *S. staphylolyticus*, which encodes the lysostaphin gene (Gargis *et al.*, 2010, Heinrich *et al.*, 1987).

Whilst the mis-identification of cytosine at position 456 was not found to alter the translation of proline₁₅₂, mis-identification of cytosine at position 96, was found to result in the translation of methionine₃₂ rather than isoleucine₃₂. The presence of a guanine rather than cytosine at position 96 was unlikely to have significantly altered the physicochemical properties of recombinant lysostaphin, however increased the predicted mass of the protein by 18 Da. This mass increment was not particularly significant; however knowledge of this amino acid substitution was useful during characterisation of recombinant lysostaphin, in which the correct amino acid sequence was required (Section 4.4).

Once transformed into *E. coli* BL21(DE3), all five pET vector constructs were found to express a recombinant protein with a molecular weight that corresponded with the expected weight of cloned recombinant lysostaphin (with or without *N*- or *C*-terminal His-tag sequences). Expression of pET constructs 4 and 5, which featured *pelB* leader sequences, were also found to lead to effective translocation of recombinant lysostaphin to the periplasmic space. In the majority of experiments recombinant lysostaphin was hyper-expressed in a largely soluble form, even when *E. coli* BL21(DE3) was cultured in different expression media.

Following expression, it was found that recombinant lysostaphin could be successfully purified using IMAC, HIC, GF and CXC to achieve a high level of purity. However the most efficient purification could be achieved using IMAC or CXC in a single chromatographic step. Single-stage purification was essential to ensure that purified recombinant lysostaphin could be obtained rapidly so as to prevent sample degradation or modification during purification or storage. CXC provided selective purification of recombinant lysostaphin from contaminating

anionic proteins present within the cell lysate. This trait was exploited to further advantage in Chapter 3.

N-terminally His-tagged recombinant lysostaphin (construct 1) was most commonly expressed and was purified using IMAC due to the high purity that the technique could provide. However this technique was used with caution as several recombinant proteins expressed in *E. coli* have exhibited *N*-terminal His-tag heterogeneity (She *et al.*, 2010, Du *et al.*, 2005a, Du *et al.*, 2005b). Unusual retention behaviour was observed during IMAC purification of recombinant lysostaphin, therefore retention behaviour was examined further (Section 4.2) to assess whether potential His-tag modifications interfered with the efficiency of purification.

Once purified, the structure and heterogeneity of recombinant lysostaphin could be investigated further by using a variety of chromatographic approaches to separate recombinant protein isoforms for further high-resolution characterisation using proteomic techniques, as described in Chapters 3 and 4.

3 Separation of Recombinant Lysostaphin Isoforms

3.1 Introduction

Following protein purification, a recombinant protein preparation should be assessed to establish whether the protein population is homogeneous. In the biotechnological and pharmaceutical industry, assessment of product heterogeneity is critical to ensure that the resulting protein demonstrates stability and consistency. However, as reported in Chapter 1, recombinant protein preparations may be composed of protein variants which demonstrate considerable charge heterogeneity. Such charge variants arise during expression or purification, as a consequence of chemical or enzymatic reactions (Pabst *et al.*, 2008, Weitzhandler *et al.*, 2001). The separation of protein charge variants is therefore of growing importance and can be achieved using a number of electrophoretic and chromatographic techniques. As charge variants differ in their pI, electrophoretic separations featuring isoelectric focusing (IEF) such as 2D-PAGE and capillary electrophoresis (CE) can be used to separate protein variants.

High-resolution HPLC is commonly used to detect protein variants, as the technique can reveal subtle modifications of protein structure (Jacobson *et al.*, 1997). IEX is particularly popular due to its ability to separate and resolve charge variants (Weitzhandler *et al.*, 2001, Ren *et al.*, 2009). The charge heterogeneity of recombinant proteins is typically assessed using CXC. CXC separates proteins according to surface charge distribution and can resolve protein isoforms according to localised charge differences, caused by the presence or absence of chemical or enzymatic modifications. For instance, CXC is commonly used to assess the charge heterogeneity of recombinant monoclonal antibody variants which exhibit local charge differences and elution profiles due to the presence or absence of oligosaccharides (Gaza-Bulsecu *et al.*, 2008, Lyubarskaya *et al.*, 2006).

Once separated, chromatographic fractions containing resolved charge variants can be isolated for subsequent analysis more conveniently than when using electrophoretic techniques. Due to the ability of IEX to provide high-resolution separation of recombinant protein variants, IEX was used to assess the charge heterogeneity of purified recombinant lysostaphin. This research was performed with a number of aims:

Aims:

- To resolve and separate recombinant lysostaphin isoforms using an appropriate analytical ion exchange column.
- To optimise chromatographic separation of recombinant lysostaphin isoforms
- To investigate factors affecting charge heterogeneity of recombinant lysostaphin during recombinant protein expression

3.2 Methods

3.2.1 Buffers

All buffer compositions are outlined in Appendix 7.136.

3.2.2 Equipment

All equipment used during the separation of recombinant lysostaphin isoforms is outlined in Appendix 7.137.

3.2.3 Sample preparation

Sample preparation is described in Appendix 7.139.

3.3 Column selection

3.3.1 Introduction

In Section 2.5.3.5, CXC was shown to provide efficient purification of recombinant lysostaphin. During purification, conditions were optimised to provide capture and purification of the target protein. Such preparative chromatography achieved resolution using columns that provided low efficiency, yet high selectivity (Jungbauer, 2005). However during analytical chromatography, protein separation is optimised for informative purposes by using columns which provide maximum efficiency. Following the success of CXC during purification, it was therefore hoped that recombinant lysostaphin isoforms could be separated effectively using analytical IEX. In this section, chromatographic separations were performed using a number of IEX columns developed to provide high-resolution protein separation. Recombinant lysostaphin was applied to ProPac™ and ProSwift™ ion exchange columns to establish which type of stationary phase composition and ion exchange functionality could provide separation of recombinant lysostaphin variants.

Chromatographic separations were initially performed using ProPac® WCX-10, SCX-10 and SAX-10 columns, however a ProPac® MAb SCX beta test column also became available for separations in the later stages of this research. ProPac™ IEX columns are composed of a non-porous, tentacle-type polymeric stationary phase, which consists of 10 µm diameter polystyrene particles (55% cross-linked). Polymeric supports can tolerate a wide pH range and offer high mechanical stability which is beneficial during IEX. Furthermore, the polymethacrylate stationary phase is coated in a hydrophilic film to prevent non-specific hydrophobic interactions with the analyte (Weitzhandler *et al.*, 2001). Minimisation of non-specific interactions ultimately leads to higher yields (Melter *et al.*, 2007).

To provide ion exchange functionality, the pellicular stationary phase particles of ProPac® SCX-10 and MAb SCX were grafted with sulphonate functional groups, whilst the ProPac® WCX-10 and SAX-10 were derivatised with carboxylate and quaternary amine groups respectively. These grafted functional groups confer high selectivity upon the column, however the nature of pellicular stationary phase composition reduces the surface area for derivatisation and therefore decreases column capacity (Melter *et al.*, 2007).

Chromatographic separations were also performed using ProSwift™ ion exchange columns which are composed of polymethacrylate monoliths. Recombinant lysostaphin was applied to ProSwift® WCX-1S and SCX-1S columns, which had been chemically grafted with

carboxylate and sulphonate groups respectively (Evenhuis *et al.*, 2008). ProSwift™ columns offer high resolution yet faster mass transfer and high loading capacity than their ProPac™ counterparts (Rao *et al.*, 2010). Like ProPac™ ion exchange columns, ProSwift™ columns also exhibit stability over a wide range of pH due to their polymethacrylate composition (Nordborg and Hilder, 2009).

ProPac™ Ion Exchange columns have previously been used to provide high-resolution separation of monoclonal antibody (mAb), cytochrome C, ribonuclease A and haemoglobin variants (Melter *et al.*, 2007, Heckenberg *et al.*, 2002). It has also been reported that protein isoforms differing by a single charged residue can be resolved using ProPac™ ion exchange columns, permitting evaluation of protein micro- and macro-heterogeneity (Heckenberg *et al.*, 2002). Monolithic ion exchange columns, such as ProSwift™ Ion Exchange can also be used to resolve protein isoforms, however they tend to be less frequently employed during IEX applications than particle columns, despite sharing the same advantages (Nordborg *et al.*, 2009).

Aims:

- To confirm that recombinant lysostaphin does not bind to analytical anion exchange columns.
- To establish whether recombinant lysostaphin isoforms can be resolved using strong or weak cation exchange columns.
- To compare the degree of separation and resolution of protein isoforms provided by weak or strong ion exchange functionalities.
- To assess whether ProPac™ or ProSwift™ ion exchange columns provided better resolution and separation of protein isoforms.

3.3.1 Methods

3.3.1.1 Column selection

A number of initial separations were performed to assess the separative capacity and resolution of ProPac[®] SAX-10, SCX-10 and WCX-10 columns using the DX500 chromatography system (Appendix 7.168) or an Ultimate[™] 3000 chromatography system (Appendix 7.169). The performance of the ProPac[®] WCX-10 (4 x 500 mm) column was also validated (Appendix 7.170). Additional separations were performed using the ProSwift[®] SCX-1S (Appendix 7.171) and ProSwift[®] WCX-1S columns (Appendix 7.172). Separations were also performed using ProPac[®] MAb SCX beta test columns to provide column validation (Appendix 7.173) and separation of recombinant lysostaphin variants (Appendix 7.174).

3.3.2 Results

In this section, chromatographic separations were performed using a number of IEX columns developed to provide high-resolution protein separation. Recombinant lysostaphin was applied to ProPac™ and ProSwift™ ion exchange columns to establish which type of stationary phase composition and ion exchange functionality could provide separation of recombinant lysostaphin variants.

3.3.2.1 Protein separation using ProPac® SAX-10 column and DX500 chromatography system

Purified recombinant lysostaphin was applied to a variety of ion exchange columns to establish, whether the protein would bind to the resin. In Section 2.5.3.4, it was determined that recombinant lysostaphin was not retained during AXC and could only be retained by a preparative CXC column. To provide extra confirmation of this finding, recombinant lysostaphin was injected onto an analytical ProPac® SAX-10 (4 x 250 mm) column. As shown in Figure 3.1, recombinant lysostaphin did not bind to the column and the sample appeared to elute from the column at the start of the separation without being retained. The chromatogram also showed two spikes which probably occurred as a result of the air bubbles passing through the UV detector.

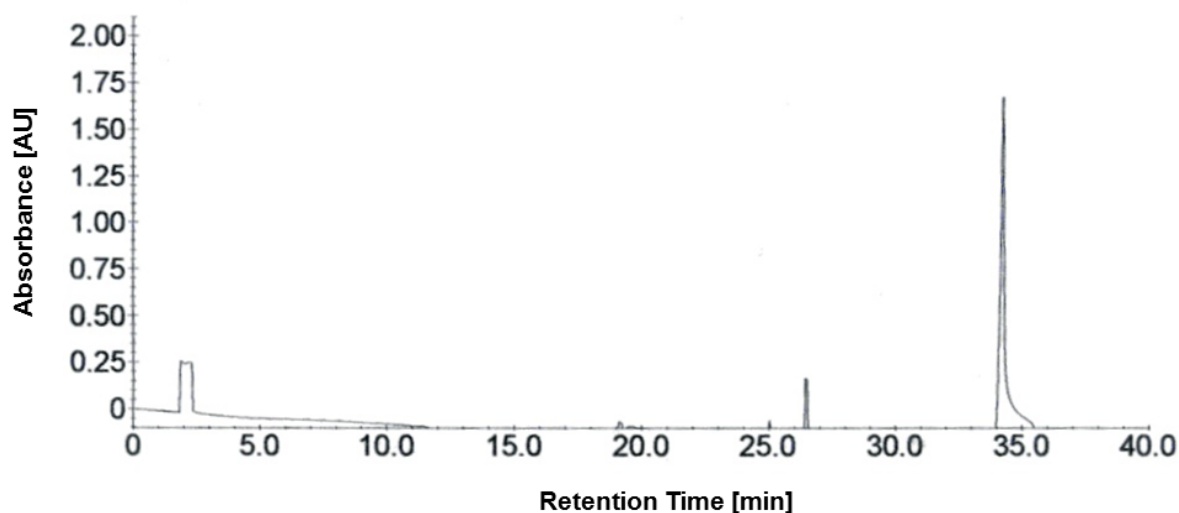


Figure 3.1: Separation of 5.5 mg of C-terminally His-tagged recombinant lysostaphin (construct 4; preparation 1) using a ProPac® SAX column (4 x 250 mm). Recombinant lysostaphin did not bind to this column as demonstrated by a breakthrough peak at the start of the separation. Absorbance was recorded at a wavelength of 280 nm.

3.3.2.2 Protein separation using ProPac® SCX-10 column and DX500 chromatography system

As recombinant lysostaphin did not bind to a SAX column, the purified sample was applied to a ProPac® SCX (4 x 250 mm) column. As Figure 3.2 shows, recombinant lysostaphin bound to a strong cation exchange resin. Despite being retained on the column, recombinant lysostaphin isoforms were not resolved by the SCX column.

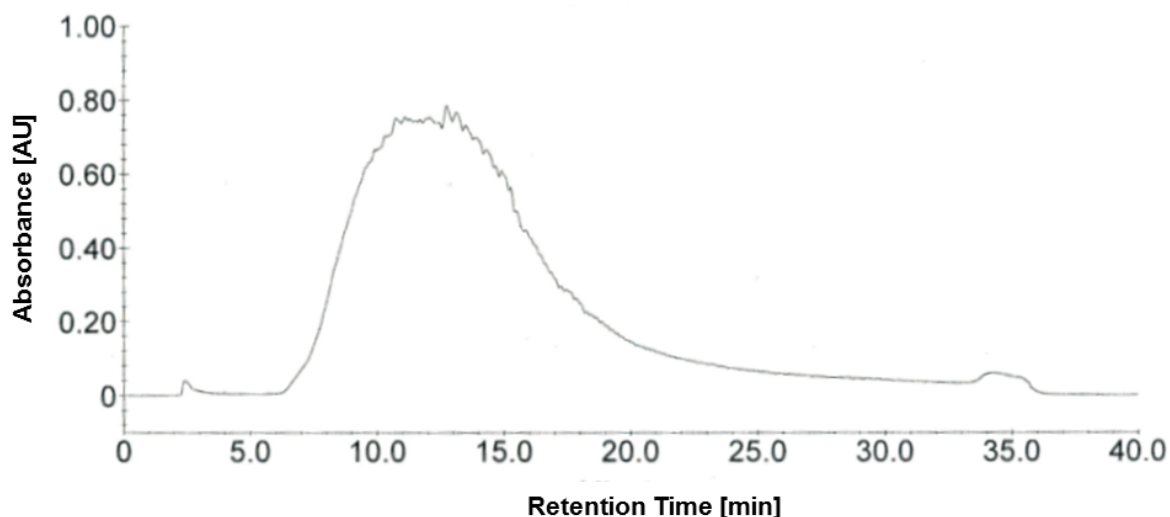


Figure 3.2: Separation of 5.5 mg of C-terminally His-tagged recombinant lysostaphin (construct 4; preparation 1) using a ProPac® SCX-10 column (4 x 250 mm). Recombinant lysostaphin bound to this column, resulting in a large peak eluting between 6.0 and 20.0 minutes. Absorbance was recorded at a wavelength of 280 nm.

3.3.2.3 Protein separation using ProPac® WCX-10 column and DX500 chromatography system

Consequently purified recombinant lysostaphin was applied to a ProPac WCX® (4 x 250 mm) column to establish if protein variants could be resolved using a WCX column. As demonstrated in Figure 3.3, recombinant lysostaphin was retained by the WCX column and it appeared that charge-distinct protein isoforms could be resolved as shoulder peaks during the WCX separation. SDS-PAGE analysis provided further confirmation that the peak observed during WCX separation reflected the presence of purified recombinant lysostaphin (Figure 3.4).

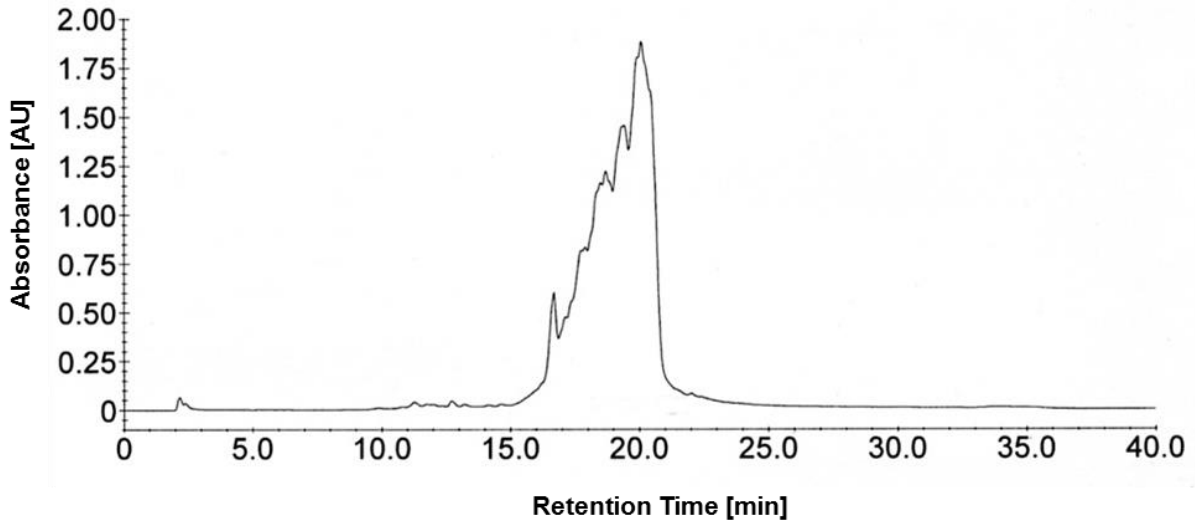


Figure 3.3: Separation of 5.5 mg of C-terminally His-tagged recombinant lysostaphin (construct 4; preparation 1) using a ProPac® WCX-10 column (4 x 250 mm). Recombinant lysostaphin bound to this column, resulting in a large peak eluting between 16.0 and 21.5 minutes. Additional shoulder peaks present within this peak indicated the resolution of protein isoforms. Absorbance was recorded at a wavelength of 280 nm.

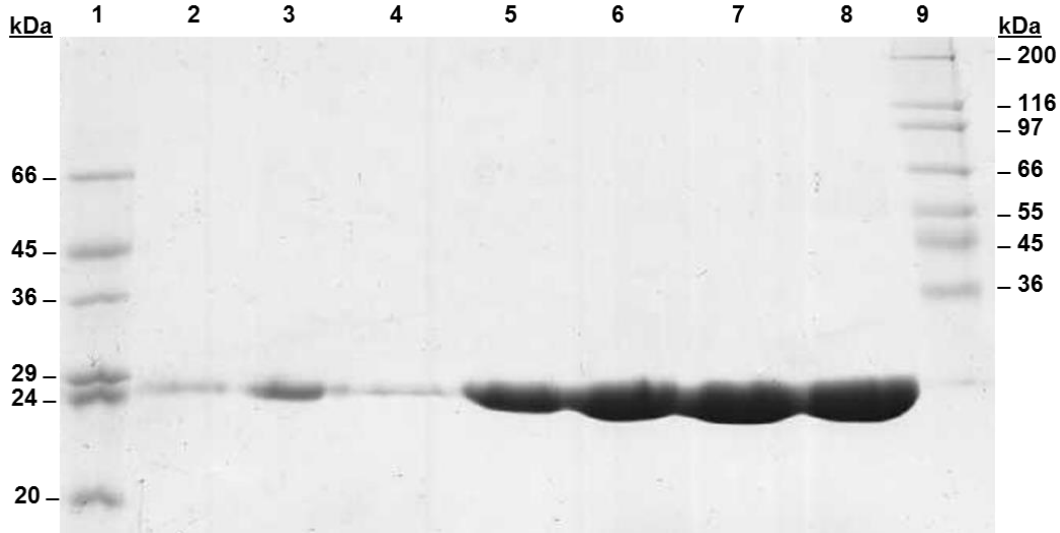


Figure 3.4: PAGE analysis of fractions eluted during WCX separation of purified C-terminally His-tagged recombinant lysostaphin (construct 4; preparation 1). Recombinant lysostaphin was expressed in *E. coli* BL21(DE3) cultured in AIM and was preparatively purified using IMAC prior to WCX separation. Following WCX separation, the eluted fractions were analysed by 12% (v/v) SDS-PAGE at neat concentration and whilst fraction collection is not indicated in Figure 3.3, corresponding retention times are provided in brackets. Lane 1: Sigma low molecular weight markers; Lane 2: Fraction 15 (15 min); Lane 3: Fraction 16 (16 min); Lane 4: Fraction 17 (17 min); Lane 5: Fraction 18 (18 min); Lane 6: Fraction 19 (19 min); Lane 7: Fraction 20 (20 min); Lane 8: Fraction 21 (21 min); Lane 9: Sigma high molecular weight markers.

Due to the success of this initial WCX separation, C-terminally His-tagged recombinant lysostaphin (construct 3) was also applied to the column as further assessment of the degree of separation and resolution provided by the ProPac® WCX-10 column. Figure 3.5 provided further evidence that the presence of protein isoforms could be established using this WCX column. During the early stages of the WCX separation (3-22 min), the UV trace at 280 nm appeared to be fairly erratic, suggesting interference by low level baseline noise, potentially due to mobile phase contaminants. Between 22 and 31 min, more authentic chromatographic peaks were observed indicating the presence of multiple protein isoforms. Further peaks were observed at retention times of 32 and 34 min indicating the resolution and separation of recombinant lysostaphin or protein contaminants.

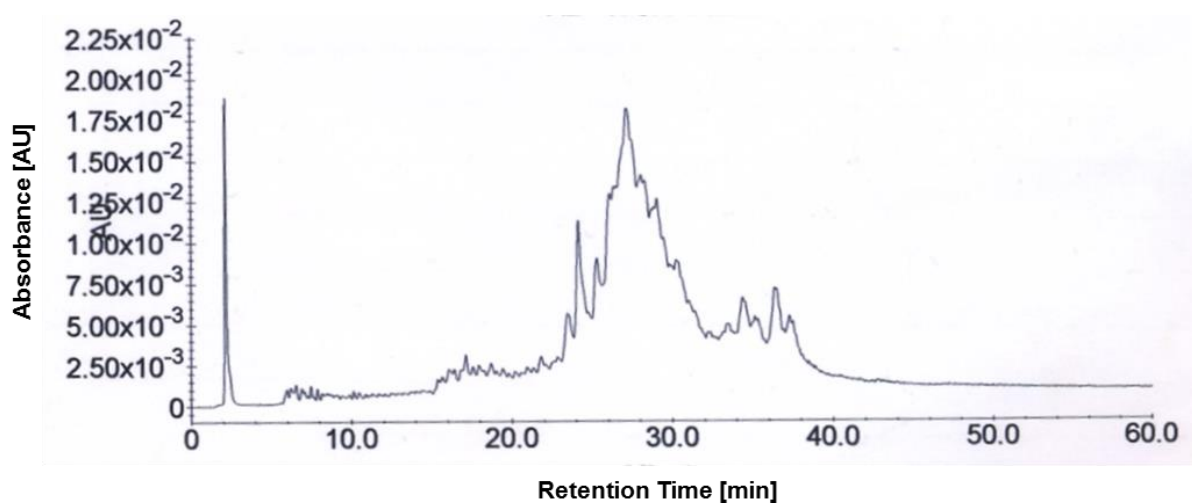


Figure 3.5: Separation of 0.8 mg of C-terminally His-tagged recombinant lysostaphin (construct 3; preparation 2) using a ProPac® WCX-10 column (4 x 250 mm). Recombinant lysostaphin bound to this column, resulting in the elution of multiple peaks between 22.0 and 39.0 minutes. The presence of multiple peaks indicates resolution of recombinant lysostaphin isoforms or possibly the presence of basic protein contaminants. The erratic UV trace between 6 and 22 min is likely to have reflected low level of baseline noise. UV absorbance was recorded at a wavelength of 280 nm.

Another preparation of C-terminally His-tagged recombinant lysostaphin (construct 3) which had been purified using preparative HIC and GF was also applied to the ProPac® WCX-10 column to separate protein variants. As shown in Figure 3.6, multiple peaks were resolved during WCX separation indicating the presence of recombinant lysostaphin isoforms. The wide distribution of peaks indicates that recombinant lysostaphin may have started to degrade, producing a greater number of charge variants. This theory is supported by PAGE analysis of the purified protein preparation (Figure 2.21) which demonstrated the presence of lower molecular weight bands which were likely to represent protein degradation. As the

protein preparation had been purified to near homogeneity using HIC and GF it was less likely that many of peaks represented protein contaminants. Unfortunately the protein concentration within fractions was not high enough to permit successful SDS-PAGE analysis of the eluted protein.

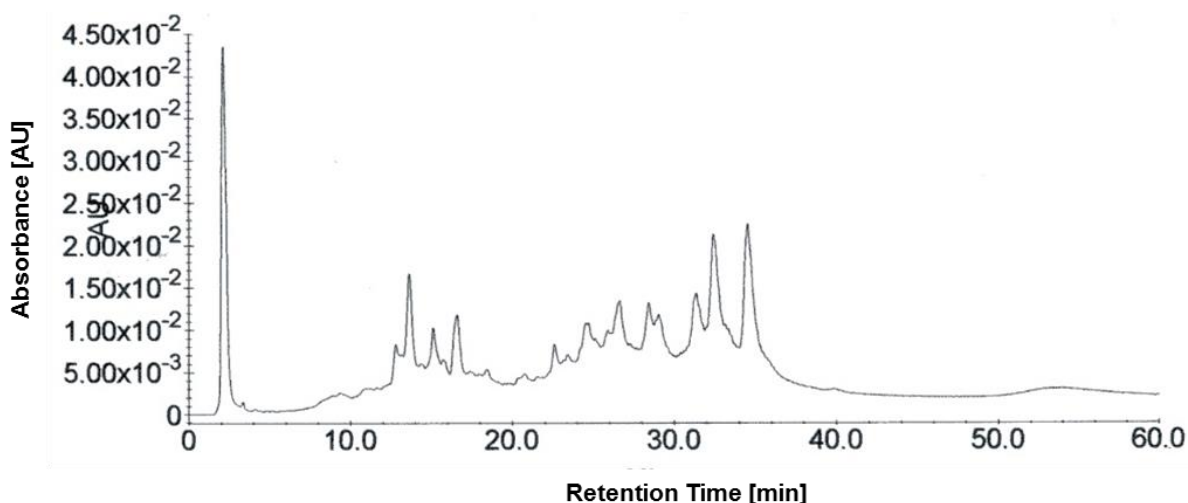


Figure 3.6: Separation of 0.1 mg of C-terminally His-tagged recombinant lysostaphin (construct 3; preparation 3) using a ProPac[®] WCX-10 column (4 x 250 mm). Recombinant lysostaphin bound to this column, resulting in the elution of multiple peaks between 12.0 and 36.0 min. The presence of multiple peaks indicated degradation of recombinant lysostaphin or possibly the presence of basic protein contaminants. UV absorbance was recorded at a wavelength of 280 nm.

3.3.2.4 Protein separation using ProPac[®] WCX-10 column and Ultimate[™] 3000 chromatography system

To permit optimisation of flow rates, fraction collection and data acquisition, WCX separation was also performed using an Ultimate[™] 3000 system. As shown in Figure 3.7, the ProPac[®] WCX-10 column provided resolution of multiple protein isoforms when performing chromatography using the Ultimate[™] 3000 chromatography system. A number of protein isoforms were observed, in addition to a number of peaks which may have reflected the presence of recombinant lysostaphin or other contaminating basic proteins. In addition the UV trace was subject to slight baseline shifting, possibly due to issues with mobile phase composition or instrumental operation, which was not desirable.

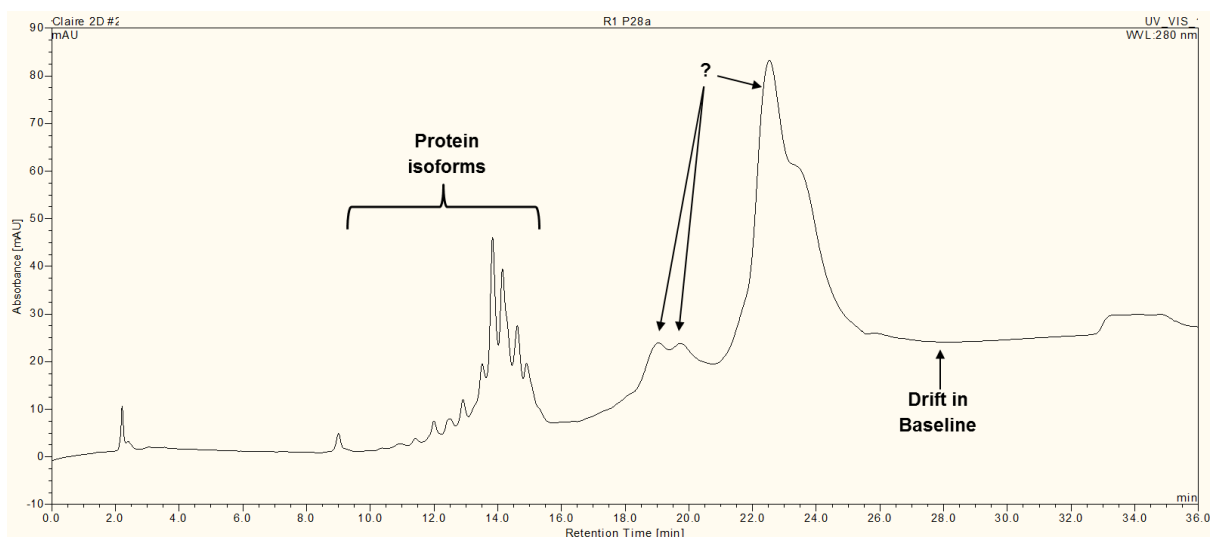


Figure 3.7: Separation of 0.1 mg of *N*-terminally His-tagged recombinant lysostaphin (construct 1; preparation 4) using a ProPac® WCX-10 column (4 x 250 mm). Recombinant lysostaphin bound to this column, resulting in the elution of multiple peaks between 10 and 16 min. The UV trace increased after 16 min revealing further peaks, which may have reflected recombinant lysostaphin or the presence of contaminating proteins. The UV trace also displayed base line drifting, which was indicative of instrumental or mobile phase composition issues. UV absorbance was recorded at a wavelength of 280 nm.

To establish whether the eluted peaks contained recombinant lysostaphin, selected WCX fractions were concentrated using TCA precipitation, as indicated in Figure 3.8. The concentrated fractions were analysed by SDS-PAGE which revealed that the majority of the peaks contained recombinant lysostaphin (Figure 3.9). Due to loss of protein during TCA precipitation, recombinant lysostaphin could not be detected in some of the analysed fractions.

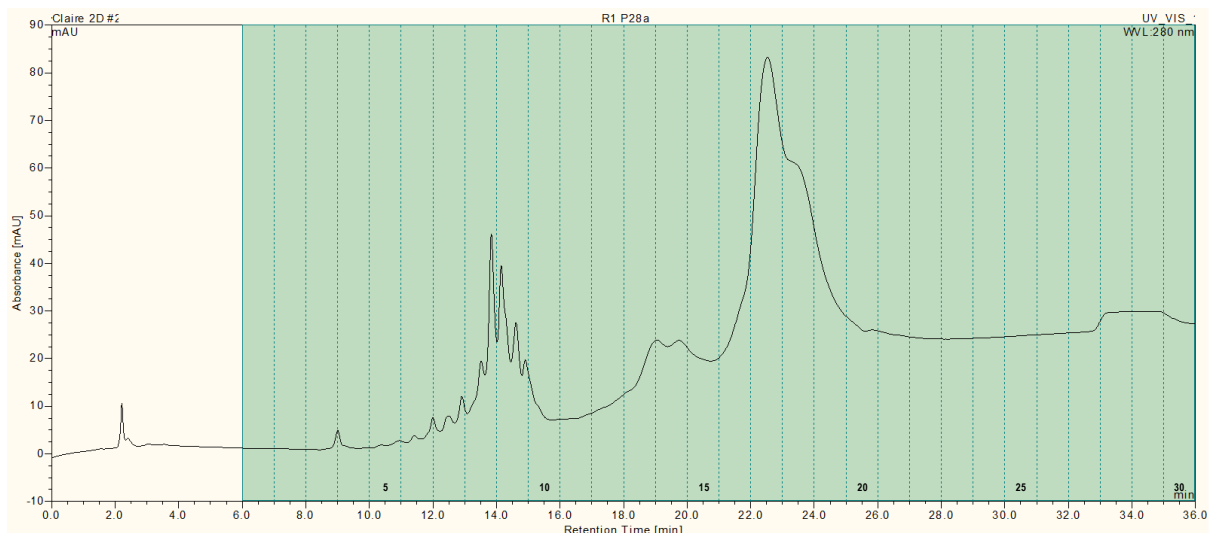


Figure 3.8: Separation of 0.1 mg of *N*-terminally His-tagged recombinant lysostaphin (construct 1; preparation 4) using a ProPac® WCX-10 column (4 x 250 mm). Fractions 9, 13, 14, 16, 17, 18, 23 and 24 were concentrated by TCA precipitation and subjected to SDS-PAGE analysis.

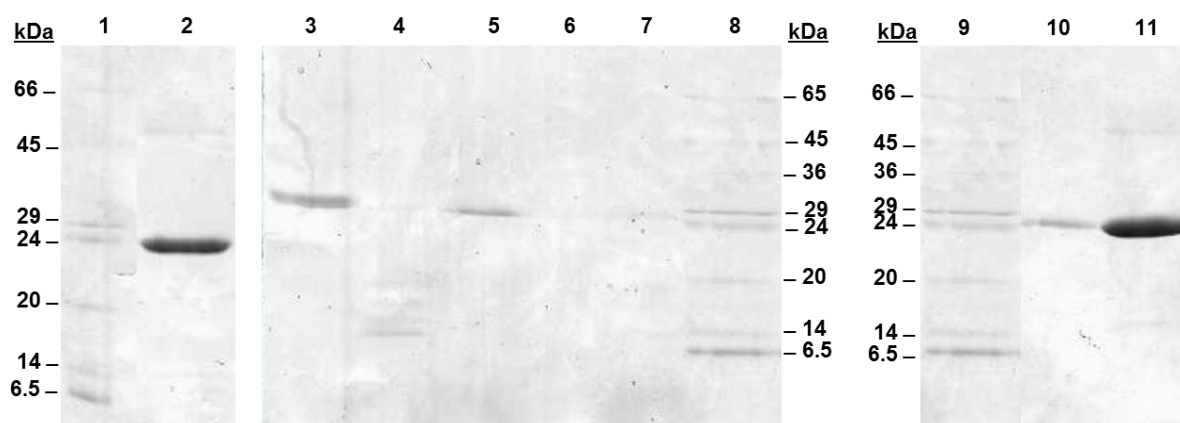


Figure 3.9: PAGE analysis of fractions eluted during WCX separation of purified *N*-terminally His-tagged recombinant lysostaphin (construct 1; preparation 4). Recombinant lysostaphin was expressed in *E. coli* BL21 (DE3) cultured in AIM and was preparatively purified using IMAC prior to WCX separation. Lane 1: Sigma low molecular weight markers; Lane 2: Fraction 9; Lane 3: Fraction 13; Lane 4: Fraction 14; Lane 5: Fraction 16; Lane 6: Fraction 23; Lane 7: Fraction 24; Lane 8: Sigma low molecular weight markers; Lane 9: Sigma low molecular weight markers; Lane 10: Fraction 18; Lane 11: Fraction 17.

3.3.2.5 Validation of ProPac® WCX-10 column

Following chromatographic issues during the separation of recombinant lysostaphin, the ProPac® WCX-10 was validated by applying a cytochrome C protein standard to the column. As shown in Figure 3.10, cytochrome C variants were separated and resolved effectively using ProPac® WCX-10. Repeated injection of cytochrome C demonstrated that the

ProPac® WCX-10 can provide very reproducible separations under optimal operational conditions.

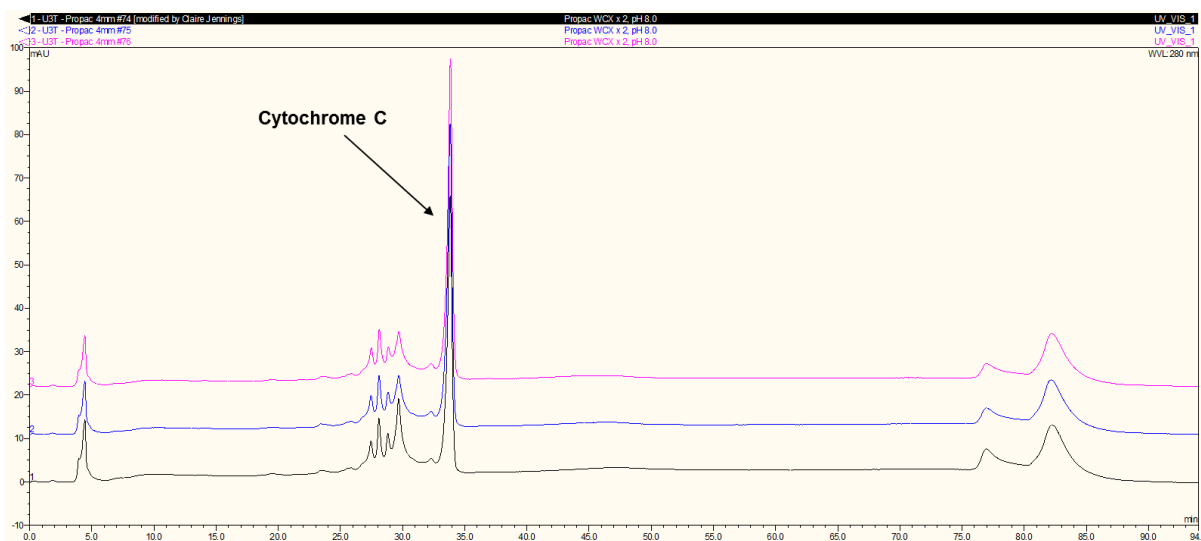


Figure 3.10: Separation of a cytochrome C standard protein solution during validation of a ProPac® WCX column (4 x 250 mm) . Cytochrome C was applied to the column three times and was separated efficiently and reproducibly by the ProPac® WCX column. Peaks representing cytochrome C are indicated. UV absorbance was recorded at a wavelength of 280 nm.

3.3.2.6 Protein separation using ProSwift® SCX-1S column and an Ultimate™ 3000 system

Recombinant lysostaphin could evidently bind to ProPac® SCX and WCX columns, therefore the purified protein was also applied to ProSwift™ ion exchange column to establish whether recombinant lysostaphin isoforms could be effectively resolved using monolithic ion exchange columns as well. Recombinant lysostaphin was initially applied to a ProSwift® SCX-1S column and the protein bound to the column (Figure 3.11). Whilst recombinant lysostaphin was strongly retained by the column, protein eluted during the wash phase rather than the linear gradient. Separation of protein isoforms could therefore not be achieved.

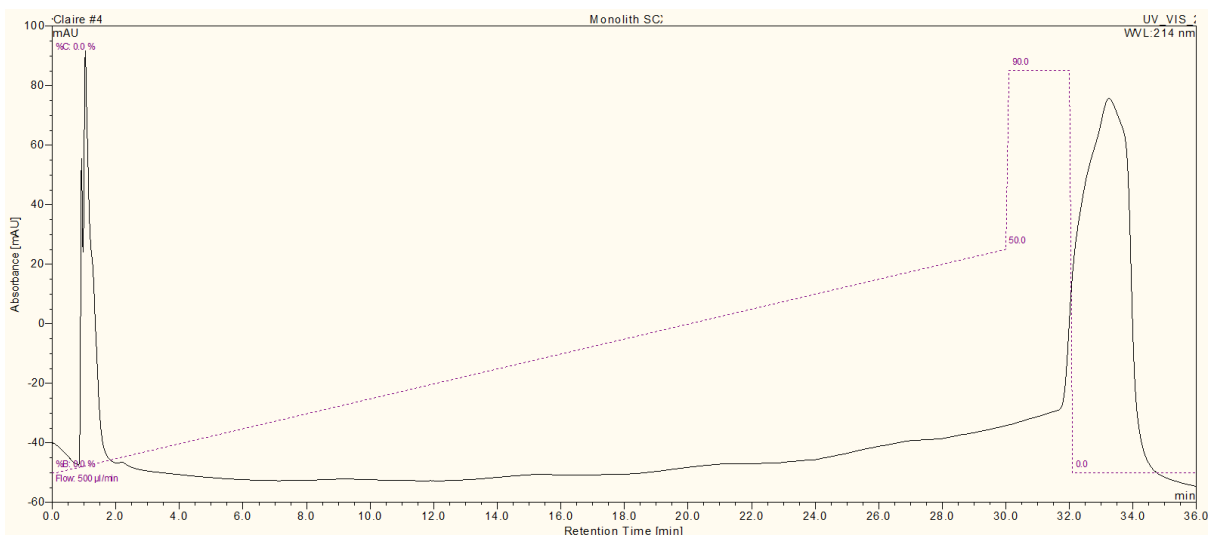


Figure 3.11: Separation of 0.2 mg of *N*-terminally His-tagged recombinant lysostaphin (construct 1; preparation 4) using a ProSwift® SCX-1S column (4.6 x 500 mm). Recombinant lysostaphin bound strongly to this column however charge isoforms were not resolved within the main peak. UV absorbance was recorded at a wavelength of 214 nm.

3.3.2.7 Protein separation using ProSwift® WCX-1S column and an Ultimate™ 3000 system

Due to previous successful resolution of protein isoforms using the ProPac® WCX-10 column, purified recombinant lysostaphin was also applied to a single ProSwift® WCX-1S column. Figure 3.12 demonstrates that the ProSwift® WCX-1S provided successful separation of protein isoforms within the linear gradient elution phase of the separation. However protein also eluted during the wash phase of the separation indicating that recombinant lysostaphin was strongly retained by the column, without achieving further resolution of protein isoforms.

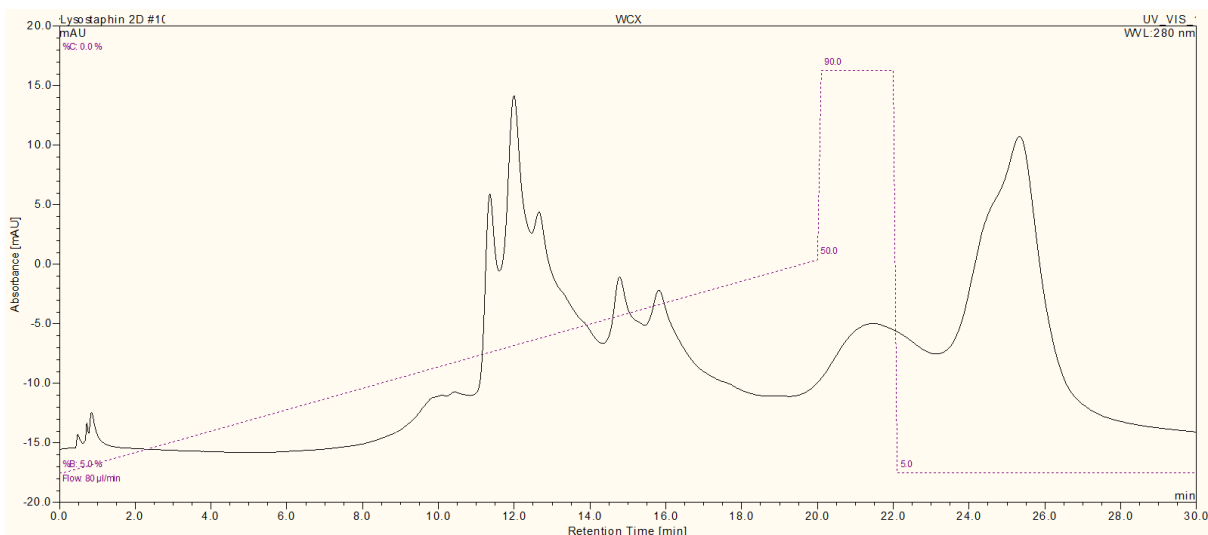


Figure 3.12: Separation of 0.1 mg of C-terminally His-tagged recombinant lysostaphin (construct 3; preparation 4) using a ProSwift® WCX column (2 x 50 mm). Purified recombinant lysostaphin was applied to the column and appeared to be retained on the column, with multiple peaks eluting during the course of separation. A large proportion of the sample eluted during the wash phase minimising the efficiency of separation. UV absorbance was recorded at a wavelength of 280 nm.

3.3.2.8 Validation of ProPac® MAb SCX beta test column

Later in the course of this research, a ProPac® MAb SCX beta test column became available for the separation of protein variants. The column was initially validated by performing multiple separations of a protein standard mix. As shown in Figure 3.13, RNase A, cytochrome C and lysozyme were resolved efficiently and reproducibly using the beta test ProPac® MAb column.

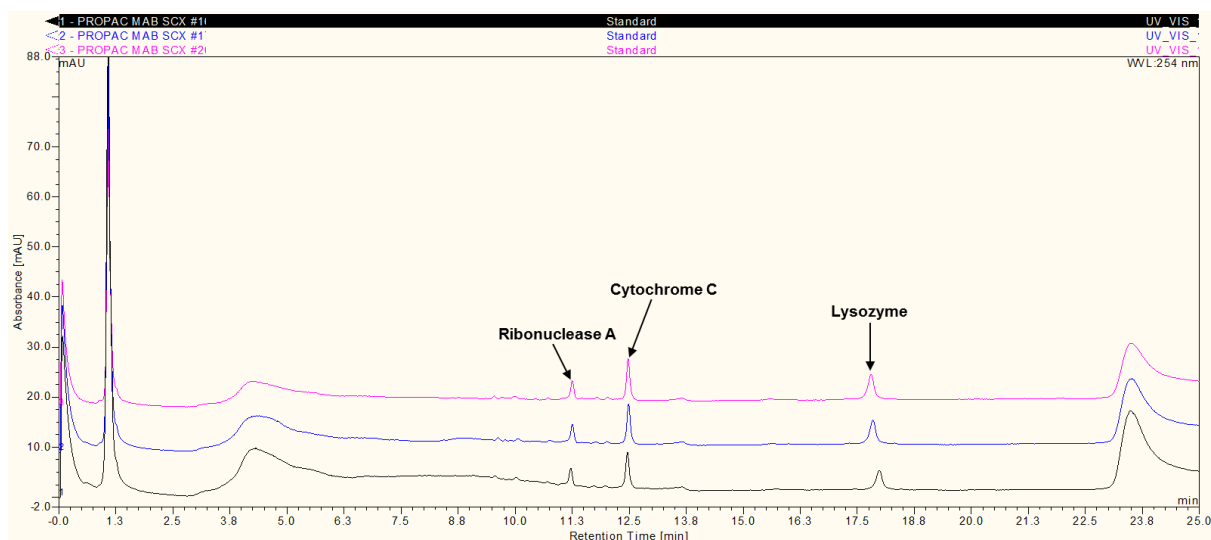


Figure 3.13: Separation of standard proteins during beta testing of a ProPac[®] MAb SCX column (4 x 250 mm). Peaks representing RNase A, cytochrome C, lysozyme are indicated. UV absorbance was recorded at a wavelength of 280 nm.

3.3.2.9 Protein separation using ProPac[®] MAb SCX beta test column and an Ultimate[™] 3000 system

Following validation of the beta test ProPac[®] MAb SCX, a sample of purified recombinant lysostaphin was applied to the column (Figure 3.14). The ProPac[®] SCX MAb column provided excellent separation of the lysostaphin isoforms, with fairly narrow peak width and separation of peaks. The degree of separation achieved using the ProPac[®] SCX MAb column was comparable and if not better than that achieved using the ProPac[®] WCX, even following method development as described in Section 3.4.

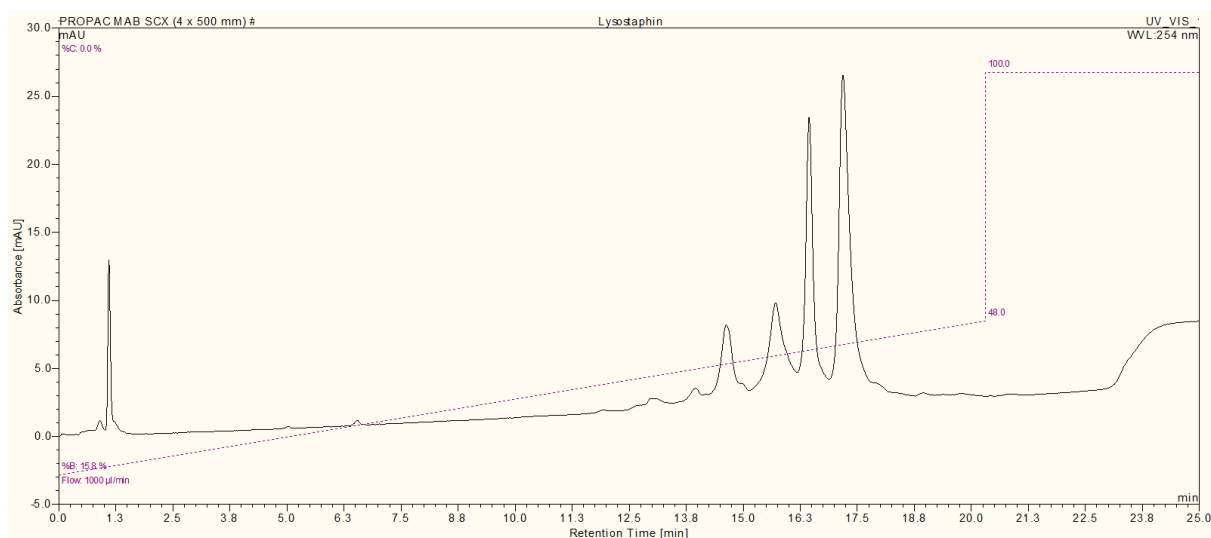


Figure 3.14: Separation of 16 µg of C-terminally his-tagged recombinant lysostaphin (construct 3; preparation 5) using a single ProPac MAb SCX column (4 x 250 mm)

3.3.3 Discussion

Initial separations performed using ProPac™ and ProSwift™ columns provided an insight into the separation and resolving powers of analytical ion exchangers. As expected, recombinant lysostaphin was not retained by the ProPac® SAX column and therefore could not provide separation of protein variants. However recombinant lysostaphin was retained by ProPac® SCX and WCX columns and whilst the SCX column did not provide resolution of protein isoforms, the WCX column did. Initial separations using the ProPac® WCX indicated that the column could separate and resolve a number of protein isoforms, which had a molecular weight corresponding with that of recombinant lysostaphin. This result indicated that recombinant lysostaphin preparations are indeed heterogeneous, emphasising the importance of the resolution, separation and characterisation of protein isoforms.

Whilst the ProPac® WCX separation provided good resolution and separation of protein isoforms, separation of recombinant lysostaphin was complicated by the quality of the recombinant protein preparation and initial chromatographic issues, which lead to baseline drifting. Purified protein preparations which had undergone lengthy purification appeared to have been affected by degradation, interfering with successful analysis of protein heterogeneity. To prevent this, subsequent separations were performed using recombinant lysostaphin preparations which had only been purified using a single purification step. Baseline drifting also interfered with the quality of analysis by complicating the identification of resolved peaks. Optimisation of chromatographic separations led to correction of baseline drifting.

Protein separations were also performed using monolithic ProSwift™ columns, with the intention of achieving rapid, high-resolution separation of protein variants. Recombinant lysostaphin was strongly retained by the ProSwift® SCX column, however resolution and separation was not accomplished. The ProSwift® WCX column also retained recombinant lysostaphin and whilst the column provided resolution of protein isoforms, it did not provide efficient separation. Overall ProSwift™ ion exchange columns did not appear to offer appropriate separation or resolution of recombinant lysostaphin variants, therefore subsequent separations were primarily focused on the use of ProPac™ ion exchange columns.

Development and availability of a beta-test ProPac® MAb column in the later stages of this research provided further evidence that ProPac™ ion exchange columns could provide effective separation and resolution of protein isoforms. The ProPac® MAb provided excellent

resolution of recombinant lysostaphin isoforms, therefore this column was employed during culture studies, as described in Section 3.5.3.13. Like the ProPac[®] WCX column, the ProPac[®] MAb column demonstrated very good reproducibility between separations as shown during column validation.

During this work, separations were performed using either a DX500 or an Ultimate[™] 3000 chromatography system. Whilst both systems could be used to provide chromatographic separation during initial column selection, the single gradient pump setup of DX500 chromatography system did not offer the flexibility and versatility of operation that was required for the optimisation of protein separation and subsequent chromatographic characterisation of protein isoforms. For instance, unlike the DX500 system, the Ultimate[™] 3000 system permitted microflow rates, which facilitated optimisation of protein separation and a variety of fraction collection modes, assisting the collection of resolved protein variants in an appropriate manner. In addition, the availability of dual pumps and switching valves on the Ultimate[™] 3000 system provide the ability to perform multidimensional separations, as described in Section 3.4.3.7.

Ultimate[™] 3000 chromatography systems were therefore used to optimise the separation of recombinant lysostaphin isoforms so that the heterogeneity of the recombinant expression products could be investigated. At this stage it was not possible to make definitive conclusions about the nature of recombinant lysostaphin variants, due to the variability of the obtained results. The variability of results was augmented by the separation of different recombinant lysostaphin constructs, which influenced the charge and inherent structure of the analysed protein. It was however known that the heterogeneity of recombinant lysostaphin could be further investigated through application and optimisation of protein separation using ProPac[™] ion exchange columns.

3.4 Optimisation of protein isoform separation

3.4.1 Introduction

Unlike other analytical techniques, chromatographic separations must be developed for specific applications in order to maximise performance, reliability and reproducibility. It was therefore essential that the chromatographic performance of protein separation was optimised for the separation of recombinant lysostaphin variants. Optimal chromatographic performance can be achieved by empirical optimisation of mobile phase conditions, such as pH or stationary phase conditions, such as column length and diameter. In addition gradient functions, fraction collection, sample concentration and formulation must also be optimised to ensure that the protein isoforms are separated efficiently and in a manner which prevents sample degradation and facilitates downstream analysis and characterisation.

It was evident that recombinant lysostaphin charge variants could be separated using ProPac™ ion exchange columns, however, it was unclear whether alternative column dimensions could enhance the analysis of recombinant lysostaphin variants. Protein separations were primarily performed using 4 mm i.d ProPac® WCX-10 columns, which provided high-resolution separation of larger amounts of recombinant lysostaphin. To enhance resolution and efficiency of separation, column diameter should be reduced to achieve higher and faster sample permeability (Gu *et al.*, 2007). Unfortunately a 2 mm version of the ProPac® WCX-10 column was not initially available; however separation of isoforms could be performed using a ProPac® SCX-10 column (2 x 250 mm) due to the lower flow rates used. ProPac® WCX-10 columns (2 x 250 mm) were later acquired, in addition to a further ProPac® WCX-10 column (4 x 250 mm), therefore separations could also be performed over an extended column length, which should provide increased resolution and capacity.

Initial protein separations were performed using sodium phosphate buffers adjusted to pH 7.0. As IEX is dramatically influenced by protein charge which is inherently affected by pH, it was important that protein separation was also tested using mobile phase buffers adjusted to pH 6.0 or pH 8.0 to establish whether separation was enhanced. In addition, altering mobile phase buffering agents can enhance resolution in a quicker and more economical manner than stationary phase optimisation. Careful optimisation of mobile phase gradients could also improve chromatographic performance by increasing separation efficiency and reducing the retention of strongly bound compounds. Extension of chromatographic gradients could enhance separation, however would increase duration of separation and

mobile phase consumption, which could be problematic if a large number of samples had been prepared.

Chromatographic conditions were initially established for the binding and separation of recombinant lysostaphin after applying purified protein to the column. It was unclear how much protein should be applied to the column to obtain sufficient concentrations of separated protein isoforms for subsequent analysis. Therefore experiments were performed to assess appropriate sample loading concentrations without over-loading the column and decreasing peak resolution. Recombinant lysostaphin had also been prepared in a lyophilised state, which could remain stable in the long-term, but tended to precipitate upon resuspension. Chromatographic separations were therefore performed on the resuspended protein to see whether sample precipitation interfered with protein separation. Furthermore protein separation was also performed upon cell lysate to establish whether recombinant lysostaphin isoforms could be directly purified and separated using analytical CXC columns, rather than preparative columns, as described in Section 2.5.3.5.

Fraction collection also required optimisation to ensure that all resolved protein isoforms were collected in an appropriate manner, whilst minimising co-elution of protein isoforms. Due to the availability of an autosampler with fractionation capabilities it was possible to evaluate the performance of fraction collection by time or peak recognition. Subsequent 2D-LC analysis of separated protein isoforms could also be performed using second-dimensional reverse phase separation to assess the purity and heterogeneity of separated protein isoforms.

Through the course of chromatographic optimisation it was also possible to gain insight into the chromatographic behaviour of recombinant lysostaphin isoforms and the heterogeneity of alternative cationic recombinant proteins. Factors influencing the heterogeneity of recombinant lysostaphin, such as culture temperature and expression media could also be investigated.

Aims:

- To assess the influence of column length and diameter upon the efficiency and resolution of protein isoform separation.
- To evaluate the influence of mobile phase pH, mobile phase composition and gradient functions upon protein isoform separation.

- To optimise sample preparation by testing whether the heterogeneity of recombinant lysostaphin could be monitored most efficiently by direct separation of purified, lyophilised or crude preparations.
- To assess the influence of sample concentration upon the separation, resolution and abundance of protein isoforms.
- To optimise fraction collection by time or peak recognition.
- To perform 2D-LC analysis to assess purity and heterogeneity of separated protein isoforms.

3.4.2 Methods

3.4.2.1 Optimisation of protein isoform separation

All separations were performed using the Ultimate™ 3000 Titanium system unless specified otherwise. Separations were performed to permit optimisation of sample loading conditions (Appendix 7.175), sample preparation (Appendix 7.176), gradient conditions (Appendix 7.177), mobile phase conditions (Appendix 7.178), column length (Appendix 7.179) and column diameter (Appendix 7.180). Experiments were also performed to optimise fraction collection by time (Appendix 7.181) or peak recognition (Appendix 7.182).

3.4.2.2 Separation of protein isoforms using optimised conditions

Once chromatographic separation had been optimised, various experiments were performed to analyse purified recombinant lysostaphin (Appendix 7.183) and the influence of culture temperature upon the charge heterogeneity of recombinant lysostaphin (Appendix 7.184). The optimised conditions were also used to analyse the charge heterogeneity of alternative recombinant protein preparations (Appendix 7.186).

3.4.2.3 Optimisation of protein separation using ProPac® MAb SCX columns

Separations were performed to permit optimisation of sample loading conditions (Appendix 7.187), gradient conditions (Appendix 7.188), mobile phase conditions (Appendix 7.189) and column length (Appendix 7.190).

3.4.3 Results

3.4.3.1 Optimisation of protein isoform separation using the ProPac® WCX column

As the ProPac® WCX columns provided good resolution separation of protein isoforms in initial experiments, further experiments were performed to optimise chromatographic conditions to achieve greater resolution. These experiments focused on optimising sample loading conditions, sample preparation, mobile phase conditions and gradient functions.

3.4.3.2 Optimisation of sample loading conditions

Initial applications of recombinant lysostaphin to ProPac® WCX columns resulted in the resolution and separation of lysostaphin isoforms. During these separations anywhere between 0.1 and 14 mg of recombinant lysostaphin was applied to the column. Each application provided separation and resolution of protein isoforms, however it was unclear how much protein should be applied to the column to allow not only detection of protein isoforms, but also their subsequent characterisation. Following the application of 9.1 mg of recombinant lysostaphin, it was evident that a fairly high concentration of lysostaphin should be applied to the column to permit resolution of low abundance protein isoforms. As shown in Figure 3.15, nine low abundance protein isoforms could be resolved during the separation, in addition to two more abundant protein variants.

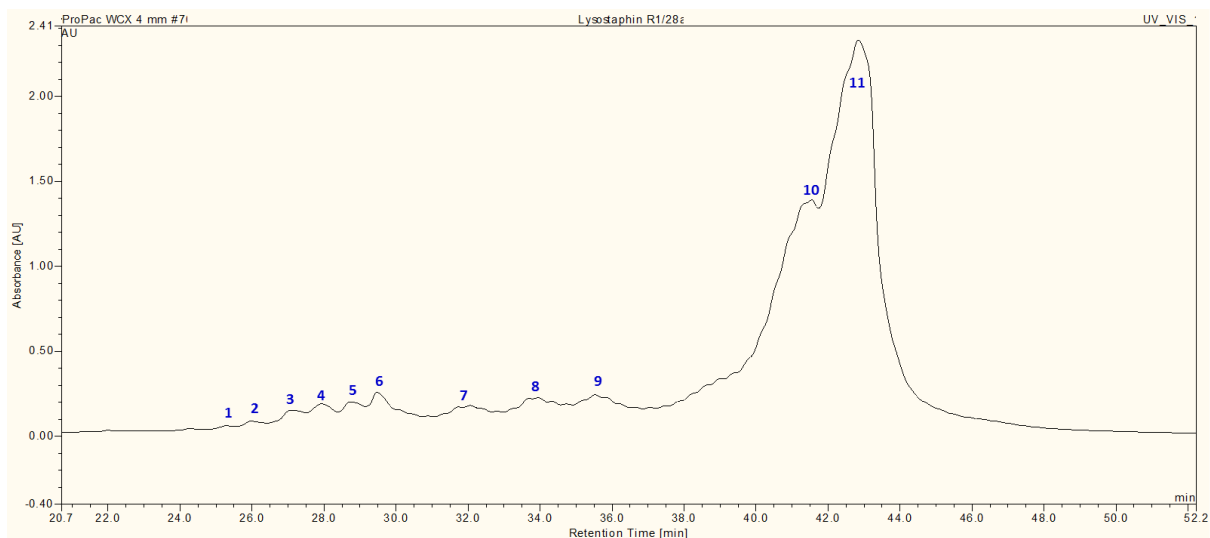


Figure 3.15: Separation of *N*-terminally His-tagged recombinant lysostaphin (construct 1) using a ProPac® WCX-10 column (4 x 250 mm). The application of 9.1 mg of recombinant lysostaphin (preparation 9) resulted in the elution of multiple peaks between 24 and 44 min. Eleven peaks were resolved during the separation, as indicated.

To increase the concentration of low abundance protein isoforms, the amount of applied protein was increased further. However Figure 3.16 indicates that an increased amount of protein resulted in substantial peak broadening, leading to decreased resolution of protein isoforms, particularly in the case of highly abundant isoforms. Peak broadening was not desirable as it interfered with the visualisation of protein variants and decreased the separative capacity provided by the column.

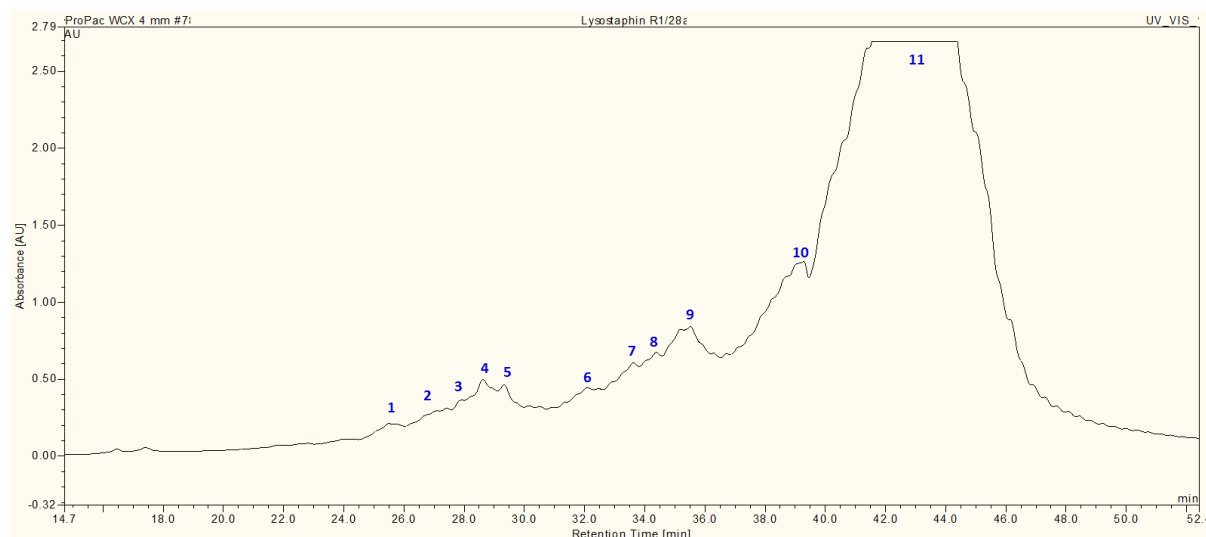


Figure 3.16: Separation of *N*-terminally His-tagged recombinant lysostaphin (construct 1) using a ProPac[®] WCX-10 column (4 x 250 mm). The application of 14.0 mg of recombinant lysostaphin (preparation 8) resulted in the elution of multiple peaks between 24 and 47 min. Eleven peaks were resolved during the separation, as indicated.

As these results provided evidence to support the application of either lower or higher amounts of recombinant lysostaphin, further comparative separations were performed to directly assess the resolution of protein isoforms following the application of different amounts of protein (Figure 3.17). Figure 3.17 indicates that the injection of lower amounts of protein resulted in better resolution and peak width following elution of highly abundant isoforms, though poor resolution of less abundant isoforms. As shown in previous separations, the injection of higher amounts of recombinant lysostaphin provided better resolution of less abundant isoforms, however peak broadening lead to decreased resolution of highly abundant isoforms.

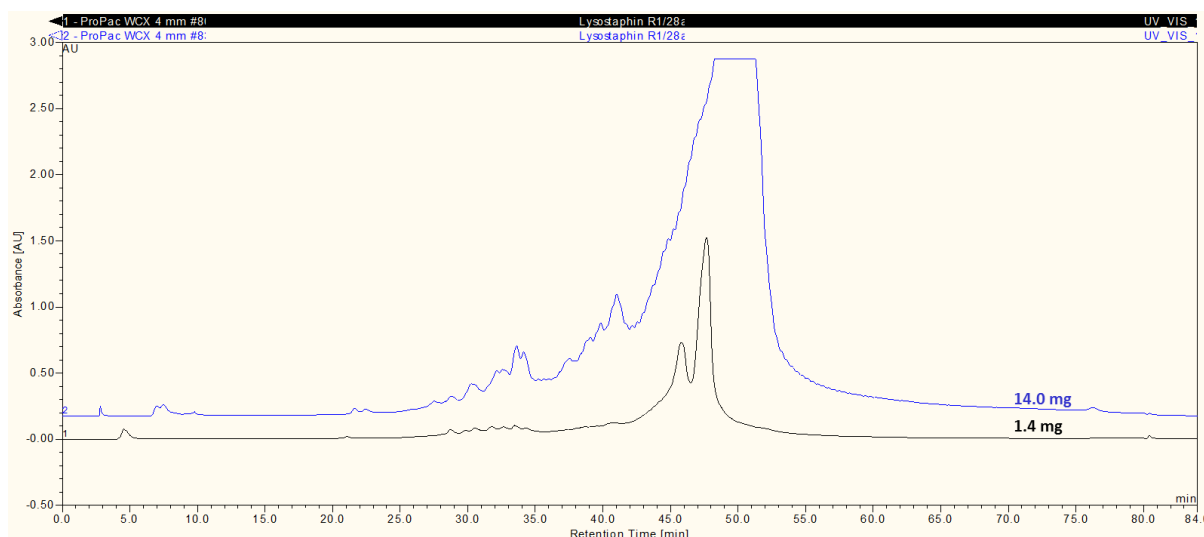


Figure 3.17: Comparative separation of *N*-terminally His-tagged recombinant lysostaphin (construct 1) using a ProPac[®] WCX-10 column (4 x 500 mm). The application of 14.0 mg and 1.4 mg of recombinant lysostaphin (preparation 8) resulted in the elution of multiple peaks, however the resolution and peak width of high abundance isoforms was better following application of a smaller amount of protein. Conversely, the resolution of low abundance isoforms was enhanced by the application of larger amounts of protein.

3.4.3.3 Optimisation of sample preparation

The majority of protein separations were performed using recombinant lysostaphin preparations which had been purified and concentrated via ultrafiltration. As described in Section 2.5.3.8, recombinant lysostaphin was purified from multiple batch cultures using large-scale IMAC purification and the resulting protein was dialysed and lyophilised. The lyophilised purified protein was resuspended to allow separation of protein isoforms. PAGE analysis indicated that the lyophilised protein preparation was reasonably pure, with signs of only slight degradation (Appendix 7.191).

The resuspension of lyophilised recombinant lysostaphin was complicated by poor solubility, which lead to sample precipitation upon resuspension in 18.2 MΩ/cm H₂O. Prior to chromatography, the resuspended protein samples were briefly centrifuged to remove visible precipitates from the sample. Due to the insolubility of the lyophilised recombinant lysostaphin it was difficult to achieve a high protein sample concentration, which meant that it was not possible to visualise less abundant protein isoforms without increasing the sample injection volume (Figure 3.18). In addition, the WCX separation of the resuspended sample resulted in an atypical peak distribution and peak broadening, suggesting that sample

preparation influenced the the charge of the expressed protein, potentially through aggregation or degradation.

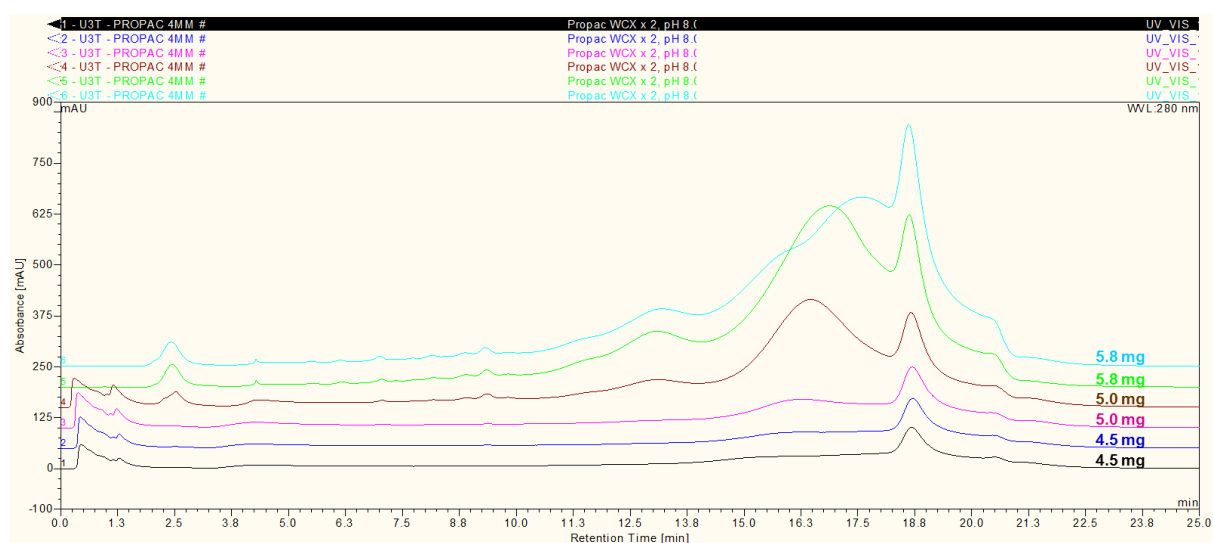


Figure 3.18: Comparison of WCX separations following injection of increasing amounts of *N*-terminally His-tagged recombinant lysostaphin (construct 1; preparation 10).

Each separation was performed in duplicate by applying injection volumes containing 4.5, 5.0 or 5.8 mg of resuspended recombinant lysostaphin. Low abundance isoforms were not resolved until at least 5.0 mg of sample was applied to the column. More abundant peaks appeared to be poorly resolved due to peak broadening. Injection of larger amounts of recombinant lysostaphin appeared to provide enhanced resolution of protein isoforms, however the separation still resulted in a broad, atypical peak (Figure 3.19). These results indicated that the separation of recombinant lysostaphin isoforms should be performed with freshly prepared protein preparations which have not undergone lengthy sample preparation by dialysis or lyophilisation.

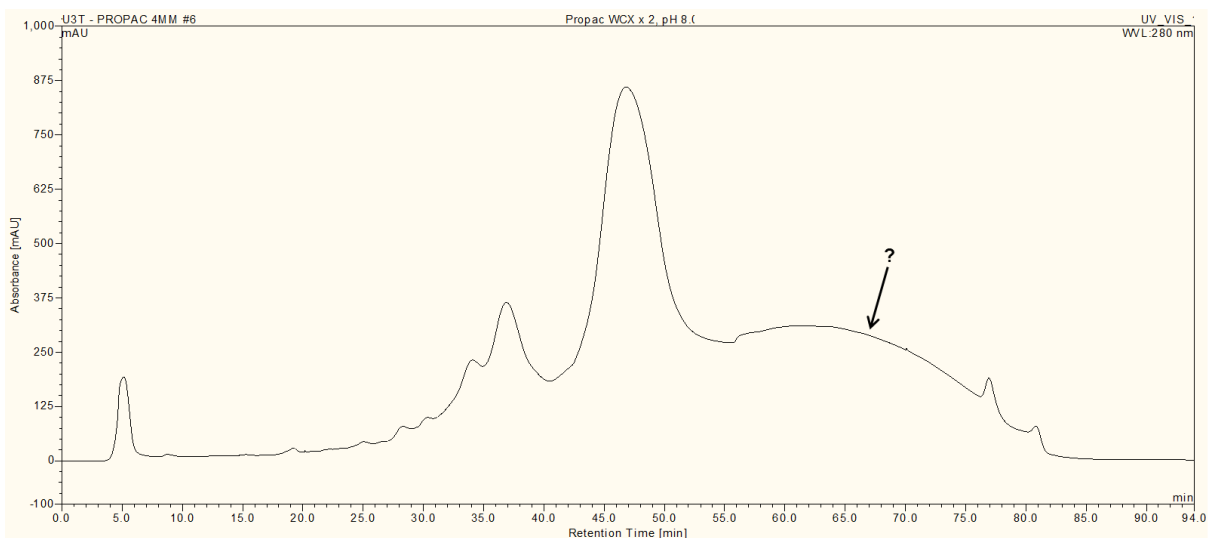


Figure 3.19: WCX separation following injection of 8.3 mg of *N*-terminally His-tagged recombinant lysostaphin (construct 1; preparation 10).

3.4.3.4 Optimisation of gradient conditions

Altering the duration of a linear gradient alters gradient steepness which can alter the degree of separation of protein isoforms. The duration of the 0 -50% linear gradient was altered so that the effect could be assessed. Recombinant lysostaphin was applied to the WCX column and separations were performed where the gradient ranged between 60 and 240 minutes (Figure 3.20 and Figure 3.21). As shown in Figure 3.20, increasing the gradient duration from 60 to 90 min resulted in marginally increased separation of protein isoforms.

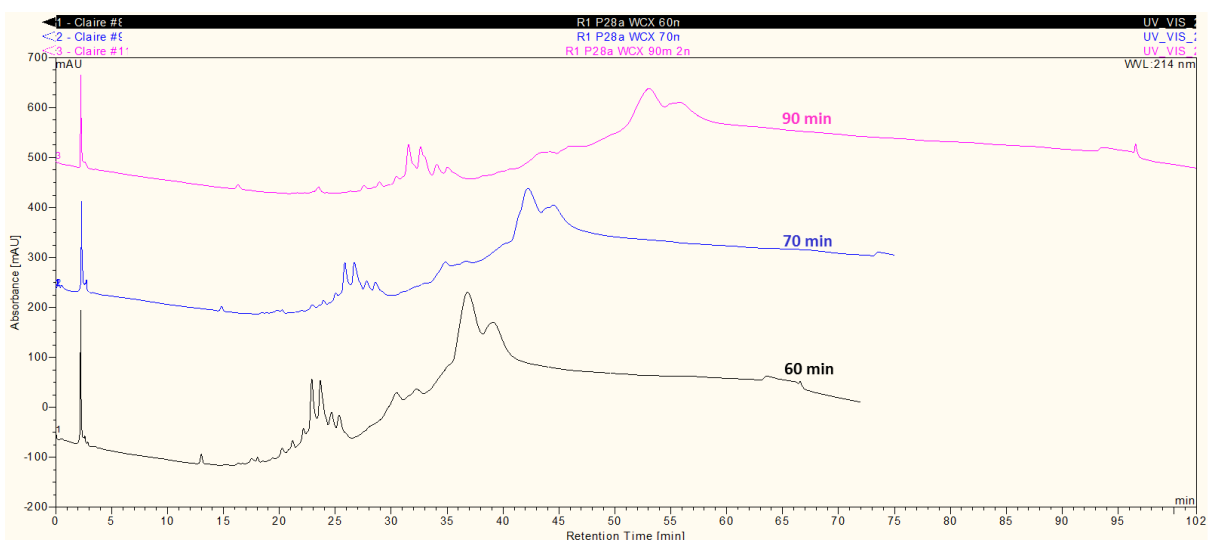


Figure 3.20: Effect of linear gradient duration on separation of 0.2 mg of *N*-terminally His-tagged recombinant lysostaphin (construct 1; preparation 4) using a ProPac WCX-10 (2 x 250 mm). Linear gradients of 60, 70 and 90 min were examined.

The gradient duration was increased further to 120 and 240 min respectively. Figure 3.21 indicates that the greatest degree of separation could be achieved with a 240 min linear gradient, however this extended gradient also led to peak broadening and therefore resulted in reduced peak resolution. Overall the 60 min linear gradient provided the least separation of protein isoforms, whilst 70, 90 and 120 minute linear gradients provided a slightly greater degree of separation with minimal loss of resolution. To minimise the total duration of separation, a 70 min linear gradient was applied in subsequent optimised separations to provide optimal separation and resolution within a reasonable amount of time.

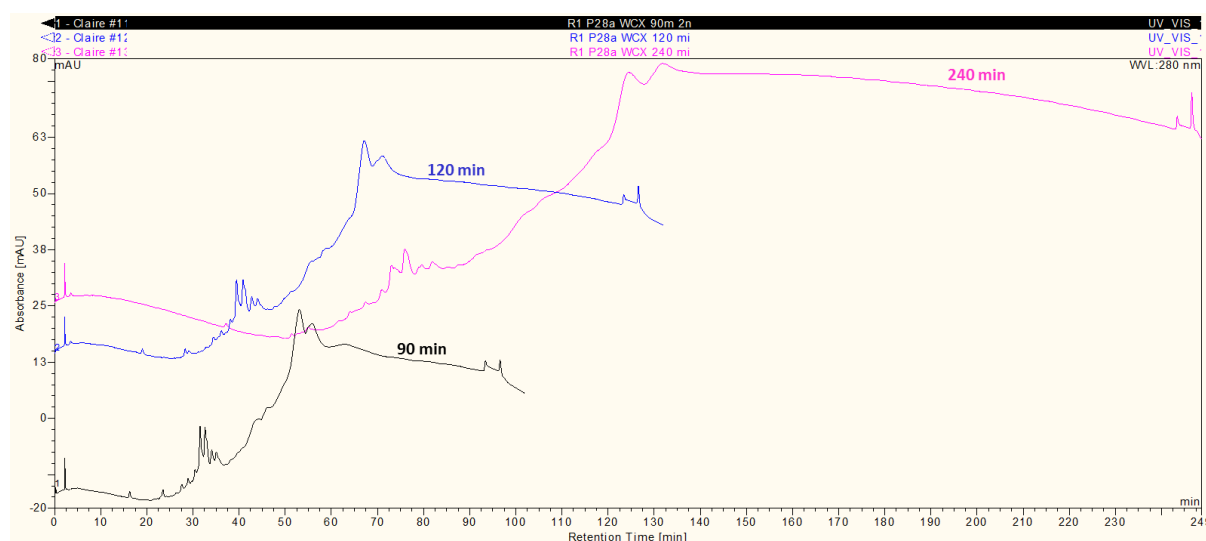


Figure 3.21: Effect of linear gradient duration on separation of 0.2 mg of *N*-terminally His-tagged recombinant lysostaphin (construct 1; preparation 4) using a ProPac WCX-10 (2 x 250 mm). Linear gradients of 90, 120 and 240 min were examined.

These initial gradient experiments were performed whilst applying a 0-50% B elution gradient, therefore recombinant lysostaphin was also separated using a steeper elution gradient to assess the influence upon separation and resolution of protein isoforms. Recombinant lysostaphin was therefore separated under a 0-90% B elution gradient, as shown in Figure 3.22. The application of a steeper elution gradient decreased retention times, however also decreased the resolution of protein isoforms.

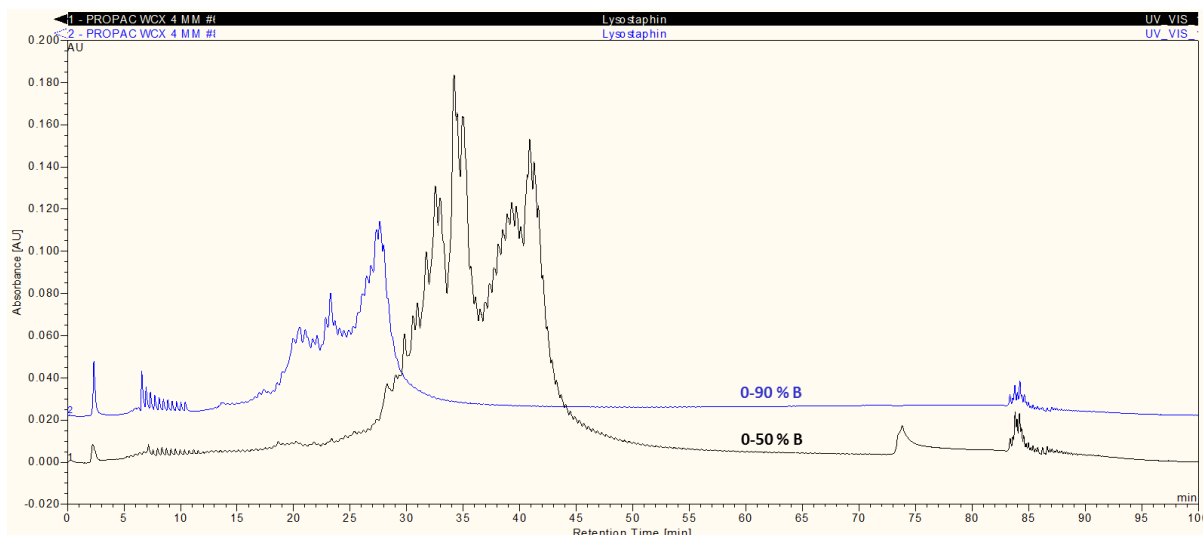


Figure 3.22: Effect of linear gradient steepness upon upon separation of 0.1 mg of *N*-terminally His-tagged recombinant lysostaphin (construct 1; preparation 7) using a ProPac WCX-10 (4 x 250 mm).

3.4.3.5 Optimisation of mobile phase conditions

IEX separations were initially performed using mobile phase buffers containing sodium phosphate buffered to pH 7.0. Whilst successful separation of protein isoforms could be achieved at pH 7.0, separations were also performed using mobile phase which had been buffered to pH 6.0 or pH 8.0, to establish how the utilisation of more acidic or basic mobile phase influenced the separation of recombinant lysostaphin isoforms.

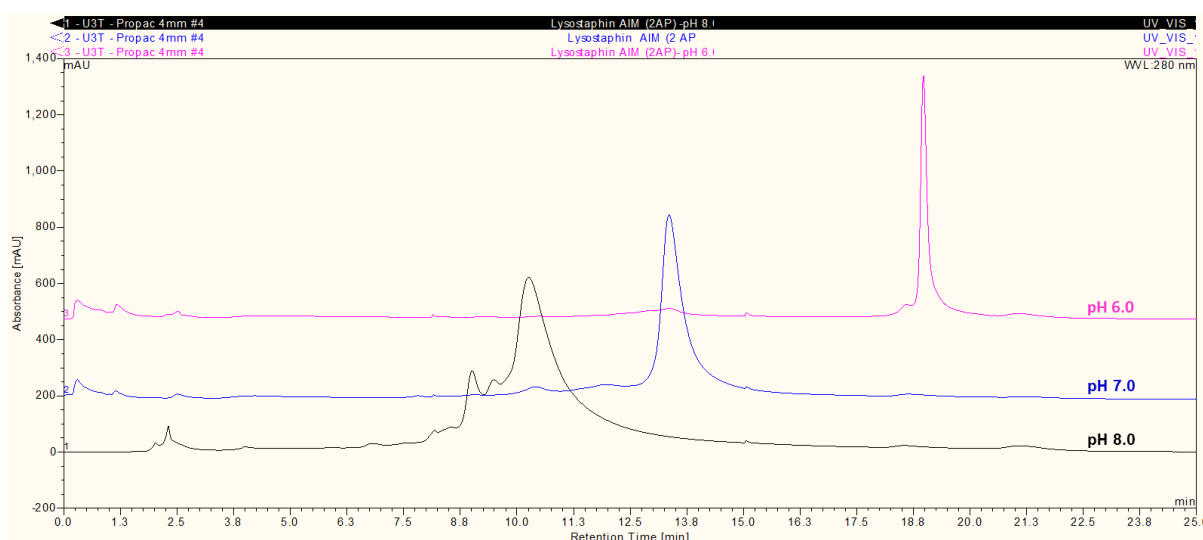


Figure 3.23: Comparative separation of 9.5 mg of *N*-terminally His-tagged recombinant lysostaphin (construct 1; preparation 4) using mobile phase buffered to pH 6.0, pH 7.0 or pH 8.0. WCX separation performed at pH 8.0 resulted in earlier elution and better separation of recombinant lysostaphin isoforms. WCX separation performed at pH 6.0 resulted in later elution and poorer separation of protein isoforms.

As shown in Figure 3.23, reduction of mobile phase pH lengthened peak retention time and did not enhance peak separation, whilst increasing mobile phase pH decreased peak retention time and enhanced resolution of protein isoforms. As pH 8.0 buffers provided more efficient separation of protein isoforms than pH 7.0 buffers, pH 8.0 buffers were used during subsequent WCX separations.

3.4.3.6 Optimisation of column length

To enhance sample loading capacity and resolution, comparative WCX separations were performed using a single ProPac[®] WCX-10 (4 x 250 mm) column or two ProPac[®] WCX-10 (4 x 500 mm) columns. As shown in Figure 3.24, WCX separation using a longer 500 mm column provided slightly enhanced resolution of protein isoforms and increased sample capacity. Two ProPac[®] WCX-10 (4 x 250 mm) columns were therefore used in subsequent experiments to provide higher resolution investigation of protein heterogeneity under different culture conditions.

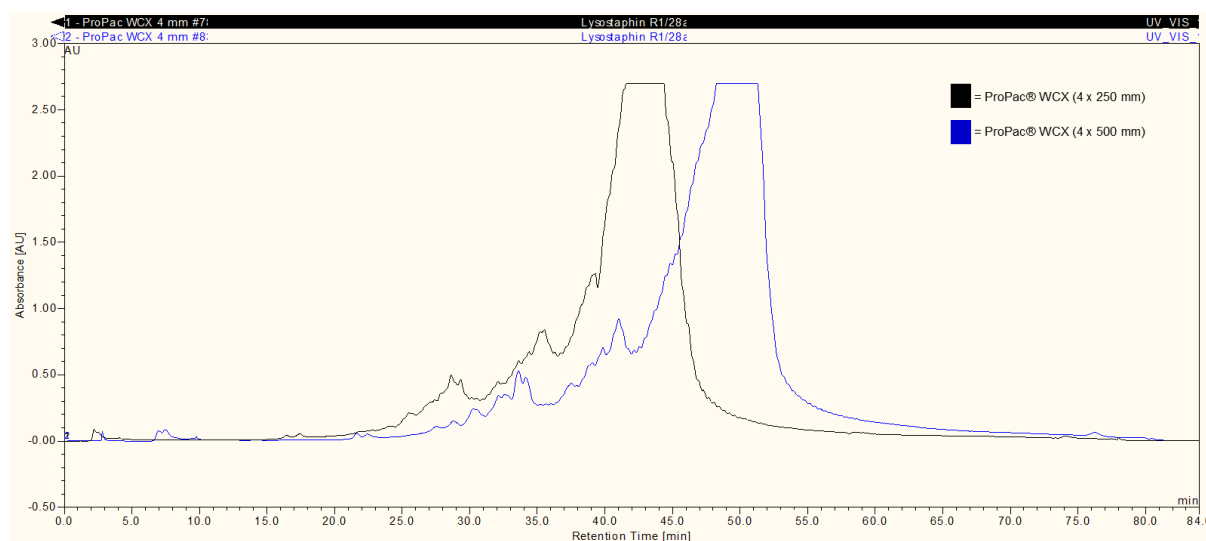


Figure 3.24: Comparative separation of 14.0 mg of *N*-terminally His-tagged recombinant lysostaphin (construct 1; preparation 8) using a ProPac[®] WCX-10 (4 x 250 mm) column or ProPac[®] WCX-10 (4 x 500 mm) column. WCX separation performed using the ProPac[®] WCX-10 (4 x 500 mm) column provided slightly enhanced resolution of protein isoforms and greater sample capacity than the ProPac[®] WCX-10 (4 x 250 mm) column.

3.4.3.7 Optimisation of column diameter

Peak resolution can be further enhanced by the use of a column with a narrower internal diameter, which minimises sample diffusion and therefore band broadening during chromatography. A 2.0 mm version of the ProPac[®] WCX-10 column was not available

initially, therefore some experiments were performed using a ProPac® SCX-10 (2 x 250 mm) column. Although the ProPac® SCX-10 (4 x 250 mm) column had not demonstrated separation of protein isoforms, it was hoped that the 2.0 mm version of the column would have provided better separation and resolution of protein isoforms. Figure 3.25 shows that improved resolution of protein isoforms was indeed achieved using the ProPac® SCX-10 (2 x 250 mm) column.

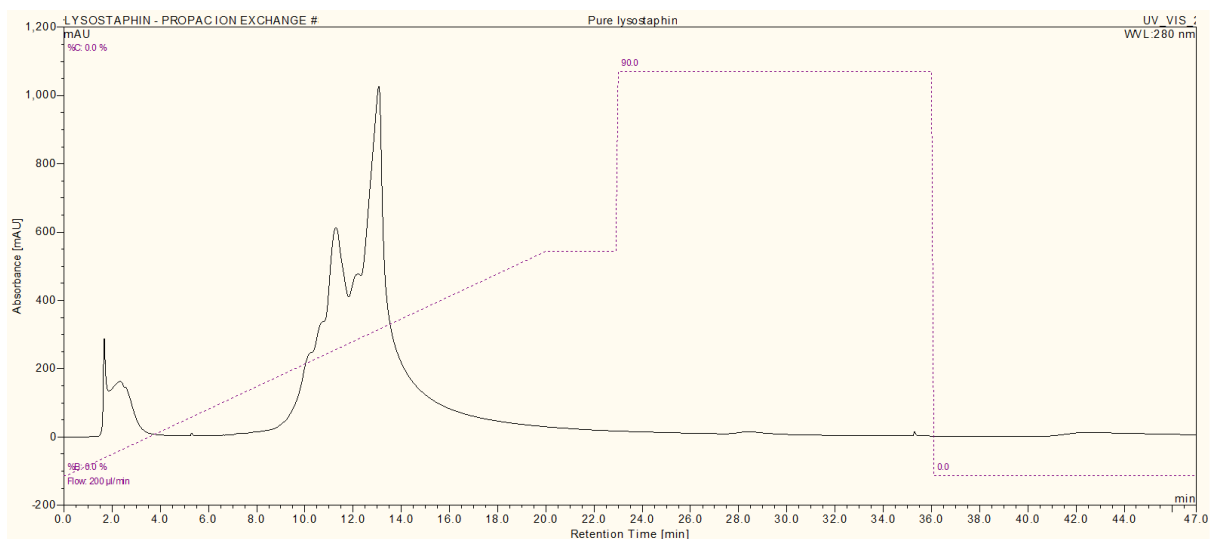


Figure 3.25: Separation of 7.8 mg of purified recombinant lysostaphin (construct 1; preparation 11) using a ProPac® SCX (2 x 250 mm) column.

The use of a lower flow rate increased the efficiency of separation, which could be achieved over a much shorter gradient. Furthermore fractionation could be easily performed within the system auto sampler, which permitted subsequent 2D-LC analysis of the fractions eluted during SCX separation (Figure 3.26). As shown by the 2D retention map, the eluted peaks appeared to be composed entirely of recombinant lysostaphin isoforms, which was not surprising considering that the separations were performed on a purified recombinant lysostaphin preparation.

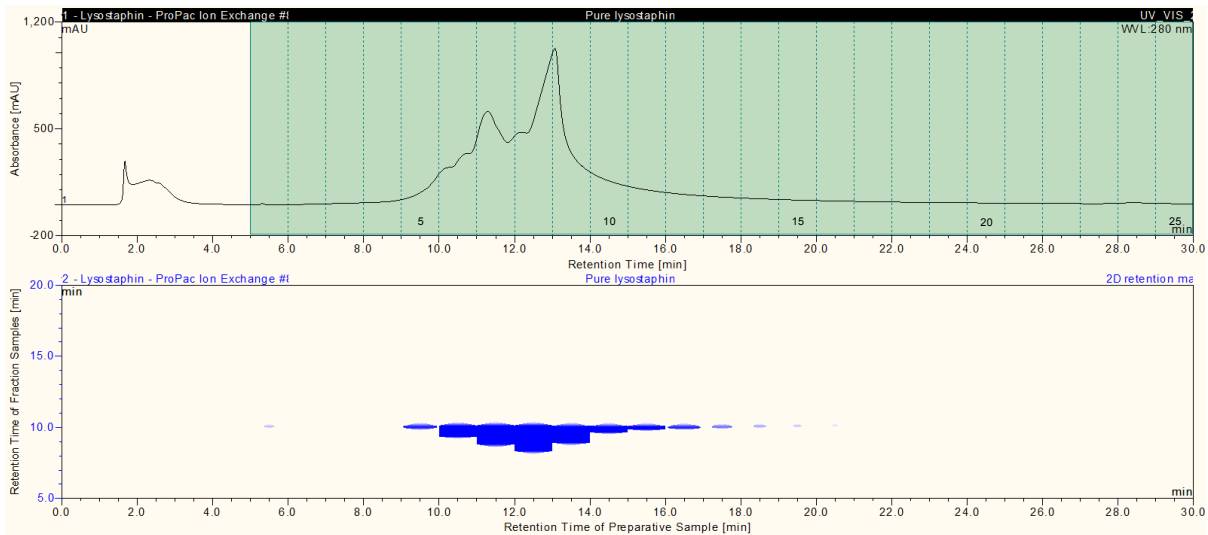


Figure 3.26: 2D-LC separation of 7.8 mg of purified recombinant lysostaphin (construct 1; preparation 11). Charge variants were separated using a ProPac® SCX (2 x 250 mm) column. Fractions collected during SCX separation were separated using a ProSwift™ RP-4H (1 x 250 mm) column.

Closer examination of RP separations performed in the 2nd dimension largely indicated that the WCX fractions contained protein isoforms which did not differ significantly in their hydrophobicity (Figure 3.27). However peak broadening observed upon RP separation of fractions 7, 8, and 9 indicated that slightly less hydrophobic protein isoforms were partially resolved during the separation.

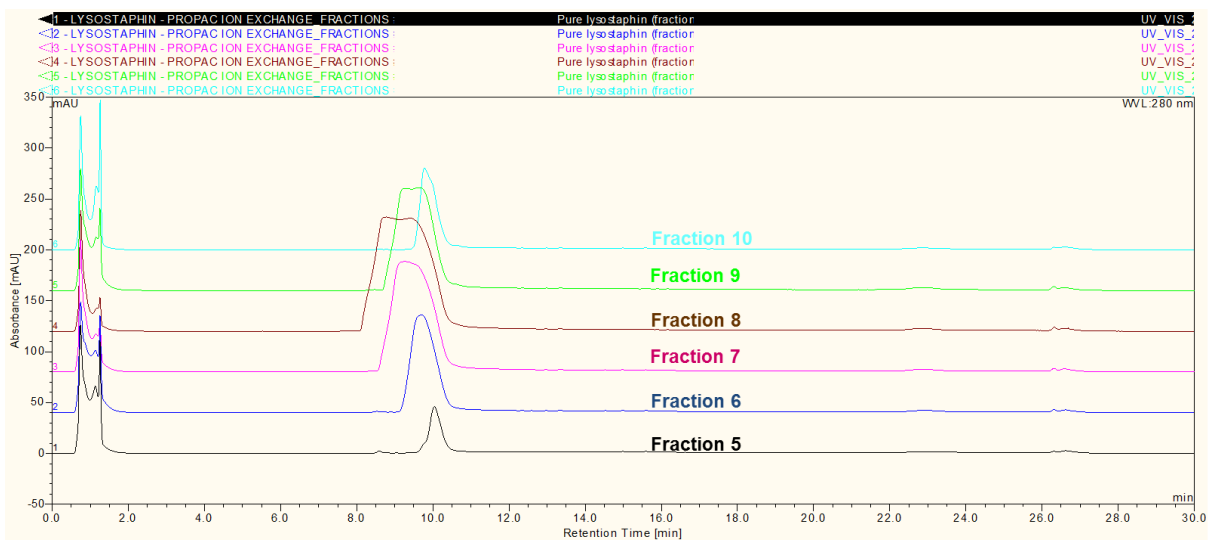


Figure 3.27: Comparison of RP separations performed on SCX fractions 5-10 using a ProSwift™ RP-4H (1 x 250 mm) column.

In a later experiment, cell lysate was applied directly to the ProPac® SCX (2 x 250 mm) column to establish whether recombinant lysostaphin could be purified and separated

straight from cell lysate without prior purification. Figure 3.28 indicates that recombinant lysostaphin protein isoforms could be separated directly from cell lysate without prior purification. This efficient mode of sample preparation was used extensively in subsequent separations to eliminate purification and storage stages, which could have contributed to the development of increased sample heterogeneity.

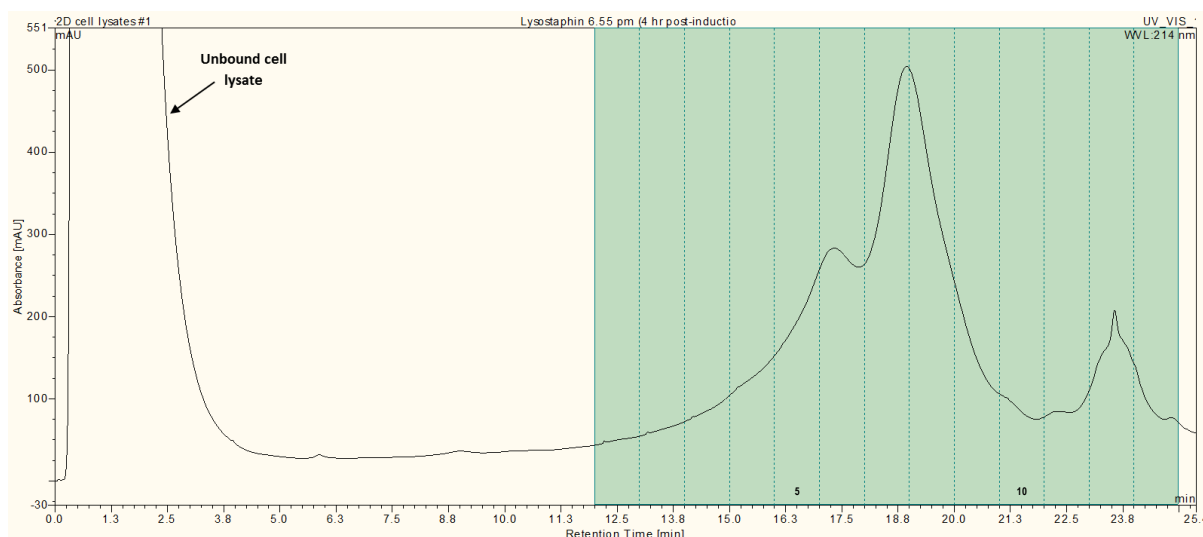


Figure 3.28: Separation of recombinant lysostaphin (construct 1) from *E. coli* cell lysate using a ProPac® SCX (2 x 250 mm) column. Cellular constituents, which could not bind to the SCX column, eluted within the first few minutes of the separation. Protein isoforms appeared to elute during the linear elution gradient, however the elution of some peaks following column washing suggested that some of the protein or UV-absorbing cationic contaminants were retained more strongly.

2D-LC analysis of fractions collected during SCX separation revealed that the resulting fractions were largely composed of a single protein type, however some protein contaminants were resolved in the later eluting fractions (Figure 3.29). Considering that crude cell lysate was applied to the column, it was remarkable that so few cationic protein contaminants were resolved during 2D-LC analysis. This result therefore demonstrated the high selectivity of CXC for the separation of basic proteins, such as recombinant lysostaphin.

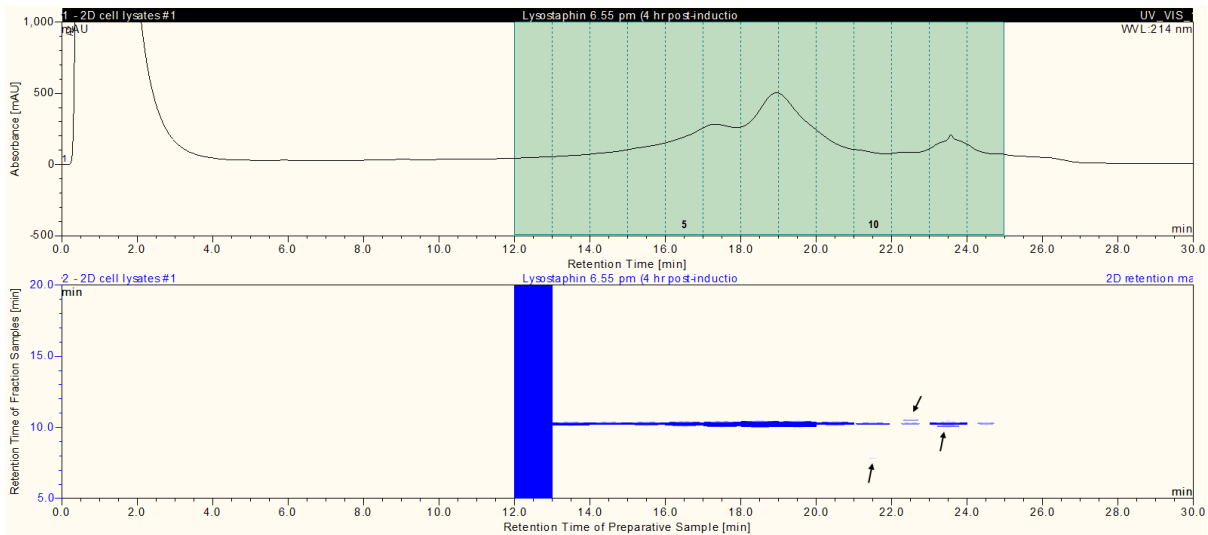


Figure 3.29: 2D-LC separation of recombinant lysostaphin (construct 1) from *E. coli* cell lysate. Recombinant lysostaphin was directly purified from cell lysate and charge variants were separated using a ProPac® SCX (2 x 250 mm) column. Fractions collected during SCX separation were separated using a ProSwift™ RP-4H (1 x 250 mm). The first RP separation had an elevated baseline which led to mis-representation of fraction 1 in the 2D retention map.

A 2.0 mm version of the ProPac® WCX-10 (2 x 250 mm) column was acquired later and proved to provide high resolution separation of recombinant lysostaphin isoforms than the ProPac® SCX-10 (2 x 250 mm) column could (Figure 3.30).

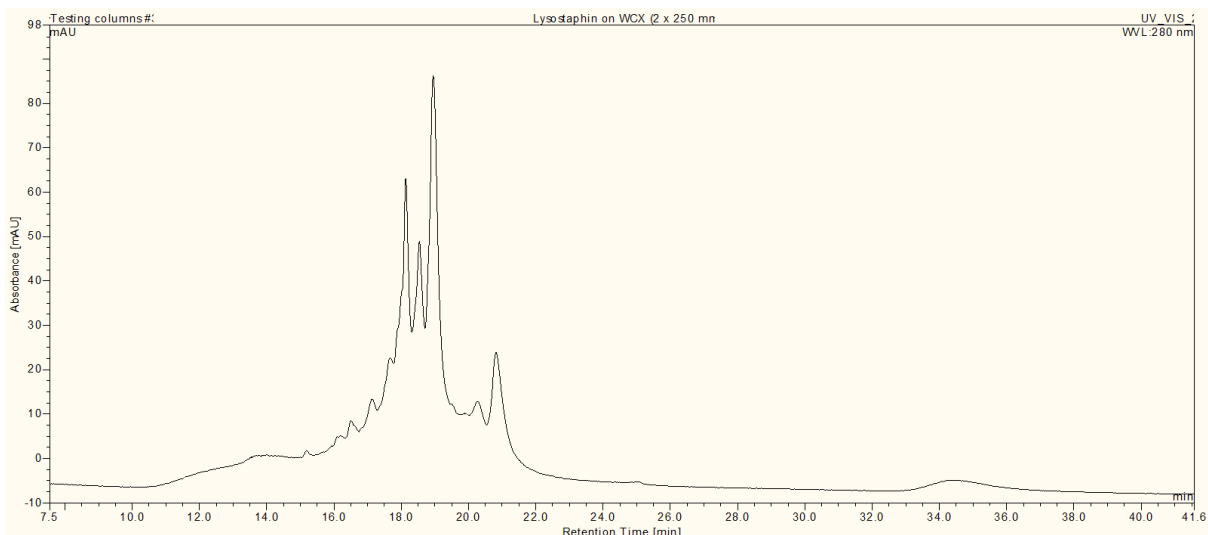


Figure 3.30: Separation of 0.3 mg of purified *N*-terminally His-tagged recombinant lysostaphin (construct 1; preparation 12) using a ProPac® WCX (2 x 250 mm) column.

A second ProPac® WCX (2 x 250 mm) column was obtained to create a ProPac® WCX (2 x 500 mm) column with greater capacity and resolving power. This longer column was

employed for the rapid high-resolution separation of recombinant protein isoforms contained within purified preparations or within cell lysate, as demonstrated in Figure 3.31.

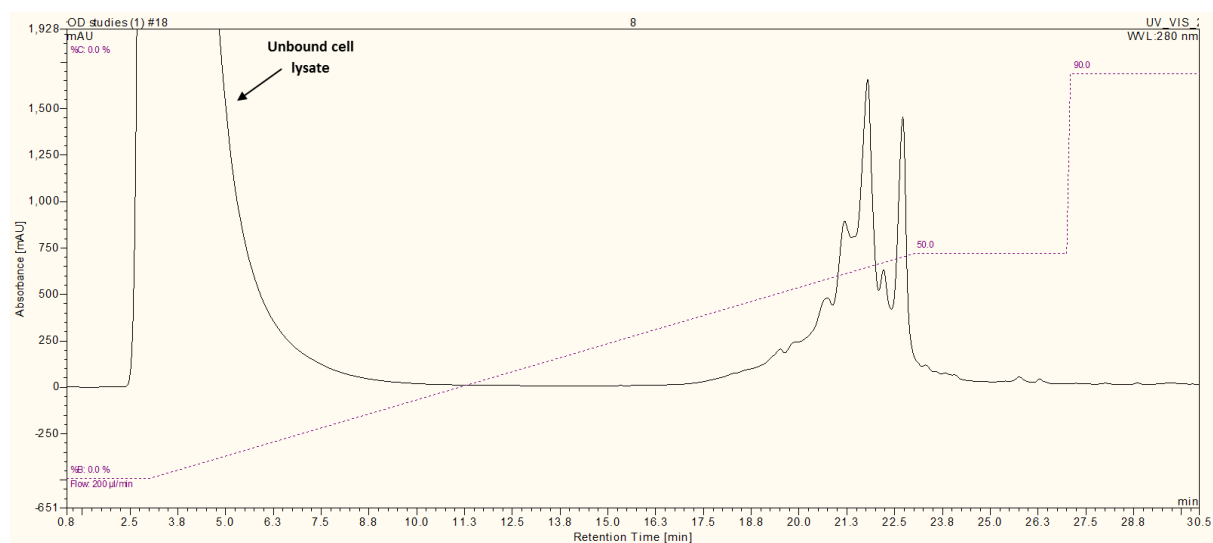


Figure 3.31: Separation of cell lysate containing recombinant lysostaphin (construct 1) using a ProPac[®] WCX (2 x 500 mm) column.

Overall these experiments indicated that high-resolution separation of recombinant lysostaphin isoforms could be achieved using a ProPac[®] WCX-10 (2 x 500 mm) column or ProPac[®] WCX-10 (4 x 500 mm) column. The ProPac[®] WCX-10 (2 x 500 mm) column was therefore used to provide rapid analysis of purified recombinant lysostaphin or cell lysate, whilst the ProPac[®] WCX-10 (4 x 500 mm) column was frequently employed to separate larger quantities of recombinant lysostaphin present within a purified preparation or cell lysate.

3.4.3.8 Optimisation of fraction collection

CXC separations were performed using fraction collection on the basis of time or peak-recognition. Fraction collection was complicated by the complexity of recombinant lysostaphin as protein isoforms did not necessarily elute as distinct peaks. A number of experiments were therefore performed to establish whether timed or peak recognition provided the most appropriate mode of collection.

3.4.3.9 Timed fraction collection

When performing fractionation by time it was essential that the onset and termination of fraction collection was triggered appropriately. The duration of timed fraction collection was selected in accordance with the duration of the linear elution gradient but also after

observing the elution of peaks during previous separation experiments. As shown in Figure 3.32, the duration of fraction collection was generally performed over an extended period of time to ensure that all of the resolved protein isoforms were appropriately collected. The duration of collection was also determined by the heterogeneity of the protein preparation, which was shown to vary considerably between separate batch cultures of recombinant lysostaphin, even following expression of the same gene construct. The onset of fractionation was often reduced to an earlier retention time to ensure that more acidic, less abundant protein isoforms were collected.

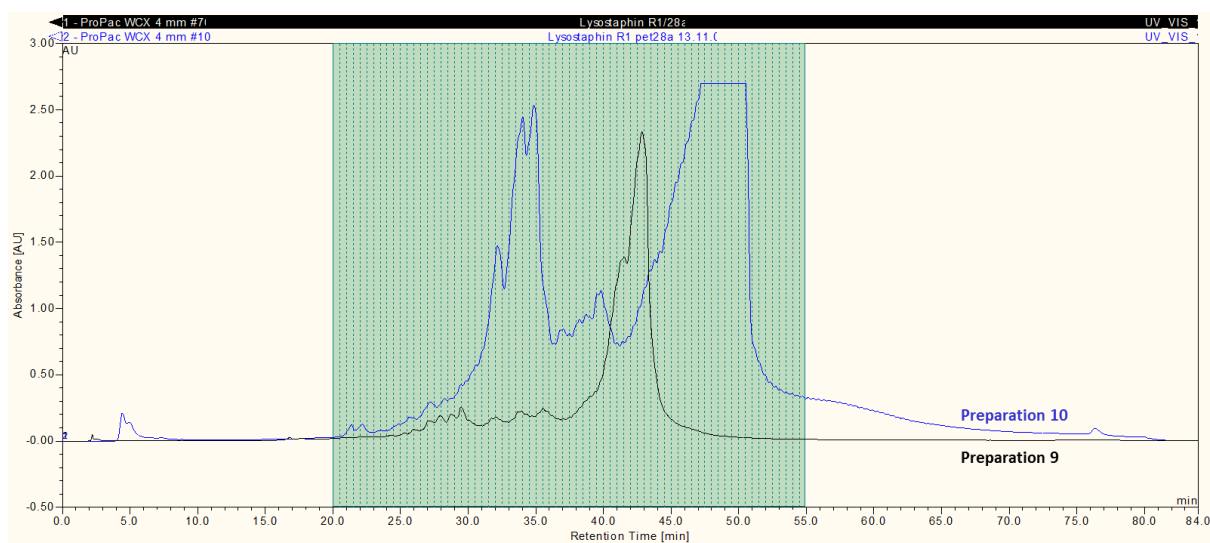


Figure 3.32: Fraction collection based upon time during the separation of different preparations of *N*-terminally His-tagged recombinant lysostaphin (construct 1). WCX analysis resulted in the separation of differently charged protein isoforms, which eluted at different retention times. During the separation of 2.4 mg of preparation 10, timed fraction collection was performed between 15 and 55 min to ensure that less abundant protein variants were collected. During the separation of 3.0 mg of preparation 9, timed fraction collection was performed between 20 and 55 min as the preparation appeared to contain fewer acidic, low-abundance protein isoforms.

3.4.3.10 Peak recognition

Peak recognition fraction collection could be performed according to UV absorbance readings acquired at 214 or 280 nm. Monitoring of absorbance at 214 nm provided the most sensitive detection of protein absorbance, through detection of the peptide backbone but also other UV-absorbing contaminants. Measurement of absorbance at 280 nm detects protein molecules according to the presence of aromatic residues, therefore offers more specific detection of protein absorbance, rather than UV-absorbing contaminants. Peak recognition fraction collection was initially performed based on absorbance at 214 nm. As shown in Figure 3.33, this led to sensitive peak recognition collection of low abundance

isoforms, however the presence of UV contaminants interfered with appropriate fraction collection of more abundant protein isoforms.

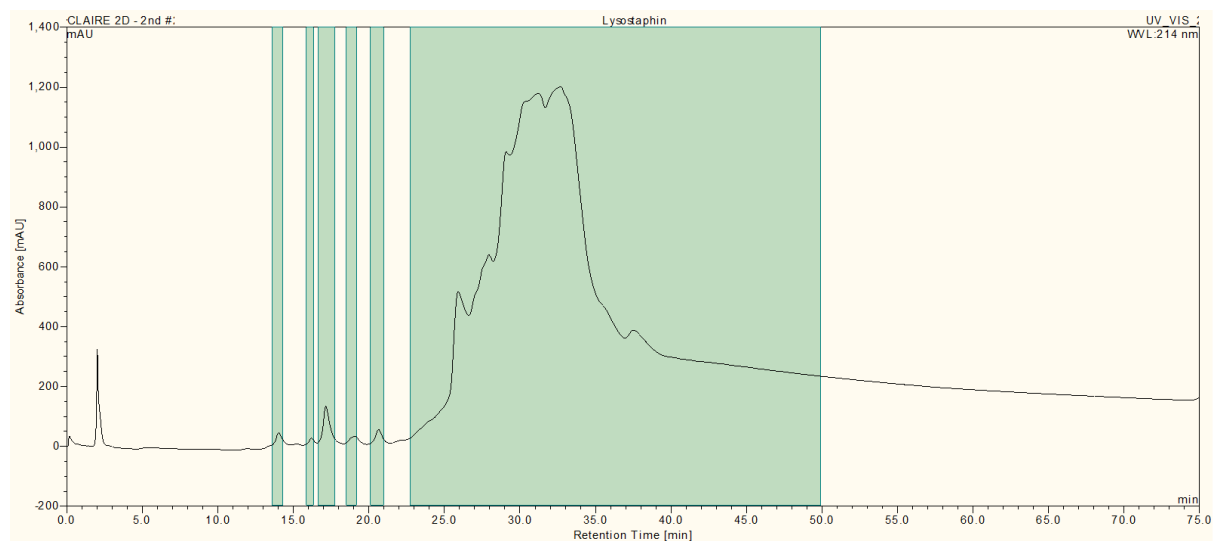


Figure 3.33: Fraction collection based upon UV absorbance at 214 nm during the separation of 0.7 mg of C-terminally His-tagged recombinant lysostaphin (construct 3; preparation 13). Collection was based upon peak recognition, which provided sensitive collection at low absorbance reading, yet lost detection sensitivity upon the elution of broad peaks with a higher absorbance. However peak recognition at 214 nm permitted collection of less abundant protein isoforms between 13 and 21 min.

When peak recognition fraction collection was based upon absorbance at 280 nm, fraction collection of protein isoforms was performed more appropriately. Figure 3.34 demonstrates that the most abundant protein isoforms were collected in separate fractions, however less abundant protein isoforms were not collected as their absorbance level did not trigger automated collection, suggesting that the peak recognition parameters required modification.

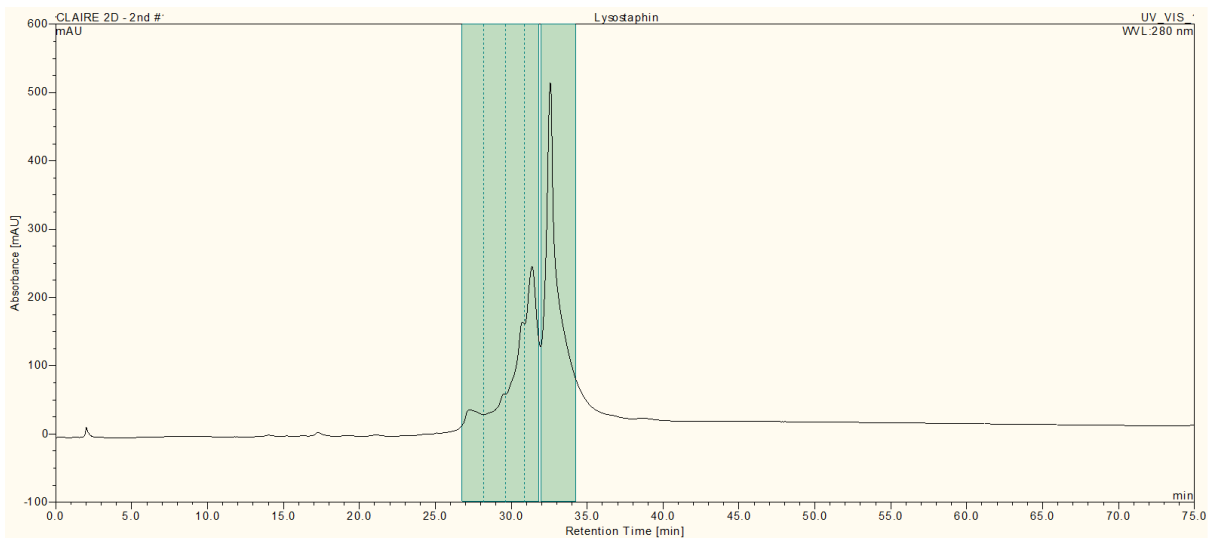


Figure 3.34: Fraction collection based upon UV absorbance at 280 nm during separation of 0.7 mg of C-terminally His-tagged recombinant lysostaphin (construct 3; preparation 13). Collection was based upon peak recognition, which provided sensitive detection of peak elution and permitted collection of protein isoform peaks within separate fractions. However peak recognition at 280 nm did not permit collection of less abundant protein isoforms.

A number of WCX separations were performed using slightly adjusted peak recognition parameters with the intention of achieving sensitive collection of eluted peaks. Despite modifying peak recognition parameters in a systematic manner, it was found that fraction collection could not be achieved correctly. This was due to an intrinsic programming error associated with the Chromeleon Version 6.8 software, which prevented the correct performance of peak recognition fraction collection. As demonstrated in Figure 3.35, fraction collection was inappropriately triggered in the absence of peak elution. Inappropriate and spurious fraction collection was not desirable as the hyper-functioning of the auto-sampler module resulted in missed collection of eluted peaks.

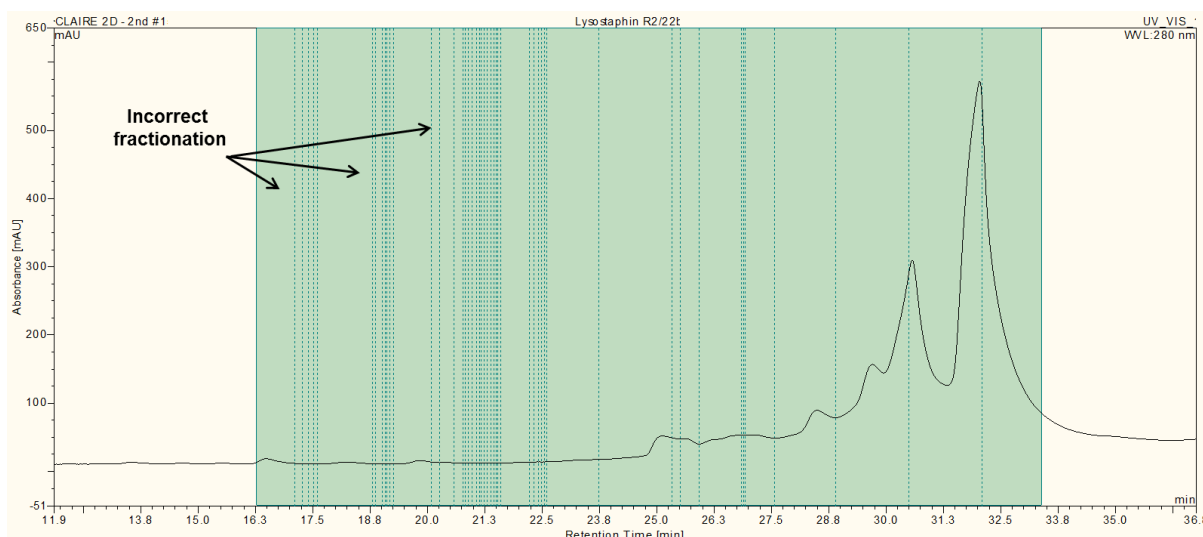


Figure 3.35: Inappropriate peak recognition fraction collection during separation of 0.7 mg of C-terminally His-tagged recombinant lysostaphin (construct 3; preparation 13). This was caused by a software fault which was subsequently corrected by Dionex Corporation.

This issue was reported to Dionex Corporation and the fault was subsequently rectified. However it was decided that time-based fraction collection would be applied in subsequent separations due to the fact that it would have been very difficult to optimise peak recognition parameters to recognise and collect small or poorly resolved peaks. Timed fraction collection was known to provide more reliable and consistent collection, regardless of peak height or resolution, therefore reducing the likelihood of missed collection of peaks during WCX separation.

3.4.3.11 Analysis of recombinant lysostaphin using optimised conditions

During the optimisation of WCX separation many experiments were performed to evaluate recombinant lysostaphin variants. It was apparent that multiple peaks could be resolved during WCX separation, reflecting the presence of protein isoforms. However it may have been possible that the detection of multiple peaks may have occurred as an artefactual phenomenon associated with separation. Therefore an eluted fraction was collected and re-applied to the column to demonstrate that the protein contained in the fraction displayed the same retention time as it did during the initial separation (Figure 3.36).

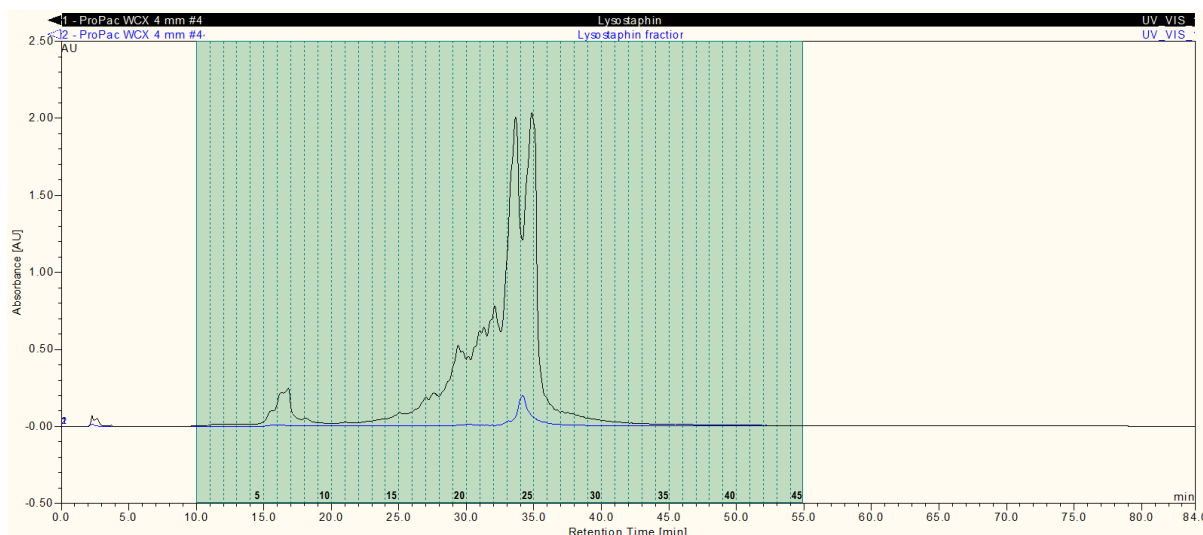


Figure 3.36: Re-application of fractions eluted during WCX separation of 0.7 mg of C-terminally His-tagged recombinant lysostaphin (construct 3; preparation 13). Fraction 25 was collected and re-applied to the column, as indicated.

Re-application of the collected fraction indicated that the eluted protein demonstrated a similar retention time as it did during the initial separation. Slight shifting in retention time was likely to reflect the fact that the protein had been eluted in an increased salt concentration, which may have influenced protein retention during the second separation.

3.4.3.12 Influence of culture temperature upon charge heterogeneity of recombinant lysostaphin

To assess whether culture temperature influenced charge heterogeneity of recombinant lysostaphin, three cultures were divided at the point of induction and fermented at either 20 or 30°C. SDS-PAGE analysis revealed that recombinant lysostaphin was hyper-expressed in all cultures (Appendix 7.191). As shown in Figure 3.37, Figure 3.38 and Figure 3.39, greater charge heterogeneity was observed amongst recombinant lysostaphin which had been expressed in cultures incubated at 30°C. SDS-PAGE analysis of selected fractions collected during WCX separation demonstrated that the major peaks were attributable to the presence of a protein with a molecular weight corresponding to that of recombinant lysostaphin (construct 1) (Appendix 7.193 - Appendix 7.204).

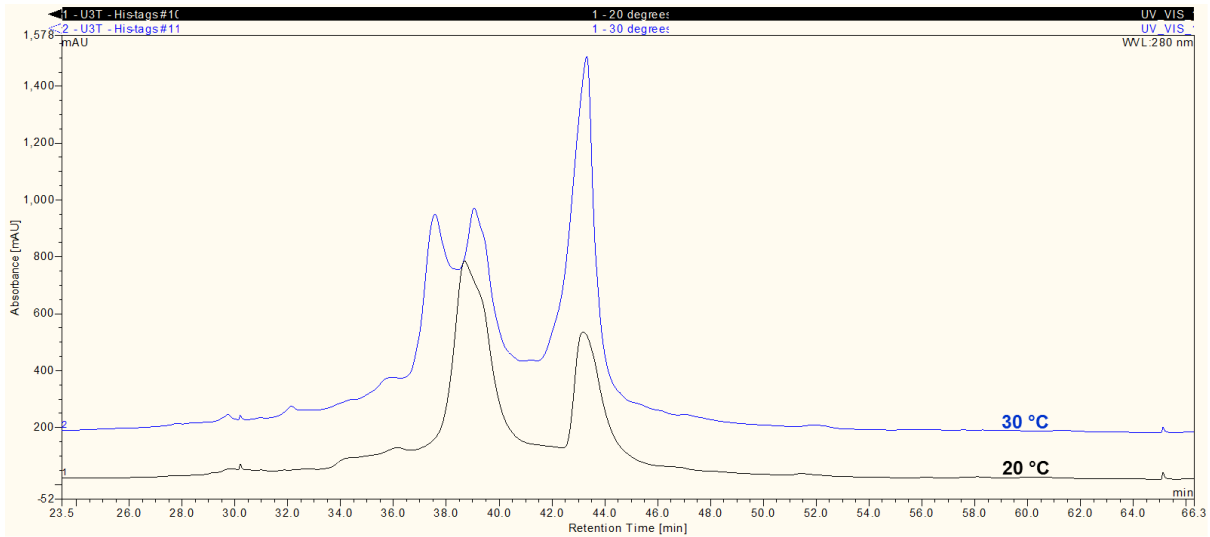


Figure 3.37: Comparison of WDX separations performed on cell lysate containing recombinant lysostaphin (construct 1) following expression at 20 or 30°C (Culture 1).

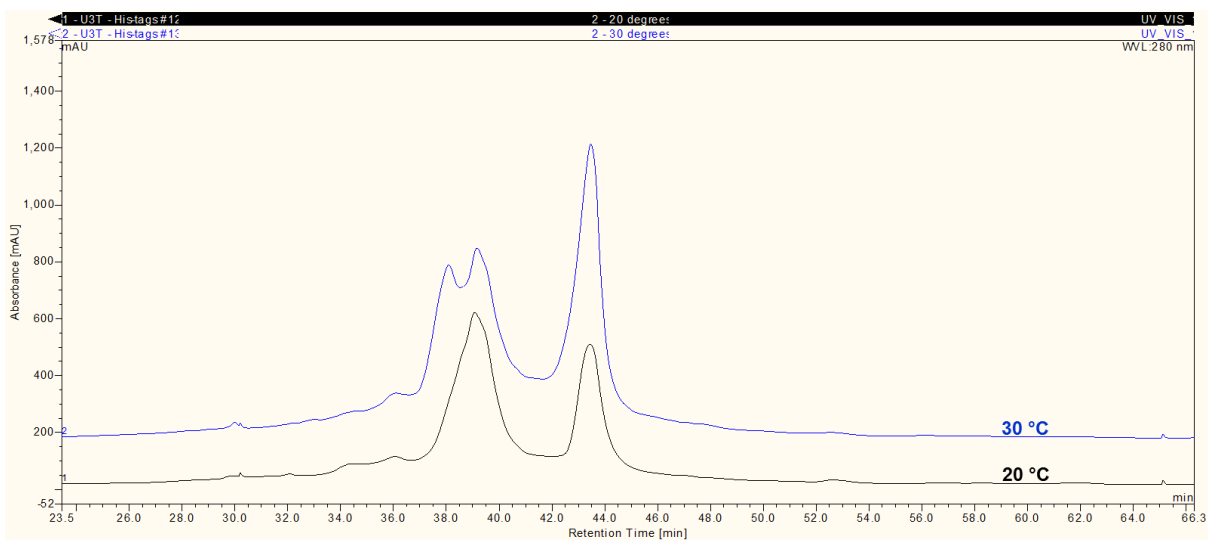


Figure 3.38: Comparison of WDX separations performed on cell lysate containing recombinant lysostaphin (construct 1) following expression at 20 or 30°C (Culture 2).

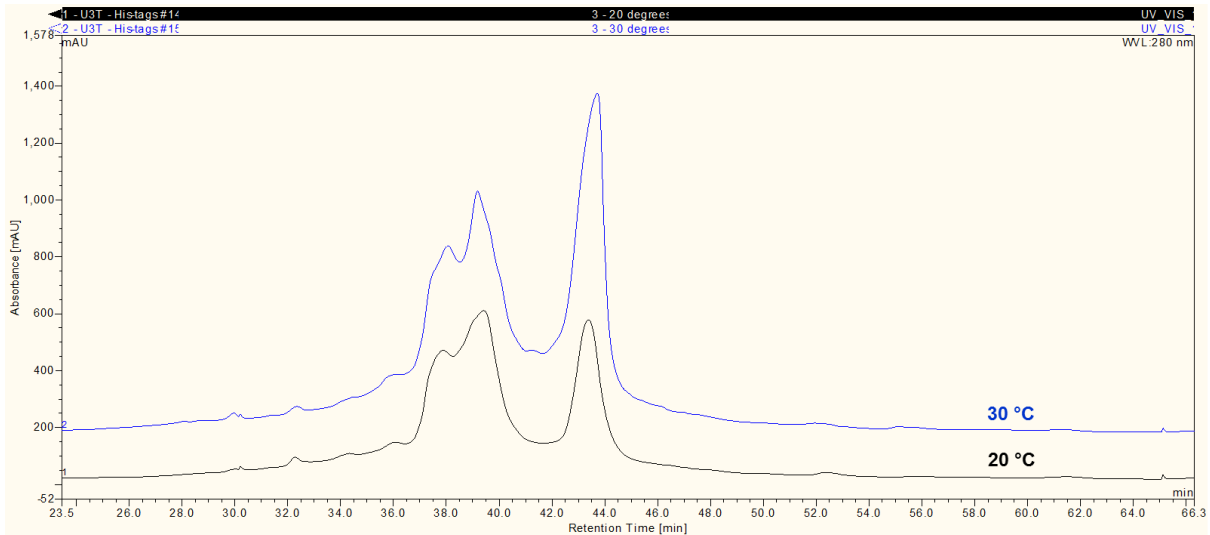


Figure 3.39: Comparison of WCX separations performed on cell lysate containing recombinant lysostaphin (construct 1) following expression at 20 or 30°C (Culture 3).

The presence of particular protein isoforms appeared to remain fairly consistent between all three cultures, however greater cell density at the point of induction appeared to increase sample heterogeneity during the expression of recombinant lysostaphin at 20°C (Figure 3.40) rather than at 30°C (Figure 3.41).

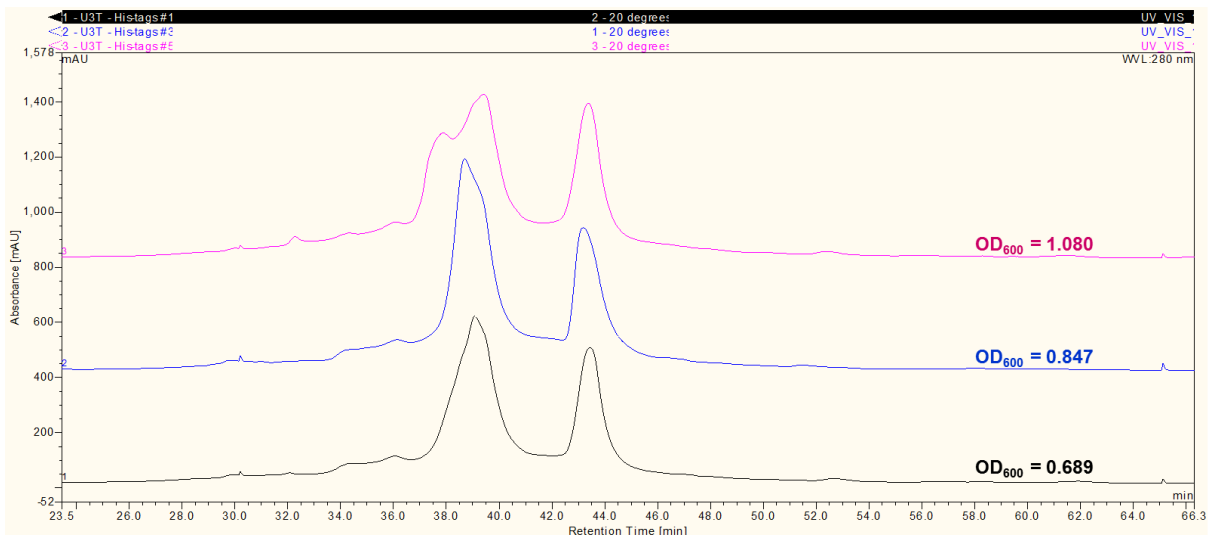


Figure 3.40: Comparison of WCX separations performed on cell lysate containing recombinant lysostaphin (construct 1) following expression at 20°C (Cultures 1, 2 and 3).

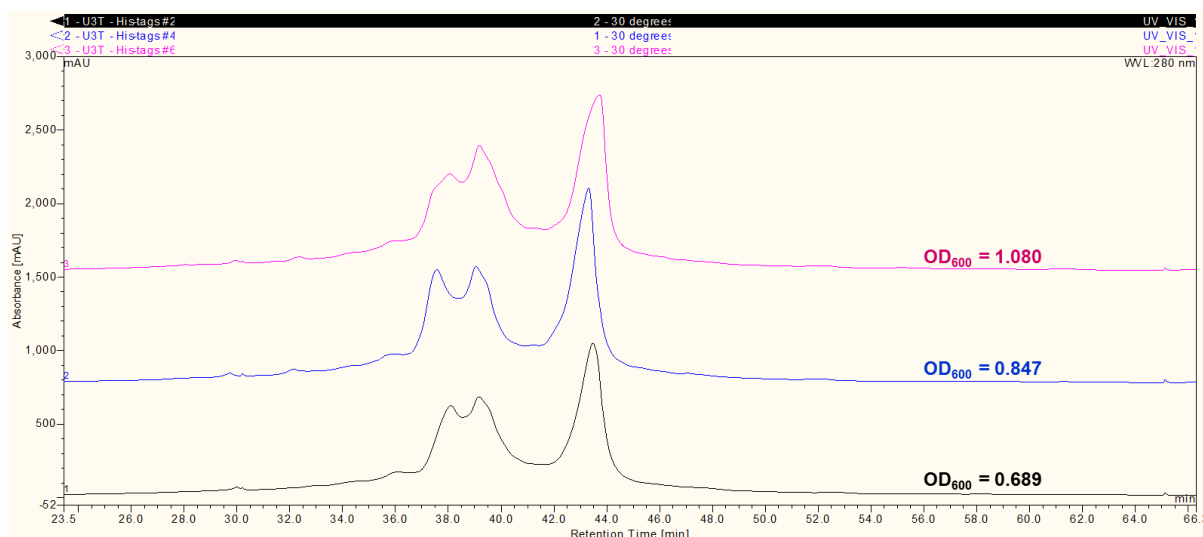


Figure 3.41: Comparison of WCX separations performed on cell lysate containing recombinant lysostaphin (construct 1) following expression at 30°C (Cultures 1, 2 and 3).

As a reduced culture temperature and a moderate optical density at the point of induction appeared to minimise the occurrence of more acidic protein isoforms, further experiments were performed under these conditions. The experiments were also performed using recombinant lysostaphin without His-tags (construct 2) rather than *N*-terminally His-tagged recombinant lysostaphin (construct 1) as this form of the protein was later found to exhibit less charge heterogeneity (Section 4.2.3.1). As shown in Figure 3.42 and Figure 3.43, the presence of particular protein isoforms remained fairly constant between cultures incubated at the same temperature and induced at similar optical densities. However the abundance of the more acidic isoform (observed at 42 min) was diminished in cultures incubated at 16°C (Figure 3.44 and Figure 3.45). Cell lysate harvested from cultures incubated at 16°C was also analysed by SDS-PAGE to confirm hyper-expression of recombinant lysostaphin (Appendix 7.205).

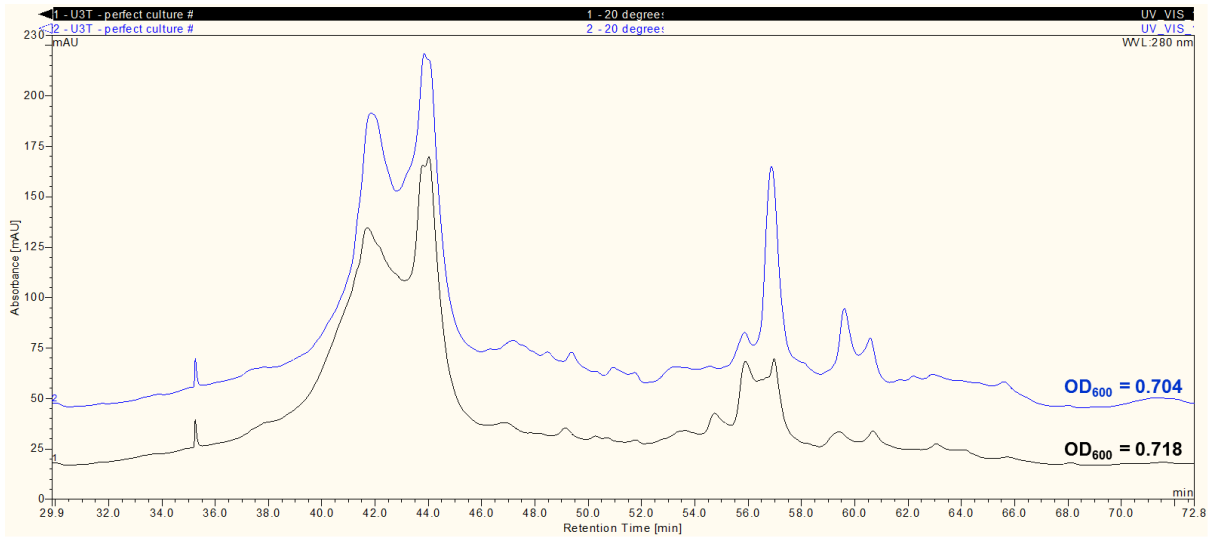


Figure 3.42: Comparison of WCX separations performed on cell lysate containing recombinant lysostaphin (construct 2) following expression at 20°C (Cultures 4 and 5).

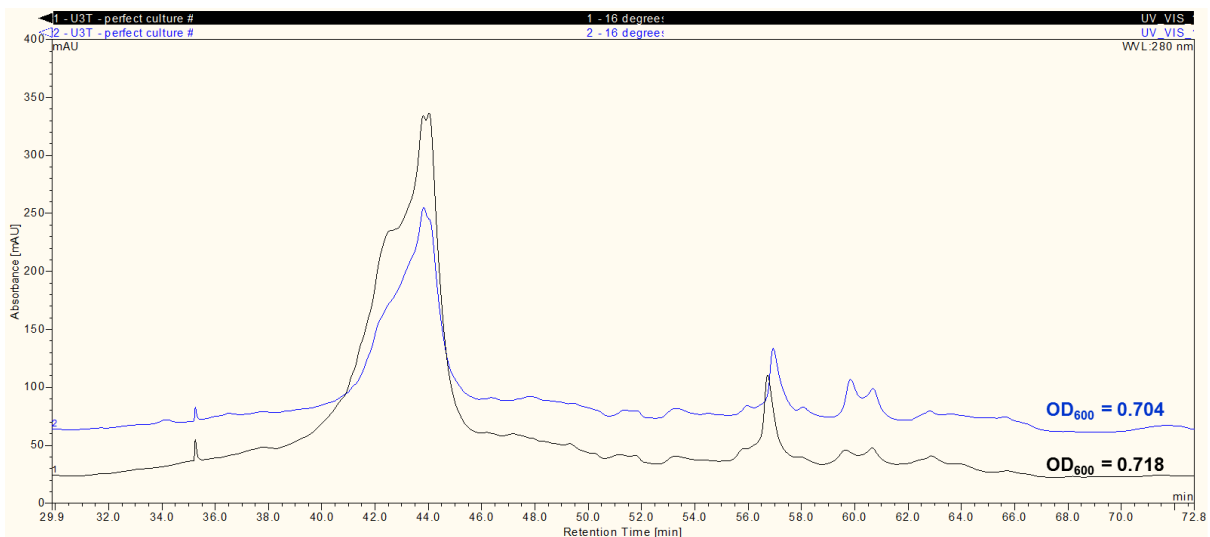


Figure 3.43: Comparison of WCX separations performed on cell lysate containing recombinant lysostaphin (construct 2) following expression at 16°C (Cultures 4 and 5).

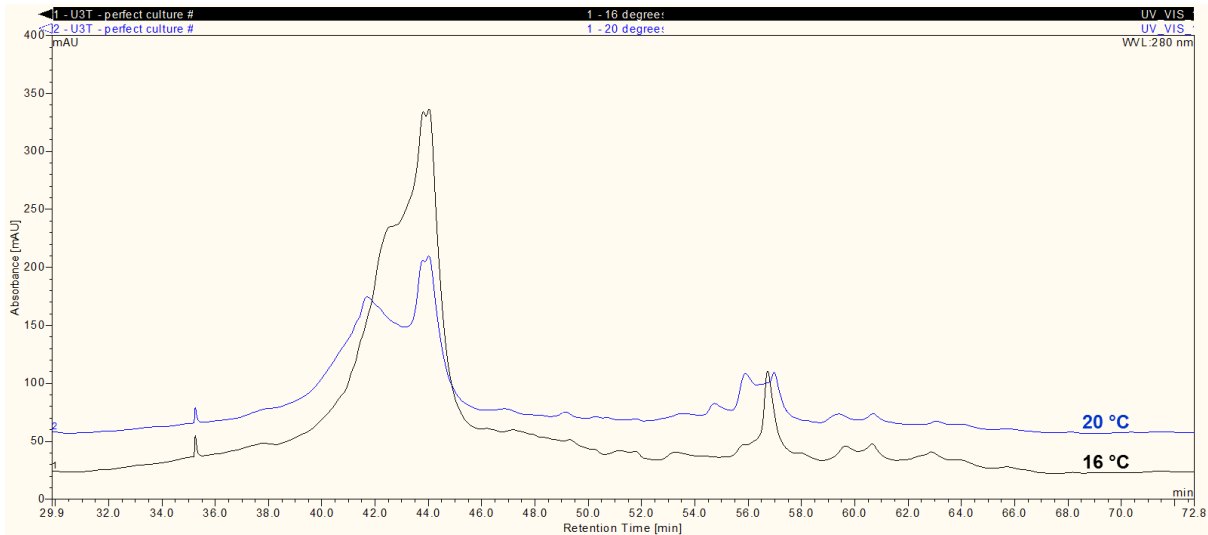


Figure 3.44: Comparison of WCX separations performed on cell lysate containing recombinant lysostaphin (construct 2) following expression at 16°C and 20°C (Culture 4).

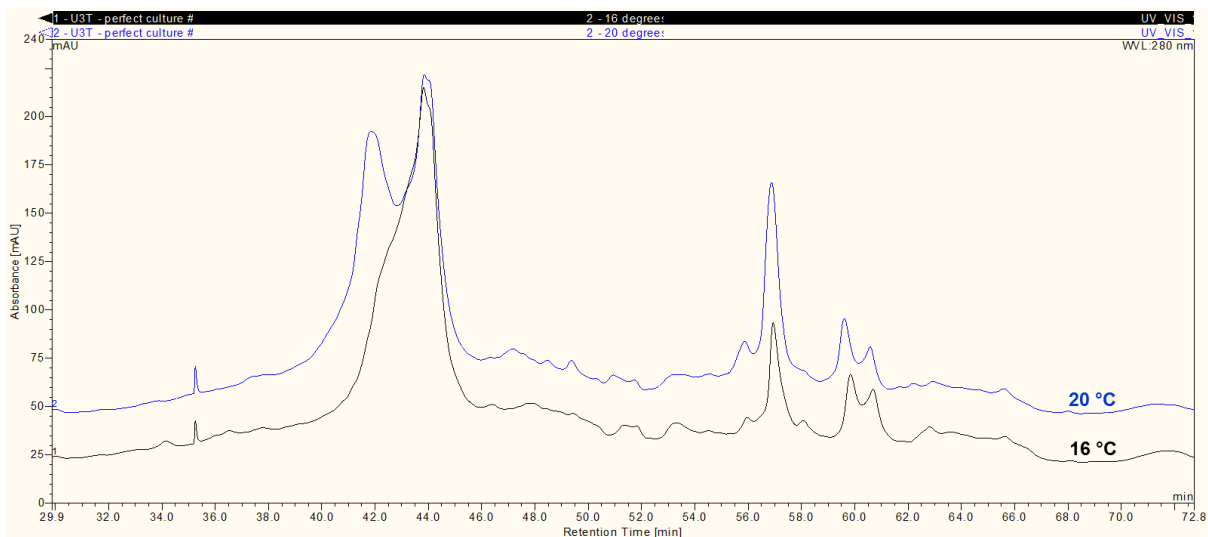


Figure 3.45: Comparison of WCX separations performed on cell lysate containing recombinant lysostaphin (construct 2) following expression at 16°C and 20°C (Culture 5).

Recombinant lysostaphin (construct 2) expressed in *E. coli* fermented at 16°C was produced as a fairly homogeneous preparation, with the resolution of a single major peak during WCX separation. However the broad width and asymmetry of the resolved single peak, suggested that protein eluted within this peak could still be fairly homogeneous. As the heterogeneity of the recombinant lysostaphin preparation was likely to increase with increased duration of culture, an additional experiment was performed to establish whether recombinant lysostaphin would demonstrate a lesser degree of heterogeneity if cell lysate was harvested after a shorter period of culture.

During the previous experiment cell lysate was harvested at 17.5 h post-induction, therefore in the subsequent experiment cell lysate was harvested at 14.0 h post-induction. Figure 3.46 however demonstrated that recombinant lysostaphin harvested at 14.0 h post-induction did not in fact demonstrate greater homogeneity.

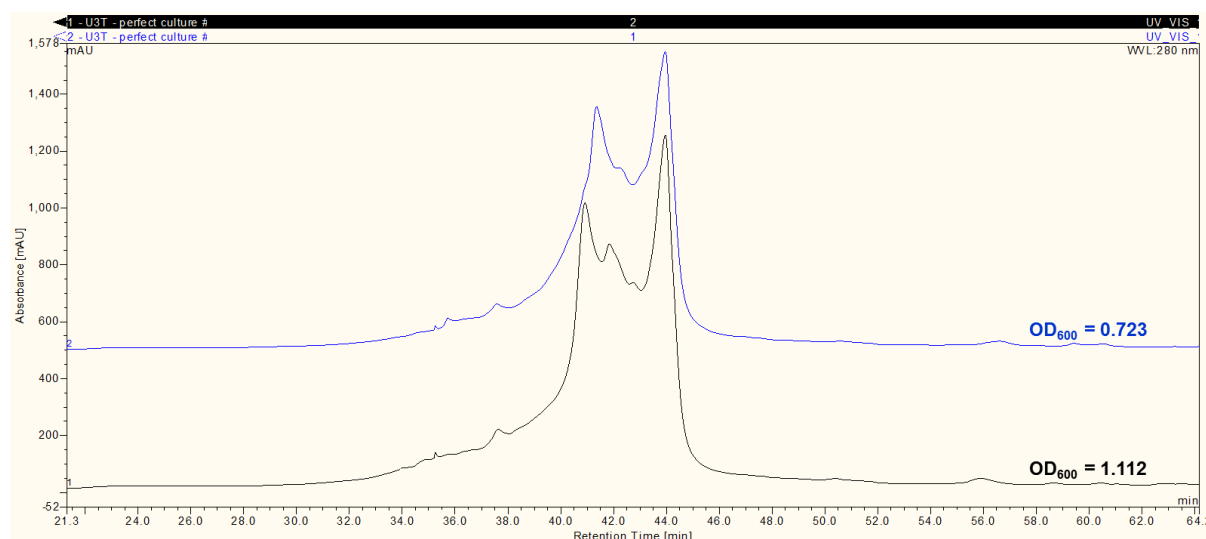


Figure 3.46: Comparison of WCX separations performed on cell lysate containing recombinant lysostaphin (construct 2) following expression at 16°C and harvest at 14.0 h post-induction (Culture 6).

3.4.3.13 Separation of alternative recombinant protein preparations

As WCX separation provided resolution of protein isoforms within recombinant lysostaphin preparations, the optimised WCX method was used to analyse alternative recombinant protein preparations to establish whether charge heterogeneity may be a common occurrence when recombinant proteins are expressed in *E. coli*. As WCX columns could only separate proteins which were basic at pH 8.0, two basic proteins were selected for analysis in the form of recombinant oxidoreductase from *Clostridium acetobutylicum* and recombinant NADPH-dependent 1-acyl dihydroxyacetone phosphate reductase (Ayr1p) from *Saccharomyces cerevisiae*.

ProtParam analysis of amino acid sequences (Appendix 7.206 and Appendix 7.207) revealed that the recombinant proteins had theoretical pI of 8.62 and 9.23 respectively (Appendix 7.208 and Appendix 7.209) and therefore were predicted to bind to the WCX column. In addition ClustalW analysis confirmed that the amino acid sequences did not share sequence homology with the amino acid sequence of recombinant lysostaphin (Appendix 7.210). Both recombinant proteins were initially expressed in *E. coli* BL21(DE3)

cultured in LB , before harvesting the cell lysate and performing SDS-PAGE analysis (Appendix 7.211). The cell lysates were then subjected to WCX analysis (Figure 3.47 and Figure 3.48).

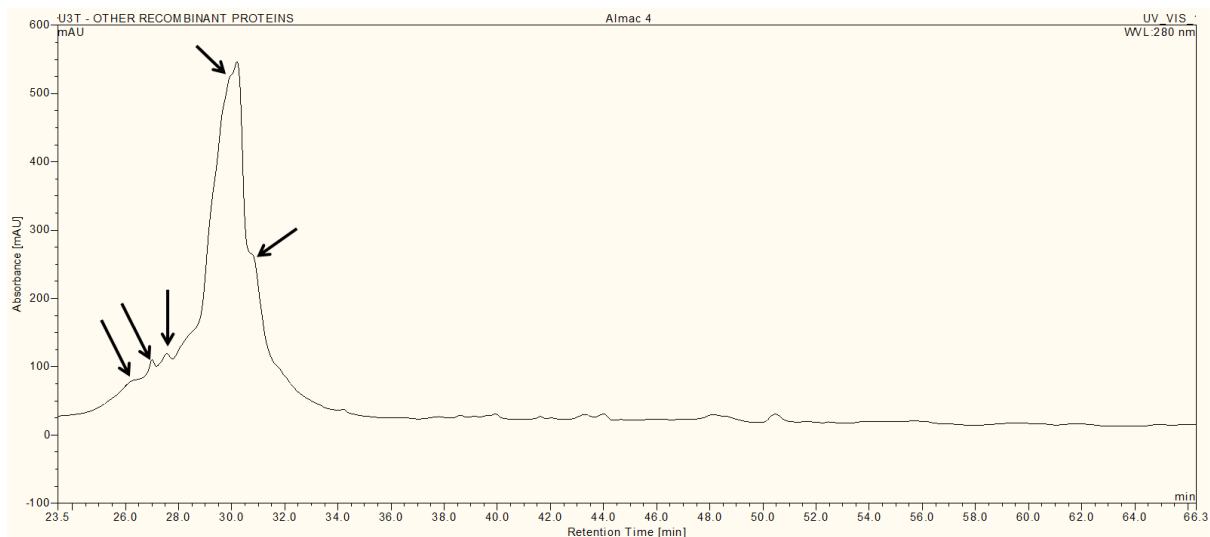


Figure 3.47: WCX separation of cell lysate containing recombinant oxidoreductase using a ProPac® WCX (4 x 500 mm) column. Cell lysate was harvested from *E. coli* BL21(DE3) which had been cultured in LB. Arrows indicate the presence of resolved charge variants.

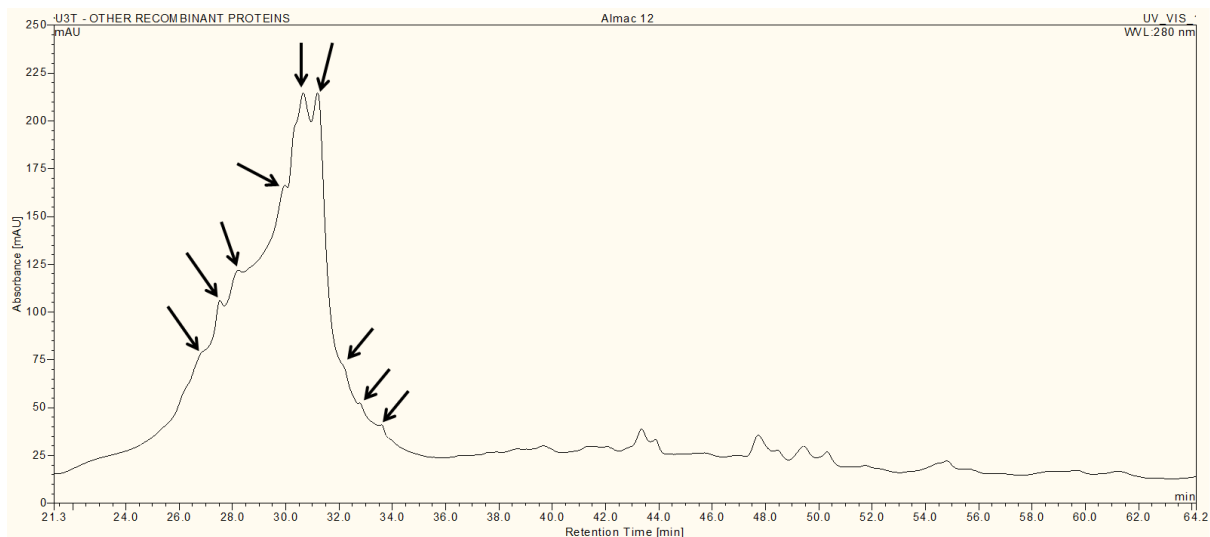


Figure 3.48: WCX separation of cell lysate containing recombinant Ayr1p using a ProPac® WCX (4 x 500 mm) column. Cell lysate was harvested from *E. coli* BL21(DE3) which had been cultured in LB. Arrows indicate the presence of resolved charge variants.

As shown in Figure 3.47 and Figure 3.48, WCX separation revealed that both recombinant protein preparations contained a predominant peak, within which minor charge variants

could be resolved. SDS-PAGE analysis confirmed that the peaks resolved during WCX separation (Appendix 7.212 and Appendix 7.214) reflected the presence of protein with a molecular weight which corresponded to the masses of recombinant oxidoreductase (28.5 kDa) and recombinant Ayr1p (32.8 kDa) (Appendix 7.213 and Appendix 7.215). Both recombinant proteins were also expressed in *E. coli* BL21(DE3) cultured in AIM and harvested cell lysates (Appendix 7.216) were subjected to WCX analysis, as shown in Figure 3.49 and Figure 3.50. Once again PAGE analysis confirmed that the peaks resolved during WCX separation (Appendix 7.217 and Appendix 7.219) reflected the presence of protein with molecular weights which corresponded to the masses of recombinant oxidoreductase (28.5 kDa) and recombinant Ayr1p (32.8 kDa) (Appendix 7.218 and Appendix 7.220).

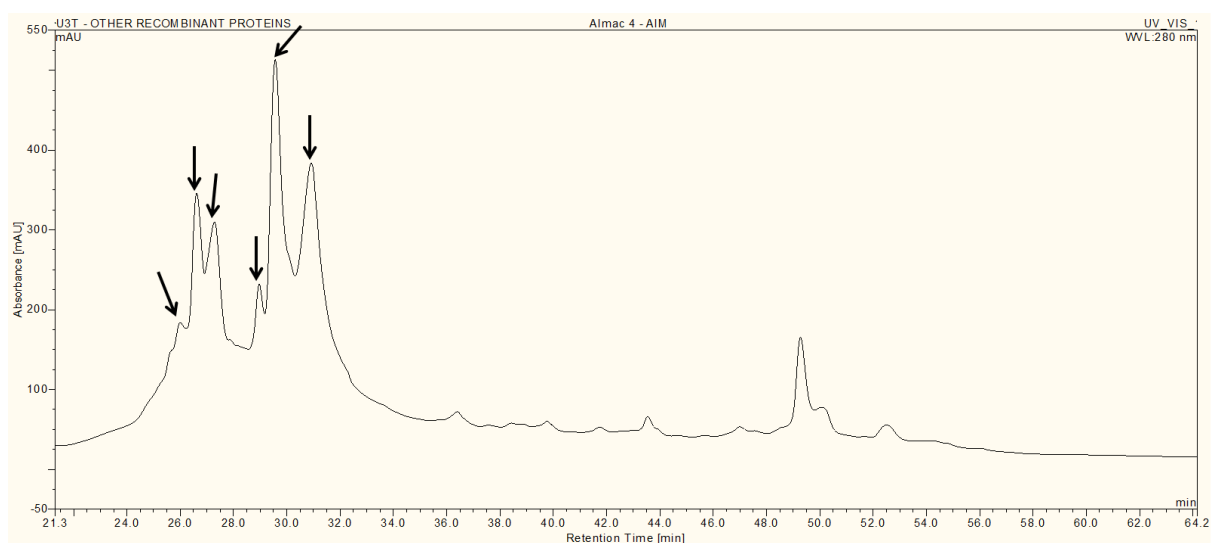


Figure 3.49: WCX separation of cell lysate containing recombinant oxidoreductase using a ProPac[®] WCX (4 x 500 mm) column. Cell lysate was harvested from *E. coli* BL21(DE3) which had been cultured in AIM. Arrows indicate the presence of resolved charge variants.

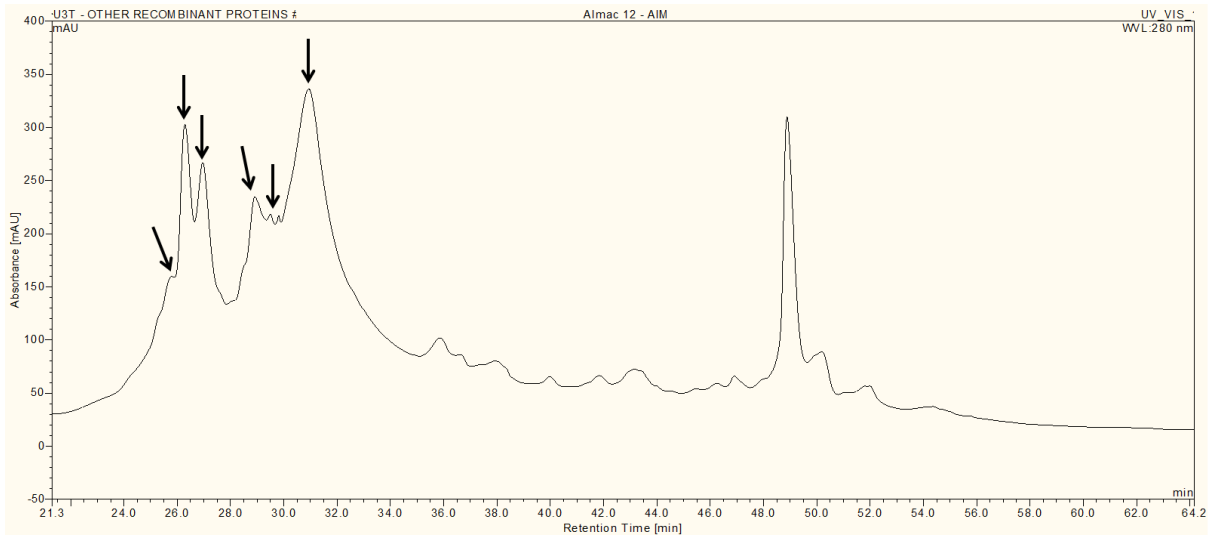


Figure 3.50: WAX separation of cell lysate containing recombinant Ayr1p using a ProPac® WAX (4 x 500 mm) column. Cell lysate was harvested from *E. coli* BL21(DE3) which had been cultured in AIM. Arrows indicate the presence of resolved charge variants.

WAX separation of recombinant oxidoreductase and recombinant Ayr1p expressed in *E. coli* cultured in AIM clearly demonstrated that charge heterogeneity is not only exhibited by recombinant lysostaphin, but also by other cationic recombinant proteins. Expression of recombinant oxidoreductase and recombinant NADPH-dependent 1-acyl dihydroxyacetone phosphate reductase (Ayr1p) by *E. coli* cultured in AIM appeared to result in greater charge heterogeneity, which may have been attributable to the expression media (Figure 3.51 and Figure 3.52). However it was more likely that the greater charge heterogeneity was attributable to differences in culture duration as recombinant proteins expressed by *E. coli* cultured in AIM were harvested at 16.0 h post-induction, whilst recombinant proteins expressed by *E. coli* cultured in LB were harvested at 19.5 h post-induction.

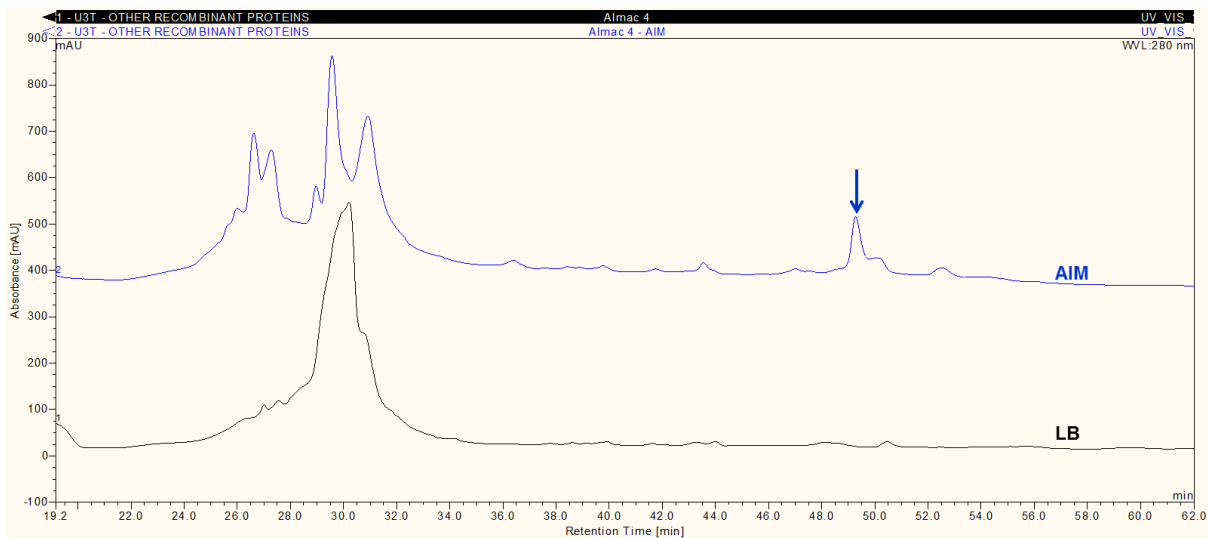


Figure 3.51: Comparison of WCX separations performed on cell lysate containing recombinant oxidoreductase expressed in *E. coli* BL21(DE3) cultured in LB or AIM. PAGE analysis revealed that the presence of an additional peak at 49 min (indicated by arrow) represented the presence of a large cationic *E. coli* protein (66-97 kDa) which was expressed upon growth in AIM.

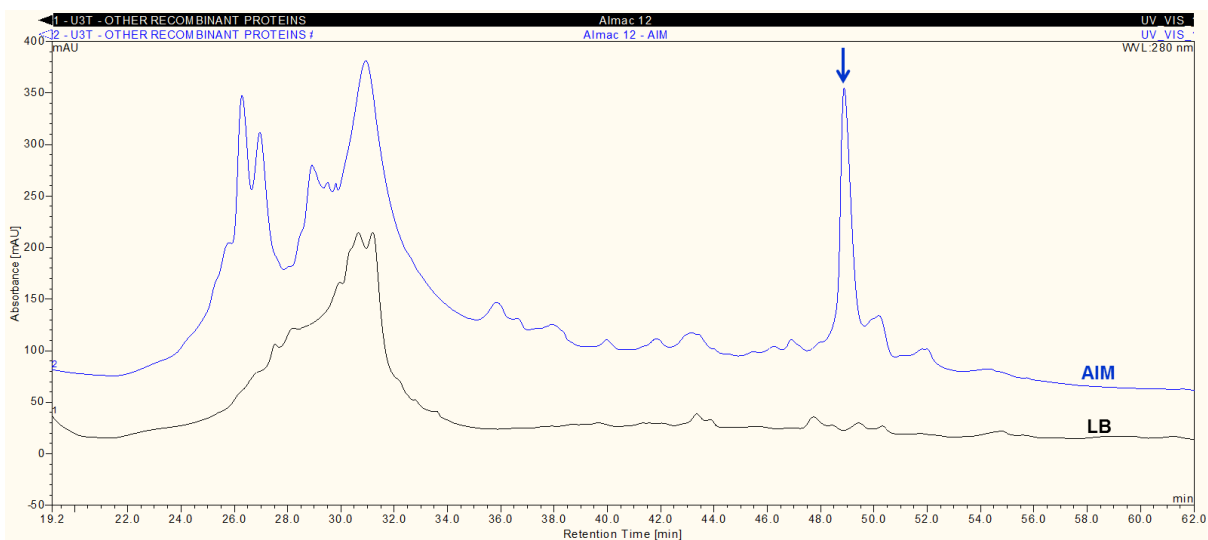


Figure 3.52: Comparison of WCX separations performed on cell lysate containing recombinant Ayr1p expressed in *E. coli* BL21(DE3) cultured in LB or AIM. PAGE analysis revealed that the presence of an additional peak at 49 min (indicated by arrow) represented the presence of a high molecular weight cationic *E. coli* protein (66-97 kDa) which was expressed upon growth in AIM.

PAGE analysis confirmed that the peaks resolved between 24 and 34 min during WCX separation reflected the presence of protein with molecular weight which corresponded to the masses of recombinant oxidoreductase (28.5 kDa) (Appendix 7.213 and Appendix 7.218) and recombinant Ayr1p (32.8 kDa) (Appendix 7.215 and Appendix 7.220). Interestingly cell lysates harvested from *E. coli* cultured in AIM appeared to contain more

contaminating cationic proteins, which were detectable during WCX separation and SDS-PAGE. This finding demonstrates that expression media can significantly influence cellular proteomic expression profiles.

3.4.3.14 Optimisation of protein isoform separation using the beta-test ProPac® MAb column

Although the ProPac® MAb column provided excellent resolution of protein isoforms, experiments were performed to establish whether separation could be optimised further by slight modification of sample loading, column length, gradient and mobile phase conditions.

3.4.3.15 Optimisation of sample loading conditions

This initial application of recombinant lysostaphin resulted in excellent resolution and separation of lysostaphin isoforms, however only a small amount of lysostaphin (16.8 µg) had been applied to the column. Consequently comparative separations were performed following injection of higher amounts of lysostaphin to establish if this would result in peak broadening and a reduction in isoform resolution and separation (Figure 3.53).

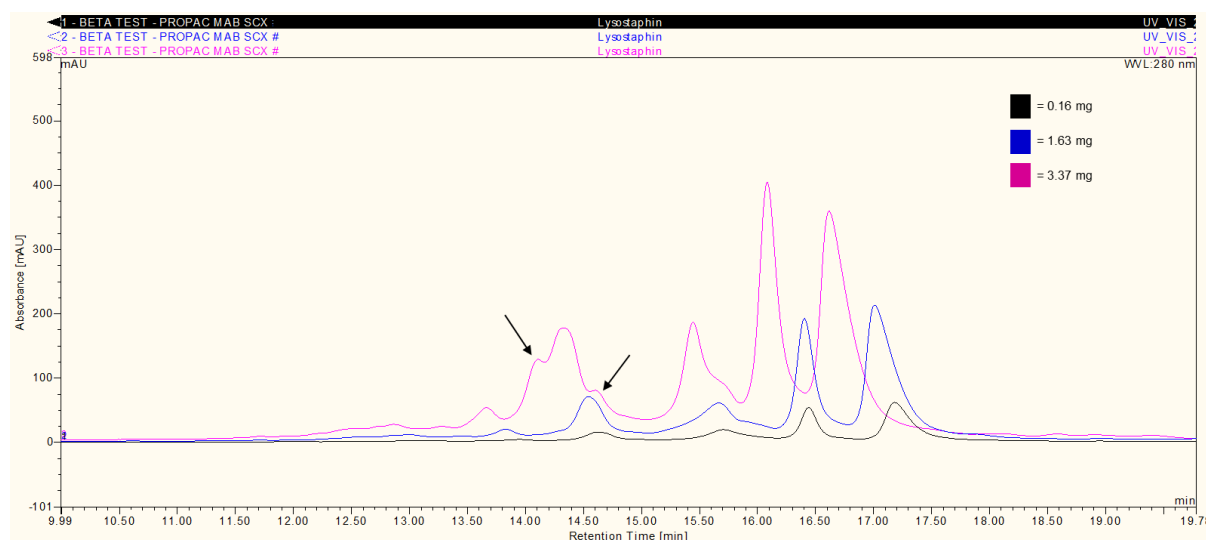


Figure 3.53: Comparison of chromatograms after injection of increasing amounts of C-terminally His-tagged recombinant lysostaphin (construct 3; preparation 5). Arrows indicate additionally resolved peaks.

Figure 3.53 demonstrates that peak height increases with the application of increasing amounts of lysostaphin, as would be expected. Adding a ten-fold higher amount of lysostaphin (1.63 mg) resulted in a very similar pattern of separation to that achieved after application of a ten-fold lower amount of lysostaphin (0.16 mg), with only slight peak

broadening observed. Application of a twenty-fold higher amount of lysostaphin (3.3 mg) also resulted minimal peak broadening and increased peak height as expected. This third application of lysostaphin was subject to slight chromatographic shifting as shown in Figure 3.53, however it is interesting to observe that additional protein isoforms were resolved with the application of a higher amount of recombinant lysostaphin (see arrows on Figure 3.53). This result highlighted the importance of optimising the amount of sample protein that was applied to the column.

3.4.3.16 Optimisation of chromatographic gradient conditions

Excellent separations of recombinant lysostaphin were achieved using the beta-testing gradient conditions suggested by Dionex. As the gradient conditions had been optimised extensively for the ProPac® WCX column, the optimised gradient conditions were applied in conjunction with the ProPac® MAb column to see if the optimised method for the ProPac® WCX-10 column could provide even greater resolution of isoforms using the beta test column. However, Figure 3.54 demonstrates that the optimised gradient conditions did not provide significantly better separation of peaks than the gradient conditions recommended during beta testing.

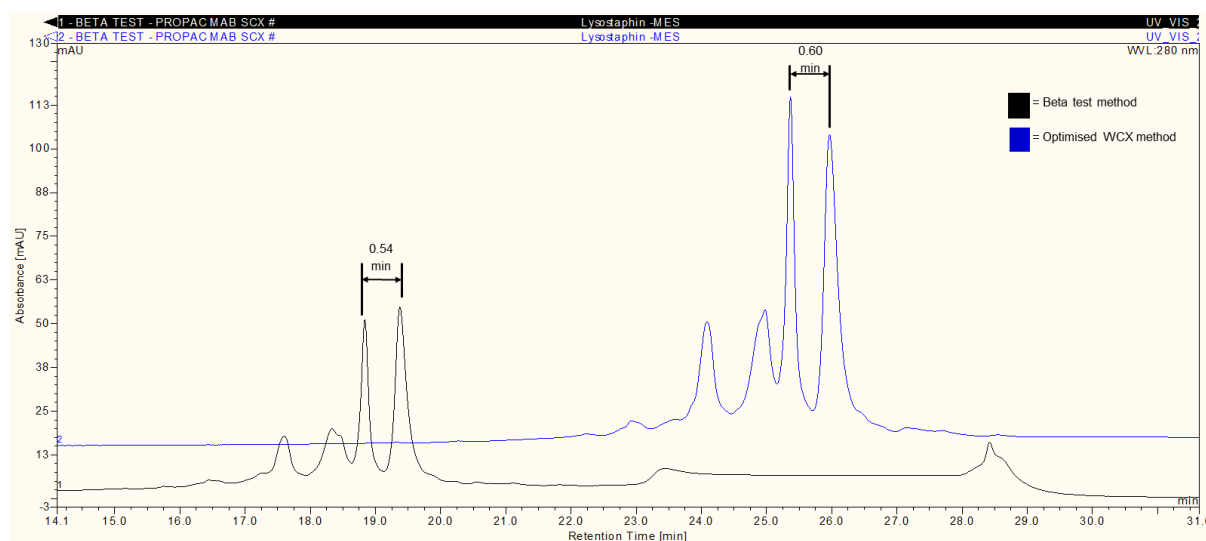


Figure 3.54: Comparison of separation efficiency of chromatographic gradient conditions during the separation of 0.3 mg of C-terminally His-tagged recombinant lysostaphin (construct 3; preparation 5) As indicated, there is very little difference in the separation efficiency of both chromatographic gradient methods.

3.4.3.17 Optimisation of mobile phase conditions

The beta test program advocated the use of MES-buffered mobile phase conditions and these conditions demonstrated very promising results. However optimised ProPac® WCX-10 separations gave an improved elution profile with sodium phosphate-buffered mobile phase conditions, therefore ProPac® MAb SCX separations were carried out using MES and sodium phosphate- buffered mobile phase conditions to compare the separation efficiency of the buffer conditions being employed (Figure 3.55).

Figure 3.55 demonstrated that separations using sodium phosphate buffers resulted in early elution of the recombinant lysostaphin isoforms, which suggested that the total chromatographic program time could be reduced considerably. However despite the benefits of early elution, the separation efficiency of the lysostaphin isoforms was significantly poorer using sodium phosphate buffers than for MES buffers. Recombinant lysostaphin isoforms were retained for an additional 10 minutes on the ProPac® MAb SCX column, however MES buffers demonstrated a much higher separation efficiency and resolution of the protein isoforms.

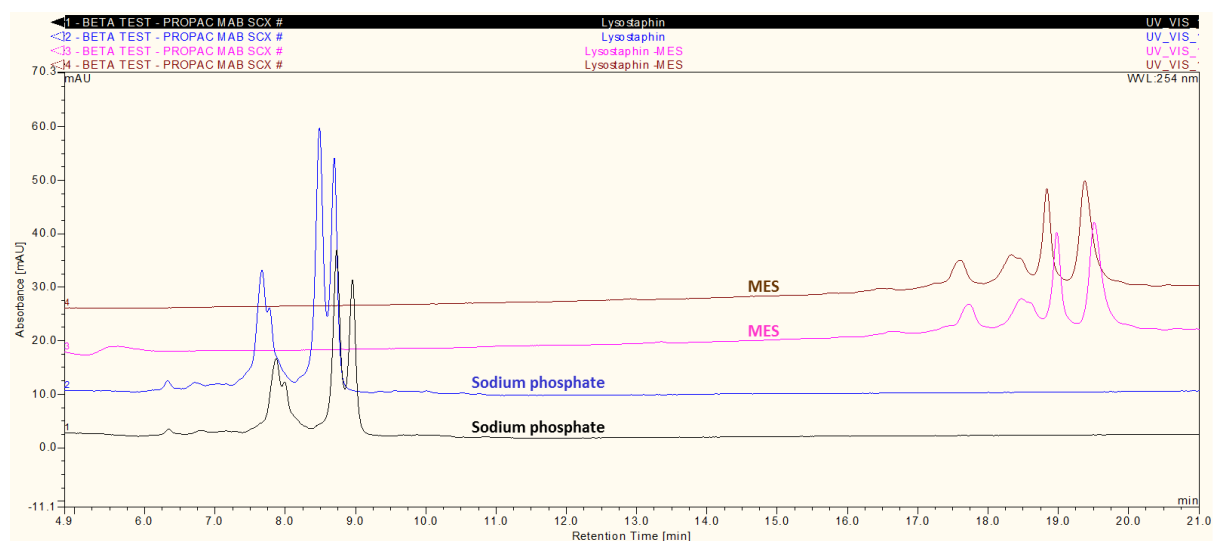


Figure 3.55: Comparison of mobile phase conditions during separation of 0.3 mg of C-terminally His-tagged recombinant lysostaphin (construct 3; preparation 5). Separations 1 and 2 were performed using an elution buffer containing 20 mM sodium phosphate, pH 8.0 and 1M NaCl, whilst separations 3 and 4 were performed using an elution buffer containing 20 mM MES, pH 6 and 1M NaCl.

3.4.3.18 Optimisation of column length

As described in Section 3.5.3.6, the in-line coupling of two 2 x 250 mm ProPac® WCX-10 columns to create a larger weak cation exchange matrix (2 x 500 mm), resulted in significant

improvements in column capacity, separation efficiency and resolution of protein isoforms. Therefore two ProPac® MAb SCX (4 x 250 mm) columns were coupled together to create a longer ProPac® MAb SCX (4 x 500 mm) column, with the expectation that the longer column volume would result in further enhancement of peak resolution. As a result of column length extension, the chromatographic method was also extended appropriately.

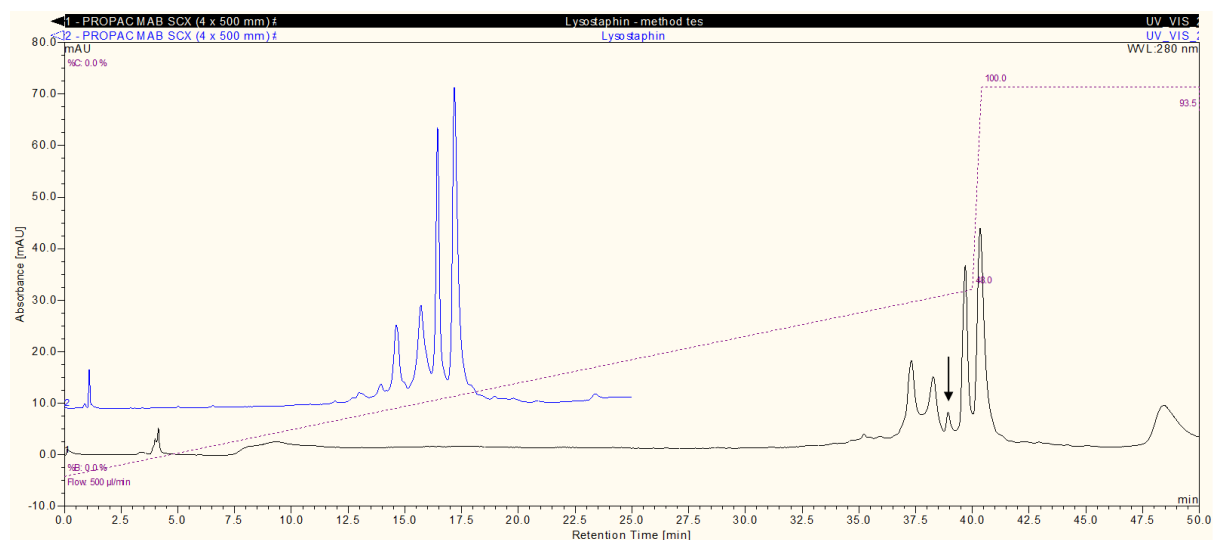


Figure 3.56: Comparison of separations of 0.7 mg of C-terminally His-tagged recombinant lysostaphin (construct 3; preparation 5) using a ProPac® MAb SCX (4 x 250 mm) or a ProPac® MAb SCX (4 x 500 mm) column. An additional isoform was resolved using the longer 4 x 500 mm column.

Figure 3.56 indicates that the longer ProPac® MAb SCX (4 x 500 mm) column does not offer significant improvements in isoform separation efficiency, however the additional column length has resolved an additional peak which was not identified using the ProPac® MAb SCX (4 x 250 mm) column. By reflecting on Figure 3.53 and Figure 3.54, it became apparent that this additional peak could not be resolved by the single ProPac® MAb SCX (4 x 250 mm) column, but was visibly present and represented by peak broadening or peak shouldering of the second major eluted peak, as shown in Figure 3.57.

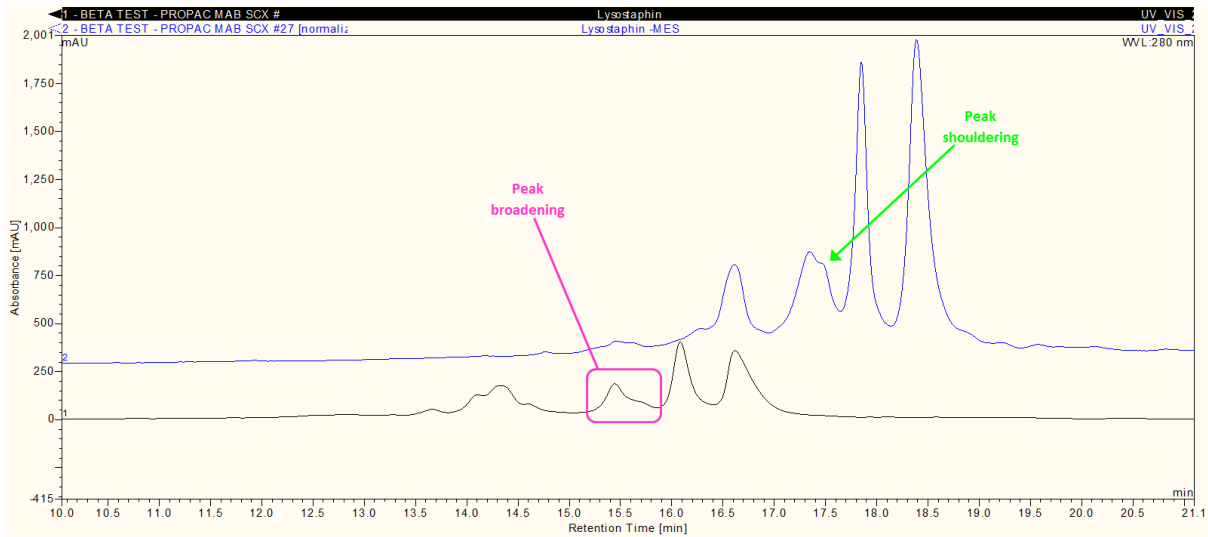


Figure 3.57: Examples of peak broadening and peak shouldering. Chromatograms show the separation of 0.2 mg (black trace) and 0.3 mg (blue trace) of C-terminally His-tagged recombinant lysostaphin (construct 3; preparation 5) on the ProPac[®] MAb SCX (4 x 500 mm) beta test column.

3.4.4 Discussion

Optimisation of protein separation was a lengthy process, which was complicated by the dynamic nature of recombinant protein production. It was only by performing many optimisation separations that greater insight into the heterogeneity of recombinant lysostaphin preparations could be achieved. For instance, the separation of higher concentrations of recombinant lysostaphin revealed that many low abundance protein isoforms could be resolved by the ProPac[®] WCX-10 (4 x 250 mm) column. However the application of larger amounts of recombinant lysostaphin could decrease the resolution of more abundant protein isoforms due to band broadening. It therefore became apparent that more abundant protein isoforms should be separated following the application of lower sample concentrations, to avoid column overloading and band broadening. Whilst separation and resolution of low abundance isoforms required the application of much higher amounts of recombinant lysostaphin.

The majority of protein separations were performed following application of recombinant lysostaphin which had been purified and stored in a liquid state prior to analysis. Lyophilised recombinant lysostaphin was produced following large-scale production of the protein and whilst this formulation provided long-term protein stability, it was found that sample precipitation interfered with the separation of protein isoforms, through atypical peak resolution and peak broadening. The separation of recombinant lysostaphin isoforms directly from cell lysate was found to provide efficient and high-resolution separation of protein isoforms however. 2D-LC analysis of protein isoforms separated from cell lysate also demonstrated that recombinant lysostaphin could be selectively purified from the cell lysate using CXC and therefore no prior purification stages were actually required, providing more efficient, real-time analysis of harvested recombinant lysostaphin preparations.

Optimisation of mobile phase conditions and gradient functions for protein separation using the ProPac[®] WCX-10 (4 x 250 mm) column indicated that greater separation could be achieved by extending gradient duration. Optimal separation was achieved using a 70 min gradient, which provided a good compromise between separation efficiency and peak resolution, which diminished with more extended gradients of 120-240 min. Increasing the steepness of the elution gradient also did not enhance resolution or separation, therefore the gradient was maintained at 0-50% of elution buffer. Altering the pH of mobile phase buffers to pH 8.0, did however increase the efficiency of protein separation by decreasing peak retention times. Therefore the pH of mobile phase buffers was increased from pH 7.0 to pH 8.0 to increase the overall efficiency of separation.

Resolution and separation power could be increased by performing separation using an extended ProPac[®] WCX-10 (4 x 500 mm) column. This extended column format provided high resolution separation of protein isoforms, but also provided the capacity to separate protein obtained from 1 L batch cultures. However separation could not be performed in a rapid manner which prevented high-throughput analysis of multiple samples. The efficiency of protein separation could however be increased by decreasing internal diameter of the column from 4 mm to 2 mm.

Although the ProPac[®] SCX-10 (4 x 250 mm) column did not provide good resolution of protein isoforms, the ProPac[®] SCX-10 (2 x 250 mm) column was found to provide higher resolution separation of recombinant lysostaphin variants within purified and crude lysate samples. 2D-LC could be performed efficiently using the smaller elution volumes achieved during SCX separation. Furthermore second dimensional RP analysis indicated that peaks eluted during SCX reflected the presence of a single protein with very few contaminants. The presence of additional protein isoforms that could not be separated by charge, could also be observed following RP analysis.

A ProPac[®] WCX-10 (2 x 250 mm) column was later acquired and was found to provide superior resolution of protein isoforms than the ProPac[®] SCX-10 (2 x 250 mm) column. The use of an extended ProPac[®] WCX-10 (2 x 500 mm) column provided more enhanced resolution and separation of protein isoforms from cell lysate within 50 min. The speed at which recombinant lysostaphin isoforms could be separated from cell lysate provided a means by which recombinant protein expression could be monitored by rapid analysis, as described in Section 3.5.3.6. Protein separation by the ProPac[®] WCX-10 (2.0 x 250 mm) columns was however limited by column capacity and therefore larger amounts of recombinant protein would have to be separated using the ProPac[®] WCX-10 (4 x 500 mm) column to achieve higher amounts of separated protein variants for characterisation experiments.

The ProPac[®] MAb SCX-10 (4 x 250 mm) column had already demonstrated excellent resolution of protein isoforms, however a few experiments were performed to establish whether resolution could be increased any further. Beta testing gradients and mobile phase conditions were found to offer better or similar separation and resolution of protein isoforms and the column possessed the capacity to separate moderate concentrations of recombinant lysostaphin. The use of an extended ProPac[®] MAb SCX-10 (4 x 500 mm) column was also found to provide slightly enhanced resolution of charge variants, however did not increase the separation efficiency. The ProPac[®] MAb SCX-10 columns did however provide rapid,

high-resolution separation of protein isoforms, which could facilitate rapid analysis of multiple samples harvested during the course of protein expression.

Due to the heterogeneity and differential abundance of recombinant lysostaphin variants, optimisation of fraction collection was essential to ensure that resolved proteins were appropriately fractionated. Whilst peak recognition-based fraction collection should have provided sensitive collection of resolved peaks, programming errors prevented appropriate fractionation. Peak recognition conditions were also difficult to optimise given that some peaks were resolved but not separated and therefore were not recognised upon elution. Time-based fraction collection was therefore found to offer more reliable collection of protein isoforms during separation .

During the course of optimisation of chromatographic conditions, it was possible to gain further insight into the influence of expression conditions upon the heterogeneity of recombinant lysostaphin. The studies provide further evidence of the variable heterogeneity within recombinant lysostaphin preparations. Repeated separation of protein eluted within a single WCX provided confirmation that the observed heterogeneity was real and that the resolution of multiple peaks did not occur as an artefactual phenomenon. However the ability to make conclusions about the origins or nature of charge heterogeneity, based on comparison of chromatograms, was limited by frequent alterations of chromatographic conditions during optimisation. It was however possible to investigate the influence of some expression conditions whilst optimising chromatographic conditions.

Investigation of the influence of incubation temperature upon product heterogeneity, revealed that higher incubation temperatures were associated with greater charge heterogeneity. An additional acidic variant was observed in cultures incubated at 30°C or cultures in which expression had been induced at higher optical densities. This observation was not especially surprising considering that post-translational processing or modification would occur faster at elevated temperatures following Arrhenius kinetics. Following this finding, incubation temperatures were reduced to 16°C which lead to the production of a more homogeneous protein preparation. Whilst WCX separation of cell lysate harvested from cultures incubated at 16°C revealed the presence of fewer protein isoforms, peak width and asymmetry suggested that the protein preparation still contained a number of charge isoforms. Nevertheless, these experiments demonstrated that the degree of product heterogeneity could be manipulated by careful selection of culture conditions.

These experiments demonstrated that the charge heterogeneity of recombinant lysostaphin was evident, however it was not clear whether other recombinant proteins expressed in *E. coli* could also exhibit charge variation. WCX separation of cell lysate containing recombinant oxidoreductase or recombinant NADPH-dependent 1-acyl dihydroxyacetone phosphate reductase (Ayr1p) suggested that the expressed protein did demonstrate micro-heterogeneity in the form of charge variants which were resolvable using the ProPac® WCX-10 (4 x 500 mm) column. Charge heterogeneity appeared to increase further upon expression of the recombinant proteins in AIM rather than LB, which indicated that expression media could influence the rate or extent of post-translational processing or modification. Furthermore investigation of the influence of expression media would be desirable as it was unclear whether the observed differences in charge heterogeneity were attributable to expression media or the duration of propagation.

Overall these experiments demonstrated that protein separation, performed under optimised chromatographic conditions could be used evaluate the charge heterogeneity of recombinant lysostaphin and other cationic recombinant proteins expressed in *E. coli*. The availability of a number of ProPac™ IEX columns provided the flexibility to perform rapid or high capacity, high-resolution separation of protein isoforms through appropriate selection of column diameter. The ability to perform rapid analysis is particularly desirable to permit culture monitoring during recombinant protein expression. Whilst one-off separations performed on whole recombinant protein preparations proved to be informative, the presence of particular charge variants could not be predicted or did not seem to follow any conclusive patterns. It was therefore thought that the charge variability could transition over time or according to culture optical density. Monitoring the influence of optical density and time could therefore be most effectively achieved by performing rapid analysis during recombinant protein expression.

3.5 Rapid analysis of recombinant lysostaphin isoforms

3.5.1 Introduction

Industrial recombinant protein production in *E. coli* is typically performed over a short, defined period of time, in which bacterial growth parameters and expression conditions are strictly controlled (Garnick *et al.*, 1988). Due to the time and cost invested in large-scale recombinant protein production it is essential that culture conditions, protein yields and product homogeneity are monitored throughout expression. By monitoring a recombinant protein production, any slight deviation in culture parameters, yields or homogeneity can be swiftly detected and addressed by adjustment and correction of culture conditions to achieve optimal expression (Dalmora *et al.*, 1997, DePhillips *et al.*, 1994). Alternatively culture analysis may demonstrate extensive product heterogeneity or poor expression yields, which would advocate termination of culture prior to performing expensive protein purification procedures.

In addition to optimisation of expression, culture analysis is desirable to establish when it is most appropriate for a recombinant product to be harvested. If a protein is harvested prematurely or too late, product yield can be dramatically reduced due to under-expression or degradation during culture (Baker *et al.*, 2002). Changes in recombinant protein expression levels are commonly assessed using techniques such as SDS-PAGE or ELISA, however these techniques do not necessarily provide accurate determination of protein concentration, particularly when analysing heterogeneous protein populations (Paasch *et al.*, 1996). Whilst SDS-PAGE and ELISA can be repeated during the course of expression, the techniques cannot be automated and do not provide real-time culture analysis. Therefore culture conditions cannot be sensitively adjusted and controlled to ensure optimal expression (Liu *et al.*, 2005, DePhillips *et al.*, 1994).

The detection and assessment of product homogeneity during recombinant protein production can only be achieved using more sensitive analytical techniques, which can provide resolution of protein variants. The assessment of the macro- and micro-heterogeneity of a recombinant protein preparation provides an insight into the consistency and stability of the recombinant product which is essential for quality control purposes (Jacobson *et al.*, 1997). Furthermore culture analysis can facilitate further investigation of protein modifications, leading to elucidation of their origin, nature, incidence and influence upon the structure and function of a recombinant protein (Dalmora *et al.*, 1997). By

identifying the source of a protein variant, measures can be taken to limit or prevent its occurrence, thereby increasing yields of the desired, unmodified recombinant protein.

Sensitive and reproducible techniques, such as HPLC and capillary electrophoresis have been commonly employed to monitor recombinant protein expression and heterogeneity. These techniques are often used to analyse a recombinant protein following its expression and purification, but are often too slow to provide on-line, real-time analysis of expression products (Baker *et al.*, 2002). However optimisation of sample preparation and analytical conditions has demonstrated that HPLC and CE can be effectively used to provide rapid and accurate detection of protein variants, as and when they occur during culture (Dalmora *et al.*, 1997, McNerney *et al.*, 1996). Due to its sensitivity, HPLC has been more commonly applied than CE during expression studies and therefore a number of rapid analysis methods have been described (Dalmora *et al.*, 1997, Londo *et al.*, 1998, Hummel *et al.*, 1989, Strege and Lagu, 1995).

In order to monitor recombinant protein expression in real-time, protein harvesting and purification procedures must be rapid enough to achieve analytical data which reflects the current state of expression. Such an optimised real-time analysis workflow would involve simple extraction of the expressed recombinant protein and a single separation stage which provides direct purification and analysis of the protein of interest. In addition, the rate of sample analysis is important as it dictates how many samples can be processed within the course of expression. Rapid analysis of samples is therefore desirable to permit high sample through-put and provide more information during each expression study.

Rapid harvesting of the recombinant protein is essential to ensure that host proteases, modifying enzymes and reactive intermediates that are present within *E. coli* do not degrade or alter the recombinant protein prior to rapid analysis. Direct recovery of a recombinant protein from a crude cell lysate is advantageous as it significantly reduces processing time and costs. Cell lysates that are acquired using cellular disruption methods, such as sonication or osmotic shock provide the best medium for reliable evaluation of protein concentration and homogeneity. Cellular disruption can be achieved fairly rapidly, therefore a cell lysate can be acquired within less than hour and subjected to rapid analysis, following one-step capture of the recombinant protein using an appropriate chromatographic or electrophoretic technique.

The selection of an appropriate analytical technique is complicated by the complex nature of crude cell lysates, which contains numerous host molecules that can interfere with

separation and detection of the target protein (Jacobson *et al.*, 1997). For instance, host contaminants may interfere with adsorption interactions or exhibit similar chromatographic behaviour as the target protein, resulting in co-elution (Viloria-Cols *et al.*, 2004). Co-elution can lead to mis-interpretation of detected peaks and may interfere with the accuracy of subsequent biological assays. It is therefore imperative that the target recombinant protein is efficiently isolated by a separation method that offers high specificity and selectivity (Kroef *et al.*, 1989).

Direct analysis of crude cell lysates may also result in column fouling, whereby cellular constituents bind to the adsorbent matrix. Fouling occurs due to electrostatic interactions between the column stationary phase and cell particulates such as nucleic acids, proteins, lipids, cellular debris and cells (Viloria-Cols *et al.*, 2004). The non-specific binding of macromolecular cell particulates can lead to aggregation which can hinder purification of the target protein, destabilize column fluidisation and reduce overall process efficiency (Feuser *et al.*, 1999). The fouled adsorbent matrix can be regenerated by extensive washing, however harsh regeneration procedures often lead to only partial recovery of column performance and therefore column fouling significantly affects the performance and life expectancy of a column (DePhillips *et al.*, 1994).

To reduce the risk of column fouling, chromatographic conditions should be carefully selected to ensure that there is ample opportunity for cellular constituents to be washed from the column without interfering with separation of the target recombinant protein. Unlike techniques such as SDS-PAGE, chromatographic separation can be developed and optimised to provide optimal performance during rapid and reproducible separation. Development of stationary phase chemistries, such as the introduction of non-porous particles and perfusive supports has further enhanced the applicability of HPLC for real-time culture analysis (Londo *et al.*, 1998).

3.5.1.1 Rapid analysis of recombinant lysostaphin

As described in Section 3.4, protein analysis was performed after following a number of harvesting and purification steps had been undertaken (Figure 3.58). Depending on culture capacity, protein harvesting could be achieved within a few hours. However protein purification, subsequent analysis and concentration stages took longer, often days to complete, delaying protein analysis and characterisation significantly. Delayed analysis was undesirable as the protein preparation may have been affected by degradation or chemical modifications which occurred artifactually during the course of sample preparation.

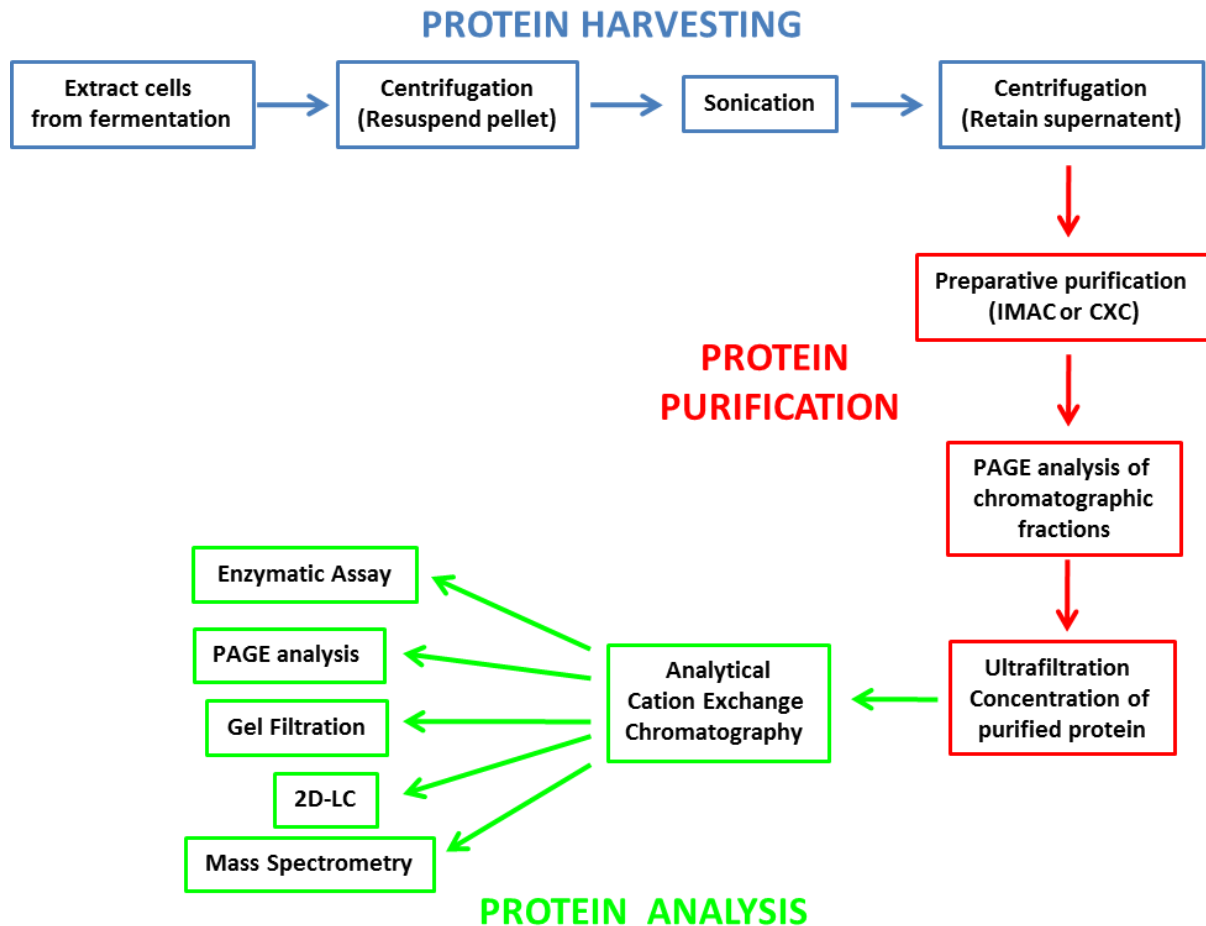


Figure 3.58: A culture analysis workflow from expression to characterisation.

However the ability of CXC to purify cationic proteins directly from cell lysate could be exploited to provide a rapid analysis workflow (Figure 3.59). The elimination of additional protein purification stages dramatically reduced the time taken to prepare recombinant lysostaphin before analysing charge heterogeneity using CXC. Depending on the volume of culture being harvested, analysis of product heterogeneity could be performed within a few hours of protein expression by applying this rapid analysis workflow. Further analysis and characterisation of the recombinant protein could then be performed immediately or following proteolytic digestion, concentration and/or buffer exchange.

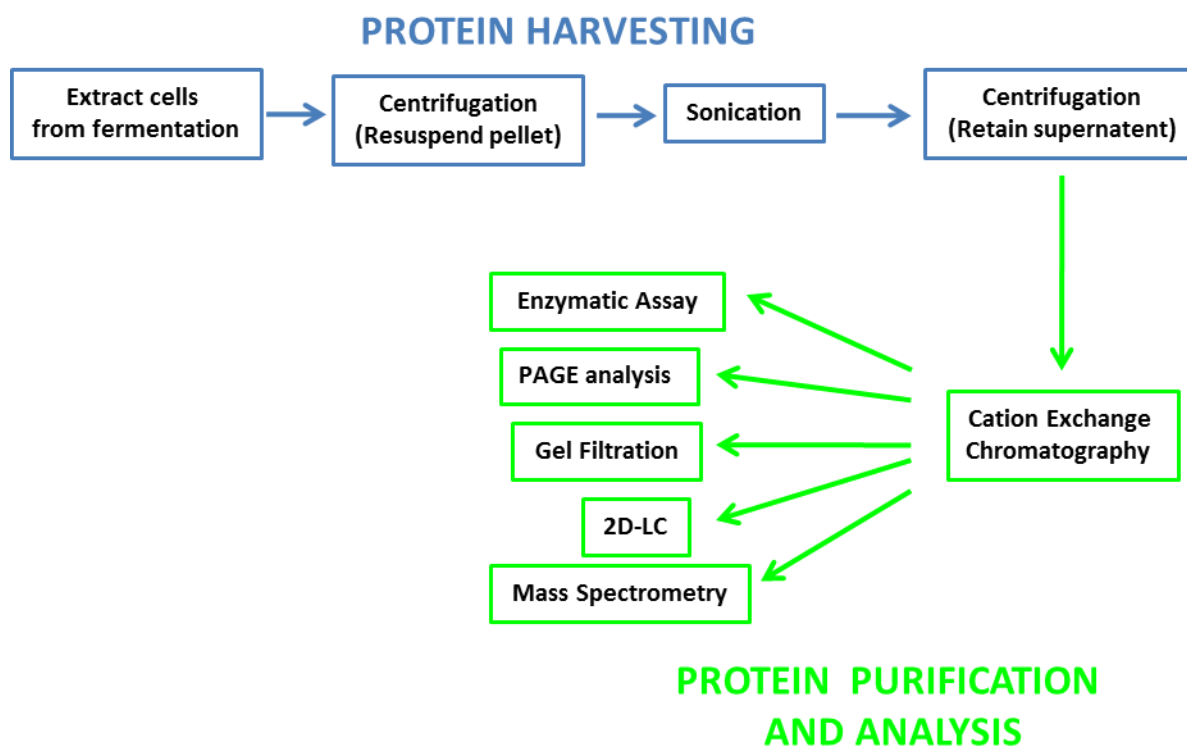


Figure 3.59: A rapid culture analysis workflow from expression to characterisation.

As chromatographic conditions had already been optimised for the binding and separation of purified recombinant, chromatographic conditions were systematically varied to permit optimised separation of crude lysate. Optimisation involved reassessment of sample preparation and chromatographic conditions.

3.5.1.2 Optimisation of sample preparation during rapid analysis

To develop a protocol for rapid analysis of recombinant protein heterogeneity, the preparation of cell lysate and the amount of recombinant lysostaphin being separated needed to be assessed and optimised. During culture analysis, it was essential that harvested samples contained enough recombinant lysostaphin to allow detection of protein isoforms using CXC. In addition to optimising cell lysate preparation, it was desirable to ensure that high sample-throughput was achieved during rapid analysis. The frequency of analysis itself was dependent on the rate of sample through-put provided by chromatographic analysis and sample throughput was ultimately limited by the duration of chromatographic separation. To circumvent this inherent limitation, different modes of sample preparation were considered to establish whether recombinant lysostaphin could be preserved in its harvested state, so that rapid analysis could be delayed until a more convenient time (Section 3.5.1.3).

3.5.1.3 Maximising sample through-put during rapid analysis

As sample throughput was limited by the duration of chromatographic separation, different modes of sample preparation were considered to permit analysis of an increased number of samples. Cell lysate was typically prepared and analysed within hours of its extraction, which became very labour intensive if multiple samples were being analysed during the course of expression, which typically spanned several days. The option of freezing samples during sample preparation was therefore considered, to allow more flexible expression analysis or repeated analysis of a sample extracted at a specific time point. For instance, pelleted *E. coli* cells could be frozen following initial extraction and centrifugation, as shown in Figure 3.60. This approach permits samples to be stored until a time when the remaining sample preparation and chromatographic analysis could be conveniently performed.

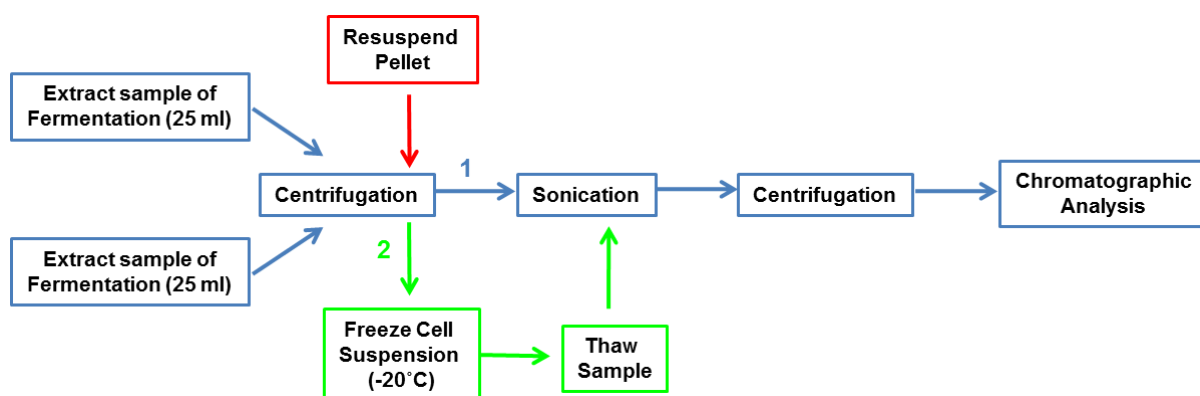


Figure 3.60: Work-flow diagram for analysis of cell lysate harvested from fresh and frozen cells. Samples of culture were extracted in duplicate, centrifuged and the resulting cell pellets were resuspended with an appropriate buffer. One of the samples was processed immediately (1), whilst the other sample was frozen (2) and processed at a convenient time.

Alternatively, additional subsequent sample preparation could be avoided by freezing a cell lysate, which could be thawed prior to chromatographic separation (Figure 3.61). As the recombinant protein remained in a reactive cellular environment, it was imperative that the samples were frozen immediately and analysed immediately after thawing to prevent any further modification or alteration of protein structure between analysis of fresh and thawed samples.

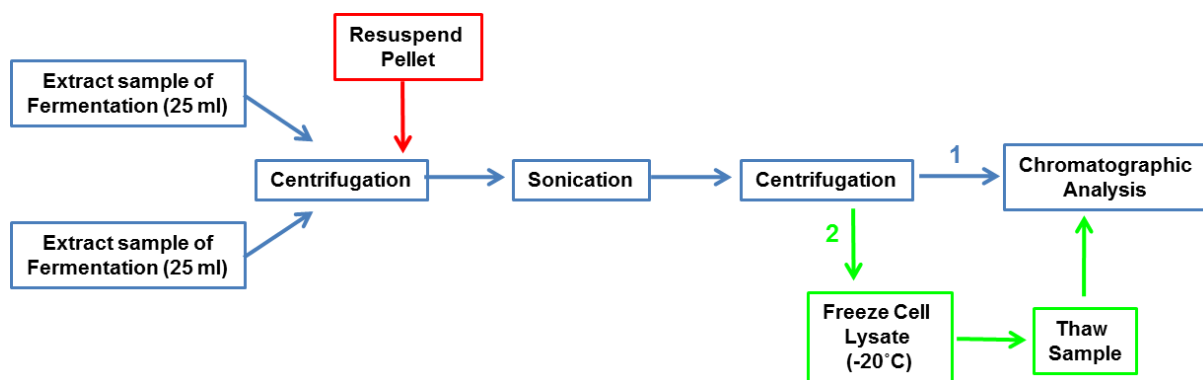


Figure 3.61: Work-flow diagram for analysis of cell lysate harvested from fresh and frozen cell lysate. Samples of culture were extracted in duplicate, centrifuged and the resulting cell pellets was resuspended with an appropriate buffer. Both samples were sonicated and centrifuged to yield cell lysate. One of the resulting cell lysates was analysed immediately (1), whilst the other sample was frozen (2) and analysed at a convenient time.

3.5.1.4 Optimisation of chromatographic conditions

In order to create an effective method for rapid analysis, chromatographic conditions required optimisation to permit real-time analysis of protein expression as it occurred during culture. Although chromatographic conditions applied whilst using the ProPac® WCX (4 x 500 mm) had been optimised for the separation of recombinant lysostaphin variants, these conditions could not be applied during rapid culture analysis for a number of reasons.

Firstly analytical separations performed using the ProPac® WCX (4 x 500 mm) were performed over an extended gradient to provide optimal separation of protein isoforms. This extended duration of separation was not suitable for rapid analysis, therefore it was essential that analysis was performed using columns with a narrower internal diameter, such as ProPac® SCX or WCX (2 x 250 mm) columns. Due to bearing a smaller internal diameter, greater resolution could be achieved whilst applying lower flow rates and shorter gradient, wash and equilibration phases, therefore increasing the speed of analysis. The application of lower flow rates was also advantageous, as eluted protein could be collected as more concentrated fractions during separation. Alternatively rapid separation could be performed using a column which could provide high resolution separation over a short duration of separation, such as the ProPac® MAb SCX (4 x 250 mm).

Secondly, chromatographic conditions required modification to accommodate the injection of crude cell lysate rather than purified, concentrated recombinant lysostaphin preparations. As cell lysate contains many cellular contaminants, sample loading stages required optimisation to ensure that interactions between cellular contaminants and the stationary phase, such as

column fouling and chromatographic interference could be avoided as much as possible. Fortunately *E. coli* cell lysate has less of a tendency to bind to chromatographic matrices than lysates harvested from eukaryotic expression hosts do (Feuser *et al.*, 1999). Cation exchange resins are also less susceptible to column fouling than anion exchange resins (Londo *et al.*, 1998). Furthermore polymeric stationary phase materials, such as those used in ProPac™ IEX columns, provide increased column stability and are less prone to degradation in the presence of crude samples (DePhillips *et al.*, 1994). In addition ProPac™ IEX columns are protected from secondary interactions due to the polymeric beads being covered in a hydrophilic coating (Dainiak *et al.*, 2002).

The aims of this work were:

- To optimise chromatographic conditions and sample preparation for the rapid separation of protein isoforms directly from cell lysate.
- To validate a rapid analysis strategy for the direct determination of recombinant lysostaphin expression levels and charge heterogeneity from cell lysate using CXC.
- To study the expression of recombinant lysostaphin over the course of bacterial culture.
- To monitor the charge heterogeneity of recombinant lysostaphin throughout expression.

3.5.2 Methods

All separations were performed using an Ultimate™ 3000 Titanium system

3.5.2.1 Optimisation of rapid analysis

Initial rapid analysis separations were performed using a ProPac® SCX (2 x 250 mm) column as described in Appendix 7.221. This rapid analysis method was used to investigate the influence of optical density at the point of induction upon charge heterogeneity (Appendix 7.222). The performance of the ProPac® SCX (2 x 250 mm) and ProPac® WCX (4 x 500 mm) columns were then compared (Appendix 7.223).

Rapid analysis was then performed using the ProPac® WCX (2 x 500 mm) column (Appendix 7.225) after optimising cell lysate preparation (Appendix 7.224) and trying to maximise sample through-put (Appendix 7.226). Chromatographic conditions were optimised further (Appendix 7.228) before investigating the influence of optical density at the point of induction again (Appendix 7.227). Using the optimised method, the influence of time upon the charge heterogeneity of recombinant lysostaphin was investigated (Appendix 7.229 and Appendix 7.230). Rapid analysis was also performed using the ProPac® MAb SCX (4 x 250 mm) column (Appendix 7.231).

3.5.3 Results

3.5.3.1 Rapid analysis of recombinant lysostaphin using a ProPac® SCX (2 x 250 mm) column

Due to the availability of a 2 mm diameter cation exchange column, initial rapid analysis separations were performed using a ProPac® SCX (2 x 250 mm) column. *E. coli* cell lysate harvested during the expression of recombinant lysostaphin was injected onto column and several peaks were separated and resolved from cellular constituents which could not bind to the SCX column (Figure 3.62). The separation was performed over 35 min, which could allow analysis of cell lysates that were harvested hourly during culture. The majority of the separated peaks were observed during the linear gradient elution, however resolved peaks were also observed following the column wash phase. As UV data was only acquired at 214 nm, it was not clear whether these peaks represented strongly retained protein or other UV-absorbing molecules.

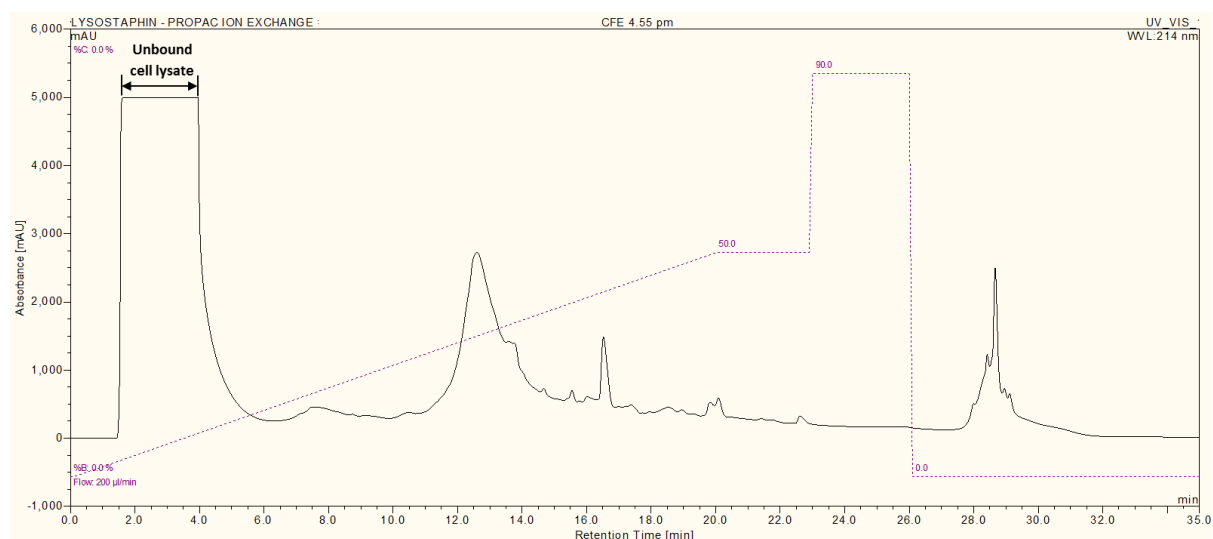


Figure 3.62: Separation of *E. coli* cell lysate containing expressed *N*-terminally His-tagged recombinant lysostaphin (construct 1) using a ProPac® SCX (2 x 250 mm) column. Cellular constituents which could not bind to the SCX column eluted within the first few minutes of the separation. Protein isoforms appeared to elute during the linear elution gradient, however the elution of some peaks following column washing suggested that some of the protein or UV-absorbing cationic contaminants were retained more strongly. UV data was acquired at a wavelength of 214 nm.

Following successful capture of cationic protein isoforms using this column, a series of separations were performed at regular intervals during the expression of recombinant lysostaphin. As shown in Figure 3.63, culture analysis could be performed in a reproducible manner, with fairly consistent sample loading and peak heights observed between separations. However some of the separations were subject to chromatographic shifting,

which slightly compromised the quality of the results.

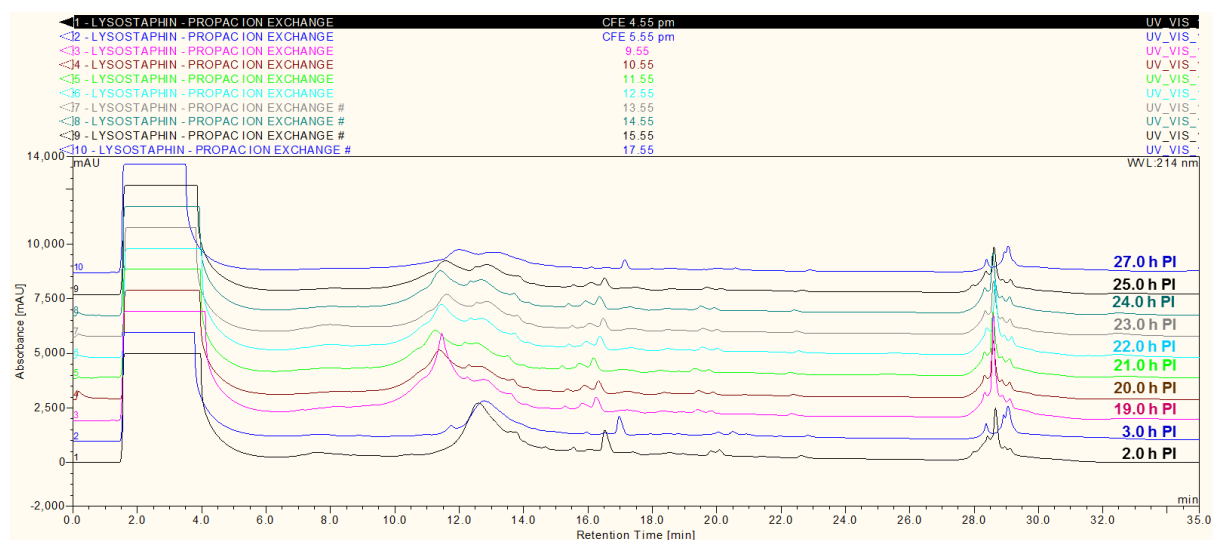


Figure 3.63: Culture analysis during the expression of *N*-terminally his-tagged recombinant lysostaphin (construct 1) in *E. coli* BL21(DE3). Cell lysates were harvested between 2.0 and 27.0 h after the induction of protein expression and applied to a ProPac® SCX (2 x 250 mm) column. Separations could be performed in a reproducible manner, however the separations were subject to chromatographic shifting.

This preliminary culture analysis provided an insight into the expression levels and charge heterogeneity of recombinant lysostaphin over the course of expression. SCX separations performed on cell lysates harvested early in the course of culture revealed that recombinant lysostaphin was hyper-expressed within 2 h of the induction of protein expression (Figure 3.64). This finding correlated with over-expression observed following SDS-PAGE analysis (Appendix 7.242). Even at this early stage of expression, several peaks were resolved indicating that the charge distribution of the separated recombinant lysostaphin was not homogeneous. Separation of cell lysate harvested 3 h after the induction of expression, demonstrated the emergence of an acidic protein variant.

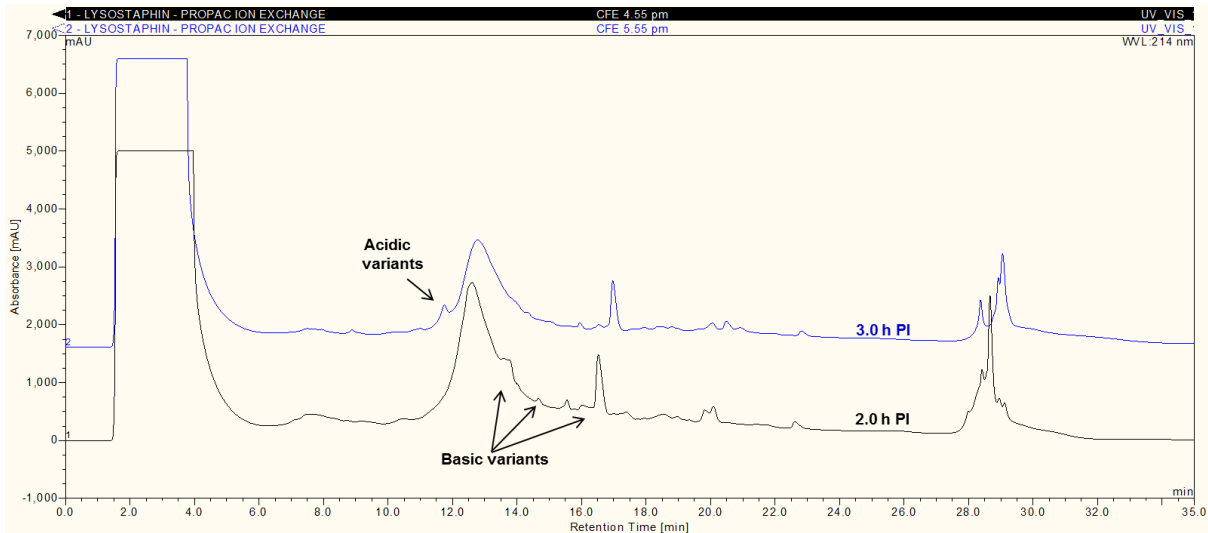


Figure 3.64: Culture analysis during the early expression of *N*-terminally His-tagged recombinant lysostaphin (construct 1) in *E. coli* BL21(DE3). SCX separation resolved a number of peaks which indicated that hyper-expression of recombinant lysostaphin had commenced within 2 h of the induction of protein expression. The resolved protein isoforms also demonstrated the presence of basic variants and the emergence of an acidic variant by 3 h post-induction.

Following an interval of 16 h, cell lysate was harvested again at 19.0 h post-induction and separated by SCX (Figure 3.66). SCX analysis indicated that recombinant lysostaphin was being constitutively hyper-expressed in *E. coli*, which was in concurrence with SDS-PAGE findings (Appendix 7.242). By 19 h post-induction, the most predominant peak was observed at a retention time of 11.5 min. This observation indicated that a more acidic protein variant had become more prevalent than the original peak observed at a retention time of 12.5 min in cell lysates harvested at 2 and 3 h. This original peak was still evident in cell lysates harvested between 19 and 22 h, however the relative abundance of this protein isoform appeared to have decreased.

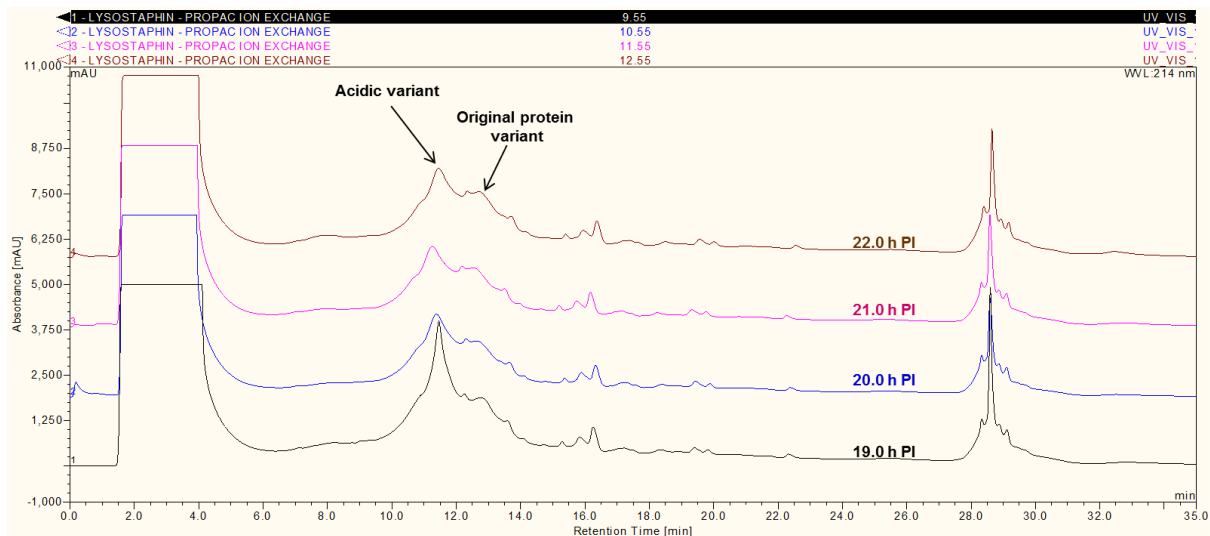


Figure 3.65: Culture analysis during the expression of *N*-terminally His-tagged recombinant lysostaphin (construct 1) in *E. coli* BL21(DE3). SCX separation resolved a number of peaks which confirmed that recombinant lysostaphin was still being expressed. An acidic peak at 11.5 min marked the emergence of a more prevalent protein isoform. The more basic original protein isoform could still be observed at 12.5 min, however the height of this peak was reduced, indicating a decreased protein abundance.

Continued analysis of cell lysates harvested after 23 h post-induction demonstrated sustained expression of recombinant lysostaphin, with continued presence of the two most prevalent protein variants (Figure 3.66). By 27 h post-induction the abundance of both protein variants appeared to have been slightly diminished indicating that expression of recombinant lysostaphin may have reduced or ceased. A reduction in protein expression, concomitant to protein degradation could have led to the observed reduction in the amount of recombinant lysostaphin present in the cell lysate.

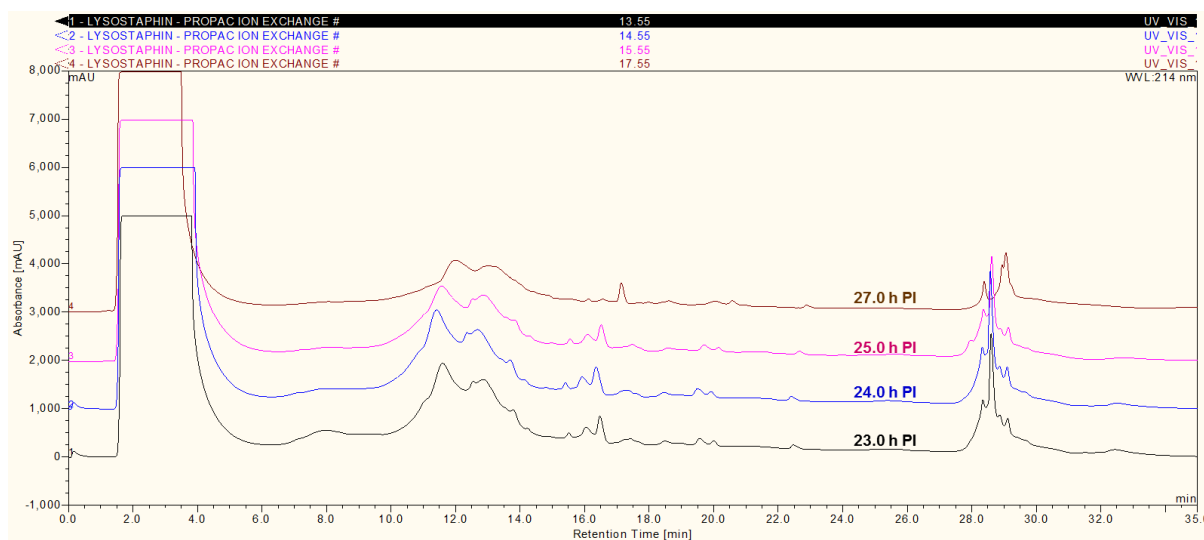


Figure 3.66: Culture analysis during later stages of expression of *N*-terminally His-tagged recombinant lysostaphin (construct 1) in *E. coli* BL21(DE3). SCX separation resolved a number of peaks which confirmed that recombinant lysostaphin was still being expressed. An acidic peak at 11.5 min marked the emergence of a more prevalent protein isoform. The more basic original protein isoform could still be observed at 12.5 min, however the height of this peak was reduced, indicating a decreased protein abundance.

This initial culture analysis demonstrated that the ProPac[®] SCX (2 x 250 mm) column could be used to provide real-time monitoring of recombinant protein. As recombinant lysostaphin is a basic protein, it binds to cation exchange columns at neutral pH and therefore this technique can be used to selectively purify the protein directly from cell lysate during culture analysis. The benefits of this technique were explained in further depth in a customer application note, entitled “Rapid Analysis of Recombinant Protein Production during Fermentation Using Dionex ProPac IMAC columns” (Appendix 7.291).

3.5.3.2 Influence of optical density at point of induction upon charge heterogeneity

Due to the success of initial culture analysis using the ProPac[®] SCX (2 x 250 mm) column, the method was used to provide further investigation of the influence of culture conditions upon product heterogeneity. The influence of optical density at the point of induction upon the expression and heterogeneity of recombinant lysostaphin was therefore investigated. The expression of recombinant lysostaphin in twenty four batch cultures which had been induced at various cell densities was monitored by SDS-PAGE (Appendix 7.253). SDS-PAGE demonstrated that hyper-expression of recombinant lysostaphin generally occurred regardless of optical density and could be detected in the majority of samples harvested at 4, 10 or 20 h post-induction.

After harvesting, the extracted cell lysates were subjected to rapid SCX analysis to assess the charge heterogeneity of the expressed recombinant lysostaphin. As shown in Figure 3.67, the presence of protein isoforms could be observed in cultures which had been induced at an $OD_{600\text{ nm}}$ of less than 0.6 and harvested at 4 h post-induction. Whilst low-level expression of recombinant protein expression prevented clear detection of protein isoforms in cultures which had been induced at very low optical densities (less than 0.06), the presence of protein variants could be detected in cultures that were induced at higher optical densities (greater than 0.06).

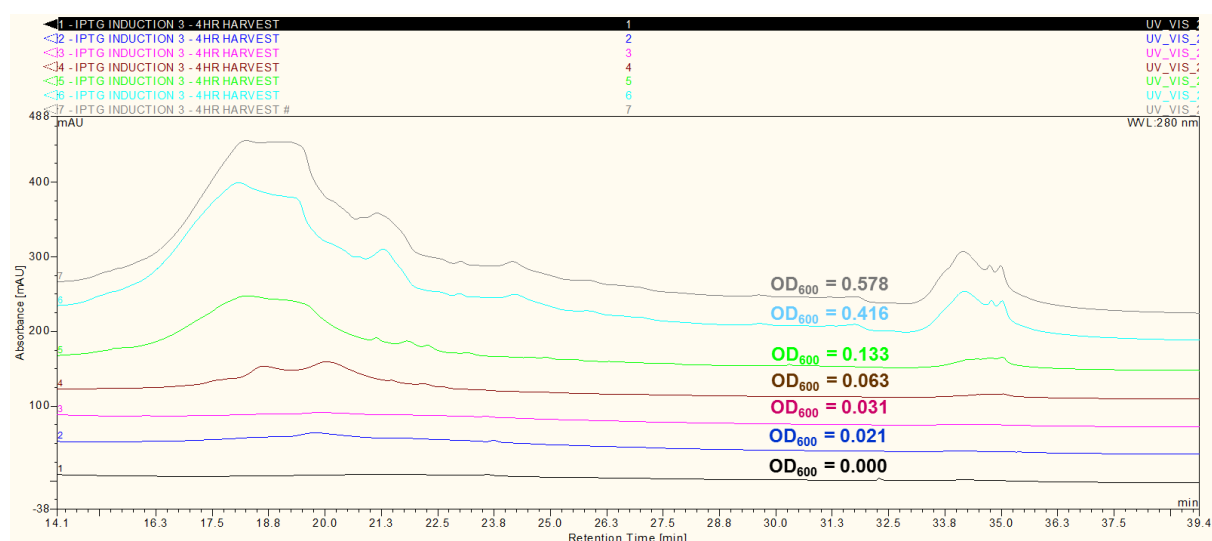


Figure 3.67: SCX analysis of cell lysates harvested 4 h after the induction of protein. Protein expression was induced at optical densities lower than the standard induction densities.

Induction of protein expression within the standard expression range ($OD_{600\text{ nm}} = 0.6-1.0$) appeared to result in higher expression levels as expected, however the heterogeneity of the protein preparation did not appear to significantly differ from that observed in cultures induced at a lower optical density (Figure 3.68). The relative abundance of protein isoforms did however appear to vary as the optical density at the point of induction increased.

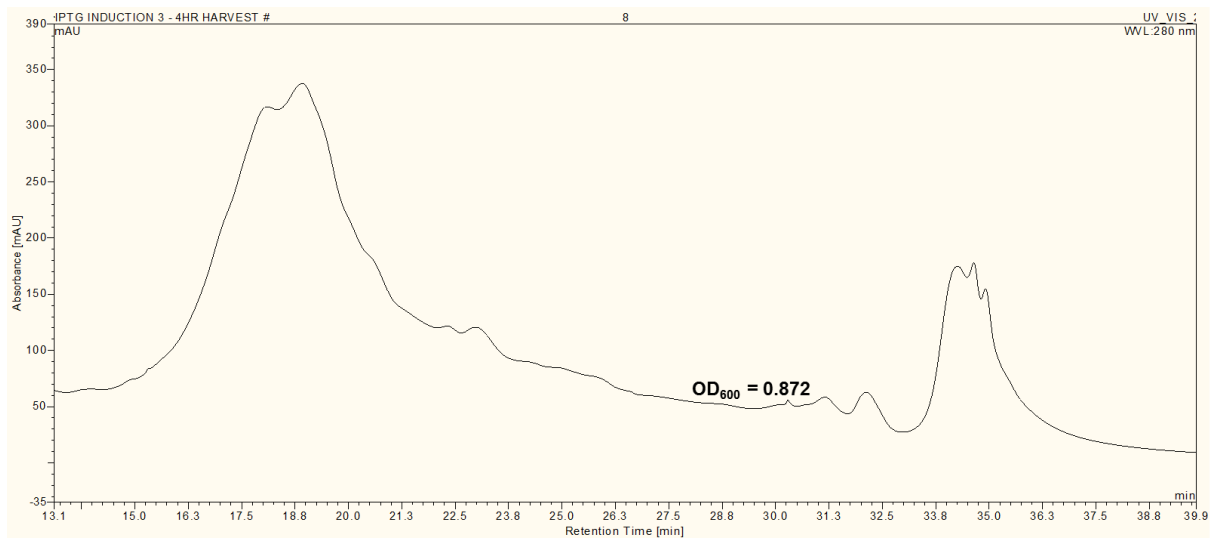


Figure 3.68: SCX analysis of cell lysate harvested 4 h after the induction of protein expression. Protein expression was induced at an optical density within the standard range.

SCX analysis of cultures harvested at 10 h post-induction revealed a similar pattern of separation, however greater expression levels could be observed in cultures in which protein expression had been induced at very low optical densities (less than 0.06) (Figure 3.69). This result was to be expected as a longer incubation time would have allowed time for a greater cell density to be reached and therefore enhanced capacity for recombinant protein production. Changes in the relative abundance of protein isoforms appeared to become more pronounced as the expression levels and the optical density at point of induction increased.

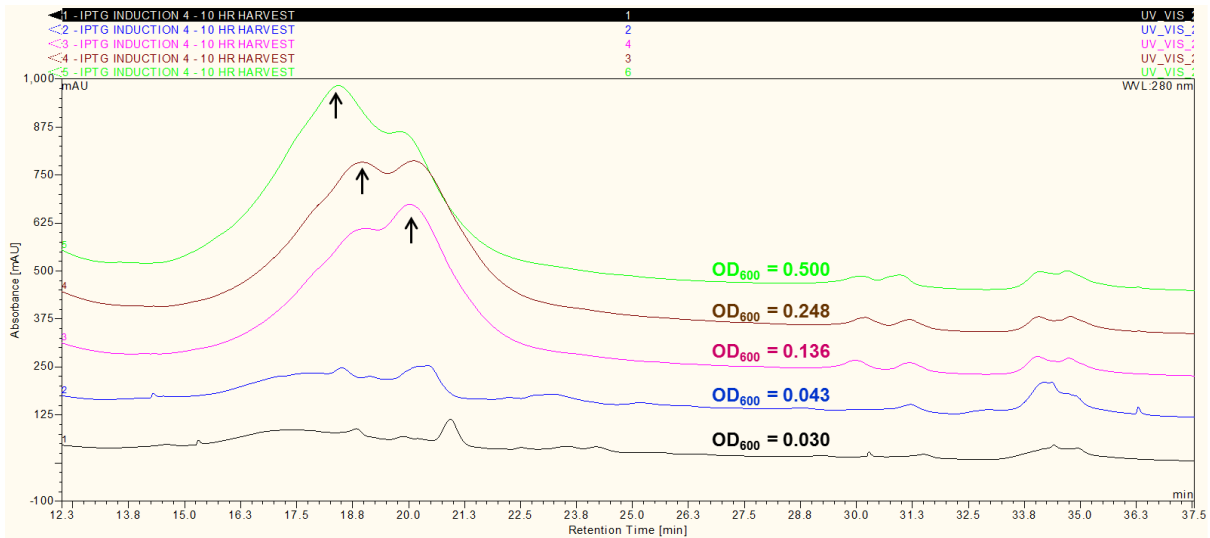


Figure 3.69: SCX analysis of cell lysates harvested 10 h after the induction of protein expression. Protein expression was induced at optical densities lower than the standard induction densities. Arrows indicate increased prevalence of more acidic or basic protein isoforms.

The difference in abundance of the more acidic protein isoform, observed at a retention time of 18 min, became increasingly evident as cell lysates induced at higher optical densities were analysed (Figure 3.70). However SDS-PAGE and SCX analysis both confirmed that recombinant lysostaphin was not expressed in a culture induced at an $OD_{600\text{ nm}}$ of 0.991.

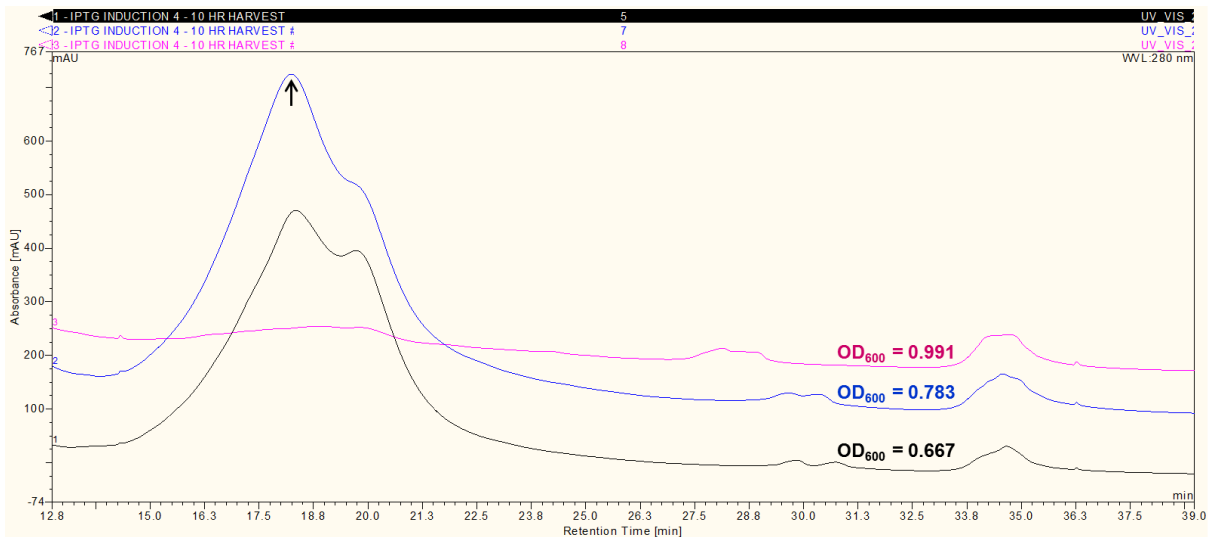


Figure 3.70: SCX analysis of cell lysate harvested 10 h after the induction of protein expression. Protein expression was induced at an optical density within the standard range. The arrow indicates the increased prevalence of a more acidic protein isoform.

When SCX analysis was performed on cell lysates harvested at 20 h post-induction of protein expression, over-expression of recombinant lysostaphin was observed in cultures

which had been induced at a low optical density (less than 0.2) (Figure 3.71). SDS-PAGE and SCX analysis revealed that there was reduced expression of recombinant lysostaphin in cultures induced at an $OD_{600\text{ nm}}$ of 0.4. These results were thought to be anomalous due to evidence of increased expression in cultures that were induced a slightly higher optical densities.

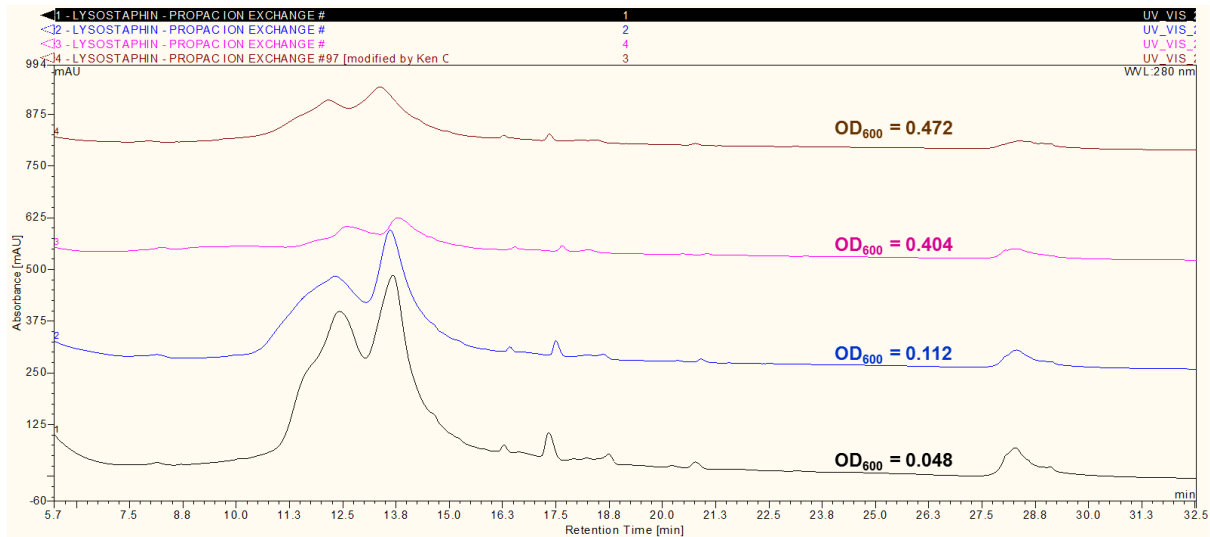


Figure 3.71: SCX analysis of cell lysates harvested 20 h after the induction of protein expression. Protein expression was induced at optical densities lower than the standard induction densities.

Hyper-expression of recombinant lysostaphin was observed in cultures which had been induced within the standard induction range ($OD_{600\text{ nm}} = 0.6-1.0$). SCX analysis demonstrated the presence of two peaks representing more acidic or basic protein isoforms (Figure 3.72). The abundance of each of these isoforms varied with differences in the optical density at point of induction, as observed during analysis of cell lysates harvested at 4 or 10 h post-induction.

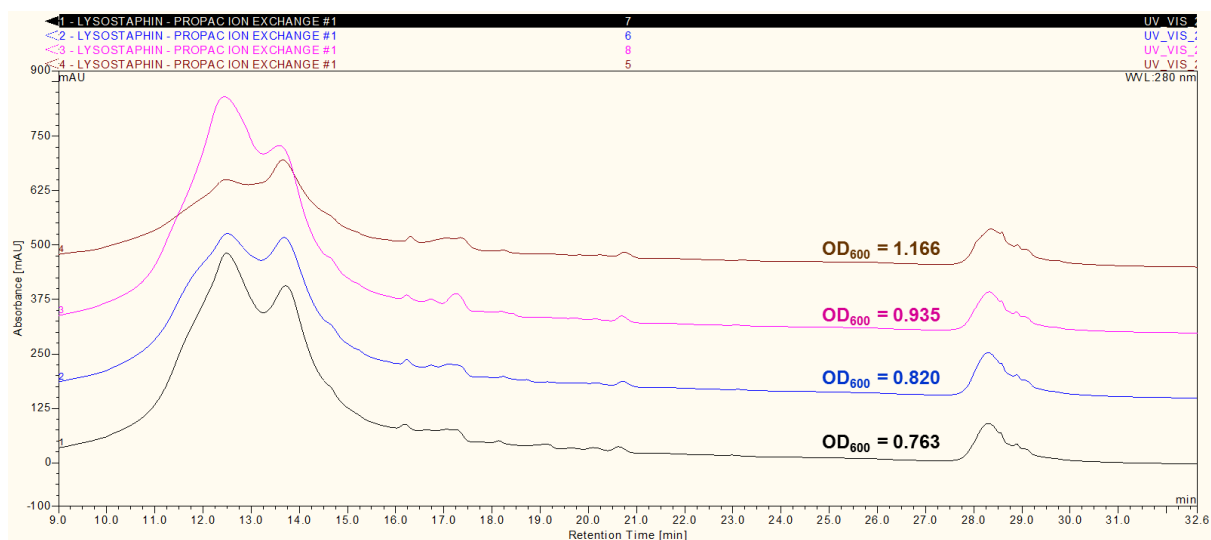


Figure 3.72: SCX analysis of cell lysate harvested 20 h after the induction of protein expression. Protein expression was induced at an optical density within the standard range.

Overall the results of these studies indicate that the optical density at which protein expression was induced was not critical to achieve expression of recombinant lysostaphin. SCX analysis indicated that the expressed protein was indeed heterogeneous, however there was no clear correlation between optical density at the point of induction and the greater prevalence of the more acidic or basic protein isoforms.

3.5.3.3 Comparative analysis of cell lysate using ProPac[®] SCX (2 x 250 mm) and ProPac[®] WCX (4 x 500 mm) columns

Although the previous experiments provided further evidence that the ProPac[®] SCX (2 x 250 mm) column could provide rapid separation of recombinant lysostaphin, it was also evident that this column provided less resolution of protein isoforms than was demonstrated by the ProPac[®] WCX (4 x 500 mm) column, despite possessing a larger internal diameter. Differences in the resolving power of the two types of column were exemplified during investigation of the influence of colony or glycerol stock-based inoculation of starter cultures upon the charge heterogeneity of expressed recombinant lysostaphin. SDS-PAGE analysis demonstrated that expression of recombinant lysostaphin could be observed in cell lysates harvested from cultures inoculated from colony or glycerol stock (Appendix 7.254).

Figure 3.73 demonstrates duplicate separations of cell lysate derived from colony or glycerol stock-based starter cultures using the ProPac[®] SCX (2 x 250 mm) column. The separations suggested that the charge heterogeneity of recombinant lysostaphin was very similar in cell

lysates extracted from cultures derived from colony- and glycerol stock-inoculated starter cultures.

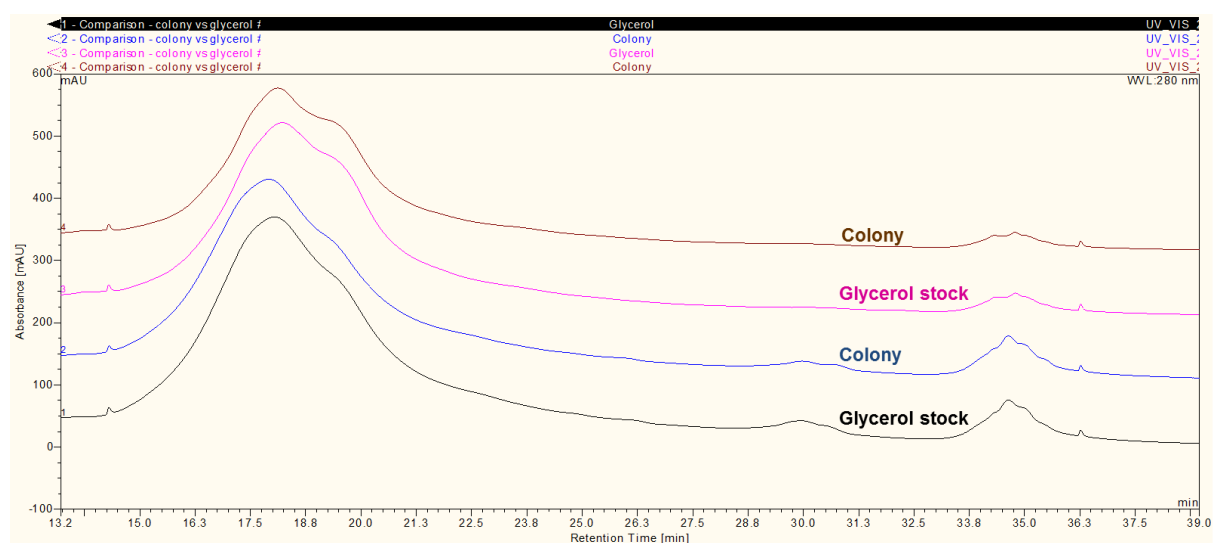


Figure 3.73: SCX separation of cell lysates derived from cultures inoculated from starter cultures, which had been inoculated from a colony or glycerol stock. The colony and glycerol stock contained *E. coli* BL21(DE3) transformed with a plasmid harbouring *N*-terminally His-tagged recombinant lysostaphin (construct 1). Starter cultures inoculated from glycerol stock or colony were inoculated into flasks containing 500 ml of LB. Protein expression was induced at an OD_{600 nm} of 1.060 in the culture derived from a colony, whilst expression was induced at an OD_{600 nm} of 1.041 in the culture derived from a glycerol stock. Each resulting cell lysate was analysed in duplicate.

However WCX separations performed using a ProPac[®] WCX (4 x 500 mm) column demonstrated that there were clear differences in the charge distribution of protein isoforms present in cell lysates extracted from cultures derived from colony- and glycerol stock-inoculated starter cultures (Figure 3.74). This enhanced resolution was desirable during rapid analysis, however the use of the ProPac[®] WCX (4 x 500 mm) column and the extended duration of separation did not support rapid analysis. At this point, the acquisition of a ProPac[®] WCX (2 x 250 mm) column became extremely desirable so as to permit higher-resolution, rapid analysis of recombinant lysostaphin charge variants.

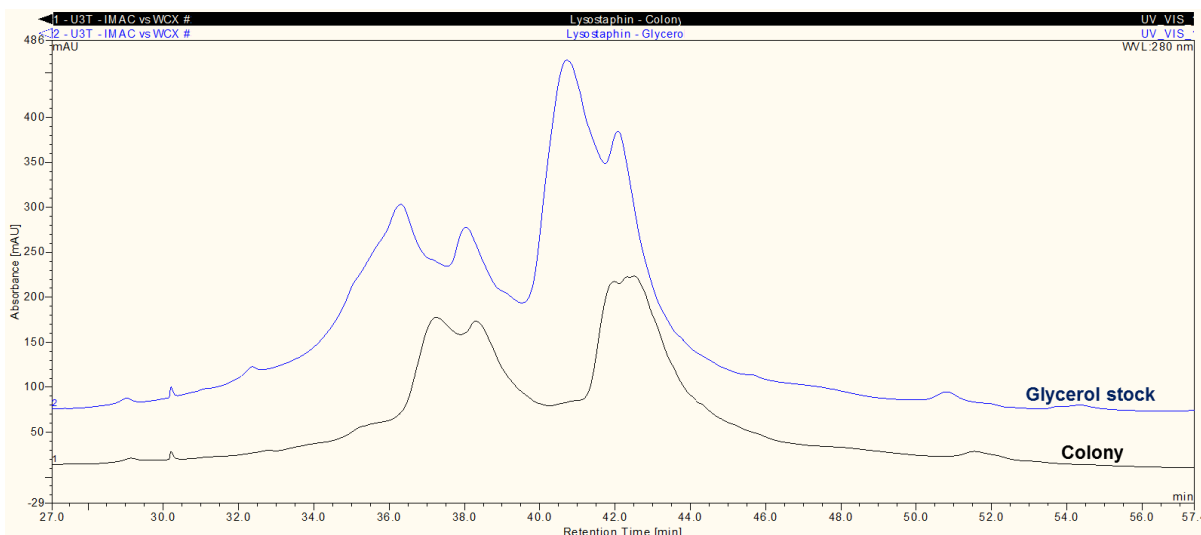


Figure 3.74: WAX separation of cell lysates derived from cultures inoculated from starter cultures, which had been inoculated from a colony or glycerol stock. The colony and glycerol stock contained *E. coli* BL21(DE3) transformed with a plasmid harbouring *N*-terminally His-tagged recombinant lysostaphin (construct 1). Starter cultures inoculated from glycerol stock or colony were inoculated into flasks containing 500 ml of LB. Protein expression was induced at an OD_{600 nm} of 1.060 in the culture derived from a colony, whilst expression was induced at an OD_{600 nm} of 1.041 in the culture derived from a glycerol stock.

The observed differences in the charge variants present in cell lysates extracted from cultures derived from colony- and glycerol stock-inoculated starter cultures appeared initially to be of concern. This concern was with regard to whether it was more appropriate to inoculate starter cultures using transformed colonies or transformed glycerol stocks and the implications of each inoculation mode upon consistency between different batch cultures and experiments. The results demonstrated in Figure 3.74 indicate that both inoculation modes could lead to different charge variants, however it was more probable that the observed differences occurred as a result of growth phase and optical density variability at the multiple points of inoculation or point of induction. Therefore glycerol-stock based inoculation remained the preferred mode of inoculation due to convenience and the fact that more cultures could be consistently inoculated using a single glycerol stock rather than a single colony.

3.5.3.4 Rapid analysis of recombinant lysostaphin using a ProPac[®] WAX (2 x 250 mm) column

In Section 3.4.3.7, ProPac[®] WAX (2 x 250 mm) columns were found to provide efficient, high resolution separation of recombinant lysostaphin isoforms within purified and crude preparations therefore could be used to perform rapid culture analysis. To improve the

quality of culture analysis it was important that sample preparation was considered and optimised to ensure that as much information could be obtained during separation of protein isoforms and during subsequent characterisation of the separated variants. A number of experiments were therefore performed to establish how much culture should be harvested at a specific time point during culture analysis to ensure that protein isoforms could be detected, but also characterised using activity assays or further LC separations.

Furthermore experiments were performed to establish whether sample through-put could be increased by freezing harvested *E. coli* or cell lysate during sample preparation (Section 3.5.3.7). Whilst such strategies could be used to enhance sample through-put, it was essential that cell lysates derived from frozen samples could be separated to achieve identical resolution of protein isoforms and charge heterogeneity, to ensure the accuracy of results.

3.5.3.5 Optimisation of cell lysate preparation during rapid analysis using a ProPac® WCX (2 x 250 mm) column

WCX separation of cell lysate harvested from 1 ml of culture yielded several distinct peaks representing the expressed isoforms of recombinant lysostaphin. However, the most abundant peak had a peak height of 55 mAU, which did not correlate with a high protein concentration. As a consequence, the separated WCX fractions could not be used for subsequent proteolytic digestion and reproducible mass spectrometric analyses. In addition, some of the less abundant isoforms were represented by peaks, which due to low absorbance readings were hard to distinguish from minor chromatographic baseline drifts (Figure 3.75).

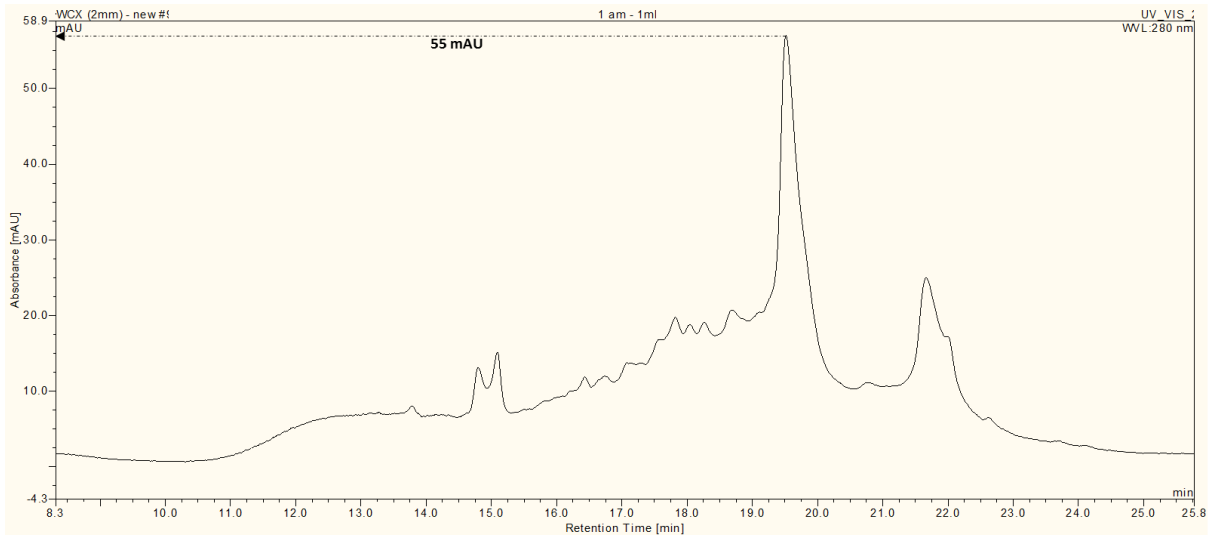


Figure 3.75: WCX separation of *N*-terminally His-tagged recombinant lysostaphin (construct 1) from cell lysate harvested from 1 ml of culture. The elution of the most abundant protein isoform was represented by a peak with a peak height of 55 mAU. The peak heights of less abundant isoforms were very low and therefore the distinction between peaks and UV base-line drifting was less clear.

Further WCX separations were performed using cell lysate harvested from larger volumes of culture (25 and 100 ml). Comparison of the WCX separations in Figure 3.76 clearly shows that higher concentrations of recombinant lysostaphin isoforms could be obtained by applying cell lysate derived from 100 ml of culture.

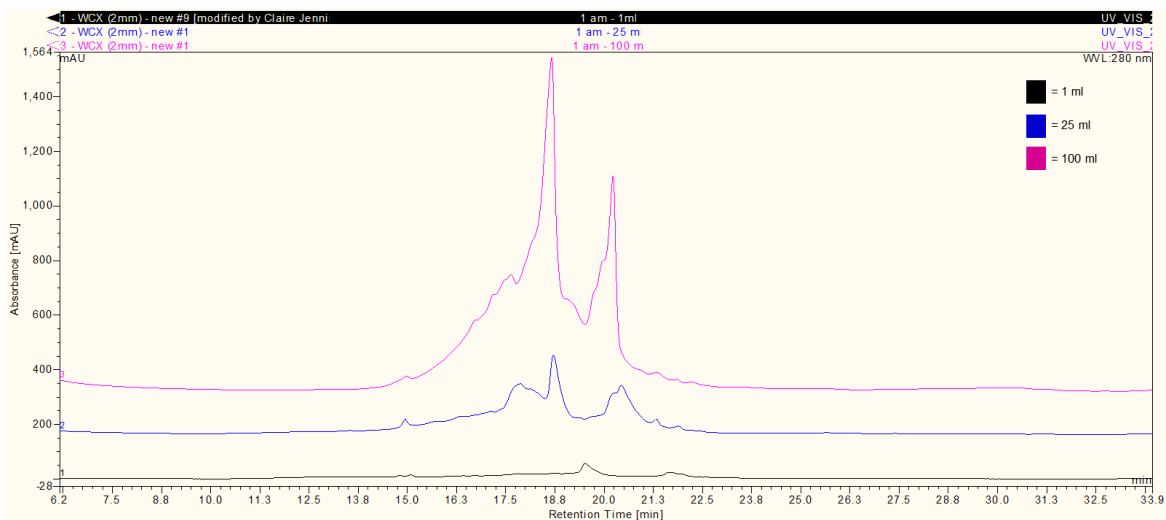


Figure 3.76: Comparison of WCX separations of *N*-terminally His-tagged recombinant lysostaphin (construct 1) from cell lysate harvested from 1, 25 and 100 ml volumes of culture.

Closer inspection of the WCX separation of recombinant lysostaphin harvested from 100 ml of culture shows that the peak representing the most abundant isoform has a peak height of

1228 mAU, which corresponds with a protein concentration which is more than adequate for proteolytic digestion and repeatable MS analysis (Figure 3.77). However harvesting 100 ml of culture would lead to volumetric depletion of 1 L batch culture after the analysis of only ten time-points, which could be problematic if protein expression lasts for several days.

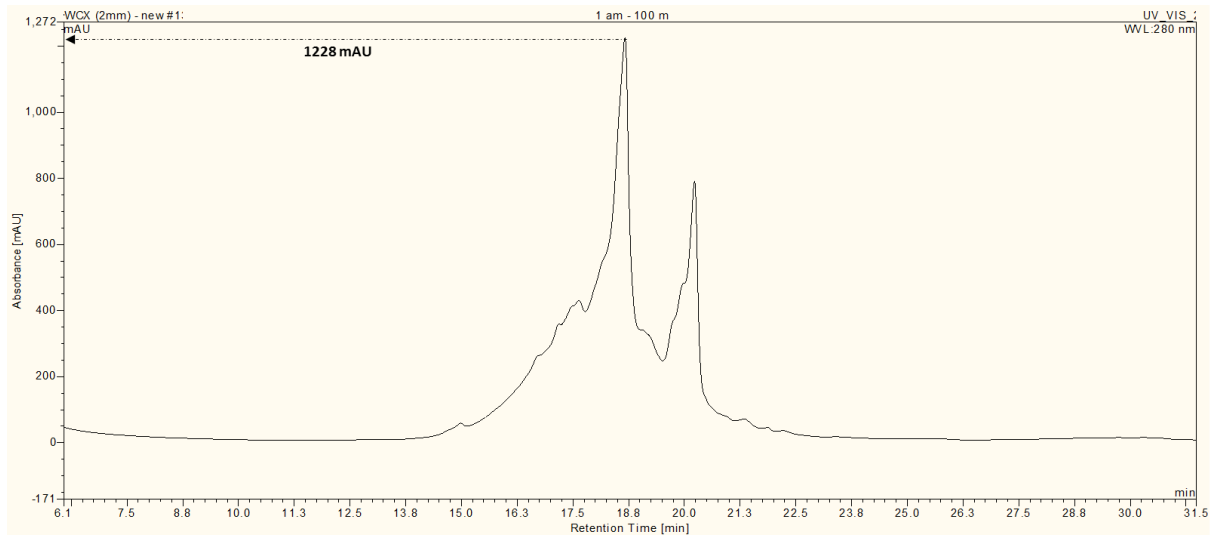


Figure 3.77: WCX separation of *N*-terminally His-tagged recombinant lysostaphin (construct 1) from cell lysate harvested from 100 ml of culture. The elution of the most abundant protein isoform was represented by a peak with a peak height of 1228 mAU. The peak heights of less abundant isoforms were also high enough to permit proteolytic digestion and reproducible MS analysis.

WCX separation of recombinant lysostaphin harvested from 25 ml of culture also provides distinct peaks representing protein isoforms which are present in high quantities (Figure 3.78). The peak representing the most abundant isoform has a peak height of 295 mAU which also corresponds with a protein concentration which would be sufficient for subsequent analysis. Harvesting 25 ml of culture would only lead to volumetric depletion of 1 L batch culture after the analysis of forty time-points, which would allow routine analysis over an extended period of protein expression.

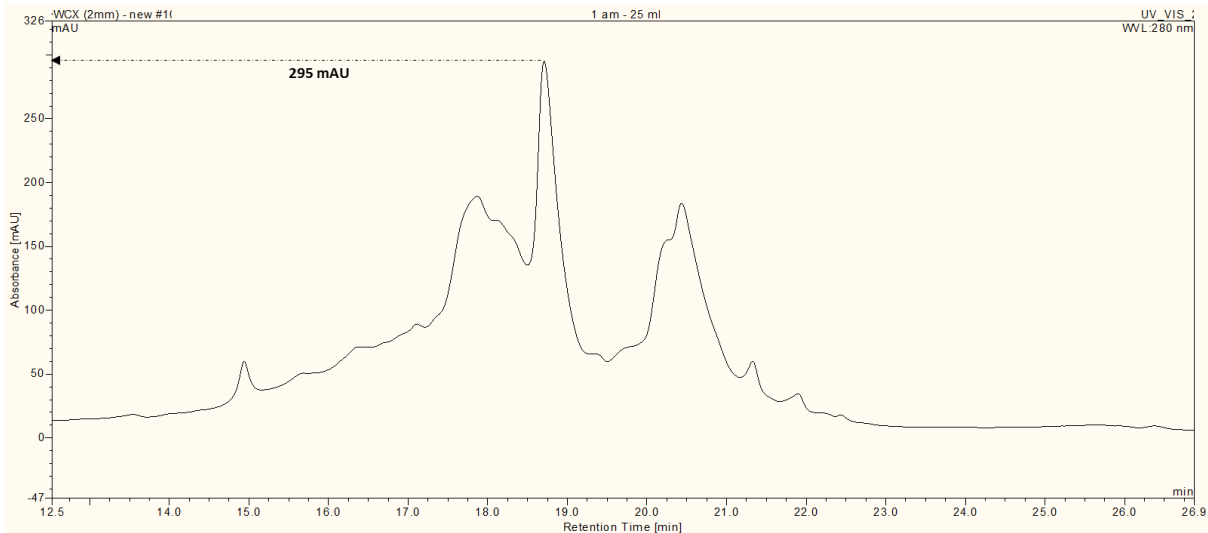


Figure 3.78: WCX separation of *N*-terminally His-tagged recombinant lysostaphin (construct 1) from cell lysate harvested from 25 ml of culture. The elution of the most abundant protein isoform was represented by a peak with a peak height of 295 mAU. The peak heights of less abundant isoforms were also high enough to permit proteolytic digestion and reproducible MS analysis.

3.5.3.6 Rapid analysis of recombinant lysostaphin using a ProPac® WCX (2 x 500 mm) column

Following the acquisition of a second ProPac® WCX (2 x 500 mm) column, both WCX columns were coupled to create a ProPac® WCX (2 x 500 mm) column. Cell lysate containing *N*-terminally His-tagged recombinant lysostaphin (construct 1) was applied to the column and separation resulted in the resolution of multiple protein isoforms (Figure 3.79). Due to the presence of two columns, the duration of column wash and equilibration phases was increased to accommodate the increased stationary phase capacity. The separation could still be achieved within 65 min, however produced enhanced resolution of protein isoforms.

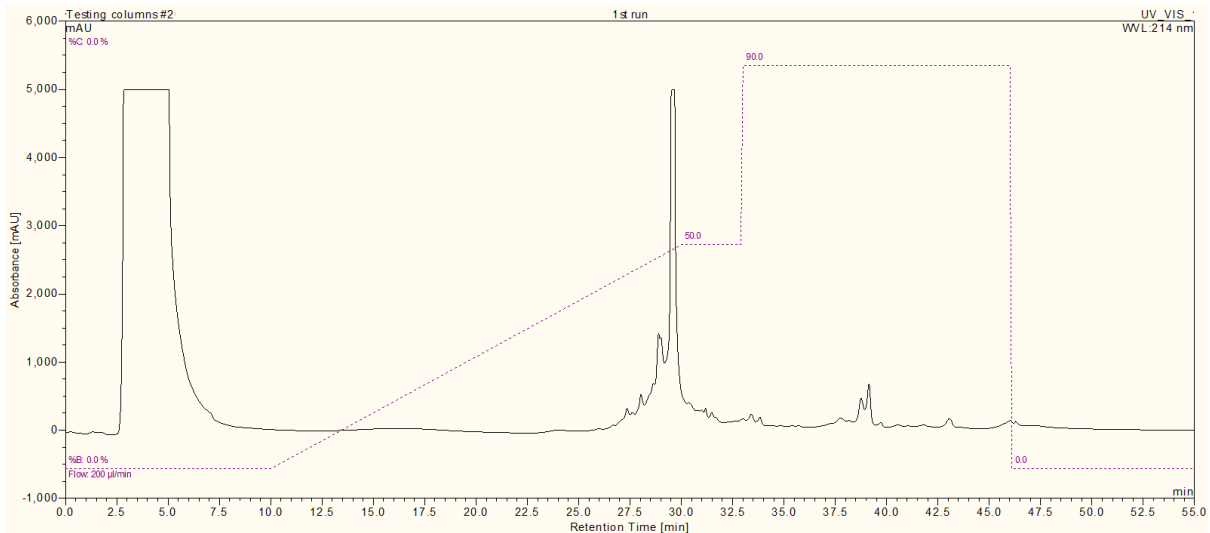


Figure 3.79: Separation of cell lysate containing *N*-terminally His-tagged recombinant lysostaphin (construct 1) using a ProPac® WCX (2 x 500 mm) column.

Repeated application of cell lysate containing *N*-terminally His-tagged recombinant lysostaphin (construct 1) demonstrated that reproducible separations could be obtained using the ProPac® WCX (2 x 500 mm) column and modified chromatographic method (Figure 3.80).

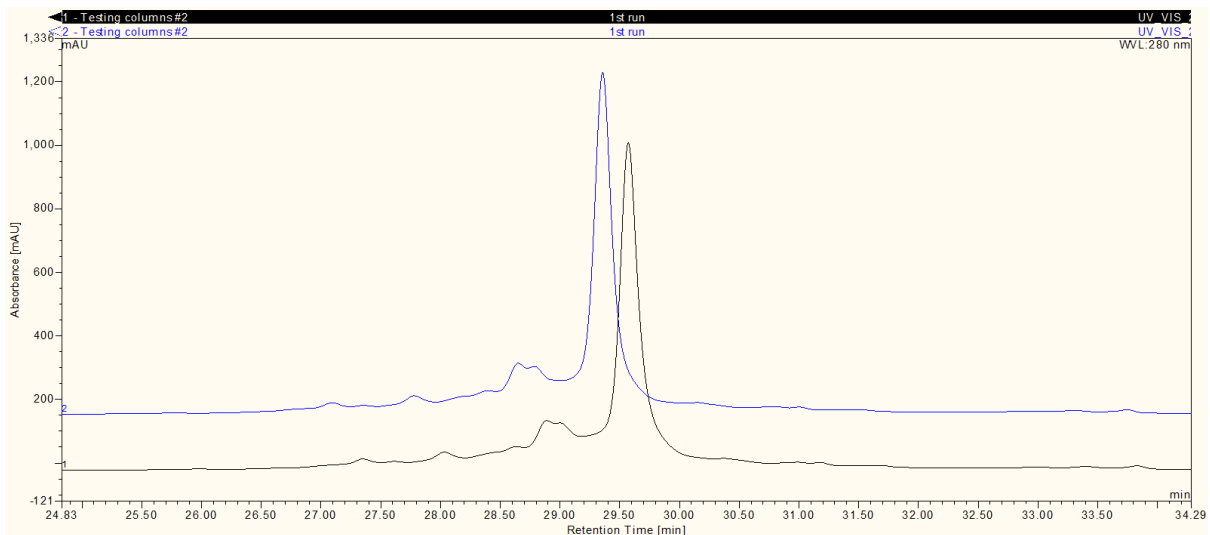


Figure 3.80: Separation of cell lysate containing *N*-terminally His-tagged recombinant lysostaphin (construct 1). Duplicate applications of the cell lysate demonstrated the reproducibility of the separation.

3.5.3.7 Maximising sample through-put during rapid analysis using a ProPac® WCX (2 x 500 mm) column

Whilst chromatographic separation methods were developed to provide rapid separation of recombinant lysostaphin, this process was ultimately delayed by the time taken to harvest cell lysate and to perform all stages of chromatographic operation, such as column elution, washing and equilibration. Rapid analysis could be performed as frequently as every hour during culture which was found to provide a good insight into the transitory nature of charge heterogeneity during protein expression. However it was not possible to perform repeated analysis of sample harvested at a specific time point, due to the continuous nature of analysis when performing hourly analysis of culture. It was therefore desirable to find a way of preserving recombinant lysostaphin in its harvested state, whilst delaying analysis for several hours or days until it became convenient to perform analysis.

As described in Section 3.5.1.3, this could theoretically have been achieved by freezing freshly harvested *E. coli* cells and resuming sample harvesting at a more convenient time. To test this strategy, cell lysates were prepared from fresh or frozen *E. coli* cell suspensions and analysed by WCX analysis to establish whether the freeze-thaw process affects the reproducibility of WCX separation results. WCX separations of recombinant lysostaphin from cell lysates derived from fresh and frozen cells were compared in Figure 3.81 and Figure 3.82. The results clearly show that the freeze-thaw process did not detrimentally affect the concentrations of protein within the samples, with no major differences in peak heights being observed between fresh and frozen preparations. However the results suggested that the freeze-thaw process subtly affected the charge of protein isoforms in the recombinant protein preparations.

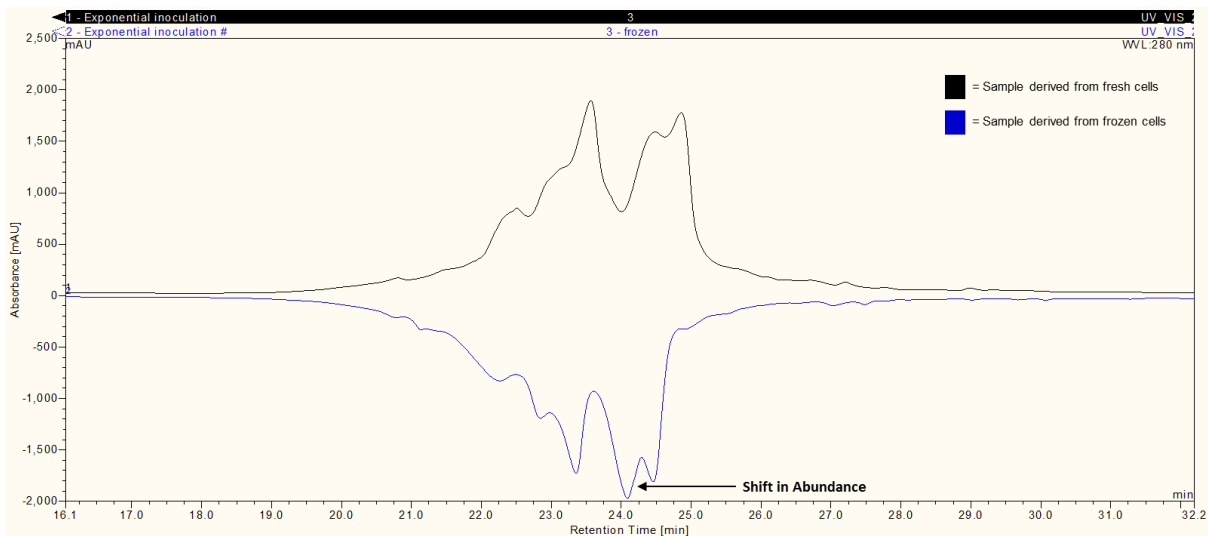


Figure 3.81: Mirrored-comparison of WCX separations of *N*-terminally His-tagged recombinant lysostaphin (construct 1) harvested from fresh and frozen *E. coli* (example 1). All of the isoforms appeared to be present in cell lysate harvested from both fresh and frozen *E. coli*, however the relative abundance of some of the conjoined peaks shifted between samples.

Comparison of WCX separations in example 1 (Figure 3.81) demonstrated that there is a shift in the relative abundance of some of the conjoined peaks between samples. In Figure 3.82, evaluation of WCX separations revealed the appearance of a double peak in the sample derived from frozen cells that was not present in the sample derived from fresh cells. Unfortunately these subtle differences between WCX separation of fresh and frozen preparations precluded the use of frozen samples in a rapid analysis protocol, as the results did not match the results obtained from fresh preparations.

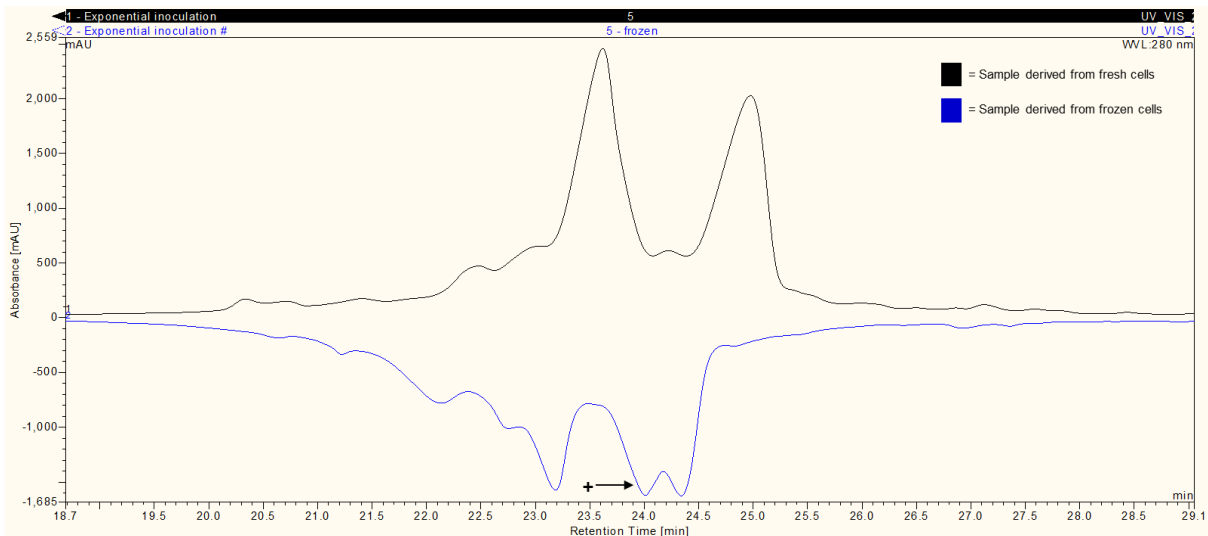


Figure 3.82: Mirrored-comparison of WCX separations of *N*-terminally His-tagged recombinant lysostaphin (construct 1) harvested from fresh and frozen *E. coli* (example 2). A major difference between the WCX separations was the appearance of a double peak (+) in the sample derived from frozen cells that was not present in the sample derived from fresh cells. Comparison of WCX separations also demonstrated a chromatographic shift in the retention times between the two separations which complicated comparison of peaks.

As *N*-terminally His-tagged recombinant lysostaphin (construct 1) was not preserved in its expressed state after freezing harvested *E. coli* cells, comparative WCX separations were performed using freshly prepared cell lysate and cell lysate which had been frozen following preparation. However, as shown in Figure 3.83, separation of the frozen cell lysate resulted in loss of several protein isoforms that were observed following separation of freshly prepared cell lysate. In addition, the abundance of the isoforms that were observed in freshly prepared cell lysate appeared to have increased, leading to the detection of two predominant isoforms following separation of the frozen cell lysate.

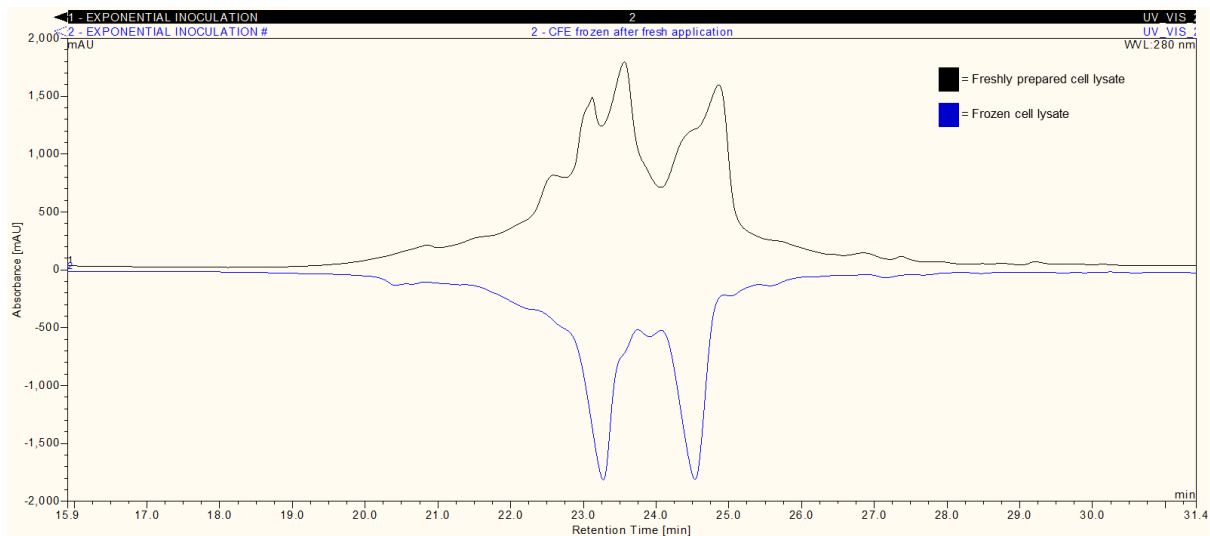


Figure 3.83: Comparison of WCX separations of *N*-terminally His-tagged recombinant lysostaphin (construct 1) harvested from fresh and frozen cell lysate (Example 1). All of the isoforms appeared to be present in cell lysate harvested from both fresh and frozen *E. coli* BL21(DE3), however the relative abundance of some of the conjoined peaks shifted between samples.

A second comparative WCX experiment also revealed differences in the charge heterogeneity of protein isoforms detected in fresh and frozen cell lysate. Once again, several protein isoforms were not detected within the frozen cell lysate, with two predominant peaks being retained (Figure 3.83). These results indicated that frozen cell lysate, could not be used to accurately represent the heterogeneity of recombinant lysostaphin during culture. This inability to preserve recombinant lysostaphin reinforced the importance of optimising and performing rapid analysis to ensure that protein heterogeneity could be monitored in real-time and as frequently as possible.

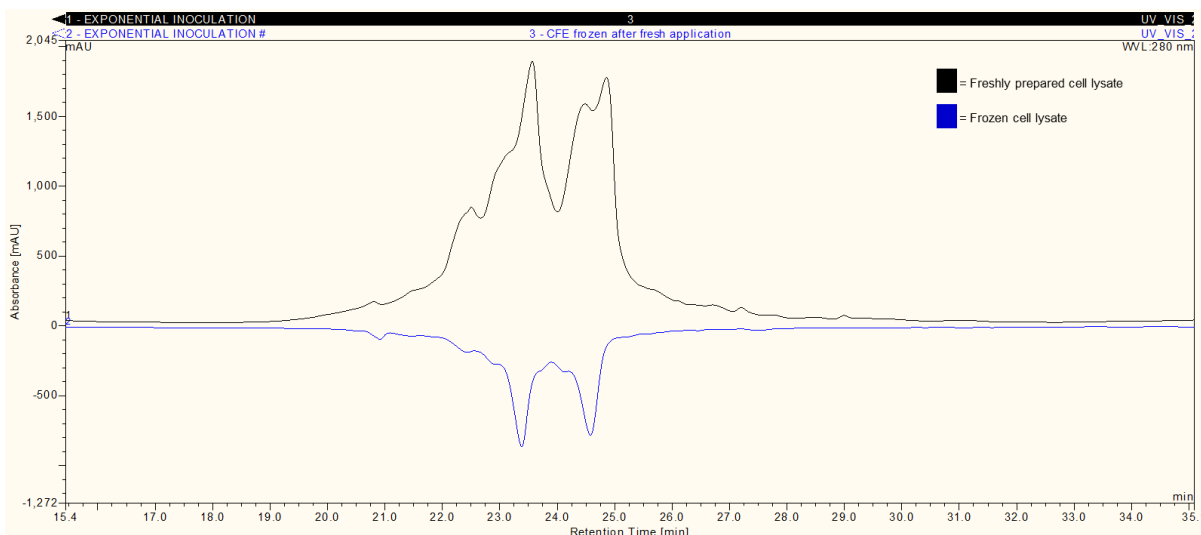


Figure 3.84: Comparison of WCX separations of *N*-terminally His-tagged recombinant lysostaphin (construct 1) harvested from fresh and frozen cell lysate (Example 2). All of the isoforms appeared to be present in cell lysate harvested from both fresh and frozen *E. coli*, however the relative abundance of some of the conjoined peaks shifted between samples.

3.5.3.8 Culture analysis using a ProPac WCX[®] (2 x 500 mm) column

Once chromatographic conditions had been optimised, multiple experiments were performed to provide further culture analysis, whilst taking advantage of the improved resolution provided by the ProPac WCX[®] (2 x 500 mm) column. Expression studies were focused upon elucidating the influence of optical density at the point of induction or time upon the resulting charge heterogeneity of recombinant lysostaphin.

3.5.3.9 Investigation of the influence of optical density at the point of induction upon the charge heterogeneity of recombinant lysostaphin

The influence of optical density upon the charge heterogeneity of recombinant lysostaphin was reinvestigated by performing three experiments in which recombinant protein expression was analysed in a total of twenty nine cultures. Expression of recombinant lysostaphin was analysed by SDS-PAGE (Appendix 7.255) and by WCX analysis to provide further information about the influence of optical density at point of induction upon product heterogeneity. Unlike the previous experiments investigating the influence of optical density upon expression and heterogeneity, which were performed on cell lysate extracted at 4, 10 or 20 h, these three experiments were performed on cell lysates harvested at 20 h exclusively.

Figure 3.85 demonstrates high resolution separation of protein isoforms expressed following induction of protein expression at optical densities lower than the standard induction densities ($OD_{600\text{ nm}} = 0.6-1.0$). WCX separation of cell lysates resulting from cultures induced at optical densities below 0.2 did not reveal the presence of clear protein isoforms indicating poor expression of *N*-terminally His-tagged recombinant lysostaphin (construct 1). However WCX separation of cell lysates harvested from cultures induced at optical densities at 0.2 and above, demonstrated clear separation of several protein isoforms. As demonstrated, in previous culture analysis experiments, the abundance of the most basic protein isoform appeared to decrease as the optical density at point of induction increased. Furthermore the abundance of the major acidic protein isoform appeared to increase with increasing optical density.

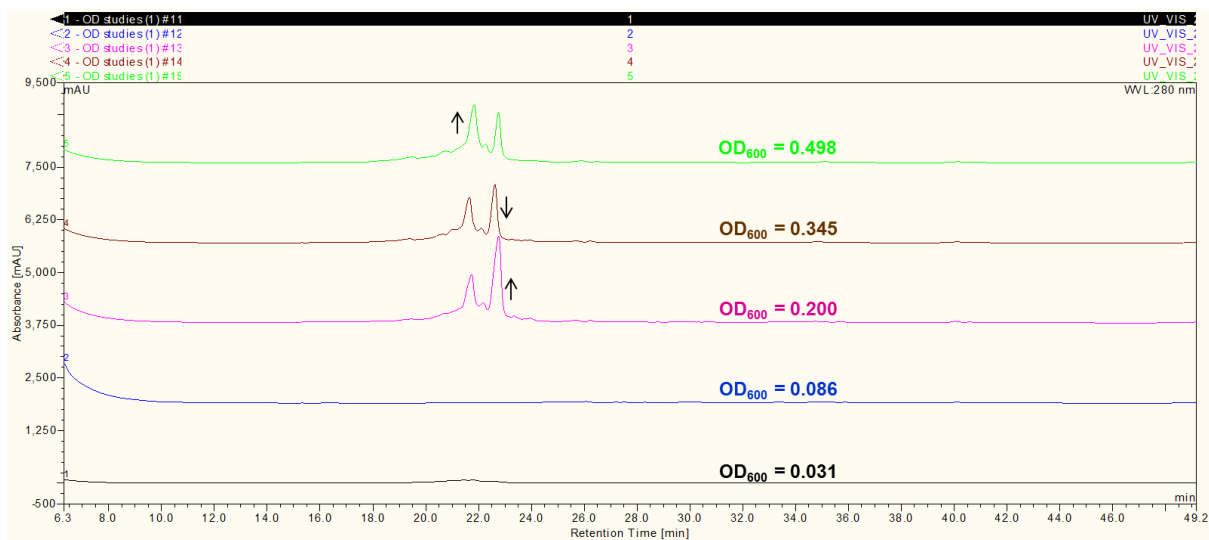


Figure 3.85: WCX analysis of *N*-terminally His-tagged recombinant lysostaphin (construct 1) from cell lysates harvested 20 h after the induction of protein expression at varying optical densities (Experiment 1). Protein expression was induced at optical densities lower than the standard induction densities. Arrows indicate changes in the abundance of the two major acidic or basic protein isoforms.

WCX separation of cell lysates harvested from cultures induced at optical densities within the standard range for protein expression, resulted in the detection of two predominant protein isoforms (Figure 3.86). In addition, a more acidic protein isoform, with a retention time of around 21.5 min, became more abundant in cultures induced at standard optical densities. These results indicated that the heterogeneity of recombinant lysostaphin also increased in cultures induced at higher optical densities. The detection of a third major protein isoform demonstrated how the increased resolution provided by the ProPac WCX[®] (2 x 500 mm) column could allow better identification of charge variants than the ProPac SCX[®]

(2 x 250 mm) column. It is likely that this third acidic isoform could not be resolved by the ProPac SCX[®] column, but instead led to the observed peak broadening.

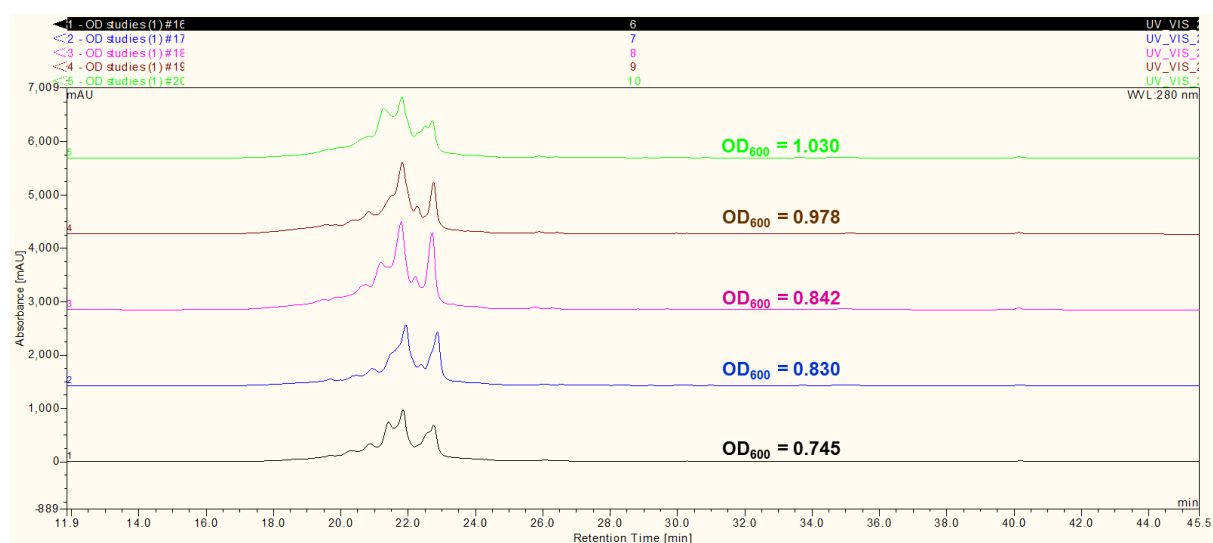


Figure 3.86: WCX analysis of *N*-terminally His-tagged recombinant lysostaphin (construct 1) from cell lysates harvested 20 h after the induction of protein expression at varying optical densities (Experiment 1). Protein expression was induced at optical densities within the standard range. Arrows indicate changes in the abundance of the two major acidic or basic protein isoforms.

In the second experiment, the enhanced resolution provided by the ProPac WCX[®] (2 x 500 mm) column elucidated the presence of further protein isoforms which were not evident during the first experiment (Figure 3.87). WCX separation of cell lysates harvested from cultures in which protein expression was induced at optical densities below 0.2 once again did not reveal any separated protein isoforms due to poor expression of *N*-terminally His-tagged recombinant lysostaphin (construct 1). Cell lysates harvested from cultures induced at optical densities above 0.2 demonstrated the presence of the two most predominant protein isoforms at retention times of 21.5 and 23.0 min. These protein isoforms were detected in the first experiment, however in the second experiment additional peaks at retention times of 20.5 and 22.5 min were also detected leading to greater charge heterogeneity. It is possible that these protein isoforms represented intermediate charge states that occurred during post-translational processing.

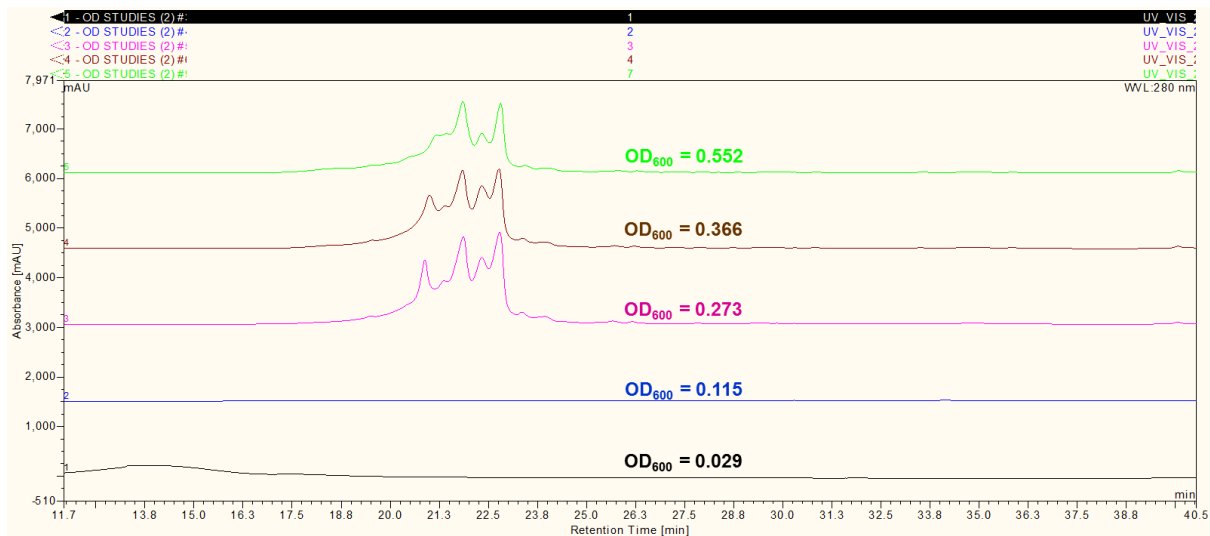


Figure 3.87: WCX analysis of *N*-terminally His-tagged recombinant lysostaphin (construct 1) from cell lysates harvested 20 h after the induction of protein expression at varying optical densities (Experiment 2). Protein expression was induced at optical densities lower than the standard induction densities. Arrows indicate changes in the abundance of the two major acidic or basic protein isoforms.

WCX separation of *N*-terminally His-tagged recombinant lysostaphin (construct 1) from cell lysates harvested from cultures induced at higher optical densities demonstrated a similar degree of heterogeneity with two or four major protein isoforms detected in all of the samples (Figure 3.88). Unlike the first experiment, the observed charge heterogeneity appeared to vary more considerably between cultures. The overall abundance of the protein isoforms appeared to have decreased slightly in cultures induced at optical densities of 0.854 and 1.558, which may have reflected decreased expression, in conjunction with degradation of recombinant lysostaphin by cellular proteases.

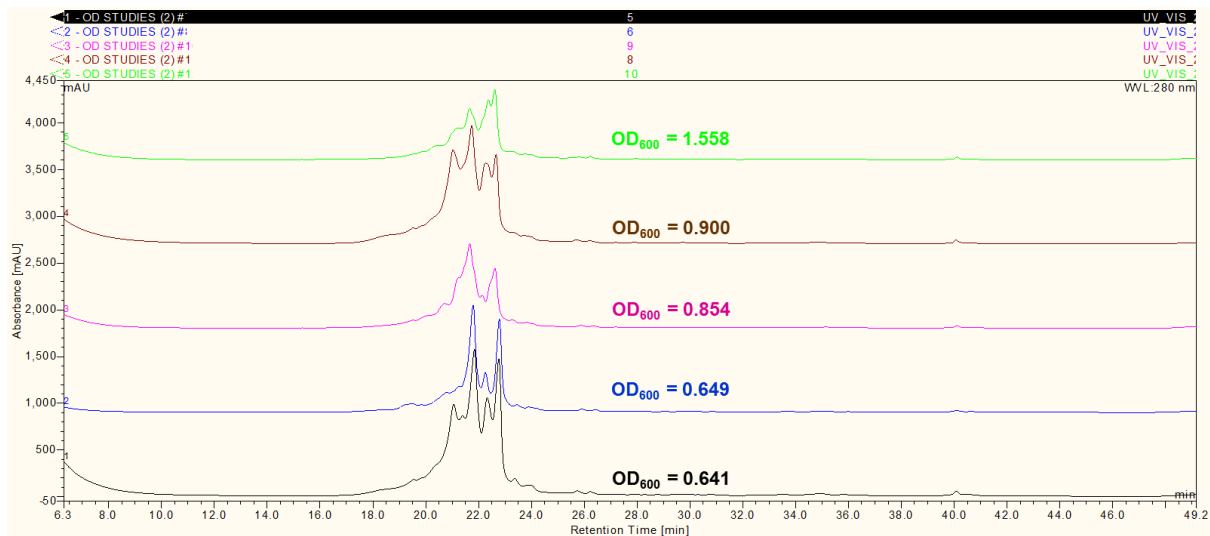


Figure 3.88: WCX analysis of *N*-terminally His-tagged recombinant lysostaphin (construct 1) from cell lysates harvested 20 h after the induction of protein expression at varying optical densities (Experiment 2). Protein expression was induced at optical densities within the standard range. Arrows indicate changes in the abundance of the two major acidic or basic protein isoforms.

The third experiment yielded similar results to the second experiment with at least four protein isoforms detected in each of the harvested cell lysates. The abundance of each of these protein isoforms appeared to vary with no apparent pattern between samples. WCX separation of cell lysates harvested from cultures induced at $OD_{600\text{ nm}}$ values below 0.6 indicated that protein isoforms with a retention time of 20.5 and 22.5 were less abundant, yet still detectable (Figure 3.89). All four protein isoforms were clearly evident in cell lysates harvested from cultures which had been induced within the standard optical density range (Figure 3.90).

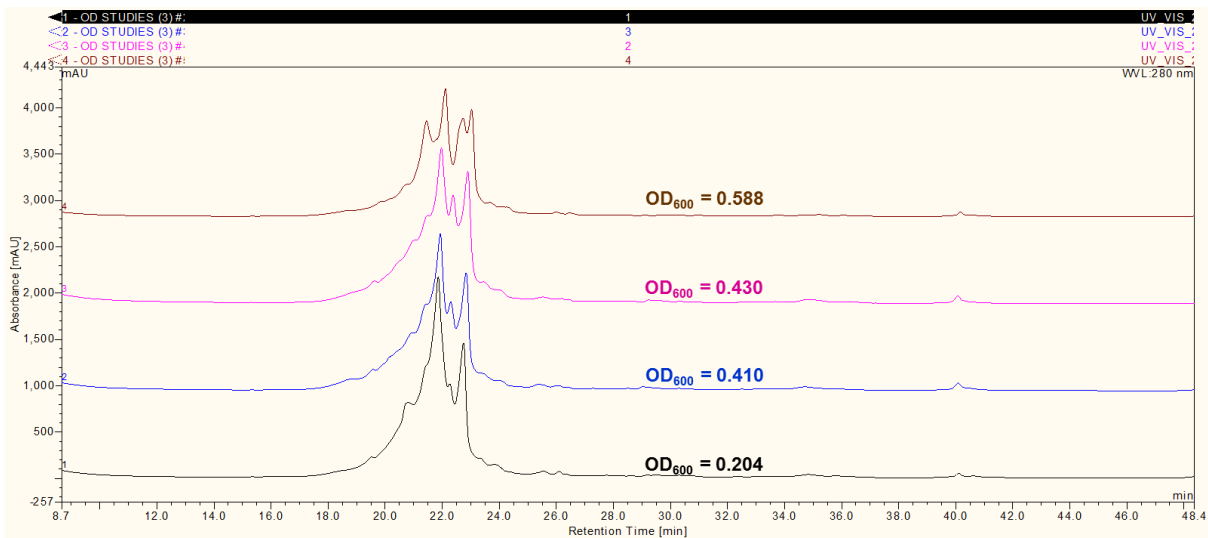


Figure 3.89: WCX analysis of *N*-terminally His-tagged recombinant lysostaphin (construct 1) from cell lysates harvested 20 h after the induction of protein expression at varying optical densities (Experiment 3). Protein expression was induced at optical densities lower than the standard induction densities. Arrows indicate changes in the abundance of the two major acidic or basic protein isoforms.

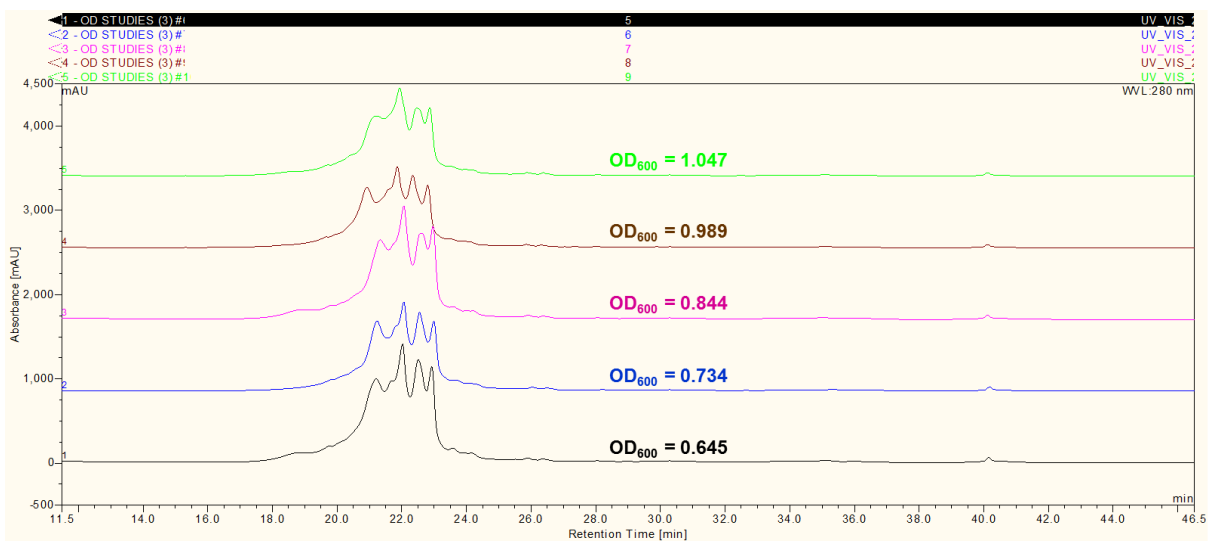


Figure 3.90: WCX analysis of *N*-terminally His-tagged recombinant lysostaphin (construct 1) from cell lysates harvested 20 h after the induction of protein expression at varying optical densities (Experiment 3). Protein expression was induced at optical densities within the standard range.

Overall these results demonstrate that more extensive visualisation of recombinant lysostaphin variants can be achieved using the ProPac WCX[®] (2 x 500 mm) column, providing a greater insight into the highly variable charge heterogeneity that can be observed following induction of protein expression at varying optical densities. The results of these experiments were however of concern, when considered that the increased charge

heterogeneity appeared to increase in cultures which were induced within the standard expression range ($OD_{600\text{ nm}} = 0.6-1.0$) and harvested 20 h following induction, as these conditions reflect those which could be routinely employed during recombinant protein production.

Although the cultures in all three experiments were fermented for exactly 20 h, the observed variability may have been attributable to differences in the optical density of the starter culture used to inoculate the main shake-flask culture. The optical density values of the starter cultures at point of inoculation were controlled as much as possible, however starter cultures with $OD_{600\text{ nm}}$ values of 1.651, 1.732 and 1.578 were used to inoculate cultures in experiments 1, 2 and 3 respectively, therefore differences in bacterial growth phase may have contributed to the observed variability.

To eliminate the introduction of variability from differences in starter culture optical density, a series of experiments were performed in which cultures were inoculated directly from a glycerol stock. To investigate whether recombinant lysostaphin could be successfully produced following direct inoculation of shake-flask cultures from a glycerol stock, cell lysates were harvested from a total of fifteen cultures during three experiments. WCX analysis of harvested cell lysates harvested in the first experiment demonstrated the presence of detectable protein isoforms (Figure 3.91). However the abundance and resolution of the detected peaks appeared to be detrimentally affected in some of the samples, due to poor expression, which was detected by SDS-PAGE analysis (Appendix 7.243).

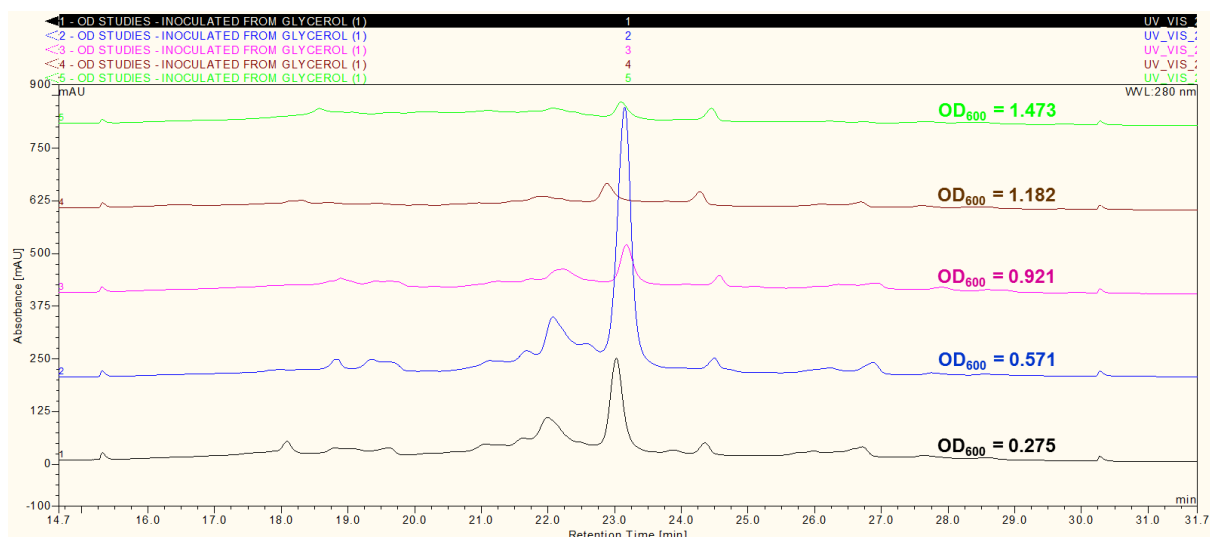


Figure 3.91: WCX analysis of *N*-terminally His-tagged recombinant lysostaphin (construct 1) from cell lysates harvested from cultures inoculated directly from a glycerol stock (Experiment 1). Cultures were harvested 20 h after the induction of protein expression at varying optical densities.

WCX analysis of cell lysates harvested in the second and third experiments also demonstrated the presence of detectable peaks, however poor protein expression was evident in some of the cell lysates (Figure 3.92 and Figure 3.93). Interestingly the more basic protein isoforms appeared to be more abundant in each of the samples and experiments, despite differences in the optical density at the point of induction. This contradicted previous experiments which suggested that higher optical densities at the point of induction correlated the increased abundance of more acidic protein isoforms.

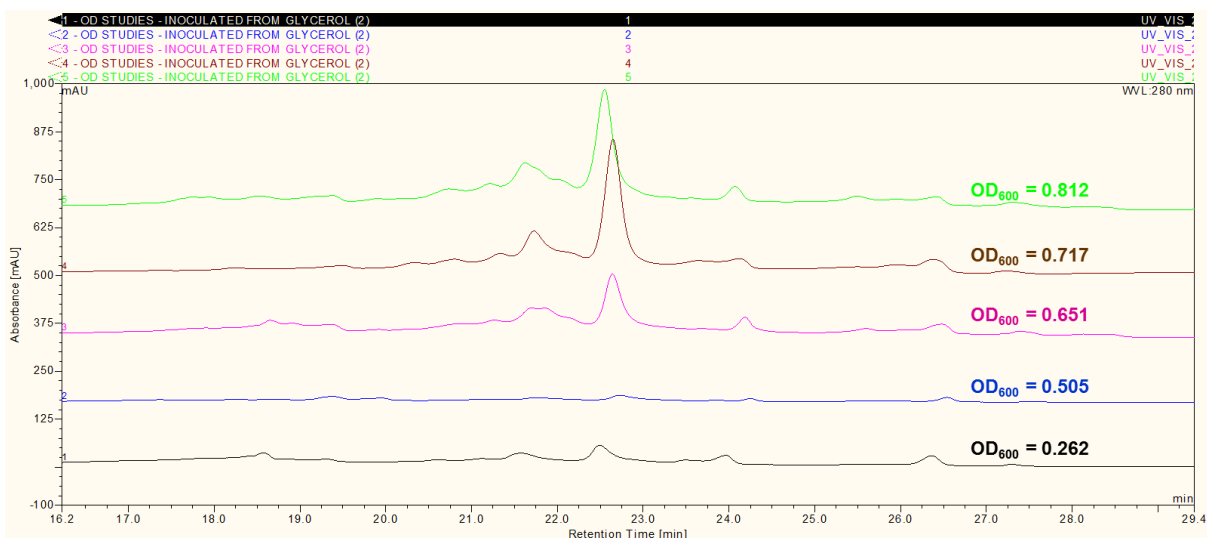


Figure 3.92: WAX analysis of *N*-terminally His-tagged recombinant lysostaphin (construct 1) from cell lysates harvested from cultures inoculated directly from a glycerol stock (Experiment 2). Cultures were harvested 20 h after the induction of protein expression at varying optical densities.

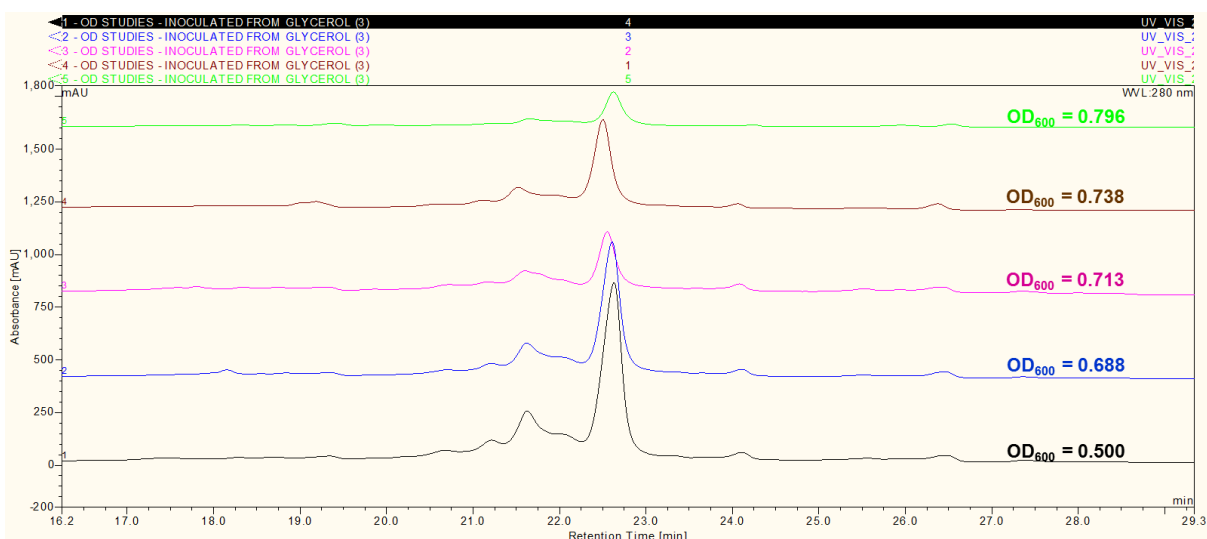


Figure 3.93: WAX analysis of *N*-terminally His-tagged recombinant lysostaphin (construct 1) from cell lysates harvested from cultures inoculated directly from a glycerol stock (Experiment 3). Cultures were harvested 20 h after the induction of protein expression at varying optical densities.

3.5.3.10 Optimisation of chromatographic conditions

As the IEX separations were frequently performed to investigate how the heterogeneity of *N*-terminally His-tagged recombinant lysostaphin (construct 1) was influenced by culture variables, such as optical density and time, chromatographic methods often remained unmodified to prevent retention time differences and allow easier comparison between experiments. However alterations to chromatographic methods were gradually applied

during the development of a rapid analysis strategy. The first such alteration featured the incorporation of a sample wash period at the start of the separation to ensure that unbound cellular contaminants did not interfere with analysis (Figure 3.94). However following separation it was evident that a 3 min wash period was not long enough to permit full elution of the unbound contaminants.

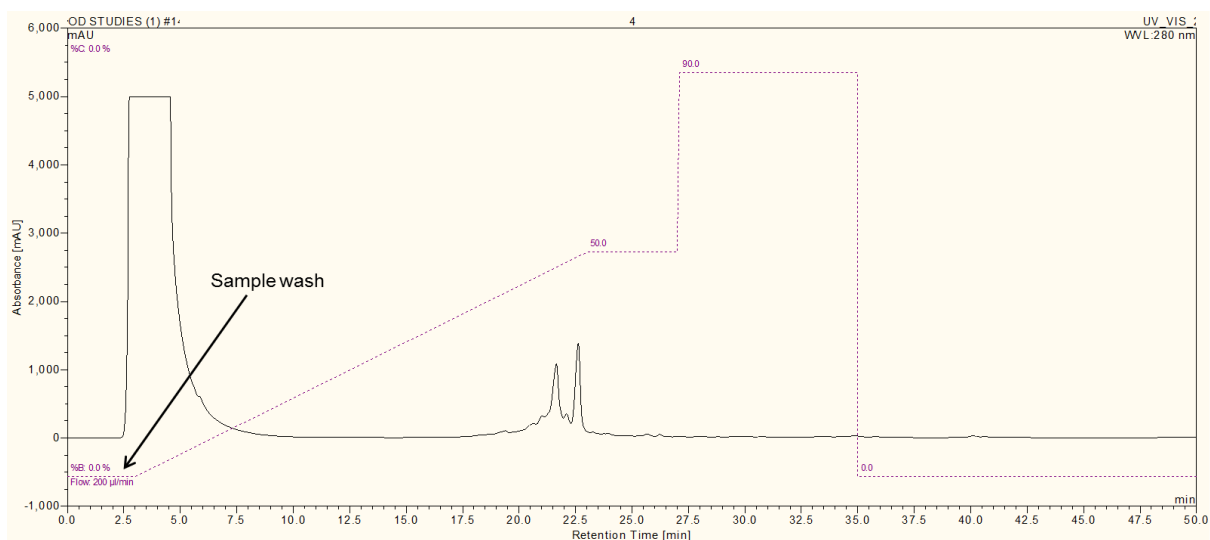


Figure 3.94: Introduction of an extended sample wash during chromatographic separation. During and following injection of cell lysate, 100% WCX buffer A was applied to the column for 3 min to ensure that any unbound cellular contaminants were washed from the column. The separation was performed on cell lysate containing *N*-terminally His-tagged recombinant lysostaphin (construct 1) using a ProPac® WCX (2 x 500 mm) column.

The wash period was therefore extended to last for 10 min following the injection of more concentrated cell lysates or to accommodate larger injection volumes. As shown in Figure 3.95, the extended sample wash period was long enough to allow unbound cellular constituents prior to the start of the linear elution gradient.

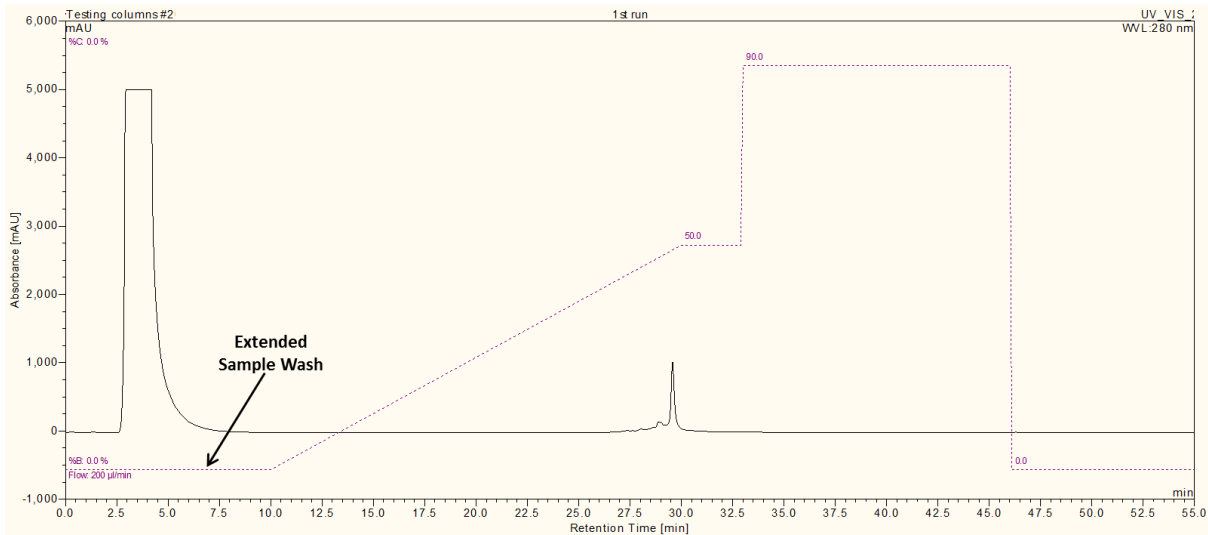


Figure 3.95: Introduction of an extended sample wash during chromatographic separation. During and following injection of cell lysate, 100% WCX buffer A was applied to the column for 10 min to ensure that any unbound cellular contaminants were washed from the column. The example separation was performed on cell lysate containing *N*-terminally His-tagged recombinant lysostaphin (construct 1) using a ProPac® WCX (2 x 500 mm) column.

During the early development of a rapid analysis strategy, the column wash period was extended to 13 min to ensure that observed peaks reflected the current state of protein expression rather than carry-over from a previous separation. With repeated culture analysis experiments, this wash period was reduced to 8 min (Figure 3.96). The equilibration period was also lengthened to minimise chromatographic shifting during culture analysis.

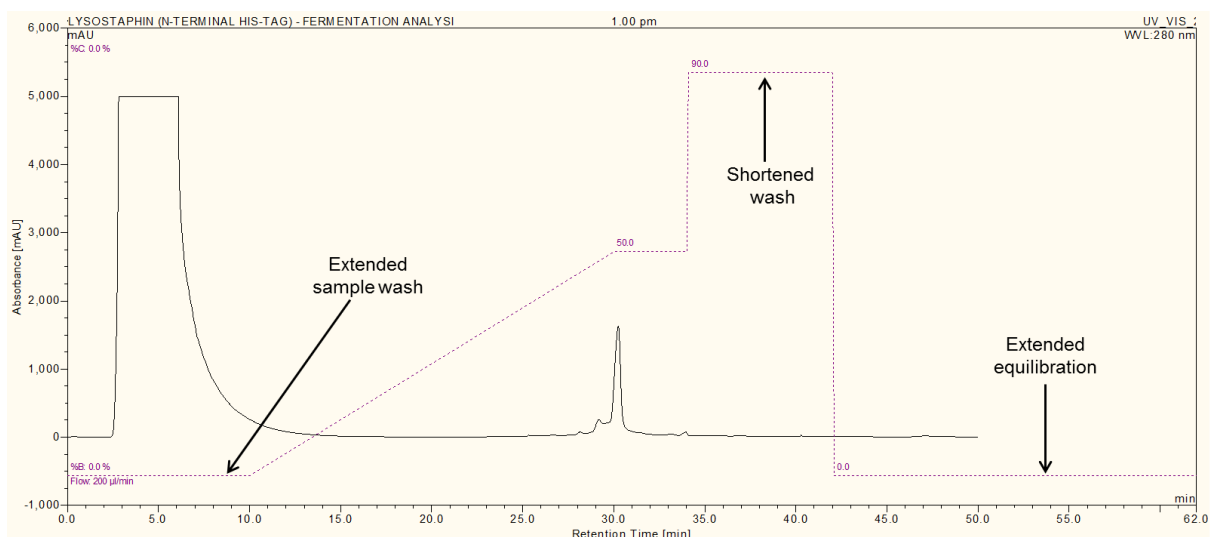


Figure 3.96: Optimised chromatographic method applied used during culture analysis. In addition to an extended sample wash, the column wash phase was shortened and the equilibration phase was lengthened to prevent chromatographic shifting during repeated analysis. The example separation was performed on cell lysate containing *N*-terminally His-tagged recombinant lysostaphin (construct 1) using a ProPac® WCX (2 x 500 mm) column.

3.5.3.11 Investigation of the influence of time upon the charge heterogeneity of recombinant lysostaphin

Expression studies focused on the influence of optical density at the point of induction provided an insight into the transitory nature of protein charge during the expression of recombinant lysostaphin. However the studies did not demonstrate a clear correlation between optical density at the point of induction and differences in the abundance and charge of particular protein isoforms. It was therefore decided that in subsequent expression studies, the charge heterogeneity of recombinant lysostaphin should be monitored using time, rather than optical density at the point of induction, as a variable.

To achieve this, the charge heterogeneity of *N*-terminally His-tagged recombinant lysostaphin (construct 1) was monitored in a single culture over a time-course of expression. To avoid swift volumetric depletion, 25 ml of culture was harvested from the culture at regular time intervals, as frequently as every 90 min. Bacterial growth during culture was monitored by UV spectrometry during the course of culture analysis (Appendix 7.244). The growth of the *E. coli* BL21(DE3) followed typical bacterial growth kinetics, entering death phase after 28 h of culture (Appendix 7.246). Despite entering death phase, expression of *N*-terminally His-tagged recombinant lysostaphin (construct 1) was detected by SDS-PAGE for at least 28 h following induction of protein expression (Appendix 7.247).

Cell lysate harvesting and culture analysis was performed between 1.5 and 30.0 h following the induction of protein expression. As evidenced by Figure 3.97, expressed recombinant lysostaphin isoforms were successfully detected and separated throughout the culture analysis. Due to the number of WCX separations performed, visual representation of the compared chromatograms was less clear, however it was evident that the presence of two predominant protein isoforms could be detected through the course of expression.

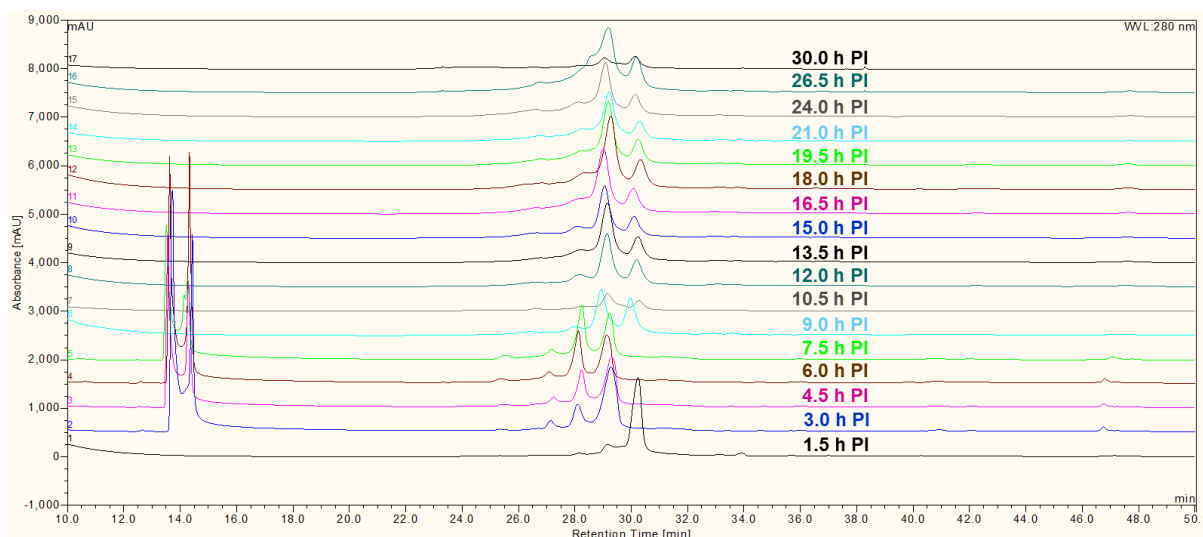


Figure 3.97: WCX analysis of *N*-terminally His-tagged recombinant lysostaphin (construct 1) over an expression time-course. Cell lysate was harvested from a 1L LB culture at regular intervals between 1.5 h and 30.0 h post-induction.

Due to the continuous nature of analysis, chromatographic issues such as retention time shifting or the presence of anomalous peaks could not be corrected immediately by re-analysing the sample. For instance, WCX analysis of cell lysates harvested at 3.0, 4.5, 6.0 and 7.5 h post-induction were subject to retention time shifting which falsely represented the peaks as more acidic protein isoforms (Figure 3.98). The degree of retention time deviation may have been caused by slight fluctuations in system back pressure during early WCX separations. The presence of additional noisy peaks between 13.5 and 15.0 min provided further evidence that the WCX separations did not provide accurate chromatographic representations. The source of the noisy peaks was unknown.

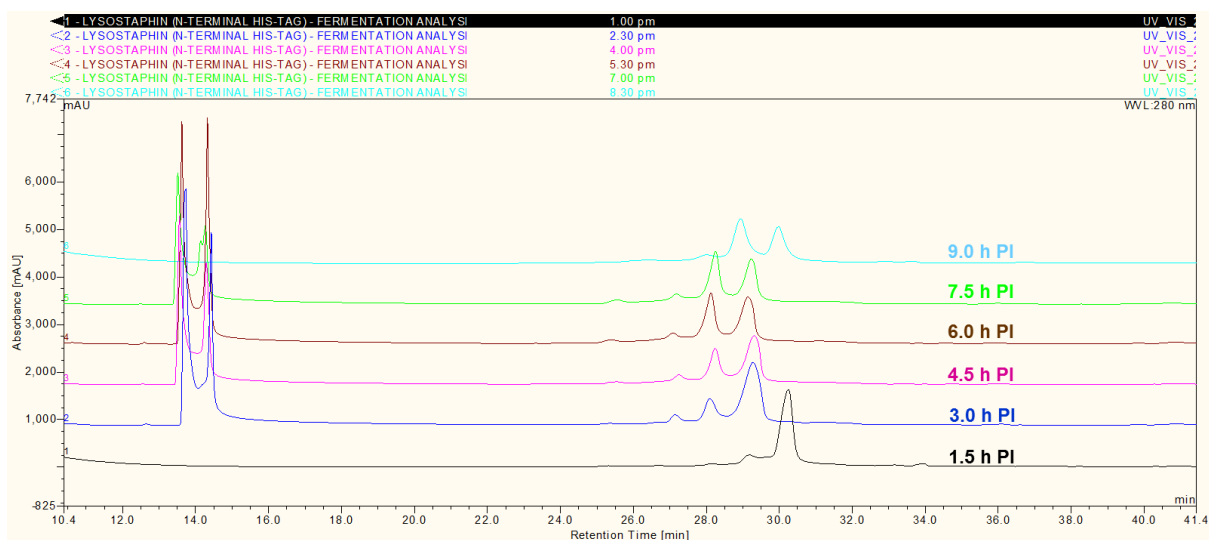


Figure 3.98: Comparison of chromatograms produced by WCX separation of *N*-terminally His-tagged recombinant lysostaphin (construct 1) performed during early culture analysis. WCX separation of cell lysates harvested at 3.0, 4.5, 6.0 and 7.5 h post-induction demonstrated detection of noisy peaks and retention time shifting.

Due to the apparent inaccuracy of WCX separation, cell lysates harvested at 3.0, 4.5, 6.0 and 7.5 h post-induction, were re-applied to the ProPac WCX[®] (2 x 500 mm) column once the final separation had been performed on cell lysate harvested at 30.0 h post-induction (Figure 3.99). The cell lysates were stored at 4°C until analysis could be performed to demonstrate that the observed peaks should have displayed retention times that corresponded with those detected during WCX separation of cell lysates harvested at 1.5 and 9.0 h.

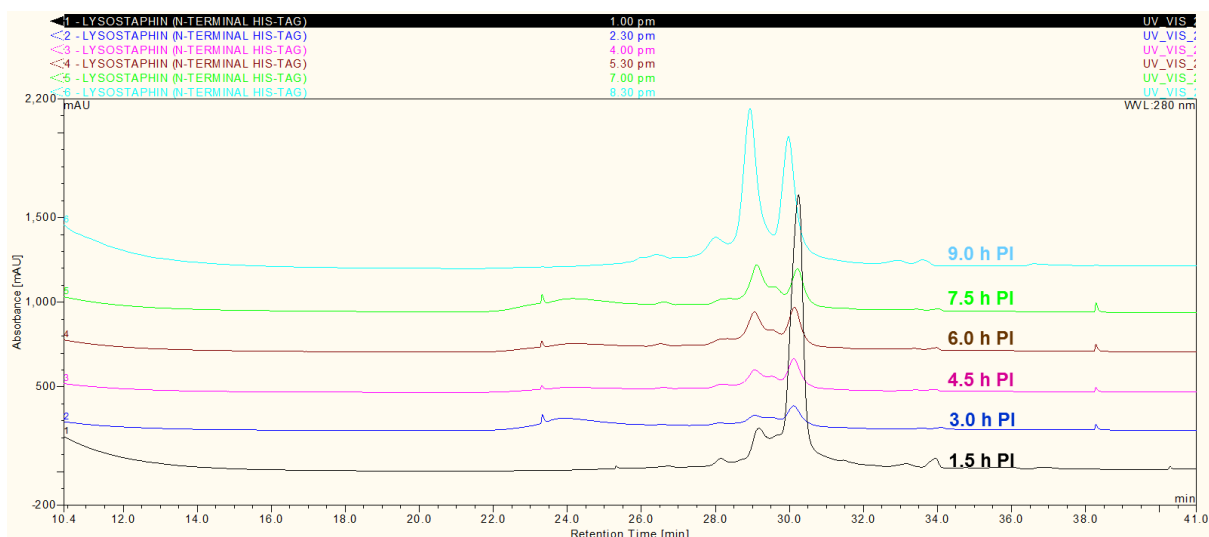


Figure 3.99: Comparison of chromatograms produced by WCX separation performed following re-application of cell lysates analysed during early culture analysis. WCX separation of cell lysates harvested at 3.0, 4.5, 6.0 and 7.5 h post-induction demonstrated detection of noisy peaks and retention time shifting.

Re-application of cell lysates demonstrated that noisy peaks between 13.5 and 15.0 min were not detected during these WCX separations, indicating that their original presence was anomalous. More importantly, repeated separation demonstrated that the peaks detected in the cell lysates did indeed display the same retention time as peaks demonstrated in cell lysates harvested at 1.5 and 9.0 h post-induction. Due to the delay in re-analysis, the protein isoforms appear to have undergone partial degradation evidenced by reduced peak heights and the presence of a broad low intensity peak which eluted between 23 and 26 min. Degradation of recombinant lysostaphin variants would result in a gradual decrease in the charge of the proteolytic fragments, leading to the detection of a broad peak representing an extremely heterogeneous mixture of increasingly acidic molecules.

To allow clearer comparison of charge variants and their relative abundance during culture, chromatograms produced following re-analysis of cell lysates harvested at 3.0, 4.5, 6.0 and 7.5 h post-induction were compared against other WCX separations performed on cell lysates harvested between 1.5 and 30.0 h post-induction (Figure 3.100). The compared chromatograms revealed a much clearer pattern of charge heterogeneity, which demonstrated a clear shift in the relative abundance of the two prominent acidic and basic protein isoforms. However due to the reduced peak height of peaks detected during re-analysis of cell lysates harvested at 3.0, 4.5, 6.0 and 7.5 h post-expression, visualisation of the detected protein isoforms was less clear.

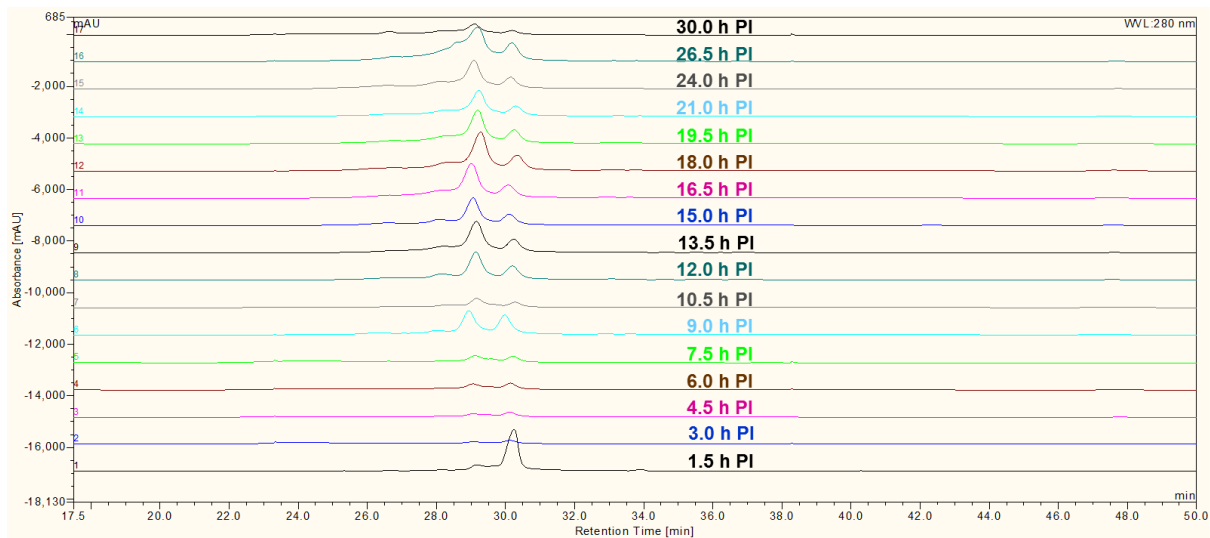


Figure 3.100: WCX analysis of *N*-terminally His-tagged recombinant lysostaphin (construct 1) over an expression time-course. Cell lysate was harvested from a 1L LB culture at regular intervals between 1.5 h and 30.0 h post-induction.

To counteract differences in peak height, the predominant basic peak at 30 min detected during separation of cell lysate harvested at 3.0 h post-induction was normalised against the same basic peak eluting at approximately 30 min in the rest of the WCX chromatograms. Normalisation resulted in better alignment of protein isoform peaks facilitating comparison of WCX separations. In addition the development of more acidic peaks could be monitored as their presence increased during the course of expression (Figure 3.101).

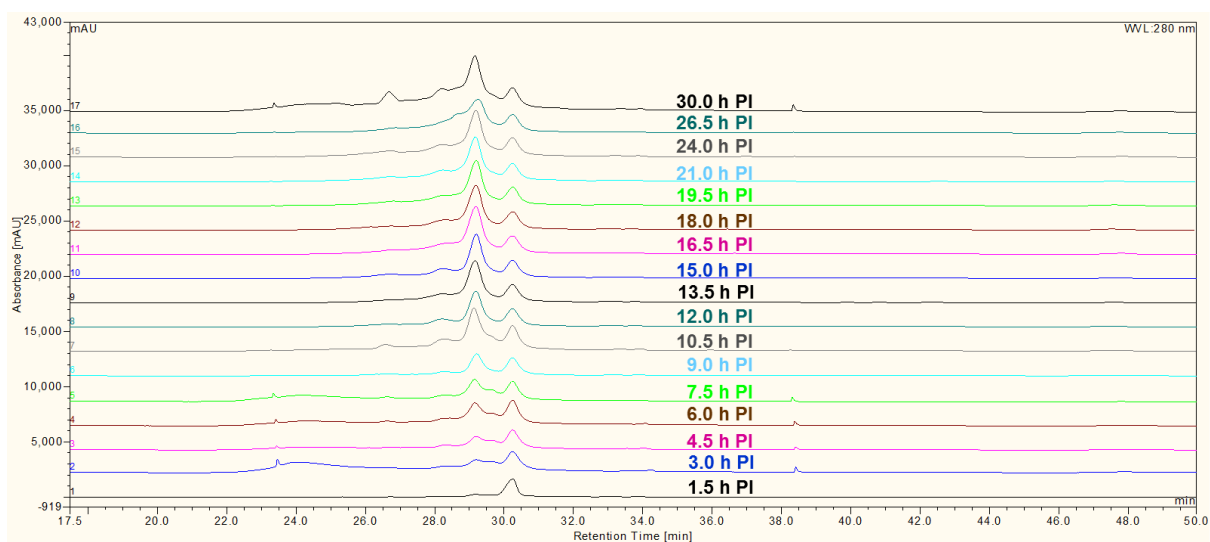


Figure 3.101: Comparison of normalised WCX chromatograms following separation of cell lysate containing *N*-terminally His-tagged recombinant lysostaphin (culture 1) during culture analysis. Cell lysate was harvested from a 1L LB culture at regular intervals between 1.5 h and 30.0 h post-induction. Separated peaks were normalised against the predominant basic peak at 30.25 min

To gain enhanced visualisation of charge variants expressed during the early stages of recombinant protein expression, selected WCX separations were compared in further detail (Figure 3.102). At 1.5 h post-induction, WCX separation of the harvested cell lysate revealed the presence of a single major protein isoform (tR = 30.25) and two minor acidic isoforms (tR = 28.15 and 29.18). This result suggested that the major peak reflected the presence of *N*-terminally His-tagged recombinant lysostaphin (construct 1) in the form that *E. coli* preferentially produces upon induction of protein expression. As the two minor peaks demonstrated much lower peak heights, the peaks reflected less abundant protein isoforms whose charge was attributable to synthesis by *E. coli* or post-translational processing or modification of one of the other abundant protein isoforms.

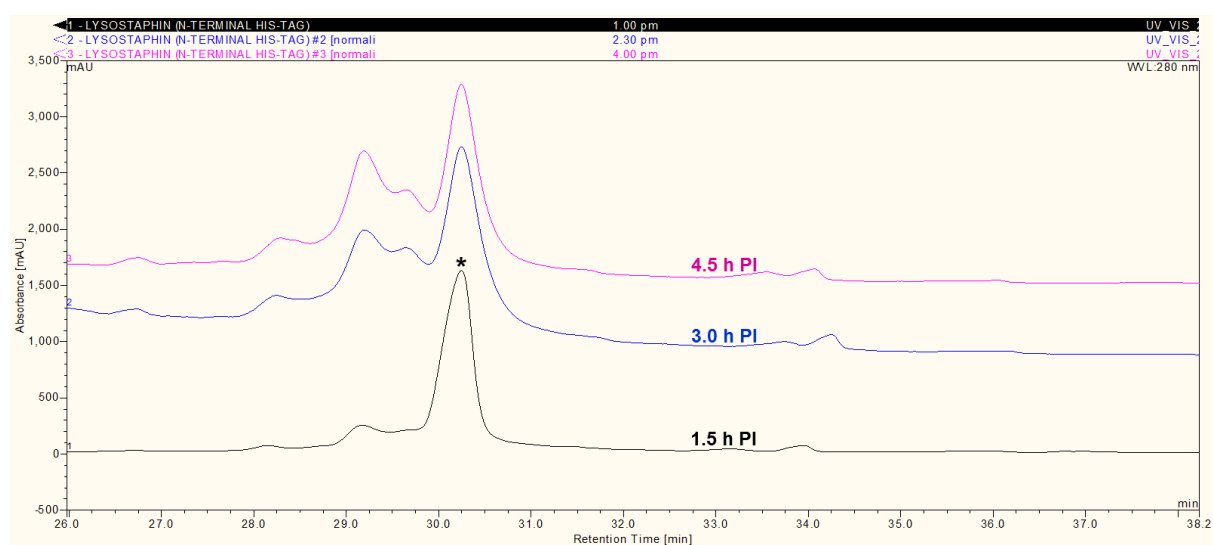


Figure 3.102: Comparison of WCX separations of cell lysates harvested between 1.5 and 4.5 h post-induction. Separated peaks were normalised against the predominant basic peak at 30.2 min, indicated by an asterisk. A non-normalised comparative chromatogram is presented in Appendix 7.256.

WCX separation of cell lysate harvested at 3.0 and 4.5 h post-induction revealed that the major protein isoform (tR = 30.25) at remained detectable, however minor acidic isoforms (tR = 28.15, 29.07 and 29.52) were represented by peaks of increasing height. The increased charge heterogeneity of the *N*-terminally His-tagged recombinant lysostaphin (construct 1) appeared to suggest increased production of alternative forms of the recombinant product, or more probable that the increased culture had allowed more time for the original basic protein isoform molecules to become steadily converted to more acidic variants through some form of post-translational processing.

As the culture progressed, the abundance of the more acidic isoforms rapidly increased, creating near equilibrium between the two prominent protein isoforms (Figure 3.103). However with time, the height of the peak representing the major acidic protein isoform (tR = 28.9-29.1) started to increase beyond the height of the peak representing the major basic protein isoform (tR = 30.1). The shift in the prevalence of the more acidic protein isoforms probably signified an accumulation of a recombinant lysostaphin variant which was being produced in a constitutive manner through post-translational processing. The peak height of the major basic peak also remained high, theoretically due to continued hyper-expression of recombinant lysostaphin by *E. coli* BL21(DE3).

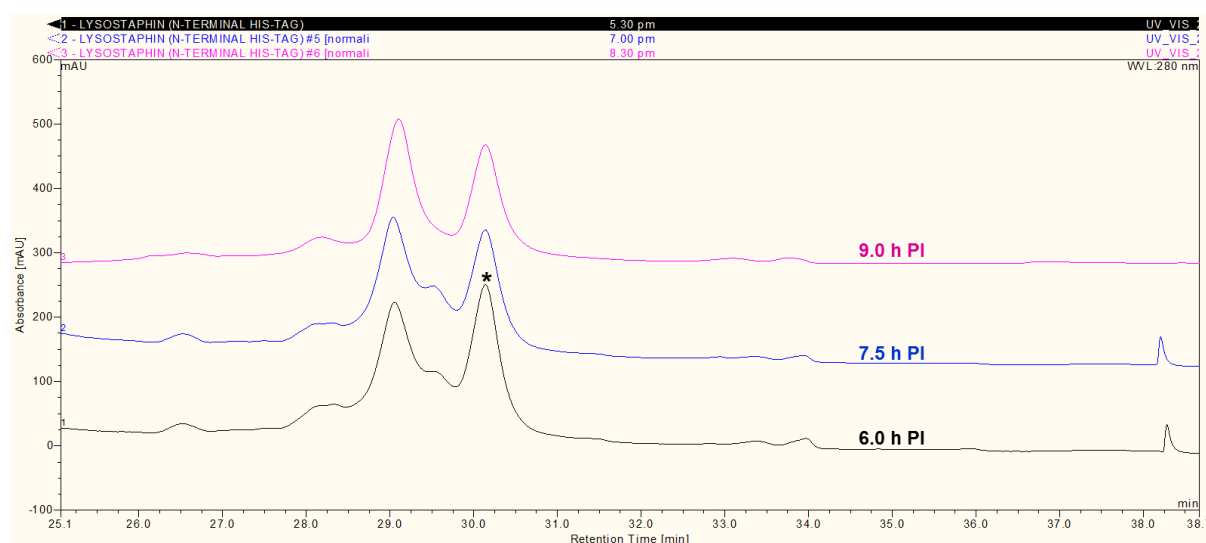


Figure 3.103: Comparison of WCX separations of cell lysates harvested between 6.0 and 9.0 h post-induction. Separated peaks were normalised against the predominant basic peak at 30.1 min, indicated by an asterisk. A non-normalised comparative chromatogram is presented in Appendix 7.257

The major acidic protein isoform remained the most prevalent form of *N*-terminally His-tagged recombinant lysostaphin (construct 1) present in cell lysates between 7.5 and 26.5 h post-induction. This extended prevalence is demonstrated in Figure 3.104, indicating that if the more basic peak represents a post-translationally processed form of *N*-terminally His-tagged recombinant lysostaphin, the modification or structural alteration tends to remain consistent over time. It was evident that other minor acidic variants were present, however prevalence of these variants remained low, suggesting that these forms of the protein were not readily produced through synthesis or post-translational processing.

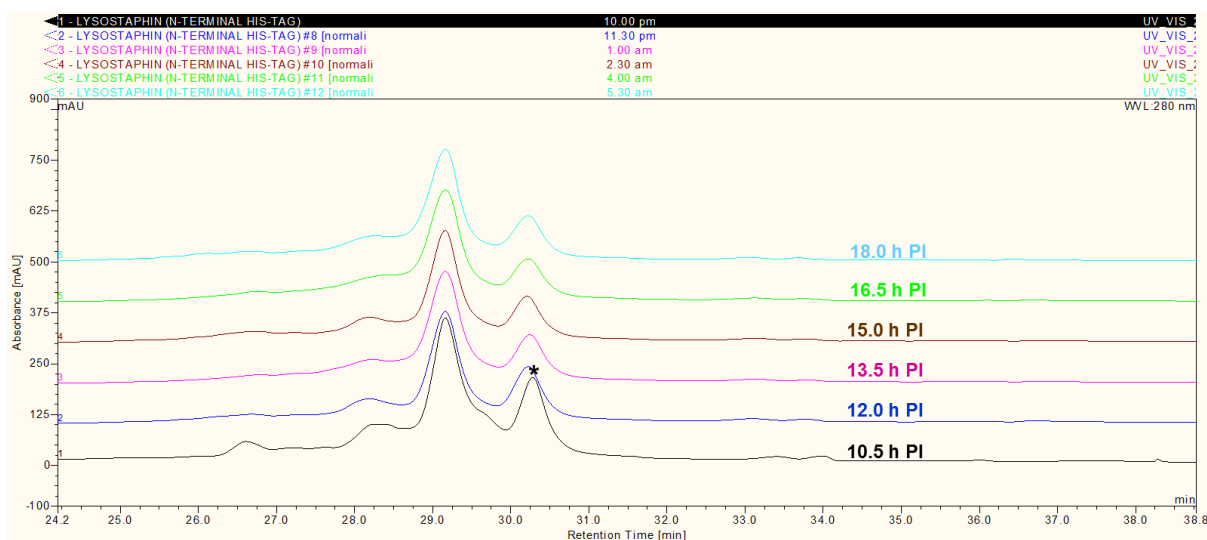


Figure 3.104: Comparison of WCX separations of cell lysates harvested between 10.5 and 18.0 h post-induction. Separated peaks were normalised against the predominant basic peak at 30.2 min, indicated by an asterisk. A non-normalised comparative chromatogram is presented in Appendix 7.258.

During the final stages of culture analysis, the major acidic protein isoform remained most abundant variant present within the analysed cell lysates (Figure 3.105). WCX separation of cell lysate harvested at 26.5 h post-induction revealed the resolution of a shoulder peak (tR = 28.53), possibly signifying the emergence of a new acidic protein isoform. However analysis of cell lysate harvested at 30.0 h post-induction suggested that the newly resolved acidic variant may have been rapidly converted to the more acidic protein isoform present (tR = 28.17). Furthermore, the peak height of even more acidic peak (tR = 26.62) increased fairly dramatically. This peak had previously been observed in low abundance in previous WCX separations and was thought to reflect the presence of a degradation product or a much more acidic protein isoform.

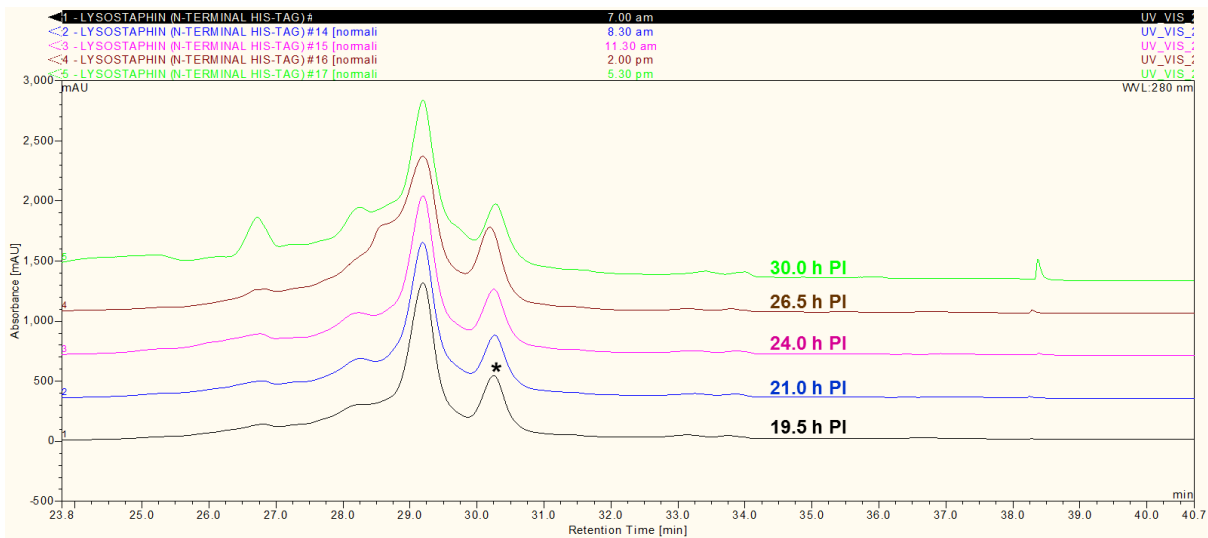


Figure 3.105: Comparison of WCX separations of cell lysates harvested between 19.5 and 30.0 h post-induction. Separated peaks were normalised against the predominant basic peak at 30.2 min. A non-normalised comparative chromatogram is presented in Appendix 7.259.

Further observation of Figure 3.104 indicates a slight issue with normalising peaks during comparison of WCX separation following culture analysis. By normalising peaks detected during WCX separation of cell lysate harvested at 30 h post-induction against the basic peak detected during a previous WCX separation, the apparent UV trace was increased proportionally to values which were in accordance with previous separations. Whilst this manipulation of the UV data allowed better comparison and visualisation of the resolved protein isoforms, it however lead to mis-representation of protein expression levels at 30.0 h post-induction. When non-normalised chromatograms were compared, it was evident that levels of recombinant lysostaphin isoforms within the cell lysate appear to have decreased dramatically, suggesting either poor sample loading during chromatography or that cellular level of recombinant lysostaphin had decreased due to reduced expression and the degradative action of cellular proteases (Figure 3.106).

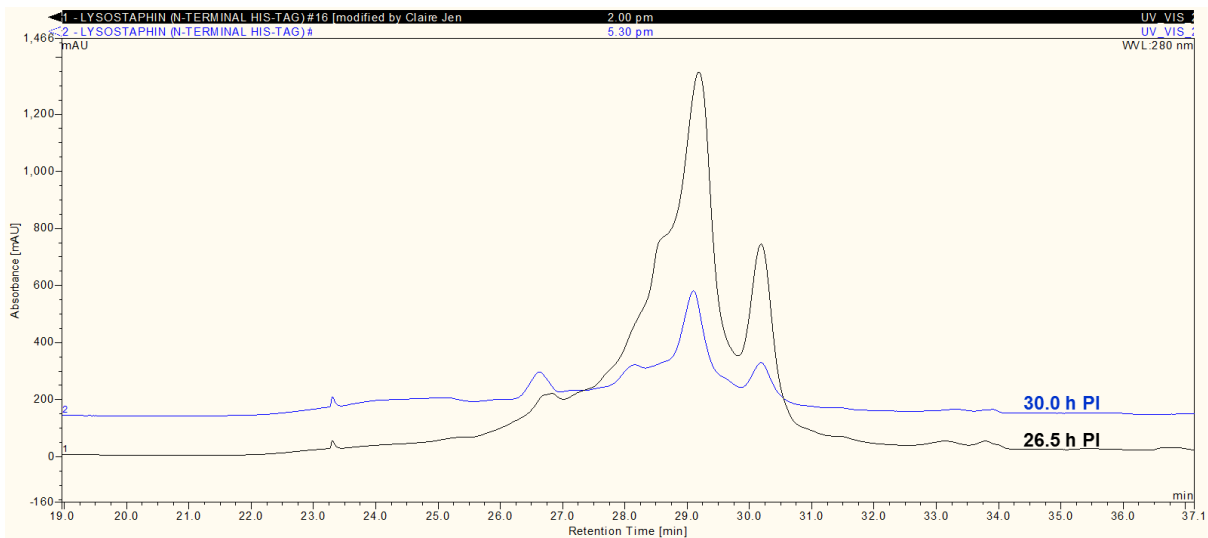


Figure 3.106: Comparison of WCX separations of cell lysates harvested at 26.5 and 30.0 h post-induction.

Following culture analysis, fractions eluted during WCX separation were analysed by SDS-PAGE to confirm that the detected peaks represented *N*-terminally His-tagged recombinant lysostaphin (construct 1). Figure 3.107 clearly indicates how a protein with a molecular weight of around 29 kDa was detected by SDS-PAGE after analysis of a fraction collected following elution of the major basic peak (tR = 30.25).

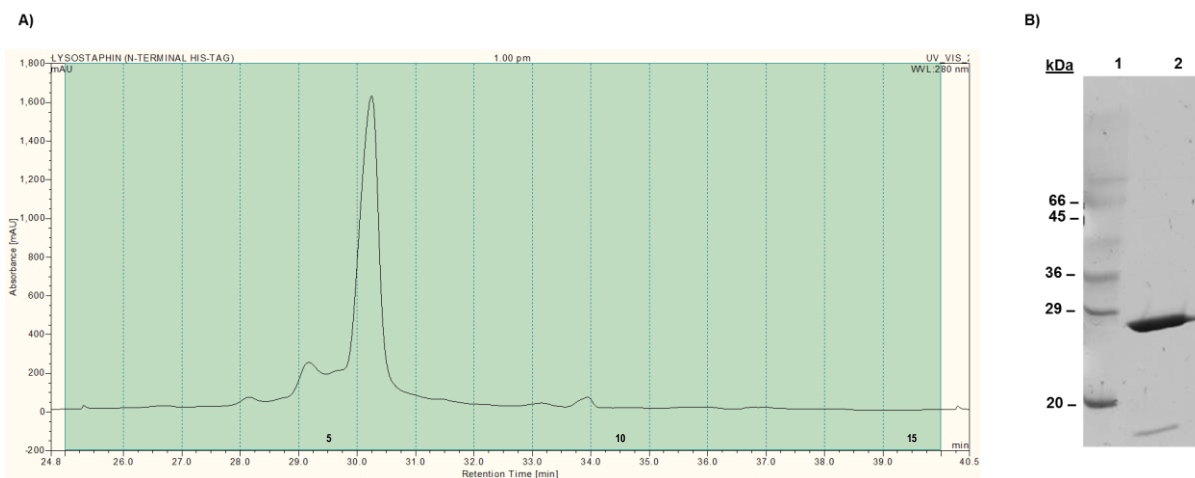


Figure 3.107: Analysis of cell lysate harvested at 1.5 h post-induction. A) WCX separation of *N*-terminally His-tagged recombinant lysostaphin (construct 1). B) SDS-PAGE analysis of WCX fractions. Lane 1: Sigma low molecular weight markers; Lane 2: Fraction 6.

SDS-PAGE of fractions eluted during other WCX separations proved to be more informative than initially anticipated due to the resolution of distinct molecular weight isoforms. As shown in Figure 3.108, Fraction 3, which was known to contain acidic protein isoforms appeared to contain two protein isoforms with distinct differences in molecular weight. The presence of

two mass distinct isoforms in Fraction 3 was likely to have been attributable to the elution of two peaks into the fraction. The other analysed fractions were only found to contain a single protein band, indicating that the fraction only contained recombinant lysostaphin molecules with very similar mass.

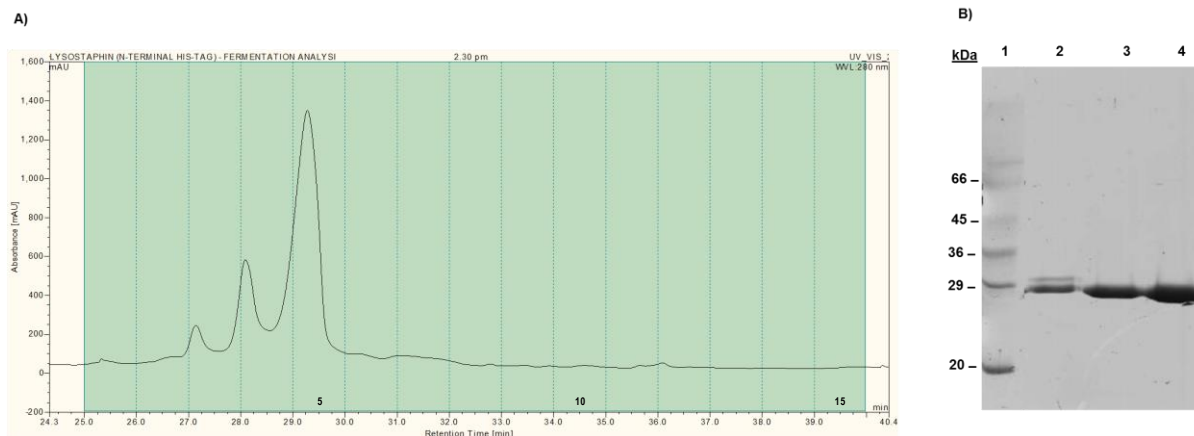


Figure 3.108: Analysis of cell lysate harvested at 3.0 h post-induction. A) WCX separation of *N*-terminally His-tagged recombinant lysostaphin (construct 1). B) SDS-PAGE analysis of WCX fractions. Lane 1: Sigma low molecular weight markers; Lane 2: Fraction 3; Lane 3: Fraction 4; Lane 4: Fraction 5.

SDS-PAGE analysis of fractions eluted during the WCX separation of cell lysates harvested at other time points also produced duplicate protein bands indicating that the molecular weight heterogeneity of expressed *N*-terminally His-tagged recombinant lysostaphin was more complex than anticipated. WCX separations and corresponding SDS-PAGE analyses are presented in Appendix 7.260-Appendix 7.273. SDS-PAGE analysis demonstrated that molecular weight heterogeneity was typically associated with the more acidic protein isoforms, however retention time variability and the elution of multiple peaks into single fractions did not provide a clear association between each peak and molecular weight heterogeneity.

3.5.3.12 Extended investigation of the influence of time upon the charge heterogeneity of recombinant lysostaphin

Despite issues with the presentation of the data, this study provided an excellent insight into the changing charge heterogeneity of *N*-terminally His-tagged recombinant lysostaphin (construct 1) over time. Therefore a second extended culture study was performed to act as secondary confirmation of these findings, but also to study the increasing heterogeneity of recombinant lysostaphin in the later stages of culture beyond 30 h post-induction. Extended culture analysis was important given that the expression of recombinant lysostaphin had been shown to occur for as long as 85.5 h after the induction of protein expression by SDS-

PAGE analysis (Appendix 7.251). Figure 3.109 demonstrates a slightly more complex pattern of charge heterogeneity, nevertheless, it is still possible to see that the formation of basic and acidic protein isoforms followed the same pattern as in the previous time-course culture experiment.

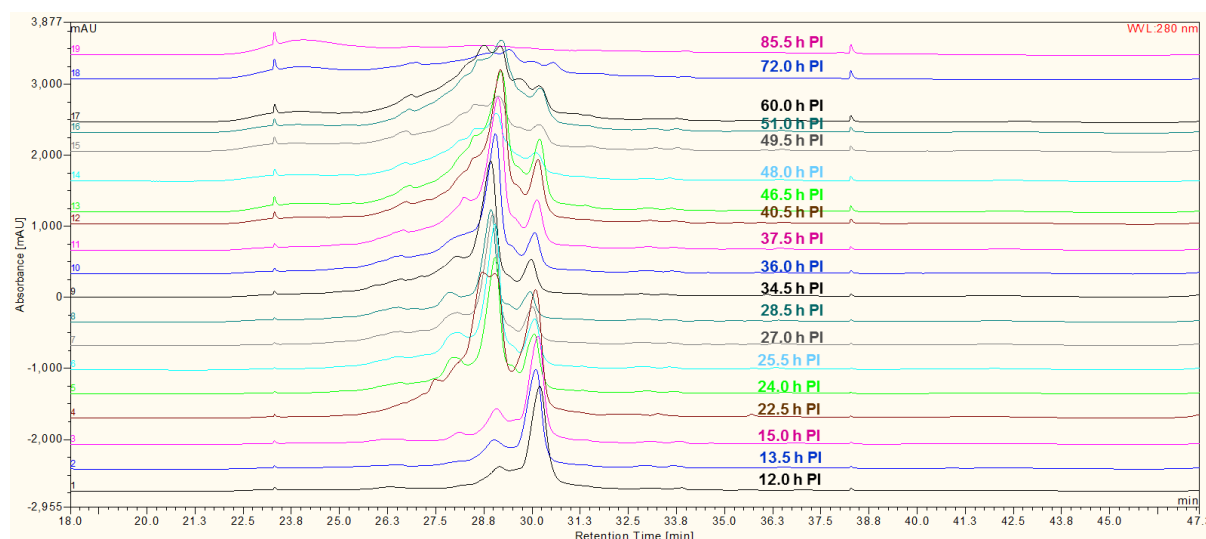


Figure 3.109: WCX analysis of *N*-terminally His-tagged recombinant lysostaphin (construct 1) over an extended culture time-course. Cell lysate was harvested from a 1L LB culture at regular intervals between 12.0 and 85.5 h post-induction.

As the study involved the analysis of cell lysate extracted at nineteen time points during culture, comparison of all of the WCX separations in a single chromatogram was less easy to interpret. Therefore Figure 3.110, Figure 3.111, and Figure 3.112 provide evidence of the distinct phases of protein isoform formation that were observed during the extended culture analysis. In Figure 3.110, it is evident that between 12.0 and 15.0 h post-induction, the major basic protein isoform (tR = 30.1-30.2) was abundantly expressed. This was unexpected as the previous study indicated that by 12.0 h post-induction, a more acidic protein isoform should have become the most prevalent isoform. The observed differences in protein isoform formation may have been attributable to differences in bacterial growth rate during culture, which was found to be much slower during UV spectrophotometric monitoring (Appendix 7.248, Appendix 7.249, Appendix 7.250 and Appendix 7.252).

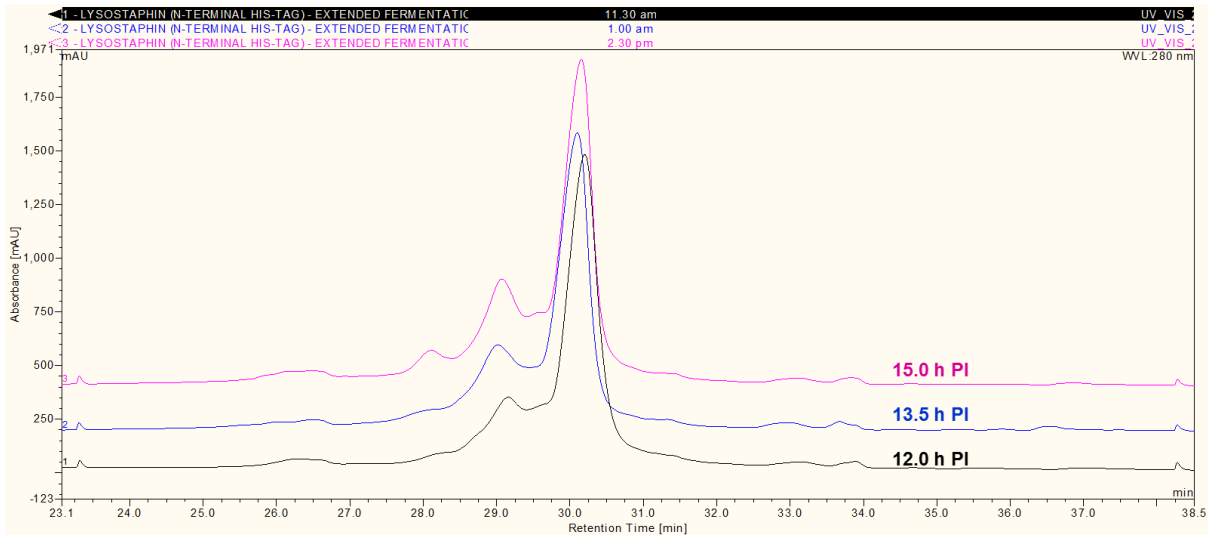


Figure 3.110: Comparison of WCX separations of cell lysates harvested between 12.0 and 15.0 h post-induction.

As the culture progressed, the relative abundance of acidic and basic protein isoforms shifted in the same manner as observed in the previous time-course experiment. WCX separation of cell lysate harvested at 22.5 h post-induction demonstrated the presence of duplex peak (tR = 28.72-29.04) (Figure 3.111). This was an unusual finding, which due to its unique appearance, may have reflected a temporary transition state that occurred during the conversion of a more basic protein isoform to a more acidic one. By 24.0 h post-induction, the acidic protein isoform had become the most prevalent protein isoform as reflected by a single peak (tR = 28.9-29.1), and continued to remain most prevalent through the remainder of culture analysis.

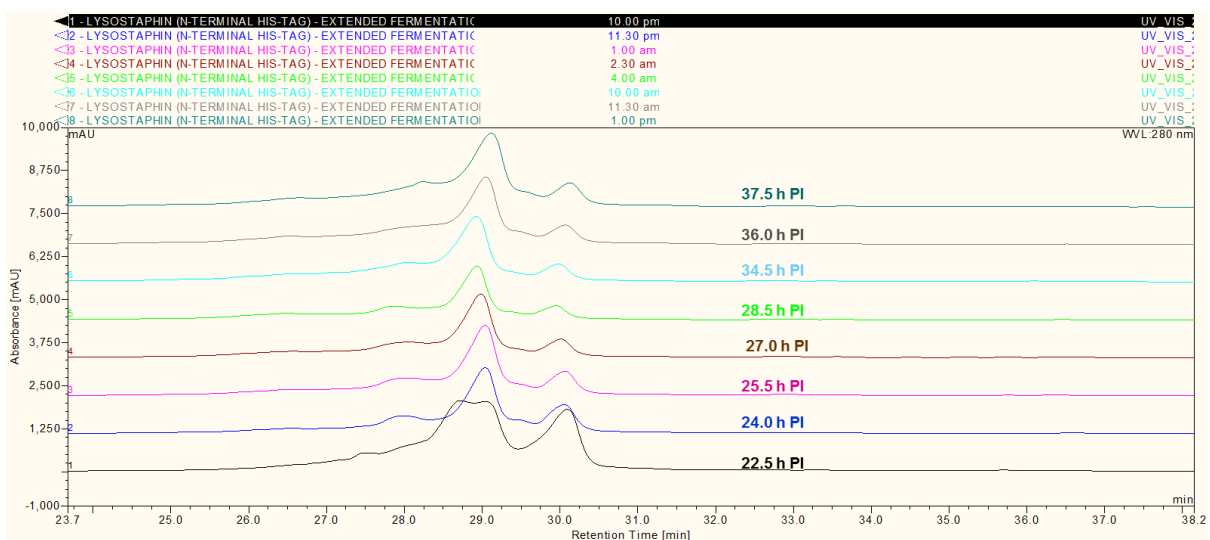


Figure 3.111: Comparison of WCX separations of cell lysates harvested between 22.5 and 37.5 h post-induction.

In the latter stages of culture analysis, it became apparent that charge heterogeneity of *N*-terminally His-tagged recombinant lysostaphin (construct 1) became more complex (Figure 3.112). At 40.5 and 46.5 h post-induction, the more acidic major protein isoform ($t_R = 28.9$ - 29.1) remained the most prevalent protein isoform. By 48.0 h post-induction the abundance of all of the protein isoforms appeared to have dramatically reduced suggesting that the expression of recombinant lysostaphin may have reduced. However the presence of multiple, poorly resolved peaks suggested that post-translational processing or modifications of *N*-terminally His-tagged recombinant lysostaphin (construct 1) continued to occur in the absence of heterologous expression. By 72.0 and 85.5 h, the harvested cell lysate appeared to contain a much reduced concentration of recombinant protein and therefore WCX separation could not clearly resolve defined protein isoforms. It was evident that recombinant protein expression must have ceased and that the action of cellular proteases had lead to the degradation of protein isoforms at this late stage of culture.

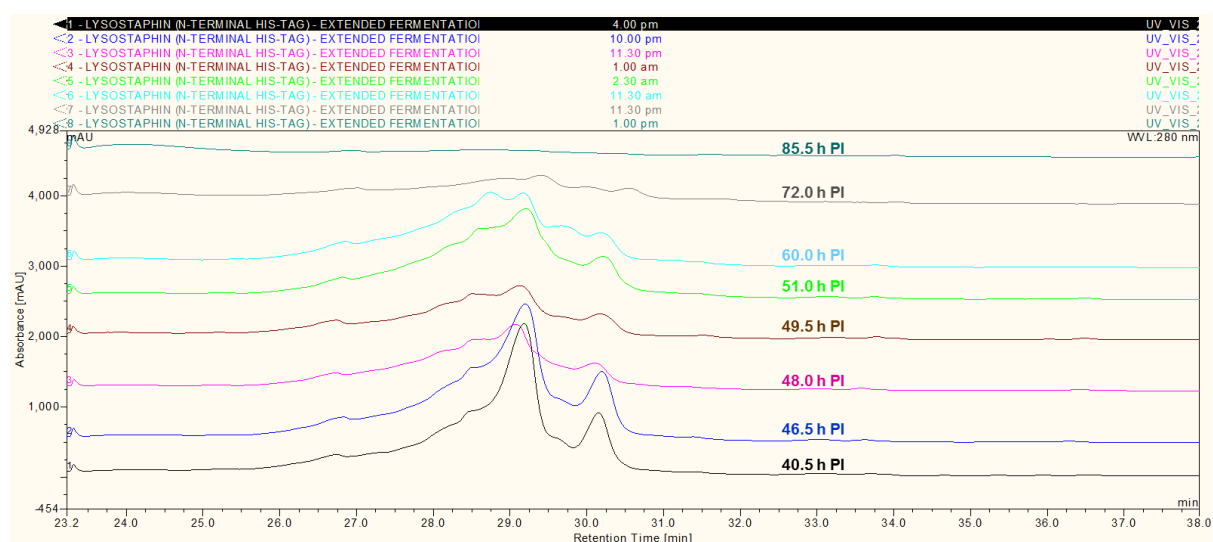


Figure 3.112: Comparison of WCX separations of cell lysates harvested between 40.5 and 85.5 h post-induction.

Following extended culture analysis, selected collected fractions were analysed by SDS-PAGE to confirm that the detected peaks reflected the presence of a protein with a molecular weight which corresponded to the weight of *N*-terminally His-tagged recombinant lysostaphin (construct 1). As shown in Figure 3.113, the detected peak was found to contain a protein with a molecular weight of less than 45 kDa. SDS-PAGE analysis of fractions eluted during other WCX separations performed during culture analysis confirmed that the detected protein had a molecular weight of approximately 29 kDa (Appendix 7.274-Appendix 7.290). Interestingly molecular weight heterogeneity was not evident following SDS-PAGE of fractions collected during this extended culture analysis experiment.

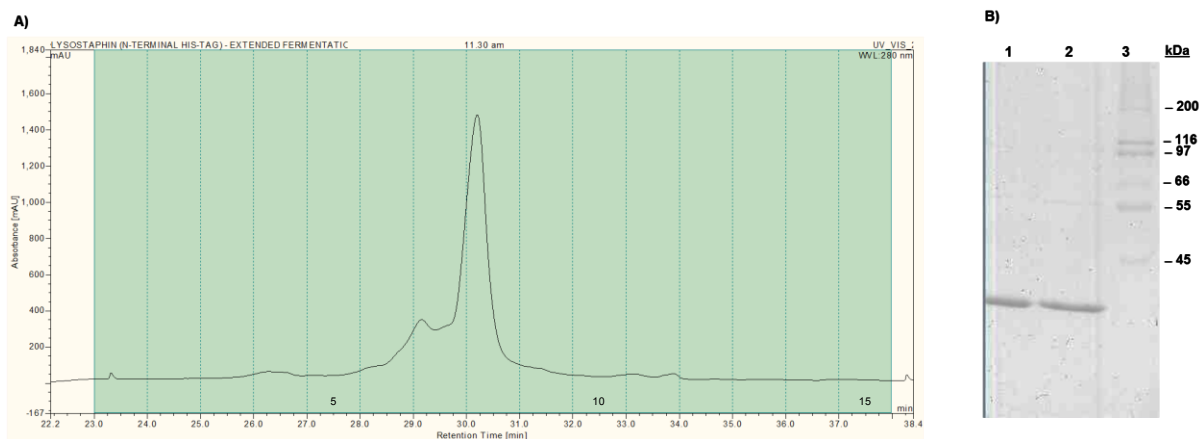


Figure 3.113: Analysis of cell lysate harvested at 12.0 h post-induction. A) WAX separation of *N*-terminally His-tagged recombinant lysostaphin (construct 1). B) SDS-PAGE analysis of WAX fractions. Lane 1: Fraction 7: Lane 2: Fraction 8: Lane 3: Sigma low molecular weight markers.

3.5.3.13 Rapid analysis of recombinant lysostaphin using a ProPac[®] MAb SCX (4 x 250 mm) column

As the ProPac[®] MAb column had previously been shown to provide excellent resolution of recombinant lysostaphin isoforms within a fairly short separation time (Section 3.3.2.9), the column was used to perform rapid culture analysis. Culture analysis was performed on cell lysates, which had previously been analysed using the ProPac[®] WAX (2 x 500 mm) column (Section 3.5.3.11). Comparison of SCX separations demonstrated that the ProPac[®] MAb SCX column could indeed be used to provide rapid culture analysis during recombinant protein expression (Figure 3.114).

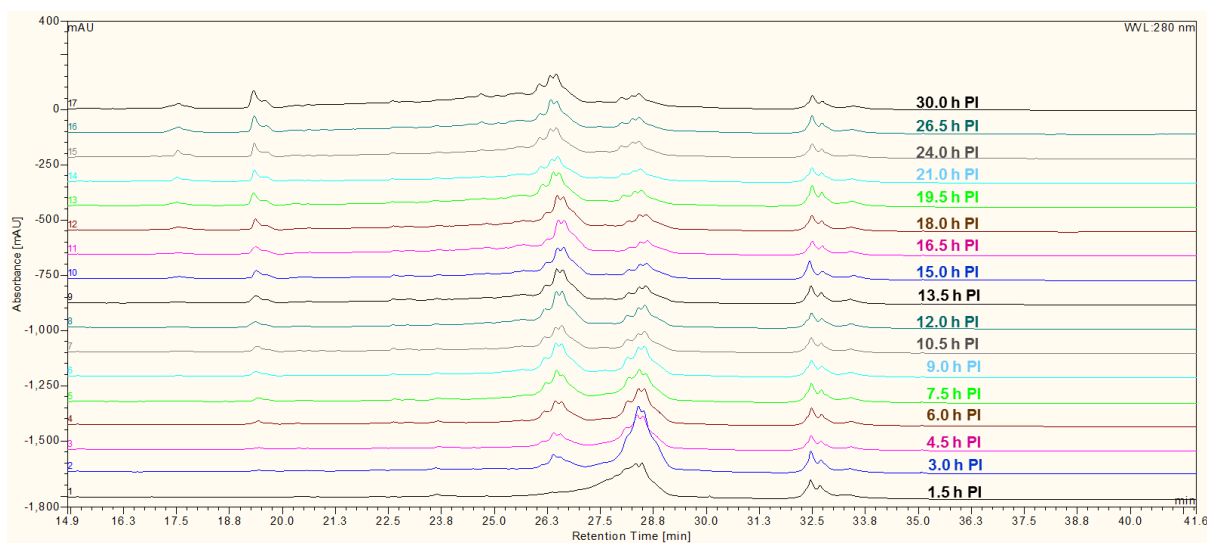


Figure 3.114: SCX analysis of *N*-terminally His-tagged recombinant lysostaphin (construct 1) over an expression time-course. Cell lysate was harvested from a 1L LB culture at regular intervals between 1.5 h and 30.0 h post-induction.

On initial assessment of the compared chromatograms, it appeared that SCX separations may not have provided very good resolution of protein isoforms, due to asymmetrical and erratic appearance of the eluted peaks. However further examination of the SCX separations revealed that the separations did in fact provide an indication of the greater micro-heterogeneity of *N*-terminally His-tagged recombinant lysostaphin (construct 1). Comparison of SCX chromatograms also suggested that the SCX separations were very reproducible, demonstrating consistent retention times and peak alignment between samples (Figure 3.115).

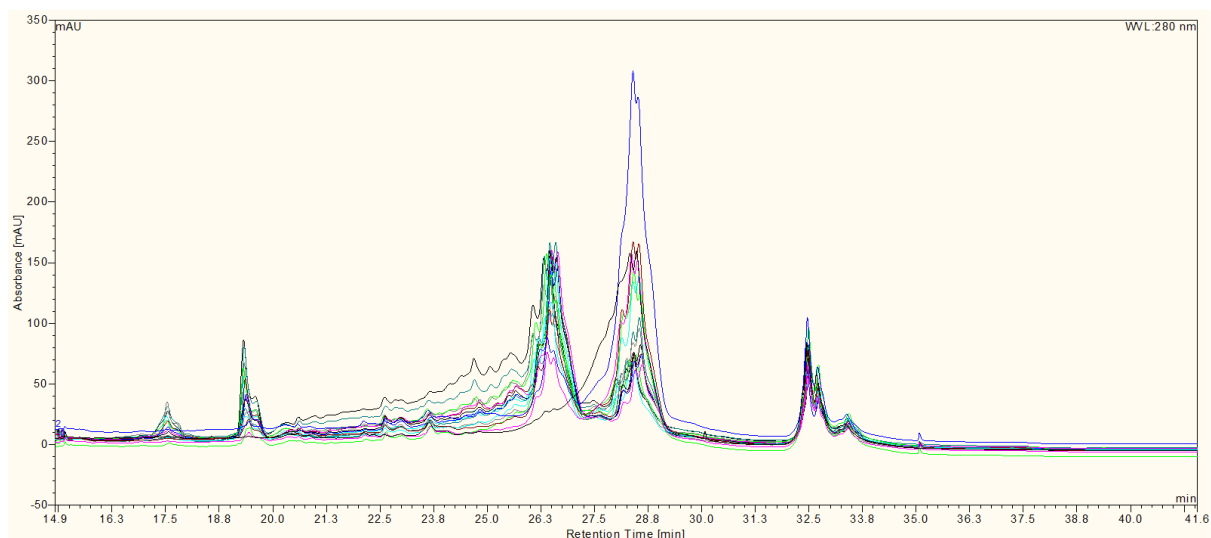


Figure 3.115: Reproducibility of SCX separations over a expression time-course. Cell lysate was harvested from a 1L LB culture at regular intervals between 1.5 h and 30.0 h post-induction. SCX separations showed a high degree of reproducibility.

During the early stages of culture analysis, SCX analysis demonstrated the same pattern of protein isoform formation that was detected by WCX analysis using the ProPac[®] WCX (2 x 500 mm) (Figure 3.116). Separation of cell lysate harvested at 1.5 h post-induction resulted in the detection of a major peak (tR= 28.48), which harboured a few minor shoulder peaks within the peak area. Between 3.0 and 6.0 h post-induction, analysed cell lysate was found to contain additional acidic protein isoforms which steadily increased in abundance over time.

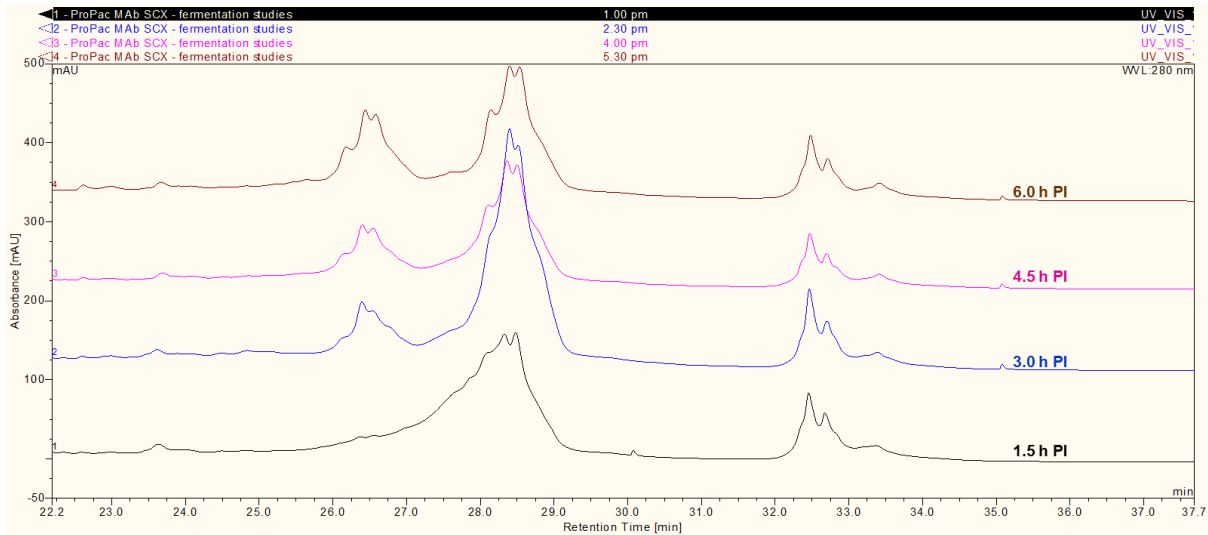


Figure 3.116: Comparison of SCX separations of cell lysates harvested between 1.5 and 6.0 h post-induction.

SCX analysis of cell lysates harvested between 7.5 and 18.0 h post-induction, demonstrated that the observed charge heterogeneity of *N*-terminally His-tagged recombinant lysostaphin (construct 1) remained fairly constant, with only slight alterations in the micro-heterogeneity of each eluted peak, observed between samples (Figure 3.117). Comparison of separations achieved using the ProPac[®] MAb SCX (4 x 500 mm) and the ProPac[®] WCX (2 x 500 mm) indicated that both columns detected the presence of both major peaks, however the protein micro-heterogeneity within each peak was not readily resolved using the ProPac[®] WCX (2 x 500 mm) column.

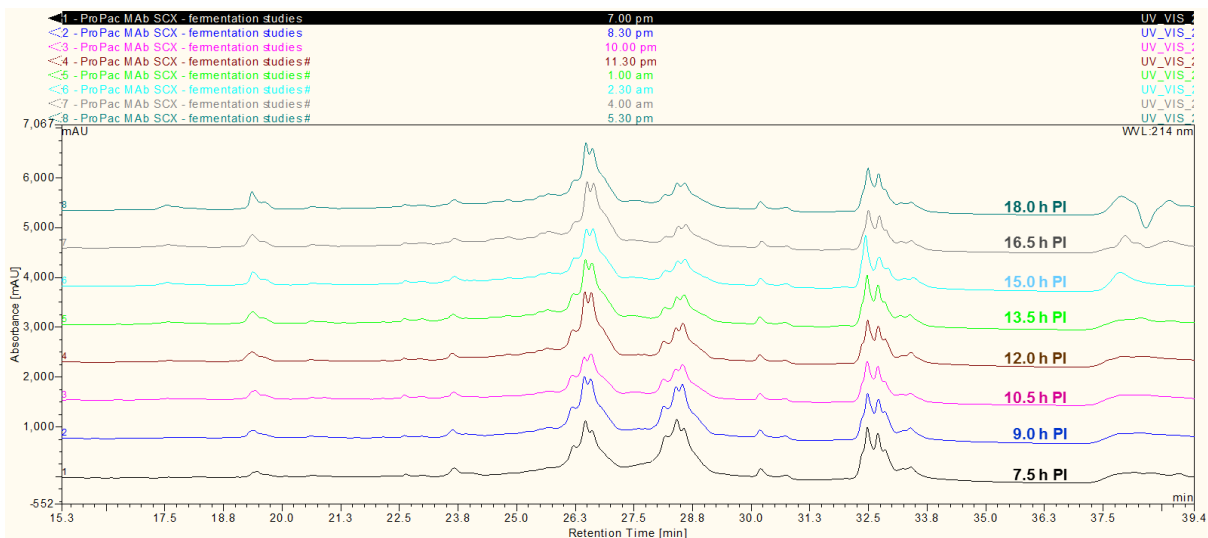


Figure 3.117: Comparison of SCX separations of cell lysates harvested between 7.5 and 18.0 h post-induction.

In the final stages of culture analysis, the emergence of minor acidic protein isoforms became more evident (Figure 3.118). Overall SCX analysis confirmed earlier results of culture analysis observed during WCX analysis, however provided greater resolution of protein isoforms present within eluted peaks. In effect SCX analysis revealed that the expression of recombinant lysostaphin leads to the production of a number of protein isoforms, which can be separated or resolved on the grounds of major or minor charge differences.

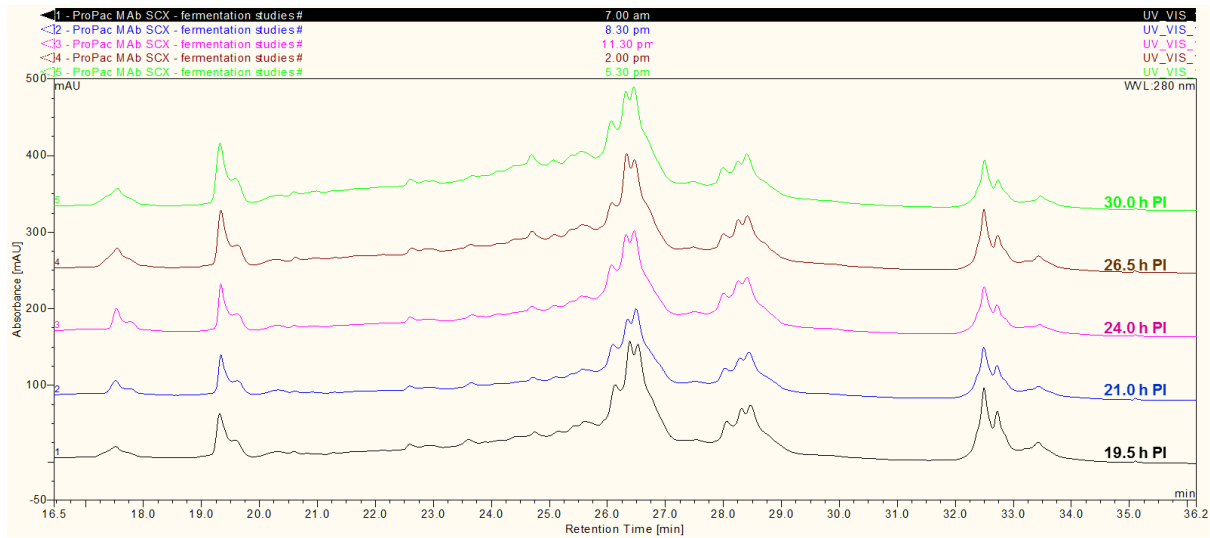


Figure 3.118: Comparison of SCX separations of cell lysates harvested between 19.5 and 30.0 h post-induction.

3.5.4 Discussion

Separation and isolation of protein variants often requires the use of several different analytical techniques. The use of multiple chromatographic stages increases overall processing time substantially and therefore prohibits real-time analysis of recombinant protein heterogeneity. Development of a rapid, reproducible chromatographic method, which could permit separation of protein isoforms and elucidate small changes in protein concentration or heterogeneity, was therefore extremely desirable. This work described the development and optimisation of a rapid and reproducible method which demonstrated a real-time insight into the transitioning charge heterogeneity of recombinant lysostaphin during its culture.

Initial culture analysis was performed using a ProPac[®] SCX (2 x 250 mm) column, which provided resolution of protein isoforms using a rapid separation method. Single-step isolation and purification of recombinant lysostaphin could be achieved readily following the application of freshly harvested cell lysate to the SCX column, due to the basicity of the recombinant protein. The ProPac[®] SCX (2 x 250 mm) column could be used to gain an insight into the charge heterogeneity of recombinant lysostaphin over time, as published (Appendix 7.291). In addition to monitoring charge heterogeneity over time, analysis was performed on cell lysates resulting from shake-flask cultures in which protein expression had been induced at various optical densities. Although culture analysis using the ProPac[®] SCX (2 x 250 mm) column did not really demonstrate any clear patterns of protein variant formation, the analysis did indicate that multiple basic and more acidic protein isoforms could be detected during culture.

Despite successful culture analysis, the resolution of protein isoforms achieved using the ProPac[®] SCX (2 x 250 mm) was inferior to that achieved using the ProPac[®] WCX (4 x 500 mm) column. As WCX separations performed using the ProPac[®] WCX (4 x 500 mm) column could not provide rapid analysis of recombinant lysostaphin, a ProPac[®] WCX (2 x 250 mm) column was acquired specifically for rapid culture analysis. As it was not possible to acquire a second ProPac[®] WCX (2 x 250 mm) column immediately, initial separations were performed using a single WCX column with the intention of optimisation rapid analysis conditions. Comparative separations suggested that the extraction of cell lysate from 25 ml of culture could provide sufficient material to achieve detectable peaks during WCX separation, without encountering volumetric depletion during culture analysis. WCX separations also demonstrated that recombinant lysostaphin derived from cell lysate which had been frozen or prepared from frozen cells did not demonstrate the same charge as

recombinant lysostaphin isolated from freshly prepared cell lysate, questioning the reliability of frozen samples.

Once a second ProPac[®] WCX (2 x 250 mm) had been acquired, a ProPac[®] WCX (2 x 500 mm) column was created and provided reproducible and high-resolution separation of *N*-terminally His-tagged recombinant lysostaphin variants. Chromatographic conditions were adjusted to accommodate the loading of cell lysate and to ensure that the chromatographic separation featured appropriate wash and equilibration phases to reduce the risk of carry-over and retention time shifting. Once chromatographic conditions had been optimised, a number of studies were performed to provide further insight into the influence of time and optical density at the point of induction upon the expression and charge heterogeneity of *N*-terminally His-tagged recombinant lysostaphin (construct 1). Culture analysis using the ProPac[®] WCX (2 x 500 mm) column demonstrated that powerful evaluation of the quality, abundance and diversity of the expressed recombinant lysostaphin variants, in a reproducible and high through-put manner.

Although enhanced resolution could be achieved using the ProPac[®] WCX (2 x 500 mm), the investigation of the influence of optical density upon the heterogeneity of *N*-terminally His-tagged recombinant lysostaphin did not yield a clear correlation between bacterial growth phase and presence of particular protein isoforms. It did however become apparent that the heterogeneity of recombinant lysostaphin increased with increased optical density at the point of induction. Greatest heterogeneity appeared to be associated with using standard expression conditions, such as following prolonged culture (> 4 h) and induction of protein expression at an optical density within the standard range ($OD_{600\text{ nm}} = 0.6-1.0$). This finding was particularly concerning given that many recombinant proteins could be produced using comparable conditions leading to similar degree of charge heterogeneity.

To minimise the variability of bacterial growth phase that was introduced at each culture inoculation, cultures were then directly inoculated from a glycerol stock, however this strategy was limited by poor protein expression and therefore could not be implemented in further experiments. Due to the inability to control optical density between batch cultures, subsequent rapid analysis experiments were performed on single batch cultures which were studied over a time-course. Time-course culture analysis yielded much more informative results, which suggested that the charge heterogeneity of *N*-terminally His-tagged recombinant lysostaphin isoforms transitioned over time leading to the formation of increasingly acidic protein isoforms.

Although some retention time shifting was observed during culture analysis, normalisation of results provided more appropriate comparison of eluted peaks. Whilst normalisation of results facilitated interpretation of detected peaks, it also led to some mis-representation of protein isoform abundance in the later stages of analysis. This finding emphasized that the culture analysis results should be interpreted carefully and appropriately to provide reliable data. When data normalisation was not applied to the results, it was possible to observe reductions in the concentration and abundance of protein isoforms, whilst also giving an indication of possible degradation products that may have occurred as the culture progressed.

Overall culture analysis performed over time, revealed a time-dependent pattern of charge heterogeneity in which certain acidic protein isoforms emerged with time. This pattern was observed again during extended culture analysis of a second culture, providing secondary confirmation of a consistent pattern of variant formation. Interestingly protein variant formation appeared to occur at a much slower rate in the second culture, possibly due the decreased bacterial growth rate which was observed during UV spectrophotometric monitoring of growth (Appendix 7.249 and Appendix 7.252). Further examination of protein variant formation is provided in Section 3.6.

SDS-PAGE analysis of protein eluted during culture analysis provided confirmation that a protein with a molecular weight of around 29 kDa was isolated during separation, indicating that *N*-terminally His-tagged recombinant lysostaphin (construct 1) had been specifically retained and purified. Interestingly SDS-PAGE analysis also indicated that some of the eluted peaks contained protein isoforms demonstrating molecular weight heterogeneity. Due to the co-elution of peaks into single fractions during collection, it was not possible to establish exactly which peaks correlated with the observed molecular weight heterogeneity, however it was found to be more readily associated with more acidic protein isoforms. This finding suggested that not all of the recombinant lysostaphin variants could be separated on the basis of charge, indicating the need for subsequent analysis by orthogonal chromatographic approaches and mass spectrometric analysis.

The greater extent of protein heterogeneity was elucidated further during culture analysis performed using the ProPac[®] MAb SCX (4 x 250 mm) column. Despite the ProPac[®] WCX (2 x 500 mm) column providing good resolution of protein isoforms during analysis of cell lysates extracted periodically over a 30 h period, the ProPac[®] MAb SCX (4 x 250 mm) column was found to provide even better resolution of recombinant lysostaphin variants. The ProPac[®] MAb SCX (4 x 250 mm) column provided evidence that the peaks detected

during separation using the ProPac® WCX (2 x 500 mm) column were composed of a number of protein variants, which explained why molecular weight heterogeneity could be observed during the SDS-PAGE analysis of apparently homogeneous peaks.

Overall these rapid analysis experiments demonstrated the importance of extensive culture analysis during recombinant protein expression. This work demonstrated that an insight into the charge heterogeneity of recombinant lysostaphin could be achieved using a variety of analytical cation exchange columns, with varying degrees of peak resolution. Analysis could be performed rapidly through optimisation of chromatographic conditions, sample preparation and careful selection of column stationary phase and diameter. As extracted cell lysate could not be preserved for delayed analysis, the rapid, immediate separation of freshly prepared cell lysate became increasingly important to provide reliable and consistent real-time analysis.

Although culture analysis was only performed upon cell lysate harbouring *N*-terminally His-tagged recombinant lysostaphin (construct 1), this reproducible method could have been applied to the other cytoplasmically expressed recombinant lysostaphin constructs (constructs 2 and 3) without any alteration of the optimised conditions. Furthermore, this optimised rapid analysis strategy could be used to analyse other basic recombinant proteins, such as recombinant oxidoreductase and recombinant NADPH-dependent 1-acyl dihydroxyacetone phosphate reductase (Ayr1p) which also possess the ability to bind to cation exchange resins..

This culture analysis strategy could also be applied to the analysis of recombinant lysostaphin which had been targeted to the periplasmic space (Constructs 4 and 5). As described in Appendix 7.78, periplasmic extraction of recombinant lysostaphin was achieved using a lengthy osmotic shock disruption method, which could be completed in approximately 1 h and therefore precluded rapid analysis of periplasmic recombinant proteins. However Dalmora *et al*, (1997) developed an analytical method for the direct analysis of human growth hormone following periplasmic extraction and RP-HPLC (Dalmora *et al.*, 1997). In this method, an optimised osmotic shock extraction strategy was employed, permitting periplasmic extraction within 30 min. It would therefore be possible to perform rapid analysis of periplasmically expressed recombinant lysostaphin using an optimised osmotic shock extraction method, which involved shorter centrifugation times.

3.6 Discussion

In Chapter 3, separation of recombinant lysostaphin preparations demonstrated that the recombinant protein was indeed heterogeneous. As a basic protein, recombinant lysostaphin was found to bind to cation exchange resins, which is unusual considering that most cellular proteins are anionic. Greater resolution and separation of protein isoforms could be achieved using pellicular rather than monolithic stationary phase resins, and therefore ProPac™ IEX were selected in preference over ProSwift™ IEX columns. The most superior resolution of protein isoforms was achieved using a ProPac® MAb SCX column, however as this column was only released in the later stages of this research, high-resolution, reproducible separation was mainly achieved using ProPac® WCX-10 columns.

Protein separation was achieved using several HPLC systems and whilst high quality separation of protein isoforms could be achieved using Dionex® DX500 HPLC system, greater flexibility and versatility during analysis could be achieved using Ultimate™ 3000 HPLC systems. The ability to use micro and nano flow rates facilitated rapid analysis using narrower bore columns and characterisation using LC/MS, as described in Section 4.4.2. Furthermore the ability to fractionate within the autosampler provided greater flexibility during fraction collection and provided the opportunity to perform 2D-LC analysis. 2D-LC analysis provided further confirmation that CXC was highly selective for recombinant lysostaphin, but also indicated that recombinant lysostaphin preparations feature protein isoforms which differ in hydrophobicity as well as charge.

Through column selection and optimisation of chromatographic conditions, it became apparent that separation of recombinant lysostaphin isoforms would be more complicated than expected. Sample preparation was of critical concern as a significant delay between expression and CXC analysis could increase the heterogeneity of the preparation or decrease the stability of the protein. The majority of the optimisation experiments were performed using purified recombinant lysostaphin which had been purified by a single purification technique. Multi-stage purification of recombinant lysostaphin prior to separation was found to be detrimental to peak resolution and therefore was avoided. The use of recombinant lysostaphin which had been derived from a combination of multiple batch cultures was also avoided as it became clear that charge heterogeneity could vary from batch-to-batch.

Lyophilisation of purified recombinant lysostaphin appeared to diminish protein solubility and it was found that sample precipitation interfered with the availability and ability of

recombinant lysostaphin to be separated by CXC analysis. However it was found that recombinant lysostaphin present within freshly harvested cell lysate could be directly and selectively purified and separated by analytical CXC, even in the presence of a milieu of contaminating cellular proteins. This was a critical finding as recombinant lysostaphin could now be analysed in its expressed state, whilst eliminating concerns over protein instability or the occurrence of chemical modifications, such as oxidation, deamidation or glycation, which could potentially occur during purification or storage (Jiang *et al.*, 2009, Mironova *et al.*, 2001, Mironova *et al.*, 2003, Pikal *et al.*, 1991, Lagerwerf *et al.*, 1996).

Frequent expression of recombinant lysostaphin within *E. coli* BL21(DE3) provided access to reasonable quantities of cell lysate and purified recombinant lysostaphin which facilitated optimisation of chromatographic separations. Optimisation of mobile phase conditions, through the implementation of extended elution gradients and pH 8.0 mobile phase buffers was found to enhance the resolution and separation of protein isoforms. In addition, optimisation of stationary phase conditions, through extension of column length or reduction of column internal diameter also helped to improve the resolution and efficiency of protein separation. Ultimately the selection of column dimensions was determined by the amount of protein available and the speed at which separation needed to be achieved.

Separation of protein isoforms present within purified recombinant lysostaphin or cell lysate derived from large shake-flask cultures, was readily achieved using the ProPac[®] WCX-10 (4 x 500 mm) column. Separations performed using this column provided evidence that greater charge heterogeneity was associated with higher incubation temperatures or induction of protein expression at higher optical densities. Furthermore the extent of charge heterogeneity could be controlled by manipulation of expression and harvest conditions. Separation of recombinant oxidoreductase and recombinant NADPH-dependent 1-acyl dihydroxyacetone phosphate reductase (Ayr1p) demonstrated that charge heterogeneity was not restricted to recombinant lysostaphin, and suggested that a significant number of recombinant proteins expressed in *E. coli* may be subject to post-translational processing or modification. This critical finding therefore had wider ramifications for industrial and biopharmaceutical production of recombinant proteins in *E. coli*.

Differences in charge heterogeneity could be observed following multiple separations of recombinant lysostaphin and also appeared to be influenced by the choice of expression media. However conclusive arguments about the nature and origin of such charge heterogeneity could not be made given that chromatograms and peak elution profiles could not often be compared due to frequent adjustment of chromatographic conditions during

optimisation of separation. Furthermore it was not possible to express recombinant lysostaphin using *E. coli* growing at identical growth rates or cell densities, therefore different optical densities at the point of inoculation or induction may have contributed to charge heterogeneity. The heterogeneity of recombinant lysostaphin also varied according to the duration of culture propagation, which was not controlled during initial separation experiments.

The influence of time and optical density upon charge heterogeneity only became apparent through rapid analysis of protein isoforms present within cell lysate using the ProPac® WCX-10 (2 x 500 mm) column and ProPac® MAb SCX-10 (4 x 500 mm) columns. WCX analysis of charge heterogeneity of *N*-terminally His-tagged recombinant lysostaphin (construct 1) expressed within cultures induced at various optical densities did not reveal any clear association between bacterial growth and the presence of particular charge variants. Rapid analysis of recombinant lysostaphin harvested from a single culture monitored over time, did however reveal a time-dependent pattern of charge heterogeneity, in which particular acidic charge variants emerged over time. Extended culture analysis of a second culture demonstrated the same pattern of variant formation, which provided secondary confirmation of this phenomenon. Protein variant formation did however occur at a slower rate in the second culture, which may have been attributable to a slower bacterial growth rate, which had been observed during spectrophotometric monitoring of growth.

The finding that charge variants emerged in a particular manner during the expression of recombinant lysostaphin provided an explanatory mechanism for how acidic and basic charge variants were detected during previous CXC separations (Figure 3.120). The early detection of the most basic peak would suggest the expression of the protein in the “native” state that *E. coli* preferentially synthesised¹. The emergence of more acidic peaks may have reflected conversion of the more basic “native” protein to a more acidic variant through PTM or truncation of *N*- or *C*-terminal amino acids. This “conversion” theory was supported by the fact that abundance of the acidic variant was found to increase as the abundance of the basic variant decreased.

The results of culture analysis would also suggest that the conversion of the basic variant to the acidic variant occurred in a constitutive manner, as the abundance of the acidic variant

¹ The term “native” could only be used tentatively as it was not known whether the protein eluted within the basic peak corresponded with the expected mass or primary sequence of recombinant lysostaphin however.

appeared to consistently increase over time. More acidic variants emerged in the later stages of culture analysis, however the production of these variants did not appear to be as prolific and occurred at a time when the expression of *N*-terminally His-tagged recombinant lysostaphin appeared to have decreased. This finding would suggest that the most acidic peaks may have reflected acidic polypeptides generated through host cell proteolysis of the recombinant product.

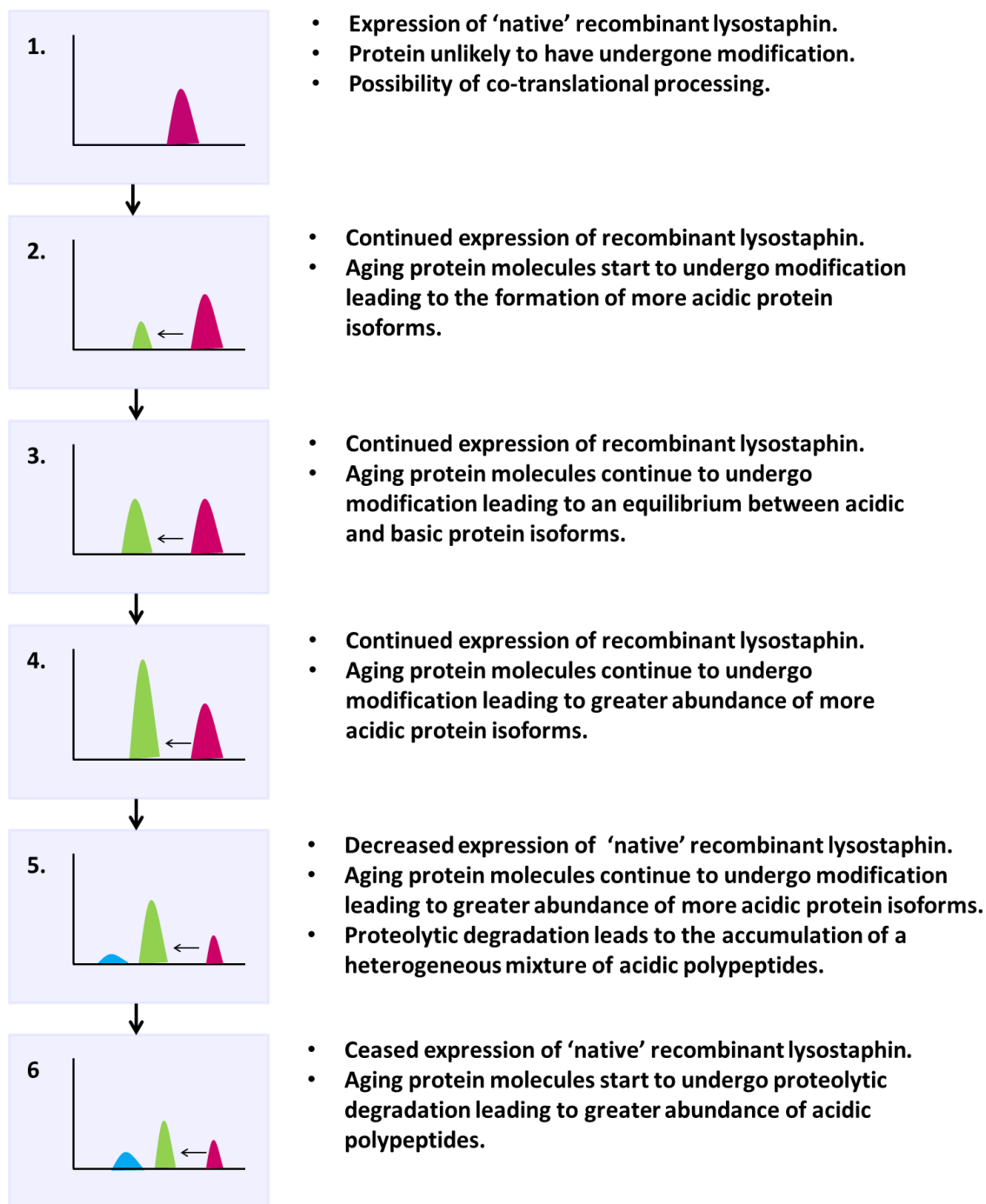


Figure 3.119: Development and detection of charge variants during the expression of N-terminally His-tagged recombinant lysostaphin (construct 1). Stages 1-6 represent the development of the charge variants observed during culture analysis

Whilst this proposed mechanism of charge variant formation seemed to give the most appropriate explanation of peaks detected during culture analysis, it was important to remember that this theory was fairly simplistic. For instance, culture analysis using the ProPac[®] MAb SCX analysis demonstrated that eluted peaks displayed much more micro-heterogeneity than culture analysis performed using the ProPac[®] WCX column had

suggested. Therefore this theory does not explain the formation of all charge variants produced during the expression of recombinant lysostaphin. This theory does however give a rational explanation as to why abundance of particular charge variants appeared to differ so dramatically during separation of recombinant lysostaphin preparations expressed and harvested at different times and optical densities.

Assuming that the time-dependent pattern of charge heterogeneity occurred whenever recombinant lysostaphin was expressed in *E. coli*, Figure 3.120 predicts how optical density at the point of induction would influence the detection of particular protein isoforms. Expression levels of recombinant lysostaphin will have been dependent on cell density at the point of induction of protein expression. The high optical density associated with log or stationary phase cells will have led to the greatest expression of recombinant lysostaphin within a short space of time, whilst less expression of recombinant lysostaphin would be produced in lag or death phase cultures. As time progressed, recombinant lysostaphin will have been expressed at levels that were determined by transitioning cell growth phase physiology. Over time the expressed product will have undergone conversion to a more acidic form, with the abundance of the acidic variant dependent on initial expression levels. If cell lysate was harvested and analysed after a short period of expression, separation chromatograms would only demonstrate high abundance of acidic variants in cultures which had been induced at a high optical density.

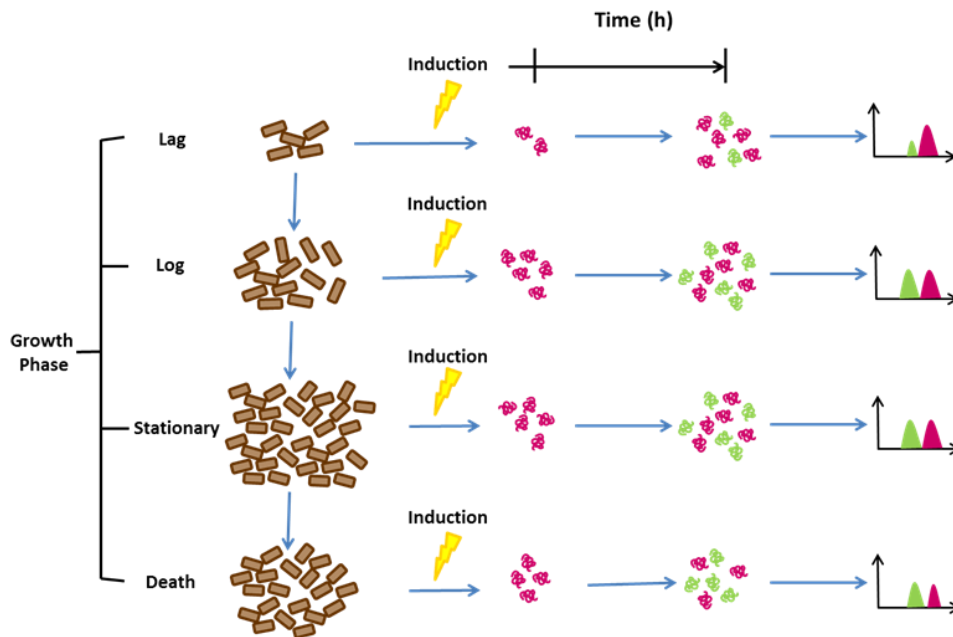


Figure 3.120: Charge variant formation following induction of recombinant lysostaphin expression at different growth phases and short expression duration. “Native” basic recombinant lysostaphin variants are denoted in pink, whilst converted acidic variants are denoted in green.

If recombinant lysostaphin was harvested after moderate expression duration, lag or log phase cultures will have become log and stationary phase cultures, therefore enhancing the expression of “native” basic recombinant lysostaphin variants. Whilst stationary and death phase cultures will have started to produce less of the basic recombinant lysostaphin variant. Increased production of recombinant lysostaphin would have ultimately lead to much greater abundance of the converted acidic variant within the culture at the point of harvest (Figure 3.121).

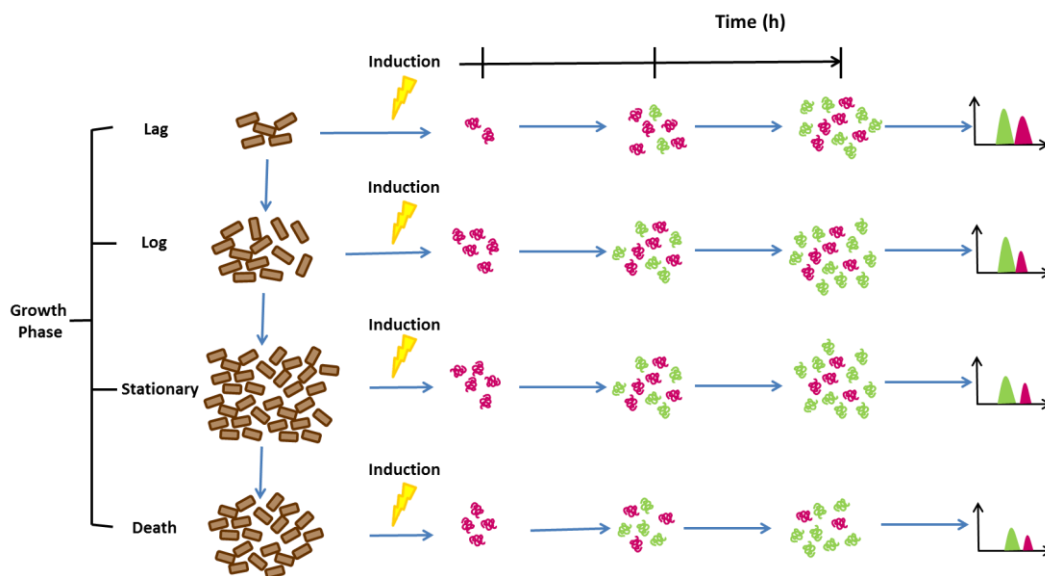


Figure 3.121: Charge variant formation following induction of recombinant lysostaphin expression at different growth phases and moderate expression duration. “Native” basic recombinant lysostaphin variants are denoted in pink, whilst converted acidic variants are denoted in green.

Analysis of recombinant lysostaphin harvested after a lengthy culture would correspond with lower levels of the “native” basic recombinant lysostaphin variant as its expression will have diminished in cultures induced at log, stationary or death phase. However the basic variant would have been more abundant in cultures which were induced at lag phase. A longer period of expression would have been associated with greater accumulation of the converted product, however the accumulation of these recombinant lysostaphin variants will have started to diminish in cultures in which expression was induced at stationary or death phase, due to host cell stress responses and proteolysis (Gill *et al.*, 2000).

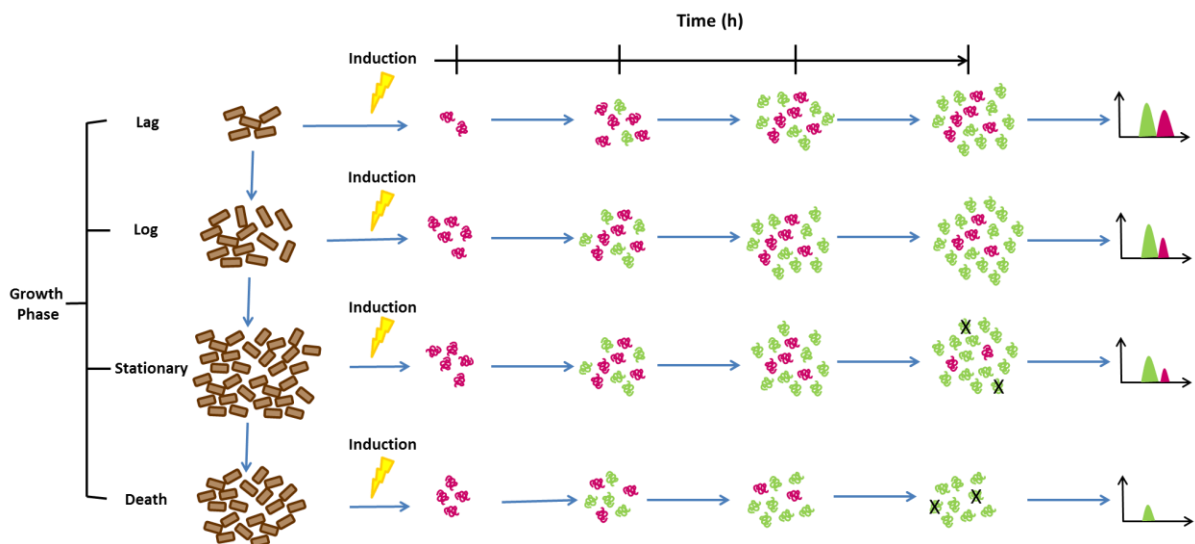


Figure 3.122: Charge variant formation following induction of recombinant lysostaphin expression at different growth phases and long expression duration. “Native” basic recombinant lysostaphin variants are denoted in pink, whilst converted acidic variants are denoted in green. Proteolysis of variants is denoted by X.

The pattern of charge variant formation observed during analysis could therefore explain the variable nature of charge heterogeneity observed during separation of *N*-terminally His-tagged recombinant lysostaphin (construct 1) harvested from cultures induced at various optical densities. Further analysis of cultures induced at different optical densities would however be desirable to provide further evidence supporting these concepts. In addition to optical density, elevated temperatures during expression would increase the rate at which product conversion occurred. Expression was performed at 20°C during culture analysis, therefore reduction of the culture temperature to 16°C would be likely to reduce the rate at which post-translational processing or modification occurred.

The differences in protein charge could be attributable to a number of causes, including protein aggregation, loss of *N*-terminal or *C*-terminal amino acids or PTM of charged residues. Examination of charged residues within the amino acid sequence of recombinant lysostaphin would suggest that there are multiple charged residues, which could be modified during expression (Figure 3.123).



Figure 3.123: Charged amino acid residues within the amino acid sequence of N-terminally His-tagged recombinant lysostaphin. Some residues are positively charged, including lysine (L) and arginine(R), whilst others are negatively charged, such as aspartate (D) and glutamate (E). The imidazole group of histidine (H) is less likely to possess a positive charge above pH 6.0 however.

Closer examination of amino acid residues at the *N*- and *C*-termini suggests that cleavage of the *C*-terminal lysine₁₆, would reduce the overall charge of the protein leading to detection of acidic charge variants. The amino acids at the *N*-terminus of the protein do not have charged side chain groups therefore cleavage of the first four residues would not influence the charge of the protein. As the imidazole group of histidine has a pKa value of 6.02, histidine residues in the *N*-terminal His-tag sequence would be unlikely to possess a positive charge at neutral pH, therefore loss of these histidine residues would not necessarily reduce the charge of the protein.

The net charge of recombinant lysostaphin may also be influenced by *N*-terminal processing during translation. Provided that the *N*-formyl group of *N*-formylmethionine has been removed by the action of PDF, the *N*-terminal methionine possesses a positively charged free α -amino group at its terminus. Depending on the action of metAPs, recombinant lysostaphin may or may not feature an *N*-terminal methionine residue; however a positive charge is likely to become exposed at the free α -amino group of the *N*-terminal residue. Retention of the *N*-formylmethionine or addition of an *N*-acetyl, *N*-methyl, *N*-gluconoyl or *N*-phosphogluconoyl groups would neutralise the positive charge at the *N*-terminal amino group or introduce a negative charge in the case of phosphogluconoylation (Charbaut *et al.*, 2002). Any of these *N*-terminal modifications could therefore explain loss of charge associated with acidic recombinant lysostaphin variants.

Side chain modification of any of the charge side chain residues could also lead to the formation of acidic recombinant protein variants through chemical or enzymatic reactions. As deamidation involves the conversion of neutral asparagine residues to negatively charged aspartate residues, this modification could produce acidic variants that would not be detectable by PAGE analysis due to the 0.98 Da mass increments that the modification

imposes. Glycation can also produce more acidic protein variants by neutralisation of positively charged lysine and arginine residues (Luthra and Balasubramanian, 1993). Meanwhile oxidation affects most amino acids, though preferentially occurs at aromatic amino acid residues, such as tryptophan, histidine, phenylalanine and tyrosine. Charged amino acids such as arginine and lysine can also become oxidated to produce carbonyl derivatives, which are known to occur during lipid peroxidation or glycation reactions (Requena *et al.*, 2001). Oxidation may therefore neutralise positive charges, producing acidic protein variants.

Enzyme-catalysed side chain modifications may have also contributed to the formation of acidic protein variants during culture. Acetylation of lysine residues is known to increase the net negative charge of a protein (Shaw *et al.*, 2010). When mono- and di-methyl groups are transferred to lysine residues these alkyl amines can become protonated. The addition of a trimethyl group to lysine is always positively charged however (Gooley and Packer, 1997). Therefore depending on protonation state, methylation can also produce acidic variants through neutralisation of ϵ -amino charges or can preserve a positive charge. Often the overall charge of an amino acid is typically only altered by around 0.5 pKa units, therefore methylation often has a negligible impact upon the isoelectric point of a protein, however may alter the hydrophobicity of the protein (Chiang *et al.*, 1996). Whilst phosphorylation of amino acids, such as serine and threonine is known to introduce negative phosphate groups to the protein, leading to the development of acidic variants

An additional source of charge variance could be attributable to the presence of apoprotein and holoprotein forms of *N*-terminally His-tagged recombinant lysostaphin (construct 1). It would seem likely that a zinc molecule would become integrated into the structure of recombinant lysostaphin following expression, however this is not necessarily guaranteed, particularly if PTMs or amino acid substitutions inhibit zinc binding (Hann *et al.*, 2006). The presence of zinc would augment the charge of recombinant lysostaphin, due to the molecule's 2^+ charge state and conversely the apoprotein would have a reduced charge. On these grounds it would seem unlikely that the removal of the bound zinc molecule would lead to the emergence of more acidic variants over time. However this does not rule out the possibility that the presence of an apoprotein form of recombinant lysostaphin could be detected as a low abundance acidic peak during CXC separation. Recombinant lysostaphin, as a zinc glycyI-endopeptidase was investigated further in Section 4.1.1.3.

Although protein heterogeneity can be detected using more traditional techniques, such as 2D-PAGE, these findings demonstrated that rapid analysis is essential to detect the time-

dependent development of charge heterogeneity within recombinant protein preparations expressed in *E. coli*. Rapid analysis provided an important insight into the transitioning charge variants expressed during the production of *N*-terminally His-tagged recombinant lysostaphin (construct 1). Further rapid analysis experiments would be desirable to establish whether the charge heterogeneity of *C*-terminally His-tagged recombinant lysostaphin (construct 3 and 4) and recombinant lysostaphin without His-tags (construct 2 and 5) exhibits the same pattern of charge variant formation. Furthermore rapid analysis of alternative cationic recombinant proteins, such as recombinant oxidoreductase and recombinant NADPH-dependent 1-acyl dihydroxyacetone phosphate reductase (Ayr1p) would assess whether the observed pattern of charge isoform formation occurs upon their culture as well.

Although separation of recombinant lysostaphin provided information about the development of charge variants, the exact structure of these variants could only be achieved through characterisation of the separated variants. Characterisation of the structure of recombinant lysostaphin variants was essential to provide further understanding of charge variant formation. The elucidation of protein mass and PTM detection could be achieved most sensitively using LC-MS analysis (Section 4.4). Characterisation of protein activity, retention behaviour and stability could also be achieved through further chromatographic analysis and activity assays, as described in Chapter 4.

4 Characterisation of Recombinant Lysostaphin

Separation of recombinant lysostaphin demonstrated that the protein preparations displayed charge heterogeneity. Whilst a pattern of charge variant development was identified following culture analysis, it was not clear how the charge variants occurred. Therefore a number of experiments were performed to investigate the function and biophysical characteristics of recombinant lysostaphin, with the hope that the nature and origins of post-translational processing or modification could be elucidated.

The functional activity of recombinant lysostaphin was assessed by performing turbidometric assays. Evidence of staphylolytic activity was essential to provide additional confirmation that the recombinant product displayed the activity associated with native lysostaphin. Turbidometric assays were also performed to establish whether separated charge variants possessed the desired staphylolytic activity, as the presence of fusion tags, covalent attachment of PTMs or C-terminal truncation may have disrupted enzyme activity.

The biophysical characteristics of recombinant lysostaphin were investigated further through the application of a number of chromatographic techniques including GF, IMAC and RP (as part of LC-MS analysis). GF was used to evaluate the stability of recombinant lysostaphin, to assess whether aggregated or mis-folded protein species may have contributed to the observed charged heterogeneity of recombinant lysostaphin during separation of protein isoforms. IMAC purification was performed to investigate the nickel binding affinity of recombinant lysostaphin, after *N*-terminally His-tagged recombinant lysostaphin (construct 1) demonstrated unusual retention behaviour whilst establishing the capacity of analytical IMAC columns (Section 2.5.3.11). The mass of recombinant lysostaphin isoforms was also assessed using high resolution LC-MS analysis. Intact mass measurements were determined to establish whether the mass of separated charge variants corresponded with the expected mass of recombinant lysostaphin (construct 1).

Aims:

- To measure the staphylolytic activity of recombinant lysostaphin preparations and separated recombinant lysostaphin charge variants.
- To assess the stability of recombinant lysostaphin using GF
- To evaluate the retention behaviour of recombinant lysostaphin during IMAC purification.
- To determine intact mass measurements for separated recombinant lysostaphin charge variants using UHR-LC-MS.

4.1 Activity of recombinant lysostaphin

4.1.1 Introduction

As described in Section 1.4, Lysostaphin is an extracellular glycyglycine endopeptidase which can lyse staphylococcal cells through specific hydrolysis of the pentaglycine cross-bridges present within peptidoglycan (Heath Farris *et al.*, 2003, Surovtsev *et al.*, 2007). Cell walls of both Gram-positive and negative bacteria feature peptidoglycan as a major structural component, as it provides rigidity and strength to protect the cell from osmotic lysis and acts as scaffold for cell wall assembly (Grundling and Schneewind, 2006). The catalytic action of lysostaphin therefore leads to cell rupture and loss of the bacterial cell wall envelope.

Peptidoglycan is a complex molecule, which has a sugar backbone consisting of *N*-acetylglucosamine (NAG) and *N*-acetyl-muramic acid (NAM) residues that are cross-linked with 1,4-glycosidic bonds (Figure 4.1) (Donovan *et al.*, 1996). The D-lactyl moiety of NAM residues forms an amide bond linkage with short polypeptides, which are composed of L- and D-amino acids (Grundling and Schneewind, 2006). As the C-terminus of the polypeptides is typically composed of two D-alanine residues, neighbouring wall peptides become cross-linked by transpeptidation, which strengthens the bacterial cell wall and generates a 3D network of peptidoglycan (Grundling and Schneewind, 2006). In Gram-negative bacteria and some Gram-positive bacteria, such as *S. aureus*, these cross-links involve the incorporation of glycine-rich linker sequences (Bochtler *et al.*, 2004).

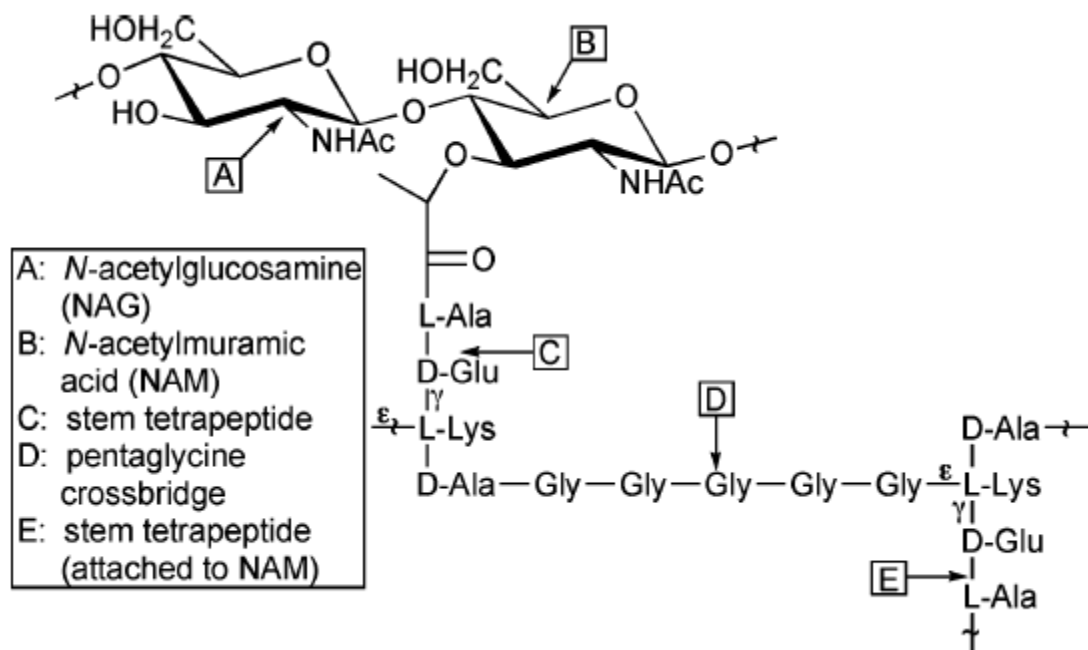


Figure 4.1: Structure of peptidoglycan in *S. aureus*. The diagram demonstrates the sugar backbone of peptidoglycan and side chain tetrapeptides. Adjacent wall peptides become cross-linked between the ϵ -amino group of L-Lys and the carboxyl group of D-Ala via a pentaglycine cross-linker. Figure taken from Warfield *et al* (2006).

Specific peptidoglycan hydrolases exist to cleave nearly every amide bond within the peptidoglycan structure (Bochtler *et al.*, 2004). These enzymes are typically categorised as glycosidases, amidases and endopeptidases (Donovan *et al.*, 1996). Lysostaphin is primarily regarded as a glycyl-glycine endopeptidase, but has also been reported to possess β -*N*-acetyl glucosaminidase and *N*-acetyl-muramyl-L-alanine amidase activities (Kumar, 2008, Wadström and Vesterberg, 1971). The substrate specificities of these functions are indicated in Figure 4.2. Lysostaphin is also reported to catalyse the transpeptidation of glycine peptides, therefore may participate in cell wall remodelling (Gargis *et al.*, 2010, Surovtsev *et al.*, 2007, Sloan *et al.*, 1977, Park *et al.*, 1995).

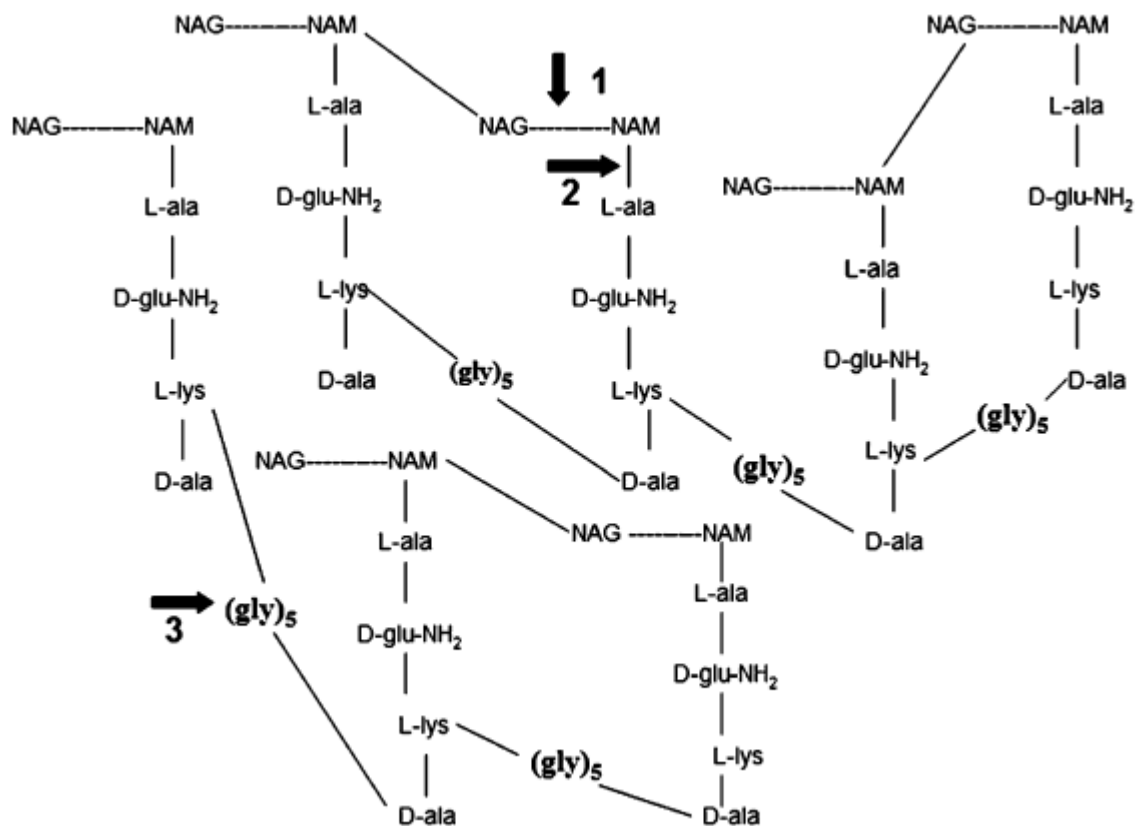


Figure 4.2: A diagram demonstrating the enzymatic activities of lysostaphin within the structure of peptidoglycan. Lysostaphin possesses multiple enzyme activities, acting as: 1) endo- β -N-acetyl glucosaminidase, 2) N-acetyl-muramyl-L-alanine amidase and 3) glycylglycine endopeptidase. The glycylglycine endopeptidase activity leads to solubilisation of the pentaglycine bridges. Figure from Kumar, (2008)

4.1.1.1 Staphylolytic activity of lysostaphin

Much research involving lysostaphin has focused primarily upon the glycyl-glycine endopeptidase activity of the protein, which is not functionally unique as other lysostaphin-type peptidases natively expressed in other Gram-positive bacteria can also specifically hydrolyse glycine-rich sequences. Due to their homology of function, glycyl-glycine endopeptidase orthologues, such as ALE-1 from *S. capitis* and LytM from *S. aureus* also share considerable sequence homology with lysostaphin. Structural and functional analysis of these lysostaphin-type peptidases and their catalytic domains has therefore enhanced understanding of the mechanisms by which lysostaphin targets and cleaves the cell walls of staphylococcal strains.

Mature lysostaphin consists of two domains – a C-terminal cell wall targeting domain (CWT) and the catalytic glycyl-glycine endopeptidase domain. The C-terminal CWT consists of 92 amino acids, which facilitate rapid pro-enzyme processing and selectively direct the

interaction between lysostaphin and the pentaglycine cross-links of peptidoglycan cell walls (Figure 4.3) (Climo *et al.*, 1998, DeHart *et al.*, 1995). The selectivity and substrate specificity of the CWT domain is critical for the efficacy of lysostaphin as it ensures that the protein can discriminate between host and target cells (Wu *et al.*, 2003). This function is essential as *S. staphylolyticus* and *S. aureus* have a very similar peptidoglycan structure, which suggests that the selectivity of the CWT is likely require a complex interaction between the lysostaphin and peptidoglycan.

```
MAATHEHSAQWLNNYKKGYGYGPYPLGINGGMHYGVDFFMNIGTPVKAISSGKIVEAGWSNYGGGNQIGLIEN  
DGVHRQWYMHLISKYNVKVGDYVKAGQIIGWSGSTGYSTAPHLHFQRMVNSFSNSTAQDPMFLKSAGYGKA  
GGTVTPPTNTGWKTNKYGTLYKSESASFPTNDIITRTTGPFRSMPQSGVLKAGQTIHYDEVMKQDGHVWVG  
YTGNSGQRIYLPVRTWNKSTNTLGVWGTIK
```

Figure 4.3: Amino acid sequence of mature lysostaphin indicating the sequence which encodes the cell wall targeting domain (green). The CWT domain was identified based on research described by Baba *et al.*, (1996).

As described in Section 2.3.1, *S. staphylolyticus* is rendered resistant to lysostaphin through co-expression of lysostaphin immunity factor (lif) encoded by an endopeptidase resistance gene (epr). Expression of lif results in the incorporation of serine residues into the third and fifth positions of each polyglycine cross-bridge (Kiri *et al.*, 2002). As lysostaphin is unable to hydrolyse glycyl-serine or seryl-glycine bonds, host cells become resistant to the lytic action of the protein (Warfield *et al.*, 2006). Whilst the incorporation of serine residues into cross bridges confers resistance to lysostaphin upon *S. staphylolyticus*, it is also likely that other cell wall structural components, such as teichoic acids and carbohydrates help the CWT domain discriminate between host and target cells (Grundling *et al.*, 2006, Baba and Schneewind, 1996).

Once directed to the staphylococcal cell wall, the catalytic glycyl-glycine endopeptidase domain specifically hydrolyses the pentaglycine cross-links of the peptidoglycan, which are typically composed of five glycine residues (Heinrich *et al.*, 1987). Specific lysis of proliferating or quiescent cells can occur, regardless of cellular metabolic state (Szweda *et al.*, 2001, Yang *et al.*, 2007). Analysis of staphylococcal surface proteins released during lysostaphin catalysis has suggested that hydrolytic cleavage occurs specifically between the third and fourth *N*-terminal residues of the pentaglycine cross bridge (Fedorov *et al.*, 2003). The catalytic endopeptidase domain is located at the *N*-terminus of the mature protein sequence, as indicated in Figure 4.4.

MAATHEHSAQWLNNYKKGYGYPYPLGINGGMHYGVDFFMNIGTPVKAISSGKIVEAGWSNYGGGNQIGLIE
NDGVHRQWYMHLSKYNVKVGDYVKAGQIIGWSGSTGYSTAPHLHFQRMVNSFSNSTAQDPMFPLKSAGYGK
AGGTVTPNTGWKTNKYGTLYKSESASFPTNDIITRTTGPFRRMPQSGVLKAGQTIHYDEVKQDGHVWV
GYTGNSGQRIYLPVRTWVKSTNTLGLVWGVIK

Figure 4.4: Amino acid sequence of mature lysostaphin indicating the sequence which encodes the catalytic glycyl-glycine endopeptidase domain (pink) and cell wall targeting domain (green). The CWT domain was identified based on research described by Baba *et al.*, (1996) and the catalytic glycyl-glycine endopeptidase domain was outlined by Warfield *et al.* (2006).

4.1.1.2 Elastolytic activity of lysostaphin

Lysostaphin has also been found to exhibit elastolytic activity, by binding to and degrading elastin, a major component of the mammalian extracellular matrix. When cross-linked, elastin is an extremely hydrophobic protein that is resistant to proteolysis and degradation. Glycine residues constitute one-third of the amino acids in the structure of elastin, which may explain the elastolytic activity of lysostaphin on the grounds of the enzyme's preference for glycine-rich sequences (Park *et al.*, 1995). Kinetic studies have indicated that elastolytic activity proceeds with relatively slow kinetics, is influenced by pH and can be inhibited by zinc chelators (Sugai, 1997, Park *et al.*, 1995).

Studies by Park *et al.* (1995) indicate that elastolytic and staphylolytic activities of the protein are dependent on separate distinct binding domains, however both activities are reliant on the presence of zinc as lysostaphin is a zinc metalloprotease (Park *et al.*, 1995). Park *et al.*, (1995) proposed that the Ala-Ala-Thr-His-Glu sequence of the mature lysostaphin sequence may be a catalytic domain for elastolysis (Figure 4.5). The identification of this sequence was based on sequence homology between lysostaphin, bacterial zinc metalloproteins and mammalian matrix metalloproteinases (MMPs) which also exhibited the ability to degrade elastin.

MAATHEHSAQWLNNYKKGYGYPYPLGINGGMHYGVDFMNIPTVKAISSGKIVEAGWS
NYGGGNQIGLIENDGVHRQWYMHLKSKYNVKGVDYVKAGQIIGWSGSTGYSTAPHLHFQRM
VNSFSNSTAQDPMFLKSAGYKAGGTVTPTNTGWKTNKYGTLYKSESASFTPNTDIITR
TTGPFRSMPQSGVLKAGQTIHYDEVMKQDGHVWVGYTGNSGQRIYLPVRTWNKSTNTLG
VLWGTIK

Figure 4.5: Amino acid sequence of mature lysostaphin indicating the Ala-Ala-Thr-His-Glu sequence, a proposed catalytic site for elastolytic activity (blue).

Further investigation of ionogenic residues within the sequence of lysostaphin indicated that the protein active site is likely to contain a glutamate and a histidine residue. These residues are believed to participate in general acid-base catalysis, whilst under the influence of environmental pH, regional hydrophobicity and electrostatic effects from proximal residues (Surovtsev *et al.*, 2007). Using crystal structure and sequence data from other lysostaphin-type enzymes, such as LytM, the active site glutamate residue was localised to the elastolytic catalytic site proposed by Park *et al.* (1995) as indicated in Figure 4.6. Furthermore Surovtsev *et al.* (2007) proposed that the identified active site could be involved in both elastolytic and staphylolytic catalysis (Surovtsev *et al.*, 2007).

MAATHEHSAQWLNNYKKGYGYPYPLGINGGMHYGVDFMNIPTVKAISSGKIVEAGWSNYGGGN
QIGLIENDGVHRQWYMHLKSKYNVKGVDYVKAGQIIGWSGSTGYSTAPHLHFQRMVNSFSNSTAQDPM
PFLKSAGYKAGGTVTPTNTGWKTNKYGTLYKSESASFTPNTDIITRTTGPFRSMPQSGVLKAGQTI
HYDEVMKQDGHVWVGYTGNSGQRIYLPVRTWNKSTNTLGVWGTIK

Figure 4.6: Amino acid sequence of mature lysostaphin indicating the proposed active site glutamate and histidine residues (orange). The residues occur within the putative elastolytic catalytic site domain (blue) and are thought to participate in general acid-base catalysis (orange).

4.1.1.3 Lysostaphin as a zinc metalloprotein

Lysostaphin is known to be a zinc metalloprotease, containing one zinc atom per protein molecule (Trayer and Buckley, 1979). Metalloproteins play important roles in biological systems and their function and stability is greatly influenced by the metal ion bound within the protein structure (Kaltashov *et al.*, 2006). The metal coordination sites within the protein structure can form catalytic, cocatalytic, structural or protein interface zinc binding sites (Auld, 2001). Although lysostaphin is widely regarded as a zinc-metalloprotease, the zinc-binding region of the protein has not been fully elucidated.

Following investigation into the elastolytic properties of lysostaphin, it was speculated that the zinc binding domain of lysostaphin could be conferred within or proximal to the Ala-Ala-

Thr-His-Glu sequence of the protein, as indicated in Figure 4.6 (Park *et al.*, 1995). This theory was further supported by the finding that exogenous addition of zinc could inhibit the elastolytic activity of lysostaphin. Although the exact mechanism of zinc inhibition is unclear, it was thought that the addition of exogenous zinc may have displaced the tightly bound endogenous zinc cation, detrimentally influencing the structure of the enzyme and interfering with catalytic activity. Furthermore staphylolytic and elastolytic activities are inhibited by zinc chelators indicating that the zinc-binding domain is of critical importance during catalytic activity (Park *et al.*, 1995).

However the sequence outlined by Park *et al.* (1995) appears to differ from those outlined as zinc-binding domains in lysostaphin-type enzymes. Lysostaphin was originally classified as an M37 family metalloprotease, but like LytM can also be classified under the M23 peptidase family (Bardelang *et al.*, 2009). Considering the close homology between the sequence of lysostaphin and lysostaphin-type peptidases such as LytM, it could be possible that lysostaphin harbours the same or a similar series of conserved metal-chelating residues. Crystal structures of lysostaphin-type peptidases have therefore provided greater insight into the functional and structural domains, which may be responsible for the zinc binding and catalytic activity of lysostaphin.

Lysostaphin-type peptidases and D-Ala-D-Ala metallopeptidases are known to possess similar active sites and a central zinc cation, which is tetra-coordinated by two histidine residues, an aspartate residue and asparagine residue or a water molecule. These conserved ligands occur in the order: histidine, aspartate, histidine and the zinc cation is coordinated via the N ϵ , the O δ and the N δ respectively (Bochtler *et al.*, 2004). Due to the sequence homology between lysostaphin and LytM, it is possible that these zinc binding domain ligands may be conserved within the structure of lysostaphin.

Should lysostaphin feature the same conserved zinc binding ligands as LytM, then it is likely that the zinc binding domain is critical for catalytic activity as postulated by Park *et al.* (1995). Histidine, aspartate and glutamate residues bind strongly with zinc and provide coordination sites which are available to water or substrate complexes, providing catalytic function (Vallee and Auld, 1990). These residues also control local protein folding, structure and conformation and therefore influence the mode of action and specificity of catalytic action. The presence of a single zinc molecule indicates that the zinc-binding domain is not cocatalytic, as cocatalytic sites are composed of several coordinated metal ions (Auld, 2001) Structural zinc atoms are coordinated with four cysteine residues to provide high stability. As

lysostaphin is cysteine-less protein, the bound zinc is not exclusively responsible for structural conformation of the protein (Vallee and Auld, 1990).

4.1.1.4 Activity of recombinant lysostaphin

As discussed in Section 2.3.1, lysostaphin is inactive or exhibits reduced activity when expressed as an unprocessed prepro- or pro-enzyme, therefore it was imperative that recombinant lysostaphin was expressed in a mature, active form. With the help of recombinant DNA technology, only the DNA sequence encoding mature lysostaphin was cloned and expressed, therefore it was extremely likely that recombinant lysostaphin would exhibit the expected staphylolytic activity. To confirm the presence of catalytic activity, an assay was developed which would allow fairly rapid identification of enzyme activity.

The staphylolytic activity of lysostaphin has traditionally been assessed using a turbidometric assay in which the lysis of staphylococcal cells is monitored spectrophotometrically over a fixed time course (Schindler and Schuhardt, 1964). Variation upon this spectrophotometric method has led to the development of alternative dye release based monitoring to provide greater sensitivity and reproducibility (Zhou *et al.*, 1988). In recent years, more advanced assays have been developed whereby lysostaphin interactions could be examined kinetically and thermodynamically (Surovtsev *et al.*, 2007). Furthermore, more sensitive assays in which hydrolysis of specific peptide substrates by lysostaphin which can be monitored by colorimetry or fluorescence spectrometry (Kline *et al.*, 1994, Warfield *et al.*, 2006).

For the purposes of this work, a simple turbidometric assay was selected to confirm activity of recombinant lysostaphin. The assay was developed based on methods described by Iversen & Grov, (1973) and Kusuma & Kokai-Kun (2005) (Iversen and Grov, 1973, Kusuma and Kokai-Kun, 2005). Once optimised the assay was used to investigate the activity of recombinant lysostaphin and achieve a number of research objectives.

Aims:

- To establish a turbidometric assay that could be used to assess the staphylolytic activity of recombinant lysostaphin.
- To assess whether recombinant lysostaphin constructs exhibited staphylolytic activity.
- To evaluate whether staphylolytic activity was influenced by expression media, expression location or sample processing and purification.

- To perform turbidometric assay of charge variants separated during WCX analysis.
- To perform bioinformatics analysis of lysostaphin amino acid sequences to establish the location of possible zinc binding residues.

4.1.2 Methods

4.1.2.1 Media

All media compositions are outlined in Appendix 7.292.

4.1.2.2 Buffers

All buffer compositions are outlined in Appendix 7.293.

4.1.2.3 Bacterial strains

Staphylococcus aureus subsp. *aureus* (NCIMB 12703) was grown for harvesting of cells for assay of lysostaphin activity. Cultured *S. aureus* was stored in 50% (v/v) glycerol at -80°C and as lenticules stored at -20°C.

4.1.2.4 Sample preparation

Sample preparation is described in Appendix 7.294.

4.1.2.5 Equipment

All equipment used to assess the activity of recombinant lysostaphin is outlined in Appendix 7.296.

4.1.2.6 Homology-based identification of consensus zinc binding residues in the amino acid sequence of recombinant lysostaphin

The amino acid sequence of glycyl-glycine endopeptidase LytM from *Staphylococcus aureus* (Q99WV0) was retrieved from the NCBI protein database (Appendix 7.323) and was subjected to ClustalW alignment against the mature sequence of recombinant lysostaphin without any fusion tags (Appendix 7.322). ClustalW alignment was developed by the European Bioinformatics Institute and was made available at <http://www.ebi.ac.uk/Tools/msa/clustalw2/>.

4.1.2.7 Lysostaphin assay

S. aureus was cultured and harvested prior to assay, as described in Appendix 7.298 and Appendix 7.299 respectively. The protein concentrations of purified recombinant lysostaphin

preparations were established using UV spectrophotometry (Appendix 7.23). Lysostaphin enzyme solutions of 2, 4, 6, 8 and 10 $\mu\text{g/ml}$ were prepared following dilution with assay buffer to give a total volume of 5 ml. A blank solution (0 $\mu\text{g/ml}$) was also prepared using 5 ml of assay buffer. The blank and test solutions were then incubated in a waterbath at 37°C for at least 5 min prior to performing the assay to allow temperature equilibration. A *S. aureus* cell suspension was then prepared by defrosting harvested *S. aureus* cells, before diluting with assay buffer to give an $\text{OD}_{620 \text{ nm}}$ of 1.3-1.5 when determined spectrophotometrically. The spectrometer was zeroed by reading the absorbance of a cuvette containing 1 ml of assay buffer at a wavelength of 620 nm. The assay was performed using a spectrophotometer coupled to a waterbath, to ensure that absorbance readings were taken at 37°C. Following equilibration, 1 ml of *S. aureus* suspension was added to each of the blank and test solutions at 1 min intervals and mixed by swirling. The absorbance at 620 nm at 0 min (T_0) was determined for each blank and test solution before incubating for 10 min at 37°C and determining the absorbance again after ten minutes (T_{10}).

4.1.2.8 Assay of recombinant lysostaphin

Assays were primarily performed to assess the activity of *N*-terminally His-tagged recombinant lysostaphin (construct 1) as this was the most commonly analysed form of the protein (Appendix 7.300). However assays were also performed to assess the influence of expression media (Appendix 7.301), expression location (Appendix 7.302), purification (Appendix 7.303) and lyophilisation (Appendix 7.304) upon the activity of recombinant lysostaphin. Charge variants were also assayed following routine WCX separation (Appendix 7.305) and following WCX separation during culture analysis (Appendix 7.306).

4.1.3 Results

4.1.3.1 Homology-based identification of consensus zinc binding residues in the amino acid sequence of recombinant lysostaphin

According to published literature, the zinc binding domain of lysostaphin had not been fully elucidated; however zinc binding residues had been identified from the crystal structure of a lysostaphin-type peptidase called LytM (Figure 4.7).

```
      10           20           30           40           50           60
MKKLTAAAIA TMGFATFTMA HQADAAETTN TQQAHTLMST QSQDVSYGTY YTIDSNGDYH

      70           80           90           100          110          120
HTPDGNWNQA MFDNKEYSYT FVDAQGHthy FYNCYPKNAN ANSGSQTYVN PATAGDNDYH

      130          140          150          160          170          180
TASQSQQHIN QYGYQSNVGP DASYYSHSNN NQAYNSHDGN GKVNYPNGTS NQNGGSASKA

      190          200          210          220          230          240
TASGHAKDAS WLTSRKQLQP YGQYHGGGAH YGVYAMPEN SPVYSLTDGT VVQAGWSNYG

      250          260          270          280          290          300
GGNQVTIKEA NSNNYQWYMH NNRLTVSAGD KVKAGDQIAY SGSTGNSTAP HVHFQRMSGG

      310
IGNQYAVDPT SYLQSR
```

Figure 4.7: Amino acid sequence of glycyl-glycine endopeptidase LytM from *Staphylococcus aureus* (Q99WV0). Consensus zinc binding residues were identified from the crystal structure of LytM by Firczuk *et al* (2005). Metal chelating residues are indicated in red at histidine₂₁₀, aspartate₂₁₄ and histidine₂₉₃.

As the glycyl-glycine endopeptidase LytM shares sequence and functional homology with lysostaphin a bioinformatics experiment was performed to establish whether the sequence of recombinant lysostaphin harboured the consensus zinc binding residues which had been identified in the amino acid sequence of LytM and other lysostaphin-type peptidases. The amino acid sequences of the glycyl-glycine endopeptidase LytM was obtained (Appendix 7.323) and subjected to ClustalW alignment (Figure 4.8) against the amino acid sequence constituting the putative mature enzyme (Appendix 7.322).

```

Lysostaphin  ---MAATHEHSAQWLNNYKKGYGYGPYPLGINGGMHYGVDFFMNIGTPVKAISSGKIVEA
LytM         SKATASGHAKDASWLTSRKQLQPYGQYHG---GGAHYGVDYAMPENSPVYSLDGTVVQA
              *: * :.*.*.. *:  ** *   ** *****: *  .:** :*:.*.:**

Lysostaphin  GWSNYGGGNQIGLIENDGVHRQWYMHLKYNVKVGDYVKAGQIIGWSGSTGYSTAPHLHF
LytM         GWSNYGGGNQVTIKEANSNNYQWYMHNNRLTVSAGDKVKAGDQIAYSGSTGNSTAPHVHF
              *****: : * :. : ***** .: .*..** *****: *.:***** *****:**

Lysostaphin  QRMVNSFSNSTAQDPMFPLKSAGYGKAGGTVTPTPTNGWKTNKYGTLYKSESASFTPNTD
LytM         QRMSGGIGNQYAVDPTSYLQSR-----
              *** ..:.*. * ** .:**

Lysostaphin  IITRTTGPFRRSMPQSGVLKAGQTIHYDEVKQDGHVWVGYTGNNSGQRIYLPVRTWNKSTN
LytM         -----

Lysostaphin  TLGVLWGTIK-
LytM         -----

```

Figure 4.8: Clustal W Alignment of lysostaphin and LytM (truncated) sequences. Consensus zinc binding residues are indicated in red. The alignment suggested that the sequences shared homology, with an alignment score of 411 being achieved during ClustalW analysis.

Without obtaining the crystal structure of recombinant lysostaphin or performing mass spectrometric analysis of the zinc binding residues, it was not possible to provide conclusive confirmation that these residues acted as metal chelating residues in recombinant lysostaphin, However ClustalW alignment provided an insight into the potential residues which may dictate zinc binding within the tertiary structure of recombinant lysostaphin.

4.1.3.2 Growth of *S. aureus* for turbidometric assay

Prior to turbidometric assay of staphylolytic activity, *S. aureus* cells were cultured and harvested. To achieve greater cell density, *S. aureus* cells were harvested at the end of the exponential growth phase which was found to occur at an OD_{600 nm} of 0.8 (Figure 4.9).

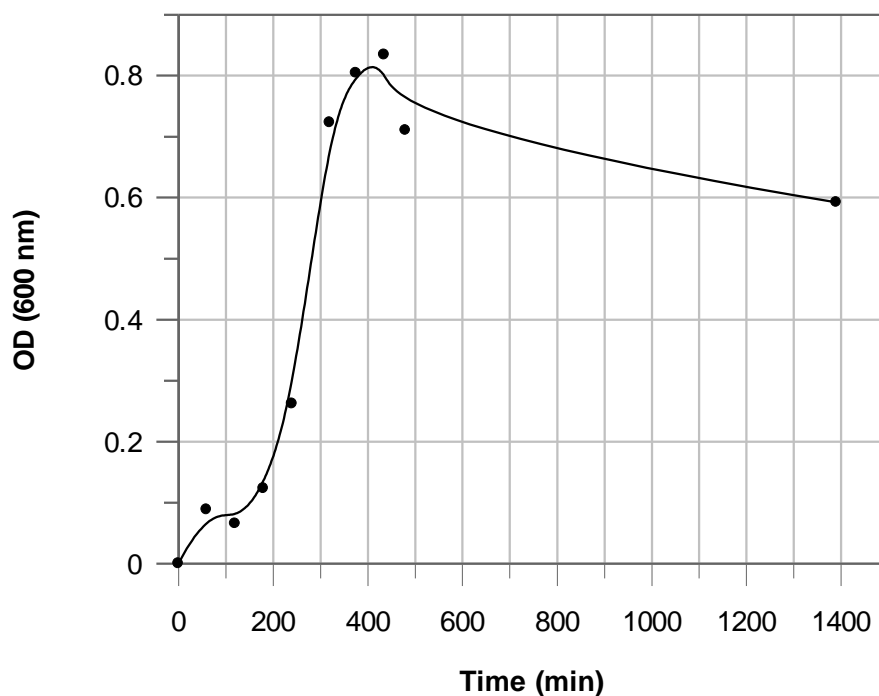


Figure 4.9: Growth of *Staphylococcus aureus* (NCIMB 12703) in liquid culture at 37°C. Bacterial growth in 1 L broth culture was monitored spectrophotometrically for over 23 h. Acquired spectrophotometric readings are tabulated in Appendix 7.324

4.1.3.3 Assay of staphylolytic activity of recombinant lysostaphin

Turbidometric assays were performed periodically to assess whether the recombinant lysostaphin preparations exhibited the expected staphylolytic activity. As recombinant lysostaphin preparations were primarily used to optimise or perform chromatographic separations, assays were not performed on every preparation that was produced. Nevertheless every recombinant lysostaphin preparation that was assayed at the correct protein concentrations, demonstrated a high level of staphylolytic activity. Assays were primarily performed on recombinant lysostaphin constructs which had undergone intensive chromatographic analysis, such as *N*-terminally His-tagged recombinant lysostaphin (construct 1) or to assess other factors, such as expression media, expression location or sample processing upon the activity of recombinant lysostaphin preparations.

4.1.3.4 Assay of *N*-terminally His-tagged recombinant lysostaphin (construct 1)

As *N*-terminally His-tagged recombinant lysostaphin (construct 1) was most commonly expressed and analysed during this research, several assays were performed on this form of recombinant lysostaphin. Repeated assay of *N*-terminally His-tagged recombinant lysostaphin revealed that the protein possessed staphylolytic activity in all preparations (Figure 4.10). Activity levels in some of the preparations (4, 15 and 17) did however appear to be slightly lower than that exhibited by preparation 6 and preparations used in other assay experiments. It was thought that the observed lower activity was due to slight differences in the state of staphylococcal cells harvested for the assay.

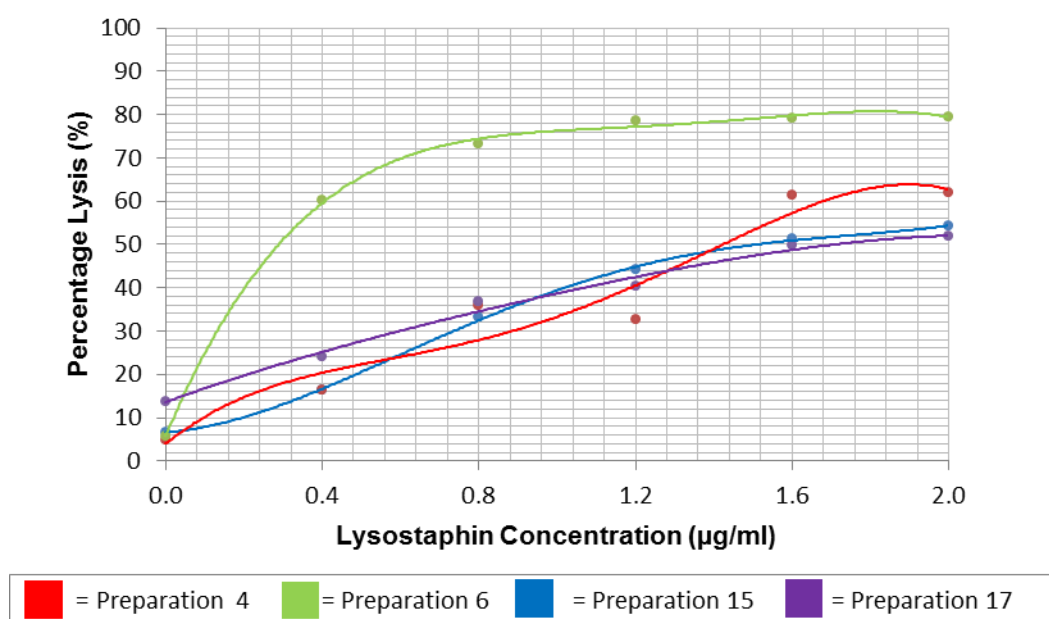


Figure 4.10: Percentage lysis of *S. aureus* following turbidometric assay of the staphylolytic activity of *N*-terminally His-tagged recombinant lysostaphin preparations (construct 1). Each recombinant lysostaphin preparation was expressed in *E. coli* BL21(DE3) cultured in AIM. UV spectrometric readings are tabulated in Appendix 7.325, Appendix 7.326, Appendix 7.327 and Appendix 7.328.

4.1.3.5 Influence of expression media upon the activity of recombinant lysostaphin

Assays were performed on *N*-terminally His-tagged recombinant lysostaphin preparations (construct 1) which had been derived from *E. coli* BL21(DE3) which had been cultured in LB or AIM. The choice of LB or AIM as expression media did not appear to have a significant influence upon the staphylolytic activity of the *N*-terminally His-tagged recombinant lysostaphin (Figure 4.11). Both experiments were performed using the same batch of *S. aureus* substrate cells, which was found to maintain consistency between results.

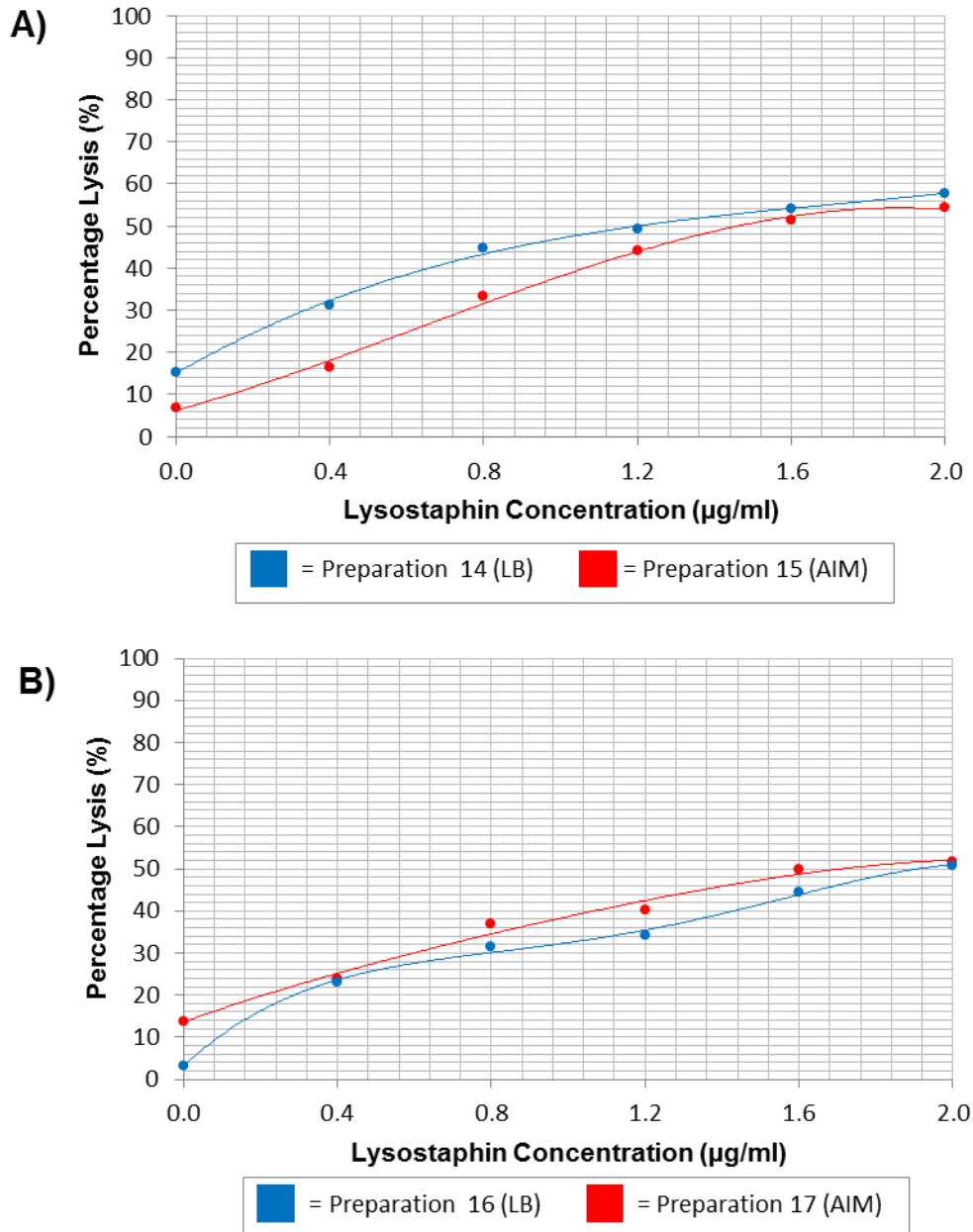


Figure 4.11: Percentage lysis of *S. aureus* following turbidometric assay of the staphylolytic activity of *N*-terminally His-tagged recombinant lysostaphin (construct 1) expressed in *E. coli* BL21(DE3) cultured in LB or AIM. A) Experiment 1. B) Experiment 2. UV spectrometric readings are tabulated in Appendix 7.327, Appendix 7.328, Appendix 7.329 and Appendix 7.330.

4.1.3.6 Influence of expression location upon the activity of recombinant lysostaphin

All of the previous assays were performed on recombinant lysostaphin preparations which had been expressed in the cytoplasm of *E. coli*. Periplasmically expressed C-terminally His-tagged recombinant lysostaphin (construct 4) also exhibited a high level of staphylolytic

activity (Figure 4.12). This result demonstrated that recombinant lysostaphin which had been targeted to the periplasm was also active.

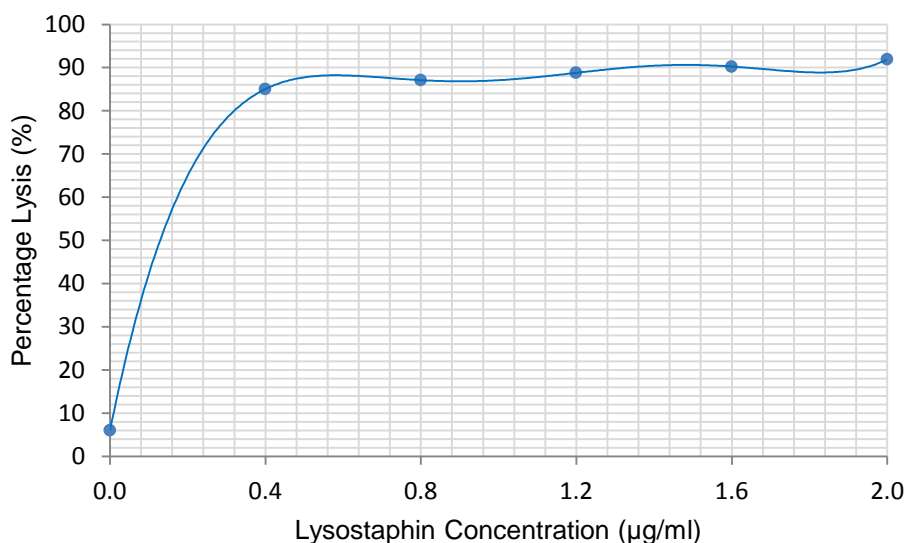


Figure 4.12: Percentage lysis of *S. aureus* following turbidometric assay of the staphylolytic activity of C-terminally his-tagged recombinant lysostaphin (construct 4). UV spectrometric readings are tabulated in Appendix 7.331.

4.1.3.7 Influence of purification upon the activity of recombinant lysostaphin

As described in Chapter 2.5, recombinant lysostaphin could be purified using a number of purification techniques. IMAC and CXC provided fairly rapid purification of recombinant lysostaphin, whilst the application of a combination of purification techniques, such as HIC and GF took longer to achieve the desired level of purification, which was shown to result in sample degradation (Section 2.5.3.3). It would therefore seem likely that lengthy purification of recombinant lysostaphin would lead to degradation and loss of catalytic activity. However, as shown in Figure 4.13, recombinant lysostaphin (construct 3) demonstrated staphylolytic activity despite lengthy purification using HIC and GF.

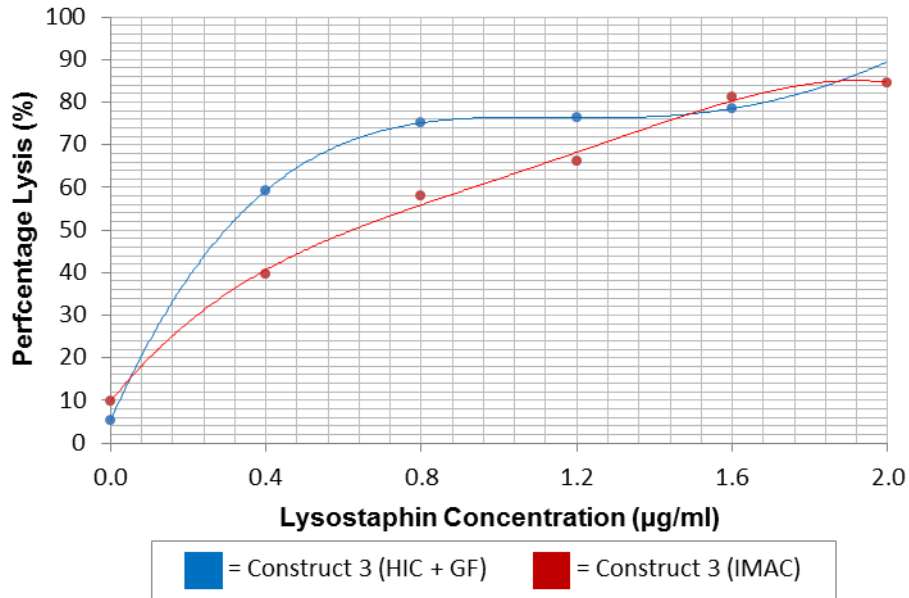


Figure 4.13: Percentage lysis of *S. aureus* following turbidometric assay of the staphylolytic activity of C-terminally his-tagged recombinant lysostaphin (construct 3). Recombinant lysostaphin preparations were purified by IMAC or HIC and GF. UV spectrometric readings are tabulated in Appendix 7.325 and Appendix 7.332.

These experiments also revealed that C-terminally His-tagged recombinant lysostaphin (construct 3) also displayed staphylolytic activity (Figure 4.13). Therefore these results indicated that the presence of a C-terminal His-tag sequence did not interfere with catalytic activity, despite the sequence being located juxtaposed to the cell wall targeting domain sequence.

4.1.3.8 Influence of lyophilisation upon the activity of recombinant lysostaphin

During large-scale production of N-terminally His-tagged recombinant lysostaphin (construct 1), IMAC purified protein was dialysed and lyophilised to concentrate the sample. Lyophilisation was found to detrimentally affect the solubility of the purified protein, however assay of the lyophilised product demonstrated that the protein retained staphylolytic activity (Figure 4.14).

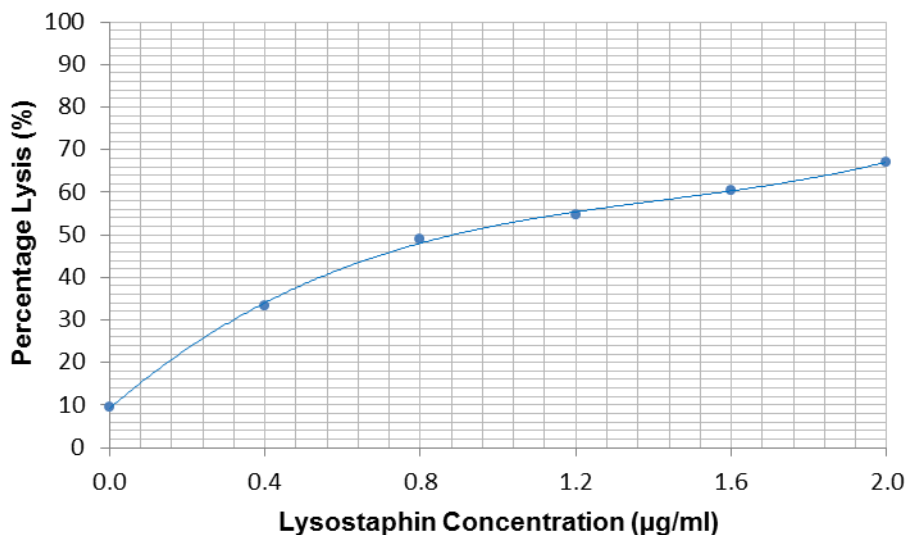


Figure 4.14: Percentage lysis of *S. aureus* following turbidometric assay of the staphylolytic activity of lyophilised *N*-terminally His-tagged recombinant lysostaphin (construct 1). UV spectrometric readings are tabulated in Appendix 7.334.

4.1.3.9 Assay of charge variants following WCX separation

To assess whether the activity of recombinant lysostaphin was specific to particular charge variants, assays were performed to assess the activity of recombinant lysostaphin variants which had been separated by WCX. Prior to WCX separation, recombinant lysostaphin (construct 1) was expressed and purified using IMAC. Following IMAC, selected fractions were rapidly concentrated to permit assay and WCX separation of charge variants (Figure 4.15). Cell lysates and IMAC fractions were analysed by SDS-PAGE (Appendix 7.319 and Appendix 7.321).

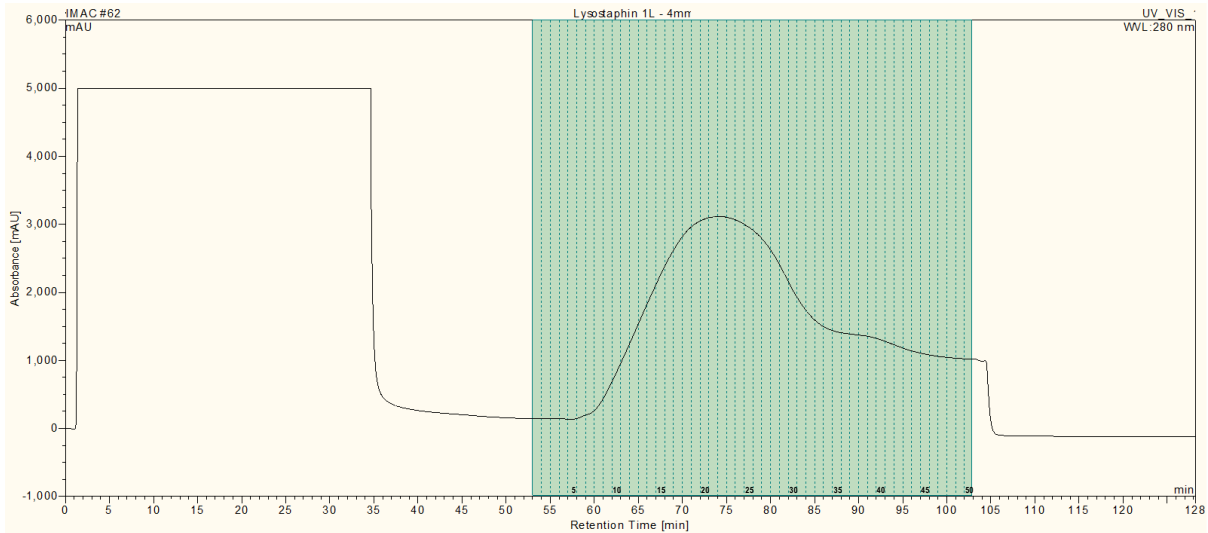


Figure 4.15: IMAC purification of *N*-terminally His-tagged recombinant lysostaphin (construct 1). Fractions 20-23 were assayed and subjected to WCX separation.

Before WCX separation, the activity of the concentrated, purified recombinant lysostaphin was assessed first to ensure that the more complex preparation exhibited activity. As shown in Figure 4.16, the activity of the recombinant lysostaphin preparation generally increased with the application of higher protein concentrations.

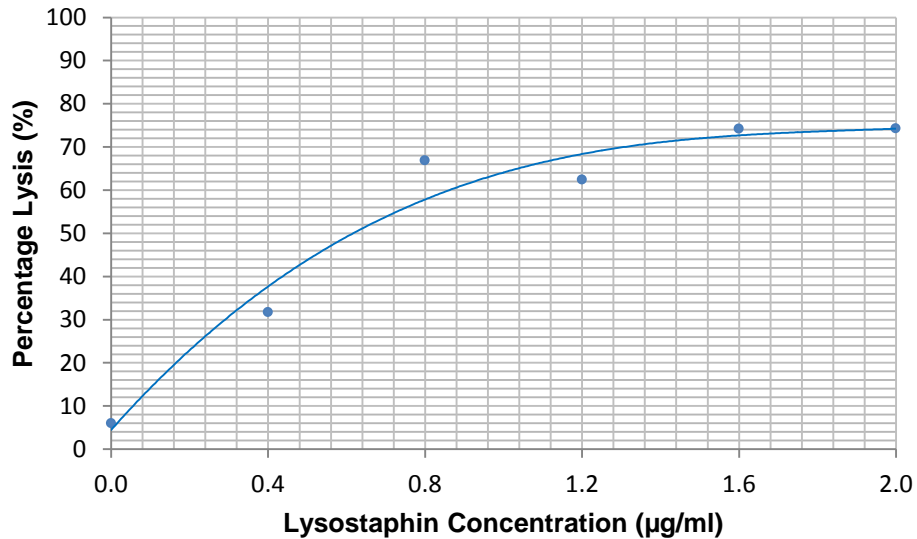


Figure 4.16: Percentage lysis of *S. aureus* following turbidometric assay of the staphylolytic activity of *N*-terminally His-tagged recombinant lysostaphin (construct 1).

Concentrated recombinant lysostaphin was then separated by WCX, which revealed the presence of two major peaks (Figure 4.17).

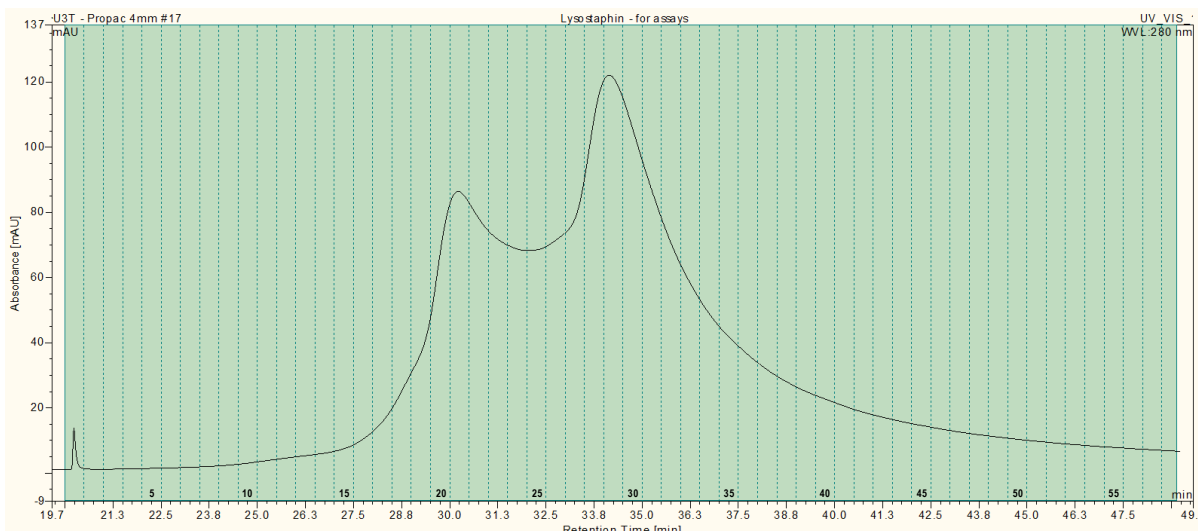


Figure 4.17: WDX separation of 0.3 mg of purified N-terminally His-tagged recombinant lysostaphin (construct 1). Fractions 21 and 29 were assayed for activity.

A selected fraction from each of the peaks was desalted and assayed for activity. Due to limited protein concentrations it was not possible to perform assays using the full range of recombinant lysostaphin concentrations. However the performed assays demonstrated that the protein contained in both fractions exhibited staphylolytic activity (Figure 4.18).

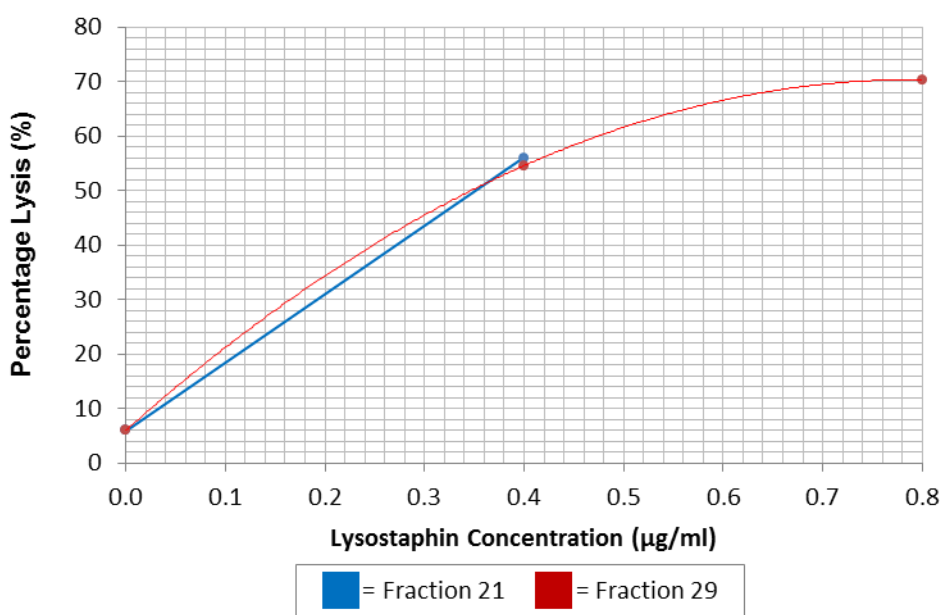


Figure 4.18: Percentage lysis of *S. aureus* following turbidometric assay of the staphylolytic activity of N-terminally His-tagged recombinant lysostaphin (construct 1) separated by WDX. UV spectrometric readings are tabulated in Appendix 7.336 and Appendix 7.337

To provide further confirmation of these results, an additional WDX separation was performed after applying a higher concentration of recombinant lysostaphin to the column.

WCX separation resulted in separation of much higher quantities of charge variants (Figure 4.19).

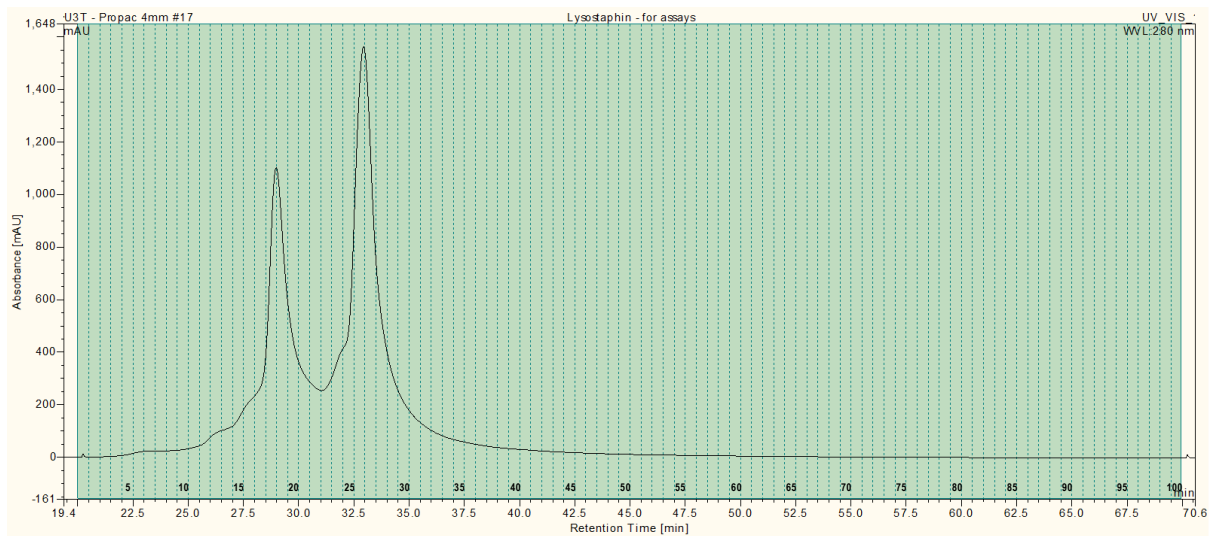


Figure 4.19: WCX separation of 2.1 mg of purified *N*-terminally His-tagged recombinant lysostaphin (construct 1). Fractions 19 and 26 were assayed for activity.

Selected fractions were desalted and assayed over the full range of recombinant lysostaphin concentrations (Figure 4.20). Assay of WCX separated protein peaks demonstrated that the charge variants that eluted within both peaks exhibited high levels of staphylolytic activity.

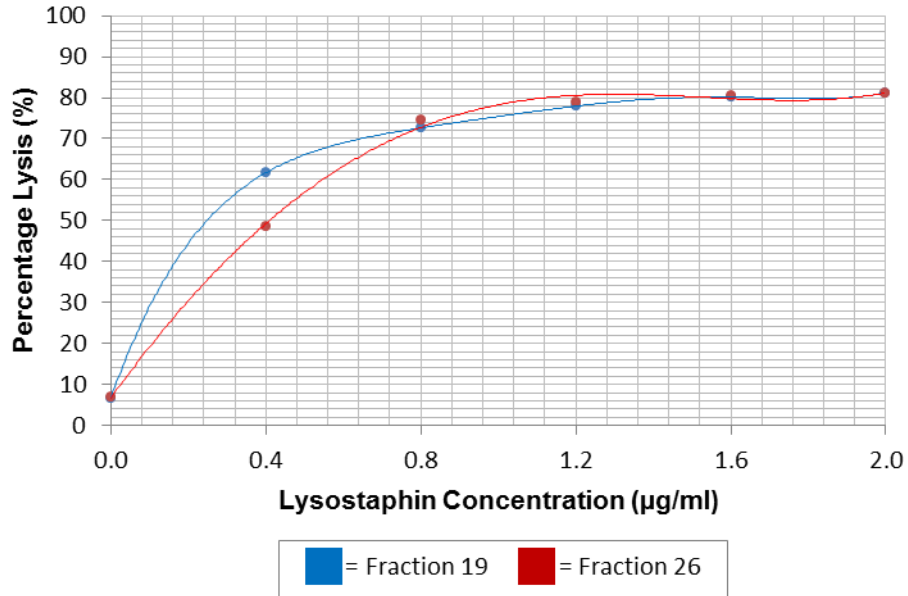


Figure 4.20: Percentage lysis of *S. aureus* following turbidometric assay of the staphylolytic activity of *N*-terminally His-tagged recombinant lysostaphin (construct 1) separated by WCX. UV spectrometric readings are tabulated in Appendix 7.338 and Appendix 7.339.

4.1.3.10 Assay of charge variants following WCX separation during culture analysis

Following extended culture analysis (Section 3.5.3.12) selected fractions were desalted, concentrated and assayed for activity. In the majority of cases, the selected fractions only contained enough protein to allow assay of activity at low recombinant lysostaphin concentrations (0.4 µg/ml) and consequently activity was not noticeably observed (data not shown). However noticeable activity could be observed in one of the fractions assayed following WCX separation of cell lysate harvested during culture analysis (Figure 4.21).

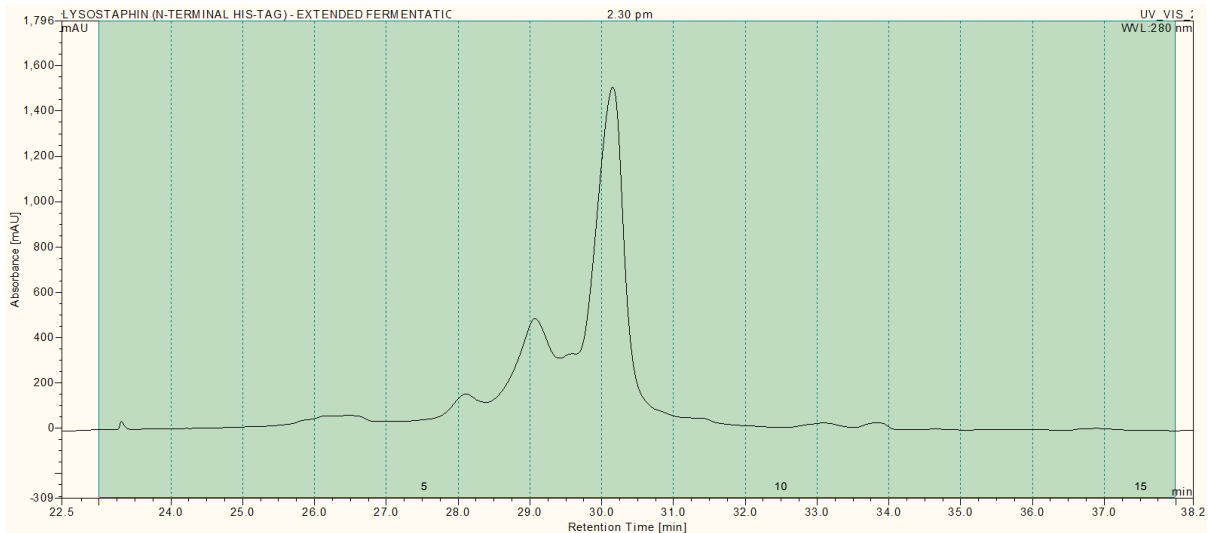


Figure 4.21: WAX separation of *N*-terminally His-tagged recombinant lysostaphin (construct 1) harvested at 15.0 h post-induction during extended culture analysis. Fraction 8 was assayed for activity.

Low level staphylolytic activity was observed in the presence of a low concentration of recombinant lysostaphin (0.4 $\mu\text{g/ml}$) (Figure 4.22). This result indicated that protein concentrations obtained during culture analysis were not sufficient enough to provide conclusive evidence of staphylolytic activity. Confirmatory evidence of activity could only be obtained by increasing cell lysate concentrations during culture analysis, which was not feasible as the culture was being subjected to frequent sampling over an extended period of time.

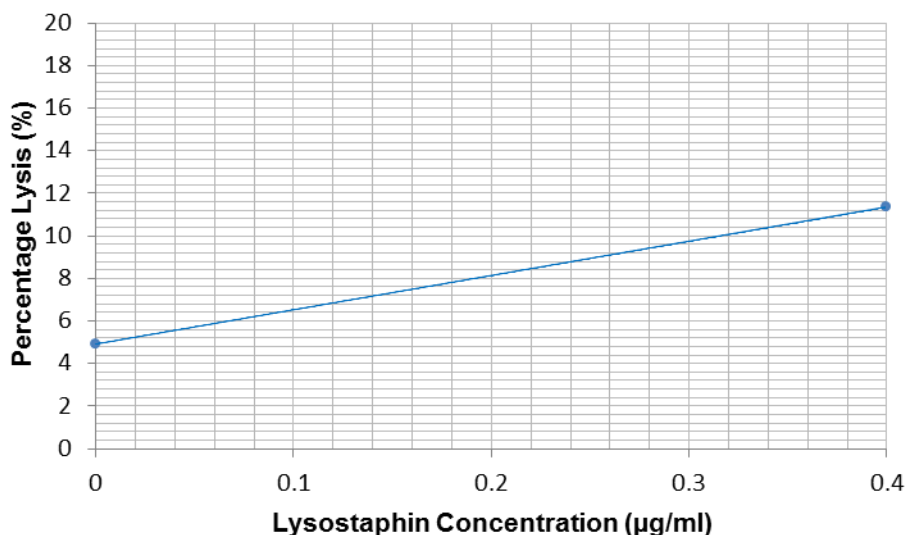


Figure 4.22: Percentage lysis of *S. aureus* following turbidometric assay of the staphylolytic activity of *N*-terminally His-tagged recombinant lysostaphin (construct 1) separated by WAX analysis. UV spectrometric readings are tabulated in Appendix 7.340.

4.1.4 Discussion

Bioinformatics comparison of the amino acid sequences composing recombinant lysostaphin and a lysostaphin-type peptidase, LytM, revealed that the amino acid sequence of recombinant lysostaphin contains the same amino acid residues that compose the zinc binding domain of LytM. ClustalW analysis identified these residues as being histidine₂₁₀, aspartate₂₁₄ and histidine₂₉₃, which along with a water molecule, tetrahedrally coordinate with zinc (Figure 4.23). This triad of amino acid residues indicates that the bound zinc is intended for catalytic rather than structural purposes. As zinc cannot participate in redox reactions, it can function as a Lewis acid-type catalyst, therefore facilitates proteolytic action (Christianson and Alexander, 1989, McCall *et al.*, 2000). Furthermore these residues modulate the nucleophilicity of the zinc bound water, whilst promoting zinc ion complexation (Christianson and Alexander, 1989).

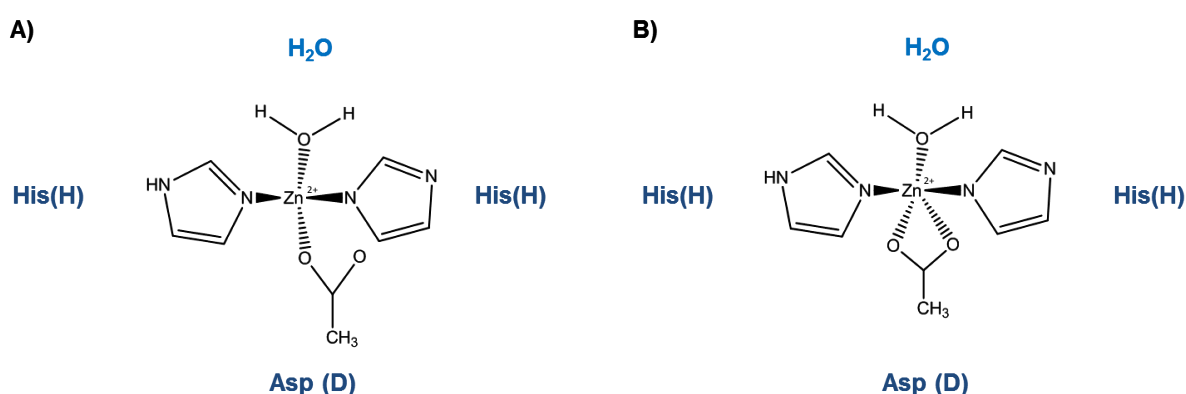


Figure 4.23: Tetrahedral coordination of zinc within the structure of recombinant lysostaphin. Histidine₂₁₀, aspartate₂₁₄ and histidine₂₉₃ and H₂O are known to tetrahedrally coordinate with zinc. Aspartate can form ligands with zinc in: A) monodentate mode or B) bidentate mode. Chemical structures drawn using ChemDraw Std 12.

As zinc binding is highly involved in the staphylolytic and elastolytic activity of recombinant lysostaphin, the observed staphylolytic activity of the enzyme indicated that the protein structure did indeed feature the presence of a zinc cofactor (Park *et al.*, 1995). To assess the enzymatic activity of recombinant lysostaphin, a turbidometric assay was developed to evaluate the staphylolytic activity of the protein. An appropriate strain of *S. aureus* was acquired and cultured to achieve substrate cells for the assay. Lysostaphin is known to lyse staphylococcal cells regardless of their growth state, though *S. aureus* was harvested at the late exponential growth phase prior to turbidometric assay to provide high cell density and experimental consistency (Yang *et al.*, 2007). Despite attempting to eliminate assay

inconsistencies, slight variations in cellular growth state did appear to interfere with observed activity levels however.

Assay of *N*-terminally His-tagged recombinant lysostaphin (construct 1) and *C*-terminally His-tagged recombinant lysostaphin (construct 3 and 4) verified that both forms of the protein possessed staphylolytic activity despite the addition of a fusion tag. Staphylolytic activity of *C*-terminally His-tagged recombinant lysostaphin was particularly encouraging considering that the cell wall targeting domain of the protein was located adjacent to the *C*-terminal His-tag sequence, and therefore the fusion tag sequence could have interfered with enzyme activity. Furthermore, the activity of recombinant lysostaphin did not appear to be influenced by the choice of expression media or expression location, following targeting of the protein to the periplasm.

Sample processing also did not appear to influence staphylolytic activity, with *C*-terminally His-tagged recombinant lysostaphin (construct 3) remaining active despite being purified by HIC and GF over an extended period of time. Extended sample handling and purification was found to decrease the stability of the protein (Section 2.5.3.3), however the staphylolytic activity of the protein appeared to remain intact. Lyophilisation of recombinant lysostaphin (construct 1) also did not appear to affect staphylolytic activity even though the solubility of the purified protein was adversely affected.

The majority of assays were performed using recombinant lysostaphin preparations which had been purified but not separated and therefore were likely to be composed of a variety of charge isoforms. Turbidometric assays were therefore performed on protein which had been separated as distinct charge variants during WCX separation, to establish whether staphylolytic activity was exclusive to specific charge variants. Due to differences in protein abundance and concentration, it was not possible to obtain comprehensive assay results initially, however once sample protein concentrations were increased prior to WCX separation; it was possible to obtain evidence that the eluted charge-distinct variants demonstrated staphylolytic activity. This finding confirmed that the absence or presence of zinc was unlikely to have led to the formation of the most predominant charge variants.

Evidence of the staphylolytic activity of distinct charge variants suggested that post-translational processing or modification of *N*-terminally His-tagged recombinant lysostaphin (construct 1) did not interfere with the activity of the protein isoforms. It is therefore likely that any potential modifications or proteolytic events did not occur within regions of the recombinant lysostaphin amino acid sequence that encoded enzymatic activity. However

high-resolution separation of charge variants using the ProPac[®] MAb SCX column (Section 3.5.3.13) suggested that peaks resolved during WCX separation may be more heterogeneous than expected. Therefore assay of apparently homogeneous protein eluted during WCX separation may not have represented the activity of all protein isoforms present within the sample.

Furthermore analysing the activity of charge variants which had been separated following IMAC purification may have not provided the complete representation of product heterogeneity. For instance, protein binding affinity during IMAC purification was questioned following unusual retention behaviour, as reported in Section 2.5.4. Further investigation of *N*-terminal His-tag heterogeneity and retention behaviour was described in Section 4.2 and indicated that the charge heterogeneity of recombinant lysostaphin may lead to inefficient purification of particular charge isoforms and therefore the purified recombinant lysostaphin preparation may not have contained all of the expressed charge isoforms. Certain charge isoforms may also not have been separated and assayed due to only pooling and concentrating a few of the peak fractions that eluted during IMAC purification.

More reliable purification of charge isoforms could therefore be achieved using CXC separation, as was performed during culture analysis. Unfortunately evidence of staphylolytic activity of charge variants separated during culture analysis was not really possible due to the availability of limited protein concentrations. Staphylolytic activity could only be determined conclusively using higher protein concentrations (0.8-2.0 µg/ml), however such protein concentrations could not be achieved without increasing the concentration of cell lysate applied during WCX separation, which was not feasible due to the frequency of sampling during culture analysis. Furthermore differences in relative abundance of different protein isoforms over time also limited the availability of adequate protein concentrations of less abundant isoforms. The implementation of a more sensitive assay technique would therefore be required to monitor enzyme activity during culture analysis.

The use of a turbidometric assay provided convenient, economical and fairly rapid assessment of staphylolytic activity, however the application of more sophisticated assay techniques would have provided a greater insight into enzyme kinetics during activity. A more sensitive assay was developed by Warfield *et al.*, (2006) who synthesised internally quenched substrates which could be quantitated using fluorescence resonance energy transfer (FRET) assays, whereby substrate cleavage leads to an increase in detected fluorescence (Warfield *et al.*, 2006, Bardelang *et al.*, 2009). In addition to providing more sensitive detection of staphylolytic activity, monitoring the cleavage of specific synthesised

substrates eliminates variability associated with the use of *S. aureus* cells, which may differ slightly in their growth phase physiology.

Overall these experiments provided confirmation that recombinant lysostaphin exhibited the expected staphylolytic activity. Further assays of other recombinant lysostaphin constructs (constructs 2 and 5) would have been desirable to provide greater insight into the influence of protein structure upon enzyme activity. Assay of separated charge variants also indicated that potential post-translational processing or modification of recombinant lysostaphin does not appear to adversely affect staphylolytic activity. However further investigation of the activity of charge variants separated using the higher resolution ProPac[®] MAb SCX column, using a more sensitive assay, would provide further insight into the influence of culture conditions upon the staphylolytic activity of recombinant lysostaphin. Although the elastolytic activity of recombinant lysostaphin was not investigated in these experiments, evidence of elastolytic activity was observed during experiments performed during related work, following tryptic digestion of *N*-terminally His-tagged recombinant lysostaphin (construct 1) (Appendix 7.341, associated data not shown).

4.2 IMAC analysis of recombinant lysostaphin

4.2.1 Introduction

IMAC is a highly selective purification technique, which can purify recombinant proteins to an extremely high degree. This selectivity is based upon specific metal affinity between immobilised metal ions and an oligohistidine affinity tag. Initial developments in metal affinity tag engineering involved attaching proteins to either very short tags, such as HisTrp or long extensions featuring up to 8 repeats of the peptide Ala-His-Gly-His-Arg-Pro (Gaberc-Porekar and Menart, 2001). Hochuli *et al* then engineered recombinant proteins with oligohistidine His-tags consisting of five or six consecutive histidine residues, which were efficiently purified in combination with a nitriloacetic acid-nickel(II) (NTA-Ni(II)) matrix (Hochuli *et al.*, 1988). NTA-Ni(II) matrices selectively bind adjacent histidine residues, therefore this type of matrix is now commonly used for His-tag purification. Penta-histidine and hexa-histidine tags provide high selectivity as the majority of natively expressed proteins do not harbour oligohistidine sequences and therefore the tags have become extremely popular (Knecht *et al.*, 2009).

The exact interaction mechanisms involved in binding of metal ions and oligohistidine His-tags are not known at present. Several reports suggest that protein binding involves a cooperative mechanism in which multipoint interactions between the proteins and the immobilised metal ions. The work of Knecht *et al*, indicated that the histidine residues in an oligohistidine tag each offer varying contributions to the overall binding. It is thought that binding commences after a monovalent interaction is established. Due to the vicinal presence of additional imidazole groups, a secondary ligand binds to the metal ion, creating multiple divalent interactions prior to elution (Figure 4.24). More specifically, Knecht *et al* reported that the 1st and 3rd or the 1st and 6th histidine residues provide a greater contribution to divalent interactions than the 2nd, 4th and 6th residues do (Figure 4.25) (Knecht *et al.*, 2009).

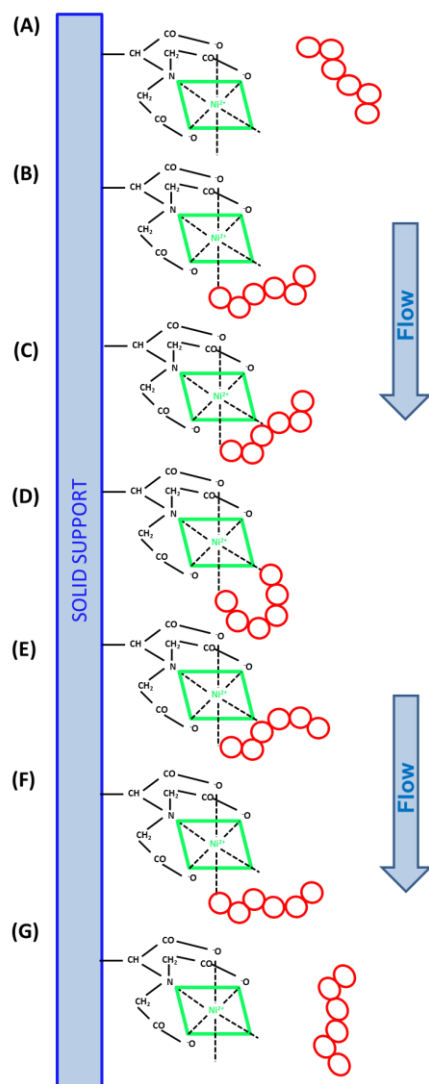


Figure 4.24: Representation of binding process involved in protein retention during IMAC purification using a Ni²⁺-NTA support, as proposed by Knecht *et al* (2008). The recombinant protein is applied to the column and the hexa-histidine tag sequence comes within proximity of the bound nickel ion (A). The His-tag sequence makes contact with the nickel via a monovalent interaction (B). Due to a high local ligand concentration, a second imidazole forms a divalent complex with the nickel (C). The His-tag sequence undergoes consecutive dissociation and reassociation of imidazole groups (D and E). Upon the application of elution buffer, divalent interactions become monovalent (F) until the His-tag dissociates fully from the nickel ion (G). Figure adapted from Knecht *et al* (2008).

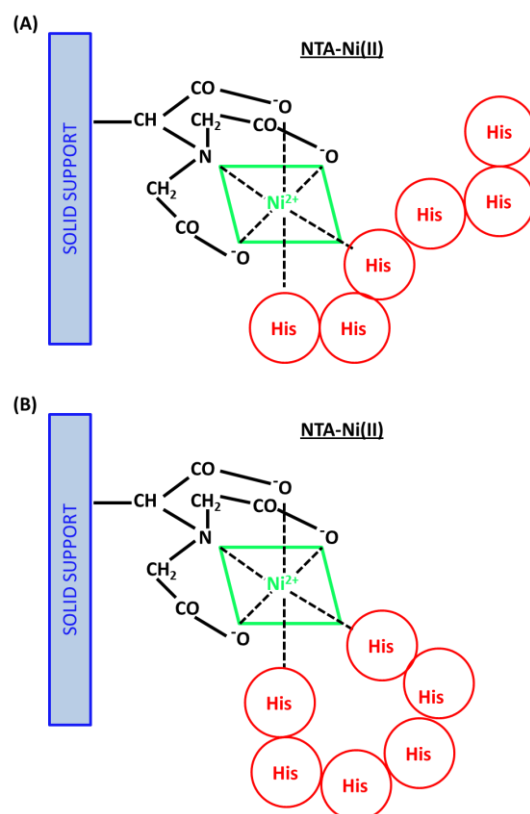


Figure 4.25: Proposed divalent binding interactions between a His-tag sequence and immobilised nickel ions on an NTA matrix. Knecht *et al*, (2008) reported that A) the first and third histidine residues and B) the first and sixth histidine residues provide a greater contribution to protein binding than the other histidine residues in the hexahistidine sequence. Figure adapted from Knecht *et al*, (2008).

The influence of His-tags upon catalytic activity may reflect altered protein folding kinetics. The presence of a His-tag sequence may affect the solubility, oligomerization or aggregation state of the protein and therefore alter active site conformation, which could detrimentally influence enzyme kinetics (Narmandakh and Bearne, 2010). Changes in protein conformation, due to the presence of His-tags may also adversely affect protein retention during IMAC. For instance, the His-tag sequence may become inaccessible due to steric hindrance caused by inappropriate protein folding and therefore lead to poor retention during purification (Knecht *et al.*, 2009). Furthermore differences in protein folding may lead to variable metal affinities, depending on whether single or multiple histidyl residues are accessible on the protein surface or protein interior. Histidine residues are mildly hydrophobic therefore only a few histidine residues tend to be located on the surface of the protein (Gaberc-Porekar and Menart, 2001). Binding affinity is also influenced by the spatial distribution of the histidyl residues and how distant or vicinal to each other they are (Hemdan *et al.*, 1989, Ueda *et al.*, 2003).

If a His-tag is concealed at the *N*- or *C*-terminus of a protein, then altering the position of the His-tag to the opposite terminus of the protein may improve His-tag accessibility and restore correct folding and activity (Lee and Kim, 2009). The position of the oligohistidine tag sequence can be important, as incorrect positioning of the tag may allow effective purification, but could prevent appropriate processing of the protein (Ueda *et al.*, 2003). For instance, the addition of a *C*-terminal His-tag to a recombinant β -lactamase altered the *N*-terminal sequence due to interfering with the action of a signal peptidase (Ledent *et al.*, 1997). Alternatively the presence of an *N*-terminal His-tag may interfere with protein synthesis, leading to premature termination and truncation of the expressed recombinant protein, increasing product heterogeneity. Conversely the insertion of an *N*-terminal His-tag may stabilise the *N*-terminus of the protein and reduce the rate of protein turnover and heterogeneity (Ueda *et al.*, 2003).

Recombinant protein heterogeneity can also be increased by the presence of PTMs, which are known to occur within the His-tag region of the protein sequence (Table 4.1). To date numerous studies have demonstrated that the amino terminus of the protein can undergo α -*N*-6 gluconoylation or α -*N*-6 phosphogluconoylation, following the addition of a gluconic acid or a phosphogluconic acid molecule (Du *et al.*, 2005a, Yan *et al.*, 1999a, Yan *et al.*, 1999b, Geoghegan *et al.*, 1999, Kim *et al.*, 2001, Du *et al.*, 2005b). Alternatively serine residues within the His-tag sequence can undergo phosphorylation (Du *et al.*, 2005a, Du *et al.*, 2005b, She *et al.*, 2010). Multiple phosphorylations may occur within the His-tag region, if the His-tag sequence features several serine residues.

Table 4.1: Modifications occurring at the N-terminal His-tag sequences of recombinant proteins.

Protein	Tag Sequence	Modifications Observed	Reference
FK506-binding protein (FKBP)	GHHHHHHHHHHSSGHIEGR	1 α -N-6 gluconoylation	Yan <i>et al</i> , 1999(a)
Spo0F	GHHHHHHHHHHSSGHIEGR	1 α -N-6 gluconoylation	Yan <i>et al</i> , 1999(a)
FK506- binding protein (FKBP)	GHHHHHHHHHHSSGHIEGR	1 α -N-6 gluconoylation	Yan <i>et al</i> , 1999(b)
G-protein-coupled receptor kinase 2 (GRK-2)	GSSHHHHHHSSGLVPRGSHM	1 α -N-6 gluconoylation 1 α -N-6 phosphogluconoylation	Geoghegan <i>et al</i> , 1999
C-terminal SH2 domain of p85 α (C-p85)	GSSHHHHHH	1 α -N-6 gluconoylation 1 α -N-6 phosphogluconoylation	Geoghegan <i>et al</i> , 1999
C-terminal SH2 domain of human ZAP-70 (C-ZAP)	GSSHHHHHHSSGLVPRGSHM	1 α -N-6 gluconoylation 1 α -N-6 phosphogluconoylation	Geoghegan <i>et al</i> , 1999
Src tyrosine kinase (SH3 domain)	GSSHHHHHH	1 α -N-6 gluconoylation	Kim <i>et al</i> , 2001
Aurora 2 catalytic domain	GSSHHHHHHSSGLVPRGSHMK	1-5 phosphorylations on Ser	Du <i>et al</i> , 2005(a)
Aurora A catalytic domain	GSSHHHHHHSSGLVPRGSH	1-5 phosphorylations on Ser	Du <i>et al</i> , 2005(b)
PAK1 catalytic domain	GSSHHHHHHSSGLVPR	1-4 phosphorylations on Ser	Du <i>et al</i> , 2005(b)
PAK7 catalytic domain	GSSHHHHHHSSGLVPR	1-2 phosphorylations on Ser 1 α -N-6 gluconoylation	Du <i>et al</i> , 2005(b)
PKA catalytic subunit	GSSHHHHHHSSGLVORGSH	1-5 phosphorylations on Ser	Du <i>et al</i> , 2005(b)
NE2398 CBS domain	GSSHHHHHHSSGRENLYFQGH	1 phosphorylation on Ser	She <i>et al</i> , 2010
RPA3416 CBS domain	GSSHHHHHHSSGRENLYFQG	1 phosphorylation on Ser	She <i>et al</i> , 2010

Table 4.1: Modifications occurring at the *N*-terminal His-tag sequences of recombinant proteins (continued)

Protein	Tag Sequence	Modifications Observed	Reference
PH0267 CBS domain	GSSHHHHHHSSGRENLYFQG	1 phosphorylation on Ser	She <i>et al</i> , 2010
Atu1752 CBS domain	GSSHHHHHHSSGRENLYFQG	1 phosphorylation on Ser	She <i>et al</i> , 2010
AF0847 CBS domain	GSSHHHHHHSSGRENLYFQG	1 phosphorylation on Ser	She <i>et al</i> , 2010
TV1335 CBS domain	GSSHHHHHHSSGRENLYFQGH	1 phosphorylation on Ser	She <i>et al</i> , 2010
MJ0653 CBS domain	GSSHHHHHHSSGRENLYFQGH	1 phosphorylation on Ser	She <i>et al</i> , 2010
SF0624 non-CBS domain	GSSHHHHHHSSGRENLYFQG	None	She <i>et al</i> , 2010
Altronate hydrolase SAF domain	GSSHHHHHHSSGRENLYFQG	None	She <i>et al</i> , 2010
Transcriptional regulator	GSSHHHHHHSSGRENLYFQG	None	She <i>et al</i> , 2010

Modifications of these charged groups should theoretically alter the thermodynamic and kinetic behaviour of the His-tag sequence and therefore also that of the recombinant protein. The addition of such a modification may lead to steric hindrance and protein misfolding, which could interfere with purification or enzyme activity. Most importantly the addition of phosphate groups on serine residues or gluconic acid at the *N*-terminus will interfere with the metal binding affinity of these ligands, but may also prevent adjacent histidine residues from participating in metal binding. In view of all these complications, it is essential that the retention behaviour of each recombinant protein should be investigated to establish if there are any factors which could interfere with IMAC purification.

4.2.1.1 Recombinant lysostaphin and *N*-terminal His-tag heterogeneity

As described in Chapter 2.4, recombinant lysostaphin was expressed with either no His-tag sequence or with an *N*- or *C*-terminal His-tag. The lysostaphin gene was cloned into pET expression system vectors, pET-28a and pET-22b vectors which encode particular fusion

tag sequences that can be engineered into a recombinant protein through careful selection of restriction enzymes during cloning. The pET-28a vector encodes an *N*-terminal His-tag, whilst the pET-22b vector sequence encodes a *C*-terminal His-tag sequence (Sommer *et al.*, 2004). The *N*-terminal His-tag sequence is followed by a thrombin cleavage site, which facilitates enzymatic removal of the tag. Proteases can however be expensive and do not necessarily provide complete cleavage of the recombinant product.

Fusion tags can also be unexpectedly cleaved by host-cell proteases following expression, which has the potential to interfere with subsequent purification (LaVallie and McCoy, 1995). Random cleavage of His-tag sequences by proteases can also increase the heterogeneity of a protein preparation, as well as altering protein charge and behaviour (Mohanty and Wiener, 2004). In Section 2.5.3, recombinant lysostaphin was successfully purified from harvested cell lysate using either a Chelating Sepharose™ Fast Flow column or ProPac® IMAC-10 column. The successful purification of recombinant lysostaphin indicated that the His-tag sequences remained intact; therefore it was unlikely that the entire His-tag sequence had been lost through unexpected cleavage by host-cell proteases.

Following purification, recombinant lysostaphin (constructs 1 and 3) were assayed for activity and both preparations were found to exhibit staphylolytic activity. These results indicated that the presence of a *N*-or *C*-terminal His-tag did not appear to interfere with the activity of either preparation. Furthermore, the location of the His-tag sequence did not appear to interfere with expression yields and therefore reasonable amounts of recombinant lysostaphin could be purified during IMAC purification. The amount of protein that could be purified using IMAC, was largely dependent on expression media volume and column diameter. Typically 5-20 mg of fusion protein is yielded per litre of LB culture and purity of over 90% can be obtained (Shih *et al.*, 2002).

ProPac® IMAC-10 columns were found to provide a higher degree of purification and more rapid separation of recombinant lysostaphin than Chelating Sepharose™ Fast Flow columns, however the capacity of the columns was initially unknown. Whilst testing the capacity of ProPac® IMAC-10 columns, it became apparent that some of the chromatographic peaks obtained during IMAC separation, were subject to severe retention time shifting. Although retention time shifting may arise due variation in mobile phase pH or ionic strength, it was thought that the apparent shifting may have been explained by another reason, such as *N*-terminal His-tag heterogeneity or protein aggregation.

To investigate this finding further, comparative IMAC purifications of *N*-terminally His-tagged recombinant lysostaphin (construct 1), recombinant lysostaphin without any His-tags

(construct 2) and C-terminally His-tagged recombinant lysostaphin (construct 3) were performed using a ProPac[®] IMAC-10 (4 x 250 mm) column. Even though construct 2 did not feature a His-tag sequence, cell lysate was subjected to IMAC purification to establish whether recombinant lysostaphin could demonstrate inherent metal affinity during IMAC. It is known that the sequence of lysostaphin possesses metal affinity for zinc, which like nickel is an intermediate Lewis acid. Therefore theoretically the expressed recombinant lysostaphin should bind zinc following expression, preventing the metal binding ligands from binding to stationary phase nickel ions. However it has been found that the bound zinc metal may become displaced by stationary phase nickel ions during IMAC, leading to a reduction in the activity of recombinant lysostaphin (Warfield, 2006).

Evidently the presence of *N*- and *C*-terminal hexahistidine tags within the sequence of recombinant lysostaphin provides metal affinity permitting IMAC purification of the protein. Histidine residues exhibit the strongest interaction with immobilised metal ions, as electron donor groups within the imidazole ring act as electron donor groups and form coordination bonds with the transition metal (Terpe, 2003, Sundberg and Martin, 1974). Even in the absence of His-tag sequences, the amino acid sequence of recombinant lysostaphin is not completely devoid of putative electron donor histidine residues. As shown in Figure 4.26, construct 2 features nine histidine residues, which will display an affinity for transition metal ions. It is therefore likely that some of the histidine residues within the sequence of mature lysostaphin would be exposed on the surface of the molecule and therefore could contribute to the metal affinity of the molecule.

Table 4.2: Ligands and functional groups involved in protein retention and their retention strengths. *Retention strength comparison based on work by Ueda *et al* (2003).

Ligand	Retention Strength*
<i>N</i> -Terminus	++
Arginine	+
Asparagine	-
Cysteine (reduced form)	++++
Glutamine	-
Histidine	++++
Lysine	+
Phenylalanine	+
Tryptophan	+
Tyrosine	+

The use of an *N*-terminal His-tag may also predispose recombinant lysostaphin to a PTM of the His-tag sequence. For instance, the *N*-terminal His-tag sequence of construct 1 possesses five serine residues, which could theoretically become phosphorylated (Figure 4.26). The *C*-terminal His-tag sequence of construct 3 does not have any serine residues therefore is unlikely to become phosphorylated.

Recombinant lysostaphin could also become susceptible to gluconoylation or phosphogluconoylation of the *N*-terminus. The incidence of this amino terminal modification, is however likely to be dependent on the *N*-terminal amino acid residue. It is likely that the initiator methionine residue is removed by a methionine aminopeptidase following expression; therefore modification of the amino terminus is more likely to occur at the *N*-terminal glycine residue in Construct 1 or the *N*-terminal alanine residue in Constructs 2 and 3. However it is possible that the *N*-terminal alanine residues may not exhibit reactivity for this type of modification as Geoghegan *et al*,(1999) proposed that this modification may be limited to sequences which are similar to Gly-Ser-Ser-[His]⁶- (Geoghegan *et al.*, 1999).

IMAC retention and purification of recombinant lysostaphin was therefore examined in further detail, to investigate the possibility of such modifications.

Aims:

- To assess whether *N*-terminally His-tagged recombinant lysostaphin (construct 1), recombinant lysostaphin without His-tags (construct 2) and *C*-terminally His-tagged

recombinant lysostaphin (construct 3) exhibit different degrees of charge heterogeneity using WCX separation.

- To study the retention behaviour of *N*-terminally His-tagged recombinant lysostaphin (construct 1), through repeated purifications.
- To compare the retention behaviour of *N*-terminally His-tagged recombinant lysostaphin against that of *C*-terminally His-tagged recombinant lysostaphin (construct 3).
- To establish whether recombinant lysostaphin without any His-tags exhibits retention during IMAC purification.
- To analyse protein eluted during IMAC purification using WCX analysis.

4.2.2 Methods

4.2.2.1 Buffers

All buffer compositions are outlined in Appendix 7.342.

4.2.2.2 Equipment

All equipment used during IMAC analysis of recombinant lysostaphin is outlined in Appendix 7.343.

4.2.2.3 Sample preparation

Sample preparation is described in Appendix 7.345.

4.2.2.4 WCX analysis of His-tag heterogeneity

WCX separation was performed using a 0.5 ml/min flow rate and a ProPac[®] WCX-10 (4 x 500 mm) column. Cell lysate (500 µl) was loaded onto the column and the cellular debris was eluted whilst maintaining an isocratic gradient of 0% B for 10 min. Protein isoforms were separated by applying a linear gradient of 0-50% B over 70 min. The column was then washed using 90% B for 9 min and then the column was equilibrated at 0 % B for 15 min. UV data was acquired at 214 and 280 nm throughout the separation and fractions were collected by time, every 30 s between 30 and 65 min. Following separation, fractions containing eluted protein were stored at 4°C until they could be analysed by SDS-PAGE (Appendix 7.15).

4.2.2.5 WCX analysis of IMAC purified protein

IMAC purification was performed as described in Appendix 7.346 and eluted fractions were concentrated as described in Appendix 7.347. WCX separation was performed using a 0.2 ml/min flow rate and a ProPac[®] WCX-10 (2.0 x 500 mm) column. Purified and concentrated protein samples were injected onto the column in 100 µl injection volumes. Protein was separated by applying a linear gradient of 0-50% B over 20 min. An isocratic gradient was maintained for a further 3 min, before washing the column using 90% B for 13 min. The column was then equilibrated at 0% B for 11 min. UV data was acquired at 214 and 280 nm throughout the separation.

4.2.3 Results

4.2.3.1 WCX analysis of His-tag heterogeneity

Following optimisation of separation conditions, various recombinant lysostaphin constructs were subjected to WCX separation using a ProPac WCX-10 (4 x 500 mm) column. Figure 4.27 demonstrates that *N*-terminally His-tagged recombinant lysostaphin (construct 1) demonstrated greater heterogeneity than *C*-terminally His-tagged recombinant lysostaphin (construct 3) and recombinant lysostaphin with no His-tags (construct 2), which appeared to be composed of fewer charge isoforms. Fractions were collected during each of the WCX separations and were subjected to PAGE analysis to confirm that the peaks being interpreted reflected protein with a molecular weight which corresponded to that of the recombinant lysostaphin construct being expressed (Appendix 7.348-Appendix 7.353).

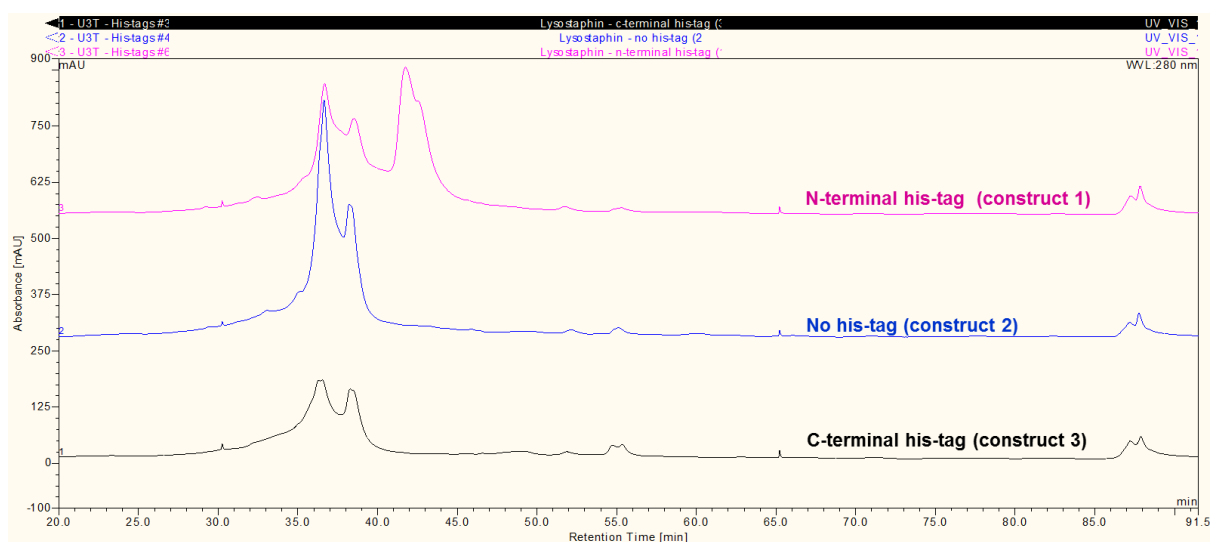


Figure 4.27: Comparison of WCX chromatograms obtained following separation of *N*-terminally His-tagged recombinant lysostaphin (construct 1), *C*-terminally His-tagged recombinant lysostaphin (construct 3) and recombinant lysostaphin without any His-tags (construct 3). Each construct was expressed in *E. coli* BL21(DE3) which had been cultured in LB. Protein expression was induced at OD_{600 nm} values of 1.010 (construct 1), 0.821 (construct 2) and 0.852 (construct 3), before harvesting the cultures at 16.25 h post-induction.

Assessment of this chromatogram would suggest a number of factors may be involved in the charge heterogeneity of recombinant lysostaphin preparations. As constructs 1, 2 and 3 all featured the same mature lysostaphin amino acid sequence it would be expected that the proteins would exhibit a similar charge during WCX analysis. However as constructs 1 and 3 featured charged His-tag sequences, it would be expected that the charge of these fusion

proteins would differ slightly from that of the non-His-tagged recombinant lysostaphin. *N*-terminally His-tagged recombinant lysostaphin (construct 1) has a theoretical pI of 9.72 and therefore should have exhibited the greatest charge due to the extra charge provided by the *N*-terminal His-tag. *C*-terminally His-tagged recombinant lysostaphin (construct 3) has a theoretical pI of 9.52, which was slightly less than that of recombinant lysostaphin without any His-tags (construct 2) at 9.59.

These differences in theoretical pI values became evident during WCX separation of each of the recombinant lysostaphin preparations, through the resolution of a number of charge isoforms, which were designated A-D (Table 4.3 and Figure 4.28). Surprisingly each WCX separation featured the resolution of acidic peaks A and B, indicating that the *N*-terminally His-tagged recombinant lysostaphin (construct 1) preparation also featured protein isoforms with the same or similar charge to that of *C*-terminally His-tagged recombinant lysostaphin (construct 3) and recombinant lysostaphin without any His-tags (construct 2). This result would suggest that a proportion of the protein molecules within the *N*-terminally His-tagged recombinant lysostaphin (construct 1) preparation may have lost charge through modification or truncation. Peaks C and D reflected the presence of more protein isoforms which would theoretically reflect the presence of protein isoforms with a more preserved or less processed or modified *N*-terminal His-tag sequence.

Table 4.3: Retention time (min) values of identified peaks following WCX separation of recombinant lysostaphin with *N*-terminal, *C*-terminal or no His-tag sequences. Peaks which were not observed during WCX separation are represented by “X”.

Construct	Fusion Tag	Theoretical pI	Peak Retention Time (min)			
			A	B	C	D
1	<i>N</i> -terminal His-tag	9.72	36.67	38.53	41.75	42.53
2	None	9.59	36.64	38.23	X	X
3	<i>C</i> -terminal His-tag	9.52	36.53	38.28	X	X

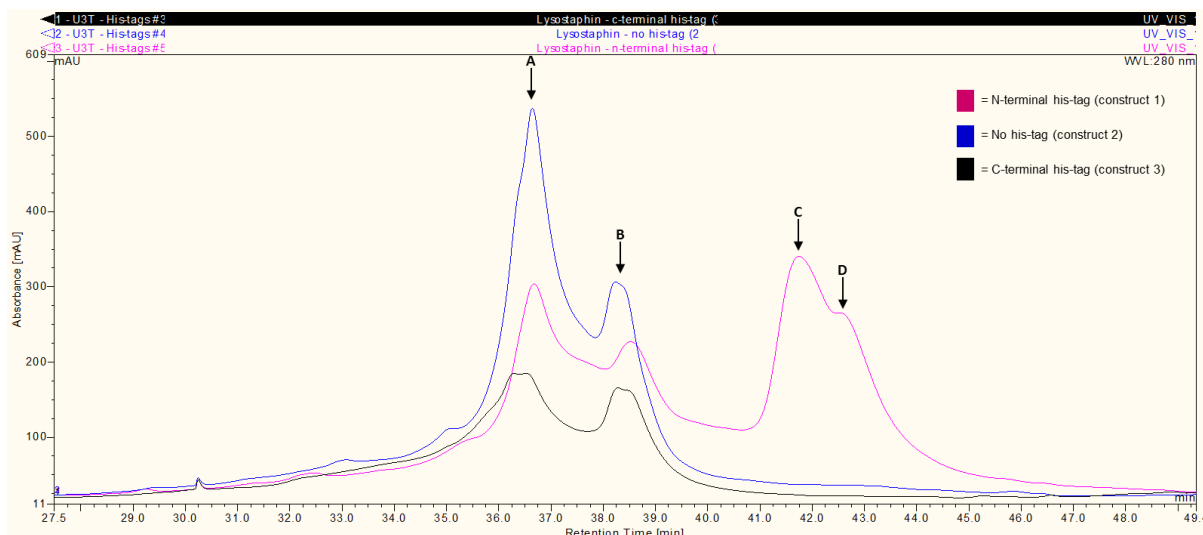


Figure 4.28: Comparison of WCX chromatograms obtained following separation of *N*-terminally His-tagged recombinant lysostaphin (construct 1), *C*-terminally His-tagged recombinant lysostaphin (construct 3) and recombinant lysostaphin without any His-tags (construct 2). Multiple peaks were observed during WCX separation and were designated A-D as indicated.

As WCX separation of *C*-terminally His-tagged recombinant lysostaphin (construct 3) and recombinant lysostaphin without any tags (construct 2) also featured peaks A and B, it was evident that both preparations also exhibited charge heterogeneity due to some form of post-translational processing or modification. It is interesting to note that the more basic protein isoforms (peaks C and D) were observed during this experiment, but also during culture analysis (Section 3.5) and therefore these variants appeared to be exclusive to *N*-terminally His-tagged recombinant lysostaphin (construct 1) preparations. These observations were however taken with caution given that certain conditions may have varied between cultures. Although expression media and incubation times were controlled in each culture, optical densities at the point of induction were not identical and therefore the presence and relative abundance of each peak would have been likely to vary over the course of culture.

4.2.3.2 IMAC Purification of *N*-terminally His-tagged recombinant lysostaphin

As *N*-terminally His-tagged recombinant lysostaphin (construct 1) preparations exhibited greater charge heterogeneity during WCX separation, it seemed likely that *N*-terminal His-tag heterogeneity might interfere with the efficiency of IMAC purification. Unusual protein binding efficiency was observed during the optimisation of IMAC purification using the ProPac[®] IMAC column (4 x 250 mm) column, as reported in Section 2.5.4. Experiments were performed to assess the capacity of the ProPac[®] IMAC column by applying various

volumes of cell lysate to the column. As shown in Figure 4.29, the peak height increased with increased volumes of CFE being applied to the column.

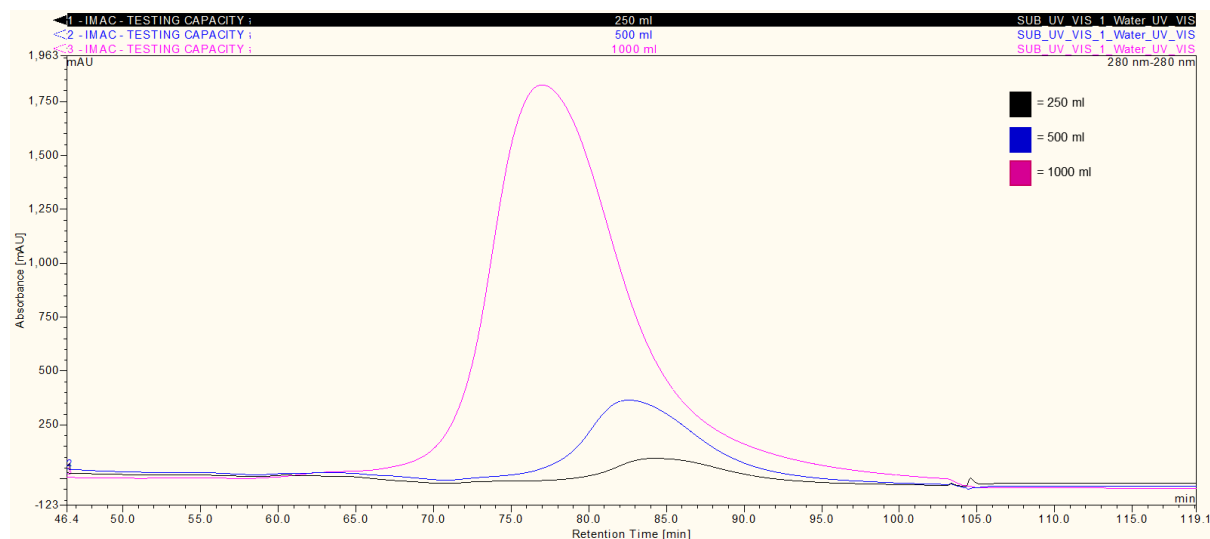


Figure 4.29: Comparison of IMAC purifications following consecutive applications of 0.25 L, 0.50 L and 1 L

Peak fractions from the IMAC purification of CFE from 1 L of *E. coli* batch culture were pooled and concentrated so that the purification yield could be quantitated by UV spectrometry. However UV spectrometry revealed that only 2.8 mg of *N*-terminally tagged recombinant lysostaphin (construct 1) was purified by the ProPac[®] IMAC-10 column, which was unexpectedly low considering the volume of *E. coli* culture that had been harvested. In addition, the application of doubling quantities of cell lysate to the column did not result in proportionally increased peak heights. These unusual results suggested that the column may have had a poor binding capacity or that the *N*-terminally His-tagged form of recombinant lysostaphin demonstrated poor binding efficiency.

In order to investigate further, another preparation of cell lysate containing *N*-terminally His-tagged recombinant lysostaphin (construct 1) was produced and applied to the ProPac[®] IMAC-10 column. The application of cell lysate resulted in the elution of a peak (peak A) representing purified recombinant lysostaphin (Figure 4.30).

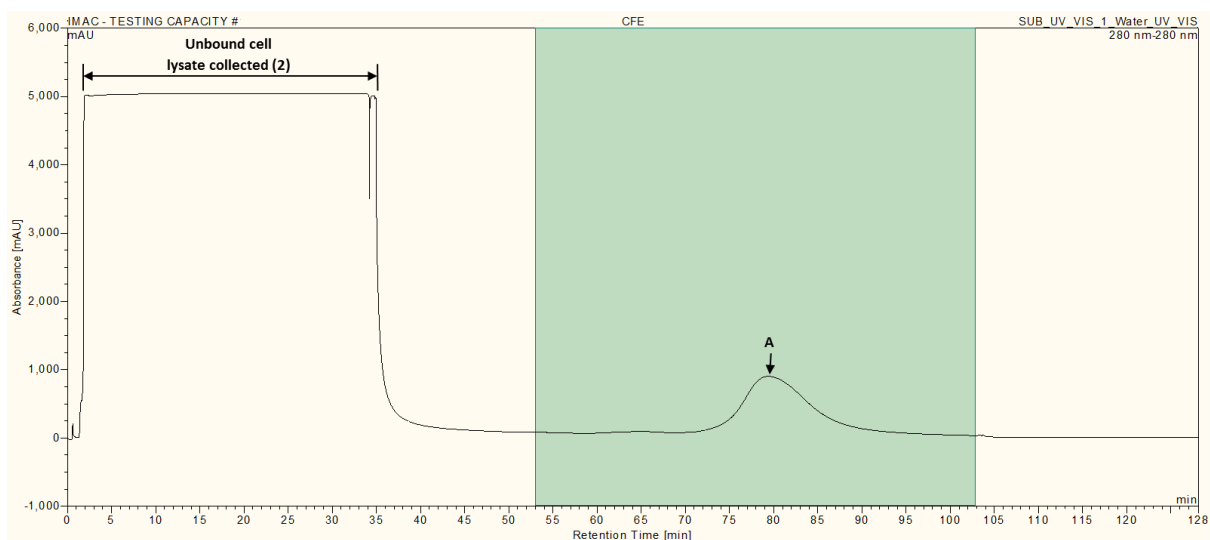


Figure 4.30: IMAC purification of *N*-terminally His-tagged recombinant lysostaphin from cell lysate. The purification yielded a single peak (A) representing purified recombinant lysostaphin. The initial unbound cell lysate was collected manually, as indicated in the figure.

The eluted column flow-through from the initial application of cell lysate was collected and re-applied to the column (Figure 4.31) to see whether more protein would bind to the column. Interestingly, re-application of unbound cell lysate (2) to the column resulted in two peaks (B and C). Retention time comparison indicated that purified protein eluted in peak B demonstrated a weaker binding affinity than peak A, whilst the purified protein eluted in peak C demonstrated a stronger binding affinity than peak A did. The peak height of peak C was approximately double the height of peak A indicating that a higher quantity of recombinant protein was purified from the cell lysate upon its second application to the column. This implied that the capacity of the column was greater than the initial purification of recombinant protein from cell lysate (1) had suggested.

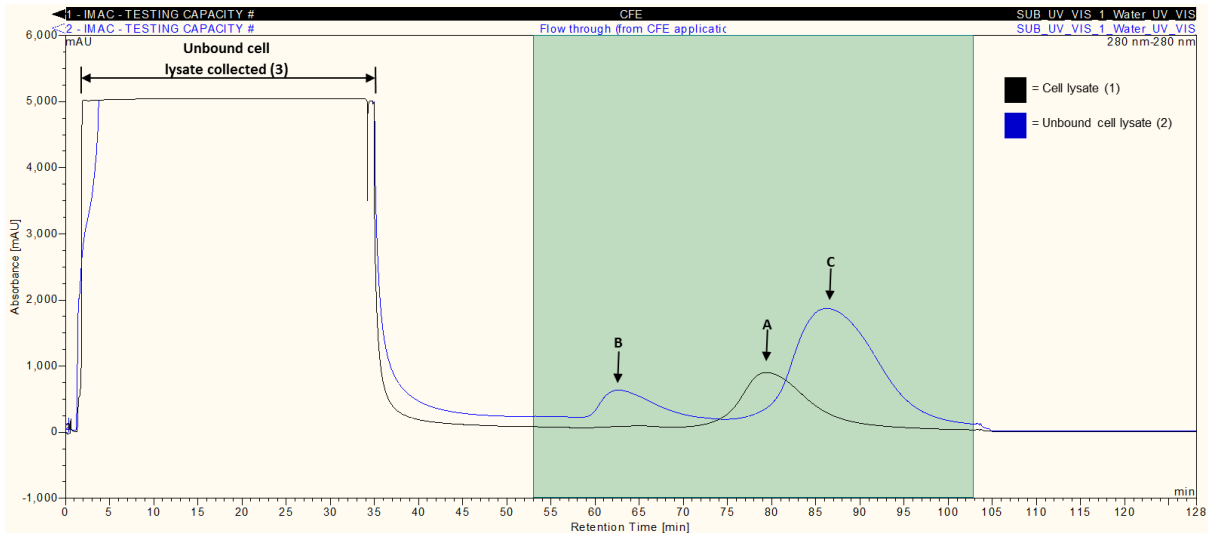


Figure 4.31: Comparison of elution peaks following the application of cell-free lysate and re-application of unbound cell lysate (2) flow-through. The re-application of unbound cell lysate (2) resulted in elution of two peaks (B and C) at retention times which were lower and higher than that of the elution of peak A after initial application of cell lysate (1). Unbound cell lysate (3) was again collected manually as indicated.

Collected unbound cell lysate (3) was again collected and subsequently re-applied to the column to see if any more recombinant protein could be purified from cell lysate (Figure 4.32). By this third IMAC purification, it was evident that the amount of recombinant protein left in the cell lysate had been significantly reduced by the previous purifications, as evidenced by a reduction in amount of recombinant protein that had bound to the ProPac™ column. The third IMAC purification resulted in the elution of peaks D and E, which have similar retention times to peaks B and C from the second IMAC purification. As the quantity of bound and unbound protein had reduced significantly by the third re-application of cell lysate, unbound cell lysate (4) was not re-applied to the column.

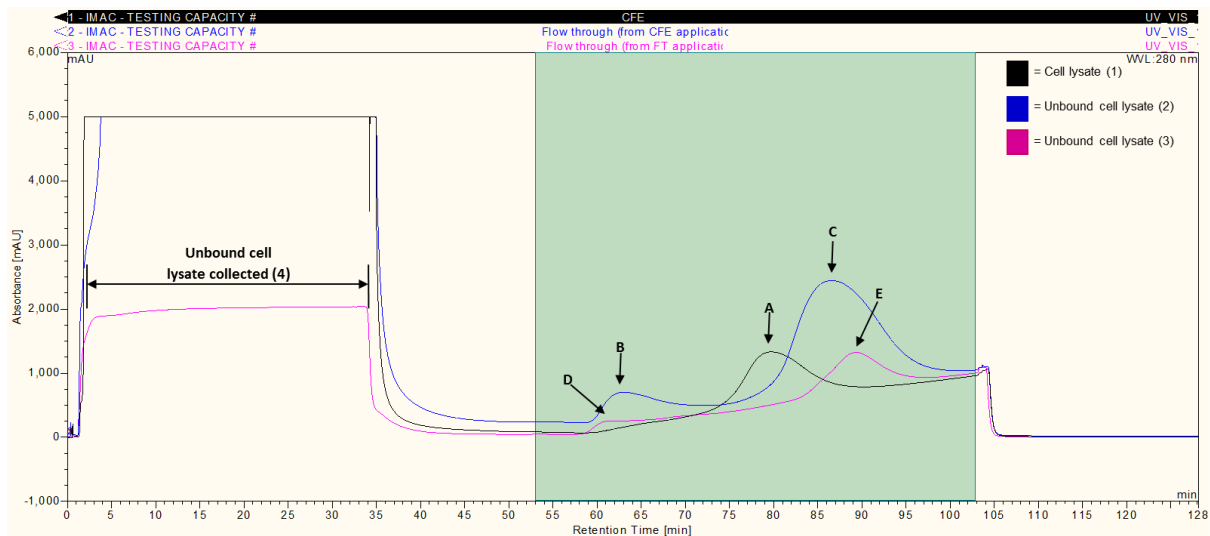


Figure 4.32: Comparison of elution peaks following the application of cell lysate (1), re-application of unbound cell lysate (2), followed by a re-application of secondary unbound cell lysate (3). Unbound cell lysate (4) was again collected manually as indicated and eluted peaks D and E are indicated alongside peaks A, B and C

4.2.3.3 PAGE analysis of IMAC samples and fractions

All of the applied and collected samples were analysed by PAGE to check for the presence of *N*-terminally His-tagged recombinant lysostaphin (Figure 4.33). PAGE analysis verified that the concentration of recombinant lysostaphin (construct 1) in the cell lysate reduced with each sequential IMAC purification and analysis of unbound cell lysate (4) suggests that recombinant lysostaphin had been largely removed from the applied cell extract by the third IMAC purification.

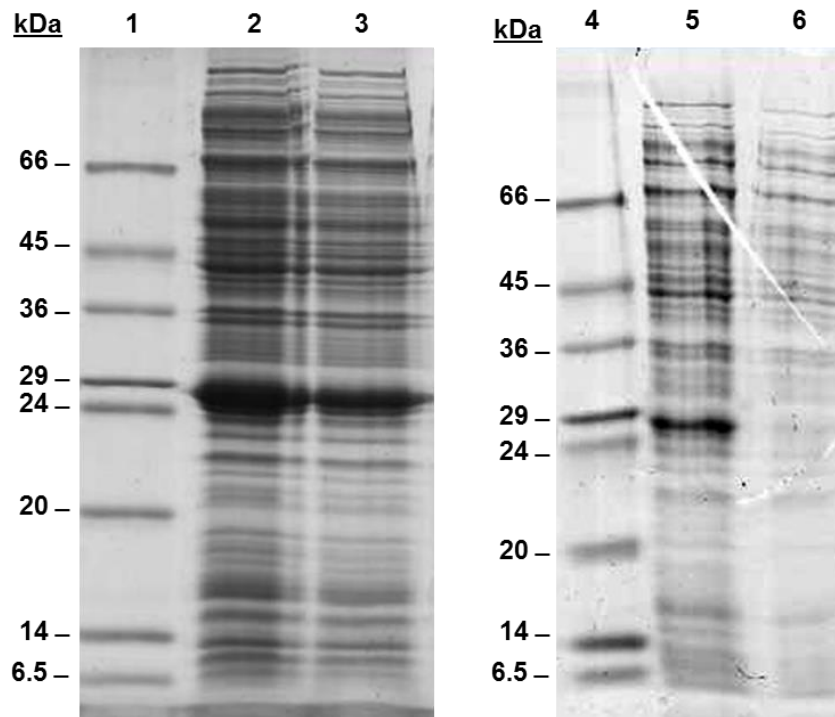


Figure 4.33: PAGE analysis of IMAC samples. Lane 1: Sigma low molecular weight markers; Lane 2: Cell lysate (1); Lane 3: Unbound cell lysate (2); Lane 4: Sigma low molecular weight markers; Lane 5: Unbound cell lysate (3); Lane 6: Unbound cell lysate (4)

To ensure that the hyper-expressed *N*-terminally His-tagged recombinant lysostaphin (construct 1) had been specifically purified from the *E. coli* cell lysate, resulting IMAC fractions were analysed by PAGE. Selected fractions from the elution of Peak A from IMAC purification of cell lysate (1) were therefore desalted, concentrated and analysed by PAGE (Figure 4.34 and Figure 4.35).

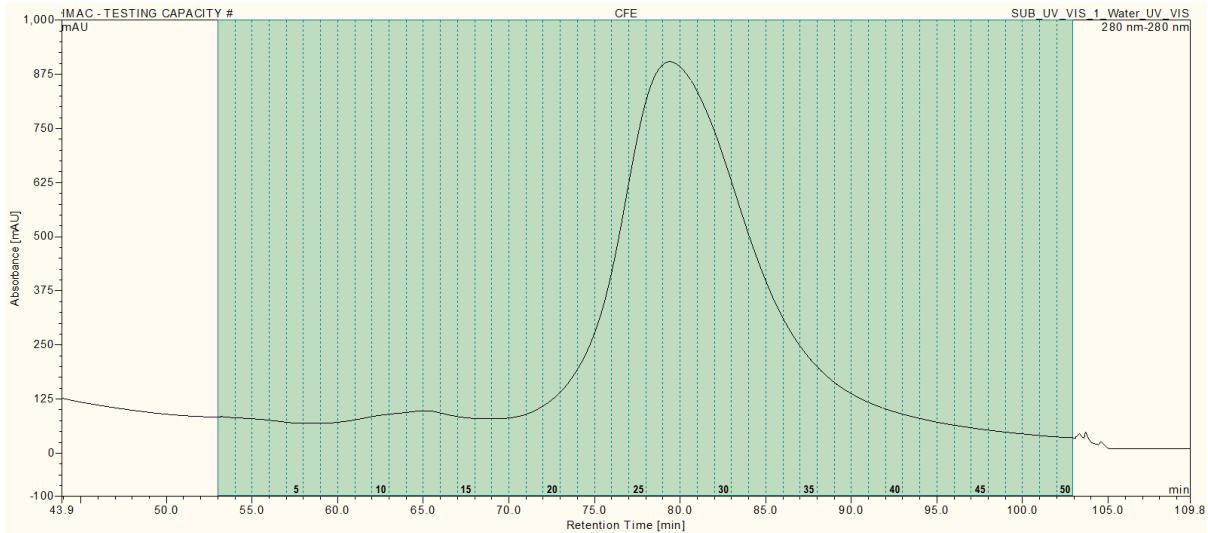


Figure 4.34: IMAC purification of *N*-terminally His-tagged recombinant lysostaphin (construct 1) from cell lysate (1). Fractions 19-39 were collected during the elution of peak A. The fractions were pooled, desalted and concentrated prior to PAGE analysis.

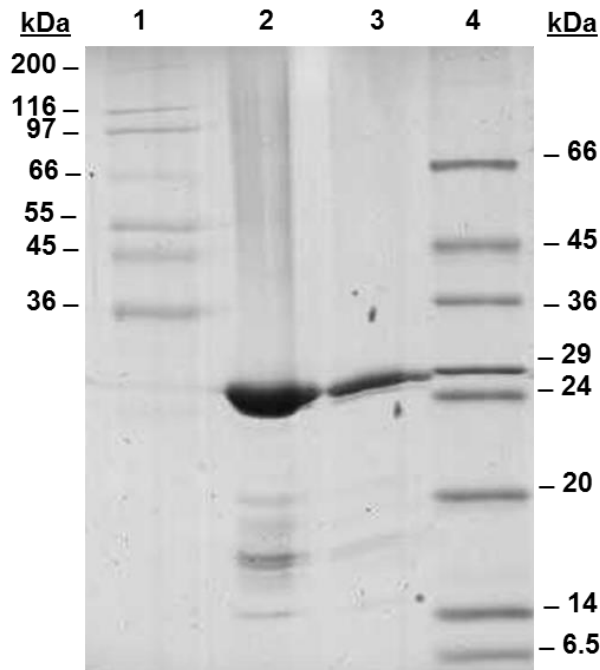


Figure 4.35: PAGE analysis of peak A from IMAC purification of cell lysate (1). Lane 1: Sigma high molecular weight markers; Lane 2: purified recombinant lysostaphin (1:10); Lane 3: purified recombinant lysostaphin (1:100); Lane 4: Sigma low molecular weight markers.

PAGE analysis of protein eluted within Peak A demonstrated that the IMAC purification specifically purified a recombinant protein with a molecular weight of around 29 kDa, which corresponded with the molecular weight of *N*-terminally His-tagged recombinant lysostaphin (construct 1). Selected fractions resulting from the elution of Peak B and C from IMAC purification of unbound cell lysate (2), as indicated in Figure 4.36, were also analysed by PAGE (Figure 4.37).

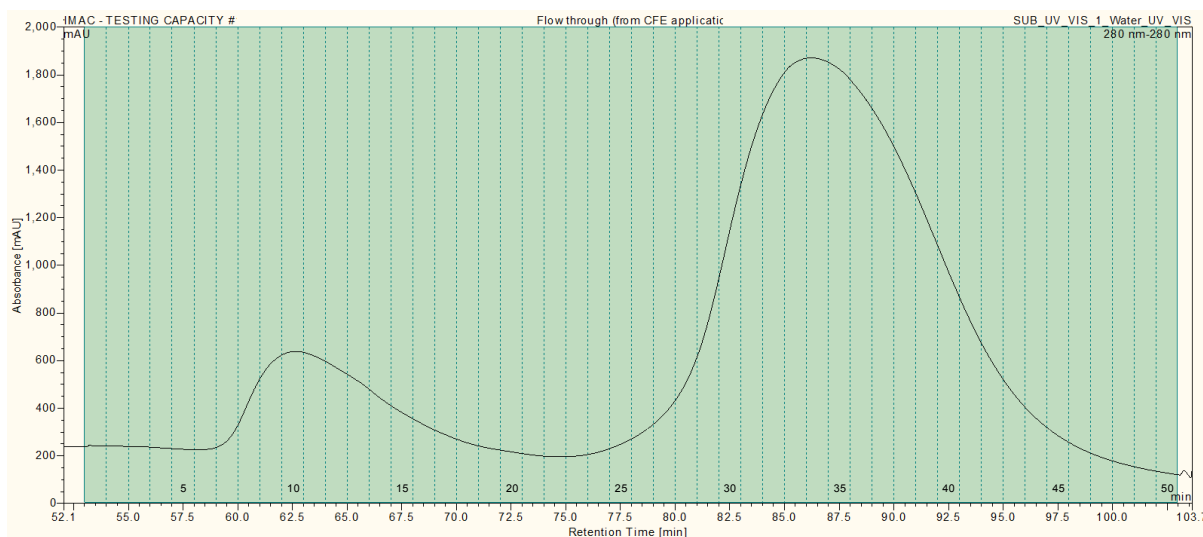


Figure 4.36: IMAC purification of *N*-terminally His-tagged recombinant lysostaphin (construct 1) from unbound cell lysate (2). Fractions 7, 10, 13 were desalted and concentrated prior to PAGE analysis of peak B, whilst fractions 32, 35 and 38 were desalted and concentrated prior to PAGE analysis of peak C.

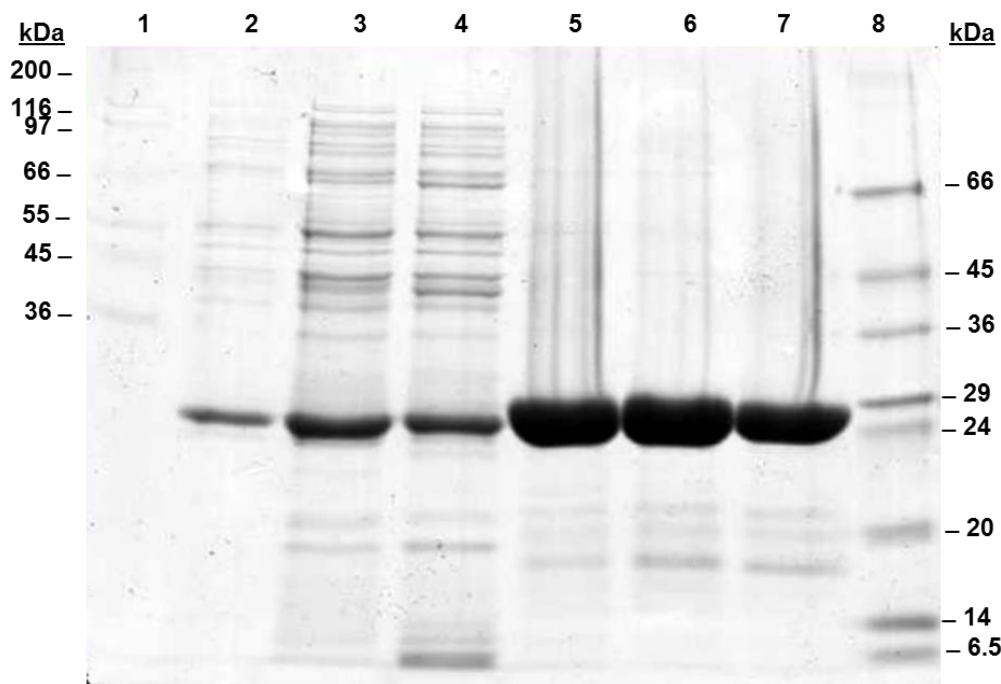


Figure 4.37: PAGE analysis of peak B and C from IMAC purification of unbound cell lysate (2). Lane 1: Sigma high molecular weight markers; Lane 2: Fraction 7 (peak B); Lane 3: Fraction 10 (peak B); Lane 4: Fraction 13 (peak B); Lane 5: Fraction 32 (peak C); Lane 6: Fraction 35 (peak C); Lane 7: Fraction 38 (peak C); Lane 8: Sigma low molecular weight markers.

Again PAGE analysis demonstrates that IMAC peaks B and C contained a purified protein with a molecular weight of 24-29 kDa which corresponded with the molecular weight of *N*-terminally His-tagged recombinant lysostaphin (29.3 kDa). IMAC peak B was predominantly composed of recombinant lysostaphin, but also appears to have been contaminated with several proteins with higher molecular weights. It could be possible that these contaminating proteins interfered with the binding of recombinant lysostaphin, which resulted in the early elution of some of the recombinant lysostaphin. Fractions collected during the elution of IMAC peak C did not appear to contain as many contaminating proteins, which may explain why the recombinant lysostaphin seemed to bind more strongly to the IMAC stationary phase.

4.2.3.4 WCX analysis of IMAC purified protein

The previous experiments demonstrated that *N*-terminally His-tagged recombinant lysostaphin (construct 1) was not entirely extracted from cell lysate upon initial purification attempts. Subsequent IMAC purification of collected unbound cell lysate revealed that additional recombinant protein could be purified from cell lysate and that it bound to the

column with variable affinities. It was possible that the observed variable binding affinities reflected the differential IMAC binding of different recombinant lysostaphin isoforms. To assess this theory, selected fractions collected during the elution of peak A and E were pooled and concentrated (Figure 4.38). The concentrated protein was then subjected to WCX analysis (Figure 4.39).

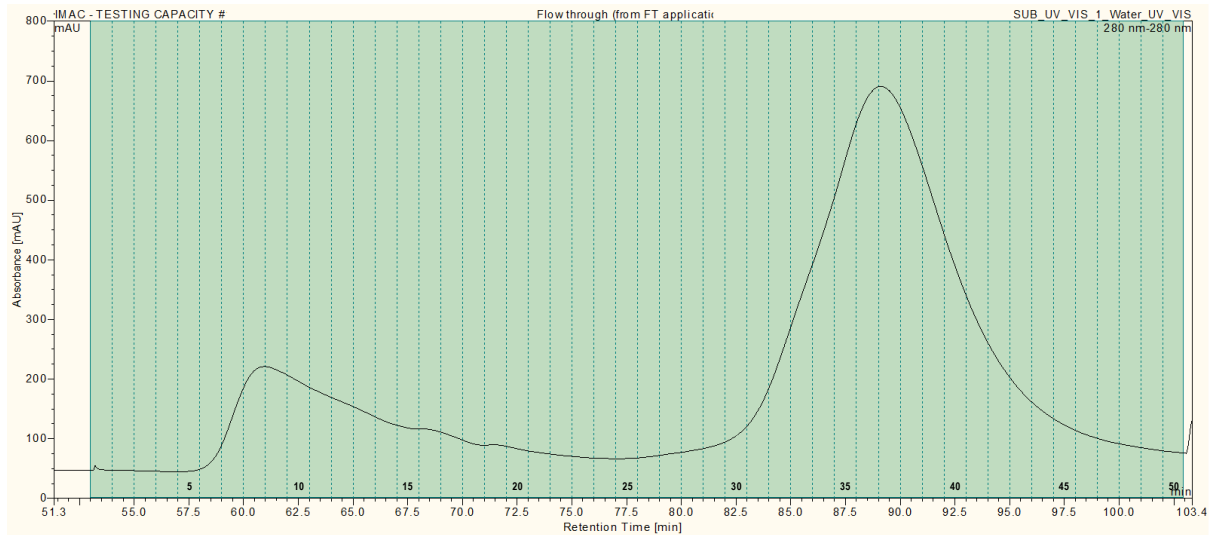


Figure 4.38: IMAC purification of *N*-terminally His-tagged recombinant lysostaphin (construct 1) from unbound cell lysate (3). Fractions 35 and 36 were desalted and concentrated prior to WCX analysis of peak E.

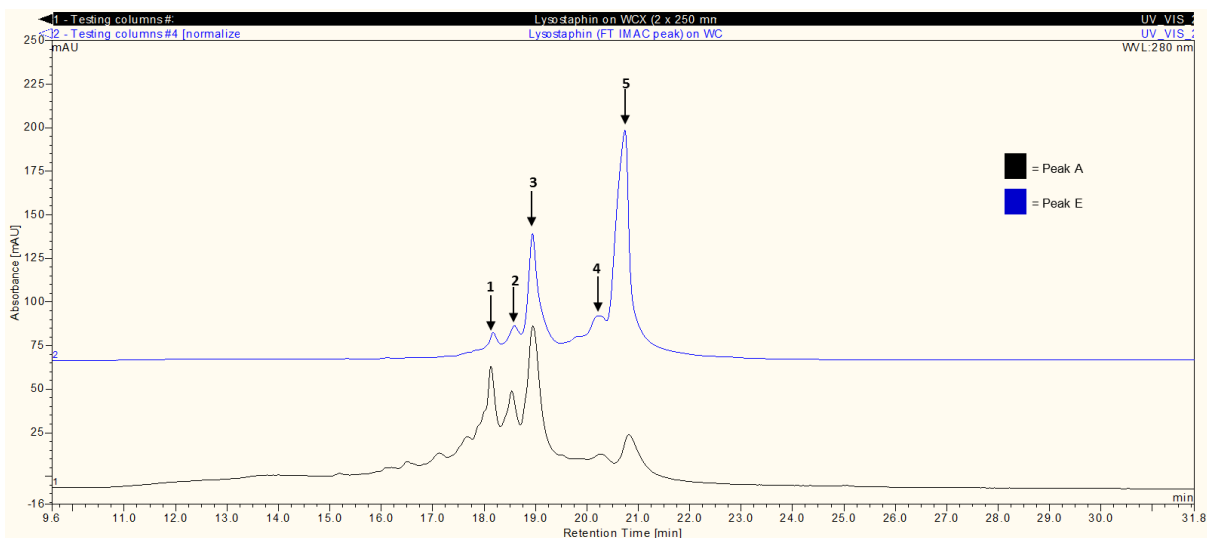


Figure 4.39: Comparison of WCX separations of IMAC purified *N*-terminally His-tagged recombinant lysostaphin (construct 1) from peaks A and E. Both separations reveal 5 distinct peaks (1-5 indicated by arrows)

WCX analysis showed that both IMAC peaks reflect the presence of five distinct charge variants. However the difference in IMAC retention times of peak A and peak E could be explained by clear differences in the relative abundances of WCX peaks 1 and 5. Basic WCX peak 5 appeared to be significantly more abundant in the protein collected during elution of IMAC peak A during the initial IMAC purification of cell lysate (1). On the other hand, acidic WCX peak 1 is appreciably more abundant in the protein collected during elution of IMAC peak E during the third IMAC purification of unbound cell lysate (3). These results suggest that stronger binding affinity, as exhibited by the retention of peak E, is associated with greater prevalence of more basic recombinant lysostaphin isoforms.

4.2.3.5 IMAC purification of C-terminally His-tagged recombinant lysostaphin

IMAC purification of *N*-terminally His-tagged recombinant lysostaphin provided interesting results which suggested that the relative quantities of different charge isoforms in a preparation may have affected the binding affinity between recombinant lysostaphin and the IMAC stationary phase. These charge isoforms may differ due to post-translational processing or modification within the *N*-terminal His-tag region of the protein, which would alter the IMAC binding affinity of the protein. As a consequence of these findings, C-terminally His-tagged recombinant lysostaphin was prepared and purified using IMAC to establish whether this form of the protein exhibited unusual IMAC binding characteristics as well (Figure 4.40).

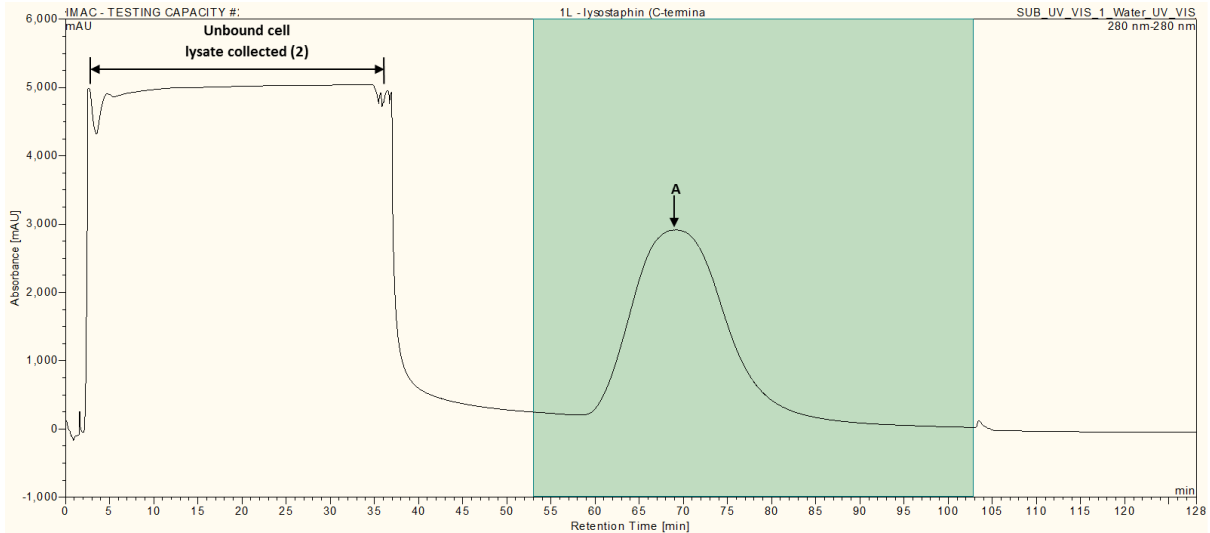


Figure 4.40: IMAC purification of C-terminally His-tagged recombinant lysostaphin from cell lysate (1). The purification yielded a single peak (A) representing purified recombinant lysostaphin. The initial unbound cell lysate was collected manually, as indicated in the figure.

Figure 4.40 shows that a large quantity of C-terminally His tagged-lysostaphin (construct 3) was purified on the initial IMAC purification. The quantity of purified protein was three times greater than that achieved during the initial IMAC purification of N-terminally His-tagged recombinant lysostaphin (construct 1), as shown in Figure 4.34. However the shorter retention time of peak A, suggested that binding of C-terminally His-tagged recombinant lysostaphin to the IMAC stationary phase was not as strong as that of N-terminally His-tagged recombinant lysostaphin (Figure 4.41).

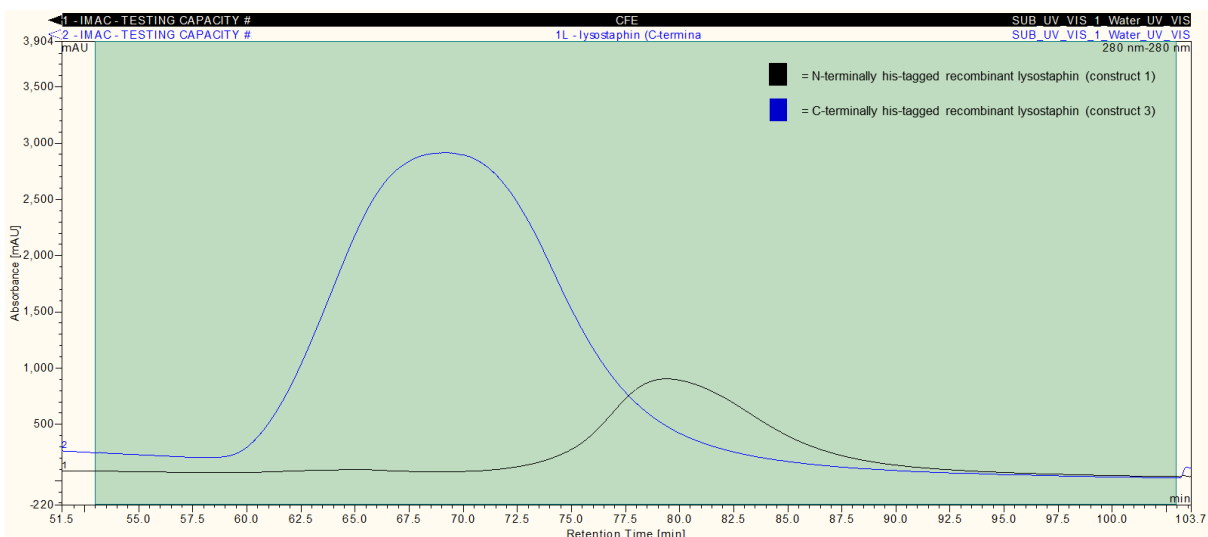


Figure 4.41: Comparison of initial IMAC purifications of N-terminally His-tagged recombinant lysostaphin (construct 1) and C-terminally His-tagged recombinant lysostaphin (construct 3) from cell lysate (1). The initial purification of C-terminally His-tagged recombinant lysostaphin purified a greater amount of protein than the initial purification of N-terminally His-tagged recombinant lysostaphin.

Unbound cell lysate (2) was collected manually and re-applied to the IMAC column to assess whether any more recombinant lysostaphin could be purified from the cell lysate (Figure 4.42). A very small quantity of recombinant protein bound to the column on the re-application of cell lysate, indicating that the majority of recombinant protein had already been purified from the cell lysate in the previous purification. This application resulted in elution of a peak (B) at a retention time which was slightly higher than that of the elution of peak A after initial application of cell lysate. Unbound cell lysate (3) was again collected manually as indicated.

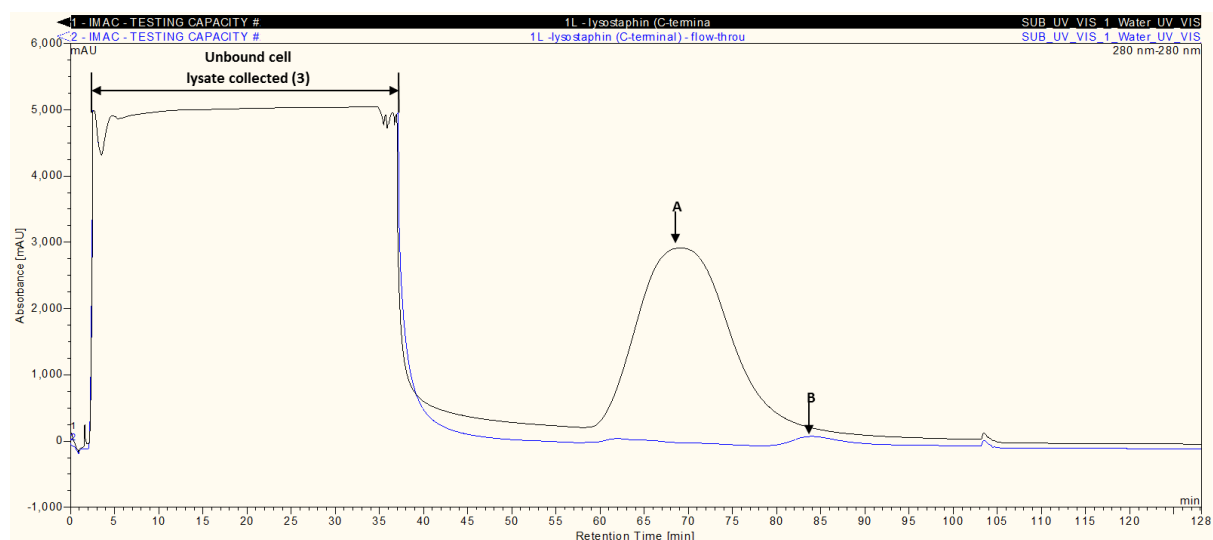


Figure 4.42: Comparison of elution peaks following the application of cell lysate (1) and re-application of unbound cell lysate (2) flow-through. The re-application of unbound cell lysate resulted in the resolution of peak B as indicated.

4.2.3.6 PAGE analysis of IMAC samples and fractions

All of the applied and collected samples were analysed by PAGE to check for the presence of recombinant lysostaphin (Figure 4.43). PAGE analysis verified that the concentration of recombinant lysostaphin in the cell lysate reduced with each sequential IMAC purification.

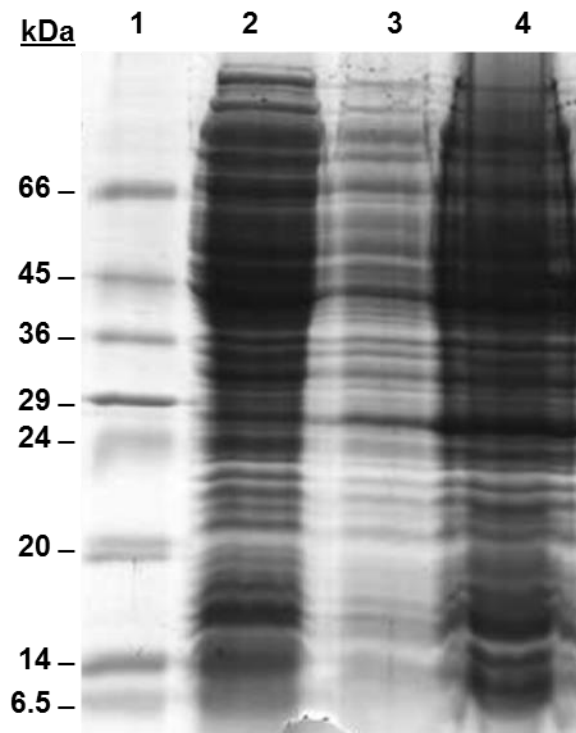


Figure 4.43: PAGE analysis of IMAC samples. Lane 1: Sigma low molecular weight markers; Lane 2: Unbound cell lysate (3); Lane 3: Unbound cell lysate (2); Lane 4: Cell lysate (1)

To ensure that the hyper-expressed recombinant lysostaphin had been specifically purified from the *E. coli* cell lysate, resulting IMAC fractions were also analysed by PAGE. Selected fractions from the elution of Peak A from IMAC purification of cell lysate (1) were selected as annotated in Figure 4.45 and analysed by PAGE (Figure 4.45).

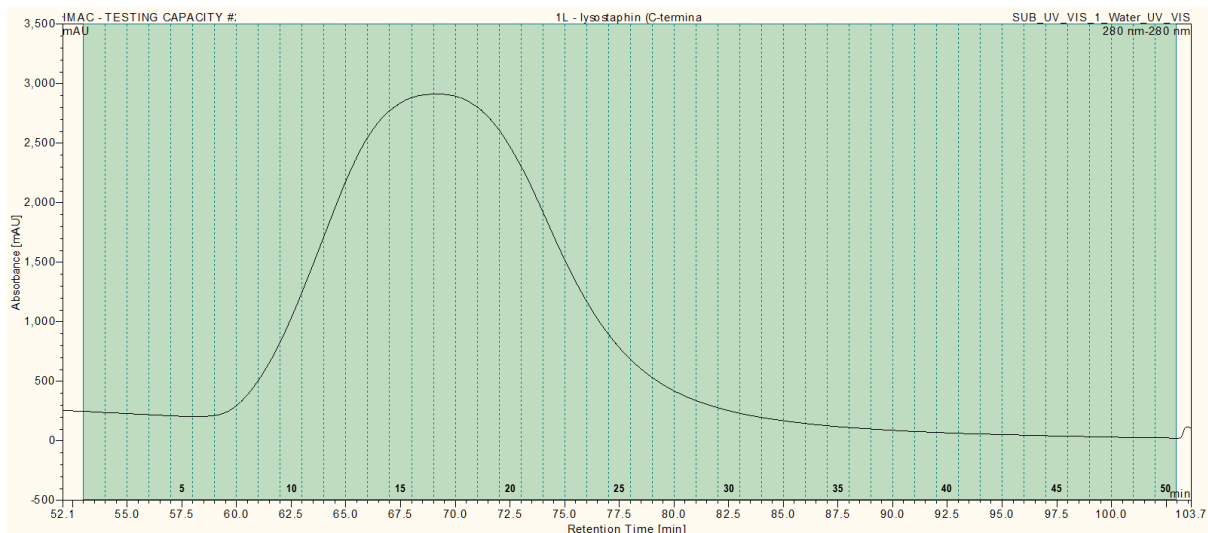


Figure 4.44: IMAC purification of recombinant lysostaphin from cell lysate (1). Fractions 4, 7, 10, 13, 16, 19, 22 and 25 fractions represent fractions that were analysed by PAGE.

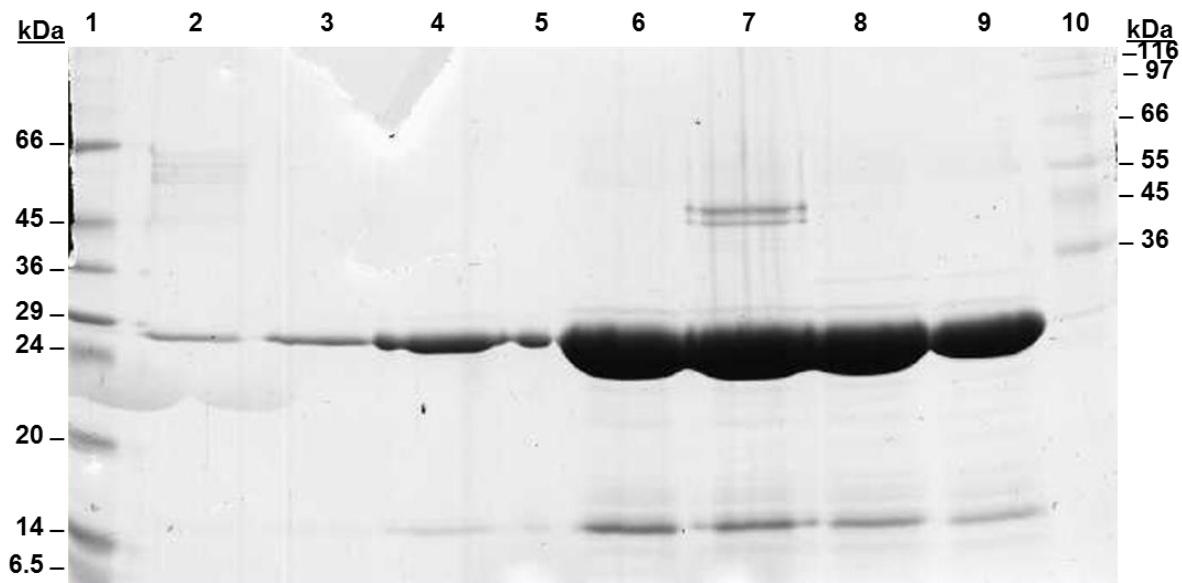


Figure 4.45: PAGE analysis of peak A from IMAC purification of cell lysate (1). Lane 1: Sigma low molecular weight markers; Lane 2: Fraction 4; Lane 3: Fraction 7; Lane 4: Fraction 10; Lane 5: Fraction 13; Lane 6: Fraction 16; Lane 7: Fraction 19; Lane 8: Fraction 22; Lane 9: Fraction 25; Lane 10: Sigma high molecular weight markers.

4.2.3.7 WCX analysis of IMAC purified protein

IMAC purification of C-terminally His-tagged recombinant lysostaphin (construct 1) appeared to be more efficient, in that a much higher quantity of the expressed recombinant protein in the cell lysate could bind to the column on the first application. IMAC peak B eluted after a

slightly longer retention time than IMAC peak A and therefore the protein collected during the elution of peaks A and B was subjected to WCX analysis. A fraction was selected from IMAC peak A and was desalted and concentrated prior to WCX analysis (Figure 4.46). Multiple fractions from the elution of IMAC peak B were also desalted and concentrated for subsequent WCX separation (Figure 4.47)

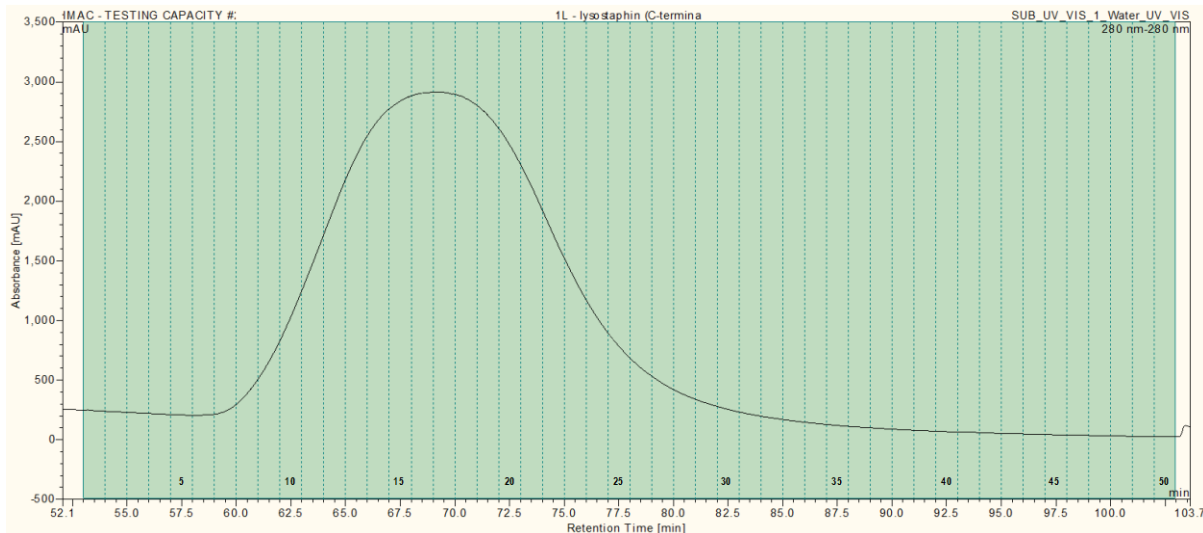


Figure 4.46: IMAC purification of C-terminally tagged recombinant lysostaphin (construct 3) from cell lysate (1). Fraction 17 was desalted and concentrated prior to WCX analysis of peak A.

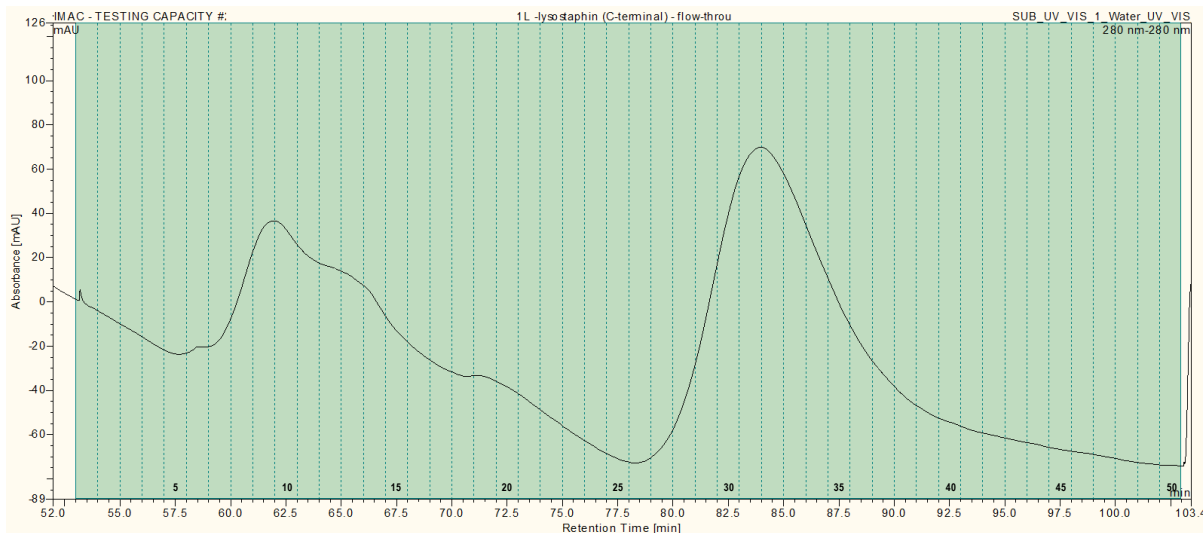


Figure 4.47: IMAC purification of C-terminally tagged recombinant lysostaphin (construct 3) from unbound cell lysate (2). Fractions 30-33 that were pooled, desalted and concentrated prior to WCX analysis of peak B.

WCX analysis showed that both IMAC peaks reflected the presence of one major distinct charge variant and around four minor more acidic charge variants (Figure 4.48). The major peak has a higher peak height in the separation of IMAC peak A than that of peak B, however this is related to the presence of a much lower protein concentration. The only noticeable difference observed in Figure 4.48 concerns the retention time of the major peak, which is slightly shorter during WCX separation of Peak B. This may reflect the purification of a slightly more acidic protein isoform, which exhibits slightly enhanced binding during IMAC purification.

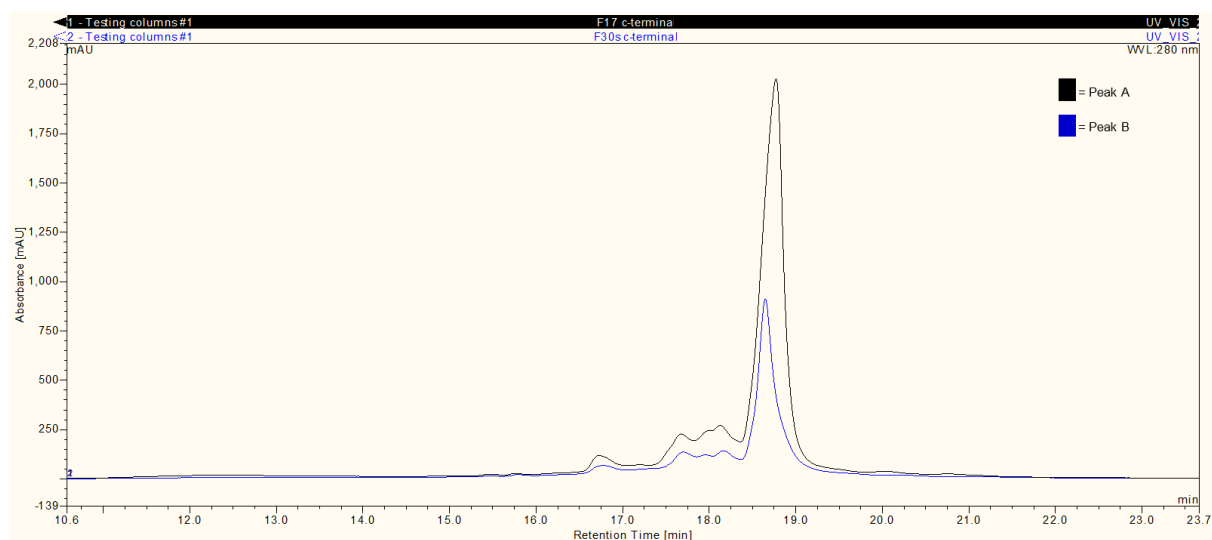


Figure 4.48: Comparison of WCX separations of IMAC purified C-terminally His-tagged recombinant lysostaphin (construct 3) from peaks A and B. Both separations reveal several minor peaks and one major distinct peak.

4.2.3.8 IMAC purification of recombinant lysostaphin

IMAC purification specifically binds His-tagged proteins, however in some cases non-His-tagged proteins can bind to the IMAC stationary phase. This form of unexpected binding may explain the variability of binding and differences in IMAC peak retention times observed during IMAC purification of C-terminally and N-terminally His-tagged proteins. Therefore recombinant lysostaphin with no His-tag sequence (construct 2) was harvested and applied to the ProPac[®] IMAC-10 column to establish whether the protein could bind to the column (Figure 4.49).

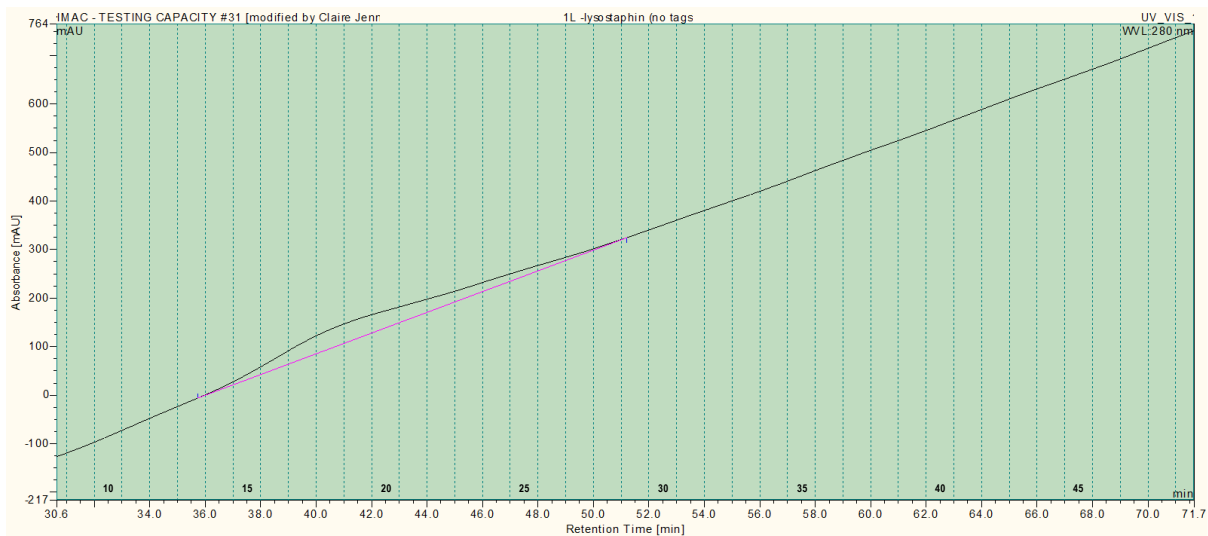


Figure 4.49: IMAC purification of recombinant lysostaphin with no His-tag (construct 2) from cell lysate. The purification yielded peak A as indicated. The rising baseline represented an increasing imidazole concentration with progression of the elution gradient. Fractions 20-26 were collected and subjected to SDS-PAGE analysis.

Protein eluted during the IMAC purification was collected and analysed by SDS-PAGE to ensure that the eluted protein possessed a molecular weight which corresponded with that of recombinant lysostaphin (construct 2), as demonstrated in Figure 4.50.

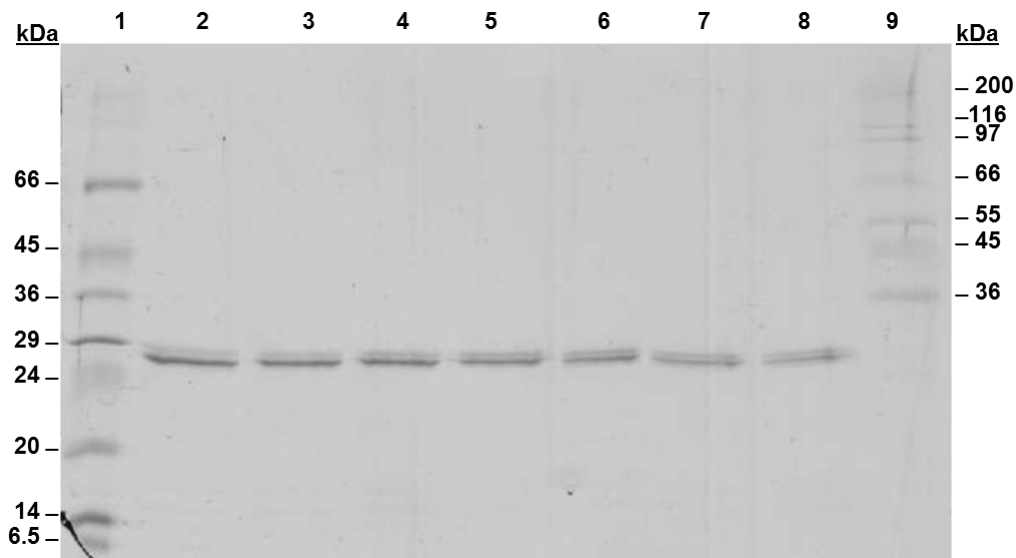


Figure 4.50: PAGE analysis of IMAC fractions. Lane 1: Sigma low molecular weight markers; Lane 2: Fraction 20; Lane 3: Fraction 21; Lane 4: Fraction 22; Lane 5: Fraction 23; Lane 6: Fraction 24; Lane 7: Fraction 25; Lane 8: Fraction 26; Lane 9: Sigma high molecular weight markers.

This initial purification of recombinant lysostaphin (construct 2) demonstrated that the recombinant protein possessed a slight ability to bind to the IMAC stationary phase, as demonstrated by peak A in Figure 4.49. The low concentration of purified protein suggests that the cell lysate may contain a small sub-population of recombinant lysostaphin, which can bind to an IMAC column. This finding was not very surprising considering that recombinant lysostaphin is a zinc metalloprotein. The protein which eluted in peak A may therefore have represented recombinant lysostaphin which did not harbour a zinc molecule and therefore the zinc binding domain of the protein was accessible for binding with the immobilised nickel bound to the IMAC stationary phase.

As this purification indicated that only a small proportion of the recombinant lysostaphin preparation was available for nickel binding, IMAC purification was performed again following production of a greater amount of recombinant lysostaphin. By applying an increased quantity of recombinant lysostaphin to the column, it should have been possible to purify larger concentrations of recombinant lysostaphin molecules which possessed IMAC binding affinity in the absence of a His-tag binding sequence. As demonstrated in Figure 4.51, IMAC purification of a more concentrated preparation of recombinant lysostaphin (construct 2) resulted in the elution of two peaks, A and B.

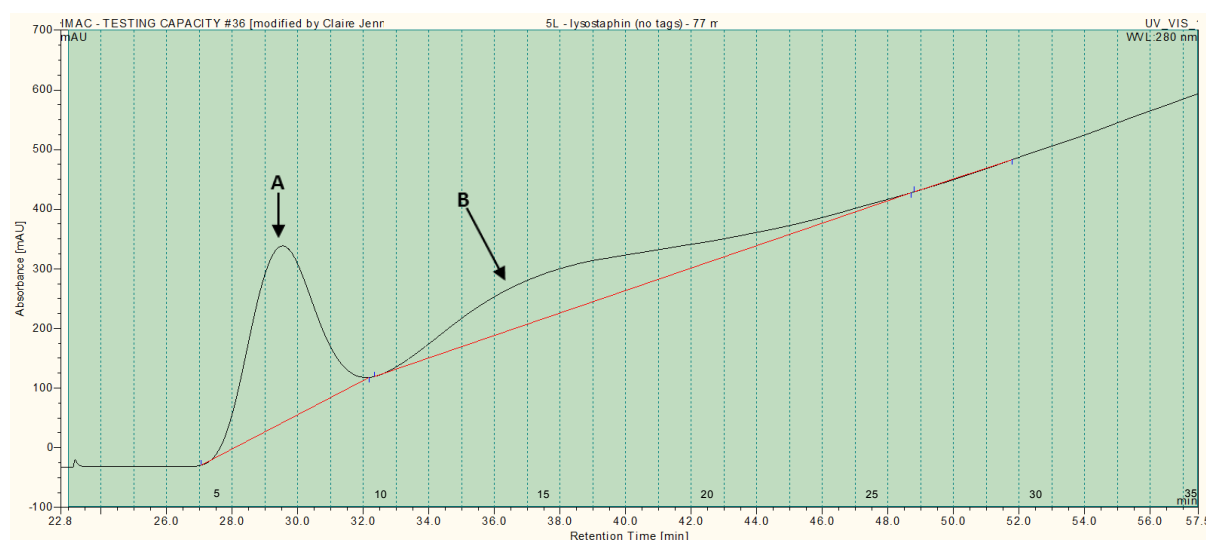


Figure 4.51: IMAC purification of recombinant lysostaphin with no His-tags (construct 2) from cell lysate. The cell lysate was harvested from 5 L of culture to achieve a higher protein concentration. The purification yielded peaks A and B, as indicated and unbound cell lysate (1) was collected manually at the start of the separation. The rising baseline represented an increasing imidazole concentration with progression of the elution gradient.

4.2.3.9 PAGE analysis of IMAC samples and fractions

All of the applied and collected samples were analysed by PAGE to check for the presence of recombinant lysostaphin (construct 2). PAGE analysis demonstrated that the majority of the recombinant lysostaphin present in the cell lysate did not bind to the column (Figure 4.52).

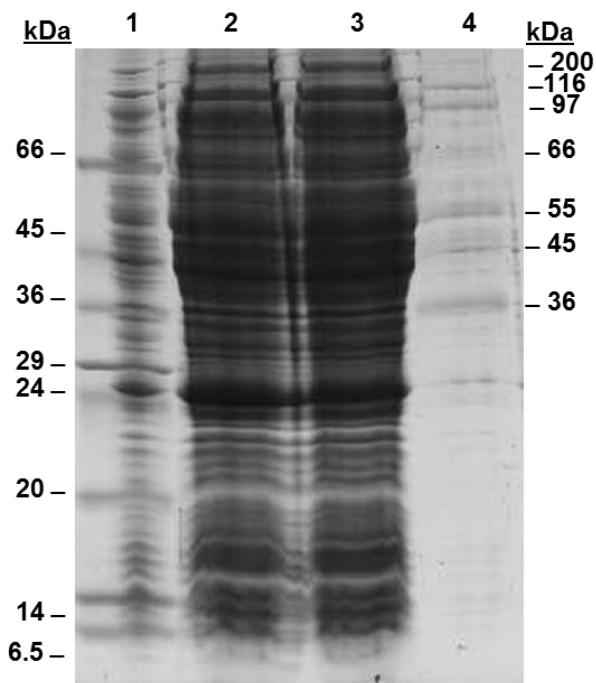


Figure 4.52: PAGE analysis of IMAC samples. Lane 1: Sigma low molecular weight markers (poor resolution due to protein contamination from adjacent lane); Lane 2: Cell lysate (1); Lane 3: Unbound cell lysate (2); Lane 4: Sigma high molecular weight markers

IMAC fractions were also analysed by PAGE to ensure that the IMAC peaks B and C reflected the presence of purified recombinant lysostaphin (construct 2). Fractions selected for PAGE analysis are indicated in Figure 4.53 and PAGE demonstrated that IMAC peaks B and C were composed of a purified protein with a molecular weight which corresponded with the 27.0 kDa mass of recombinant lysostaphin without any His-tags (Figure 4.54).

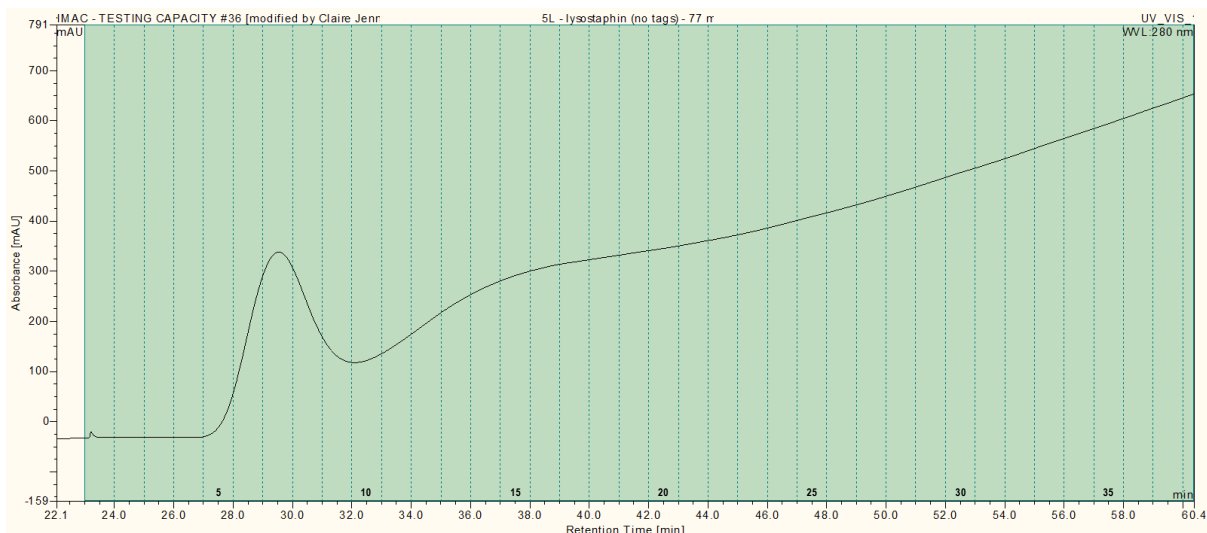


Figure 4.53: IMAC purification of recombinant lysostaphin (construct 2) from cell lysate (1). Fractions 7, 9, 11, 13, 15, 17 and 19 were analysed by PAGE.

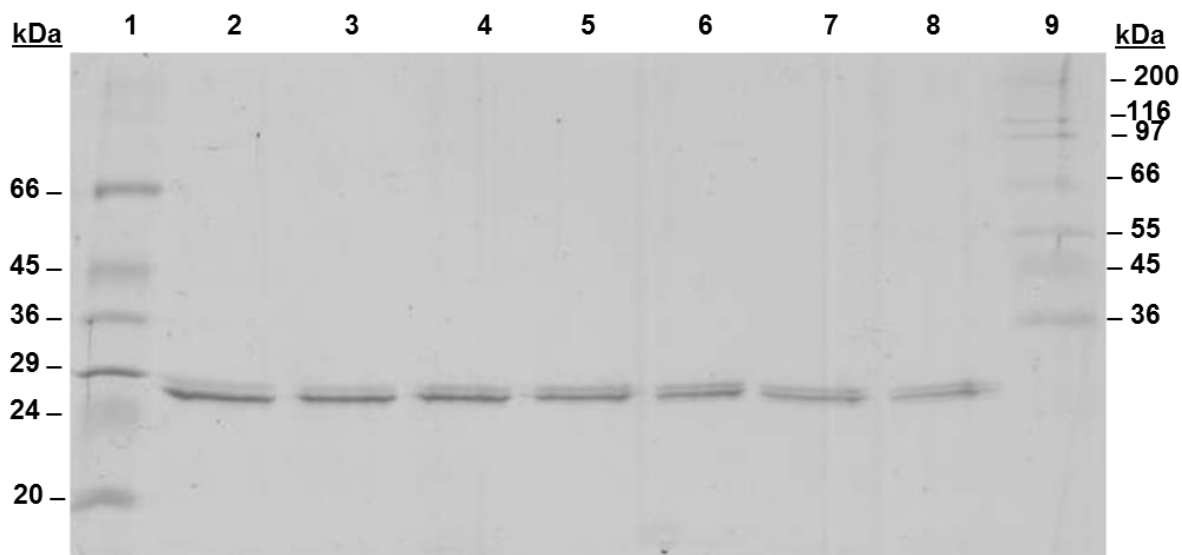


Figure 4.54: PAGE analysis of IMAC fractions. Lane 1: Sigma low molecular weight markers; Lane 2: Fraction 7 (peak A); Lane 3: Fraction 9 (peak A); Lane 4: Fraction 11 (peak B); Lane 5: Fraction 13 (peak B); Lane 6: Fraction 15 (peak B); Lane 7: Fraction 17 (peak B); Lane 8: Fraction 19 (peak B); Lane 9: Sigma high molecular weight markers

Protein eluted during IMAC purification was collected and subjected to WCX analysis, however chromatographic issues resulted in the poor resolution of peaks (data not shown). These results do however indicate that the sequence of mature recombinant lysostaphin possesses IMAC binding affinity, which is likely to be associated with the inherent metal binding ability of the protein. The results also indicate that a small proportion of recombinant

lysostaphin preparations may be composed of protein molecules, which do not possess zinc in their structure and therefore are available to participate during IMAC purification.

4.2.4 Discussion

Overall this work has provided further insight into the heterogeneous nature of recombinant lysostaphin preparations and the implications that charge heterogeneity has upon protein purification using IMAC. IMAC is a popular technique due to its ability to provide a very high degree of protein purity in an efficient manner. Whilst IMAC has been shown to purify recombinant lysostaphin to a very high degree, the series of experiments performed in this work indicate that protein heterogeneity can interfere with the efficiency of IMAC purification. Therefore caution should be taken when performing IMAC purification of recombinant lysostaphin but also other recombinant proteins, which may possess unknown charge heterogeneity

WCX separation of cell lysate containing recombinant lysostaphin expressed without or with C-terminal or *N*-terminal His-tags, revealed that each of the preparations demonstrated charge heterogeneity. *N*-terminally His-tagged recombinant lysostaphin (construct 1) demonstrated the greatest charge heterogeneity during WCX separation, whilst C-terminally His-tagged recombinant lysostaphin (construct 3) and recombinant lysostaphin without any His-tags (construct 2) demonstrated a lesser yet similar degree of charge heterogeneity. PAGE analysis confirmed that the observed peaks reflected the elution of charge-distinct protein isoforms with a molecular weight which corresponded with the expected masses of recombinant lysostaphin (constructs 1-3). Furthermore all of the analysed preparations exhibited retention behaviour that correlated with their respective theoretical isoelectric points.

Intriguingly WCX separation revealed that all of the recombinant lysostaphin preparations demonstrated the presence of the same or similarly charged acidic protein isoforms (peak A and B). This was a surprising finding considering that *N*-terminally His-tagged recombinant lysostaphin (construct 1) molecules were expected to possess a greater charge. This result therefore indicated that a proportion of the protein molecules within the *N*-terminally His-tagged recombinant lysostaphin (construct 1) preparation may have lost charge through modification or truncation. WCX separation of *N*-terminally His-tagged recombinant lysostaphin (construct 1) also revealed the presence of more basic peaks (peaks C and D), which may have reflected the presence of protein isoforms with a more preserved or less processed or modified *N*-terminal His-tag sequence. This experiment and previous WCX separations suggested that these more basic charge isoforms were exclusively formed within *N*-terminally His-tagged recombinant lysostaphin (construct 1) preparations.

Comparison of amino acid sequences in Section 4.2.1.1 indicated that the *N*-terminal His-tag sequence features serine residues which could be susceptible to phosphorylation. Phosphorylation of serine residues replaces neutral hydroxyl groups within the serine side chain with negatively charged phosphate groups (Rogakou *et al.*, 1998). Phosphorylation of serine groups within the *N*-terminal His-tag sequence may therefore lead to the formation of more acidic variants of *N*-terminally His-tagged recombinant lysostaphin (construct 1). α -*N*-6 gluconoylation of the *N*-terminus leads to loss of the positively charged free α -amino group at the *N*-terminal amino acidic residue. This modification could also lead to the formation of acidic variants of *N*-terminally His-tagged recombinant lysostaphin. Furthermore α -*N*-6 phosphogluconoylation would introduce an additional negatively charged phosphate group to the protein, resulting in the production of even more acidic protein variants. These modifications can be sensitively detected using MS analysis as discussed in Chapter 5.

Although *N*-terminally His-tagged recombinant lysostaphin (construct 1) exhibited the most charge heterogeneity, *C*-terminally His-tagged recombinant lysostaphin (construct 3) and recombinant lysostaphin without His-tags (construct 2) also demonstrated charge heterogeneity which was likely to have reflected some form of post-translational processing or modification. Culture analysis of the expression of these forms of recombinant lysostaphin would be desirable to establish whether the charge heterogeneity of recombinant lysostaphin increased over time, as was found to be the case for *N*-terminally His-tagged recombinant lysostaphin (Sections 3.5.3.11 and 3.5.3.12). Culture analysis would also provide more informative analysis of charge heterogeneity over time and would minimise concerns over culture conditions and batch-to-batch variability.

His-tag sequences are commonly used to facilitate highly specific binding during IMAC purification; however these experiments suggest that the *N*-terminal His-tag sequence should be used with caution. *N*-terminal His-tag sequences have already been found to undergo modification during expression in *E. coli* (Table 4.1) and these experiments would suggest the presence of an *N*-terminal His-tag is associated with such a modification or loss of charged *N*-terminal amino acids. Removal of the *N*-terminal His-tag sequence may therefore be desirable and can be accomplished using a site-specific protease, which should not interfere with the activity of recombinant lysostaphin. Cleavage is typically performed using a recombinant protease with an affinity tag which will permit subsequent removal by affinity purification (Terpe, 2006). However protease cleavage can be expensive and incomplete cleavage may increase preparation complexity further.

Alternatively the use of C-terminally His-tagged recombinant lysostaphin preparation (construct 3) may provide a less complex source of recombinant lysostaphin which can still be purified using IMAC. C-terminally His-tagged recombinant lysostaphin (construct 3) was shown to possess staphylolytic activity and therefore, despite being positioned adjacent to the C-terminal cell wall targeting domain sequence, the presence of a C-terminal His-tag sequence does not interfere with protein activity (Section 4.1.3.7). Furthermore as WCX analysis indicated that C-terminally His-tagged recombinant lysostaphin displays less charge heterogeneity than N-terminally His-tagged recombinant lysostaphin, it may be possible to create more homogeneous protein preparations by expressing these constructs using optimised culture conditions, as described in Section 3.4.3.12. Culture analysis during the expression of these constructs would provide a greater insight into how this could be achieved through optimisation of expression media, temperature and harvest points.

In this work, IMAC provided purification of recombinant lysostaphin, but also an insight into the differential retention behaviour which occurred as a consequence of charge heterogeneity. Although purification is the primary application of IMAC, the technique has also been used for topographic purposes to assess the surface localisation, accessibility and frequency of histidine residues within a protein (Hemdan *et al.*, 1989). As a consequence, IMAC has proven useful for the differentiation of modified recombinant protein variants, due to differences in the number of accessible histidine residues and therefore binding strength (Gaberc-Porekar and Menart, 2001, Ueda *et al.*, 2003).

As N-terminally His-tagged recombinant lysostaphin (construct 1) possessed considerable charge heterogeneity, it seemed likely that the charge-distinct protein isoforms would display different binding characteristics during IMAC purification. This theory was confounded by unusual protein binding patterns observed whilst testing the capacity of the ProPac[®] IMAC column. During these initial studies, the capacity of the column appeared poor and the application of increasing amounts of cell lysate did not result in proportionally increased peak heights. These results therefore suggested that N-terminally His-tagged recombinant lysostaphin (construct 1) exhibited poor binding efficiency.

To investigate this phenomenon further, a series of IMAC purifications were performed in which the column flow-through was reapplied to the column to see if further binding could be achieved. Initial application of cell lysate resulted in a typical peak (peak A) which appeared to display moderate binding strength during elution. Subsequent IMAC purification of unbound cell lysate resulted in the appearance of two peaks (peak B and C), which exhibited lesser and greater binding strength, when peak retention times were compared to that of protein eluted as peak A. A third IMAC purification performed following reapplication of

unbound cell lysate resulted in the retention of two more peaks (peaks D and E). Protein eluted within peaks D and E also exhibited lesser and greater binding strength, than that exhibited by protein purified during the first IMAC purification.

PAGE analysis of cell lysates provided confirmation that *N*-terminally His-tagged recombinant lysostaphin (construct 1) was not fully removed from the cell lysate until after three consecutive IMAC purifications had been performed. PAGE analysis of IMAC fractions also provided confirmation that the peaks observed during purification contained a protein with a molecular weight, which corresponded to that of recombinant lysostaphin (construct 1). Overall these results indicated that the charge heterogeneity of recombinant lysostaphin isoforms lead to incomplete and sequential purification of different protein isoforms upon repeated applications of cell lysate to the column.

The results also suggest that recombinant lysostaphin protein isoforms possess different binding strengths leading to different retention properties during IMAC purification. To establish whether retention time differences were attributable to different charge variants, WCX analysis was performed on protein eluted at different retention times (peak A and E). WCX indicated that the stronger binding affinity exhibited by protein eluted in peak E was associated with greater prevalence of more basic recombinant lysostaphin isoforms, whilst the moderate binding affinity exhibited by protein eluted in peak A was associated with the greater abundance of more acidic protein isoforms.

As *C*-terminally His-tagged recombinant lysostaphin (construct 3) appeared to possess a lesser degree of charge heterogeneity, IMAC purifications were also performed using this form of the protein. An initial purification resulted in the purification of a much larger quantity of protein, than was achieved during the initial purification of *N*-terminally His-tagged recombinant lysostaphin (construct 1). Reapplication of unbound cell lysate resulted in the elution of a much smaller peak during the second IMAC purification, which indicated that the protein was efficiently purified during the first purification. PAGE analysis confirmed that the observed peaks reflected the high-quality purification of a protein with a molecular weight which corresponded to that of *C*-terminally His-tagged recombinant lysostaphin (construct 3). Although the peaks resolved during repeated IMAC purification exhibited different retention times, WCX analysis did not suggest the retention time differences were attributable to differences in the abundance of particular charge variants.

It is evident that the retention behaviour of fusion proteins during IMAC is not very easy to predict due to the complexity of protein adsorption. During IMAC, protein adsorption is based upon multipoint interactions between specific groups on a protein structure and

individual binding sites distributed across the surface of the stationary phase. The strength of binding affinity is therefore largely dependent on the distribution of surface binding sites and the random, heterogeneous binding that occurs during multipoint interactions, resulting in a variety of binding energies (Johnson *et al.*, 1996, Johnson and Arnold, 1995). Greatest binding affinity is achieved when surface arrangements best match the distribution of functional groups within the protein structure, whilst less favourable arrangements result in lower affinity.

Multipoint interactions leading to protein adsorption are hindered if the His-tag sequence is not accessible on the protein surface (Terpe, 2006, Du *et al.*, 2008). As recombinant lysostaphin (constructs 1 and 3) can be purified using IMAC, it is likely that the *N*-terminal and *C*-terminal His-tag sequences are sufficiently exposed during purification. However the variable binding efficiency observed during purification of *N*-terminally His-tagged recombinant lysostaphin would suggest that some of the charge variants detected during WCX separation exhibit variable binding affinities. Loss of several amino acids from the *N*-terminus of the protein could contribute to reduced binding affinity if some of the histidine residues that compose the hexahistidine tag were lost through host proteolysis.

PTM of residues within the His-tag sequence would also be likely to influence binding affinities during IMAC purification. As the nucleophilic *N*-terminal amino groups possess metal binding affinity, neutralisation of this group by α -*N*-6 gluconoylation or α -*N*-6 phosphogluconoylation would weaken binding affinity slightly (Geoghegan *et al.*, 1999). Phosphorylation of serine residues within the His-tag sequence could have a more profound influence upon binding affinity due to the nature of the *N*-terminal His-tag sequence. Although serine residues do not participate in protein retention, the addition of negatively charged phosphate groups in close vicinity to the hexa-histidine residues may lead to steric hindrance of metal affinity, as demonstrated in Figure 4.55.

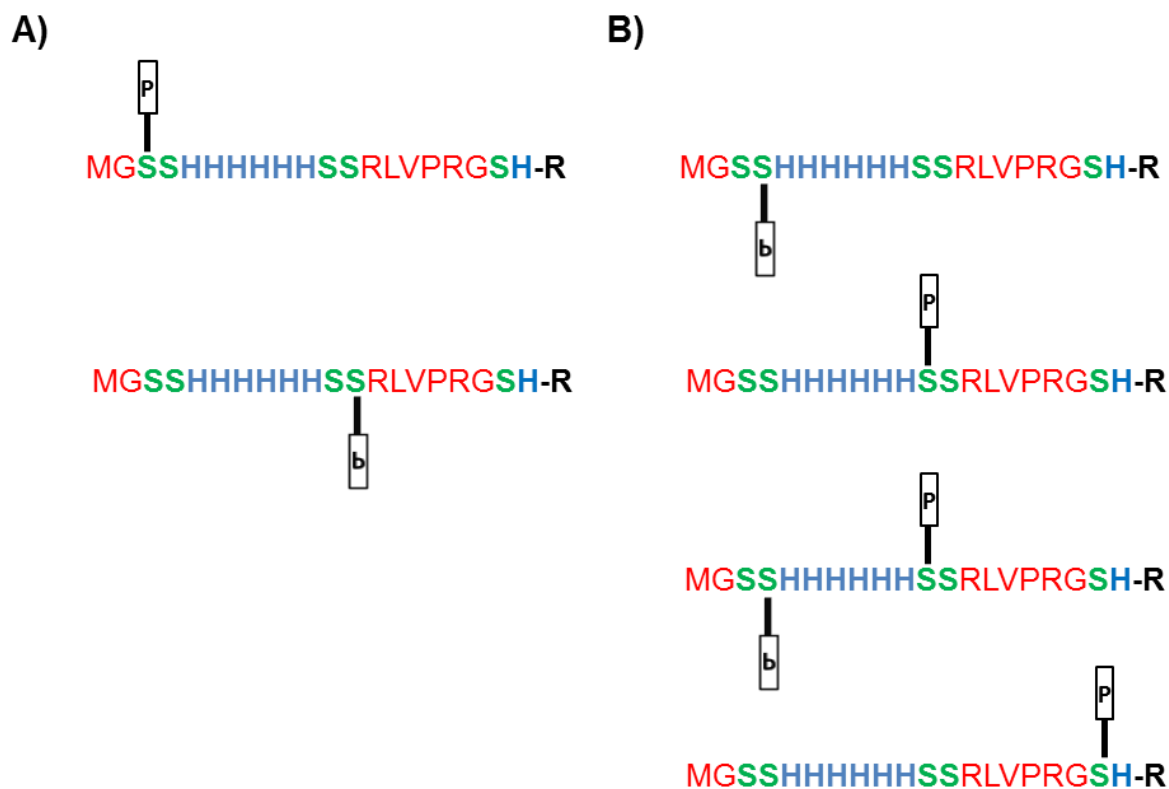


Figure 4.55: Sites of phosphorylation in *N*-terminal His-tag sequences and the influence upon binding affinity. A) Phosphorylation of Ser₃ or Ser₁₂ would be more likely to interfere with binding affinity through steric hindrance of preferred multipoint interactions involving His₅ and His₁₀, as postulated by Knecht *et al.*, (2009). B) Phosphorylation of Ser₄, Ser₁₁ or Ser₁₉ would be less likely to interfere with binding affinity.

Knecht *et al.*, (2009) identified that the 1st and 3rd or the 1st and 6th histidine residues within the hexa-histidine sequence provide the greater contribution to divalent interactions than the 2nd, 4th and 5th histidine residues do (Knecht *et al.*, 2009). Therefore phosphorylation of the side group's serine residues at the same axial rotation as the imidazole groups of the 1st and 6th residues could potentially weaken binding affinity through steric hindrance. As the *N*-terminal His-tag sequence contains five serine residues, up to five phosphorylations could possibly occur. Variation in the number and position of phosphorylation sites would therefore lead to varying binding affinities, such as those demonstrated by recombinant lysostaphin.

Although modification or truncation of the *N*-terminus could explain the variability of binding affinity, it was not clear why the sequential application of cell lysate did not initially result in the binding of protein molecules with the greatest binding strength. It is likely that this phenomenon was associated with heterogeneity of protein binding, high sample loading and

associated negative cooperative binding (Johnson *et al.*, 1996). Negative cooperative binding occurs when single-point binding of a ligand, decreases the affinity of the ligand for a second binding site. This phenomenon is commonly observed when large amounts of protein are loaded onto column, as overpopulation of binding sites prevents the protein from achieving surface arrangements that best match the distribution of functional groups on the protein structure. Net binding energy steadily decreases with increasing protein coverage, as less favourable binding sites become heavily populated (Johnson *et al.*, 1996).

These principles could explain the variability of binding affinity observed during IMAC purification, as postulated in Figure 4.56. Theoretically the presence of large amounts of protein would prevent stronger multipoint interactions from readily occurring as secondary binding sites would not necessarily be available due to overpopulation of binding sites. Therefore initial application of cell lysate would result in largely single-point, moderately strong interactions. Following the initial purification, the protein concentration of the cell lysate would decrease and therefore re-application of the cell lysate to the column would allow more multi-point interactions to occur due to the availability of more favourable binding sites. Weaker interactions would have also occurred at less favourable binding sites, as the stationary phase binding sites became more heavily populated at favourable sites.

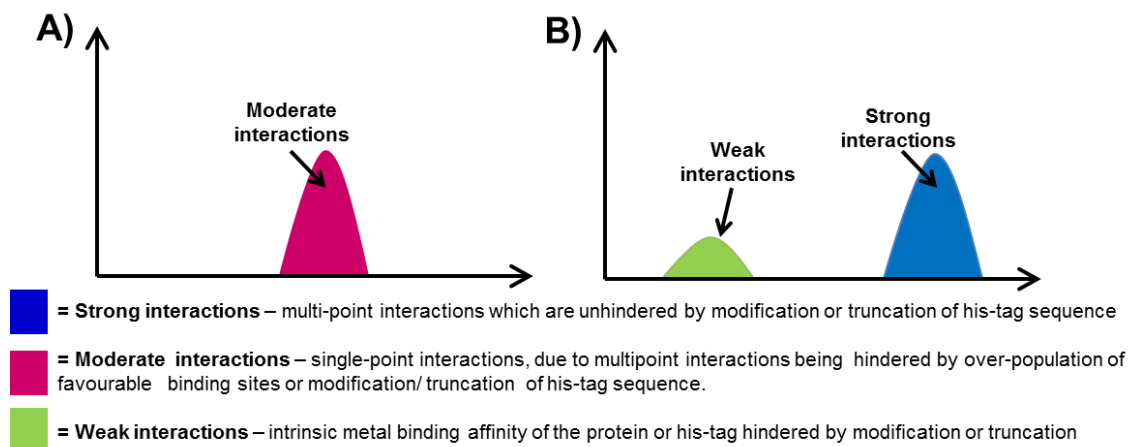


Figure 4.56: Model of variable binding interactions of during IMAC purification of recombinant lysostaphin (construct 1). A) Upon initial application of cell lysate, the ligand participated in single point interactions with the stationary phase, resulting in moderate interaction strength. Multipoint interactions may have been hindered by over-population of stationary phase binding sites or through modification or truncation of the His-tag sequence. B) Upon reduction in protein concentration, reapplication of cell lysate allowed stronger multipoint interactions to occur due to the increased availability of favourable binding sites. Weak interactions could also occur with lesser binding strength due to the greater availability of less favourable binding sites.

WCX separation of IMAC purified protein would also suggest that particular charge variants influenced binding affinity by influencing whether single or multi-point interactions could occur. Upon WCX separation, the eluted IMAC peaks were found to contain a number of charge variants, which could be explained by the heterogeneous nature of IMAC binding (Johnson and Arnold, 1995). The greater prevalence of acidic variants was associated with more moderate binding, which could reflect steric hindrance of multi-point binding due to modifications or truncation of the His-tag sequence. The presence of more basic recombinant lysostaphin isoforms was correlated with stronger binding affinity, which would support the theory that increased protein basicity was associated with protein variants with preserved His-tag sequences, which had not undergone modification or truncation. More comprehensive WCX analysis of protein eluted during these IMAC purification experiments would be desirable to support this retention behaviour model and provide additional confirmation of these findings.

Although this model of retention behaviour was developed by examining retention behaviour observed during the purification of *N*-terminally His-tagged recombinant lysostaphin (construct 1), the same principles can be applied to retention behaviour observed during the IMAC purification of *C*-terminally His-tagged recombinant lysostaphin (construct 3). WCX separation of purified protein eluted following IMAC purification of *C*-terminally His-tagged recombinant lysostaphin (construct 3), did not reveal any associations between charge variants and retention behaviour. However secondary application of cell lysate resulted in the elution of protein which displayed slightly greater binding affinity than protein eluted during the initial purification. Once again this result can be explained by over-population of the stationary phase during the initial purification, which will have reduced the incidence of stronger multipoint interactions. By the second purification, a greater number of favourable binding sites will have become available therefore permitting stronger multi-point interactions.

To ensure that retention time differences were not caused by chromatographic conditions, stationary and mobile phase conditions were kept as constant as possible. For instance, the stationary phase was stripped and charged with nickel ions prior to purification to ensure that charging insufficiencies did not lead to binding variability between purifications. Furthermore mobile phase conditions were kept constant to ensure that fluctuations in pH or imidazole concentrations did not lead to altered retention properties. IMAC was performed at neutral pH, which would ensure that imidazole nitrogens of histidine residues were present in their non-protonated form and therefore available for complexation (Sundberg and Martin, 1974).

Mobile phase buffers were also of high ionic strength to minimise non-specific electrostatic interactions (Gaberc-Porekar and Menart, 2001).

It was however less easy to control other factors, which may have occurred as a consequence of IMAC purification. For example, IMAC purifications are typically performed under aerobic and mildly oxidative conditions, which may lead to undesirable protein oxidation. Several amino acids are susceptible to metal-catalysed oxidation and therefore the presence of stationary phase metal ions can lead to destruction of amino acid side chains or result in cleavage of the protein backbone through metal-catalysed reactions within the internal column environment (Gaberc-Porekar and Menart, 2001). Furthermore the use of imidazole buffers is known to result in protein aggregation, which was investigated in Section 4.3. In light of these potential reactive factors, it could not be guaranteed that the structure of the zinc-binding domain or folding of recombinant lysostaphin had not been disrupted during the course of IMAC purification.

Experiments were also performed to establish whether recombinant lysostaphin without His-tags (construct 2) could bind to the column during IMAC purification. As a zinc metalloprotease, it is known that lysostaphin possesses metal affinity which could interact during IMAC purification. Whilst metal binding domains are only supposed to accept a specific metal ion, experiments by Warfield *et al* (2008) suggested that bound zinc molecules within the structure of recombinant lysostaphin can become substituted by nickel ions during IMAC purification (Warfield *et al.*, 2006, Clark *et al.*, 2009). This result would suggest that unoccupied zinc binding domains of recombinant lysostaphin may be able to interact with the nickel stationary phase. Alternatively IMAC is known to remove metal ions from metalloproteins, therefore bound nickel may have displaced bound zinc within the structure of recombinant lysostaphin (Terpe, 2003).

Application of concentrated cell lysate revealed that a small proportion of a recombinant lysostaphin (construct 2) preparation could bind fairly weakly to the column. This indicated that a small proportion of recombinant lysostaphin preparations may not contain the bound zinc molecule that was required for catalytic activity. Furthermore apoprotein forms of recombinant lysostaphin may have been detected as low abundance charge variants during WCX separation. Although WCX separation of the bound recombinant lysostaphin could not be achieved, PAGE analysis revealed that the peaks resolved during IMAC purification did contain a protein with a molecular weight that corresponded with that of recombinant lysostaphin (construct 2). Comparative WCX and IMAC purification of recombinant lysostaphin within a single cell lysate would have provided an insight into whether IMAC

purification perturbed the structure of recombinant lysostaphin through removal or replacement of metal ions or through oxidative damage.

Overall these experiments demonstrated that the charge heterogeneity of a recombinant preparation can complicate and interfere with the efficiency of IMAC purification. Whilst the presence of a C-terminal His-tag does not appear to interfere with IMAC purification of recombinant lysostaphin, the addition of an N-terminal His-tag leads to increased charge heterogeneity and inefficient IMAC purification due to the charge variants exhibiting variable binding affinities. To achieve improved product heterogeneity, removal of the N-terminal His-tag sequence or the use of a C-terminal His-tag sequence would be advisable. Alternatively a high degree of purification of recombinant lysostaphin could be achieved using CXC in the absence of His-tag sequences. As recombinant lysostaphin without His-tag sequences also exhibits charge heterogeneity, optimisation of culture and harvest conditions would be required to produce the protein in a more homogeneous state.

4.3 GF analysis of recombinant lysostaphin

4.3.1 Introduction

4.3.1.1 Aggregation during recombinant protein expression

Recombinant protein production in *E. coli* can be compromised by protein mis-folding and aggregation, which lead to poor yields and formation of insoluble inclusion bodies (Ghosh Moulick *et al.*, 2007). As recombinant protein expression puts excessive demands on cellular metabolism and translational apparatus, the host environment undergoes cellular stress. Should levels of denatured protein accumulate, then inclusion bodies form, often adversely affecting enzyme activity and potentially downstream processing (Sorensen and Mortensen, 2005, Cserjan-Puschmann *et al.*, 2006). Inclusion body formation is most likely to occur when the rate of heterologous expression dramatically exceeds that of host protein expression. This may also be due to protein folding regimes being overwhelmed, inappropriate translational speeds, expression location and culture conditions, such as temperature.

Eukaryotic proteins expressed heterologously in *E. coli* are more susceptible to misfolding and protein aggregation, due to differences between prokaryotic and eukaryotic chaperones (Haacke *et al.*, 2009). Molecular chaperones minimise protein aggregation by shielding exposed hydrophobic regions of non-native proteins and assisting the folding of newly synthesised and partially folded proteins into their native states (Haacke *et al.*, 2009, Derlinden *et al.*, 2008). The eukaryotic cytosol contains chaperones which are highly capable of cotranslational folding protein polypeptides as they leave the ribosome. Chaperones present in the bacterial cytosol may be incompatible with eukaryotic folding regimes, therefore simultaneous co-expression of molecular chaperones has been employed to try and improve the yield and quality of recombinant products derived from eukaryotic genes.

In addition to differences in molecular chaperones, differences in translational speeds can lead to protein aggregation. Prokaryotic translation rates are faster than eukaryotic translation rates, leading to greater conformational possibilities. During slow growth in *E. coli*, polypeptide elongation occurs at a rate of around 1 amino acid per second (aa/s), whilst during fast growth, elongation rates can increase to around 20 aa/s. Eukaryotic polypeptide elongation rates are thought to remain fairly constant and at a considerably slower rate of 3-8 aa/s (Siller *et al.*, 2010). The speed of recombinant protein translation can be further influenced by codon bias, as the translation of rare codons can lead to ribosomal pausing

and therefore a reduced protein synthesis rate. Slow translational speeds may restrict incorrect folding, whilst faster translational speeds may expose the emerging nascent polypeptide to a greater number of conformational influences.

In addition to increasing the rate of protein translation, the increased incubation temperatures required for recombinant protein expression support aggregate formation by encouraging hydrophobic interactions. As hydrophobic interactions are temperature dependent, reducing culture temperature can minimise hydrophobic interactions and also reduce the incidence of protein misfolding by decreasing translation rates. Induction temperatures as low as 18°C can be used, however misfolded proteins may still result as the reduced temperature can also adversely affect the biochemical activities of molecular chaperones and intrinsic folding rates (Siller *et al.*, 2010).

The location of protein expression also influences the likelihood of protein aggregation. When expressed intracellularly, proteins may exist in a reduced form, however upon cell lysis the proteins become exposed to an oxidizing environment which encourages disulfide bond formation (Hale *et al.*, 2004). When cysteine residues form disulphide bonds, covalent cross-linking creates protein aggregation and affects overall protein conformation. Furthermore the incidence of PTMs, such as deamidation, glycation and oxidation, can also lead to intramolecular cross-linking and therefore protein aggregates (Nagaraj *et al.*, 1996, Manning *et al.*, 2010, Cromwell *et al.*, 2006).

4.3.1.2 Aggregation during protein purification

It is evident that several factors lead to incorrect folding and aggregation of a recombinant protein during protein expression. However the recombinant protein preparation also remains susceptible to conformational changes during protein purification procedures. It is therefore important that the recombinant protein is processed quickly and considerately to ensure that product stability is not jeopardised during purification. Environmental temperature changes may of course influence protein stability; however the sample is unlikely to undergo heat denaturation during purification, as temperatures are generally conserved or controlled at cool or ambient temperatures.

The ionic strength and pH of buffer solutions used during protein purification therefore has a greater influence upon protein folding during purification. Fortunately the ionic strength and pH of buffers is typically selected to ensure that the structural and functional integrity of the protein is not unnecessarily perturbed during purification (Gadgil *et al.*, 2007). However in

some instances acidic buffers may be required to achieve elution during chromatography, which would increase the incidence of aggregation (Cromwell *et al.*, 2006). Sometimes elution buffers are supplemented with non-ionic surfactants, which minimise undesirable adsorption and aggregation during purification, though may result in oxidation (Manning *et al.*, 2010). Following purification, the protein may also encounter aggregation during ultrafiltration. During ultrafiltration, the protein concentration at the membrane surface can be much greater than that of the sample solution, leading to membrane fouling through aggregation formation within the membrane region (Cromwell *et al.*, 2006).

4.3.1.3 Aggregation during storage and formulation

Following purification, a recombinant product is stored until required for its intended application. Storage temperature is the most critical factor determining preservation of protein structure and prevention of protein aggregation. As mentioned previously high-temperatures lead to thermal denaturation, protein unfolding and aggregation. Likewise proteins can also become susceptible to cold denaturation, as proteins can retain mobility at -10°C. A storage temperature of below -30°C is therefore required to prevent cold denaturation (Manning *et al.*, 2010). However freezing temperatures also induce stress upon the protein structure by altering the pH and ionic strength, which influences the conformational and colloidal stability (Kueltoz *et al.*, 2008).

Ionic strength and pH can be altered during freezing, through crystallization of buffer salts leading to changes in protein conformation (Manning *et al.*, 2010). Furthermore the warming and cooling rates associated with the freeze-thaw process influence freeze concentration and the surface area of the ice water interface. When frozen, a sample undergoes freeze concentration as water is lost from the sample, leading to concentration of the solute, which increases protein interactions and therefore increases the likelihood of protein aggregation (Manning *et al.*, 1989). Freeze concentration tends to be more problematic with larger volumes and concentrations of a protein. Conversely increased sample protein concentrations decrease the amount of protein which is exposed to the ice-water interface (Kueltoz *et al.*, 2008). This is problematic as when surface-labile proteins are exposed to the ice-water interface, they can undergo surface induced denaturation (Manning *et al.*, 1989).

Due to the stress that the freeze-thaw process imposes upon protein structure, repeated freeze-thaw cycles are avoided as much as possible. A purified recombinant protein sample may however undergo freeze-drying to produce a dried solid state, which remains stable over the long-term. Although the removal of water by freeze-drying should theoretically

minimise protein degradation, the freeze-dry process can put stress upon protein structure. A protein may unfold during lyophilisation and aggregate during rehydration, producing protein dimers and high-molecular mass multimers (HMM) (Dalmora *et al.*, 1997). As a result, sucrose is frequently used as an excipient during protein formulation, as it can act as a stabilising agent in liquid and lyophilised protein formulations (Allison *et al.*, 1996). Protein stability is enhanced as the sucrose increases the thermal transition temperature of proteins, inhibiting unfolding and therefore irreversible aggregation. Although the addition of sucrose may increase the recovery of folded protein molecules, its presence may lead to glycation of the recombinant product (Gadgil *et al.*, 2007).

4.3.1.4 Protein structure and aggregation

The susceptibility to protein aggregation is also determined by protein structure. For instance, some proteins interact strongly or weakly *in vivo* to form oligomers or protein complexes. In addition, multimeric protein assemblies often interact with other biomolecules and participate in signal transduction and substrate binding (Heck and van den Heuvel, 2004). Protein oligomerisation is thought to improve protein stability, minimising the risk of proteolysis and thermal denaturation. The addition of a non-covalent cofactor can also induce subunit association which further enhances resistance towards chemical and thermal denaturation. Metal cofactors reduce conformational heterogeneity and encourage transition to the folded state (Kaltashov *et al.*, 2006). The incidence of aggregation and insolubility of recombinant proteins may also be reduced by the presence of fusion tags, such as GST and MBP, which were developed to enhance the solubility of the expressed protein (Cheng and Lee, 2010).

4.3.1.5 Aggregation of recombinant lysostaphin

As recombinant lysostaphin demonstrated charge heterogeneity, recombinant protein preparations were analysed for signs of protein aggregation. It is important to assess whether a recombinant protein preparation is affected by aggregation, as protein aggregates and particulates may elicit an immune response if clinically administered (Rosenberg, 2006, Cromwell *et al.*, 2006). As protein cross-linking and aggregation can influence the charge of a protein, it was therefore possible that the protein isoforms detected during CXC separation reflected the presence of dimeric or larger HMMs (Cromwell *et al.*, 2006). Furthermore, in Section 2.4.3.2, SDS-PAGE analysis of *N*-terminally His-tagged recombinant lysostaphin

(construct 1) suggested that hyper-expression may result in the production of soluble and insoluble fractions.

Unlike the expression of eukaryotic genes in *E. coli*, the expression of recombinant lysostaphin is advantaged by the fact that the gene is derived from a prokaryotic origin, *S. staphylolyticus*. Therefore it is less likely that protein folding will be detrimentally affected by the absence of suitable prokaryotic chaperones. In addition, the prokaryotic origin of lysostaphin will mean that native lysostaphin and recombinant lysostaphin are translated at a similar elongation rates in *S. staphylolyticus* and *E. coli* respectively. Expression of recombinant lysostaphin was performed under standard expression temperatures of 30°C or 20°C. If expression was performed at 37°C, the optimal growth temperature for *E. coli*, aggregate formation would have been encouraged. As expression was performed at 30°C or 20°C, these temperatures would make the expressed recombinant lysostaphin less susceptible to protein misfolding.

As the amino acid sequence of recombinant lysostaphin does not contain any cysteine residues, the structure of the protein will not contain any disulphide bonds and therefore the protein should not be susceptible to this form of covalent aggregation. Covalent aggregation could however occur through oxidation and cross-linking of tyrosine residues, forming bityrosine (Cromwell *et al.*, 2006). The amino acid sequence of *N*-terminally His-tagged recombinant lysostaphin (construct 1) contains sixteen tyrosine residues which have the potential become cross-linked in such a manner. Reversible protein aggregation can also occur following relatively weak, non-covalent protein interactions. The reversibility of the interactions often result from alterations in pH or protein concentration (Cromwell *et al.*, 2006).

N-terminally His-tagged recombinant lysostaphin is regarded as a stable protein *in vitro* following calculation of the proteins instability index by ProParam analysis (Appendix 7.82). In Section 4.1, recombinant lysostaphin was found to exhibit the expected staphylolytic activity, which indicated that the protein was unlikely to be mis-folded or aggregated to a state that interfered with activity. Furthermore, the presence of a bound zinc ion should also theoretically minimise the incidence of protein aggregation, through the strength of zinc metal coordination. The zinc binding domain of recombinant lysostaphin is known to be a catalytic zinc site, which is distinct from a structural zinc site and therefore should not act to stabilize the tertiary structure of recombinant lysostaphin (McCall *et al.*, 2000). However as recombinant lysostaphin is devoid of cysteine residues it seems logical that the bound zinc molecule will influence the stability and conformation of the protein.

During the purification of recombinant lysostaphin, it became apparent that certain conditions could affect the solubility of the protein (Sections 2.5.3.3 and 2.5.3.8). For instance, purified protein preparations could not be concentrated by ASF without protein precipitation. In some instances it was possible to regain solubility by adding salts to the resuspension, however this solution was not compatible with subsequent CXC analysis. As ASF could not be used, protein concentration and buffer exchange was achieved through ultrafiltration. During ultrafiltration, recombinant lysostaphin was exchanged into water and whilst visible aggregation was rarely observed, it was possible that non-visible aggregated particles may have been present within the concentrated sample. The development of a rapid analysis strategy therefore minimised the incidence of protein aggregation by eliminating the requirement for ultrafiltration (Section 3.5).

Following the expression of recombinant lysostaphin, the temperature of the protein was maintained at around 4°C during storage or 22°C whilst handling. Freezing of samples was avoided where possible to minimise stress upon the protein structure. However purified recombinant lysostaphin was frozen following large-scale IMAC purification and dialysis, prior to lyophilisation. Although lyophilisation provided long-term stability of recombinant lysostaphin, it was not possible to completely resuspend the lyophilised protein prior to CXC separation. The macroscopic particulates could be removed by brief centrifugation, however this interfered with subsequent IMAC and CXC analysis through poor peak resolution and height.

During the development of a rapid analysis strategy, harvested cells and cell lysates were frozen to try and maximise sample throughput (Section 3.5.3.7). However it was found that the freeze-thaw process interfered with the charge of recombinant lysostaphin isoforms, possibly through freeze concentration or cold denaturation. Following separation of recombinant lysostaphin isoforms, eluted fractions were stored at 4°C as frozen storage would not have been suitable considering that the samples were within sodium phosphate buffers. Sodium phosphate is known to crystallise out during freezing, which would therefore alter the pH and ionic strength of the samples, potentially leading to protein interactions and potentially aggregation (Kuelzto *et al.*, 2008).

In this work, gel filtration was used to assess whether protein aggregation occurred during the recombinant expression of lysostaphin. Protein aggregation of recombinant protein preparations is almost exclusively analysed using gel filtration (Rosenberg, 2006). In Section 2.5.3.3, preparative GF was used to provide secondary purification of recombinant lysostaphin. However preparative GF provides poor resolution of protein aggregates due to larger amounts of protein being loaded, therefore an analytical GF column was used to

provide enhanced resolution of smaller amounts of protein. GF can typically resolve protein species that demonstrate approximately 25% difference in their hydrodynamic radii, and resolution is further reduced if dilute samples are being analysed (Cromwell *et al.*, 2006). Resolution is inversely related to the dynamic range over which molecular masses can be separated, therefore GF typically has a limited dynamic range (Arakawa *et al.*, 2010). It is therefore important that a GF resin is selected, which provides a good compromise between dynamic range and resolution.

Analysis of potential aggregation of recombinant lysostaphin was performed with an analytical GF column, which could provide enhanced resolution. The Agilent Zorbax® GF-250 (4.6 x 250 mm) column is a surface-stabilised, hydrophilic column commonly designed for the separation of proteins. This column has a dynamic range of between 4 and 400 kDa, however provides linear separation between 10 and 250 kDa, therefore should provide good separation of recombinant lysostaphin (27.0-29.3 kDa) and any aggregated species. The stationary phase is composed of 4 µm spherical silica particles, providing efficient and high resolution separation. In addition the separation can be performed at 1.0 ml/min which permits fairly rapid separation. This column was therefore used to analyse recombinant lysostaphin preparations to assess for presence of mass distinct protein species, with a number of aims:

Aims:

- To assess the stability of recombinant lysostaphin preparations during storage and formulation.
- To establish whether recombinant lysostaphin becomes aggregated following purification using gel filtration.
- To evaluate whether protein isoforms separated using CXC exhibited aggregation using gel filtration.

4.3.2 Methods

4.3.2.1 Buffers

All buffer compositions are outlined in Appendix 7.354.

4.3.2.2 Equipment

All equipment used during GF analysis of recombinant lysostaphin is outlined in Appendix 7.355.

4.3.2.3 Sample preparation

Sample preparation is described in Appendix 7.357.

4.3.2.4 PAGE analysis of protein stability after prolonged storage

Purified and concentrated recombinant lysostaphin preparations were stored in solution at 4°C until required for analysis. During analysis the preparations were transferred to ice to ensure that the protein was stored at cool temperatures as much as possible. Following prolonged storage, a selection of recombinant lysostaphin preparations (preparations 3, 4, 6, 13 and 19) were subjected to 12% (w/v) SDS-PAGE analysis (Appendix 7.15) to establish whether the protein remained stable and retained its expected molecular weight during storage.

4.3.2.5 GF Analysis

GF analysis was performed on fractions which had eluted following IMAC purification of recombinant lysostaphin under non-denaturing (Appendix 7.359) and denaturing conditions (Appendix 7.360). GF analysis was also performed on fractions eluted following WCX separation of recombinant lysostaphin isoforms (Appendix 7.361).

4.3.3 Results

4.3.3.1 PAGE analysis of protein stability after prolonged storage

Following purification, several recombinant lysostaphin preparations were stored in solution at 4°C for prolonged periods of time. The samples were removed from storage occasionally to obtain an aliquot for chromatographic separation or assay. Whilst removed, the samples were stored on ice and swiftly returned to 4°C to ensure that the protein was not subjected to fluctuations in temperature. To assess whether the recombinant lysostaphin preparations remained stable during storage, the samples were analysed by SDS-PAGE. As shown in Figure 4.57, the majority of the samples remained remarkably stable despite prolonged storage at 4°C.

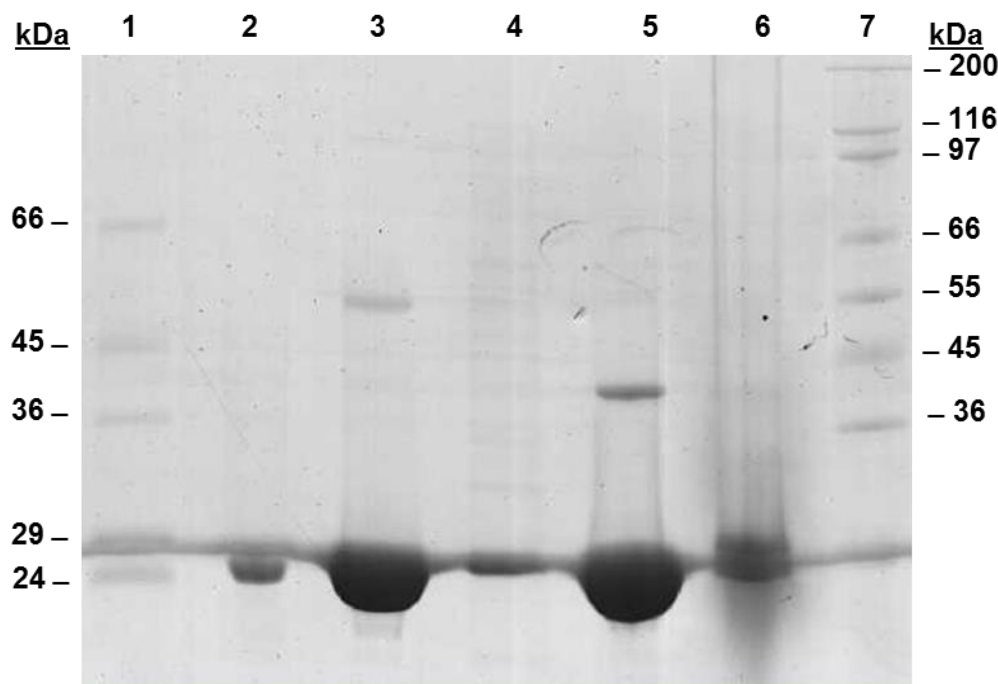


Figure 4.57: PAGE analysis of recombinant lysostaphin preparations following storage at 4°C. Lane 1: Sigma low molecular weight markers; Lane 2: N-terminally His-tagged recombinant lysostaphin (construct 1; preparation 19) at 311 days post-expression; Lane 3: C-terminally His-tagged recombinant lysostaphin (construct 3, preparation 4) at 140 days post-expression; Lane 4: C-terminally His-tagged recombinant lysostaphin (construct 3, preparation 3) at 260 days post-expression; Lane 5: C-terminally His-tagged recombinant lysostaphin (construct 3. Preparation 13) at 225 days post-expression; Lane 6: N-terminally His-tagged recombinant lysostaphin (construct 1, preparation 6) at 90 days post-expression; Lane 7: Sigma high molecular weight markers.

Some preparations of recombinant lysostaphin (construct 3) seemed to retain their expected molecular weights upon analysis at 140 to 260 days, which suggested that the protein

remained stable in solution, whilst stored at 4°C. Intriguingly one preparation of recombinant lysostaphin (construct 1) appeared to maintain its expected molecular weight for up to 311 days, whilst another preparation appeared to have undergone degradation after only 90 days storage. The latter sample was analysed more frequently during the optimisation of protein separation, therefore it is likely that this protein was subjected to mild temperature fluctuations on a more regular basis than the other samples were.

4.3.3.2 Influence of lyophilisation on the solubility of recombinant lysostaphin

As described in Section 3.4.3.3, lyophilised recombinant lysostaphin did not resuspend very well after freeze-drying, which complicated downstream processing. Figure 4.58 demonstrates how protein adsorption was dramatically reduced following application of *N*-terminally His-tagged recombinant lysostaphin (construct 1) which could only be partially solubilised following lyophilisation. Poor peak heights were observed following application of between 100 and 1000 µg of re-suspended lyophilised recombinant lysostaphin. However the application of liquid preparations of between 8 and 40 µg of recombinant lysostaphin demonstrated significantly greater adsorption, which could typically be observed during IMAC purification.

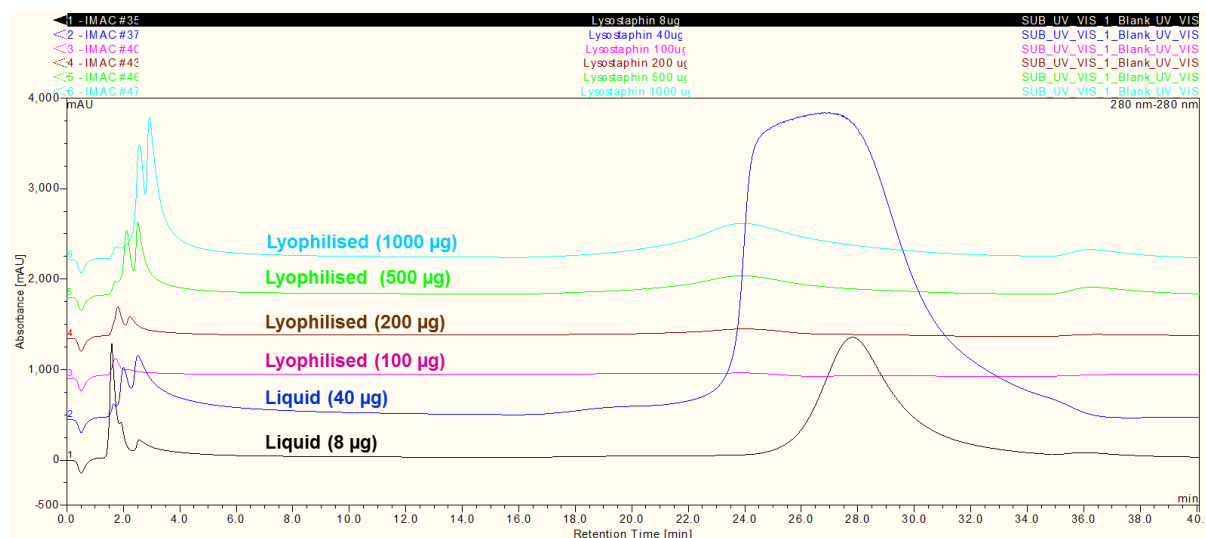


Figure 4.58: Comparison of protein binding concentrations following IMAC purification of fresh recombinant lysostaphin (construct 1) and re-suspended lyophilised recombinant lysostaphin (construct 1). IMAC purification revealed apparent inconsistencies between protein concentration and protein binding with fresh and lyophilised samples.

It was thought that this apparent lack of binding occurred as a result of the lyophilised recombinant protein not fully solubilising in water. Precipitation of the recombinant lysostaphin would have led to heterogeneous distribution of the protein within the sample, which would have compromised injection of the correct concentrations of protein within the sample, due to precipitation.

4.3.3.3 GF of fractions eluted following IMAC purification

Recombinant lysostaphin (construct 1) was purified by IMAC, as demonstrated in Figure 4.59. IMAC resulted in the elution of a very broad peak, from which fractions were collected and a single fraction was taken and subjected to GF

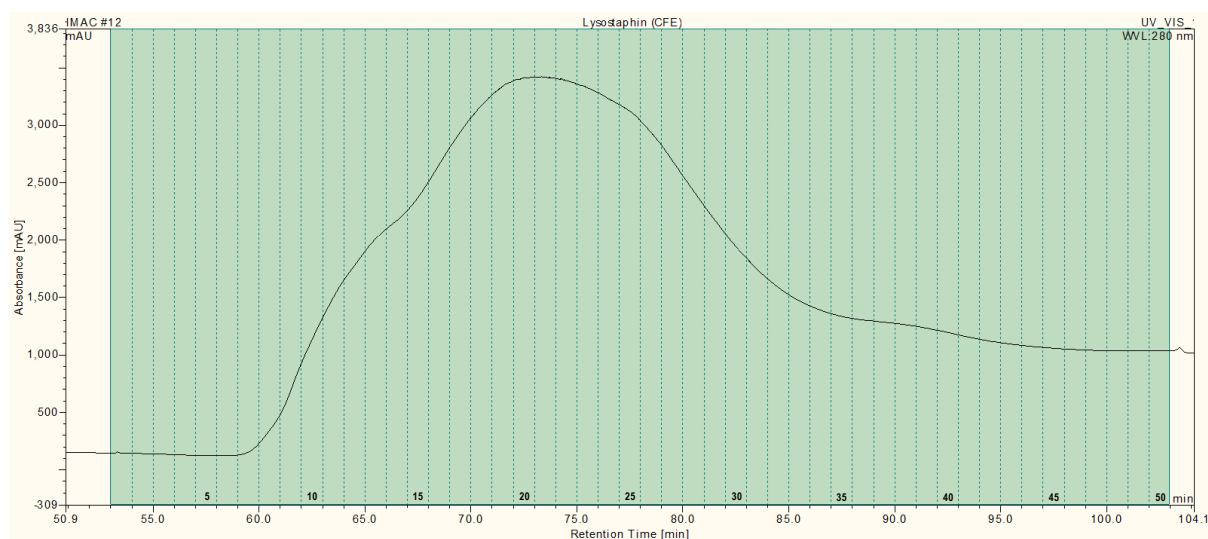


Figure 4.59: IMAC purification of N-terminally His-tagged recombinant lysostaphin (construct 1). Fraction 13 was selected for GF separation.

GF separation resulted in the elution of two major peaks and the resolution of multiple minor peaks, which indicated that a number of different molecular weight species were present within the eluted IMAC fraction (Figure 4.60). This result was rather unexpected and it was unclear whether the difference in molecular weight could be attributable to aggregation, which may have occurred following expression, during purification or during storage, as GF was performed 24 h after IMAC purification.

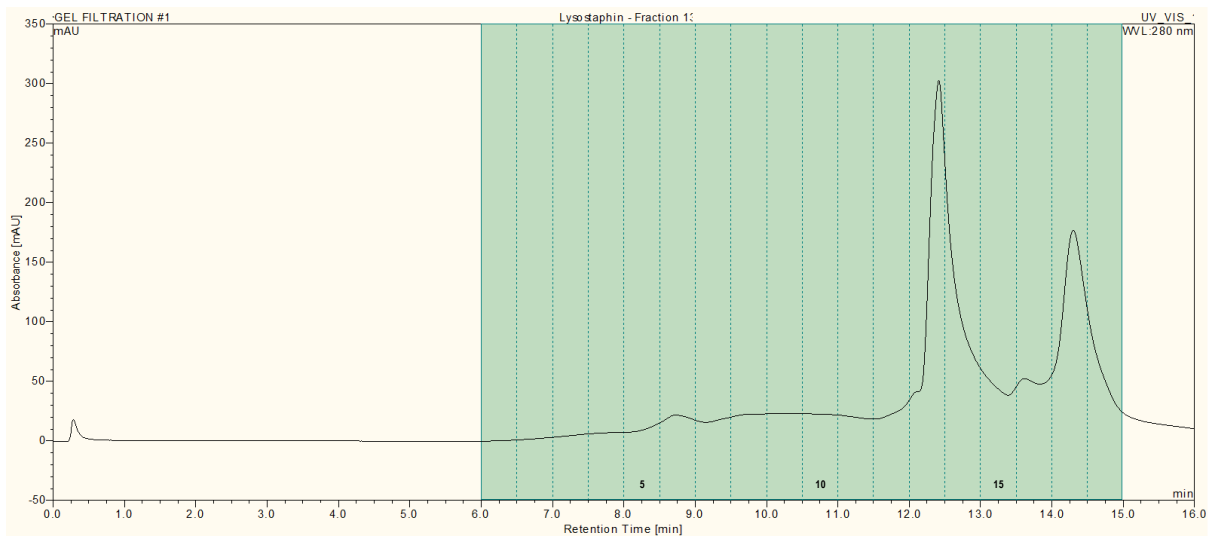


Figure 4.60: Gel filtration of IMAC fraction 13. Multiple peaks were resolved during GF demonstrating that the fraction was composed of different molecular weight species. Fractions 13-17 were subjected to PAGE analysis.

To assess whether differences in molecular weight species could be detected during PAGE analysis, selected fractions were subjected to PAGE analysis (Figure 4.61). PAGE analysis indicated that the GF peaks reflected a protein with a molecular weight of just over 26 kDa, which corresponded with the mass of recombinant lysostaphin (29.3 kDa). The bands did not reveal any difference in the molecular weights of protein eluted during GF, despite resolution of distinct molecular weight species. However the denaturing conditions applied during SDS-PAGE will have disrupted aggregated species.

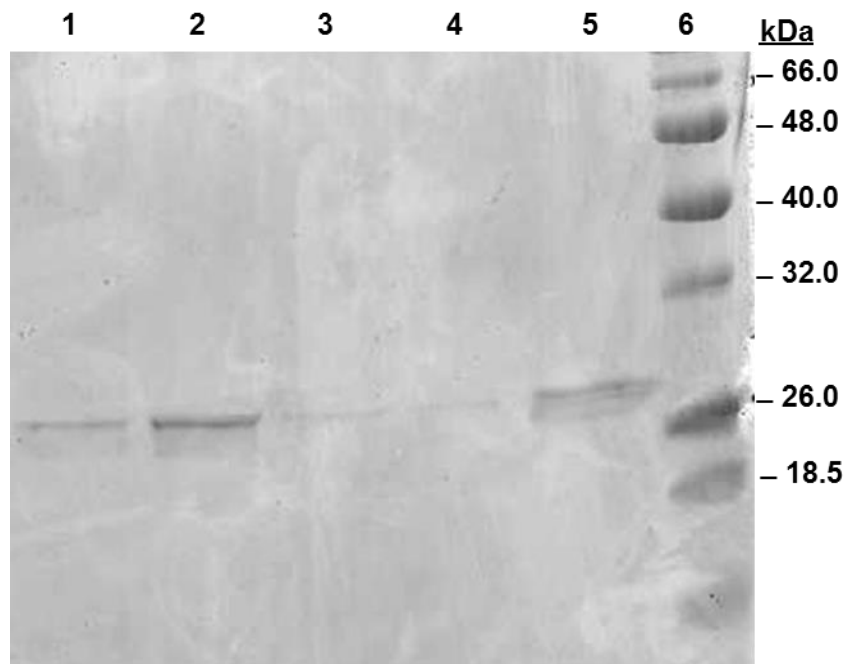


Figure 4.61: PAGE analysis of selected GF fractions. Lane 1: Fraction 13; Lane 2: Fraction 14; Lane 3: Fraction 15; Lane 4: Fraction 16; Lane 5: Fraction 17; Lane 6: NEB broad molecular weight markers.

4.3.3.4 GF of fractions eluted following IMAC purification under denaturing conditions

To establish whether different molecular weight species formed through aggregation following expression or during IMAC purification, IMAC was performed under denaturing conditions by supplementing the chromatographic buffers with urea. IMAC purification resulted in a broad peak from which eluted protein was collected and selected fractions were subjected to GF analysis (Figure 4.62).

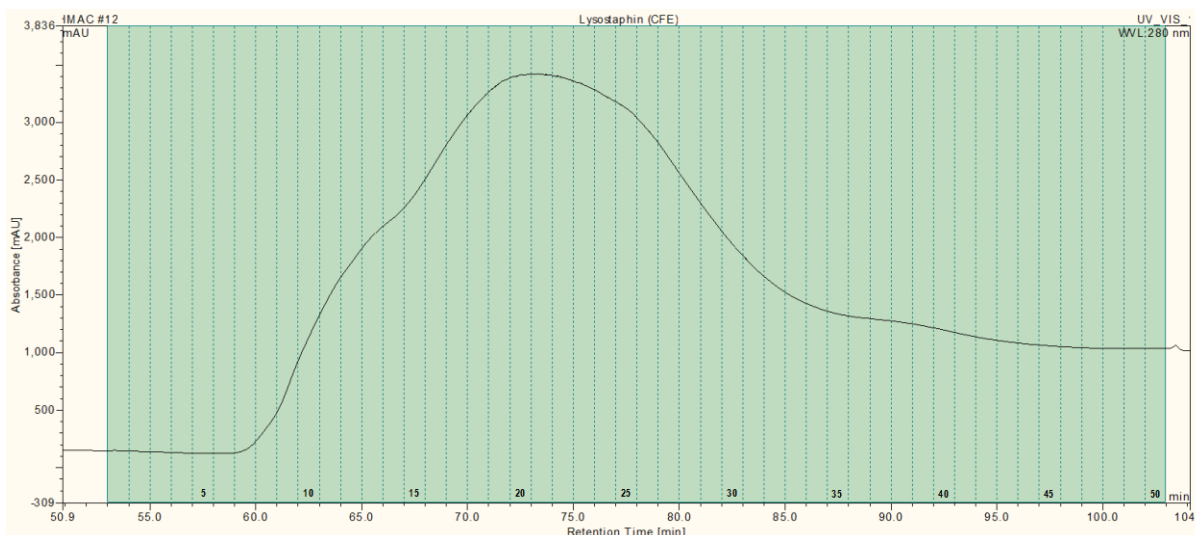


Figure 4.62: IMAC purification of *N*-terminally His-tagged recombinant lysostaphin (construct 1) under denaturing conditions. Fractions 12, 24, 32 and 36 were subjected to GF separation.

Theoretically if the multiple peaks observed previously resulted from aggregated species, then the supplementation of IMAC buffers with high concentrations of urea, should have dissociated the pre-formed aggregated species. In addition, by supplementing the buffers during IMAC, the risk of aggregation during purification and storage was reduced and therefore GF analysis should have revealed fewer peaks. This however was not the case with the elution of multiple peaks during GF (Figure 4.63). This result indicated that the major peak eluting at 12.3 min may have reflected native recombinant lysostaphin, whilst peaks eluting after 13 min reflected smaller molecular weight species, which may have resulted from protein truncation or degradation.

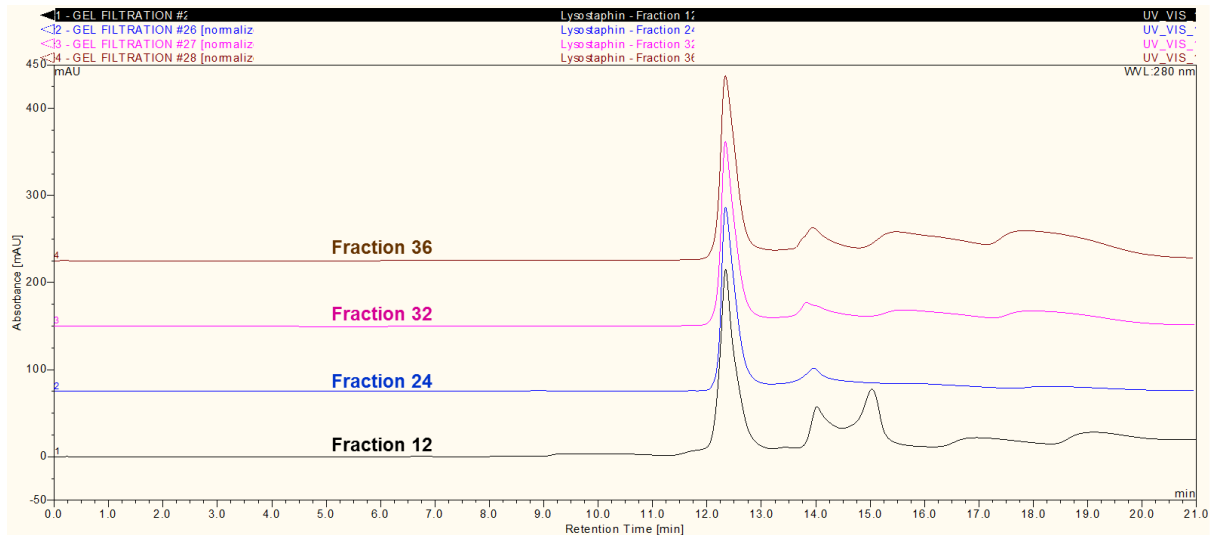


Figure 4.63: Gel filtration of IMAC fractions. Multiple peaks were resolved during GF demonstrating that each fraction was composed of different molecular weight species.

Interestingly GF separation of fraction 12 resulted in greater abundance of smaller protein species, which in conjunction with the previous experiment, suggest that smaller protein isoforms are more poorly retained during IMAC. IMAC binding of recombinant lysostaphin was investigated further in Section 4.2. The apparent molecular mass heterogeneity observed during GF analysis of each IMAC fraction may have also been attributable to the charge heterogeneity of recombinant lysostaphin, which may have increased the complexity of peaks eluted during GF separation.

4.3.3.5 GF of fractions eluted following WCX separation of recombinant lysostaphin isoforms

In order to minimise sample heterogeneity and to assess whether charge distinct WCX peaks occur as a consequence of protein aggregation, WCX fractions from a selected WCX separation were subjected to GF analysis. WCX separation of *E. coli* cell lysate harvested at 10.5 h post-induction during culture analysis yielded four distinct peaks representing different charge isoforms (Figure 4.64).

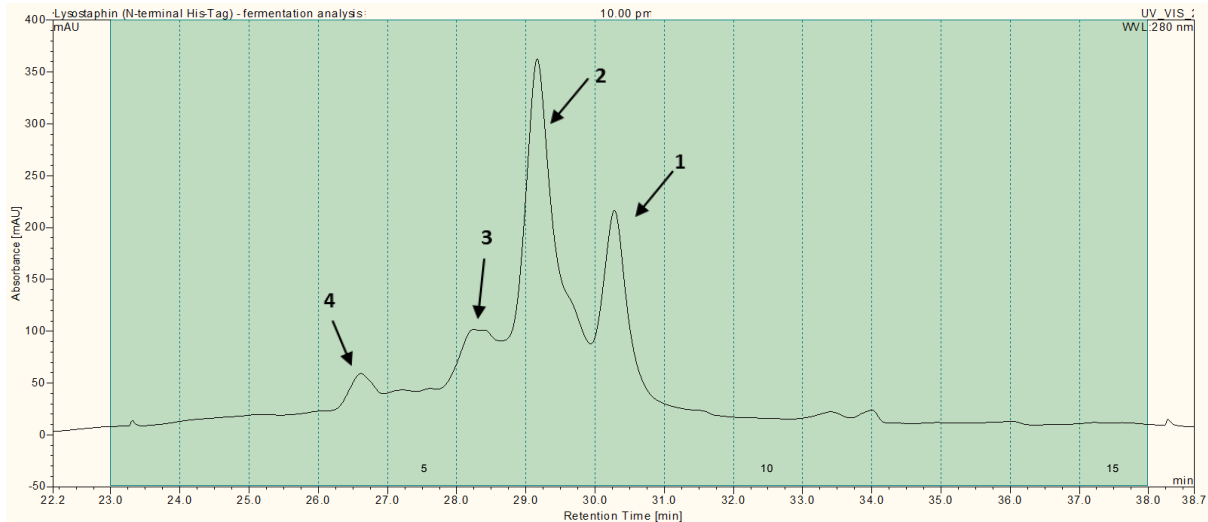


Figure 4.64: WCX separation of *N*-terminally His-tagged recombinant lysostaphin (construct 1) from *E. coli* cell lysate harvested at 10.5 h post-induction. WCX peaks of interest are indicated by arrows (1-4). The charge isoforms are labelled in order of development during culture analysis. Fractions 6, 7 and 8 were selected for SDS-PAGE analysis.

Despite differences in charge, SDS-PAGE analysis of the major peaks eluted during WCX separation did not indicate that the peaks contained different molecular weight protein isoforms (Figure 4.65).

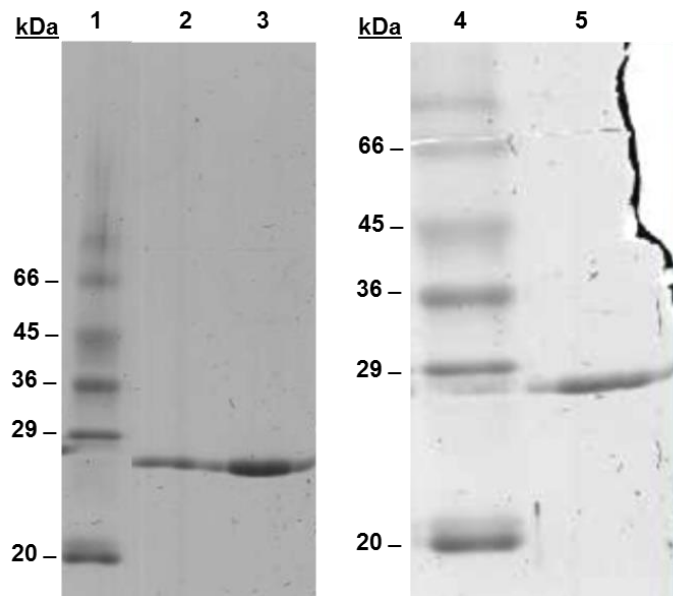


Figure 4.65: PAGE analysis of selected WCX fractions. Lane 1: Sigma low molecular weight markers; Lane 2: Fraction 6; Lane 3: Fraction 7; Lane 4: Sigma low molecular weight markers; Lane 5: Fraction 8.

Although PAGE analysis did not reveal any evidence of molecular weight heterogeneity, the charge-distinct protein isoforms were subjected to GF analysis. Comparison of GF results suggested that in addition to differences in charge, each GF separation indicated that each WCX peak contained protein isoforms which had subtle differences in molecular weight as well (Figure 4.66).

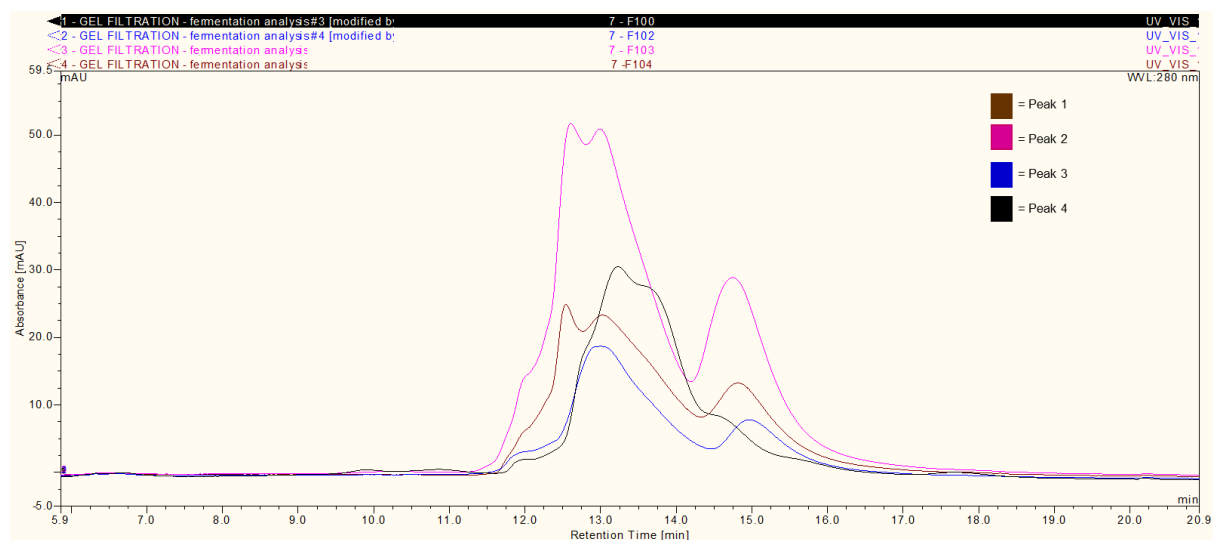


Figure 4.66: Comparison of chromatograms following gel filtration of WCX fractions. GF results suggest that each WCX peak was composed of protein isoforms of relatively similar molecular weights, however in some of the peaks there were additionally resolved molecular weight-distinct species.

Interpretation of the GF chromatograms revealed the presence of at least seven size-variable peaks or peak-shoulders (A-G), which are detailed in Table 4.4.

Table 4.4: Retention time (min) values of identified peaks or peak-shoulders (A-G) following gel filtration analysis of fractionated WCX peaks. Peaks which are absent in the GF separation are represented by “X”.

Analysed WCX peak	Retention time (min) of Identified GF Peaks						
	A	B	C	D	E	F	G
1	11.960	12.540	13.100	X	X	X	14.814
2	11.967	12.607	13.067	X	X	X	14.747
3	11.880	X	13.020	X	X	X	14.980
4	11.907	X	X	13.230	13.787	14.667	X

Individual examination of each gel filtration chromatogram shows that there were slight differences in protein molecular weights that could not be sufficiently separated, but could be resolved using the selected gel filtration resin and chromatographic conditions. GF analysis of peak 1, the peak which was found to be observed earliest during culture analysis, revealed the resolution of four peaks (Figure 4.67).

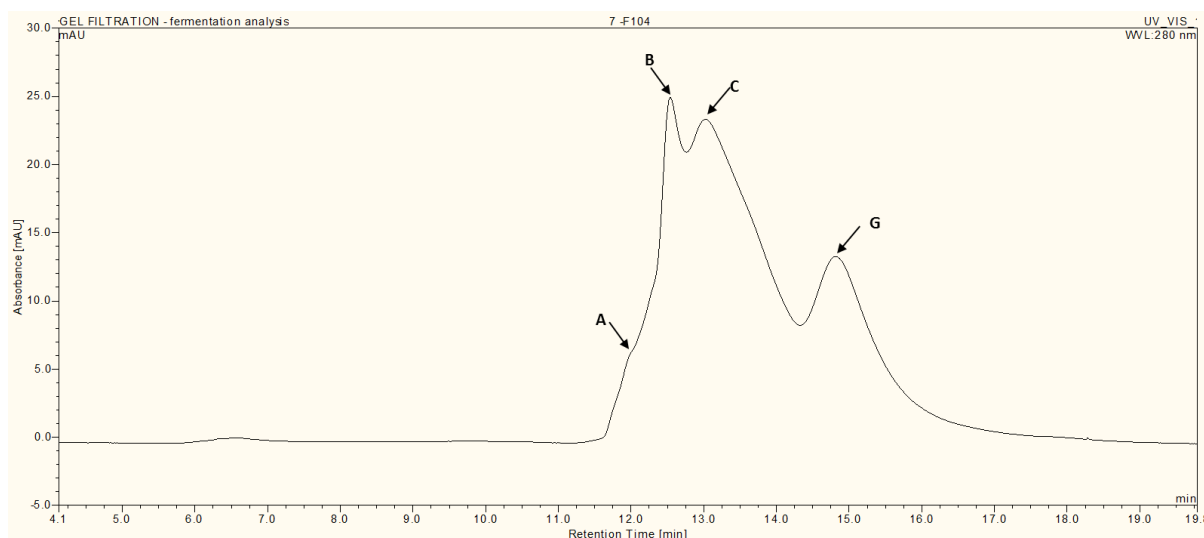


Figure 4.67: GF separation of WCX peak 1. All four isoform peaks were identified and annotated as A, B, C and G.

The same peaks were also resolved after gel filtration of WCX peak 2 (Figure 4.68). Peak A was slightly more evident, whilst peak G appeared to represent an increasingly abundant isoform. Peak B and C eluted at very similar retention times, whilst peak C also gained greater peak height.

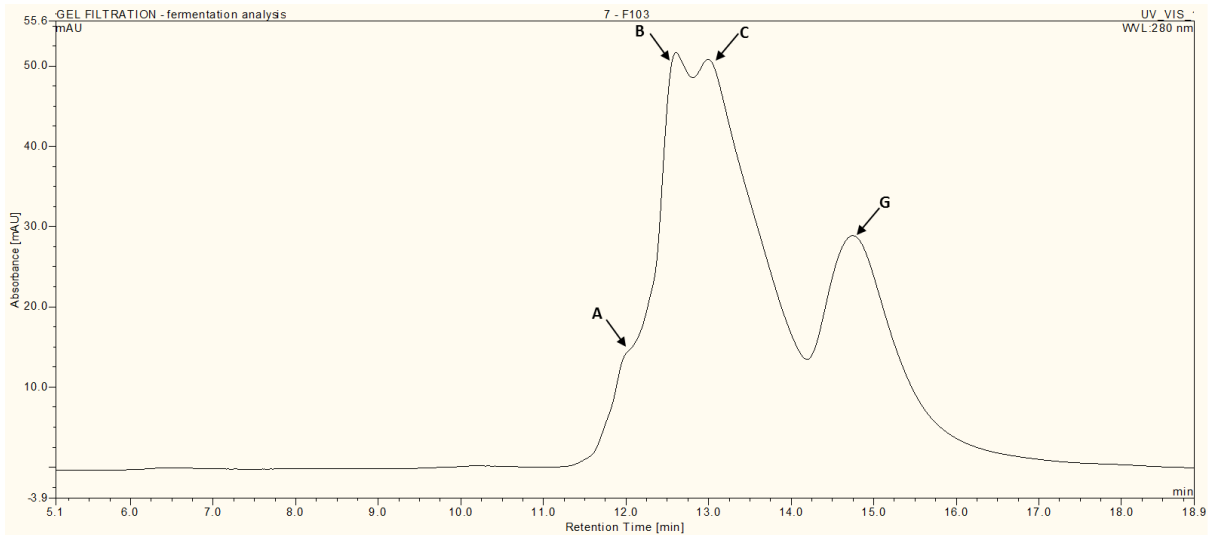


Figure 4.68: GF separation of WCX peak 2. Two major peaks were resolved with four different molecular weight isoforms (annotated as A, B, C and G and indicated by arrows).

Gel filtration of WCX peak 3 demonstrated the separation of two distinct peaks, C and G (Figure 4.69). The longer retention time of peak G indicated that the peak represents a protein isoform with a significantly lower mass than that of the protein isoform represented by peak C. Peak A also appeared more evident; however this was due to the absence of peak B. The loss of peak B indicated that peak 3 contained a greater proportion of protein isoforms with a slightly decreased molecular mass.

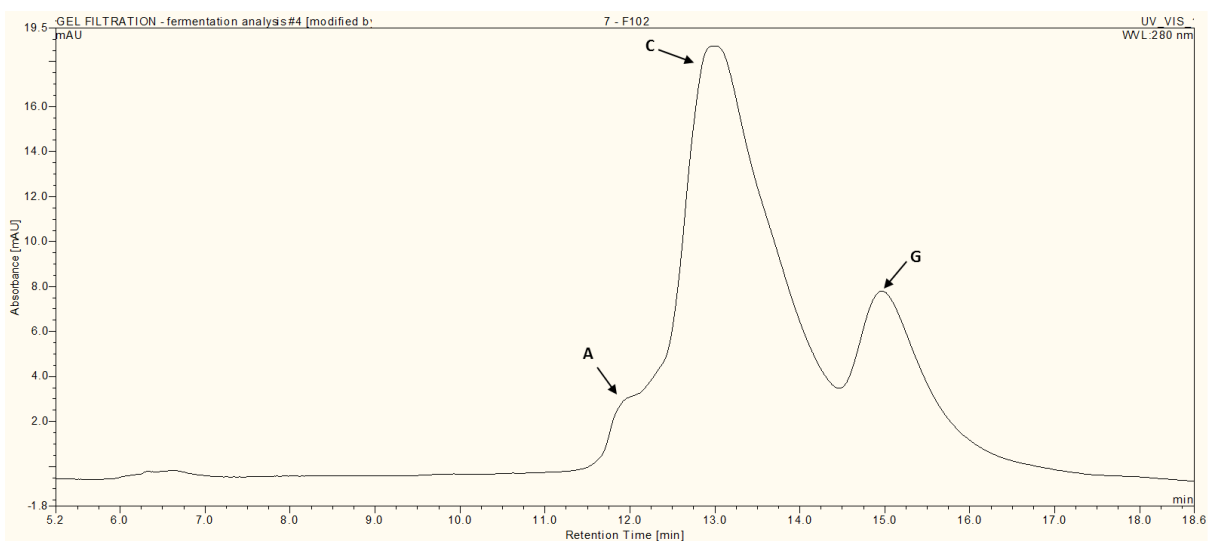


Figure 4.69: GF separation of WCX peak 3. Two distinct peaks were resolved (C and G) with shoulder peak A also remaining apparent. Size isoforms have been annotated A, C and G and are indicated by arrows.

Gel filtration of WCX peak 4 demonstrated a single peak, which was composed of at least four protein isoforms, which had not been separated but had slight differences in molecular weight (Figure 4.70). These isoforms presented as peak shoulders which were identified in Figure 4.70. Isoform D and E appeared to be the most abundant isoforms in WCX peak 4, whilst peak A represented the largest molecular weight isoform and peak F the smallest molecular weight isoform.

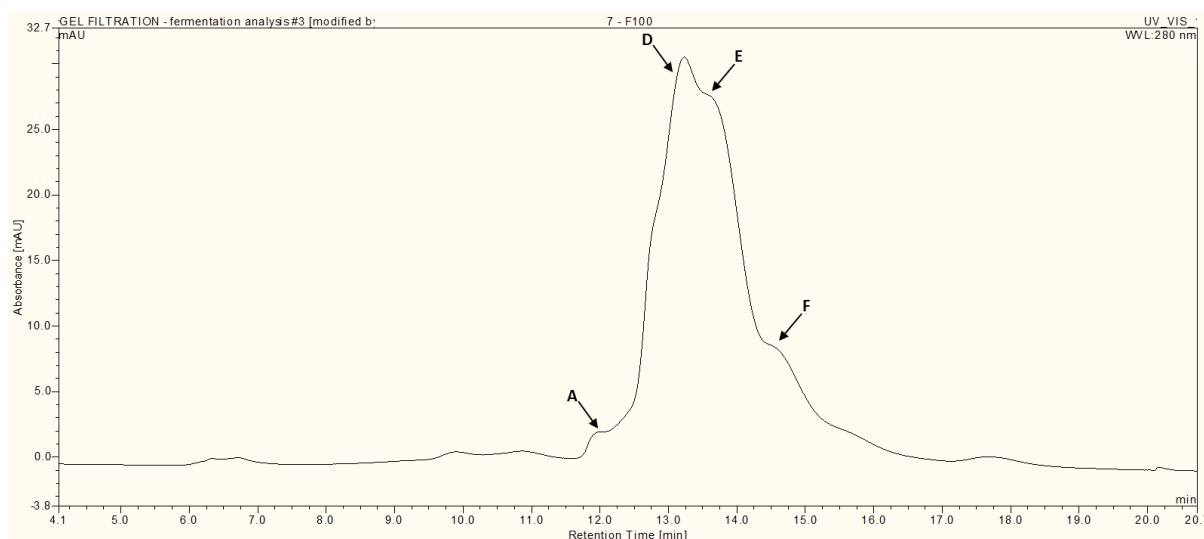


Figure 4.70: GF separation of WCX peak 4. A single peak is present, however this peak is composed of at least four unresolvable protein isoforms which are likely to differ slightly in molecular weight (size isoforms have been annotated (A, D, E and F) and indicated by arrows).

Overall these results indicate that WCX peaks 3 and 4, which became apparent later in the course of culture analysis, were predominantly composed of protein isoforms with a slightly smaller molecular weight. These differences in molecular weight would alter the charge of the protein, leading to the observed resolution of increasingly acidic protein isoforms during WCX separation. To establish whether these findings could be observed from protein which was obtained later in culture analysis, GF analysis was also performed on charge-distinct protein isoforms which had been separated during other WCX separations, such as those harvested at 21.0 and 24.0 h post-induction of protein expression (Figure 4.71 and Figure 4.72 respectively).

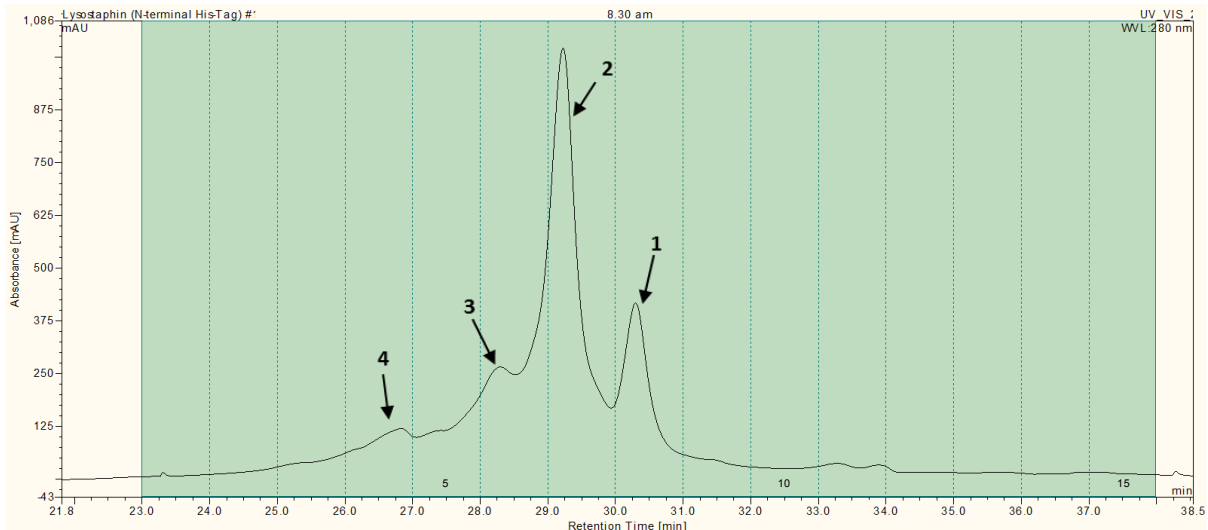


Figure 4.71: WAX separation of *N*-terminally His-tagged recombinant lysostaphin (construct 1) from *E. coli* cell lysate harvested at 21.0 hours post-induction. WAX peaks are indicated by arrows (1-4). Fractions 6, 7 and 8 were subjected to gel filtration analysis.

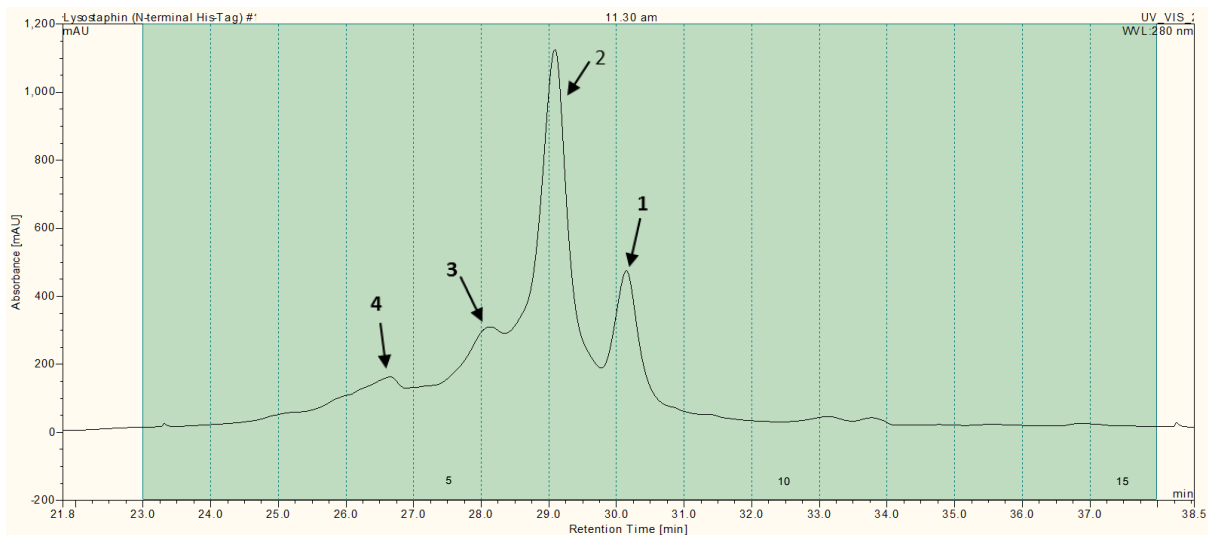


Figure 4.72: WAX separation of *N*-terminally His-tagged recombinant lysostaphin (construct 1) from *E. coli* cell lysate harvested at 24.0 hours post-induction. WAX peaks are indicated by arrows (1-4). Fractions 6 and 8 were subjected to gel filtration analysis.

Once again, fractions containing the most prominent peaks were analysed by SDS-PAGE (Figure 4.73). However in both instances, PAGE analysis indicated that peaks 2 and 3 demonstrated molecular weight heterogeneity, which could be resolved by 12% SDS-PAGE. This was an unexpected result, which was also observed following PAGE analysis of peaks resolved during some other WAX separations performed during culture analysis.

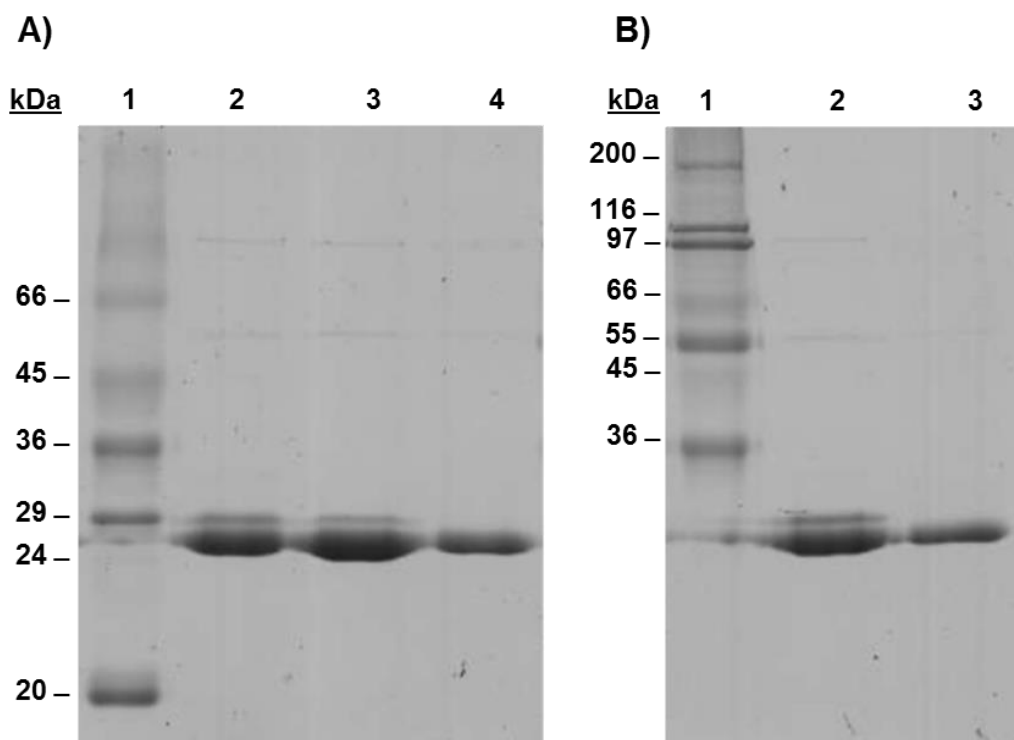


Figure 4.73: PAGE analysis of WCX fractions prior to gel filtration analysis. A) Fractions eluted during WCX separation of cell lysate harvested at 21 h post-induction. Lane 1: Sigma low molecular weight markers; Lane 2: Peak 2/3; Lane 3: Peak 3, Lane 4: Peak 4. **B)** Fractions eluted during WCX separation of cell lysate harvested at 24 h post-induction. Lane 1: Sigma high molecular weight markers; Lane 2: Peak 2/3; Lane 3: Peak 4.

As PAGE analysis clearly showed variance in the molecular weight of a sub-population of protein eluted in certain WCX peaks, gel filtration was performed on selected fractions from WCX separations of *N*-terminally His-tagged recombinant lysostaphin (construct 1) analysed at 21 h and 24 h post-induction (Figure 4.74 and Figure 4.75). Surprisingly GF analysis did not indicate the presence of an additional peak reflecting the presence of a higher molecular weight isoform. Instead the resolved peaks all exhibited retention times which corresponded with peaks observed during GF analysis of WCX fractions eluted following separation of cell lysate harvested at 10.5 h post-induction. However the most abundant peak demonstrated a retention time which was between those observed for peak B and C, therefore could not be definitely assigned as being of the same molecular weight species.

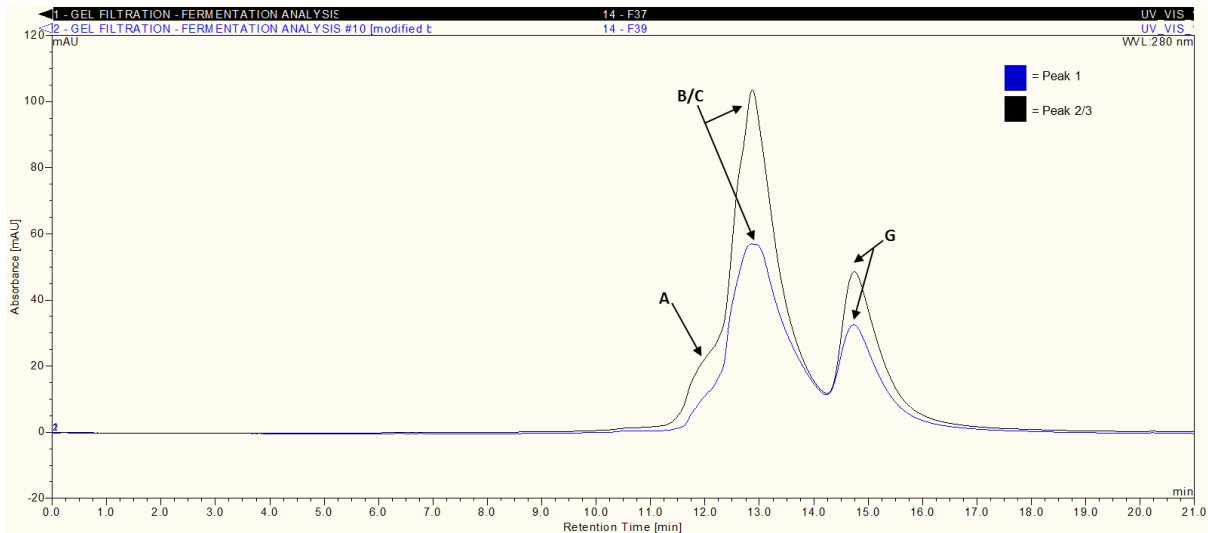


Figure 4.74: Comparison of chromatograms following GF separation of WCX fractions resulting from WCX analysis of *N*-terminally His-tagged recombinant lysostaphin (construct 1) harvested at 21 h post-induction. GF analysis results suggested that the analysed WCX fractions were composed of protein isoforms of very similar molecular weights. Identified peaks were annotated A, B, C and G as indicated by arrows.

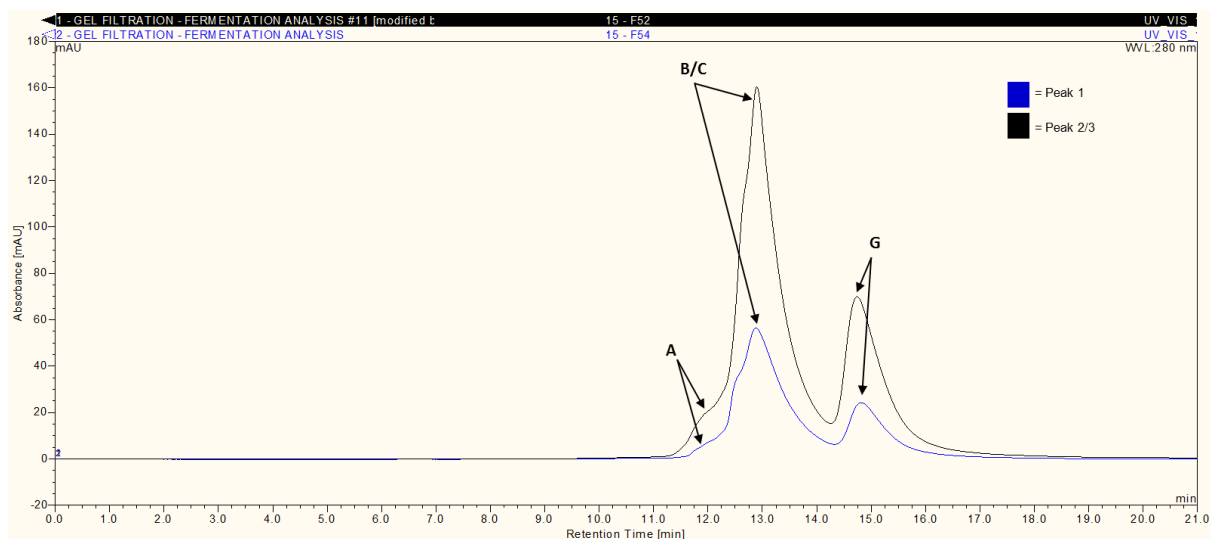


Figure 4.75: Comparison of chromatograms following GF separation of WCX fractions resulting from WCX analysis of *N*-terminally His-tagged recombinant lysostaphin (construct 1) harvested at 24 hr post-induction. Gel filtration results suggest that the analysed WCX fractions were composed of protein isoforms of very similar molecular weights. Identified peaks were annotated A, B, C and G as indicated by arrows.

Comparison of all the GF separations performed on fractions collected during WCX separations of cell lysates harvested at 10.5, 21.0 and 24.0 h post-induction demonstrated that all WCX peaks were composed of several protein isoforms which differed slightly in their

molecular weights. Seven peaks or peak shoulders were identified and the retention times of these were collated and compared in Table 4.5.

Table 4.5: Retention time (min) values of identified peaks or peak-shoulders (A-G) following GF analysis of fractionated WCX peaks. Peaks which were absent during GF separation are represented by “X”.

Sample	WCX peak	Retention time (min) of identified GF Peaks						
		A	B	C	D	E	F	G
10.5 h post-induction	1	11.960	12.540	13.100	X	X	X	14.814
	2	11.967	12.607	13.067	X	X	X	14.747
	3	11.880	X	13.020	X	X	X	14.980
	4	11.907	X	X	13.230	13.787	14.667	X
21.0 h post-induction	1	11.920	12.860		X	X	X	14.734
	2/3	11.793	12.873		X	X	X	14.747
24.0 h post-induction	1	11.774	12.880		X	X	X	14.814
	2/3	11.887	12.900		X	X	X	14.740

Table 4.5 demonstrates that the largest molecular weight isoform (Peak A) was present in all samples analysed by gel filtration, with very close retention times achieved in all samples. Closer examination of the GF chromatograms suggested that peak A may have in fact reflected the presence of the additional faint increased molecular weight band observed during PAGE analysis (Figure 4.73). For instance, the peak height of peak A was considerably higher during GF separation of fractions, which had demonstrated the presence of a higher molecular weight band during PAGE analysis. It therefore could be possible that this higher molecular weight protein isoform was present in all of the WCX peaks, however was not always detectable by PAGE analysis due to low abundance.

Further examination of PAGE analysis may even suggest that the higher molecular weight band may represent the “native” *N*-terminally His-tagged recombinant lysostaphin (construct 1), as the observed molecular weight was nearer to the 29 kDa size marker than the stronger protein band was. Peaks B-G may have therefore reflected truncated or degraded forms of recombinant lysostaphin. Peaks B and C appeared to occur in the majority of samples, however peak retention times tended to deviate anywhere between 12.5 and 13.1 min, which complicated identification of distinct isoforms. Peaks D, E and F were only distinguishable after gel filtration of WCX peak 4, which was separated from cell lysate

harvested at 10.5 h post-induction. Due to the isolated observation of these peaks, it seemed likely that these peaks had occurred transiently, possibly during the formation of the lowest mass protein isoform (peak G).

Through interpretation of these results it became apparent that peaks containing charge isoforms that were separated by WCX analysis, also demonstrated considerable mass heterogeneity. This was an unusual finding as it seemed unlikely that protein which could demonstrate the same apparent charge, would also differ in mass. Fortunately as the cell lysates separated by the ProPac[®] WCX (2 x 500 mm) column were also separated by using a higher resolution ProPac[®] MAb SCX (4 x 500 mm) column, it became apparent that recombinant lysostaphin isoforms could demonstrate both macro- and micro-heterogeneity with regard to protein charge (Figure 4.76).

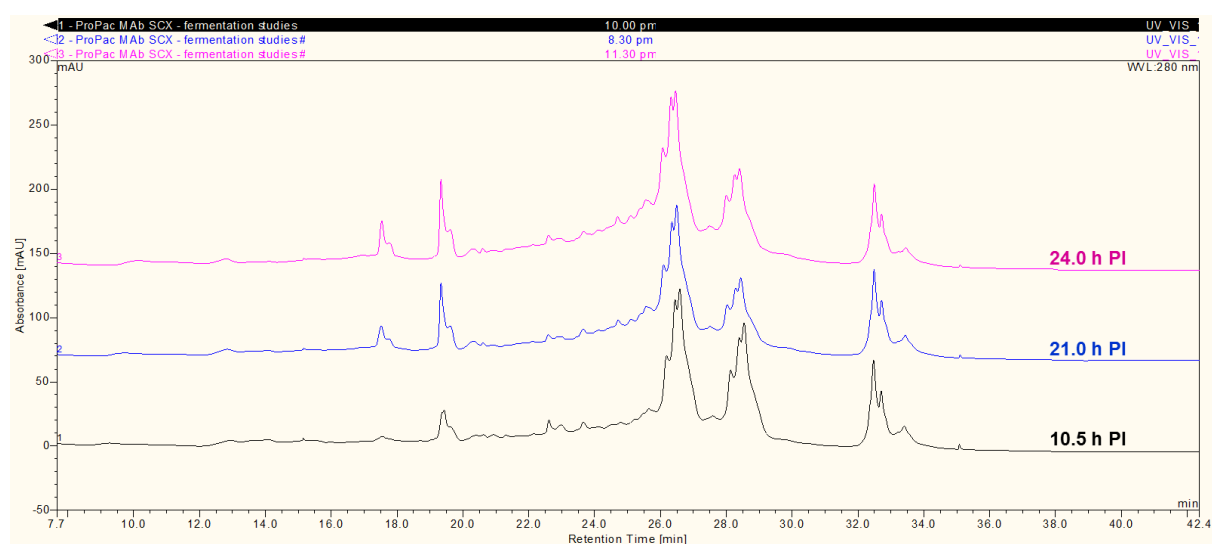


Figure 4.76: Comparison of chromatograms following SCX separation of *N*-terminally His-tagged recombinant lysostaphin (construct 1) from cell lysate harvested at 10.5, 21.0 and 24.0 h post-induction during culture analysis. SCX separation using the ProPac[®] MAb SCX (4 x 500 mm) column demonstrated that greater charge heterogeneity could be observed within the harvested recombinant lysostaphin preparations.

Closer examination of SCX separations during culture analysis revealed that peaks that would have appeared homogeneous during WCX separation, were in fact heterogeneous (Figure 4.77). The ProPac[®] MAb SCX (4 x 500 mm) resolved at least three protein isoforms within the peaks that reflected more acidic or basic forms of recombinant lysostaphin when separated by the ProPac[®] WCX (2 x 500 mm). Due to slight differences in charge, these minor protein isoforms were likely to reflect the detection of the molecular weight species that were observed during GF separation of WCX fractions.

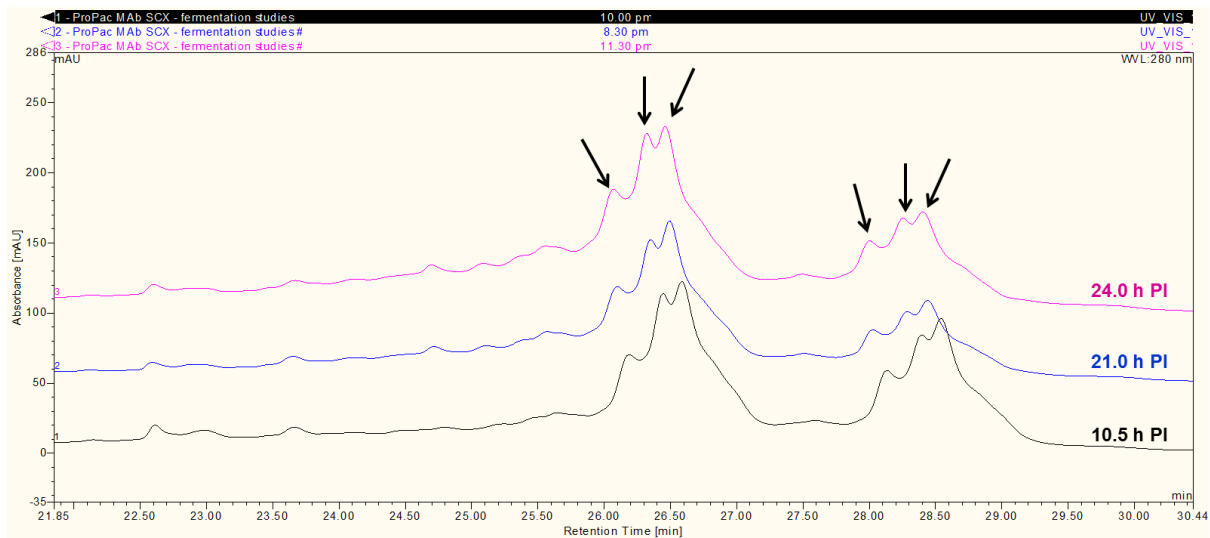


Figure 4.77: Comparison of chromatograms following SCX separation of cell lysate harvested at 10.5, 21.0 and 24.0 h post-induction during culture analysis. Closer examination of peaks separated using the ProPac[®] MAb SCX (4 x 500 mm) column suggested that the peaks observed during WCX separation were likely to be composed of multiple protein isoforms, which differed slightly in charge.

4.3.4 Discussion

Through repeated expression, purification and separation of recombinant lysostaphin preparations, it was possible to gain an insight into the stability of the protein. If maintained in a soluble state, recombinant lysostaphin (constructs 1 and 3) were found to remain stable in liquid formulation for prolonged periods of time, provided that it was stored at 4°C and not subjected to repeated fluctuations in temperature during usage. However lyophilised recombinant lysostaphin preparations were not found to respond well to solubilisation and protein precipitation was found to interfere with sample loading concentrations during chromatographic analysis. Due to the insolubility of lyophilised recombinant lysostaphin, subsequent chromatographic analysis was performed using only freshly prepared liquid preparations or cell lysates, which ensured better solubility and ease of preparation.

GF analysis following protein purification via IMAC also provided an insight into molecular mass heterogeneity of the purified recombinant product. GF separation of a single fraction eluted during IMAC, resulted in the elution of two major and a number of minor peaks. SDS-PAGE analysis confirmed that the eluted peaks contained a protein with a molecular mass which corresponded to that of *N*-terminally His-tagged recombinant lysostaphin (29.3 kDa). However PAGE analysis did not give an indication of any significant differences in molecular mass due to the denaturing conditions used during analysis, which would prevent detection of non-covalent interactions (Price and Nairn, 2009). More appropriate estimation of native masses and oligomerisation states would have been achievable using clear-native PAGE (CN-PAGE) or higher resolution blue-native PAGE (BN-PAGE) (Wittig and Schägger, 2005, Wittig *et al.*, 2006).

In order to establish whether aggregated species contributed to the observation of mass distinct species during GF analysis, IMAC purification was performed under denaturing conditions to dissociate molecules which may have aggregated during expression or during purification. In addition, elution using buffers containing urea also minimised the risk of aggregation during storage prior to GF analysis. Given the denaturing conditions, it would be expected that GF separation would resolve fewer peaks, particularly those with shorter retention times, reflecting the presence of larger dimeric or oligomeric species. However this was not the case as the largest molecular weight major peak remained present, whilst there was a reduction in the abundance of smaller molecular species instead. This finding was likely to have reflected minor differences in culture conditions, which would lead to differences in product heterogeneity.

These initial GF experiments indicated that purified recombinant lysostaphin preparations could demonstrate molecular mass heterogeneity. However it was also evident that the charge heterogeneity of the recombinant lysostaphin purified during IMAC increased the complexity of peaks eluted during GF and therefore it would be more appropriate if GF analysis was performed on protein which had undergone prior WCX separation. GF analysis of peaks eluted during WCX separation of cell lysates harvested during culture analysis also demonstrated the resolution of a number of molecular mass species. Although GF separation did not result in separation of distinct molecular mass species, seven distinct peaks or peak shoulders were resolved within the samples. Further examination of the peaks resolved during GF analysis, indicated that although the peaks resolved during WCX separation contained charge-distinct protein isoforms, they also contained protein isoforms which differed slightly in mass.

The mass heterogeneity observed within peaks which eluted during WCX separation was a much unexpected finding as the recombinant lysostaphin preparation had already been separated into fairly distinct charge isoforms. It would seem rational that proteins that differed in molecular mass would also differ in charge and vice-versa. Furthermore it was unclear as to why multiple molecular mass species could be observed within all of the analysed samples, regardless of the charge that the protein exhibited during WCX separation. However as culture analysis of cell lysates was performed using both the ProPac[®] WCX (2 x 500 mm) and higher-resolution ProPac[®] MAb SCX (4 x 500 mm) it became clear that recombinant lysostaphin could demonstrate both macro- and micro-heterogeneity with regard to charge. The observed micro-heterogeneity detected during ProPac[®] MAb SCX separation therefore explained why molecular weight species of a similar charge could be detected.

The apparent differences in mass were compounded by SDS-PAGE analysis which indicated that some of the peaks resolved during WCX separation could also contain mass-distinct protein isoforms that were resolvable by PAGE analysis. This finding had not been noticeably observed until SDS-PAGE analysis was performed on a substantial number of fractions, which had been generated from WCX separations performed during culture analysis. Although SDS-PAGE is not a high-resolution technique, SDS-PAGE and Coomassie blue staining are known to provide resolution to within 1-2% of a 50 kDa protein, which would equate to a difference of 4.5-9 amino acids (Price and Nairn, 2009). The technique could therefore be used to detect post-translational processing or proteolysis, which resulted in the loss of 4 or more amino acids. Recombinant lysostaphin may therefore be susceptible to truncation through proteolytic action.

Intriguingly the presence of the increased molecular mass protein isoform resolved during SDS-PAGE, was also not noticeably apparent following GF separation. The most reasonable explanation for this finding was that this protein may have actually been detected in all of the samples, as peak A, the highest molecular weight protein resolved during GF analysis. However due to being of a low protein concentration, this high-molecular weight protein may have been present but not always necessarily detectable during PAGE or GF analysis. In addition the greater abundance of slightly smaller molecular weight species, reflected by resolution of peaks B and C often hindered the resolution of peak A during GF analysis.

Furthermore SDS-PAGE analysis suggested that this protein may possess molecular weight which more correctly corresponded with the 29.3 kDa mass of *N*-terminally His-tagged recombinant lysostaphin (construct 1). This minor protein may therefore reflect the presence of native, unmodified recombinant lysostaphin, which contradicted theories involving “native” protein expression that were developed following culture analysis in Section 3.6. Alternatively this minor, higher-molecular mass protein species may have represented a post-translationally modified form of the protein, which could explain the increased mass yet apparent decreased charge of the protein.

As SDS-PAGE is a low-resolution technique it was not possible to make any definite conclusions about the cause of this finding. To gain a better indication of the degree of mass difference between the observed peaks, comparison could have been made with standard proteins. In addition, the application of some protein standards could have been used to confirm that the mobile phase conditions did not promote protein adsorption, whilst in the presence of high phosphate concentrations. However estimation of protein mass using standards has been known to lead to overestimation of protein mass, particularly of those bearing modifications (Arakawa *et al.*, 2010). Mass spectrometric analysis would therefore provide greater, more sensitive determination of protein mass, as described in Section 4.4.

Overall these experiments indicated that the Agilent Zorbax[®] GF-250 column could be used to provide separation of protein isoforms with significant differences in mass, however could only provide resolution of protein variants with only minor differences in molecular weight. The Agilent Zorbax[®] GF-250 column is more commonly used to separate a mixture of proteins with different molecular weights or oligomeric proteins, which would display a much more dramatic difference in molecular weight. GF analysis using this column indicated that charge variants observed during WCX separation of recombinant lysostaphin were unlikely to reflect aggregated, oligomeric species. However GF analysis of protein eluted during

WCX separation indicated that recombinant lysostaphin preparations may display considerable charge and mass heterogeneity, which could be attributable to protein truncation, through proteolysis or post-translational processing. As resolution is inversely related to the dynamic range of a GF resin, the selection of a GF column with a decreased dynamic range would hopefully provide increased resolution of these closely related molecular mass isoforms.

4.4 LC-MS analysis of recombinant lysostaphin

4.4.1 Introduction

In this work, intact recombinant lysostaphin was analysed using LC-MS analysis. Intact mass measurements were acquired using a MaXis Ultra-high resolution (UHR) quad-TOF mass spectrometer. The MaXis system was introduced in 2008 and can achieve mass accuracy to within less than 1 ppm and mass resolution of over 40,000 kDa. Given the accuracy and resolution of the instrument, intact mass measurements could provide a valuable insight into the how PTMs or sequence variation contributed to the heterogeneity of recombinant lysostaphin.

Aims:

- To establish accurate intact mass measurements for recombinant lysostaphin variants.

4.4.2 Methods

4.4.2.1 Buffers

All buffer compositions are outlined in Appendix 7.363

4.4.2.2 Equipment

All equipment used during LC-MS analysis of recombinant lysostaphin is outlined in Appendix 7.364.

4.4.2.3 Sample preparation

Sample preparation is described in Appendix 7.366.

4.4.2.4 Intact LC-MS analysis

Recombinant lysostaphin isoforms were separated by WCX (Appendix 7.368) and selected eluted fractions were concentrated prior to LC-MS analysis (Appendix 7.369). Online LC separation of intact protein was performed using a 2.5 μ l/min flow rate and a PepSwift[®] PS-DVB column. Following concentration, the protein samples were diluted 1:1 with RP Buffer A and 1 μ l of the diluted sample was injected onto the column. An isocratic gradient of 4% B was applied for 3 min at the start of separation following injection of the sample. Protein separation was achieved by applying a linear gradient of 4-90% B over 9 min. The column was then washed using 90% B for 8 min and then the column was equilibrated at 4% B for 6.5 min.

Separated proteins were delivered to the MaXis UHR-TOF via an ESI source. The MaXis was operated in positive mode under the following conditions: capillary voltage: 4500 V; nebuliser gas flow: 1.0 bar; drying gas: 4.0 L/min; drying temperature: 180°C; spectra rate: 1.0 Hz. The acquired MS spectrum was analysed using Data Analysis Version 4.0 SP1 (253) (Bruker Daltonics, UK) and were subjected to Maximum Entropy (MaxEnt) deconvolution using the following conditions: low mass: 10000; high mass: 35000; data point spacing: 5 and instrument resolving power: 20000². Acquired intact mass measurements were

² Intact MS/MS analysis was performed at the North East Proteome Analysis Facility (NEPAF) with assistance from Mr David Blinco

compared against theoretical intact protein mass values determined using ProtParam prediction (Section 2.4.2.6).

4.4.3 Results

4.4.3.1 Intact MS analysis of recombinant lysostaphin

Prior to intact MS analysis, a purified recombinant lysostaphin preparation was subjected to WCX separation (Figure 4.78). As previous experiments demonstrated that less abundant isoforms were not well resolved if low concentrations of protein were applied to the column (Section 3.4.3.2), the WCX separation was performed following injection of 31 mg of protein to ensure that less abundant protein isoforms could also be resolved. The injection of a high amount of protein resulted in the resolution of several peaks with high absorbance readings and significant peak broadening due to column or detector overloading.

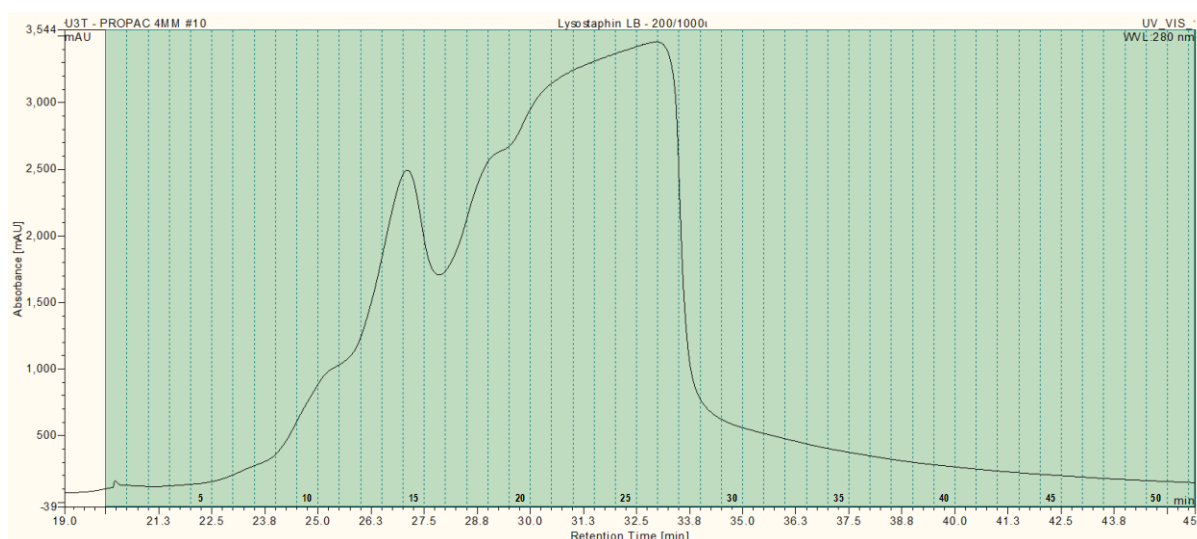


Figure 4.78: WCX separation of 31 mg of N-terminally His-tagged recombinant lysostaphin (construct 1) using a ProPac® WCX-10 (4 x 500 mm) column. Fractions 14 and 25 were subjected to intact MS analysis

The separation did however resolve at least three peaks which contained charge distinct protein isoforms, which could be subjected to intact MS analysis. Fractions were collected during the separation and selected fractions were therefore analysed to determine intact mass measurements. Intact MS analysis generated a mass spectrum which revealed the presence of a charge envelope reflecting the presence of intact protein with an estimated mass of approximately 29049.7 Da (Figure 4.79). Figure 4.79 also demonstrated that the MaXis UHR-TOF instrument could provide extremely high-resolution and high-accuracy mass data.

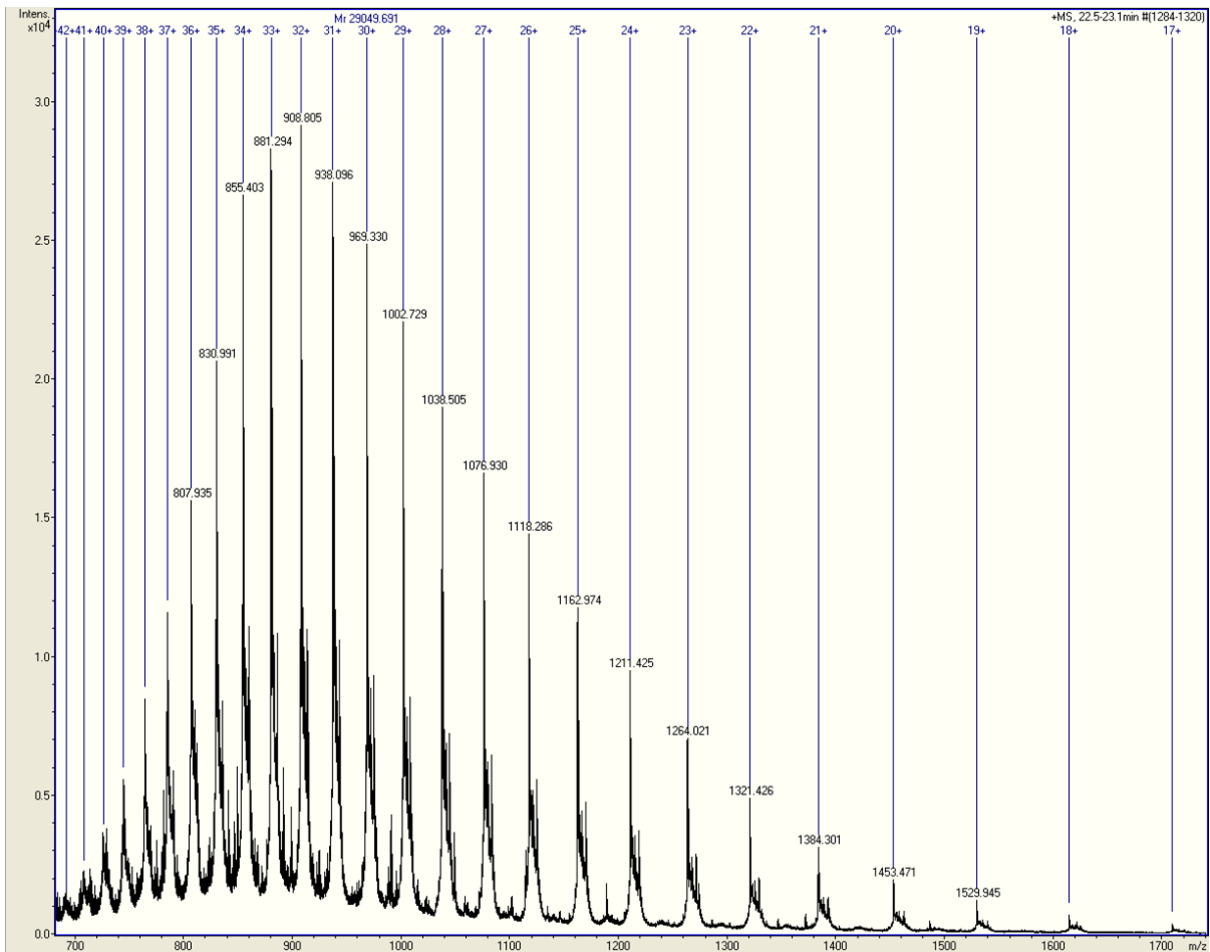


Figure 4.79: Acquired mass spectrum following LC-MS of intact protein eluted within WCX fraction 14.

Closer examination of a peak within the charge envelope (m/z 938.1, 31+) indicated isotopic resolution of less abundant species of the same charge state (Figure 4.80). This finding indicated that even though charge isoforms had been separated by WCX separation, the eluted protein still demonstrated micro-heterogeneity, which could be clearly resolved by the maXis.

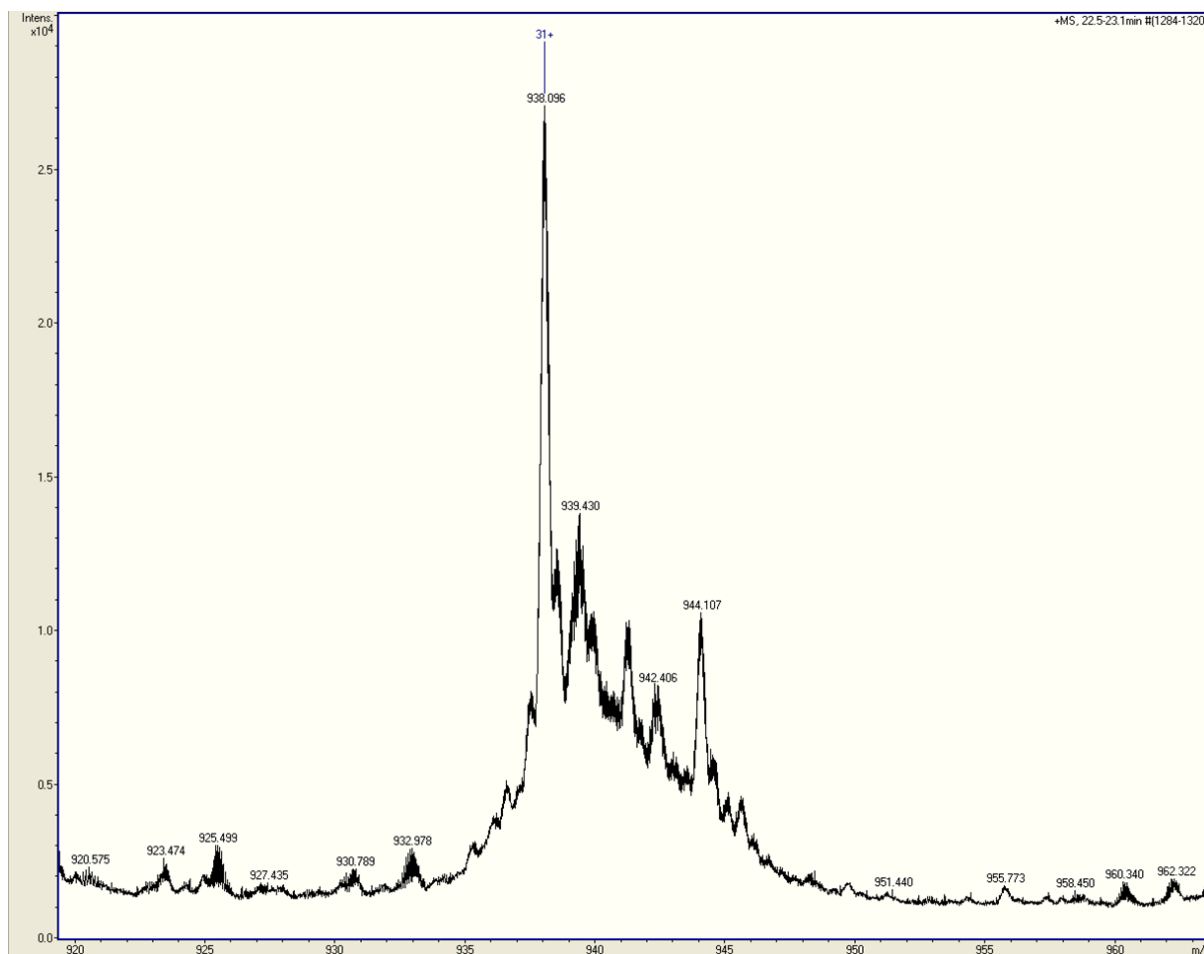


Figure 4.80: Enlarged base peak region (m/z 938.1, 31+) within charge state envelope of protein eluted within Fraction 14. Several less abundant peaks could be observed at the same charge state, indicating microheterogeneity within the sample.

The acquired mass spectrum was subjected to MaxEnt deconvolution to provide accurate masses of proteins detected within the resolved peaks (Figure 4.81). Deconvolution revealed that Fraction 14 was composed of a number of protein variants with a molecular weight similar to that of *N*-terminally His-tagged recombinant lysostaphin (construct 1) at 29337.8 Da. The mass associated with the most abundant peak, indicated that Fraction 14 was predominantly composed of a protein isoform with a mass of 29050.5 Da. The mass of this protein isoform reflected the loss of 287.3 Da from the overall expected molecular weight of *N*-terminally His-tagged recombinant lysostaphin (construct 1) in its apoprotein state.

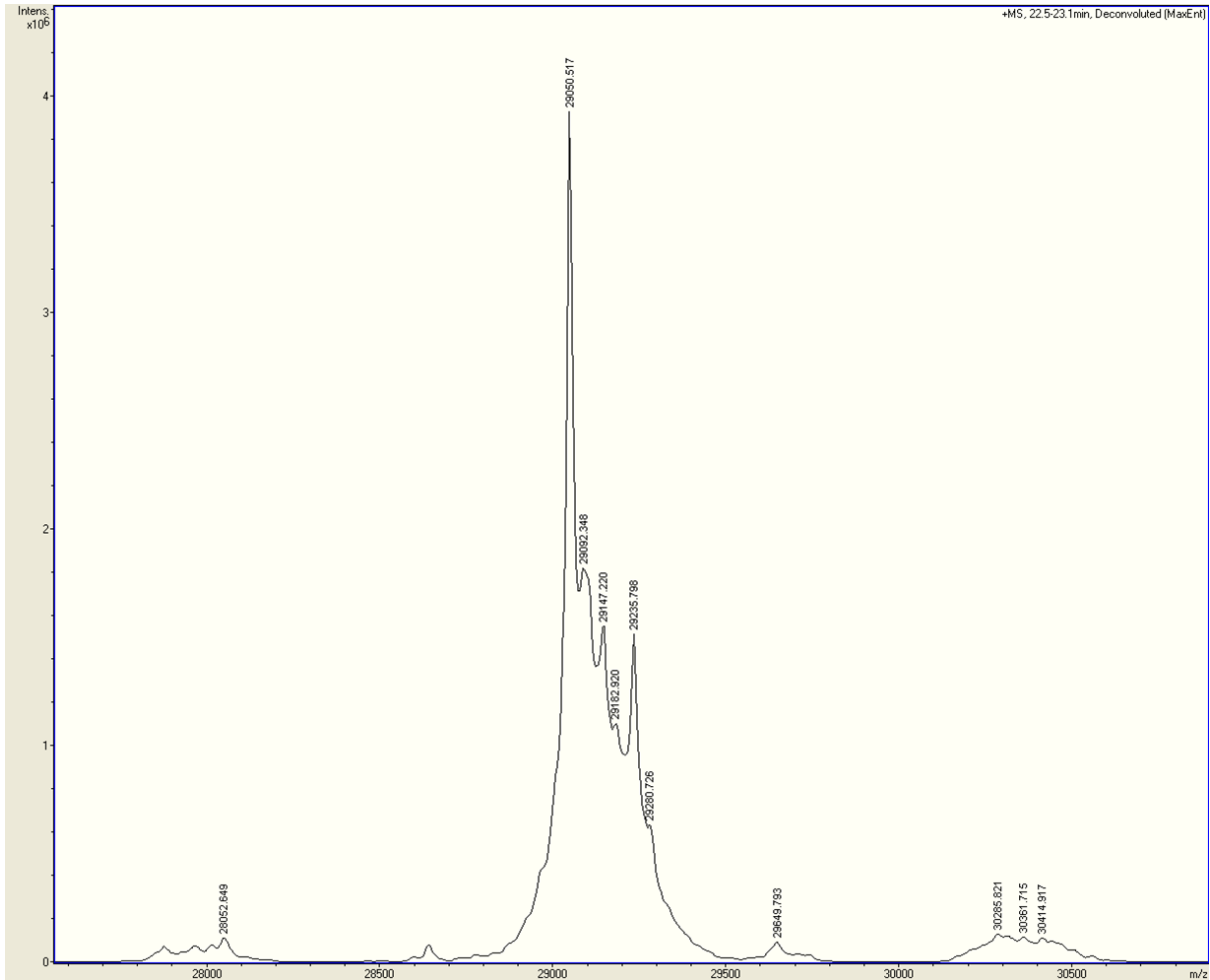


Figure 4.81: Deconvoluted mass spectrum following LC-MS of intact protein eluted within WCX fraction 14. MaxEnt deconvolution revealed that Fraction 14 contained multiple protein species with a molecular weight similar to that of *N*-terminally His-tagged recombinant lysostaphin (construct 1).

Intact MS analysis of protein eluted in WCX fraction 25 also produced a high-resolution mass spectrum, which contained a charge envelope reflecting the presence of intact protein with an estimated mass of approximately 29106.8 Da (Figure 4.82).

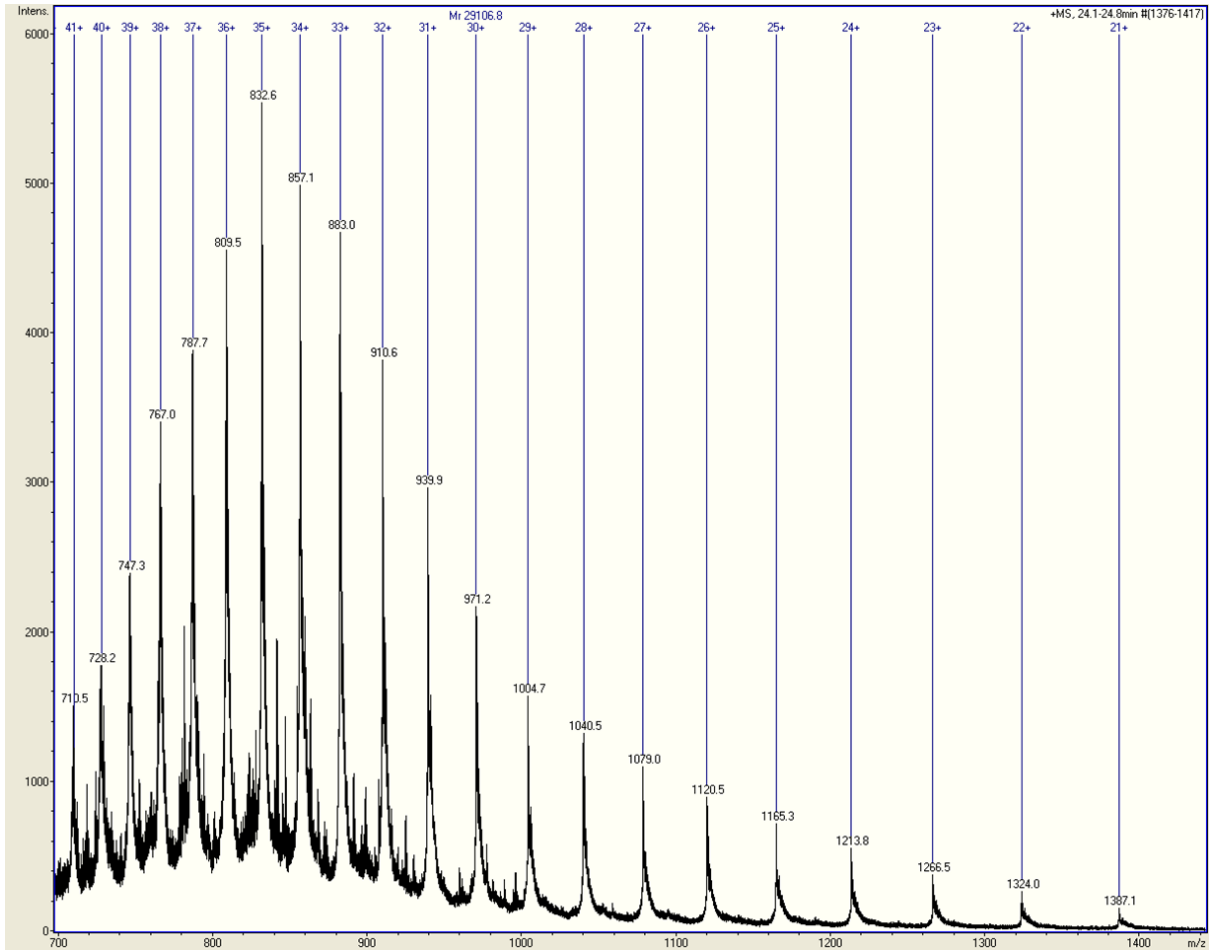


Figure 4.82: Acquired mass spectrum following LC-MS of intact protein eluted within WCX fraction 25.

Closer examination of a peak within the charge envelope (m/z 939.9, 31+) indicated isotopic resolution of less abundant species of the same charge state (Figure 4.83). Once again the complexity of the charge envelope indicated that the protein eluted within WCX fraction 25 displayed micro-heterogeneity despite prior separation of charge isoforms by WCX. The fraction appeared to be slightly less heterogeneous than protein contained within Fraction 14 however.

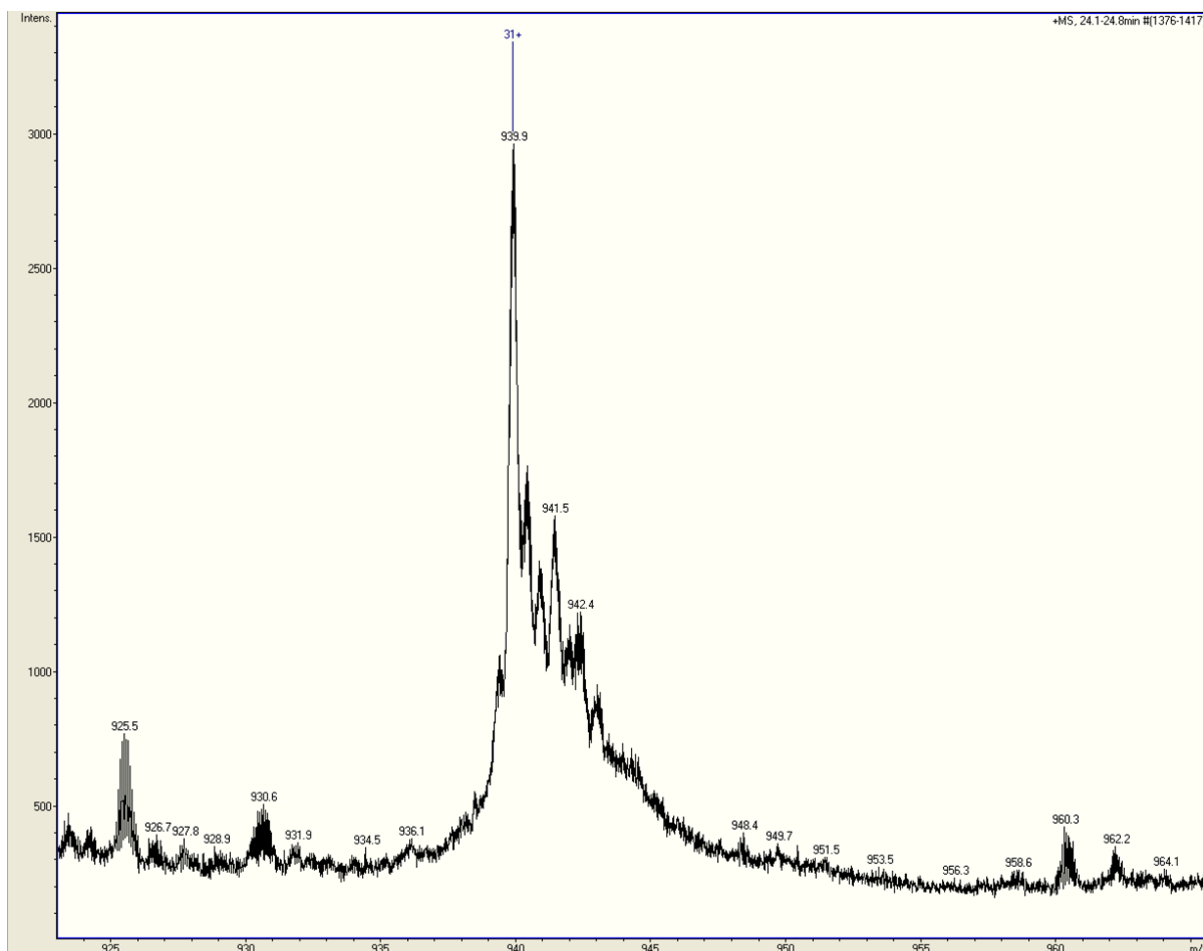


Figure 4.83: Enlarged base peak region (m/z 939.3, 31+) within charge state envelope of protein eluted within Fraction 25. Several less abundant peaks could be observed at the same charge state, indicating microheterogeneity within the sample.

The acquired mass spectrum was subjected to MaxEnt deconvolution to provide accurate masses of proteins detected within the resolved peaks (Figure 4.84). Deconvolution revealed that Fraction 25 was predominantly composed of a protein variant with a molecular weight of 29107.7 Da. Once again this mass was similar to the molecular weight of *N*-terminally His-tagged recombinant lysostaphin (construct 1), which had a predicted molecular weight of 29337.8 Da. This result would indicate that the most abundant protein isoform present within Fraction 25 had a mass which was 230.1 Da less than the predicted mass of *N*-terminally His-tagged recombinant lysostaphin (construct 1) in its apoprotein state.

Deconvolution of the mass spectrum also revealed lesser abundance of protein species with higher molecular weights ranging between 29150.7 and 29630.0 Da, which may have reflected less processed or modified forms of recombinant lysostaphin. Furthermore a protein species with a molecular weight of 29336.9 Da could be observed at low abundance

within the deconvoluted mass spectrum, reflecting a protein species with a mass that was extremely close to the expected 29337.8 Da mass of *N*-terminally His-tagged recombinant lysostaphin (construct 1) in its apoprotein state.

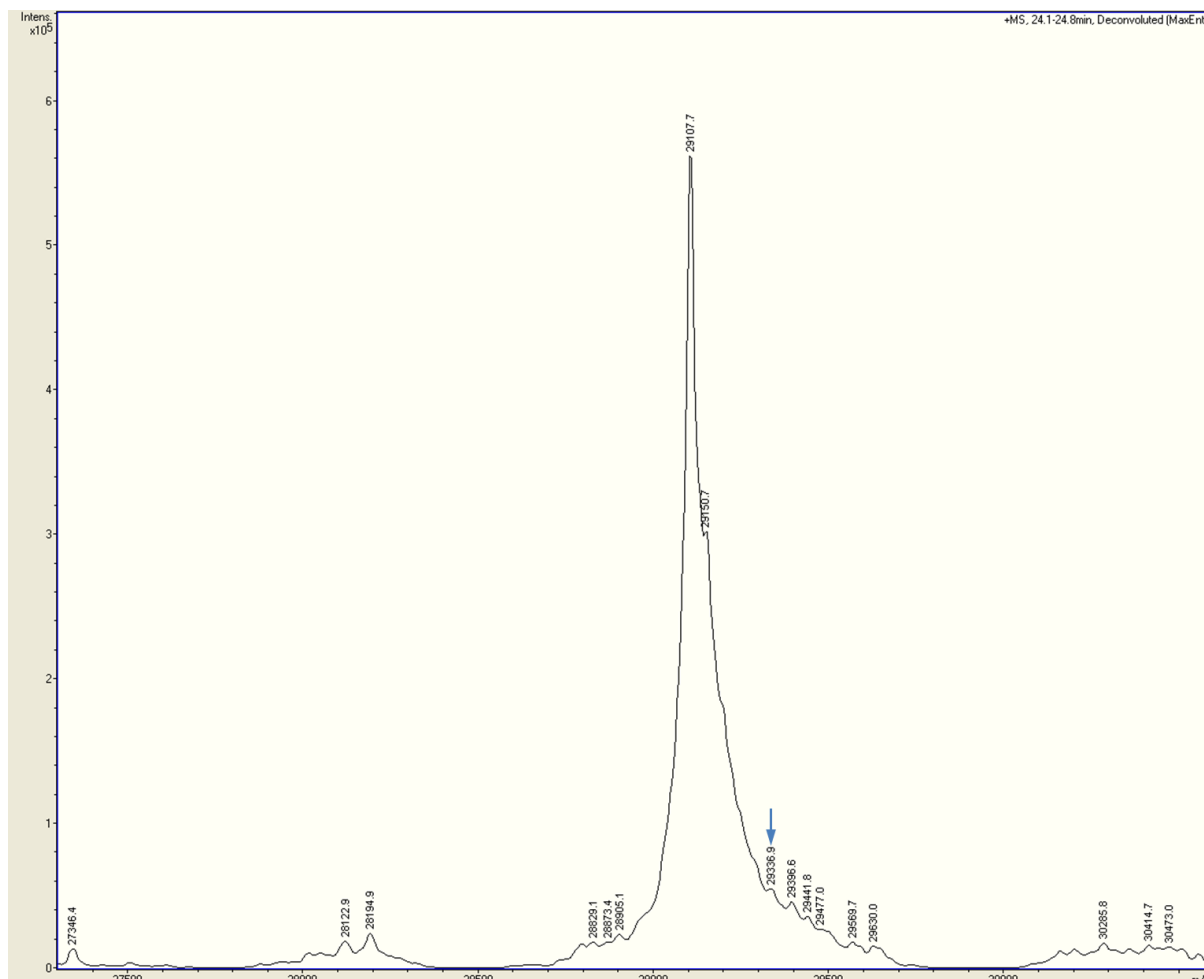


Figure 4.84: Deconvoluted mass spectrum following LC-MS of intact protein eluted within WCX fraction 25. MaxEnt deconvolution revealed that Fraction 25 contained multiple protein species with a molecular weight similar to that of recombinant lysostaphin (construct 1). The arrow indicates the presence of a low abundance protein species with a molecular weight which was very close to that of *N*-terminally His-tagged recombinant lysostaphin (construct 1), which had a mass of 29337.8 Da in its apoprotein state.

Intact mass measurements indicated that protein eluted in WCX Fractions 14 and 25 was predominantly composed of protein isoforms with molecular weights that were at least 230.1 and 287.3 Da less than the expected mass of *N*-terminally His-tagged recombinant lysostaphin (construct 1) in its apoprotein state, respectively. This would suggest loss of amino acids from either the *N*- or *C*-terminus of the protein.

Unfortunately due to instrumental issues, MS/MS analysis could not be performed on the precursor ions detected during these experiments to provide sequence data. Therefore the acquired intact mass measurements were compared with the theoretical masses of *N*-terminally His-tagged recombinant lysostaphin (construct 1) with loss of amino acids from the *N*- or *C*-terminus (Figure 4.85 and Figure 4.86). Theoretical mass values of *N*-terminally His-tagged recombinant lysostaphin (construct 1) with loss of *N*-terminal residues, loss of *C*-terminal residues and loss of both *N*- and *C*-terminal residues were established using ProParam analysis and are presented in Table 4.6, Table 4.7 and Table 4.8 respectively.

Table 4.6: Theoretical masses and pI of recombinant lysostaphin (construct 1) sequence variants following sequential loss of *N*-terminal amino acid residues. ProtParam results are presented in Appendix 7.370-Appendix 7.375.

Sequence variant	Apoprotein mass (Da)	Number of Amino Acids	Theoretical pI
Intact protein sequence	29337.8	267	9.72
ΔM_1	29206.7	266	9.72
ΔM_1-G_2	29149.6	265	9.72
ΔM_1-S_3	29062.5	264	9.72
ΔM_1-S_4	28975.4	263	9.72
ΔM_1-H_5	28838.3	262	9.72
ΔM_1-H_6	28701.2	261	9.72

Table 4.7: Mass and theoretical pI of recombinant lysostaphin sequence variants following sequential loss of *C*-terminal amino acid residues. ProtParam results are presented in Appendix 7.376-Appendix 7.381.

Sequence variant	Apoprotein mass (Da)	Number of Amino Acids	Theoretical pI
Intact protein sequence	29337.8	267	9.72
ΔK_{267}	29209.7	266	9.68
$\Delta I_{266}-K_{267}$	29096.5	265	9.68
$\Delta T_{265}-K_{267}$	28995.4	264	9.68
$\Delta G_{264}-K_{267}$	28938.4	263	9.68
$\Delta W_{263}-K_{267}$	28752.1	262	9.68
$\Delta L_{262}-K_{267}$	28639.0	261	9.68

Table 4.8: Mass and theoretical pI of recombinant lysostaphin sequence variants following loss of N-terminal and C-terminal amino acid residues. ProtParam results are presented in Appendix 7.382-Appendix 7.392.

Sequence variant	Apoprotein mass (Da)	Number of amino acids	Theoretical pI
Intact protein sequence	29337.8	267	9.72
$\Delta M_1 + \Delta K_{267}$	29078.5	265	9.68
$\Delta M_1 + \Delta I_{266} - K_{267}$	28965.3	264	9.68
$\Delta M_1 + \Delta T_{265} - K_{267}$	28864.2	263	9.68
$\Delta M_1 + \Delta G_{264} - K_{267}$	28807.2	262	9.68
$\Delta M_1 - G_2 + \Delta K_{267}$	29021.4	264	9.68
$\Delta M_1 - G_2 + \Delta I_{266} - K_{267}$	28908.3	263	9.68
$\Delta M_1 - G_2 + \Delta T_{265} - K_{267}$	28807.2	262	9.68
$\Delta M_1 - S_3 + \Delta K_{267}$	28934.4	263	9.68
$\Delta M_1 - S_3 + \Delta I_{266} - K_{267}$	28821.2	262	9.68
$\Delta M_1 - S_4 + \Delta K_{267}$	28847.3	262	9.68
$\Delta M_1 - S_4 + \Delta I_{266} - K_{267}$	28734.1	261	9.68

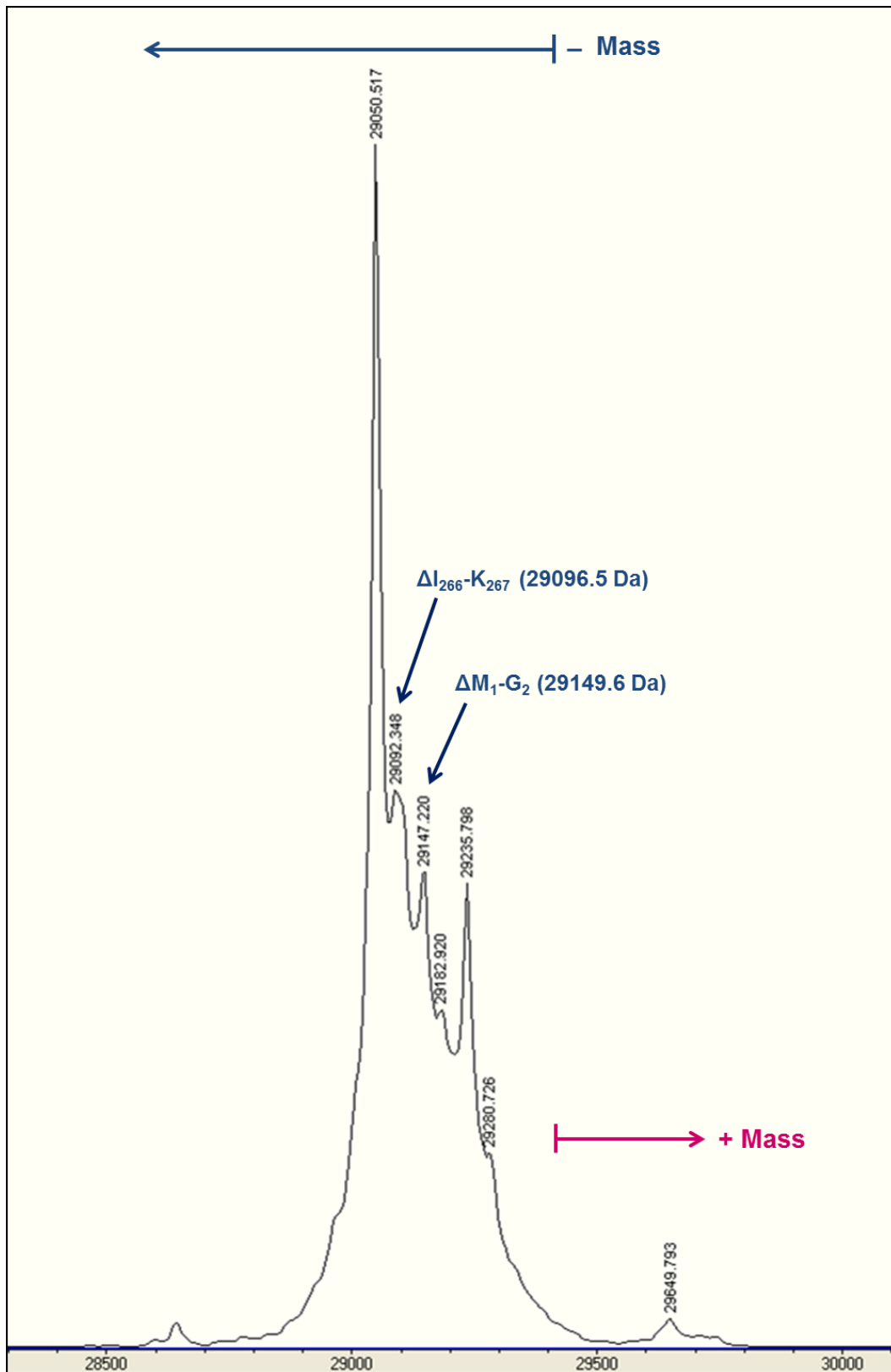


Figure 4.85: Deconvoluted mass spectrum following LC-MS analysis of intact protein eluted within WCX fraction 14. Selected detected masses correlated (within 5 Da) to the theoretical masses of truncated recombinant lysostaphin (construct 1) variants in an apo protein state.

Comparison of intact mass measurements obtained during LC-MS analysis of protein eluted in Fraction 14 during WCX separation and theoretical masses of full-length and truncated forms of *N*-terminally His-tagged recombinant lysostaphin (Appendix 7.393-Appendix 7.395) indicated that the most predominant mass was not directly associated with the loss of particular *N*- or *C*- terminal amino acids (Figure 4.85). Other less abundant protein species may have been attributable to the loss of *N*-terminal glycine₂ or *C*-terminal isoleucine₂₆₆ from recombinant lysostaphin (construct 1). Mass associations were made allowing a variation of up to 5 Da between theoretical and acquired mass values, therefore all of these mass comparisons may not have reflected the true composition of protein species detected during LC-MS analysis, given the mass accuracy of the MaXis UHR-TOF instrument.

Comparison of intact mass measurements obtained during LC-MS of protein eluted in Fraction 25 during WCX separation and theoretical masses of full-length and truncated forms of *N*-terminally His-tagged recombinant lysostaphin (Appendix 7.396-Appendix 7.398) did not suggest that the most predominant mass was specifically attributable to the loss of particular residues (Figure 4.86). However one of the detected low abundance mass species, presented with a mass within 0.9 Da of the theoretical mass of full-length recombinant lysostaphin (construct 1) in its apoprotein state. Other less abundant protein species may have also been attributable to the loss of *N*-terminal glycine₂ or both *N*-terminal glycine₂ and *C*-terminal isoleucine₂₆₆. Once again mass associations were made allowing a variation of up to 5 Da between theoretical and acquired mass values, therefore all of these mass comparisons may not have reflected the true composition of protein species detected during LC-MS analysis.

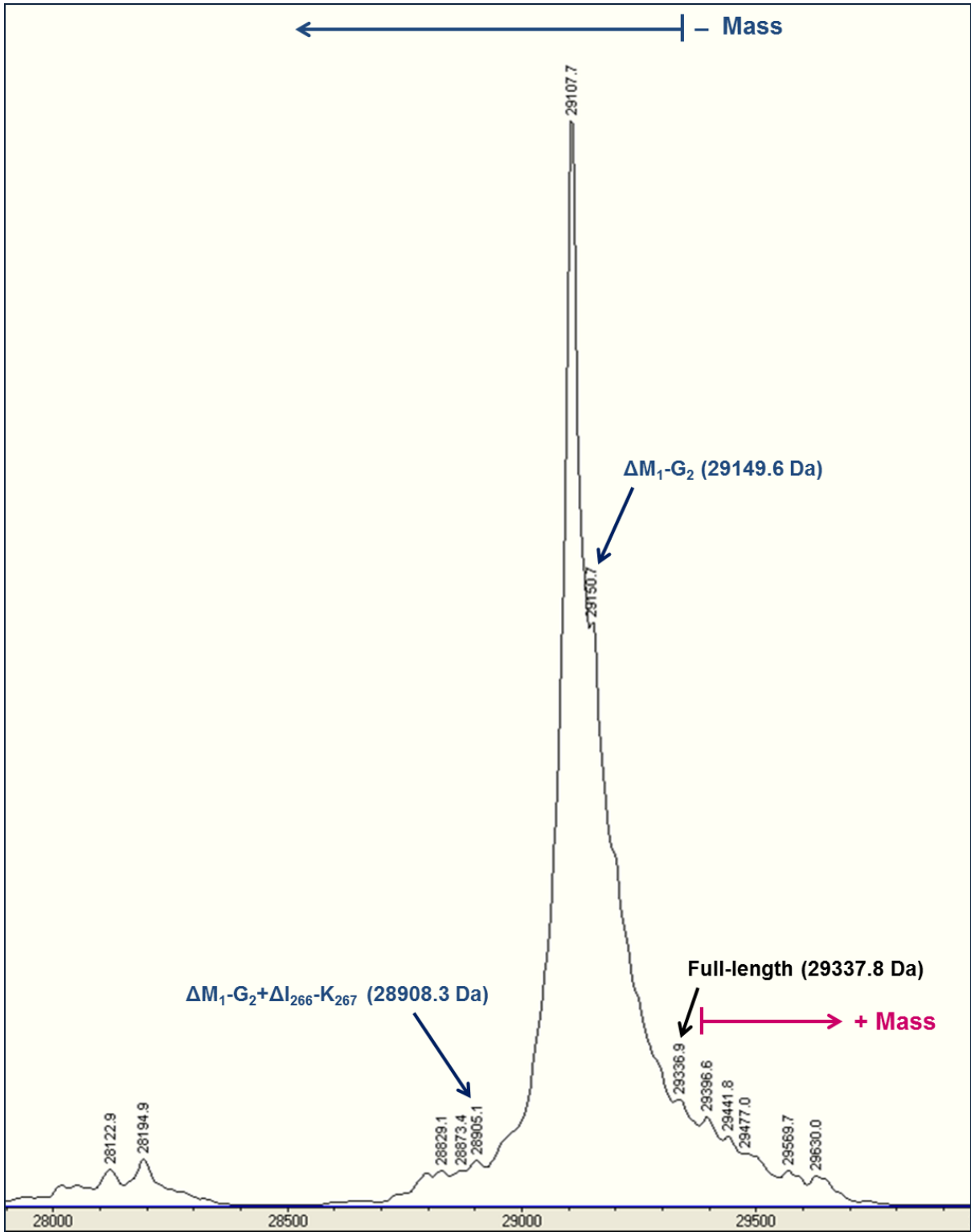


Figure 4.86: Deconvoluted mass spectrum following LC-MS analysis of intact protein eluted within WCX fraction 25. Selected detected masses correlated (within 5 Da) to the theoretical masses of truncated recombinant lysostaphin (construct 1) variants in an apo-protein state.

4.4.4 Discussion

LC-MS analysis of intact protein separated by WCX proved successful and informative. The high resolving power and mass accuracy of the MaXis UHR-TOF mass spectrometer provided high resolution mass spectra from which accurate intact protein mass measurements could be determined. The acquired mass spectra revealed that both WCX fractions contained a heterogeneous mixture of protein, despite prior separation of charge isoforms by WCX. This finding was not especially surprising considering that additional heterogeneity was also resolved during SCX separation (Section 3.5.3.13) and GF separation (Section 4.3.3.5). Furthermore column over-loading during WCX separation led to band broadening, which decreased the ability of the column to efficiently separate distinct charge variants prior to intact LC-MS analysis.

Fortunately the MaXis UHR-TOF could resolve the heterogeneous mixture of proteins present within WCX fractions 14 and 25. LC-MS analysis of intact protein present within WCX fraction 14 indicated that the most predominant protein isoform had a mass of 29050.5 Da, reflecting loss of 287.3 Da from the expected mass of *N*-terminally His-tagged recombinant lysostaphin (construct 1) in an apoprotein state. This loss could have reflected the loss of several amino acids from either the *N*- or *C*-terminus of the protein, or possibly both termini. Loss of *C*-terminal lysine₂₆₇ seemed rational, as the loss of a charged lysine residue from the *C*-terminus would decrease the pI of the protein isoform, leading to separation of a more acidic protein isoform, as was known to have eluted into WCX fraction 14.

LC-MS analysis of intact protein present within WCX fraction 25 also indicated that the most predominant protein isoform had a mass of 29107.7 Da, reflecting loss of 230.1 Da from the expected mass of *N*-terminally His-tagged recombinant lysostaphin (construct 1) in an apoprotein state. These losses would also reflect the loss of several amino acids from either the *N*- or *C*-terminus of the protein, or possibly both termini. Given that the average mass of an amino acid is 110 Da, such a mass decrement would signify the loss of two or three amino acids from the sequence of *N*-terminally His-tagged recombinant lysostaphin (construct 1). As fraction 25 predominantly contained more basic protein isoforms, it seemed logical that loss of amino acids would have occurred at the *N*-terminus of recombinant lysostaphin, which features neutral or hydrophobic amino acid residues.

Comparison of deconvoluted intact protein masses and theoretical masses for full-length and truncated forms of recombinant lysostaphin (construct 1) did not provide a clear identification

of detected mass species. However during LC-MS analysis of protein eluted into Fraction 25, a protein species with a mass within 0.9 Da of the theoretical mass of full-length recombinant lysostaphin (construct 1) was observed. This finding supported the theory that the intact recombinant lysostaphin was present within the protein preparation, but only at low abundance. Unfortunately the most predominant protein species masses detected in Fraction 14 and Fraction 25 were not directly associated with the masses of truncated protein variants. However evaluation of mass associations identified in Figure 4.85 and Figure 4.86 would suggest that the some of the detected protein species could be associated with the loss of *N*-, *C*- or *N*- and *C*-terminal residues.

Identification of detected protein species was complicated further by slight differences between the theoretical and detected masses. Given the high mass accuracy of the MaXis UHR-TOF, it seemed unlikely that mass errors as great as 5 Da would occur. Data analysis would have been complicated further if mass comparisons were based on average metalloprotein masses, due to variance in zinc isotopic masses and uncertainty over retention of the water molecule within the coordination sphere of the zinc binding domain. However as mobile phase conditions used during RP separation were acidic, it is very likely that recombinant lysostaphin became denatured during separation, leading to dissociation of the bound zinc molecule (Hann *et al.*, 2006). For this reason, detected masses were only compared against theoretical average apoprotein masses, rather than theoretical metalloprotein masses.

Overall LC-MS analysis indicated that the separated recombinant lysostaphin variants were predominantly composed of protein species with a mass that was significantly less than theoretical values of full-length recombinant lysostaphin (construct 1) in an apoprotein state. Due to the extent of mass loss, it seemed probable that the most predominant variants detected in Fraction 14 and 25 represented truncated forms of *N*-terminally His-tagged recombinant lysostaphin (construct 1). Both deconvoluted mass spectra also revealed the presence of a number of peaks reflecting the presence of intact proteins with a mass greater than the theoretical masses of recombinant lysostaphin (construct 1). These augmented masses may have reflected the presence of protein contaminants with a similar mass to that of recombinant lysostaphin or may have reflected post-translationally modified forms of the recombinant lysostaphin (construct 1).

To identify PTMs which could explain the heterogeneity of recombinant lysostaphin, the acquisition of supporting sequence data was required. Unfortunately it was not possible to

perform MS/MS analysis of intact protein using the MaXis UHR-TOF due to instrumental issues during these experiments. However subsequent LC-MS/MS analysis could be used to localise and quantify PTMs, which may further increment or decrement the mass of truncated forms of recombinant lysostaphin (construct 1).

4.5 Discussion

Chromatographic analysis of recombinant lysostaphin produced some interesting findings which provided further insight into the nature of the expressed protein. Turbidometric assay of the staphylolytic activity of recombinant lysostaphin demonstrated that enzyme preparations were active despite their charge heterogeneity. As lysostaphin is a zinc metalloprotease and is dependent on zinc for staphylolytic and elastolytic activity, the observed activity suggested that the bound zinc cofactor was indeed present (Park *et al.*, 1995). Bioinformatic comparison of the sequence of recombinant lysostaphin with LytM, a lysostaphin type endopeptidase, revealed that the amino acid sequence of recombinant lysostaphin contains the same amino acid residues that compose the zinc binding domain of LytM. This finding provided further knowledge about the structure and mass of recombinant lysostaphin in its metalloprotein state.

Enzyme activity was studied using a simple turbidometric assay in which the lysis of *S. aureus* was monitored over a fixed time course. The presence of an *N*- or *C*-terminal His-tag was not found to interfere with the activity of recombinant lysostaphin, which was encouraging considering that the cell wall targeting domain of the protein is located juxtaposed to the *C*-terminal His-tag sequence. Furthermore, the activity of recombinant lysostaphin did not appear to be influenced by the choice of expression media or expression location, with recombinant lysostaphin found to be active following translocation to the periplasm. Recombinant lysostaphin even retained its expression following lengthy purification and lyophilisation, which was surprising considering that prolonged storage, purification and lyophilisation were found to interfere with the stability of the protein.

Initial assays were performed on recombinant lysostaphin preparations, which had been purified by IMAC, which in retrospect was less reliable given that a proportion of the expressed recombinant lysostaphin may not have bound to the IMAC column and therefore may have not been available for assay. Furthermore assay of whole preparations may not have reflected the activity of individual charge variants; therefore additional experiments were performed to establish whether staphylolytic activity was restricted to particular variants. The assays revealed that charge variants separated during WCX analysis did demonstrate staphylolytic activity, which suggested that post-translational processing or modification of *N*-terminally His-tagged recombinant lysostaphin (construct 1) did not interfere with staphylolytic activity. Conversely, this result would suggest that any potential modifications or proteolytic events did not occur within the regions of the protein sequence that encoded catalytic activity.

However these experiments may not have accounted for the activity of all charge variants, as the assays were performed on apparently homogeneous protein variants separated by the ProPac[®] WCX (2 x 500 mm) column, which were found to be more heterogeneous when separated by the higher resolution ProPac[®] MAb SCX column (4 x 500 mm) (Section 3.5.3.13). As recombinant lysostaphin preparations were found to exhibit macro- and micro-heterogeneity, which could be resolved but not necessarily separated, it may not be possible to analyse the activity of every charge variant, especially when present at low concentrations. The application of a more sophisticated assay, such as a FRET assay would provide more sensitive assessment of staphylolytic activity and enzyme kinetics displayed by separated charge variants, even at low concentrations (Warfield *et al.*, 2006). In addition to providing more sensitive detection of staphylolytic activity, monitoring the cleavage of specific, synthesised substrates would eliminate variability associated with the use of *S. aureus* cells, which can differ in their growth phase physiology and interfere with the reproducibility of turbidometric assays.

Using chromatographic separations and LC-MS analysis, the retention behaviour, stability and mass of recombinant lysostaphin was investigated. The retention behaviour of recombinant lysostaphin was investigated following the observation of poor binding efficiency whilst testing the capacity of a ProPac[®] IMAC-10 column. Further IMAC purifications demonstrated that the charge heterogeneity of recombinant lysostaphin (construct 1) could interfere with the efficiency of IMAC purification. It is therefore imperative that caution is taken when using IMAC to purify recombinant proteins expressed in *E. coli*, particularly if the homogeneity of the preparation is not known.

WCX separation demonstrated that *N*-terminally His-tagged recombinant lysostaphin (construct 1) was found to demonstrate greater charge heterogeneity, whilst *C*-terminally His-tagged recombinant lysostaphin (construct 3) and recombinant lysostaphin without His-tags (construct 2) both demonstrated a lesser, yet similar degree of charge heterogeneity. The peaks eluted during WCX separation corresponded with the theoretical pI of each of form of recombinant lysostaphin, however it was interesting to observe that the *N*-terminally His-tagged recombinant lysostaphin (construct 1) preparation contained variants with the same charge as observed during separation of recombinant lysostaphin (constructs 2 and 3). This result indicated that a high proportion of the *N*-terminally His-tagged recombinant lysostaphin preparation may have undergone truncation. Alternatively the formation of more acidic variants may be attributable to phosphorylation, gluconoylation or phosphogluconoylation of the *N*-terminal His-tag sequence (Du *et al.*, 2005a, Du *et al.*, 2005b, She *et al.*, 2010).

Further IMAC purifications suggested that the charge heterogeneity of *N*-terminally His-tagged recombinant lysostaphin (construct 1) was associated with unusual retention behaviour, in which sequential application of cell lysate resulted in the retention of protein which displayed differential binding affinities. WCX analysis of the purified protein indicated that strongest retention was associated with the greater abundance of more basic protein isoforms, whilst moderate retention was associated with greater abundance of more acidic isoforms. IMAC purification of *C*-terminally His-tagged recombinant lysostaphin (construct 3) was associated with more normal retention behaviour permitting more efficient purification of recombinant lysostaphin (construct 3). Variable binding affinity was also observed during the purification of *C*-terminally His-tagged recombinant lysostaphin (construct 1), however WCX separation of purified protein suggested that this was likely to be attributable to high column loading rather than *C*-terminal His-tag heterogeneity.

Overall it was thought that the observed variable binding affinities could be attributable to negative cooperative binding during application of larger amounts of protein, whereby protein molecules with a stronger binding affinity cannot achieve multipoint adsorption due to a lack of favourable binding sites. The strength of binding affinity could be influenced by PTMs within the His-tag sequence, such as phosphorylation of serine residues, which, depending on location could interfere with multipoint binding interactions during IMAC. Application of large amounts of recombinant lysostaphin without a His-tag (construct 2) indicated that a small proportion of the preparation could bind to the IMAC column in the absence of a His-tag. This finding may have indicated that a small proportion of the preparation did not contain a bound zinc molecule and therefore could bind to the nickel ions on the stationary phase. Alternatively IMAC purification may have perturbed the structure of recombinant lysostaphin through removal or replacement of metal ions or through oxidative damage (Warfield *et al.*, 2006).

These experiments indicated that caution must be taken during IMAC purification to ensure that charge heterogeneity and protein structure does not interfere with the ability to purify a His-tagged recombinant protein in an efficient manner. The additional charge heterogeneity associated with the *N*-terminal His-tag sequence of recombinant lysostaphin would suggest that removal of the *N*-terminal His-tag sequence or use of alternative forms of recombinant lysostaphin (construct 2 and 3) would be advisable. Both *C*-terminally His-tagged recombinant lysostaphin (construct 3) and recombinant lysostaphin without His-tags (construct 2) are active and are likely to be less heterogeneous than the *N*-terminally His-tagged form of the protein. Both forms of the protein could be purified by CXC which would

be the preferred option, or using IMAC in the case of C-terminally His-tagged recombinant lysostaphin (construct 3).

Further chromatographic studies revealed that recombinant lysostaphin preparations remained stable for long periods of time whilst in liquid formulation and stored at 4°C. Lyophilised recombinant lysostaphin also possessed long-term stability however lost solubility following resuspension which interfered with peak resolution during WCX analysis and contraindicated its usage. SDS-PAGE of recombinant lysostaphin preparations indicated that the purified protein was homogeneous, however the use of denaturing conditions during SDS-PAGE prevented the detection of larger dimeric or oligomeric species. GF was therefore performed on recombinant lysostaphin (construct 1) which had been purified by IMAC under non-denaturing and denaturing conditions; to detect and dissociate potentially aggregated species. GF analysis resulted in the elution of a number of peaks, which did not seem to indicate aggregated species but rather more subtle mass heterogeneity within the purified recombinant lysostaphin preparation.

As it was thought that the molecular weight heterogeneity observed during GF analysis was attributable to the charge heterogeneity of the purified recombinant lysostaphin preparation, further GF separations were performed on protein variants which had been separated by WCX during culture analysis. However molecular weight heterogeneity was also resolved during GF analysis of charge distinct protein variants which had been separated by WCX. This was an unexpected finding considering that the complexity of the preparation had been reduced by WCX and it would be expected that differences in mass may also be associated with differences in charge. The macro- and micro-heterogeneity resolved by ProPac[®] MAB SCX separations did however provide an explanation for the presence of different molecular weight species with a similar charge.

Molecular weight heterogeneity was also observed during culture analysis following SDS-PAGE analysis, which was quite surprising considering that the detected protein appeared to possess a molecular weight which corresponded more closely with the molecular weight of recombinant lysostaphin (construct 1). This finding provided the first indication that the bulk of the recombinant lysostaphin (construct 1) preparation may have undergone truncation, through loss of *N*-terminal or *C*-terminal amino acid residues. It was initially expected that the mass differences observed during SDS-PAGE analysis would be evident during GF separation, however this was found not to be the case. Closer examination of the GF chromatograms suggested that the higher molecular weight species may have in fact been

detected as a low abundance peak observed in all of the samples, however low concentrations may have interfered with prior detection by SDS-PAGE.

Overall GF analysis indicated that recombinant lysostaphin (construct 1) preparations could demonstrate molecular weight heterogeneity as well as charge heterogeneity. Associated SDS-PAGE analysis also suggested that the bulk of the recombinant lysostaphin may actually be composed of a truncated form of the protein rather than the full length “native” recombinant lysostaphin that was initially expected to be expressed. GF separations performed using the Zorbax[®] GF-250 column were therefore informative, however greater resolution of molecular weight species could have been achieved using a GF column with a smaller dynamic range or through LC-MS analysis.

LC-MS analysis using the MaXis UHR-TOF system provided high resolution and high accuracy mass spectra from which accurate intact protein mass measurements could be achieved. LC-MS analysis of charge distinct protein isoforms indicated that that eluted protein was heterogeneous despite prior WCX separation. This finding was not surprising considering that the column was overloaded with sample and that greater heterogeneity had already been observed during SCX and GF separations performed using ProPac[®] MAb SCX and Zorbax[®] GF-250 columns. The obtained mass spectra indicated that protein eluted during WCX separation was largely composed of protein with a mass below the expected mass of *N*-terminally His-tagged recombinant lysostaphin (construct 1).

LC-MS analysis of more acidic protein variants eluted within WCX fraction 14 indicated that the most predominant variant has a mass of 29050.5 Da, reflecting loss of 287.3 Da from the expected mass of recombinant lysostaphin (construct 1) in an apoprotein state. The most predominant protein species detected in Fraction 14 could be more definitively associated with loss of both *N*- and *C*-terminal residues. Loss of *C*-terminal lysine₂₆₇ would provide a logical explanation for the observed acidity of the protein during WCX analysis.

LC-MS analysis of more basic protein variants eluted within WCX fraction 25 indicated that the most predominant variant has a mass of 29107.7 Da, reflecting loss of 230.1 Da from the expected mass of recombinant lysostaphin (construct 1) in an apoprotein state. However the most predominant protein species was less definitively associated with loss of *C*-terminal residues and therefore loss of *N*-terminal residues seemed more probable. As fraction 25 contained more basic protein isoforms, it seemed logical that truncation could have occurred at the *N*-terminus of recombinant lysostaphin, which features neutral or hydrophobic amino acid residues.

Comparison of deconvoluted intact protein masses and theoretical masses for full-length and truncated forms of recombinant lysostaphin (construct 1) resulted in the identification of a few closely related masses. For instance, LC-MS analysis of WCX fraction 25 demonstrated the presence of a low abundance protein with a mass of 29336.9 Da which may have reflected the presence of unmodified and unprocessed recombinant lysostaphin (construct 1) in an apoprotein state. This finding supported previous theories that the intact recombinant lysostaphin was present within the protein preparation, but only at low abundance.

Associations between theoretical truncated masses and the determined masses of less abundant protein species provided further indication that recombinant lysostaphin (construct 1) may have become truncated at the *N*- and *C*-termini during expression. However as theoretical and detected protein masses differed slightly, these identifications could not be confirmed as such a mass error would not occur given the high mass accuracy of the MaXis UHR-TOF. It therefore seemed likely that the separated charge variants may have undergone loss of *N*-terminal or *C*-terminal residues, in conjunction with mass increments or decrements associated with the addition of PTMs.

LC-MS analysis of *N*-terminally His-tagged recombinant lysostaphin (construct 1) would provide further knowledge about the truncation events and PTMs. Unfortunately it was not possible to perform MS/MS and MS_n analysis using the MaXis UHR-TOF due to instrumental issues. However following rectification of these issues, it is likely that sensitive MS/MS and MS_n analysis could be performed using the MaXis UHR-TOF system as recombinant lysostaphin has a fairly low mass, therefore high sequence coverage and characterisation of sequence modifications could be achievable. However PTMs which result in minimal mass shifting, such as deamidation (+0.98 Da) would probably not be detectable by intact protein analysis and would therefore analysis of fragmented protein would be more sensitive (Xie *et al.*, 2009). Ideally a combination of both analyses would be applied to achieve maximal MS/MS sequence coverage and characterise the protein structure fully. The application of de novo sequencing or MALDI-MS would also provide sensitive analysis of *N*-terminal and *C*-terminal sequences (Bruni *et al.*, 2005, Yamaguchi *et al.*, 2004).

Overall these studies provided greater insight into the influence of heterogeneity upon the activity, behaviour, stability and mass of recombinant lysostaphin. Product heterogeneity did not appear to affect the staphylolytic activity of recombinant lysostaphin, however interfered with the ability to efficiently purify *N*-terminally His-tagged recombinant lysostaphin (construct 1). *N*-terminally His-tagged recombinant lysostaphin (construct 1) was also shown to

demonstrate mass heterogeneity during GF and intact protein LC-MS analysis, which was thought to be largely attributable to protein truncation. The implications of which are discussed further in Chapter 5.

5 Discussion

5.1 Cloning, expression and purification of recombinant lysostaphin

During this research recombinant lysostaphin was analysed extensively using chromatographic techniques. However prior to chromatographic analysis, the mature lysostaphin domain from *S. staphylolyticus* was amplified and cloned in *E. coli* using a combination of PCR and gene cloning techniques. Cloning of the mature lysostaphin domain was uneventful and led to the production of five pET vector constructs, which could be used to express recombinant lysostaphin with or without *N*- or *C*-terminal His-tags, within the cytoplasm or the periplasm of *E. coli* BL21(DE3). However sequencing of the pET vector constructs 1, 2 and 3 led to the elucidation of two nucleotide mis-matches within the lysostaphin gene sequence published by Heinrich *et al.*, (1987). These nucleotide mis-matches were confirmed by the work of Gargis *et al.* (2010), who sequenced the pACK1 plasmid of *S. staphylolyticus*, which encodes the lysostaphin gene (Gargis *et al.*, 2010, Heinrich *et al.*, 1987).

Whilst the mis-identification of cytosine at position 456 was not found to alter the translation of proline₁₅₂, mis-identification of cytosine at position 96, was found to result in the translation of methionine₃₂ rather than isoleucine₃₂. The presence of a guanine rather than cytosine at position 96 was unlikely to have significantly altered the physicochemical properties of recombinant lysostaphin, however increased the predicted mass of the protein by 18 Da. This mass increment was not particularly significant; however knowledge of this amino acid difference would be useful during characterisation of recombinant lysostaphin, in which the correct amino acid sequence would be required for accurate peptide identification during LC-MS/MS analysis. Given that the sequence of the pACK1 plasmid was only published in 2010, it is unlikely that many past characterisation studies will have been performed with knowledge of these amino acid mis-identifications.

Once transformed into *E. coli* BL21(DE3), all five pET vector constructs were found to express a recombinant protein with a molecular weight that corresponded with the expected weight of cloned recombinant lysostaphin (with or without *N*- or *C*-terminal His-tag sequences). Expression of pET constructs 4 and 5, which featured *pelB* leader sequences, was also found to lead to effective translocation of recombinant lysostaphin to the periplasmic space. In the majority of experiments recombinant lysostaphin was hyper-expressed in a largely soluble form, even when *E. coli* BL21(DE3) was cultured in a variety of expression media and at several different incubation temperatures. Time-course experiments suggested that recombinant lysostaphin expression persisted for between 24

and 85 h after the induction of protein expression and was largely determined by bacterial growth rates. Expression of recombinant lysostaphin was also observed following induction of protein expression at OD_{600 nm} values above and below the recommended range (0.6-1.0).

Following expression, it was found that recombinant lysostaphin could be efficiently purified using IMAC or CXC to achieve a high level of purity. Single-stage purification was essential to ensure that purified recombinant lysostaphin could be obtained rapidly so as to prevent sample degradation or modification during purification or storage. *N*-terminally His-tagged recombinant lysostaphin (construct 1) was most commonly expressed and was purified using IMAC due to the high purity that the technique could provide. However this technique was used with caution as several publications reported that the *N*-terminally His-tagged sequences could become modified by phosphorylation, gluconoylation and phosphogluconoylation (She *et al.*, 2010, Du *et al.*, 2005a, Du *et al.*, 2005b). These concerns were confounded by the observation of unusual retention behaviour, whilst testing the capacity of an analytical ProPac[®] IMAC-10 column, which suggested that recombinant lysostaphin may exhibit *N*-terminal His-tag heterogeneity.

5.2 Separation of recombinant lysostaphin

The ability of CXC to bind recombinant lysostaphin was an unusual finding considering that the majority of cellular proteins are anionic and therefore would bind during AXC. Nonetheless, the basicity of recombinant lysostaphin proved extremely useful during the purification and separation of recombinant lysostaphin isoforms. Greater resolution and separation of protein isoforms could be achieved using pellicular rather than monolithic stationary phase resins, and therefore ProPac[™] IEX were selected in preference over ProSwift[®] IEX columns. The most superior resolution of protein isoforms could be achieved using the ProPac[®] MAb SCX columns, however as this column was only released in the later stages of this research, high-resolution, reproducible separation was achieved using ProPac[®] WCX-10 columns.

Optimisation of protein separation was primarily achieved using Ultimate[™] 3000 HPLC systems which provided flexibility to perform one-dimensional or two-dimensional separation using various column formats and fraction collection settings. Two-dimensional separation could be easily achieved and provided further confirmation that recombinant lysostaphin variants could be selectively separated from purified and crude preparations. Second dimensional RP separations also indicated that recombinant lysostaphin preparations contained protein variants which differed in their hydrophobicity as well as charge. Greater

resolution of product heterogeneity was achieved using ProPac[®] MAb SCX separations or through intact protein LC-MS however.

Enhanced resolution and separation of protein isoforms was achieved through optimisation of mobile and stationary phase conditions. Adjustment of mobile phase pH from 7.0 to 8.0 and extension of gradient duration to 70 min was found to provide the most efficient separation using the ProPac[®] WCX-10 (4 x 250 mm) column. The use of an extended ProPac[®] WCX-10 (4 x 500 mm) column or a narrower bore ProPac[®] WCX-10 (2 x 500 mm) was found to provide enhanced separation. Column dimensions were ultimately selected according to amount of protein available for analysis and the speed at which analysis needed to be performed.

Sample preparation was of paramount importance during this research due to the unknown origins of charge heterogeneity, which may have arisen during expression, purification or storage. Whilst purified preparations of recombinant lysostaphin provided material which could be used to steadily optimise mobile and stationary phase conditions, reliable assessment of charge heterogeneity could not be achieved due to retention time variability and differences in expression and harvest conditions. In addition, lyophilised preparations could not be reliably separated, despite demonstrating staphylolytic activity and providing long-term stability. The ability to efficiently and selectively separate recombinant lysostaphin charge variants, directly from cell lysate therefore provided a convenient and reliable source of recombinant lysostaphin for analysis.

Separation of protein isoforms present within purified recombinant lysostaphin or cell lysate derived from large shake-flask cultures, was readily achieved using the ProPac[®] WCX-10 (4.0 x 500 mm) column and demonstrated that recombinant lysostaphin preparation can demonstrate considerable charge heterogeneity. Greater charge heterogeneity was associated with higher incubation temperatures or induction of protein expression at higher optical densities. Knowledge of these contributing factors lead to a series of experiments that demonstrated that expression at 16°C and earlier protein harvesting was associated in a more homogeneous protein preparation. It was therefore evident that like product yield, product heterogeneity must be manipulated and monitored during recombinant protein expression, to yield a homogeneous product.

WCX analysis of other cationic recombinant protein preparations, including recombinant oxidoreductase and recombinant NADPH-dependent 1-acyl dihydroxyacetone phosphate reductase (Ayr1p) demonstrated that charge heterogeneity was not restricted to recombinant lysostaphin. Post-translational processing or modification of recombinant proteins expressed

in *E. coli* is not uncommon, as evidenced by publications cited in Section 1.2.1. However it was surprising that two other basic recombinant proteins, which do not share functional or sequence homology with recombinant lysostaphin, could also demonstrate charge heterogeneity upon WCX separation. These findings indicate that charge heterogeneity, post-translational processing and modification of recombinant proteins could be a widespread phenomenon, which must be acknowledged during the industrial and biopharmaceutical production of recombinant proteins within *E. coli*.

The influence of time and optical density at the point of induction upon the charge heterogeneity of recombinant lysostaphin only became apparent through rapid analysis of protein isoforms present within cell lysate using the ProPac[®] WCX-10 (2.0 x 500 mm) column and ProPac[®] MAb SCX-10 (4.0 x 500 mm) columns. Rapid analysis of *N*-terminally His-tagged recombinant lysostaphin (construct 1) revealed a time-dependent pattern of charge heterogeneity, in which particular acidic charge variants emerged over time. Extended culture analysis of a second culture demonstrated the same pattern of variant formation, providing secondary confirmation of this finding. Protein variant formation did however occur at a slower rate which corresponded with the slower bacterial growth rate of the culture. Rapid analysis therefore provided comprehensive evaluation of the time-dependent nature of charge variant formation during the course of expression.

The time-dependent pattern of charge variant formation provided an explanatory mechanism for the emergence of acidic and basic protein isoforms during the expression of recombinant lysostaphin and explained the variable nature of charge heterogeneity observed when cultures were induced at various optical densities. With a knowledge of how charge variant formation occurs and factors affecting the degree of charge heterogeneity, it would be possible to adjust expression and harvesting conditions to produce a more homogeneous product. For instance, reduced optical densities at the point of induction (> 1.0 AU), reduced expression temperatures (16°C) and early harvest of the recombinant product (>3h post-induction) would provide a more homogeneous product. The use of AIM should be avoided on the grounds that the time and optical density at auto-induction could not be monitored precisely, unlike IPTG induction.

This research also demonstrated the power of existing IEX column chemistries to resolve charge heterogeneity within recombinant protein preparations. Using various column formats, ProPac[®] WCX and SCX columns provided separation and resolution of charge variants to provide an insight into heterogeneity of recombinant lysostaphin. In addition, rapid analysis also provided a robust and efficient method that could be used to provide rapid, real-time analysis of recombinant protein production. The greatest separation and

resolution was demonstrated using the ProPac[®] MAb SCX column in the later stages of research. The resolution of this column provided explanations for many questions encountered during the characterisation of recombinant lysostaphin. Therefore it is hoped that further developments of ProPac[®] MAb SCX column format and chemistries will provide even greater resolution and separation of charge variants in the near future.

5.3 Activity of recombinant lysostaphin

Functional analysis of recombinant lysostaphin demonstrated that purified and lyophilised preparations demonstrated staphylolytic activity. Staphylolytic activity was not affected by the presence of *N*- or *C*-terminal His-tags, the choice of expression media or translocation to the periplasmic space. Furthermore turbidometric assay of charge variants which had been separated by WCX, revealed that putative post-translational processing or modification of recombinant lysostaphin did not interfere with staphylolytic activity. Confirmed staphylolytic activity of all assayed samples indicated that the expressed protein structure contained zinc, which is essential for the catalytic activity of lysostaphin and suggested that protein truncation or the presence of fusion tags or PTMs does not interfere with enzyme activity. Bioinformatic analysis also suggested that the zinc cofactor may have bound at conserved zinc binding domain residues which are common to lysostaphin-type enzymes, such as LytM (Bochtler *et al.*, 2004).

Although separated charge variants demonstrated staphylolytic activity, it could not be guaranteed that every charge variant present within the micro-heterogeneity of recombinant lysostaphin preparations possessed staphylolytic activity. Product micro-heterogeneity could be resolved during ProPac[®] MAb SCX separation, however separation of distinct charge variants at sufficient concentrations to enable assay would be difficult to achieve, particularly using a turbidometric assay. The implementation of a more sensitive assay, which could assess enzyme kinetics, at a low concentration of recombinant lysostaphin, would therefore be desirable to achieve greater functional characterisation of recombinant lysostaphin. For the purposes of this research, a simple turbidometric assay sufficed and demonstrated the potent anti-staphylococcal activity of recombinant lysostaphin.

5.4 IMAC analysis of recombinant lysostaphin

Recombinant lysostaphin was analysed during a number of chromatographic studies in which the retention behaviour, stability and mass were investigated. Retention behaviour was investigated after poor binding efficiency was observed during IMAC purification. Sequential IMAC purifications demonstrated that the charge heterogeneity of *N*-terminally

His-tagged recombinant lysostaphin (construct 1) interfered with binding efficiency during IMAC and therefore to achieve full purification, cell lysate had to be applied to the column several times, leading to the observation of unusual retention behaviour. WCX analysis of purified protein indicated that a greater abundance of more basic variants was associated with stronger binding affinity, whilst more moderate binding affinity was associated with a greater abundance of more acidic variants.

C-terminally His-tagged recombinant lysostaphin (construct 3) exhibited much greater binding efficiency during IMAC purification. Although some unusual retention behaviour was observed during IMAC purification, WCX separation did not suggest that protein binding affinity was associated with charge heterogeneity, but rather high sample loading. It was thought that unusual retention behaviour observed during IMAC purification could be attributed to high sample loading and the principles of negative cooperative binding, whereby protein molecules with a stronger binding affinity cannot achieve multipoint adsorption due to a lack of favourable binding sites. Furthermore, it was thought that truncation or modification of *N*-terminal His-tag residues may compromise the strength of binding affinity.

WCX separation of *N*-terminally His-tagged recombinant lysostaphin (construct 1) revealed that the protein preparations demonstrated greater charge heterogeneity than *C*-terminally His-tagged recombinant lysostaphin (construct 3) and recombinant lysostaphin without His-tags (construct 2) which both exhibited a lesser, yet similar degree of charge heterogeneity. The observed charge variants appeared to reflect the respective theoretical pIs of the proteins, however it was interesting to note that the *N*-terminally His-tagged recombinant lysostaphin (construct 1) preparation contained variants with the same charge as observed during separation of recombinant lysostaphin (constructs 2 and 3). This result suggested that *N*-terminally His-tagged recombinant lysostaphin preparations may have undergone truncation. Alternatively the formation of more acidic variants may be attributable to phosphorylation, gluconoylation or phosphogluconoylation of the *N*-terminal His-tag sequence (She *et al.*, 2010, Du *et al.*, 2005a, Du *et al.*, 2005b).

Overall these results indicated that great care must be taken when using IMAC to purify a recombinant protein expressed in *E. coli*, particularly if the homogeneity of the product is uncertain. *N*-terminally His-tagged recombinant lysostaphin (construct 1) was associated with inefficient IMAC purification, therefore removal of the *N*-terminal His-tag sequence would be advisable. Alternatively expression and purification of *C*-terminally His-tagged recombinant lysostaphin (construct 3) or recombinant lysostaphin without His-tags (construct 2) using IMAC or preferably CXC would be advisable to improve the efficiency of purification and minimise the heterogeneity of the recombinant protein preparation.

5.5 GF analysis of recombinant lysostaphin

Recombinant lysostaphin was found to display long-term stability in liquid formulation when stored at 4°C which was extremely useful during the optimisation of protein separation. Lyophilised preparations also provided long-term stability, however issues with protein insolubility interfered with the capacity to analyse the resuspended recombinant lysostaphin. GF analysis of recombinant lysostaphin which had been purified by IMAC under non-denaturing and denaturing conditions indicated that the protein was unlikely to be aggregated. GF separation of protein which had been separated by WCX during culture analysis also did not suggest the presence of aggregated species, however did indicate that protein eluted within peaks separated during WCX analysis demonstrated subtle mass heterogeneity. The observed heterogeneity was thought to be attributable to micro-heterogeneity which could only be observed following separation using the ProPac[®] MAb SCX column.

Mass heterogeneity was also detected during SDS-PAGE performed following culture analysis, which revealed the presence of a low abundance protein with a molecular weight corresponding more closely to that of recombinant lysostaphin (construct 1). This finding indicated that the bulk of recombinant lysostaphin preparations may in fact be composed of a truncated form of the protein. Closer examination of GF chromatograms provided further evidence that full-length “native” lysostaphin may be present in the majority of samples however was often undetectable during SDS-PAGE due to being present at such low concentrations. Whilst GF analysis proved to be very informative, high resolution analysis of mass heterogeneity could not be achieved using the Zorbax[®] GF-250 column.

5.6 LC-MS analysis of recombinant lysostaphin

High resolution analysis of mass heterogeneity could be obtained through LC-MS analysis of intact recombinant lysostaphin (construct 1) using a MaXis UHR-TOF system. LC-MS analysis revealed that the intact protein samples were heterogeneous despite prior separation by WCX. This finding was not surprising considering that previous SCX and GF separations performed using the ProPac[®] MAb SCX and Zorbax[®] GF-250 columns had demonstrated additional charge and mass heterogeneity. The obtained mass spectra indicated that protein eluted during WCX separation was largely composed of protein with a mass below the expected mass of *N*-terminally His-tagged recombinant lysostaphin (construct 1), suggesting that the protein had undergone truncation.

LC-MS analysis of more acidic protein variants eluted within WCX fraction 14 demonstrated that the most predominant variant has a mass of 29050.5 Da, reflecting loss of 287.3 Da from the expected mass of recombinant lysostaphin (construct 1) in an apoprotein state. Such a loss may have reflected the loss of several amino acids from either the *N*- or *C*-terminus of the protein, or possibly both termini. Loss of *C*-terminal lysine₂₆₇ would provide a logical explanation for the observed acidity of the protein during WCX analysis.

LC-MS analysis of more basic protein variants eluted within WCX fraction 25 indicated that the most predominant variant has a mass of 29107.7 Da, reflecting loss of 230.1 Da from the expected mass of *N*-terminally His-tagged recombinant lysostaphin (construct 1) in an apoprotein state. Once again this loss may have indicated the loss of several amino acids from either the *N*- or *C*-terminus of the protein, or possibly both termini. As fraction 25 contained more basic protein isoforms, it seemed logical that truncation could have occurred at the *N*-terminus of recombinant lysostaphin, which features neutral or hydrophobic amino acid residues.

The acquired intact mass measurements were found to correlate with some of the theoretical mass measurements of full-length and truncated forms recombinant lysostaphin (construct 1) in an apoprotein state. For instance, during LC-MS analysis of WCX fraction 25, a low abundance protein was detected with a mass of 29336.9 Da which was extremely close to the mass of full-length recombinant lysostaphin (construct 1). This finding supported the theory that the intact recombinant lysostaphin was present within the protein preparations, but only at low abundance. Due to the high mass accuracy provided by the MaXis UHR-TOF-system and slight differences between theoretical and acquired masses it was evident that nature of resolved protein variants could not be elucidated without confirmatory sequence data acquired by LC-MS/MS.

Nonetheless the acquired mass measurements indicated that the majority of the *N*-terminally His-tagged recombinant lysostaphin (construct 1) preparation had undergone truncation of *N*- *C*- or *N*- and *C*-terminal residues. It also seemed likely that the intact mass measurements reflected protein truncation, in conjunction with mass increments or decrements associated with the addition of PTMs. These findings would provide an explanation for the micro- and macro-heterogeneity observed during chromatographic separation of recombinant lysostaphin preparations. Further confirmation of these theories could be achieved by performing MS/MS analysis of intact protein or digested peptides in combination with MS_n analysis, 100% sequence coverage should be obtainable, permitting full characterisation of sequence variants and PTMs. *N*- and *C*-terminal sequences could also be investigated by MALDI-MS or by using MS/MS data to perform *de novo* sequencing.

5.7 Heterogeneity of recombinant lysostaphin

This research has demonstrated that recombinant lysostaphin displays considerable heterogeneity when expressed in *E. coli*. Charge heterogeneity within recombinant lysostaphin preparations became evident whilst optimising CXC separation following cloning, expression and purification of recombinant lysostaphin (construct 1, 2, 3 and 4). Recombinant lysostaphin was expressed within the cytoplasm of *E. coli* or was translocated to the periplasmic space, however charge heterogeneity was still observed upon CXC separation of periplasmically expressed C-terminally His-tagged recombinant lysostaphin (construct 4). The charge heterogeneity of recombinant lysostaphin (construct 5), which had been successfully translocated to the periplasm in a soluble form, was not investigated however, as the other forms of recombinant lysostaphin were more convenient to harvest and purify during initial studies.

Through continued expression, purification and separation of recombinant lysostaphin it became apparent that the charge heterogeneity of recombinant lysostaphin could be extremely variable and therefore could be attributable to a number of factors, including amino acid sequence and expression conditions, such as temperature, location and media. To minimise variables, analysis was primarily focused on N-terminally His-tagged recombinant lysostaphin (construct 1), which could be conveniently harvested from the cytoplasm of *E. coli* and purified efficiently using IMAC or CXC. Repeated CXC separation of N-terminally His-tagged recombinant lysostaphin (construct 1) demonstrated that most preparations were associated with the presence of a number of acidic and basic protein variants. It also became apparent that the abundance of such variants was dependent upon time and optical density at the point of induction of protein expression.

Rapid analysis of shake-flask cultures which were incubated for between 30 and 85.5 h post-induction, demonstrated a time-dependent pattern of charge variant formation (Sections 3.5.3.11 and 3.5.3.12). In this pattern, recombinant protein expression was marked by the presence of more basic charge variants, which appeared to undergo conversion to produce a more acid charge variant. A conversion mechanism was proposed as the initial increase in abundance of basic variants was followed by a steady increase in acidic variants, which appeared to occur in proportion to a steady decrease in the abundance of basic variants. The expression level of the basic variant was not found to decrease completely, which supported the theory that this variant reflected the 'native' state in which *E. coli* translated recombinant lysostaphin (construct 1) during the course of expression.

The term 'native' state could only be used tentatively, as it was not clear whether *E. coli* translated *N*-terminally His-tagged recombinant lysostaphin exactly as encoded by the pET vector construct (construct 1). This could only be confirmed by performing a series of characterisation experiments to assess the mass of *N*-terminally His-tagged recombinant lysostaphin. The mass of *N*-terminally His-tagged recombinant lysostaphin was investigated through SDS-PAGE, GF separation and LC-MS analysis, which provided an increasing degree of mass resolution. SDS-PAGE generally indicated that recombinant lysostaphin preparations were homogeneous, however SDS-PAGE analysis of recombinant lysostaphin harvested during culture analysis indicated that a small proportion of the preparation actually had a mass which appeared closer to the expected mass of recombinant lysostaphin (construct 1) (Section 3.5.3.11). This was an unexpected finding, as the mass determination by SDS-PAGE was assumed to be fairly inaccurate considering the fairly low resolution of the technique. In addition it seemed unusual that the majority of the protein preparation appeared to be of a lesser mass. This finding therefore provided the first indication that *N*-terminally His-tagged recombinant lysostaphin (construct 1) may become truncated upon expression in *E. coli*.

GF analysis provided further confirmation of mass heterogeneity within recombinant lysostaphin (construct 1) preparations, which seemed unlikely to be attributable to aggregated species. Correlation of SDS-PAGE and GF results suggested that most recombinant lysostaphin preparations contained a low abundance protein with a mass closer to the expected mass of recombinant lysostaphin. The greater abundance of lower molecular weight species further supported the theory that recombinant lysostaphin (construct 1) may have undergone truncation. Mass heterogeneity was even observed following WCX separation of charge variants, which was a little surprising, however correlated with separations performed using the ProPac[®] MAb SCX column in which macro- and micro-heterogeneity was clearly observed.

High-resolution analysis of mass could be achieved through LC-MS analysis of intact recombinant lysostaphin. LC-MS analysis revealed that protein which had been separated by WCX still displayed mass heterogeneity and that the most predominant protein isoforms possessed masses which were 287.3 Da and 230.1 Da less than the expected mass of *N*-terminally His-tagged recombinant lysostaphin (construct 1), which had a mass of 29337.8 Da. As the more acidic protein variant was associated with loss of 287.3 Da it was postulated that this loss may be associated with cleavage of the C-terminal lysine₂₆₇ residue and additional uncharged residues from the *N*- or C-terminus. The more basic protein variant

was therefore only thought to be associated with loss of uncharged amino acids from the *N*-terminus of the protein.

LC-MS, GF and SDS-PAGE analysis all indicated that recombinant lysostaphin preparations may have contained a low abundance protein variant with a molecular weight close to the theoretical mass of *N*-terminally His-tagged recombinant lysostaphin (construct 1). These results therefore indicated that the 'native' protein that was predicted to be expressed during culture was in fact a truncated form of the protein. On the grounds of LC-MS data, it seemed likely however that the 'native' protein detected during culture analysis had a very similar charge to that of full-length recombinant lysostaphin, possibly due to loss of uncharged *N*-terminal residues. Further explanation of the charge and mass heterogeneity of *N*-terminally His-tagged recombinant lysostaphin (construct 1) is provided in Figure 5.1.

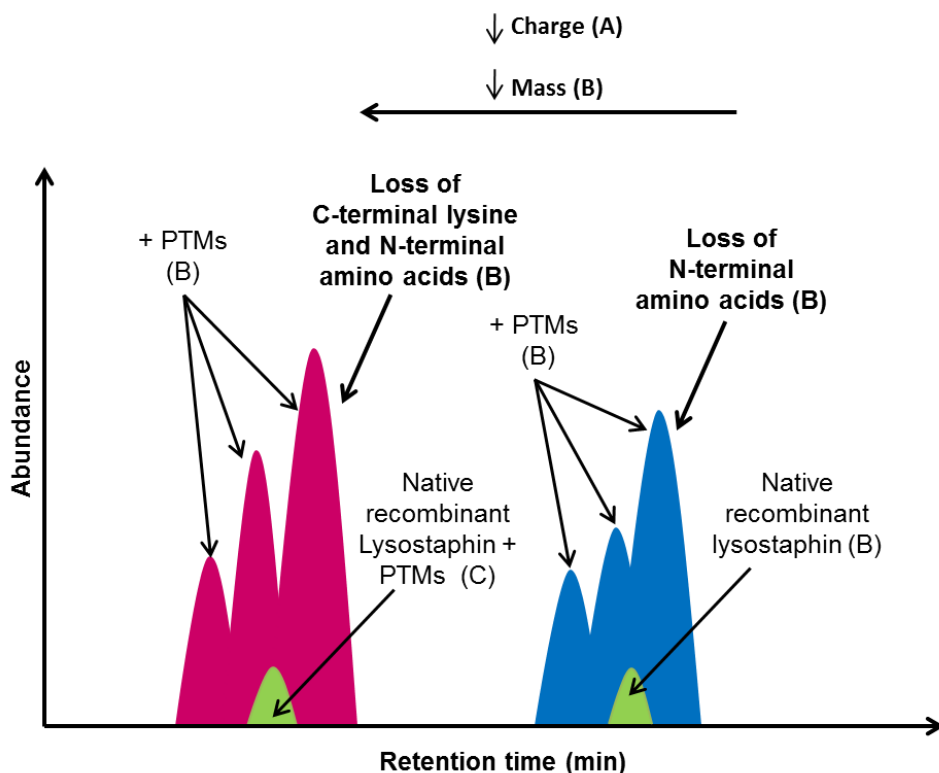


Figure 5.1: Explanation of observed charge and mass heterogeneity within *N*-terminally His-tagged recombinant lysostaphin (construct 1) preparations. Comparison of results obtained during CXC separation (A), LC-MS analysis (B), GF analysis and SDS-PAGE (C) provided the proposed explanations. Macro- and micro-heterogeneity observed during separation of recombinant lysostaphin using the ProPac[®] MAb SCX column (A) revealed a number of acidic and basic peaks upon which these explanations are based. LC-MS analysis (B) revealed that acidic and basic peaks were likely to be associated with loss of amino acids from the *N*- or *C*-terminus, but also PTMs resulting in mass decrements or increments. LC-MS analysis (B), GF analysis and SDS-PAGE (C) suggested that full-length recombinant lysostaphin may be present as a low abundance basic variant and a low abundance variant with PTMs which reduce protein charge.

Further confirmation of these explanations is required and could be achieved through MS/MS analysis of intact and digested recombinant lysostaphin. Additional validation of these results is also essential considering that these concepts have been derived from data which was obtained following analysis of *N*-terminally His-tagged recombinant lysostaphin (construct 1), which had been expressed in different shake-flask cultures. Correlation between LC-MS, CXC, GF and SDS-PAGE analysis results does however favour these explanations.

5.8 Truncation of recombinant lysostaphin

The theoretical mass of *N*-terminally His-tagged recombinant lysostaphin was calculated on the basis that the *N*-terminal methionine residue was retained. The *N*-terminal methionine residue is not always retained as methionine aminopeptidases (MetAPs) co-translationally process the removal of the *N*-terminal methionine as the nascent polypeptide emerges from the ribosome. In a few instances, the *N*-terminal methionine residue has found to not be removed during recombinant production (Table 1.6); therefore the theoretical mass of *N*-terminally His-tagged recombinant lysostaphin was calculated based on the maximum number of amino acids which could be translated within the polypeptide. The intact protein masses obtained during LC-MS analysis suggested that the *N*-terminal methionine was likely to have been co-translationally removed during expression, in addition to post-translational removal of additional *N*- or *C*-terminal residues.

Truncation of *N*-terminally His-tagged recombinant lysostaphin (construct 1) may have arisen as a consequence of cloning and expressing only the mature lysostaphin encoding domain, rather than the gene encoding preprolysostaphin. In *S. staphylolyticus* lysostaphin is expressed extracellularly as a catalytically active 27 kDa mature enzyme, following conversion from prolysostaphin by a cell wall-associated cysteine protease (Grundling and Schneewind, 2006). Prolysostaphin is itself derived from signal peptidase cleavage of the *N*-terminal signal peptide of 42 kDa preprolysostaphin upon signal peptide-mediated translocation from the cytoplasm to the periplasm. The presence of the *N*-terminal signal peptide region of preprolysostaphin and the prepropeptide of prolyostaphin therefore shields the *N*-terminal residues of mature lysostaphin from proteolytic cleavage, as the proenzyme translocates from the cytoplasm to periplasm and to extracellular space.

An alternative explanation for the truncation of *N*-terminally His-tagged recombinant lysostaphin may be dependent on the elastolytic activity of lysostaphin. Although recombinant lysostaphin is produced to take advantage of its potent staphylolytic activity, the elastolytic activity of the enzyme is often disregarded. As the amino acid sequence of elastin is glycine rich, it is likely that lysostaphin's elastolytic activity is attributable to the enzymes preference for glycine-rich sequences (Park *et al.*, 1995). Elastolytic activity of lysostaphin proceeds under slow kinetics, however could theoretically auto-catalyse cleavage of peptide bonds associated with hydrophobic or aromatic amino acids which are accessible within the structure of recombinant lysostaphin (Park *et al.*, 1995, Mecham *et al.*, 1997). Evidence of such an interaction was observed in related work following peptide identification of tryptically digested *N*-terminally His-tagged recombinant lysostaphin (construct 1) (Appendix 7.341, associated data not shown).

As explained in Section 4.1.1.2, elastolytic activity is dependent on the presence of zinc and a distinct catalytic binding domain, featuring an Ala-Ala-Thr-His-Glu sequence in the *N*-terminal portion of mature lysostaphin (Figure 5.2). The tertiary conformation of recombinant lysostaphin is likely to be primarily dictated by the zinc binding domain residues within the protein, however in the absence of the crystal structure of lysostaphin it is hard to predict how the protein will fold. It does however seem feasible that the elastolytic catalytic domain could interact with the *C*-terminal residues if they became proximal. If auto-elastolytic activity was responsible for proteolysis of cleavage of peptide bonds within the sequence of recombinant lysostaphin, then expression of recombinant prolysostaphin may help to reduce elastolytic activity, as prolysostaphin is known to be 4.5 fold less active than mature lysostaphin (Thumm and Götz, 1997).

MGSSHHHHHSSRLVPRGSHMAATHESAQWLNNYKKGYPYPL
 GINGGMHYGVDFFMNIGTPVKAISSGKIVEAGWSNYGGGNQIGLIEND
 GVHRQWYMHLISKYNVKVG DYVKAGQIIGWSGSTGYSTAPHLHFQRMV
 NSFSNSTAQDPMPFLKSAGYGKAGGTVTPTNTGWKTNKYGTLYKSE
 SASFTPNTDIITRTTGPFERSMPQSGVLKAGQTIHYDEVMKQDGHVWVG
 YTGNSGQRIYLPVRTWNKSTNTLGVLWGVIK

Figure 5.2: Amino acid sequence of *N*-terminally His-tagged recombinant lysostaphin (construct 1) indicating the *N*-terminal His-tag sequence (red), proposed catalytic site for elastolytic activity (green) and zinc binding domain residues (blue) as determined by ClustalW analysis performed in Section 4.1.3.1.

Protein truncation can also result during expression due to a number of reasons, such as codon bias or proteolytic processing. As lysostaphin is derived from a prokaryotic source, extreme codon bias would not be expected during the expression of recombinant lysostaphin in *E. coli*. *S. staphylolyticus* has a GC content of 35%, whilst *E. coli* BL21(DE3) has a slightly higher GC content of 50.8% and therefore codon bias is unlikely to exert a significant influence on protein expression (Sloan *et al.*, 1982). If codon bias did occur, then premature termination of protein translation would occur, yielding an abnormal protein, which would be rapidly recognised and degraded by host cell proteases.

The cytoplasm of *E. coli* does however possess a number of proteases which can degrade abnormal or foreign proteins. Cellular proteasomes survey the cellular environment to detect incomplete proteins, mis-sense proteins, post-synthetically damaged proteins, denatured proteins, mis-folded proteins or genetically-engineered proteins (Goldberg, 2003). In prokaryotes, such as *E. coli*, degradation involves a number of ATP-dependent proteases, such as Lon (La), HflB (FtsH), ClpAP, ClpXP and ClpYQ (Hs1UV), which have distinct

substrate specificities (Gottesman *et al.*, 1998). Although peptide bond hydrolysis does not require ATP hydrolysis, the ATP dependence is thought to be required to permit substrate unfolding to facilitate degradation (Starkova *et al.*, 1998). The proteases are co-ordinately induced along with molecular chaperones, as part of a heat-shock response, which is initiated when large amounts of unfolded or foreign proteins are expressed (Goldberg, 2003).

Protein unfolding is a critical factor in proteolysis and therefore chaperones enhance the process of protein degradation. Proteolysis therefore occurs in a progressive manner in which the substrate is unravelled from a 'degradation signal' which is present somewhere in the amino acid sequence of the protein. The selectivity of intracellular proteolysis depends on the ability of the enzyme to detect a specific 'degradation signal' which is typically determined by C- or N-terminal sequences or chemical damage such as oxidation, glycation or deamidation (Goldberg, 2003, Keiler and Sauer, 1996). The level of degradation by the proteases is then determined by protein stability, which is weaker if a protein has been mis-folded or has an absent co-factor (Prakash *et al.*, 2004, Goldberg, 2003).

GF analysis suggested that N-terminally His-tagged recombinant lysostaphin (construct 1) was unlikely to be aggregated and therefore it was less likely that the protein was mis-folded following expression. Zinc is known to bind tightly within the structure of metalloproteins and therefore the structure of recombinant lysostaphin would be preserved by the presence of the zinc cofactor. However as demonstrated by Figure 5.2, the genetically engineered N-terminal His-tag sequence or C-terminal residues may have been accessible to proteases and therefore may provide a degradation signal, which leads to progressive degradation of recombinant lysostaphin, which was believed to be observed during the later stages of culture analysis (Section 3.5.3.11). The speed and consistency at which acidic charge variants developed would also suggest that an enzymatic mechanism of conversion was involved. Proteolytic activity would also be enhanced by increased temperatures or richness of expression media, which would explain why charge heterogeneity was increased at higher temperatures or within complex media such as AIM or LB (Swamy and Goldberg, 1982).

5.9 PTM of recombinant lysostaphin

LC-MS analysis of N-terminally His-tagged recombinant lysostaphin (construct 1) revealed that intact mass measurements could not be exclusively attributable to the loss of specific N- or C-terminal residues and therefore it was thought that PTM of recombinant lysostaphin variants could provide an explanation for additional mass increments or decrements. This theory was supported by the additional mass and charge micro-heterogeneity, which was observed during GF and SCX analysis, performed using the ProPac[®] MAb SCX and Zorbax[®]

GF-250 columns. Whilst mass heterogeneity could be attributable to PTM of any amino acid residue, charge heterogeneity would only be caused by modification of charged amino acid residues. As discussed in Section 3.6, there are multiple charged residues within the sequence of recombinant lysostaphin which may have become modified by enzymatic or chemical modifications.

WCX analysis revealed that *N*-terminally His-tagged recombinant lysostaphin (construct 1) exhibited greater heterogeneity than *C*-terminally His-tagged or non-tagged forms of recombinant lysostaphin, which would suggest that the *N*-terminal His-tag sequence may have undergone modification. Furthermore, *N*-terminally His-tagged recombinant lysostaphin (construct 1) exhibited unusual retention behaviour and poor binding capacity during IMAC purification, indicating *N*-terminal His-tag heterogeneity. *N*-terminal His-tag heterogeneity is not unknown, as reported in Table 4.1 and therefore it was possible that the *N*-terminal His-tag sequence may have undergone phosphorylation of serine residues or modification of the α -amino acid, in the form of gluconoylation or phosphogluconoylation.

Phosphorylation of serine residues and gluconoylation or phosphogluconoylation of the α -amino acid would lead to the development of acidic recombinant lysostaphin variants, through the introduction of negative charges or neutralisation of the positively charged α -amino terminus. Given that α -*N*-6 gluconoylation and α -*N*-6 phosphogluconoylation result in mass increments of 178 Da and 258 Da respectively, such modifications would have to have occurred in conjunction with loss of several *N*-terminal or *C*-terminal residues. The occurrence of such α -*N*-terminal modifications could trigger *N*-terminal proteolysis or conversely *N*-terminal proteolysis may minimise the occurrence of such modifications. Phosphorylation of serine residues would seem more logical considering that the addition of single or multiple negatively charged phosphate groups could interfere with the binding affinity of the *N*-terminal His-tag sequence during IMAC purification.

Other *N*-terminal modifications may have led to the development of more acidic recombinant lysostaphin variants, such as the retention of *N*-formylmethionine or addition of *N*-acetyl or *N*-methyl groups. The retention of *N*-formylmethionine is unlikely considering the loss of mass detected during LC-MS analysis, however *N*-acetylation of *N*-terminal residues may feasibly occur to stabilise the structure of recombinant lysostaphin following removal of *N*-terminal methionine or glycine residues (Charbaut *et al.*, 2002). Chemical modification of amino acid side chain groups, such as oxidation, deamidation or glycation could also produce acidic variants, and if present at *N*- or *C*-terminal sequences, could act as a degradation signal for proteolysis. Given the chemical nature of these modifications, it is

however unclear whether more complex multi-stage modifications such as glycation could lead to the formation of acidic recombinant lysostaphin variants, as readily and consistently as was observed during culture analysis. Smaller, less complex chemical modifications such as oxidation or deamidation would therefore seem more likely.

Enzyme-catalysed side chain modification would be able to occur readily and in a more consistent manner, therefore would have led to the formation of acidic recombinant lysostaphin variants. Phosphorylation and acetylation are known to increase the net charge of a protein, whilst methylation can either neutralise ϵ -amino charges upon the addition of mono- or di-methyl groups, or introduce a positively charged tri-methyl group (Gooley and Packer, 1997). The majority of these modifications would have decreased the charge of *N*-terminally His-tagged recombinant lysostaphin (construct 1), but would have also increased the mass of the protein (Table 5.1). These modifications would therefore have had to occur along with truncation events, which reduced the mass of the protein.

Table 5.1: N-terminal and side chain modifications and their monoisotopic mass increments

Modification location	Modification	Mass increment (Da)
N-terminal	Formylation	27.99
	Acetylation	42.01
	Gluconoylation	178.05
	Phosphogluconoylation	258.02
Side chain	Phosphorylation	79.97
	Acetylation	42.01
	Methylation	14.02
	- Dimethylation	28.04
	- Trimethylation	43.06
	Glycation	162.05
	Deamidation	0.98
Oxidation	15.99	

Elucidation and confirmation of PTMs and sequence variation contributing the observed charge and mass heterogeneity could be achieved by MS/MS analysis of intact and digested recombinant lysostaphin. It is possible that recombinant lysostaphin, like other recombinant proteins, may be only partially modified at a particular site or affected by several kinds of PTM, which complicates identification (Hepner *et al.*, 2005, Lahnstein *et al.*, 1993). The presence of multiple modifications would however help to explain the charge and mass heterogeneity of recombinant lysostaphin.

5.10 Consequences of product heterogeneity

Even though this research has raised a number of concerns over the heterogeneity of recombinant lysostaphin, it does not necessarily mean that *E. coli* usage should be discontinued during the production of recombinant lysostaphin for industrial, research or even potential therapeutic purposes. For instance, recombinant lysostaphin was shown to exhibit potent staphylolytic activity during activity assays, which demonstrated that the enzyme is of importance for research or diagnostic purposes where the heterogeneity of the protein mixture is not of concern or importance. IMAC purification of N-terminally His-tagged forms of recombinant lysostaphin would however have to be performed with caution, to ensure complete purification of the protein.

In terms of therapeutic efficacy, recombinant lysostaphin was shown to provide potent staphylolytic activity, which shows great promise for the treatment of blood-borne and biofilm-associated staphylococcal infections. Furthermore, the loss of *N*- or *C*-terminal amino acids would be unlikely to initiate an immunogenic response upon therapeutic administration of recombinant lysostaphin. However without performing immunological studies, it is unclear whether potential PTMs of recombinant lysostaphin would contravene its use as a therapeutic agent. The identification of PTMs affecting the structure of recombinant lysostaphin would however be extremely desirable so that their presence could be prevented or eliminated. Prevention or elimination of PTMs is largely dependent on the nature of the modification which may be reversible or irreversible, necessitating removal of the modified amino acid.

Overall *E. coli* has been shown to produce large amounts of recombinant lysostaphin in an economical manner; however the observed heterogeneity would contravene drug quality standards. Further investigation of the heterogeneity is therefore essential to establish whether a more homogeneous recombinant lysostaphin preparation can be produced, without resorting to the use of less well characterised expression hosts, such as *L. lactis* or *Bacillus sphaericus* (Mierau *et al.*, 2005a, Climo *et al.*, 2001).

Charge heterogeneity observed during CXC separation of other basic recombinant proteins, recombinant oxidoreductase and recombinant NADPH-dependent 1-acyl dihydroxyacetone phosphate reductase (Ayr1p) is however more concerning as it indicates that product heterogeneity may be a widespread phenomenon that affects many recombinant proteins which are expressed in *E. coli*. Further more stringent characterisation of biologically important recombinant proteins is therefore required to assess whether the origins of heterogeneity follow the same or different mechanisms. Such information would then permit optimisation of expression and harvesting conditions or the development of additional genetically and metabolically engineered expression strains (Aon *et al.*, 2008).

5.11 Detection and remediation of product heterogeneity

As product heterogeneity was believed to arise as a consequence of His-tag heterogeneity, proteolysis of *N*- and *C*-terminal sequences, PTMs and culture duration, remediation would be focused on these key areas. As the *N*-terminal His-tag sequence was associated with greater charge heterogeneity and unusual retention behaviour, chemical or enzymatic removal of this His-tag sequence or use of a *C*-terminal His-tag would be the simplest way to reduce product heterogeneity (Ueda *et al.*, 2003). Alternatively if *N*-terminal His-tag heterogeneity was found to be attributable to phosphorylation of serine residues within the His-tag sequence then a modified vector sequence, devoid of serine residues could be used during cloning and expression instead (Lomas-Lopez *et al.*, 2008).

The detection of proteolytic action could be monitored through combined AXC and CXC separation of cell lysate, in which cellular proteases would be likely to bind to an anion exchange resin, whilst recombinant lysostaphin would bind to the cation exchange resin. If cell lysate was rapidly analysed from the start of culture analysis, it would be likely that the induction of heat-shock response proteins could be detected by AXC, concomitant to the induction of recombinant lysostaphin expression, detected by CXC. Fractionated peaks which corresponded with up-regulated proteases could then be subjected to LC-MS based protein identification to elucidate the origins of proteolysis. Upon detection of a specific protease which could contribute to truncation of *N*-terminally His-tagged recombinant lysostaphin (construct 1), expression conditions could be adjusted by the use of protease inhibitors or an expression strain which is deficient in that particular protease (Strauch and Beckwith, 1988)

To protect the *N*-terminal residues of mature lysostaphin from proteolytic action, recombinant prolysostaphin could be expressed in *E. coli* and purified prior to *in vitro* conversion to mature lysostaphin by addition of a cysteine protease (Wandersman, 1989). The protein would have to be expressed as prolysostaphin rather than preprolysostaphin, as the signal peptide sequence of preprolysostaphin is specific to translocation of the inner membrane of *S. staphylolyticus* rather than *E. coli*. Even though prokaryotic signal peptides share a canonical design, signal peptides expressed within Gram-positive bacteria tend to be longer than those expressed within Gram-negative bacteria therefore it is unknown whether the signal peptide of preprolysostaphin can translocate the cell wall of *E. coli* (von Heijne, 1990, Chan, 1996). Given the basicity of recombinant mature lysostaphin, it would be hoped that the cleaved mature enzyme could be efficiently separated and purified from any uncleaved prolysostaphin, which would be acidic on the grounds of the high number of negatively

charged glutamate residues within the repetitive sequences that encode the propeptide region.

Alternatively targeted expression of recombinant lysostaphin within the periplasm may protect the *N*-terminal residues of the protein, due to the addition of an *N*-terminal PelB leader sequence. Recombinant lysostaphin (constructs 4 and 5) were cloned and expressed within the periplasm of *E. coli*, however these forms of the protein were not investigated fully. The presence of a PelB leader sequence would theoretically protect *N*-terminal residues until the leader sequence was cleaved by signal peptidases upon translocation through the inner membrane. However it is not clear whether the action of cytoplasmic proteases may cleave PelB leader sequence leading to ineffective translocation. Recombinant lysostaphin may also become susceptible to the action of proteases within the periplasm.

Following LC-MS/MS identification and localisation of PTMs affecting the structure of recombinant lysostaphin, product heterogeneity could be remediated through prevention or removal of the modifications. PTM prevention can be achieved through site-directed mutagenesis of known modification sites to prevent a particular PTM forming at a specific amino acid residue (Lu *et al.*, 1999). Alternatively enzyme-mediated side chain modification, such as methylation, acetylation and phosphorylation could be removed by treating the enzyme with demethylases, deacetylases and dephosphorylases respectively (Walsh and Jefferis, 2006, Paik *et al.*, 2007). This approach would however require additional purification and characterisation of recombinant lysostaphin, to ensure that the contaminating enzyme had been removed and that the modification had been successfully removed.

Chemical modifications are however often more insidious and may involve several stages of development. For instance, during deamidation the primary modification mechanism results in the irreversible formation of a metastable, five-membered succinimide ring intermediate, which ultimately yields aspartic acid (Reissner and Aswad, 2003). Whilst deamidation may not elicit immunogenicity, it can interfere with the stability of a protein therefore is undesirable. The occurrence of advanced glycation can result in the irreversible addition of a glucose moiety at lysine or arginine residues, which may elicit an immune response (Wilton *et al.*, 2006). The removal of chemical modifications may therefore be more difficult unless a specific enzyme is available, such as an amadoriase, which can deglycate proteins (Capuano *et al.*, 2007) .

As charge heterogeneity increases over the course of culture, product heterogeneity can be minimised by harvesting the protein shortly after induction of protein expression. The micro-heterogeneity of recombinant lysostaphin may be reduced further by utilising different *E. coli*

expression strains, such as *E. coli* Tuner or *E. coli* Tuner pLysS, which have been engineered to achieve homogeneous distribution of IPTG or tighter control of the *lac* promoter. By using such strains, induction of protein expression may occur in a more synchronised manner within the heterogeneous microbial cell population (Zhang *et al.*, 2007, Strauss *et al.*, 2001). The addition of pLysS also minimises leaky expression, which would prevent the premature expression and potential early modification of recombinant protein prior to induction of protein expression (Vincentelli *et al.*, 2003).

5.12 Recombinant lysostaphin as a zinc glycyl-glycine endopeptidase

During this research, the consequences of the presence of zinc within the structure of recombinant lysostaphin were largely unknown. It is known that lysostaphin is a zinc metalloprotease, in which the zinc molecule is essential for catalytic activity, but is also likely to help modulate protein structure in the absence of cysteine residues. As recombinant lysostaphin was found to exhibit staphylolytic activity, the bound zinc molecule will have been present in the majority of the protein population. This knowledge was extremely useful as it suggested that charge variants observed during CXC separation were less likely to be attributable to the presence of apo- and metalloprotein forms of recombinant lysostaphin.

This finding was partially supported by IMAC purification of recombinant lysostaphin (construct 2) which suggested that only a small proportion of the recombinant protein preparation possessed metal affinity. Whilst many amino acids can act as metal ion ligands, the inherent metal affinity of the zinc binding domain of recombinant lysostaphin would be most likely to participate in retention during IMAC. This theory was supported by the work of Warfield *et al.* (2006), who found that lysostaphin could bind nickel ions. However nickel binding was also thought to occur as a consequence of zinc displacement during the course of IMAC purification, therefore the incidence of metal affinity during IMAC may have been more attributable to zinc displacement (Warfield *et al.*, 2006).

Through functional analysis of recombinant lysostaphin, it was possible to gain further insight into structural conformation of the zinc binding domain of recombinant lysostaphin. ClustalW comparison of the amino acid sequences encoding recombinant lysostaphin and a lysostaphin-type peptidase, LytM, revealed that the zinc binding domain of recombinant lysostaphin was likely to involve histidine₃₃, aspartate₃₇ and histidine₁₁₆, which along with a water molecule, tetrahedrally coordinate with zinc. Knowledge about this zinc binding domain enhanced knowledge about the activity of recombinant lysostaphin as a zinc metalloprotease but also provided an insight into protein structure.

5.13 Conclusions

In summary this research has shown that when recombinant lysostaphin is expressed in *E. coli*, the resulting active protein can demonstrate considerable charge heterogeneity. Using a variety of chromatographic modes, including IEX, GF, IMAC, HIC and RP, several variants of recombinant lysostaphin were resolved indicating differences in charge, mass and hydrophobicity. The degree of charge heterogeneity observed was influenced by a number of factors, including expression temperature, amino acid sequence, optical density at point of induction and duration of culture. Rapid analysis of *N*-terminally His-tagged recombinant lysostaphin (construct 1) demonstrated that charge variant formation occurred in a time-dependent manner whereby basic protein variants become steadily converted to more acidic variants.

LC-MS analysis of intact *N*-terminally His-tagged recombinant lysostaphin (construct 1) indicated that the protein was likely to have become truncated during expression. Comparison of WCX and LC-MS analysis suggest that amino acids were lost from the *N*-terminus to produce basic variants, whilst loss of *C*-terminal lysine₂₆₇ may have explained the detection of more acidic variants. As intact mass measurements acquired during LC-MS analysis of intact recombinant lysostaphin (construct 1) did not match exactly with theoretical intact protein masses, it was thought that the protein variants were also subject to enzymatic or chemical PTMs. These conclusions were made, using supporting evidence that was acquired during GF, SDS-PAGE and CXC analysis. Additional LC-MS/MS analysis would be desirable to confirm these findings.

Overall these findings are of concern during the production of recombinant lysostaphin and other recombinant proteins which are expressed in *E. coli*. However this research suggested that chromatography can be used to sensitively detect and monitor of product heterogeneity, so that a more homogeneous product could be produced by careful adjustment of expression, harvest and formulation conditions.

5.14 Further work

To extend this research further, a variety of experiments could be performed to gain further insight into protein variant formation and the origins of truncation events and PTMs. As rapid analysis of cell lysate during the course of expression provided the most comprehensive evaluation of charge variant formation, further rapid analysis experiments should be performed upon forms of recombinant lysostaphin (constructs 1, 2 and 3) expressed within the cytoplasm of *E. coli*. Optimisation of periplasmic lysate expression conditions would also permit rapid analysis of recombinant lysostaphin (constructs 4 and 5) which have been translocated to the periplasm. This would permit assessment of the influence of cellular location upon the charge heterogeneity of recombinant lysostaphin, but would also allow further assessment of the lesser charge heterogeneity of C-terminally His-tagged and non-tagged forms of recombinant lysostaphin.

Further rapid analysis of cell lysate harvested from cultures grown using different expression media, temperatures and *E. coli* strains, such as *E. coli* Tuner or *E. coli* Tuner pLysS, may permit more regulated and homogeneous production of recombinant lysostaphin. Rapid analysis of cell lysate harvested during the expression of other basic recombinant proteins, such as recombinant oxidoreductase and recombinant NADPH-dependent 1-acyl dihydroxyacetone phosphate reductase (Ayr1p) would also be desirable to establish whether charge variant formation follows a similar pattern to that of recombinant lysostaphin (construct 1).

To provide the most sensitive detection of charge variants, rapid analysis should be performed using the ProPac[®] MAb SCX column, whilst applying more optimised fraction collection settings to ensure that charge variants are most appropriately fractionated.

Most importantly, LC-MS/MS analysis of separated charge variants would be essential to establish whether amino acids are being lost from the N- and C-termini of recombinant lysostaphin (construct 1). In addition LC-MS/MS analysis would permit elucidation of the type, location and abundance of PTMs affecting the structure of recombinant lysostaphin. The MaXis UHR-TOF demonstrated excellent resolution of protein species; therefore analysis using this instrument should provide high sequence coverage following MS/MS of intact proteins. LC-MS/MS analysis of digested peptides would complement top-down analysis and provide confirmation of sequence data. The use of targeted MSn should also increase sequence coverage, whilst *de novo* sequencing would facilitate elucidation of N- or C-terminal sequences.

Identification of PTMs and sequence variation could ultimately facilitate remediation of charge and mass heterogeneity. Cloning and expression of prolystostaphin may protect the *N*-terminal His-tag sequence from potential proteolysis or PTM. Whilst IEX separation of cell lysate harvested during the early stages of culture could lead to the detection of up-regulation of cellular proteases during the heat-shock response. LC-MS based protein identification could then be used to identify specific proteases responsible for the truncation of recombinant lysostaphin, which could advocate the use of protease inhibitors or a protease-deficient expression strain.

6 References

- ALLISON, S. D., DONG, A. & CARPENTER, J. F. 1996. Counteracting effects of thiocyanate and sucrose on chymotrypsinogen secondary structure and aggregation during freezing, drying, and rehydration. *Biophysical Journal*, 71, 2022-2032.
- AON, J. C., CAIMI, R. J., TAYLOR, A. H., LU, Q., OLUBOYEDE, F., DALLY, J., KESSLER, M. D., KERRIGAN, J. J., LEWIS, T. S., WYSOCKI, L. A. & PATEL, P. S. 2008. Suppressing Post-translational Gluconoylation of Heterologous Proteins by Metabolic Engineering of *Escherichia coli*. *Applied and Environmental Microbiology*, 74, 950-958.
- APOSTOL, I., AITKEN, J., LEVINE, J., LIPPINCOTT, J., DAVIDSON, J. S. & ABBOTT-BROWN, D. 1995. Recombinant protein sequences can trigger methylation of N-terminal amino acids in *Escherichia coli*. *Protein Science*, 4, 2616-2618.
- APOSTOL, I., LEVINE, J., LIPPINCOTT, J., LEACH, J., HESS, E., GLASCOCK, C. B., WEICKERT, M. J. & BLACKMORE, R. 1997. Incorporation of Norvaline at Leucine Positions in Recombinant Human Hemoglobin Expressed in *Escherichia coli*. *Journal of Biological Chemistry*, 272, 28980-28988.
- ARAKAWA, T., EJIMA, D., LI, T. & PHILO, J. S. 2010. The critical role of mobile phase composition in size exclusion chromatography of protein pharmaceuticals. *Journal of Pharmaceutical Sciences*, 99, 1674-1692.
- ARFIN, S. M. & BRADSHAW, R. A. 1988. Cotranslational processing and protein turnover in eukaryotic cells. *Biochemistry*, 27, 7979-7984.
- AULD, D. S. 2001. Zinc coordination sphere in biochemical zinc sites. *BioMetals*, 14, 271-313.
- BABA, T. & SCHNEEWIND, O. 1996. Target cell specificity of a bacteriocin molecule: a C-terminal signal directs lysostaphin to the cell wall of *Staphylococcus aureus* *EMBO Journal*, 15, 4789-4797.
- BAKER, K. N., RENDALL, M. H., PATEL, A., BOYD, P., HOARE, M., FREEDMAN, R. B. & JAMES, D. C. 2002. Rapid monitoring of recombinant protein products: a comparison of current technologies. *Trends in Biotechnology*, 20, 149-156.
- BARDELANG, P., VANKEEMMELBEKE, M., ZHANG, Y., JARVIS, H., ANTIADOU, E., ROCHETTE, S., THOMAS, N. R., PENFOLD, C. & JAMES, R. 2009. Design of a polypeptide FRET substrate that facilitates study of the antimicrobial protease lysostaphin. *Biochemical Journal*, 418, 615-624.
- BARIOLA, P. A., RUSSELL, B. A., MONAHAN, S. J. & STROOP, S. D. 2007. Identification and quantification of N_α-acetylated *Y. pestis* fusion protein F1-V expressed in *Escherichia coli* using LC-MS. *Journal of Biotechnology*, 130, 11-23.
- BLATTNER, F. R., PLUNKETT, G., BLOCH, C. A., PERNA, N. T., BURLAND, V., RILEY, M., COLLADO-VIDES, J., GLASNER, J. D., RODE, C. K., MAYHEW, G. F., GREGOR, J., DAVIS, N. W., KIRKPATRICK, H. A., GOEDEN, M. A., ROSE, D. J., MAU, B. & SHAO, Y. 1997. The Complete Genome Sequence of *Escherichia coli* K-12. *Science*, 277, 1453-1462.
- BOCHTLER, M., ODINTSOV, S. G., MARCYJANIAK, M. & SABALA, I. 2004. Similar active sites in lysostaphins and D-Ala-D-Ala metallopeptidases. *Protein Science*, 13, 854-861.
- BOGOSIAN, G., VIOLAND, B., DORWARD-KING, E., WORKMAN, W., JUNG, P. & KANE, J. 1989. Biosynthesis and incorporation into protein of norleucine by *Escherichia coli*. *Journal of Biological Chemistry*, 264, 531-539.
- BONEKAMP, F. & JENSEN, K. F. 1988. The AGG codon is translated slowly in *E. coli* even at very low-expression levels. *Nucleic Acids Research*, 16, 3013-3024.
- BOYLE-VAVRA, S., CAREY, R. B. & DAUM, R. S. 2001. Development of vancomycin and lysostaphin resistance in a methicillin-resistant *Staphylococcus aureus* isolate. *Journal of Antimicrobial Chemotherapy*, 48, 617-625.

- BRUNI, R., GIANFRANCESCHI, G. & KOCH, G. 2005. On Peptide De Novo Sequencing: A New Approach. *Journal of Peptide Science*, 11, 225-234.
- BUNN, W. J., HEATH, H. E., LEBLANC, P. A. & SLOAN, G. L. 1998. Wall-associated processing of extracellular enzymes of *Staphylococcus simulans* biovar *staphylolyticus*. *FEMS Microbiology Letters*, 165, 123-127.
- BYLUND, F., CASTAN, A., MIKKOLA, R., VEIDE, A. & LARSSON, G. 2000. Influence of scale-up on the quality of recombinant human growth hormone. *Biotechnology and Bioengineering*, 69, 119-128.
- CAPUANO, E., FEDELE, F., MENNELLA, C., VISCIANO, M., NAPOLITANO, A., LANZUISE, S., RUOCCO, M., LORITO, M., DELCASTILLO, M. D. & FOGLIANO, V. 2007. Studies on the Effect of Amadoriase from *Aspergillus fumigatus* on Peptide and Protein Glycation In Vitro. *Journal of Agricultural and Food Chemistry*, 55, 4189-4195.
- CHAN, E.-C. 1996. Expression and Purification of Recombinant Lysostaphin in *Escherichia coli*. *Biotechnology Letters* 18, 833-838.
- CHARBAUT, E., REDEKER, V., ROSSIER, J. & SOBEL, A. 2002. N-terminal acetylation of ectopic recombinant proteins in *Escherichia coli*. *FEBS Letters*, 529, 341-345.
- CHENG, C.-H. & LEE, W.-C. 2010. Protein solubility and differential proteomic profiling of recombinant *Escherichia coli* overexpressing double-tagged fusion proteins. *Microbial Cell Factories*, 9, 63.
- CHIANG, P., GORDON, R., TAL, J., ZENG, G., DOCTOR, B., PARDHASARADHI, K. & MCCANN, P. 1996. S-Adenosylmethionine and methylation. *The FASEB Journal*, 10, 471-480.
- CHOI, J. H., KEUM, K. C. & LEE, S. Y. 2006. Production of recombinant proteins by high cell density culture of *Escherichia coli*. *Chemical Engineering Science*, 61, 876-885.
- CHOI, J. H. & LEE, S. Y. 2004. Secretory and extracellular production of recombinant proteins using *Escherichia coli*. *Applied Microbiology and Biotechnology*, 64, 625-635.
- CHOU, C. 2007. Engineering cell physiology to enhance recombinant protein production in *Escherichia coli*. *Applied Microbiology and Biotechnology*, 76, 521-532.
- CHRISTIANSON, D. W. & ALEXANDER, R. S. 1989. Carboxylate-histidine-zinc interactions in protein structure and function. *Journal of the American Chemical Society*, 111, 6412-6419.
- CISANI, G., VARALDO, P. E., GRAZI, G. & SORO, O. 1982. High-level potentiation of lysostaphin anti-staphylococcal activity by lysozyme. *Antimicrobial Agents and Chemotherapy*, 21, 531-535.
- CLARK, K. M., VAN DER DONK, W. A. & LU, Y. 2009. Expressed protein ligation for metalloprotein design and engineering. In: SIDNEY P. COLOWICK, TOM W. MUIR & ABELSON, J. N. (eds.) *Methods in Enzymology*. Academic Press.
- CLIMO, M. W., EHLERT, K. & ARCHER, G. L. 2001. Mechanism and Suppression of Lysostaphin Resistance in Oxacillin-Resistant *Staphylococcus aureus*. *Antimicrobial Agents and Chemotherapy*, 45, 1431-1437.
- CLIMO, M. W., PATRON, R. L., GOLDSTEIN, B. P. & ARCHER, G. L. 1998. Lysostaphin Treatment of Experimental Methicillin-Resistant *Staphylococcus aureus* Aortic Valve Endocarditis. *Antimicrobial Agents and Chemotherapy*, 42, 1355-1360.
- CLOGSTON, C. L., HSU, Y.-R., BOONE, T. C. & LU, H. S. 1992. Detection and quantitation of recombinant granulocyte colony-stimulating factor charge isoforms: Comparative analysis by cationic-exchange chromatography, isoelectric focusing gel electrophoresis, and peptide mapping. *Analytical Biochemistry*, 202, 375-383.
- CROMWELL, M., HILARIO, E. & JACOBSON, F. 2006. Protein aggregation and bioprocessing. *The AAPS Journal*, 8, E572-E579.
- CSERJAN-PUSCHMANN, M., CLEMENTSCHITSCH, F., STRIEDNER, G., POTSCHACHER, F., KERN, J. & BAYER, K. 2006. Modulation of inclusion body (IB) formation kinetics by different induction regimes in *E. coli* fed batch cultivations. *Microbial Cell Factories*, 5, P22.

- D'ALAYER, J., EXPERT-BEZANÇON, N. & BÉGUIN, P. 2007. Time- and temperature-dependent acetylation of the chemokine RANTES produced in recombinant *Escherichia coli*. *Protein Expression and Purification*, 55, 9-16.
- DAINIYAK, M. B., GALAEV, I. Y. & MATTIASSON, B. 2002. Direct capture of product from fermentation broth using a cell-repelling ion exchanger. *Journal of Chromatography A*, 942, 123-131.
- DAJCS, J. J., HUME, E. B. H., MOREAU, J. M., CABALLERO, A. R., CANNON, B. M. & O'CALLAGHAN, R. J. 2000. Lysostaphin Treatment of Methicillin-Resistant *Staphylococcus aureus* Keratitis in the Rabbit. *Investigative Ophthalmology & Visual Science*, 41, 1432-1437.
- DAJCS, J. J., THIBODEAUX, B. A., GIRGIS, D. O., SHAFFER, M. D., DELVISCO, S. M. & O'CALLAGHAN, R. J. 2002. Immunity to Lysostaphin and Its Therapeutic Value for Ocular MRSA Infections in the Rabbit. *Investigative Ophthalmology & Visual Science*, 43, 3712-3716.
- DALEY, M. J. & OLDHAM, E. R. 1992. Lysostaphin: immunogenicity of locally administered recombinant protein used in mastitis therapy. *Veterinary Immunology and Immunopathology*, 31, 301-312.
- DALMORA, S., DE OLIVEIRA, J. E., AFFONSO, R., GIMBO, E., RIBELA, M. T. C. P. & BARTOLINI, P. 1997. Analysis of recombinant human growth hormone directly in osmotic shock fluids. *Journal of Chromatography A*, 782, 199-210.
- DEHART, H. P., HEATH, H. E., HEATH, L. S., LEBLANC, P. A. & SLOAN, G. L. 1995. The lysostaphin endopeptidase resistance gene (epr) specifies modification of peptidoglycan cross bridges in *Staphylococcus simulans* and *Staphylococcus aureus*. *Applied and Environmental Microbiology*, 61, 1475-1479.
- DEMAIN, A. L. & VAISHNAV, P. 2009. Production of recombinant proteins by microbes and higher organisms. *Biotechnology Advances*, 27, 297-306.
- DEPHILLIPS, P., BUCKLAND, B., GBEWONYO, K., YAMAZAKI, S. & SITRIN, R. 1994. Reversed-phase high-performance liquid chromatography assay for recombinant acidic fibroblast growth factor in *E. coli* cell suspensions and lysate samples. *Journal of Chromatography A*, 663, 43-51.
- DERLINDEN, E. V., BERNAERTS, K. & IMPE, J. F. V. 2008. Dynamics of *Escherichia coli* at elevated temperatures: effect of temperature history and medium. *Journal of Applied Microbiology*, 104, 438-453.
- DONG, M.-S., BELL, L. C., GUO, Z., PHILLIPS, D. R., BLAIR, I. A. & GUENGERICH, F. P. 1996. Identification of Retained N-Formylmethionine in Bacterial Recombinant Mammalian Cytochrome P450 Proteins with the N-Terminal Sequence MALLAVFL...: Roles of Residues 3-5 in Retention and Membrane Topology. *Biochemistry*, 35, 10031-10040.
- DONOVAN, R., ROBINSON, C. & GLICK, B. 1996. Optimizing inducer and culture conditions for expression of foreign proteins under the control of the lac promoter. *Journal of Industrial Microbiology* 16, 145 - 154.
- DU, H., ZHANG, Z., WANG, J., YAO, X. & HU, Z. 2008. Novel approaches to predict the retention of histidine-containing peptides in immobilised metal-affinity chromatography. *Proteomics*, 8, 2185-2195.
- DU, P., LOULAKIS, P., LUO, C., MISTRY, A., SIMONS, S. P., LEMOTTE, P. K., RAJAMOHAN, F., RAFIDI, K., COLEMAN, K. G., GEOGHEGAN, K. F. & XIE, Z. 2005a. Phosphorylation of serine residues in histidine-tag sequences attached to recombinant protein kinases: A cause of heterogeneity in mass and complications in function. *Protein Expression and Purification*, 44, 121-129.
- DU, P., LOULAKIS, P., XIE, Z., SIMONS, S. P. & GEOGHEGAN, K. F. 2005b. Tandem mass spectrometry of multiply phosphorylated forms of a 'histidine-tag' derived from a recombinant protein kinase expressed in bacteria. *Rapid Communications in Mass Spectrometry* 19, 547-551.
- EITEMAN, M. A. & ALTMAN, E. 2006. Overcoming acetate in *Escherichia coli* recombinant protein fermentations. *Trends in Biotechnology*, 24, 530-536.

- ESPOSITO, G., MICHELUTTI, R., VERDONE, G., VIGLINO, P., ÁNDEZ, H. H., ROBINSON, C. V., AMORESANO, A., PIAZ, F. D., MONTI, M., PUCCI, P., MANGIONE, P., STOPPINI, M., MERLINI, G., FERRI, G. & BELLOTTI, V. 2000. Removal of the N-terminal hexapeptide from human β 2-microglobulin facilitates protein aggregation and fibril formation. *Protein Science*, 9, 831-845.
- EVENHUIS, C. J., BUCHBERGER, W., HILDER, E. F., FLOOK, K. J., POHL, C. A., NESTERENKO, P. N. & HADDAD, P. R. 2008. Separation of inorganic anions on a high capacity porous polymeric monolithic column and application to direct determination of anions in seawater. *Journal of Separation Science*, 31, 2598-2604.
- EWING, B., HILLIER, L., WENDL, M. C. & GREEN, P. 1998. Base-calling of Automated Sequencer Traces Using *Phred*. I. Accuracy Assessment *Genome Research*, 8, 175-185.
- EYKAMP, W. 1991. Ultrafiltration. In: BAKER, R. W. (ed.) *Membrane separation systems: recent developments and future directions*. William Andrew.
- FAN, W., PLAUT, K., BRAMLEY, A. J., BARLOW, J. W. & KERR, D. E. 2002. Adenoviral-Mediated Transfer of a Lysostaphin Gene into the Goat Mammary Gland. *Journal of Dairy Science*, 85, 1709-1716.
- FAN, W., PLAUT, K., BRAMLEY, A. J., BARLOW, J. W., MISCHLER, S. A. & KERR, D. E. 2004. Persistency of Adenoviral-Mediated Lysostaphin Expression in Goat Mammary Glands. *Journal of Dairy Science*, 87, 602-608.
- FANG, P., LI, X., WANG, J., XING, L., GAO, Y., NIU, L. & TENG, M. 2010. Crystal Structure of the Protein L-Isoaspartyl Methyltransferase from *Escherichia coli*. *Cell Biochemistry and Biophysics*, 58, 163-167.
- FEDOROV, T. V., SUROVTSEV, V. I., PLETNEV, V. Z., BOROZDINA, M. A. & GUSEV, V. V. 2003. Purification and Some Properties of Lysostaphin, a Glycylglycine Endopeptidase from the Culture Liquid of *Staphylococcus simulans* biovar *staphylolyticus*. *Biochemistry (Moscow)*, 68, 50-53.
- FEUSER, J., WALTER, J., KULA, M.-R. & THÖMMES, J. 1999. Cell/adsorbent interactions in expanded bed adsorption of proteins. *Bioseparation*, 8, 99-109.
- FIRCZUK, M., MUCHA, A. & BOCHTLER, M. 2005. Crystal Structures of Active LytM. *Journal of Molecular Biology*, 354, 578-590.
- FORSBERG, G., PALM, G., EKEBACKE, A., JOSEPHSON, S. & HARTMANIS, M. 1990. Separation and characterization of modified variants of recombinant human insulin-like growth factor I derived from a fusion protein secreted from *Escherichia coli*. *Biochemical Journal*, 271, 357-363.
- GABERC-POREKAR, V. & MENART, V. 2001. Perspectives of immobilized-metal affinity chromatography. *Journal of Biochemical and Biophysical Methods*, 49, 335-360.
- GADGIL, H. S., BONDARENKO, P. V., PIPES, G., REHDER, D., MCAULEY, A., PERICO, N., DILLON, T., RICCI, M. & TREUHEIT, M. 2007. The LC/MS analysis of glycation of IgG molecules in sucrose containing formulations. *Microbial Cell Factories*, 96, 2607-2621.
- GAIER, W., VOGEL, R. F. & HAMMES, W. P. 1992. Cloning and expression of the lysostaphin gene in *Bacillus subtilis* and *Lactobacillus casei*. *Letters in Applied Microbiology*, 14, 72-76.
- GARGIS, A. S., TATE, A. H., HEATH, L. S., HEATH, H. E., LEBLANC, P. A. & SLOAN, G. L. 2010. Complete nucleotide sequences of plasmids pACK1 and pACK3 from *Staphylococcus simulans* biovar *staphylolyticus*. *Plasmid*, 64, 104-109.
- GARNICK, R. L., SOLLI, N. J. & PAPA, P. A. 1988. The role of quality control in biotechnology: an analytical perspective. *Analytical Chemistry*, 60, 2546-2557.
- GAZA-BULSECO, G., BULSECO, A., CHUMSAE, C. & LIU, H. 2008. Characterization of the glycosylation state of a recombinant monoclonal antibody using weak cation exchange chromatography and mass spectrometry. *Journal of Chromatography B*, 862, 155-160.

- GELLERFORS, P., PAVLU, B., AXELSSON, K., NYHLÉN, C. & JOHANSSON, S. 1990. Separation and Identification of Growth Hormone Variants with High Performance Liquid Chromatography Techniques. *Acta Pædiatrica*, 79, 93-100.
- GEOGHEGAN, K. F., DIXON, H. B. F., ROSNER, P. J., HOTH, L. R., LANZETTI, A. J., BORZILLERI, K. A., MARR, E. S., PEZZULLO, L. H., MARTIN, L. B., LEMOTTE, P. K., MCCOLL, A. S., KAMATH, A. V. & STROH, J. G. 1999. Spontaneous alpha-N-6-Phosphogluconoylation of "His Tag" in *Escherichia coli*: The Cause of Extra Mass of 258 or 178 Da in Fusion Proteins. *Analytical Biochemistry* 267, 169-184.
- GEORGIU, G. 1988. Optimizing the production of recombinant proteins in microorganisms. *AIChE Journal*, 34, 1233-1248.
- GHOSH MOULICK, R., BHATTACHARYA, J., ROY, S., BASAK, S. & DASGUPTA, A. K. 2007. Compensatory secondary structure alterations in protein glycation. *Biochimica et Biophysica Acta (BBA) - Proteins & Proteomics*, 1774, 233-242.
- GILL, R. T., VALDES, J. J. & BENTLEY, W. E. 2000. A Comparative Study of Global Stress Gene Regulation in Response to Overexpression of Recombinant Proteins in *Escherichia coli*. *Metabolic Engineering*, 2, 178-189.
- GOLDBERG, A. L. 2003. Protein degradation and protection against misfolded or damaged proteins. *Nature*, 426, 895-899.
- GOOLEY, A. A. & PACKER, N. H. 1997. The Importance of Protein Co- and Post-translational Modifications in Proteome Projects *In*: WILKINS, M. R. (ed.) *Proteome research: new frontiers in functional genomics*. Springer.
- GOTTESMAN, S., ROCHE, E., ZHOU, Y. & SAUER, R. T. 1998. The ClpXP and ClpAP proteases degrade proteins with carboxy-terminal peptide tails added by the SsrA-tagging system. *Genes & Development*, 12, 1338-1347.
- GRUNDLING, A., MISSIAKAS, D. M. & SCHNEEWIND, O. 2006. *Staphylococcus aureus* Mutants with Increased Lysostaphin Resistance. *Journal of Bacteriology*, 188, 6286-6297.
- GRUNDLING, A. & SCHNEEWIND, O. 2006. Cross-Linked Peptidoglycan Mediates Lysostaphin Binding to the Cell Wall Envelope of *Staphylococcus aureus*. *Journal of Bacteriology*, 188, 2463-2473.
- GRUTTER, M. G., MARKI, W. & WALLISER, H. P. 1985. Crystals of the complex between recombinant N-acetylglucosaminidase and subtilisin. A preliminary characterization. *Journal of Biological Chemistry*, 260, 11436-11437.
- GU, C., LIN, L., CHEN, X., JIA, J., REN, J. & FANG, N. 2007. Effects of inner diameter of monolithic column on separation of proteins in capillary-liquid chromatography. *Journal of Chromatography A*, 1170, 15-22.
- HAACKE, A., FENDRICH, G., RAMAGE, P. & GEISER, M. 2009. Chaperone over-expression in *Escherichia coli*: Apparent increased yields of soluble recombinant protein kinases are due mainly to soluble aggregates. *Protein Expression and Purification*, 64, 185-193.
- HALE, J. E., BUTLER, J. P., GELFANOVA, V., YOU, J.-S. & KNIERMAN, M. D. 2004. A simplified procedure for the reduction and alkylation of cysteine residues in proteins prior to proteolytic digestion and mass spectral analysis. *Analytical Biochemistry*, 333, 174-181.
- HANN, S., OBINGER, C., STINGEDER, G., PAUMANN, M., FURTMULLER, P. G. & KOELLENSPERGER, G. 2006. Studying metal integration in native and recombinant copper proteins by hyphenated ICP-DRC-MS and ESI-TOF-MS capabilities and limitations of the complementary techniques. *Journal of Analytical Atomic Spectrometry*, 21, 1224-1231.
- HARA, S., LIU, N., MENG, S.-Y. & LU, H. S. 1996. Isolation and structural characterization of recombinant human neu differentiation factor expressed in *Escherichia coli*. *Biochimica et Biophysica Acta (BBA) - Protein Structure and Molecular Enzymology*, 1292, 168-176.
- HARRISON, E. F. & ZYGMUNT, W. A. 1967. Lysostaphin in Experimental Renal Infections. *Journal of Bacteriology*, 93, 520-524.

- HEATH FARRIS, M., HEATH, L. S., HEATH, H. E., LEBLANC, P. A., SIMMONDS, R. S. & SLOAN, G. L. 2003. Expression of the genes for lysostaphin and lysostaphin resistance in streptococci. *FEMS Microbiology Letters*, 228, 115-119.
- HECK, A. J. R. & VAN DEN HEUVEL, R. H. H. 2004. Investigation of intact protein complexes by mass spectrometry. *Mass Spectrometry Reviews*, 23, 368-389.
- HECKENBERG, A., FARNAN, D. & WEITZHANDLER, M. 2002. Cation-exchange separation of C-Terminal Processing of a Humanized Monoclonal Antibody on a Grafted Polymeric Stationary Phase. Sunnyvale, California: Dionex Corporation.
- HEINRICH, P., ROSENSTEIN, R., BOHMER, M., SONNER, P. & GOTZ, F. 1987. The molecular organization of the lysostaphin gene and its sequences repeated in tandem *Molecular and General Genetics* 1987, 563-569.
- HEMDAN, E. S., ZHAO, Y. J., SULKOWSKI, E. & PORATH, J. 1989. Surface topography of histidine residues: a facile probe by immobilized metal ion affinity chromatography. *Proceedings of the National Academy of Sciences of the United States of America*, 86, 1811-1815.
- HEPNER, F., CSASZAR, E., ROITINGER, E., POLLAK, A. & LUBEC, G. 2006. Mass spectrometrical analysis of recombinant human growth hormone Norditropin® reveals amino acid exchange at M14_V14 rhGH. *PROTEOMICS*, 6, 775-784.
- HEPNER, F., CSZASAR, E., ROITINGER, E. & LUBEC, G. 2005. Mass spectrometrical analysis of recombinant human growth hormone (Genotropin®) reveals amino acid substitutions in 2% of the expressed protein. *Proteome Science*, 3, 1.
- HOCHULI, E., BANNWARTH, W., DOBELI, H., GENTZ, R. & STUBER, D. 1988. Genetic Approach to Facilitate Purification of Recombinant Proteins with a Novel Metal Chelate Adsorbent. *Nature Biotechnology*, 6, 1321-1325.
- HONDA, S., ASANO, T., KAJIO, T. & NISHIMURA, O. 1989. *Escherichia coli*-derived human interferon- γ with Cys---Tyr---Cys at the N-terminus is partially N $_{\alpha}$ -acylated. *Archives of Biochemistry and Biophysics*, 269, 612-622.
- HSU, Y.-R., CHANG, MENDIAZ, E. A., HARA, S., CHOW, D. T., MANN, M. B., LANGLEY, K. E. & LU, H. S. 1998. Selective Deamidation of Recombinant Human Stem Cell Factor during in Vitro Aging: Isolation and Characterization of the Aspartyl and Isoaspartyl Homodimers and Heterodimers. *Biochemistry*, 37, 2251-2262.
- HUBER, M. M. & HUBER, T. W. 1989. Susceptibility of methicillin-resistant *Staphylococcus aureus* to lysostaphin. *Journal of Clinical Microbiology*, 27, 1122-1124.
- HUMMEL, M., HERBST, H. & STEIN, H. 1989. Gene synthesis, expression in *Escherichia coli* and purification of immunoreactive human insulin-like growth factors I and II. *European Journal of Biochemistry*, 180, 555-561.
- HWANG, D. S., YOO, H. J., JUN, J. H., MOON, W. K. & CHA, H. J. 2004. Expression of Functional Recombinant Mussel Adhesive Protein Mgfp-5 in *Escherichia coli*. *Applied and Environmental Microbiology*, 70, 3352-3359.
- INVITROGEN. 2010. *RE: Zero Blunt PCR Cloning Kit - A high efficiency system for cloning blunt-ended PCR products*
- IOANNOU, Y., GILES, I, LAMBRIANIDES, A., RICHARDSON, C., PEARL, L.H., LATCHMAN, D.S., ISENBERG., D.A., RAHMAN, A. 2006. A novel expression system of domain I of human β 2 glycoprotein I in *Escherichia coli* *BMC Biotechnology*, 6.8.
- IVERSEN, O.-J. & GROV, A. 1973. Studies on Lysostaphin. Separation and Characterization of Three Enzymes. *European Journal of Biochemistry*, 38, 293-300.
- JACOBSON, F. S., HANSON, J. T., WONG, P.-Y., MULKERRIN, M., DEVENEY, J., REILLY, D. & WONG, S. C. 1997. Role of high-performance liquid chromatographic protein analysis in developing fermentation processes for recombinant human growth hormone, relaxin, antibody fragments and lymphotoxin. *Journal of Chromatography A*, 763, 31-48.
- JENZSCH, M., GNOTH, S., KLEINSCHMIDT, M., SIMUTIS, R. & LÜBBERT, A. 2006. Improving the batch-to-batch reproducibility in microbial cultures during recombinant

- protein production by guiding the process along a predefined total biomass profile. *Bioprocess and Biosystems Engineering*, 29, 315-321.
- JIANG, H., WU, S.-L., KARGER, B. L. & HANCOCK, W. S. 2009. Mass spectrometric analysis of innovator, counterfeit, and follow-on recombinant human growth hormone. *Biotechnology Progress*, 25, 207-218.
- JOHNSON, I. 1983. Human insulin from recombinant DNA technology. *Science*, 219, 632-637.
- JOHNSON, R. D. & ARNOLD, F. H. 1995. Review: Multipoint binding and heterogeneity in immobilized metal affinity chromatography. *Biotechnology and Bioengineering*, 48, 437-443.
- JOHNSON, R. D., WANG, Z. G. & ARNOLD, F. H. 1996. Surface Site Heterogeneity and Lateral Interactions in Multipoint Protein Adsorption. *The Journal of Physical Chemistry*, 100, 5134-5139.
- JUNGBAUER, A. 2005. Chromatographic media for bioseparation. *Journal of Chromatography A*, 1065, 3-12.
- KALTASHOV, I. A., ZHANG, M., EYLES, S. J. & ABZALIMOV, R. R. 2006. Investigation of structure, dynamics and function of metalloproteins with electrospray ionization mass spectrometry. *Analytical and Bioanalytical Chemistry*, 386, 472-81.
- KANE, J. F., VIOLAND, B. N., CURRAN, D. F., STATEN, N. R. & DUFFIN, K. L. 1992. Novel in-frame two codon translational hop during synthesis of bovine placental lactogen in a recombinant strain of *Escherichia coli* *Nucleic Acids Research*, 20, 6707-6712.
- KANG, H. A., CHOI, E. S., HONG, W. K., KIM, J. Y., KO, S. M., SOHN, J. H. & RHEE, S. K. 2000. Proteolytic stability of recombinant human serum albumin secreted in the yeast *Saccharomyces cerevisiae*. *Applied Microbiology and Biotechnology*, 53, 575-582.
- KARA, B., GRANT, G., LIDDELL, J. & ALDRIDGE, P.. 2006. *RE: Meeting at Avecia Biologics, Billingham, UK.* .
- KEILER, K. C. & SAUER, R. T. 1996. Sequence Determinants of C-terminal Substrate Recognition by the Tsp Protease. *Journal of Biological Chemistry*, 271, 2589-2593.
- KELLEY, D. R., SCHATZ, M. C. & SALZBERG, S. L. 2010. Quake: quality-aware detection and correction of sequencing errors. *Genome Biology*, 11, R116.
- KERR, D. E., PLAUT, K., BRAMLEY, A. J., WILLIAMSON, C. M., LAX, A. J., MOORE, K., WELLS, K. D. & WALL, R. J. 2001. Lysostaphin expression in mammary glands confers protection against staphylococcal infection in transgenic mice. *Nature Biotechnology*, 19, 66-70.
- KIM, K. M., YI, E. C., BAKER, D. & XHANG, K. Y. J. 2001. Post-translational modification of the N-terminal His tag interferes with the crystallization of the wild-type and mutant SH3 domains from chicken src tyrosine kinase. *Acta Crystallographica D* 57, 759-762.
- KIRI, N., ARCHER, G. & CLIMO, M. W. 2002. Combinations of Lysostaphin with β -Lactams Are Synergistic against Oxacillin-Resistant *Staphylococcus epidermidis*. *Antimicrobial Agents and Chemotherapy*, 46, 2017-2020.
- KLEIN, M., KRÖNKE, M. & KRUT, O. 2006. Expression of lysostaphin in HeLa cells protects from host cell killing by intracellular *Staphylococcus aureus*. *Medical Microbiology and Immunology*, 195, 159-163.
- KLINE, S. A., DELAHARPE, J. & BLACKBURN, P. 1994. A Colorimetric Microtiter Plate Assay for Lysostaphin Using a Hexaglycine Substrate. *Analytical Biochemistry*, 217, 329-331.
- KNECHT, S., RICKLIN, D., EBERLE, A. N. & ERNST, B. 2009. Oligohis-tags: mechanisms of binding to Ni²⁺-NTA surfaces. *Journal of Molecular Recognition*, 22, 270-279.
- KOKAI-KUN, J. F., CHANTURIYA, T. & MOND, J. J. 2007. Lysostaphin as a treatment for systemic *Staphylococcus aureus* infection in a mouse model *Journal of Antimicrobial Chemotherapy*, 60, 1051-1059.
- KOKAI-KUN, J. F., WALSH, S. M., CHANTURIYA, T. & MOND, J. J. 2003. Lysostaphin Cream Eradicates *Staphylococcus aureus* Nasal Colonization in a Cotton Rat Model. *Antimicrobial agents and Chemotherapy*, 47, 1589-1597.

- KROEF, E. P., OWENS, R. A., CAMPBELL, E. L., JOHNSON, R. D. & MARKS, H. I. 1989. Production scale purification of biosynthetic human insulin by reversed-phase high-performance liquid chromatography. *Journal of Chromatography A*, 461, 45-61.
- KUJELTZO, L. A., WANG, W., RANDOLPH, T. W. & CARPENTER, J. F. 2008. Effects of solution conditions, processing parameters, and container materials on aggregation of a monoclonal antibody during freeze–thawing. *Journal of Pharmaceutical Sciences*, 97, 1801-1812.
- KUHNERT, P., BOERLIN, P. & FREY, J. 2000. Target genes for virulence assessment of *Escherichia coli* isolates from water, food and the environment. *FEMS Microbiology Reviews*, 24, 107-117.
- KUMAR, J. 2008. Lysostaphin: an antistaphylococcal agent. *Applied Microbiology and Biotechnology*, 80, 555-561.
- KUSUMA, C. M. & KOKAI-KUN, J. F. 2005. Comparison of Four Methods for Determining Lysostaphin Susceptibility of Various Strains of *Staphylococcus aureus*. *Antimicrobial Agents and Chemotherapy*, 49, 3256-3263.
- LAGERWERF, F. M., WEERT, M. V. D., HEERMA, W. & HAVERKAMP, J. 1996. Identification of Oxidized Methionine in Peptides. *Rapid Communications in Mass Spectrometry*, 10, 1905-1910.
- LAHNSTEIN, J. M., DYER, S., GOSS, N., DUNCAN, M. & NORTON, R. S. 1993. N-terminal modification of malarial antigens from *E. coli*. *Techniques in Protein Chemistry IV*, 83-90.
- LAVALLIE, E. R. & MCCOY, J. M. 1995. Gene fusion expression systems in *Escherichia coli*. *Current Opinion in Biotechnology*, 6, 501-506.
- LEDENT, P., DUEZ, C., VANHOVE, M., LEJEUNE, A., FONZÉ, E., CHARLIER, P., RHAZIFILALI, F., THAMM, I., GUILLAUME, G., SAMYN, B., DEVREESE, B., VAN BEEUMEN, J., LAMOTTE-BRASSEUR, J. & FRÈRE, J.-M. 1997. Unexpected influence of a C-terminal-fused His-tag on the processing of an enzyme and on the kinetic and folding parameters. *FEBS Letters*, 413, 194-196.
- LEE, J. & KIM, S.-H. 2009. High-throughput T7 LIC vector for introducing C-terminal poly-histidine tags with variable lengths without extra sequences. *Protein Expression and Purification*, 63, 58-61.
- LEONARD, C. K., SPELLMAN, M. W., RIDDLE, L., HARRIS, R. J., THOMAS, J. N. & GREGORY, T. J. 1990. Assignment of intrachain disulfide bonds and characterization of potential glycosylation sites of the type 1 recombinant human immunodeficiency virus envelope glycoprotein (gp120) expressed in Chinese hamster ovary cells. *Journal of Biological Chemistry*, 265, 10373-10382.
- LINTON, D., DORRELL, N., HITCHEN, P., G., AMBER, S., KARLYSHEV, A., V., MORRIS, H., R., DELL, A., VALVANO, M., A., AEBI, M. & WREN, B., W. 2005. Functional analysis of the *Campylobacter jejuni* N-linked protein glycosylation pathway. *Molecular Microbiology*, 55, 1695-1703.
- LIPSHUTZ, R. J., TAVERNER, F., HENNESSY, K., HARTZELL, G. & DAVIS, R. 1994. DNA Sequence Confidence Estimation. *Genomics*, 19, 417-424.
- LISCHWE, M. A., NEWTON, R. C., HUANG, J. J., YATES, R. A., BRETH, L. A. & LARSEN, B. S. 1993. *Escherichia coli*: Derived Murine Interleukin-1 β with N-Terminus Partially N $_c$ -Acetylated. *Protein Expression and Purification*, 4, 499-502.
- LIU, H., PAN, H.-C., PENG, L. & CAI, S.-X. 2005. RP-HPLC determination of recombinant human interferon Ω in the *Pichia pastoris* fermentation broth. *Journal of Pharmaceutical and Biomedical Analysis*, 38, 734-737.
- LIU, P., TARNOWSKI, M., A., O'MARA, B., W., WU, W., ZHANG, H., TAMURA, J., K., ACKERMAN, M., S., TAO, L., GRACE, M., J. & RUSSELL, R., J. 2009. Characterization of S-thiolation on secreted proteins from *E. coli* by mass spectrometry. *Rapid Communications in Mass Spectrometry*, 23, 3343-3349.
- LOMAS-LOPEZ, R., COZZONE, A. J. & DUCLOS, B. 2008. A modified His-tag vector for the production of recombinant protein kinases. *Analytical Biochemistry*, 377, 272-273.

- LONDO, T., LYNCH, P., KEHOE, T., MEYS, M. & GORDON, N. 1998. Accelerated recombinant protein purification process development: Automated, robotics-based integration of chromatographic purification and analysis. *Journal of Chromatography A*, 798, 73-82.
- LU, H. S., FAUSSET, P. R., NARHI, L. O., HORAN, T., SHINAGAWA, K., SHIMAMOTO, G. & BOONE, T. C. 1999. Chemical Modification and Site-Directed Mutagenesis of Methionine Residues in Recombinant Human Granulocyte Colony-Stimulating Factor: Effect on Stability and Biological Activity. *Archives of Biochemistry and Biophysics*, 362, 1-11.
- LUTHRA, M. & BALASUBRAMANIAN, D. 1993. Nonenzymatic glycation alters protein structure and stability. *Journal of Biological Chemistry*, 268, 18119-18127.
- LYUBARSKAYA, Y., HOUDE, D., WOODARD, J., MURPHY, D. & MHATRE, R. 2006. Analysis of recombinant monoclonal antibody isoforms by electrospray ionization mass spectrometry as a strategy for streamlining characterization of recombinant monoclonal antibody charge heterogeneity. *Analytical Biochemistry*, 348, 24-39.
- MALIK, A., RUDOLPH, R. & SOHLING, B. 2006. A novel fusion protein system for the production of native human pepsinogen in the bacterial periplasm. *Protein Expression and Purification*, 47, 662-671.
- MANNING, M., CHOU, D., MURPHY, B., PAYNE, R. & KATAYAMA, D. 2010. Stability of Protein Pharmaceuticals: An Update. *Pharmaceutical Research*, 27, 544-575.
- MANNING, M. C., PATEL, K. & BORCHARDT, R. T. 1989. Stability of Protein Pharmaceuticals. *Pharmaceutical Research*, 6, 903-918.
- MARSHAK, D. R. 1996. *Strategies for protein purification and characterisation: a laboratory course manual*, CSHL Press.
- MARTINEZ, A., KNAPPSKOG, P. M., OLAFSDOTTIR, S., DØSKELAND, A., EIKEN, H., SVEBAK, R., BOZZINI, M., APOLD, J. & FLATMARK, T. 1995. Expression of recombinant human phenylalanine hydroxylase as fusion protein in *Escherichia coli* circumvents proteolytic degradation by host cell proteases. Isolation and Characterization of the wild-type enzyme. *Biochemical Journal*, 1, 589-597.
- MCCALL, K. A., HUANG, C.-C. & FIERKE, C. A. 2000. Function and Mechanism of Zinc Metalloenzymes. *The Journal of Nutrition*, 130, 1437S-1446S.
- MCCORMICK, C., DAJCS, J. J., REED, J., MARQUART, M. & O'CALLAGHAN, R. 2006. The Effectiveness of Lysostaphin Therapy for Experimental Coagulase-Negative *Staphylococcus Endophthalmitis*. *Current Eye Research*, 31, 225-230.
- MCNERNEY, T. M., WATSON, S. K., SIM, J.-H. & BRIDENBAUGH, R. L. 1996. Separation of recombinant human growth hormone from *Escherichia coli* cell pellet extract by capillary zone electrophoresis. *Journal of Chromatography A*, 744, 223-229.
- MCNULTY, D. E., CLAFFEE, B. A., HUDDLESTON, M. J. & KANE, J. F. 2003. Mistranslational errors associated with the rare arginine codon CGG in *Escherichia coli*. *Protein Expression and Purification*, 27, 365-374.
- MECHAM, R. P., BROEKELMANN, T. J., FLISZAR, C. J., SHAPIRO, S. D., WELGUS, H. G. & SENIOR, R. M. 1997. Elastin Degradation by Matrix Metalloproteinases. *Journal of Biological Chemistry*, 272, 18071-18076.
- MELTER, L., STRÖHLEIN, G., BUTTÉ, A. & MORBIDELLI, M. 2007. Adsorption of monoclonal antibody variants on analytical cation-exchange resin. *Journal of Chromatography A*, 1154, 121-131.
- MERCK4BIOSCIENCES. 2010a. *pET-28a(+)* DNA [Online]. Available: http://www.merck-chemicals.com/usa/life-science-research/pet-28a-plus-dna/EMD_BIO-69864/p_2tOb.s1OkacAAAEjWhI9.zLX.
- MERCK4BIOSCIENCES. 2010b. *pET Expression System 22b* [Online]. Available: http://www.merck-chemicals.com/life-science-research/pet-expression-system-22b/EMD_BIO-70765/p_oOib.s1LxAoAAAEW8GEfVhTm?attachments=VMAP.
- MIERAU, I., LEIJ, P., VAN SWAM, I., BLOMMESTEIN, B., FLORIS, E., MOND, J. & SMID, E. 2005a. Industrial-scale production and purification of a heterologous protein in

- Lactococcus lactis* using the nisin-controlled gene expression system NICE: The case of lysostaphin. *Microbial Cell Factories*, 4, 15.
- MIERAU, I., OLIEMAN, K., MOND, J. & SMID, E. 2005b. Optimization of the *Lactococcus lactis* nisin-controlled gene expression system NICE for industrial applications. *Microbial Cell Factories*, 4, 16.
- MIRONOVA, R., NIWA, T., DIMITROVA, R., BOYANOVA, M. & IVANOV, I. 2003. Glycation and Post-translational Processing of Human Interferon- γ Expressed in *Escherichia coli*. *Journal of Biological Chemistry*, 278, 51068-51074.
- MIRONOVA, R., NIWA, T., HAYASHI, H., DIMITROVA, R. & IVANOV, I. 2001. Evidence for non-enzymatic glycosylation in *Escherichia coli*. *Molecular Microbiology*, 39, 1061-1068.
- MIRONOVA, R., SREDOVSKA, A., IVANOV, I. & NIWA, T. 2008. Maillard Reaction Products in the *Escherichia coli*-derived Therapeutic Protein Interferon Alfacon-1. *Annals of the New York Academy of Sciences*, 1126, 181-184.
- MITRA, A., HRUSKA, K. S., WELLNITZ, O., KERR, D. E., CAPUCO, A. V. & WALL, R. J. 2003. Expression of Lysostaphin in Milk of Transgenic Mice Affects the Growth of Neonates. *Transgenic Research*, 12, 597-605.
- MOGUILLEVSKY, N., VARSALONA, F., GUILLAUME, J.-P., GILLES, P., BOLLEN, A. & ROOBOL, K. 1993. Production of authentic human proapolipoprotein A-I in *Escherichia coli*: Strategies for the removal of the amino-terminal methionine. *Journal of Biotechnology*, 27, 159-172.
- MOHANTY, A. K. & WIENER, M. C. 2004. Membrane protein expression and production: effects of polyhistidine tag length and position. *Protein Expression and Purification*, 33, 311-325.
- NAGARAJ, R. H., SHIPANOVA, I. N. & FAUST, F. M. 1996. Protein Cross-linking by the Maillard Reaction. *Journal of Biological Chemistry*, 271, 19338-19345.
- NAKAGAWA, S., YAMADA, T., KATO, K. & NISHIMURA, O. 1987. Enzymatic Cleavage of Amino Terminal Methionine from Recombinant Human Interleukin 2 and Growth Hormone by Aminopeptidase M. *Nature Biotechnology*, 5, 824-827.
- NARAYANAN, N. & CHOU, C. P. 2009. Alleviation of Proteolytic Sensitivity To Enhance Recombinant Lipase Production in *Escherichia coli*. *Applied and Environmental Microbiology*, 75, 5424-5427.
- NARMANDAKH, A. & BEARNE, S. L. 2010. Purification of recombinant mandelate racemase: Improved catalytic activity. *Protein Expression and Purification*, 69, 39-46.
- NISHIMURA, O., SUENAGA, M., OHAMAE, H., TSUJI, S., MASATO SUENAGA & FUJINO, M. 1998. An efficient chemical method for removing N-terminal extra methionine from recombinant methionylated human growth hormone. *Chemical Communications*, 1135-1136.
- NORDBORG, A. & HILDER, E. 2009. Recent advances in polymer monoliths for ion-exchange chromatography. *Analytical and Bioanalytical Chemistry*, 394, 71-84.
- NORDBORG, A., ZHANG, B., HE, X. Z., HILDER, E. F. & HADDAD, P. R. 2009. Characterization of monoclonal antibodies using polymeric cation exchange monoliths in combination with salt and pH gradients. *Journal of Separation Science*, 32, 2668-2673.
- ODDONE, G. M., LAN, C. Q., RAWSTHORNE, H., MILLS, D. A. & BLOCK, D. E. 2007. Optimization of fed-batch production of the model recombinant protein GFP in *Lactococcus lactis*. *Biotechnology and Bioengineering*, 96, 1127-1138.
- OLUOLA, O., KONG, L., FEIN, M. & WEISMAN, L. E. 2007. Lysostaphin in the Treatment of Neonatal *Staphylococcus aureus* Infection. *Antimicrobial Agents and Chemotherapy*, 51, 2198-2200.
- PAASCH, B. D., REED, B. R., KECK, R., SANDLUND, B. K., GILKERSON, E. & SHALABY, R. 1996. An evaluation of the accuracy of four ELISA methods for measuring natural and recombinant human interferon- γ . *Journal of Immunological Methods*, 198, 165-176.

- PABST, T. M., CARTA, G., RAMASUBRAMANYAN, N., HUNTER, A. K., MENSAH, P. & GUSTAFSON, M. E. 2008. Separation of protein charge variants with induced pH gradients using anion exchange chromatographic columns. *Biotechnology Progress*, 24, 1096-1106.
- PAIK, W. K., PAIK, D. C. & KIM, S. 2007. Historical review: the field of protein methylation. *Trends in Biochemical Sciences*, 32, 146-152.
- PARK, P. W., SENIOR, R. M., GRIFFIN, G. L., BROEKELMANN, T. J., MUDD, S. M. & MECHAM, R. P. 1995. Binding and degradation of elastin by the staphylolytic enzyme lysostaphin. *The International Journal of Biochemistry & Cell Biology*, 27, 139-146.
- PATRON, R. L., CLIMO, M. W., GOLDSTEIN, B. P. & ARCHER, G. L. 1999. Lysostaphin Treatment of Experimental Aortic Valve Endocarditis Caused by a *Staphylococcus aureus* Isolate with Reduced Susceptibility to Vancomycin. *Antimicrobial agents and Chemotherapy*, 43, 1754-1755.
- PAVLOVIC, M., GIRARDIN, E., KAPETANOVIC, L., HO, K. & TROUVIN, J.-H. 2008. Similar Biological Medicinal Products Containing Recombinant Human Growth Hormone: European Regulation. *Hormone Research*, 69, 14-21.
- PIKAL, M. J., DELLERMAN, K. M., ROY, M. L. & RIGGIN, R. M. 1991. The Effects of Formulation Variables on the Stability of Freeze-Dried Human Growth Hormone. *Pharmaceutical Research*, 8, 427-436.
- POLEVODA, B. & SHERMAN, F. 2007. Methylation of proteins involved in translation. *Molecular Microbiology*, 65, 590-606.
- PRAKASH, S., TIAN, L., RATLIFF, K. S., LEHOTZKY, R. E. & MATOUSCHEK, A. 2004. An unstructured initiation site is required for efficient proteasome-mediated degradation. *Nature Structural and Molecular Biology*, 11, 830-837.
- PRICE, N. C. & NAIRN, J. 2009. *Exploring proteins: a student's guide to experimental skills and methods*, Oxford University Press.
- PROUDFOOT, A. E. I., BROWN, S. C., BERNARD, A. R., BONNEFOY, J.-Y. & KAWASHIMA, E. H. 1993. Recombinant human IL-6 expressed in *E. coli* undergoes selective N-terminal degradation: Evidence that the protein consists of a stable core and a nonessential flexible N-terminal. *Journal of Protein Chemistry*, 12, 489-497.
- QUICKEL, K. E., JR., SELDEN, R., CALDWELL, J. R., NORA, N. F. & SCHAFFNER, W. 1971. Efficacy and Safety of Topical Lysostaphin Treatment of Persistent Nasal Carriage of *Staphylococcus aureus*. *Applied and Environmental Microbiology*, 22, 446-450.
- RAO, S., WOODRUFF, A., REY, M., FLOOK, K., THAYER, J. & POHL, C. 2010. Separation of Monoclonal Antibodies by Weak Cation-Exchange Chromatography Using ProPac and ProSwift Columns. Sunnyvale, California: Dionex.
- RATHORE, A. S., SOBACKE, S. E., KOCOT, T. J., MORGAN, D. R., DUFIELD, R. L. & MOZIER, N. M. 2003. Analysis for residual host cell proteins and DNA in process streams of a recombinant protein product expressed in *Escherichia coli* cells. *Journal of Pharmaceutical and Biomedical Analysis*, 32, 1199-1211.
- RECSEI, P. A., GRUSS, A. D. & NOVICK, R. P. 1987. Cloning, Sequence, and Expression of the Lysostaphin Gene from *Staphylococcus simulans*. *Proceedings of the National Academy of Sciences*, 84, 1127-1131.
- REISSNER, K. J. & ASWAD, D. W. 2003. Deamidation and isoaspartate formation in proteins: unwanted alterations or surreptitious signals? *Cellular and Molecular Life Sciences*, 60, 1281-1295.
- REN, D., RATNASWAMY, G., BEIERLE, J., TREUHEIT, M. J., BREMS, D. N. & BONDARENKO, P. V. 2009. Degradation products analysis of an Fc fusion protein using LC/MS methods. *International Journal of Biological Macromolecules*, 44, 81-85.
- REQUENA, J. S. R., CHAO, C.-C., LEVINE, R. L. & STADTMAN, E. R. 2001. Glutamic and amino adipic semialdehydes are the main carbonyl products of metal-catalyzed oxidation of proteins. *Proceedings of the National Academy of Sciences of the United States of America*, 98, 69-74.

- RICHMOND, C. S., GLASNER, J. D., MAU, R., JIN, H. & BLATTNER, F. R. 1999. Genome-wide expression profiling in *Escherichia coli* K-12. *Nucleic Acids Research*, 27, 3821-3835.
- ROGAKOU, E. P., PILCH, D. R., ORR, A. H., IVANOVA, V. S. & BONNER, W. M. 1998. DNA Double-stranded Breaks Induce Histone H2AX Phosphorylation on Serine 139. *Journal of Biological Chemistry*, 273, 5858-5868.
- ROSE, K., REGAMEY, P. O., ANDEREGG, R., WELLS, T. N. & PROUDFOOT, A. E. 1992. Human interleukin-5 expressed in *Escherichia coli* has N-terminal modifications. *Biochemical Journal*, 286 825-8.
- ROSENBERG, A. 2006. Effects of protein aggregates: An immunologic perspective. *The AAPS Journal*, 8, E501-E507.
- SANDMAN, K., GRAYLING, R. A. & REEVE, J. N. 1995. Improved N-terminal Processing of Recombinant Proteins Synthesized in *Escherichia coli*. *Nature Biotechnology*, 13, 504-506.
- SANGER, F., NICKLEN, S. & COULSON, A. R. 1977. DNA sequencing with chain-terminating inhibitors. *Proceedings of the National Academy of Sciences*, 74, 5463-5467.
- SHELLEKENS, H. 2005. Follow-on biologics: challenges of the 'next generation'. *Nephrology Dialysis Transplantation*, 20, 31-36.
- SCHINDLER, V. T. & SCHUHARDT, C. A. 1964. Lysostaphin: A new bacteriolytic agent for the *Staphylococcus*. *Proceedings of the National Academy of Sciences* 51, 414-421.
- SCHNEIDER, E. L., KING, D. S. & MARLETTA, M. A. 2005. Amino Acid Substitution and Modification Resulting from *Escherichia coli* Expression of Recombinant *Plasmodium falciparum* Histidine-Rich Protein II. *Biochemistry*, 44, 987-995.
- SCORER, C. A., CARRIER, M. J. & ROSENBERGER, R. F. 1991. Amino acid misincorporation during high-level expression of mouse epidermal growth factor in *Escherichia coli*. *Nucleic Acids Research*, 19, 3511-3516.
- SHAH, A., MOND, J. J. & WALSH, S. 2004. Lysostaphin-coated catheters eradicate *Staphylococcus aureus* challenge and block surface colonization. *Antimicrobial agents and Chemotherapy*, 48, 2704-2707.
- SHARMA, R., SHARMA, P. R., CHOUDHARY, M. L., PANDE, A. & KHATRI, G. S. 2006. Cytoplasmic expression of mature glycyglycine endopeptidase lysostaphin with an amino terminal hexa-histidine in a soluble and catalytically active form in *Escherichia coli*. *Protein Expression and Purification*, 45, 206-215.
- SHAW, B. F., ARTHANARI, H., NAROVLYANSKY, M., DURAZO, A., FRUEH, D. P., POLLASTRI, M. P., LEE, A., BILGICER, B., GYGI, S. P., WAGNER, G. & WHITESIDES, G. M. 2010. Neutralizing Positive Charges at the Surface of a Protein Lowers Its Rate of Amide Hydrogen Exchange without Altering Its Structure or Increasing Its Thermostability. *Journal of the American Chemical Society*, 132, 17411-17425.
- SHE, Y.-M., XU, X., YAKUNIN, A. F., DHE-PAGANON, S., DONALD, L. J., STANDING, K. G., LEE, D. C., JIA, Z. & CYR, T. D. 2010. Mass Spectrometry Following Mild Enzymatic Digestion Reveals Phosphorylation of Recombinant Proteins in *Escherichia coli* Through Mechanisms Involving Direct Nucleotide Binding. *Journal of Proteome Research*, 9, 3311-3318.
- SHIH, Y.-P., KUNG, W.-M., CHEN, J.-C., YEH, C.-H., WANG, A. H. J. & WANG, T.-F. 2002. High-throughput screening of soluble recombinant proteins. *Protein Science*, 11, 1714-1719.
- SILLER, E., DEZWAAN, D. C., ANDERSON, J. F., FREEMAN, B. C. & BARRAL, J. M. 2010. Slowing Bacterial Translation Speed Enhances Eukaryotic Protein Folding Efficiency. *Journal of Molecular Biology*, In Press, Corrected Proof.
- SLOAN, G. L., ROBINSON, J. M. & KLOOS, W. E. 1982. Identification of "*Staphylococcus staphylolyticus*" NRRL B-2628 as a Biovar of *Staphylococcus simulans*. *International Journal of Systematic Bacteriology* 32, 170-174.

- SLOAN, G. L., SMITH, E. C. & LANCASTER, J. H. 1977. Lysostaphin endopeptidase-catalysed transpeptidation reactions of the imino-transfer type. *Biochemical Journal*, 167, 293-296.
- SOINI, J., FALSCHLEHNER, C., LIEDERT, C., BERNHARDT, J., VUORISTO, J. & NEUBAUER, P. 2008. Norvaline is accumulated after a down-shift of oxygen in *Escherichia coli* W3110. *Microbial Cell Factories*, 7, 30.
- SOLSTAD, T. & FLATMARK, T. 2000. Microheterogeneity of recombinant human phenylalanine hydroxylase as a result of nonenzymatic deamidations of labile amide containing amino acids. *European Journal of Biochemistry*, 267, 6302-6310.
- SOMMER, C. A., SILVA, F. H. & NOVO, M. T. M. 2004. Teaching molecular biology to undergraduate biology students: An illustration of protein expression and purification. *Biochemistry and Molecular Biology Education*, 32, 7-10.
- SORENSEN, H. & MORTENSEN, K. 2005. Soluble expression of recombinant proteins in the cytoplasm of *Escherichia coli*. *Microbial Cell Factories*, 4, 1.
- SPECHT, B., OUDENAMPSEN-KRÜGER, E., INGENDOH, A., HILLENKAMP, F., LEZIUS, A. G. & SPENER, F. 1994. N-terminal variants of fatty acid-binding protein from bovine heart overexpressed in *Escherichia coli*. *Journal of Biotechnology*, 33, 259-269.
- STARK, F. R., THORNSVARD, C., FLANNERY, E. P. & ARTENSTEIN, M. S. 1974. Systemic Lysostaphin in Man - Apparent Antimicrobial Activity in a Neutropenic Patient. *New England Journal of Medicine*, 291, 239-240.
- STARKOVA, N. N., KOROLEVA, E. P., RUMSH, L. D., GINODMAN, L. M. & ROTANOVA, T. V. 1998. Mutations in the proteolytic domain of *Escherichia coli* protease Lon impair the ATPase activity of the enzyme. *FEBS Letters*, 422, 218-220.
- STRAUCH, K. L. & BECKWITH, J. 1988. An *Escherichia coli* mutation preventing degradation of abnormal periplasmic proteins. *Proceedings of the National Academy of Sciences*, 85, 1576-1580.
- STRAUSS, E., KINSLAND, C., GE, Y., MCLAFFERTY, F. W. & BEGLEY, T. P. 2001. Phosphopantothencysteine Synthetase from *Escherichia coli*. *Journal of Biological Chemistry*, 276, 13513-13516.
- STREGE, M. A. & LAGU, A. L. 1995. Analysis of recombinant human growth hormone in *Escherichia coli* fermentation broth by micellar high-performance liquid chromatography. *Journal of Chromatography A*, 705, 155-161.
- STRIEMER, C. C., GABORSKI, T. R., MCGRATH, J. L. & FAUCHET, P. M. 2007. Charge- and size-based separation of macromolecules using ultra-thin silicon membranes. *Nature*, 445, 749-753.
- SUENAGA, M., OHMAE, H., OKUTANI, N., KUROKAWA, T., ASANOM, T., YAMADA, T., NISHIMURA, O. & FUJINO, M. 1999. Further studies on the chemical cleavage of an N-terminal extra methionine from recombinant methionylated proteins. *Journal of the Chemical Society: Perkins Transactions* 1, 1, 3727-3733.
- SUGAI, M. 1997. Peptidoglycan hydrolases of the *Staphylococci*. *Journal of Infection and Chemotherapy*, 3, 113-127.
- SUGASE, K., LANDES, M. A., WRIGHT, P. E. & MARTINEZ-YAMOUT, M. 2008. Overexpression of post-translationally modified peptides in *Escherichia coli* by co-expression with modifying enzymes. *Protein Expression and Purification*, 57, 108-115.
- SUGIMOTO, S., YAMAGUCHI, K. & YOKOO, Y. 1990. Isolation and characterization of recombinant eel growth hormone expressed in *Escherichia coli*. *Journal of Chromatography A*, 515, 483-494.
- SUNDBERG, R. J. & MARTIN, R. B. 1974. Interactions of histidine and other imidazole derivatives with transition metal ions in chemical and biological systems. *Chemical Reviews*, 74, 471-517.
- SUROVTSEV, V., BORZENKOV, V., FEDOROV, T. & SMOTROV, O. 2007. Ionogenic groups in the active site of lysostaphin. Kinetic and thermodynamic data compared with X-ray crystallographic data. *Biochemistry (Moscow)*, 72, 989-993.

- SWAMY, K. H. & GOLDBERG, A. L. 1982. Subcellular distribution of various proteases in *Escherichia coli*. *Journal of Bacteriology*, 149, 1027-1033.
- SWARTZ, J. R. 2001. Advances in *Escherichia coli* production of therapeutic proteins. *Current Opinion in Biotechnology*, 12, 195-201.
- SZWEDA, P., KOTLOWSKI, R. & KUR, J. 2005. New effective sources of the *Staphylococcus simulans* lysostaphin. *Journal of Biotechnology*, 117, 203-213.
- SZWEDA, P., PLADZYK, R., KOTLOWSKI, R. & KUR, J. 2001. Cloning, Expression, and Purification of the *Staphylococcus simulans* Lysostaphin Using the Intein-Chitin-Binding Domain (CBD) System. *Protein Expression and Purification*, 22, 467-471.
- TAKAO, T., KOBAYASHI, M., NISHIMURA, O. & SHIMONISHI, Y. 1987. Chemical characterization of recombinant human leukocyte interferon A using fast atom bombardment mass spectrometry. *Journal of Biological Chemistry*, 15, 3541-3547.
- TERPE, K. 2003. Overview of tag protein fusions: from molecular and biochemical fundamentals to commercial systems. *Applied Microbiology and Biotechnology*, 60, 523-533.
- TERPE, K. 2006. Overview of bacterial expression systems for heterologous protein production: from molecular and biochemical fundamentals to commercial systems. *Applied Microbiology and Biotechnology*, 72, 211-222.
- THUMM, G. & GÖTZ, F. 1997. Studies on polysostaphin processing and characterization of the lysostaphin immunity factor (Lif) of *Staphylococcus simulans* biovar *staphylolyticus*. *Molecular Microbiology*, 23, 1251-1265.
- TRAYER, H. R. & BUCKLEY, C. E. 1979. Molecular properties of Lysostaphin, a bacteriolytic agent specific for *Staphylococcus aureus*. *Journal of Biological Chemistry*, 245, 4842-4846.
- TROEBERG, L., TANAKA, M., WAIT, R., SHI, Y. E., BREW, K. & NAGASE, H. 2002. *E. coli* Expression of TIMP-4 and Comparative Kinetic Studies with TIMP-1 and TIMP-2: Insights into the Interactions of TIMPs and Matrix Metalloproteinase 2 (Gelatinase A). *Biochemistry*, 41, 15025-15035.
- TSAI, L. B., LU, H. S., KENNEY, W. C., CURLESS, C. C., KLEIN, M. L., LAI, P.-H., FENTON, D. M., ALTROCK, B. W. & MANN, M. B. 1988. Control of misincorporation of de novo synthesized norleucine into recombinant interleukin-2 in *E. coli*. *Biochemical and Biophysical Research Communications*, 156, 733-739.
- TSUMOTO, K., EJIMA, D., KUMAGAI, I. & ARAKAWA, T. 2003. Practical considerations in refolding proteins from inclusion bodies. *Protein Expression and Purification*, 28, 1-8.
- TURNER, M. S., WALDHERR, F., LOESSNER, M. J. & GIFFARD, P. M. 2007. Antimicrobial activity of lysostaphin and a *Listeria monocytogenes* bacteriophage endolysin produced and secreted by lactic acid bacteria. *Systematic and Applied Microbiology*, 30, 58-67.
- UEDA, E. K. M., GOUT, P. W. & MORGANTI, L. 2003. Current and prospective applications of metal ion-protein binding. *Journal of Chromatography A*, 988, 1-23.
- VALLEE, B. L. & AULD, D. S. 1990. Zinc coordination, function, and structure of zinc enzymes and other proteins. *Biochemistry*, 29, 5647-5659.
- VAN DOREN, S. R., WEI, S., GAO, G., DAGUE, B. B., PALMIER, M. O., BAHUDHANAPATI, H. & BREW, K. 2008. Inactivation of N-TIMP-1 by N-terminal acetylation when expressed in bacteria. *Biopolymers*, 89, 960-968.
- VILORIA-COLS, M. E., HATTI-KAUL, R. & MATTIASSON, B. 2004. Agarose-coated anion exchanger prevents cell-adsorbent interactions. *Journal of Chromatography A*, 1043, 195-200.
- VINCENTELLI, R., BIGNON, C., GRUEZ, A., CANAAN, S., SULZENBACHER, G., TEGONI, M., CAMPANACCI, V. R. & CABBILLAU, C. 2003. Medium-Scale Structural Genomics: Strategies for Protein Expression and Crystallization. *Accounts of Chemical Research*, 36, 165-172.
- VIOLAND, B. N., SCHLITTLER, M. R., LAWSON, C. Q., KANE, J. F., SIEGEL, N. R., SMITH, C. E., KOLODZIEJ, E. W. & DUFFIN, K. L. 1994. Isolation of *Escherichia coli*

- synthesized recombinant eukaryotic proteins that contain 6-N-acetyllysine. *Protein Science*, 3, 1089-1097.
- VON HEIJNE, G. 1990. The signal peptide. *Journal of Membrane Biology* 115, 195-201.
- VUILLARD, L., BRAUN-BRETON, C. & RABILLOUD, T. 1995. Non-detergent sulphobetaines: A new class of mild solubilization agents for protein purification *Biochemical Journal*, 305, 337-343.
- WACKER, M., LINTON, D., HITCHEN, P. G., NITA-LAZAR, M., HASLAM, S. M., NORTH, S. J., PANICO, M., MORRIS, H. R., DELL, A., WREN, B. W. & AEBI, M. 2002. N-Linked Glycosylation in *Campylobacter jejuni* and its functional transfer into *E. coli*. *Science*, 29, 1790-1793.
- WADSTRØM, T. & VESTERBERG, O. 1971. Studies on Endo- β -N-acetylglucosaminidase, staphylolytic peptidase, and N-acetylmuramyl-L-alanine amidase in Lysostaphin and from *Staphylococcus aureus*. *Acta Pathologica Microbiologica Scandinavica Section B Microbiology and Immunology*, 79B, 248-264.
- WALENCKA, E., SADOWSKA, B. & ROZALSKA, S. 2005. Lysostaphin as a Potential Therapeutic Agent for Staphylococcal Biofilm Eradication. *Polish Journal of Microbiology*, 54, 191-200.
- WALENCKA, E., SADOWSKA, B., RÓŻALSKA, S., HRYNIEWICZ, W. & RÓŻALSKA, B. 2006. *Staphylococcus aureus* biofilm as a target for single or repeated doses of oxacillin, vancomycin, linezolid and/or lysostaphin. *Folia Microbiologica*, 51, 381-386.
- WALL, R. J., POWELL, A. M., PAAPE, M. J., KERR, D. E., BANNERMAN, D. D., PURSEL, V. G., WELLS, K. D., TALBOT, N. & HAWK, H. W. 2005. Genetically enhanced cows resist intramammary *Staphylococcus aureus* infection. *Nature Biotechnology*, 23, 445-451.
- WALSH, C. T. 2006. Post-translational modifications of proteins - Expanding Nature's Inventory. Roberts and Company Publishers.
- WALSH, C. T., GARNEAU-TSODIKOVA, S. & GATTO, G. J. 2005. Protein Posttranslational Modifications: The Chemistry of Proteome Diversifications. *Angewandte Chemie International Edition*, 44, 7342-7372.
- WALSH, G. & JEFFERIS, R. 2006. Post-translational modifications in the context of therapeutic proteins. *Nature Biotechnology*, 24, 1241 - 1252.
- WALSH, S., KOKAI-KUN, J., SHAH, A. & MOND, J. 2004. Extended Nasal Residence Time of Lysostaphin and an Anti-Staphylococcal Monoclonal Antibody by Delivery in Semisolid or Polymeric Carriers. *Pharmaceutical Research*, 21, 1770-1775.
- WANDERSMAN, C. 1989. Secretion, processing and activation of bacterial extracellular proteases. *Molecular Microbiology*, 3, 1825-1831.
- WARFIELD, R., BARDELANG, P., SAUNDERS, H., CHAN, W. C., PENFOLD, C., JAMES, R. & THOMAS, N. R. 2006. Internally quenched peptides for the study of lysostaphin: an antimicrobial protease that kills *Staphylococcus aureus*. *Organic & Biomolecular Chemistry*, 4, 3626-3638.
- WEITZHANDLER, M., FARNAN, D., ROHRER, J. S. & AVDALOVIC, N. 2001. Protein variant separations using cation exchange chromatography on grafted, polymeric stationary phases. *Proteomics*, 1, 179-185.
- WENDLAND, J. 2003. PCR-based methods facilitate targeted gene manipulations and cloning procedures. *Current Genetics*, 44, 115-123.
- WESTERS, L., WESTERS, H. & QUAX, W. J. 2004. *Bacillus subtilis* as cell factory for pharmaceutical proteins: a biotechnological approach to optimize the host organism. *Biochimica et Biophysica Acta (BBA) - Molecular Cell Research*, 1694, 299-310.
- WILLIAMSON, C. M., BRAMLEY, A. J. & LAX, A. J. 1994. Expression of the lysostaphin gene of *Staphylococcus simulans* in a eukaryotic system. *Applied and Environmental Microbiology*, 60, 771-776.
- WILTON, R., YOUSEF, M. A., SAXENA, P., SZPUNAR, M. & STEVENS, F. J. 2006. Expression and purification of recombinant human receptor for advanced glycation endproducts in *Escherichia coli*. *Protein Expression and Purification*, 47, 25-35.

- WINGFIELD, P. T., GRABER, P., ROSE, K., SIMONA, M. G. & HUGHES, G. J. 1987a. Chromatofocusing of N-terminally processed forms of proteins : Isolation and characterization of two forms of interleukin-1 β and of bovine growth hormone. *Journal of Chromatography A*, 387, 291-300.
- WINGFIELD, P. T., MATTALIANO, R. J., MACDONALD, H. R., CRAIG, S., CLORE, G. M., GRONENBORN, A. M. & SCHMEISSNER, U. 1987b. Recombinant-derived interleukin-1 α stabilized against specific deamidation. *Protein Engineering Design and Selection*, 1, 413-417.
- WITTIG, I., BRAUN, H. P. & SCHAGGER, H. 2006. Blue native PAGE. *Nature Protocols*, 1, 418 - 428.
- WITTIG, I. & SCHÄGGER, H. 2005. Advantages and limitations of clear-native PAGE. *Proteomics*, 5, 4338-4346.
- WU, J., CHANG, S., GONG, X., LIU, D. & MA, Q. 2006. Identification of N-terminal acetylation of recombinant human prothymosin α in *Escherichia coli*. *Biochimica et Biophysica Acta (BBA) - General Subjects*, 1760, 1241-1247.
- WU, J. A., KUSUMA, C., MOND, J. J. & KOKAI-KUN, J. F. 2003. Lysostaphin Disrupts *Staphylococcus aureus* and *Staphylococcus epidermidis* Biofilms on Artificial Surfaces. *Antimicrobial agents and Chemotherapy*, 47, 3407-3414.
- XIE, H., GILAR, M. & GEBLER, J. C. 2009. Characterization of Protein Impurities and Site-Specific Modifications Using Peptide Mapping with Liquid Chromatography and Data Independent Acquisition Mass Spectrometry. *Analytical Chemistry*, 81, 5699-5708.
- XIE, M., SHAHROKH, Z., KADKHODAYAN, M., HENZEL, W. J., POWELL, M. F., BORCHARDT, R. T. & SCHOWEN, R. L. 2003. Asparagine deamidation in recombinant human lymphotoxin: Hindrance by three-dimensional structures. *Journal of Pharmaceutical Science*, 92, 869-880.
- XU, Y., YASIN, A., TANG, R., SCHARER, J., MOO-YOUNG, M. & CHOU, C. 2008. Heterologous expression of lipase in *Escherichia coli* is limited by folding and disulfide bond formation. *Applied Microbiology and Biotechnology*, 81, 79-87.
- YAMAGUCHI, M., NAKAZAWA, T., KUYAMA, H., OBAMA, T., ANDO, E., OKAMURA, T.-A., UEYAMA, N. & NORIOKA, S. 2004. High-Throughput Method for N-Terminal Sequencing of Proteins by MALDI Mass Spectrometry. *Analytical Chemistry*, 77, 645-651.
- YAN, Z., CALDWELL, G. W. & MCDONELL, P. A. 1999a. Identification of a Gluconic Acid Derivative Attached to the N-Terminus of Histidine-Tagged Proteins Expressed in Bacteria. *Biochemical and Biophysical Research Communications*, 262, 793-800.
- YAN, Z., CALDWELL, G. W., MCDONELL, P. A., JONES, W. J., AUGUST, A. & MASUCCI, J. A. 1999b. Mass Spectrometric Determination of a Novel Modification of the N-Terminus of Histidine-Tagged Proteins Expressed in Bacteria. *Biochemical and Biophysical Research Communications*, 259, 271-282.
- YANG, X.-Y., LI, C.-R., LOU, R.-H., WANG, Y.-M., ZHANG, W.-X., CHEN, H.-Z., HUANG, Q.-S., HAN, Y.-X., JIANG, J.-D. & YOU, X.-F. 2007. *In vitro* activity of recombinant lysostaphin against *Staphylococcus aureus* isolates from hospitals in Beijing, China. *Journal of Medical Microbiology*, 56, 71-76.
- ZHANG, H., LU, L., YAN, X. & GAO, P. 2007. Effect of the population heterogeneity on growth behavior and its estimation. *Science in China Series C: Life Sciences*, 50, 535-547.
- ZHANG, J. & GREASHAM, R. 1999. Chemically defined media for commercial fermentations. *Applied Microbiology and Biotechnology*, 51, 407-421.
- ZHANG, Z., TAN, M., XIE, Z., DAI, L., CHEN, Y. & ZHAO, Y. 2011. Identification of lysine succinylation as a new post-translational modification. *Nature Chemical Biology*, 7, 58-63.
- ZHOU, R., CHEN, S. & RECSEI, P. 1988. A dye release assay for determination of lysostaphin activity. *Analytical Biochemistry*, 171, 141-144.

7 Appendix

7.1 Cloning, Expression and Purification of Recombinant Lysostaphin

Appendix 7.1: Bacterial strains used during cloning, expression and characterisation of recombinant lysostaphin

Bacteria	Strain	Source
<i>Escherichia coli</i>	TOP10	Invitrogen, UK
<i>Escherichia coli</i>	XL-1 Blue	Agilent, UK
<i>Escherichia coli</i>	BL21(DE3)	Merck4Biosciences, UK
<i>Staphylococcus simulans</i>	b.v <i>staphylolyticus</i>	DSMZ, Germany
<i>Staphylococcus aureus</i>	b.v <i>aureus</i>	DSMZ, Germany

Appendix 7.2: Preparation of media

All media were prepared using 18.2 MΩ/cm H₂O (unless specified otherwise) and sterilised by autoclaving. Any solutions which could not be autoclaved were sterilised by filtration. To achieve the correct stated pH, the pH of solutions was adjusted using HCl or NaOH and a pH meter. Solid media was stored at 4°C, whilst liquid media was stored at room temperature.

Appendix 7.3: Storage of bacterial strains

Glycerol stocks of bacterial strains were prepared by mixing 0.5 ml of bacterial culture broth with 0.5 ml of 50 % (v/v) glycerol. *E. coli* Top 10, *E. coli* XL1-Blue and *Staphylococcus aureus* were stored in 50 % (v/v) glycerol at -80°C. *Staphylococcus staphylolyticus* was stored in 50 % (v/v) glycerol at -80°C.

Appendix 7.4: Growth of bacteria on agar plates

The bacteria were streaked or plated onto agar plates and incubated overnight at 37°C. Bacterial colonies were then picked using a sterile wire loop and inoculated into liquid cultures.

Appendix 7.5: Streaking of bacterial strains

Before streaking, agar plates were surface dried at 65°C for 10 min by placing them open and face down in an oven. Using a sterile wire loop, a loop-full of bacterial glycerol stock was streaked onto the agar plate. The agar plate was then inverted and incubated at 37°C overnight.

Appendix 7.6: Plating of bacterial suspensions

Before plating, agar plates were surface dried at 65°C for 10 min by placing them open and face down in an oven. A sterile glass spreader was used to spread bacterial suspension evenly on the surface of the agar. The glass spreader was immersed in 70% (v/v) ethanol and passed through a blue Bunsen flame to remove the excess ethanol and ensure sterilisation of the glass spreader. Once the bacterial suspension had fully absorbed into the agar, the agar plate was inverted and incubated overnight at 37°C.

Appendix 7.7: Measurement of bacterial growth

Bacterial growth in liquid culture was measured at 600 nm using a Visible light spectrophotometer. Prior to each measurement, 1 ml of sterile culture media was added to a cuvette and used to blank the spectrophotometer, before measuring the absorbance of 1 ml of the culture in a fresh cuvette.

Appendix 7.8: Preparation of chemical solutions and buffers

All solutions were prepared using 18.2 M Ω /cm H₂O which had been purified by a Milli-Q water purification system and stored at room temperature, unless specified otherwise. Following preparation, all solutions were autoclaved at 121 °C. Alternatively when solutions could not be autoclaved, solutions were sterilised by filtration using 0.2 μ m filters (Sartorius Stedim Biotech, Germany). To achieve the correct stated pH, the pH of solutions was adjusted using HCl or NaOH and a pH meter.

Appendix 7.9: Chemicals and media

Acros	Disodium phosphate Iron chloride Lactose Monosodium phosphate Potassium dihydrogen orthophosphate Sodium molybdate <i>N,N,N',N'</i> -Tetramethylethylenediamine (TEMED)
BDH	Bacto-peptone Beef extract Bromophenol blue Nickel (II) chloride Trypticase soy yeast extract
Fisher BioReagents	Acrylamide/Bisacrylamide (37.5:1, 40 % solution) Coomassie Blue R-250 Methanol Phenol
Fisher Chemicals	Acetic acid, glacial Acetone Acetonitrile(LC-MS grade) Ammonium chloride Ammonium sulphate Calcium carbonate Ethanol Glycerol 2-(<i>N</i> -morpholino)ethanesulfonic acid (MES) Sodium sulphate Trifluoroacetic acid
Fluka	Ammonium bicarbonate
Melford Laboratories Ltd	Agarose (High gel strength) Ampicillin Dithiothreitol Ethylene diamine tetraacetic acid (EDTA) Glycine Isopropyl β -D-1-thiogalactopyranoside (IPTG) Kanamycin Sodium chloride Sodium dodecylsulphate (SDS) Sodium phosphate dibasic Tris (Hydroxymethyl) aminomethane (Tris-HCl) Tryptone

	Yeast extract
Oxoid	Agar biological no. 1
Riedel-deHaen	Hydrochloric acid
Sigma	Ammonium dihydrogen phosphate Ammonium sulphate Ammonium persulphate (APS) Bovine serum albumin, Fraction V (BSA) Bradford's reagent Bromophenol blue Calcium chloride anhydrous Cobalt chloride Cupric chloride Dipotassium phosphate Ethidium bromide Ferrous sulphate Glucose 4-(2-hydroxyethyl)-1-piperazineethanesulfonic acid (HEPES) Hydrogen borate Imidazole Isopropanol (2-propanol) Manganous sulphate Magnesium chloride Nickel sulphate β -mercaptoethanol Potassium chloride Potassium phosphate monobasic Potassium sulphate Sodium acetate Sodium hydroxide Sodium phosphate monobasic Sodium sulphite Sodium selenite Sucrose Urea Zinc sulphate

Appendix 7.10: Equipment used during this research

Purpose	Equipment	Manufacturer
General	Milli-Q water purification system	Millipore Corporation, USA
	Chemi doc XRS gel documentation system	BioRad, UK
	Prestige [®] Medical 2100 Classic autoclave	Prestige Medical, UK
	Priorclave front loading autoclave	Priorclave, UK
	UV-visible Helios α spectrophotometer.	Spectronic Unicam, UK
	UV-visible Pharmacia Ultrospec 2000	Pharmacia, UK
	Cecil 2000 Series Visible Spectrophotometer	Cecil Instruments, UK
	Jenway Ion Meter 3340	Jenway, UK
Cloning /Expression	Techne TC-512 thermal cycler	Jencons Plc, UK
	Gene Pulser Xcell [™] Electroporation System	BioRad, UK
	Static incubator	Weiss Gallenkamp, UK
	Orbital shaking incubator	Weiss Gallenkamp, UK
	Bench top micro-centrifuge (1-15)	Sigma-Aldrich, UK
	Refrigerated bench top centrifuge (3K18C)	Sigma-Aldrich, UK
	Sorvall [®] RC5B Plus	ThermoScientific, UK
	MSE Soniprep 150-ultrasonicator	MSE, UK
	Mini-sub cell electrophoresis kit	Bio-Rad, UK
	Mini-protean 3 cell electrophoresis kit	Bio-Rad, UK
	Centrifugal evaporator RVC 2-18	Martin Christ, Germany
Purification	ÄKTA [™] Prime Plus System	GE Healthcare, UK
	Microtube peristaltic pump (MP3)	Eyela, China
	Ultimate [™] 3000 LC system	Dionex, UK
	Christ [®] Alpha 1-2 freeze drier.	Martin Christ, Germany
Separation	Ultimate [™] Titanium system	Dionex, UK
Chromatography	Ultimate [™] 3000 Titanium system	Dionex, UK
	Ultimate [™] 3000 LC system	Dionex, UK
	ISCO Foxy [®] Jr fraction collector	Teledyne ISCO, USA
LC-MS	MaXis Hybrid Quad TOF	Bruker Daltonics, UK

Appendix 7.11: Chromatographic columns used during this research

Application	Separation	Column	Mode	Stationary Phase	Dimension (mm)	Manufacturer
Protein Purification	IMAC	Chelating Sepharose™ Fast Flow, XK 16/20	Preparative	Porous	16.0 x 50.0	GE Healthcare, UK
	IMAC	Chelating Sepharose™ Fast Flow, XK 50/20	Preparative	Porous	50.0 x 12.0	GE Healthcare, UK
	IMAC	ProPac® IMAC-10	Analytical	Pellicular	2.0 x 250	Dionex, UK
	IMAC	ProPac® IMAC-10	Analytical	Pellicular	4.0 x 250	Dionex, UK
	HIC	Phenyl Sepharose™ High Performance, XK 16/20	Preparative	Porous	16.0 x 45.0	GE Healthcare, UK
	GF	HiLoad 16/60 Superdex 200 prep grade	Preparative	Porous	16.0 x 600.0	GE Healthcare, UK
	AXC	Source™ 30Q media XK 16/20	Preparative	Porous	16.0 x 40.0	GE Healthcare, UK
	CXC	Source™ 30S media, XK 16/20	Preparative	Porous	16.0 x 32.0	GE Healthcare, UK
Protein Separation	WCX	ProPac® WCX-10	Analytical	Pellicular	2.0 x 250	Dionex, UK
	WCX	ProPac® WCX-10	Analytical	Pellicular	4.0 x 250	Dionex, UK
	WCX	ProSwift® WCX-1S	Analytical	Monolithic	2.0 x 50	Dionex, UK
	SAX	ProPac® SAX-10	Analytical	Pellicular	2.0 x 250	Dionex, UK
	SCX	ProPac® SCX-10	Analytical	Pellicular	2.0 x 250	Dionex, UK
	SCX	ProPac® SCX-10	Analytical	Pellicular	4.0 x 250	Dionex, UK
	SCX	ProSwift® SCX-1S	Analytical	Monolithic	4.6 x 50	Dionex, UK
	SCX	ProPac® MAb SCX	Analytical	Pellicular	4.0 x 250	Dionex, UK
Protein Characterisation	GF	Zorbax® GF-250	Analytical	Porous	4.6 x 250	Agilent, UK
	RP	PepSwift® PS-DVB	Analytical	Monolithic	0.2 x 50	Dionex, UK

Appendix 7.12: Buffers and solutions

50 x TAE buffer (1L)

Tris-base	242.0 g
Glacial acetic acid	57.1 ml
EDTA (5 mM)	100.0 ml

The pH was adjusted to pH 8.0 and the solution was stored at 4°C.

EDTA (1L)

EDTA (500 mM)	186.1 g
---------------	---------

To dissolve the EDTA, the pH of the solution was adjusted to pH 8.0.

6 x Bromophenol blue loading buffer (10 ml)

Bromophenol blue (0.25% w/v)	0.025 g
Glycerol (30% w/v)	3.000 g

The solution was stored at 4°C.

6 x Xylene cyanol loading buffer (10 ml)

Xylene cyanol (0.25% w/v)	0.025 g
Glycerol (30 % w/v)	3.000 g

The solution was stored at 4°C.

Ethidium bromide solution (100 ml)

Ethidium bromide (10 mg/ml)	100 µl
-----------------------------	--------

The solution was protected from light.

SDS-PAGE Buffer B (200 ml)

Tris-HCl (2M)	150 ml
SDS (10 %)	8 ml
18.2 Ω/cm H ₂ O	42 ml

The pH of the buffer was adjusted to pH 8.8 prior to the addition of SDS. The solution was stored at 4°C.

SDS-PAGE Buffer C (200 ml)

Tris-HCl (1M)	100 ml
SDS (10%)	8 ml
18.2 Ω /cm H ₂ O	92 ml

The pH of the buffer was adjusted to pH 6.8 prior to the addition of SDS. The solution was stored at 4°C.

SDS-PAGE loading buffer (10 ml)

Tris-HCl, pH 6.8 (1M)	0.6 ml
50% (w/v) glycerol	5.0 ml
10% (w/v) sodium dodecyl sulphate (SDS)	2.0 ml
β -mercaptoethanol (14.4 mM)	0.5 ml
18.2 Ω /cm H ₂ O	0.9 ml
1% (w/v) bromophenol blue (BPB)	1.0 ml

The pH of the buffer was adjusted to pH 6.8 prior to the addition of SDS. The solution was stored as aliquots at -20°C.

SDS-PAGE solubilising cracking buffer (10 ml)

SDS-PAGE loading buffer	7.6 ml
Urea	2.4 g

The solution was stored at 4°C.

10 x SDS-PAGE running buffer (1 L)

Tris-HCl, pH 8.0	30.2 g
Glycine	144.0 g
SDS	10.0 g

The pH of the buffer was adjusted to pH 8.0 prior to the addition of SDS. The solution was stored at room temperature and diluted 1:10 with 18.2 Ω /cm H₂O during SDS-PAGE.

SDS-PAGE stain

Methanol	450.0 ml
----------	----------

Glacial acetic acid	100.0 ml
Coomassie Blue (R250)	1.0 g

The SDS-PAGE stain was stored at room temperature. The stain could be filtered through filter paper and re-used.

SDS-PAGE de-stain

Methanol	100 ml
Glacial acetic acid	100 ml
18.2 Ω /cm H ₂ O	800 ml

De-stain was stored at room temperature. Polyacrylamide gels were placed in de-stain overnight or until protein bands could be clearly resolved.

Appendix 7.13: Analytical agarose gel electrophoresis

A 1 % agarose gel was prepared by dissolving 0.3 g agarose in 30 ml of 1 x TAE buffer under heat using a Bunsen burner. Once dissolved and allowed to cool for a short period of time, the agarose was poured in a continuous movement into a sealed mini-gel casting tray containing an 8-well comb, on a level work surface. Diluted 1x TAE buffer was poured into the reservoirs of the electrophoresis tank and over the gel and casting tray which was placed onto the back plate of the tank. After allowing the gel to soak, the 8-well comb was carefully removed from the gel and DNA samples were loaded using a Gilson pipette. Samples were loaded by combining 5 μ l of DNA with 1 μ l of bromophenol blue or xylene cyanol loading buffer. Loading buffers were selected based on the molecular weight of the DNA being analysed to prevent co-migration of DNA and dye molecules. The samples were run alongside a 1 kb size standard (Appendix 7.17).

Electrophoresis was performed at 100 V and 1.20 mA for 45 min. The gel was removed from the tank, stained with ethidium bromide solution for 10 min and washed with distilled H₂O. The DNA bands were visualised by transferring the gel to a Chemi doc XRS UV gel documentation system with Quantity One™ software. Hard copies of the gel images were obtained from a linked Mitsubishi Video Copy Processor printer.

Appendix 7.14: Preparative agarose gel electrophoresis

Agarose gel electrophoresis was performed as described in Appendix 7.13; however the gels were stained only using freshly prepared ethidium bromide solution to avoid DNA contamination. The gel was visualised using white UV-light and the DNA band of interest was excised from the gel using a scalpel. DNA was then extracted from the gel by gel extraction (Appendix 7.44).

Appendix 7.15: SDS-PAGE

SDS-PAGE was performed using 12 % (w/v) polyacrylamide gels which were prepared following polymerisation of a resolving gel and a stacking gel. The resolving gel was prepared by combining 3.0 ml of acrylamide (40%), 4.5 ml of 18.2 Ω /cm H₂O, 2.5 ml of SDS-PAGE Buffer B, 50 μ l of 10 % (w/v) ammonium persulphate (APS) and 10 μ l of tetramethylethylenediamine (TEMED) before casting the mixture between two glass plates. Once cast the resolving gel was overlaid with 18.2 Ω /cm H₂O and allowed to set for 20 min. A stacking gel was then prepared containing 0.5 ml of acrylamide (30%), 2.5 ml of 18.2 Ω /cm H₂O, 1.0 ml of SDS-PAGE Buffer C, 30 μ l of APS (10%), 10 μ l of TEMED and a few drops of 1% bromophenol blue. The stacking gel was used to overlay the resolving gel, after blotting away residual 18.2 M Ω H₂O, and a 10-well comb was added to the gel. The gel was allowed to set for 20 min and once polymerised, the comb was removed and the wells were washed with distilled water to remove any polyacrylamide gel debris.

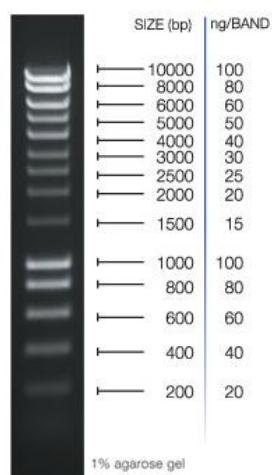
The gel was loaded into the PAGE tank and 1 L of 1 x SDS-PAGE running buffer was added to the tank. Loading buffer (5 μ l) was added to 20 μ l of protein sample and electrophoresed against a protein size standard. A number of protein size standards were used during this research based on their availability and were prepared as described in Appendix 7.16.

During protein expression experiments, the solubility of protein samples could be tested by resuspending insoluble cellular protein in solubilising cracking buffer (described further in Appendix 7.77). Prior to SDS-PAGE, protein samples and standards were transferred to a boiling water bath and heated for 3 min prior to loading onto the SDS-PAGE gel using a 25 μ l Hamilton syringe. Electrophoresis was performed at 200 V and 60 mA for 60 min. The gels were then stained with SDS-PAGE stain for 10-15 min and then de-stained using SDS-PAGE de-stain overnight. Protein bands were visualised and photographed using a Chemi doc XRS UV gel documentation system with a GS 800 densitometer. Hard copies of the gel images were obtained from a linked Mitsubishi Video Copy Processor printer.

Appendix 7.16: Protein size standards used during SDS-PAGE analysis

Size standard	Loading composition	Reference	Supplier
Sigma low range	8 μ l standard 4 μ l loading buffer	Appendix 7.18	Sigma-Aldrich, UK
Sigma high range	8 μ l standard 4 μ l loading buffer	Appendix 7.18	Sigma-Aldrich, UK
NZY broad range	5 μ l standard 5 μ l loading buffer	Appendix 7.19 Appendix 7.20	NZYtech, Portugal
NEB pre-stained broad range	15 μ l standard	Appendix 7.21 Appendix 7.22	NE Biolabs, USA

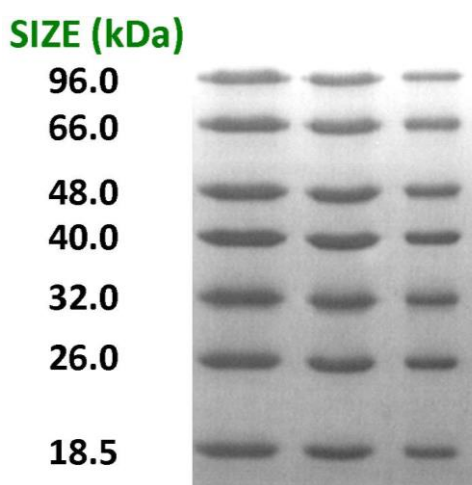
Appendix 7.17: Size standards for agarose gel electrophoresis. The DNA standards composing Hyperladder I (Bioline Ltd) range between 200 and 10,000 bp.



Appendix 7.18: Sigma low- and high-range size standards for SDS-PAGE (Sigma-Aldrich, UK). Low and high molecular standards were composed of a number of protein standards.

Proteins	Source	Molecular Weight (Da)	High Range	Low Range
Myosin	Rabbit muscle	200,000	X	
β -galactosidase	<i>E. coli</i>	116,000	X	
Phosphorylase b	Rabbit muscle	97,000	X	
Albumin	Bovine serum	66,000	X	X
Glutamic dehydrogenase	Bovine liver	55,000	X	
Ovalbumin	Chicken egg	45,000	X	X
Glyceraldehyde-3-phosphate dehydrogenase	Rabbit muscle	36,000	X	X
Carbonic anhydrase	Bovine erythrocytes	29,000		X
Trypsinogen	Bovine pancreas	24,000		X
Trypsin inhibitor	soybean	20,000		X
α -Lactoalbumin	Bovine milk	14,200		X
Aprotinin	Bovine lung	6,500		X

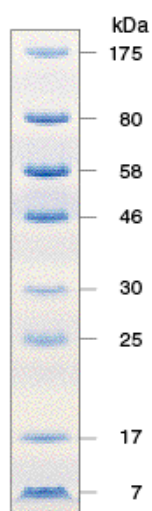
Appendix 7.19: Visual representation of NZY broad-range size standard for SDS-PAGE (NZYtech, Portugal). The molecular weights of the size standard ranged between 18.5 and 96 kDa.



Appendix 7.20: NZY broad-range size standard for SDS-PAGE (NZYtech, Portugal). The molecular weights of size standard ranged between 18.5 and 96 kDa.

Protein	Source	Molecular Weight (Da)
Xylanase U4	<i>Clostridium Thermocellum</i>	96000
Albumin	Bovine serum	66000
Phosphomannose isomerase	<i>Cellvibrio mixtus</i>	48000
Cellulase 5A	<i>Cellvibrio mixtus</i>	40000
Cellulase M9	<i>Clostridium Thermocellum</i>	32000
Family 4 Carbohydrate esterase	<i>Clostridium Thermocellum</i>	26000
Xyloglucan-binding domain M6	<i>Clostridium Thermocellum</i>	18500

Appendix 7.21: Visual representation of NEB pre-stained broad-range protein standard for SDS-PAGE (NE Biolabs, USA). The molecular weights of size standard ranged between 7 and 175 kDa.



Appendix 7.22: NEB pre-stained broad-range protein standard for SDS-PAGE (NE Biolabs, USA). The molecular weights of size standard ranged between 7 and 175 kDa.

Proteins	Source	Molecular Weight (Da)
MBP- β -galactosidase	<i>E. coli</i>	175000
MBP-paramyosin	<i>E. coli</i>	80000
MBP-CBD	<i>E. coli</i>	58000
CBD-Mxe Intein-2CD	<i>E. coli</i>	46000
CBD-Mxe Intein	<i>E. coli</i>	30000
CBD-BmFKBP13	<i>E. coli</i>	25000
Lysozyme	Chicken egg white	17000
Aprotonin	Bovine lung	7000

Appendix 7.23: UV spectrophotometric quantification of DNA and protein concentrations

DNA and protein concentrations were accurately quantified using a UV-visible Helios α Spectronic Unicam spectrophotometer, which was programmed to scan between 200 and 350 nm. The spectrophotometer was zeroed with 18.2 M Ω /cm H₂O prior to use. For DNA samples, a 1:14 dilution of the sample was prepared to a minimum volume of 70 μ l, whilst protein samples were diluted to 1:10, 1:100 or 1:1000 (by serial dilution) with a minimum volume of 70 μ l. The samples were then transferred to a 50 μ l quartz cuvette and scanned in the spectrophotometer. The absorbance reading at 260 nm was used to quantitate double-stranded DNA concentrations using the following formula:

$$[\text{dsDNA}] \mu\text{g}/\mu\text{l} = (A_{260}) \times 50 \times \text{dilution} / 1000$$

The absorbance reading at 280 nm was used to quantitate protein concentrations using the following formula:

$$[\text{protein}] \mu\text{g}/\mu\text{l} = ((A_{280}) \times \text{dilution}) / \text{molecular extinction coefficient} \times \text{molecular weight}$$

If absorbance readings exceeded 1.0, the samples were diluted ten-fold to ensure that the absorbance reading was between 0 and 1.0 to ensure accurate quantitation.

When sample concentrations were limited, sample concentration was determined using a UV vis spectrophotometer and plastic cuvettes, so that the sample could be used for subsequent applications.

Appendix 7.24: Detection of protein using Bradford's reagent

To test for the presence of protein, 20 μl of sample was mixed with 200 μl of Bradford's reagent within a 96-well microtitre plate. A transition in colour from brown to blue denoted the presence of protein.

7.1.1 Cloning of the gene encoding lysostaphin

Appendix 7.25: Media

Luria-Bertani (LB) Broth (1 L)

Tryptone	10.0 g
Yeast extract	5.0 g
NaCl	10.0 g

The pH was adjusted to pH 7.0 using NaOH, before autoclaving the media and storing it at room temperature.

LB agar (100 ml)

LB broth	100 ml
Agar (bacteriological agar no. 1)	2.0 g

The media was autoclaved to make the agar soluble and allowed to cool to less than 50°C, before pouring into petri dishes and leaving to set for ~ 20 min.

Luria-Bertani (LB) low salt media (1L)

Tryptone	10.0 g
Yeast extract	5.0 g
Sodium chloride	5.0 g

The pH of the media was adjusted to pH 7.0 using NaOH, prior to autoclaving.

Trypticase soy yeast extract medium (1L)

Trypticase soy broth	30.0 g
Yeast extract	3.0 g

The pH of the media was adjusted to be within the range of pH 7.0-7.2 before autoclaving.

Trypticase soy yeast extract agar (100 ml)

Trypticase soy yeast extract medium	100 ml
Agar (bacteriological agar no. 1)	1.5 g

The media was autoclaved to make the agar soluble and allowed to cool to less than 50°C, before pouring into petri dishes and leaving to set for ~ 20 min.

SOC medium

SOB media (100 ml):

Tryptone	2.0 g
Yeast extract	0.5 g
NaCl (5M)	0.20 ml
KCl (1M)	0.25 ml

Each chemical was dissolved sequentially in 90 ml of 18.2 MΩ/cm H₂O. The pH of the media was adjusted to pH 7.0 using NaOH, before bringing the volume to 100 ml using 18.2 MΩ/cm H₂O. The SOB media was divided into 10 ml aliquots and autoclaved. Following sterilisation, SOB media was stored at room temperature.

The following chemicals were aseptically added to each 10 ml aliquot of SOB media to give SOC medium:

MgCl ₂ (1M)	0.1 ml
MgSO ₄ (1M)	0.1 ml
Filter sterilised glucose (1 M)	0.2 ml

Appendix 7.26: Enzyme and buffer composition

During gene cloning, a number of enzymes and their associated reaction buffers were employed, as described in Appendix 7.27 and Appendix 7.28.

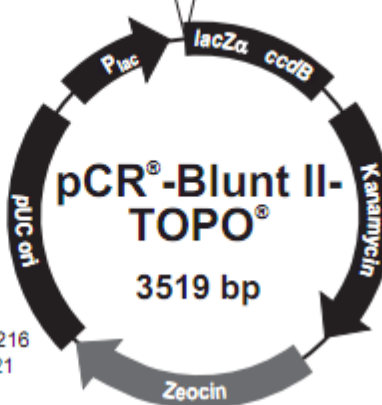
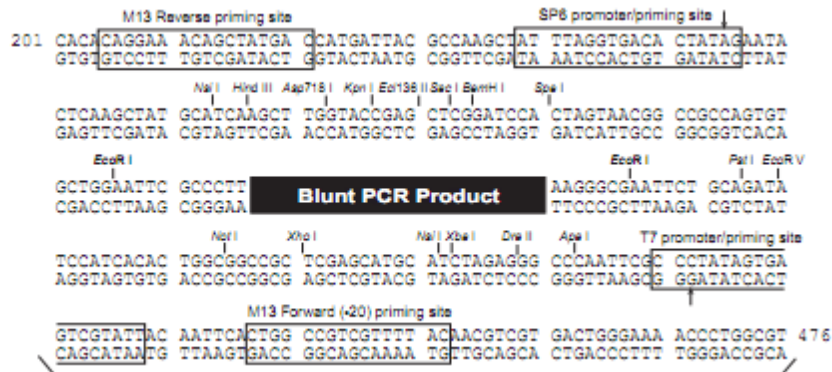
Appendix 7.27: Enzymes used during gene cloning

Enzyme	Enzyme Units per μ l	Supplier
KOD Hot Start Polymerase	1	Merck4Biosciences, UK
T4 DNA ligase	4	New England Biolabs, UK
<i>Eco</i> RI	10	New England Biolabs, UK
<i>Nde</i> I	20	New England Biolabs, UK
<i>Nco</i> I	10	New England Biolabs, UK
<i>Xho</i> I	20	New England Biolabs, UK

Appendix 7.28: Reaction buffers and compositions

Buffer	Composition	Supplier
10 x KOD Hot Start Polymerase buffer	20 mM Tris-HCl 8 mM MgCl ₂ 7.5 mM DTT (\approx 50 μ g/ml)	Merck4Biosciences, UK
10 x Ligation buffer	60 mM Tris-HCl, pH 7.5 60 mM MgCl ₂ 50 mM NaCl 1 mg/ml BSA 70 mM β -mercaptoethanol 1 mM ATP 20 mM dithiothreitol 10 mM spermidine	New England Biolabs, UK
10 x Buffer 4	50 mM potassium acetate 20 mM Tris-acetate 10 mM magnesium acetate 1 mM dithiothreitol, pH 7.9	New England Biolabs, UK

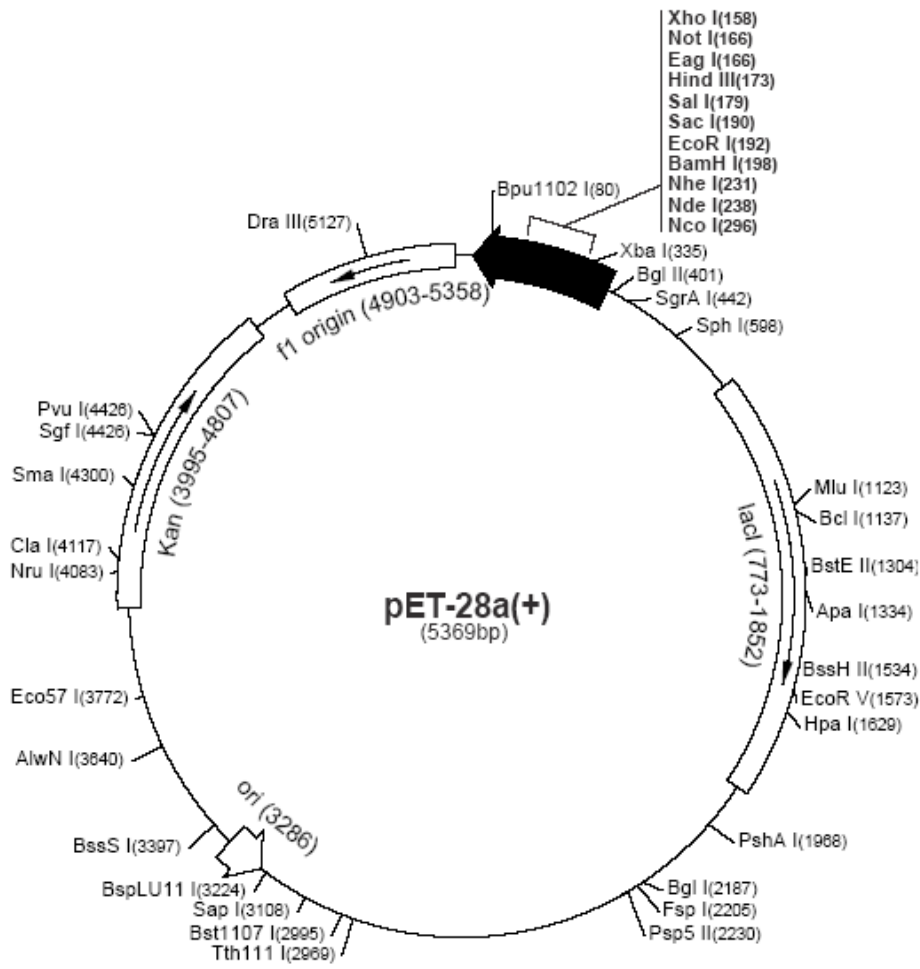
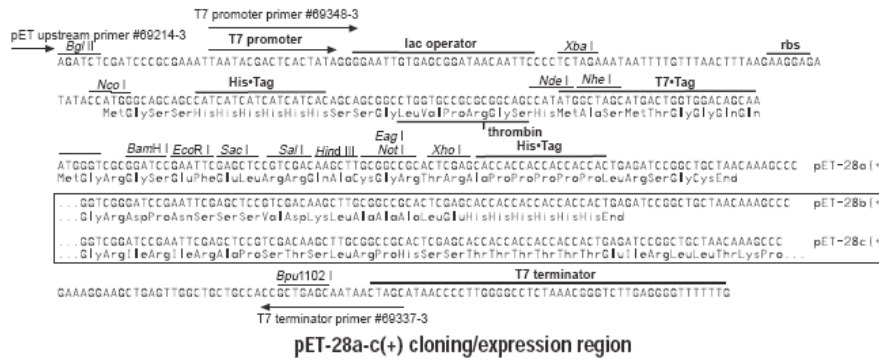
Appendix 7.29: pCR-Blunt vector map (Invitrogen, 2010)



Comments for pCR[®]-Blunt II-TOPO[®]
3519 nucleotides

lac promoter/operator region: bases 95-216
 M13 Reverse priming site: bases 205-221
 LacZ-alpha ORF: bases 217-576
 SP6 promoter priming site: bases 239-256
 Multiple Cloning Site: bases 269-399
 TOPO[®]-Cloning site: bases 336-337
 T7 promoter priming site: bases 406-425
 M13 (-20) Forward priming site: bases 433-448
 Fusion joint: bases 577-585
ccdB lethal gene ORF: bases 586-888
kan gene: bases 1099-2031
 kan promoter: bases 1099-1236
 Kanamycin resistance gene ORF: bases 1237-2031
 Zeocin resistance ORF: bases 2238-2612
 pUC origin: bases 2724-3397

Appendix 7.31: pET-28a cloning/ expression region and vector map (Merck4Biosciences, 2010a)



Appendix 7.32: Composition of Qiagen® kit buffer solutions

Qiagen kits: DNeasy® Mini Spin Kit
 QIAprep® Spin Miniprep Kit
 QIAquick® Gel Extraction Kit
 Qiagen® Plasmid Maxi Kit

Qiagen® kit buffer	Function	Buffer composition
Enzymatic lysis buffer	Lysis	20 mM Tris-HCl, pH 8.0 2 mM sodium EDTA 1.2% Triton X100 20 mg/ml lysozyme
AL	Lysis	Concentrated solution containing guanidinium chloride 200 µl ethanol (96-100%) Full composition not provided by manufacturer
AW1	Neutralisation	Concentrated solution containing guanidinium chloride 30 ml ethanol (96-100%) Full composition not provided by manufacturer
AW2	Wash	30 ml ethanol (96-100%) Full composition not provided by manufacturer
P1	Resuspension	50 mM Tris-HCl, pH 8.0 10 mM EDTA, 100 µg/ml RNase A
P2	Lysis	200 mM NaOH 1 % SDS (w/v)
P3	Neutralization	3 M potassium acetate, pH 5.0
N3	Neutralization	25-50 % guanidinium chloride 10-25 % acetic acid Full composition not provided by manufacturer
EB	Elution	Full composition not provided by manufacturer
PE	Wash	Full composition not provided by manufacturer
QG	Agarose gel solubilisation	50-100 % guanidinium chloride Full composition not provided by manufacturer

Appendix 7.32: Composition of Qiagen® kit buffer solutions (continued)

Qiagen® kit buffer	Function	Buffer composition
PB	Wash	25-50 % guanidinium chloride 25-50 % isopropanol Full composition not provided by manufacturer
QBT	Equilibration	750 mM NaCl 50 mM MOPS, pH 7.0 15 % isopropanol (v/v) 0.15 % Triton® X-100 (v/v)
QC	Wash	1 M NaCl 50 mM MOPS, pH 7.0 15 % isopropanol (v/v)
QF	Elution	1.25 M NaCl 50 mM Tris-HCl, pH 8.5 15 % isopropanol (v/v)

Appendix 7.33: Growth of *S. staphylolyticus* for isolation of genomic DNA

An ampoule of dried culture of *S. staphylolyticus* was rehydrated with trypticase soy yeast extract media and streaked onto trypticase soy yeast extract agar plates and grown overnight at 37°C. A single colony of *S. staphylolyticus* was then inoculated from the agar plate into 50 ml of trypticase soy yeast extract medium using a sterile wire loop. The culture was incubated overnight at 37°C with orbital shaking at 200 rpm. Cells were harvested after 16 h and genomic DNA was purified using DNeasy mini spin kit.

Appendix 7.34: Purification of genomic DNA from *S. staphylolyticus* using a DNeasy Mini Spin kit

Cells (0.5 ml) were harvested in a microcentrifuge tube by centrifugation at 5000 x g and the supernatant was discarded. The bacterial cell pellet was resuspended in 180 µl of enzymatic lysis buffer, before incubation at 37°C for at least 30 min. Following incubation, 25 µl of proteinase K and 200 µl of buffer AL were added to the microcentrifuge tube and mixed by vortexing. The tube was then incubated for 30 min at 70°C, before adding 200 µl of ethanol (96-100%, v/v) and mixing thoroughly by vortexing to produce a homogeneous solution. A DNeasy® mini spin column was placed in a 2 ml collection tube and the mixture

was pipetted into the column and centrifuged at 6000 x g for 1 min, before discarding the flow-through and collection tube. The DNeasy[®] mini spin column was placed into a fresh 2 ml collection tube and 500 µl of buffer AW1 was added to the column before recentrifuging for 1 min at 6,000 x g. The flow-through and collection tube were discarded and the column was placed in a fresh 2 ml collection tube, before adding 500 µl of buffer AW2 and centrifuging for 3 min at 20,000 x g to dry the DNeasy[®] membrane. The flow-through and collection tube were discarded, prior to placing the DNeasy[®] spin column into a clean 1.5 ml microcentrifuge tube. Sterile 18.2 MΩ/cm H₂O (200 µl) was added directly to the DNeasy membrane, before incubating at room temperature for 1 min and then centrifuging for 1 min at ≥ 6,000 x g. The eluant was retained and a second elution was acquired in a fresh microcentrifuge tube, by applying a further 200 µl of sterile 18.2 MΩ/cm H₂O to the DNeasy[®] membrane and centrifuging for 1 min at ≥ 6,000 x g. The purified genomic DNA was analysed by agarose gel electrophoresis (Appendix 7.13)..

Appendix 7.35: Lysostaphin gene from *Staphylococcus staphylolyticus* (X06121). The 15 tandem repeats in the polysostaphin sequence are hi-lighted, with the initial 14 identical repeats (encoding A-E-V-E-T-S-K-A-P-V-E-N-T) hi-lighted in green, whilst the 15th repeat (encoding A-E-V-E-T-S-K-A-L-V-Q-N-R) is hi-lighted in red. The mature lysostaphin gene sequence is indicated in blue.

GAAAATTCCAAAAAAAACCTACTTTCTTAATATTGATTCATATTATTTAACACAATCAGTT
 AGAATTTCAAAAATCTTAAAGTCAATTTTTGAGTGTGTTTGTATATTCATCAAAGCCAATC
 AATATTATTTACTTTCTTCATCGTTAAAAAATGTAATATTTATAAAAATATGCTATTCTCATAA
 ATGTAATAATAAATTAGGAGGTATTAAGGTTGAAGAAAACAAAAACAATTATTATACGAC
 ACCTTTAGCTATTGGACTGAGTACATTTGCCTTAGCATCTATTGTTTATGGAGGGATTCAA
 ATGAAACACATGCTTCTGAAAAAGTAATATGGATGTTTCAAAAAAGTAGCTGAAGTAG
 GACTTCAAAACCCCGTAGAAAATACAGCTGAAGTAGAGACTTCAAAAGCTCCAGTA
 GAAAATACAGCTGAAGTAGAGACTTCAAAAGCTCCAGTAGAAAATACAGCTGAAGTAGA
 GACTTCAAAAGCTCCAGTAGAAAATACAGCTGAAGTAGAGACTTCAAAAGCTCCGGTAG
 AAAATACAGCTGAAGTAGAGACTTCAAAAGCTCCGGTAGAAAATACAGCTGAAGTAGAG
 ACTTCAAAAGCCCGTAGAAAATACAGCTGAAGTAGAGACTTCAAAAGCTCCAGTAGA
 AAATACAGCTGAAGTAGAGACTTCAAAAGCTCCGGTAGAAAATACAGCTGAAGTAGAGA
 CTTCAAAAGCCCGTAGAAAATACAGCTGAAGTAGAGACTTCAAAAGCTCCAGTAGAA
 AATACAGCTGAAGTAGAGACTTCAAAAGCTCCGGTAGAAAATACAGCTGAAGTAGAGAC
 TCAAAAGCCCGTAGAAAATACAGCTGAAGTAGAGACTTCAAAAGCCCTGGTTCAA
 ATAGAACAGCTTTAAGAGCTGCAACACATGAACATTCAGCACAAATGGTTGAATAATTACA
 AAAAAGGATATGGTTACGGTCCTTATCCATTAGGTATAAATGGCGGTATCCACTACGGAGT
 TGATTTTTTATGAATATTGGAACACCAGTAAAAGCTATTTCAAGCGGAAAAATAGTTGAA
 GCTGGTTGGAGTAATTACGGAGGAGGTAATCAAATAGGTCTTATTGAAAATGATGGAGTG
 CATAGACAATGGTATATGCATCTAAGTAAATATAATGTTAAAGTAGGAGATTATGTCAAAGC
 TGGTCAAATAATCGGTTGGTCTGGAAGCACTGGTTATTCTACAGCACCACATTTACACTTC
 CAAAGAATGGTTAATTCATTTCAAATCAACTGCCAAGATCCAATGCCTTTCTTAAAGA
 GCGCAGGATATGAAAAGCAGGTGGTACAGTAACTCCAACGCCAATACAGGTTGGAAA
 ACAAACAATATGGCACACTATATAATCAGAGTCAGCTAGCTTCACACCTAATACAGATAT
 AATAACAAGAACGACTGGTCCATTTAGAAGCATGCCGCAGTCAGGAGTCTTAAAAGCAG
 GTCAAACAATTCATTATGATGAAGTGATGAAACAAGACGGTCATGTTGGGTAGGTTATAC
 AGGTAACAGTGGCCAACGTATTTACTTGCCTGTAAGAACATGGAATAAATCTACTAATACT
 TTAGGTGTTCTTTGGGGAACATAAAGTGAGCGCGCTTTTTATAAACTTATATGATAATTAG
 AGCAAATAAAAATTTTTCTCATTCCCTAAAGTTGAAGCTTTTCGTAATCATGTCATAGCGTT
 TCCTGTGTGAAATTGCTTAGCCTCACAATCCACACAACATACGAGCCGGAACATAAAGT
 GCTAAGCCT

Appendix 7.36: PCR amplification of lysostaphin gene

The lysostaphin gene was amplified by PCR from template *S. staphylolyticus* genomic DNA under the conditions described in Appendix 7.37. Each 50 μ l PCR reaction contained 5 μ l of 10 x KOD Hot Start Polymerase buffer, 1 μ l of template genomic DNA from *S. staphylolyticus*, 3 μ l of MgSO₄ (25 mM), 1 μ l of KOD Hot Start DNA polymerase (1U/ μ l), 5 μ l of dNTPs (2 mM each), 1.5 μ l of sense 5' primer (LSNdeIFP or LS NcoIFP) or 1.5 μ l of antisense 3' primer (LSXhoISRP or LSXhoINSRP) and 32 μ l of PCR grade H₂O. PCR amplification was performed using a Techne TC-512 thermal cycler. Agarose gel electrophoresis was performed to determine the molecular weight of the PCR products (Appendix 7.13). The concentration of the PCR products was determined from the agarose gel bands using the analysis tool of the Bio-Rad Gel Doc 2000 Quantity One™ software prior to ligation.

Appendix 7.37: PCR conditions used for the amplification of the lysostaphin gene

Cycles	Temperature (°C)	Time (min:sec)
Initial Denaturation	95	02:00
5	95	00:20
	54	00:10
	70	00:30
14	95	00:20
	69.6 \leq 2°C (decreasing by 0.5°C every cycle)	00:10
	70	00:30
20	95	00:20
	62.6 \leq 2°C	00:10
	70	00:30
Final Extension	70	10:00
Final Hold	10	Hold

Appendix 7.38: Ligation of PCR product and pCR-Blunt vector

Ligation reactions were prepared containing 1 μ l of pCR-Blunt (25 ng), 5 μ l of PCR product, 1 μ l of 10 x ligation buffer, 2 μ l of 18.2 M Ω /cm H₂O and 1 μ l of T4 DNA ligase (4U/ μ l). The reaction was incubated at 16°C for 16 h in a thermal cycler. Following incubation, the

recombinant plasmid was transformed into electrocompetent *E. coli* using electroporation on a Gene Pulser X-cell electroporator.

Appendix 7.39: Growth of *E. coli* TOP10/ XL1-BLUE for preparation of electrocompetent cells

E. coli TOP10 was streaked onto LB agar and *E. coli* XL1-Blue was streaked onto LB agar supplemented with 125 µg/ ml tetracycline, and the plates were incubated at 37°C overnight. A single colony of *E. coli* TOP10/ XL1-Blue was inoculated from an agar plate into 50 ml of pre-warmed low-salt LB broth, using a sterile wire loop. The culture was incubated at 37°C with orbital shaking at 200 rpm and the growth was monitored spectrophotometrically by measuring the optical density (OD) of the cells at 600 nm. Cells were harvested during exponential phase at an OD_{600 nm} in the range of 0.5-0.6. In order to obtain the correct OD_{600 nm}, 1 ml of the culture was transferred into a cuvette and the OD was determined using a visible-light spectrophotometer set at a wavelength of 600 nm. The spectrophotometer had previously been zeroed using a cuvette of sterile LB media.

Appendix 7.40: Preparation of electrocompetent cells

Once an OD_{600 nm} of 0.5-0.6 had been obtained, the *E. coli* XL1-Blue/ TOP10 were harvested. The cells were placed on ice for 20 min and then centrifuged at 4000 x g for 15 min at 4°C. Following centrifugation the supernatant was discarded and the pellet was resuspended in 25 ml of ice cold 18.2 MΩ/cm H₂O. The resuspension was then centrifuged at 4000 x g for 15 min at 4°C and the pellet was resuspended in 12.5 ml of ice cold 18.2 MΩ/cm H₂O. The resuspension was centrifuged at 4000 x g for 15 min at 4°C and the pellet was resuspended in 5 ml of ice cold 18.2 MΩ/cm H₂O. The resuspension was centrifuged again at 4000 x g for 15 min at 4°C and the pellet was finally resuspended in 200 µl of ice cold 18.2 MΩ/cm H₂O. The cells were separated into 40 µl aliquots and transformed by electroporation.

Appendix 7.41: Transformation of electrocompetent cells

To perform electroporation, 2 µl of ligation reaction was added to 40 µl of electrocompetent cells and the mixture was transferred to an ice cold sterile 2 mm electroporation cuvette (BioRad, UK). The cells were gently tapped down to the bottom of the cuvette and the

cuvette was dried before being enclosed in a BioRad ShockPod of a Gene Pulser Xcell™ Electroporation System. The cells were electroporated with 2500 volts at a pulse time constant of 4.8-4.9 msec. Following electroporation, 200 µl of SOC medium was aseptically added to recover the cells. The cells were then incubated for 1 h at 37°C then spread on LB agar plates supplemented with 50 µg/ml kanamycin and incubated overnight at 37°C. After overnight incubation, transformed *E.coli* colonies were inoculated into 5 ml LB media supplemented with 50 µg/ml kanamycin and incubated overnight at 37°C and 200 rpm prior to plasmid DNA extraction using a QIAprep® spin miniprep kit.

Appendix 7.42: Extraction of plasmid DNA using QIAprep spin miniprep kit

Following overnight culture of transformed *E. coli* colonies, the cells were pelleted by centrifugation at 4000 x g in microcentrifuge tubes. The pelleted cells were resuspended in 250 µl of buffer P1, before adding 250 µl of buffer P2 and mixing thoroughly by inverting the tube 4-6 times. After mixing, 350 µl of Buffer N3 was added and mixed thoroughly by inverting the tube 4-6 times. The sample was centrifuged at 17,900 x g for 10 min before decanting the supernatant into a QIAprep® spin column. The column was then centrifuged at 17,900 x g for 60 s and the flow-through was discarded. The sample was washed by applying 0.5 ml of buffer PB to the column, prior to centrifuging at 17,900 x g for 60 s. The flow-through was discarded and 0.75 ml of buffer PE was added to the column before centrifuging at 17,900 x g for 60 s and then discarding the flow-through. To remove any residual wash buffer, the column was centrifuged at 17,900 x g for a further 60 s and the column was transferred to a clean microcentrifuge tube. The DNA was eluted by adding 50 µl of 18.2 MΩ/cm H₂O to the column, leaving it to stand for 1 min and then centrifuging at 17,900 x g for 1 min. The eluted DNA was analysed by agarose gel electrophoresis to ensure that purification was successful and then the plasmid DNA was restriction digested to check for the presence of the insert DNA.

Appendix 7.43: Restriction digestion of plasmid DNA

Restriction digestions were performed in accordance with instructions provided by the enzyme manufacturers. Prior to digestion, the amount of DNA was determined by UV spectrometry and for each µg of DNA, 5 units of enzyme were used for the digestion performed at 37°C for 2 h. Enzyme unit values are described in Appendix 7.27. All digestions were performed using 10 x Buffer 4 and the reactions were supplemented with

BSA (0.1 mg/ml) when using *Xho*I. As the enzymes used were stored in glycerol, it was ensured that the glycerol concentration of the reaction did not exceed 10% (v/v). When required, the restriction enzymes were inactivated by heating the samples at 65°C for 10 min.

A number of restriction digestions were performed during gene cloning. To establish whether extracted DNA from pCR-Blunt clones contained the appropriate insert DNA fragment, a restriction digestion with *Eco*RI was performed. Samples which were found to contain the insert DNA were subjected to a second, confirmatory restriction digest using both *Nde*I and *Xho*I or *Nco*I and *Xho*I, depending on the gene construct being analysed. To assess the orientation of insert ligation within pCR-Blunt, single *Xho*I restriction digests were also performed. Digested samples were then subjected to analytical or preparative agarose gel electrophoresis.

Appendix 7.44: Gel extraction of DNA

Following excision of gel containing the DNA of interest, the gel was weighed so that 3 volumes of Buffer QG could be added to 1 volume of gel. The sample was incubated at 50°C for 10 min or until the gel had dissolved completely. To aid solubility, the sample was mixed by vortexing every 2-3 min during the incubation. Once dissolved, 1 gel volume of isopropanol was added to the sample and mixed. A QIAquick® spin column was placed into a 2 ml collection tube and the sample was applied to the QIAquick® column to bind the DNA, before centrifuging at 17,900 x g for 1 min. The flow-through was discarded and the QIAquick® column was placed back into the collection tube. To remove traces of agarose, 0.5 ml of buffer QG was added to the column and centrifuged for 1 min. To wash the DNA, 0.75 ml of Buffer PE was added to the column and centrifuged for 1 min, before discarding the flow-through and centrifuging at 17,900 x g for an additional 1 min. The column was transferred to a clean microcentrifuge tube and the DNA was eluted by adding 50 µl of 18.2 MΩ/cm H₂O. The eluted DNA was analysed by agarose gel electrophoresis.

Appendix 7.45: Growth of *E. coli* pET vector transformants for preparation of pET vector DNA

A glycerol stock of *E. coli* which had been previously transformed with pET-22b was streak plated onto LB agar supplemented with 100 µg/ml ampicillin, and incubated at 37°C overnight. A glycerol stock of *E. coli* which had been previously transformed with pET-28a

was streak plated onto LB agar supplemented with 50 µg/ml kanamycin, and incubated at 37°C overnight. Following incubation, a single colony was extracted from each of the agar plates and inoculated into separate conical flasks containing 50 ml of LB supplemented with either 50 µg/ml kanamycin or 100 µg/ml ampicillin, depending on the pET-vector being used. The LB cultures were incubated at 37°C and 200 rpm overnight in preparation for extraction of plasmid DNA.

Appendix 7.46: Preparation of pET vector DNA

Following culture of *E. coli* transformed with pET vector DNA, 5 ml of cells were removed from the culture and pelleted by centrifugation at 4000 x g. Plasmid DNA was extracted using the QIAprep[®] spin miniprep kit (Appendix 7.42) or using a Plasmid Maxi Kit.

When using the Plasmid Maxi Kit, 5 ml starter cultures of *E. coli* transformed with pET vector DNA were inoculated and incubated overnight at 37°C and shaken vigorously at 250 rpm. The starter culture was diluted 1/1000 into 100 ml of LB supplemented with an appropriate antibiotic and cultured at 37°C and 250 rpm for 12-16 hours. The cells were harvested by centrifugation at 6000 x g for 15 min at 4°C and then the supernatant was discarded. The bacterial pellet was resuspended in 10 ml of buffer P1 and then 10 ml of Buffer P2 was added to the resuspension before mixing by inversion 4-6 times and incubating at room temperature for 5 min. Buffer P3 was chilled and then 10 ml of the buffer was added to the sample and mixed immediately but in a gentle manner by inversion 4-6 times, before incubating on ice for 20 min. The sample was centrifuged at ≥20000 x g for 30 min at 4°C and the supernatant containing the plasmid DNA was removed promptly. The supernatant was centrifuged again at ≥ 20000 x g for 15 min at 4°C and once again the supernatant that contained the plasmid DNA was removed swiftly.

A Qiagen[®]-tip 500 was equilibrated by applying 10 ml of Buffer QBT, before allowing the column to empty by gravity flow. The supernatant was applied to the Qiagen[®]-tip and was allowed to enter the resin by gravity flow. The Qiagen[®]-tip was washed twice with 30 ml of Buffer QC and then the DNA was eluted through the application of 15 ml of Buffer QF. The DNA was precipitated by adding 10.5 ml of room temperature isopropanol to the eluted DNA, before mixing and centrifuging immediately at ≥ 15000 x g for 30 min at 4°C. The supernatant was carefully decanted and the DNA pellet was washed with 5 ml of room temperature 70% (v/v) ethanol and centrifuged at ≥ 15000 x g for 10 min. Without disturbing the pellet, the resulting supernatant was decanted and the pellet was air-dried for 5-10 min and the DNA was dissolved in a suitable volume of 18.2 MΩ/cm H₂O. The eluted plasmid

DNA was analysed by agarose gel electrophoresis to check the success of extraction and DNA purity (Appendix 7.13). The pET vector DNA was restriction digested (Appendix 7.43) and gel extracted (Appendix 7.44), prior to ligation (Appendix 7.47).

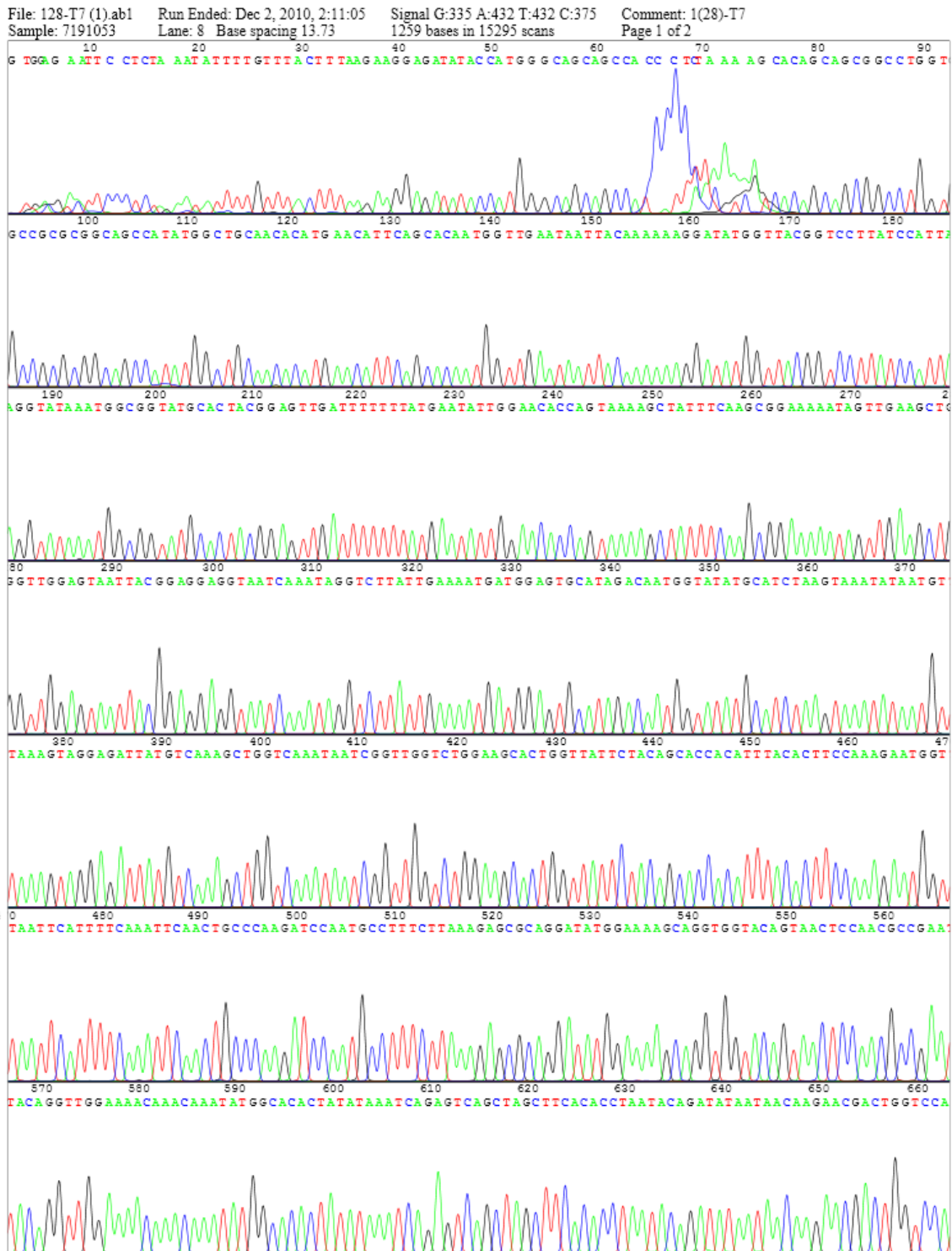
Appendix 7.47: Ligation of insert and pET vector DNA

The ligation reaction contained 50 ng of pET-vector DNA, 1.0 µl T4 DNA ligase buffer (10X), 20 ng of insert DNA, 0.5 µl of T4 DNA ligase (4 U/µl) and 18.2 MΩ/cm H₂O to bring the total volume of the reaction to 10 µl. The reaction was incubated at 16°C for 16 h in a thermal cycler. Following incubation, the recombinant plasmid was transformed into electrocompetent *E. coli* using electroporation and plated on agar plates supplemented with either 50 µg/ml kanamycin or 100 µg/ml ampicillin depending on the antibiotic resistance of the pET-vector being used. Following culture of transformant colonies, plasmid DNA was extracted (Appendix 7.42). Extracted plasmid DNA was restriction digested to establish if the plasmid DNA harboured the gene insert (Appendix 7.43).

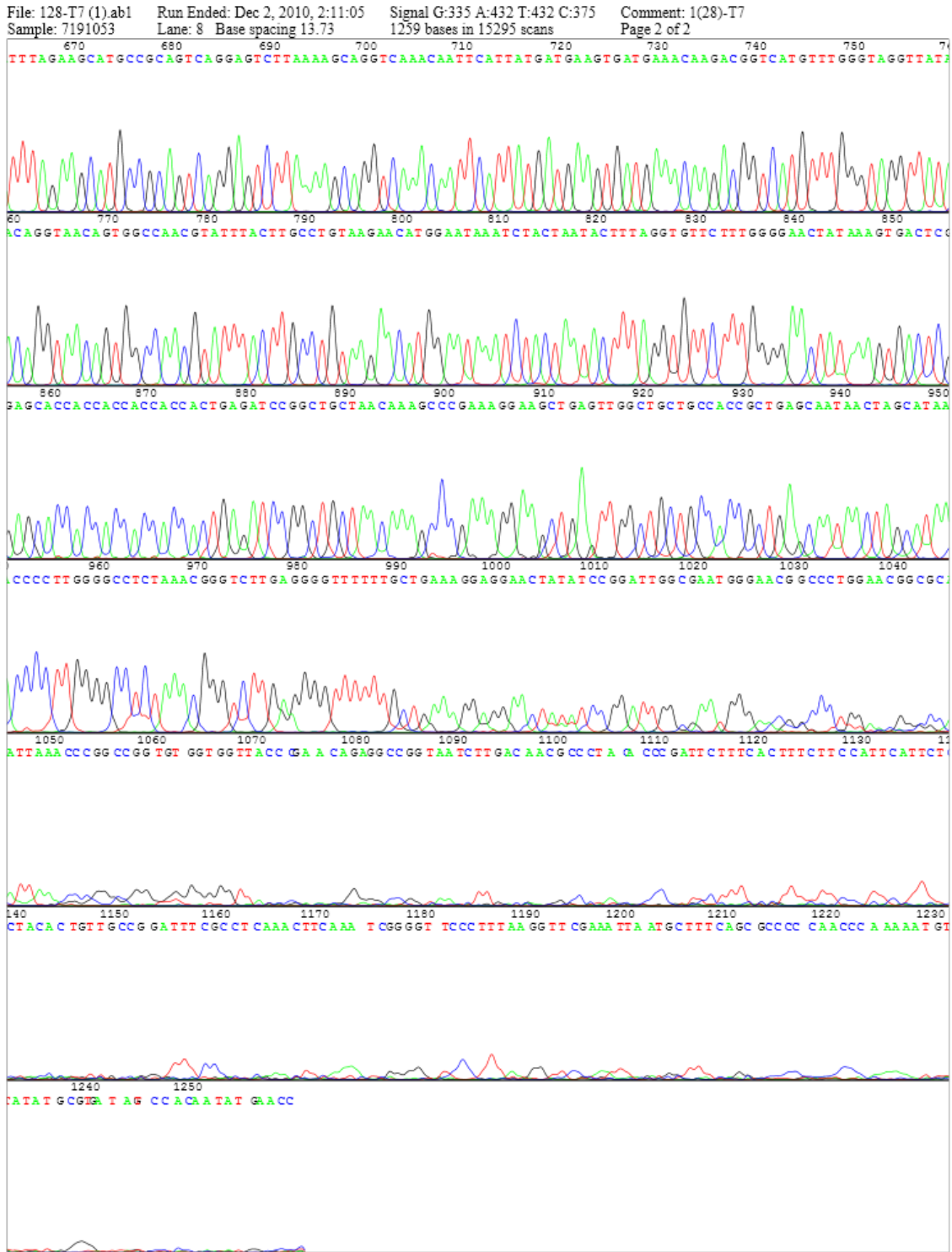
Appendix 7.48: Preparation of plasmid DNA for sequencing

Prior to sequencing, plasmid DNA was extracted from 8 ml of cultured transformed *E. coli* (Appendix 7.42). Plasmid DNA was eluted in 50 µl of 18.2 MΩ/cm H₂O. The concentration of the plasmid DNA was established by UV spectrometry (Appendix 7.23) and 30 µl of plasmid DNA, at a concentration of 30-100 ng/µg, was sent for single read sequencing at GATC Biotech (UK). The resulting data was examined and the expected and observed DNA sequences were aligned using ClustalW. ClustalW alignment was developed by the European Bioinformatics Institute and was made available at <http://www.ebi.ac.uk/Tools/msa/clustalw2/>. To assess the influence of nucleotide substitutions upon the translated amino acid sequence of the mature lysostaphin domain, original and substituted DNA sequences were translated in silico by Translate tool (Expasy Proteomics Server, Swiss Institute of Bioinformatics), available at <http://expasy.org/tools/dna.html>. The resulting amino acids sequences were then compared using ClustalW alignment.

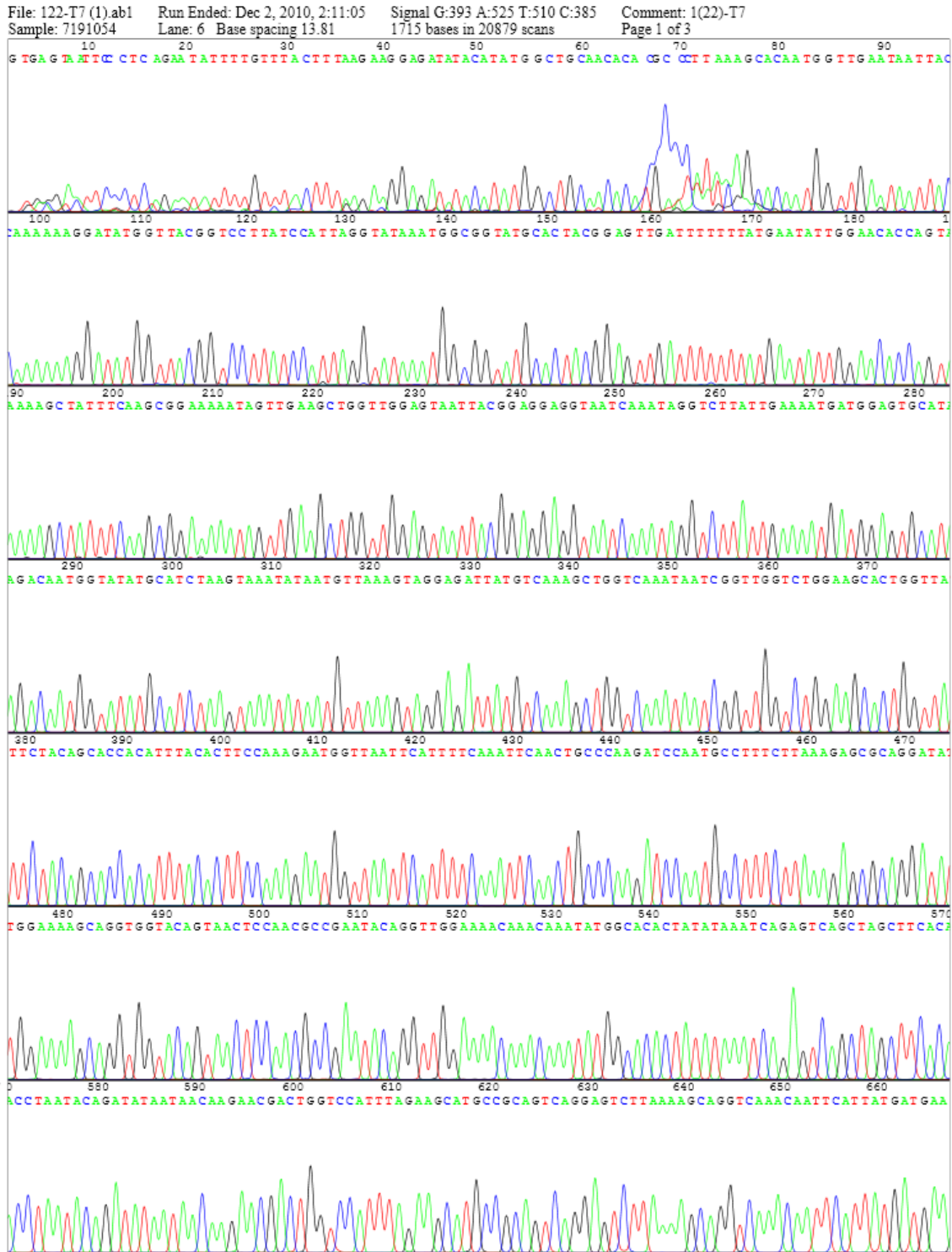
Appendix 7.49: Chromatographic representation of sequence data for recombinant pET-28a DNA encoding *N*-terminally His-tagged recombinant lysostaphin (construct 1)



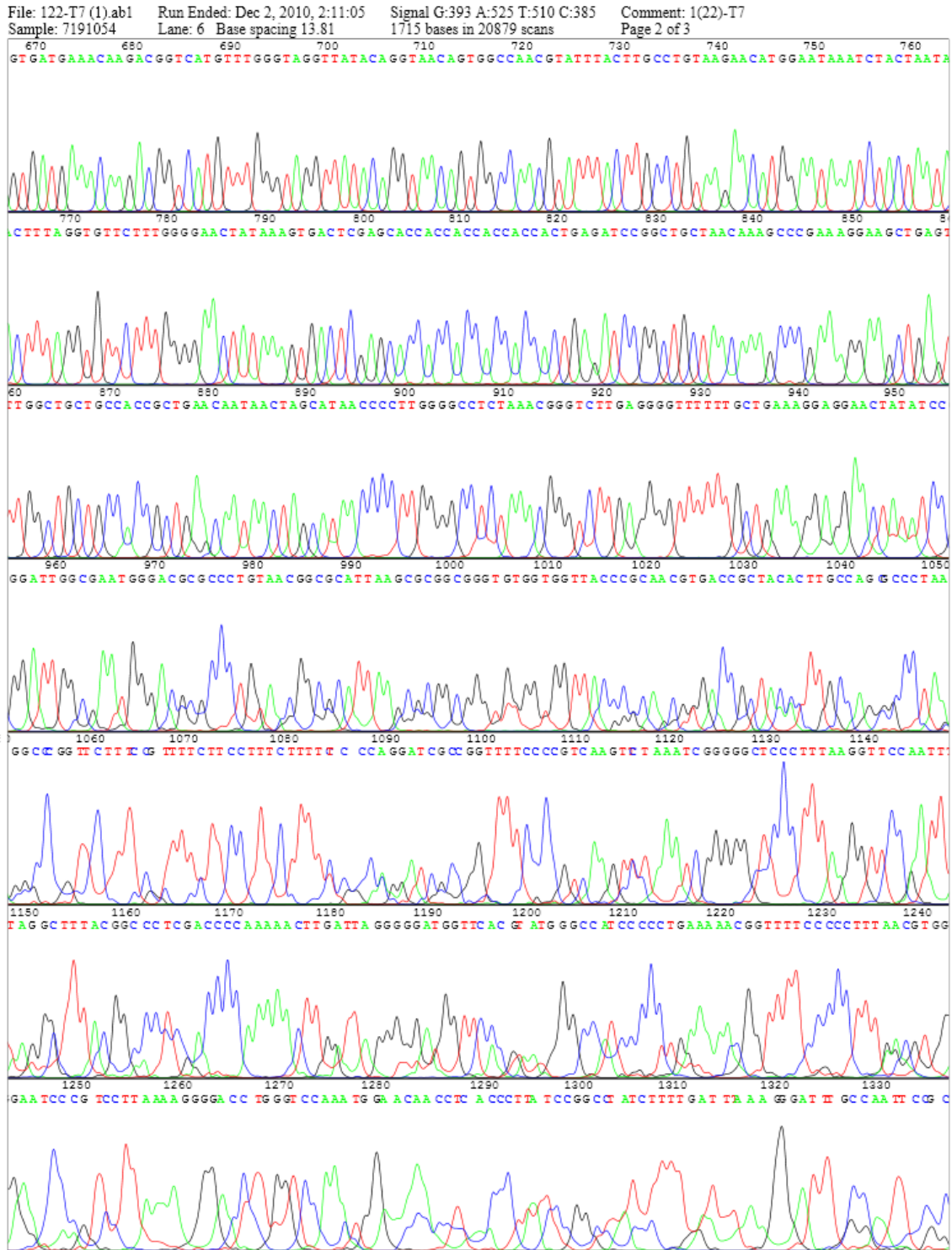
Appendix 7.49: Chromatographic representation of sequence data for recombinant pET-28a DNA encoding N-terminally His-tagged recombinant lysostaphin (continued)



Appendix 7.50: Chromatographic representation of sequence data for recombinant pET-22b DNA encoding recombinant lysostaphin (construct 2)



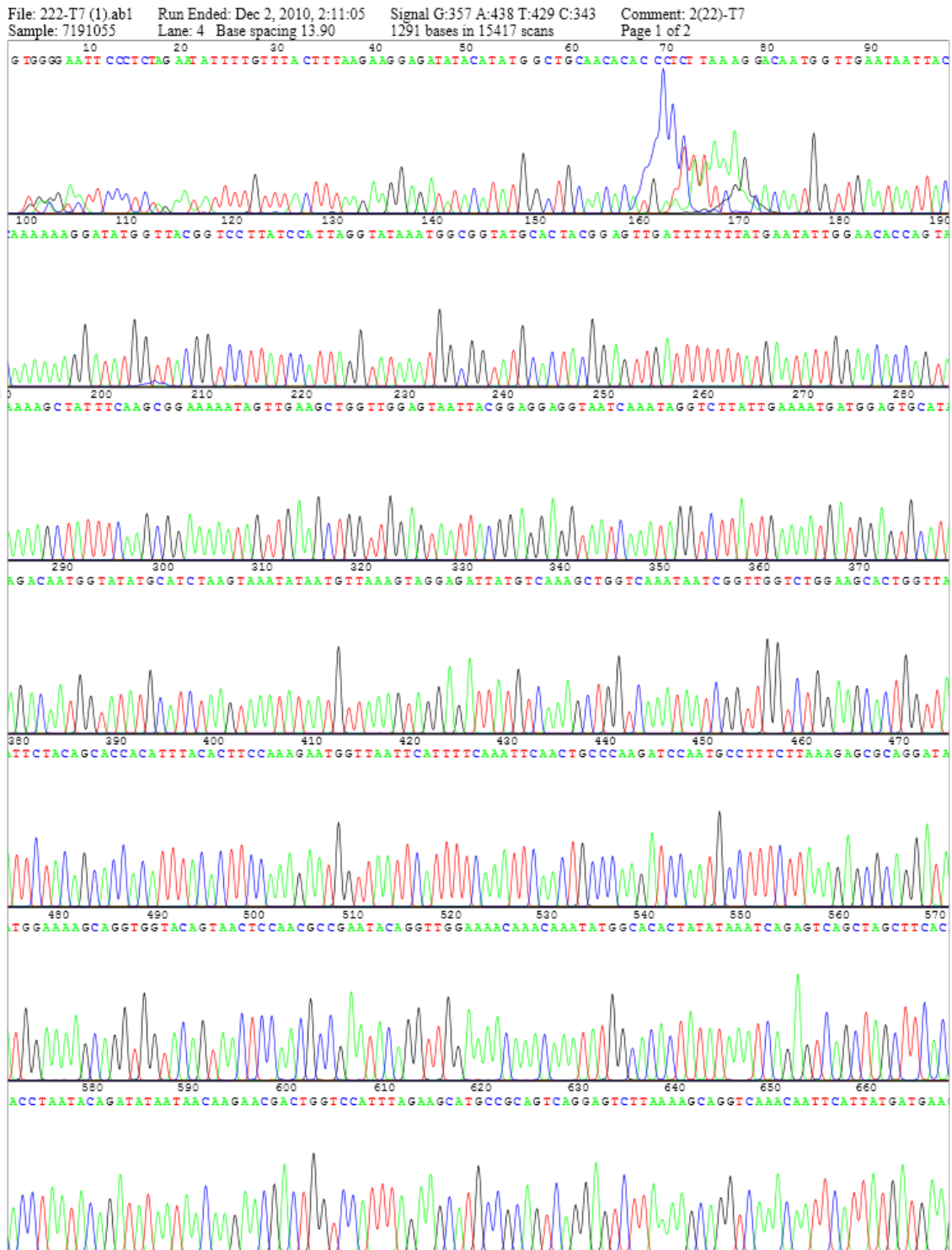
Appendix 7.50: Chromatographic representation of sequence data for recombinant pET-22b DNA encoding recombinant lysostaphin (construct 2) (continued).



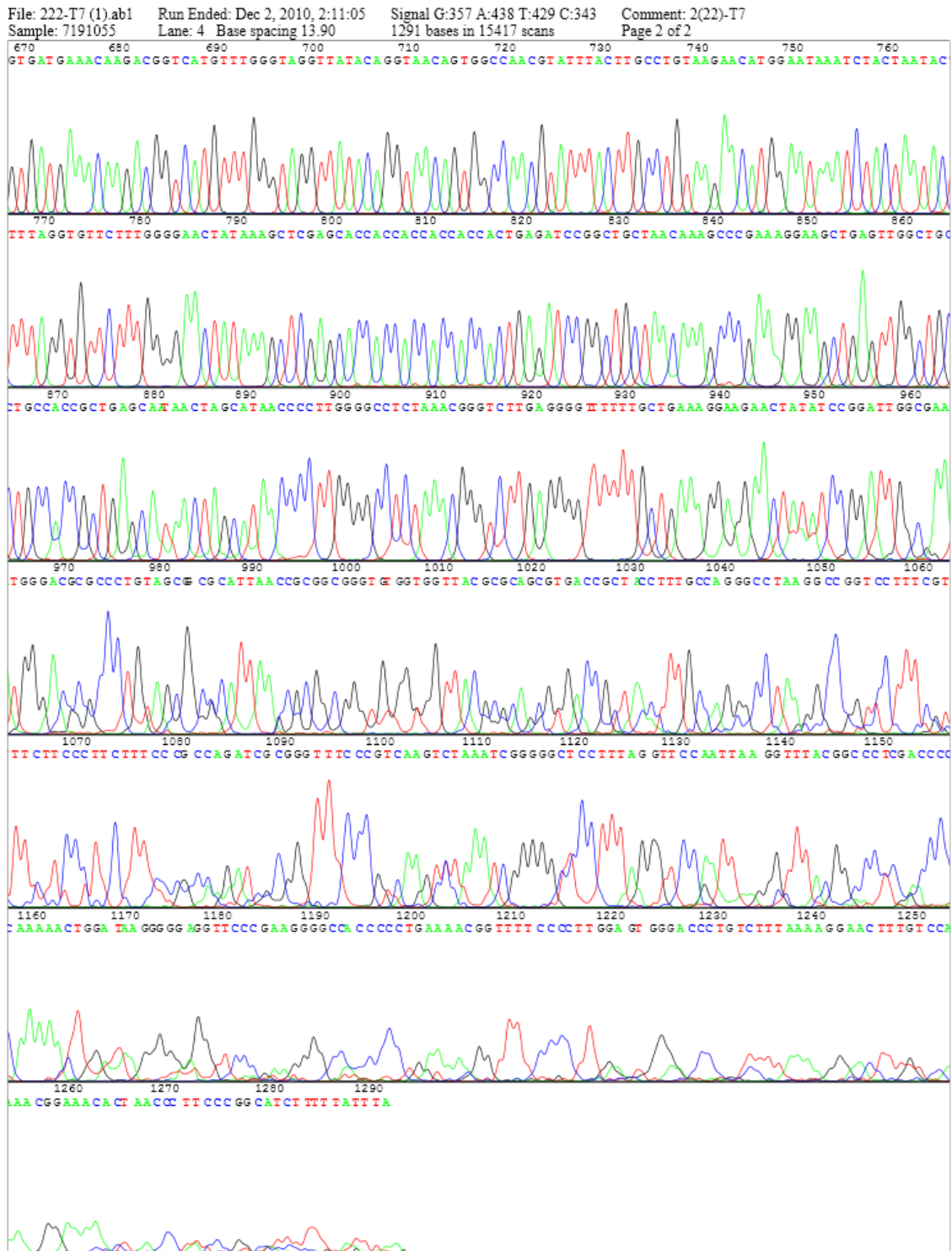
Appendix 7.50: Chromatographic representation of sequence data for recombinant pET-22b DNA encoding recombinant lysostaphin (construct 2) (continued).



Appendix 7.51: Chromatographic representation of sequence data for recombinant pET-22b DNA encoding C-terminally His-tagged recombinant lysostaphin (construct 3)



Appendix 7.51: Chromatographic representation of sequence data for recombinant pET-22b DNA encoding C-terminally His-tagged recombinant lysostaphin (construct 3) (continued).



Appendix 7.52: The known mature lysostaphin domain encoding sequence incorporating the *N*-terminal His-tag encoding sequence in red (construct 1).

ATGGGCAGCAGCCATCATCATCATCACAGCAGCGGCCTGGTGCCGCGCGGCAGCCATA
TGGCTGCAACACATGAACATTCAGCACAATGGTTGAATAATTACAAAAAGGATATGGTTAC
GGTCCTTATCCATTAGGTATAAATGGCGGTATCCACTACGGAGTTGATTTTTTTATGAATATTG
GAACACCAGTAAAAGCTATTTCAAGCGGAAAAATAGTTGAAGCTGGTTGGAGTAATTACGG
AGGAGGTAATCAAATAGGTCTTATTGAAAATGATGGAGTGCATAGACAATGGTATATGCATCT
AAGTAAATATAATGTTAAAGTAGGAGATTATGTCAAAGCTGGTCAAATAATCGGTTGGTCTGG
AAGCACTGGTTATTCTACAGCACCATTTACTTCCAAGAATGGTTAATTCATTTCAAAT
TCAACTGCCCAAGATCCAATGCCTTTCTAAAGAGCGCAGGATATGGAAAAGCAGGTGGTAC
AGTAACTCCAACGCCCAATACAGGTTGGAAAACAAACAAATATGGCACACTATATAAATCAGA
GTCAGCTAGCTTCACACCTAATACAGATATAATAACAAGAACGACTGGTCCATTTAGAAGCAT
GCCGCAGTCAGGAGTCTTAAAAGCAGGTCAAACAATTCATTATGATGAAGTATGAAACAA
GACGGTCATGTTTGGGTAGGTTATACAGGTAACAGTGGCCAACGTATTTACTTGCCTGTAAG
AACATGGAATAAATCTACTAATACTTTAGGTGTTCTTTGGGGAACATAAAAGTGA

Appendix 7.53: Sequence data acquired following sequencing of plasmid DNA containing the gene sequence encoding the *N*-terminally His-tagged mature lysostaphin domain (construct 1). The *N*-terminal His-tag encoding sequences are denoted in red, whilst the mature lysostaphin domain encoding sequence is denoted in blue.

GTGGAGAATTCCTCTAAATATTTGTTTACTTTAAGAAGGAGATATACC**ATGGGCAGCAGCCACCCTCTA**
AAAGCACAGCAGCGGCCTGGTGCCGCGCGGCAGCCAT**ATGGCTGCAACACATGAACATTCAGCACA**
TGGTTGAATAATTACAAAAAGGATATGGTTACGGTCCTTATCCATTAGGTATAAATGGCGGTATGCACT
ACGGAGTTGATTTTTTTATGAATATTGGAACACCAGTAAAAGCTATTTCAAGCGGAAAAATAGTTGAA
GCTGGTTGGAGTAATTACGGAGGAGGTAATCAAATAGGTCTTATTGAAAATGATGGAGTGCATAGACA
ATGGTATATGCATCTAAGTAAATATAATGTTAAAGTAGGAGATTATGTCAAAGCTGGTCAAATAATCGGT
TGGTCTGGAAGCACTGGTTATTCTACAGCACCATTTACTTCCAAGAATGGTTAATTCATTTCAA
ATTCAACTGCCCAAGATCCAATGCCTTTCTAAAGAGCGCAGGATATGGAAAAGCAGGTGGTACAGTA
ACTCCAACGCCGAATACAGGTTGGAAAACAAACAAATATGGCACACTATATAATCAGAGTCAGCTAG
CTTCACACCTAATACAGATATAATAACAAGAACGACTGGTCCATTTAGAAGCATGCCGCAGTCAGGAGT
CTTAAAAGCAGGTCAAACAATTCATTATGATGAAGTATGAAACAAGACGGTCATGTTTGGGTAGGTT
ATACAGGTAACAGTGGCCAACGTATTTACTTGCCTGTAAGAACATGGAATAAATCTACTAATACTTTAGG
TGTTCTTTGGGGAACATAAAAGTGACTCGAGCACCACCACCACCACCCTGAGATCCGGCTGCTAACAA
AGCCCGAAAGGAAGCTGAGTTGGCTGCTGCCACCGCTGAGCAATAACTAGCATAACCCCTGGGGCCT
CTAAACGGGTCTTGAGGGGTTTTTTGCTGAAAGGAGGAACTATATCCGGATTGGCGAATGGGAACGGC
CCTGGAACGGCGCATTAAACCCGGCCGGTGTGGTGGTTACCCGAACAGAGGCCGGTAATCTTGACAAC
GCCCTACACCCGATTCTTTCACTTTCTCCATTCTCTACTGTTGCCGATTTGCCTCAAACCTCA
AATCGGGGTTCCCTTTAAGGTTCAAATAATGCTTTCAGCGCCCCCAACCCAAAAATGTATATGCGTGAT
AGTCCACAATATGAACC

Appendix 7.54: DNA sequence encoding recombinant lysostaphin (construct 2).

ATGGCTGCAACACATGAACATTCAGCACAATGGTTGAATAATTACAAAAAGGATATGG
TTACGGTCCTTATCCATTAGGTATAAATGGCGGTATCCACTACGGAGTTGATTTTTTATG
AATATTGGAACACCAGTAAAAGCTATTTCAAGCGGAAAAATAGTTGAAGCTGGTTGGA
GTAATTACGGAGGAGGTAATCAAATAGGTCTTATTGAAAATGATGGAGTGCATAGACAA
TGGTATATGCATCTAAGTAAATATAATGTTAAAGTAGGAGATTATGTCAAAGCTGGTCAA
TAATCGGTTGGTCTGGAAGCACTGGTTATTCTACAGCACCATTTACTTCCAAAGAA
TGGTTAATTCATTTCAAATTCAACTGCCCAAGATCCAATGCCTTTCTTAAAGAGCGCAG
GATATGGAAAAGCAGGTGGTACAGTAACTCCAACGCCCAATACAGGTTGGAAAACAAA
CAAATATGGCACACTATATAAATCAGAGTCAGCTAGCTTCACACCTAATACAGATATAATA
ACAAGAACGACTGGTCCATTTAGAAGCATGCCGCAGTCAGGAGTCTTAAAAGCAGGTC
AAACAATTCATTATGATGAAGTGATGAAACAAGACGGTCATGTTTGGGTAGGTTATACA
GGTAACAGTGGCCAACGTATTTACTTGCCTGTAAGAACATGGAATAAATCTACTAATACT
TTAGGTGTTCTTTGGGGAACATAAAGTGA

Appendix 7.55: Sequence data acquired following sequencing of plasmid DNA containing the gene sequence encoding recombinant lysostaphin (construct 2). The recombinant lysostaphin gene sequence is denoted in blue

GTGAGTAATTCCTCAGAATATTTTGTACTTTAAGAAGGAGATATACAT**ATGGCTGCAACACACGC**
CCTTAAAGCACAATGGTTGAATAATTACAAAAAGGATATGGTTACGGTCCTTATCCATTAGGTATA
AATGGCGGTATGCACTACGGAGTTGATTTTTTATGAATATTGGAACACCAGTAAAAGCTATTTCAA
GCGGAAAAATAGTTGAAGCTGGTTGGAGTAATTACGGAGGAGTAATCAAATAGGTCTTATTGAA
AATGATGGAGTGCATAGACAATGGTATATGCATCTAAGTAAATATAATGTTAAAGTAGGAGATTATG
TCAAAGCTGGTCAAATAATCGGTTGGTCTGGAAGCACTGGTTATTCTACAGCACCACATTTACTT
CCAAAGAATGGTTAATTCATTTTCAAATCACTGCCCAAGATCCAATGCCTTTCTTAAAGAGCGCA
GGATATGGAAAAGCAGGTGGTACAGTAACTCCAACGCCGAATACAGGTTGGAAAACAAACAATA
TGGCACACTATATAAATCAGAGTCAGCTAGCTTACACCTAATACAGATATAATAACAAGAACGACT
GGTCCATTTAGAAGCATGCCGCAGTCAGGAGTCTTAAAAGCAGGTCAAACAATTCATTATGATGAA
GTGATGAAACAAGACGGTCATGTTTGGGTAGGTTATACAGGTAACAGTGGCCAACGTATTTACTTG
CCTGTAAGAACATGGAATAAATCTACTAATACTTTAGGTGTTCTTTGGGGAECTATAAAGTGACTCG
AGCACCACCACCACCACCCTGAGATCCGGCTGCTAACAAAGCCCGAAAGGAAGCTGAGTTGGCTG
CTGCCACCGCTGAACAATAACTAGCATAACCCCTTGGGGCCTCTAACGGGTCTTGAGGGGTTTTTT
GCTGAAAGGAGGAECTATATCCGGATTGGCGAATGGGACGCGCCCTGTAACGGCGCATTAAAGCGCG
GCGGGTGTGGTGGTTACCCGCAACGTGACCGCTACACTTGCCAGCGCCCTAAGGCCCGTTCTTTC
CGTTTTCTCCTTCTTCTCCAGGATCGCCGTTTTCCCGTCAAGTTCTAAATCGGGGGCTCCCT
TTAAGGTTCCAATTTAGGCTTTACGGCCCTCGACCCAAAAACTTGATTAGGGGGATGGTTCACGTAT
GGGCATCCCCCTGAAAAACGGTTTTCCCCCTTAACTGGGAATCCCGTCTTAAAAGGGGACCTG
GGTCCAATGGAACAACCTCACCTTATCCGGCCTATCTTTTGATTTAAAGGGATTTGCCAATCCGC
CTTTGGTAAAAAAGGCGGTTTAAACAAAATAACCGAATTTACAAAATTAACCGTTCAATTTAGGGCCT
TTTCGGAAAATGGCGGAACCCCTTGTGTTTTCCAAAACCAAAAATGACCCCTCGAAAAACCCCT
GTAGGCCTTTTATTTAAAAGGGAAAAGTTACTCTGTCTGGGCCCTATCTTTTGGAAATTCCTTTTGT
TCACAAACGGGTAAAAGACGACAGATGCGAGTCAGGAAAGCCTCCAACCTGCCTGATCCCTTACCC
CCATTTAGACTGCGCCTAACAAAAAGGCGCTCACGATGTGTGAAACCAGAAAAGTGGAGAATTGTAT
AGATTGAAATGCTACTAGGGAGCCCTGCGTTCGGTACCCGAG

Appendix 7.56: DNA sequence encoding C-terminally His-tagged recombinant lysostaphin (construct 3). The C-terminal His-tag sequence is denoted in red.

ATGGCTGCAACACATGAACATTCAGCACAATGGTTGAATAATTACAAAAAGGATATGGTTACGG
TCCTTATCCATTAGGTATAAATGGCGGTATCCACTACGGAGTTGATTTTTTTATGAATATTGGAACA
CCAGTAAAAGCTATTTCAAGCGGAAAAATAGTTGAAGCTGGTTGGAGTAATTACGGAGGAGGTA
ATCAAATAGGTCTTATTGAAAATGATGGAGTGCATAGACAATGGTATATGCATCTAAGTAAATATAA
TGTTAAAGTAGGAGATTATGTCAAAGCTGGTCAAATAATCGGTTGGTCTGGAAGCACTGGTTATT
CTACAGCACCATTTACACTTCCAAAGAATGGTTAATTCATTTTTCAAATCAACTGCCCAAGATCC
AATGCCTTTCTTAAAGAGCGCAGGATATGGAAAAGCAGGTGGTACAGTAACTCCAACGCCCAATA
CAGGTTGGAAAACAAACAAATATGGCACACTATATAAATCAGAGTCAGCTAGCTTACACCTAATA
CAGATATAATAACAAGAACGACTGGTCCATTTAGAAGCATGCCGCAGTCAGGAGTCTTAAAAGCA
GGTCAAACAATTCATTATGATGAAGTGATGAAACAAGACGGTCATGTTGGGTAGGTTATACAGG
TAACAGTGGCCAACGTATTTACTTGCCTGTAAGAACATGGAATAAATCTACTAATACTTTAGGTGTT
CTTTGGGGAACATAAAGCTCGAG **CACCACCACCACCACCTGA**

Appendix 7.57: Sequence data acquired following sequencing of plasmid DNA containing the gene sequence encoding C-terminally His-tagged recombinant lysostaphin (construct 3). The C-terminal His-tag sequences are denoted in red, whilst the recombinant lysostaphin gene sequence is denoted in blue.

GTGGGGAATCCCTCTAGAATATTTGTTTACTTTAAGAAGGAGATATACAT **ATGGCTGCAACACACC**
CTCTTAAAGGACAATGGTTGAATAATTACAAAAAGGATATGGTTACGGTTCCTTATCCATTAGGTAT
AAATGGCGGTATGCACTACGGAGTTGATTTTTTTATGAATATTGGAACACCAGTAAAAGCTATTTCA
AGCGGAAAAATAGTTGAAGCTGGTTGGAGTAATTACGGAGGAGGTAATCAAATAGGTCTTATTGA
AAATGATGGAGTGCATAGACAATGGTATATGCATCTAAGTAAATATAATGTTAAAGTAGGAGATTAT
GTCAAAGCTGGTCAAATAATCGGTTGGTCTGGAAGCACTGGTTATTCTACAGCACCATTTACACT
TCCAAAGAATGGTTAATTCATTTCAAATCAACTGCCCAAGATCCAATGCCTTTCTTAAAGAGCGC
AGGATATGGAAAAGCAGGTGGTACAGTAACTCCAACGCCGAATACAGGTTGGAAAACAAACAAAT
ATGGCACACTATATAAATCAGAGTCAGCTAGCTTACACCTAATACAGATATAATAACAAGAACGAC
TGGTCCATTTAGAAGCATGCCGCAGTCAGGAGTCTTAAAAGCAGGTCAAACAATTCATTATGATGA
AGTGATGAAACAAGACGGTCATGTTGGGTAGGTTATACAGGTAACAGTGGCCAACGTATTTACTT
GCCTGTAAGAACATGGAATAAATCTACTAATACTTTAGGTGTTCTTTGGGGAACATAAAGCTCGAG
CACCACCACCACCACCTGAGATCCGGCTGCTAACAAAGCCCGAAAGGAAGCTGAGTTGGCTGCT
GCCACCGCTGAGCAATAACTAGCATAACCCCTGGGGCCTCTAACGGGTCTTGAGGGGTTTTTTGC
TGAAAGGAAGAACTATATCCGGATTGGCGAATGGGACGCGCCCTGTAGCGGCGCATTAAACGCGGC
GGGTGTGGTGGTTACGCGCAGCGTGACCGCTACCTTTGCCAGGGCCTAAGGCCGTCTTTTCGTTT
CTTCCCTTCTTTCCCGCCAGATCGCGGGTTTCCCGTCAAGTCTAAATCGGGGCTCCTTTAGGTTCCA
ATTAAGGTTTACGGCCCTCGACCCCAAAAAGTGGATAAGGGGGAGGTTCCCGAAGGGGCCACCCCC
TGAAAACGGTTTTTCCCTTGGAGTGGGACCCTGTCTTTAAAAGGAACCTTTGTCAAACGGAAACACT
AACCTTCCCGGCATCTTTTATTTA

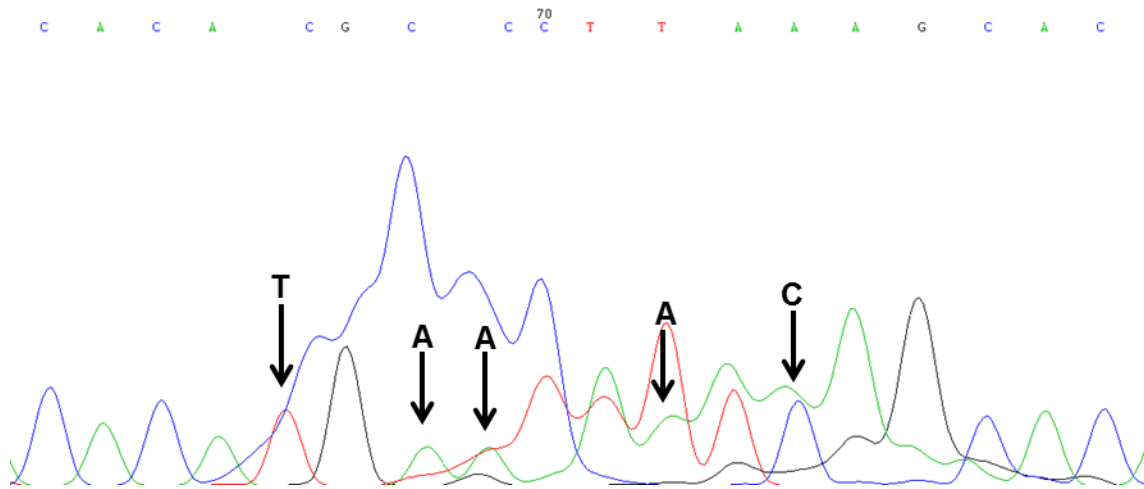
Appendix 7.58: ClustalW alignment of the known mature lysostaphin domain encoding sequence (with no His-tag encoding sequence added) and the acquired DNA sequence from pET construct 2. The known mature lysostaphin domain encoding sequence (with no His-tag encoding sequence added) is presented in Appendix 7.54. The sequence acquired from construct 2 is presented in Appendix 7.55.

```

Expected      ATGGCTGCAACACATGAACATTCAGCACAAATGGTTGAATAAATTACAAAAAGGATATGGT 60
Lysostaphin  ATGGCTGCAACACACGCCCTTAAAGCACAAATGGTTGAATAAATTACAAAAAGGATATGGT 60
*****
Expected      TACGGTCCTTATCCATTAGGTATAAATGGCGGTATCCACTACGGAGTTGATTTTTTTATG 120
Lysostaphin  TACGGTCCTTATCCATTAGGTATAAATGGCGGTATGCACACTACGGAGTTGATTTTTTTATG 120
*****
Expected      AATATTGGAAACACCAGTAAAAGCTATTTCAAGCGGAAAAATAGTTGAACTGGTTGGAGT 180
Lysostaphin  AATATTGGAAACACCAGTAAAAGCTATTTCAAGCGGAAAAATAGTTGAACTGGTTGGAGT 180
*****
Expected      AATTACGGAGGAGGTAATCAAATAGGTCTTATTGAAAATGATGGAGTGCATAGACAATGG 240
Lysostaphin  AATTACGGAGGAGGTAATCAAATAGGTCTTATTGAAAATGATGGAGTGCATAGACAATGG 240
*****
Expected      TATATGCATCTAAGTAAATATAATGTTAAAGTAGGAGATTATGTCAAAGCTGGTCAAATA 300
Lysostaphin  TATATGCATCTAAGTAAATATAATGTTAAAGTAGGAGATTATGTCAAAGCTGGTCAAATA 300
*****
Expected      ATCGGTTGGTCTGGAAGCACTGGTATTCTACAGCACACATTTACACTTCCAAAGAATG 360
Lysostaphin  ATCGGTTGGTCTGGAAGCACTGGTATTCTACAGCACACATTTACACTTCCAAAGAATG 360
*****
Expected      GTTAATTCATTTTCAAATTCAACTGCCCAAGATCCAATGCCTTTCTTAAAGAGCGCAGGA 420
Lysostaphin  GTTAATTCATTTTCAAATTCAACTGCCCAAGATCCAATGCCTTTCTTAAAGAGCGCAGGA 420
*****
Expected      TATGGAAGAGCAGGTGGTACAGTAACTCCAACGCCCAATACAGGTTGGAAAACAAACAAA 480
Lysostaphin  TATGGAAGAGCAGGTGGTACAGTAACTCCAACGCCCAATACAGGTTGGAAAACAAACAAA 480
*****
Expected      TATGGCACACTATATAAATCAGAGTCAGCTAGCTTCACACCTAATACAGATATAATAACA 540
Lysostaphin  TATGGCACACTATATAAATCAGAGTCAGCTAGCTTCACACCTAATACAGATATAATAACA 540
*****
Expected      AGAACGACTGGTCCATTTAGAAAGCATGCCGAGTCAGGAGTCTTAAAAGCAGGTCAAACA 600
Lysostaphin  AGAACGACTGGTCCATTTAGAAAGCATGCCGAGTCAGGAGTCTTAAAAGCAGGTCAAACA 600
*****
Expected      ATTCATTATGATGAAGTGATGAAACAAGACGGTCATGTTTGGGTAGGTTATACAGGTAAC 660
Lysostaphin  ATTCATTATGATGAAGTGATGAAACAAGACGGTCATGTTTGGGTAGGTTATACAGGTAAC 660
*****
Expected      AGTGGCCAACGTATTTACTTGCCTGTAAAGAATGGAATAAATCTACTAATACTTTAGGT 720
Lysostaphin  AGTGGCCAACGTATTTACTTGCCTGTAAAGAATGGAATAAATCTACTAATACTTTAGGT 720
*****
Expected      GTTCTTTGGGGAACATAAAAGTGA 744
Lysostaphin  GTTCTTTGGGGAACATAAAAGTGA 744
*****

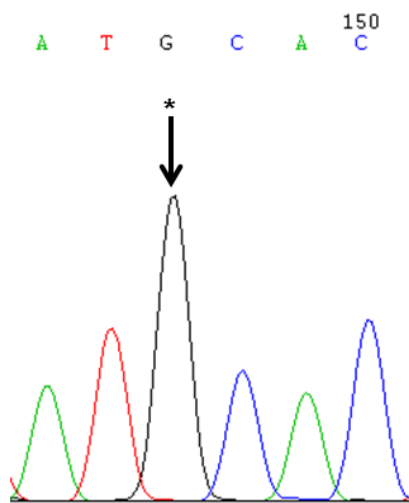
```

Appendix 7.59: Mis-identification of nucleotides during sequencing of pET construct
2. Mis-identified bases are indicated with the expected nucleotide,

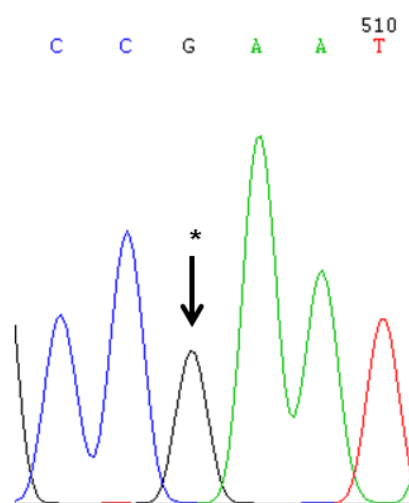


Appendix 7.60: Sequence data supporting base differences supported by ClustalW.
The positions of substituted nucleotides are marked by an asterisk.

A) C → G at position 147



B) C → G at position 507



Appendix 7.61: ClustalW alignment of the known mature lysostaphin domain encoding sequence (with C-terminal His-tag encoding sequence added) and the acquired DNA sequence from pET construct 3. The known mature lysostaphin domain encoding sequence (with C-terminal His-tag encoding sequence added) is presented in Appendix 7.56. The sequence acquired from construct 3 is presented in Appendix 7.57

```

Expected      ATGGCTGCAACACATGAACATTCAGCACAAATGGTTGAATAATTACAAAAAGGATATGGT 60
C-terminally ATGGCTGCAACACACCCTCTTAAAGGACAAATGGTTGAATAATTACAAAAAGGATATGGT 60
*****      .:*.:.** *****

Expected      TACGGTCCTTATCCATTAGGTATAAATGGCGGTATCCACTACGGAGTTGATTTTTTTATG 120
C-terminally TACGGTCCTTATCCATTAGGTATAAATGGCGGTATGCACTACGGAGTTGATTTTTTTATG 120
*****      *****

Expected      AATATTGGAACACCAGTAAAAGCTATTTCAAGCGGAAAAATAGTTGAAGCTGGTTGGAGT 180
C-terminally AATATTGGAACACCAGTAAAAGCTATTTCAAGCGGAAAAATAGTTGAAGCTGGTTGGAGT 180
*****

Expected      AATTACGGAGGAGGTAATCAAATAGGTCTTATTGAAAATGATGGAGTGCATAGACAATGG 240
C-terminally AATTACGGAGGAGGTAATCAAATAGGTCTTATTGAAAATGATGGAGTGCATAGACAATGG 240
*****

Expected      TATATGCATCTAAGTAAATATAATGTTAAAGTAGGAGATTATGTCAAAGCTGGTCAAATA 300
C-terminally TATATGCATCTAAGTAAATATAATGTTAAAGTAGGAGATTATGTCAAAGCTGGTCAAATA 300
*****

Expected      ATCGGTTGGTCTGGAAGCACTGGTTATTCTACAGCACCAATTTACACTTCCAAAGAATG 360
C-terminally ATCGGTTGGTCTGGAAGCACTGGTTATTCTACAGCACCAATTTACACTTCCAAAGAATG 360
*****

Expected      GTTAATTCATTTTCAAATTCAACTGCCCAAGATCCAATGCCTTTCTTAAAGAGCGCAGGA 420
C-terminally GTTAATTCATTTTCAAATTCAACTGCCCAAGATCCAATGCCTTTCTTAAAGAGCGCAGGA 420
*****

Expected      TATGGAAGCAGGTGGTACAGTAACTCCAACGCCAATACAGGTTGGAAGCAAAACAAA 480
C-terminally TATGGAAGCAGGTGGTACAGTAACTCCAACGCCAATACAGGTTGGAAGCAAAACAAA 480
*****

Expected      TATGGCACTATATAAATCAGAGTCAGCTAGCTTACACCTAATACAGATATAATAACA 540
C-terminally TATGGCACTATATAAATCAGAGTCAGCTAGCTTACACCTAATACAGATATAATAACA 540
*****

Expected      AGAACGACTGGTCCATTTAGAAGCATGCCGAGTCAGGAGTCTTAAAAGCAGGTCAAACA 600
C-terminally AGAACGACTGGTCCATTTAGAAGCATGCCGAGTCAGGAGTCTTAAAAGCAGGTCAAACA 600
*****

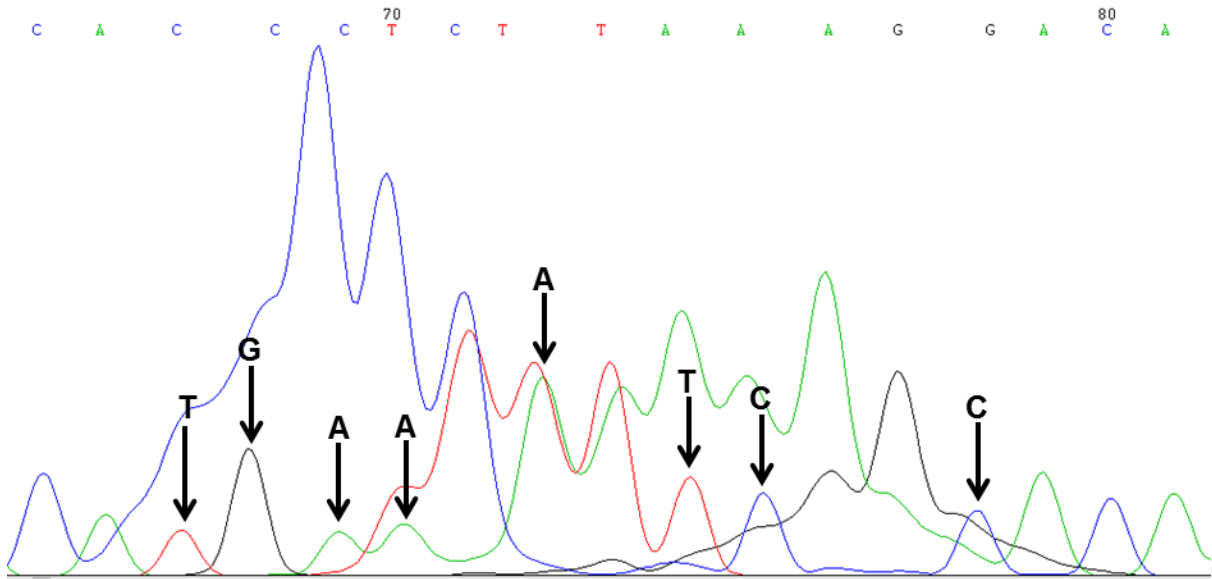
Expected      ATTCATTATGATGAAGTGATGAAACAAGACGGTCATGTTTGGGTAGGTTATACAGGTAAC 660
C-terminally ATTCATTATGATGAAGTGATGAAACAAGACGGTCATGTTTGGGTAGGTTATACAGGTAAC 660
*****

Expected      AGTGGCCAACGTATTTACTTGCCTGTAAAGACATGGAATAAATCTACTAATACTTTAGGT 720
C-terminally AGTGGCCAACGTATTTACTTGCCTGTAAAGACATGGAATAAATCTACTAATACTTTAGGT 720
*****

Expected      GTTCTTTGGGGAACATAAAGCTCGAGCACCAACCACCACCCTGA 768
C-terminally GTTCTTTGGGGAACATAAAGCTCGAGCACCAACCACCACCCTGA 768
*****

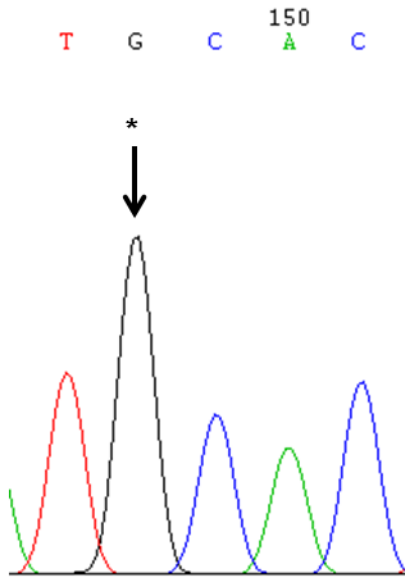
```

**Appendix 7.62: Mis-identification of nucleotides during sequencing of pET construct
3. Mis-identified bases are indicated**

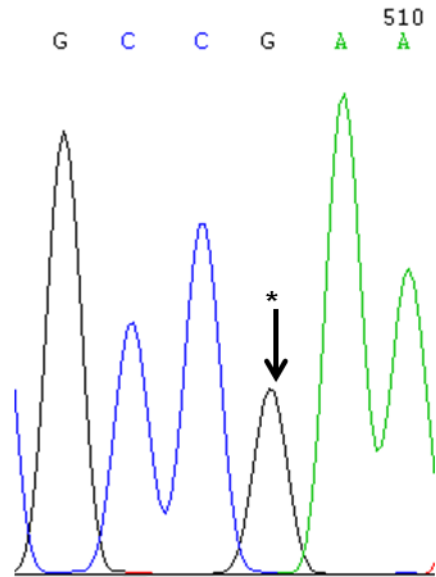


**Appendix 7.63: Sequence data supporting base differences supported by ClustalW.
The positions of substituted bases are marked by an asterisk.**

A) C → G at position 148



B) C → G at position 508



Appendix 7.64: ClustalW alignment of the mature lysostaphin gene sequence from *Staphylococcus staphylolyticus* (X06121) and the complete sequence of the PACK1 plasmid from *Staphylococcus simulans* bv. *Staphylolyticus* (gi|291246341|ref|NC_013944.1)

```

gi|291246341|ref|NC_013944.1| X06121      GGTTCAAAATAGAACAGCTTTAAGAGCTGCAACACATGAACATTCAGCAC 51000
-----AGAGCTGCAACACATGAACATTCAGCAC 28
*****

gi|291246341|ref|NC_013944.1| X06121      AATGGTTGAATAATTACAAAAAAGGATATGGTTACGGTCCTTATCCATTA 51050
AATGGTTGAATAATTACAAAAAAGGATATGGTTACGGTCCTTATCCATTA 78
*****

gi|291246341|ref|NC_013944.1| X06121      GGTATAAATGGCGGTATGCACTACGGAGTTGATTTTTTTTATGAATATTGG 51100
GGTATAAATGGCGGTATGCACTACGGAGTTGATTTTTTTTATGAATATTGG 128
*****

gi|291246341|ref|NC_013944.1| X06121      AACACCAGTAAAAGCTATTTCAAGCGGAAAAATAGTTGAAGCTGGTTGGA 51150
AACACCAGTAAAAGCTATTTCAAGCGGAAAAATAGTTGAAGCTGGTTGGA 178
*****

gi|291246341|ref|NC_013944.1| X06121      GTAATTACGGAGGAGTAATCAAATAGGTCTTATTGAAAATGATGGAGTG 51200
GTAATTACGGAGGAGTAATCAAATAGGTCTTATTGAAAATGATGGAGTG 228
*****

gi|291246341|ref|NC_013944.1| X06121      CATAGACAATGGTATATGCATCTAAGTAAATATAATGTTAAAGTAGGAGA 51250
CATAGACAATGGTATATGCATCTAAGTAAATATAATGTTAAAGTAGGAGA 278
*****

gi|291246341|ref|NC_013944.1| X06121      TTATGTCAAAGCTGGTCAAATAATCGGTTGGTCTGGAAGCACTGGTTATT 51300
TTATGTCAAAGCTGGTCAAATAATCGGTTGGTCTGGAAGCACTGGTTATT 328
*****

gi|291246341|ref|NC_013944.1| X06121      CTACAGCACCACATTTACACTTCCAAGAATGGTTAATTCATTTTCAAAT 51350
CTACAGCACCACATTTACACTTCCAAGAATGGTTAATTCATTTTCAAAT 378

gi|291246341|ref|NC_013944.1| X06121      TCAACTGCCAAGATCCAATGCCTTTCTTAAAGAGCGCAGGATATGGAAA 51400
TCAACTGCCAAGATCCAATGCCTTTCTTAAAGAGCGCAGGATATGGAAA 428
*****

gi|291246341|ref|NC_013944.1| X06121      AGCAGGTGGTACAGTAACTCCAACGCCGAATACAGGTTGGA AAAACA 51450
AGCAGGTGGTACAGTAACTCCAACGCCGAATACAGGTTGGA AAAACA 478
*****

gi|291246341|ref|NC_013944.1| X06121      AATATGGCACACTATATAAATCAGAGTCAGCTAGCTTCACACCTAATACA 51500
AATATGGCACACTATATAAATCAGAGTCAGCTAGCTTCACACCTAATACA 528
*****

gi|291246341|ref|NC_013944.1| X06121      GATATAATAACAAGAACGACTGGTCCATTTAGAAGCATGCCGAGTCAGG 51550
GATATAATAACAAGAACGACTGGTCCATTTAGAAGCATGCCGAGTCAGG 578
*****

gi|291246341|ref|NC_013944.1| X06121      AGTCTTAAAAGCAGGTCAAACAATTCATTATGATGAAGTGATGAAACAAG 51600
AGTCTTAAAAGCAGGTCAAACAATTCATTATGATGAAGTGATGAAACAAG 628
*****

gi|291246341|ref|NC_013944.1| X06121      ACGGTCATGTTGGGTAGGTTATACAGGTAACAGTGGCCAACGTATTTAC 51650
ACGGTCATGTTGGGTAGGTTATACAGGTAACAGTGGCCAACGTATTTAC 678
*****

gi|291246341|ref|NC_013944.1| X06121      TTGCTGTAAGAACATGGAATAAATCTACTAATACTTTAGGTGTTCTTTG 51700
TTGCTGTAAGAACATGGAATAAATCTACTAATACTTTAGGTGTTCTTTG 728
*****

gi|291246341|ref|NC_013944.1| X06121      GGGAACTATAAAGTGAGCGCGCTTTTATAAACTTATATGATAATTAGAG 51750
GGGAACTATAAAGTGA----- 744
*****

```

Appendix 7.65: DNA sequence encoding the mature lysostaphin domain. Substituted guanine bases are indicated in blue (position 96 and 456).

ATGGCTGCAACACATGAACATTCAGCACAATGGTTGAATAATTACAAAAAGGATATGGTTACGGTCC
TTATCCATTAGGTATAAATGGCGGTATGCACTACGGAGTTGATTTTTTATGAATATTGGAACACCCAGT
AAAAGCTATTTCAAGCGGAAAAATAGTTGAAGCTGGTTGGAGTAATTACGGAGGAGGTAATCAAATA
GGTCTTATTGAAAATGATGGAGTGCATAGACAATGGTATATGCATCTAAGTAAATATAATGTTAAAGTA
GGAGATTATGTCAAAGCTGGTCAAATAATCGGTTGGTCTGGAAGCACTGGTTATTCTACAGCACCACA
TTTACACTTCCAAAGAATGGTTAATTCATTTTCAAATTCAACTGCCCAAGATCCAATGCCTTTCTTAAA
GAGCGCAGGATATGGAAAAGCAGGTGGTACAGTAACTCCAACGCCGAATACAGGTTGGAAAACAA
ACAAATATGGCACACTATATAAATCAGAGTCAGCTAGCTTCACACCTAATACAGATATAATAACAAGAA
CGACTGGTCCATTTAGAAGCATGCCGCAGTCAGGAGTCTTAAAAGCAGGTCAAACAATTCATTATGAT
GAAGTGATGAAACAAGACGGTCATGTTTGGGTAGGTTATACAGGTAACAGTGGCCAACGTATTTACT
TGCCTGTAAGAACATGGAATAAATCTACTAATACTTTAGGTGTTCTTTGGGGAAGTATAAAGTGA

Appendix 7.66: Amino acid sequence encoding the mature lysostaphin domain with mis-identified amino acids (indicated in red)

MAATHEHSAQWLNNYKKGYGYGPYPLGINGG^IIHYGVDFFMNIGTPVKAISSGKIVEAGWS
NGGGNQIGLIENDGVHRQWYMHLISKYNVKVGDYVKAGQIIGWSGSTGYSTAPHLHFQRM
VNSFSNSTAQDPMPFLKSAGYGKAGGTVTPT^PNNTGWKTNKYGTLYKSESASFTPNTDIIT
RTTGPF^RSMPQSGVLKAGQTIHYDEVMKQDGHVWVG^YTGNSGQRIYLPVRTW^NKSTNT
LG VLVG^TIK-

Appendix 7.67: Amino acid sequence encoding the mature lysostaphin domain with substituted amino acids (indicated in red)

MAATHEHSAQWLNNYKKGYGYGPYPLGINGG^MIHYGVDFFMNIGTPVKAISSGKIVEAGW
SNYGGNQIGLIENDGVHRQWYMHLISKYNVKVG^DYVKAGQIIGWSGSTGYSTAPHLHFQ
RMVNSFSNSTAQDPMPFLKSAGYGKAGGTVTPT^PNNTGWKTNKYGTLYKSESASFTPNTDI
ITRTTGPF^RSMPQSGVLKAGQTIHYDEVMKQDGHVWVG^YTGNSGQRIYLPVRTW^NKSTN
TLG VLVG^TIK-

7.1.2 Expression of recombinant lysostaphin

Appendix 7.68: Media

Luria-Bertani (LB) Broth (1L)	(as described in Section 2.3.2.1/Appendix 7.25)
LB agar (100 ml)	(as described in Section 2.3.2.1/Appendix 7.25)
SOC media	(as described in Section 2.3.2.1/Appendix 7.25)

MDG starter media (10 ml)

Sterile 18.2 MΩ/cm H ₂ O	9.55 ml
MgSO ₄ (1M)	20.00 µl
1000 x metals [¶]	2.00 µl
Glucose (40%, w/v)	125.00 µl
Aspartate (25%, w/v)	100.00 µl
50 x M ⁺	200.00 µl
Antibiotic	100.00 µg/ml

The chemicals were aseptically added to a sterile universal tube to create starter cultures.

[¶]**1000 x metals (100 ml)** was prepared by sequentially dissolving the following chemicals in deionized 18.2 MΩ H₂O to achieve a final volume of 1 litre:

Sterile 18.2 MΩ/cm H ₂ O	36.0 ml
FeCl ₃ -6H ₂ O [†]	50.0 ml
CaCl ₂ (1M) anhydrous	2.0 ml
MnCl ₂ -4H ₂ O (1M)	1.0 ml
Zn-SO ₄ -7H ₂ O (1 M)	1.0 ml
CoCl ₂ -6H ₂ O (0.2 M)	1.0 ml

CuCl ₂ -2H ₂ O (0.1M)	2.0 ml
NiCl ₂ -6H ₂ O (0.2 M)	1.0 ml
Na ₂ MoO ₄ -5H ₂ O (0.1 M)	2.0 ml
Na ₂ SeO ₃ -5H ₂ O (0.1M)	2.0 ml
H ₃ BO ₃ (0.1 M) anhydrous	2.0 ml

†FeCl₃-6H₂O was dissolved in a 100-fold dilution of HCl (~0.12 M HCl) before filter sterilisation using a 0.2 µm filter.

Each of the other solutions was autoclaved separately and aseptically combined to formulate 1000 x metals.

*50 x M (100 ml) was prepared by sequentially dissolving the following chemicals in deionized 18.2 MΩ H₂O to achieve a final volume of 100ml:

Na ₂ SO ₄ anhydrous	3.6 g
NH ₄ Cl anhydrous	13.4 g
KH ₂ PO ₄ anhydrous	17.0 g
Na ₂ HPO ₄ anhydrous	17.7 g

The solution was autoclaved before and between use.

ZYM-5052 auto-induction media (AIM) (500 ml)

ZY‡	478.5 ml
MgSO ₄ (1M)	1.0 ml
1000 x metals††	0.5 ml
50 x M*	1.0 ml
Antibiotic	100.0 µg/ml
50 x 5052*	1.0 ml

The chemicals were aseptically added to a 2 L baffled flask.

NH₄Cl 5.0 g

The salt solution was divided into 200 ml aliquots, which were sterilized by autoclaving.

The MgSO₄ and CaCl₂ solutions were prepared separately, sterilized by autoclaving and were aseptically combined with the solutions after diluting the 5 x M9 salts to 980 ml with sterile H₂O. The glucose was sterilised by passing it through a 0.22 µm filter before being added to the diluted M9 salts.

Terrific broth (TB) (1 L)

To 900 ml of 18.2 MΩ/cm H₂O, the following chemicals were added:

Tryptone 12 g

Yeast extract 24 g

Glycerol 4 ml

The solutes were shaken until they had dissolved, before autoclaving the media for 20 min at 15 psi on liquid cycle. The solution was allowed to cool to 60 °C or less and before adding 100 ml of a sterile solution of 0.17 M KH₂PO₄/0.72 M K₂HPO₄ (made by dissolving 2.31 g of KH₂PO₄ and 12.54 g of K₂HPO₄ in 90 ml of deionized H₂O, before autoclaving the solution for 20 minutes at 15 psi).

Appendix 7.69: Chemicals

MgSO₄ (100 ml)

MgSO₄ 26.65 g

The MgSO₄ was dissolved in 18.2 MΩ/cm H₂O and then autoclaved before and between use.

Glucose (20 ml)

Glucose (40%, w/v) 8.0 g

The glucose was sterilised by filter sterilisation using a 0.2 µm filter (Sartorius, Germany), prior to use.

Aspartate (20 ml)

Aspartate (25% w/v) 5.0 g

The pH was adjusted to 7.0 using NaOH, prior to autoclaving.

CaCl₂ (100 ml)

CaCl₂ (1M) 14.7 g

The CaCl₂ was dissolved in 18.2 MΩ/cm H₂O and then autoclaved before and between use.

MgCl₂-CaCl₂ (200 ml)

MgCl₂ (80 mM) 3.25 g

CaCl₂ (0.02 M) 0.59 g

The chemicals were dissolved sequentially in 18.2 MΩ/cm H₂O and then autoclaved before and between use.

CaCl₂ (200 ml)

CaCl₂ (0.1 M) 2.9 g

The CaCl₂ was dissolved in 18.2 MΩ/cm H₂O and then autoclaved before and between use.

EDTA (50 ml)

EDTA, pH 8.0 (0.5 M) 9.3 g

The EDTA was dissolved in 18.2 MΩ/cm H₂O and the pH was adjusted to 8.0. The solution was autoclaved before and between use.

Appendix 7.70: Buffers

De-salting buffer (50 ml)

Tris-HCl, pH 8.0 (25 mM) 0.15 g

The tris-base was dissolved in 18.2 MΩ/cm H₂O and the pH of the buffer was adjusted to pH 8.0, using HCl, prior to autoclaving.

Osmotic-shock buffer (100 ml)

Tris-HCl, pH 8.0 (10 mM) 0.12 g

Sucrose (20%, w/v) 20.00 g

The chemicals were dissolved sequentially in 18.2 MΩ/cm H₂O prior to autoclaving.

Resuspension buffers

During cytoplasmic protein extraction, harvested *E. coli* was resuspended in a buffer that was compatible with the subsequent protein purification by various modes of chromatography. The appropriate buffers are indicated in Appendix 7.71.

Appendix 7.71: Resuspension buffers used to resuspend *E. coli* during cytoplasmic protein extraction prior to protein purification

Type of chromatography	Column	Buffer
IMAC	Chelating Sepharose Fast Flow IMAC	IMAC buffer A (Appendix 7.105)
	ProPac [®] IMAC-10	IMAC buffer A (Appendix 7.105)
HIC	Phenyl Sepharose HP	HIC buffer A (Appendix 7.105)
AXC	Source [™] 30Q	AXC buffer A (Appendix 7.105)
	ProPac [®] SAX	IEX buffer A (Appendix 7.105)
CXC	Source [™] 30S	CXC buffer A (Appendix 7.105)
	ProPac [®] WCX/SCX	IEX buffer A (Appendix 7.136)
		WCX buffer A (Appendix 7.136)
		SCX buffer A (Appendix 7.136)
ProPac [®] MAb SCX	MAb SCX buffer A (Appendix 7.136)	

Appendix 7.72: Preparation of chemically competent *E. coli* BL21

To produce competent cells for transformation, a bacterial colony was transferred into a 100 ml LB broth in a 1 L conical flask and grown until an OD_{600 nm} of 0.35-0.4 was reached. The cells were transferred to two cold, sterile universal tubes and stored on ice for 10 min. The universal tubes were centrifuged at 4000 x g for 10 min at 4°C, and following centrifugation the supernatant discarded into a Virkon solution, as viable cells may have been present. The supernatant was discarded to leave a dry pellet, which was re-suspended in 15 ml of ice-cold MgCl₂ -CaCl₂ by gently swirling. The cells were recovered by centrifugation at 4000 x g for 10 min at 4°C, before the supernatant was discarded into Virkon and the pellet resuspended by swirling in 1 ml of ice cold 0.1 M CaCl₂. The competent cells were aliquoted into 50 µl volumes and used directly for transformation. To any remaining cells, sterile glycerol was added to 15% (v/v) and the cells then stored at -80°C until required for subsequent transformations.

Appendix 7.73: Transformation of chemically competent *E. coli* BL21

Competent cells were mixed with 2.5 µl of ligation and incubated on ice for 30 min. The cells were then transferred to a water bath at 42°C for 90 sec, before incubating on ice for at least 2 min. The cells were recovered through aseptic addition of 200 µl of SOC medium and then incubated at 37°C for 45 min. The recovered cells were aseptically plated onto LB media, supplemented with an appropriate antibiotic, and incubated overnight at 37°C to allow growth of transformed bacterial colonies.

Appendix 7.74: Preparation of media for shake flask cultures

In order to minimise batch-to-batch variability during culture, the expression media was prepared, ensuring that chemical constituents were weighed as accurately as possible. The pH of the media was verified prior to sterilisation of the media. Small-scale cultures were performed using between 50 and 100 ml of expression media. To provide sufficient aeration to the cultures, small-scale batch cultures were performed in suitable Erlenmeyer flasks, ensuring that the expression media volume did not exceed more than 20% of the volumetric capacity of the flask. Large-scale batch cultures containing 1L of expression media were performed in 2 L baffled Erlenmeyer flasks to provide increased aeration. Where multiple 1L batch cultures were used in a single experiment, expression media was prepared as a single large volume to ensure consistency of media formulation between cultures.

Appendix 7.75: Recombinant protein expression following auto-induction

Transformed *E. coli* BL21 colonies or glycerol stocks were used to inoculate MDG starter cultures, which were incubated overnight at 37°C and 200 rpm. A 1% (v/v) inoculum of the MDG starter culture was aseptically transferred into an appropriate volume of ZYM-5052 autoinduction media. The culture was incubated at 37°C and 200 rpm, whilst being monitored spectrophotometrically until an OD_{600 nm} of 0.6-1.0 had been obtained. At the appropriate OD_{600 nm}, the incubation conditions were adjusted to 30°C and 100 rpm shaking overnight, before the cell-free extract was extracted by cytoplasmic or periplasmic extraction methods, depending on the location of protein expression. The cell-free extract was then analysed by SDS-PAGE (Appendix 7.15) to establish whether the target protein had been overexpressed in a soluble form.

Appendix 7.76: Recombinant protein expression following IPTG induction

IPTG-induced protein expression was performed using LB, TB or MM. Transformed *E. coli* BL21(DE3) colonies or glycerol stocks were used to inoculate starter cultures containing 10 ml of the chosen expression media, supplemented with an appropriate antibiotic. The starter cultures were incubated overnight at 37°C and 200 rpm, before aseptic transfer of a 1% (v/v) inoculum into an appropriate volume of expression media, supplemented with an antibiotic. The culture was incubated at 37°C and 200 rpm, whilst the optical density of the culture was monitored by spectrometry during growth. Once an OD_{600 nm} of 0.6-1.0 was obtained, IPTG to a concentration of 240 µg/ml was added to the culture to induce protein expression. At the appropriate OD_{600 nm}, the culture was incubated at 30°C and 100 rpm overnight. A cell-

free extract was then extracted by cytoplasmic or periplasmic extraction methods, depending on the location of protein expression.

Appendix 7.77: Cytoplasmic protein extraction

Following culture, the *E. coli* BL21(DE3) were harvested by centrifugation at 4000 x g for 15 min at 4°C to pellet the cells. The bacterial cell pellet was resuspended in an appropriate resuspension buffer. The resuspension buffer was selected to facilitate subsequent purification of the recombinant protein by chromatography, as indicated in Appendix 7.71. The resuspended cells were lysed by sonication at amplitude of 15 microns amplitude at 10 sec intervals for 2 min, whilst on ice. After sonication, the cells were centrifuged at 24000 x g for 20 min at 4°C and the resulting supernatant (cell-free extract, CFE) was decanted from the pellet and retained. The residual cell pellet was mixed with 300 µl of solubilising (cracking) buffer to provide an initial indication of protein solubility during protein expression. The solubilised samples and neat and diluted CFE samples were boiled for 3 min and then analysed by PAGE to establish whether the target protein had been overexpressed in a soluble form.

Appendix 7.78: Periplasmic protein extraction

Following culture, the *E. coli* BL21(DE3) were placed on ice for 10 min, before being centrifuged at 4000 x g for 10 min to pellet the cells. The bacterial cell pellet was gently resuspended in 5 ml of 10 mM Tris-HCl, pH 8.0 containing 20 % (w/v) sucrose. After re-suspension, 0.25 ml of 0.5 M EDTA, pH 8.0 was added to the mixture and incubated on ice for 30 min. After incubation, the suspension was transferred to a 50 ml centrifuge tube and centrifuged for 10 min at 4000 x g. The resulting bacterial pellet was resuspended by gentle vortexing in 4 ml of ice cold 18.2 MΩ/cm H₂O and incubated on ice for 30 min. Following incubation the mixture was centrifuged at 30000 x g at 4 °C for 10 min. The sucrose and salts were then removed from the supernatant by gel filtration using PD10 columns (Appendix 7.79).

Appendix 7.79: Desalting of cell-free extract using gel filtration (PD10 columns)

A PD10 gel filtration column was prepared by resuspending 2 g of Sephadex™ G-25 (medium gel filtration matrix) in 15 ml of de-salting buffer in a 20 ml plastic universal tube. A plastic PD-10 column was prepared by cutting off the bottom of the column and inserting a filter at the bottom to prevent loss of resin during filtration. The contents were transferred to the PD-10 column, homogenised, then allowed to settle. After adding the resin, a 10 ml

syringe plunger was used to encourage the excess buffer to leave the column. Another filter was then placed on top of the resin and caps were placed on the top and bottom of the column to prevent dehydration prior to use.

Extracted CFE (2.5 ml) was then applied to the column and allowed to flow through the column by gravity, without collecting the flow-through. The desalted recombinant protein was eluted by applying 3.5 ml of desalting buffer to the column, whilst retaining the eluate. To remove sucrose and salts from the column, 6.0 ml of desalting buffer was then applied to the column, without collecting the flow-through. This process was repeated until all of the extracted CFE had been desalted and collected. Neat and diluted cell-free extract was then analysed by PAGE to establish whether the target protein had been overexpressed in a soluble form.

Appendix 7.80: Nucleotide sequence of *N*-terminally His-tagged recombinant lysostaphin (construct 1). The *N*-terminal His-tag region is presented in red.

ATGGGCAGCAGCCATCATCATCATCACAGCAGCCGCCTGGTGCCGCGCGGCAGCCATATGGCT
GCAACACATGAACATTCAGCACAAATGGTTGAATAATTACAAAAAGGATATGGTTACGGTCCTTATCCAT
TAGGTATAAATGGCGGTATGCACTACGGAGTTGATTTTTTATGAATATTGGAACACCAGTAAAAGCTAT
TTCAAGCGGAAAAATAGTTGAAGCTGGTTGGAGTAATTACGGAGGAGGTAATCAAATAGGTCTTATTGA
AAATGATGGAGTGCATAGACAATGGTATATGCATCTAAGTAAATATAATGTTAAAGTAGGAGATTATGTCA
AAGCTGGTCAAATAATCGGTTGGTCTGGAAGCACTGGTTATTCTACAGCACCCACATTTACACTTCCAAA
GAATGGTTAATTCATTTTCAAATTCAACTGCCCAAGATCCAATGCCTTTCTTAAAGAGCGCAGGATATGG
AAAAGCAGGTGGTACAGTAACTCCAACGCCGAATACAGGTTGGAAAACAAACAAATATGGCACACTATA
TAAATCAGAGTCAGCTAGCTTACACCTAATACAGATATAATAACAAGAACGACTGGTCCATTTAGAAGC
ATGCCGCGAGTCAGGAGTCTTAAAAGCAGGTCAAACAATTCATTATGATGAAGTGATGAAACAAGACGG
TCATGTTTGGGTAGGTTATACAGGTAACAGTGGCCAACGTATTACTTGCCTGTAAGAACATGGAATAA
ATCTACTAATACTTAGGTGTTCTTTGGGGAACATAAAGTGA

Appendix 7.81: Predicted amino acid sequence of *N*-terminally His-tagged recombinant lysostaphin (construct 1).

MGSSHHHHHSSRLVPRGSHMAATHEHSAQWLNNYKKGYGYPYPLGINGGMHYG
VDFFMNIGTPVKAISSGKIVEAGWSNYGGGNQIGLIENDGVHRQWYMHLISKYNVKG
DYVKAGQIIGWSGSTGYSTAPHLHFQRMVNSFSNSTAQDPMPFLKSAGYGKAGGTVT
PTPNTGWKTNKYGTLYKSESASFTPNTDIITRTTGPFRSMPQSGVLKAGQTIHYDEVM
KQDGHVWVGYTGNSGQRIYLPVRTWNKSTNTLGVLVWGTIK-

Appendix 7.82: ProtParam analysis of *N*-terminally His-tagged recombinant lysostaphin (construct 1) with a retained *N*-terminal methionine residue

User-provided sequence:

```

      10      20      30      40      50      60
MGSSHHHHHH SSRLVPRGSH MAATHEHSAQ WLNNYKKGYG YGPYPLGING GMHYGVDFFM

      70      80      90     100     110     120
NIGTPVKAIS SGKIVEAGWS NYGGGNQIGL IENDGVHRQW YMHL SKYNVK VGDYVKAGQI

     130     140     150     160     170     180
IGWSGSTGYS TAPHLHFQRM VNSFSNSTAQ DPMPFLKSAG YGKAGGTVTP TPNTGWKTNK

     190     200     210     220     230     240
YGTLYKSESA SFTPNTDIIT RTTGPFRSMP QSGVLKAGQT IHYDEVKMQD GHVWVGYTGN

     250     260
SQQRIYLPVR TWNKSTNITLGLVWGIIK

```

Number of amino acids: 267

Molecular weight: 29337.8

Theoretical pI: 9.72

Amino acid composition:

[CSV format](#)

Ala (A)	12	4.5%
Arg (R)	8	3.0%
Asn (N)	16	6.0%
Asp (D)	7	2.6%
Cys (C)	0	0.0%
Gln (Q)	10	3.7%
Glu (E)	5	1.9%
Gly (G)	37	13.9%
His (H)	16	6.0%
Ile (I)	13	4.9%
Leu (L)	12	4.5%
Lys (K)	16	6.0%
Met (M)	9	3.4%
Phe (F)	7	2.6%
Pro (P)	13	4.9%
Ser (S)	24	9.0%
Thr (T)	22	8.2%
Trp (W)	8	3.0%
Tyr (Y)	16	6.0%
Val (V)	16	6.0%
Pyl (O)	0	0.0%
Sec (U)	0	0.0%
(B)	0	0.0%
(Z)	0	0.0%
(X)	0	0.0%

Appendix 7.82: ProtParam analysis of *N*-terminally His-tagged recombinant lysostaphin (construct 1) with a retained *N*-terminal methionine residue (continued).

Total number of negatively charged residues (Asp + Glu): 12
Total number of positively charged residues (Arg + Lys): 24

Atomic composition:

Carbon	C	1312
Hydrogen	H	1971
Nitrogen	N	373
Oxygen	O	380
Sulfur	S	9

Formula: C₁₃₁₂H₁₉₇₁N₃₇₃O₃₈₀S₉
Total number of atoms: 4045

Extinction coefficients:

Extinction coefficients are in units of M⁻¹ cm⁻¹, at 280 nm measured in water.

Ext. coefficient	67840
Abs 0.1% (=1 g/l)	2.312

Estimated half-life:

The *N*-terminal of the sequence considered is M (Met).

The estimated half-life is: 30 hours (mammalian reticulocytes, in vitro).
>20 hours (yeast, in vivo).
>10 hours (Escherichia coli, in vivo).

Instability index:

The instability index (II) is computed to be 33.26
This classifies the protein as stable.

Aliphatic index: 58.39

Grand average of hydropathicity (GRAVY): -0.566

Appendix 7.83: Nucleotide sequence of recombinant lysostaphin (construct 2)

ATGGCTGCAACACATGAACATTCAGCACAATGGTTGAATAATTACAAAAAGGATATGGTTACGGTCCTTATCC
ATTAGGTATAAATGGCGGTATGCACTACGGAGTTGATTTTTTATGAATATTGGAACACCAGTAAAAAGCTATTTCC
AAGCGGAAAAATAGTTGAAGCTGGTTGGAGTAATTACGGAGGAGGTAATCAAATAGGTCTTATTGAAAATGATG
GAGTGCATAGACAATGGTATATGCATCTAAGTAAATATAATGTTAAAGTAGGAGATTATGTCAAAGCTGGTCAAA
TAATCGGTTGGTCTGGAAGCACTGGTTATTCTACAGCACCACATTTACACTTCCAAAGAATGGTTAATTCATTTT
CAAATCAACTGCCCAAGATCCAATGCCTTTCTTAAAGAGCGCAGGATATGGAAAAGCAGGTGGTACAGTAAC
TCCAACGCCGAATACAGGTTGGAAAACAAACAAATATGGCACACTATATAAATCAGAGTCAGCTAGCTTCACAC
CTAATACAGATATAATAACAAGAACGACTGGTCCATTTAGAAGCATGCCGCAGTCAGGAGTCTTAAAAGCAGGT
CAAACAATTCATTATGATGAAGTGATGAAACAAGACGGTCATGTTTGGGTAGGTTATACAGGTAACAGTGGCCA
ACGTATTACTTGCCTGTAAGAACATGGAATAAATCTACTAATACTTTAGGTGTTCTTTGGGGAACATAAAGTG
A

Appendix 7.84: Predicted amino acid sequence of recombinant lysostaphin (construct 2)

MAATHEHSAQWLNNYKKGYGYPYPLGINGGMHYGVDFFMNIGTPVKAISSGKIVEAGWSNYGGGNQIG
LIENDGVHRQWYMHLSKYNVKVDYVKAGQIIGWSGSTGYSTAPHLHFQRMVNSFSNSTAQDPMPFLKS
AGYGKAGGTVPTPNTGWKTNKYGTLYKSESASFTPNTDIIIRTTGPFRSMPQSGVLKAGQTIHYDEVK
QDGHVWVGYTGNSGQRIYLPVRTWNKSTNTLGVLVGTLK-

Appendix 7.85: ProtParam analysis of recombinant lysostaphin (construct 2) with a retained N-terminal methionine residue

User-provided sequence:

```

      10      20      30      40      50      60
MAATHEHSAQ WLNNYKKGYG YGPYPLGING GMHYGVDFFM NIGTPVKAIS SGKIVEAGWS

      70      80      90     100     110     120
NYGGGNQIGL IENDGVHRQW YMHLSKYNVK VGDYVKAGQI IGWSGSTGYS TAPHLHFQRM

     130     140     150     160     170     180
VNSFSNSTAQ DPMPFLKSAG YGKAGGTVTP TPNTGWKTNK YGTLYKSESA SFTPNTDIIT

     190     200     210     220     230     240
RTTGPFRRSMP QSGVLKAGQT IHYDEVKMQD GHVWVGYTGN SGQRIYLPVR TWNKSTNTLG

VLWGTIK

```

Number of amino acids: 247

Molecular weight: 27075.4

Theoretical pI: 9.59

Amino acid composition:

Ala (A)	12	4.9%
Arg (R)	6	2.4%
Asn (N)	16	6.5%
Asp (D)	7	2.8%
Cys (C)	0	0.0%
Gln (Q)	10	4.0%
Glu (E)	5	2.0%
Gly (G)	35	14.2%
His (H)	9	3.6%
Ile (I)	13	5.3%
Leu (L)	11	4.5%
Lys (K)	16	6.5%
Met (M)	8	3.2%
Phe (F)	7	2.8%
Pro (P)	12	4.9%
Ser (S)	19	7.7%
Thr (T)	22	8.9%
Trp (W)	8	3.2%
Tyr (Y)	16	6.5%
Val (V)	15	6.1%
Pyl (O)	0	0.0%
Sec (U)	0	0.0%
(B)	0	0.0%
(Z)	0	0.0%
(X)	0	0.0%

Total number of negatively charged residues (Asp + Glu): 12

Total number of positively charged residues (Arg + Lys): 22

Appendix 7.85: ProtParam analysis of recombinant lysostaphin (construct 2) with a retained N-terminal methionine residue (continued).

Atomic composition:

Carbon	C	1218
Hydrogen	H	1831
Nitrogen	N	333
Oxygen	O	355
Sulfur	S	8

Formula: $C_{1218}H_{1831}N_{333}O_{355}S_8$

Total number of atoms: 3745

Extinction coefficients:

Extinction coefficients are in units of $M^{-1} \text{ cm}^{-1}$, at 280 nm measured in water.

Ext. coefficient 67840

Abs 0.1% (=1 g/l) 2.506

Estimated half-life:

The N-terminal of the sequence considered is M (Met).

The estimated half-life is: 30 hours (mammalian reticulocytes, in vitro).

>20 hours (yeast, in vivo).

>10 hours (Escherichia coli, in vivo).

Instability index:

The instability index (II) is computed to be 32.68

This classifies the protein as stable.

Aliphatic index: 60.36

Grand average of hydropathicity (GRAVY): -0.499

Appendix 7.86: Nucleotide sequence of C-terminally His-tagged recombinant lysostaphin (construct 3). The C-terminal His-tag region is presented in green.

ATGGCTGCAACACATGAACATTCAGCACAATGGTTGAATAATTACAAAAAGGATATGGTT
ACGGTCCTTATCCATTAGGTATAAATGGCGGTATGCACTACGGAGTTGATTTTTTTATGAA
TATTGGAACACCAGTAAAAGCTATTTCAAGCGGAAAAATAGTTGAAGCTGGTTGGAGTAA
TTACGGAGGAGGTAATCAAATAGGTCTTATTGAAAATGATGGAGTGCATAGACAATGGTAT
ATGCATCTAAGTAAATATAATGTTAAAGTAGGAGATTATGTCAAAGCTGGTCAAATAATCGG
TTGGTCTGGAAGCACTGGTTATTCTACAGCACCACATTTACACTTCCAAAGAATGGTTAA
TTCATTTTCAAATCAACTGCCCAAGATCCAATGCCTTTCTTAAAGAGCGCAGGATATGGA
AAAGCAGGTGGTACAGTAACTCCAACGCCGAATACAGGTTGGAAAACAAACAAATATGG
CACACTATATAAATCAGAGTCAGCTAGCTTCACACCTAATACAGATATAATAACAAGAACGA
CTGGTCCATTTAGAAGCATGCCGCAGTCAGGAGTCTTAAAAGCAGGTCAAACAATTCATT
ATGATGAAGTGATGAAACAAGACGGTCATGTTTGGGTAGGTTATACAGGTAACAGTGGC
CAACGTATTTACTTGCCTGTAAGAACATGGAATAAATCTACTAATACTTTAGGTGTTCTTTG
GGGAACTATAAAGCTCGAGCACCACCACCACCACACTGA

Appendix 7.87: Predicted amino acid sequence of C-terminally His-tagged recombinant lysostaphin (construct 3)

MAATHEHSAQWLNNYKKGYGYGPYPLGINGGMHYGVDFFMNIGTPVKAISSGKIVEAG
WSNYGGGNQIGLIENDGVHRQWYMHLISKYNVKVGDYVKAGQIIGWSGSTGYSTAPHL
HFQRMVNSFSNSTAQDPMPFLKSAGYGKAGGTVTPNTGWKTNKYGTLYKSESASF
TPNTDII TRTTGPFRSMPQSGVLKAGQTIHYDEVKQDGHVWVGYTGNSGQRIYLPVR
TWNKSTNTLGV LWGTIKLEHHHHH-

Appendix 7.88: ProtParam analysis of C-terminally His-tagged recombinant lysostaphin (construct 3) with a retained N-terminal methionine residue

User-provided sequence:

```
      10      20      30      40      50      60
MAATHEHSAQ WLNNYKKGYG YGPYPLGING GMHYGVDFFM NIGTPVKAIS SGKIVEAGWS

      70      80      90     100     110     120
NYGGGNQIGL IENDGVHRQW YMHLSKYNVK VGDYVKAGQI IGWSGSTGYS TAPHLHFQRM

     130     140     150     160     170     180
VNSFSNSTAQ DPMPFLKSAG YGKAGGTVTP TPNTGWKTNK YGTLYKSESA SFTPNTDIIT

     190     200     210     220     230     240
RTTGPFRSMP QSGVLKAGQT IHYDEVMKQD GHVWVGYTGN SGQRIYLPVR TWNKSTNLTG

     250
VLWGTIKLEH HHHHH
```

Number of amino acids: 255

Molecular weight: 28140.5

Theoretical pI: 9.52

Amino acid composition: [CSV format](#)

Ala (A)	12	4.7%
Arg (R)	6	2.4%
Asn (N)	16	6.3%
Asp (D)	7	2.7%
Cys (C)	0	0.0%
Gln (Q)	10	3.9%
Glu (E)	6	2.4%
Gly (G)	35	13.7%
His (H)	15	5.9%
Ile (I)	13	5.1%
Leu (L)	12	4.7%
Lys (K)	16	6.3%
Met (M)	8	3.1%
Phe (F)	7	2.7%
Pro (P)	12	4.7%
Ser (S)	19	7.5%
Thr (T)	22	8.6%
Trp (W)	8	3.1%
Tyr (Y)	16	6.3%
Val (V)	15	5.9%
Pyl (O)	0	0.0%
Sec (U)	0	0.0%
(B)	0	0.0%
(Z)	0	0.0%
(X)	0	0.0%

Total number of negatively charged residues (Asp + Glu): 13

Total number of positively charged residues (Arg + Lys): 22

Appendix 7.88: ProtParam analysis of C-terminally His-tagged recombinant lysostaphin (construct 3) with a retained N-terminal methionine residue (continued).

Atomic composition:

Carbon	C	1265
Hydrogen	H	1891
Nitrogen	N	353
Oxygen	O	365
Sulfur	S	8

Formula: $C_{1265}H_{1891}N_{353}O_{365}S_8$

Total number of atoms: 3882

Extinction coefficients:

Extinction coefficients are in units of $M^{-1} \text{ cm}^{-1}$, at 280 nm measured in water.

Ext. coefficient 67840

Abs 0.1% (=1 g/l) 2.411

Estimated half-life:

The N-terminal of the sequence considered is M (Met).

The estimated half-life is: 30 hours (mammalian reticulocytes, in vitro).

>20 hours (yeast, in vivo).

>10 hours (Escherichia coli, in vivo).

Instability index:

The instability index (II) is computed to be 31.34

This classifies the protein as stable.

Aliphatic index: 60.00

Grand average of hydropathicity (GRAVY): -0.558

Appendix 7.89: Nucleotide sequence of C-terminally His-tagged recombinant lysostaphin (construct 4). The C-terminal His-tag region is presented in green.

ATGGCTGCAACACATGAACATTCAGCACAAATGGTTGAATAATTACAAAAAGGATATGGTT
ACGGTCCTTATCCATTAGGTATAAATGGCGGTATGCACTACGGAGTTGATTTTTTATGAA
TATTGGAACACCAGTAAAAGCTATTTCAAGCGGAAAAATAGTTGAAGCTGGTTGGAGTAA
TTACGGAGGAGGTAATCAAATAGGTCTTATTGAAAATGATGGAGTGCATAGACAATGGTA
TATGCATCTAAGTAAATATAATGTTAAAGTAGGAGATTATGTCAAAGCTGGTCAAATAATCG
GTTGGTCTGGAAGCACTGGTTATTCTACAGCACCACATTTACACTTCCAAAGAATGGTTA
ATTCATTTTCAAATTTCAACTGCCCAAGATCCAATGCCTTTCTTAAAGAGCGCAGGATATG
GAAAAGCAGGTGGTACAGTAACTCCAACGCCGAATACAGGTTGGAAAACAAACAAATAT
GGCACACTATATAAATCAGAGTCAGCTAGCTTCACACCTAATACAGATATAATAACAAGAA
CGACTGGTCCATTTAGAAGCATGCCGCAGTCAGGAGTCTTAAAAGCAGGTCAAACAATT
CATTATGATGAAGTGATGAAACAAGACGGTCATGTTTGGGTAGGTTATACAGGTAACAGT
GGCCAACGTATTTACTTGCCTGTAAGAACATGGAATAAATCTACTAATACTTTAGGTGTTT
TTTGGGGAACATAAAGCTCGAGCACCACCACCACCACCCTGA

Appendix 7.90: Predicted amino acid sequence of C-terminally His-tagged recombinant lysostaphin (construct 4)

MAATHEHSAQWLNNYKKGYGYGPYPLGINGGMHYGVDFFMNIGTPVKAISSGKIVEAGWS
NYGGGNQIGLIENDGVHRQWYMHL SKYNVKVGDYVKAGQIIGWSGSTGYSTAPHLHFQR
MVNSFSNSTAQDPMPFLKSAGYGKAGGTVTPTPNTGWKTNKYGTLYKSESASFTPNTDIIT
RTTGPFERSMPQSGVLKAGQTIHYDEV MKQDGHVWVG YTGNSGQRIYLPVRTWNKSTNTL
GVLWGTIKLEHHHHH-

Appendix 7.91: ProtParam analysis of C-terminally His-tagged recombinant lysostaphin (construct 4) with a retained N-terminal methionine residue

User-provided sequence:

```
      10      20      30      40      50      60
MAATHEHSAQ WLNNYKKGYG YGPYPLGING GMHYGVDFFM NIGTPVK AIS  SGKIVEAGWS

      70      80      90     100     110     120
NYGGGNQIGL IENDGVHRQW YMHL SKY NVK  VGDYVKAGQI IGWSGSTGYS TAPHLHFQRM

     130     140     150     160     170     180
VNSFSNSTAQ DPMPFLKSAG YGKAGGTVTP TPNTGWKTNK YGTLYKSESA SFTPNTDIIT

     190     200     210     220     230     240
RTTGPFRSMP QSGVLKAGQT IHYDEVKQD  GHVWVGYTGN SGQRIYLPVR TWNKSTNLTG

     250
VLWGTIKLEH HHHHH
```

Number of amino acids: 255

Molecular weight: 28140.5

Theoretical pI: 9.52

Amino acid composition:

[CSV format](#)

Ala (A)	12	4.7%
Arg (R)	6	2.4%
Asn (N)	16	6.3%
Asp (D)	7	2.7%
Cys (C)	0	0.0%
Gln (Q)	10	3.9%
Glu (E)	6	2.4%
Gly (G)	35	13.7%
His (H)	15	5.9%
Ile (I)	13	5.1%
Leu (L)	12	4.7%
Lys (K)	16	6.3%
Met (M)	8	3.1%
Phe (F)	7	2.7%
Pro (P)	12	4.7%
Ser (S)	19	7.5%
Thr (T)	22	8.6%
Trp (W)	8	3.1%
Tyr (Y)	16	6.3%
Val (V)	15	5.9%
Pyl (O)	0	0.0%
Sec (U)	0	0.0%
(B)	0	0.0%
(Z)	0	0.0%
(X)	0	0.0%

Total number of negatively charged residues (Asp + Glu): 13

Total number of positively charged residues (Arg + Lys): 22

Appendix 7.91: Prot Param analysis of C-terminally His-tagged recombinant lysostaphin (construct 4) with a retained N-terminal methionine residue (continued).

Atomic composition:

Carbon	C	1265
Hydrogen	H	1891
Nitrogen	N	353
Oxygen	O	365
Sulfur	S	8

Formula: $C_{1265}H_{1891}N_{353}O_{365}S_8$

Total number of atoms: 3882

Extinction coefficients:

Extinction coefficients are in units of $M^{-1} cm^{-1}$, at 280 nm measured in water.

Ext. coefficient 67840

Abs 0.1% (=1 g/l) 2.411

Estimated half-life:

The N-terminal of the sequence considered is M (Met).

The estimated half-life is: 30 hours (mammalian reticulocytes, in vitro).

>20 hours (yeast, in vivo).

>10 hours (Escherichia coli, in vivo).

Instability index:

The instability index (II) is computed to be 31.34

This classifies the protein as stable.

Aliphatic index: 60.00

Grand average of hydropathicity (GRAVY): -0.558

Appendix 7.92: Nucleotide sequence of recombinant lysostaphin (construct 5)

ATGGCTGCAACACATGAACATTCAGCACAATGGTTGAATAATTACAAAAAGGATATGGTTACGGT
CCTTATCCATTAGGTATAAATGGCGGTATGCACTACGGAGTTGATTTTTTATGAATATTGGAACAC
CAGTAAAAGCTATTTCAAGCGGAAAAATAGTTGAAGCTGGTTGGAGTAATTACGGAGGAGGTAAT
CAAATAGGTCTTATTGAAAATGATGGAGTGCATAGACAATGGTATATGCATCTAAGTAAATATAATGT
TAAAGTAGGAGATTATGTCAAAGCTGGTCAAATAATCGGTTGGTCTGGAAGCACTGGTTATTCTAC
AGCACCATTTACACTTCCAAAGAATGGTTAATTCATTTTCAAATTCAACTGCCCAAGATCCAAT
GCCTTTCTTAAAGAGCGCAGGATATGGAAAAGCAGGTGGTACAGTAACTCCAACGCCGAATACA
GGTTGGAACAACAACAATATGGCACACTATATAAATCAGAGTCAGCTAGCTTCACACCTAATACA
GATATAATAACAAGAACGACTGGTCCATTTAGAAGCATGCCGCAGTCAGGAGTCTTAAAAGCAGG
TCAAACAATTCATTATGATGAAGTGATGAAACAAGACGGTCATGTTTGGGTAGGTTATACAGGTAA
CAGTGGCCAACGTATTTACTTGCCTGTAAGAACATGGAATAAATCTACTAATACTTTAGGTGTTCTT
TGGGGAACATAAAGTGA

Appendix 7.93: Predicted amino acid sequence of recombinant lysostaphin (construct 5)

MAATHEHSAQWLNNYKKGYGYGPYPLGINGGMHYGVDFFMNIGTPVKAISSGKIVEAGWSNYGGG
NQIGLIENDGVHRQWYMHLISKYNVKVGDYVKAGQIIGWSGSTGYSTAPHLHFQRMVNSFSNSTAQD
PMPFLKSAGYGKAGGTVTPPTNTGWKTNKYGTLYKSESASFTPNTDIITRTTGPFRRSMPQSGVLKAG
QTIHYDEVKQDGHVWVGYTGNVSGQRIYLPVRTWNKSTNTLGVLVGTLK-

Appendix 7.94: ProtParam analysis of recombinant lysostaphin (construct 5) with a retained *N*-terminal methionine residue

User-provided sequence:

```
      10      20      30      40      50      60
MAATHEHSAQ WLNNYKKGYG YGPYPLGING GMHYGVDFFM NIGTPVKAIS SGKIVEAGWS

      70      80      90     100     110     120
NYGGGNQIGL IENDGVHRQW YMHLISKYNVK VGDYVKAGQI IGWSGSTGYS TAPHLHFQRM

     130     140     150     160     170     180
VNSFNSSTAQ DPMPFLKSAG YGKAGGTVTP TPNTGWKTNK YGTLYKSESA SFTPNTDIIT

     190     200     210     220     230     240
RTTGPFRRSMP QSGVLKAGQT IHYDEVKQD GHVWVGYTGN SGQRIYLPVR TWNKSTNTLG

VLWGTIK
```

Number of amino acids: 247

Molecular weight: 27075.4

Theoretical pI: 9.59

Amino acid composition: [CSV format](#)

Ala (A)	12	4.9%
Arg (R)	6	2.4%
Asn (N)	16	6.5%
Asp (D)	7	2.8%
Cys (C)	0	0.0%
Gln (Q)	10	4.0%
Glu (E)	5	2.0%
Gly (G)	35	14.2%
His (H)	9	3.6%
Ile (I)	13	5.3%
Leu (L)	11	4.5%
Lys (K)	16	6.5%
Met (M)	8	3.2%
Phe (F)	7	2.8%
Pro (P)	12	4.9%
Ser (S)	19	7.7%
Thr (T)	22	8.9%
Trp (W)	8	3.2%
Tyr (Y)	16	6.5%
Val (V)	15	6.1%
Pyl (O)	0	0.0%
Sec (U)	0	0.0%
(B)	0	0.0%
(Z)	0	0.0%
(X)	0	0.0%

Total number of negatively charged residues (Asp + Glu): 12

Total number of positively charged residues (Arg + Lys): 22

Appendix 7.94: ProtParam analysis of recombinant lysostaphin (construct 5) with a retained N-terminal methionine residue (continued).

Atomic composition:

Carbon	C	1218
Hydrogen	H	1831
Nitrogen	N	333
Oxygen	O	355
Sulfur	S	8

Formula: $C_{1218}H_{1831}N_{333}O_{355}S_8$
Total number of atoms: 3745

Extinction coefficients:

Extinction coefficients are in units of $M^{-1} cm^{-1}$, at 280 nm measured in water.

Ext. coefficient	67840
Abs 0.1% (=1 g/l)	2.506

Estimated half-life:

The N-terminal of the sequence considered is M (Met).

The estimated half-life is: 30 hours (mammalian reticulocytes, in vitro).
>20 hours (yeast, in vivo).
>10 hours (Escherichia coli, in vivo).

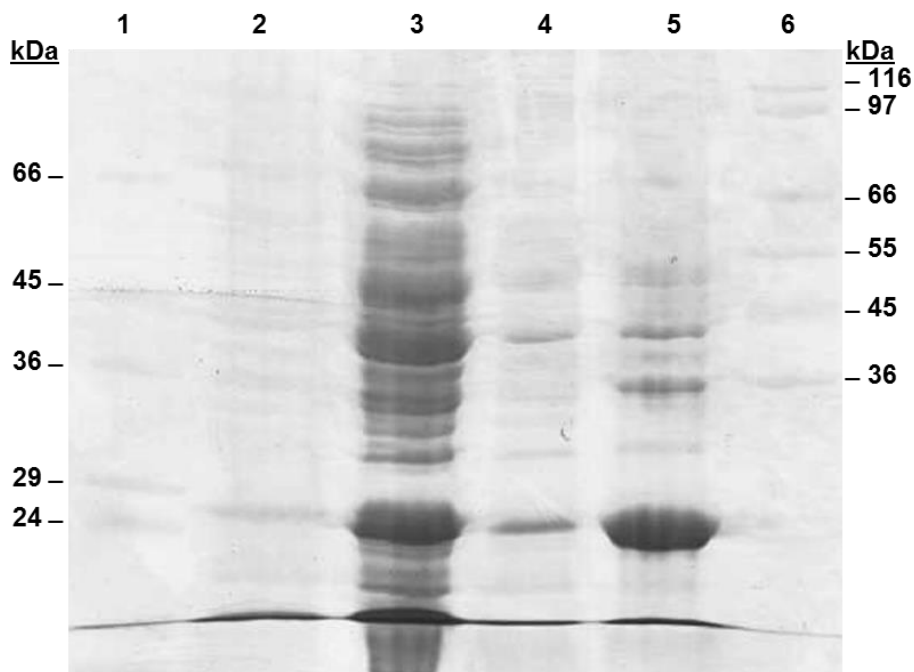
Instability index:

The instability index (II) is computed to be 32.68
This classifies the protein as stable.

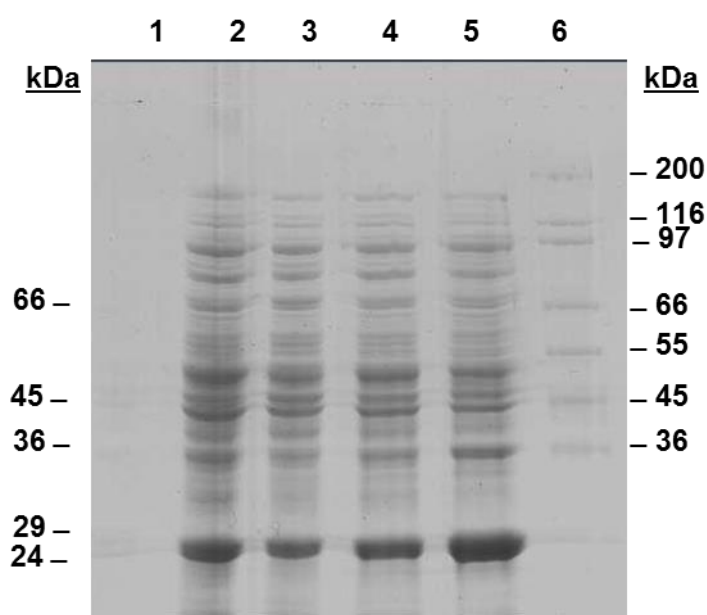
Aliphatic index: 60.36

Grand average of hydropathicity (GRAVY): -0.499

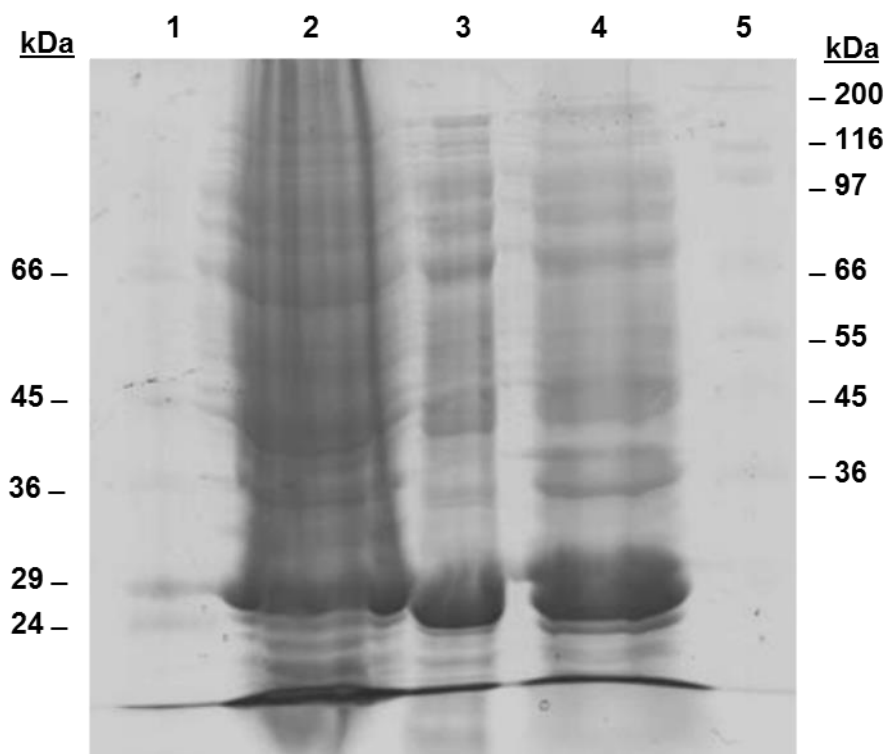
Appendix 7.95: Cytoplasmic expression of recombinant lysostaphin (construct 2) by *E. coli* BL21(DE3) cultured in AIM. Lane 1: Sigma low molecular weight markers; Lane 2: CFE (1:100); Lane 3: CFE (neat); Lane 4: CFE (1:10); Lane 5: CFE in solubilising buffer; Lane 6: Sigma high molecular weight markers.



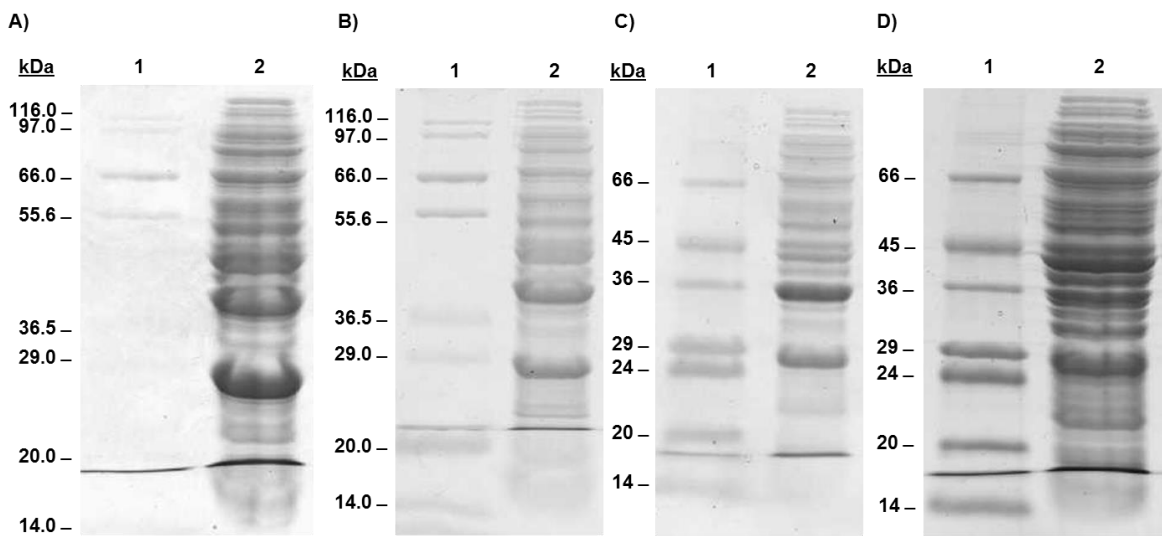
Appendix 7.96: Cytoplasmic expression of C-terminally His-tagged recombinant lysostaphin in *E. coli* BL21(DE3) cultured in AIM. Lane 1: Sigma low molecular weight markers; Lane 2: CFE (neat); Lane 3: CFE (1:10); Lane 4: CFE (1:100); Lane 5: CFE in solubilising buffer; Lane 6: Sigma high molecular weight markers.



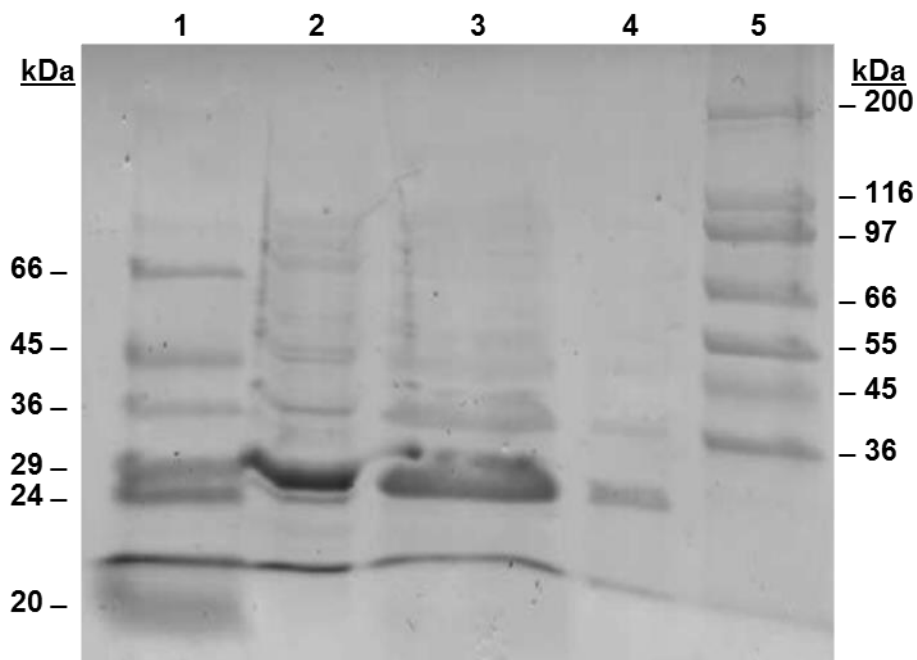
Appendix 7.97: Periplasmic expression of C-terminally His-tagged recombinant lysostaphin (construct 4) in *E. coli* BL21 (DE3) cultured in AIM. Lane 1: Sigma low molecular weight markers; Lane 2: periplasmic lysate in solubilising buffer sample; Lane 3: periplasmic lysate (neat); Lane 4: periplasmic lysate (1:10); Lane 5: Sigma high molecular weight markers.



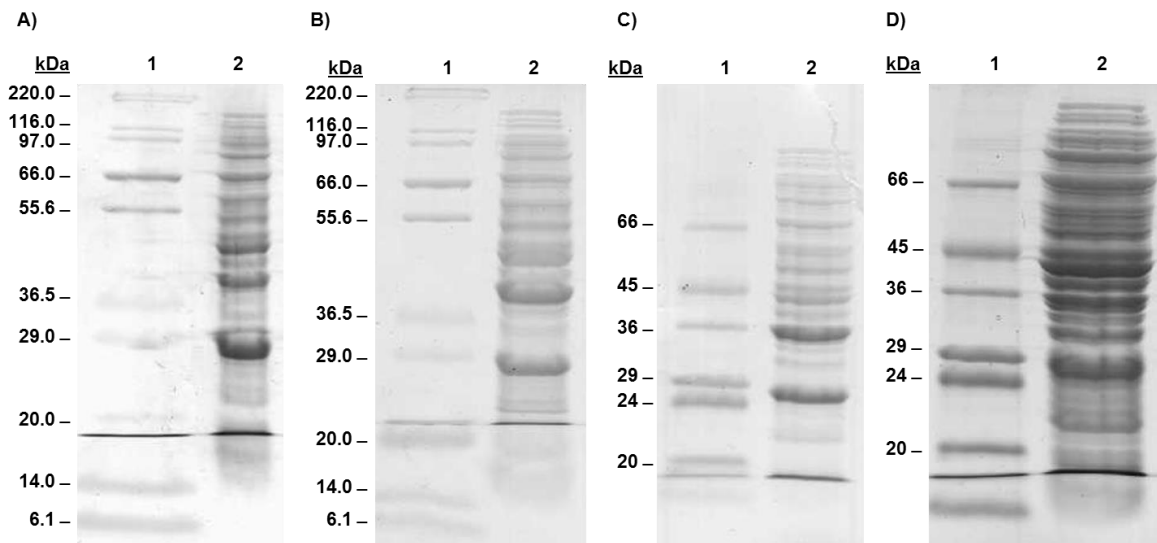
Appendix 7.98: Periplasmic expression of C-terminally His-tagged recombinant lysostaphin (construct 4). *E. coli* BL21(DE3) harbouring plasmid DNA encoding construct 4 was cultured and the expressed C-terminally recombinant lysostaphin was harvested from periplasm on several separate occasions (A-D). In each instance, a hyper-expressed protein was observed with a molecular weight of around 28 kDa, which was likely to represent recombinant lysostaphin. The harvested cell lysates also showed evidence of larger proteins with molecular weights of around 36 kDa and 45 kDa, which were especially prevalent in the harvested periplasmic lysate. A) Lane 1: NZY broad range size marker; Lane 2: periplasmic lysate (neat). B) Lane 1: NZY broad range size marker; Lane 2: periplasmic lysate (neat). C) Lane 1: Sigma low molecular weight markers; Lane 2: periplasmic lysate (neat). D) Lane 1: Sigma low molecular weight markers; Lane 2: periplasmic lysate (neat).



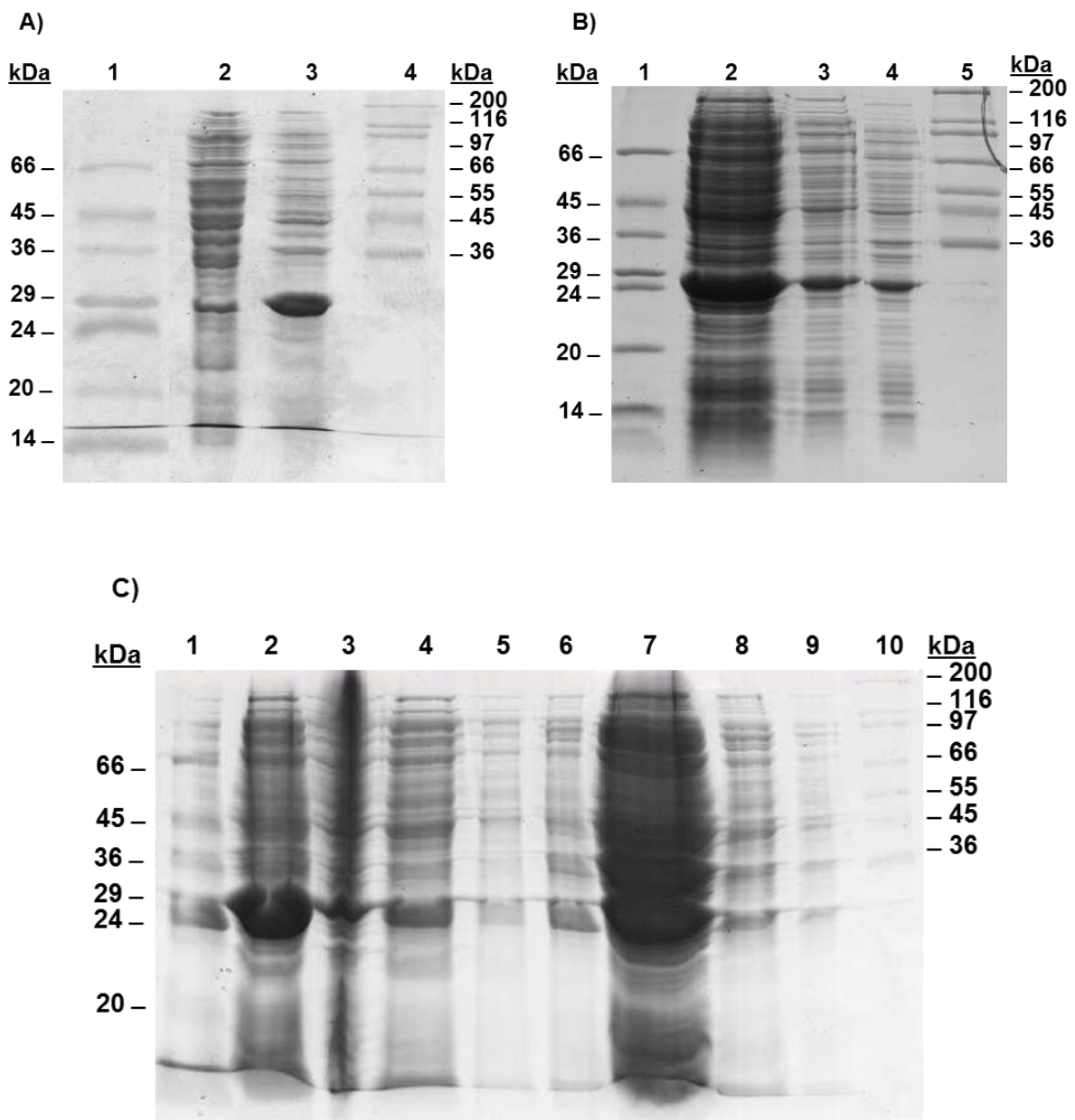
Appendix 7.99: Periplasmic expression of recombinant lysostaphin (construct 5) by *E. coli* BL21(DE3) cultured in AIM. Lane 1: Sigma low molecular weight markers; Lane 2: periplasmic cell lysate in solubilising buffer; Lane 3: periplasmic lysate (neat); Lane 4: periplasmic lysate (1:10); Lane 5: Sigma high molecular weight markers.



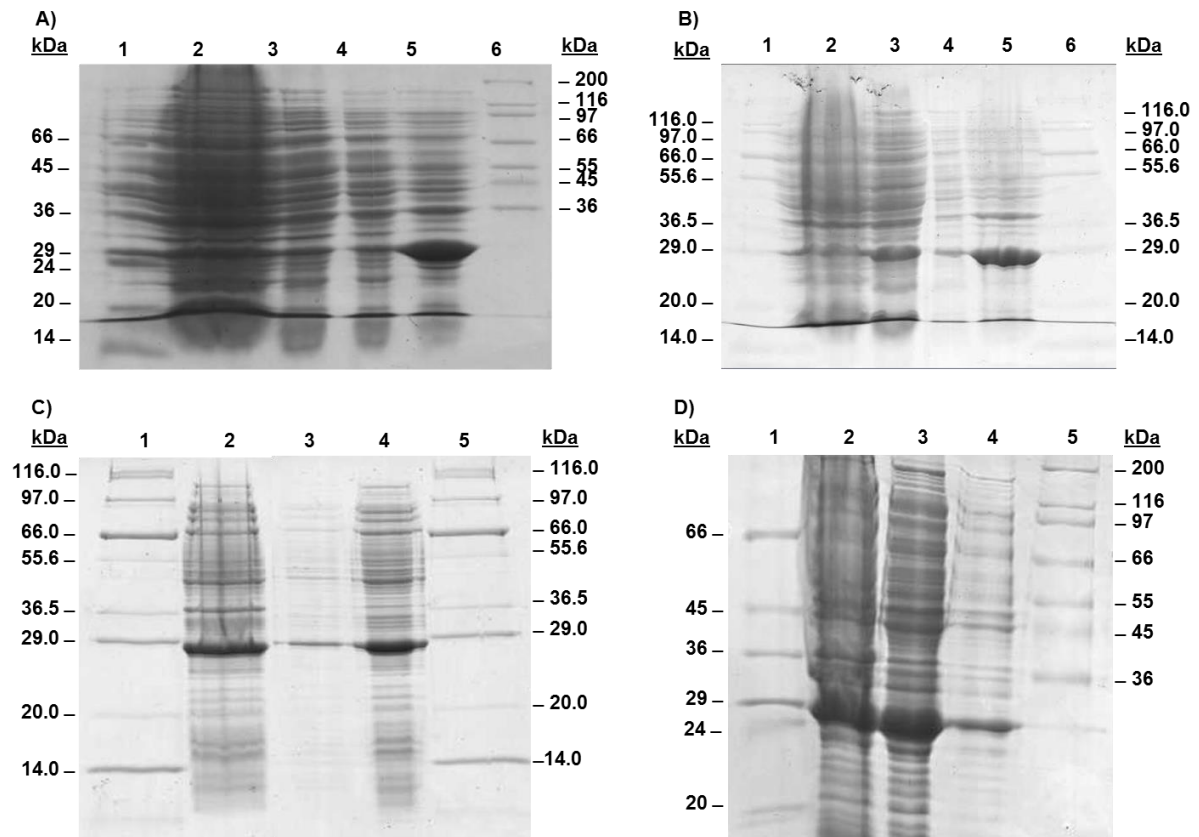
Appendix 7.100: Periplasmic expression of recombinant lysostaphin (construct 5) in *E. coli* BL21(DE3) cultured in AIM media. Recombinant lysostaphin was harvested from periplasm on several separate occasions (A-D). In each instance, a hyper-expressed protein was observed with a molecular weight of around 27 kDa, which was likely to represent recombinant lysostaphin. The harvested cell lysates also showed evidence of larger proteins with molecular weights of around 36 kDa and 45 kDa, which were especially prevalent in the harvested periplasmic lysate. A) Lane 1: NZY broad range size marker; Lane 2: periplasmic lysate (neat). B) Lane 1: NZY broad range size marker; Lane 2: periplasmic lysate (neat). C) Lane 1: Sigma low molecular weight markers; Lane 2: periplasmic lysate (neat). D) Lane 1: Sigma low molecular weight markers; Lane 2: periplasmic lysate (neat).



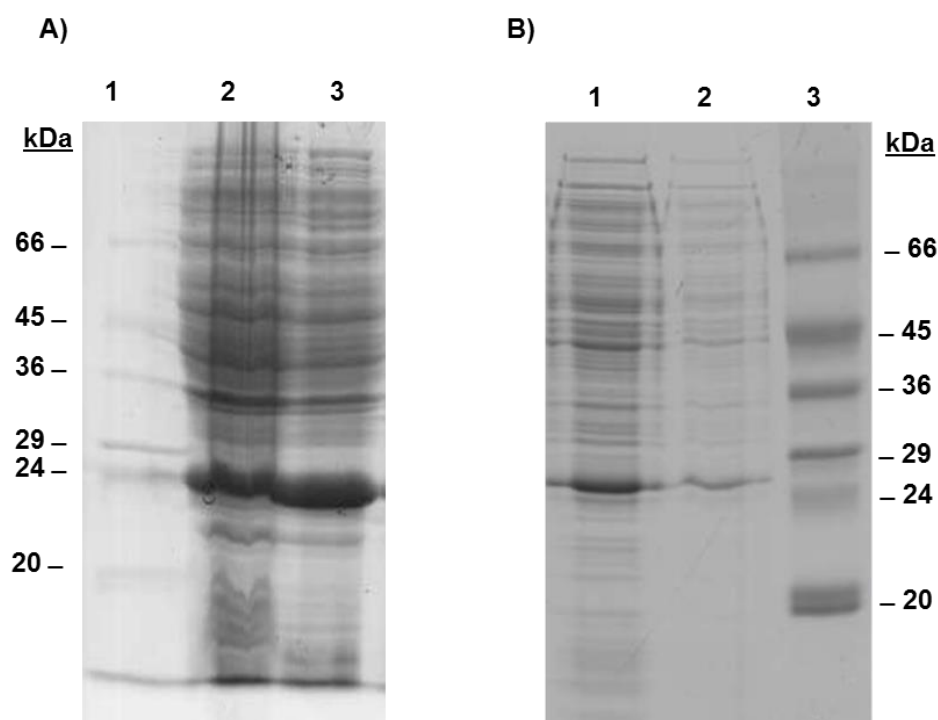
Appendix 7.101: Expression of *N*-terminally His-tagged recombinant lysostaphin (construct 1) using different expression media. In each instance, over-expression of protein with a molecular weight of around 29 kDa, was observed indicating the presence of *N*-terminally His-tagged recombinant lysostaphin. A) Recombinant protein expression in AIM; Lane 1: Sigma low molecular weight markers; Lane 2: CFE (1:10); Lane 3: CFE in solubilising buffer, Lane 4: Sigma high molecular weight markers. B) Recombinant protein expression in LB. Lane 1: Sigma low molecular weight markers; Lane 2: CFE (neat); Lane 3: CFE (1:10); Lane 4: CFE in solubilising buffer; Lane 5: Sigma high molecular weight markers. C) Recombinant protein expression in TB; Lane 1: Sigma low molecular weight markers; Lane 2: CFE in solubilising buffer, Lane 3: CFE (neat), Lane 4: CFE (1:10), Lane 5: CFE (1:100); Recombinant protein expression in MM; Lane 6: CFE in solubilising buffer, Lane 7: CFE (neat), Lane 8: CFE (1:10), Lane 9: CFE (1:100); Lane 10: Sigma high molecular weight markers.



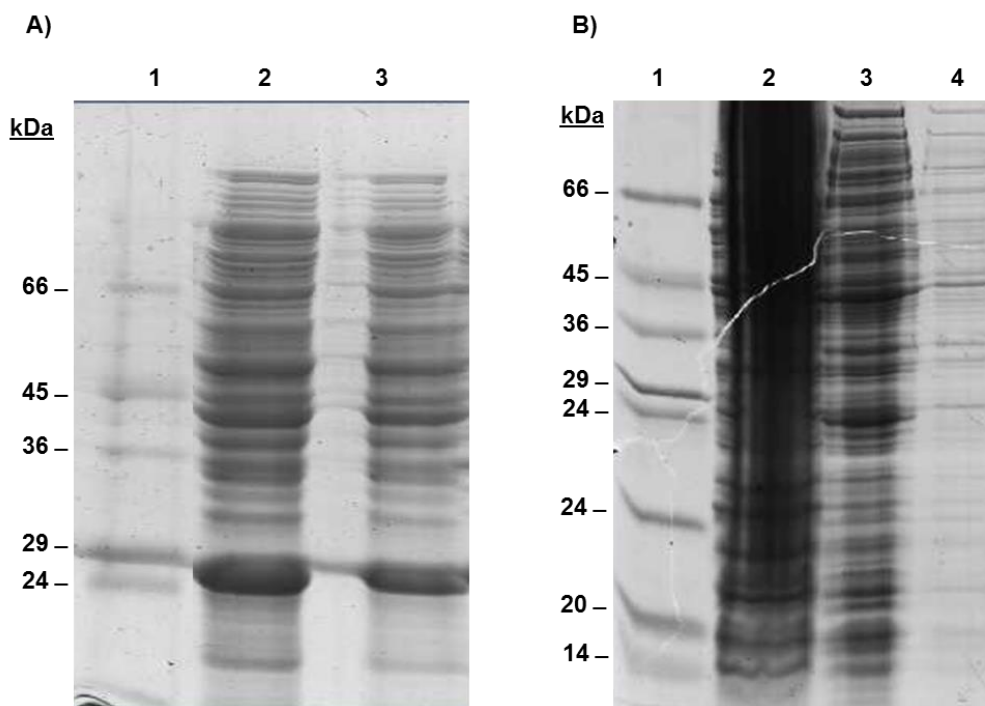
Appendix 7.102: Cytoplasmic expression of N-terminally His-tagged recombinant lysostaphin (construct 1) in *E. coli* BL21(DE3) in AIM or LB. CFE was analysed by SDS-PAGE. A) Expression of construct 1 in AIM. Lane 1: Sigma low molecular weight markers; Lane 2: CFE (neat); Lane 3: CFE (1:10); Lane 4: CFE (1:100); Lane 5: CFE in solubilising buffer; Lane 6: Sigma high molecular weight markers. B) Expression of construct 1 in AIM. Lane 1: NZY broad range size markers; Lane 2: CFE (neat); Lane 3: CFE (1:10); Lane 4: CFE (1:100); Lane 5: CFE in solubilising buffer; Lane 6: NZY broad range size markers; C) Expression of construct 1 in LB. Lane 1: NZY broad range size markers; Lane 2: CFE (1:10); Lane 3: CFE (1:100); Lane 4: CFE in solubilising buffer; Lane 5: NZY broad range size markers. D) Expression of construct 1 in LB. Lane 1: Sigma low molecular size markers; Lane 2: CFE in solubilising buffer; Lane 3: CFE (neat); Lane 4: CFE (1:10); Lane 5: Sigma high molecular weight size markers.



Appendix 7.103: Expression of recombinant lysostaphin (construct 2) using different expression media. In each instance, over-expression of protein with a molecular weight of around 28 kDa, was observed indicating the presence of recombinant lysostaphin. A) Recombinant protein expression in AIM; Lane 1: Sigma low molecular weight markers; Lane 2: CFE (neat); Lane 3: CFE (1:10), B) Recombinant protein expression in LB. Lane 1: CFE (neat); Lane 2: CFE (1:10); Lane 3: Sigma low molecular weight markers.



Appendix 7.104: Expression of C-terminally His-tagged recombinant lysostaphin (construct 3) in *E. coli* BL21(DE3) using different expression media. In each instance, over-expression of protein with a molecular weight of around 28 kDa, was observed indicating the presence of C-terminally His-tagged recombinant lysostaphin. A) Recombinant protein expression in AIM; Lane 1: Sigma low molecular weight markers; Lane 2: CFE (neat); Lane 3: CFE (1:10), B) Recombinant protein expression in LB. Lane 1: Sigma low molecular weight markers; Lane 2: CFE (neat); Lane 3: CFE (1:10); Lane 4: CFE (1:100).



7.1.3 Purification of recombinant lysostaphin

Appendix 7.105: Buffers

Resuspension buffer (1 L)

Tris-HCl, pH 8.0 (10 mM) 1.21 g

Tris-base was dissolved in 18.2 M Ω /cm H₂O and the pH of the buffer was adjusted to pH 8.0 using HCl. The buffer was autoclaved prior to use.

HIC buffer A (1L)

Tris-HCl, pH 8.0 (10 mM) 1.21 g

(NH₄)₂SO₄ (1.5 M) 198.21 g

Tris-base and ammonium sulphate were dissolved in 18.2 M Ω /cm H₂O and the pH of the buffer was adjusted to pH 8.0 using HCl. The buffer was autoclaved prior to use.

HIC buffer B (1 L)

Tris-HCl, pH 8.0 (10 mM) 1.21 g

Tris-base was dissolved in 18.2 M Ω /cm H₂O and the pH of the buffer was adjusted to pH 8.0 using HCl. The buffer was autoclaved prior to use.

Column storage buffer (1 L)

EtOH (20%, v/v) 200 ml

EtOH was added to 800 ml of 18.2 M Ω /cm H₂O.

GF buffer (1L)

Tris-HCl, pH 8.0 (25 mM) 3.03 g

NaCl (200 mM) 11.68 g

Tris-base and NaCl were dissolved in 18.2M Ω /cm H₂O and the pH of the buffer was adjusted to pH 8.0 using HCl. The buffer was autoclaved prior to use.

AXC buffer A (1 L)

Tris-HCl, pH 8.0 (25 mM) 3.03 g

Tris-base was dissolved in 18.2 MΩ/cm H₂O and the pH of the buffer was adjusted to pH 8.0 using HCl. The buffer was autoclaved prior to use.

AXC buffer B (1 L)

Tris-HCl, pH 8.0 (25 mM) 3.03 g

NaCl (1 M) 58.44 g

Tris-base and NaCl were dissolved in 18.2 MΩ/cm H₂O and the pH of the buffer was adjusted to pH 8.0 using HCl. The buffer was autoclaved prior to use.

CXC buffer A (1 L)

HEPES (50 mM) 11.9 g

HEPES was dissolved in 18.2 MΩ/cm H₂O and the pH of the buffer was adjusted to pH 8.0 using NaOH. The buffer was autoclaved prior to use.

CXC buffer B (1L)

HEPES (50 mM) 11.90 g

NaCl (1.0 M) 58.44 g

HEPES and NaCl were dissolved in 18.2 MΩ/cm H₂O and the pH of the buffer was adjusted to pH 8.0 using NaOH. The buffer was autoclaved prior to use.

CXC storage buffer (1L)

EtOH (20%) 200.0 ml

NaC₂H₃O₂ (0.2 M) 16.4 g

EtOH and sodium acetate were added to an appropriate volume of 18.2 MΩ/cm H₂O.

IMAC buffer A (1 L)

Sodium phosphate (20 mM) 100 ml of 200 mM stock solution

Imidazole (10 mM)	0.68 g
NaCl (500 mM)	29.20 g

Sodium phosphate stock solution, imidazole and NaCl were combined and dissolved in 18.2 MΩ/cm H₂O, before the pH of the buffer was adjusted to pH 7.4 using NaOH. The buffer was autoclaved prior to use.

IMAC buffer B (1L)

Sodium phosphate (20 mM)	100 ml of 200 mM stock solution
Imidazole (500 mM)	34.04 g
NaCl (500 mM)	29.20 g

Sodium phosphate stock solution, imidazole and NaCl were combined and dissolved in 18.2 MΩ/cm H₂O, before the pH of the buffer was adjusted to pH 7.4 using NaOH. The buffer was autoclaved prior to use.

Appendix 7.106: Chemicals

EDTA (1 L)

EDTA (100 mM)	37.22 g
---------------	---------

EDTA was dissolved in 18.2 MΩ/cm H₂O and the pH of the buffer was adjusted to pH 8.0 using NaOH. The solution was autoclaved prior to use.

NaH₂PO₄ stock solution (1 L)

NaH ₂ PO ₄ ·H ₂ O (200 mM)	27.6 g
Na ₂ HPO ₄ ·H ₂ O (200 mM)	28.4 g

NaH₂PO₄·H₂O and Na₂HPO₄·H₂O were dissolved in 18.2 MΩ/cm H₂O to create two separate solutions. Appropriate volumes of each solution were combined to create buffers with appropriate pH and molarity. The stock solution was autoclaved prior to use.

NiSO₄ (1 L)

NiSO ₄ (100 mM)	
----------------------------	--

NiSO₄ was dissolved in 18.2 MΩ/cm H₂O.

Appendix 7.107: Equipment

Protein purifications were performed using an ÄKTA™ prime plus purification system, a FPLC system, a peristaltic pump or an Ultimate™ 3000 Titanium system.

The ÄKTA™ prime plus purification system consisted of a gradient pump, buffer selection valves, a UV and conductivity detector and a fraction collector. The system was fitted with a 100 µl injection loop. Data collection and analysis was performed using PrimeView™ 5.0 evaluation software.

The FPLC system consisted of a Pharmacia LKB pump P-500, a Pharmacia LKB controller LCC-501 plus, buffer selection valves, a Unicord VW 2251 detector and a Pharmacia LKB Frac-100 fraction collector. Data collection and analysis was performed using FPLC director™ version 1.03 software.

Large-scale IMAC purifications were performed using an Eylea microtube peristaltic pump (MP3). Chromatographic flow was manually adjusted to provide flow rates of 0-10 ml/min. Protein elution was monitored by Bradford's assay during each step elution (Appendix 7.24).

The Ultimate™ 3000 Titanium system consisted of an analytical titanium pump, a thermal compartment with two column change valves, a VWD detector and a WPS-3000 Biocompatible autosampler. The autosampler was fitted with 250 µl syringe and a 1 ml injection loop. Although the autosampler could accommodate fractionation, fractionation was performed using an ISCO Foxy® Jr Fraction collector in this instance. Data collection and analysis was performed using a Chromeleon® Chromatography Data System software with fractionation license.

Chromatographic separations were performed using a number of separation modes and columns, as described in Appendix 7.108.

Appendix 7.108: Chromatography columns used during purification of recombinant lysostaphin

Separation Mode	Column	Chromatography System	Dimension (mm)
IMAC	Chelating Sepharose™ Fast Flow, XK 16/20	ÄKTA™ prime plus	16.0 x 50
	Chelating Sepharose™ Fast Flow, XK 50/20	Peristaltic pump	50.0 x 12
	ProPac® IMAC-10	Ultimate™ 3000	2.0 x 250
	ProPac® IMAC-10	Ultimate™ 3000	4.0 x 250
HIC	Phenyl Sepharose™ High Performance, XK 16/20	ÄKTA™ prime plus	16.0 x 55
GF	HiLoad™ 16/60 Superdex 200prep grade	FPLC	16.0 x 600
CXC	Source™ 30S media, XK 16/20	ÄKTA™ prime plus	16.0 x 32
AXC	Source™ 30Q media XK 16/20	ÄKTA™ prime plus	16.0 x 40

Appendix 7.109: Ammonium sulphate fractionation

Extracted cell lysate was mixed with 20% (w/v) ammonium sulphate at 4°C until dissolved. The solution was centrifuged at 4000 x g and 4°C for 5 min before retaining the supernatant and re-suspending the resulting pellet in 10 ml of resuspension buffer. The ammonium sulphate concentration of the supernatant was increased to 30% (w/v) and the solution was mixed at 4°C until the ammonium sulphate had dissolved. The solution was centrifuged at 4000 x g for 5 min before retaining the supernatant and re-suspending the resulting pellet in 10 ml of resuspension buffer. This process was repeated whilst steadily increasing the saturation of ammonium sulphate from 30% to 40% and then 60% (w/v). The resuspended pellets from each stage of fractionation and the remaining supernatant were analysed by SDS-PAGE to establish the ammonium sulphate concentration at which recombinant lysostaphin became insoluble.

To concentrate a sample during protein purification, recombinant lysostaphin was precipitated through the addition of 50 or 60% (w/v) ammonium sulphate, before mixing at 4°C until dissolved. Once dissolved, the precipitation was centrifuged at 4000 x g for 5 min. The pellet was resuspended in a buffer which was compatible with the subsequent chromatographic purification method.

Appendix 7.110: HIC using Phenyl Sepharose™ High Performance media and an ÄKTA™ purification system

An XK 16/20 column was packed with Phenyl Sepharose™ High Performance media and incorporated into an ÄKTA™ purification system. The column was packed to a bed height of approximately 5.5 cm and had previously been equilibrated with 100 ml of HIC buffer A at a flow rate of 5.0 ml/min. CFE was loaded onto the column at a flow rate of 2.0 ml/min via buffer line C. Following application, 100% of HIC buffer A was applied to the column for 10 min at flow rate of 2.0 ml/min using the same buffer line, to ensure that the CFE had been fully loaded onto to column. The target protein was eluted by applying a linear gradient from 0-100% of HIC buffer B over 50 min at 5.0 ml/min. Absorbance at 280 nm was monitored throughout the separation and the data was acquired using PrimeView™ software. The column eluate was collected as fractions in 5 ml volumes and using the chromatogram produced, fractions were selected and analysed by SDS-PAGE (Appendix 7.15). After use, the column was stored in EtOH after flowing 100 ml of column storage buffer through the column at 5.0 ml/min.

Appendix 7.111: GF using HiLoad 16/60 Superdex 200 media and a FPLC system

A gel filtration column packed with HiLoad 16/60 Superdex 200 prep grade was equilibrated with GF buffer at a flow rate of 1 ml/ min using an FPLC system. Following HIC purification and ultrafiltration, concentrated protein (0.5 ml) was manually loaded on to the gel filtration column by injection. The target protein was eluted over 120 min using an isocratic flow rate of 1 ml/ min. Absorbance at 280 nm was monitored throughout the separation and the data was acquired using FPLCdirector™ software. Fractions were collected in 5 ml volumes and fractions thought to contain the target protein were analysed by SDS-PAGE (Appendix 7.15). The column was stored in 20% (v/v) EtOH.

Appendix 7.112: AXC using Source™ 30Q media and an ÄKTA™ purification system

An XK 16/20 column was packed with Source™ 30Q media and incorporated into an ÄKTA™ purification system. The column was packed to a bed height of approximately 4.0 cm and had previously been equilibrated with 100 ml of AXC buffer A at a flow rate of 5.0 ml/min. CFE was loaded onto the column at a flow rate of 2.0 ml/min via buffer line C. Following application, 100% of AXC buffer A was applied to the column for 10 min at flow rate of 2.0 ml/min using the same buffer line, to ensure that the CFE had been fully loaded

onto to column. The target protein was eluted by applying a linear gradient from 0-100% of AXC buffer B over 50 min at 5.0 ml/min. Absorbance at 280 nm was monitored throughout the separation and the data was acquired using PrimeView™ software. The column eluate was collected as fractions in 5 ml volumes. The purification process was monitored using PrimeView™ software. Using the chromatogram produced, fractions were selected and analysed by SDS-PAGE (Appendix 7.15). After use, the column was stored in EtOH after flowing 100 ml of column storage buffer through the column at 5.0 ml/min.

Appendix 7.113: CXC using Source™ 30S media and an ÄKTA™ purification system

An XK 16/20 column was packed with Source™ 30S media and incorporated into an ÄKTA™ purification system. The column was packed to a bed height of approximately 3.2 cm and had previously been equilibrated with 100 ml of CXC buffer A at a flow rate of 5.0 ml/min. CFE was loaded onto the column at a flow rate of 2.0 ml/min via buffer line C. Following application, 100% of CXC buffer B was applied to the column for 10 min at a flow rate of 2.0 ml/min using the same buffer line, to ensure that the CFE had been fully loaded onto the column. The target protein was eluted by applying a linear gradient from 0-100% of CXC buffer B over 50 min at 5.0 ml/min. Absorbance at 280 nm was monitored throughout the separation and the data was acquired using PrimeView™ software. The column eluate was collected as fractions in 5 ml volumes. The purification process was monitored using PrimeView™ software. Using the chromatogram produced, fractions were selected and analysed by SDS-PAGE (Appendix 7.15). After use, the column was stored in EtOH and sodium acetate, after flowing 100 ml of CXC storage buffer through the column at 5.0 ml/min.

Appendix 7.114: IMAC using Chelating Sepharose™ Fast Flow media and an ÄKTA™ purification system

An XK 16/20 column was packed with Chelating Sepharose™ Fast Flow media and incorporated into an ÄKTA™ purification system. Prior to sample loading, the nickel column had been stripped and charged by sequentially applying 30 ml of 18.2 MΩ/cm H₂O, 30 ml EDTA (100mM), 30 ml of 18.2 MΩ/cm H₂O and 30 ml NiSO₄ (0.1M) at a rate of 5.0 ml/min. The column was then equilibrated with 100 ml of IMAC buffer A at 5.0 ml/min. CFE was loaded onto the column (via buffer line C) at a flow rate of 2.0 ml/min. Following application, 100% of IMAC buffer A was applied to the column for 10 min at a flow rate of 2.0 ml/min using the same buffer line, to ensure that the CFE had been fully loaded onto to column. The

target protein was eluted by applying a linear gradient from 0-100% of IMAC buffer B over 50 min at 5.0 ml/min. Absorbance at 280 nm was monitored throughout the separation and the data was acquired using PrimeView™ software. The column eluate was collected as fractions in 5 ml volumes and fractions thought to contain the target protein were analysed by SDS-PAGE. After use, the column was stored in EtOH after flowing 100 ml of column storage buffer through the column at 5.0 ml/min.

Appendix 7.115: IMAC using Chelating Sepharose™ Fast Flow media and a peristaltic pump

An XK 50/20 column packed with 250 ml of Chelating Sepharose™ Fast Flow media was prepared and used to perform IMAC purification, with the assistance of a peristaltic pump. The nickel column was stripped and charged by sequentially applying 300 ml of 18.2 MΩ/cm H₂O, 300 ml EDTA (100mM), 300 ml of 18.2 MΩ/cm H₂O and 300 ml NiSO₄ (0.1M) at a rate of 5-10 ml/min. The column was then equilibrated with 1000 ml of IMAC buffer A at 5-10 ml/min. CFE was loaded onto the column and the target protein was eluted by applying a step gradient featuring elution buffers containing 50 mM, 100 mM, 200 mM, 300 mM, 400 mM and 500 mM imidazole. At each stage of the step gradient, protein elution was monitored using Bradford's reagent (Appendix 7.24) and the concentration of the imidazole gradient was only increased when Bradford's reagent confirmed that protein elution had ceased. The column eluate at each stage of the step elution was collected and precipitated with ammonium sulphate or dialysed (Appendix 7.109 or Appendix 7.118) and lyophilised to concentrate the eluted protein (Appendix 7.119). The purified protein was analysed by SDS-PAGE. After use, the column was stored in 20% (v/v) EtOH.

Appendix 7.116: IMAC using a ProPac® IMAC-10 column (2 x 250 mm) and an Ultimate™ 3000 system

Prior to purification, the ProPac® IMAC-10 column was stripped and charged through manual injection of 500 µl of EDTA (100 mM) and 1000 µl of NiSO₄ (100 mM). Purified recombinant lysostaphin (preparation 9) was loaded onto the column through automated injection of 8 µg and then 40 µg. During the first 10 min, IMAC buffer A was applied to the column at a flow rate of 0.25 ml/min, to remove non-binding proteins and cellular contaminants. The bound protein was eluted by applying a linear gradient from 0-100% of IMAC buffer B over 20 min at a flow rate of 0.25 ml/min. Fractions were collected by time, every 60 s during this linear

gradient. The column was re-equilibrated for 10 min with 100% of IMAC buffer A at a flow rate of 0.25 ml/ min. UV absorbance was recorded at 214 and 280 nm throughout the purification and the acquired data was analysed using Chromeleon software. The column eluate was collected as fractions in 0.25 ml volumes and fractions thought to contain the target protein were analysed by SDS-PAGE.

Appendix 7.117: IMAC using a ProPac[®] IMAC-10 column (4 x 250 mm) and an Ultimate[™] 3000 system

Prior to purification, the ProPac[®] IMAC-10 column was stripped and charged through manual injection of 500 µl of EDTA (100 mM) and 1000 µl of NiSO₄ (100 mM), CFE (66 ml) was loaded onto the column (via buffer line C) at a flow rate of 1.0 ml/min. Following application of the cell lysate, 100% of IMAC buffer A was applied to the column for 20 min at a flow rate of 1.0 ml/min, to remove non-binding proteins and cellular contaminants. The target protein was eluted by applying a linear gradient from 0-100% of IMAC buffer B over 50 min at 0.5 ml/min. The column was re-equilibrated for 25 min with 100% of IMAC buffer A at a flow rate of 1.0 ml/ min. UV absorbance was recorded at 214 and 280 nm throughout the purification and the acquired data was analysed using Chromeleon[™] software. The column eluate was collected as fractions in 0.25 ml volumes and fractions thought to contain the target protein were analysed by SDS-PAGE (Appendix 7.15).

Appendix 7.118: Dialysis

Dialysis tubing (Sigma Aldrich, USA) was cut into 30 cm strips and boiled for 20 min in 18.2 MΩ/cm H₂O over a Bunsen burner. The boiled dialysis tubing was then rinsed internally and externally four times with 18.2 MΩ/cm H₂O to remove residual surface contaminants, such as glycerol and sodium azide. The washed tubing was used for dialysis immediately or stored in 18.2 MΩ/cm H₂O at 4°C until required.

The prepared dialysis tubing was filled with the eluate following elution with an IMAC elution buffer containing 200 mM imidazole and sealed to prevent leakage. The sealed dialysis tubing was placed into beakers containing 3 L of 18.2 MΩ/cm H₂O and stirred at 4°C for 1 h. It was ensured that the volume of dialysed protein solution did not exceed 1/200 of the volume of the 18.2 MΩ/cm H₂O. After 1 h, the dialysate was replaced with fresh 18.2 MΩ/cm

H₂O and the samples were dialysed for a further 2 h, before exchanging the dialysate and continuing dialysis for a further 3 h. Following 6 h of dialysis, the dialysate was replaced again and dialysis was continued overnight. Following dialysis, the desalted protein solution was lyophilised to concentrate the purified recombinant lysostaphin.

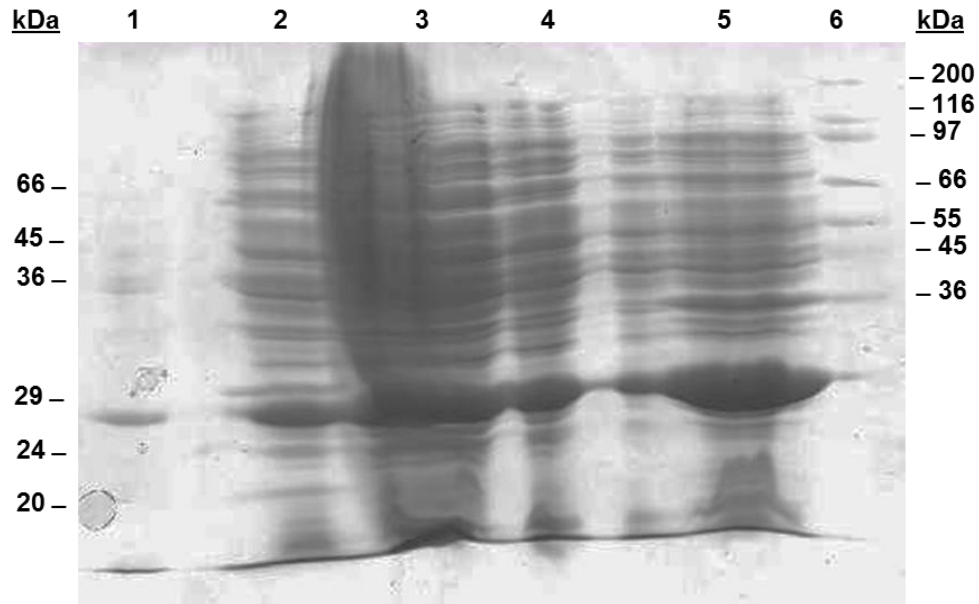
Appendix 7.119: Lyophilisation

Following dialysis, 25 ml aliquots of the protein solution were transferred to Petri dishes, sealed with adhesive tape and frozen at -20°C. The frozen samples were then transferred to a freeze-drier until they had reached complete lyophilisation.

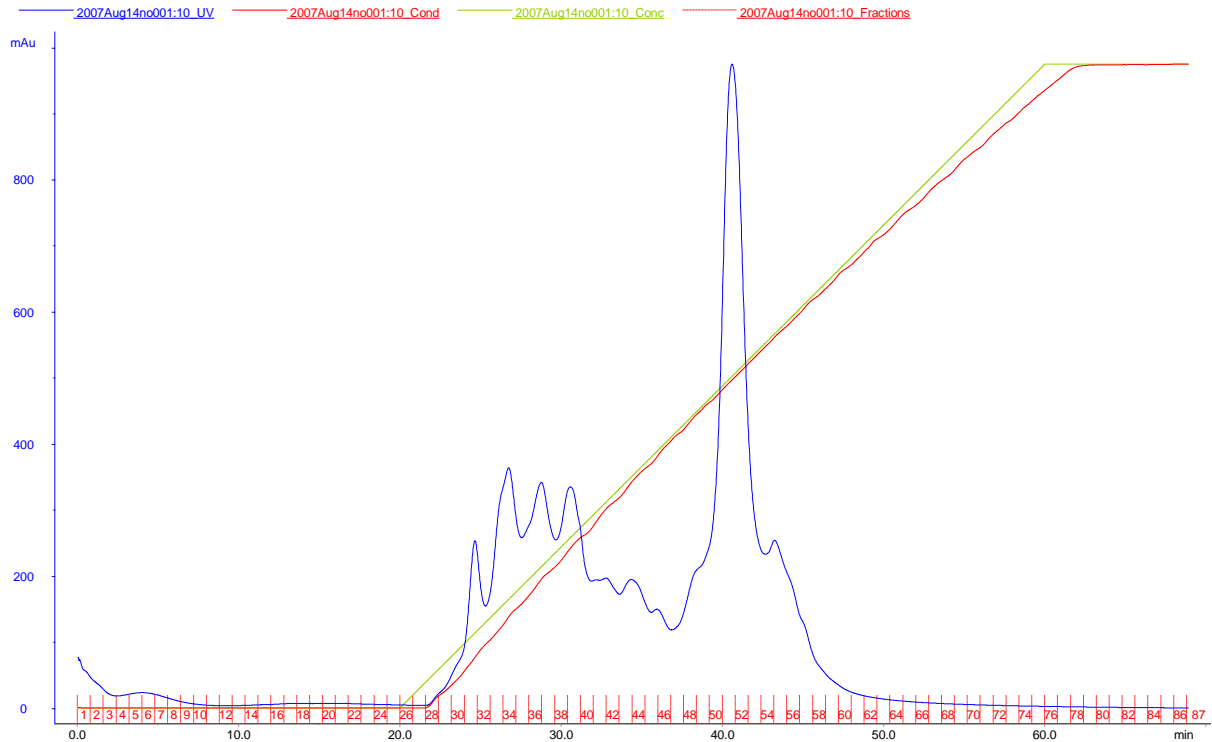
Appendix 7.120: Ultrafiltration

Following purification, chromatographic fractions were analysed by SDS-PAGE to establish which fractions contained the target protein. The fractions containing the target protein were pooled and concentrated using Vivaspin 20 ml ultrafiltration columns with a 10 kDa membrane to remove salts and other contaminating micromolecules (Sartorius Stedim, Germany). After adding the pooled fractions to the column, the column was centrifuged at 4000 x g and 4°C until the volume had been reduced from 20 ml to 0.5 ml. The flow-through was retained and Bradford's reagent was used to confirm that protein had not passed through the ultrafiltration membrane. Once the protein volume had been reduced to 0.5 ml, the protein was washed three times with 20 ml of 18.2 MΩ/cm H₂O by continuing to centrifuge at 4000 x g and 4°C. After the third wash with 18.2 MΩ/cm H₂O, the protein was stored as a 0.5 ml volume at 4°C.

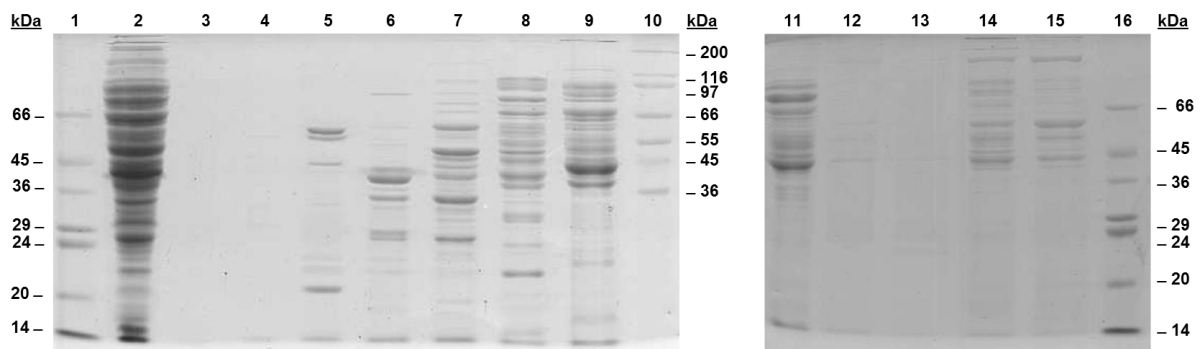
Appendix 7.121: Expression of recombinant lysostaphin (construct 2) in *E. coli* BL21(DE3) cultured in AIM. Over-expression of protein with a molecular weight of around 27 kDa was observed indicating the presence of recombinant lysostaphin. Lane 1: Sigma low molecular weight markers; Lane 2: CFE (neat); Lane 3: CFE (1:10); Lane 4: CFE (1:100); Lane 5: CFE in solubilising cracking buffer; Lane 6: Sigma high molecular weight markers.



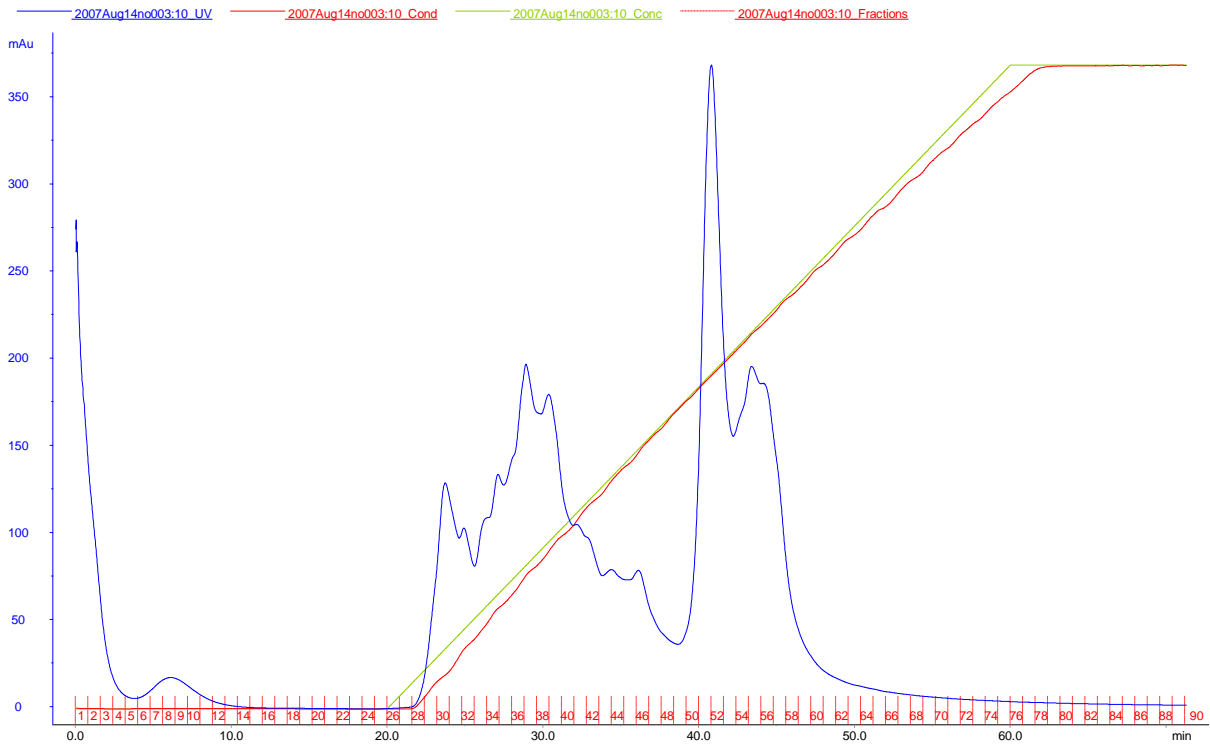
Appendix 7.122: Purification of C-terminally His-tagged recombinant lysostaphin (construct 4) using AXC. Cell lysate extracted from recombinant *E. coli* BL21(DE3) cultured in AIM was applied to the Source™ 30Q column. Bound protein was eluted by applying an increasing NaCl concentration (0-1.0 M).



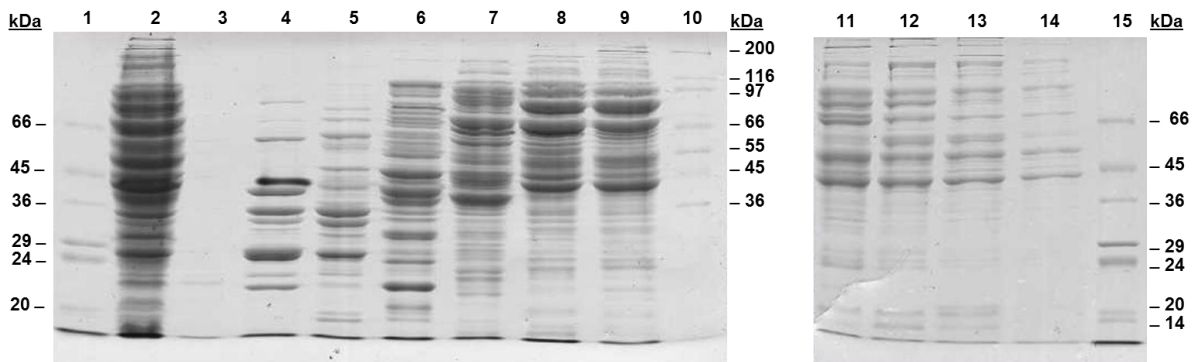
Appendix 7.123: SDS-PAGE analysis of fractions eluted during AXC of cell-lysate containing C-terminally His-tagged recombinant lysostaphin (construct 4). Lane 1: Sigma low molecular weight markers; Lane 2: dialysed lysate (neat); Lane 3: Fraction 26; Lane 4: Fraction 28; Lane 5: Fraction 30; Lane 6: Fraction 32; Lane 7: Fraction 34; Lane 8: Fraction 36; Lane 9: Fraction 38; Lane 10: Sigma high molecular weight markers; Lane 11: Fraction 40; Lane 12: Fraction 42; Lane 13: Fraction 54; Lane 14: Fraction 44; Lane 15: Fraction 46; Lane 16: Sigma low molecular weight markers.



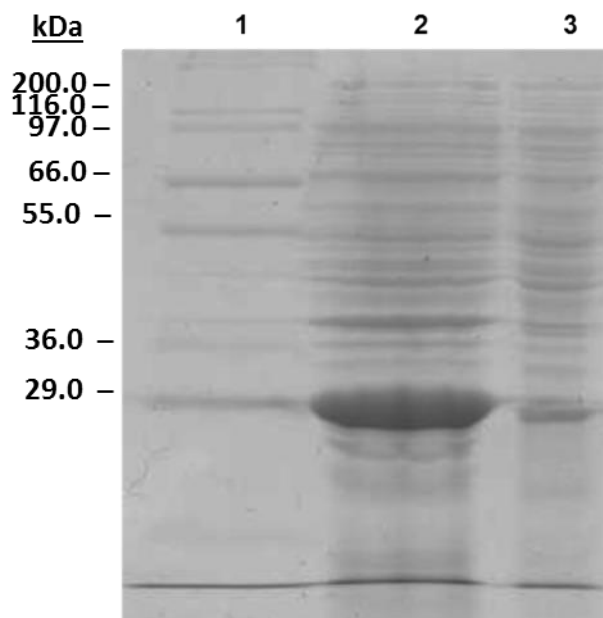
Appendix 7.124: Purification of recombinant lysostaphin (construct 5) using AXC. Cell lysate extracted from recombinant *E. coli* BL21(DE3) cultured in AIM was applied to the Source™ 30Q column. Bound protein was eluted by applying an increasing NaCl concentration (0-1.0 M).



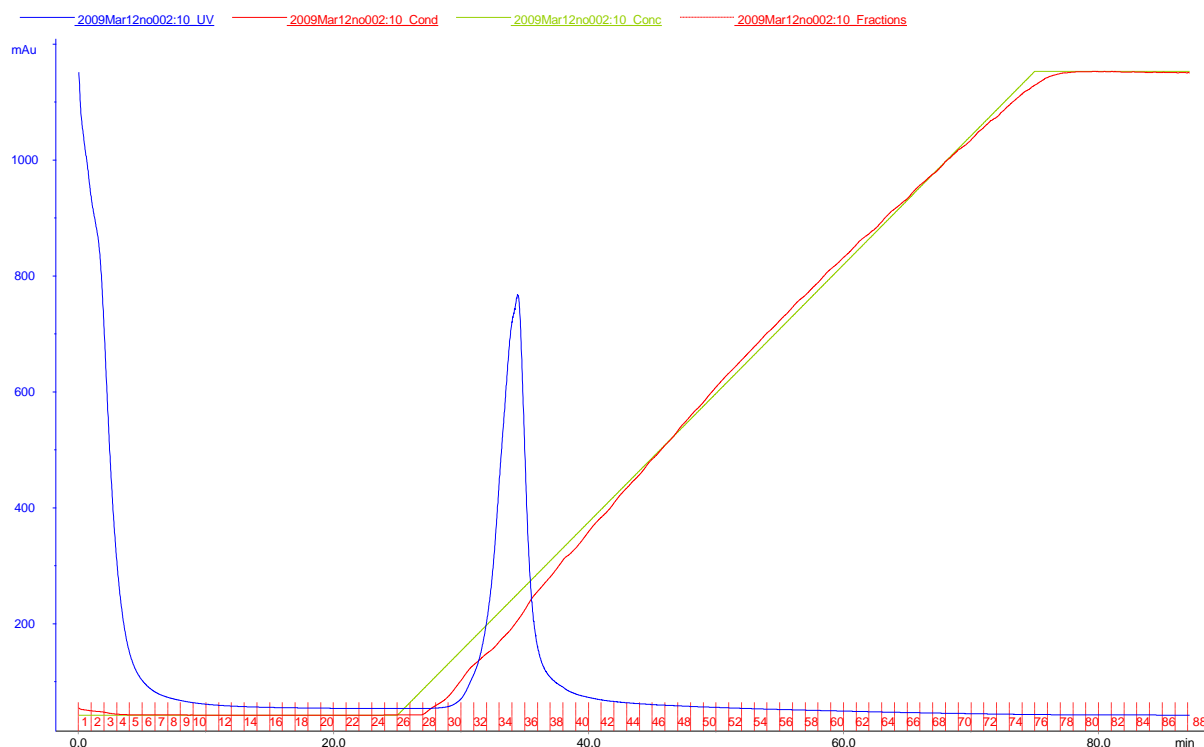
Appendix 7.125: SDS-PAGE analysis of fractions eluted during AXC of cell-lysate containing recombinant lysostaphin (construct 5). Lane 1: Sigma low molecular weight markers; Lane 2: dialysed lysate (neat); Lane 3: Fraction 29; Lane 4: Fraction 31; Lane 5: Fraction 33; Lane 6: Fraction 35; Lane 7: Fraction 37; Lane 8: Fraction 39; Lane 9: Fraction 41; Lane 10: Sigma high molecular weight markers; Lane 11: Fraction 43; Lane 12: Fraction 45; Lane 13: Fraction 47; Lane 14: fraction 49; Lane 15: Sigma low molecular weight markers.



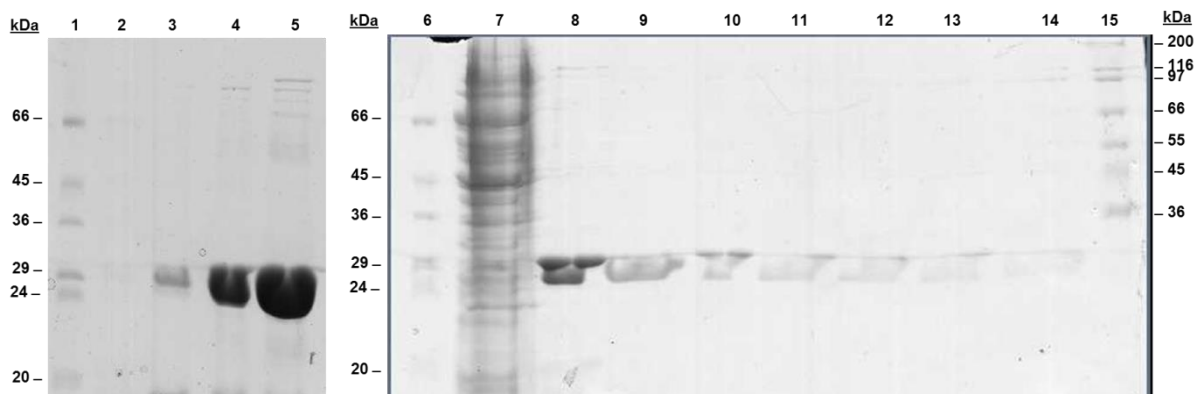
Appendix 7.126: Expression of C-terminally His-tagged recombinant lysostaphin (construct 3) in *E. coli* BL21(DE3) cultured in AIM. Over-expression of protein with a molecular weight of around 28 kDa was observed indicating the presence of C-terminally His-tagged recombinant lysostaphin. Lane 1: Sigma high molecular weight markers; Lane 2: CFE (neat); Lane 3: CFE (1:10).



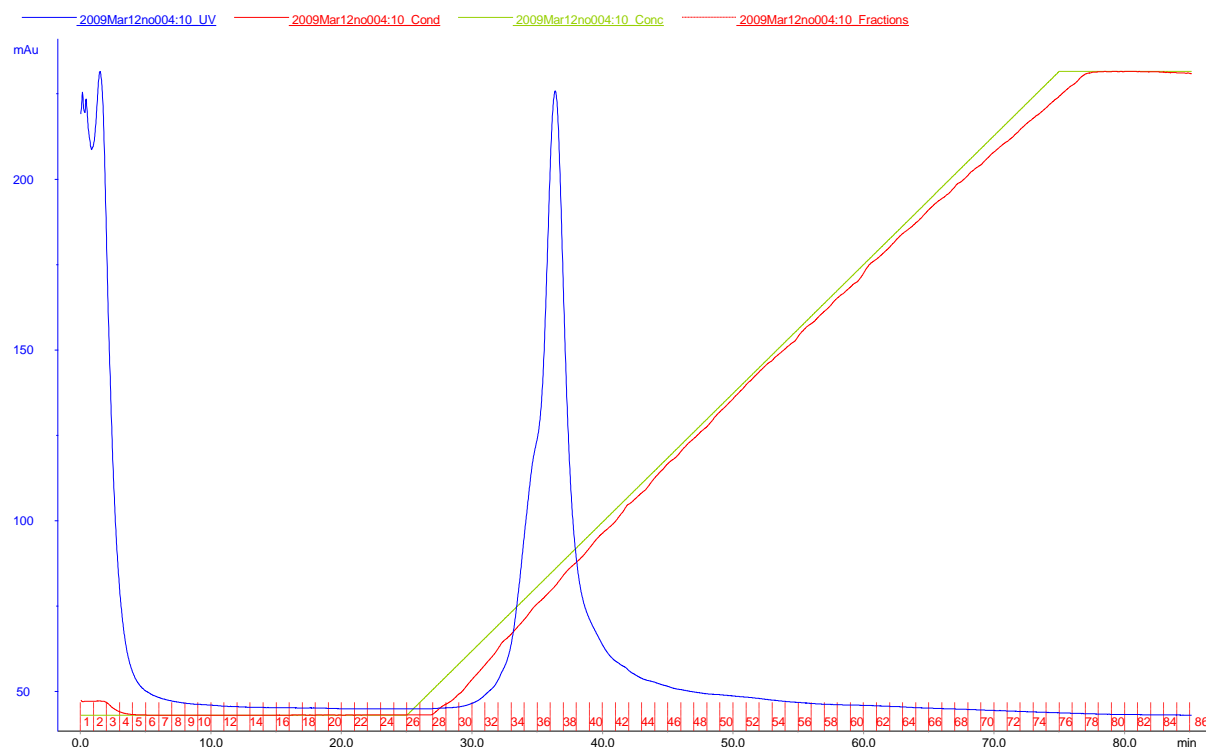
Appendix 7.127: Purification of *N*-terminally His-tagged recombinant lysostaphin (construct 1) using CXC. Cell lysate extracted from recombinant *E. coli* BL21(DE3) cultured in TB was applied to the Source™ 30s column. Bound protein was eluted by applying an increasing NaCl concentration (0-1.0 M).



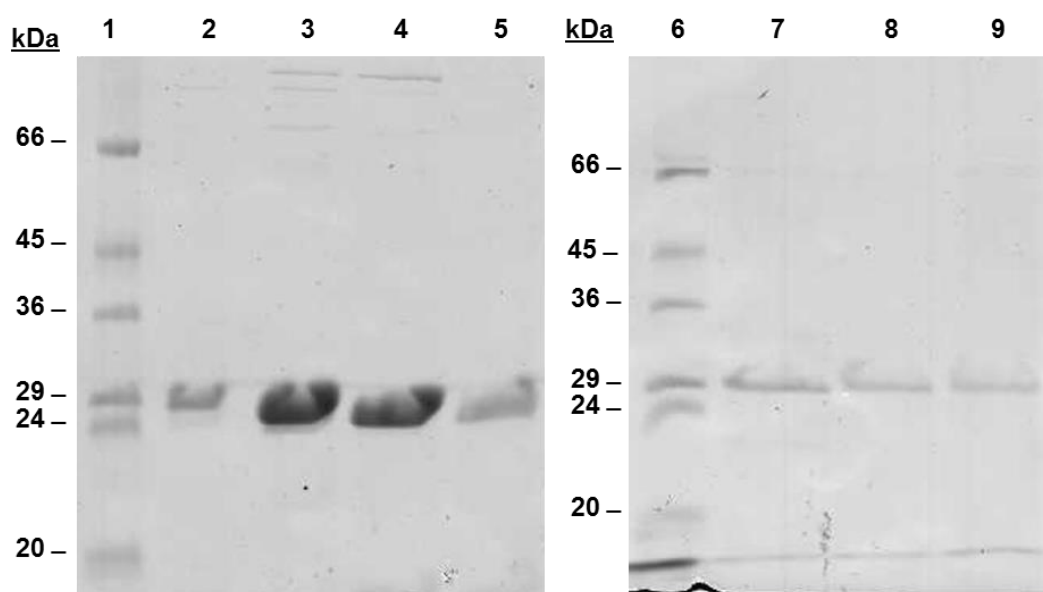
Appendix 7.128: SDS-PAGE analysis of CXC fractions following purification of *N*-terminally His-tagged recombinant lysostaphin (construct 1) derived from *E. coli* BL21(DE3) cultured in TB. Lane 1: Sigma low molecular weight markers; Lane 2: Fraction 20; Lane 3: Fraction 22; Lane 4: Fraction 24; Lane 5: Fraction 26; Lane 6: Sigma low molecular weight markers; Lane 7: Column flow through; Lane 8: Fraction 28; Lane 9: Fraction 30; Lane 10: Fraction 32; Lane 11: Fraction 34; Lane 12: Fraction 36; Lane 13: Fraction 38; Lane 14: Fraction 40; Lane 15: Sigma high molecular weight markers.



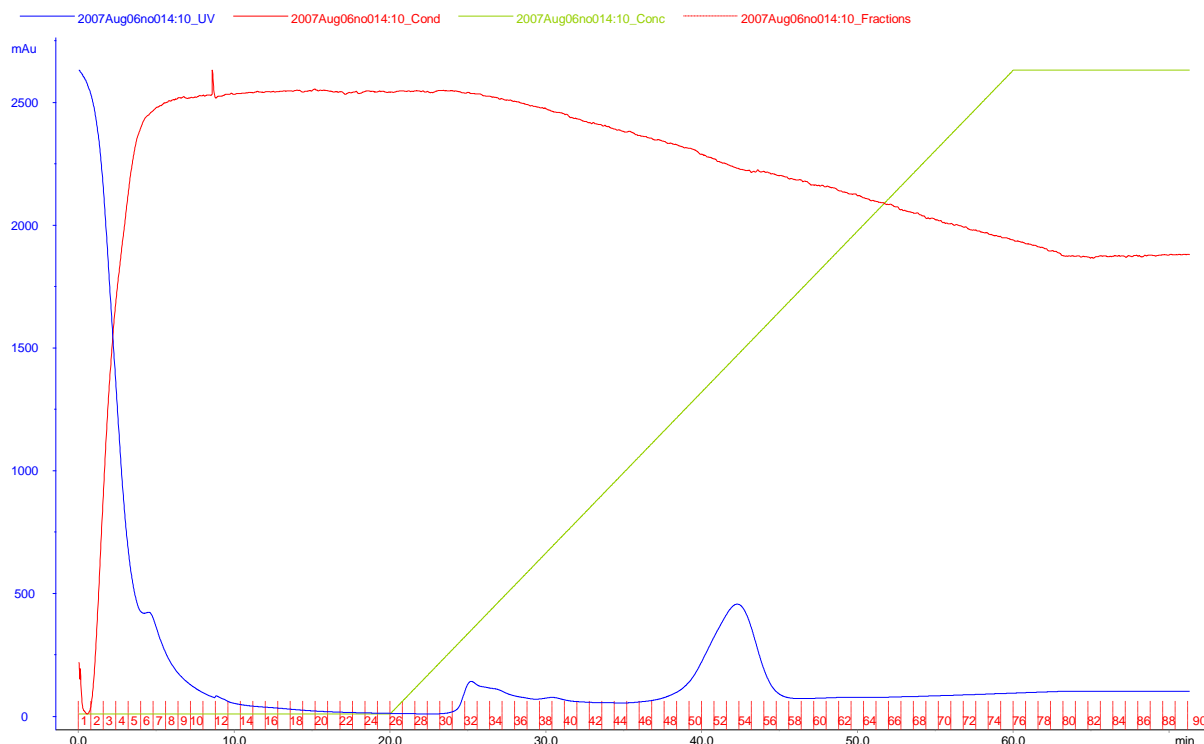
Appendix 7.129: Purification of *N*-terminally His-tagged recombinant lysostaphin (construct 1) using CXC. Cell lysate extracted from recombinant *E. coli* BL21(DE3) cultured in MM was applied to the Source™ 30s column. Bound protein was eluted by applying an increasing NaCl concentration (0-1.0 M).



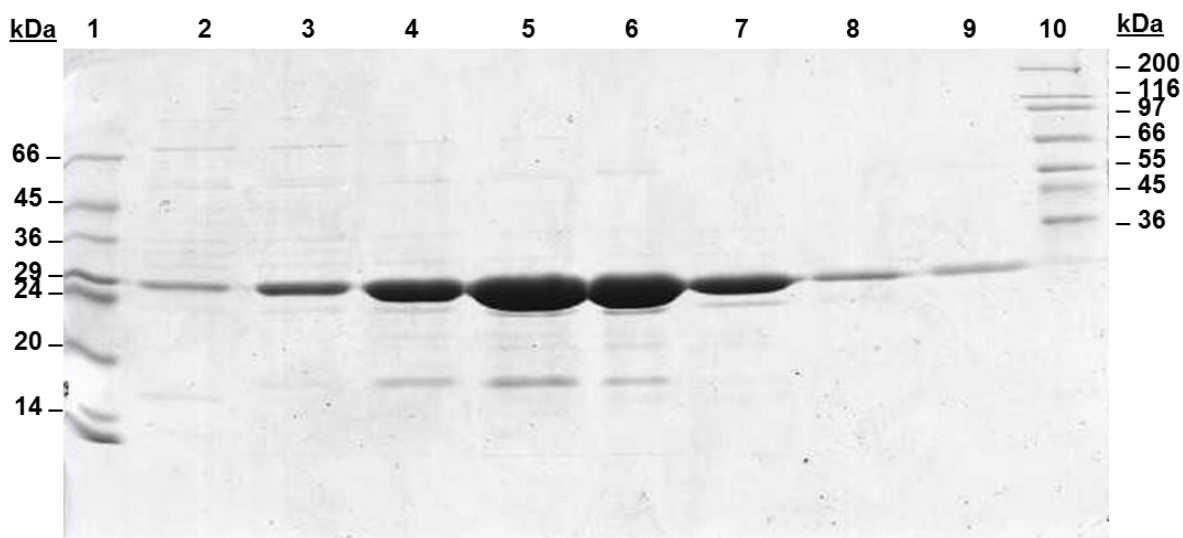
Appendix 7.130: SDS-PAGE analysis of CXC fractions following purification of *N*-terminally His-tagged recombinant lysostaphin (construct 1) derived from *E. coli* BL21(DE3) cultured in MM. Lane 1: Sigma low molecular weight markers; Lane 2: Fraction 29; Lane 3: Fraction 31; Lane 4: Fraction 33; Lane 5: Fraction 35; Lane 6: Sigma low molecular weight markers; Lane 7: Fraction 37; Lane 8: Fraction 39; Lane 9: Fraction 41.



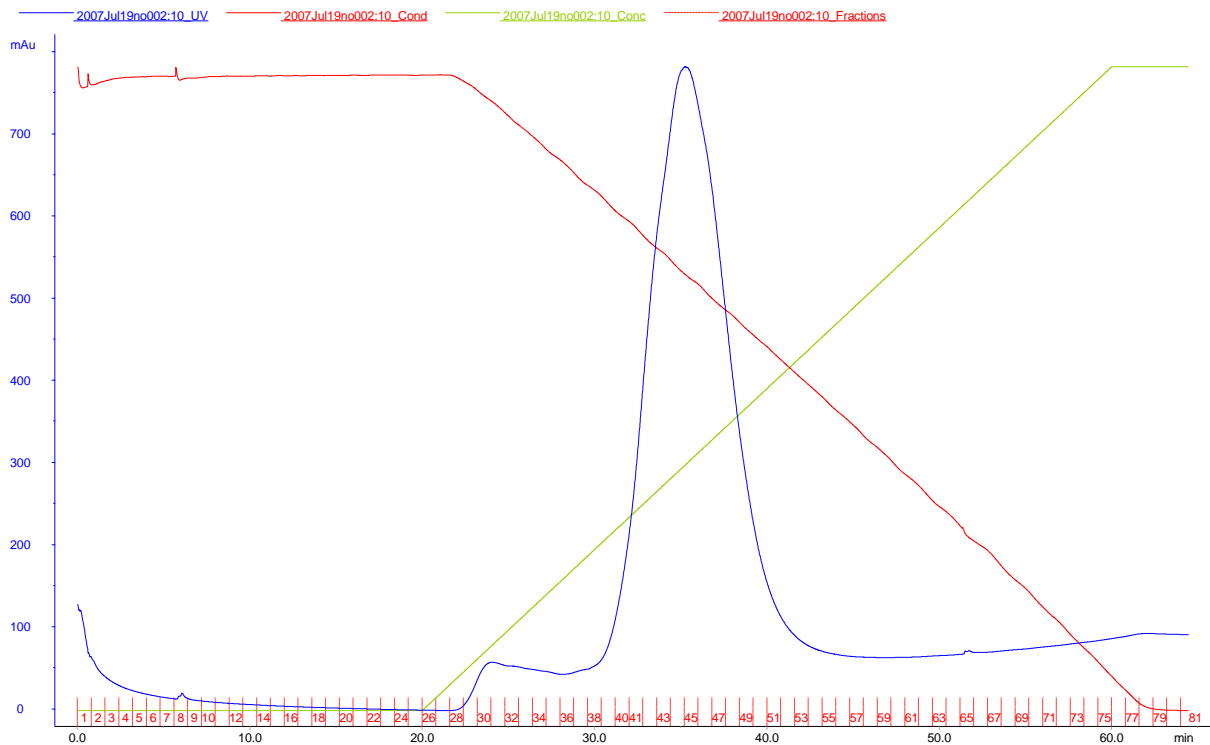
Appendix 7.131: Purification of *N*-terminally His-tagged recombinant lysostaphin (construct 1; preparation 19) using IMAC. Cell lysate extracted from recombinant *E. coli* BL21(DE3) cultured in AIM was applied to the Chelating Sepharose™ Fast Flow media column. Bound protein was eluted by applying an increasing imidazole concentration (20-500 mM).



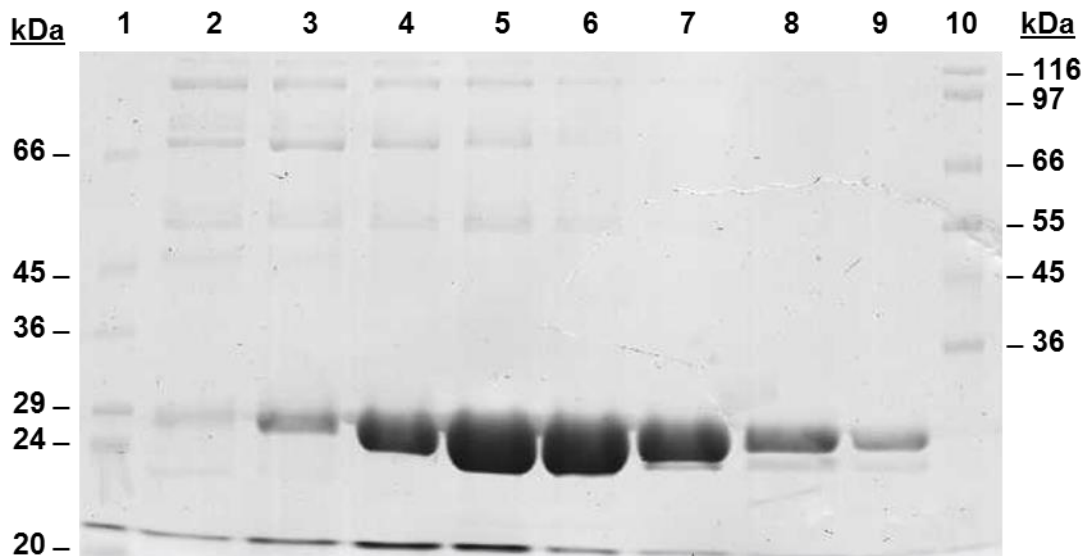
Appendix 7.132: SDS-PAGE analysis of fractions following IMAC purification of *N*-terminally His-tagged recombinant lysostaphin (construct 1; preparation 19) derived from *E. coli* BL21(DE3) cultured in AIM. Lane 1: Sigma low molecular weight markers; Lane 2: Fraction 46; Lane 3: Fraction 48; Lane 4: Fraction 50; Lane 5: Fraction 52; Lane 6: Fraction 54; Lane 7: Fraction 56; Lane 8: Fraction 58; Lane 9: Fraction 60; Lane 10: Sigma high molecular weight markers.



Appendix 7.133: Purification of C-terminally His-tagged recombinant lysostaphin (construct 4) using IMAC. Cell lysate extracted from recombinant *E. coli* BL21(DE3) was applied to the Chelating Sepharose™ Fast Flow media column. Bound protein was eluted by applying an increasing imidazole concentration (20-500 mM).



Appendix 7.134: SDS-PAGE analysis of GF fractions following IMAC purification of C-terminally His-tagged recombinant lysostaphin (construct 4) derived from *E. coli* BL21(DE3) cultured in AIM. Lane 1: Sigma low molecular weight markers; Lane 2: Fraction 45; Lane 3: Fraction 47; Lane 4: Fraction 49; Lane 5: Fraction 51; Lane 6: Fraction 53; Lane 7: Fraction 55; Lane 8: Fraction 57; Lane 9: Fraction 59; Lane 10: Sigma high molecular weight markers.



Appendix 7.135: Dionex Customer Application Note entitled "Rapid His-tag purification of recombinant proteins using Dionex ProPac IMAC columns". Available at <http://www.dionex.com/en-us/webdocs/86266-CAN107-LC-Recombinant-Proteins> 15April2010-LPN2495.pdf.



Rapid His-Tag Purification of Recombinant Proteins Using Dionex ProPac IMAC Columns

CAN
107

Dr. Claire Jennings, Prof. Gary W. Black
Biomolecular and Biomedical Research Centre, School of Applied Sciences, Northumbria University

Introduction

Immobilized-metal-affinity chromatography (IMAC) stationary phases are typically used for the capture/release enrichment of proteins in the purification of His-tag recombinant proteins. The IMAC approach captures His-tagged proteins, which have an affinity for the immobilized metal bound to the IMAC column. Release of the bound His-tagged protein is achieved by exposure to an elution buffer containing a high concentration of imidazole. Typical materials used for this purification are medium-pressure, porous resins such as agarose or cross-linked dextran containing a chelation function, which can be charged with the appropriate metal for the purification. From 500 to 1000 mL cultures, 5 to over 50 mg of protein can be obtained depending on the expression and fermentation process. The columns used at this level of protein production are usually 16 × 200 mm (30 mL total volume) with a flow rate of around 5 mL/min.

A typical purification protocol would include the following steps:

1. Wash with EDTA and 30 mL water; then, add 30 mL of 100 mM EDTA, followed by 30 mL water to obtain a total volume of 90 mL
2. Charge with 30 mL of 100 mM nickel sulfate (NiSO_4)
3. Equilibrate with 100 mL loading buffer
4. Load with sample
5. Wash the column with 200 mL loading buffer
6. Elute with imidazole

The process outlined here takes up to 3 h and will release the protein in around 50 mL of buffer containing high concentrations of imidazole and sodium chloride. As a result, further concentration and buffer-exchange steps must be performed, which are quite lengthy processes, to get the protein into a more manageable volume and buffer conditions.

The Dionex ProPac® IMAC-10 column is an HPLC resin column using 10 µm pellicular polystyrene beads with isolated poly(IDA) grafts on a hydrophilic boundary layer. The capacity of a 4 × 250 mm column is compatible with the levels of protein expected from 1 L cultures. For higher levels, 9 and 22 mm columns are available.

As the ProPac column is a pressure-stable column, flow rates of 2 mL/min are easily achieved during the washing stages and the low-dead-volume of the column (around 1 mL due to the pellicular structure) allows many column volumes to be used for washing, and reduced flow to be used during elution to increase the concentration of the purified protein.

Equipment

UltiMate® 3000 Titanium system consisting of:

- Analytical titanium pump
- Thermal compartment with two column change valves
- VWD detector

WPS-3000 Biocompatible autosampler with fractionation, 250 µL syringe, 1 mL loop

ISCO Foxy® Jr. Fraction collector

Chromeleon® Chromatography Data System software with fractionation license

Dionex ProPac IMAC-10, 4.0 mm i.d. × 250 mm

Agilent Zorbax® GF-250, 4 µm, 4.6 × 250 mm

Now sold under the
Thermo Scientific brand

Thermo
SCIENTIFIC

 **DIONEX**

Passion. Power. Productivity.

This is a Customer submitted application note published as is. No ISO data available for included figures.

Appendix 7.135: Dionex Customer Application Note entitled “Rapid His-tag purification of recombinant proteins using Dionex ProPac IMAC columns”. Available at <http://www.dionex.com/en-us/webdocs/86266-CAN107-LC-Recombinant-Proteins> 15April2010-LPN2495.pdf (continued).

Preparation of Samples

Using genomic DNA from *S. staphylolyticus* as a template, the mature lysostaphin ORF from the lysostaphin precursor (glycylglycine endopeptidase) sequence (Gen Bank Accession No. X06121) was amplified using PCR. The gene was first cloned in pCR-Blunt® vector using the Zero Blunt Cloning system (Invitrogen Ltd, UK) and then subcloned in the pET vector cloning system using pET-28a vector (Invitrogen Ltd, UK).

Pel10Acm, a carbohydrate module encoded in the pel10A gene originating from *P. cellulosa* was amplified using PCR. The PCR product was cloned into pGEM®-T Easy vector (Promega, UK) and then subcloned in the pET vector cloning system using pET-28a vector (Invitrogen Ltd, UK).

Recombinant pET vector DNA encoding lysostaphin and Pel10Acm was transformed into *E. coli* BL21(DE3) for protein expression. The transformed *E. coli* BL21(DE3) was used to inoculate an LB starter culture which was incubated overnight at 37 °C and 200 rpm. The LB starter culture was then inoculated into a 1 L flask of LB media. The inoculated LB media was incubated at 37 °C and 200 rpm until an o.d.600 of 0.6–1.0 was obtained. At this point, protein expression was induced by addition of 0.24 µg/mL IPTG and incubation at 30 °C and 100 rpm. The cell-free extract was harvested through centrifugation of cells at 4000 x g for 15 min. The resulting cell pellet was resuspended in IMAC buffer A and sonicated at 14 mA every 10 s for a total of 2 min. The sonicated cells were centrifuged at 24,000 x g for 20 min and the resulting cell-free extract was applied to the nickel columns for purification of recombinant lysostaphin and Pel10Acm.

Methods

Washing and charging the column can be done with simple 1 mL loop injections. The loading of the column with concentrated cell lysate is done using line C of the quaternary titanium pump.

Chromatographic Conditions– UltiMate 3000 Titanium System

Column: Dionex ProPac IMAC-10, 4.0 mm i.d. x 250 mm (P/N 063278)
 Mobile Phase: A) Sodium phosphate (20 mM), Sodium chloride (500 mM), Imidazole (20 mM), pH 7.4
 B) Sodium phosphate (20 mM), Sodium chloride (500 mM), Imidazole (500 mM), pH 7.4
 Gradient: See Table 1
 Flow Rate: See Table 1
 Sample Volume: 66 mL (loading via line buffer line C)
 Detection: Absorbance at 280 nm
 Column Preparation: Column stripped and charged through loading of 500 µL EDTA (manual 500 µL injection), 1000 µL of nickel sulfate (manual 1000 µL injection)

The concentrated cell lysate of 33 mL, was pumped onto the column at 1 mL/min. Following sample loading, the column was washed with the loading buffer before elution with an imidazole gradient at 0.5 mL/min.

Time (min)	Flow (mL/min)	%B	%C
0.000	1.000	0.0	0.0
0.100	1.000	0.0	0.0
0.200	1.000	0.0	100.0
33.000	1.000	0.0	100.0
33.100	1.000	0.0	0.0
53.000	0.500	0.0	0.0
103.000	0.500	100.0	0.0
103.100	1.000	0.0	0.0
128.000	1.000	0.0	0.0



Appendix 7.135: Dionex Customer Application Note entitled “Rapid His-tag purification of recombinant proteins using Dionex ProPac IMAC columns”. Available at <http://www.dionex.com/en-us/webdocs/86266-CAN107-LC-Recombinant-Proteins> 15April2010-LPN2495.pdf (continued).

Results

The purification procedure takes approximately 2.15 h compared to 3 h using the previous media. The length of purification is dependent on sample volume and therefore, the method duration can be easily reduced to accommodate lower sample volumes. In addition to time efficiency, the ProPac IMAC column produced a more concentrated end product, which is important for postpurification sample processing. In this example, the protein was collected in a total volume of 8 mL, which was concentrated and desalted within a few hours. An IMAC purification was performed using a Chelating Sepharose™ Fast Flow, XK 16/20 column. The purification used the same amount of protein and was eluted in a total volume of 50 mL, which required concentration over several days. The less time spent concentrating the purified protein dramatically reduces the total purification time. The elution profiles for the recombinant proteins Pel10Acm and lysostaphin are shown in Figures 1 and 2.

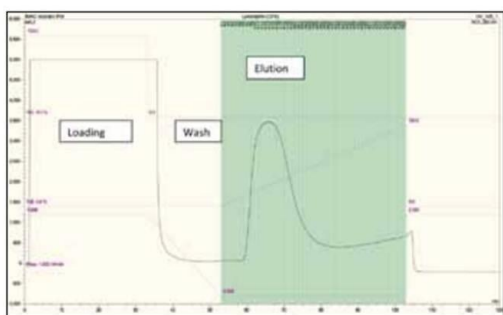


Figure 1. IMAC Purification of Pel10Acm from an *E. coli* cell-free extract.

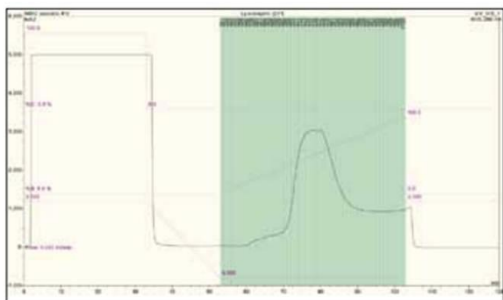


Figure 2. IMAC purification of lysostaphin from an *E. coli* cell-free extract.

The collected lysostaphin protein fractions contained 9.5 mg of the purified recombinant protein in an 8 mL elution buffer. A duplicate sample was applied to a Chelating Sepharose Fast Flow IMAC column and collected a similar amount of protein in a 50 mL elution buffer. The two methods produced similar purification results as shown by the amount of protein collected and the subsequent analysis by gel filtration (Figure 3).

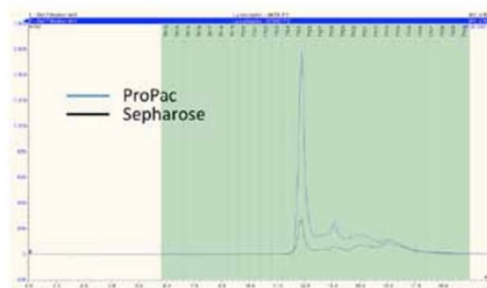


Figure 3. Gel filtration analysis of lysostaphin from ProPac and Sepharose IMAC columns. 50 mM PO_4 , 100 mM NaCl, pH 7.0 with a flow rate of 0.25 mL/min, 30 μ L of the collected fractions injected, UV detection at 280 nm.

Gel filtration analysis of the purified lysostaphin samples from the ProPac and the Sepharose columns are shown in Figure 3. The ProPac sample is more concentrated but both purified samples show a similar profile with no indication of aggregation.

Conclusion

The Dionex ProPac IMAC column can be used to successfully and rapidly purify His-Tagged recombinant proteins from cell-free extracts harvested from up to 1 L of *E. coli* fermentation cultures.

The ProPac IMAC column achieved the purification in 90 min compared with 3 h previously. Purification time may be reduced further through the application of a more concentrated sample with a smaller sample volume. The released protein was collected in 8 mL buffer, which is a more manageable volume compared to the 50 mL released from the Chelating Sepharose Fast Flow column. With larger collection volumes, a lengthy concentration step is required. Concentration of 50 mL using ultrafiltration spin columns may take several days. Dialysis to remove the high salt concentration will also require several buffer exchanges. The smaller collection volumes reduce the time required for these steps considerably.

7.2 Separation of Recombinant Lysostaphin Isoforms

Appendix 7.136: Buffers

IEX buffer A (1 L)

Sodium phosphate (20 mM)	100 ml of 200 mM stock solution
--------------------------	---------------------------------

The stock solution was mixed with 900 ml of 18.2 MΩ/cm H₂O and the pH of the buffer was adjusted to pH 7.0 using NaOH. The buffer was autoclaved prior to use.

IEX buffer B (1L)

Sodium phosphate (20 mM)	100 ml of 200 mM stock solution
NaCl (1.0 M)	58.44 g

The stock solution and NaCl were added to 18.2 MΩ/cm H₂O to achieve a total volume of 1 L. The pH of the buffer was adjusted to pH 7.0 using NaOH. The buffer was autoclaved prior to use.

MAb SCX buffer A (1 L)

MES (20 mM)	3.9 g
-------------	-------

MES was dissolved in 18.2 MΩ/cm H₂O and the pH of the buffer was adjusted to pH 6.4 using NaOH. The buffer was autoclaved prior to use.

MAb SCX buffer B (1 L)

MES (20 mM)	3.90 g
NaCl (1.0 M)	58.44 g

MES and NaCl were dissolved in 18.2 MΩ/cm H₂O and the pH of the buffer was adjusted to pH 6.4 using NaOH. The buffer was autoclaved prior to use.

WCX buffer A (1 L)

Sodium phosphate (20 mM) 100 ml of 200 mM stock solution

The stock solution was mixed with 900 ml of 18.2 MΩ/cm H₂O and the pH of the buffer was adjusted to pH 7.0 using NaOH. The buffer was autoclaved prior to use.

WCX buffer B (1 L)

Sodium phosphate (20 mM) 100 ml of 200 mM stock solution

NaCl (1.0 M) 58.44 g

The stock solution and NaCl were added to 18.2 MΩ/cm H₂O to achieve a total volume of 1L. The pH of the buffer was adjusted to pH 7.0 using NaOH. The buffer was autoclaved prior to use.

SCX buffer A (1 L)

Sodium phosphate (20 mM) 100 ml of 200 mM stock solution

The stock solution was mixed with 900 ml of 18.2 MΩ/cm H₂O and the pH of the buffer was adjusted to pH 8.0 using NaOH. The buffer was autoclaved prior to use.

SCX buffer B (1 L)

Sodium phosphate (20 mM) 100 ml of 200 mM stock solution

NaCl (1.0 M) 58.44 g

The stock solution and NaCl were added to 18.2 MΩ/cm H₂O to achieve a total volume of 1L. The pH of the buffer was adjusted to pH 7.0 using NaOH. The buffer was autoclaved prior to use.

RP buffer A (1 L)

Acetonitrile (LC/MS grade) (2.0%, v/v) 20.0 ml

Trifluoroacetic acid (TFA) (0.1%, v/v) 1.0 ml

The volume was made up to 1 L with LC/MS grade H₂O

RP buffer B (1 L)

Acetonitrile (LC/MS grade) (90%, v/v)	900.0 ml
Trifluoroacetic acid (TFA) (0.09%, v/v)	1.0 ml

The volume was made up to 1 L with LC/MS grade H₂O

Appendix 7.137: Equipment

Initial ion exchange separations were performed using a Dionex DX500 HPLC system consisting of a GP40 Gradient Pump, an AD25 variable wavelength absorbance detector, an LC20 Chromatography Enclosure. Fractions were collected using a Foxy Jr fraction collector. The system was operated using a Dionex PeakNet Chromatography Workstation and acquired data was collected using PeakNet Version 5.01. UV data was acquired at 280 nm throughout each separation.

Subsequent separations were performed using one of two Ultimate™ 3000 Titanium systems. Both systems consisted of a dual gradient titanium pump, a thermal compartment with two column change valves, a VWD detector and a WPS-3000 Biocompatible autosampler. The thermal compartment was maintained at 25°C, unless specified otherwise. The system was fitted with a PEEK fluidic pathway and the autosampler was fitted with a 250 µl syringe and a 1 ml injection loop. Although both autosamplers could accommodate fractionation, fractionation was performed using an ISCO Foxy® Jr Fraction collector when using one of the systems, due to the use of higher flow rates (0.5-1.0 ml). Data collection and analysis was performed using Chromeleon® Chromatography Data system software with fractionation license. UV data was acquired at 214 and 280 nm throughout each separation.

Chromatographic separations were performed using a number of analytical columns, as described in Appendix 7.138.

Appendix 7.138: Analytical columns and mobile phase compositions used during separation of recombinant lysostaphin isoforms

Column	IEX mode	Dimensions	Mobile Phase
ProPac [®] WCX-10	WCX	2.0 x 250	WCX buffer A and B
ProPac [®] WCX-10	WCX	4.0 x 250	IEX buffer A and B <u>or</u> WCX buffer A and B
ProSwift [®] WCX-1S	WCX	2.0 x 50	IEX buffer A and B
ProPac [®] SAX-10	SAX	2.0 x 250	IEX buffer A and B
ProPac [®] SCX-10	SCX	2.0 x 250	IEX buffer A and B <u>or</u> SCX buffer A and B
ProSwift [®] SCX-1S	SCX	4.6 x 50	IEX buffer A and B
ProPac [®] SCX-10	SCX	4.0 x 250	IEX buffer A and B
ProPac [®] MAb SCX	SCX	4.0 x 250	MAb SCX Buffer A and B
ProSwift [®] RP-4H	RP	1.0 x 250	RP buffer A and B

Appendix 7.139: Sample preparation

Recombinant lysostaphin was harvested from *E. coli* BL21(DE3) cultured in either LB or AIM and purified using either IMAC or HIC and GF. Following purification, the purified protein was concentrated using ultrafiltration. Further details about preparation of recombinant lysostaphin is provided in Appendix 7.140.

The ProPac[®] WCX-10 column was validated using a Cytochrome C standard (LC Packings, UK). Prior to use the lyophilised cytochrome C was resuspended in 200 µl of LC/MS grade H₂O and stored at -20°C between use.

The ProPac[®] MAb SCX column was validated using a standard protein mix composed of a mixture of Lysozyme (0.25 mg/ml), Ribonuclease A (1.0 mg/ml) and Cytochrome C (0.20 mg/ml). The lyophilized standard was provided by Dionex, UK for beta-testing purposes. Prior to use, the standard protein mix was resuspended in 200 µl of LC/MS grade H₂O and 10 µl of standard was injected onto the column during each standard separation. Following resuspension the standard samples was re-refrigerated at 2-8°C.

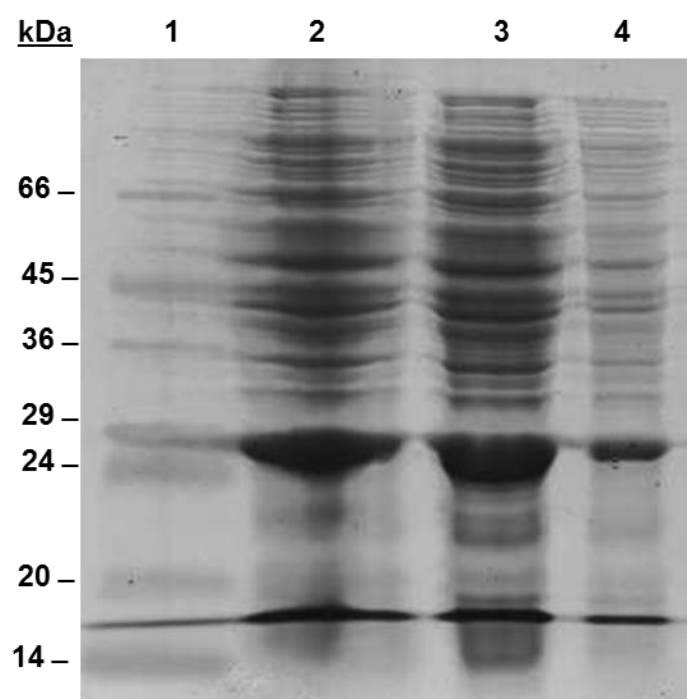
Appendix 7.140: Purified recombinant lysostaphin preparations

Preparation ID	Construct	Expression media	Mode of purification	Protein concentration ($\mu\text{g}/\mu\text{l}$)	Related results
1	4	AIM	IMAC	55.42	Appendix 7.97 Appendix 7.133 Appendix 7.134
2	3	AIM	IMAC	8.67	Appendix 7.141 Figure 2.26 Figure 2.27
3	3	AIM	HIC, GF	1.46	Appendix 7.142 Figure 2.17 Figure 2.18 Figure 2.19 Figure 2.20 Figure 2.21
4	1	AIM	IMAC	37.80	Appendix 7.143 Appendix 7.144 Appendix 7.145
5	3	LB	IMAC	16.34	Appendix 7.146 Figure 2.37 Figure 2.39
6	1	AIM	IMAC	157.85	Appendix 7.147 Appendix 7.148 Appendix 7.149
7	1	AIM	IMAC	55.35	Appendix 7.150 Appendix 7.151 Appendix 7.152
8	1	AIM	IMAC	140.12	Appendix 7.153 Appendix 7.154 Appendix 7.155
9	1	AIM	IMAC	91.68	Appendix 7.156 Appendix 7.157 Appendix 7.158
10	1	LB	IMAC	16.69	Appendix 7.159 Appendix 7.160 Appendix 7.161

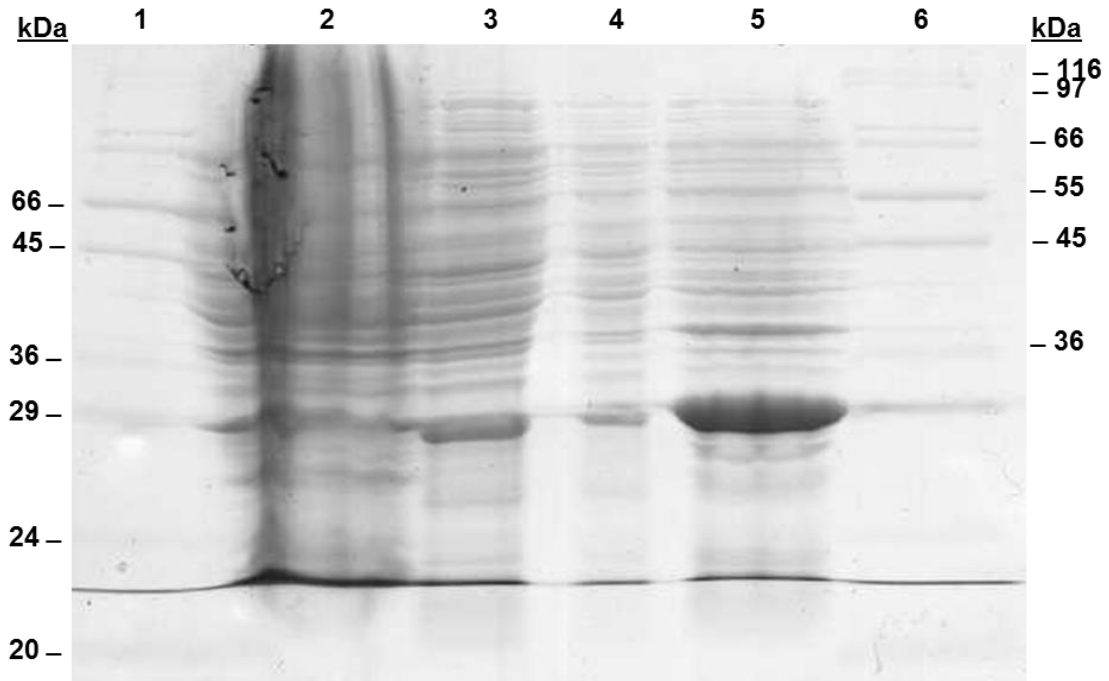
Appendix 7.140: Purified recombinant lysostaphin preparations (continued)

Preparation ID	Construct	Expression media	Mode of purification	Protein concentration ($\mu\text{g}/\mu\text{l}$)	Related results
11	1	LB	IMAC	39.35	Appendix 7.162 Appendix 7.163 Appendix 7.164
12	1	LB	IMAC	5.71	Appendix 7.165 Appendix 7.166 Figure 4.29
13	3	AIM	IMAC/GF	19.08	Appendix 7.167 Figure 2.26 Figure 2.27 Figure 2.28 Figure 2.29

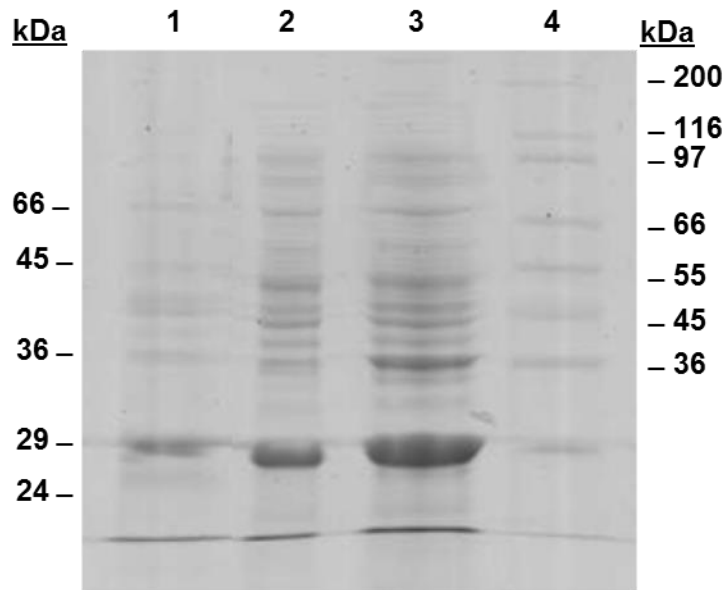
Appendix 7.141: SDS-PAGE analysis of cell lysate containing C-terminally His-tagged recombinant lysostaphin (construct 3, preparation 2) expressed in *E.coli* BL21(DE3) cultured in AIM. Lane 1: Sigma low molecular weight markers; Lane 2: CFE (neat); Lane 3: CFE (1:10 dilution), Lane 4: CFE (1:100 dilution).



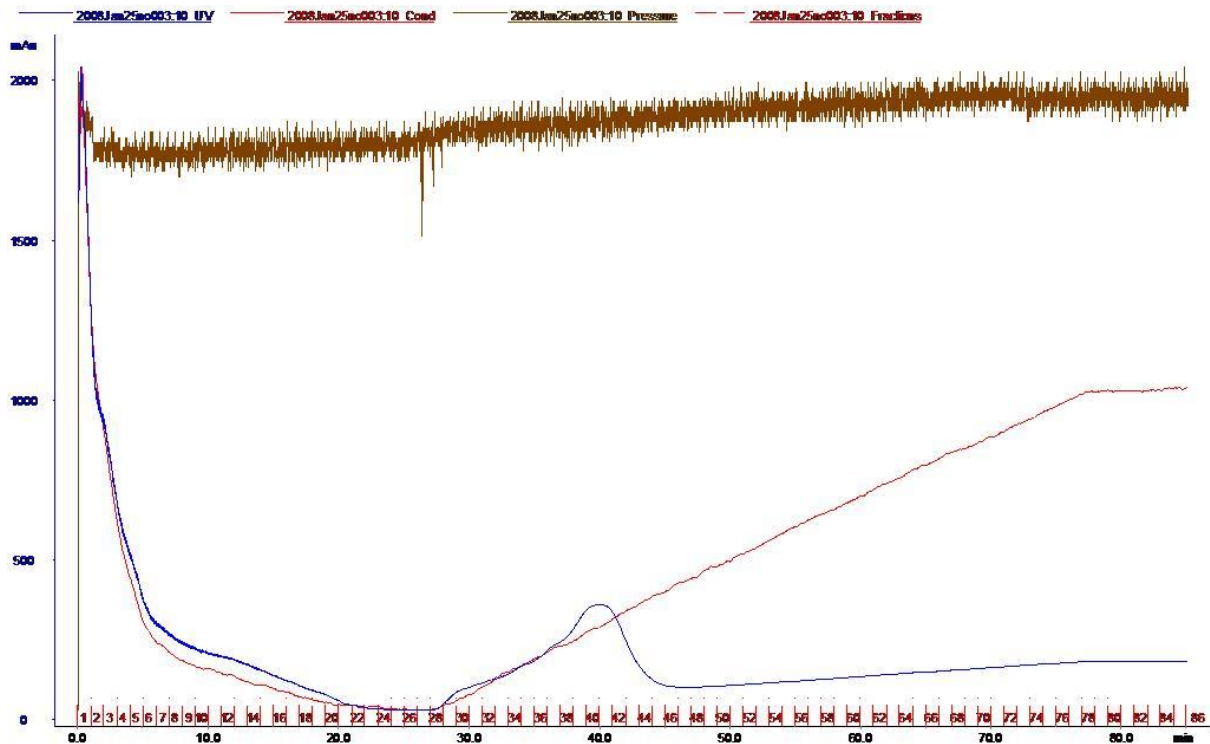
Appendix 7.142: SDS-PAGE analysis of cell lysate containing C-terminally His-tagged recombinant lysostaphin (construct 3, preparation 3) expressed in *E.coli* BL21(DE3) cultured in AIM. Lane 1: Sigma low molecular weight markers; Lane 2: CFE (neat); Lane 3: CFE (1:10 dilution), Lane 4: CFE (1:100 dilution); Lane 5: CFE in solubilising cracking buffer; Lane 6: Sigma high molecular weight markers



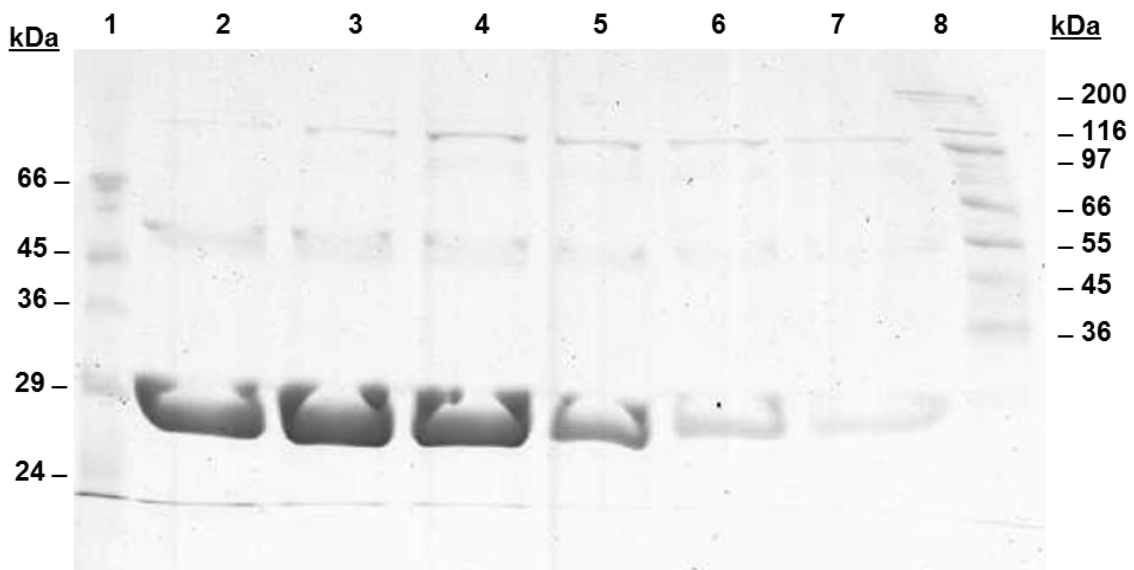
Appendix 7.143: SDS-PAGE analysis of cell lysate containing N-terminally His-tagged recombinant lysostaphin (construct 1, preparation 4) expressed in *E.coli* BL21(DE3) cultured in AIM. Lane 1: Sigma low molecular weight markers; Lane 2: CFE (1:10); Lane 3: CFE (neat), Lane 4: Sigma high molecular weight markers



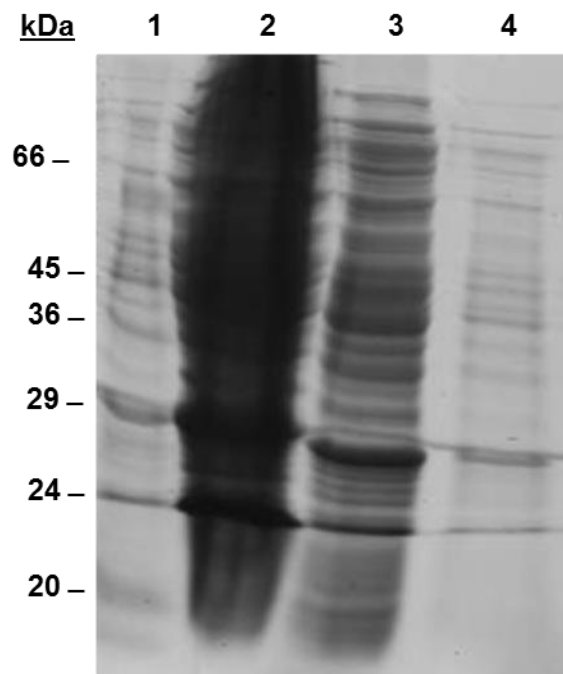
Appendix 7.144: IMAC purification of *N*-terminally His-tagged recombinant lysostaphin (construct 1, preparation 4) using a Chelating Sepharose™ Fast Flow media column and ÄKTA™ prime plus system. Bound protein was eluted by applying an increasing imidazole concentration (20-500 mM). Fractions were collected every 60 s throughout the separation. Fractions 38-48 were pooled and concentrated.



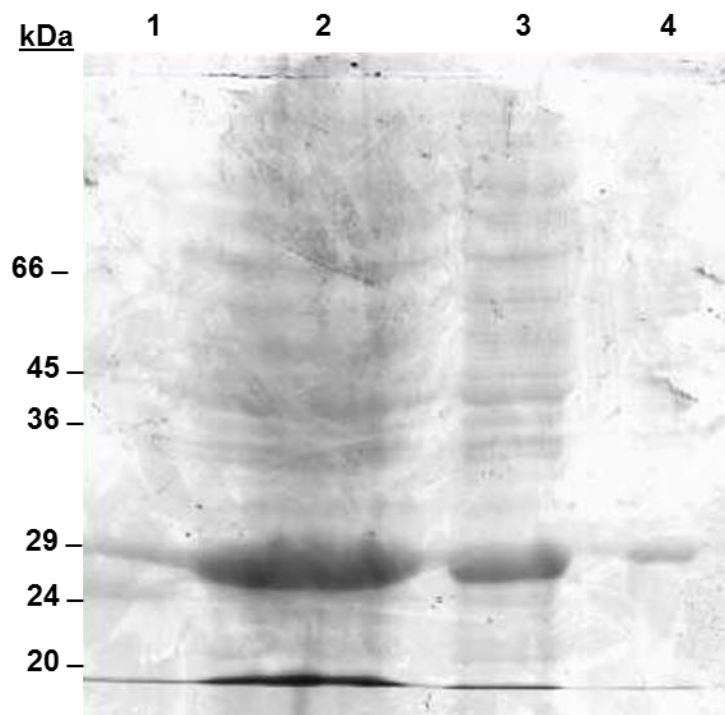
Appendix 7.145: SDS-PAGE analysis of fractions eluted during IMAC of cell-lysate containing *N*-terminally His-tagged recombinant lysostaphin (construct 1, preparation 4). Lane 1: Sigma low molecular weight markers; Lane 2: Fraction 38; Lane 3: Fraction 40; Lane 4: Fraction 42; Lane 5: Fraction 44; Lane 6: Fraction 46; Lane 7: Fraction 48; Lane 8: Sigma high molecular weight markers.



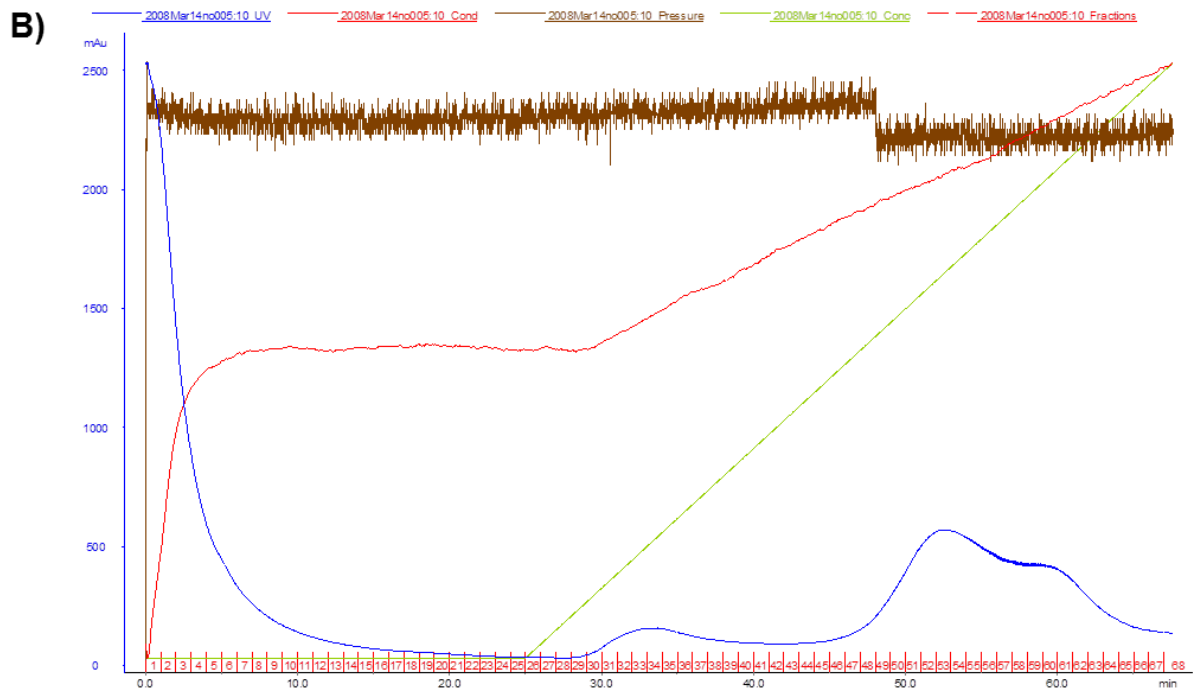
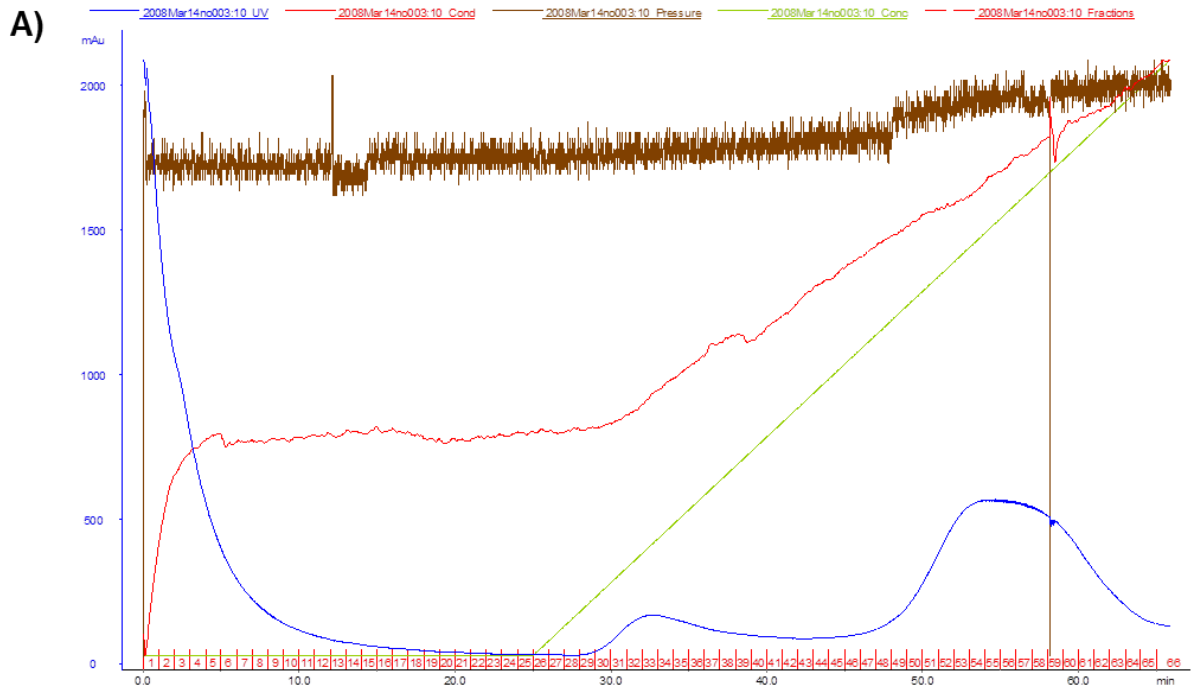
Appendix 7.146: SDS-PAGE analysis of cell lysate containing C-terminally His-tagged recombinant lysostaphin (construct 3, preparation 5) expressed in *E.coli* BL21(DE3) cultured in AIM. Lane 1: Sigma low molecular weight markers; Lane 2: CFE (neat); Lane 3: CFE (1:10 dilution), Lane 4: CFE (1: 100 dilution).



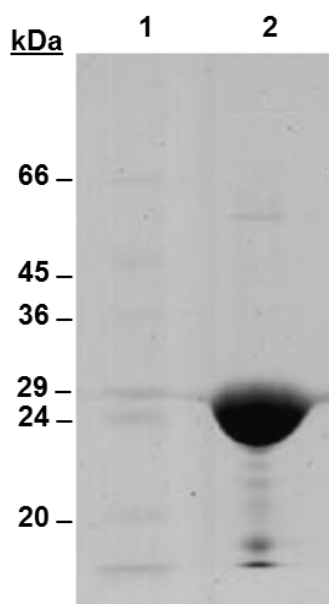
Appendix 7.147: SDS-PAGE analysis of cell lysate containing N-terminally His-tagged recombinant lysostaphin (construct 1, preparation 6) expressed in *E.coli* BL21(DE3) cultured in AIM. Lane 1: Sigma low molecular weight markers; Lane 2: CFE (neat); Lane 3: CFE (1:10 dilution), Lane 4: CFE (1:100 dilution).



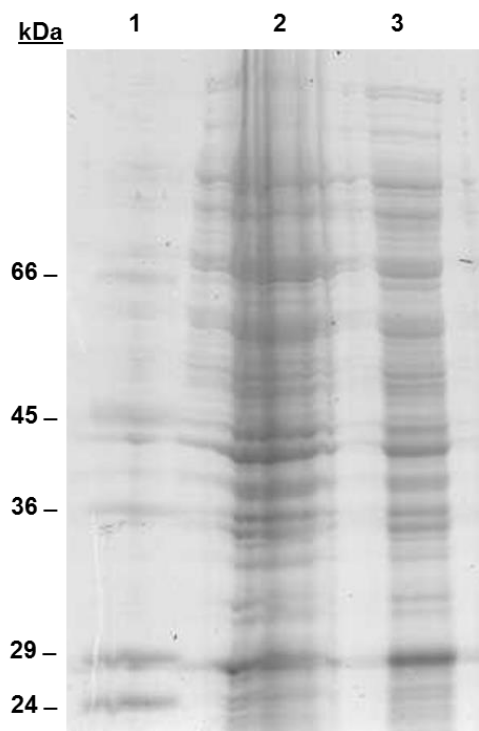
Appendix 7.148: IMAC purification of recombinant lysostaphin (construct 1, preparation 6) using a Chelating Sepharose™ Fast Flow media column and ÄKTA™ prime plus system. Cell lysate was applied to the column on two consecutive occasions (A and B). Bound protein was eluted by applying an increasing imidazole concentration (20-500 mM). Fractions were collected every 60 s throughout the separations. Fractions 48-63 collected during the first purification (A) and fractions 40-52 collected during the second purification (B) were pooled and concentrated.



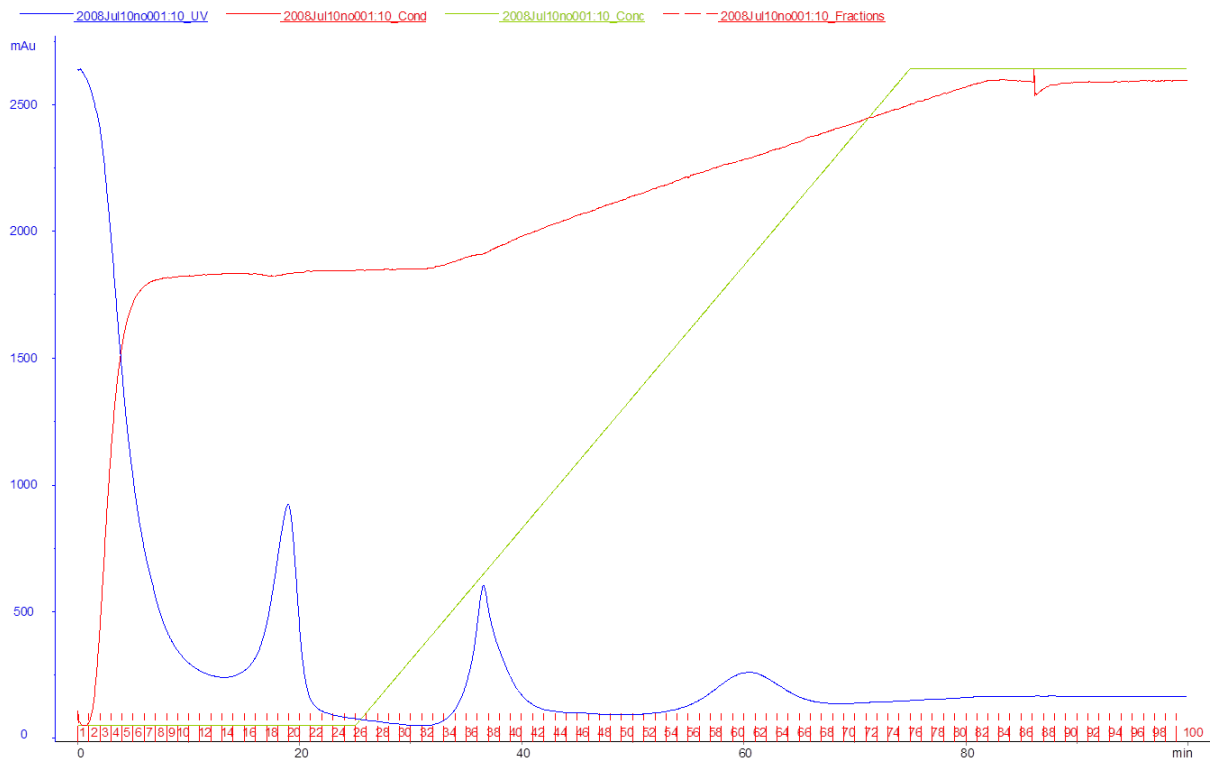
Appendix 7.149: SDS-PAGE analysis of purified, concentrated *N*-terminally His-tagged recombinant lysostaphin (construct 1, preparation 6). Lane 1: Sigma low molecular weight markers; Lane 2: concentrated protein (neat).



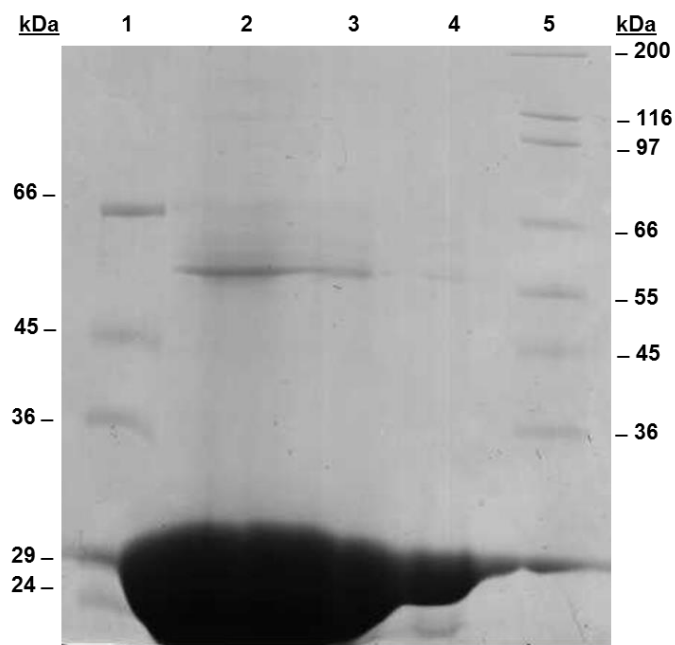
Appendix 7.150: SDS-PAGE analysis of cell lysate containing *N*-terminally His-tagged recombinant lysostaphin (construct 1, preparation 7) expressed in *E.coli* BL21(DE3) cultured in AIM. Lane 1: Sigma low molecular weight markers; Lane 2: CFE (neat); Lane 3: CFE (1:10).



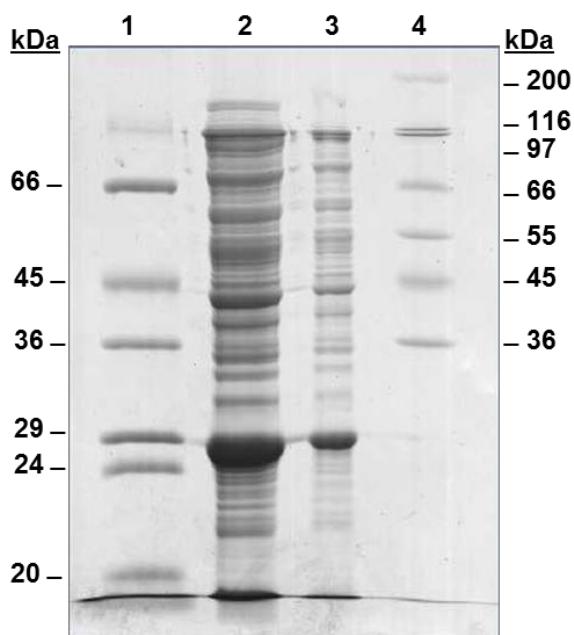
Appendix 7.151: IMAC purification of recombinant lysostaphin (construct 1, preparation 7) using a Chelating Sepharose™ Fast Flow media column and ÄKTA™ prime plus system. Bound protein was eluted by applying an increasing imidazole concentration (20-500 mM). Fractions were collected every 60 s throughout the separation. Fractions 58-70 were pooled and concentrated.



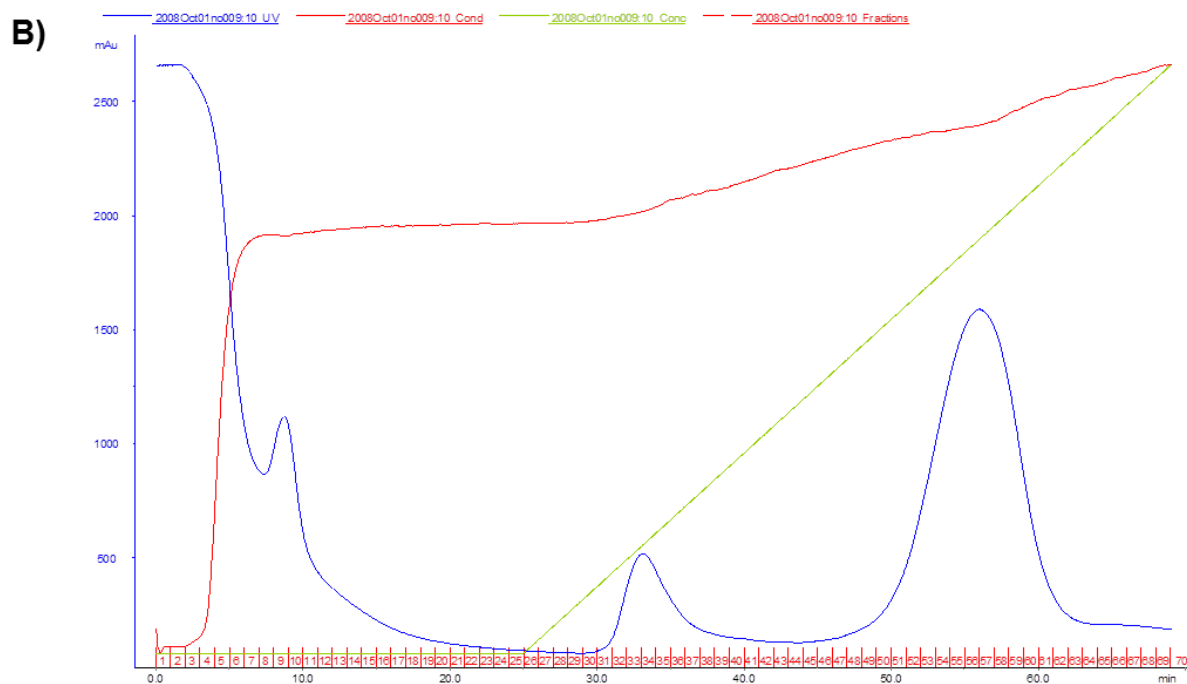
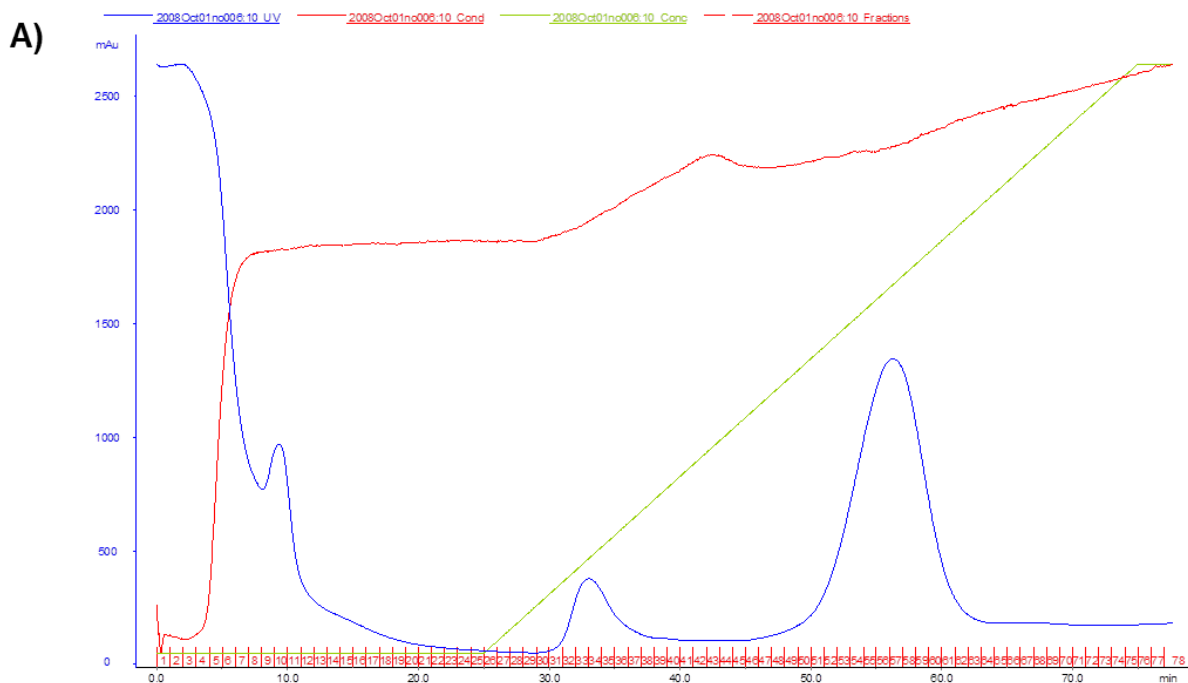
Appendix 7.152: SDS-PAGE analysis of purified, concentrated *N*-terminally His-tagged recombinant lysostaphin (construct 1, preparation 7). Lane 1: Sigma low molecular weight markers; Lane 2: concentrated protein (1:2); Lane 3: concentrated protein (1:10), Lane 4: concentrated protein (1:100); Lane 5: Sigma high molecular weight markers.



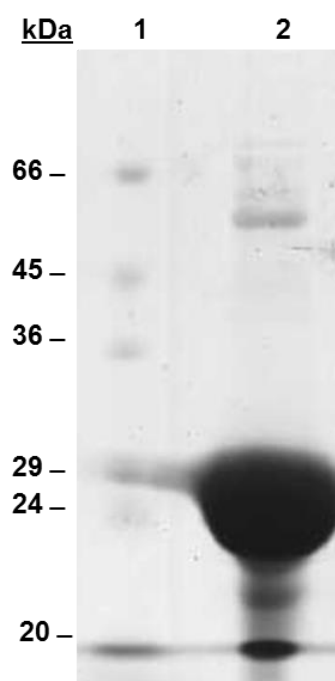
Appendix 7.153: SDS-PAGE analysis of cell lysate containing *N*-terminally His-tagged recombinant lysostaphin (construct 1, preparation 8) expressed in *E.coli* BL21(DE3) cultured in AIM. Lane 1: Sigma low molecular weight markers; Lane 2: CFE (neat); Lane 3: CFE (1:10), Lane 4: Sigma high molecular weight markers.



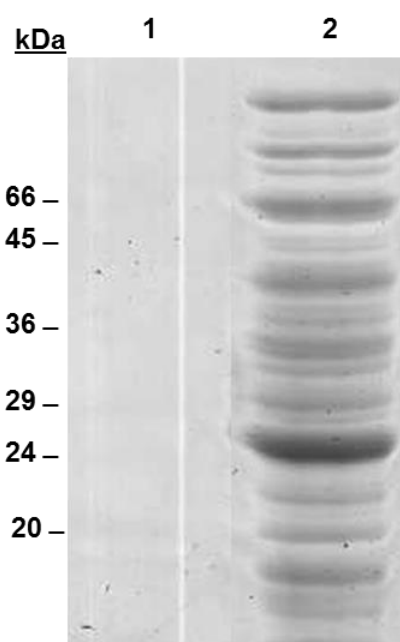
Appendix 7.154: IMAC purification of recombinant lysostaphin (construct 1, preparation 8) using a Chelating Sepharose™ Fast Flow media column and ÄKTA™ prime plus system. Fractions were collected every 60 s throughout the separations. Cell lysate was applied to the column on two consecutive occasions (A and B). Bound protein was eluted by applying an increasing imidazole concentration (20-500 mM). Fractions 52-62 collected during purifications A and B were pooled and concentrated.



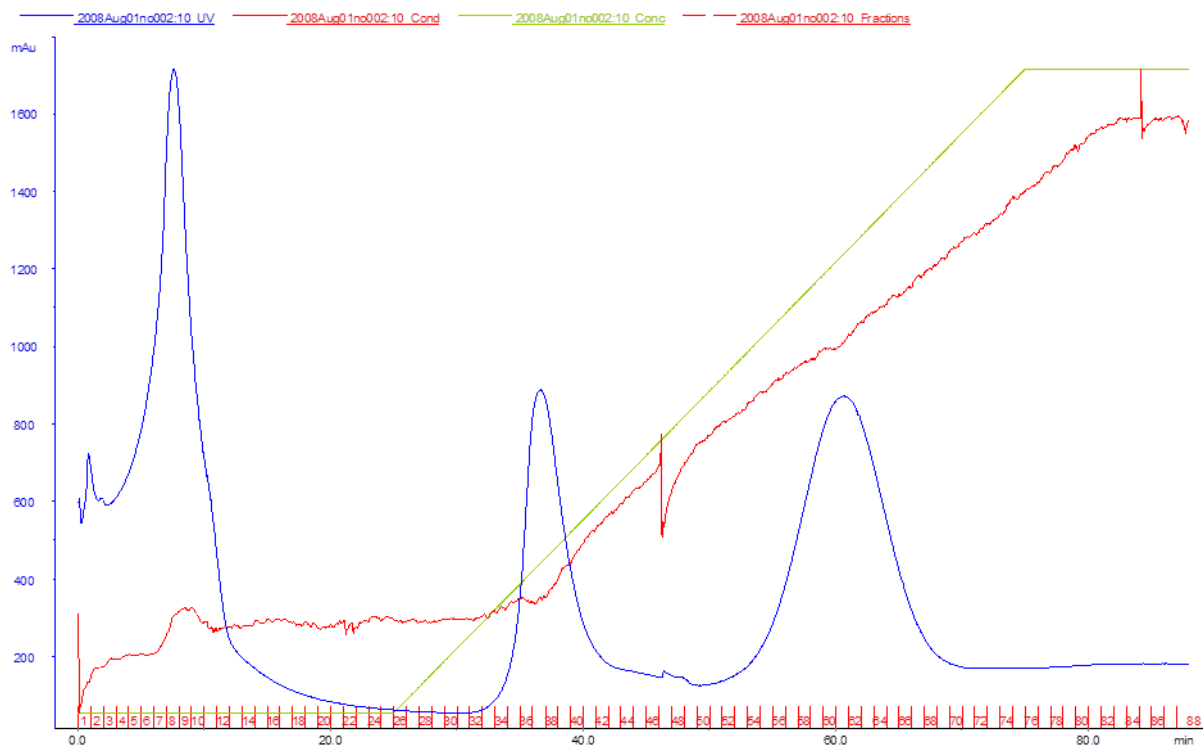
Appendix 7.155: SDS-PAGE analysis of purified, concentrated *N*-terminally His-tagged recombinant lysostaphin (construct 1, preparation 8). Lane 1: Sigma low molecular weight markers; Lane 2: concentrated protein (1:10).



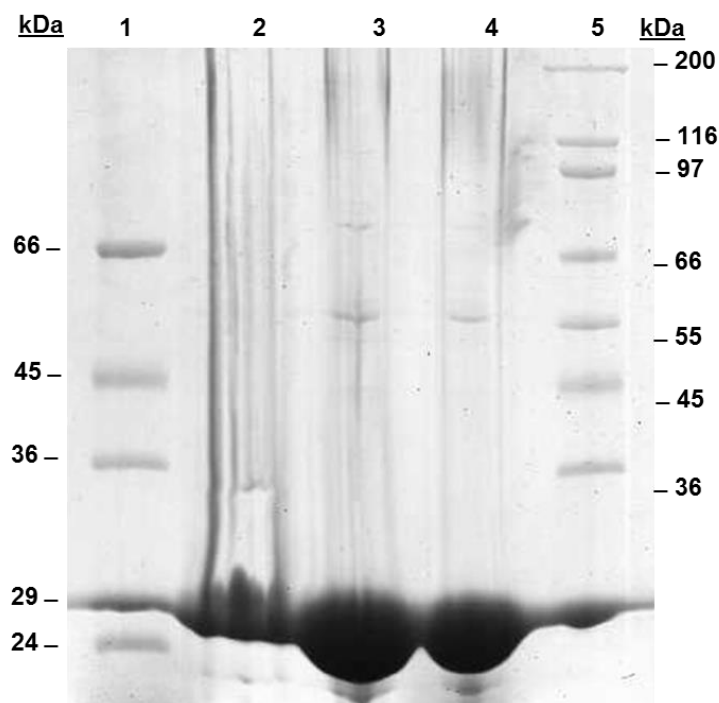
Appendix 7.156: SDS-PAGE analysis of cell lysate containing *N*-terminally His-tagged recombinant lysostaphin (construct 1, preparation 9) expressed in *E.coli* BL21(DE3) cultured in AIM. Lane 1: Sigma low molecular weight markers; Lane 2: CFE (neat).



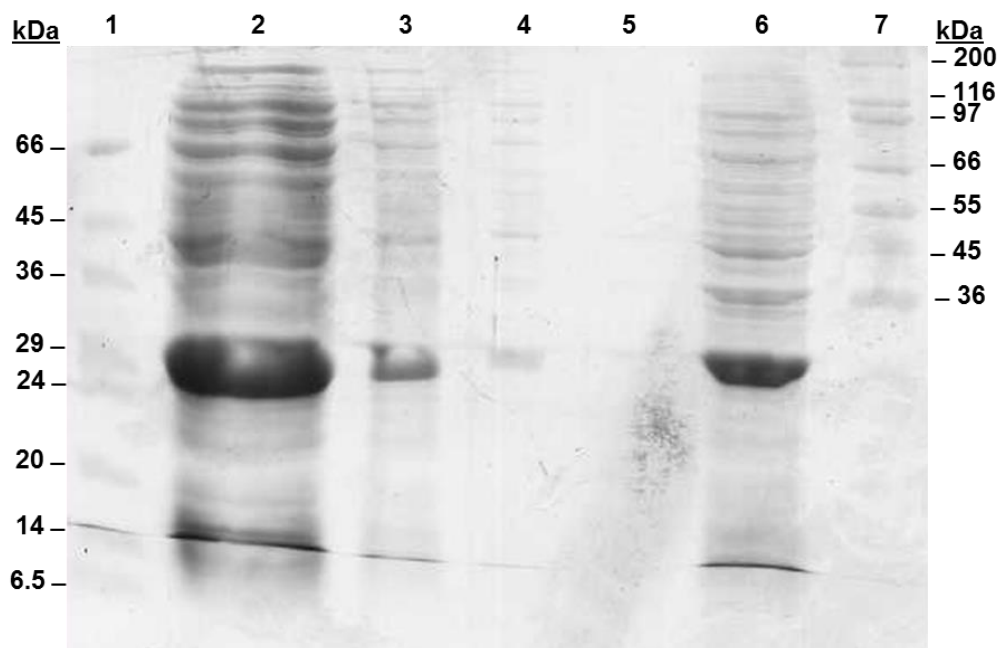
Appendix 7.157: IMAC purification of recombinant lysostaphin (construct 1, preparation 9) using a Chelating Sepharose™ Fast Flow media column and ÄKTA™ prime plus system. Bound protein was eluted by applying an increasing imidazole concentration (20-500 mM). Fractions were collected every 60 s throughout the separation. Fractions 56-70 were pooled and concentrated.



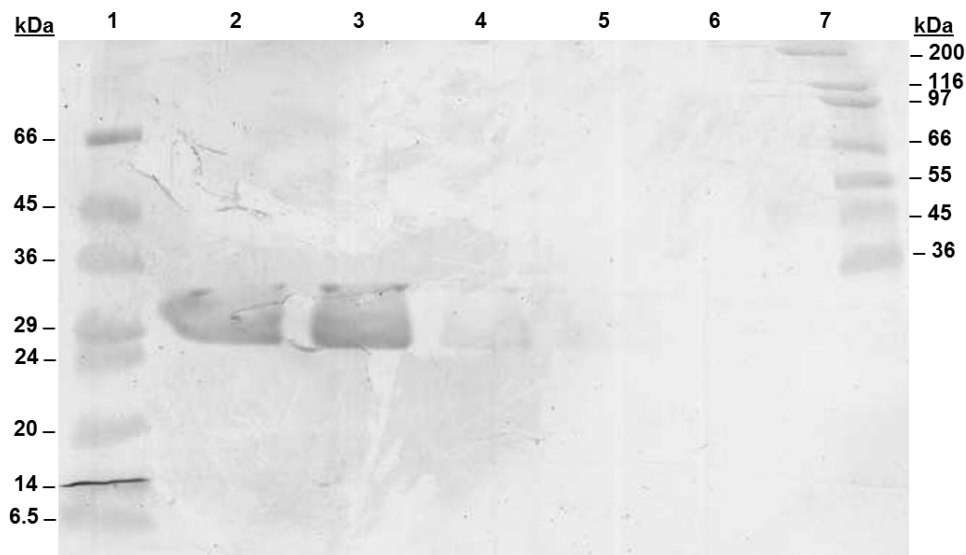
Appendix 7.158: SDS-PAGE analysis of purified, concentrated *N*-terminally His-tagged recombinant lysostaphin (construct 1, preparation 9). Lane 1: Sigma low molecular weight markers; Lane 2: concentrated protein (neat); Lane 3: concentrated protein (1:10); Lane 4: concentrated protein (1:100); Lane 5: Sigma high molecular weight markers



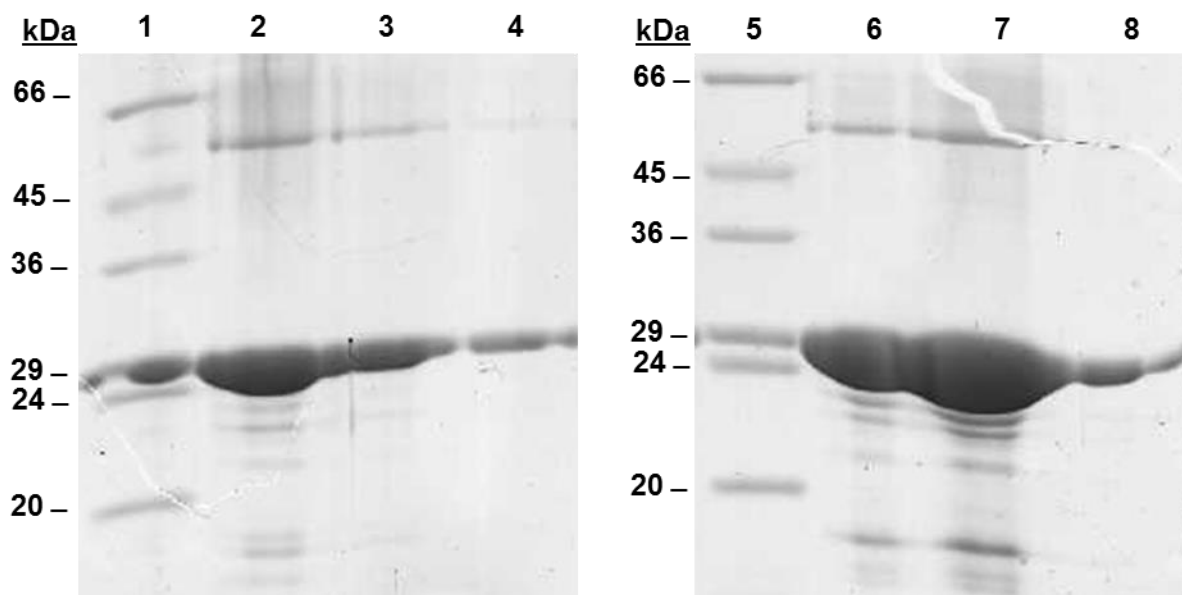
Appendix 7.159: SDS-PAGE analysis of cell lysate containing *N*-terminally His-tagged recombinant lysostaphin (construct 1, preparation 10) expressed in *E.coli* BL21(DE3) cultured in 14 x 1 L LB. Lane 1: Sigma low molecular weight markers; Lane 2: CFE (neat); Lane 3: CFE (1:10), Lane 4: CFE (1:100); Lane 5: CFE (1:1000); Lane 6: CFE in solubilising buffer; Lane 7: Sigma high molecular weight markers



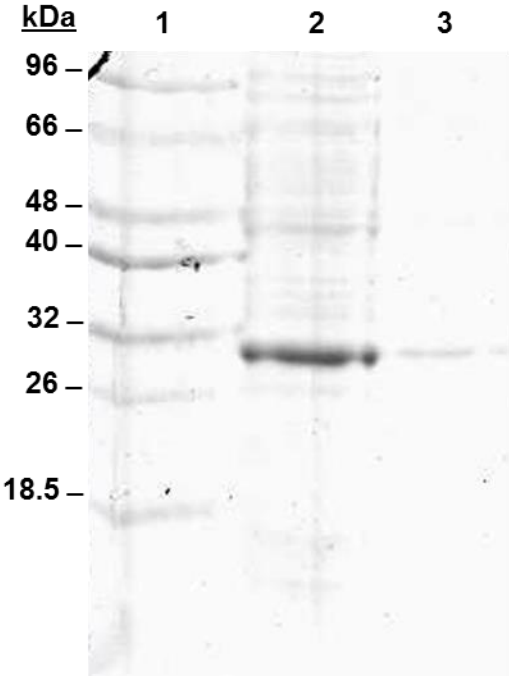
Appendix 7.160: SDS-PAGE analysis of purified N-terminally His-tagged recombinant lysostaphin (construct 1, preparation 10) following large-scale IMAC purification. Lane 1: Sigma low molecular weight markers; Lane 2: 200 mM imidazole (elution A); Lane 3: 200 mM imidazole (elution B), Lane 4: 300 mM imidazole; Lane 5: 400 mM imidazole; Lane 6: 500 mM imidazole; Lane 7: Sigma high molecular weight markers.



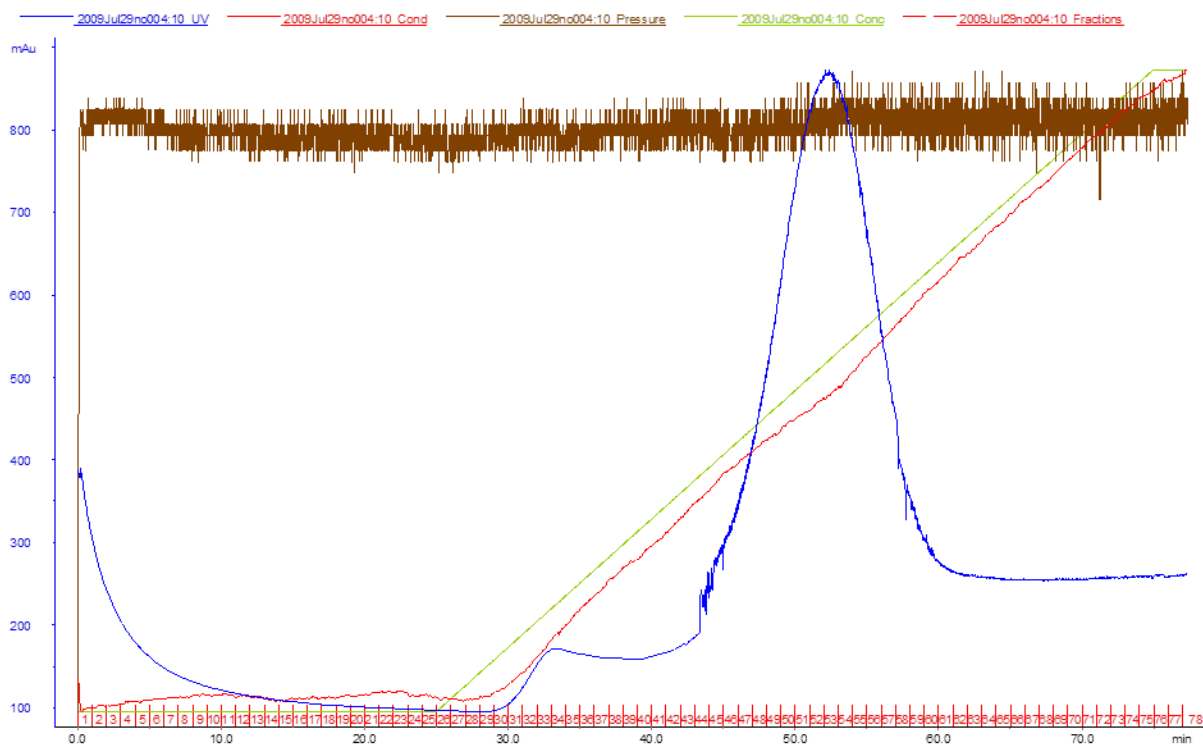
Appendix 7.161: SDS-PAGE analysis of purified freeze-dried recombinant lysostaphin (construct 1, preparation 10). Lane 1: Sigma low molecular weight markers; Lane 2: lysostaphin expressed in LB media (neat); Lane 3: lysostaphin expressed in LB media (1/10), Lane 4: lysostaphin expressed in LB (1/100); Lane 5: Sigma low molecular weight markers; Lane 6: lysostaphin expressed in AIM media (neat); Lane 7: lysostaphin expressed in AIM media (1/10); Lane 8: lysostaphin expressed in AIM media (1/100).



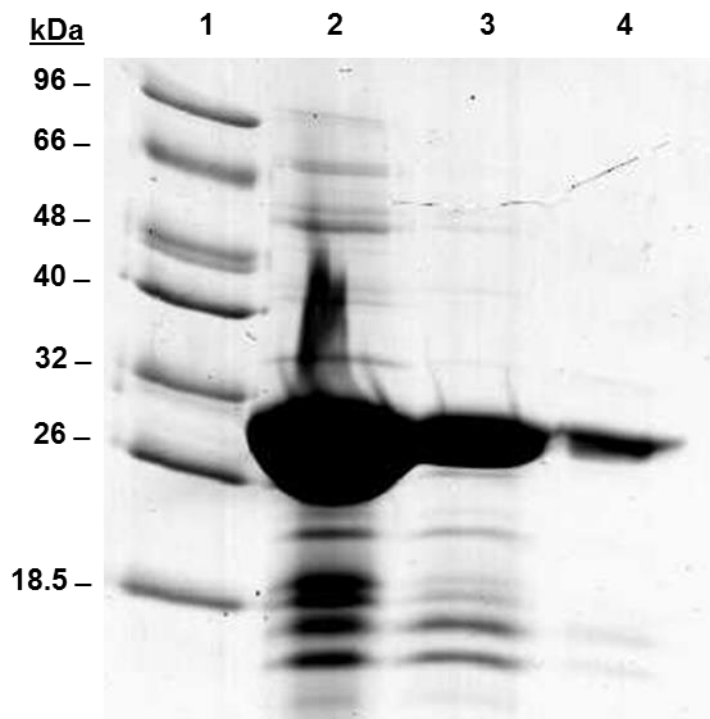
Appendix 7.162: SDS-PAGE analysis of cell lysate containing N-terminally His-tagged recombinant lysostaphin (construct 1, preparation 11) expressed in *E.coli* BL21(DE3) cultured in LB. Lane 1: NZY broad size markers; Lane 2: CFE (1:10); Lane 3: CFE (1:100).



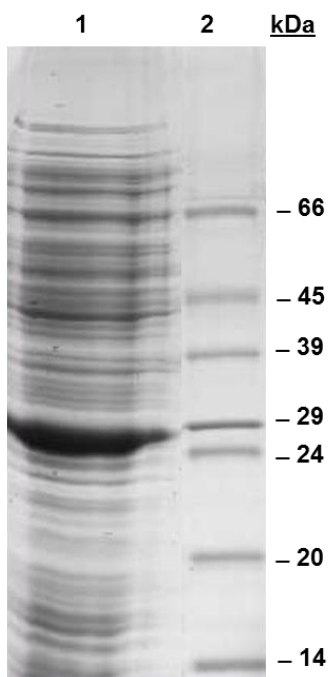
Appendix 7.163: IMAC purification of recombinant lysostaphin (construct 1, preparation 11) using a Chelating Sepharose™ Fast Flow media column and ÄKTA™ prime plus system. Bound protein was eluted by applying an increasing imidazole concentration (20-500 mM). Fractions were collected every 60 s throughout the separation. Fractions 44-60 were pooled and concentrated.



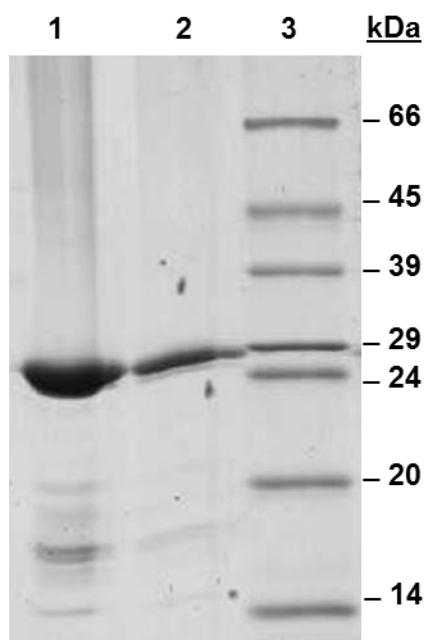
Appendix 7.164: SDS-PAGE analysis of purified, concentrated *N*-terminally His-tagged recombinant lysostaphin (construct 1, preparation 11). Lane 1: NZY broad range size markers; Lane 2: concentrated protein (1:10); Lane 3: concentrated protein (1:100); Lane 4: concentrated protein (1:1000).



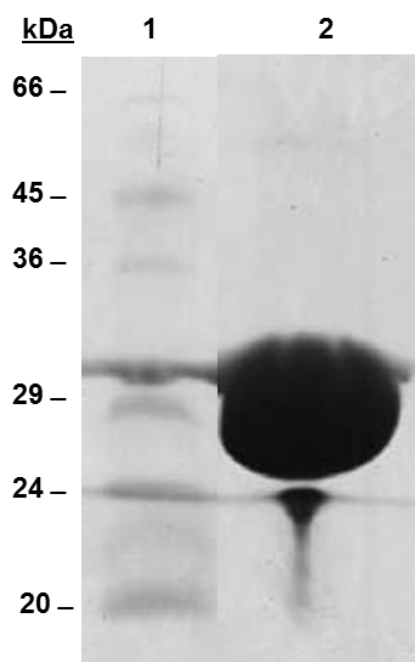
Appendix 7.165: SDS-PAGE analysis of cell lysate containing *N*-terminally His-tagged recombinant lysostaphin (construct 1, preparation 12) expressed in *E.coli* BL21(DE3) cultured in LB. Lane 1: CFE (neat); Lane 2: Sigma low molecular weight markers.



Appendix 7.166: SDS-PAGE analysis of purified, concentrated *N*-terminally His-tagged recombinant lysostaphin (construct 1, preparation 12). Lane 1: concentrated protein (1:10); Lane 2: concentrated protein (1:100); Lane 3: Sigma low molecular weight markers



Appendix 7.167: SDS-PAGE analysis of purified, concentrated *N*-terminally His-tagged recombinant lysostaphin (construct 1, preparation 13). Lane 1: Sigma low molecular weight markers; Lane 2: concentrated protein (neat).



7.2.1 Column selection

Appendix 7.168: Protein separation using ProPac® SAX-10, SCX-10 and WCX-10 columns and DX500 chromatography system

Initial ion exchange separations were performed using a 0.5 ml/ min flow rate and linear gradient from 0-50% IEX buffer B in 60 min. The ion exchange column was washed at 90% B for 10 min and then the column was equilibrated at 0% B for 10 min. Mobile phase buffers were degassed for 15 min prior to system equilibration. Manual injections of 100 µl of recombinant lysostaphin (construct 4, preparation 1 or construct 3, preparations 2 or 3) were delivered to the system. Fractions were collected using a Foxy Jr fraction collector and fraction collection was initiated manually upon peak elution.

Appendix 7.169: Protein separation using ProPac® WCX-10 column and Ultimate™ 3000 chromatography system

WCX separation was performed using a 0.5 ml/ min flow rate and linear gradient from 0-50% IEX buffer B in 30 min. The WCX column was washed at 90% B for 2 min and then the column was equilibrated at 0 % B for 4 min. A 5 µl injection of a 1:2 dilution of purified recombinant lysostaphin (construct 1, preparation 4) was applied to the system. Fractions were collected by time, every 60 s between 6 and 36 min. Following separation, fractions containing eluted protein were analysed by SDS-PAGE.

Appendix 7.170: Validation of ProPac® WCX-10 column

Multiple WCX separations were performed to validate a ProPac® WCX-10 column (4.0 x 250 mm). The separations were performed using a 0.5 ml/ min flow rate and linear gradient from 0-50% B over 70 min. The WCX column was washed at 90% B for 4 min and then the column was equilibrated at 0% B for 20 min. A 50 µl injection of cytochrome C standard was injected onto the system.

Appendix 7.171: Protein separation using ProSwift® SCX-1S column and an Ultimate™ 3000 system

SCX separation was performed using a 0.5 ml/ min flow rate and linear gradient from 0-50% IEX buffer B in 30 min. The ProSwift® SCX-1S column was washed at 90% B for 2 min and

then the column was equilibrated with 0 % B for 4 min. A 5 µl of injection of purified concentrated recombinant lysostaphin (construct 1, preparation 4) was delivered onto the system. Fractions were collected by time, every 60 s between 6 and 28 min.

Appendix 7.172: Protein separation using ProSwift® WCX-1S column and an Ultimate™ 3000 system

WCX separation was performed using an 80 µl/ min flow rate and linear gradient from 5-50% IEX buffer B in 20 min. The ProSwift® WCX-1S column was washed at 90% B for 2 min and then the column was equilibrated at 5 % B for 8 min. A 30 µl injection of a 1:10 dilution of purified recombinant lysostaphin (construct 1, preparation 4) was applied to the system. Fractions were collected by time, every 60 s between 2 and 22 min.

Appendix 7.173: Validation of ProPac® MAb SCX beta test column

The ProPac® MAb SCX-1S column was validated according to a beta-test protocol provided by Dionex, UK. During each separation, 10 µl of standard protein mix was injected onto the column. Each separation was performed using a flow rate of 1.0 ml/min. The column was equilibrated for 10 min using 100% MAb SCX buffer A, before applying a linear gradient of 0-48% MAb SCX buffer B in 20.3 min. The column was then washed for 5 min using 100% MAb SCX buffer B.

Appendix 7.174: Protein separation using the ProPac® MAb SCX beta test column

Purified recombinant lysostaphin was separated using the beta-test protocol (Appendix 7.173). During the separation, 10 µl of a 1:10 dilution of purified recombinant lysostaphin (construct 3, preparation 5) was applied to the column.

7.2.2 Optimisation of protein isoform separation

Appendix 7.175: Optimisation of sample loading conditions

Separations were performed using ProPac® WCX-10 column (4 x 250 mm) or ProPac® WCX-10 column (4 x 500 mm) column at a flow rate of 0.5 ml/min. Separation was achieved by applying a linear gradient from 0-50% WCX Buffer B in 70 min. The column was washed at 90% B for 4 min before being equilibrated with 0% B for 10 min. Manual 100 µl injections of recombinant lysostaphin (construct 1, preparation 8 or 9) were delivered to the Dionex DX500 HPLC system. Fractions were collected using a Foxy Jr fraction collector every 30 s between 15 and 55 min.

Appendix 7.176: Optimisation of sample preparation

Separations were performed using a ProPac® WCX-10 column (4 x 500 mm) column at a flow rate of 1.0 ml/min. Separation was achieved by applying a linear gradient from 0-50% B in 15 min. The column was washed at 90% IEX Buffer B for 2 min before being equilibrated with 0% B for 8 min. Automated injections of 270, 300 or 350 µl of recombinant lysostaphin (construct 1, preparation 10) were delivered to the system.

Appendix 7.177: Optimisation of gradient conditions

Gradient duration experiments were performed using a ProPac® WCX-10 column (4 x 250 mm) at a flow rate of 0.5 ml/min. Separation was achieved by applying a linear gradient from 0-50% IEX buffer B for either 60, 70, 90, 120 or 240 min. The column was washed at 90% B for 3 min before being equilibrated with 0% B for 9 min. Automated 5 µl injections of recombinant lysostaphin (construct 1, preparation 4) were delivered to the system.

Gradient steepness experiments were performed using ProPac® WCX-10 column (4 x 250 mm) at a flow rate of 0.5 ml/min. Separation was achieved by applying a linear gradient from 0-50% or 0-90% IEX buffer B for 70 min. The column was washed at 90% B for 10 min before being equilibrated with 0% B for 20 min. Manual 20 µl injections of a 1:10 dilution of recombinant lysostaphin (construct 1, preparation 7) were delivered to the Dionex DX500 HPLC system.

Appendix 7.178: Optimisation of mobile phase conditions

Separation was performed as described in Appendix 7.176 with injection of 260 µl of recombinant lysostaphin (construct 1, preparation 4).

Appendix 7.179: Optimisation of column length

Separations were performed as described in Appendix 7.175 following manual injection of 100 µl of recombinant lysostaphin (construct 1, preparation 8).

Appendix 7.180: Optimisation of column diameter

First dimensional SCX separation of purified recombinant lysostaphin was performed using a ProPac[®] SCX-10 column (2 x 250 mm) at a flow rate of 0.2 ml/min. Separation was achieved by applying a linear gradient from 0-50% SCX Buffer B in 20 min. The column was washed at 90% B for 13 min before being equilibrated with 0% B for 11 min. An automated 200 µl injection of recombinant lysostaphin (construct 1, preparation 11) was delivered to the system. Fractions were collected using a Foxy Jr fraction collector every 60 s between 5 and 35 min. The thermal compartment was maintained at 40°C.

Second dimensional RP separations were performed using a ProSwift[®] RP-4H (1 x 250 mm) column at a flow rate of 0.3 ml/min. Separation was achieved by applying a linear gradient from 13-65% RP Buffer B in 20 min. The column was washed at 90% B for 3 min before being equilibrated with 13% B for 6 min. An automated 60 µl injection of each SCX fraction was then delivered to the system

First dimensional SCX separations of cell lysate were performed using a ProPac[®] SCX-10 column (2 x 250 mm) at a flow rate of 0.2 ml/min. Cell lysate was prepared as described in Appendix 7.233. Separation was achieved by applying a linear gradient from 0-50% SCX Buffer B in 20 min. An isocratic gradient was maintained at 50% B for 1 min before washing the column at 90% B for 3 min. The column was then equilibrated with 0% B for 11 min. An automated 100 µl injection of cell lysate containing recombinant lysostaphin (construct 1) was delivered to the system. Cell lysate harvested at 4 h post-induction was prepared as described in Appendix 7.233. Fractions were collected using a Foxy Jr fraction collector every 60 s between 12 and 35 min. Second dimensional separation was performed as described above.

WCX separation of purified recombinant lysostaphin was performed using the ProPac® WCX-10 column (2 x 250 mm) column at a flow rate of 0.2 ml/min. Separation was achieved by applying a linear gradient from 0-50% WCX Buffer B in 20 min. An isocratic gradient was maintained at 50% B for 2.9 min before washing the column at 90% B for 13 min. The column was then equilibrated with 0% B for 11 min. An automated 50 µl injection of recombinant lysostaphin (construct 1, preparation 12) was delivered to the system. WCX separation of cell lysate was performed as described in Appendix 7.224.

Appendix 7.181: Optimisation of fraction collection by time

Separation of recombinant lysostaphin (construct 1, preparation 9) was performed using a ProPac® WCX-10 column (4 x 250 mm) column, whilst separation of recombinant lysostaphin (construct 1, preparation 10) was achieved using ProPac® WCX-10 column (4 x 500 mm) column. Separation was performed as described in Appendix 7.175, however 100 µl of a 1:3 dilution of preparation 9 or 150 µl of preparation 10 were delivered to the Dionex DX500 HPLC system. During the separation of preparation 9, fractions were collected every 30 s between 15 and 55 min, whilst fractions were collected every 30 s between 20 and 55 min during separation of preparation 10.

Appendix 7.182: Optimisation of fraction collection by peak recognition

Initial separations of recombinant lysostaphin was performed using a ProPac® WCX-10 column (2 x 250 mm) at a flow rate of 150 µl/min. Automated 20 µl injections of recombinant lysostaphin (construct 3, preparation 13) were delivered to the system. Separation was achieved by applying a linear gradient from 0-50% IEX buffer B over 70 min. The column was washed at 90% B for 3 min before being equilibrated with 0% B for 9 min. Fraction collection was performed by peak recognition between 3 and 50 min using default settings. Fractions were not collected outside of peaks and collection was based upon UV absorbance at 214 nm or 280 nm. During the next separation, peak recognition settings were modified from default values, with peak start threshold decreased from 10 to 5 mAU, peak start/end true times increased from 1 s to 3 s and threshold no peak end increased from 100 mAU to 2000 mAU.

Appendix 7.183: Analysis of recombinant lysostaphin using optimised conditions

Separation was performed as described in Appendix 7.175 using a ProPac[®] WCX-10 (4 x 250 mm) column however 20 µl of purified recombinant lysostaphin (construct 3, preparation 13) was delivered to the Dionex DX500 HPLC system. Fraction 25 collected during WCX separation was re-applied to the column and separated using the same conditions.

Appendix 7.184: Influence of culture temperature upon charge heterogeneity of recombinant lysostaphin

To assess the influence of temperature upon the charge heterogeneity of recombinant lysostaphin a number of cultures were setup and incubated at 16, 20 or 30°C (Appendix 7.185). Recombinant protein expression was performed in LB as described in Appendix 7.232. Some of the cultures were aseptically split at the point of induction to ensure the cells cultured at different temperatures were induced at the same optical density. The duration of expression was adjusted according to the results obtained. Cell lysate was harvested as described in Appendix 7.77 and applied directly to the ProPac[®] WCX (4 x 500 mm) column.

Separation of cell lysate was performed using a ProPac[®] WCX-10 column (4 x 500 mm) column at flow rate of 0.5 ml/min. Following sample injection, an isocratic gradient of 0% WCX buffer B was applied before separating protein isoforms by applying a linear gradient from 0-50% WCX Buffer B in 70 min. The column was washed at 90% B for 9 min and then equilibrated with 0% B for 15 min. An automated 500 µl injection of cell lysate containing recombinant lysostaphin (construct 1) was delivered to the system

Appendix 7.185: Culture conditions

Culture	Construct	Temperature (°C)	Induction optical density (OD _{600 nm})	Duration of Expression (h)
1	1	20	0.847	16.0
	1	30		
2	1	20	0.689	16.0
	1	30		
3	1	20	1.080	16.0
	1	30		
4	2	16	0.718	17.5
		20		
5	2	16	0.704	17.5
		20		
6	2	16	1.112	14.0
7	2	16	0.723	14.0

Appendix 7.186: Separation of alternative recombinant protein preparations

The genes encoding recombinant oxidoreductase from *Clostridium acetobutylicum* (gi:15004706) and recombinant NADPH-dependent 1-acyl dihydroxyacetone phosphate reductase (Ayr1p) from *Saccharomyces cerevisiae* (gi:6322067), were synthesised or amplified and cloned into pET-YSBLIC using ligation-independent cloning and *E. coli* TOP10³. The recombinant pET-YSBLIC was transformed into *E. coli* BL21(DE3) and the recombinant proteins were expressed in LB and AIM, as described in Appendix 7.76 and Appendix 7.75 respectively. *E. coli* cultures grown in LB were induced at OD_{600 nm} values of 0.788 and 0.747 for recombinant oxidoreductase and recombinant Ayr1p respectively and cell lysate was harvested 19.5 h post-induction. *E. coli* cultures grown in AIM were induced at OD_{600 nm} values of 1.228 and 0.912 for recombinant oxidoreductase and recombinant Ayr1p respectively and cell lysate was harvested 16.0 h post-induction.

Harvested cell lysate was directly applied to the ProPac[®] WCX (4 x 500 mm) column and the protein preparation was separated as described in Appendix 7.184. ProtParam analysis was performed on the amino acid sequences of both recombinant proteins (Appendix 7.206 and Appendix 7.207) to ensure that the expected charge of the expressed protein would permit

³ These basic recombinant proteins were cloned and transformed in to *E. coli* BL21(DE3) by Dr Meng Zhang at Northumbria University.

binding during WCX. ClustalW analysis was also performed to establish whether the selected proteins shared sequence homology, as described in Appendix 7.48.

Appendix 7.187: Optimisation of sample loading conditions

Separation was performed as described in Appendix 7.173 using the ProPac[®] MAb SCX beta test (4 x 250 mm) column. During each separation, 10, 100 or 200 µl of recombinant lysostaphin (construct 3, preparation 5) was injected onto the column.

Appendix 7.188: Optimisation of chromatographic gradient conditions

The first separation was performed as described in Appendix 7.173 using the ProPac[®] MAb SCX beta test (4 x 250 mm) column. During each separation 200 µl of a 1:10 dilution of recombinant lysostaphin (construct 3, preparation 5) was injected onto the column.

The second separation was performed using a ProPac[®] WCX-10 column (2 x 250 mm) at a flow rate of 500 µl/min. Following injection of 200 µl of a 1:10 dilution of recombinant lysostaphin (construct 3, preparation 5), an isocratic gradient was maintained for 3 min at 0% B. Separation was achieved by applying a linear gradient of 0-50% MAb SCX buffer B over 20 min. The column was washed at 90% B for 4 min before being equilibrated with 0% B for 8 min.

Appendix 7.189: Optimisation of mobile phase conditions

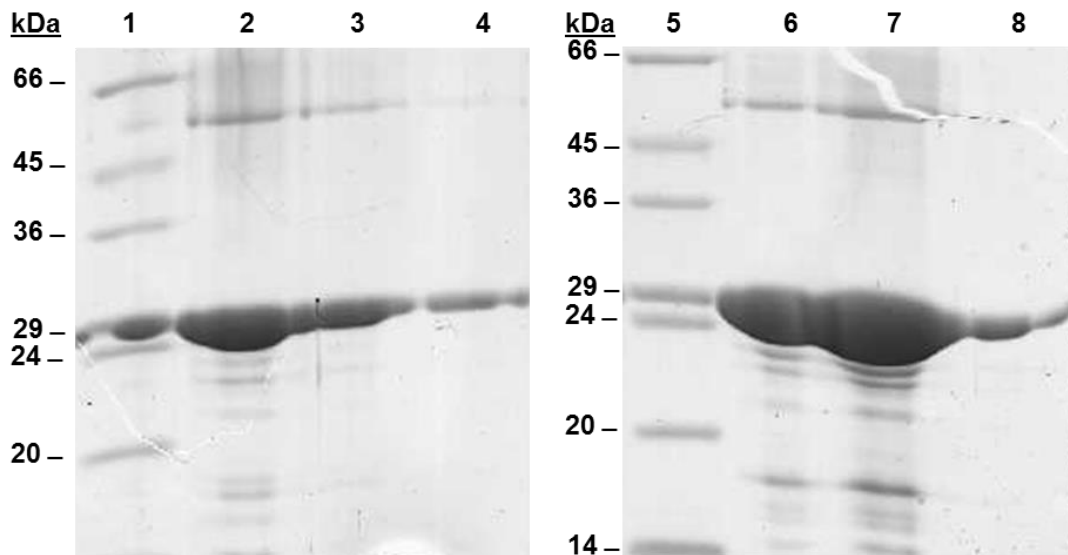
Separation was performed as described in Appendix 7.173 using the ProPac[®] MAb SCX beta test (4 x 250 mm) column. However two separations were performed using MAb SCX buffer A and B and two separations were performed using WCX buffer A and B. During each separation, 20 µl of recombinant lysostaphin (construct 3, preparation 5) was injected onto the column.

Appendix 7.190: Optimisation of column length

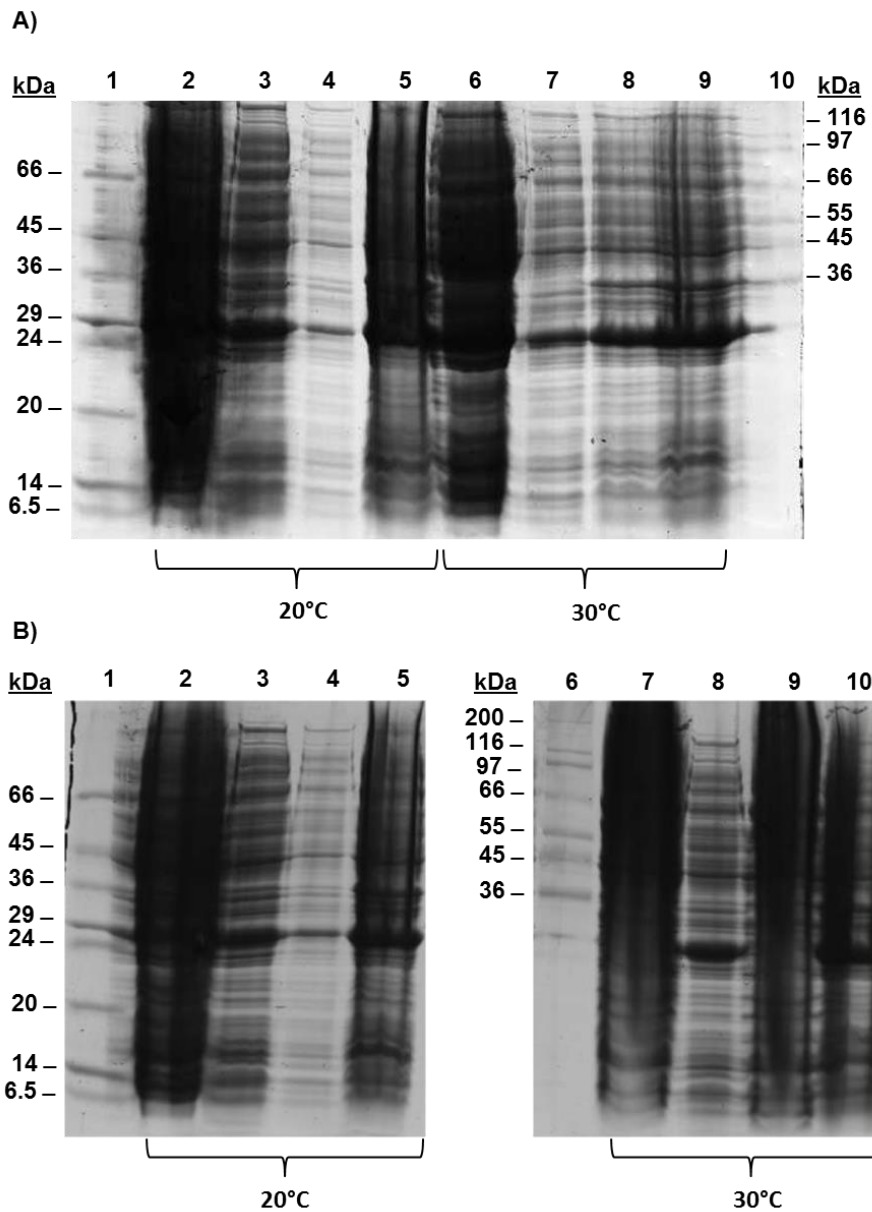
The first separation was performed as described in Appendix 7.173 using the ProPac® MAb SCX (4 x 250 mm) column. During each separation 40 µl of recombinant lysostaphin (construct 3, preparation 5) was injected onto the column.

The second separation was performed using a ProPac® WCX-10 column (4 x 500 mm) at a flow rate of 1.0 ml/min. Prior to injection of 40 µl of recombinant lysostaphin (construct 3, preparation 5), an isocratic gradient was maintained for 10 min at 0% B. Separation was achieved by applying a 0-48% MAb SCX buffer B over 40.0 min. The column was then washed for 10 min using 100% B before reequilibrating at 0% B for 10 min.

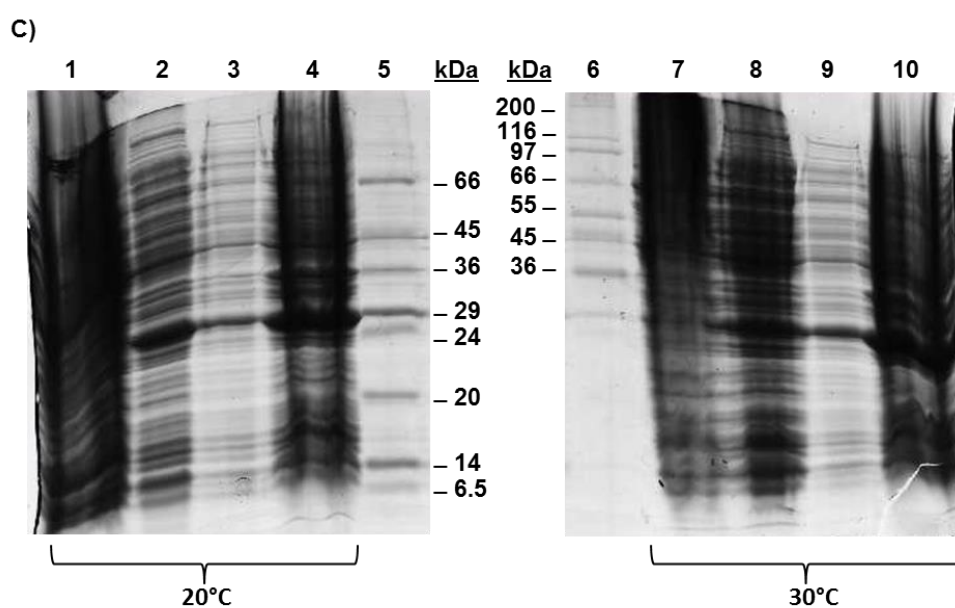
Appendix 7.191: SDS-PAGE analysis of resuspended *N*-terminally His-tagged recombinant lysostaphin (construct 1) following IMAC, dialysis and lyophilisation. Recombinant lysostaphin was produced using *E. coli* BL21(DE3) which had been cultured in either LB or AIM. Lane 1: Sigma low molecular weight markers; Lane 2: construct 1 expressed in LB (neat); Lane 3: construct 1 expressed in LB (1:10); Lane 4: construct 1 expressed in LB (1:100); Lane 5: Sigma low molecular weight markers; Lane 6: construct 1 expressed in AIM (neat); Lane 7: construct 1 expressed in AIM (1:10); Lane 8: construct 1 expressed in AIM (1:100).



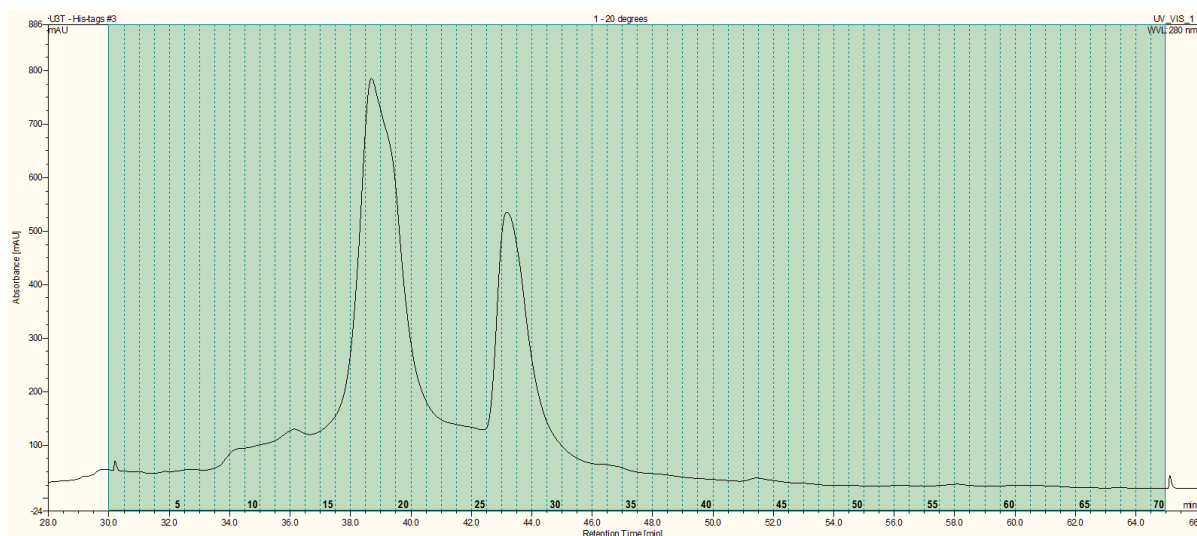
Appendix 7.192: Expression of recombinant lysostaphin at different post-induction temperatures. Three cultures containing 500 ml of LB were inoculated with a starter culture harbouring *E.coli* BL21(DE3) transformed with a plasmid containing *N*-terminally His-tagged recombinant lysostaphin (construct 1). Protein expression was induced in cultures 1, 2 and 3 at OD_{600 nm} values of 0.847, 0.689, and 1.080 respectively. Following IPTG induction, each culture was aseptically split and the resulting six 250 ml cultures were incubated at 30°C or 20°C. Cell lysates were harvested 16 h after induction of protein expression and were analysed by 12% (w/v) SDS-PAGE. A) Culture 1. Lane 1: Sigma low molecular weight markers; Lane 2: CFE (neat) [20°C]; Lane 3: CFE (1:10) [20°C]; Lane 4: CFE (1:100) [20°C]; Lane 5: CFE in solubilising buffer [20°C]; Lane 6: CFE (neat) [30°C]; Lane 7: CFE (1:10) [30°C]; Lane 8: CFE (1:100) [30°C]; Lane 9: CFE in solubilising buffer [30°C]; Lane 10: Sigma high molecular weight markers. B) Culture 2. Lane 1: Sigma low molecular weight markers; Lane 2: CFE (neat) [20°C]; Lane 3: CFE (1:10) [20°C]; Lane 4: CFE (1:100) [20°C]; Lane 5: CFE in solubilising buffer [20°C]; Lane 6: Sigma high molecular weight markers; Lane 7: CFE(neat) [30°C]; Lane 8: CFE (1:10) [30°C]; Lane 9: CFE (1:100) [30°C]; Lane 10: CFE in solubilising buffer [30°C].



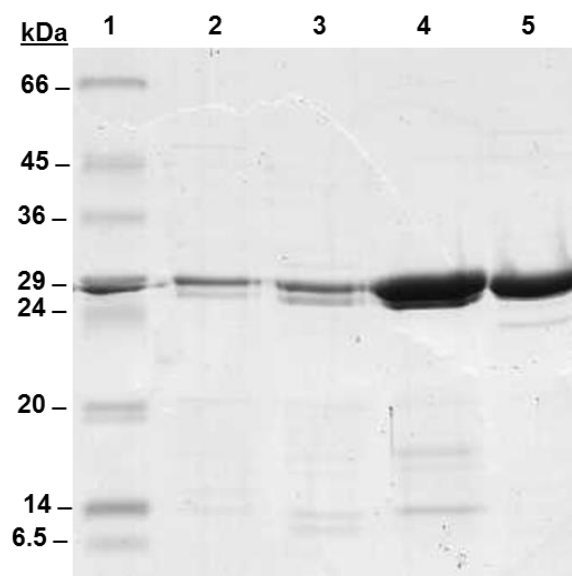
Appendix 7.192 (continued): Expression of recombinant lysostaphin at different post-induction temperatures. Three cultures containing 500 ml of LB were inoculated with a starter culture harbouring *E.coli* BL21(DE3) transformed with a plasmid containing *N*-terminally His-tagged recombinant lysostaphin (construct 1). Protein expression was induced in cultures 1, 2 and 3 at OD_{600 nm} values of 0.847, 0.689, and 1.080 respectively. Following IPTG induction, each culture was aseptically split and the resulting six 250 ml cultures were incubated at 30°C or 20°C. Cell lysates were harvested 16 h after induction of protein expression and were analysed by 12% (w/v) SDS-PAGE. C) Culture 3. Lane 1: CFE (neat) [20°C]; Lane 2: CFE(1:10) [20°C]; Lane 3: CFE (1:100) [20°C]; Lane 4: CFE in solubilising buffer [20°C]; Lane 5: Sigma low molecular weight markers; Lane 6: Sigma high molecular weight markers; Lane 7: CFE (neat) [30°C]; Lane 8: CFE (1:10) [30°C]; Lane 9: CFE (1:100) [30°C]; Lane 10: CFE in solubilising buffer [30°C].



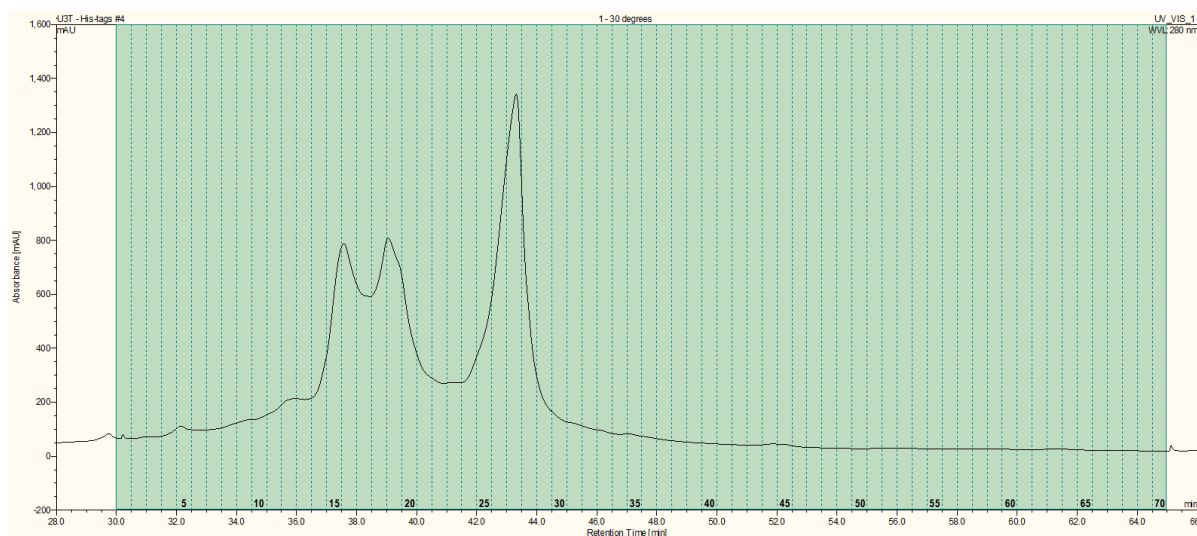
Appendix 7.193: WCX separation of cell lysate containing *N*-terminally His-tagged recombinant lysostaphin (construct 1) following expression at 20°C (Culture 1). Fractions 9, 13, 18 and 27 were analysed by SDS-PAGE.



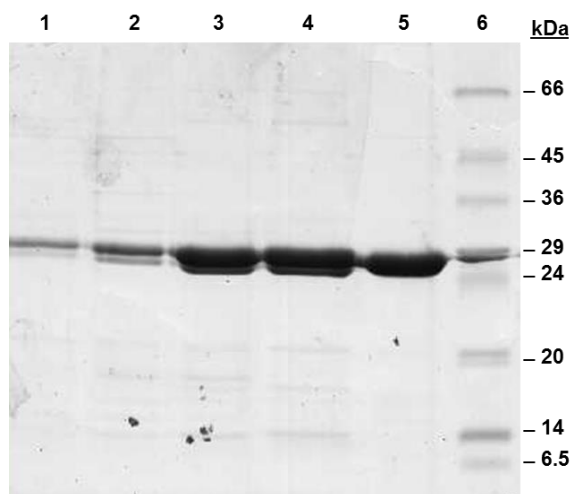
Appendix 7.194: SDS-PAGE analysis of WCX fractions following separation of *N*-terminally His-tagged recombinant lysostaphin (construct 1) after expression at 20°C (Culture 1). Lane 1: Sigma low molecular weight markers; Lane 2: Fraction 9; Lane 3: Fraction 13; Lane 4: Fraction 18; Lane 5: Fraction 27.



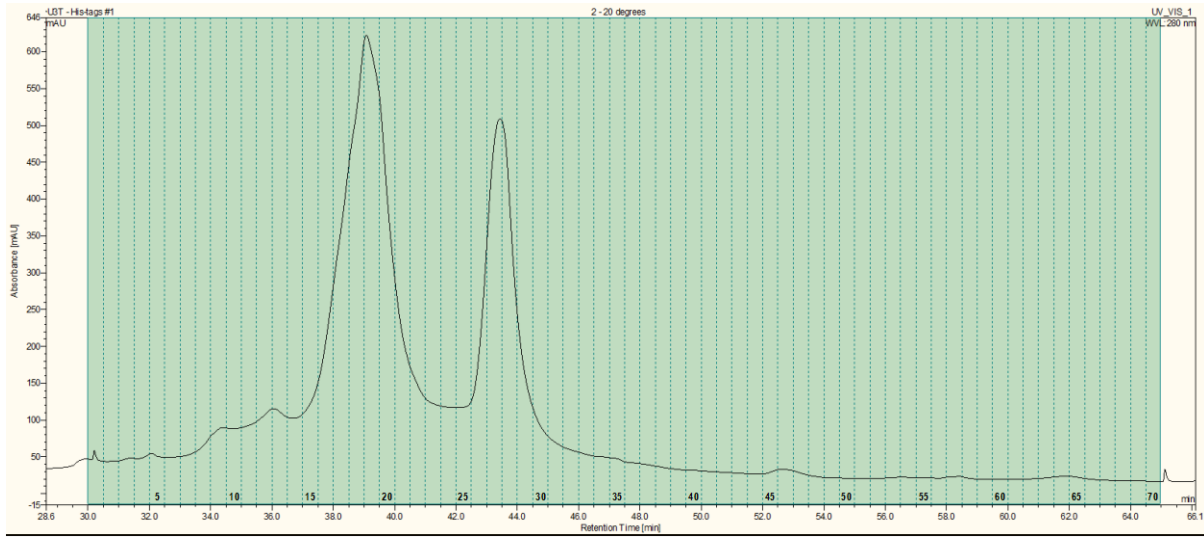
Appendix 7.195: WCX separation of cell lysate containing *N*-terminally His-tagged recombinant lysostaphin (construct 1) following expression at 30°C (Culture 1). Fractions 5, 12, 16, 19 and 27 were analysed by PAGE.



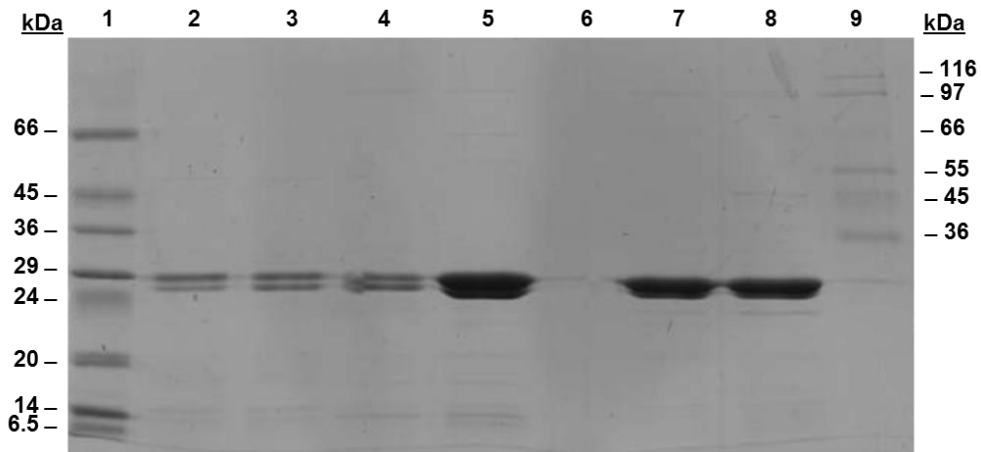
Appendix 7.196: SDS-PAGE analysis of WCX fractions following separation of *N*-terminally His-tagged recombinant lysostaphin (construct 1) after expression at 30°C (Culture 1). Lane 1: Fraction 5; Lane 2: Fraction 12; Lane 3: Fraction 16; Lane 4: Fraction 19; Lane 5: Fraction 27; Lane 6: Sigma low molecular weight markers.



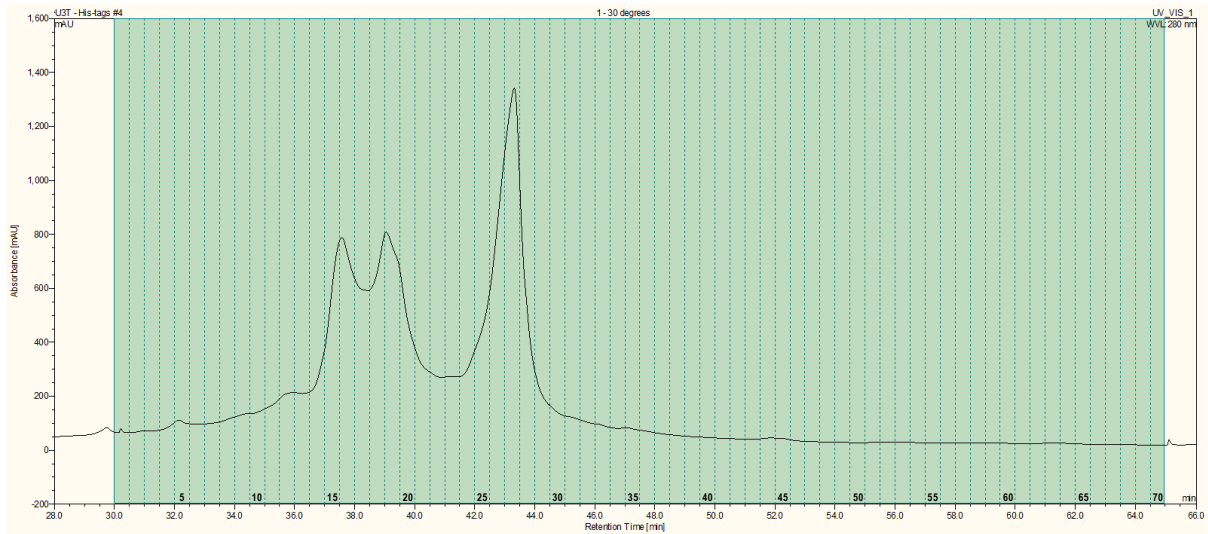
Appendix 7.197: WCX separation of cell lysate containing *N*-terminally His-tagged recombinant lysostaphin (construct 1) following expression at 20°C (Culture 2). Fractions 9, 12, 13, 18, 19, 27 and 28 were analysed by SDS-PAGE.



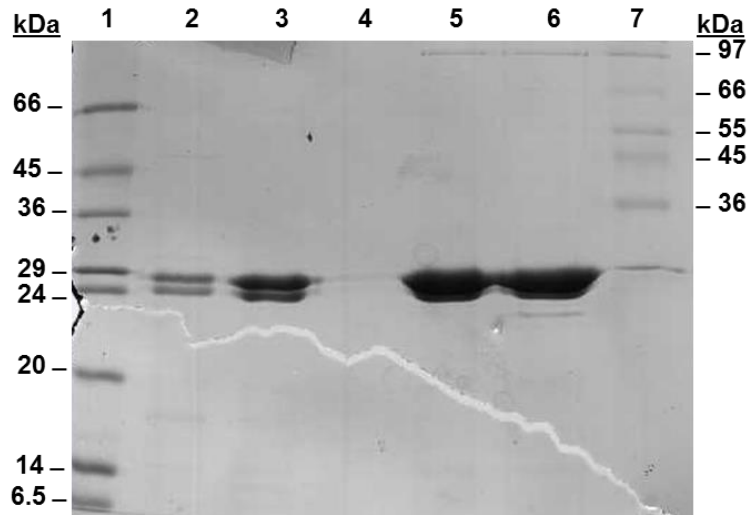
Appendix 7.198: SDS-PAGE analysis of WCX fractions following separation of *N*-terminally His-tagged recombinant lysostaphin (construct 1) after expression at 20°C (Culture 2). Lane 1: Sigma low molecular weight markers; Lane 2: Fraction 9; Lane 3: Fraction 12; Lane 4: Fraction 13; Lane 5: Fraction 18; Lane 6: Fraction 19; Lane 7: Fraction 27; Lane 8: Fraction 28; Lane 9: Sigma high molecular weight markers.



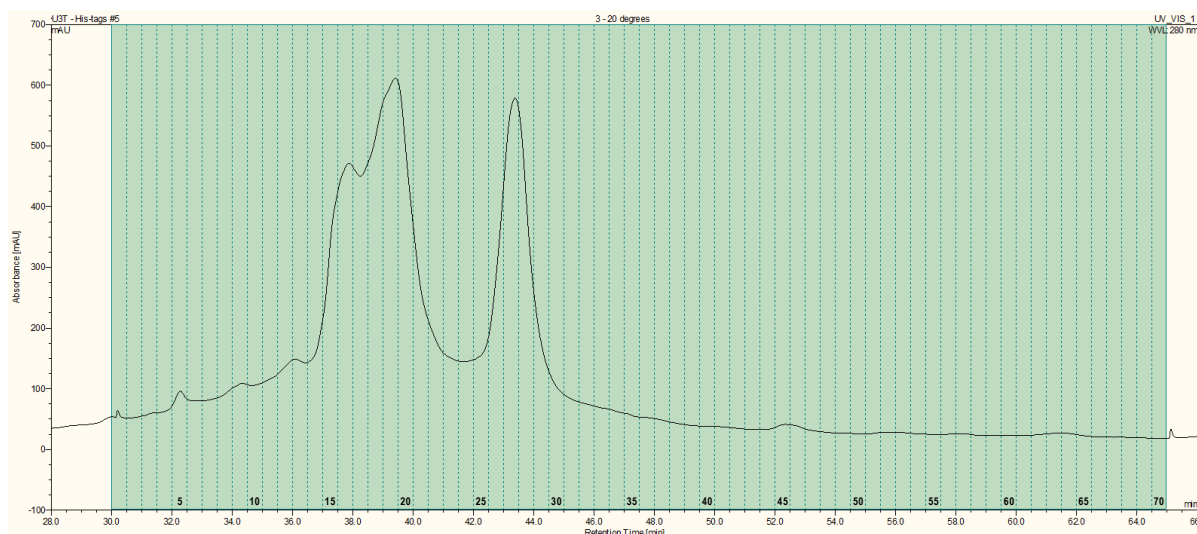
Appendix 7.199: WCX separation of cell lysate containing *N*-terminally His-tagged recombinant lysostaphin (construct 1) following expression at 30°C (Culture 2). Fractions 13, 17, 19, 27 and 28 were analysed by SDS-PAGE.



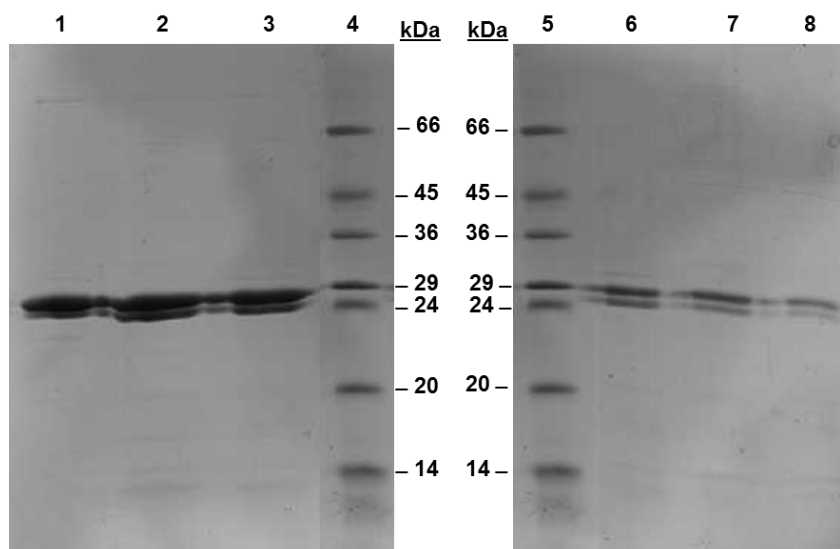
Appendix 7.200: SDS-PAGE analysis of WCX fractions following separation of *N*-terminally His-tagged recombinant lysostaphin (construct 1) after expression at 30°C (Culture 2). Lane 1: Sigma low molecular weight markers; Lane 2: Fraction 13; Lane 3: Fraction 17; Lane 4: Fraction 19; Lane 5: Fraction 27; Lane 6: Fraction 28; Lane 7: Sigma high molecular weight markers.



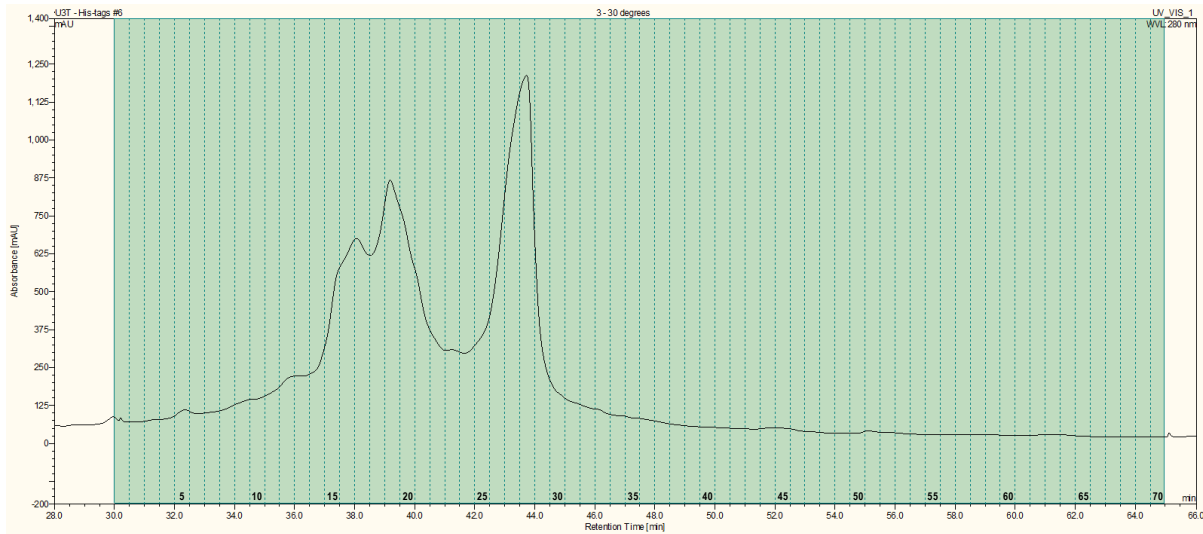
Appendix 7.201: WCX separation of cell lysate containing *N*-terminally His-tagged recombinant lysostaphin (construct 1) following expression at 20°C (Culture 3). Fractions 5, 9, 13, 16, 19 and 27 were analysed by SDS-PAGE.



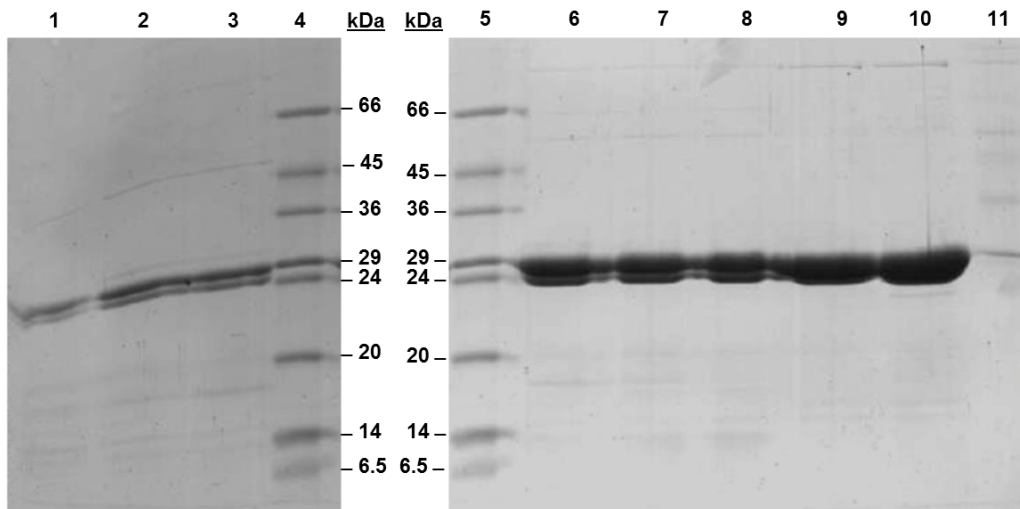
Appendix 7.202: SDS-PAGE analysis of WCX fractions following separation of *N*-terminally His-tagged recombinant lysostaphin (construct 1) after expression at 20°C (Culture 3). Lane 1: Fraction 5; Lane 2: Fraction 9; Lane 3: Fraction 13; Lane 4: Sigma low molecular weight markers; Lane 5: Sigma low molecular weight markers; Lane 6: Fraction 16; Lane 7: Fraction 19; Lane 8: Fraction 27.



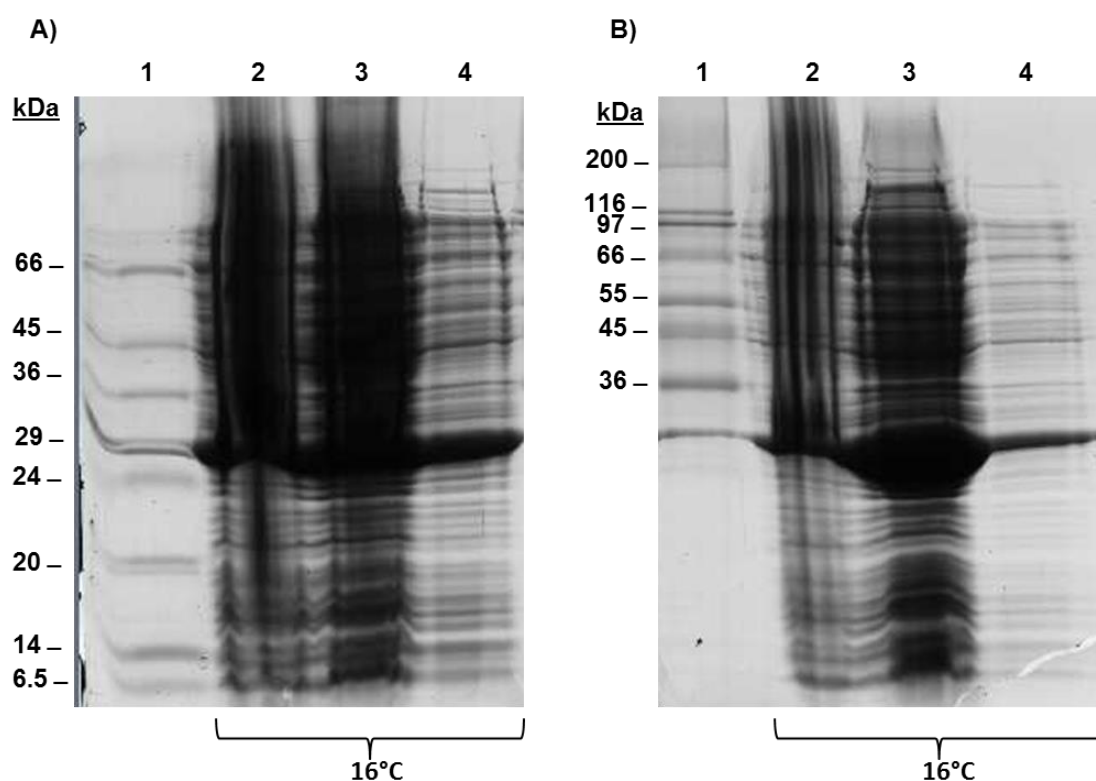
Appendix 7.203: WCX separation of cell lysate containing *N*-terminally His-tagged recombinant lysostaphin (construct 1) following expression at 30°C (Culture 3). Fractions 5, 12, 13, 16, 17, 19, 27 and 28 were analysed by SDS-PAGE.



Appendix 7.204: SDS-PAGE analysis of WCX fractions following separation of *N*-terminally His-tagged recombinant lysostaphin (construct 1) after expression at 30°C (Culture 3). Lane 1: Fraction 5; Lane 2: Fraction 12; Lane 3: Fraction 13; Lane 4: Sigma low molecular weight markers; Lane 5: Sigma low molecular weight markers; Lane 6: Fraction 16; Lane 7: Fraction 17; Lane 8: Fraction 19; Lane 9: Fraction 27; Lane 10: Fraction 28; Lane 11: Sigma high molecular weight markers.



Appendix 7.205: Expression of recombinant lysostaphin at 16°C. Two cultures containing 500 ml of LB were inoculated with a starter culture harbouring *E.coli* BL21(DE3) transformed with a plasmid containing *N*-terminally His-tagged recombinant lysostaphin (construct 1). Protein expression was induced in cultures 1 and 2 at OD_{600 nm} values of 1.112 and 0.723 respectively. Following IPTG induction, the cultures were incubated at 16°C. Cell lysates were harvested 14 h after induction of protein expression and were analysed by SDS-PAGE. A) Culture 1. Lane 1: Sigma low molecular weight markers; Lane 2: CFE (neat); Lane 3: CFE (1:10); Lane 4: CFE (1:100); B) Culture 2. Lane 1: Sigma high molecular weight markers; Lane 2: CFE (neat); Lane 3: CFE (1:10); Lane 4: CFE (1:100).



Appendix 7.206: Predicted amino acid sequence of recombinant oxidoreductase from *Clostridium acetobutylicum* (ATCC 8S4) (NP_149166.1).

```
MKEYKYTVITGASSGIGYEAAKAFKRGKLNLIARRREKLEELKKEILHYNRSLKVIVKSIDLSITSNV
YSLYDELKNYNIETLVNNAGFGDYSKVNNQNLEKVESMLSLNIEALVILSSLFVRDYEKIEGTQLINISS
AGGYTIVPNAVIYCATKFFVSSFTEGLARELIEAKSNLKAKVLAPAATETEFGKVASDVKEYDYQEKFKH
YHTSKQMAEFLIKLYDNDYIVGKVDRNSFKFTLQNPFDYA
```

Appendix 7.207: Predicted amino acid sequence of recombinant AyrP1, a dehydrogenase from *Saccharomyces cerevisiae* (S288c) (NP_012142.1).

MSELQSQPKKIAVWTGASGGIGYEVTKELARNGYLVYACARRLEPMAQLAIQFGNDSIKPYKLDISKPEE
IVTFSGFLRANLPDGKLDLLYNNAGQSCTFPALDATDAAVEQCCKVNVFGHINMCRELSEFLIKAKGTIV
FTGSLAGVVSFPFGSIYSASKAAIHQYARGLHLEMKPFNVRVINAITGGVATDIADKRPLPETSINYFPE
GREAFNSRKTMAKDNKMPADAYAKQLVKDILSTSDPVDVYRGTFANIMRFVMIFVPYWLEKGLSKKFK
LDKVNNALKSKQKNKDD

Appendix 7.208: ProtParam analysis of recombinant oxidoreductase from *Clostridium acetobutylicum* (NP_149166.1)

User-provided sequence:

```

      10      20      30      40      50      60
MKEYKYTVIT GASSGIGYEA AKAFAKRGKN LIIIARRREK LEELKKEILH YNRSCLKVIVK

      70      80      90     100     110     120
SIDLSITSNV YSLYDELKNY NIETLVNNG FGDYSKVNQ NLEKVESMLS LNIEALVILS

     130     140     150     160     170     180
SLFVRDYEKI EGTQLINISS AGGYTIVPNA VIYCATKFFV SSFTEGLARE LIEAKSNLKA

     190     200     210     220     230     240
KVLAPAATET EFGKVASDVK EYDYQEKFKH YHTSKQMAEF LIKLYDNDYI VGKVDRNSFK

     250
FTLQNPIFDY A

```

Molecular weight: 28507.6

Theoretical pI: 8.62

Amino acid composition:

[CSV format](#)

Ala (A)	20	8.0%
Arg (R)	8	3.2%
Asn (N)	17	6.8%
Asp (D)	10	4.0%
Cys (C)	1	0.4%
Gln (Q)	5	2.0%
Glu (E)	21	8.4%
Gly (G)	12	4.8%
His (H)	3	1.2%
Ile (I)	21	8.4%
Leu (L)	23	9.2%
Lys (K)	26	10.4%
Met (M)	3	1.2%
Phe (F)	12	4.8%
Pro (P)	3	1.2%
Ser (S)	20	8.0%
Thr (T)	12	4.8%
Trp (W)	0	0.0%
Tyr (Y)	17	6.8%
Val (V)	17	6.8%
Pyl (O)	0	0.0%
Sec (U)	0	0.0%
(B)	0	0.0%
(Z)	0	0.0%
(X)	0	0.0%

Appendix 7.208: ProtParam analysis of recombinant oxidoreductase from *Clostridium acetobutylicum* (NP_149166.1) (continued).

Total number of negatively charged residues (Asp + Glu): 31
Total number of positively charged residues (Arg + Lys): 34

Atomic composition:

Carbon	C	1295
Hydrogen	H	2041
Nitrogen	N	329
Oxygen	O	385
Sulfur	S	4

Formula: $C_{1295}H_{2041}N_{329}O_{385}S_4$

Total number of atoms: 4054

Extinction coefficients:

This protein does not contain any Trp residues. Experience shows that this could result in more than 10% error in the computed extinction coefficient.

Extinction coefficients are in units of $M^{-1} cm^{-1}$, at 280 nm measured in water.

Ext. coefficient	25330
Abs 0.1% (=1 g/l)	0.889, assuming all pairs of Cys residues form cystines

Ext. coefficient	25330
Abs 0.1% (=1 g/l)	0.889, assuming all Cys residues are reduced

Estimated half-life:

The N-terminal of the sequence considered is M (Met).

The estimated half-life is: 30 hours (mammalian reticulocytes, in vitro).
>20 hours (yeast, in vivo).
>10 hours (Escherichia coli, in vivo).

Instability index:

The instability index (II) is computed to be 40.01
This classifies the protein as unstable.

Aliphatic index: 95.98

Grand average of hydropathicity (GRAVY): -0.229

Appendix 7.209: ProtParam analysis of recombinant NADPH-dependent 1-acyl dihydroxyacetone phosphate reductase (Ayr1p) from *Saccharomyces cerevisiae* (NP_012142.1)

User-provided sequence:

```

      10      20      30      40      50      60
MSELQSQPKK IAVVTGASGG IGYEVTKELA RNGYLVYACA RRLEPMAQLA IQFGNDSIKP

      70      80      90     100     110     120
YKLDISKPEE IVTFSGFLRA NLPDGKLDLL YNNAGQSCTF PALDATDAAV EQCFKVNCFG

     130     140     150     160     170     180
HINMCRELSE FLIKAKGTIV FTGSLAGVVS FPFSGSIYSAS KAAIHQYARG LHLEMKPFNV

     190     200     210     220     230     240
RVINAITGGV ATDIADKRPL PETSIIYFPE GREAFNSRKT MAKDNKMPMA DAYAKQLVKD

     250     260     270     280     290
ILSTSDPVDV YRGTFANIMR FVMIFVPYWL LEKGLSKKFK LDKVNNALKS KQKNKDD

```

Number of amino acids: 297

Molecular weight: 32813.9

Theoretical pI: 9.23

Amino acid composition:

[CSV format](#)

Ala (A)	29	9.8%
Arg (R)	12	4.0%
Asn (N)	16	5.4%
Asp (D)	16	5.4%
Cys (C)	4	1.3%
Gln (Q)	9	3.0%
Glu (E)	14	4.7%
Gly (G)	20	6.7%
His (H)	3	1.0%
Ile (I)	18	6.1%
Leu (L)	25	8.4%
Lys (K)	27	9.1%
Met (M)	8	2.7%
Phe (F)	17	5.7%
Pro (P)	15	5.1%
Ser (S)	19	6.4%
Thr (T)	13	4.4%
Trp (W)	1	0.3%
Tyr (Y)	11	3.7%
Val (V)	20	6.7%
Pyl (O)	0	0.0%
Sec (U)	0	0.0%
(B)	0	0.0%
(Z)	0	0.0%
(X)	0	0.0%

Appendix 7.209: ProtParam analysis of recombinant NADPH-dependent 1-acyl dihydroxyacetone phosphate reductase (Ayr1p) from *Saccharomyces cerevisiae* (NP_012142.1) (continued).

Total number of negatively charged residues (Asp + Glu): 30
Total number of positively charged residues (Arg + Lys): 39

Atomic composition:

Carbon	C	1479
Hydrogen	H	2340
Nitrogen	N	392
Oxygen	O	426
Sulfur	S	12

Formula: C₁₄₇₉H₂₃₄₀N₃₉₂O₄₂₆S₁₂
Total number of atoms: 4649

Extinction coefficients:

Extinction coefficients are in units of M⁻¹ cm⁻¹, at 280 nm measured in water.

Ext. coefficient 22140
Abs 0.1% (=1 g/l) 0.675, assuming all pairs of Cys residues form cystines

Ext. coefficient 21890
Abs 0.1% (=1 g/l) 0.667, assuming all Cys residues are reduced

Estimated half-life:

The N-terminal of the sequence considered is M (Met).

The estimated half-life is: 30 hours (mammalian reticulocytes, in vitro).
 >20 hours (yeast, in vivo).
 >10 hours (Escherichia coli, in vivo).

Instability index:

The instability index (II) is computed to be 37.61
This classifies the protein as stable.

Aliphatic index: 85.76

Grand average of hydropathicity (GRAVY): -0.161

Appendix 7.210: Clustal W alignment of recombinant lysostaphin (construct 1), recombinant oxidoreductase and recombinant NADPH-dependent 1-acyl dihydroxyacetone phosphate reductase (Ayr1p) sequences. The alignment suggested that the sequences shared little homology, with an alignment score of 6.0 being achieved between *N*-terminally His-tagged recombinant lysostaphin (construct 1) and recombinant oxidoreductase. A low alignment score of 5.0 was also achieved between *N*-terminally His-tagged recombinant lysostaphin (construct 1) and recombinant Ayr1p. Recombinant oxidoreductase and recombinant Ayr1p shared greater sequence homology with an alignment score of 20.

```

oxidoreductase  ----MKEYKYTVITGASSGIGYEAAKAFKRGKNLIIARRREKLEELKKEILHYNRSL 55
Ayr1p          MSELQSQPKKIAVVTGASGGIGYEVTKELARNGYLVYACARRLEPMAQLAIQFGNDSIKP 60
lysostaphin    -----MGSSHHHHHSSRLVPRGSHMAATHEHSAQWLNNYKKGYG---P 43
                *: *      . : : . . . .      : : : :

oxidoreductase  KVIVKSIDLSITSNVYSLYDELKNYNIETLVNNAAGFDYSKVNQNLKVESMLSLNIEA 115
Ayr1p          YKLDISKPEEIVTFSGFLRANLPDGLDLLYNNAGQSCTFPALDATDAAVEQCQFKVNVFG 120
lysostaphin    YPLGINGGMHYGVDFFMNIGTPVKAISSGKIVEAGWSNYGGGNQIGLIEND---GVHRQW 100
                : .      . .      : * * .      : : : :

oxidoreductase  LVILSSLFVRYDYEKIEGTQLINISSAGGYTIVPNAVIYCATKFFVSSFTEGLARELIEAK 175
Ayr1p          HINMCRELSEFLIKAKGTIVFTGSLAG-VVSFPFGSIYSASKAAIHQYARGLHLEMKPFN 179
lysostaphin    YMHLKYNVKGVDYVKAGQIIGWSGSTGYSTAP----HLHFQRMVNSFNSNSTAQDPMPFL 156
                : : .      .      : : : * :      * : : : : . : : . :

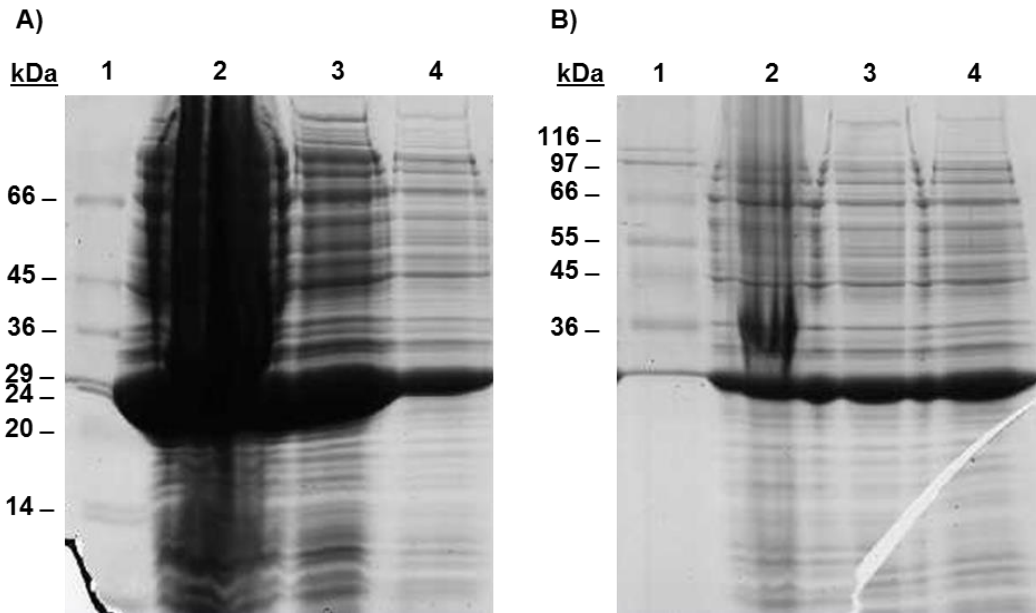
oxidoreductase  SNLKAKVLAPAATETEFGKVASDVKEYDYQEKFKHYHTSKQMAE----- 219
Ayr1p          VRVINAITGGVATDIADKRPLPETSIFYNFPREGAFNSRKTMAKDNKMPADAYAKQLVK 239
lysostaphin    KSAGYGKAGGTVTPTPNTGWKTNKYGTLYKSESASFPTNTDIIIRTTG----- 204
                . . . *      . :      : .      : . . :

oxidoreductase  -----FLIKLYDNDYIVGKVDNRSFKFTLQNPIFDYA----- 251
Ayr1p          DILSTSDPVDVYRGTAFANIMRFVMI FVPYWLLKGLSKFKLDKVNNAKLSKQKNKDD-- 297
lysostaphin    -PFRSMPQSGVLKAGQTIHYDEVMKQDGHVWVG YTGNSGQRIYLPVRTWNKSTNTLGVLW 263
                : :      : :      . : :      .

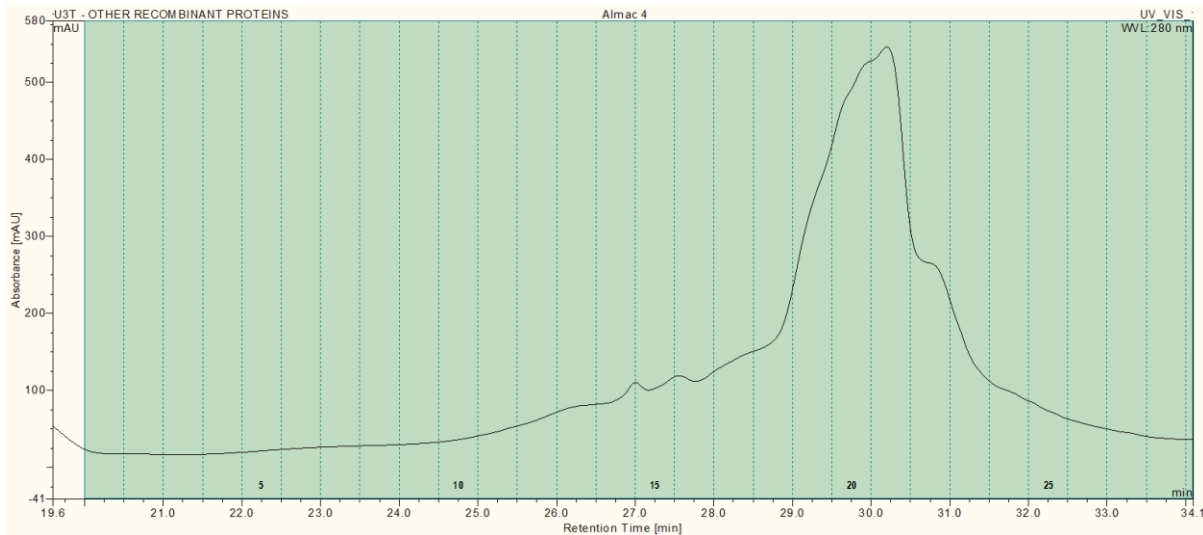
oxidoreductase  ----
Ayr1p          ----
lysostaphin    GTIK 267

```

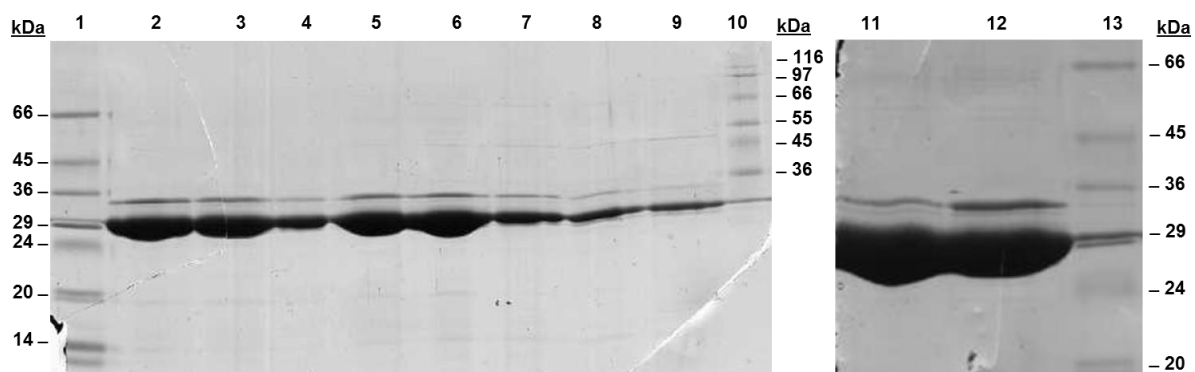
Appendix 7.211: SDS-PAGE analysis of cell lysate extracted following expression of basic recombinant proteins in *E. coli* BL21(DE3) cultured in LB. A) Expression of recombinant oxidoreductase. Lane 1: Sigma low molecular weight markers; Lane 2: CFE (neat); Lane 3: CFE (1:10); Lane 4: CFE (1:100). B) Expression of recombinant NADPH-dependent 1-acyl dihydroxyacetone phosphate reductase (Ayr1p). Lane 1: Sigma high molecular weight markers; Lane 2: CFE (neat); Lane 3: CFE (1:10); Lane 4: CFE (1:100).



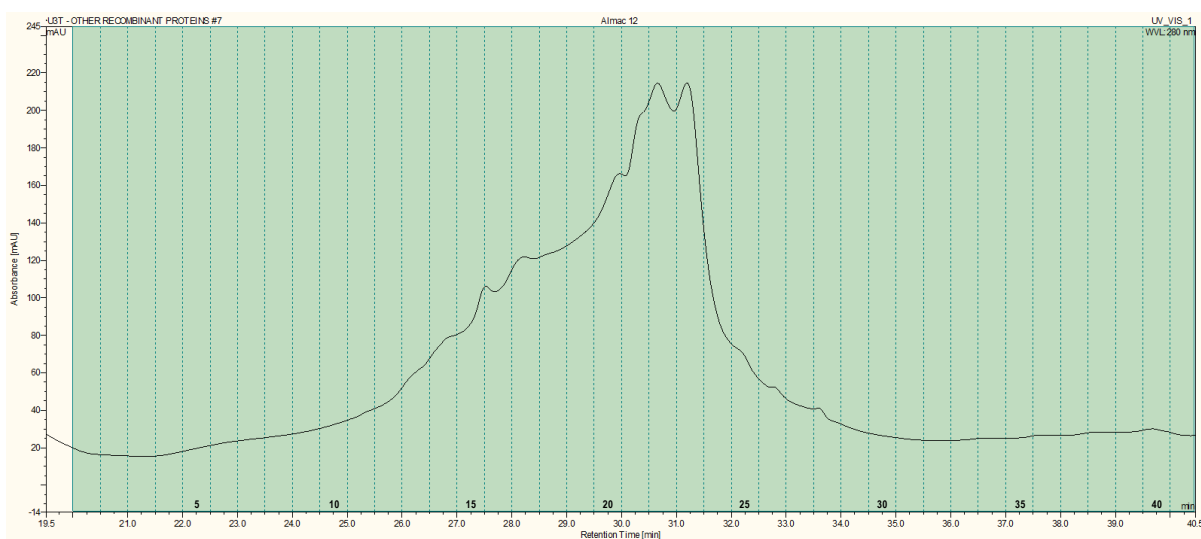
Appendix 7.212: WCX separation of cell lysate containing recombinant oxidoreductase using a ProPac® WCX (4 x 500 mm) column. Fractions 13-22 were analysed by PAGE.



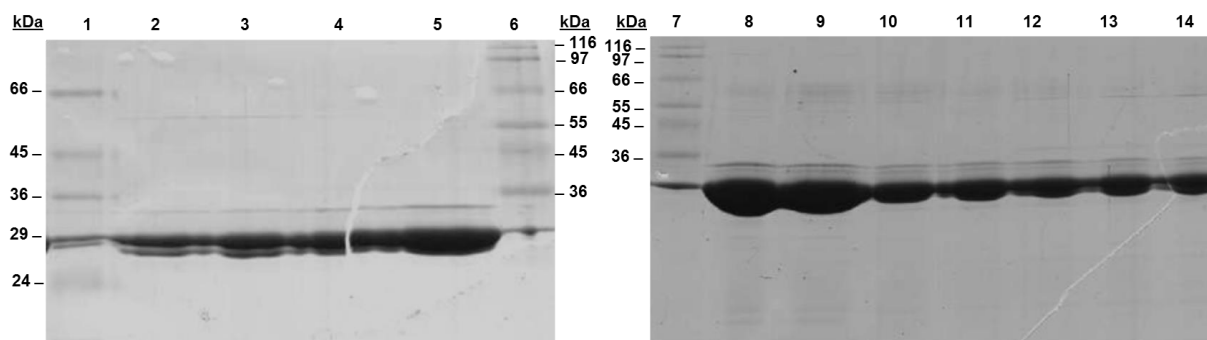
Appendix 7.213: SDS-PAGE analysis of fractions collected during WCX separation of cell lysate containing recombinant oxidoreductase. Lane 1: Sigma low molecular weight markers; Lane 2: Fraction 13; Lane 3: Fraction 14; Lane 4: Fraction 15; Lane 5: Fraction 16; Lane 6: Fraction 17; Lane 7: Fraction 18; Lane 8: Fraction 19; Lane 9: Fraction 20; Lane 10: Sigma high molecular weight markers; Lane 11: Fraction 21; Lane 12: Fraction 22; Lane 13: Sigma low molecular weight markers.



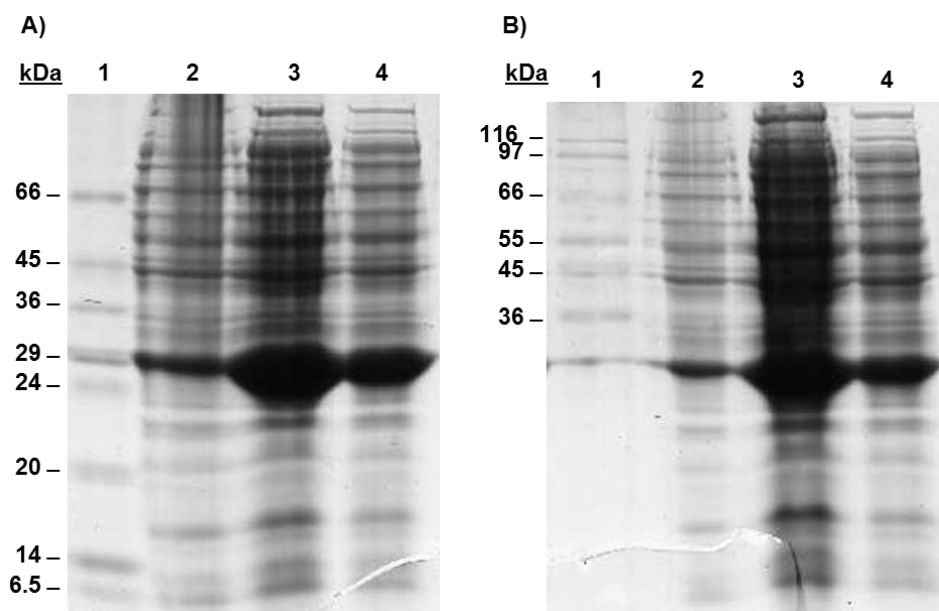
Appendix 7.214: WCX separation of cell lysate containing recombinant Ayr1p using a ProPac® WCX (4 x 500 mm) column. Fractions 13, 14, 16, 17, 20, 21, 22, 23, 25, 26 and 28 were analysed by SDS-PAGE.



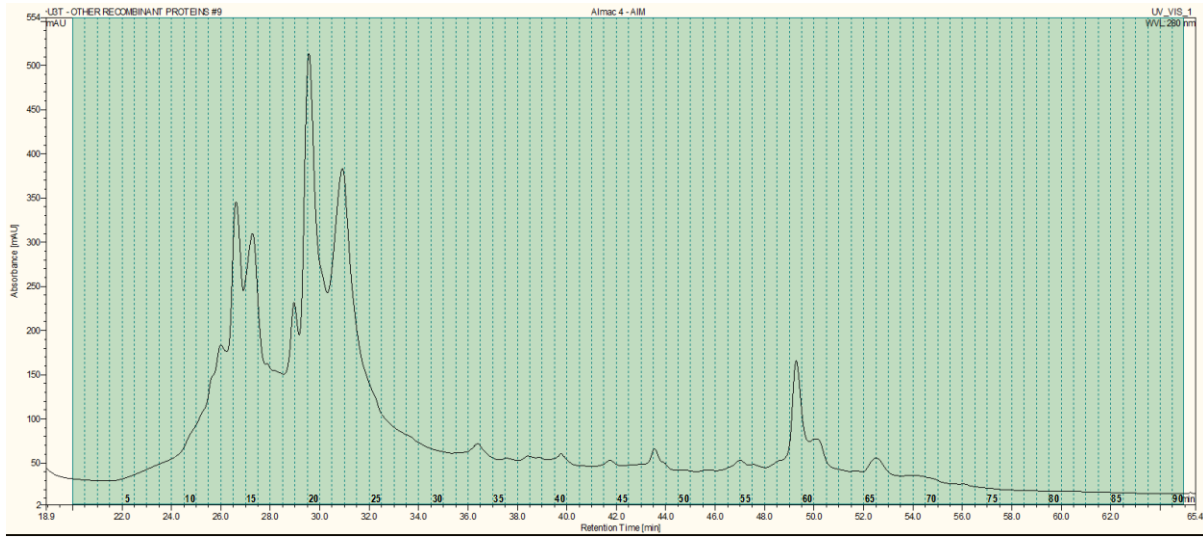
Appendix 7.215: SDS-PAGE analysis of fractions collected during WCX separation of cell lysate containing recombinant NADPH-dependent 1-acyl dihydroxyacetone phosphate reductase (Ayr1p). Lane 1: Sigma low molecular weight markers; Lane 2: Fraction 13; Lane 3: Fraction 14; Lane 4: Fraction 16; Lane 5: Fraction 17; Lane 6: Sigma high molecular weight markers; Lane 7: Sigma high molecular weight markers; Lane 8: Fraction 20; Lane 9: Fraction 21; Lane 10: Fraction 22; Lane 11: Fraction 23; Lane 12: Fraction 25; Lane 13: Fraction 26; Lane 14: Fraction 28.



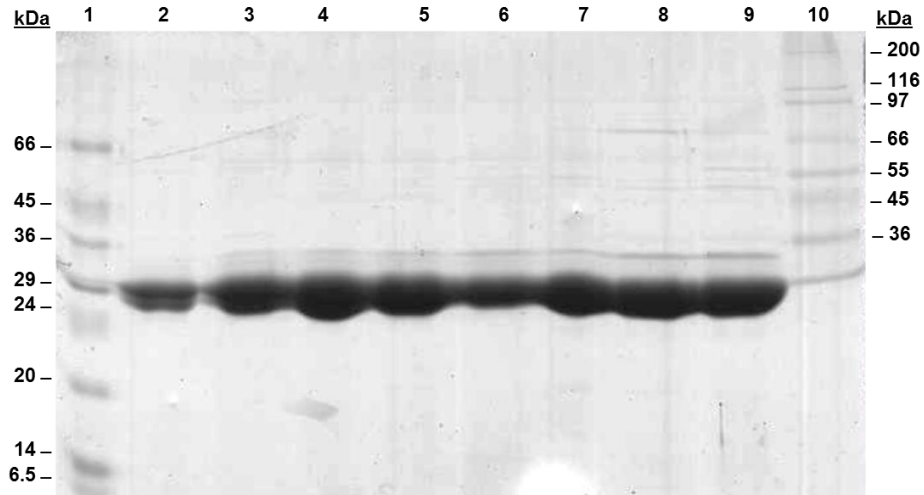
Appendix 7.216: SDS-PAGE analysis of cell lysate extracted following expression of basic recombinant proteins in *E. coli* BL21(DE3) cultured in AIM. A) Expression of recombinant oxidoreductase. Lane 1: Sigma low molecular weight markers; Lane 2: CFE (neat); Lane 3: CFE (1:10); Lane 4: CFE (1:100). B) Expression of recombinant NADPH-dependent 1-acyl dihydroxyacetone phosphate reductase (Ayr1p). Lane 1: Sigma high molecular weight markers; Lane 2: CFE (neat); Lane 3: CFE (1:10); Lane 4: CFE (1:100).



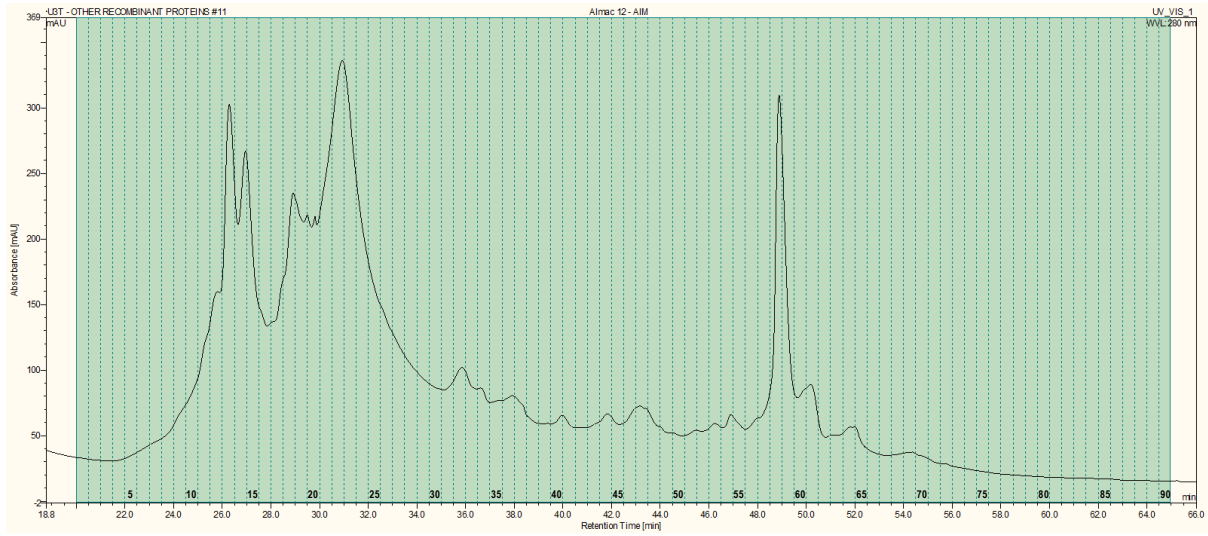
Appendix 7.217: WCX separation of cell lysate containing recombinant oxidoreductase using a ProPac® WCX (4 x 500 mm) column. Fractions 12, 13, 14, 15, 18, 20, 22 and 23 were analysed by SDS-PAGE.



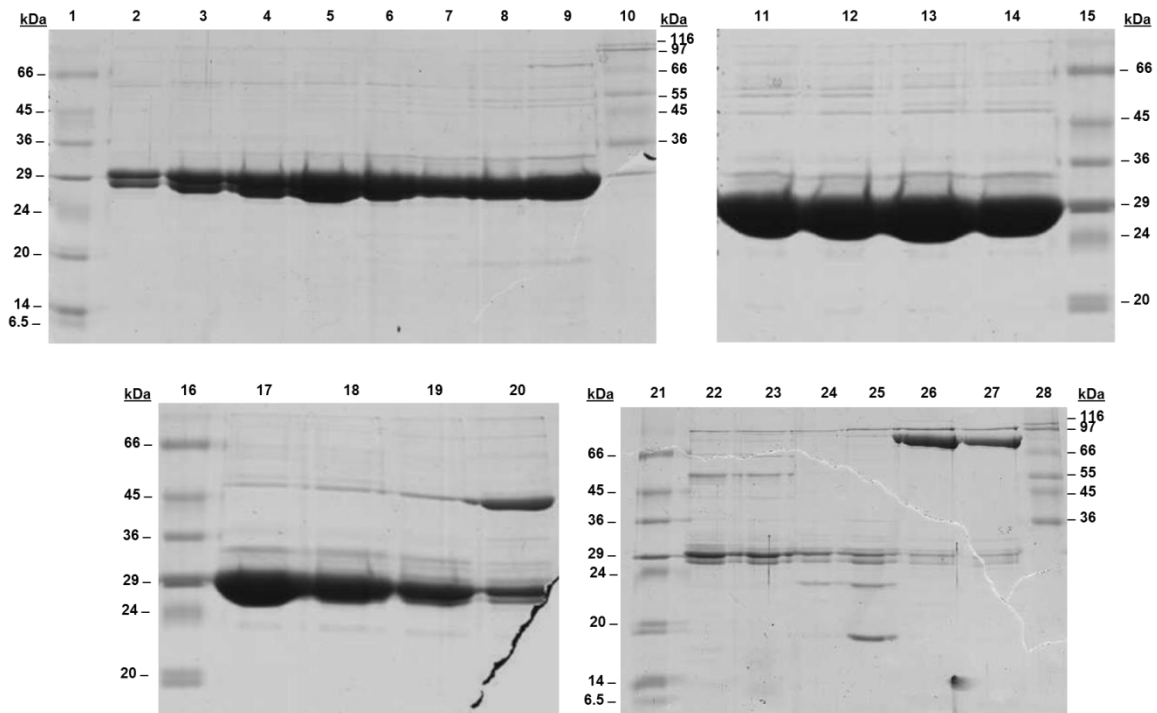
Appendix 7.218: SDS-PAGE analysis of fractions collected during WCX separation of cell lysate containing recombinant oxidoreductase. Lane 1: Sigma low molecular weight markers; Lane 2: Fraction 12; Lane 3: Fraction 13; Lane 4: Fraction 14; Lane 5: Fraction 15; Lane 6: Fraction 18; Lane 7: Fraction 20; Lane 8: Fraction 22; Lane 9: Fraction 23; Lane 10: Sigma high molecular weight markers.



Appendix 7.219: WCX separation of cell lysate containing recombinant NADPH-dependent 1-acyl dihydroxyacetone phosphate reductase (Ayr1p) using a ProPac® WCX (4 x 500 mm) column. Fractions 9, 11, 12, 13, 14, 15, 18, 19, 20, 21, 22, 23, 24, 26, 28, 32, 36, 37, 40, 44, 58 and 59 were analysed by SDS-PAGE.



Appendix 7.220: SDS-PAGE analysis of fractions collected during WCX separation of cell lysate containing recombinant NADPH-dependent 1-acyl dihydroxyacetone phosphate reductase (Ayr1p). Lane 1: Sigma low molecular weight markers; Lane 2: Fraction 9; Lane 3: Fraction 11; Lane 4: Fraction 12; Lane 5: Fraction 13; Lane 6: Fraction 14; Lane 7: Fraction 15; Lane 8: Fraction 18; Lane 9: Fraction 19; Lane 10: Sigma high molecular weight markers; Lane 11: Fraction 20; Lane 12: Fraction 21; Lane 13: Fraction 22; Lane 14: Fraction 23; Lane 15: Sigma low molecular weight markers; Lane 16: Sigma low molecular weight markers; Lane 17: Fraction 24; Lane 18: Fraction 26; Lane 19: Fraction 28; Lane 20: Fraction 32; Lane 21: Sigma low molecular weight markers; Lane 22: Fraction 36; Lane 23: Fraction 37; Lane 24: Fraction 40; Lane 25: Fraction 44; Lane 26: Fraction 58; Lane 27: Fraction 59; Lane 28: Sigma high molecular weight markers.



7.2.3 Rapid analysis of recombinant lysostaphin isoforms

Appendix 7.221: Rapid analysis of recombinant lysostaphin using a ProPac® SCX (2 x 250 mm) column

SCX analysis was performed using a 0.2 ml/min flow rate and linear gradient from 0-50% SCX buffer B in 20 min. Cell lysate containing recombinant lysostaphin (construct 1) was harvested as described in Appendix 7.236, before applying 200 µl of cell lysate to the column. The gradient remained at 50% B for 2.9 min, before the ProPac® SCX column was washed for 3 min by applying 90% B. The column was then equilibrated at 0% B for 11 min.

Appendix 7.222: Influence of optical density at point of induction upon charge heterogeneity

Cell lysate containing recombinant lysostaphin (construct 1) was harvested as described in Appendix 7.235 before applying 500 µl of cell lysate to the ProPac® SCX (2 x 250 mm) column. SCX analysis was performed using a 0.2 ml/min flow rate and linear gradient from 0-50% SCX buffer B in 20 min. The gradient remained at 50% B for 2.9 min, before the ProPac® SCX column was washed for 13 min by applying 90% B. The column was then equilibrated at 0% B for 11 min. Fractions were collected every 60 s between 14 and 36 min.

Appendix 7.223: Comparative analysis of cell lysate using a ProPac® SCX (2 x 250 mm) and ProPac® WCX (4 x 500 mm) columns

Expression was performed as described in Appendix 7.240 using baffled flasks containing 500 ml LB. Once inoculated into 500 ml LB cultures, protein expression was induced at OD_{600 nm} values of 1.060 and 1.041 for cultures derived from colony-based and glycerol stock-based inoculation respectively. Twenty-one hours after the induction of protein expression, cell lysate was harvested from both cultures, as described in Appendix 7.77. The resulting cell lysate (500 µl) was then analysed by SCX and WCX analysis.

SCX analysis was performed using a 0.2 ml/min flow rate and linear gradient from 0-50% SCX buffer B in 20 min. The gradient remained at 50% B for 3 min, before the ProPac® SCX column was washed for 13 min by applying 90% B. The column was then equilibrated at 0% B for 11 min. Fraction collection was optionally performed during separation, by collecting fractions every 60 s between 14 and 36 min.

WCX analysis was performed using a 0.5 ml/min flow rate and linear gradient from 0-50% WCX buffer B in 70 min. Prior to the linear gradient, the column was washed with 100% A for 10 min to ensure that cellular contaminants were washed from the column following application of cell lysate. Following the linear elution gradient, the ProPac® WCX column was washed for 13 min by applying 90% IEX buffer B. The column was then equilibrated at 0% IEX buffer B for 15 min. Fraction collection was optionally performed during separation, by collecting fractions every 30 s between 15 and 35 min.

Appendix 7.224: Optimisation of cell lysate preparation during rapid analysis using a ProPac® WCX (2 x 250 mm) column

Cell lysate containing recombinant lysostaphin (construct 1) was harvested from 1, 25 or 100 ml volumes of culture. Expression was performed as described in Appendix 7.76 using baffled flasks containing 250 ml LB. Cell lysate was harvested from 1 ml aliquots of culture by centrifugation of cells at 4000 x g for 5 min using a benchtop microfuge. The supernatant was discarded and the pelleted cells were resuspended in 100 µl of WCX buffer A. Cell lysate was harvested from 25 or 100 ml volumes of culture using conditions described in Appendix 7.77. The harvested cell lysate (100 µl) was then applied to the ProPac® WCX (2 x 250 mm) column. WCX analysis was performed using a 0.2 ml/min flow rate and linear gradient from 0-50% WCX buffer B in 20 min. The gradient remained at 50% B for 2.9 min, before the column was washed for 13 min by applying 90% B. The column was then equilibrated at 0% B for 11 min.

Appendix 7.225: Rapid analysis of recombinant lysostaphin using a ProPac® WCX (2 x 500 mm) column

Cell lysate containing recombinant lysostaphin (construct 2) was harvested from 5 x 1L cultures. Expression was performed as described in Appendix 7.76 using LB. Cell lysate was harvested as described in Appendix 7.77. WCX analysis was performed using a 0.2 ml/min flow rate. The harvested cell lysate (100 µl) was then applied to a ProPac® WCX (2 x 500 mm) column and an isocratic gradient of 0% WCX buffer B was maintained for 10 min. Separation was achieved by applying a linear gradient from 0-50% WCX buffer B over 30 min. The gradient remained at 50% B for 2.9 min, before the column was washed for 13 min by applying 90% B. The column was then equilibrated at 0% B for 19 min.

Appendix 7.226: Maximising sample through-put during rapid analysis using a ProPac® WCX (2 x 500 mm) column

Expression of recombinant lysostaphin (construct 1) was performed as described in Appendix 7.76, using multiple flasks containing 100 ml LB. Cell lysate was harvested from the cultures, as described in Appendix 7.239, however prior to harvest, the cultures were divided into 50 ml volumes. Cell lysate was harvested from one of the 50 ml cultures immediately and analysed by WCX. Cell lysate was extracted from the other 50 ml culture immediately and the resulting cell lysate was frozen and thawed prior to WCX analysis. Alternatively pelleted *E. coli* was frozen during the preparation of cell lysate so that the cell lysate could be fully extracted and analysed later.

WCX analysis was performed using a 0.2 ml/min flow rate. The harvested cell lysate (500 µl) was then applied to a ProPac® WCX (2 x 500 mm) column and an isocratic gradient of 0% WCX buffer B was maintained for 4 min. Separation was achieved by applying a linear gradient of 0-50% WCX buffer B in 20 min. The gradient remained at 50% B for 2.9 min, before the column was washed for 13 min by applying 90% B and then the column was then equilibrated at 0% B for 25 min.

Appendix 7.227: Investigation of the influence of optical density at the point of induction upon the charge heterogeneity of recombinant lysostaphin

Cell lysate containing recombinant lysostaphin (construct 1) was harvested from twenty-nine cultures as described in Appendix 7.239, before applying 200 µl of cell lysate to a ProPac® WCX (2 x 500 mm) column. WCX analysis was performed using a 0.2 ml/min flow rate. Following sample injection, an isocratic gradient of 0% WCX buffer B was maintained for 3 min. Separation was achieved by applying a linear gradient from 0-50% WCX buffer B in 20 min. The gradient remained at 50% B for 4 min, before the column was washed for 8 min by applying 90% B and the column was then equilibrated at 0% B for 20 min. Fractions were collected every 60 s between 15 and 30 min. Cell lysate was also harvested from cultures which had been inoculated directly from glycerol stock (Appendix 7.241).

Appendix 7.228: Optimisation of chromatographic conditions

Chromatographic conditions were gradually optimised by increasing the duration of the initial isocratic gradient (0% WCX buffer B) from 3 to 10 min to ensure that unbound cellular contaminants were washed from the column following application of cell lysate. The wash

period (90% WCX buffer B) was also decreased from 13 to 8 min and the equilibration period was extended to 20 min.

Appendix 7.229: Investigation of the influence of time upon the charge heterogeneity of recombinant lysostaphin

Cell lysate containing recombinant lysostaphin (construct 1) was harvested periodically from a 1 L culture, as described in Appendix 7.237, before applying 500 µl of cell lysate to a ProPac® WCX (2 x 500 mm) column. WCX analysis was performed using a 0.2 ml/min flow rate. Following sample injection, an isocratic gradient of 0% WCX buffer B was maintained for 10 min. Separation was achieved by applying a linear gradient from 0-50% WCX buffer B in 20 min. The gradient remained at 50% B for 4 min, before the column was washed for 8 min by applying 90% B and the column was then equilibrated at 0 % B for 20 min. Fractions were collected every 60s between 23 and 38 min. The collected fractions were analysed by SDS-PAGE as described in Appendix 7.15.

Appendix 7.230: Extended investigation of the influence of time upon the charge heterogeneity of recombinant lysostaphin

Cell lysate containing recombinant lysostaphin (construct 1) was harvested periodically from a 1 L culture, as described in Appendix 7.238 and, before applying 500 µl of cell lysate to a ProPac® WCX (2 x 500 mm). WCX separation was performed as described in Appendix 7.229. Collected fractions were subjected to SDS-PAGE analysis, as described in Appendix 7.15.

Appendix 7.231: Rapid analysis of recombinant lysostaphin using a ProPac® MAb SCX (4 x 250 mm) column

Cell lysate containing recombinant lysostaphin (construct 1) was harvested periodically from a 1 L culture, as described in Appendix 7.237, before applying 500 µl of cell lysate to a ProPac® MAb SCX (2 x 500 mm). The separation was performed at 1.0 ml/min and following sample injection, an isocratic gradient of 0% MAb SCX buffer B was maintained for 10 min. Separation was achieved by applying a linear gradient from 0-50% B in 20 min. The column was washed for 5 min by applying 90% B and the column was then equilibrated at 0% B for 10 min. Fractions were collected every 30 s between 15 and 35 min. The collected fractions were analysed by SDS-PAGE as described in Appendix 7.15.

Appendix 7.232: Recombinant protein expression using different post-induction temperatures

To investigate the influence of post-induction temperatures upon the expression of recombinant lysostaphin, recombinant protein expression was performed at different temperatures. Cultures were typically incubated at 30°C following induction of protein expression, however in this instance, cultures were incubated at 20°C or 16°C. In these experiments, 500 ml of LB supplemented with kanamycin was inoculated with 5 ml of starter culture. The starter cultures were composed of 10 ml of LB, supplemented with kanamycin, which had been inoculated from a glycerol stock containing *E. coli* BL21(DE3) transformed with recombinant pET-28a encoding *N*-terminally His-tagged recombinant lysostaphin (construct 1). The expression cultures were incubated at 37°C and 200 rpm, until exponential growth had been achieved, at which point, protein expression was induced through the addition of IPTG. In the initial experiment, this was achieved at an OD_{600 nm} value of 0.847. The 500 ml culture was aseptically split following the addition of IPTG, so that 250 ml cultures could be incubated at 30°C and 100 rpm or 20°C and 100 rpm, allowing comparison of expression levels and charge heterogeneity at each temperature. Cell lysates were harvested from each culture, 16 h after induction of protein expression and the resulting cell lysates were extracted and analysed by PAGE and IEX (Appendix 7.15 and Appendix 7.184).

In a subsequent experiment, two cultures were incubated at 16°C following the induction of protein expression. As previously, LB starter cultures were inoculated from an *E. coli* BL21(DE3) glycerol stock transformed with a recombinant pET-28a encoding *N*-terminally His-tagged recombinant lysostaphin (construct 1). Two flasks containing 500 ml of LB supplemented with kanamycin were inoculated with 5 ml of a starter culture, before incubation at 37°C and 200 rpm. Protein expression was induced in cultures 1 and 2 at OD_{600 nm} values of 1.112 and 0.723 respectively. Following induction the cultures were incubated at 16°C and 100 rpm for 14 h. After 14 h the cultures were harvested and the resulting cell lysates were analysed by PAGE and IEX (Appendix 7.15 and Appendix 7.184).

Appendix 7.233: Monitoring of expression of recombinant lysostaphin (1)

In order to monitor expression of recombinant lysostaphin over time, ten 2 L non-baffled flasks containing 50 ml of LB, supplemented with kanamycin, were inoculated with 0.5 ml of LB starter culture. The starter culture had been incubated overnight at 37°C and 200 rpm following inoculation from a glycerol stock of *E. coli* BL21(DE3) harbouring recombinant pET-

28a encoding *N*-terminally His-tagged recombinant lysostaphin (construct 1). The flasks were incubated at 37°C and 200 rpm for 4.5 h. The OD_{600 nm} of a single culture was established as being 0.658, therefore IPTG was added to all of the cultures to induce protein expression in a synchronised manner. One of the cultures was harvested at the point of induction, whilst the remaining cultures were incubated for longer periods of time after reducing the incubation temperature and shaking speed to 30°C and 100 rpm respectively. The remaining nine cultures were harvested between 2 and 25 h after the induction of protein expression. Cytoplasmic cell lysates were extracted and analysed by SDS-PAGE (Appendix 7.15).

Appendix 7.234: Monitoring of expression of recombinant lysostaphin (2)

To assess the influence of optical density at the point of induction upon protein expression, twenty-nine cultures were analysed following induction at varying optical densities, during three separate experiments. Starter cultures containing 10 ml of LB, supplemented with kanamycin were inoculated from a glycerol stock containing *E. coli* BL21(DE3) transformed with recombinant pET-28a encoding *N*-terminally His-tagged recombinant lysostaphin (construct 1). The cultures were incubated overnight at 37°C and 200 rpm, until OD_{600 nm} values of 1.651, 1.732, and 1.578 were obtained in experiments 1, 2 and 3 respectively. At which point, 0.5 ml of the starter culture was inoculated into flasks containing 50 ml of LB, supplemented with kanamycin. The cultures were incubated at 37°C and 200 rpm until protein expression was induced at an OD_{600 nm} value ranging between 0 and 1.6. Following induction, the cultures were incubated at 30°C and 100 rpm for 20 h. At 20 h post-induction, the cultures were harvested and the resulting cell lysates were analysed by SDS-PAGE and IEX (Appendix 7.15 and Appendix 7.227). Cell lysate was harvested as described in Appendix 7.239.

Appendix 7.235: Monitoring of expression of recombinant lysostaphin (3)

To assess the influence of optical density at the point of induction upon protein expression, eight cultures were analysed following induction at varying optical densities, during three separate experiments. In each experiment, cultures were harvested either 4 h post - induction (experiment 1), 12 h post-induction (experiment 2) or 20 h post-induction (experiment 3). Starter cultures containing 10 ml of LB, supplemented with kanamycin were inoculated from a glycerol stock containing *E. coli* BL21(DE3) transformed with recombinant pET-28a encoding *N*-terminally His-tagged recombinant lysostaphin (construct 1). The

cultures were incubated overnight at 37°C and 200 rpm, before inoculating 1 ml of a single starter culture into eight flasks containing 100 ml of LB, supplemented with kanamycin. The cultures were incubated at 37°C and 200 rpm until induction of protein expression, at which point incubation temperature and shaking speed were reduced to 30°C and 100 rpm. Induction of protein expression was induced at OD_{600 nm} values ranging between 0 and 1.2. Cell lysates were harvested at 4, 10 or 20 h following induction of protein expression and the resulting lysates were analysed by SDS-PAGE and IEX (Appendix 7.15 and Appendix 7.222). Cell lysate was harvested as described in Appendix 7.77.

Appendix 7.236: Monitoring of expression of recombinant lysostaphin (4)

To monitor recombinant protein production over the duration of protein expression, a single 1L shake-flask culture was cultured and analysed until 27 hours after the induction of protein expression. LB starter cultures supplemented with kanamycin, were inoculated from a glycerol stock containing *E. coli* BL21(DE3) transformed with recombinant pET-28a encoding *N*-terminally His-tagged recombinant lysostaphin (construct 1), before being incubated overnight at 37°C and 200 rpm. A baffled flask containing 1 L of LB, supplemented with kanamycin was inoculated with 10 ml of the starter culture, prior to incubation at 37°C and 200 rpm. At an OD_{600 nm} of 0.808, protein expression was induced through the addition of IPTG and the incubation conditions were adjusted to 30°C and 100 rpm. Samples (30 ml) of the culture were extracted at 2, 3, 19, 20, 21, 22, 23, 24, 25, and 27 h post-induction before extracting the cytoplasmic cell lysate and performing analysis by SDS-PAGE and IEX (Appendix 7.15 and Appendix 7.221). The cytoplasmic extraction of cell lysate was performed using real-time monitoring extraction method (Appendix 7.239).

Appendix 7.237: Monitoring of expression of recombinant lysostaphin (5)

Further analysis of recombinant protein expression and bacterial growth was performed by monitoring a single batch culture until 30 h after the induction of protein expression. An LB starter culture supplemented with kanamycin, was inoculated from a glycerol stock containing *E. coli* BL21(DE3) transformed with recombinant pET-28a encoding *N*-terminally His-tagged recombinant lysostaphin (construct 1) and incubated overnight at 37°C and 200 rpm. After 7 h of incubation, the starter culture had an OD_{600 nm} of 0.646 and therefore 5 ml of the culture was used to inoculate a baffled flask containing 1 L of LB, supplemented with kanamycin. The batch culture was incubated at 37°C and 200 rpm, whilst the growth of the culture was monitored spectrophotometrically until the point of IPTG induction at an OD_{600 nm}

at 0.644. The incubation conditions were adjusted to 30°C and 100 rpm and 50 ml of the culture was aseptically extracted at regular intervals between 1.5 and 30 h after the induction of protein expression. At each time-point, the OD_{600 nm} of the culture was recorded and the cytoplasmic cell lysate was extracted for analysis by SDS-PAGE and IEX (Appendix 7.15 and Appendix 7.229). The cytoplasmic extraction of cell lysate was performed using real-time monitoring extraction method (Appendix 7.239).

Appendix 7.238: Monitoring of expression of recombinant lysostaphin (6)

Extended culture analysis of recombinant protein expression and bacterial growth was performed by monitoring a single batch culture until 85.5 hours after the induction of protein expression. An LB starter culture supplemented with kanamycin, was inoculated from a glycerol stock containing *E. coli* BL21(DE3) transformed with recombinant pET-28a encoding *N*-terminally His-tagged recombinant lysostaphin (construct 1) and incubated overnight at 37°C and 200 rpm. The starter culture was incubated until an OD_{600 nm} of 0.610 had been obtained, at which point, 5 ml of the culture was used to inoculate a baffled flask containing 1 L of LB, supplemented with kanamycin. The batch culture was incubated at 37°C and 200 rpm, whilst bacterial growth was monitored spectrophotometrically until the point of IPTG induction at an OD_{600 nm} of 0.846. The incubation conditions were adjusted to 30°C and 100 rpm and 50 ml of the culture was aseptically extracted at regular intervals between 12.0 and 85.5 h after the induction of protein expression. At each time-point, the OD_{600 nm} of the culture was recorded and the cytoplasmic cell lysate was extracted for analysis by SDS-PAGE and IEX (Appendix 7.15 and Appendix 7.230). The cytoplasmic extraction of cell lysate was performed as described in Appendix 7.239.

Appendix 7.239: Cytoplasmic protein extraction during real-time culture analysis

To enable real-time culture analysis, as described in Section 3.5.1, cytoplasmic protein extraction was optimised to obtain analysable cell lysates in a shorter period of time. During analysis, 50 ml of the culture was harvested by centrifugation at 4000 x g for 10 min at 4°C to pellet the cells. The bacterial cell pellet was resuspended in a suitable volume of an appropriate resuspension buffer. The resuspension buffer was selected to facilitate subsequent purification or separation of the recombinant protein by chromatography, as indicated in Appendix 7.71. The resuspended cells were lysed by sonication at 15 microns amplitude at 5 sec intervals for 1 min, whilst on ice. After sonication, the cells were

centrifuged at 24000 x g for 10 min at 4°C and the resulting supernatant (CFE) was decanted from the pellet and retained for subsequent analysis.

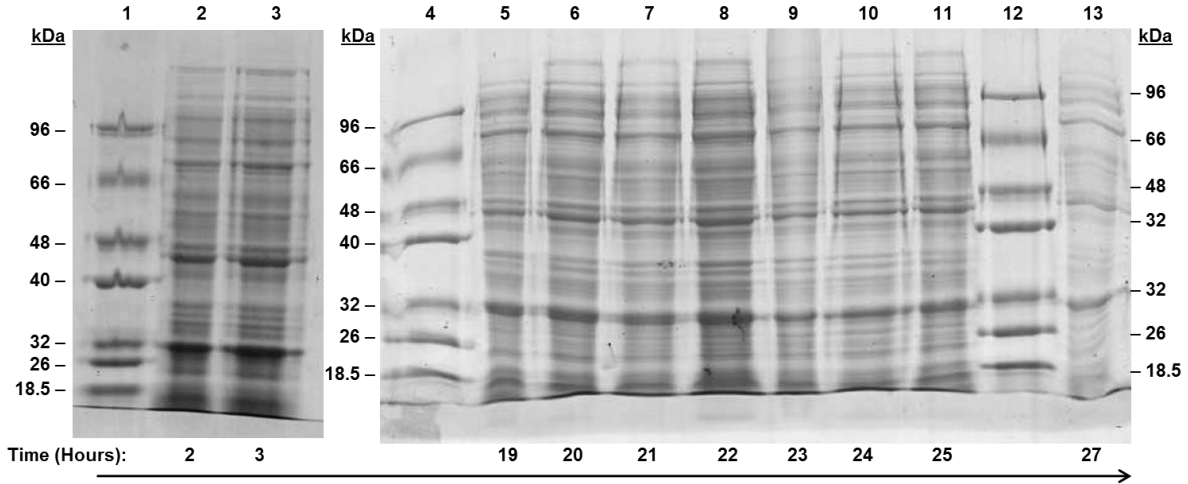
Appendix 7.240: Expression of recombinant lysostaphin following different modes of inoculation

To investigate the influence of inoculation modes upon the expression of recombinant lysostaphin, various expression experiments were performed following inoculation with colony or glycerol stock derived recombinant *E. coli* BL21(DE3). Colonies transformed with *E. coli* BL21(DE3) harbouring recombinant pET-28a encoding *N*-terminally His-tagged recombinant lysostaphin (construct 1) were cultured as described in Appendix 7.75. Glycerol stocks containing *E. coli* BL21(DE3) harbouring recombinant pET-28a encoding *N*-terminally His-tagged recombinant lysostaphin (construct 1) were prepared as described in Appendix 7.3. Starter cultures were inoculated with either transformed colonies or a glycerol stock using sterile technique and recombinant protein expression was performed as described in Appendix 7.76.

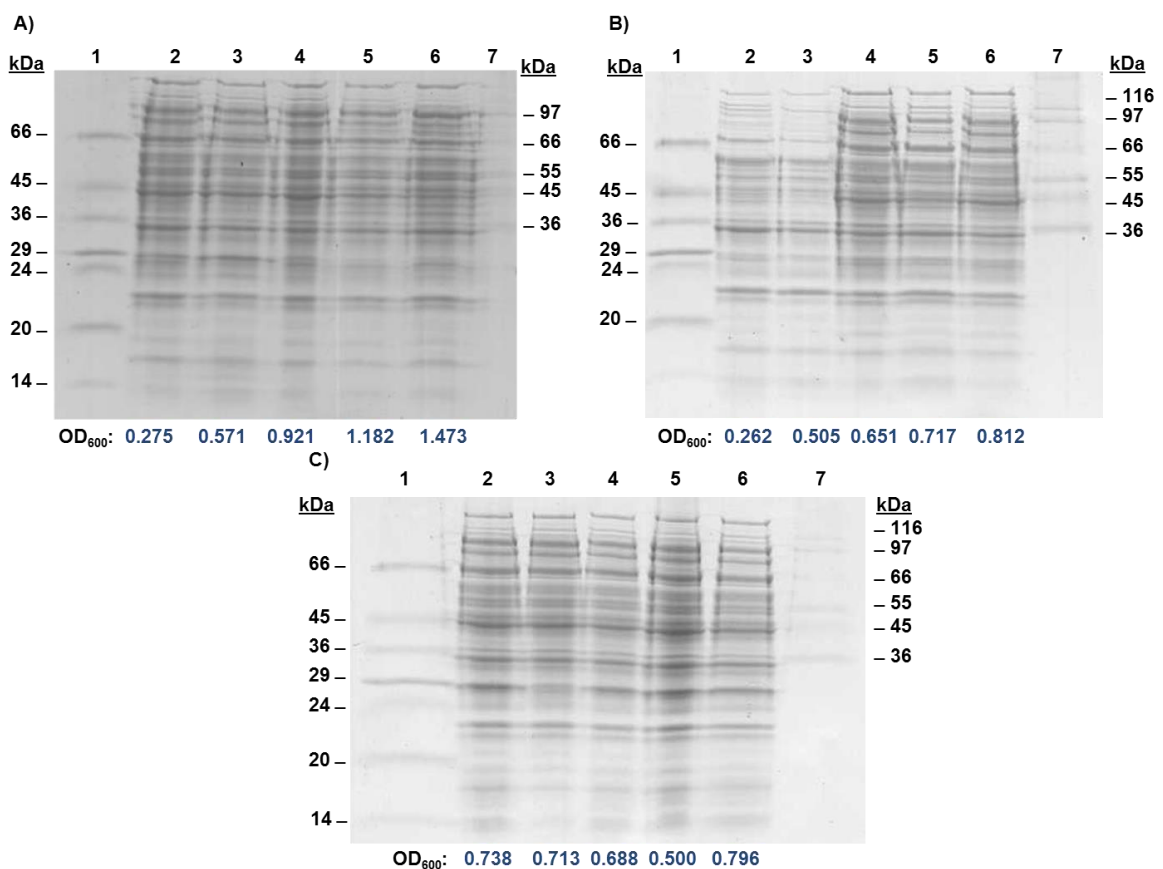
Appendix 7.241: Expression of recombinant lysostaphin in the absence of starter cultures.

To minimise the growth phase variability during recombinant protein expression, expression of recombinant lysostaphin was attempted by inoculating expression media directly from a glycerol stock rather than via starter cultures. During three separate experiments, a total of fifteen flasks containing 50 ml of LB supplemented with kanamycin were inoculated directly from a glycerol stock containing *E. coli* BL21(DE3) transformed with recombinant pET-28a encoding *N*-terminally His-tagged recombinant lysostaphin (construct 1). The flasks were incubated at 37°C and 200 rpm until induction of protein expression. IPTG was added to the cultures at OD_{600 nm} values of between 0.2 and 1.5 and following induction, the cultures were incubated at 30°C and 100 rpm. The cultures were harvested 18 h after induction of protein expression and cytoplasmic cell lysates were extracted, as described in Appendix 7.77. The resulting cell lysates were analysed by SDS-PAGE and IEX, as reported in Appendix 7.15 and Appendix 7.227.

Appendix 7.242: Expression of *N*-terminally His-tagged recombinant lysostaphin over time. Lane 1: NZY molecular weight markers; Lane 2: Sample 1 (2 h PI); Lane 3: Sample 2 (3 h PI); Lane 4: NZY molecular weight markers; Lane 5: Sample 3 (19 h PI); Lane 6: Sample 4 (20 h PI); Lane 7: Sample 5: (21 h PI); Lane 8: Sample 6 (22 h PI); Lane 9: Sample 7 (23 h PI); Lane 10: Sample 8 (24 h PI); Lane 11: Sample 9 (25 h PI); Lane 12: NZY molecular weight markers; Lane 13: Sample 10 (27 h PI).



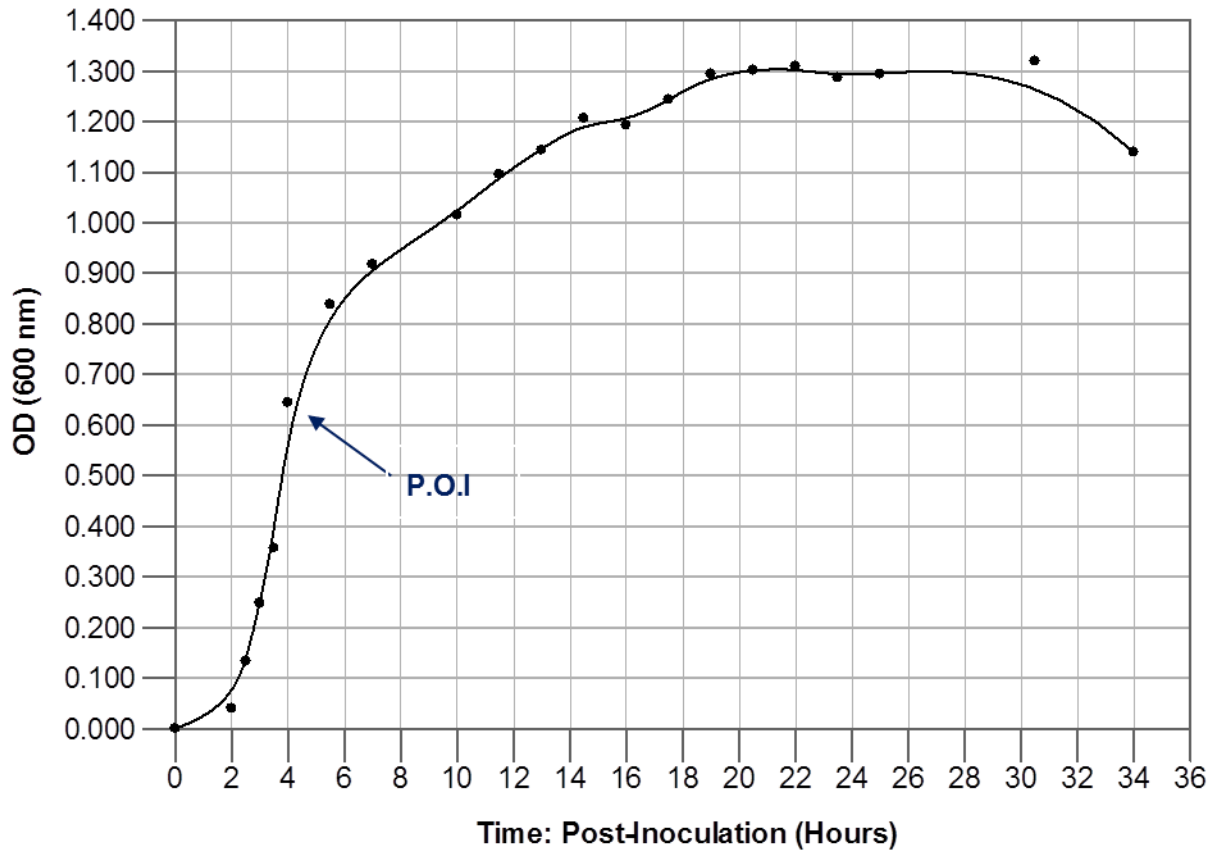
Appendix 7.243: Expression of recombinant lysostaphin in the absence of starter cultures. During three separate experiments, fifteen cultures containing 50 ml LB were inoculated with 1.5 ml of a glycerol stock containing *E. coli* BL21(DE3) transformed with *N*-terminally His-tagged recombinant lysostaphin (construct 1). The cultures were incubated and protein expression was induced at various optical densities. Cell lysates were extracted from the cultures 18 h after the induction of the protein expression and analysed by SDS-PAGE. A) Experiment 1. Lane 1: Sigma low molecular weight markers; Lane 2: Sample 1; Lane 3: Sample 2; Lane 4: Sample 3; Lane 5: Sample 4; Lane 6; Sample 5; Lane 7: Sigma high molecular weight markers. B) Experiment 2. Lane 1: Sigma low molecular weight markers; Lane 2: Sample 1; Lane 3: Sample 2; Lane 4: Sample 3; Lane 5: Sample 4; Lane 6; Sample 5; Lane 7: Sigma high molecular weight markers. C) Experiment 3. Lane 1: Sigma low molecular weight markers; Lane 2: Sample 1; Lane 3: Sample 2; Lane 4: Sample 3; Lane 5: Sample 4; Lane 6; Sample 5; Lane 7: Sigma high molecular weight markers.



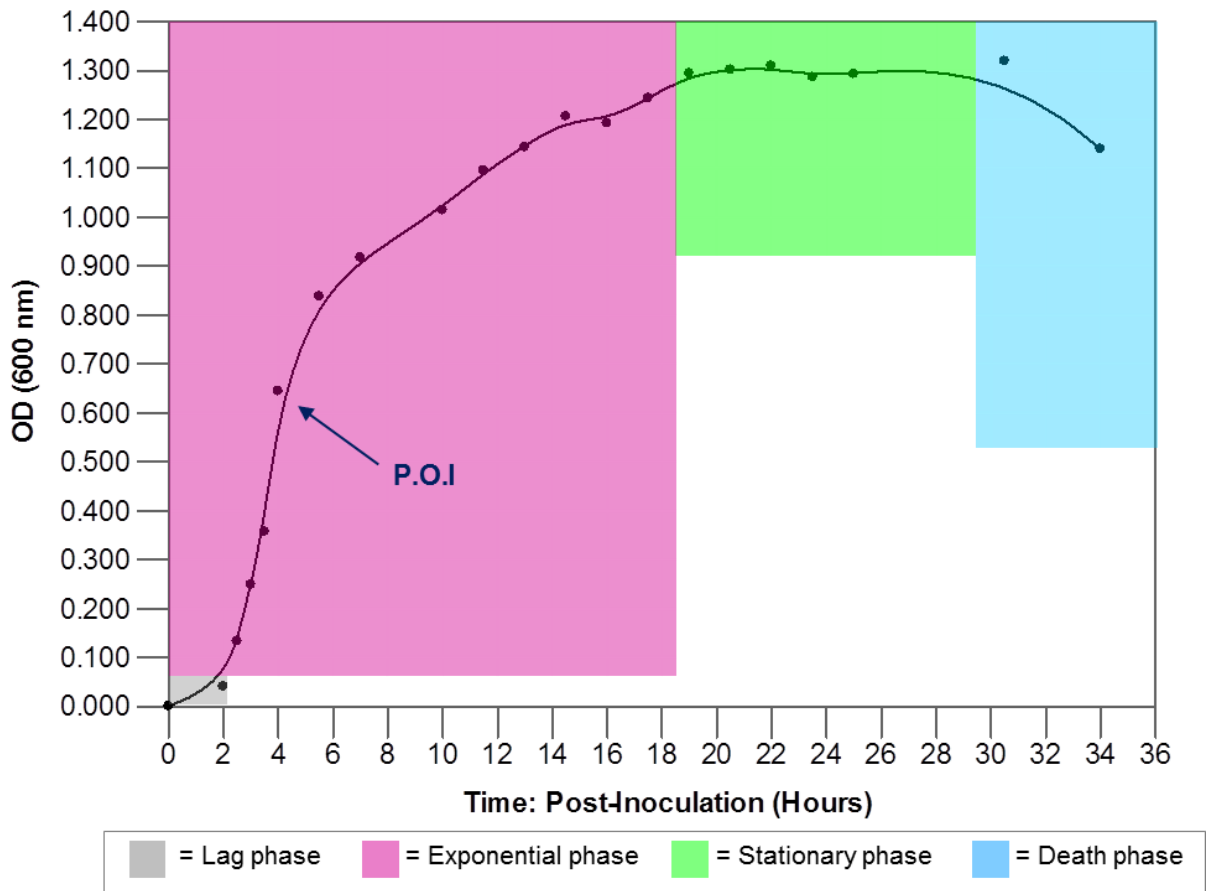
Appendix 7.244: Optical density measurements recorded following culture inoculation and induction of protein expression.

Sample ID	Time: Post-Inoculation (Hours)	Time: Post-Induction (Hours)	OD_{600 nm}
-	2.0	-2.0	0.040
-	2.5	-1.5	0.133
-	3.0	-1.0	0.248
-	3.5	-0.5	0.357
-	4.0	0.0	0.644
1	5.5	1.5	0.838
2	7.0	3.0	0.917
3	8.5	4.5	0.870
4	10.0	6.0	1.014
5	11.5	7.5	1.095
6	13.0	9.0	1.143
7	14.5	10.5	1.206
8	16.0	12.0	1.192
9	17.5	13.5	1.243
10	19.0	15.0	1.294
11	20.5	16.5	1.301
12	22.0	18.0	1.309
13	23.5	19.5	1.286
14	25.0	21.0	1.293
15	28.0	24.0	1.168
16	30.5	26.5	1.319
17	34.0	30.0	1.139

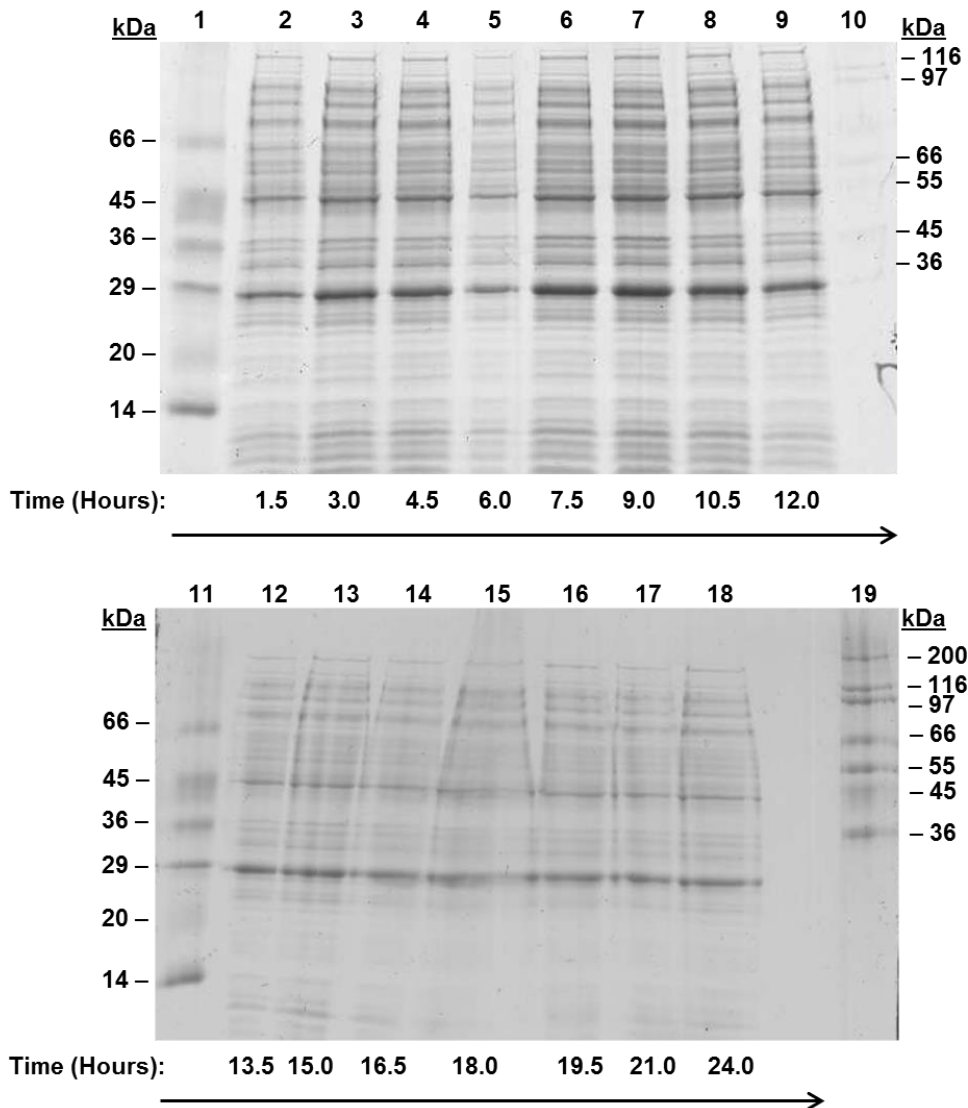
Appendix 7.245: Growth of *E. coli* BL21(DE3) pre- and post-induction of recombinant lysostaphin expression. The *E. coli* was grown in LB media supplemented with kanamycin (10 µg/ml) and incubated at 37 °C with orbital shaking at 200 rpm. At an OD_{600 nm} of 0.644, protein expression was induced (Point of Induction = P.O.I) through the addition of IPTG (240 µg/ml) and the culture was incubated at 30°C with orbital shaking at 100 rpm.



Appendix 7.246: Growth phases of *E. coli* BL21(DE3) pre- and post-induction of N-terminally His-tagged recombinant lysostaphin (construct 1) expression (Point of Induction = P.O.I).



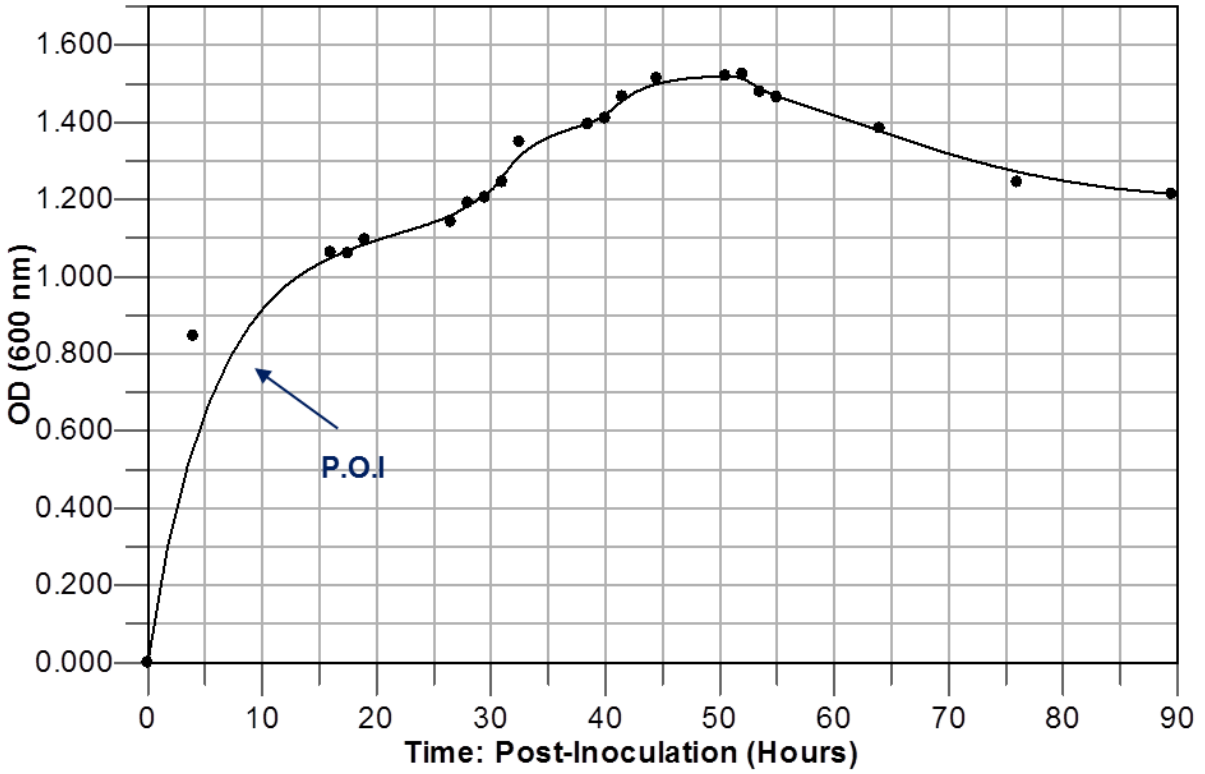
Appendix 7.247: Expression of N-terminally His-tagged recombinant lysostaphin (construct 1). Samples of the culture were extracted at regular time points after induction and the resulting cell lysates were analysed by SDS-PAGE. Lane 1: Sigma low molecular weight markers; Lane 2: Sample 1 (1.5 h PI); Lane 3: Sample 2 (3.0 h PI); Lane 4: Sample 3 (4.5 h PI); Lane 5: Sample 4 (6.0 h PI); Lane 6: Sample 5 (7.5 h PI); Lane 7: Sample 6 (9.0 h PI); Lane 8: Sample 7 (10.5 h PI); Lane 9: Sample 8 (12.0 h PI); Lane 10: Sigma high molecular weight markers; Lane 11: Sigma low molecular weight markers; Lane 12: Sample 9 (13.5 h PI); Lane 13: Sample 10 (15 h PI); Lane 14: Sample 11 (16.5 h PI); Lane 15: Sample 12 (18.0 h PI); Lane 16: Sample 13 (19.5 h PI); Lane 17: Sample 14 (21 h PI); Lane 18: Sample 15 (24.0 h PI); Lane 19: Sigma high molecular weight markers.



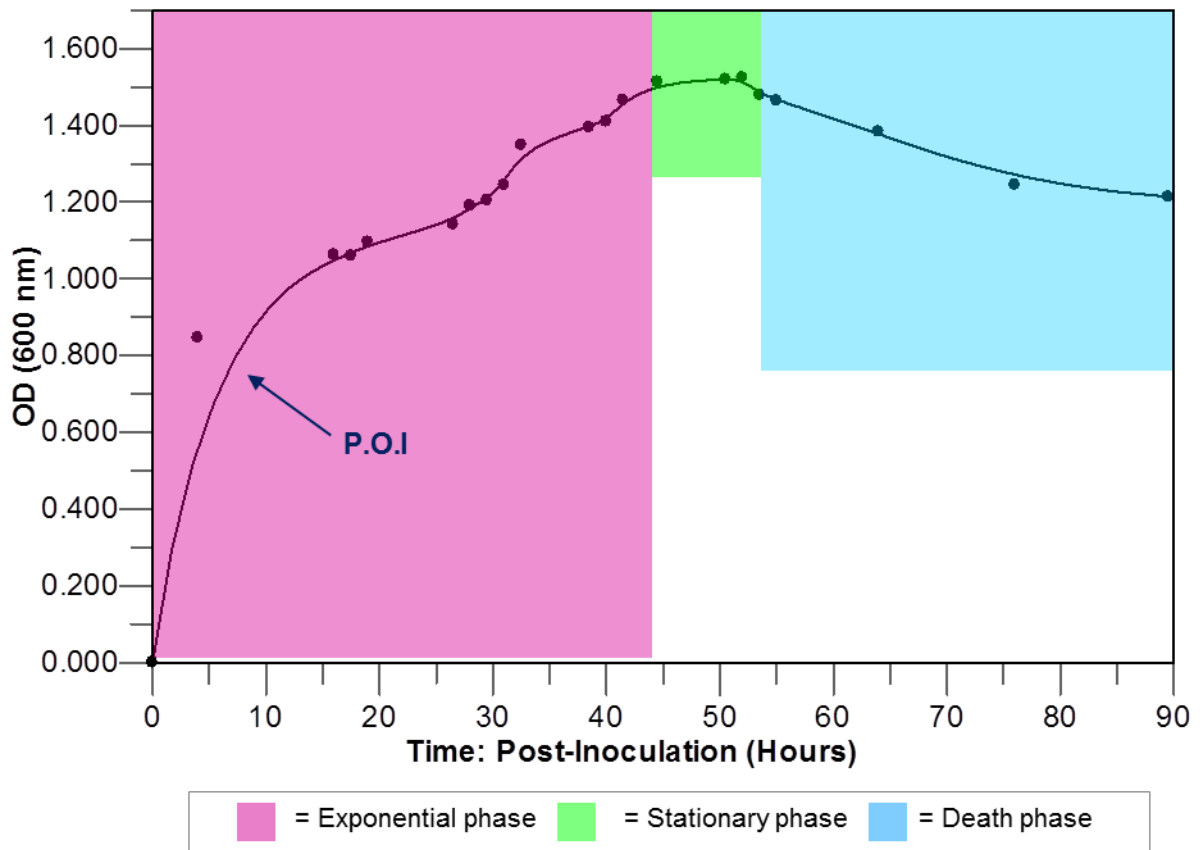
Appendix 7.248: Optical density measurements recorded following culture inoculation and induction of protein expression.

Sample ID	Time: Post-Inoculation (Hours)	Time: Post-Induction (Hours)	OD_{600 nm}
1	16.0	12.0	1.062
2	17.5	13.5	1.060
3	19.0	15.0	1.096
4	26.5	22.5	1.142
5	28.0	24.0	1.191
6	29.5	25.5	1.204
7	31.0	27.0	1.245
8	32.5	28.5	1.349
9	38.5	34.5	1.395
10	40.0	36.0	1.410
11	41.5	37.5	1.466
12	44.5	40.5	1.514
13	50.5	46.5	1.520
14	52.0	48.0	1.525
15	53.5	49.5	1.479
16	55.0	51.0	1.465
17	64.0	60.0	1.384
18	76.0	72.0	1.245
19	89.5	85.5	1.214

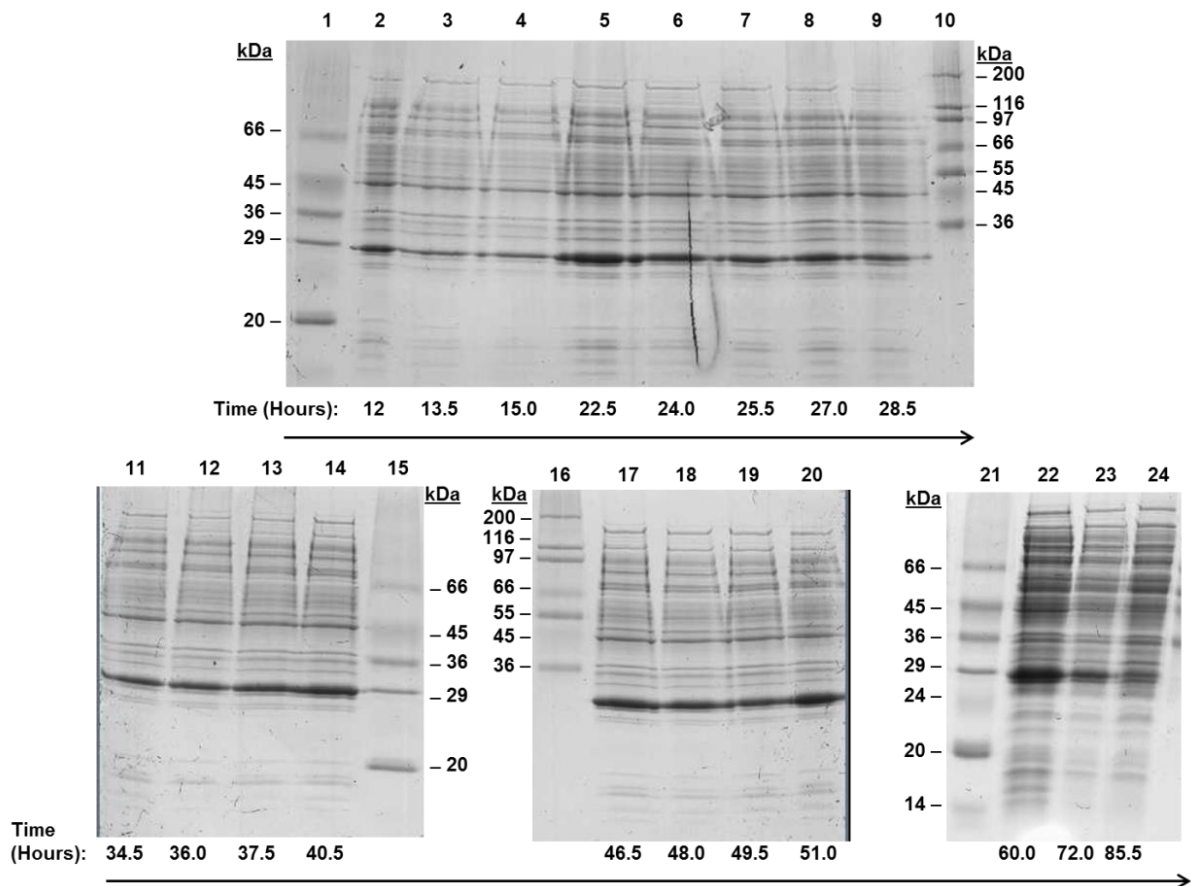
Appendix 7.249: Growth of *E. coli* BL21(DE3) pre- and post-induction of *N*-terminally His-tagged recombinant lysostaphin (construct 1) expression. The *E. coli* BL21(DE3) was grown in LB media supplemented with kanamycin (10 µg/ml) and incubated at 37°C with orbital shaking at 200 rpm. At an OD_{600 nm} of 0.846, protein expression was induced (Point of Induction = P.O.I) through the addition of IPTG (240 µg/ml) and culture was incubated 30°C with orbital shaking at 100 rpm.



Appendix 7.250: Growth phases of *E. coli* BL21(DE3) pre- and post-induction of recombinant lysostaphin expression.

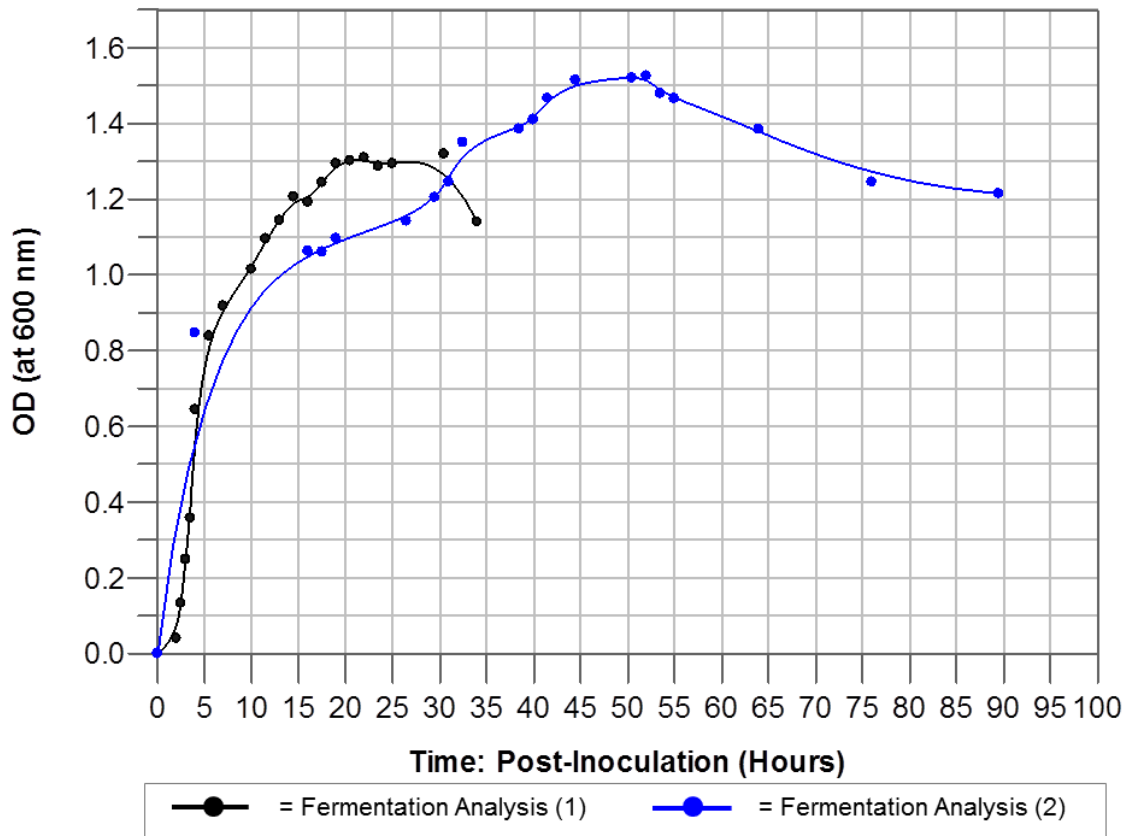


Appendix 7.251: Extended culture and expression of *N*-terminally His-tagged recombinant lysostaphin (construct 1). Lane 1: Sigma low molecular weight markers; Lane 2: Sample 1 (12.0 h PI); Lane 3: Sample 2 (13.5 h PI); Lane 4: Sample 3: (15.0 h PI); Lane 5: Sample 4 (22.5 h PI); Lane 6: Sample 5 (24.0 h PI); Lane 7: Sample 6 (25.5 h PI); Lane 8: Sample 7 (27.0 h PI); Lane 9: Sample 8 (28.5 h PI); Lane 10: Sigma high molecular weight markers; Lane 11: Sample 9 (34.5 h PI); Lane 12: Sample 10 (36 h PI); Lane 13: Sample 11 (37.5 h PI); Lane 14: Sample 12 (40.5 h PI); Lane 15: Sigma low molecular weight markers; Lane 16: Sigma high molecular weight markers; Lane 17: Sample 13 (46.5 h PI); Lane 18: Sample 14 (48.0 h PI); Lane 19: Sample 15 (49.5 h PI); Lane 20: Sample 16 (51.0 h PI); Lane 21: Sigma low molecular weight markers; Lane 21: Sample 17 (60 h PI); Lane 23: Sample 18 (72.0 h PI); Lane 24: Sample 19 (85.5 h PI)

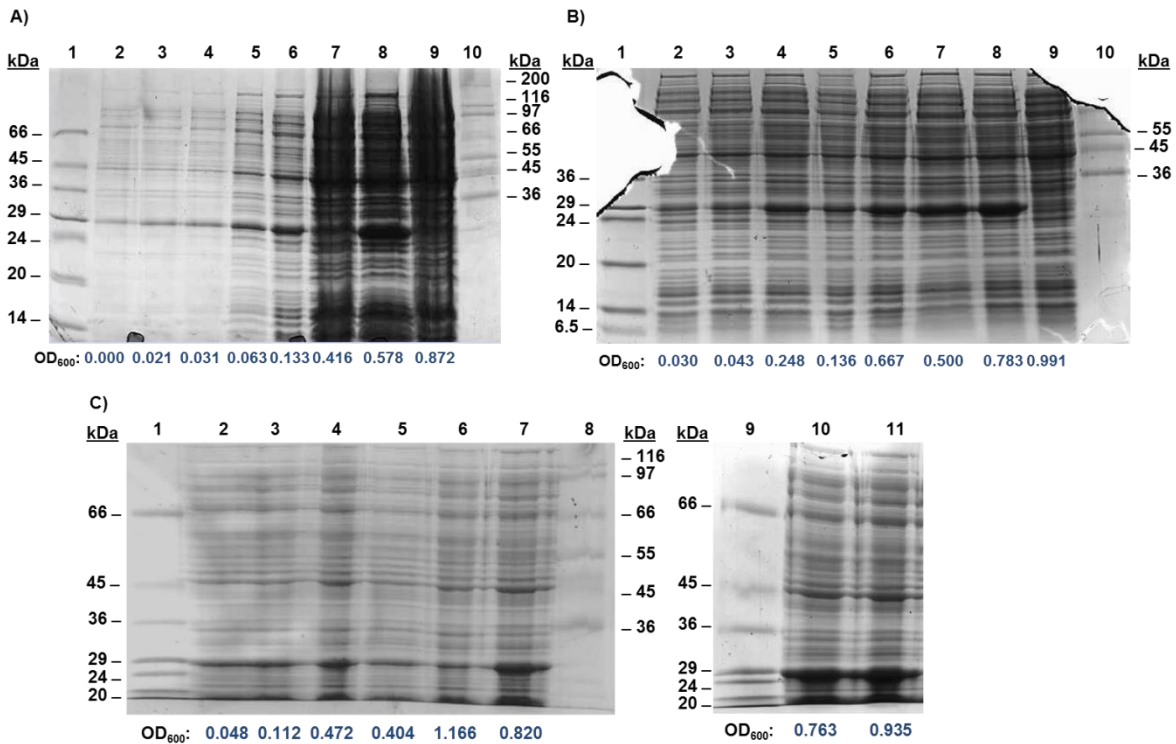


Appendix 7.252: Comparison of growth of *E. coli* BL21(DE3) pre- and post-induction of recombinant lysostaphin expression, during culture analysis (experiments 1 and 2).

The *E. coli* BL21(DE3) was grown in LB media supplemented with kanamycin (10 µg/ml) and incubated at 37 °C with orbital shaking at 200 rpm. At OD_{600 nm} values of 0.644 and 0.846 , protein expression was induced in cultures 1 and 2 respectively, through the addition of IPTG (240 µg/ml). The cultures were subsequently incubated at 30°C with orbital shaking at 100 rpm.

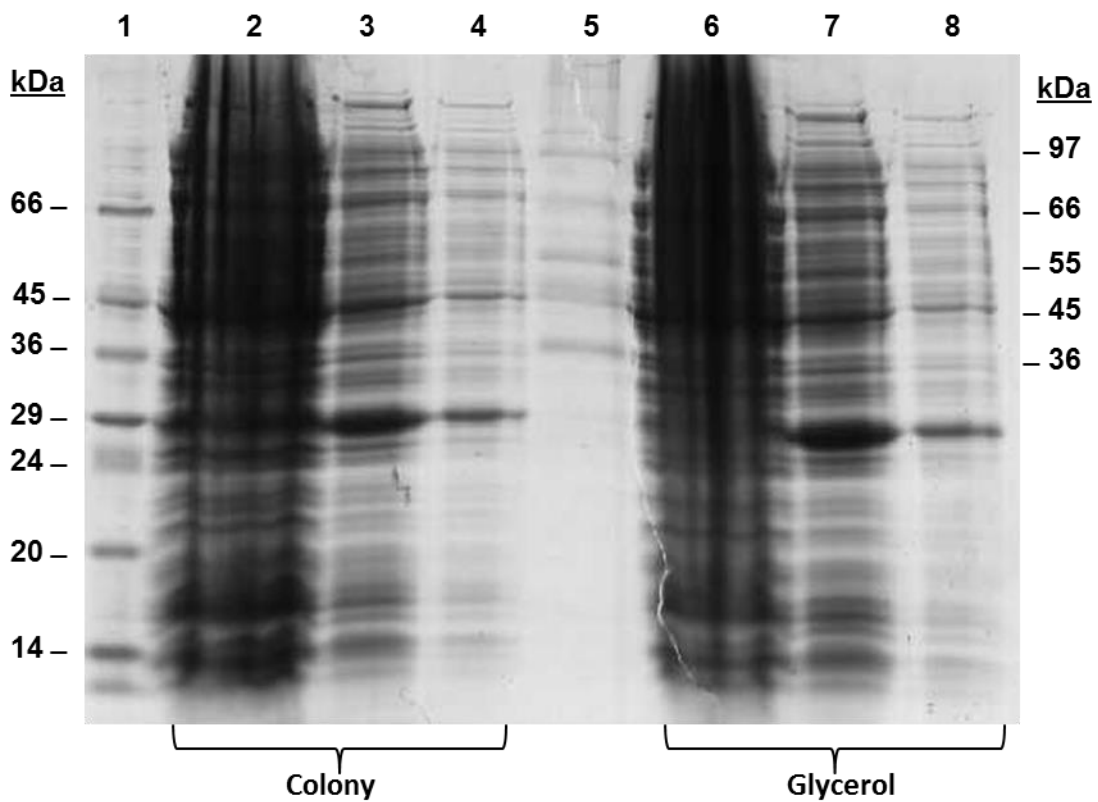


Appendix 7.253: Expression of recombinant lysostaphin at different time-points following IPTG induction according to optical density of cultures. During three separate experiments, twenty four cultures containing 100 ml of LB were inoculated using LB starter cultures. The LB starter cultures were inoculated using a single glycerol stock containing *E. coli* BL21(DE3) transformed with *N*-terminally His-tagged recombinant lysostaphin (construct 1). The cultures were incubated at 37°C, before inducing recombinant protein expression through the addition of IPTG. Each culture was induced at a different optical density (OD_{600 nm}) to assess whether the optical density of the culture at the point of induction, had an influence on protein expression. In each experiment, the cultures were harvested at 4, 10 or 20 h post-induction (PI) and the resulting cell lysates were analysed by 12% (v/v) SDS-PAGE. A) Experiment 1 – cell lysates harvested at 4 h post-induction. Lane 1: Sigma low molecular weight markers; Lane 2: Culture 1; Lane 3: Culture 2; Lane 4: Culture 3; Lane 5: Culture 4; Lane 6: Culture 5; Lane 7: Culture 6; Lane 8: Culture 7; Lane 9; Culture 8; Lane 10: Sigma high molecular weight markers. B) Experiment 2 – cell lysates harvested at 10 h post-induction. Lane 1: Sigma low molecular weight markers; Lane 2: Culture 1; Lane 3: Culture 2; Lane 4: Culture 3; Lane 5: Culture 4; Lane 6: Culture 5; Lane 7: Culture 6; Lane 8: Culture 7; Lane 9; Culture 8; Lane 10: Sigma high molecular weight markers. C) Experiment 3 – cell lysates harvested at 20 h post-induction. Lane 1: Sigma low molecular weight markers; Lane 2: Culture 1; Lane 3: Culture 2; Lane 4: Culture 3; Lane 5: Culture 4; Lane 6: Culture 5; Lane 7: Culture 6; Lane 8: Sigma high molecular weight markers; Lane 8: Sigma low molecular weight markers; Lane 9: Sigma low molecular weight markers; Lane 10: Culture 7; Lane 11: Culture 8.

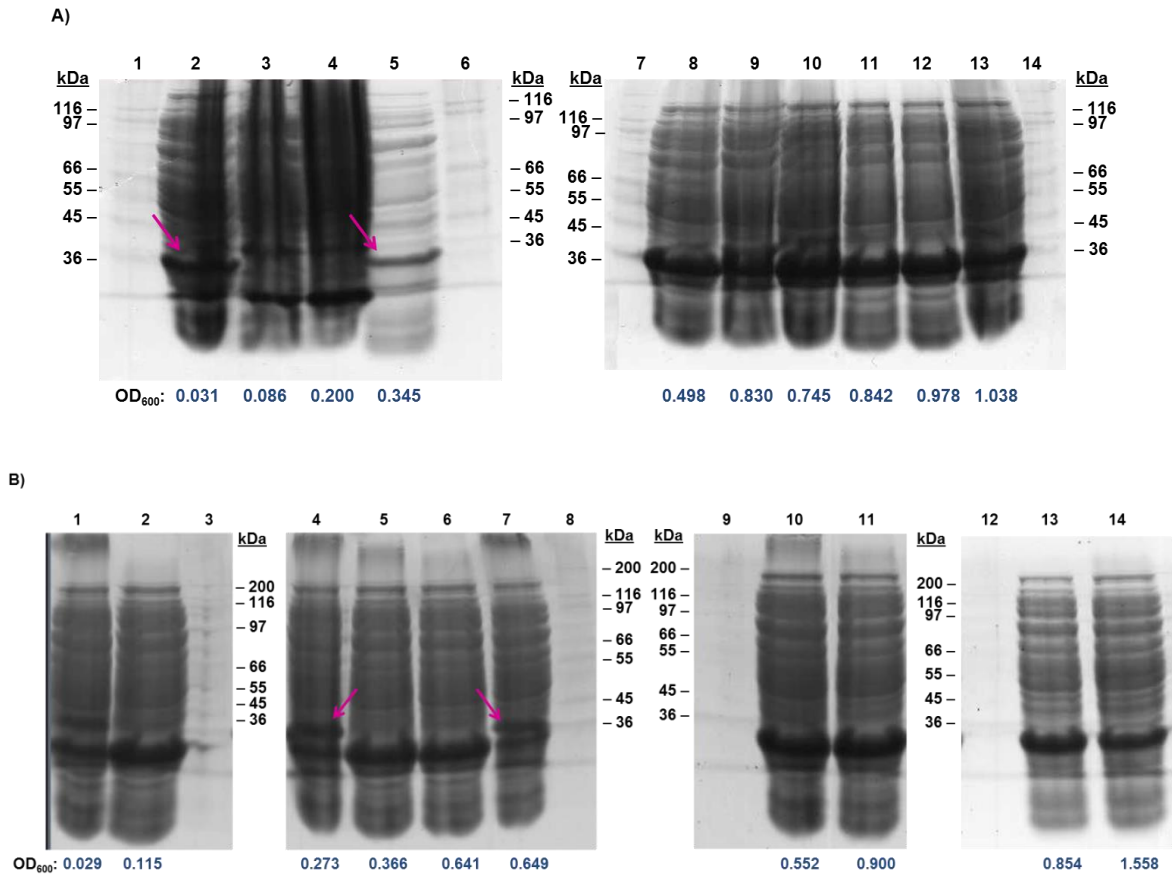


Appendix 7.254: Expression of recombinant lysostaphin following inoculation of LB media using LB starter cultures inoculated from glycerol stock or colony. LB starter cultures were inoculated using an *E.coli* BL21(DE3) glycerol stock or colony transformed with *N*-terminally His-tagged recombinant lysostaphin (construct 1).

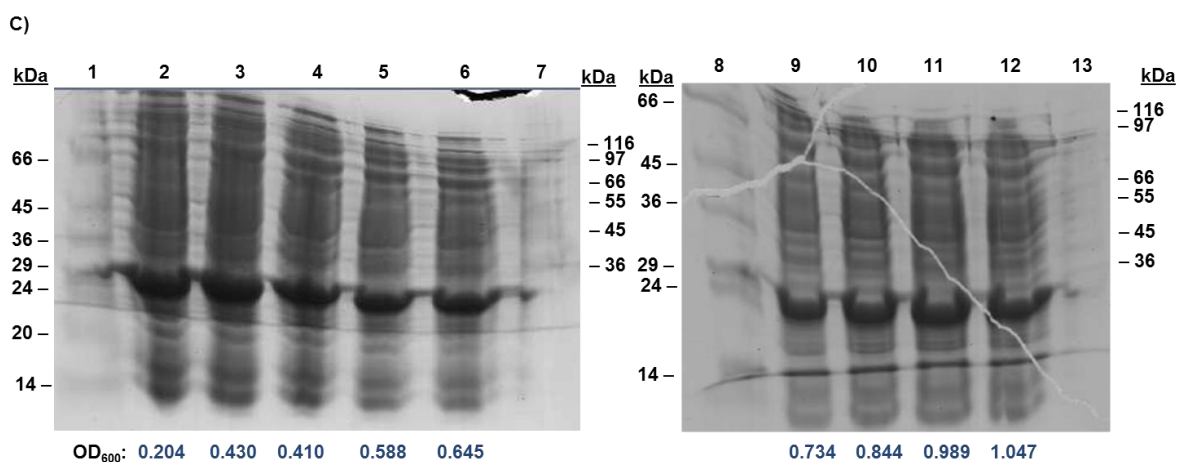
Protein expression was induced once OD_{600 nm} values of 1.041 and 1.060 had been obtained for glycerol stock-inoculated and colony-inoculated cultures respectively. Cell lysate was harvested 21 h after induction of protein expression and was analysed by 12% w/v SDS-PAGE. Lane 1: Sigma low molecular weight markers; Lane 2: CFE following colony inoculation (neat); Lane 3: CFE following colony inoculation (1:10); Lane 4: CFE following colony inoculation (1:100); Lane 5: Sigma high molecular weight markers; Lane 6: CFE following glycerol inoculation (neat); Lane 7: CFE following glycerol inoculation (1:10); Lane 8: CFE following glycerol inoculation (1:100).



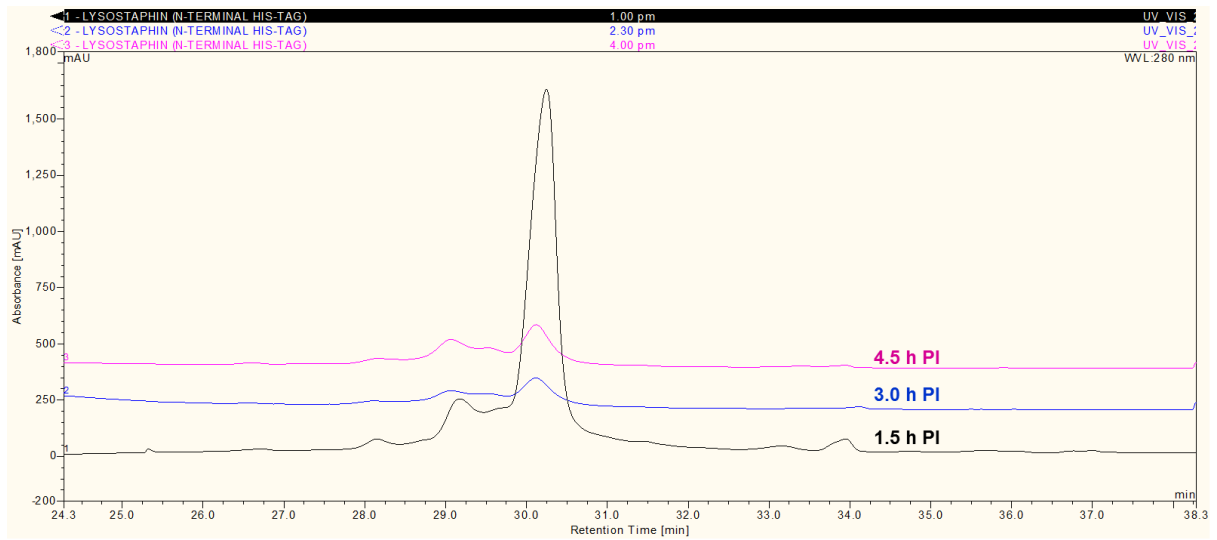
Appendix 7.255: Expression of recombinant lysostaphin following IPTG induction according to optical density of cultures. During three separate experiments, twenty nine cultures containing 100 ml of LB were inoculated using a single glycerol stock containing *E. coli* BL21(DE3) transformed with *N*-terminally His-tagged recombinant lysostaphin (construct 1). The cultures were incubated at 37°C, before inducing recombinant protein expression through the addition of IPTG. Each culture was induced at a different optical density ($OD_{600\text{ nm}}$) to assess whether the optical density of the culture at the point of induction had an influence on protein expression. In each experiment, the cultures were harvested at 20 h post-induction (PI) and the resulting cell lysates were analysed by 12% (w/v) SDS-PAGE. Arrows indicate over-expression of non-recombinant proteins. A) Experiment 1. Lane 1: Sigma high molecular weight markers; Lane 2: Culture 1; Lane 3: Culture 2; Lane 4: Culture 3; Lane 5: Culture 4; Lane 6: Sigma high molecular weight markers; Lane 7: Sigma high molecular weight markers; Lane 8: Culture 5; Lane 9: Culture 6; Lane 10: Culture 7; Lane 11: Culture 8; Lane 12: Culture 9; Lane 13: Culture 10; Lane 14: Sigma high molecular weight markers. B) Experiment 2. Lane 1: Culture 1; Lane 2: Culture 2; Lane 3: Sigma high molecular weight markers; Lane 4: Culture 3; Lane 5: Culture 4; Lane 6: Culture 5; Lane 7: Culture 6; Lane 8: Sigma high molecular weight markers; Lane 9: Sigma high molecular weight markers; Lane 10: Culture 7; Lane 11: Culture 8; Lane 12: Sigma high molecular weight markers; Lane 13: Culture 9; Lane 14: Culture 10.



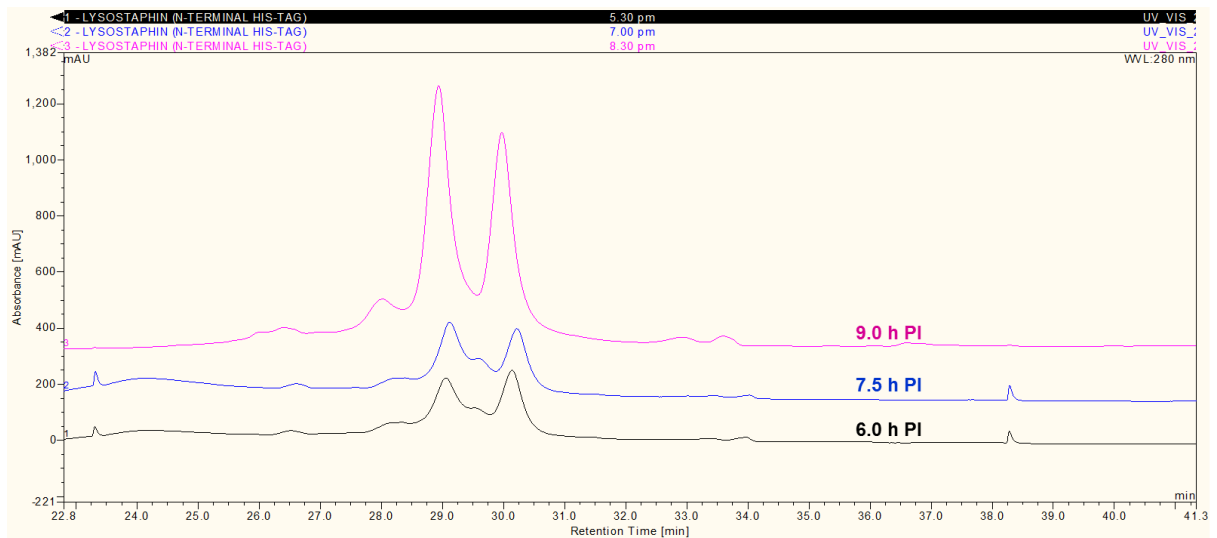
Appendix 7.255 (continued): Expression of recombinant lysostaphin following IPTG induction according to optical density of cultures. During three separate experiments, twenty nine cultures containing 100 ml LB were inoculated using a single glycerol stock containing *E. coli* BL21(DE3) transformed with *N*-terminally His-tagged recombinant lysostaphin (construct 1). The cultures were incubated at 37°C, before inducing recombinant protein expression through the addition of IPTG. Each culture was induced at a different optical density ($OD_{600\text{ nm}}$) to assess whether the optical density of the culture at the point of induction, had an influence on protein expression. In each experiment, the cultures were harvested at 20 h post-induction (PI) and the resulting cell lysates were analysed by 12% (w/v) SDS-PAGE. Arrows indicate over-expression of non-recombinant proteins. C) Experiment 3. Lane 1: Sigma low molecular weight markers; Lane 2: Culture 1; Lane 3: Culture 2; Lane 4: Culture 3; Lane 5: Culture 4; Lane 6: Culture 5; Lane 7: Sigma high molecular weight markers; Lane 8: Sigma low molecular weight markers; Lane 9: Culture 6; Lane 10: Culture 7; Lane 11: Culture 8; Lane 12: Culture 9; Lane 13: Sigma high molecular weight markers.



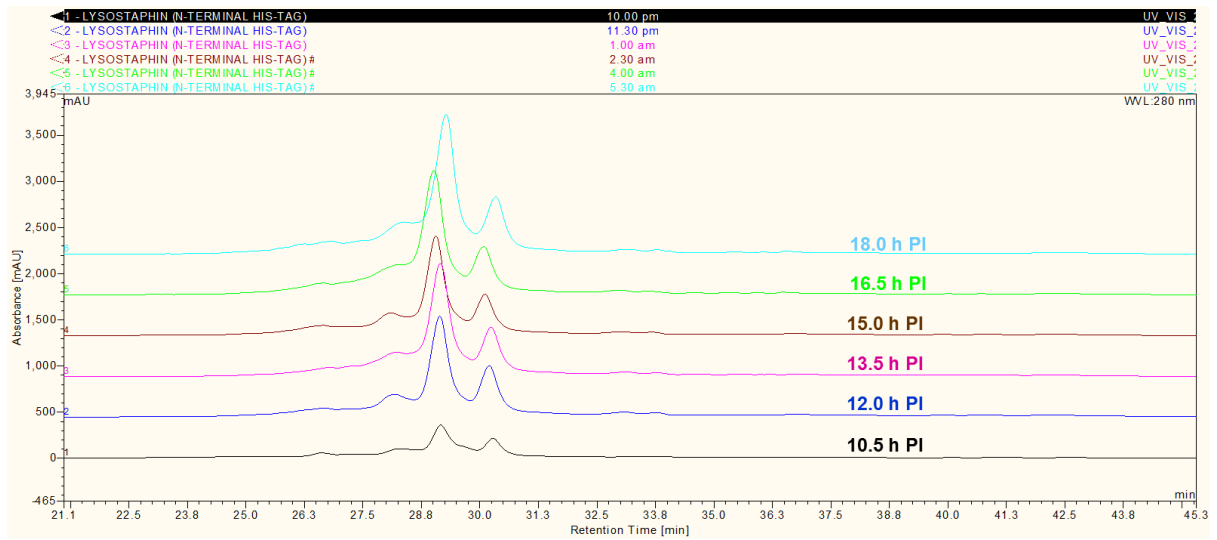
Appendix 7.256: Comparison of WCX separations of cell lysates harvested between 1.5 and 4.5 h post-induction.



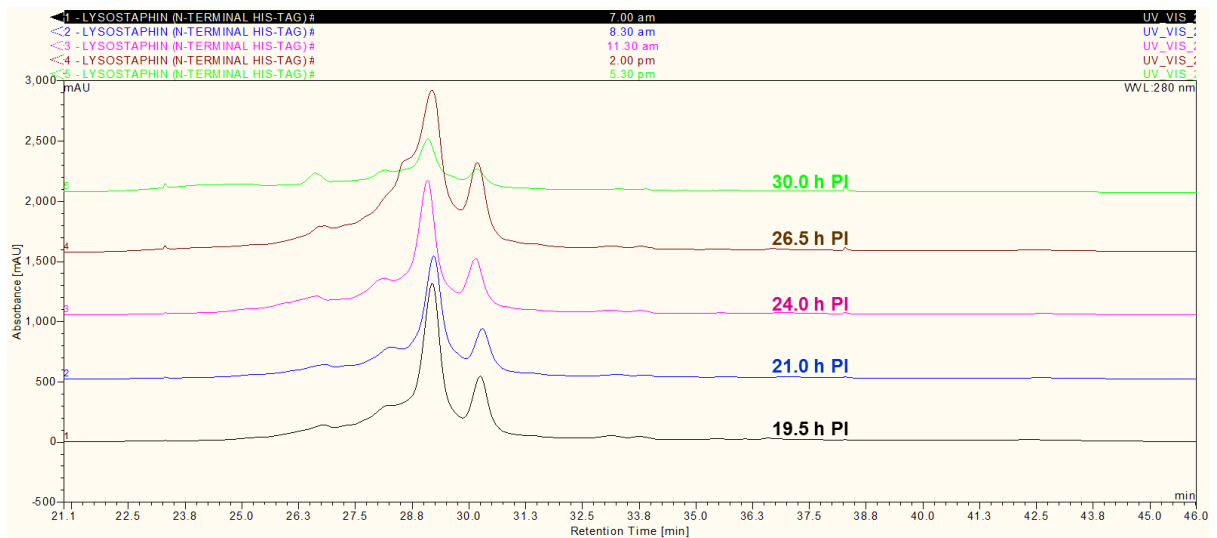
Appendix 7.257: Comparison of WCX separations of cell lysates harvested between 6.0 and 9.0 h post-induction.



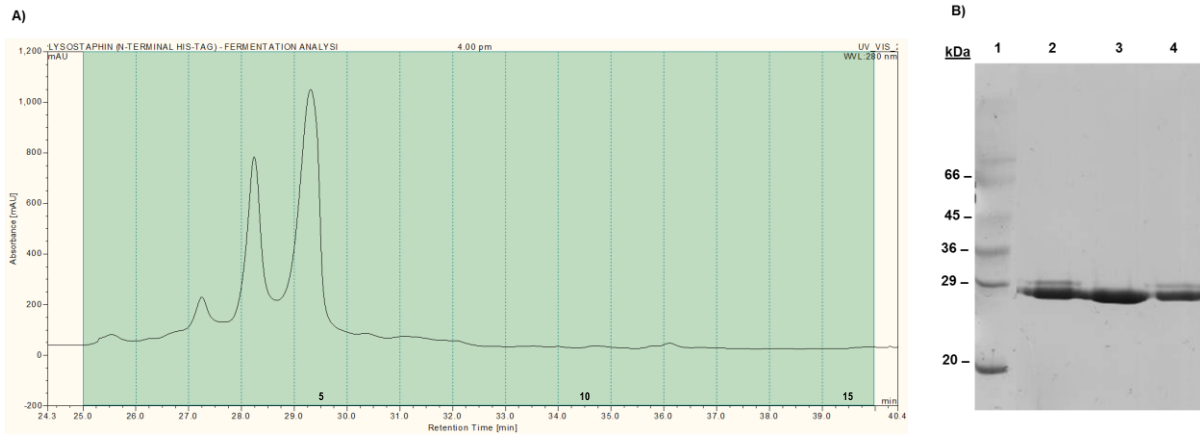
Appendix 7.258: Comparison of WCX separations of cell lysates harvested between 10.5 and 18.0 h post-induction.



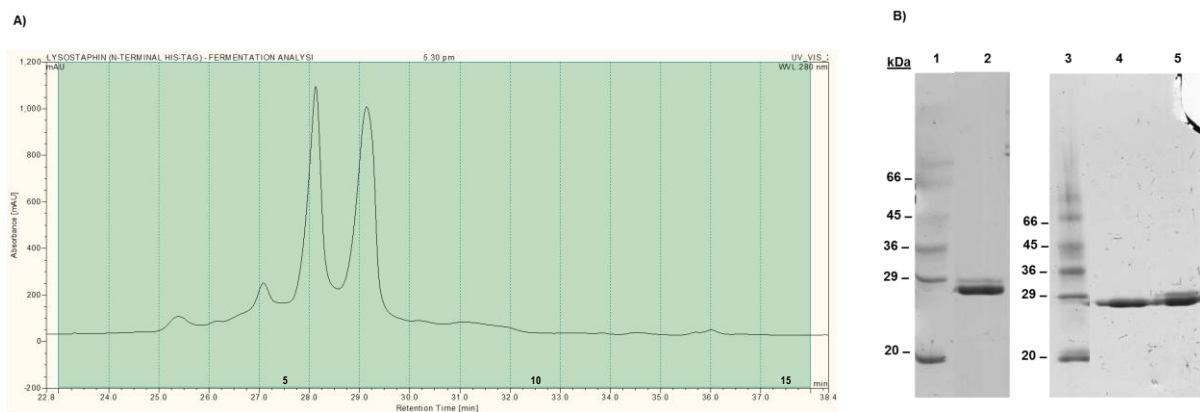
Appendix 7.259: Comparison of WCX separations of cell lysates harvested between 19.5 and 30.0 h post-induction.



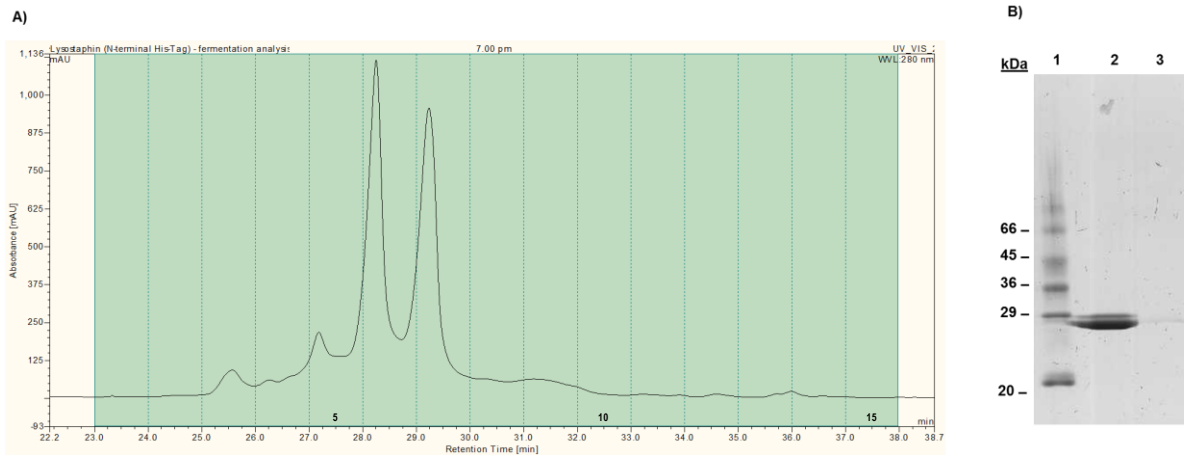
Appendix 7.260: Analysis of cell lysate harvested at 4.5 h post-induction. A) WCX separation of *N*-terminally His-tagged recombinant lysostaphin (construct 1). B) SDS-PAGE analysis of WCX fractions. Lane 1: Sigma low molecular weight markers; Lane 2: Fraction 3; Lane 3: Fraction 4; Lane 4: Fraction 5.



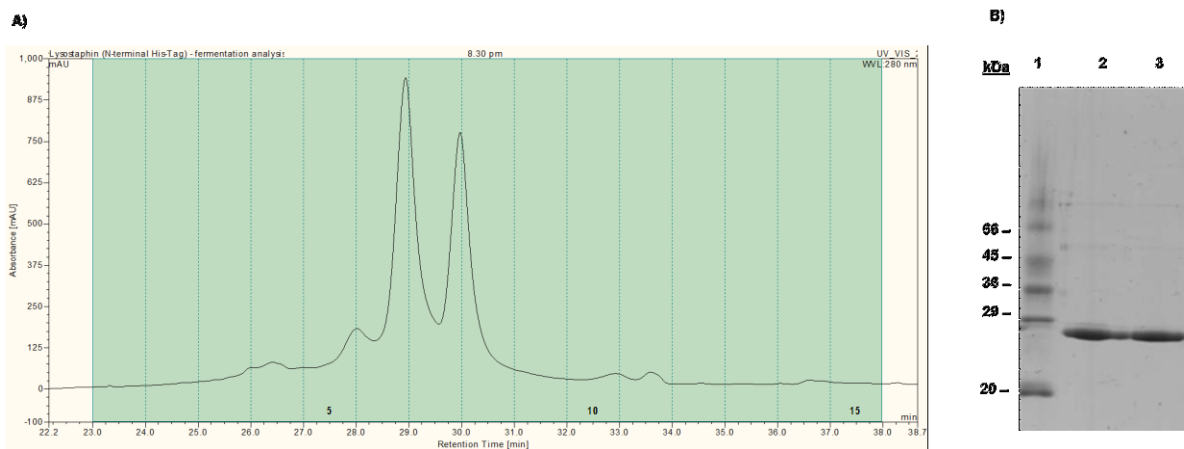
Appendix 7.261: Analysis of cell lysate harvested at 6.0 h post-induction. A) WCX separation of *N*-terminally His-tagged recombinant lysostaphin (construct 1). B) SDS-PAGE analysis of WCX fractions. Lane 1: Sigma low molecular weight markers; Lane 2: Fraction 5; Lane 3: Sigma low molecular weight markers; Lane 4: Fraction 6; Lane 5: Fraction 7.



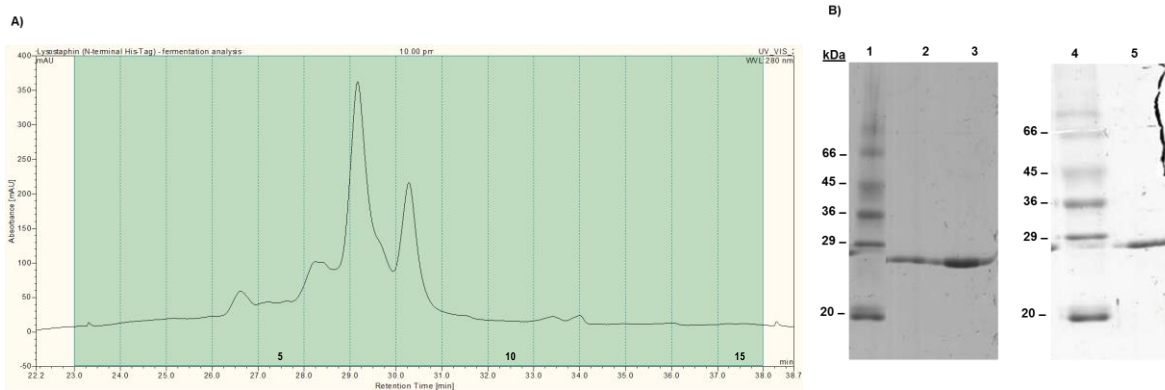
Appendix 7.262: Analysis of cell lysate harvested at 7.5 h post-induction. A) WCX separation of *N*-terminally His-tagged recombinant lysostaphin (construct 1). B) SDS-PAGE analysis of WCX fractions. Lane 1: Sigma low molecular weight markers; Lane 2: Fraction 6; Lane 3: Fraction 3.



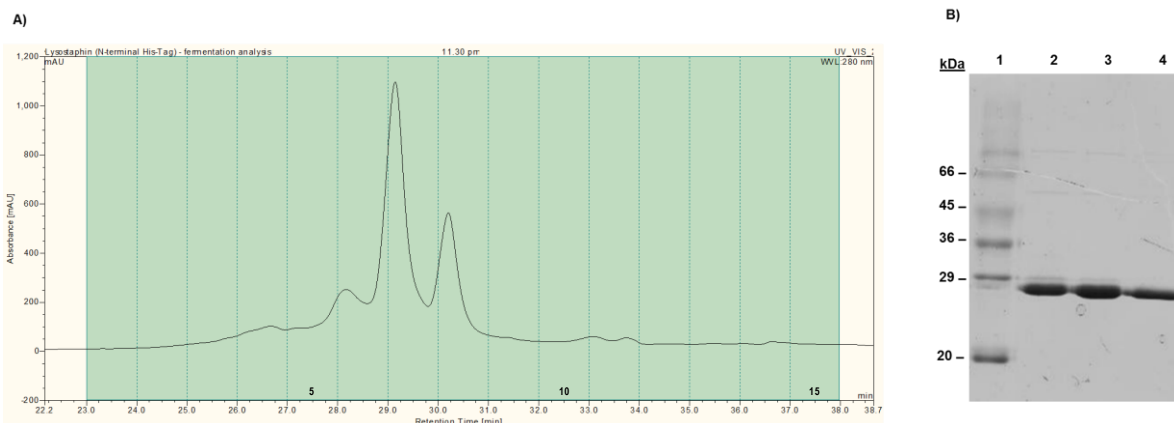
Appendix 7.263: Analysis of cell lysate harvested at 9.0 h post-induction. A) WCX separation of *N*-terminally His-tagged recombinant lysostaphin (construct 1). B) SDS-PAGE analysis of WCX fractions. Lane 1: Sigma low molecular weight markers; Lane 2: Fraction 6; Lane 3: Fraction 7.



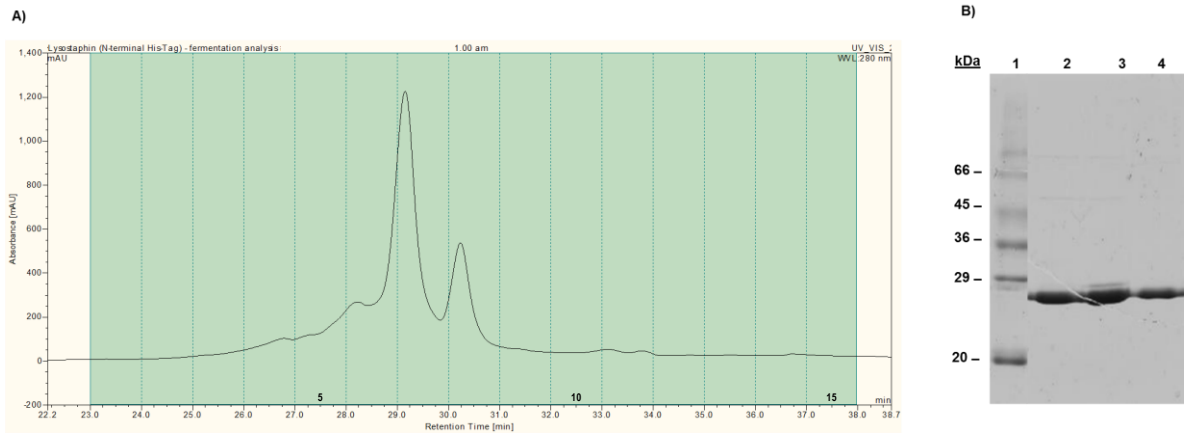
Appendix 7.264: Analysis of cell lysate harvested at 10.5 h post-induction. A) WCX separation of *N*-terminally His-tagged recombinant lysostaphin (construct 1). B) SDS-PAGE analysis of WCX fractions. Lane 1: Sigma low molecular weight markers; Lane 2: Fraction 6; Lane 3: Fraction 7; Lane 4: Sigma low molecular weight markers; Lane 5: Fraction 8.



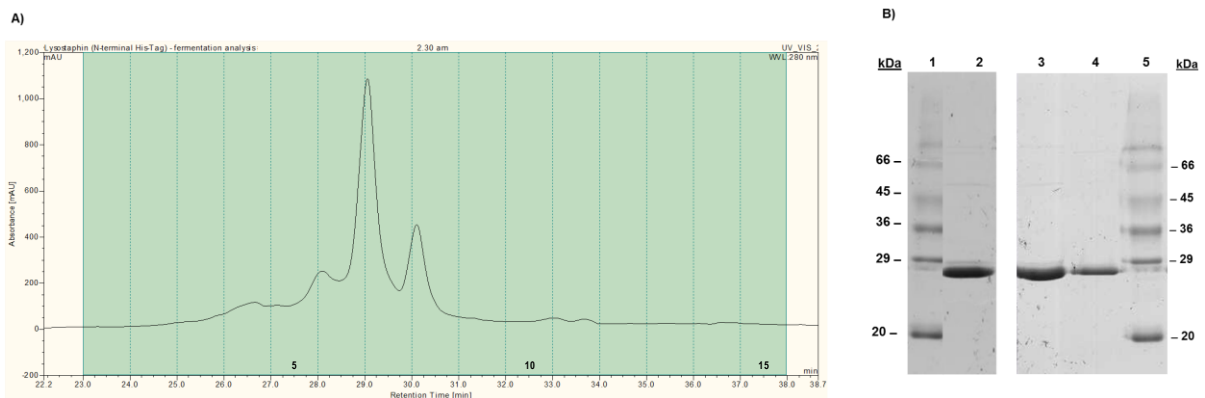
Appendix 7.265: Analysis of cell lysate harvested at 12.0 h post-induction. A) WCX separation of *N*-terminally His-tagged recombinant lysostaphin (construct 1). B) SDS-PAGE analysis of WCX fractions. Lane 1: Sigma low molecular weight markers; Lane 2: Fraction 6; Lane 3: Fraction 7; Lane 4: Fraction 8.



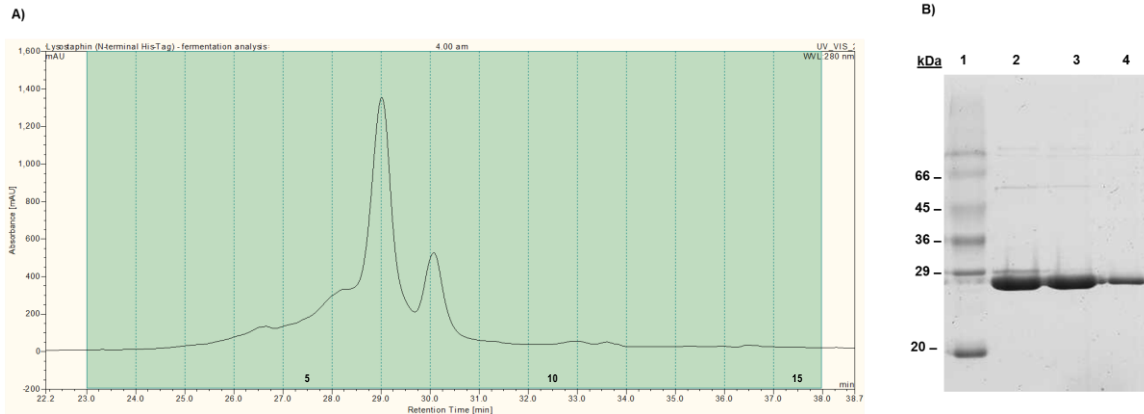
Appendix 7.266: Analysis of cell lysate harvested at 13.5 h post-induction. A) WCX separation of *N*-terminally His-tagged recombinant lysostaphin (construct 1). B) SDS-PAGE analysis of WCX fractions. Lane 1: Sigma low molecular weight markers; Lane 2: Fraction 6; Lane 3: Fraction 7; Lane 4: Fraction 8.



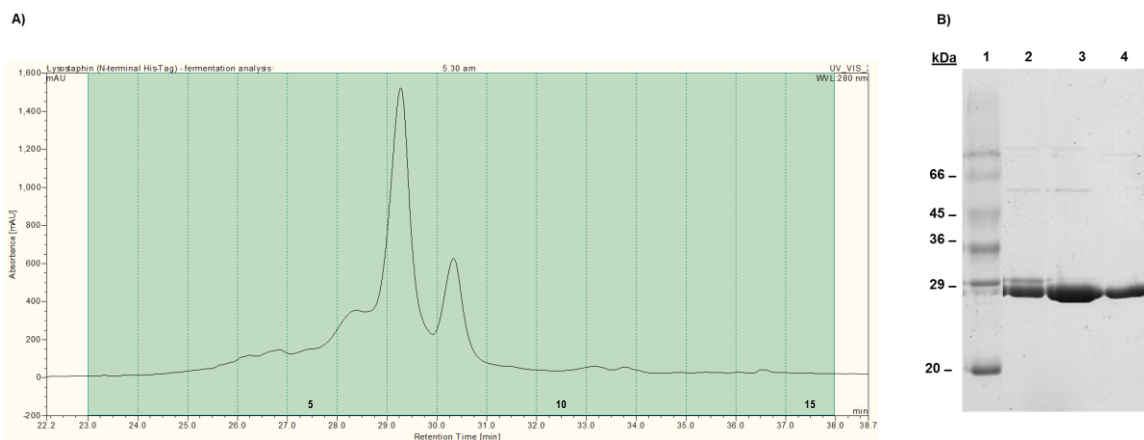
Appendix 7.267: Analysis of cell lysate harvested at 15.0 h post-induction. A) WCX separation of *N*-terminally His-tagged recombinant lysostaphin (construct 1). B) SDS-PAGE analysis of WCX fractions. Lane 1: Sigma low molecular weight markers; Lane 2: Fraction 6; Lane 3: Fraction 7; Lane 4: Fraction 8; Lane 5: Sigma low molecular weight markers.



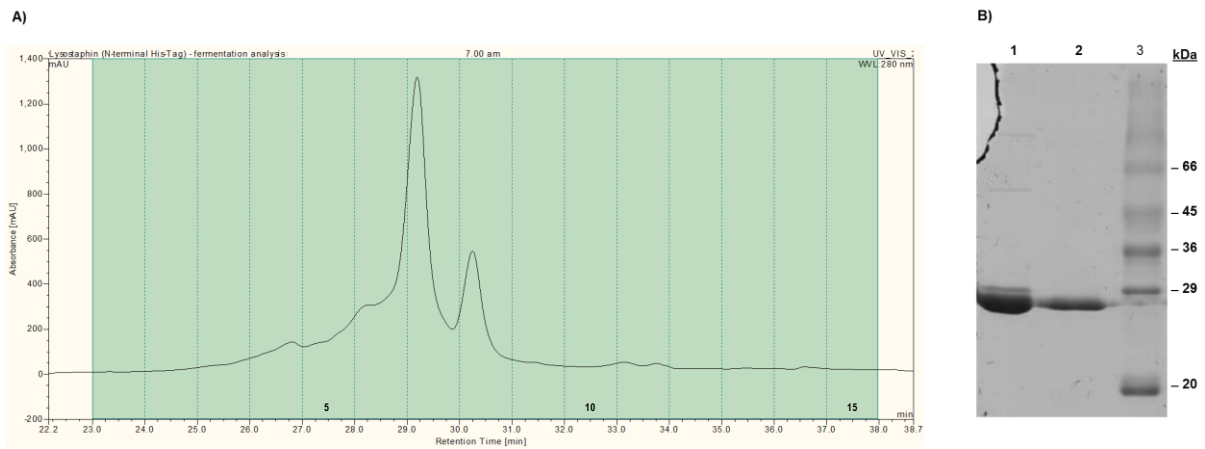
Appendix 7.268: Analysis of cell lysate harvested at 16.5 h post-induction. A) WCX separation of *N*-terminally His-tagged recombinant lysostaphin (construct 1). B) SDS-PAGE analysis of WCX fractions. Lane 1: Sigma low molecular weight markers; Lane 2: Fraction 6; Lane 3: Fraction 7; Lane 4: Fraction 8.



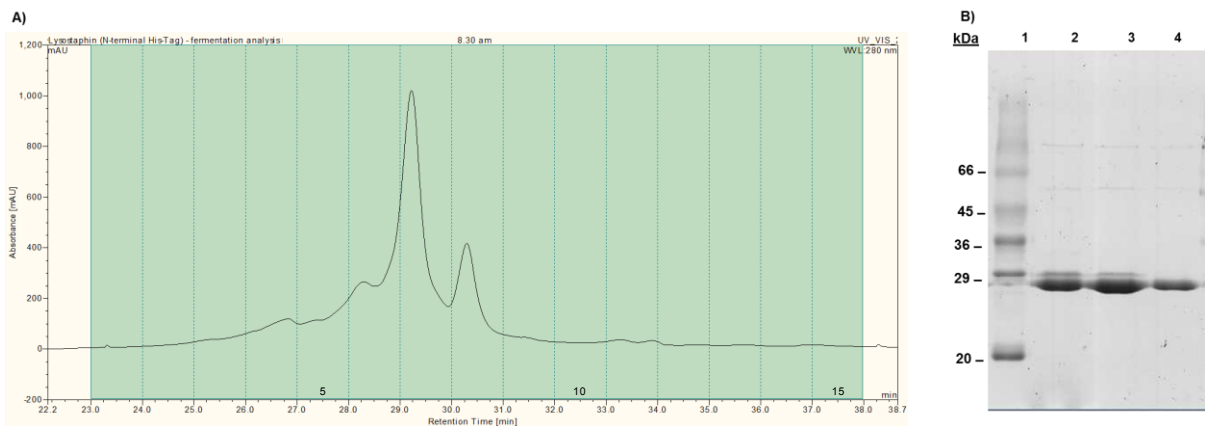
Appendix 7.269: Analysis of cell lysate harvested at 18.0 h post-induction. A) WCX separation of *N*-terminally His-tagged recombinant lysostaphin (construct 1). B) SDS-PAGE analysis of WCX fractions. Lane 1: Sigma low molecular weight markers; Lane 2: Fraction 6; Lane 3: Fraction 7; Lane 4: Fraction 8.



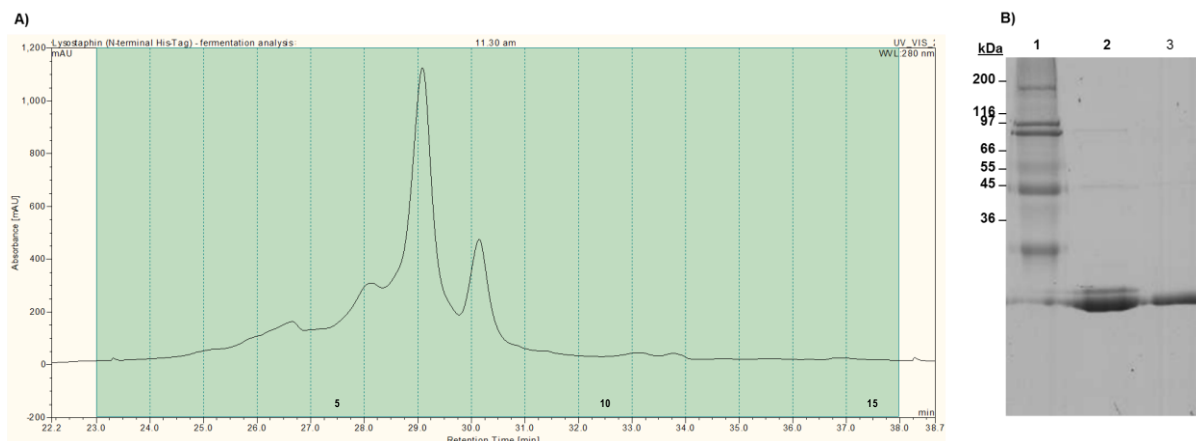
Appendix 7.270: Analysis of cell lysate harvested at 19.5 h post-induction. A) WCX separation of *N*-terminally His-tagged recombinant lysostaphin (construct 1). B) SDS-PAGE analysis of WCX fractions. Lane 1: Fraction 7; Lane 2: Fraction 8; Lane 3: Sigma low molecular weight markers.



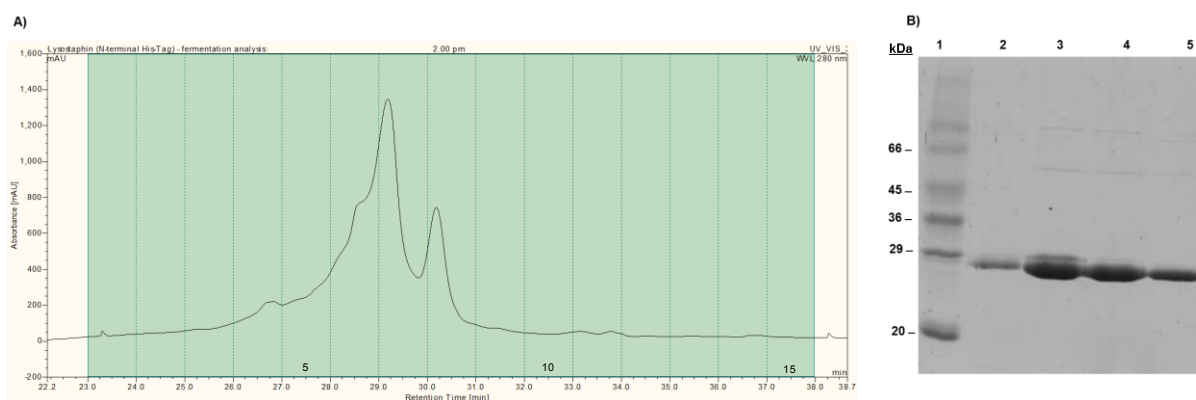
Appendix 7.271: Analysis of cell lysate harvested at 21.0 h post-induction. A) WCX separation of *N*-terminally His-tagged recombinant lysostaphin (construct 1). B) SDS-PAGE analysis of WCX fractions. Lane 1: Sigma low molecular weight markers; Lane 2: Fraction 6; Lane 3: Fraction 7; Lane 4: Fraction 8.



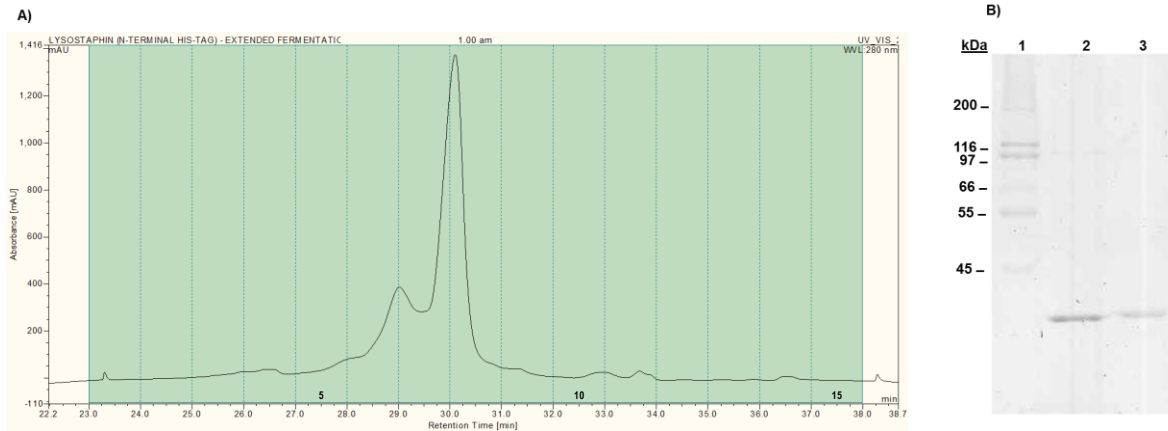
Appendix 7.272: Analysis of cell lysate harvested at 24.0 h post-induction. A) WCX separation of *N*-terminally His-tagged recombinant lysostaphin (construct 1). B) SDS-PAGE analysis of WCX fractions. Lane 1: Sigma high molecular weight markers; Lane 2: Fraction 6; Lane 3: Fraction 8.



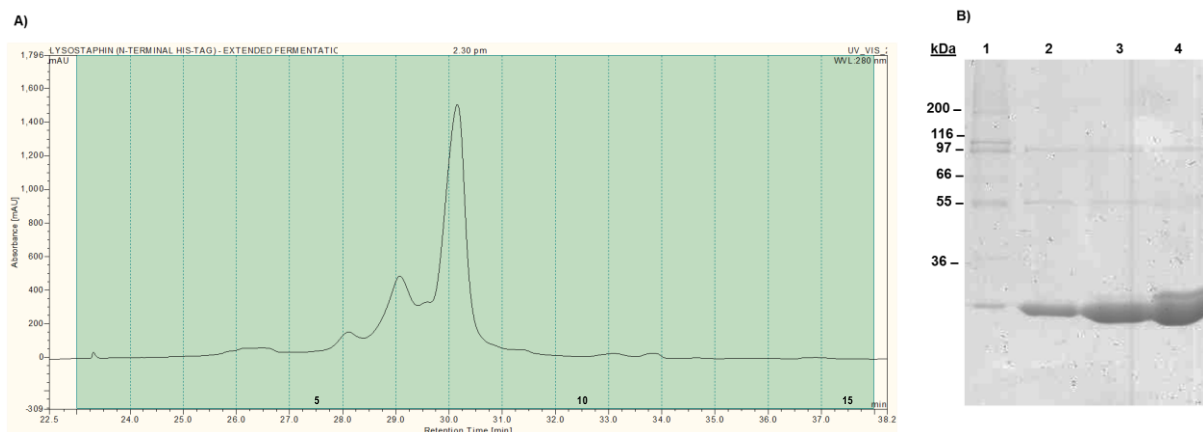
Appendix 7.273: Analysis of cell lysate harvested at 26.5 h post-induction. A) WCX separation of *N*-terminally His-tagged recombinant lysostaphin (construct 1). B) SDS-PAGE analysis of WCX fractions. Lane 1: Sigma low molecular weight markers; Lane 2: Fraction 4; Lane 3: Fraction 6; Lane 4: Fraction 7; Lane 5: Fraction 8.



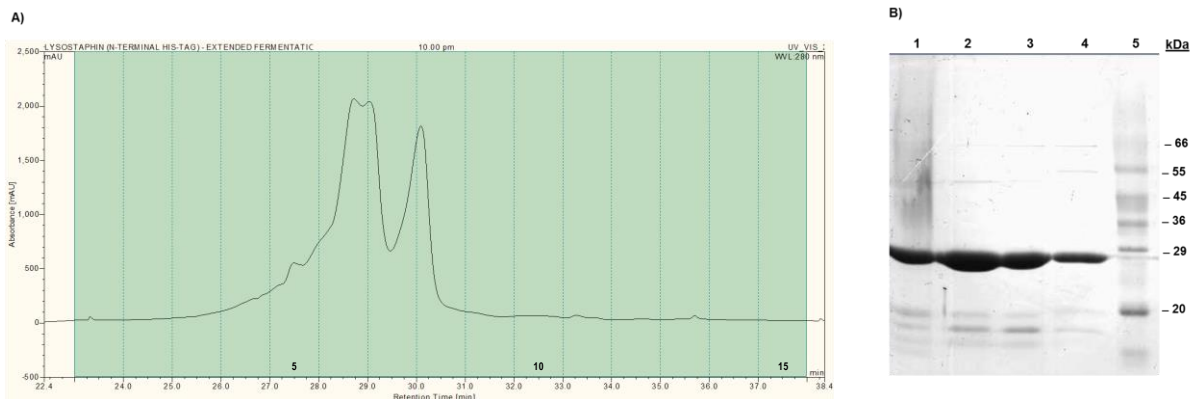
Appendix 7.274: Analysis of cell lysate harvested at 13.5 h post-induction. A) WCX separation of *N*-terminally His-tagged recombinant lysostaphin (construct 1). B) SDS-PAGE analysis of WCX fractions. Lane 1: Sigma high molecular weight markers; Lane 2: Fraction 6; Lane 3: Fraction 7.



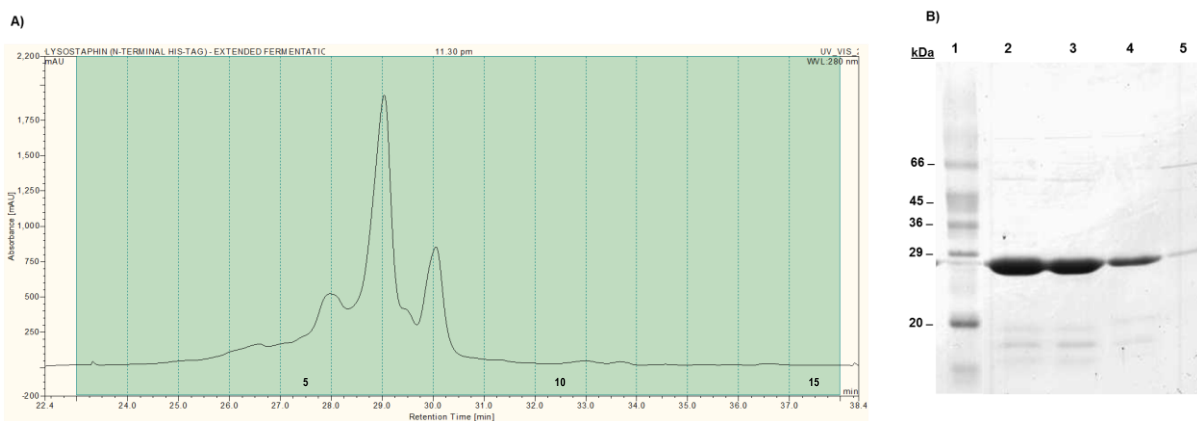
Appendix 7.275: Analysis of cell lysate harvested at 15.0 h post-induction. A) WCX separation of *N*-terminally His-tagged recombinant lysostaphin (construct 1). B) SDS-PAGE analysis of WCX fractions. Lane 1: Sigma high molecular weight markers; Lane 2: Fraction 6; Lane 3: Fraction 7; Lane 4: Fraction 8.



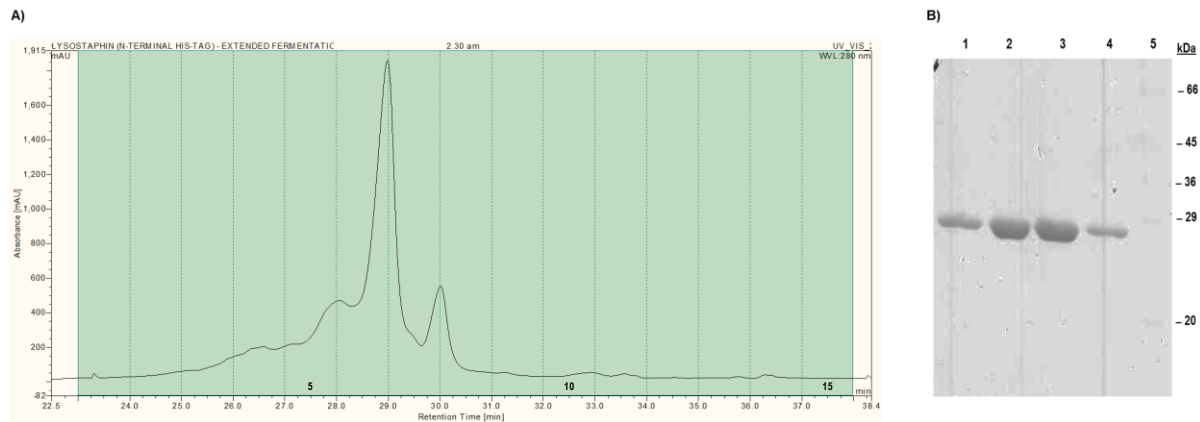
Appendix 7.276: Analysis of cell lysate harvested at 22.5 h post-induction. A) WCX separation of *N*-terminally His-tagged recombinant lysostaphin (construct 1). B) SDS-PAGE analysis of WCX fractions. Lane 1: Fraction 5; Lane 2: Fraction 6; Lane 3: Fraction 7; Lane 4: Fraction 8; Lane 5: Sigma low molecular weight markers.



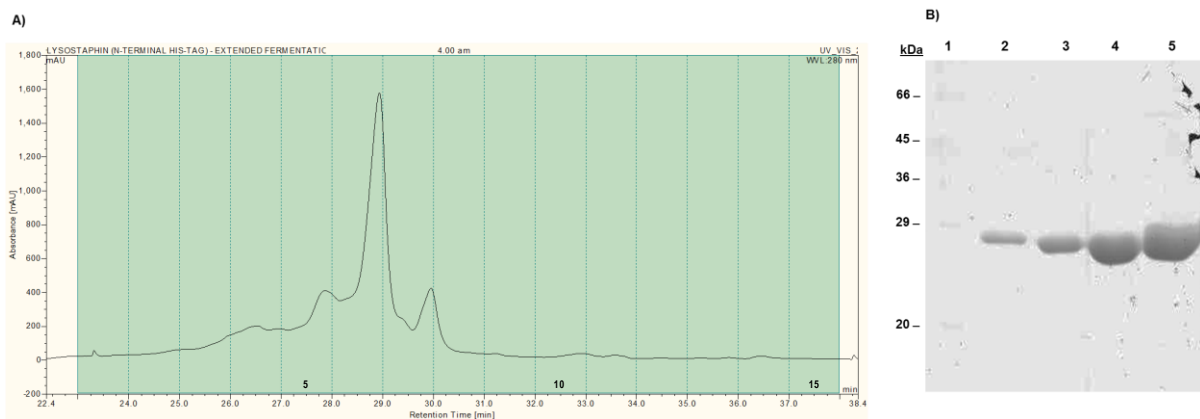
Appendix 7.277: Analysis of cell lysate harvested at 24.0 h post-induction. A) WCX separation of *N*-terminally His-tagged recombinant lysostaphin (construct 1). B) SDS-PAGE analysis of WCX fractions. Lane 1: Sigma low molecular weight markers; Lane 2: Fraction 5; Lane 3: Fraction 6; Lane 4: Fraction 7; Lane 5: Fraction 8.



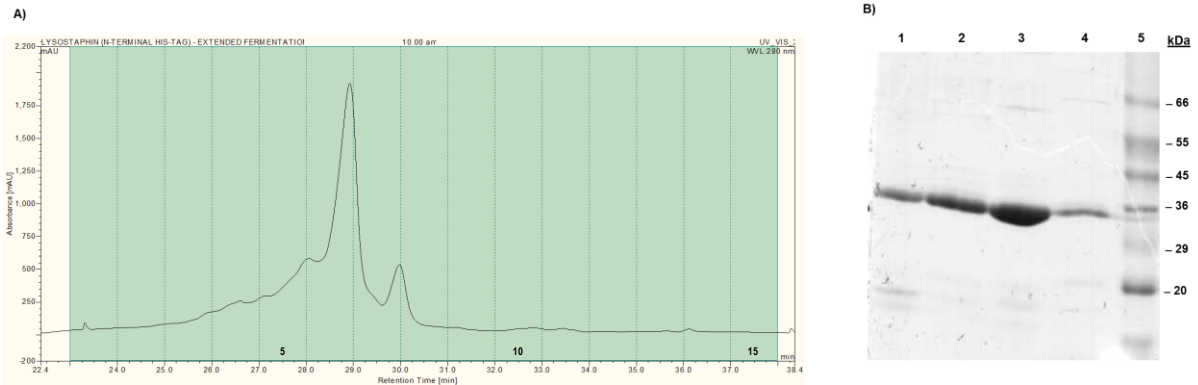
Appendix 7.278: Analysis of cell lysate harvested at 27.0 h post-induction. A) WCX separation of *N*-terminally His-tagged recombinant lysostaphin (construct 1). B) SDS-PAGE analysis of WCX fractions. Lane 1: Fraction 4; Lane 2: Fraction 6; Lane 3: Fraction 7; Lane 4: Fraction 8; Lane 5: Sigma low molecular weight markers.



Appendix 7.279: Analysis of cell lysate harvested at 28.5 h post-induction. A) WCX separation of *N*-terminally His-tagged recombinant lysostaphin (construct 1). B) SDS-PAGE analysis of WCX fractions. Lane 1: Sigma low molecular weight markers; Lane 2: Fraction 4; Lane 3: Fraction 5; Lane 4: Fraction 6; Lane 5: Fraction 7.



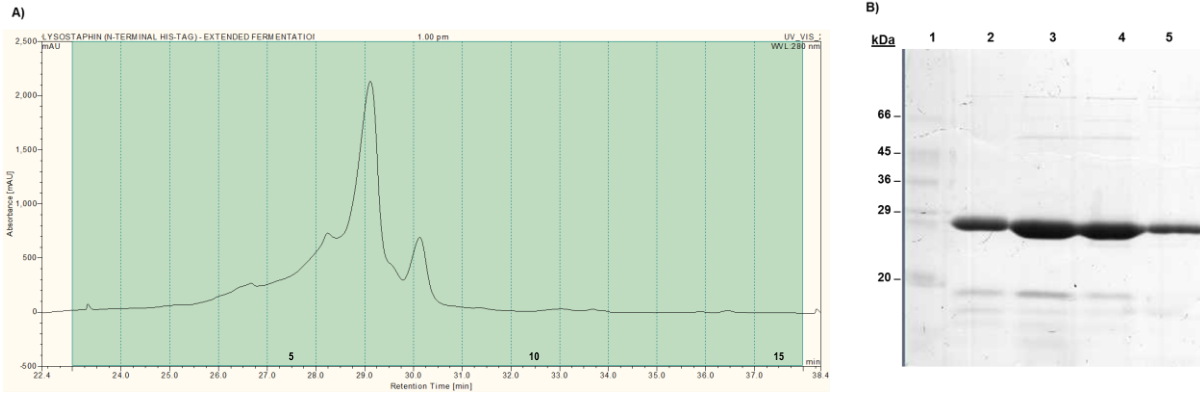
Appendix 7.280: Analysis of cell lysate harvested at 34.5 h post-induction. A) WCX separation of *N*-terminally His-tagged recombinant lysostaphin (construct 1). B) SDS-PAGE analysis of WCX fractions. Lane 1: Fraction 4; Lane 2: Fraction 5; Lane 3: Fraction 6; Lane 4: Fraction 8; Lane 5: Sigma low molecular weight markers.



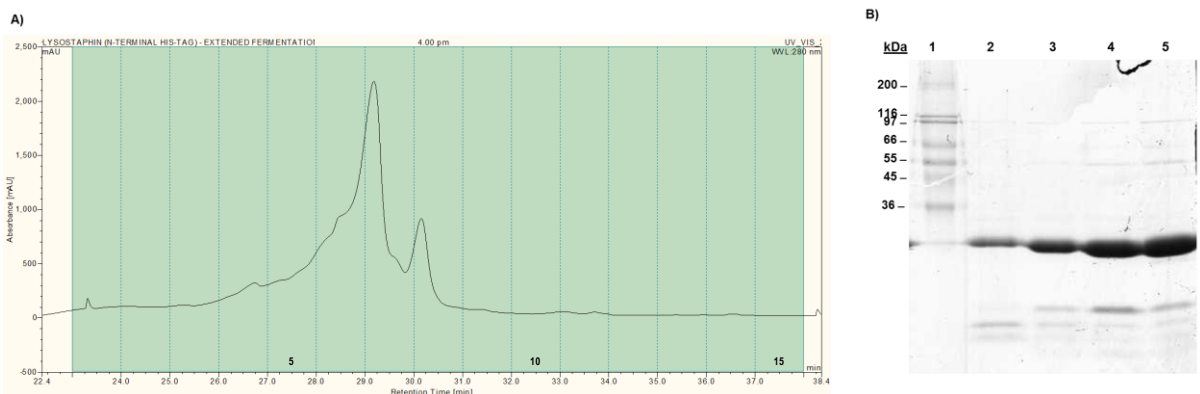
Appendix 7.281: Analysis of cell lysate harvested at 36.0 h post-induction. A) WCX separation of *N*-terminally His-tagged recombinant lysostaphin (construct 1). B) SDS-PAGE analysis of WCX fractions. Lane 1: Sigma low molecular weight markers; Lane 2: Fraction 4; Lane 3: Fraction 5; Lane 4: Fraction 6.



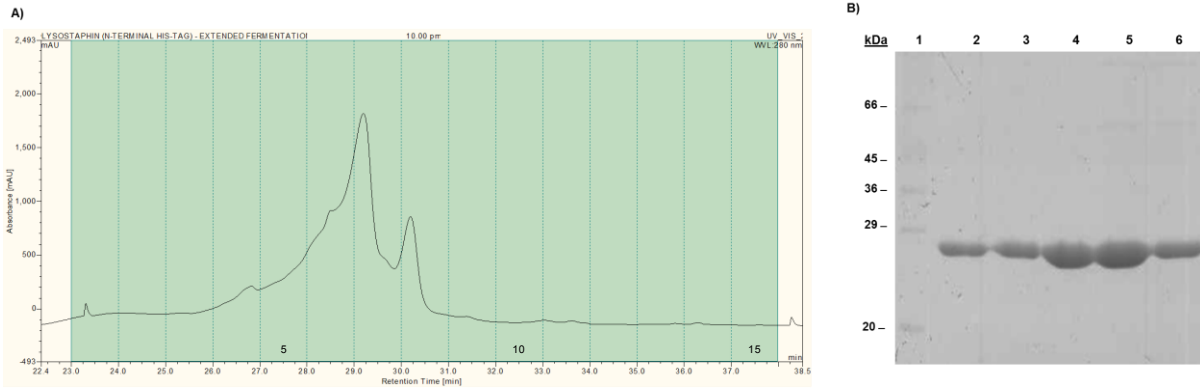
Appendix 7.282: Analysis of cell lysate harvested at 37.5 h post-induction. A) WCX separation of *N*-terminally His-tagged recombinant lysostaphin (construct 1). B) SDS-PAGE analysis of WCX fractions. Lane 1: Sigma low molecular weight markers; Lane 2: Fraction 5; Lane 3: Fraction 6; Lane 4: Fraction 7; Lane 5: Fraction 8.



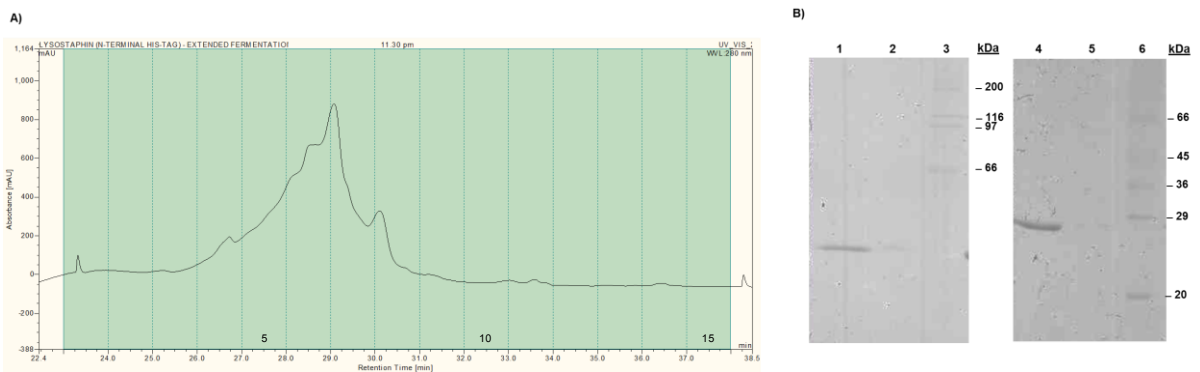
Appendix 7.283: Analysis of cell lysate harvested at 40.5 h post-induction. A) WCX separation of *N*-terminally His-tagged recombinant lysostaphin (construct 1). B) SDS-PAGE analysis of WCX fractions. Lane 1: Sigma high molecular weight markers; Lane 2: Fraction 4; Lane 3: Fraction 5; Lane 4: Fraction 6; Lane 5: Fraction 7.



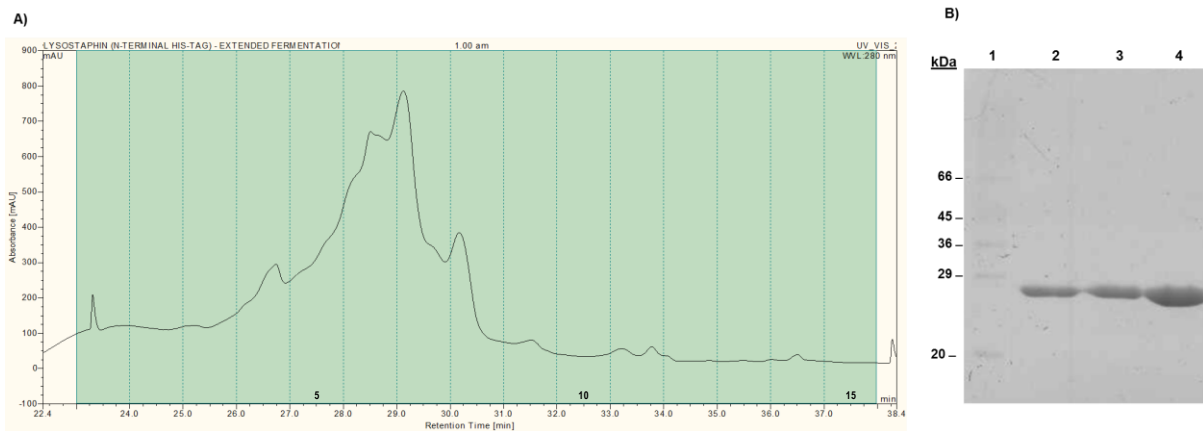
Appendix 7.284: Analysis of cell lysate harvested at 46.5 h post-induction. A) WCX separation of *N*-terminally His-tagged recombinant lysostaphin (construct 1). B) SDS-PAGE analysis of WCX fractions. Lane 1: Sigma low molecular weight markers; Lane 2: Fraction 4; Lane 3: Fraction 5; Lane 4: Fraction 6; Lane 5: Fraction 7; Lane 6: Fraction 8.



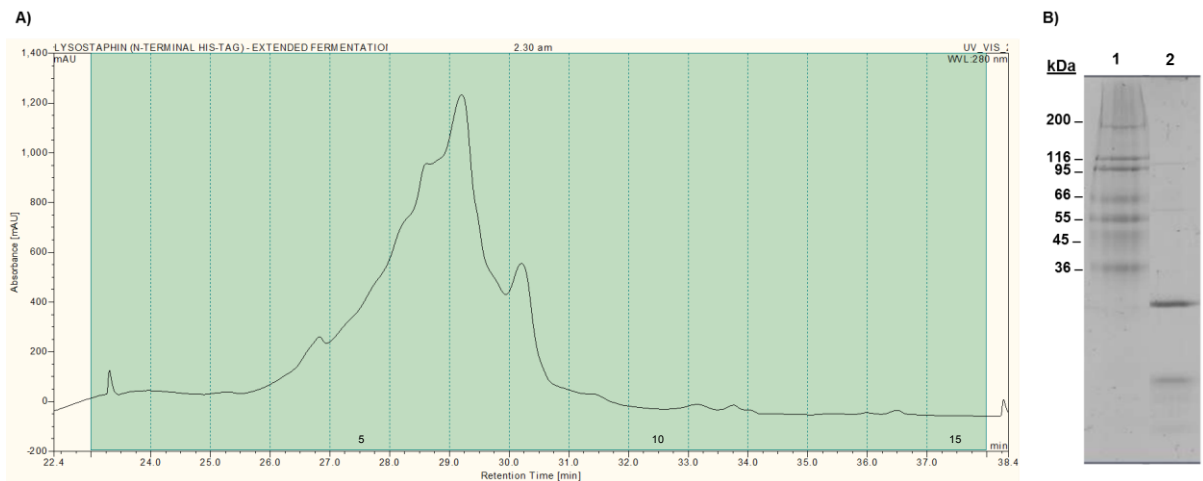
Appendix 7.285: Analysis of cell lysate harvested at 48.0 h post-induction. A) WCX separation of *N*-terminally His-tagged recombinant lysostaphin (construct 1). B) SDS-PAGE analysis of WCX fractions. Lane 1: Fraction 6; Lane 2: Fraction 4; Lane 3: Sigma high molecular weight markers; Lane 4: Fraction 7; Lane 5: Fraction 8; Lane 6: Sigma low molecular weight markers.



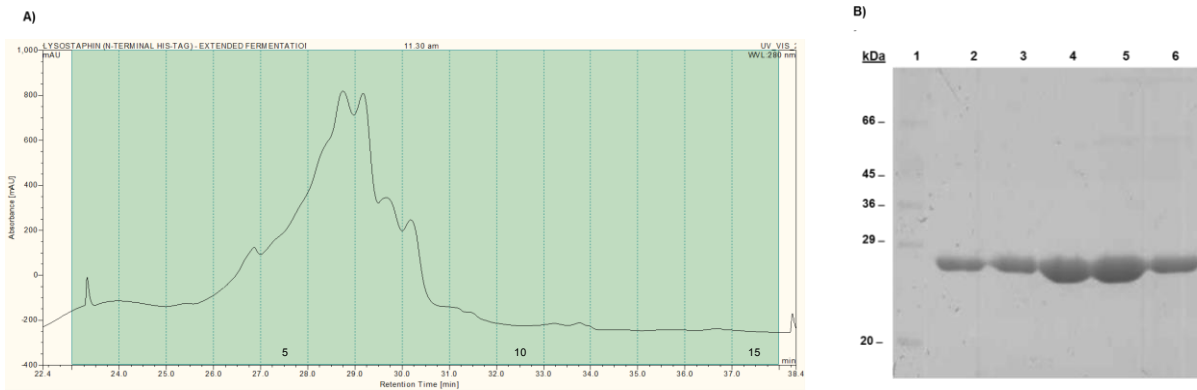
Appendix 7.286: Analysis of cell lysate harvested at 49.5 h post-induction. A) WCX separation of *N*-terminally His-tagged recombinant lysostaphin (construct 1). B) SDS-PAGE analysis of WCX fractions. Lane 1: Sigma low molecular weight markers; Lane 2: Fraction 4; Lane 3: Fraction 6; Lane 4: Fraction 7.



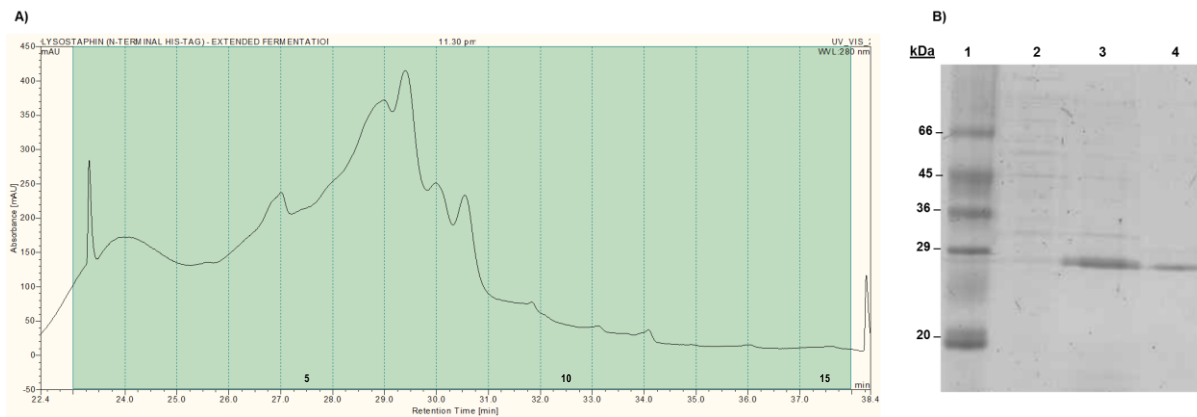
Appendix 7.287: Analysis of cell lysate harvested at 51.0 h post-induction. A) WCX separation of *N*-terminally His-tagged recombinant lysostaphin (construct 1). B) SDS-PAGE analysis of WCX fractions. Lane 1: Sigma high molecular weight markers; Lane 2: Fraction 7.



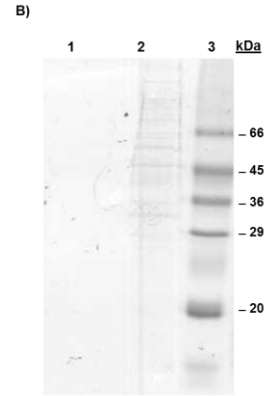
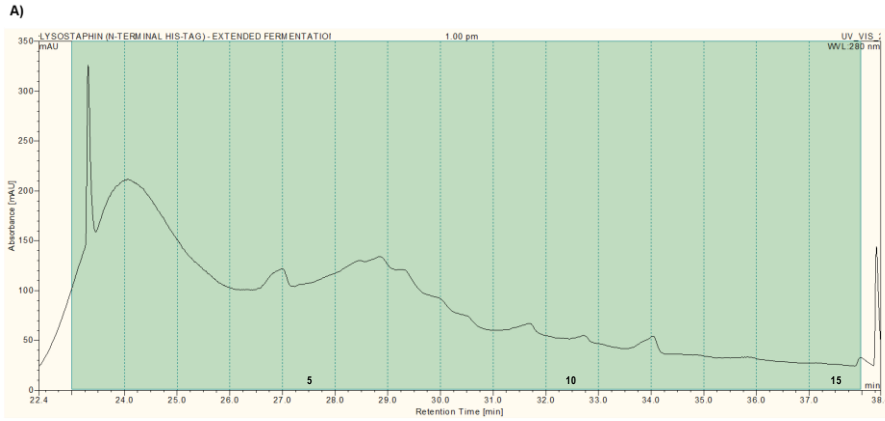
Appendix 7.288: Analysis of cell lysate harvested at 60.0 h post-induction. A) WCX separation of *N*-terminally His-tagged recombinant lysostaphin (construct 1). B) SDS-PAGE analysis of WCX fractions. Lane 1: Sigma low molecular weight markers; Lane 2: Fraction 4; Lane 3: Fraction 5; Lane 4: Fraction 6; Lane 5: Fraction 7; Lane 6: Fraction 8.



Appendix 7.289: Analysis of cell lysate harvested at 72.0 h post-induction. A) WCX separation of *N*-terminally His-tagged recombinant lysostaphin (construct 1). B) SDS-PAGE analysis of WCX fractions. Lane 1: Sigma low molecular weight markers; Lane 2: Fraction 1; Lane 3: Fraction 4; Lane 4: Fraction 7.



Appendix 7.290: Analysis of cell lysate harvested at 85.5 h post-induction. A) WCX separation of *N*-terminally His-tagged recombinant lysostaphin. B) SDS-PAGE analysis of WCX fractions. Lane 1: Fraction 1; Lane 2: Fraction 2; Lane 3: Sigma low molecular weight markers.



Appendix 7.291: Dionex customer application note entitled “Rapid Analysis of Recombinant Protein Production During Fermentation Using Dionex ProPac SCX Columns”. Available at <http://www.dionex.com/en-us/webdocs/109791-CAN110-IC-RecombinantProtein-Fermentation-19Jan2011-LPN2683.pdf>



Rapid Analysis of Recombinant Protein Production During Fermentation Using Dionex ProPac SCX Columns

CAN
110

Dr. Claire Jennings, Professor Gary W. Black
Biomolecular and Biomedical Research Centre, School of Applied Sciences, Northumbria University

Introduction

Production of recombinant proteins using bacterial or mammalian cell culture involves lengthy fermentations that usually undergo very little monitoring of the protein that is expressed. During fermentation, the desired protein may suffer from delayed expression or modifications, yielding undesired variants or aggregates. Real-time monitoring of protein expression is difficult due to the requirement for time-consuming cell harvesting, protein extraction, and purification procedures prior to analysis. On a laboratory scale, the cost and implications of a failed fermentation are insignificant compared to the massive costs involved in industrial scale protein fermentations. Therefore, the development of a laboratory scale, real-time analysis workflow is extremely desirable.

Using strong cation-exchange chromatography, a reproducible method was developed for rapid analysis of recombinant lysostaphin expression in *Escherichia coli*. Lysostaphin is a glycyglycine endopeptidase that is secreted in *Staphylococcus staphylolyticus*. The extracellular enzyme is a zinc metalloprotease that can specifically degrade the peptidoglycan cell wall of staphylococcal strains. As a result, lysostaphin shows great potential as a novel antimicrobial agent for the treatment of blood-borne and biofilm associated infections caused by multidrug resistant staphylococcal strains. Prior characterization of recombinant lysostaphin is essential, however, to establish the homogeneity, stability, and potential immunogenicity of recombinant preparations. In fact, all therapeutic proteins produced by recombinant DNA technology must be thoroughly characterized to satisfy strict regulatory requirements.

Equipment

UltiMate® 3000 Titanium System including:
Biocompatible micro pump
Thermal compartment with two column change valves
VWD detector with micro cell
WPS-3000 Biocompatible Autosampler with fractionation, 250 µL syringe, 100 µL loop
Chromeleon® Chromatography Data System (CDS) software with fractionation license
ProPac® SCX-10, 2.0 mm × 250 mm (Dionex)



Passion. Power. Productivity.

This is a customer-submitted application note published as is. No ISO data available for included figures.

Appendix 7.291: Dionex customer application note entitled “Rapid Analysis of Recombinant Protein Production During Fermentation Using Dionex ProPac SCX Columns”. Available at <http://www.dionex.com/en-us/webdocs/109791-CAN110-IC-RecombinantProtein-Fermentation-19Jan2011-LPN2683.pdf> (continued).

Reagents and Standards

Using genomic DNA from *S. staphylolyticus* as a template, the mature lysostaphin ORF from lysostaphin precursor (glycylglycine endopeptidase) sequence (GenBank Accession Number X06121) was amplified using PCR. The gene was firstly cloned in pCR[®]-Blunt vector using the Zero Blunt[®] cloning system (Invitrogen Ltd., U.K.) and then subcloned in the pET vector cloning system using pET-28a vector (EMD4Biosciences, U.S.A.).

Recombinant pET vector DNA encoding N-terminal His-tagged recombinant lysostaphin was transformed into *E. coli* BL21(DE3) for protein expression. Transformed *E. coli* BL21 (DE3) was used to inoculate an LB starter culture, supplemented with 50 µg/ml kanamycin, which was incubated overnight at 37 °C and 200 rpm. The LB starter culture was then inoculated into a 1 L flask of LB media, supplemented with 50 µg/ml kanamycin. The inoculated LB media was incubated at 37 °C and 200 rpm until an OD₅₀₀ of 0.6 to 1.0 had been obtained. Once within the correct optical density range, protein expression was induced through the addition of 0.24 µg/mL IPTG and fermentation conditions were altered to 30 °C and 100 rpm.

At the point of induction, 30 mL of cells were aseptically removed from the 1 L fermentation and cell-free lysate was harvested by centrifugation at 4000 × G for 10 min. The resulting cell pellet was resuspended in 0.75 ml of SCX buffer A and sonicated at 14 mA

for a total of 1 min using 10 s intervals. The sonicated cells were centrifuged at 24,000 × G for 10 min and 200 µL of the resulting cell-free extract was subjected to SCX analysis. Cell-free extract was harvested and analyzed at regular time points during the fermentation to monitor expression levels and charge heterogeneity of recombinant lysostaphin during expression.

Method

Chromatographic

Conditions: UltiMate 3000 Titanium System

Column: Dionex ProPac SCX-10,
2.0 mm × 250 mm (P/N 063456)

Mobile Phase: A: Sodium phosphate (20 mM), pH 7.4
B: Sodium phosphate (20 mM),
sodium chloride (1000 mM), pH 7.4

Flow Rate: 0.2 mL/min

Injection Volume: 200 µL

Detection: Absorbance at 214 and 280 nm

Gradient:	Time (min)	Flow (mL/min)	% B	% C
	0.00	0.2	0.0	0.0
	0.10	0.2	0.0	0.0
	20.00	0.2	50.0	0.0
	22.90	0.2	50.0	0.0
	23.00	0.2	90.0	0.0
	26.00	0.2	90.0	0.0
	26.10	0.2	0.0	0.0
	37.00	0.2	0.0	0.0

Results

Recombinant lysostaphin is a basic protein that binds well to cation-exchange columns, even at pH 7.4. This trait is beneficial for analysis, as most cellular proteins do not bind to a strong cation-exchange [SCX] column at this pH. When hyperexpressed, recombinant lysostaphin can contribute approximately 50% of the protein content of the cell-free extract. The small percentage of *E. coli* cellular proteins that can bind to the SCX column at this pH are individually present in much smaller amounts than the lysostaphin; therefore, they do not interfere in the analysis. The ability to purify and analyze recombinant lysostaphin directly from cell-free lysate, without any further purification steps, is advantageous as it permits rapid monitoring as the fermentation progresses.

E. coli cultures of 500 to 1000 mL can yield from 50 to over 200 mg of protein, depending on how well the protein is expressed during fermentation. PAGE analysis of cell-free lysate harvested during fermentation demonstrates that high levels of recombinant lysostaphin are present from four hours after induction of protein expression (Figure 1). At this level of protein expression, harvesting small volumes of culture provides sufficient material for analysis. As little as 1 mL of culture can provide enough material for rapid analysis; however, if subsequent analyses are to be performed, then a greater sample concentration will be necessary.

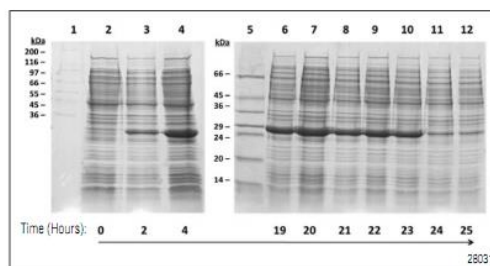


Figure 1. SDS-PAGE analysis of cell-free lysate harvested from an *E. coli* BL21 fermentation. Hyperexpression of recombinant lysostaphin was evident between 4 and 23 h post-induction. Recombinant lysostaphin has a molecular weight of 29.3 kDa. Lanes 1 and 5 contain protein molecular weight markers.

Appendix 7.291: Dionex customer application note entitled “Rapid Analysis of Recombinant Protein Production During Fermentation Using Dionex ProPac SCX Columns”. Available at <http://www.dionex.com/en-us/webdocs/109791-CAN110-IC-RecombinantProtein-Fermentation-19Jan2011-LPN2683.pdf> (continued).

From the PAGE analysis of cell lysates harvested during the fermentation process, it can be seen that expression of recombinant lysostaphin started soon after induction of protein expression. Twenty-four hours after induction of protein expression, recombinant lysostaphin expression ceased and expressed protein was removed by cellular degradative processes. Recombinant lysostaphin has a molecular weight of 29.3 kDa and this was detected by PAGE analysis, which revealed the presence of a 29 kDa protein band throughout the fermentation. However, PAGE analysis does not show how recombinant lysostaphin alters during the fermentation, yielding different charge variants. These protein variants can be observed as they occur during fermentation by analyzing the cell lysate by cation-exchange chromatography using ProPac SCX-10 columns (Figure 2).

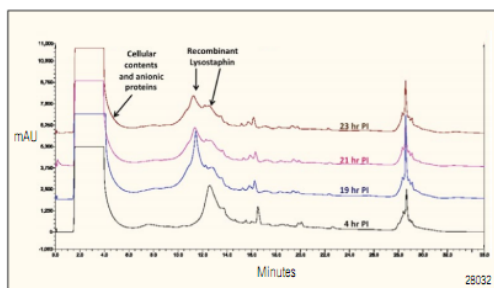


Figure 2. Comparison of SCX separations of recombinant lysostaphin from cell lysate. Chromatograms obtained by analysis of cell lysate at 4, 19, 21, and 23 h post-induction are shown.

Fermentation analysis revealed that recombinant protein expression can yield several protein variants, and that the abundance of each variant can alter dramatically over time. SCX analysis of cell lysate harvested between 4 and 19 h post-induction revealed protein isoforms displaying major differences in charge, which emphasizes the importance of real-time monitoring during fermentation. Although the protein variants differ in their charge, all of the fractions collected exhibited the expected enzymatic activity. In addition, each of the observed peaks showed no differences when analyzed by PAGE, reversed-phase HPLC, and size-exclusion chromatography. Therefore, recombinant lysostaphin produced in *E. coli* appears to display charge heterogeneity, which does not seem to be attributable to aggregation or significant alterations in molecular weight.

Conclusion

The recognition of structural variants is critical in the production of monoclonal antibodies and other therapeutic proteins. Structural variations have been previously identified using Dionex ProPac columns with a high-resolution, inert HPLC system.^{1,2} The work shown here, however, is an example of how such a system can be used for real-time monitoring of recombinant protein production. Charge heterogeneity of other cationic recombinant proteins can also be studied by direct rapid analysis of cell-free lysate during fermentation. It is possible that chromatographic analysis time can be reduced further, with a slight loss in resolution, by using a rapid analysis monolithic ion exchange column such as the ProSwift® SCX-1S 1 × 50 mm column (P/N 071977).

Reference

1. Dionex Corporation, *Analysis of Monoclonal Antibody Heterogeneity by Cation-Exchange Chromatography: Separation of C-Terminal Lysine Variants*. Application Note 127, LPN 1047, 2009, Sunnyvale, CA.
2. Weitzhandler, M.; Farnan, D.; Horvath, J.; Rohrer, J. S.; Slingsby, R. W.; Avdalovic, N.; Pohl, C. Protein Variant Separations by Cation-Exchange Chromatography on Tentacle-Type Polymeric Stationary Phases. *J. Chromatogr., A* **1998**, *828*, 365–372.

This is a customer-submitted application note published as is. No ISO data available for included figures.

UltiMate, Chromeleon, ProPac, and ProSwift are registered trademarks of Dionex Corporation. pCR-Blunt and Zero Blunt are registered trademarks of Invitrogen Corporation.

Passion. Power. Productivity.



Dionex Corporation
1228 Titan Way
P.O. Box 3603
Sunnyvale, CA
94089-3603
(408) 737-0700

North America
U.S./Canada (847) 295-7500

South America
Brazil (55) 11 3731 5140

Europe
Austria (43) 1 616 51 25 Benelux (31) 20 663 9758 (32) 9 353 4294
Denmark (45) 96 36 90 90 France (33) 1 39 30 01 10 Germany (49) 5126 991 0
Ireland (353) 1 844 0054 Italy (39) 02 51 02 1267 Sweden (46) 8 473 3360
Switzerland (41) 62 205 9966 United Kingdom (44) 1276 591722

Asia Pacific
Australia (61) 2 9420 5233 China (862) 2428 3282 India (91) 22 2764 2735
Japan (81) 6 6585 1213 Korea (82) 2 2653 2580 Singapore (65) 6299 1190
Taiwan (886) 2 8751 6555
www.dionex.com



LPN 2683 PDF 1/11
©2011 Dionex Corporation

7.3 Characterisation of Recombinant Lysostaphin

7.3.1 Activity of recombinant lysostaphin

Appendix 7.292: Media

***Micrococcus* nutrient medium (1L)**

Peptone	5.0 g
Beef extract	1.5 g
Yeast extract	3.0 g
Glucose	1.0 g

The pH was adjusted to pH 7.4, prior to autoclaving the media.

***Micrococcus* nutrient medium agar (100 ml)**

Micrococcus nutrient medium	100.0 ml
Agar (bacteriological agar no. 1)	1.2 g

The media was autoclaved to make the agar soluble and allowed to cool to less than 50°C, before pouring into Petri dishes and leaving to set for ~ 20 min.

Appendix 7.293: Buffers

Wash buffer (1L)

NaCl (0.15 M)	8.76 g
KHPO ₄ (0.01 M)	1.36 g

The pH of the solution was adjusted to pH 7.2 and autoclaved.

Assay buffer (1L)

Tris-HCl (0.05 M)	6.1 g
NaCl (0.15 M)	8.8 g

The pH of the buffer was adjusted to pH 7.5, prior to autoclaving.

IMAC buffer A (1 L) (as described in Section 2.5.2.1 / Appendix 7.105)

IMAC buffer B (1L) (as described in Section 2.5.2.1 / Appendix 7.105)

WCX buffer A (1L) (as described in Section 3.2.1 / Appendix 7.136)

IEX buffer B (1L) (as described in Section 3.2.1 / Appendix 7.136)

Appendix 7.294: Sample preparation

Experiments were performed using purified, concentrated recombinant lysostaphin samples. Purified, concentrated recombinant lysostaphin was harvested from *E. coli* BL21(DE3) cultured in either LB or AIM and purified using either IMAC or HIC and GF. Following purification, the purified protein was concentrated using ultrafiltration. Further details about preparation of recombinant lysostaphin is provided in Appendix 7.295.

Appendix 7.295: Purified recombinant lysostaphin preparations

Preparation ID	Construct	Expression media	Mode of purification	Protein concentration (µg/µl)	Related results
2	3	AIM	IMAC	8.67	Figure 2.27 Appendix 7.141 Figure 2.26
3	3	AIM	HIC, GF	1.46	Appendix 7.142 Figure 2.17 Figure 2.18 Figure 2.19 Figure 2.20 Figure 2.21
4	1	AIM	IMAC	37.80	Appendix 7.143 Appendix 7.144 Appendix 7.145
6	1	AIM	IMAC	157.85	Appendix 7.147 Appendix 7.148 Appendix 7.149
14	1	LB	IMAC	111.14	Appendix 7.307 Appendix 7.308 Appendix 7.309
15	1	AIM	IMAC	203.25	Appendix 7.310 Appendix 7.311 Appendix 7.312
16	1	LB	IMAC	312.23	Appendix 7.313 Appendix 7.314 Appendix 7.315
17	1	AIM	IMAC	257.74	Appendix 7.316 Appendix 7.317 Appendix 7.318
18	1	LB	IMAC	6.23	Appendix 7.319 Appendix 7.320 Appendix 7.321

Appendix 7.296: Equipment

IMAC purifications and WCX separations using the ProPac[®] WCX-10 (4 x 500 mm) column were performed using an Ultimate[™] 3000 Titanium system which consisted of a dual gradient pump, a thermal compartment with two column change valves, a VWD detector and a WPS-3000 biocompatible autosampler. The thermal compartment was maintained at 30°C during separation. The system was fitted with a PEEK fluidic pathway and the autosampler was fitted with a 250 µl syringe and a 1 ml injection loop. Small sample volumes were loaded onto the system via automated injection, whilst larger sample volumes were pumped into the system via buffer line C. Although the autosampler could accommodate fractionation, fractionation was performed using an ISCO Foxy[®] Jr Fraction collector in this instance. Data collection and analysis was performed using Chromeleon[®] Chromatography Data System software with fractionation license.

WCX separations using the ProPac[®] WCX-10 (2 x 500 mm) column were performed using an Ultimate[™] 3000 Titanium system which consisted of an analytical titanium pump, a thermal compartment with two column change valves, a VWD detector and a WPS-3000 biocompatible autosampler. The system was fitted with a PEEK fluidic pathway and the autosampler was fitted with a 250 µl syringe and a 500 µl injection loop. Fractionation was achieved using the WPS-3000 biocompatible autosampler, which was temperature regulated to 10°C. Data collection and analysis was performed using Chromeleon[®] Chromatography Data System software with fractionation license.

Chromatographic separations were performed using a number of analytical columns, as described in Appendix 7.297.

Appendix 7.297: Analytical columns and mobile phase compositions used whilst investigating the activity of recombinant lysostaphin

Column	Chromatographic mode	Dimensions (mm)	Mobile phase conditions
ProPac [®] IMAC-10	IMAC	4.0 x 250	IMAC buffer A and B
ProPac [®] WCX-10	WCX	2.0 x 500	IEX buffer A and B
ProPac [®] WCX-10	WCX	4.0 x 500	IEX buffer A and B

Appendix 7.298: Growth of *S. aureus* for lysostaphin assay

An ampoule of dried culture of *S. aureus* was rehydrated with *micrococcus* nutrient media and streaked onto *micrococcus* nutrient media agar plates. A single colony of *S. aureus* was inoculated from agar into 100 ml of pre-warmed *micrococcus* nutrient medium using a sterile wire loop to create a starter culture. The starter culture was incubated overnight at 37°C with orbital shaking at 150 rpm. Following overnight incubation, the starter culture was inoculated into 900 ml of pre-warmed *micrococcus* nutrient medium and incubated at 37°C with orbital shaking at 150 rpm. Growth of the *S. aureus* was measured spectrophotometrically at a wavelength of 600 nm over 24 h, in order to determine the optical density at which the end of the exponential phase occurred.

Appendix 7.299: Harvesting of *S. aureus* for lysostaphin assay

After monitoring the growth of *S. aureus* spectrophotometrically, it was found that the end of the exponential phase occurred at an OD_{600 nm} of 0.8. Therefore *S. aureus* cells were harvested at an OD_{600 nm} of 0.8 by centrifugation of the 900 ml culture at 10,000 x g and 4°C. The pelleted cells were washed and resuspended in wash buffer and stored at -20°C until required.

Appendix 7.300: Assay of N-terminally His-tagged recombinant lysostaphin (construct 1)

Assays were performed as described in Section 4.1.2.7 using preparations 4, 6, 15 and 17 which had been purified using IMAC (Appendix 7.114) and concentrated by ultrafiltration (Appendix 7.120). The protein preparations had been expressed in *E. coli* BL21(DE3) cultured in AIM (Appendix 7.75) and cell lysate was harvested as described in Appendix 7.77.

Appendix 7.301: Influence of expression media upon the activity of recombinant lysostaphin

Assays were performed as described in Section 4.1.2.7 using preparations 14, 15, 16 and 17, which had been purified using IMAC (Appendix 7.114 or Appendix 7.117) and concentrated by ultrafiltration (Appendix 7.120). Preparations 14 and 16 had been expressed in *E. coli* BL21(DE3) cultured in LB (Appendix 7.76), whilst preparations 15 and 17 were

expressed in *E. coli* BL21(DE3) cultured in AIM (Appendix 7.75). Cell lysate was harvested as described in Appendix 7.77. Each assay comparison was performed on separate occasions, however both experiments were performed on *S. aureus* substrate cells which had been harvested from the same culture.

Appendix 7.302: Influence of expression location upon the activity of recombinant lysostaphin

An assay was performed as described in Section 4.1.2.7 using preparation 1 which had been purified using IMAC (Appendix 7.114) and concentrated by ultrafiltration (Appendix 7.120). The preparation had been expressed in *E. coli* BL21(DE3) cultured in AIM (Appendix 7.75) and cell lysate was harvested as described in Appendix 7.77.

Appendix 7.303: Influence of purification upon the activity of recombinant lysostaphin

Assays were performed as described in Section 4.1.2.7 using preparations 2 and 3, which had been purified using HIC and GF or IMAC respectively (Appendix 7.110 and Appendix 7.111 or Appendix 7.114). Following purification, selected fractions were concentrated by ultrafiltration (Appendix 7.120). Preparations 2 and 3 had been expressed in *E. coli* BL21(DE3) cultured in AIM (Appendix 7.75) and cell lysate was harvested as described in Appendix 7.77.

Appendix 7.304: Influence of lyophilisation upon the activity of recombinant lysostaphin

Assays were performed as described in Section 4.1.2.7 using preparation 10, which had been purified using large-scale IMAC purification (Appendix 7.115). Following purification, selected eluted protein was dialysed (Appendix 7.118) and lyophilised (Appendix 7.119). Lyophilised recombinant lysostaphin was resuspended in 18.2 MΩ/cm H₂O prior to assay. Preparation 10 had been expressed in *E. coli* BL21(DE3) cultured in LB (Appendix 7.76) and cell lysate was harvested as described in Appendix 7.77.

Appendix 7.305: Assay of charge variants following WCX separation

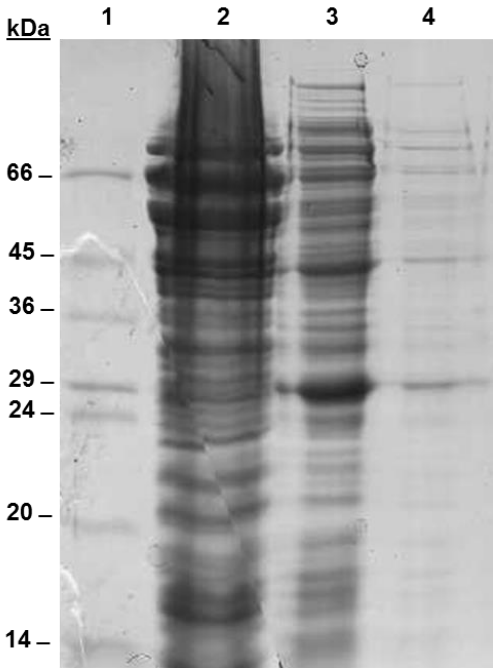
Recombinant lysostaphin (preparation 18) was purified from cell lysate which had been purified by IMAC, as described in Appendix 7.117. Preparation 18 had been expressed in *E. coli* BL21(DE3) cultured in LB (Appendix 7.76) and cell lysate was harvested as described in Appendix 7.77. Following purification selected fractions were desalted and concentrated by ultrafiltration (Appendix 7.120). The purified preparation was assayed for activity, as indicated in Section 4.1.2.7 and subjected to WCX separation.

WCX separation was performed using a 0.5 ml/ min flow rate and a ProPac[®] WCX-10 (4 x 500 mm) column. Purified, concentrated recombinant lysostaphin (300 µg) was applied to the column initially, however higher concentrations of recombinant lysostaphin (2.1 mg) were applied during the second WCX separation. Protein isoforms were separated by applying a linear gradient of 0-50% B over 70 min. The column was then washed using 90% B for 4 min and then the column was equilibrated at 0 % B for 20 min. UV data was acquired at 214 and 280 nm throughout the separation and fractions were collected by time, every 30 s between 20 and 70 min. Following separation, selected fractions were desalted, concentrated and assayed for activity, as described in Appendix 7.369 and Section 4.1.2.7.

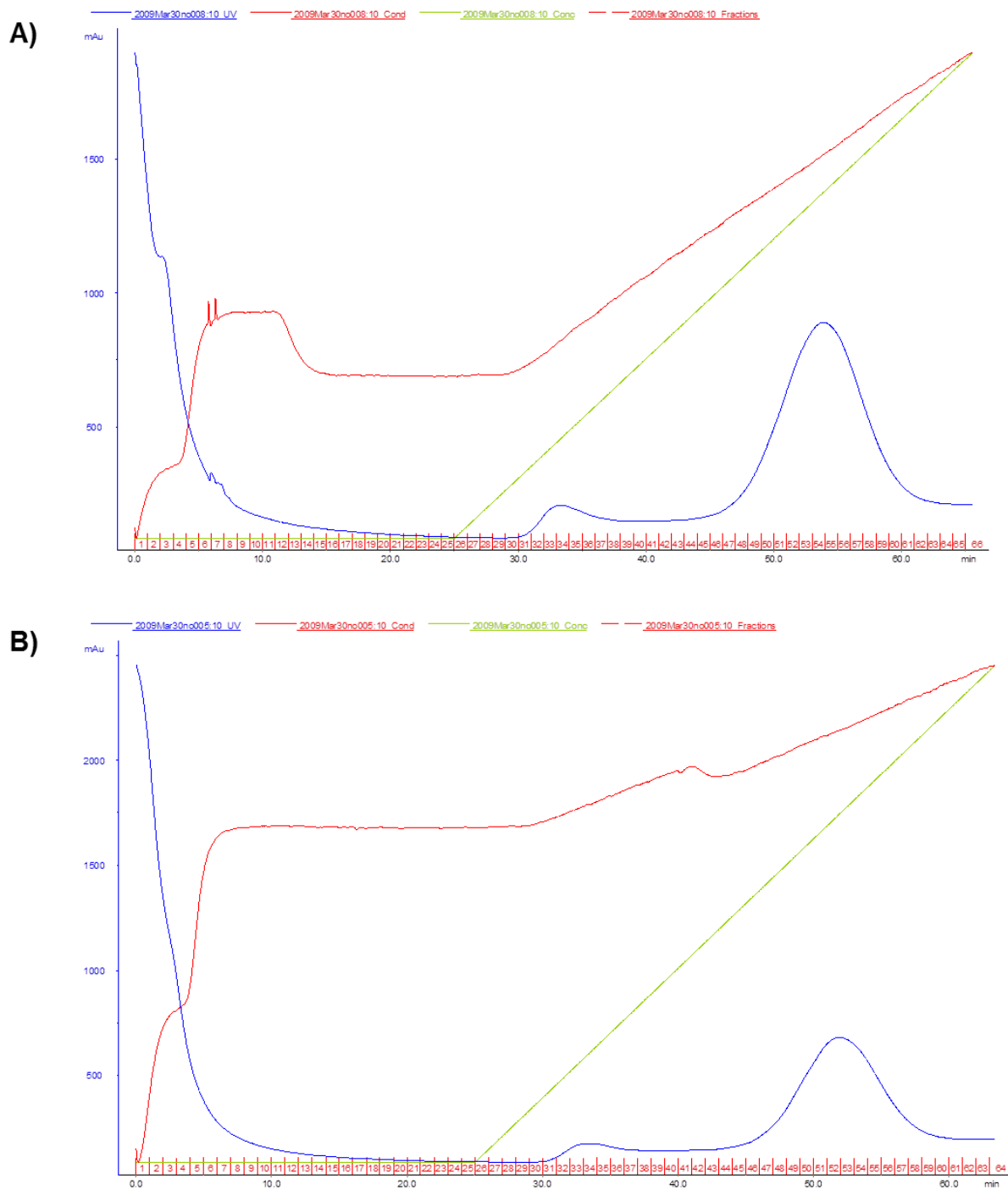
Appendix 7.306: Assay of charge variants following WCX separation during culture analysis

Recombinant lysostaphin was purified from cell lysate which had been harvested during the course of expression. The preparation was produced following expression in *E. coli* BL21(DE3) cultured in LB and cell lysate was harvested as described in Appendix 7.239. The cell lysate was subjected to WCX analysis, as described in Appendix 7.230. Charge variants separated by WCX analysis were then assayed for activity as described in Section 4.1.2.7.

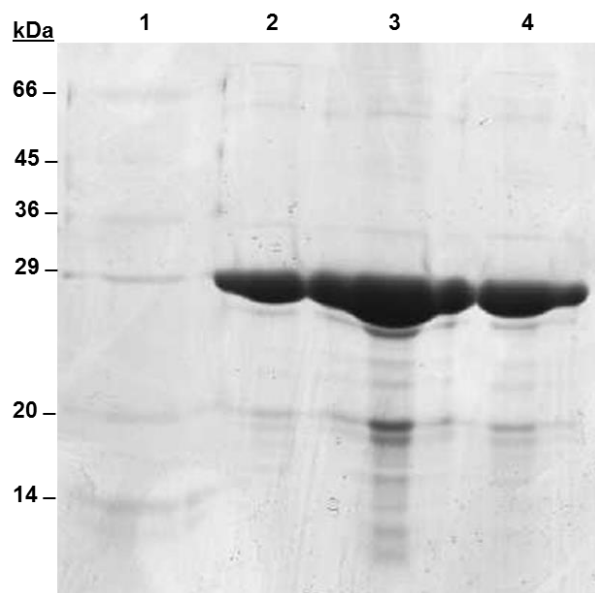
Appendix 7.307: SDS-PAGE analysis of cell lysate containing N-terminally His-tagged recombinant lysostaphin (construct 1, preparation 14) expressed in *E.coli* BL21(DE3) cultured in LB. Lane 1: Sigma low molecular markers; Lane 2: CFE (neat); Lane 3: CFE (1:10); Lane 4: CFE (1:100).



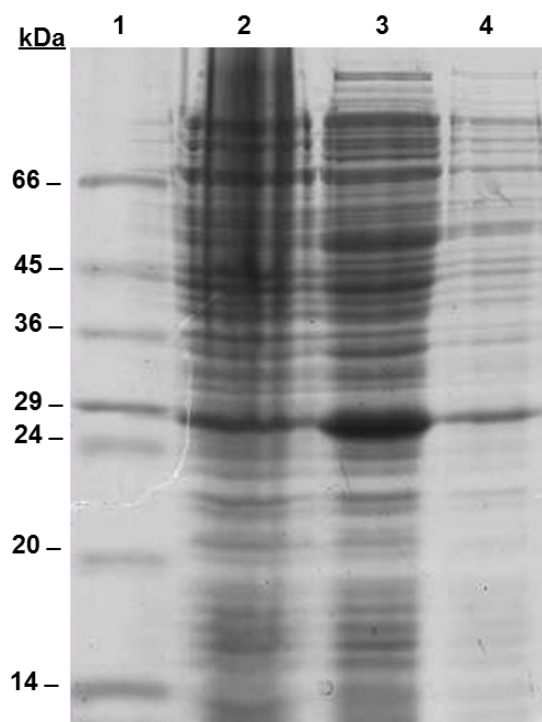
Appendix 7.308: IMAC purification of recombinant lysostaphin (construct 1, preparation 14) using a Chelating Sepharose™ Fast Flow media column and ÄKTA™ prime plus system. Fractions were collected every 60 s throughout the separations. Cell lysate was applied to the column on two consecutive occasions (A and B). Bound protein was eluted by applying an increasing imidazole concentration (20-500 mM). Fractions 48-62 collected during purification A and fractions 49-61 collected during purification B were pooled and concentrated.



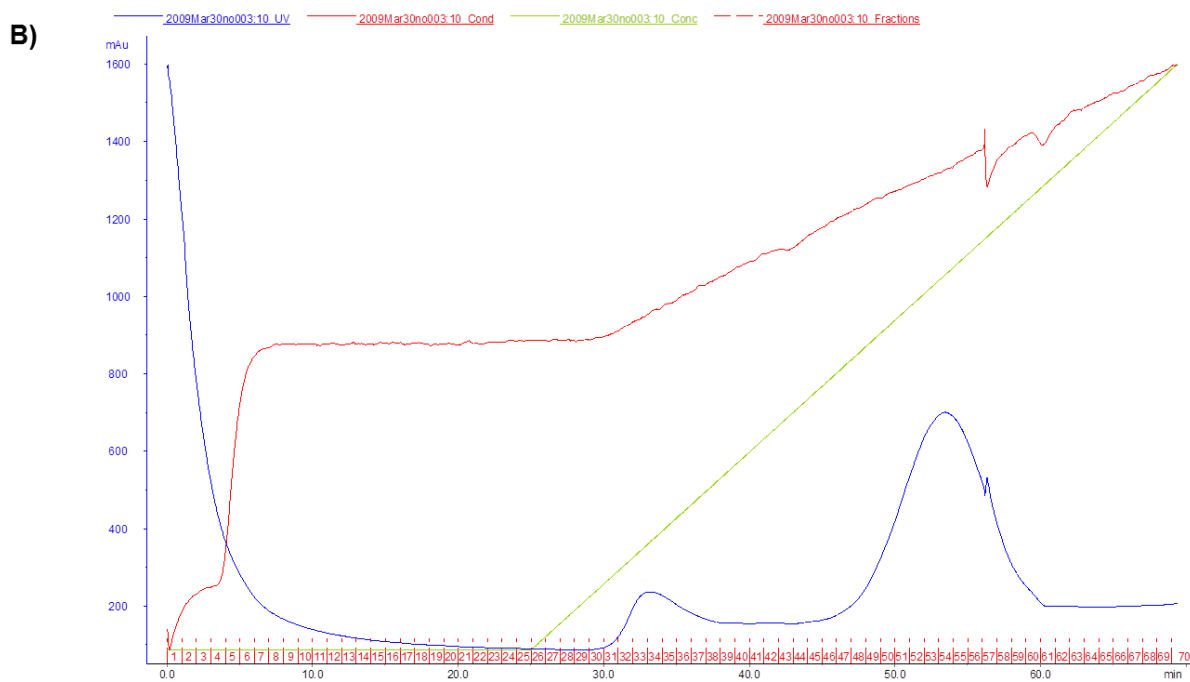
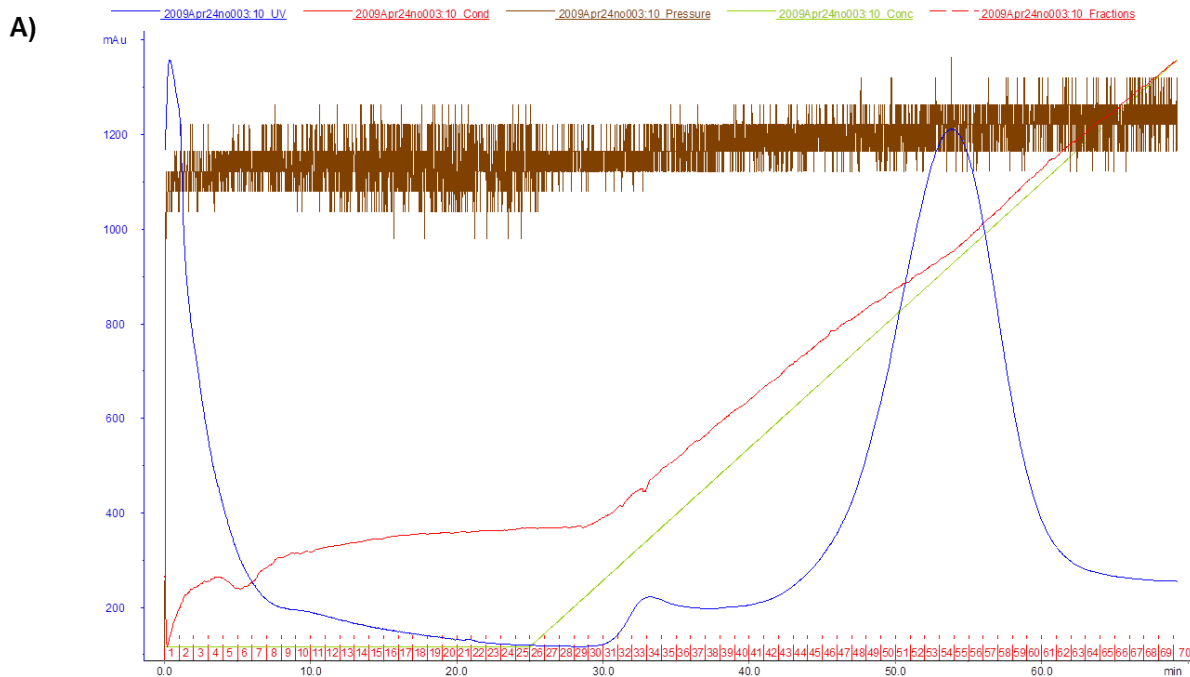
Appendix 7.309: SDS-PAGE analysis of purified, concentrated *N*-terminally His-tagged recombinant lysostaphin (construct 1, preparation 14). Lane 1: Sigma low molecular weight markers; Lane 2: concentrated protein (1:100); Lane 3: concentrated protein (1:10); Lane 4: concentrated protein (1:1000).



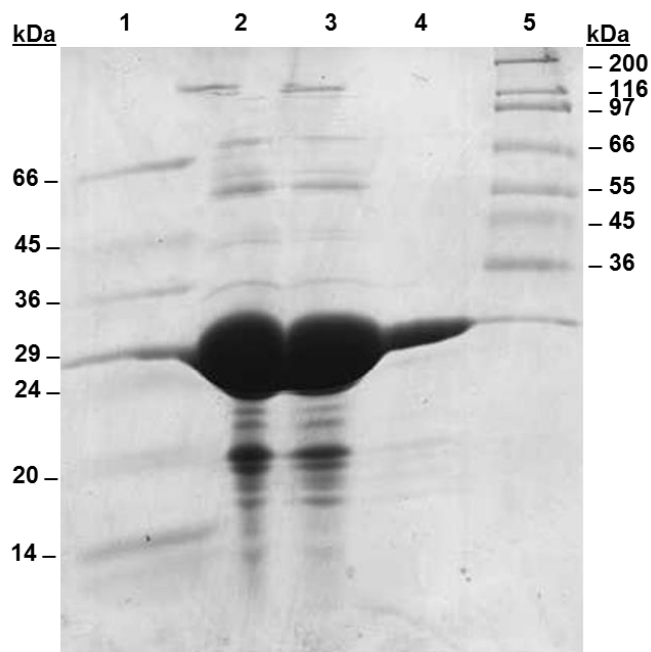
Appendix 7.310: SDS-PAGE analysis of cell lysate containing *N*-terminally His-tagged recombinant lysostaphin (construct 1, preparation 15) expressed in *E.coli* BL21(DE3) cultured in AIM. Lane 1: Sigma low molecular markers; Lane 2: CFE (neat); Lane 3: CFE (1:10); Lane 4: CFE (1:100).



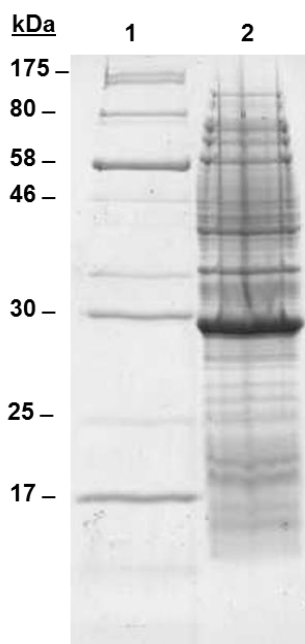
Appendix 7.311: IMAC purification of recombinant lysostaphin (construct 1, preparation 15) using a Chelating Sepharose™ Fast Flow media column and ÄKTA™ prime plus system. Fractions were collected every 60 s throughout the separations. Cell lysate was applied to the column on two consecutive occasions (A and B). Bound protein was eluted by applying an increasing imidazole concentration (20-500 mM). Fractions 43-59 collected during purification A and fractions 49-59 collected during purification B were pooled and concentrated.



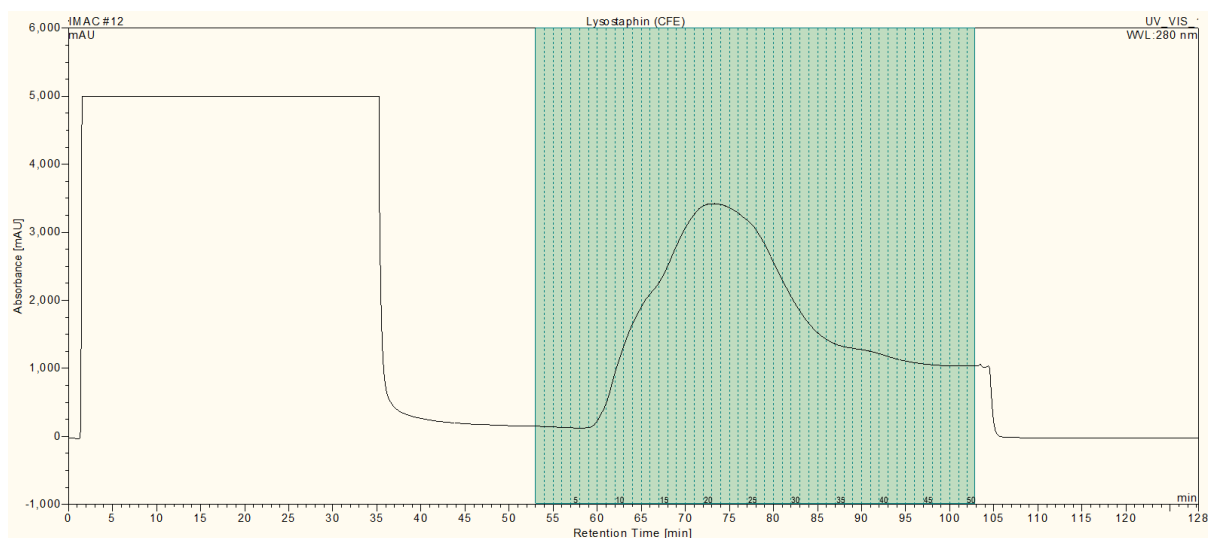
Appendix 7.312: SDS-PAGE analysis of purified, concentrated *N*-terminally His-tagged recombinant lysostaphin (construct 1, preparation 15). Lane 1: Sigma low molecular weight markers; Lane 2: concentrated protein (1:10); Lane 3: concentrated protein (1:100); Lane 4: concentrated protein (1:1000), Lane 5: Sigma high molecular weight markers.



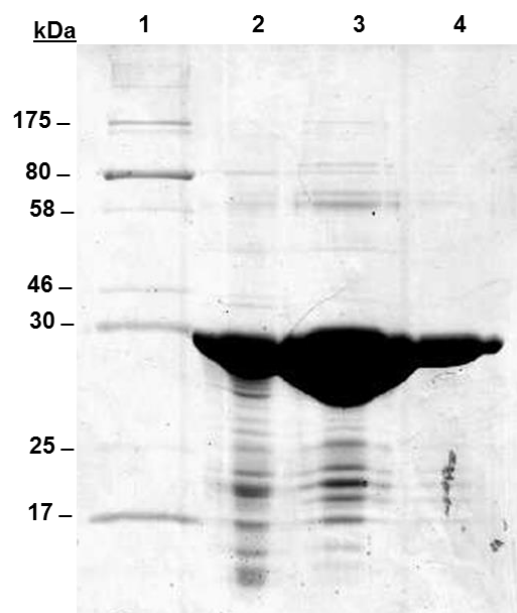
Appendix 7.313: SDS-PAGE analysis of cell lysate containing *N*-terminally His-tagged recombinant lysostaphin (construct 1, preparation 16) expressed in *E.coli* BL21(DE3) cultured in LB. Lane 1: NZY broad-range markers; Lane 2: CFE (1:10).



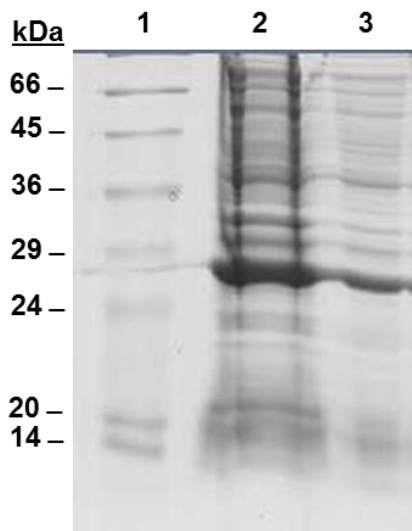
Appendix 7.314: IMAC purification of recombinant lysostaphin (construct 1, preparation 16) using a Chelating Sepharose™ Fast Flow media column and ÄKTA™ prime plus system. Bound protein was eluted by applying an increasing imidazole concentration (20-500 mM). Fractions were collected every 60 s throughout the separation. Fractions 10-34 were pooled and concentrated.



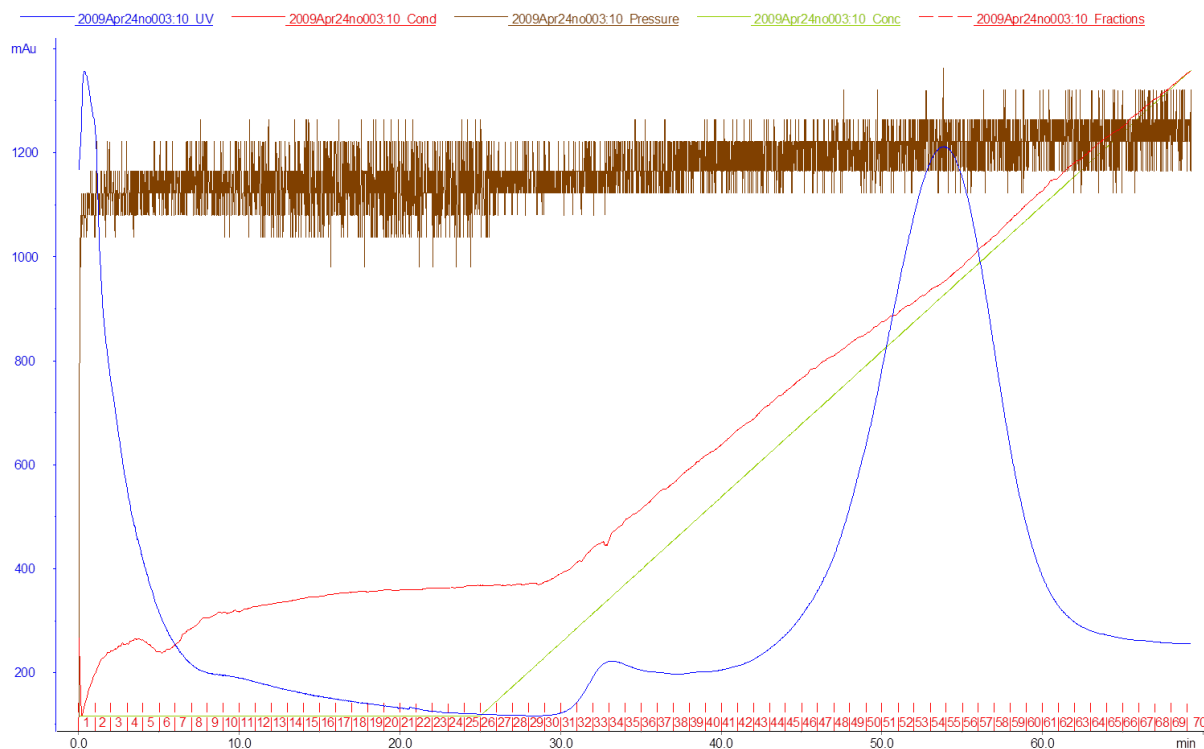
Appendix 7.315: SDS-PAGE analysis of purified, concentrated *N*-terminally His-tagged recombinant lysostaphin (construct 1, Preparation 16). Lane 1: NEB pre-stained broad-range markers; Lane 2: concentrated protein (1:10); Lane 3: concentrated protein (1:100); Lane 4: concentrated protein (1:1000).



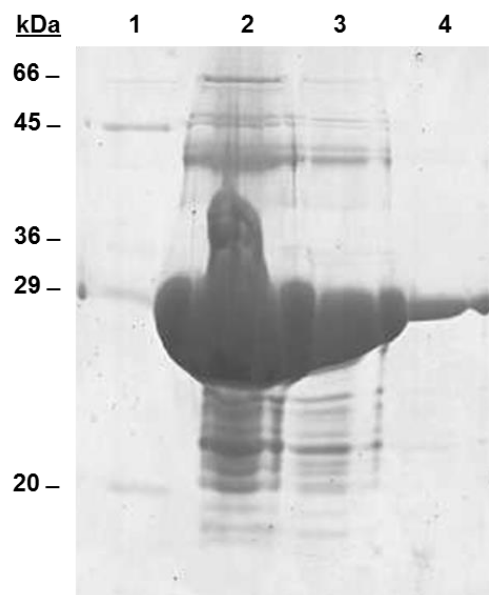
Appendix 7.316: SDS-PAGE analysis of cell lysate containing *N*-terminally His-tagged recombinant lysostaphin (construct 1, preparation 17) expressed in *E.coli* BL21(DE3) cultured in AIM. Lane 1: Sigma low molecular weight markers; Lane 2: CFE (neat); Lane 3: CFE (1:10).



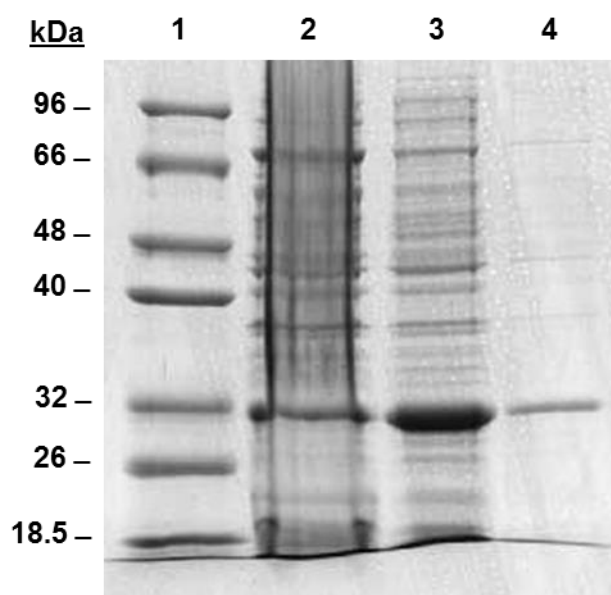
Appendix 7.317: IMAC purification of recombinant lysostaphin (construct 1, preparation 17) using a Chelating Sepharose™ Fast Flow media column and ÄKTA™ prime plus system. Bound protein was eluted by applying an increasing imidazole concentration (20-500 mM). Fractions were collected every 60 s throughout the separation. Fractions 46-63 were pooled and concentrated.



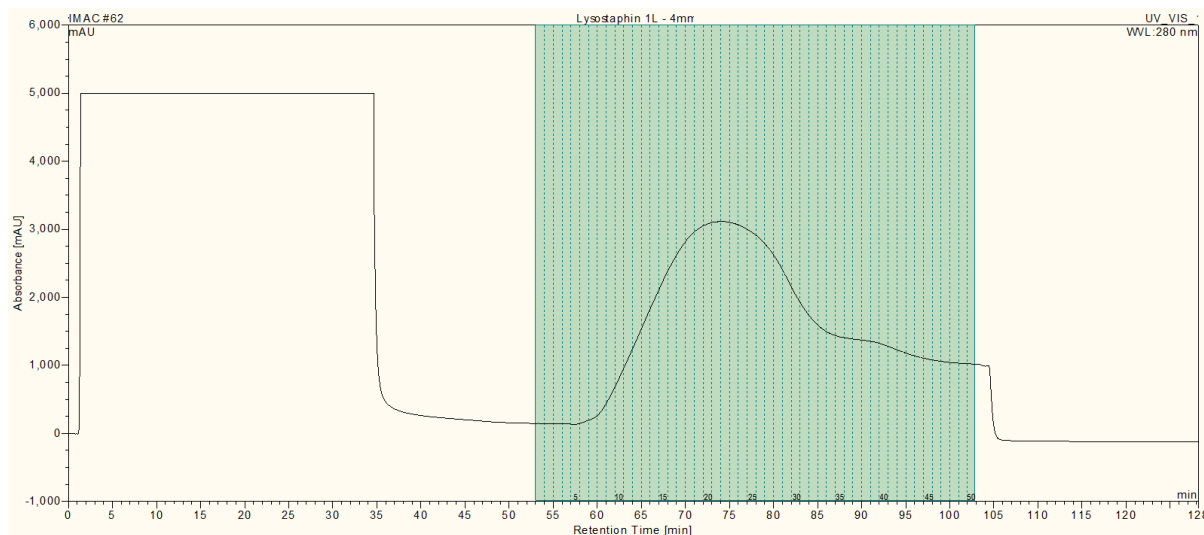
Appendix 7.318: SDS-PAGE analysis of purified, concentrated *N*-terminally His-tagged recombinant lysostaphin (construct 1, Preparation 17). Lane 1: NZY broad-range markers; Lane 2: concentrated protein (1:10); Lane 3: concentrated protein (1:100); Lane 4: concentrated protein (1:1000).



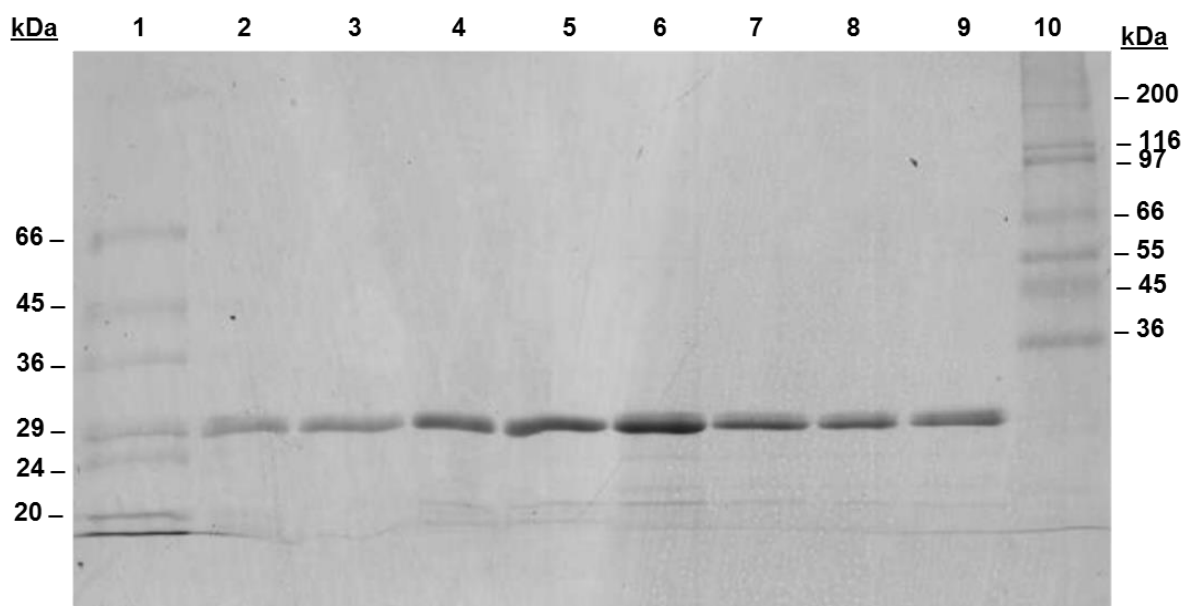
Appendix 7.319: SDS-PAGE analysis of cell lysate containing *N*-terminally His-tagged recombinant lysostaphin (construct 1, preparation 18) expressed in *E.coli* BL21(DE3) cultured in LB. Lane 1: NZY broad range size markers; Lane 2: CFE (neat); Lane 3: CFE (1:10); Lane 4: CFE (1:100).



Appendix 7.320: IMAC purification of recombinant lysostaphin (construct 1, preparation 18) using a ProPac® IMAC-10 column (4.0 x 250 mm) and Ultimate™ 3000 system. Fractions were collected by time between 53 and 103 min and fractions 8, 9, 10, 11, 35, 36, 37 and 38 were analysed by SDS-PAGE.



Appendix 7.321: SDS-PAGE analysis of IMAC fractions following purification of *N*-terminally His-tagged recombinant lysostaphin (construct 1; preparation 18) derived from *E.coli* BL21(DE3) cultured in LB, using the ProPac IMAC-10 (4 x 250 mm) column. Lane 1: Sigma low molecular weight markers; Lane 2: Fraction 8; Lane 3: Fraction 9; Lane 4: Fraction 10; Lane 5: Fraction 11; Lane 6: Fraction 35; Lane 7: Fraction 36; Lane 8: Fraction 37; Lane 9: Fraction 38; Lane 10: Sigma high molecular weight markers.



Appendix 7.322: Amino acid sequence of mature lysostaphin from *Staphylococcus staphylolyticus*

MAATHEHSAQWLNNYKKGYGYPYPLGINGGMHYGVDFFMNIGTPVKAISSGKIVEAGWSNYGG
GNQIGLIENDGVHRQWYMHLKYNVKGVDYVKAGQIIGWSGSTGYSTAPHLHFQRMVNSFSNSTA
QDPMPFLKSAGYGKAGGTVTPTNTGWKTNKYGTLYKSESASFTPNTDII TRTTGPFRRSMPQSGV
LKAGQTIHYDEVKQDGHVWVGYTGNSGQRIYLPVRTWKNKSTNTLGVLVWGTIK

Appendix 7.323: Amino acid sequence of glycyl-glycine endopeptidase LytM from *Staphylococcus aureus* (Q99WV0). Zinc binding domain residues are indicated in red.

MKKLTAAAIATMGFATFTMAHQADAAETTNTQQAHTLMSTQSQDVSYGTYTIDSNGDYHHTPDGNWNQAMF
DNKEYSYTFVDAQGHTHYFYNCYPKNANANGSGQTYVNPATAGDNNDYTASQSQQHINQYGYQSNVGPDAS
YYSHSNNNQAYNSHDGNGKVNYPNGTSNQNGGSASKATASGHAKDASWLTSRKQLQPYGQYHGGGAHYGV
DYAMPENSPVYSLTDGTVVQAGWSNYGGGNQVTIKEANSNNYQWYMHNNRRLTVSAGDKVKAGDQIAYSGST
GNSTAPHVHFQRMSGGIGNQYAVDPTS YLQSR

Appendix 7.324: Spectrophotometric monitoring of the growth of *Staphylococcus aureus* (NCIMB 12703) in liquid culture at 37°C. Bacterial growth in 1 L broth culture was monitored spectrophotometrically for over 23 h.

Time (min)	Absorbance at 600 nm
0	0.000
60	0.088
120	0.065
180	0.123
240	0.262
320	0.723
375	0.804
435	0.834
480	0.710
1390	0.592

Appendix 7.325: Percentage lysis of *S. aureus* cells by N-terminally His-tagged recombinant lysostaphin (construct 1, preparation 4) as determined by turbidometric assay

Lysostaphin (μg)	Lysostaphin concentration ($\mu\text{g/ml}$)	Absorbance at 620 nm		Percentage change in absorbance (%)
		T ₀	T ₁₀	
0	0.0	0.725	0.690	4.83
2	0.4	0.726	0.607	16.39
4	0.8	0.710	0.455	35.92
6	1.2	0.700	0.472	32.57
8	1.6	0.733	0.284	61.26
10	2.0	0.715	0.272	61.96

Appendix 7.326: Percentage lysis of *S. aureus* cells by N-terminally His-tagged recombinant lysostaphin (construct 1, preparation 6) as determined by turbidometric assay

Lysostaphin (μg)	Lysostaphin concentration ($\mu\text{g/ml}$)	Absorbance at 620 nm		Percentage change in absorbance (%)
		T ₀	T ₁₀	
0	0.0	0.314	0.296	5.73
2	0.4	0.322	0.128	60.25
4	0.8	0.327	0.088	73.09
6	1.2	0.331	0.071	78.55
8	1.6	0.335	0.070	79.10
10	2.0	0.328	0.067	79.57

Appendix 7.327: Percentage lysis of *S. aureus* cells by N-terminally His-tagged recombinant lysostaphin (construct 1, preparation 15) as determined by turbidometric assay

Lysostaphin (μg)	Lysostaphin concentration ($\mu\text{g/ml}$)	Absorbance at 620 nm		Percentage change in absorbance (%)
		T ₀	T ₁₀	
0	0.0	0.417	0.389	6.71
2	0.4	0.423	0.354	16.31
4	0.8	0.427	0.285	33.26
6	1.2	0.440	0.246	44.09
8	1.6	0.427	0.208	51.29
10	2.0	0.420	0.192	54.29

Appendix 7.328: Percentage lysis of *S. aureus* cells by N-terminally His-tagged recombinant lysostaphin (construct 1, preparation 17) as determined by turbidometric assay

Lysostaphin (μg)	Lysostaphin concentration ($\mu\text{g/ml}$)	Absorbance at 620 nm		Percentage change in absorbance (%)
		T ₀	T ₁₀	
0	0.0	0.361	0.311	13.85
2	0.4	0.370	0.281	24.05
4	0.8	0.356	0.225	36.80
6	1.2	0.343	0.205	40.23
8	1.6	0.357	0.179	49.86
10	2.0	0.359	0.173	51.81

Appendix 7.329: Percentage lysis of *S. aureus* cells by N-terminally His-tagged recombinant lysostaphin (construct 1, preparation 14) as determined by turbidometric assay

Lysostaphin (μg)	Lysostaphin concentration ($\mu\text{g/ml}$)	Absorbance at 620 nm		Percentage change in absorbance (%)
		T ₀	T ₁₀	
0	0.0	0.477	0.404	15.30
2	0.4	0.440	0.303	31.14
4	0.8	0.455	0.251	44.84
6	1.2	0.453	0.230	49.23
8	1.6	0.430	0.197	54.19
10	2.0	0.458	0.193	57.86

Appendix 7.330: Percentage lysis of *S. aureus* cells by N-terminally His-tagged recombinant lysostaphin (construct 1, preparation 16) as determined by turbidometric assay

Lysostaphin (μg)	Lysostaphin concentration ($\mu\text{g/ml}$)	Absorbance at 620 nm		Percentage change in absorbance (%)
		T ₀	T ₁₀	
0	0.0	0.363	0.351	3.31
2	0.4	0.357	0.275	22.97
4	0.8	0.347	0.238	31.41
6	1.2	0.322	0.212	34.16
8	1.6	0.355	0.197	44.51
10	2.0	0.358	0.176	50.84

Appendix 7.331: Percentage lysis of *S. aureus* cells by C-terminally His-tagged recombinant lysostaphin (construct 4, preparation 1) as determined by turbidometric assay

Lysostaphin (μg)	Lysostaphin concentration ($\mu\text{g/ml}$)	Absorbance at 620 nm		Percentage change in absorbance (%)
		T ₀	T ₁₀	
0	0.0	0.480	0.451	6.04
2	0.4	0.468	0.075	85.04
4	0.8	0.465	0.060	87.10
6	1.2	0.464	0.052	88.79
8	1.6	0.472	0.046	90.25
10	2.0	0.456	0.037	91.89

Appendix 7.332: Percentage lysis of *S. aureus* cells by C-terminally His-tagged recombinant lysostaphin (construct 3, preparation 3) as determined by turbidometric assay

Lysostaphin (μg)	Lysostaphin concentration ($\mu\text{g/ml}$)	Absorbance at 620 nm		Percentage change in absorbance (%)
		T ₀	T ₁₀	
0	0.0	0.855	0.810	5.26
2	0.4	0.832	0.339	59.25
4	0.8	0.825	0.205	75.15
6	1.2	0.816	0.193	76.15
8	1.6	0.816	0.193	78.51

Appendix 7.333: Percentage lysis of *S. aureus* cells by C-terminally His-tagged recombinant lysostaphin (construct 3, preparation 2) as determined by turbidometric assay

Lysostaphin (μg)	Lysostaphin concentration ($\mu\text{g/ml}$)	Absorbance at 620 nm		Percentage change in absorbance (%)
		T ₀	T ₁₀	
0	0.0	0.332	0.299	9.94
2	0.4	0.353	0.213	39.66
4	0.8	0.361	0.152	57.89
6	1.2	0.347	0.117	66.28
8	1.6	0.342	0.064	81.29
10	2.0	0.347	0.054	84.44

Appendix 7.334: Percentage lysis of *S. aureus* cells by N-terminally His-tagged recombinant lysostaphin (construct 1, preparation 10) as determined by turbidometric assay

Lysostaphin (μg)	Lysostaphin concentration ($\mu\text{g/ml}$)	Absorbance at 620 nm		Percentage change in absorbance (%)
		T ₀	T ₁₀	
0	0.0	0.298	0.270	9.40
2	0.4	0.337	0.225	33.23
4	0.8	0.336	0.171	49.11
6	1.2	0.330	0.149	54.85
8	1.6	0.310	0.123	60.32
10	2.0	0.335	0.110	67.16

Appendix 7.335: Percentage lysis of *S. aureus* cells by *N*-terminally His-tagged recombinant lysostaphin (construct 1, preparation 18) as determined by turbidometric assay.

Lysostaphin (μg)	Lysostaphin concentration ($\mu\text{g}/\text{ml}$)	Absorbance at 620 nm		Percentage change in absorbance (%)
		T ₀	T ₁₀	
0	0.0	0.401	0.377	5.99
2	0.4	0.366	0.250	31.69
4	0.8	0.380	0.126	66.84
6	1.2	0.343	0.129	62.39
8	1.6	0.360	0.093	74.17
10	2.0	0.396	0.102	74.24

Appendix 7.336: Percentage lysis of *S. aureus* cells by recombinant lysostaphin (fraction 21) following WCX separation. Values determined by turbidometric assay.

Lysostaphin (μg)	Lysostaphin concentration ($\mu\text{g}/\text{ml}$)	Absorbance at 620 nm		Percentage change in absorbance (%)
		T ₀	T ₁₀	
0	0.0	0.401	0.377	5.99
2	0.4	0.352	0.155	55.97

Appendix 7.337: Percentage lysis of *S. aureus* cells by recombinant lysostaphin (fraction 29) following WCX separation. Values determined by turbidometric assay.

Lysostaphin (μg)	Lysostaphin concentration ($\mu\text{g}/\text{ml}$)	Absorbance at 620 nm		Percentage change in absorbance (%)
		T ₀	T ₁₀	
0	0.0	0.401	0.377	5.99
2	0.4	0.339	0.154	54.57
4	0.8	0.354	0.105	70.34

Appendix 7.338: Percentage lysis of *S. aureus* cells by recombinant lysostaphin (fraction 19) following WCX separation. Values determined by turbidometric assay.

Lysostaphin (μg)	Lysostaphin concentration ($\mu\text{g/ml}$)	Absorbance at 620 nm		Percentage change in absorbance (%)
		T ₀	T ₁₀	
0	0.0	0.374	0.349	6.68
2	0.4	0.373	0.143	61.66
4	0.8	0.387	0.106	72.61
6	1.2	0.376	0.083	77.93
8	1.6	0.367	0.073	80.11
10	2.0	0.368	0.069	81.25

Appendix 7.339: Percentage lysis of *S. aureus* cells by recombinant lysostaphin (fraction 26) following WCX separation. Values determined by turbidometric assay.

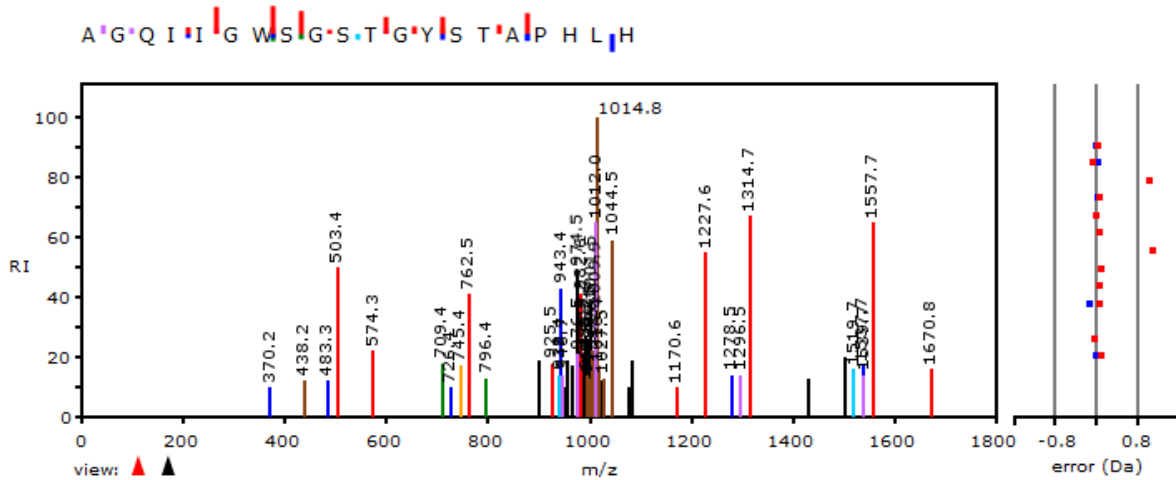
Lysostaphin (μg)	Lysostaphin concentration ($\mu\text{g/ml}$)	Absorbance at 620 nm		Percentage change in absorbance (%)
		T ₀	T ₁₀	
0	0.0	0.306	0.285	6.86
2	0.4	0.316	0.163	48.42
4	0.8	0.313	0.080	74.44
6	1.2	0.298	0.063	78.86
8	1.6	0.294	0.054	80.61
10	2.0	0.316	0.060	81.01

Appendix 7.340: Percentage lysis of *S. aureus* cells by recombinant lysostaphin (fraction 8) following WCX separation. Values determined by turbidometric assay.

Lysostaphin (µg)	Lysostaphin concentration (µg/ml)	Absorbance at 620 nm		Percentage change in absorbance (%)
		T ₀	T ₁₀	
0	0.0	0.306	0.285	6.86
2	0.4	0.316	0.163	48.42
4	0.8	0.313	0.080	74.44
6	1.2	0.298	0.063	78.86
8	1.6	0.294	0.054	80.61
10	2.0	0.316	0.060	81.01

Appendix 7.341: Evidence of elastolytic activity following LC-MS/MS analysis of tryptically digested *N*-terminally His-tagged recombinant lysostaphin (construct 1). Although the specificity of elastolytic activity is not known, elastolytic enzymes are known to catalyse the cleavage of peptide bonds associated with hydrophobic amino acids, such as alanine or aromatic amino acids, such as histidine. Acquired LC-MS/MS spectra were submitted to X!Tandem open source software. Associated data not shown.

3 - F36 - 1 in 3 d11 -40 K-SE_RE5_01_2786.2911.2911.2



7.3.2 IMAC analysis of recombinant lysostaphin

Appendix 7.342: Buffers

IMAC buffer A (1 L) (as described in Section 2.5.2.1/ Appendix 7.105)

IMAC buffer B (1L) (as described in Section 2.5.2.1/ Appendix 7.105)

WCX buffer A (1L) (as described in Section 3.2.1/ Appendix 7.136)

WCX buffer B (1L) (as described in Section 3.2.1/ Appendix 7.136)

Appendix 7.343: Equipment

IMAC purifications and WCX separations achieved using the ProPac[®] WCX-10 (4.0 x 500 mm) column were performed using an Ultimate[™] 3000 Titanium system, which consisted of an analytical titanium pump, a thermal compartment with two column change valves, a VWD detector and a WPS-3000 biocompatible autosampler. The thermal compartment was maintained at 30°C and the autosampler was fitted with a 250 µl syringe and a 1 ml injection loop. The system was fitted with a PEEK fluidic pathway. Small samples volumes were loaded onto the system via automated injection, whilst larger sample volumes were pumped into the system via buffer line C. Although the autosampler could accommodate fractionation, fractionation was performed using an ISCO Foxy[®] Jr Fraction collector in this instance. Data collection and analysis was performed using Chromeleon[®] Chromatography Data System software with fractionation license.

WCX separations using the ProPac[®] WCX-10 (2 x 500 mm) column were performed with an Ultimate[™] 3000 Titanium system which consisted of an analytical titanium pump, a thermal compartment with two column change valves, a VWD detector and a WPS-3000 biocompatible autosampler. The system was fitted with a PEEK fluidic pathway and the autosampler was fitted with a 250 µl syringe and a 500 µl injection loop. Fractionation was achieved using the WPS-3000 biocompatible autosampler, which was temperature regulated to 10°C. Data collection and analysis was performed using Chromeleon[®] Chromatography Data System software with fractionation license.

Chromatographic separations were performed using a number of analytical columns, as described in Appendix 7.344.

Appendix 7.344: Analytical columns and mobile phase compositions used whilst investigating the retention behaviour of recombinant lysostaphin

Column	Chromatographic mode	Dimensions (mm)	Mobile phase conditions
ProPac® IMAC-10	IMAC	4.0 x 250	IMAC buffer A and B
ProPac® WCX-10	WCX	2.0 x 500	IEX buffer A and B
ProPac® WCX-10	WCX	4.0 x 500	IEX buffer A and B

Appendix 7.345: Sample preparation

Experiments were performed using freshly harvested cell lysate. Cell lysates were harvested from *E. coli* BL21(DE3) which was transformed with a plasmid encoding *N*-terminally His-tagged recombinant lysostaphin (construct 1), recombinant lysostaphin (construct 2) or *C*-terminally His-tagged recombinant lysostaphin (construct 3). Recombinant protein expression was performed as described in Appendix 7.76. All cultures were grown in LB media.

IMAC purification was performed using freshly harvested cell lysate, which was prepared as described in Appendix 7.77. IMAC purification of *N*-terminally His-tagged recombinant lysostaphin (construct 1) and *C*-terminally His-tagged recombinant lysostaphin (construct 3) was performed on cell lysate harvested from 1 L of culture. IMAC purification of recombinant lysostaphin (construct 2) was performed on cell lysate harvested from 1 L of culture initially, before harvesting from 5 L of culture prior to the subsequent purification. During harvesting of cell lysate, sample volumes were kept as concentrated as possible, and diluted to a minimum volume of 33 ml using IMAC buffer A, prior to IMAC purification.

WCX separation of recombinant lysostaphin constructs was performed using freshly harvested cell lysate, which had been prepared as described in Appendix 7.77. WCX analysis was performed upon 500 µl of cell lysate which was harvested from 100 ml of culture.

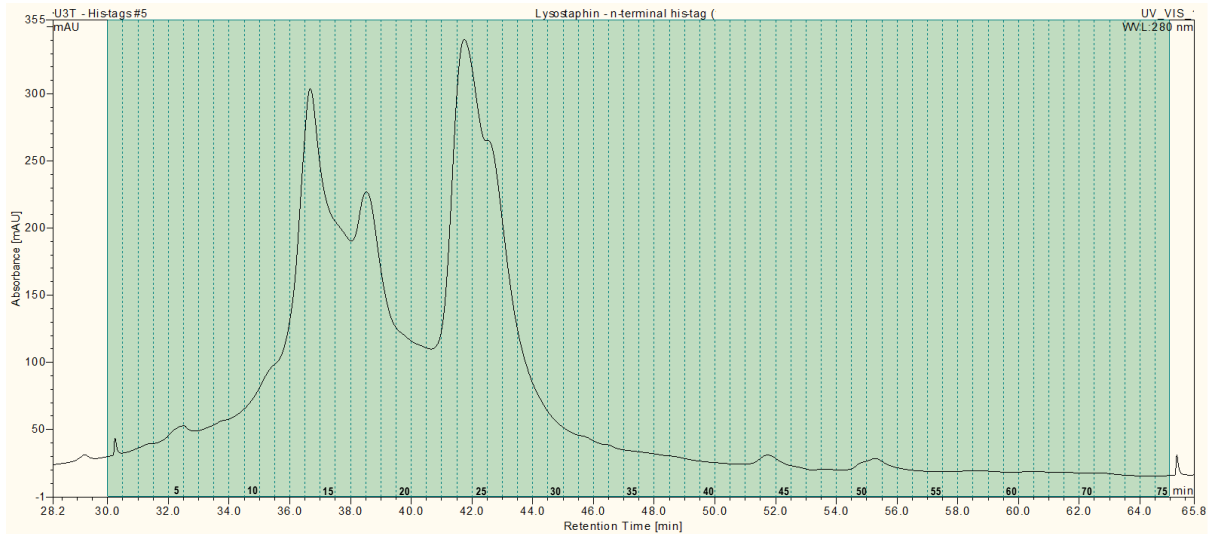
Appendix 7.346: IMAC purification

IMAC purification was performed using a ProPac[®] IMAC-10 (4.0 x 250 mm) column. Prior to purification, the ProPac[®] IMAC-10 column was stripped and charged through manual injection of 500 µl of EDTA and 1000 µl of NiSO₄. Cell lysate (33 ml) was loaded onto the column (via buffer line C) at a flow rate of 1.0 ml/min. Following application of the cell lysate, the gradient remained isocratic by applying 0% B to the column for 20 min at a flow rate of 1.0 ml/min, to remove non-binding proteins and cellular contaminants. The target protein was eluted by applying a linear gradient from 0-100% B over 50 min at 0.5 ml/min. The column was re-equilibrated for 25 min with 0% B at a flow rate of 1.0 ml/min. UV absorbance was recorded at 214 and 280 nm throughout the purification. The column eluate was collected as fractions in 0.25 ml volumes and stored at 4°C until required for subsequent analysis. Fractions thought to contain the target protein were analysed by SDS-PAGE (Appendix 7.15).

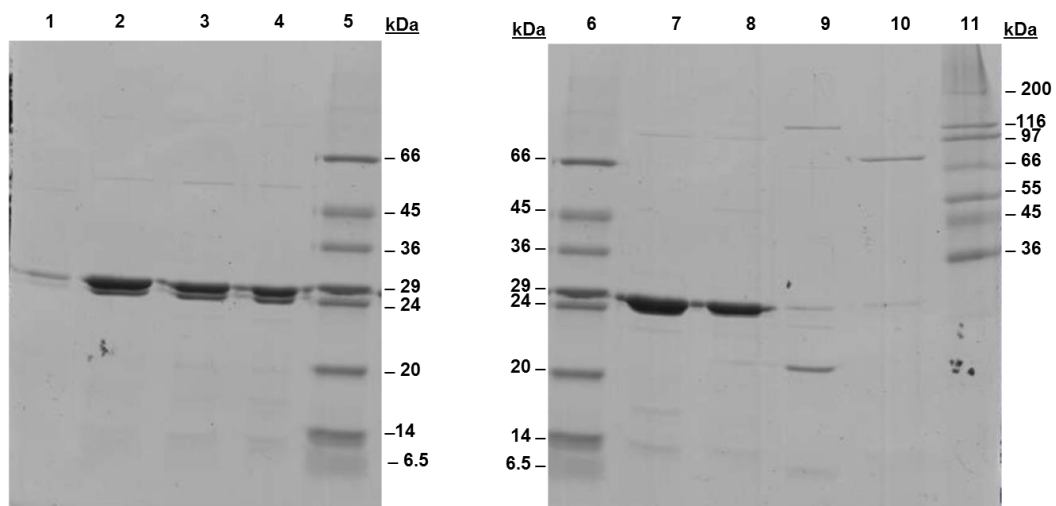
Appendix 7.347: Concentration of IMAC fractions for analysis

Following IMAC purification, selected fractions were either concentrated and desalted using Vivaspin 20 ml ultrafiltration columns with a 10 kDa membrane (Appendix 7.120) or Vivaspin 500 µl columns with 10 kDa membrane. The Vivaspin 500 µl column was placed into a filtrate container and the concentrator column was filled up to the maximum volume of 500 µl with IMAC fraction eluent. The spin column was centrifuged at 14,000 x g until the desired volume of sample had been achieved. The filtrate container was emptied and the concentrator was re-filled with 500 µl of 18.2 MΩ/cm H₂O and centrifuged at 14,000 x g until the volume had reduced to ~50 µl. This washing and desalting process was performed twice more before transferring the concentrated desalted sample from the concentrator column to a sterile microtube ready for subsequent analysis.

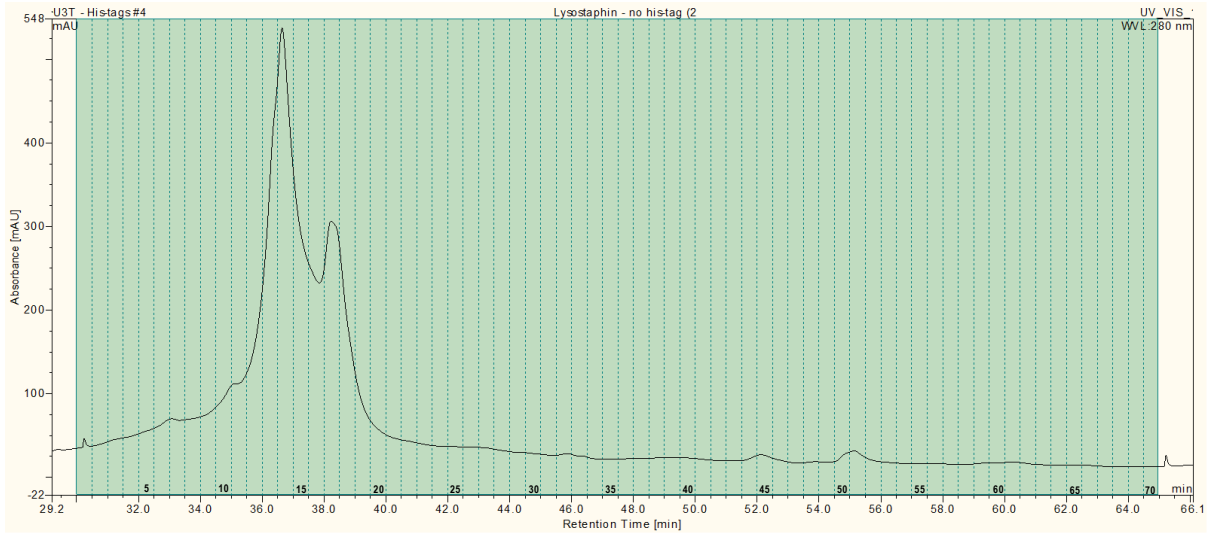
Appendix 7.348: WCX separation of *N*-terminally His-tagged recombinant lysostaphin (construct 1) using ProPac® WCX (2 x 500.0 mm). Fractions 5, 14, 17, 18, 24, 26, 44 and 51 were selected for PAGE analysis.



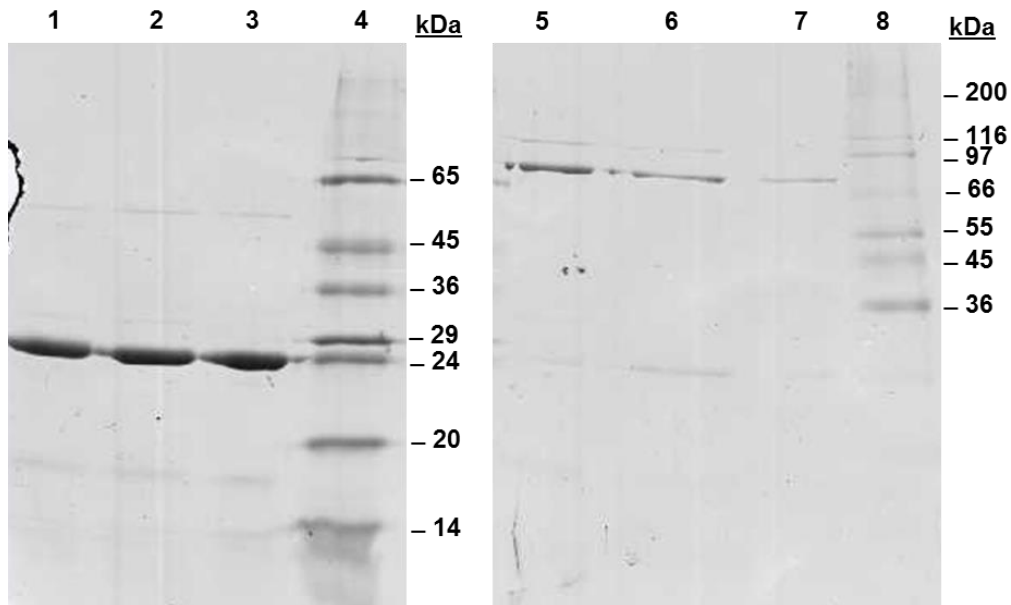
Appendix 7.349: SDS-PAGE analysis of fractions eluted during separation of *N*-terminally His-tagged recombinant lysostaphin (construct 1) using ProPac WCX column (2 x 500.0 mm). Lane 1: Fraction 5; Lane 2: Fraction 14; Lane 3: Fraction 17; Lane 4: Fraction 18; Lane 5: Sigma low molecular weight markers; Lane 6: Sigma low molecular weight markers; Lane 7: Fraction 24; Lane 8: Fraction 26; Lane 9: Fraction 44; Lane 10: Fraction 51; Lane 11: Sigma high molecular weight markers.



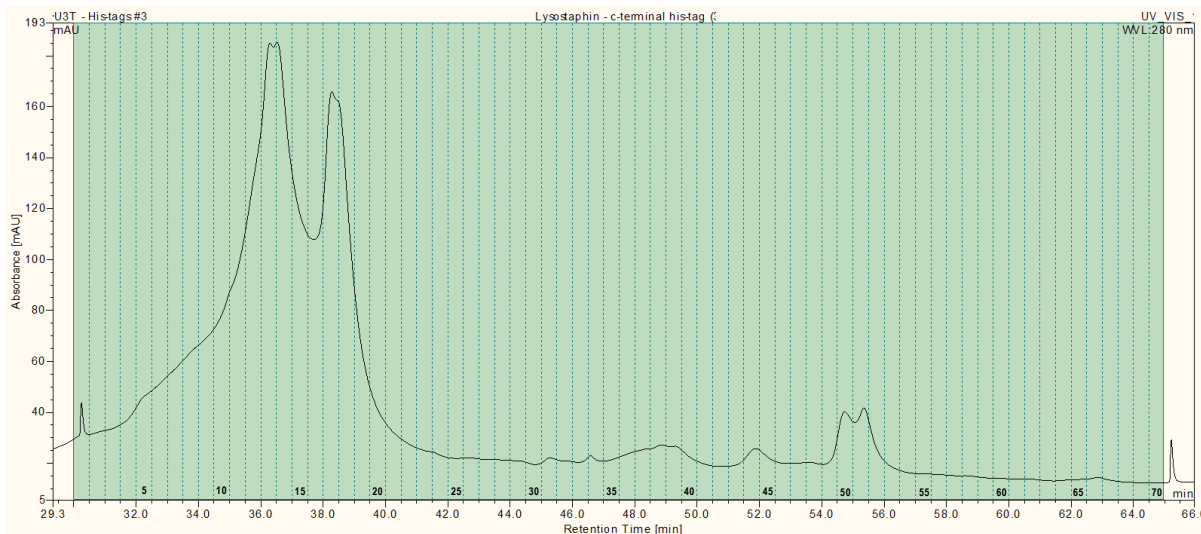
Appendix 7.350: WCX separation of recombinant lysostaphin (construct 2) using ProPac® WCX column (2 x 500.0 mm). Fractions 12, 13, 17, 45, 50 and 51 were selected for PAGE analysis.



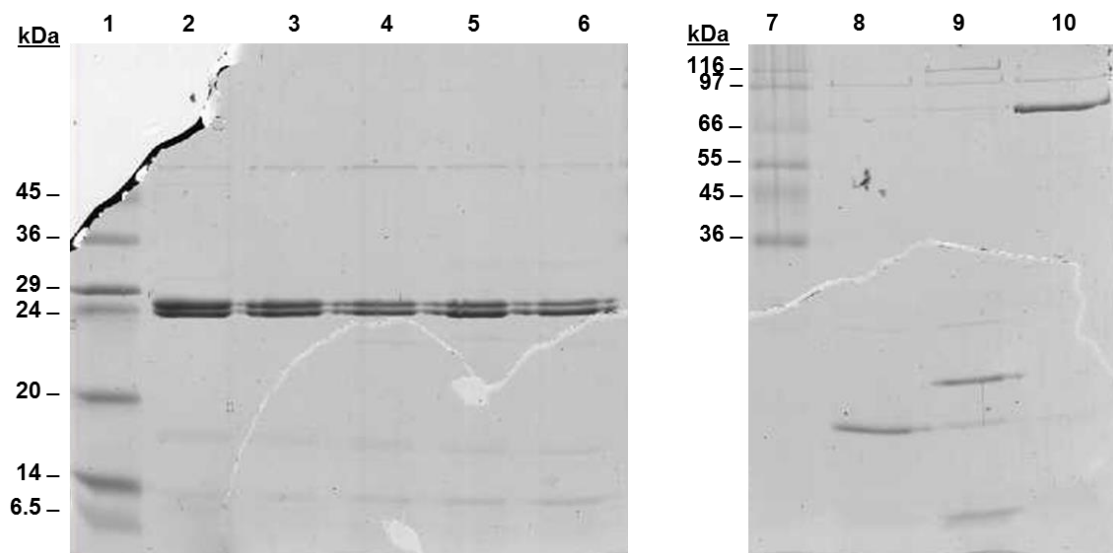
Appendix 7.351: SDS-PAGE analysis of fractions eluted during separation of recombinant lysostaphin (construct 2) using a ProPac® WCX column (2 x 500.0 mm). Lane 1: Fraction 12; Lane 2: Fraction 13; Lane 3: Fraction 17; Lane 4: Sigma low molecular weight markers; Lane 5: Fraction 45; Lane 6: Fraction 50; Lane 7: Fraction 51; Lane 8: Sigma high molecular weight markers.



Appendix 7.352: WCX separation of C-terminally His-tagged recombinant lysostaphin (construct 3) using ProPac® WCX column (2 x 500.0 mm). Fractions 13, 14, 15, 17, 18, 39, 44 and 51 were selected for PAGE analysis.



Appendix 7.353: SDS-PAGE analysis of fractions eluted during separation of C-terminally His-tagged recombinant lysostaphin (construct 3) using a ProPac® WCX column (2 x 500.0 mm). Lane 1: Sigma low molecular weight markers; Lane 2: Fraction 13; Lane 3: Fraction 14; Lane 4: Fraction 15; Lane 5: Fraction 17; Lane 6: Fraction 18; Lane 7: Sigma high molecular weight markers; Lane 8: Fraction 39; Lane 9: Fraction 44; Lane 10: Fraction 51.



7.3.3 GF Analysis of recombinant lysostaphin

Appendix 7.354: Buffers

IMAC buffer A (1 L) (as described in Section 2.5.2.1/ Appendix 7.105)

IMAC buffer B (1L) (as described in Section 2.5.2.1/ Appendix 7.105)

GF Buffer (1 L)

NaH₂PO₄·H₂O (200 mM) 27.6 g

Na₂HPO₄·H₂O (200 mM) 28.4 g

NaH₂PO₄·H₂O and Na₂HPO₄·H₂O were dissolved in 18.2 MΩ/cm H₂O to create two separate solutions. Appropriate volumes of each solution were combined to provide a sodium phosphate buffer with correct pH. If required, the pH of the buffer was adjusted to pH 8.0 using NaOH. The stock solution was autoclaved prior to use.

IMAC denaturing buffer A (1 L)

Sodium phosphate (20 mM) 100 ml of 200 mM stock solution

Imidazole (10 mM) 0.68 g

NaCl (500 mM) 29.20 g

Urea (500 mM) 30.03 g

Sodium phosphate stock solution was diluted with an appropriate volume of 18.2 Ω/cm H₂O, to account for volumetric displacement following dissolution of imidazole, NaCl, and urea. The pH of the buffer was adjusted to pH 7.4 using NaOH or HCl. The buffer was autoclaved prior to use.

IMAC denaturing buffer B (1L)

Sodium phosphate (20 mM) 100 ml of 200 mM stock solution

Imidazole (500 mM) 34.04 g

NaCl (500 mM) 29.20 g

Urea (500 mM) 30.03 g

Sodium phosphate stock solution was diluted with an appropriate volume of 18.2 Ω /cm H₂O, to account for volumetric displacement following dissolution of imidazole, NaCl, and urea. The pH of the buffer was adjusted to pH 7.4 using NaOH or HCl. The buffer was autoclaved prior to use.

IEX buffer A (1L) (as described in Section 3.2.1/ Appendix 7.136)

IEX buffer B (1L) (as described in Section 3.2.1/ Appendix 7.136)

SCX buffer A (1L) (as described in Section 3.2.1/ Appendix 7.136)

SCX buffer B (1L) (as described in Section 3.2.1/ Appendix 7.136)

Appendix 7.355: Equipment

Chromatographic separations were performed using an Ultimate™ 3000 Titanium system consisting of an analytical titanium pump, a thermal compartment with two column change valves, a VWD detector and a WPS-3000 Biocompatible autosampler. The system was fitted with a PEEK fluidic pathway and the autosampler was fitted with a 250 μ l syringe and a 1 ml injection loop. Although the autosampler could accommodate fractionation, fractionation was performed using an ISCO Foxy® Jr Fraction collector in this instance. Data collection and analysis was performed using Chromeleon® Chromatography Data System software with fractionation license.

Chromatographic separations were performed using a number of analytical columns, as described in Appendix 7.356.

Appendix 7.356: Analytical columns and mobile phase compositions used whilst investigating the stability of recombinant lysostaphin

Column	Chromatographic mode	Dimensions (mm)	Mobile phase conditions
ProPac [®] IMAC-10	IMAC	4.0 x 250	IMAC buffer A and B <u>or</u> IMAC denaturing buffer A and B
Zorbax [®] GF-250	GF	4.6 x 250	GF buffer
ProPac [®] WCX-10	WCX	2.0 x 500	IEX buffer A and B
ProPac [®] MAb SCX	SCX	4.0 x 500	SCX Buffer A and B

Appendix 7.357: Sample preparation

Experiments were performed using either purified, concentrated recombinant lysostaphin samples, freshly harvested cell lysate or purified, lyophilised recombinant lysostaphin.

Purified, concentrated recombinant lysostaphin was harvested from *E.coli* BL21(DE3) cultured in either LB or AIM and purified using either IMAC or HIC and GF. Following purification, the purified protein was concentrated using ultrafiltration. Further details about preparation of recombinant lysostaphin are provided in Appendix 7.358.

Lyophilised recombinant lysostaphin was prepared following expression of *N*-terminally His-tagged recombinant lysostaphin (construct 1) with 15 x 1 L batches of AIM (Appendix 7.75). Cell lysate was harvested according to methods described in (Appendix 7.77) and large-scale IMAC purification was performed as described in Appendix 7.115. Following purification, the resulting recombinant lysostaphin was dialysed and lyophilised (Appendix 7.118 and Appendix 7.119).

Freshly harvested lysate for IMAC purification was harvested as described in Appendix 7.77, whilst cell lysate used during WCX separation was harvested as described in Appendix 7.239. All freshly harvested cell lysates were harvested from *E. coli* BL21(DE3) transformed with recombinant pET-28a for expression of *N*-terminally His-tagged recombinant lysostaphin (construct 1) following culture in LB.

Appendix 7.358: Purified recombinant lysostaphin preparations

Preparation ID	Construct	Expression media	Mode of purification	Protein concentration ($\mu\text{g}/\mu\text{l}$)	Related results
3	3	AIM	HIC, GF	1.46	Appendix 7.142 Figure 2.17 Figure 2.18 Figure 2.19 Figure 2.20 Figure 2.21
4	3	AIM	IMAC	37.80	Appendix 7.143 Appendix 7.144 Appendix 7.145
6	1	AIM	IMAC	157.85	Appendix 7.147 Appendix 7.148 Appendix 7.149
13	3	AIM	IMAC/GF	19.08	Appendix 7.167 Figure 2.26 Figure 2.27 Figure 2.28 Figure 2.29
19	1	AIM	IMAC	Not determined	Appendix 7.362 Appendix 7.131 Appendix 7.132

Appendix 7.359: GF of fractions eluted following IMAC purification

IMAC purification was performed on cell lysate containing *N*-terminally His-tagged recombinant lysostaphin (construct 1). IMAC separation was performed as described in Appendix 7.117, however due to over-pressure during sample loading, the separation was interrupted at 20 min and the separation was recommenced without sample loading. Fractions were subsequently collected between 23 and 73 minutes and one of the fractions was selected for GF separation.

GF separation was performed using a 0.25 ml/min flow rate and an isocratic gradient over 16 min. Manual injection of 250 μl of IMAC fraction 13 was delivered to the system and UV data was acquired at 214 and 280 nm throughout the separation. Fractions were collected

using a Foxy[®] Jr fraction collector between 6 and 15 min. Selected fractions were then analysed by SDS-PAGE.

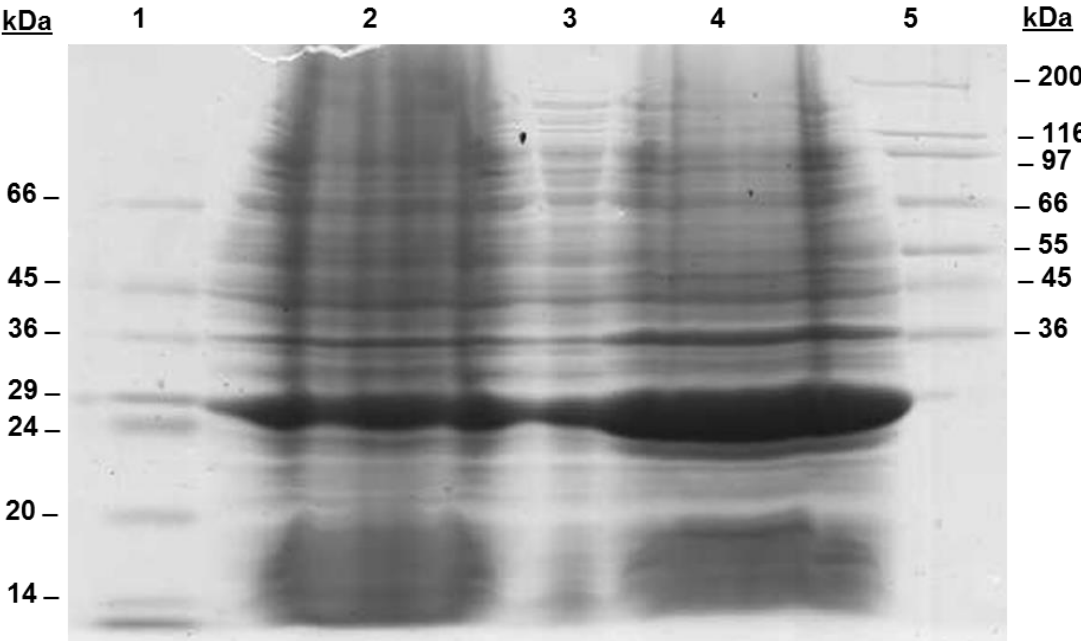
Appendix 7.360: GF of fractions eluted following IMAC purification under denaturing conditions

IMAC purification was performed on cell lysate containing *N*-terminally His-tagged recombinant lysostaphin (construct 1). IMAC separation was performed as described in Appendix 7.117, however the separation was performed using IMAC denaturing start and elution buffers. Fractions were subsequently collected using a Foxy[®] Jr Fraction collector between 53 and 103 min. Selected fractions were subjected to GF separation, performed as described in Appendix 7.359.

Appendix 7.361: GF of fractions eluted following WCX separation of recombinant lysostaphin isoforms

WCX separation was performed on cell lysate containing *N*-terminally His-tagged recombinant lysostaphin (construct 1). WCX separation was performed as described in Appendix 7.229 and fractions were subsequently collected between 23 and 38 min. Selected fractions were subjected to GF separation, performed as described in Appendix 7.359. Comparative SCX separations were performed on the same cell lysates, as described in Appendix 7.231, however fractions collected during SCX separation were not subjected to GF analysis.

Appendix 7.362: SDS-PAGE analysis of cell lysate containing N-terminally His-tagged recombinant lysostaphin (construct 1, preparation 19) expressed in *E.coli* BL21(DE3) cultured in AIM. Lane 1: Sigma low molecular weight markers; Lane 2: CFE (neat); Lane 3: CFE (1:10); Lane 4: CFE in solubilising buffer; Lane 5: Sigma high molecular weight markers.



7.3.4 LC-MS analysis of recombinant lysostaphin

Appendix 7.363: Buffers

WCX buffer A (1L) (as described in Chapter 3.2.1 /Appendix 7.136)

WCX buffer B (1L) (as described in Chapter 3.2.1 / Appendix 7.136)

RP buffer A (1 L)

Formic acid (0.1% v/v) 1 ml

The buffer was made up to 1 L using LC/MS grade H₂O.

RP buffer B (1 L)

Acetonitrile (80% v/v) 800.0 ml

Formic acid (0.05% v/v) 0.5 ml

The buffer was made up to 1 L using LC/MS grade H₂O.

Appendix 7.364: Equipment

WCX separation prior to intact MS analysis was performed using the ProPac[®] WCX-10 (4 x 500 mm) column and an Ultimate[™] 3000 Titanium system, which consisted of an analytical titanium pump, a thermal compartment with two column change valves, a VWD detector and a WPS-3000 biocompatible autosampler. The system was fitted with a PEEK fluidic pathway. The thermal compartment was maintained at 30°C and the autosampler was fitted with a 250 µl syringe and a 1 ml injection loop. Although the autosampler could accommodate fractionation, fractionation was performed using an ISCO Foxy[®] Jr Fraction collector in this instance. Data collection and analysis was performed using Chromeleon[®] Chromatography Data System software with fractionation license.

Intact MS analysis was performed using an online MaXis UHR-TOF system (Bruker Daltonics, Germany) coupled to an Ultimate[™] 3000 LC system with a PepSwift[®] monolithic

PS-DVB column. The Ultimate™ 3000 system featured a flow manager column compartment with a flow-splitter cartridge to permit low flow rates and was maintained at 60°C during separation. The MaXis UHR-TOF system was fitted with an ESI source (Bruker, UK). The instruments were controlled using Hystar™ 3.2 (Build 44) and Esquire Control™ Version 6.1 (Build 92) (Bruker Daltonics) software.

Chromatographic separations were performed using a number of analytical columns, as described in Appendix 7.365.

Appendix 7.365: Analytical columns and mobile phase compositions used during LC-MS analysis of recombinant lysostaphin

Column	Chromatographic mode	Dimensions (mm)	Mobile phase conditions
ProPac® WCX-10	WCX	4.0 x 500	WCX buffer A and B
PepSwift® PS-DVB	RP	0.2 x 50	RP buffer A and B

Appendix 7.366: Sample preparation

Intact MS analysis was performed upon purified, concentrated recombinant lysostaphin which had been harvested from *E.coli* BL21(DE3) cultured in LB (Appendix 7.76) and purified using IMAC (Appendix 7.114). Following purification, the purified protein was concentrated using ultrafiltration (Appendix 7.120). The purified and concentrated recombinant lysostaphin was then separated by WCX prior to intact MS analysis. Further details about preparation of recombinant lysostaphin is provided in Appendix 7.367.

Appendix 7.367: Purified recombinant lysostaphin preparation

Preparation ID	Construct	Expression media	Mode of purification	Protein concentration ($\mu\text{g}/\mu\text{l}$)	Related results
16	1	LB	IMAC	312.23	Appendix 7.313 Appendix 7.314 Appendix 7.315

Appendix 7.368: WCX separation of purified recombinant lysostaphin

WCX separation was performed using a 0.5 ml/min flow rate and a ProPac[®] WCX-10 (4 x 500 mm) column. Following purification and concentration, 31 mg (500 μl) of a 1:5 dilution of *N*-terminally His-tagged recombinant lysostaphin (construct 1, preparation 16) was injected onto the column. Protein isoforms were separated by applying a linear gradient of 0-50% B over 70 min. The column was then washed using 90% B for 4 min and then the column was equilibrated at 0% B for 20 min. UV data was acquired at 214 and 280 nm throughout the separation and fractions were collected by time, every 30 s between 20 and 70 min. Following separation, fractions 14 and 25 were concentrated and desalted as described in Appendix 7.369. Samples were stored at 4°C until they could be analysed by LC-MS as described in Section 4.4.2.4.

Appendix 7.369: Concentration of WCX fractions for intact MS analysis

Following WCX purification, selected fractions were desalted and concentrated using Nanosep[®] centrifugal devices with a 10 kDa membrane (Pall Gelman Laboratory, USA). The Nanosep[®] device was placed into a filtrate container and the 250 μl of eluted sample was pipetted into the concentrator device. The device was centrifuged at 14,000 x g until the volume of sample had reached a minimum volume of 20 μl . The sample was washed and desalted by applying 500 μl of 18.2 M Ω /cm H₂O to device before centrifuging at 14,000 x g for 10 min. This wash procedure was repeated five times before the resulting sample was analysed by intact LC-MS (Section 4.4.2.4).

Appendix 7.370: ProtParam analysis of *N*-terminally His-tagged recombinant lysostaphin (construct 1) with loss of *N*-terminal methionine₁

User-provided sequence:

```
      10      20      30      40      50      60
GSSHHHHHHS SRLVPRGSHM AATHEHSAQW LNNYKKGYGY GPYPLGINGG MHYGVDFFMN

      70      80      90     100     110     120
IGTPVKAISS GKIVEAGWSN YGGGNQIGLI ENDGVHRQWY MHLSKYNVKV GDYVKAGQII

     130     140     150     160     170     180
GWSGSTGYST APHLHFQRMV NSFSNSTAQD PMPFLKSAGY GKAGGTVIPT PNTGWKTKNY

     190     200     210     220     230     240
GTLYKSESAS FTPNTDIITR TTGPFRSMPQ SGVLKAGQTI HYDEVKQDGH HWVVGTYGNS

     250     260
GQRIYLPVRT WNKSTNTLGV LWGTIK
```

Number of amino acids: 266

Molecular weight: 29206.7

Theoretical pI: 9.72

Appendix 7.371: ProtParam analysis of *N*-terminally His-tagged recombinant lysostaphin (construct 1) with loss of *N*-terminal glycine₂

User-provided sequence:

```
      10      20      30      40      50      60
SSHHHHHHHS RLVPRGSHMA ATHEHSAQWL NNYKKGYGYG PYPLGINGGM HYGVDFFMNI

      70      80      90     100     110     120
GTPVKAISSG KIVEAGWSNY GGGNQIGLIE NDGVHRQWYM HLSKYNVKVG DYVKAGQIIG

     130     140     150     160     170     180
WSGSTGYSTA PHLHFQRMVN SFSNSTAQDP MPFLKSAGYG KAGGTVIPTP NTGWKTKNYG

     190     200     210     220     230     240
TLYKSESASF TPNTDIITRT TGPFRRSMPQS GVLKAGQTIH YDEVKQDGH VWVVGTYGNSG

     250     260
QRIYLPVRTW NKSTNTLGVL WGTIK
```

Number of amino acids: 265

Molecular weight: 29149.6

Theoretical pI: 9.72

Appendix 7.372: ProtParam analysis of *N*-terminally His-tagged recombinant lysostaphin (construct 1) with loss of *N*-terminal serine₃

User-provided sequence:

```
      10      20      30      40      50      60
SHHHHHHSSR LVPRGSHMAA THEHSAQWLN NYKKGYGYGP YPLGINGGMH YGVDFFMNIG

      70      80      90     100     110     120
TPVKAISSGK IVEAGWSNYG GGNQIGLIEN DGVHRQWYMH LSKYNVKVGD YVKAGQIIGW

     130     140     150     160     170     180
SGSTGYSTAP HLHFQRMVNS FSNSTAQDPM PFLKSAGYGK AGGTVTPTPN TGWKTNKYGT

     190     200     210     220     230     240
LYKSESASFT PNTDIITRIT GPFRSMPQSG VLKAGQTIHY DEVMKQDGHV WVG YTGNSGQ

     250     260
RIYLPVRTWN KSTNTLGVLW GTIK
```

Number of amino acids: 264

Molecular weight: 29062.5

Theoretical pI: 9.72

Appendix 7.373: ProtParam analysis of *N*-terminally His-tagged recombinant lysostaphin (construct 1) with loss of *N*-terminal serine₄

User-provided sequence:

```
      10      20      30      40      50      60
HHHHHHHSSRL VPRGSHMAAT HEHSAQWLNN YKKG YGYGPY PLGINGGMHY GVDFFMNIGT

      70      80      90     100     110     120
PVKAISSGKI VEAGWSNYGG GNQIGLIEND GVHRQWYMH LSKYNVKVGDY VKAGQIIGWS

     130     140     150     160     170     180
GSTGYSTAPH LHFQRMVNSF SNSTAQDPMP FLKSAGYGKA GGTVTPTPNT GWKTNKYGT L

     190     200     210     220     230     240
YKSESASFTP NTDIITRTTG PFRSMPQSGV LKAGQTIHYD EVMKQDGHVW VGYTGNSGQR

     250     260
IYLPVRTWNK STNTLGVLWG TIK
```

Number of amino acids: 263

Molecular weight: 28975.4

Theoretical pI: 9.72

Appendix 7.374: ProtParam analysis of *N*-terminally His-tagged recombinant lysostaphin (construct 1) with loss of *N*-terminal histidine₅

User-provided sequence:

```
      10      20      30      40      50      60
HHHHHSSRLV PRGSHMAATH EHSAQWLNNY KKGYGYPYP LGINGGMHYG VDFFMNIGTP

      70      80      90     100     110     120
VKAISSGKIV EAGWSNYGGG NQIGLIENDG VHRQWYMHLS KYNVKVGDYV KAGQIIGWSG

     130     140     150     160     170     180
STGYSTAPHL HFQRMVNSFS NSTAQDPMPF LKSAGYGKAG GTVIPTPNIG WKTINKYGTLY

     190     200     210     220     230     240
KSESASFTPN TDIITRTTGP FRSMPSQSVL KAGQTIHYDE VMKQDGHVWV GYTGNISGQRI

     250     260
YLPVRTWNKS TNTLGVWLTG IK
```

Number of amino acids: 262

Molecular weight: 28838.3

Theoretical pI: 9.72

Appendix 7.375: ProtParam analysis of *N*-terminally His-tagged recombinant lysostaphin (construct 1) with loss of *N*-terminal histidine₆

User-provided sequence:

```
      10      20      30      40      50      60
HHHHSSRLVP RGSMAATHE HSAQWLNNYK KKGYGYPYPL GINGGMHYGV DFFMNIGTPV

      70      80      90     100     110     120
KAISSGKIVE AGWSNYGGGN QIGLIENDGV HRQWYMHLSK YNVKVGDIYV AGQIIGWSGS

     130     140     150     160     170     180
TGYSTAPHLH FQRMVNSFSN STAQDPMPFL KSAGYGKAGG TVTPTPNIGW KTKYGTLYK

     190     200     210     220     230     240
SESASFTPNT DIITRTTGPF RSMPSQSVLK AGQTIHYDEV MKQDGHVWVG YTGNSGQRIY

     250     260
LPVRTWNKST NTLGVWLTG K
```

Number of amino acids: 261

Molecular weight: 28701.2

Theoretical pI: 9.72

Appendix 7.376: ProtParam analysis of *N*-terminally His-tagged recombinant lysostaphin (construct 1) with loss of C-terminal lysine₂₆₇

User-provided sequence:

```
      10      20      30      40      50      60
MGSSHHHHHH SSRLVPRGSH MAATHEHSAQ WLNNYKKGYG YGPYPLGING GMHYGVDFFM

      70      80      90     100     110     120
NIGTPVKAIS SGKIVEAGWS NYGGGNQIGL IENDGVHRQW YMHLSKYNVK VGDYVKAGQI

     130     140     150     160     170     180
IGWSGSTGYS TAPHLHFQRM VNSFSNSTAQ DPMPFLKSAG YGKAGGTVIP TPNTIGWKINK

     190     200     210     220     230     240
YGTLYKSESA SFTPNTDIIT RTTGPFRSMP QSGVLKAGQT IHYDEVKMQD GHVWVGYTGN

     250     260
SGQRIYLPVR TWNKSTNTLG VLWGTI
```

Number of amino acids: 266

Molecular weight: 29209.7

Theoretical pI: 9.68

Appendix 7.377: ProtParam analysis of *N*-terminally His-tagged recombinant lysostaphin (construct 1) with loss of C-terminal isoleucine₂₆₆

User-provided sequence:

```
      10      20      30      40      50      60
MGSSHHHHHH SSRLVPRGSH MAATHEHSAQ WLNNYKKGYG YGPYPLGING GMHYGVDFFM

      70      80      90     100     110     120
NIGTPVKAIS SGKIVEAGWS NYGGGNQIGL IENDGVHRQW YMHLSKYNVK VGDYVKAGQI

     130     140     150     160     170     180
IGWSGSTGYS TAPHLHFQRM VNSFSNSTAQ DPMPFLKSAG YGKAGGTVIP TPNTIGWKINK

     190     200     210     220     230     240
YGTLYKSESA SFTPNTDIIT RTTGPFRSMP QSGVLKAGQT IHYDEVKMQD GHVWVGYTGN

     250     260
SGQRIYLPVR TWNKSTNTLG VLWGT
```

Number of amino acids: 265

Molecular weight: 29096.5

Theoretical pI: 9.68

Appendix 7.378: ProtParam analysis of *N*-terminally His-tagged recombinant lysostaphin (construct 1) with loss of C-terminal threonine₂₆₅

User-provided sequence:

```
      10      20      30      40      50      60
MGSSHHHHHH SSRLVPRGSH MAATHEHSAQ WLNNYKKGYG YGPYPLGING GMHYGVDFFM

      70      80      90     100     110     120
NIGTPVKAIS SGKIVEAGWS NYGGGNQIGL IENDGVHRQW YMHLSKYNVK VGDYVKAGQI

     130     140     150     160     170     180
IGWSGSTGYS TAPHLHFQRM VNSFSNSTAQ DPMPFLKSAG YGKAGGTVTP TPNTGWKTNK

     190     200     210     220     230     240
YGTLYKSESA SFTPNTDIIT RTTGPFRSMP QSGVLKAGQT IHYDEVKQD GHVWVGYTGN

     250     260
SGQRIYLPVR TWNKSTNTLG VLWG
```

Number of amino acids: 264

Molecular weight: 28995.4

Theoretical pI: 9.68

Appendix 7.379: ProtParam analysis of *N*-terminally His-tagged recombinant lysostaphin (construct 1) with loss of C-terminal glycine₂₆₄

User-provided sequence:

```
      10      20      30      40      50      60
MGSSHHHHHH SSRLVPRGSH MAATHEHSAQ WLNNYKKGYG YGPYPLGING GMHYGVDFFM

      70      80      90     100     110     120
NIGTPVKAIS SGKIVEAGWS NYGGGNQIGL IENDGVHRQW YMHLSKYNVK VGDYVKAGQI

     130     140     150     160     170     180
IGWSGSTGYS TAPHLHFQRM VNSFSNSTAQ DPMPFLKSAG YGKAGGTVTP TPNTGWKTNK

     190     200     210     220     230     240
YGTLYKSESA SFTPNTDIIT RTTGPFRSMP QSGVLKAGQT IHYDEVKQD GHVWVGYTGN

     250     260
SGQRIYLPVR TWNKSTNTLG VLW
```

Number of amino acids: 263

Molecular weight: 28938.4

Theoretical pI: 9.68

Appendix 7.380: ProtParam analysis of *N*-terminally His-tagged recombinant lysostaphin (construct 1) with loss of C-terminal tryptophan₂₆₃

User-provided sequence:

```
      10      20      30      40      50      60
MGSSHHHHHHH SSRLVPRGSH MAATHEHSAQ WLNNYKKGYG YGPYPLGING GMHYGVDFFM

      70      80      90     100     110     120
NIGTPVKAIS  SGKIVEAGWS  NYGGGNQIGL  IENDGVHRQW  YMHLSKYNVK  VGDYVKAGQI

     130     140     150     160     170     180
IGWSGSTGYS  TAPHLHFQRM  VNSFSNSTAQ  DPMPFLKSAG  YGKAGGTVTP  TPNTGWKTNK

     190     200     210     220     230     240
YGTLYKSESA  SFTPNTDIIT  RTTGPFRSMP  QSGVLKAGQT  IHYDEVKQD   GHVWVGYTGN

     250     260
SGQRIYLPVR  TWNKSTNTLG VL
```

Number of amino acids: 262

Molecular weight: 28752.1

Theoretical pI: 9.68

Appendix 7.381: ProtParam analysis of *N*-terminally His-tagged recombinant lysostaphin (construct 1) with loss of C-terminal leucine₂₆₂

User-provided sequence:

```
      10      20      30      40      50      60
MGSSHHHHHHH SSRLVPRGSH MAATHEHSAQ WLNNYKKGYG YGPYPLGING GMHYGVDFFM

      70      80      90     100     110     120
NIGTPVKAIS  SGKIVEAGWS  NYGGGNQIGL  IENDGVHRQW  YMHLSKYNVK  VGDYVKAGQI

     130     140     150     160     170     180
IGWSGSTGYS  TAPHLHFQRM  VNSFSNSTAQ  DPMPFLKSAG  YGKAGGTVTP  TPNTGWKTNK

     190     200     210     220     230     240
YGTLYKSESA  SFTPNTDIIT  RTTGPFRSMP  QSGVLKAGQT  IHYDEVKQD   GHVWVGYTGN

     250     260
SGQRIYLPVR  TWNKSTNTLG V
```

Number of amino acids: 261

Molecular weight: 28639.0

Theoretical pI: 9.68

Appendix 7.382: ProtParam analysis of *N*-terminally His-tagged recombinant lysostaphin (construct 1) with loss of methionine₁ and lysine₂₆₇

User-provided sequence:

```
      10      20      30      40      50      60
GSSHHHHHHS SRLVPRGSHM AATHEHSAQW LNNYKKGYG YPYPLGINGG MHYGVDFFMN

      70      80      90     100     110     120
IGTPVKAISS GKIVEAGWSN YGGGNQIGLI ENDGVHRQWY MHLSKYNVKV GDYVKAGQII

     130     140     150     160     170     180
GWSGSTGYST APHLHFQRMV NSFSNSTAQD PMPFLKSAGY GKAGGTVTPT PNTGWKTKNY

     190     200     210     220     230     240
GTLYKSESAS FTPNTDIITR TTGPFRSMPQ SGVLKAGQTI HYDEVKQDG HWVVG YTGNS

     250     260
GQRIYLPVRT WNKSTNTLGV LWGTI
```

Number of amino acids: 265

Molecular weight: 29078.5

Theoretical pI: 9.68

Appendix 7.383: ProtParam analysis of *N*-terminally His-tagged recombinant lysostaphin (construct 1) with loss of methionine₁ and isoleucine₂₆₆

User-provided sequence:

```
      10      20      30      40      50      60
GSSHHHHHHS SRLVPRGSHM AATHEHSAQW LNNYKKGYG YPYPLGINGG MHYGVDFFMN

      70      80      90     100     110     120
IGTPVKAISS GKIVEAGWSN YGGGNQIGLI ENDGVHRQWY MHLSKYNVKV GDYVKAGQII

     130     140     150     160     170     180
GWSGSTGYST APHLHFQRMV NSFSNSTAQD PMPFLKSAGY GKAGGTVTPT PNTGWKTKNY

     190     200     210     220     230     240
GTLYKSESAS FTPNTDIITR TTGPFRSMPQ SGVLKAGQTI HYDEVKQDG HWVVG YTGNS

     250     260
GQRIYLPVRT WNKSTNTLGV LWGT
```

Number of amino acids: 264

Molecular weight: 28965.3

Theoretical pI: 9.68

Appendix 7.384: ProtParam analysis of *N*-terminally His-tagged recombinant lysostaphin (construct 1) with loss of methionine₁ and threonine₂₆₅

User-provided sequence:

```
      10      20      30      40      50      60
GSSHHHHHHS SRLVPRGSHM AATHEHSAQW LNNYKKG YGY GPYPLGINGG MHYGVDFFMN

      70      80      90     100     110     120
IGTPVKAISS GKIVEAGWSN YGGNQIGLI ENDGVHRQWY MHLKYNVKV GDYVKAGQII

     130     140     150     160     170     180
GWSGSTGYST APHLHFQRMV NSFSNSTAQD PMPFLKSAGY GKAGGTVTPT PNTGWKTINKY

     190     200     210     220     230     240
GTLYKSESAS FTPNTDIITR TTGPFRSMPQ SGVLKAGQTI HYDEVKQDG HWVVG YTGNS

     250     260
GQRIYLPVRT WNKSTNTLGV LWG
```

Number of amino acids: 263

Molecular weight: 28864.2

Theoretical pI: 9.68

Appendix 7.385: ProtParam analysis of *N*-terminally His-tagged recombinant lysostaphin (construct 1) with loss of methionine₁ and glycine₂₆₄

User-provided sequence:

```
      10      20      30      40      50      60
GSSHHHHHHS SRLVPRGSHM AATHEHSAQW LNNYKKG YGY GPYPLGINGG MHYGVDFFMN

      70      80      90     100     110     120
IGTPVKAISS GKIVEAGWSN YGGNQIGLI ENDGVHRQWY MHLKYNVKV GDYVKAGQII

     130     140     150     160     170     180
GWSGSTGYST APHLHFQRMV NSFSNSTAQD PMPFLKSAGY GKAGGTVTPT PNTGWKTINKY

     190     200     210     220     230     240
GTLYKSESAS FTPNTDIITR TTGPFRSMPQ SGVLKAGQTI HYDEVKQDG HWVVG YTGNS

     250     260
GQRIYLPVRT WNKSTNTLGV LW
```

Number of amino acids: 262

Molecular weight: 28807.2

Theoretical pI: 9.68

Appendix 7.386: ProtParam analysis of *N*-terminally His-tagged recombinant lysostaphin (construct 1) with loss of glycine₂ and lysine₂₆₇

User-provided sequence:

```
      10      20      30      40      50      60
SSHHHHHHSS RLVPRGSHMA ATHEHSAQWL NNYKKGYGYG PYPLGINGGM HYGVDFFMNI

      70      80      90     100     110     120
GTPVKAISSG KIVEAGWSNY GGGNQIGLIE NDGVHRQWYM HLSKYNVKVG DYVKAGQIIG

     130     140     150     160     170     180
WSGSTGYSTA PHLHFQRMVN SFSNSTAQDP MPFLKSAGYG KAGGTVIPTP NIGWKTKNYG

     190     200     210     220     230     240
TLYKSESASF TPNTDIIITRT TGPFRSMPQS GVLKAGQTIH YDEVMKQDGH VVVGYTGNNSG

     250     260
QRIYLPVRTW NKSTNTLGVL WGTI
```

Number of amino acids: 264

Molecular weight: 29021.4

Theoretical pI: 9.68

Appendix 7.387: ProtParam analysis of *N*-terminally His-tagged recombinant lysostaphin (construct 1) with loss of glycine₂ and isoleucine₂₆₆

User-provided sequence:

```
      10      20      30      40      50      60
SSHHHHHHSS RLVPRGSHMA ATHEHSAQWL NNYKKGYGYG PYPLGINGGM HYGVDFFMNI

      70      80      90     100     110     120
GTPVKAISSG KIVEAGWSNY GGGNQIGLIE NDGVHRQWYM HLSKYNVKVG DYVKAGQIIG

     130     140     150     160     170     180
WSGSTGYSTA PHLHFQRMVN SFSNSTAQDP MPFLKSAGYG KAGGTVIPTP NIGWKTKNYG

     190     200     210     220     230     240
TLYKSESASF TPNTDIIITRT TGPFRSMPQS GVLKAGQTIH YDEVMKQDGH VVVGYTGNNSG

     250     260
QRIYLPVRTW NKSTNTLGVL WGT
```

Number of amino acids: 263

Molecular weight: 28908.3

Theoretical pI: 9.68

Appendix 7.388: ProtParam analysis of *N*-terminally His-tagged recombinant lysostaphin (construct 1) with loss of glycine₂ and threonine₂₆₅

User-provided sequence:

```
      10      20      30      40      50      60
SSHHHHHHSS RLVPRGSHMA ATHEHSAQWL NNYKKGYGYG PYPLGINGGM HYGVDFFMNI

      70      80      90     100     110     120
GTPVKAISSG KIVEAGWSNY GGNQIGLIE NDGVHRQWYM HLSKYNVKVG DYVKAGQIIG

     130     140     150     160     170     180
WSGSTGYSTA PHLHFQRMVN SFSNSTAQDP MPFLKSAGYG KAGGTVTPTP NTGWKTNKYG

     190     200     210     220     230     240
TLYKSESASF TPNTDIITRT TGPFRSMPQS GVLKAGQTIH YDEVKQDGH VWVGYTGNSG

     250     260
QRIYLPVRTW NKSTNTLGVL WG
```

Number of amino acids: 262

Molecular weight: 28807.2

Theoretical pI: 9.68

Appendix 7.389: ProtParam analysis of *N*-terminally His-tagged recombinant lysostaphin (construct 1) with loss of serine₃ and lysine₂₆₇

User-provided sequence:

```
      10      20      30      40      50      60
SHHHHHHSSR LVPRGSHMAA THEHSAQWLN NYKKGYGYGP YPLGINGGMH YGVDFFMNIG

      70      80      90     100     110     120
TPVKAISSGK IVEAGWSNYG GGNQIGLIEN DGVHRQWYMH LSKYNVKVGD YVKAGQIIGW

     130     140     150     160     170     180
SGSTGYSTAP HLFHFQRMVNS FSNSTAQDPM PFLKSAGYGK AGGTVTPTPN TGWKTNKYGT

     190     200     210     220     230     240
LYKSESASF TPNTDIITRT GPFRSMPQSG VLKAGQTIHY DEVKQDGHV VWVGYTGNSGQ

     250     260
RIYLPVRTWN KSTNTLGVLW GTI
```

Number of amino acids: 263

Molecular weight: 28934.4

Theoretical pI: 9.68

Appendix 7.390: ProtParam analysis of *N*-terminally His-tagged recombinant lysostaphin (construct 1) with loss of serine₃ and isoleucine₂₆₆

User-provided sequence:

```
      10      20      30      40      50      60
SHHHHHHSSR LVPRGSHMAA THEHSAQWLN NYKKGYGYGP YPLGINGGMH YGVDFFMNIG

      70      80      90     100     110     120
TPVKAISSGK IVEAGWSNYG GGNQIGLIEN DGVHRQWYMH LSKYNVKVGD YVKAGQIIGW

     130     140     150     160     170     180
SGSTGYSTAP HLHFQRMVNS FSNSTAQDPM PFLKSAGYGK AGGTVTPTPN TGWKTNKYGT

     190     200     210     220     230     240
LYKSESASFT PNTDIITRTT GPFRSMPQSG VLKAGQTIHY DEVMKQDGHV WVG YTGNSGQ

     250     260
RIYLPVRTWN KSTNTLGVLW GT
```

Number of amino acids: 262

Molecular weight: 28821.2

Theoretical pI: 9.68

Appendix 7.391: ProtParam analysis of *N*-terminally His-tagged recombinant lysostaphin (construct 1) with loss of serine₄ and lysine₂₆₇

User-provided sequence:

```
      10      20      30      40      50      60
HHHHHHSSRL VPRGSHMAAT HEHSAQWLNN YKKG YGYGPY PLGINGGMHY GVDFFMNIGT

      70      80      90     100     110     120
PVKAISSGKI VEAGWSNYGG GNQIGLIEND GVHRQWYMH LSKYNVKVGDY VKAGQIIGWS

     130     140     150     160     170     180
GSTGYSTAPH LHFQRMVNSF SNSTAQDPM PFLKSAGYGKA GGTVTPTPNT GWKTNKYGTL

     190     200     210     220     230     240
YKSESASFTP NTDIITRTTG PFRSMPQSGV LKAGQTIHYD EVMKQDGHVW VGYTGNSGQR

     250     260
IYLPVRTW NKSTNTLGVLWG TI
```

Number of amino acids: 262

Molecular weight: 28847.3

Theoretical pI: 9.68

Appendix 7.392: ProtParam analysis of *N*-terminally His-tagged recombinant lysostaphin (construct 1) with loss of serine₄ and isoleucine₂₆₆

User-provided sequence:

```
      10      20      30      40      50      60
HHHHHHSSRL VPRGSHMAAT HEHSAQWLNN YKKGYGYPY PLGINGGMHY GVDFFMNIGT

      70      80      90     100     110     120
PVKAISSGKI VEAGWSNYGG GNQIGLIEND GVHRQWYML SKYNVKVGDY VKAGQIIGWS

     130     140     150     160     170     180
GSTGYSTAPH LHFQRMVNSF SNSTAQDPMP FLKSAGYGKA GGTVTPTPNT GWKTNKYGL

     190     200     210     220     230     240
YKSESASFTP NTDIITRTTG PFRSMPQSGV LKAGQIIHYD EVMKQDGHVW VGYTGNSGQR

     250     260
IYLPVRTWNK STNILGVLWG T
```

Number of amino acids: 261

Molecular weight: 28734.1

Theoretical pI: 9.68

Appendix 7.393: Comparison of full-length and *N*-terminally truncated apoprotein masses (Da) with intact mass measurements obtained during LC-MS of protein eluted in Fraction 14 during WCX separation.

Intact Mass (Da)	Full-length mass (29337.8 Da)	ΔM_1 (29206.7 Da)	ΔM_1-G_2 (29149.6 Da)	ΔM_1-S_3 (29062.5 Da)	ΔM_1-S_4 (28975.4 Da)	ΔM_1-H_5 (28838.3 Da)	ΔM_1-H_6 (28701.2 Da)
29050.517	-287.3	-156.2	-99.1	-12.0	75.1	212.2	349.3
29092.348	-245.5	-114.4	-57.3	29.8	116.9	254.0	391.1
29147.220	-190.6	-59.5	-2.4	84.7	171.8	308.9	446.0
29182.920	-154.9	-23.8	33.3	120.4	207.5	344.6	481.7
29235.798	-102.0	29.1	86.2	173.3	260.4	397.5	534.6
29280.726	-57.1	74.0	131.1	218.2	305.3	442.4	579.5
29649.793	312.0	443.1	500.2	587.3	674.4	811.5	948.6

Appendix 7.394: Comparison of full-length and C-terminally truncated apoprotein masses (Da) with intact mass measurements obtained during LC-MS of protein eluted in Fraction 14 during WCX separation

Intact Mass (Da)	Full-length mass (29337.8 Da)	ΔK_{267} (29209.7 Da)	$\Delta I_{266}-K_{267}$ (29096.5 Da)	$\Delta T_{265}-K_{267}$ (28995.4 Da)	$\Delta G_{264}-K_{267}$ (28938.4 Da)	$\Delta W_{263}-K_{267}$ (28752.1 Da)	$\Delta L_{262}-K_{267}$ (28639.0 Da)
29050.517	-287.3	-159.2	-46.0	55.1	112.1	298.4	411.5
29092.348	-245.5	-117.4	-4.2	96.9	153.9	340.3	453.3
29147.220	-190.6	-62.5	50.7	151.8	208.8	395.12	508.2
29182.920	-154.9	-26.8	86.4	187.5	244.5	430.8	543.9
29235.798	-102.0	26.1	139.3	240.4	297.4	483.7	596.8
29280.726	-57.1	71.0	184.2	285.3	342.3	528.6	641.7
29649.793	312.0	440.1	553.3	654.4	711.4	897.7	1010.8

Appendix 7.395: Comparison of full-length and N- and C-terminally truncated apoprotein masses (Da) with intact mass measurements obtained during LC-MS of protein eluted in Fraction 14 during WCX separation.

Intact Mass (Da)	Full-length mass (29337.8 Da)	$\Delta M_1 + \Delta K_{267}$ (29078.5 Da)	$\Delta M_1 + \Delta I_{266} - K_{267}$ (28965.3 Da)	$\Delta M_1 + \Delta T_{265} - K_{267}$ (28864.2 Da)	$\Delta M_1 + \Delta G_{264} - K_{267}$ (28807.2 Da)
29050.517	-287.3	-28.0	85.2	186.3	243.3
29092.348	-245.5	13.8	127.0	228.1	285.1
29147.22	-190.6	68.7	181.9	283.0	340.0
29182.92	-154.9	104.4	217.6	318.7	375.7
29235.798	-102.0	157.3	270.5	371.6	428.6
29280.726	-57.1	202.2	315.4	416.5	473.5
29649.793	312.0	571.3	684.5	785.6	842.6

Intact Mass (Da)	$\Delta M_1 - G_2 + \Delta K_{267}$ (29021.4 Da)	$\Delta M_1 - G_2 + \Delta I_{266} - K_{267}$ (28908.3 Da)	$\Delta M_1 - G_2 + \Delta T_{265} - K_{267}$ (28807.2 Da)	$\Delta M_1 - S_3 + \Delta K_{267}$ (28934.4 Da)	$\Delta M_1 - S_3 + \Delta I_{266} - K_{267}$ (28821.2 Da)	$\Delta M_1 - S_4 + \Delta K_{267}$ (28847.3 Da)	$\Delta M_1 - S_4 + \Delta I_{266} - K_{267}$ (28734.1 Da)
29050.517	29.1	142.2	243.3	116.1	229.3	203.2	316.4
29092.348	71.0	184.0	285.2	158.0	271.2	245.1	358.3
29147.22	125.8	238.9	340.0	212.8	326.0	299.9	413.1
29182.92	161.5	274.6	375.7	248.5	361.7	335.6	448.8
29235.798	214.4	327.5	428.6	301.4	414.6	388.5	501.7
29280.726	259.3	372.4	473.5	346.3	459.6	433.4	546.6
29649.793	628.4	741.5	842.6	715.4	828.6	802.5	915.7

Appendix 7.396: Comparison of full-length and *N*-terminally truncated apoprotein masses (Da) with intact mass measurements obtained during LC-MS of protein eluted in Fraction 25 during WCX separation.

Intact Mass (Da)	Full-length mass (29337.8 Da)	ΔM_1 (29206.7 Da)	ΔM_1-G_2 (29149.6 Da)	ΔM_1-S_3 (29062.5 Da)	ΔM_1-S_4 (28975.4 Da)	ΔM_1-H_5 (28838.3 Da)	ΔM_1-H_6 (28701.2 Da)
28829.1	-508.7	-377.6	-320.5	-233.4	-146.3	-9.2	127.9
28873.4	-464.4	-333.3	-276.2	-189.1	-102.0	35.1	172.2
28905.1	-432.7	-301.6	-244.5	-157.4	-70.3	66.8	203.9
29107.7	-230.1	-99.0	-41.9	45.2	132.3	269.4	406.5
29150.7	-187.1	-56.0	1.1	88.2	175.3	312.4	449.5
29336.9	-0.9	130.2	187.3	274.4	361.5	498.6	635.7
29396.6	58.8	189.9	247.0	334.1	421.2	558.3	695.4
29441.8	104.0	235.1	292.2	379.3	466.4	603.5	740.6
29477.0	139.2	270.3	327.4	414.5	501.6	638.7	775.8
29569.7	231.9	363.0	420.1	507.2	594.3	731.4	868.5
29630.0	292.2	423.3	480.4	567.5	654.6	791.7	928.8

Appendix 7.397: Comparison of full-length and C-terminally truncated apoprotein masses (Da) with intact mass measurements obtained during LC-MS of protein eluted in Fraction 25 during WCX separation.

Intact Mass (Da)	Full-length mass (29337.8 Da)	ΔK_{267} (29209.7Da)	$\Delta I_{266}-K_{267}$ (29096.5 Da)	$\Delta T_{265}-K_{267}$ (28995.4 Da)	$\Delta G_{264}-K_{267}$ (28938.4 Da)	$\Delta W_{263}-K_{267}$ (28752.1 Da)	$\Delta L_{262}-K_{267}$ (28639.0 Da)
28829.1	-508.7	-380.6	-267.4	-166.3	-109.3	77.0	190.1
28873.4	-464.4	-336.3	-223.1	-122.0	-65.0	121.3	234.4
28905.1	-432.7	-304.6	-191.4	-90.3	-33.3	153.0	266.1
29107.7	-230.1	-102.0	11.2	112.3	169.3	355.6	468.7
29150.7	-187.1	-59.0	54.2	155.3	212.3	398.6	511.7
29336.9	-0.9	127.2	240.4	341.5	398.5	584.8	697.9
29396.6	58.8	186.9	300.1	401.2	458.2	644.5	757.6
29441.8	104.0	232.1	345.3	446.4	503.4	689.7	802.8
29477.0	139.2	267.3	380.5	481.6	538.6	724.9	838.0
29569.7	231.9	360.0	473.2	574.3	631.3	817.6	930.7
29630.0	292.2	420.3	533.5	634.6	691.6	877.9	991.0

Appendix 7.398: Comparison of full-length and N- and C-terminally truncated apoprotein masses (Da) with intact mass measurements obtained during LC-MS of protein eluted in Fraction 25 during WCX separation.

Intact Mass (Da)	Full-length mass (29337.8 Da)	$\Delta M_1 + \Delta K_{267}$ (29078.5 Da)	$\Delta M_1 + \Delta I_{266} - K_{267}$ (28965.3 Da)	$\Delta M_1 + \Delta T_{265} - K_{267}$ (28864.2 Da)	$\Delta M_1 + \Delta G_{264} - K_{267}$ (28807.2 Da)
28829.1	-508.7	-249.4	-136.2	-35.1	21.9
28873.4	-464.4	-205.1	-91.9	9.2	66.2
28905.1	-432.7	-173.4	-60.2	40.9	97.9
29107.7	-230.1	29.2	142.4	243.5	300.5
29150.7	-187.1	72.2	185.4	286.5	343.5
29336.9	-0.9	258.4	371.6	472.7	529.7
29396.6	58.8	318.1	431.3	532.4	589.4
29441.8	104.0	363.3	476.5	577.6	634.6
29477.0	139.2	398.5	511.7	612.8	669.8
29569.7	231.9	491.2	604.4	705.5	762.5
29630.0	292.2	551.5	664.7	765.8	822.8

Appendix 7.398: Comparison of full-length and N- and C-terminally truncated apoprotein masses (Da) with intact mass measurements obtained during LC-MS of protein eluted in Fraction 25 during WCX separation (continued)

Intact Mass (Da)	$\Delta M_1-G_2+\Delta K_{267}$ (29021.4 Da)	$\Delta M_1-G_2+\Delta I_{266}-K_{267}$ (28908.3 Da)	$\Delta M_1-G_2+\Delta T_{265}-K_{267}$ (28807.2 Da)	$\Delta M_1-S_3+\Delta K_{267}$ (28934.4 Da)	$\Delta M_1-S_3+\Delta I_{266}-K_{267}$ (28821.2 Da)	$\Delta M_1-S_4+\Delta K_{267}$ (28847.3 Da)	$\Delta M_1-S_4+\Delta I_{266}-K_{267}$ (28734.1 Da)
28829.1	-192.3	-79.2	21.9	-105.3	7.9	-18.2	95.0
28873.4	-148.0	-34.9	66.2	-61.0	52.2	26.1	139.3
28905.1	-116.3	-3.2	97.9	-29.3	83.9	57.8	171.0
29107.7	86.3	199.4	300.5	173.3	286.5	260.4	373.6
29150.7	129.3	242.4	343.5	216.3	329.5	303.4	416.6
29336.9	315.5	428.6	529.7	402.5	515.7	489.6	602.8
29396.6	375.2	488.3	589.4	462.2	575.4	549.3	662.5
29441.8	420.4	533.5	634.6	507.4	620.6	594.5	707.7
29477.0	455.6	568.7	669.8	542.6	655.8	629.7	742.9
29569.7	548.3	661.4	762.5	635.3	748.5	722.4	835.6
29630.0	608.6	721.7	822.8	695.6	808.8	782.7	895.9